Virtual 45th Meeting of the
American Society of Biomechanics

ASB2021

August 10-13, 2021

The Big Book of Abstracts

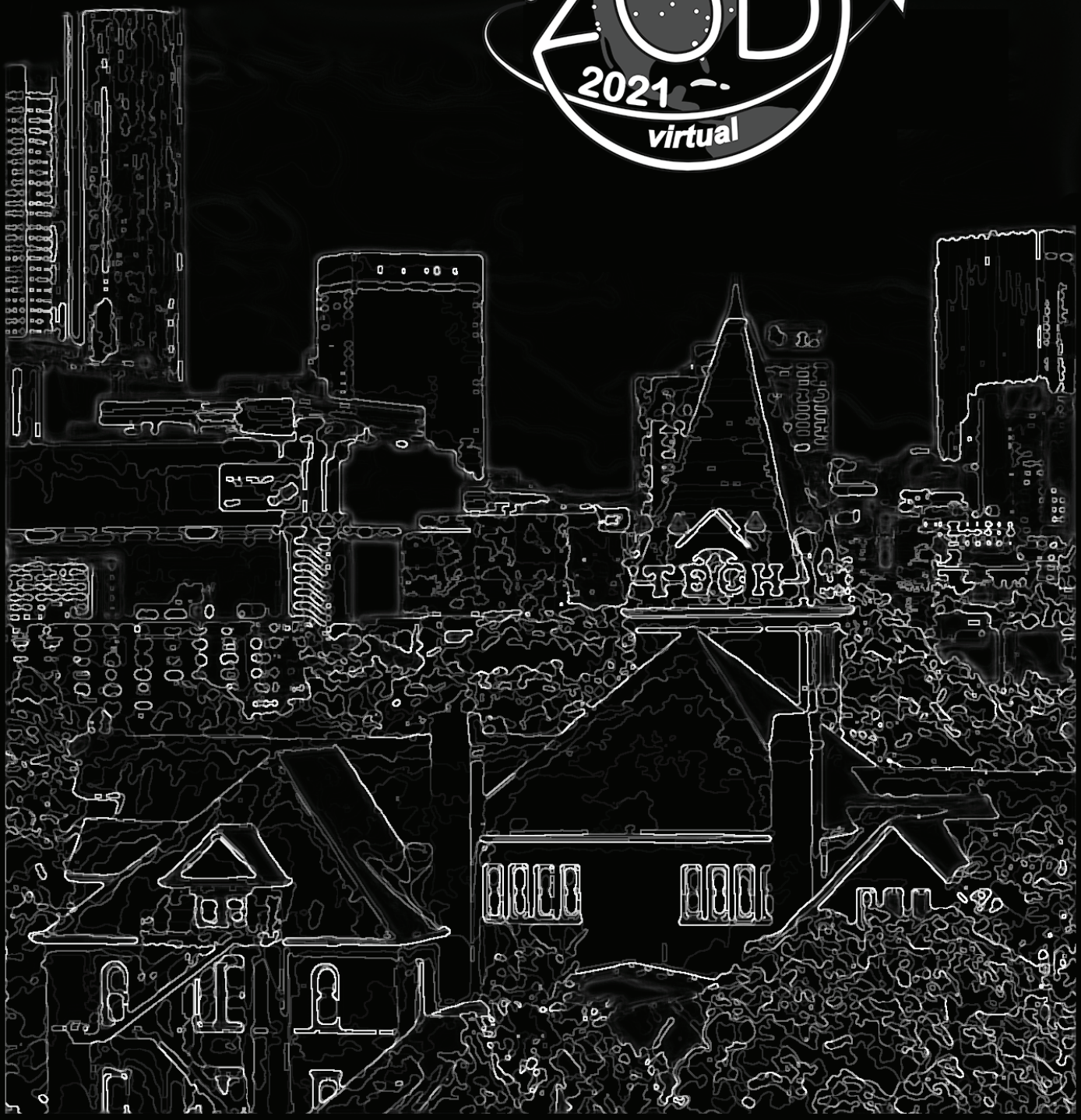

vASB2021 organizers, attendees and the American Society of Biomechanics thanks its generous sponsors:

Premium Sponsors

Conference Sponsors

IMPACT OF CALCANEAL PITCH ON MIDTARSAL JOINT KINEMATICS DURING GAIT

Paige F Paulus[1], Tom H Gale[1], Maria A Munsch[1], MaCalus V Hogan[1], and William J Anderst[1]
[1]University of Pittsburgh, Department of Orthopaedic Surgery
Email: pap82@pitt.edu

Introduction

Hindfoot kinematics during the stance phase of gait have been precisely measured using biplane radiography to provide novel insight into the dynamic kinematics of healthy and pathological feet [1, 2]. Less is known about midfoot kinematics during the gait cycle [3].

Calcaneal pitch is the angle between the inferior calcaneus and the horizontal plane (normal: 20-30°, pes planus: <18°). Diminished calcaneal pitch has been clinically associated with dysfunction such as plantar fasciitis and adult acquired flatfoot deformity [4].

The purpose of this pilot study was to explore the relationship between calcaneal pitch and talonavicular (TN) and calcaneocuboid (CC) kinematics during the stance phase of gait. We hypothesized that individuals with pes planus would have greater pronation (dorsiflexion (DF), eversion, and external rotation (ER)) and translation in CC and TN kinematics and this variation would be greater in the TN joint.

Methods

Five healthy volunteers (age: 26 to 41 years, weight: 103 to 181 lbs, and height 1.6 to 1.8 m) provided written informed consent prior to participating in this IRB-approved study. Subjects walked overground at a self-selected pace. Synchronized biplane radiographs of the foot and ankle were collected during static standing and during the full support phase of walking (heel strike (HS) to toe off (TO)) at 100 frames per second. Calcaneal pitch was measured in a static sagittal radiograph [4].

Computed Tomography scans were used to create subject-specific 3D models of the talus, calcaneus, cuboid, and navicular. A validated volumetric model-based tracking technique [5] was used to match these models to the biplane radiographic images with sub-millimeter accuracy. HS and TO were determined by a force plate under the foot.

Joint kinematics were filtered with a 4th order Butterworth filter with 10 Hz cut-off frequency and interpolated to percent stance phase. Dynamic kinematic data was normalized to the average static trial and participants grouped based on subject calcaneal pitch. Differences in kinematics between groups were evaluated using two sample t-test for static trials and statistical parametric mapping (SPM) [6] for dynamic trials with a significance set at $p < 0.05$ for all tests.

Results and Discussion

Based on calcaneal pitch assessment, two subjects were classified as normal calcaneal pitch (21.8° and 25.9°) and three were classified as pes planus (9.8° to 16.8°).

In the static standing position, the navicular was found to sit in greater dorsiflexion in relation to the talus (average difference = 24.5°, $p<0.001$) and more proximally in relation to the talus (average difference = 10.7 mm, $p<0.05$), and that the cuboid sits more medially in relation to the calcaneus (average difference = 8.4 mm, $p< 0.05$) in individuals with pes planus compared to those with normal calcaneal pitch.

The primary motion in the CC joint was dorsiflexion/plantarflexion rotation, while the primary motions in the TN joint were dorsiflexion/plantarflexion and inversion rotation (Table 1).

Table 1: Average Midtarsal Joint ROM over Stance Phase

	Talonavicular ± SD	Calcaneocuboid ± SD
Medial/Lateral Translation (mm)	4.4 ± 1.3	6.8 ± 2.4
Anterior/Posterior Translation (mm)	3.1 ± 1.1	2.3 ± 0.8
Proximal/Distal Translation (mm)	3.4 ± 0.9	7.7 ± 2.7
Dorsiflexion Rotation (°)	10.3 ± 3.8	10.0 ± 2.9
Inversion Rotation (°)	13.6 ± 3.2	7.8 ± 2.4
Internal Rotation (°)	9.6 ± 3.0	7.3 ± 3.7

During dynamic trials, the cuboid was found to move more laterally on the calcaneus ($p<0.001$) in individuals with pes planus during midstance and terminal stance (17-19% and 33-38% stance) (Figure 1).

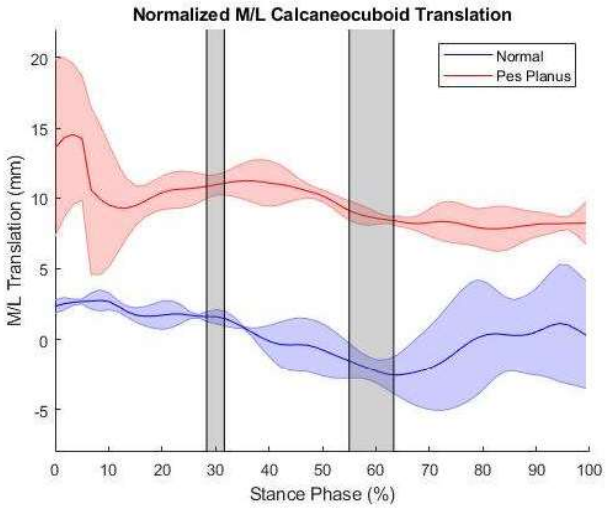

Figure 1: CC M/L translation (lateral (+), medial (-)) during dynamic trials. Gray shaded regions represent periods of significant differences ($p < 0.001$).

Significance

Results of this pilot study suggest calcaneal pitch can impact midtarsal motion during gait. This finding has implications for joint arthroplasty design and treatment of other foot pathologies. Further research on a larger cohort is justified to confirm these results.

Acknowledgments

This work was funded in part by NIH Grant R44HD066831.

References

[1] Lenz, et al, J of Biomech, 2021, [2] Yang, et al, J of Biomech, 2021 [3] Phan, et al, J. Biomech, 2019. [4] Flores, et al, RG, 2019. [5] Pitcairn et al, J. Biomech, 2020. [6] Friston, et al, Elsevier, 2007.

The Effect of Load Carrying on Gait Parameters

Mu Qiao
Department of Kinesiology, Louisiana Tech University, Ruston, LA 71272
Email: mqiao@latech.edu

Introduction

Although humans can choose gait parameters (i.e., step length and step frequency) to maintain a low-level cost of transportation, selecting gait parameters must satisfy the need to maintain balance. This work seek to explain the strategy of humans to choose gait parameters during load carrying. Load carrying can be deemed as a behavioral perturbation to probe the relationship between step length and step frequency as compared with normal walking.

The relationship between step length and step frequency could reveal the underlying mechanism among body mass, step length, and step frequency during preferred walking. The hypothesis was that load carrying would reduce walking speed by reducing step length. The alternative hypothesis was that load carrying would reduce walking speed by reducing step frequency or both of step length and step frequency.

Methods

This study recruited 42 college students (age = 22.6 ± 3.3 yrs.; body mass (m_0) = 80.2 ± 22.5 kg; body height (bh) = 1.74 ± 0.09 m, 24 males/18 females; mean ± S.D.) The Institutional Review Board of Louisiana Tech University approved all experimental procedures. Participants were asked to maintain the preferred walking speed during load carrying. The loads were weight added to the waist belt used for scuba diving (*i.e.*, 5 lbs. for each weight bag). The waist belt ensured the added weight surrounded the body's center of mass (COM) and did not hinder walking. There were three loading conditions, *i.e.*, 0 lbs. (i.e., normal condition, m_0), 15 lbs. (6.8 kg), and 30 lbs. (13.6 kg).

A photocell timing system (Brower Timing System, Draper, UT) measured participants' duration when walking from one baseline to the other baseline (i.e., 28 m) on a basketball court. To ensure participants maintained walking speed and to exclude acceleration and deceleration at the gait initiation and termination, participants chose an appropriate starting position at least 2 m behind the baseline. Participants continued walking when they passed the other baseline. An experimenter followed the participants from the starting line to the finishing line while counting the step numbers.

Results and Discussion

Load carrying affects step length but not step frequency. The load added significantly increased participants' BMI by 9% (15 lbs., $p < 0.001$) and 18% (30 lbs., $p < 0.001$), respectively (Table 1). Walking speed decreased significantly during load carrying ($p < 0.001$, Table 1). Increasing load carried by 15 lbs. (6.8 kg) and 30 lbs. (13.6 kg) decreased preferred walking speed by 3% and 5%, respectively (i.e., v decreased by 0.42 $cm \cdot s^{-1}$ per kg added, $p < 0.001$). The decrease in prefered walking speed was caused by the decrease of step length ($p < 0.001$) rather than step frequency (f, $p = 0.058$, Table 1). Increasing loads carried by 15 lbs. and 30 lbs. decreased step length by 3% and 4%, respectively (i.e., step length decreased by 2 mm per kg added, $p < 0.001$, Table 1). Hence, the null hypothesis that loading carrying would reduce walking speed by reducing step length was supported.

Load carrying did not affect step frequency during preferred walking. Humans maintain a constant tempo produced by the central pattern generator in the spinal cord without neuro inputs from the brain or peripheral areas. The unchanged step frequency (i.e., step duration) can maintain the amount of proprioceptive neurofeedback when both feet contact the ground. Although the effect size ($\eta^2 = 0.07$) of step frequency was low, the statistical power was 0.76 from the large sample size (Table 1). Hence, the unaffected step frequency is more likely to be the strategy used by humans during preferred walking.

As loads added, walking becomes unstable. To maintain balance would require humans to reduce the step length. Reducing step length could also reduce the COM's excursion and ground reaction force. Then, humans can reduce the impact absorbed at the leg joints, ligaments, and tendons and maintain the safety factor associated with injuries. The strategy that humans choose to reduce step length while maintaining step frequency under load carrying seems to balance physiological and biomechanical factors.

Significance

Characterizing gait parameters under load carrying (i.e., increased BMI) could have important implications for people with special needs, e.g., pregnant women or obese people. Understanding the mechanism of selecting spatial and temporal gait parameters would also improve the design of load carrying equipment and improve walking efficiency for firefighters as their equipment could weigh 20 kg (45 lbs.)

Table 1. The effects of load carrying on gait parameters during preferred walking.

Variable name	Symbol	unit	p	η^2	m_0 (I)	m_0 + 15 lbs. (II)	m_0 + 30 lbs. (III)
Step length	SL	m	< 0.001	0.45	0.73±0.06(II,III)	0.71±0.06(III)	0.70±0.06
Step frequency	f	Hz	0.058	0.07	1.83±0.14	1.82±0.16	1.81±0.16
Gait cycle duration	$2/f$	s	0.817	0.08	1.10±0.09	1.11±0.10	1.11±0.10
Walking speed	$v = SL \cdot f$	$m \cdot s^{-1}$	< 0.001	0.32	1.33±0.17(II,III)	1.29±0.18(III)	1.27±0.17
BMI	$m \cdot bh^{-2}$	$kg \cdot m^{-2}$	< 0.001	0.99	26.2±5.5(II,III)	28.5±5.4(III)	30.7±5.3

Data are means ± S.D. For each variable, a one-way factorial repeated measure ANOVA was performed with main factor loading conditions (i.e., m = m_0, m_0 + 15 lbs., and m_0 + 30 lbs.) *Post hoc* significant differences among conditions are listed by superscript, $p < 0.017$.

THE INFLUENCE OF SHOE AND CLEAT TYPE ON TRUNK AND PELVIS ROTATION IN YOUTH BASEBALL PITCHERS

Jacob R. Gdovin[1], Chip Wade[2], Lauren A. Luginsland[3], Charles C. Williams[4], Riley Galloway[5] and John C. Garner[6]
[1]Winthrop University, Rock Hill, SC, USA; [2]Auburn University, Auburn, AL, USA; [3]University of Mississippi, University, MS, USA; [4]University of North Florida, Jacksonville, FL, USA; [5]University of Southern Mississippi, Hattiesburg, MS, USA; [6]Troy University, Troy, AL, USA
Email: gdovinj@winthrop.edu

Introduction

Pitching a baseball is a highly dynamic movement where the lower extremity, pelvis, and trunk work in sequence to transfer energy to produce a desired ball velocity, pitch accuracy, and alleviate stress on the upper extremity. Efficiency of this movement depends on an athlete's ability to maximize the proximal-to-distal sequencing mechanism and properly time the movement of the trunk and pelvis. This linked interaction results in a summation of speed allowing the end of the distal segment to reach a maximal velocity greater than its adjacent segments by summing all the previous velocities within that sequence. While this mechanism assists in increasing ball velocity by transferring momentum from the legs, pelvis, and trunk to the distal ends of the upper extremity, movement in the most distal segment does not occur until the adjacent proximal segment reaches maximum angular velocity. Faulty mechanics, or disadvantageous trunk and pelvis orientations, may lead to a loss in the amount of momentum transferred to the throwing arm causing pitchers to compensate by increasing the amount of internal torque and therefore the injury risk within the upper extremity. Studies have looked at pelvic rotations, trunk rotations, and trunk angles during a baseball pitch and how that affects the upper extremity; however, one variable overlooked is the shoe-surface interface. Therefore, the purpose of this study was to investigate the shoe-surface interaction and how baseball specific footwear [molded cleats (MC) and turf shoes (TS)] on varying inclined surfaces (pitching mound (PM) and flat ground (FG)] affect pelvis and trunk kinematics and kinetics.

Methods

Eleven healthy male baseball pitchers (Age: 13.2 ± 1.7 years; Height: 179.0 ± 15.7 cm; Mass: 61.0 ± 14.7 kg) participated. A counterbalanced design was implemented for both footwear [New Balance 4040v3 Low Youth Baseball Cleat (MC), and New Balance 4040v3 Turf Shoe (TS)] and surface (PM and FG) conditions. Retroreflective markers were placed on each participant and pitching data was recorded and analyzed via a Vicon Nexus (Oxford, UK) 3D motion capture system with 8 wall-mounted, infrared T-series cameras collecting at 240 Hz. Participants were then given an unlimited amount of time to perform his warm-up routine, including stretching and non-throwing drills. Participants were then instructed to throw four-seam fastballs with the same technique and effort as if it were a game. Ten pitches, separated by thirty seconds of rest, were thrown from the stretch into a net ten feet away with a designated strike zone. Upon completion of ten pitches, a ten-minute rest between footwear conditions acted as a washout period where participants sat down without wearing any footwear. Following the washout period, the same experimental protocol occurred for the three remaining counterbalanced conditions.

Results and Discussion

No significant differences were found ($p > 0.05$) for the dependent variables of interest. Previous research has found that the magnitude of a horizontal force is limited by the maximum force applied into the ground [1]. This indicates cleated footwear can either "slide" or "hold" relative to the surface meaning they are displaced relative to the surface without causing a divot or can hold with minimal displacement relative to the ground, respectively [1].

Results from the current study conclude that the TS caused the trunk to reach a larger maximum angular velocity on the PM compared to the FG and the MC generated faster trunk angular velocities on FG relative to the PM.

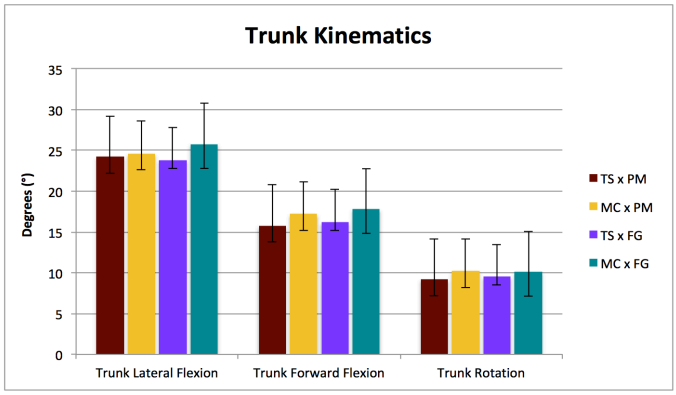

Figure 1: Trunk kinematics in all four shoe-surface conditions.

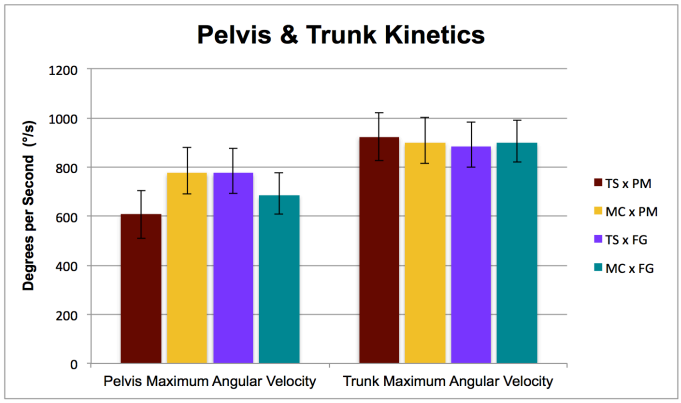

Figure 2: Trunk and pelvis kinetics in all shoe-surface conditions.

Significance

Footwear, and its interaction with the underlying playing surface, does not appear to have an effect on the amount of pelvis rotation or trunk lean in all three planes.

References

Kent, R., Forman, J. L., Crandall, J., & Lessley, D. (2015). The mechanical interactions between an American football cleat and playing surfaces in-situ at loads and rates generated by elite athletes: A comparison of playing surfaces. *Sports Biomechanics*, *14*(1), 1-17.

Margin of Stability during A Single-turn Pirouette in Amateur Female Dancers: A Pilot Study

Gordon Alderink[1], Anna Dykstra[1], Ashley Kooistra[1], Nicole Reading[1], Lauren Hickox[2], David Zeitler[1].
[1]Department of Physical Therapy, Grand Valley State University, Grand Rapids, MI, USA
[2]Department of Mechanical Engineering, Penn State University, State College, PA, USA
Email: aldering@gvsu.edu

Introduction

The pirouette (turn) is a fundamental skill performed routinely in classical ballet. In the pirouette the dancer balances on a single limb while on the toes (pointe) or on the ball of the foot (demi-point), and turns once or multiple times around the pivot axis through the stance limb [1]. The turn phase requires exquisite control of the center of mass (CoM) over a small base of support (BoS) to maintain balance on a single limb. Zaferiou et al. [3] examined whole body angular momentum and noted the importance of hip joint moments to produce and control turns. Others [3,4] used a toppling angle metric to describe control of the CoM during a turn. However, no research to date has used an inverted pendulum framework [5] and margin of stability (MoS) [6] to examine the mechanics of dynamic balance during a pirouette. Our purpose was to examine the MoS, as a measure of dynamic balance, during a single turn en dehors pirouette in female amateur ballet dancers.

Methods

Four healthy female elite amateur ballet dancers (24.3 ± 2.1 yrs.; 162.1 ± 4.1cm; 54.1 ± 5.9kg; 20.5 ± 1.3kg/m^2) participated. Approval was obtained from Grand Valley State University IRB (IRB#19-296-H). Participants performed single turn pirouettes on two force plates until five successful pirouettes were achieved without hopping or loss of balance. Sixteen MX-T40 cameras (120 Hz), Nexus motion capture software v2.81 (Vicon Motion System Ltd., Oxford Metrics, UK), and two AMTI (Advanced Mechanical Technology Inc., Watertown, MA) force plates were used to collect kinematic and kinetic data. A modified full body Plug-In Gait and Oxford Foot model marker sets were used. Trajectory and raw ground reaction force data for three representative trials per dancer were exported to Visual3D biomechanics software (C-Motion Inc., Germantown, MD) for further data reduction. The CoM/Center of pressure (CoP) angle of inclination (topple angle), the anteroposterior (A/P) and mediolateral (M/L) distance between XCoM to CoP (MoS_{CoP}), and A/P and M/L distance between XCoM and BoS center (MoS_{BoS}) were used to analyze dynamic balance during the turn phase. The XCoM is calculated from the horizontal velocity of the projected CoM onto the floor. The MoS is the distance that the XCoM moves from the CoP or BoS center. Dynamic measures were described relative to two coordinate systems: laboratory (LCS) and ankle joint center of stance leg (LFT) CS. Mean, standard deviation (SD), and coefficient of variation (CV) for each participant and across participants was calculated for topple angle and MoS measurements using JMP Pro 14 software (SAS Institute Inc., Cary, NC).

Results and Discussion

MoS_{CoP} and MoS_{Bos} had similar magnitudes along the respective axes. However, mean MoS_{BoS} and MoS_{CoP} distances were larger along the M/L than A/P axis (Table), suggesting that M/L balance is more precarious. The data show that for elite amateur dancers who successfully complete a sincle pirourette turn that the CoM is tightly controlled (i.e.,. 2-5 cm). Examination of the MoS distances, over time, demonstrated that the XCoM reached a maximum at the beginning and end of the turn phase. This finding suggests that when initiating and completing the turn, control of the CoM is in transition in terms of control. Both the beginning and end of a turn may be a time of least (most) stability as the dancer changes from double- to single-limb support. This research is the first to report on the MoS metric during a dance movement.

Table. Mean (mm ± SD, CV) for the distance between XCoM to BoS denter and XCoM to CoP along A/P (y) and M/L (x) axes of LFT CS.

Variable	Axis	Mean (mm)	CV (%)
XCoM to BoS Center	X	52.80 ± 14.51	27.49
XCoM to BoS Center	Y	19.63 ± 8.75	44.58
XCoM to CoP	X	49.37 ± 14.99	30.36
XCoM to CoP	Y	21.10 ± 3.81	18.04

The topple angle (3.3 ± 0.7°) was greatest at toe-off and before toe touch (at the end of the turn), and least during the middle of the turn, similar to what had previously been reported [3,4]. These results minic what was found using the MoS parameters, suggesting that the topple angle and MoS indices may be related.

Significance

This project's findings provide preliminary evidence that in well-trained amateur ballet dancers the CoM is tightlhy controlled during a successful one-turn pirouette. Least stability may occur during the transition from double- to single-limb support, suggesting that these may be times to focus on when analysing training exercises. These data need to be corrabortaed by testing professional dancers, and a larger data base of both female and male dancers is warranted.

Acknowledgements

Yunju Lee, PhD, Samantha Shelton.

References

1. Kim, J. et al. (2014). *Sport Biomech*, 13, pp. 215-229.
2. Zaferiou, A. et al. (2016), *J Appl Biomech*, 32, pp. 425-432.
3. Zaferiour, A. et al. (2016), *Med Probl Perform Art*, 31, pp. 96-103.
4. Lott, M., Laws, K., (2012), *J Dance Med Sci*, 16, pp. 167-274.
5. Winter, D. (1995). *Gait Posture*, 3, pp.193-214.
6. Hof, AL et al. (2005). *J. Biomech*., 38, pp.1-8.

PREMENOPAUSAL BILATERAL OOPHORECTOMY EFFECTS ON SKELETAL LOADING AND BONE MINERAL DENSITY

Emma Fortune[1]*, Omid Jahanian[1], Melissa M. Morrow[1], Virginia M. Miller[2], and Michelle M. Mielke[3]
[1]Robert D. and Patricia E. Kern Center for the Science of Health Care Delivery, [2]Departments of Surgery and Physiology and Biomedical Engineering , [3]Department of Quantitative Health Sciences, Mayo Clinic, Rochester, MN
email: *fortune.emma@mayo.edu

Introduction

One in eight women have their ovaries removed before reaching natural menopause (known as premenopausal bilateral oophorectomy; PBO) [1], which results in accelerated aging and an increased risk for low bone mineral density (BMD) and osteoporosis [2]. Physical activity under appropriate skeletal loading conditions is essential for bone health while aging. We developed an accelerometry-based skeletal loading metric and showed it was a significant predictor of hip areal BMD (aBMD) in women after natural menopause [3]. However, the relationship of skeletal loading with BMD in women after PBO is unknown. Therefore, this ongoing study is investigating the cross-sectional relationships of daily skeletal loading estimates with spine, pelvic and leg aBMD in post-menopausal women with and without a history of PBO.

Methods

Women with a history of PBO and age-matched referent women received full body DEXA scans measuring spine, pelvic, and leg aBMD, and wore ankle accelerometers for 7 days. Daily step count and loading index (the cumulative sum of each step's skeletal loading normalized to body weight) were calculated for each participant from their acceleration data [3,4]. Between group differences were assessed using ANOVA for BMI and step counts, and ANCOVA for loading index and aBMD values with BMI as a covariate. Age, BMI, daily step count and loading index for each participant were entered into stepwise multiple regression to identify significant predictors of spine, pelvic, and leg aBMD.

Results and Discussion

Compared to referent women, women with a history of PBO had larger BMIs, and lower daily steps and loading index (Table 1). Unexpectedly aBMD was higher in the PBO group, which might reflect having received hormone replacement therapy. Among referent women, loading index was the only significant predictor of spine, pelvic, and leg aBMD (Fig 1). Among the PBO women, loading index was the only significant predictor of non-dominant leg aBMD, whereas BMI was the only significant predictor of spine, pelvic, and dominant leg aBMD. This difference may be due to the strong known effects of PBO on BMI and of BMI on BMD.

Significance

These data suggest that PBO women may have lower daily step counts and loading compared to referent women, which may affect BMD maintenance. The loading metric could be used for prescribing and monitoring physical activity. Future work will include additional confounders to further elucidate the complex relationship of loading with bone health after PBO.

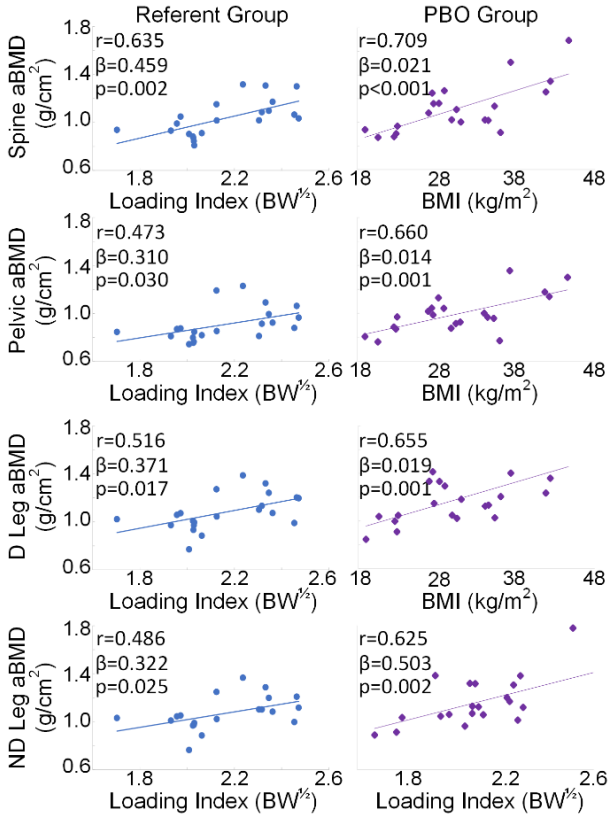

Figure 1: Regression plots of the significant linear relationships of (1) loading index with spine, pelvic, dominant (D) leg, and non-dominant (ND) leg aBMD for referent group and ND leg aBMD for PBO group, and (2) BMI with spine, pelvic, D leg aBMD for PBO group.

Acknowledgments

Funding provided by the NIH (U54 AG44170, K12 HD065987, and UL1 TR002377), and the Mayo Clinic Robert D. and Patricia E. Kern Center for the Science of Health Care Delivery.

References

[1] Howe (1984). Am J Public Health, 74. [2] Mucowski et al. (2014). Fertil Steril, 101. [3] Madansingh et al. (2019). Gait Post, 69. [4] Madansingh et al. (2020). Menopause, 27.

Table 1: Group (sample size; n), mean (SD) values for age, BMI, daily step count, daily loading index, and spine, pelvic, dominant (D) and non-dominant (ND) leg aBMD for PBO and referent groups, and p-values for between group differences.

Group (n)	Age (yrs)	BMI (kg/m²)	Steps	Loading Index (BW½)	Spine aBMD (g/cm²)	Pelvic aBMD (g/cm²)	D Leg aBMD (g/cm²)	ND Leg aBMD (g/cm²)
PBO (21)	66 (5)	31 (7)	11578 (3564)	2.13 (0.26)	1.12 (0.21)	0.99 (0.16)	1.19 (0.21)	1.17 (0.21)
Ref (21)	66 (5)	29 (6)	12715 (5745)	2.16 (0.21)	1.03 (0.15)	0.91 (0.14)	1.08 (0.15)	1.07 (0.14)
P-value	-	0.368	0.445	0.089	0.247	0.108	0.117	0.101

SHH! Quiet Running Promotes Sustained Reduction in Ground Reaction Force

Kevin D. Dames[1*], Sarah Rothstein[1], Larissa True[2], and Jacqueline A. Augustine[1]
[1]Kinesiology Department, SUNY Cortland, Cortland, NY, USA
[2]Department of Kinesiology & Dance, New Mexico State University, Las Cruces, NM, USA
email: *kevin.dames@cortland.edu

Introduction

Large vertical force loading rates are associated with running injury [1]. Real-time information about shank acceleration [2] and foot strike volume in decibels [3] can promote gait patterns that reduce impact force characteristics. Previous interventions have illustrated acute adaptations [2, 3], with one demonstrating sustained adaptations 1 month post-intervention [2]. Studies in this area have generally ignored relevant physiological performance markers (e.g., running economy) that are affected by gait mechanics. The purpose of this study was to evaluate acute and sustained responses to a foot strike volume intervention in trained female runners. We hypothesized that encouraging runners to adopt a quieter foot strike would decrease vertical ground reaction force (GRF) parameters and, secondly, improve running economy.

Methods

Fifteen female distance runners participated in this study (Table 1). Participation included three sessions: Baseline, Training, and Follow-Up. Baseline and Training sessions were separated by at least 24 hours, and the Training and Follow-Up sessions were separated by 1 week. In each, participants performed a 10-minute warmup on a treadmill, overground running trials while force data (1000 Hz) were recorded, and then a 10-minute steady-state treadmill run while expired gasses were collected. All activities were performed at the participant's self-reported preferred running speed. In the Training session only, biofeedback was provided during a 15-minute treadmill run immediately after the warmup. During this protocol, researchers instructed participants to run as quietly as possible. Average and peak decibels were shared with the participant in 3-minute intervals using a smartphone application. No other instructions or strategies to accomplish quieter running were suggested by the researchers.

Vertical force data from overground trials were low pass filtered at 50 Hz and ground contact was identified at a threshold of 10 N. Impact transient, peak vertical ground reaction force, peak and average vertical loading rates, and ground contact time were identified from five successful trials within each session. Metabolic data from the steady-state treadmill bouts were averaged over the final 3 minutes. Repeated measures analysis of variance was used to compare outcomes across the three sessions.

Table 1. Participant demographics

Parameter	Mean (SD)
Age (years)*	24 (7)
Mass (kg)	56.3 (6.6)
Height (cm)	164 (4)
Preferred running speed ($m \cdot s^{-1}$)*	2.9 (0.2)
Years of running*	9 (4)
Miles·week^{-1}*	24 (15)

Note: * indicates measure based on self-report

Results and Discussion

We accept our first hypothesis that making runners aware of their impact volume during running would decrease GRF parameters. We observed a 3.7% lower peak vertical GRF in the Follow-up compared to Baseline testing, a 13.4% decrease in the vertical instantaneous loading rate following the intervention compared to Baseline, and a 3.0% decrease in this measure at the Follow-up compared to the Training session (Table 2). This is consistent with prior interventions [2,3] and the loading rate decrease seems particularly beneficial [1]. Our findings demonstrate that simple instructions can yield immediate and sustained reductions in impact force profiles which do not influence running economy. Reduction of injury risk is desirable, but doing so at the expense of performance could discourage athletes from attempting this sort of intervention. Our findings demonstrate that a single, 15-minute bout of biofeedback can produce immediate gait adaptations that persist for at least a week. This supports the efficacy of decibel meter feedback to potentially reduce injury risk in trained female recreational runners.

Table 2. Dependent variable magnitudes by session. Mean (SD)

Parameter	Baseline	Training	Follow-Up
VGRF (BW)	2.39 (0.19)	2.34 (0.23)	2.30 (0.24)*+
IT (BW)	1.89 (0.49)	1.77 (0.56)	1.78 (0.52)
VILR ($BW \cdot s^{-1}$)	69.70 (21.62)	62.24 (22.68)	60.35 (19.30)*+
VALR ($BW \cdot s^{-1}$)	46.65 (17.87)	42.82 (16.12)	40.58 (13.94)
GCT (s)	0.27 (0.03)	0.28 (0.04)	0.28 (0.03)
VO_2 ($ml \cdot kg^{-1} min^{-1}$)	39.32 (5.75)	39.58 (5.19)	40.15 (5.64)

Note: BW: bodyweight; VGRF: peak vertical ground reaction force; IT: impact transient; VILR: vertical instantaneous loading rate; VALR: vertical average loading rate; GCT: ground contact time. * indicates a significant difference from Baseline and + indicates a significant difference from Training Session.

Significance

Runners and coaches who may not have access to a gait laboratory can use a simple method to promote, monitor, and maintain desirable gait modifications. Sound biofeedback is an intuitive method for non-specialists to understand, is easy to capture using a smartphone application, and yields meaningful gait adaptations without harming running economy.

Acknowledgments

This study was supported by a Faculty Research Program award from SUNY Cortland.

References

1. Zadpoor & Nikooyan. *Clin Biomech*, **26**, 1, 23-28.
2. Crowell & Davis. *Clin Biomech*, **26**, 1, 78-83.
3. Tate & Milner. *J Ortho Sports Phys Therapy*, **47**, 8, 565-569.

EFFECTS OF FRONT LOADED TREADMILL WALKING AT SELF-SELECTED SPEED ON DYNAMIC GAIT STABILITY

Caroline Simpkins[1], Jiyun Ahn[1], Rebecca Ban[1], Feng Yang[1]
[1]Georgia State University, Department of Kinesiology & Health, Atlanta, GA, USA
e-mail: claubacher1@student.gsu.edu

Introduction

Walking with an anterior load carriage is a common activity in daily living and occupations such as construction workers, movers, and firefighters. An anteriorly-placed load on the human body can affect gait patterns and increase the risk of falls [1]. Dynamic gait stability is a measurement of the human body's dynamic balance. Dynamic gait stability is defined based on the kinematic relationship between the body's center of mass (COM) and its base of support (BOS). It has been used to quantify the risk of falling during walking [2]. An examination of how front load carriage influences dynamic gait stability could provide more information regarding the impact of front load carriage on the risk of falls. This study aimed to explore the effects of anteriorly-loaded treadmill walking at a self-selected speed on dynamic gait stability in healthy young adults. Based on the literature, we hypothesized that front load carriage would affect dynamic gait stability during treadmill walking at a self-selected speed.

Methods

Thirty healthy young adults (24.83 ± 4.96 years) were randomly assigned to three groups: 0% or no load (Group 1), 10% body weight (*bw*) (Group 2), and 20% *bw* (Group 3). The load was assembled by filling sand bags with various weights into a fitness sandbag. Before the loaded treadmill walking, each participant walked unloaded on a treadmill for about 10 minutes to warm up and become familiar with treadmill walking. Their self-selected walking speed (in m/s) was also determined during the warm-up. Then, 26 markers were attached to the body landmarks and two more markers were applied to the sandbag (for Groups 2 and 3). Participants completed three 30-sec treadmill trials with either no load (Group 1) or their assigned load (Groups 2 and 3). The treadmill belt speed was set as the predetermined self-selected speed for each participant. Participants in Groups 2 and 3 carried their respective load against their abdomen using both hands in a symmetric posture maintaining load height with both elbows flexed about 90º.

Full-body kinematics were collected from the reflective markers through a motion capture system (Vicon, UK). Marker paths were filtered. Two transitional gait events, touchdown (TD) and liftoff (LO), were identified based on foot kinematics. The body-load system's COM position was calculated from the filtered marker paths. The two components of the COM motion state (position and velocity) were calculated relative to the rear part of the BOS (or the lead heel). Dynamic gait stability at both events was calculated as the shortest distance from the COM motion state to the limit against backward balance loss [2]. A positive/negative value of dynamic gait stability indicates a stable/unstable body against backward balance loss. Trunk angle (°) at TD and LO in the sagittal plane and step length (/body height) were also calculated from the marker paths. A positive/negative angle specifies backward/forward lean of the trunk. Dependent variables (dynamic stability at TD and LO, trunk angle at TD and LO, step length, and gait speed) were compared between groups using one-way ANOVA. SPSS 25 (IBM) was used and α level of 0.05 was applied.

Results and Discussion

One-way ANOVA did not detect significant differences associated with load group for dynamic stability at TD (p = 0.066) or LO (p = 0.108, Table 1). Significant differences were found between groups for trunk angle at TD and LO ($p < 0.001$ for both). No significant differences were observed between groups for step length (p = 0.954) or gait speed (p = 0.592). The results reject our hypothesis. To retain stability during loaded walking, adults leaned their trunk backward in the loaded groups. This action offset the potential forward shift of the COM due to the carried load. Therefore, participants can maintain the body-load system COM's position relative to the BOS. As the gait speed is not significantly different between groups, dynamic stability, which is determined by the COM-BOS kinematic relationship, was not different between groups either. This finding suggests that the central nervous system of the human body can rapidly adapt the gait pattern to the front load and maintain dynamic gait stability during treadmill walking at self-selected speed.

	Group 1	Group 2	Group 3
Stability-TD	0.04±0.04	0.03±0.04	0.00±0.02
Stability-LO	0.20±0.04	0.20±0.05	0.17±0.03
Trunk angle-TD	-1.27±5.04	4.39±1.54	8.78±2.07
Trunk angle-LO	0.48±5.52	6.11±2.14	10.35±2.76
Step length	0.34±0.08	0.33±0.06	0.33±0.03
Gait speed	1.12±0.37	1.16±0.29	1.04±0.12

Table 1: Comparisons of outcome measures between groups (mean ± SD).

Significance

Anterior load carriage of up to 20% *bw* may not significantly affect dynamic gait stability in young adults during treadmill walking at a self-selected speed. Our findings could provide useful information to design further studies to investigate the effects of front load carriage on human body stability and the risk of falls. This new information may in turn offer us guidance for developing safe load carrying tasks and working environments.

Acknowledgments

The authors thank the members at the Biomechanics Lab for the assistance with data collection and processing.

References

[1] Owings et al. (2004). *J. Biomech.*, **37**: 935-938.
[2] Yang, F. (2016). *Handbook of Human Motion*; 1-22.

EVALUATING RELATIONSHIPS BETWEEN STRIDE LENGTH AND ANKLE DORSI/PLANTARFLEXION MUSCLE ACTIVITY DURING POWERED ANKLE EXOSKELETON WALKING

Yadrianna Acosta-Sojo[1]*, Aditi Gupta[2], and Leia Stirling[1]
[1] Industrial and Operations Engineering, Center for Ergonomics, University of Michigan, Ann Arbor, MI
[2] Scientific Citizenship Initiative, Systems Biology, Harvard Medical School, Boston, MA
email: *yacosta@umich.edu

Introduction

Powered lower-body exoskeletons have the capability to assist and enhance human performance during activities of daily living, such as walking [1-2]. Studies have shown that exoskeletons can lower muscle activation during walking over time when averaging across participants [3], but not all users select similar gait characteristics when first using these systems [4]. Previous evaluation of human-exoskeleton strategy has shown that for defined stride lengths, there are decreases in muscle activity with shorter strides and increases in activity with longer strides, with the increase in muscle activity mitigated with a powered exoskeleton [5]. However, it is unclear if there is a relationship between the changes in stride length and muscle activity when stride lengths are freely selected. We hypothesized that there would be a correlation between the changes in normalized stride length and muscle activity of the medial gastrocnemius and tibialis anterior when wearing a powered ankle exoskeleton.

Methods

Fifteen healthy young adults walked on a treadmill wearing a powered ankle exoskeleton (Dephy, Maynard, MA). Participants walked at four speeds (0.5, 1.0, 1.3, 1.5 m/s) for one minute each with the exoskeleton powered off (baseline). Then, participants walked at 1.3 m/s for 10 minutes with the exoskeleton powered on (adaptation) followed by 5 minutes with the exoskeleton powered off (de-adaptation). Motion capture markers were placed on the body, and surface electromyography (EMG) sensors were placed on the tibialis anterior (TA) and medial gastrocnemius (MGAS) muscle on both legs. Heel-strike and toe-off events were detected from marker data and used to calculate the stride length. The root-mean-square (RMS) of each EMG signal was found for each stride. Stride lengths were normalized to participant leg lengths (NSL). RMS EMG and NSL data were binned into 5 walking conditions: baseline (B1), early adaptation (A1), late adaptation (A2), early de-adaptation (D1), and late de-adaptation (D2). Relationships between changes in NSL and RMS EMG data were assessed using Pearson correlations for subject-specific difference in means of NSL versus differences in means of RMS TA and RMS MGAS for the paired walking conditions (A1-B1, A2-A1, A2-B1, D1-A2, D2-B1, D2-D1). A positive ΔNSL and ΔRMS EMG indicate a longer stride length and greater muscle activation for the first condition, respectively.

Results and Discussion

The data do not support the hypothesis that there is a relationship between the changes in NSL and muscle activity for the muscles examined. No significant correlations between differences in NSL and RMS TA (Figure 1) or RMS MGAS (Figure 2) were observed. The range of ΔNSL was smaller [-0.11, 0.18] when freely selected compared to previous fixed lengths examined [5] and individuals varied in their muscle activity even with small changes in NSL. For example, when the exoskeleton was powered on (A1-B1), there were participants that decreased their NSL while maintaining, increasing, and decreasing RMS MGAS. Participants likely recruited muscles from different joints, such as the hip, to generate the differences observed in NSL.

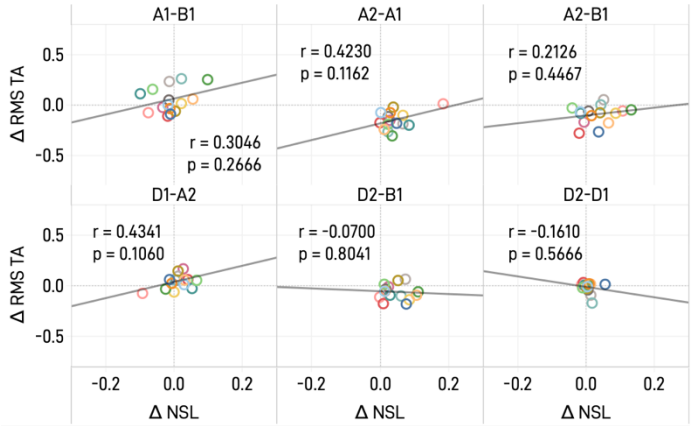

Figure 1. Scatter plots and correlation coefficients (r) with p-values (p) of the difference in NSL and RMS TA for paired walking conditions.

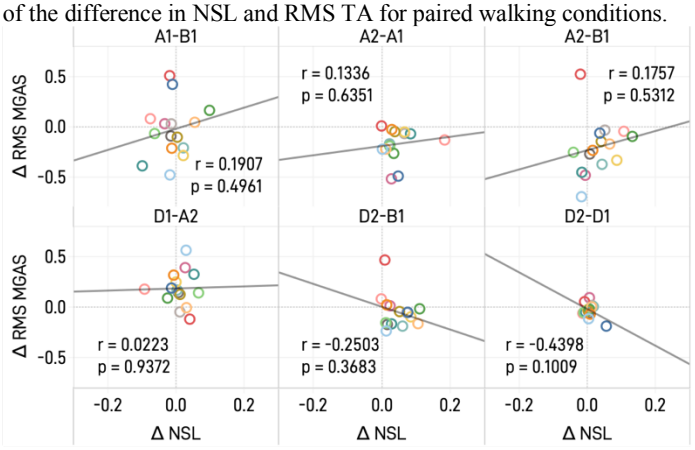

Figure 2. Scatter plots and correlation coefficients (r) with p-values (p) of the difference in NSL and RMS MGAS for paired walking conditions.

Significance

While mobility-assist exoskeletons may be designed to augment muscles of a particular joint, such as the ankle, changes in gait characteristics may be driven by muscle recruitment at other locations in the kinematic chain. Exoskeleton evaluation should consider broader changes in muscle recruitment to characterize human performance for human-exoskeleton coordination.

Acknowledgments

Thanks to the staff of the STRIVE Center, where the study was performed. The data used for this analysis was collected with support from the Army CCDC Soldier Center.

References

[1] Dollar & Herr (2008). *IEEE Trans. Robot.*, 24(1), 144-158. [2] Ferris et al. (2005). *J. Appl. Biomech.*, *21*(2), 189-197. [3] Gordon et al. (2013). *J. Neurophysiol.*, *109*(7), 1804-1814. [4] Gupta (2021). MIT Doctoral Dissertation [5] Sawicki & Ferris (2009). *J. Exp. Biol., 212*(1), 21-31.

STRUCTURAL, MATERIAL AND MECHANICAL PROPERTIES OF HUMERI AND FEMORA CORTICAL BONE FROM JUVENILE WHITE-TAILED DEER

Meir M. Barak[1*]
[1] Department of Veterinary Biomedical Sciences, College of Veterinary Medicine, Long Island University, Brookville, NY, USA
email: *Meir.Barak@liu.edu

Introduction

Plexiform bone (also called fibrolamellar bone), a primary bone tissue that is commonly found in long bones of fast-growing juvenile mammals, is remodelled as the animal matures into secondary Haversian bone [1]. The aim of this study is to determine the material (mineral content), mechanical (stiffness) and structural (primary vs. secondary bone tissue) properties of mid- and proximal diaphysis cortical bone of humeri and femora from juvenile white-tailed deer. The study is testing several hypotheses: (1) All four bone locations will reveal plexiform bone (primary bone tissue). (2) Mid-diaphysis cortical bone will have higher mineral content and consequently higher stiffness than proximal diaphysis in both the humerus and femur. (3) Femoral mineral content and stiffness will be higher than the humerus for comparable locations.

Methods

Multiple cross-sections were prepared from proximal and mid-diaphysis humeri and femora of seven juvenile white-tailed deer (juvenile state was determined by the existence of an active growth plate), and then inspected under light and electron microscopy to determine cortical bone structure. Next, multiple bone samples from these regions were crushed and ashed to quantify their mineral content. Finally, a total of 234 cubical samples (each 2^3 mm in size) were collect from the four locations and tested in compression within their elastic region along the axial, transverse and radial directions, and material stiffness (Young's modulus) was calculated.

Results and Discussion

Contrary to the prediction of the first hypothesis, while the femur proximal diaphysis and the femur and humerus mid diaphyses, revealed primary, plexiform bone, the humerus proximal diaphysis was completely remodeled into secondary, Haversian bone (fig. 1, right; compare with plexiform bone in the femur proximal diaphysis, left). Therefore, cortical bone remodeling in white-tailed deer happens at a much earlier age at the humerus proximal diaphysis compared with the femur proximal diaphysis and the femur and humerus mid-diaphyses. This finding is supported by Purdue (1983), who found the proximal diaphysis of the white-tailed deer humerus to be the most active site of growth and the last site to fuse its growth plate.

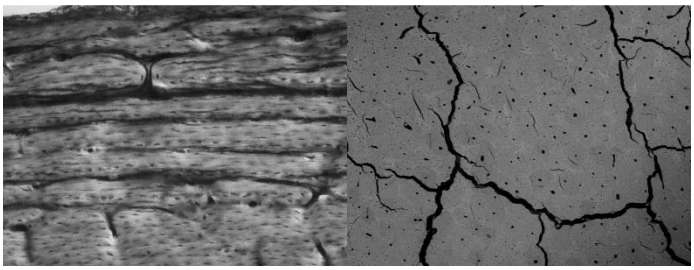

Figure 1: Primary, plexiform bone (left) and secondary, Haversian bone (right) were found at the femoral and humeral proximal diaphysis respectively.

The remodeled state of the humerus proximal diaphysis was also supported by the ashing and mechanical results. The humerus proximal diaphysis demonstrated the lowest mineral content, 63.3% (± 2.1%, Table 1). Additionally, cubical samples from the humerus proximal diaphysis tested under compression demonstrated transverse isotropic behavior (Table 1), an expected outcome for remodeled Haversian bone; where the radial and transverse orientations had non-significant differences in stiffness, but both were significantly less stiff than the axial orientation. Finally, the axial, radial and transverse stiffness values for the humerus proximal diaphysis were significantly lower than all other plexiform bone locations (Table 1), again, an expected outcome for remodeled Haversian bone, when compared to plexiform bone.

E (GPa)	Prox. F.	Mid F.	Prox. H.	Mid H.
Axial	24.5 (4.7)	28.7 (4.8)	17.9 (3.7)	26.1 (4.7)
Radial	15.6 (3.8)	16.8 (2.2)	10.3 (2.2)	14.5(2.5)
Transverse	17.8 (3.7)	21.2 (3.6)	10.9 (2.0)	18.3 (3.3)
Mineral %	68.4 (3.5)	71.0 (0.8)	63.3 (2.1)	69.6 (1.7)

Table 1. Average stiffness (E, GPa, top 3 rows) and SD in parenthesis for the 4 bone locations along the axial, radial and transverse orientations. Average % of mineral (bottom row, grey cells) and SD in parenthesis for the 4 bone regions.

In agreement with the prediction of the second hypothesis, both the humerus and femoral mid-diaphyses demonstrated higher mineral content and stiffness compared to their proximal diaphyses. One possible explanation for this finding is the higher stresses that are expected in the mid-diaphysis compared to the proximal diaphysis during normal locomotion.

Finally, in agreement with the prediction of the third hypothesis, femoral locations demonstrated higher mineral content and stiffness values compared to the humerus. These finding are supported by the fact that during quadrupedal locomotion higher loads, and stresses, are carried by the hindlimb compared to the forelimb.

Thus, the results reveal higher stiffness in the mid-diaphysis compared to the proximal diaphysis, and in the femur compared to the humerus in juvenile white-tailed deer. These findings emphasize the heterogeneous nature of bone material (mineral %), structure (primary vs. secondary bone tissue) and stiffness within the same bone and between bones of the same individual.

Significance

The findings of this study highlight the heterogeneous nature of bone material and emphasis the importance of histological and mineral content data collection whenever the mechanical properties of bone samples are compared, even within the same bone.

References

[1] Mori et al. (2005) J. Vet. Med. Sci. 67, 1223–9.
[2] Purdue (1983) J. Wildl. Manag. 47, 1207-1.

FRONTAL PLANE KINEMATICS OF THE TRIPLE STEP IN SWING DANCING

Meredith D. Wells[1] and Feng Yang[1]
[1]Department of Kinesiology and Health, Georgia State University, Atlanta, GA, USA
Email : mwells19@student.gsu.edu

Introduction

Swing dancing originated in the 1920s [1], yet remains popular today and continues to draw people to it with its social atmosphere and lively music [2]. Despite its continued popularity, swing dancing has not been thoroughly studied from the biomechanical perspective. For example, the kinematic information of swing dancing remains unknown. This lack of knowledge poses challenges in recognizing the movement patterns and restricts our ability to understand the demands placed on the body and the injuries related to swing dancing. The triple step is one of the most common movement elements in swing dancing and involves taking a small step to the side, bringing the second foot to meet the first, and taking a third step to the side with the first foot (Figure 1). The purpose of this study was to quantify the angular kinematics of the lower extremity joints during the stance phase of each of the three steps within the triple step in the frontal plane among swing dancers. It was hypothesized that significant differences in the lower extremity joint kinematics would be seen among the three steps.

Methods

Eight recreational swing dancers who finished at least 50 sessions of swing dancing in the prior year (age: 30.9 ± 4.7 years; height: 1.73 ± 0.07 m; mass: 73.6 ± 13.1 kg; swing dancing experience: 4.1 ± 3.1 years) participated in this study. Participants completed a 5-minute dance warm-up, and then performed three triple steps to the right with a partner. Participants performed the dance element on vinyl flooring, wearing standardized socks.

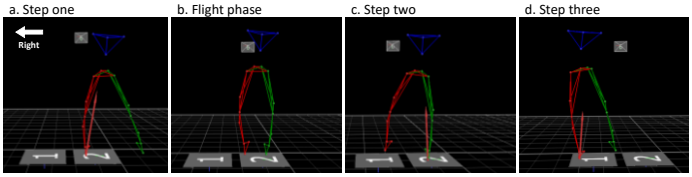

Figure 1: Representative body movement sequences of a triple step to the right and the illustration of two force plates on the dancing floor.

Lower extremity kinematics were collected via 16 reflective markers using an 8-camera motion capture system (Vicon, UK). The ground reaction forces were gathered by two force plates (AMTI, MA). Joint centres were calculated from the filtered marker paths and measured anthropometric parameters [3]. Frontal plane angles at the ankle, knee and hip during stance of each of the three steps within the triple step were calculated based on the joint center data using inverse kinematics. The stance phase of each step was determined by the vertical ground reaction force. The peak values of each joint angle in either direction (abduction vs. adduction) were determined and used as the outcome measures. One-way ANOVAs with repeated measures were used to analyze the outcome measures. The step (first vs. second vs. third) was the within-subject factor. Bonferroni post-hoc tests were run when significant step-related differences were seen. The significance level was set as 0.05.

Results and Discussion

The ANOVA indicated that the peak angles at the knee and hip joints in either direction were significant (p-values ranging from < 0.001 to 0.039), but there were no significant differences at the ankle joint. Therefore, the results partially supported our hypothesis that there would be differences among the steps at all lower extremity joints. Post-hoc tests revealed the following significant between-step differences: greater peak knee abduction during the first ($p = 0.002$) and third ($p = 0.001$) steps compared to the second step, greater peak knee adduction during the second step compared to the first ($p = 0.004$) and third ($p = 0.045$) steps, greater peak hip abduction during the second step compared to the first ($p = 0.002$) and third ($p = 0.004$) steps, and a greater peak hip adduction angle during the first step compared to the second step ($p = 0.043$) (Table 1).

The differences that occurred between steps one and two and steps two and three are likely a result of form differences. When triple stepping to the right, the first and third steps are taken with the right foot, while the second step is taken with the left foot, which may explain these kinematic differences. In addition, dancers often hop between steps one and two, leading to a brief flight phase, while there is no flight phase leading into steps one and three, which may have contributed to the kinematic differences as well.

Significance

This study provides meaningful information regarding the lower limb angular kinematics of the triple step movement in swing dance. Results indicate that the peak angular joint angles in the frontal plane are affected by the step, particularly the knee and hip. The findings from the current study may help to educate dancers and coaches about the design of training protocols and may be used to enhance performance and reduce injury risk.

References

[1] Spring H. (1997). *American Music*, **15**: 183-207.
[2] Fuller J. (2019). *Swing History*, CentralHome.com.
[3] Pai YC, et al. (2006). *J of Biomech*, **39**: 2194-2204.

Table 1. Frontal plane peak joint angles (in mean ± standard deviation) for all steps. The bold items showed an overall step-related difference.

Step	Ankle Eversion	Ankle Inversion	**Knee Abduction**	**Knee Adduction**	**Hip Abduction**	**Hip Adduction**
1	-0.74 ± 1.91	2.06 ± 2.95	-18.47 ± 4.84	-5.98 ± 2.74	1.65 ± 9.31	10.21 ± 8.59
2	-3.40 ± 6.75	0.93 ± 4.20	-1.83 ± 11.87	8.35 ± 11.52	-15.74 ± 4.78	-1.20 ± 6.32
3	-0.94 ± 2.45	1.02 ± 2.85	-20.77 ± 2.85	-1.87 ± 3.46	0.04 ± 8.26	7.05 ± 8.54

SPLIT-BELT TREADMILL TRAINING IMPROVES GAIT EFFICIENCY IN PEOPLE WITH HIP OSTEOARTHRITIS

Chun-Hao Huang[1]*, Burcu Aydemir[1], and Kharma C. Foucher[1]
[1]Depatment of Kinesiology and Nutrition, University of Illinois at Chicago
Email : *chuan26@uic.edu

Introduction

Reduced gait efficiency has been found in hip osteoarthritis (OA) measured as decreased mechanical energy exchange (MEE)[1] or increased metabolic energy expenditure.[2,3] Step length asymmetry (SLA) is commonly reported in hip OA patients[4,5] and could potentially influence gait efficiency by impacting center of mass (COM) movement. Split-belt treadmill training with error augmentation method induces step length symmetry and reduces net metabolic power in stroke patients.[6,7] This novel rehabilitation method has not been explored in the hip OA population. The purpose of this study was to determine the effect of split-belt treadmill training modifying step length on gait efficiency in people with hip OA. We hypothesized that one session of split-belt treadmill training reduces step length asymmetry, increases mechanical energy exchange, and decreases oxygen consumption during walking in people with hip OA.

Methods

We evaluated 7 women with hip OA (66 ± 5.4 yrs; 32.5 ± 6.3 kg/m^2) who provided informed consent for this IRB-approved study. We conducted split-belt treadmill testing with 4 periods: Warm-up (3 minutes), Baseline (1 minute), Adaptation (10 minutes), and post-adaptation (1 minute) with motion analysis and metabolic energy analysis. During the adaptation period, the involved limb was assigned to the slow speed belt (half of the self-selected walking speed), and the uninvolved limb was assigned to the fast speed belt (self-selected walking speed). Both belts were at the self-selected speed during the other periods.

Gait analysis was conducted using standard methods. Baseline (1 minute), beginning of adaptation (2 minutes), end of adaptation (2 minutes), and post-adaptation (1 minute) were analyzed. Oxygen consumption was measured at the same time using indirect calorimetry. O_2 rate was extracted from the cardiopulmonary diagnostic software.

We used Symmetry Index (SI): $[|X_{uninvolved}-X_{involved}|/ X_{uninvolved}] * 100\%$ to determine SLA.[8] We extracted COM by the segmental analysis method.[9] Next, the potential (Ep) and kinetic (Ek) energy were calculated by the equations: $E_p = M_{tot} \times 9.81 COM\ (z)$, $E_k = 1/2 M_{tot} (V_x^2+V_y^2+V_z^2)$.[10]
Finally, mechanical energy exchange, the percent of center of mass energy recovery was calculated by the equation: $\%Recovery = [\Delta^+ E_p + \Delta^+ E_k - \Delta^+ E_{tot}]/ [\Delta^+ E_p + \Delta^+ E_k]$.[11] %Recovery is the pendulum-like transfer between E_k and E_p and can be considered a measure of gait efficiency.

Repeated measures ANOVA was used to determine the effect of the training period on SI for step length, MEE, and O_2 rate in each period. LSD post hoc test was used to compare each condition. Spearman correlation was used to assess the relationship between the change of variables in different period. The key comparison being the baseline period to the end of adaptation period.

Results and Discussion

There was a significant effect of training period for SI for the step length ($p = 0.04$), MEE ($p = 0.01$), and O_2 rate ($p < 0.01$) in the multivariate test. Post hoc testing revealed that SI for step length significantly decreased from the baseline period (11.0 ± 4.7) to the end of adaptation period (2.5 ± 1.2) ($p < 0.01$). MEE significantly increased from the baseline period (22.7 ± 4.4 %) to the end of adaptation period (29.1 ± 5.2 %) ($p < 0.01$). O_2 rate significantly decreased from the baseline period (8.4 ± 2.3) to the end of adaptation period (6.3 ± 1.7) ($p < 0.01$) (Figure 1). Additionally, the decreasing of SI for step length was associated with the decreasing O2 rate from baseline to the end of adaptation ($R = 0.79$, $p = 0.04$).

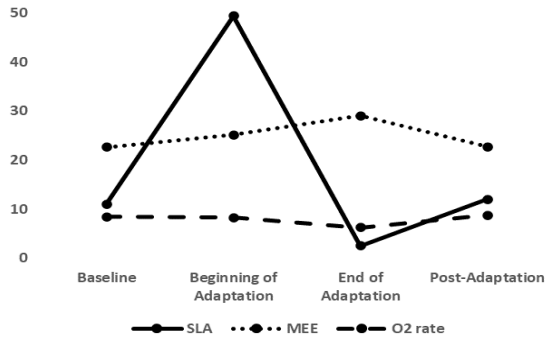

Figure 1: The improvement of SLA, MEE, and O_2 rate through the split-belt treadmill training. As SLA decreased, the MEE increased and O_2 rate decreased at the end adaptation period.

Our hypotheses were supported. Statistically significant changes in SI for step length, MEE, and O_2 rate were present after split-belt treadmill training. SLA changed significantly through split-belt treadmill training becoming more symmetric. Beneficial modifications in MEE and O_2 rate were also seen. Split-belt treadmill training could potentially become a rehabilitation strategy to improve gait efficiency in hip OA patients. Future research should examine whether effects following split-belt treadmill adaptation transfer to overground walking in hip OA population.

Significance

Improving gait efficiency through split-belt treadmill training could potentially promote better overall function and improve physical activity in people with hip OA.

Acknowledgments

This study was supported by National Institute on Aging Roybal Center for Health and Promotion and Translation Doctoral Pilot Grant.

References

(1) Queen, R.M., et al., 2016. (2)Brown, M., et al., 1980. (3) McBeath., et al., 1980. (4) Verlinden, V.J.A., et al., 2017. (5) Constantinou, M., et al., 2017. (6) Reisman, D.S., el al., 2007. (7)Finley, J.M., et al., 2013. (8) Lugade V., et al., 2010. (9) Stagni, R., et al., 2014. (10) Hallemans, A., et al., 2004. (11) Cavagna, G.A., et al., 1976.

THE IMPACT OF SAMPLING FREQUENCY ON KINETIC OUTCOMES

K. Renner[1], A. Peebles[2], R. Queen[3]
[1]Hartford Hospital Rehabilitation Network, Hartford, CT [2]Virginia Commonwealth University, Richmond, VA [3] Department of Biomedical Engineering and Mechanics, Virginia Tech, Blacksburg, VA
email: Kristen.e.renner@gmail.com

Introduction

Metrics such as peak force, loading rate (LR) and impulse are frequently reported for dynamic tasks such as walking, running, single limb landing and double limb landing. These metrics have been used to determine injury risk[1,2]. Embedded force plates are the gold-standard for assessing kinetics during various movement tasks; however, embedded force plates are not widely used in non-research settings as they are expensive and not highly portable. Portable force plates and force sensing insoles are more affordable and practical to use in non-research settings; however, these technologies have maximum data sampling rates which are lower than standard embedded force plates[3,4]. The lowest recommended sampling frequency for assessing common impact kinetic outcomes is not currently available in the literature. Therefore, the purpose of this study was to determine the effect of sampling frequency on the accuracy of common impact kinetic outcomes during landing, walking and running tasks.

Methods

The present study was a secondary analysis utilizing data from three previous studies. Each study received institutional review board approval and informed consent was signed prior to data collection. The landing protocol consisted of seven bilateral drop vertical jumps[5] and seven unilateral drop landings[6] on each limb from a 31 cm box. For the bilateral tasks, participants jumped forward toward a target placed half their body height away from the box followed by a maximum effort vertical jump[5]. Impact kinetics were measured throughout each landing task (AMTI, Watertown, MA; 1920 Hz). The treadmill running and walking protocols were performed on a fore-aft split-belt instrumented treadmill (AMTI; 1440 Hz) at preferred speed[7]. Walking was completed at a 0%, +10% and -10% incline.

All data analysis was performed using MATLAB (MathWorks Inc., Nantucket, MA) and force data was normilzed to body weight. Peak impact force, LR and impulse were computed using the vertical ground reaction force during the first landing of the bilateral drop vertical jump and during the first 200 ms of the unilateral landing[3]. For the landing tasks average LR was computed as the peak impact force divided by the time between initial contact and peak impact force[3]. Impulse was computed as the area under the force-time profile[3].

Peak impact force average LR, and impulse were computed using the vertical ground reaction force during every ground contact for 10 seconds of each treadmill running and walking trial. Peak impact force was defined as the first peak which occurred following initial contact[2]. Average LR was computed during the linear portion of the force-time profile[2]. Impulse was computed as the area under the force-time curve [4].

Data was not filtered at any stage. Outcomes were first computed using the raw force plate data, and considered the 'true value'. Then, the force plate data was consecutively down-sampled until 48 Hz was reached by keeping every 2nd, 3rd, 4th, etc. data points, which artificially creates a new sampling frequency. Outcomes were computed at each stage of the down-sampling process. Percent difference was computed at each sampling frequency relative to the true value for each trial, and then averaged across trials for each participant.

Results and Discussion

Thirty participants (15 male, 15 female) completed the landing study (70.3 ± 14.1 kg; 1.76 ± 0.07 m; 23.3 ± 2.7 years). Twenty participants (10 men, 10 women) completed in the running study (70.5 ± 12.6 kg; 1.75 ± 0.08 m; 21.9 ± 2.4 years). Six participants in the running study did not have clearly defined impact peaks and were therefore removed from this analysis. Twenty participants (10 male, 10 female) completed the walking portion of the study (67.80 ± 13.88 kg; 1.68 ± 0.05 m; 22.89 ± 3.14 years). The minimum recommended frequency to reach 90%, 95%, and 99.5% of the true value for each outcome can be found in **Table 1**.

We determined that impulse was the most unaffected by sampling frequency and can be accurately computed using data sampled as low as 100 Hz. LR was the most sensitive to sampling frequency, which is likely the result of compounding the variance in the magnitude and timing of peak impact force, as well as the variance in the timing of initial contact.

Significance

This study fills a current gap in our understanding of how sampling rate impacts kinetic outcome metrics for a variety of tasks. This information will allow researchers and clinicians to make informed choices regarding the appropriateness of using new equipment such as force sensing insoles and portable force plates based on the task to be collected, desired outcomes, and the available sampling rate.

References

1- Hewett, T.E., et al., 2005. Am J Sports Med 33, 492-501.**2-** Milner, C.E., et al., 2006. Med Sci Sports Exerc 38, 323-328. **3-** Peebles, A.T., et al., 2018. Sensors 18, 4082. **4-** Renner, K.E., et al., 2019. Sensors.19.2, 265. **5-** Bell, D.R., et al, 2014. J Athl Train 49, 435-441. **6-** Ithurburn, M.P., et al., 2017. Am J Sports Med 45, 2604-2613. **7-**Dingwell, J.B., Marin, L.C., 2006. J of biomechanics.39, 444-452.

Table 1: Minimum sampling frequency (Hz) needed to achieve 90%, 95% and 99.5% of the true value.

	Peak Impact Force			Average LR			Impulse		
% of True Value	**90**	**95**	**99.5**	**90**	**95**	**99.5**	**90**	**95**	**99.5**
Bilateral	62	96	384	192	384	1920	48	48	106
Unilateral	48	48	137	48	87	640	48	48	148
Running	160	240	1440	480	1440	1440	48	110	240
Flat Walk	48	48	720	48	48	75.8	48	48	60
-10%Walk	48	48	48	48	110.8	720	48	48	48
+10%Walk	48	48	48	62.6	75.8	720	48	48	48

Effects of Anterior Load Carriage on Dynamic Stability during Level Walking

Jiyun Ahn[1], Caroline Simpkins[1], Rebekah Buehler[1], Feng Yang[1]
[1]Department of Kinesiology and Health, Georgia State University, Atlanta, GA 30303, USA
Email: jahn12@gsu.edu

Introduction

Falls account for a large portion of workplace accidents, leading to unwanted outcomes such as injuries and economic burden [1]. Load carriage is one of the major occupational fall hazards. A recent study suggested that front load carriage is one of the load carrying approaches which significantly destabilizes the human body and increases the risk of falls during walking [2]. However, the potential effect of front load carriage on dynamic body balance during walking is still understudied. Dynamic gait stability has been widely used to quantify body balance during gait. It is defined based on the kinematic (velocity-position) relationship between the body's center of mass (COM) and its base of support (BOS) [3]. The purpose of this study was to examine the effects of anterior load carriage on dynamic gait stability during overground walking. It was hypothesized that the front load carriage would affect dynamic gait stability during overground walking.

Methods

Thirty healthy young adults (24.83 ± 4.96 y/o) were randomly assigned into three groups: no load (Group 1), 10% body weight (bw) (Group 2), and 20% bw (Group 3). Participants walked on a 10-m walkway at their self-selected speed three times without carrying any load. Then, each participant in Groups 2 and 3 walked another three times with the assigned load, which was assembled by sand bags. Participants in loaded groups carried the load against their abdomen using both hands in a symmetric posture and maintained the height of the load during walking. They were also informed to walk at their preferred speed. For individuals assigned to the unloaded group (Group 1), they walked another three trials on the ground.

The full-body kinematics were collected from 26 reflective markers on the body landmarks through a motion capture system (Vicon). Two additional markers were attached to the sandbag. The last walking trial was selected for analysis. The marker paths were filtered. Two events: touchdown (TD) and liftoff (LO), were identified based on the foot kinematics. The body-load system's COM position was calculated from the filtered marker paths [4]. The gait speed was calculated as the first order derivative of COM position with respect to time and normalized to the body height (bh). The two components of the COM motion state (i.e., its position and velocity) were calculated relative to the BOS and normalized by the foot length and the square root of the product of bh and gravitational acceleration, respectively. Dynamic gait stability at both events was calculated as the shortest distance from the COM motion state to the limit against backward balance loss [3]. The dependent variables (gait speed and dynamic stability at TD and LO) were analyzed using one-way ANOVA with the load level as the factor (0% vs. 10% vs. 20% bw). SPSS 25 (IBM) was used and a significance level of 0.05 was applied.

Results and Discussion

ANOVA did not detect a significant effect of the load level on gait speed (0.81 ± 0.1, 0.77 ± 0.06, and 0.82 ± 0.11 bh/s respectively for Groups 1, 2, and 3, $p = 0.60$). Dynamic gait stability at TD and LO were comparable among groups ($p > 0.05$ for both, Fig. 1). The results rejected our hypothesis that the anterior load carriage affects dynamic gait stability during level walking. Given that dynamic gait stability is determined by the relative position and velocity between the COM and BOS and that the speed is not different between groups, the COM position relative to the BOS should be similar between groups. The front load carriage has the potential to anteriorly shift the body-load system's COM that could change the COM-BOS kinematic relationship and thus dynamic gait stability. However, the human body was able to adjust the relative position of the COM to the BOS during loaded walking. The main strategy used to compensate the front load is to lean the trunk backward, which can offset the forward shift of the COM due to the front load. Collectively, the COM's position did not significantly differ between groups. This indicates that the central nervous system can quickly adapt to the disruptions (induced by the external load) on balance and maintain dynamic gait stability during walking. The results from our study share the same notion with previous studies that reported the walking surface (overground vs. treadmill) and body mass index (lean vs. obese) have little impact on dynamic gait stability during walking [5, 6]. Further studies are needed to examine the effect of front load carriage on dynamic gait stability when encountering an external perturbation (such as a slip or trip).

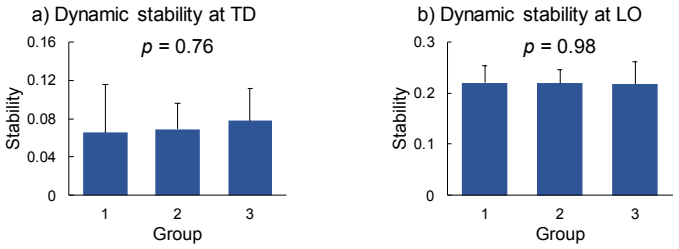

Figure 1. Comparisons of dynamic gait stability between three groups at a) TD and b) LO during overground walking.

Significance

The current study will expand our understanding of how anterior load carriage influences human gait biomechanics from the perspective of dynamic stability control.

Acknowledgements

The authors thank all members in the Biomechanics Lab at Georgia State University for assisting the data collection.

References

[1] Webster, T., Compensation and working conditions, 2000. 2000: p. 28-38.
[2] Alamoudi, M., et al., *Int. J. Ind. Ergon*, 2018. 67: p. 81-88.
[3] Yang, F., Handbook of Human Motion, 2016. pp. 1-22.
[4] Yang, F., *J Biomech*, 2008. 41(9): 1823-1831.
[5] Liu, Z.-Q. and F. Yang, *PloS one*, 2017. 12(1): p.
[6] Yang, F. and G.A. King, *J Electromyogr Kinesiol*, 2016. 31: p. 81-87.

THE EFFECT OF COGNITIVE LOAD ON BALANCE RECOVERY STRATEGIES USED DURING WALKING

Gabriella H. Small and Richard R. Neptune
Walker Department of Mechanical Engineering, The University of Texas at Austin, Austin, TX
email: gsmall@utexas.edu

Introduction

Dual-task (DT) studies often combine steady-state walking with an additional cognitive task to assess their influence on gait performance [1]. DT studies analyzing steady-state walking with challenging cognitive loads have found that healthy adults prioritize cognitive task performance at the expense of maintaining control of their balance [2]. Maintaining balance is essential during walking, with foot-placement playing a critical role [3]. As a result, errors in foot-placement can lead to a loss of balance. To recover from a loss of balance, healthy adults can use an ankle strategy that quickly moves the center of pressure but is limited by the surface area of the foot [4]. A hip strategy can also be used to adjust the mediolateral ground reaction force, although the response time is slower [4]. However, whether the addition of a cognitive load would affect the strategy used in response to a foot-placement perturbation is unknown. The purpose of this study was to determine the effect of cognitive loads on the balance recovery strategy used after a mediolateral perturbation to foot-placement in young healthy adults. We hypothesize that as the cognitive load increases, individuals will focus more on the cognitive load, causing a delay in response time to the perturbation. Furthermore, we expect this delay will cause individuals to use the faster ankle strategy rather than the hip strategy in response to the perturbation as the cognitive load increases.

Methods

A 10 camera motion capture system (VICON, Los Angeles, USA) recorded full body 3D kinematics during steady-state and perturbed treadmill walking from 15 healthy subjects (age 25 ± 4 years, 9 females) using four increasing levels of cognitive load: no load, attentive listening, spelling short 5-letter words backwards and spelling long 10-letter words backwards [5]. Subjects performed a cognitive single-task control (spelling short and long words while standing), and then walked on a treadmill during steady-state unperturbed and perturbed DT conditions at their self-selected speed (1.3 ± 0.1 m/s) and at a fixed speed (1 m/s). Medial and lateral perturbations (~3.6 cm) were applied to the left ankle just before heel strike at random steps throughout the trial using a novel perturbation device [6]. Peak ankle inversion and hip abduction moments were analyzed in Visual3D (C-Motion, Germantown, MD) and MATLAB (Mathworks Inc., Natick, MA, USA) to determine the changes in joint responses to the perturbations across the conditions. Cognitive performance was determined by the correct response rate in recorded audio data.

Results and Discussion

Contrary to our hypothesis, cognitive load did not affect the ankle inversion or hip abduction peak moments or where in the gait cycle the peaks occurred for either the medial or lateral perturbations (Fig. 1) ($p > 0.05$), indicating that the subjects did not change their recovery strategy during the DTs. Furthermore, cognitive performance in the spelling task did not change between the standing single-task (short word response rate = 1.91 ± 0.5 letter/s, long word = 1.02 ± 0.5 letter/s) and unperturbed DT (short word response rate = 1.87 ± 0.6 letter/s, long word = 1.04 ± 0.4 letter/s) ($p = 0.994$), but their cognitive performance did decrease during the perturbed DT (short word response rate = 1.67 ± 0.4 letter/s, long word = 0.90 ± 0.3 letter/s) ($p = 0.003$). Thus as previously shown, individuals appear to focus on their cognitive performance at the expense of their balance control during steady-state walking [2], but the current results show they redirect their attention to balance recovery when their foot-placement is perturbed.

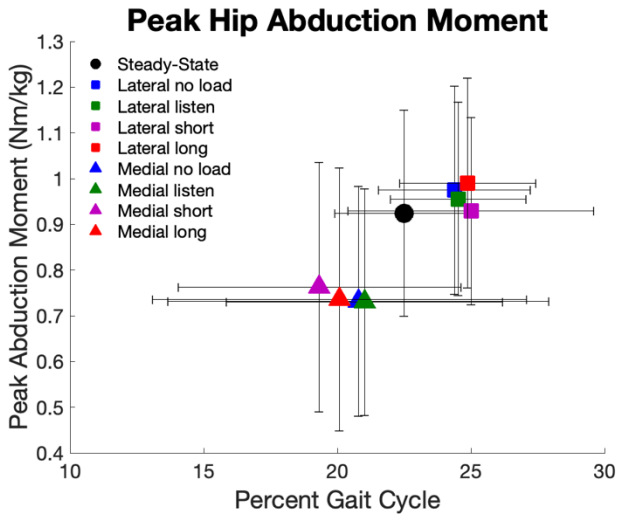

Figure 1: Peak hip abduction moments for the lateral and medial perturbed conditions across the four cognitive loads (no load, listening, spelling short and long words backwards) and where in the gait cycle the peaks occurred. Error bars represent ± 1 standard deviation.

Significance

Balance control decreased during perturbed relative to unperturbed walking, but the cognitive load had little effect on the strategy used to recover their balance after a mediolateral perturbation. In contrast to steady-state walking, young healthy adults prioritized balance control over cognitive performance when faced with foot-placement perturbations. These results provide further insight into the automatic nature of walking in healthy young individuals, which provides the foundation for future studies to determine differences in neurologically impaired populations.

Acknowledgments

This project was supported in part by the Dr. J. Parker Lamb Endowed Presidential Fellowship in Mechanical Engineering.

References

[1] Ebersbach G., et al., *Percept Mot Skills* 81(1), 1995.
[2] Small, G., et al., *J Biomech (in review)* 2021.
[3] Roelker, S., et al., *J Biomech* 95, 2019.
[4] Hof, A. et al., *J Exp. Biol.* 213, 2010.
[5] Hollman, J., et al., *Gait Posture* 32(1), 2010.
[6] Brough, L., et al., *J Biomech* 116, 2020.

KINEMATIC AND KINETIC ANALYSIS OF KNEE ARTHRODESIS- A CASE STUDY GUIDE TO REHABILITATION

Priyanka Aggarwal[1], Rajesh Malhotra[1], Deepak Gautam[1], Supriya Bali[1], Manish Gupta[1]
[1]Department of Ortho-surgery, All India Institute of Medical Sciences, Delhi, India
email: *priyanka.aggarwal@aiims.edu

Introduction

Knee arthrodesis is a limb-salvage option that gives a stable, painless joint but a fused knee can cause gait deviations along with possible limb shortening. This can make activities of daily living difficult [1]. Thus, some patients may require permanent assistance in walking and/ or shoe-raise on the fused side to balance leg-length [2]. However, less attention is paid to the presence of long-standing adaptive changes in associated joints of the kinematic chain. The expected function decreases further when rehabilitation fails to address these changes [3].

This study aims to find key points to improve an atypical compensation of dynamic trunk flexion and asymmetrical loading in a knee arthrodesis case, with prolonged use of walker support hypothesized to be its main reason.

Methods

A 65-year-old male underwent left knee arthrodesis due to a 11-month-old post-traumatic knee flexion deformity with repeated infections and failed knee extensor mechanism. This was followed by regular physiotherapy and a 2-cm external shoe-raise on left side. Even after 18 months of surgery, patient demonstrated a walker-assisted gait with reduced loading time on the left leg and excessive trunk flexion (Figure 1-Left). There was no pain and bony fusion was achieved on radiographs.

Physical examination revealed that the patient could lie prone with mild tightness of bilateral hip flexors, and weakness of bilateral trunk extensors (2-/5), bilateral hip extensors (3-/5) and left hip abductors (2-/5). A kinematic (500 Hz) and kinetic (1000 Hz) gait analysis (SMART DX-7000, BTS Bioengineering, Milan, Italy) was done to guide further rehabilitation. A conventional gait model with Helen Hayes 18-marker protocol was used [4]. Joint centres were identified by anthropometric data and regression equations. After consent, the patient walked with his walker, at self-selected walking speed, with and without shoe-raise, till clean forces were obtained for both legs.

Results and Discussion

The shoe-raise improved short-limb compensations, foot loading and cadence but not spatial-temporal asymmetry. The average loading on left limb improved (50% to 66% BW) but was still less than the right (79% BW). The left Single-limb-support phase (SLS) was only 17% of the gait cycle, while the right stance phase acquired >80% of the gait cycle. The mean velocity (0.2 m/s) remained low, but is comparable with walker-assisted studies [5].

There was dynamic trunk flexion (Table 1), sustained hip flexion (Figure 1-Right), an anterior pelvic tilt, a net internal hip extensor moment (Figure 2- Left) and an absent second peak on the left vertical GRF (Figure 2-Right). These preliminary gait findings suggest shifting of GRF vector anterior to the hip due to weak stabilizing forces (hip and knee extensors), especially in late stance, most likely secondary to knee arthrodesis or previous adaptive changes in pelvis and hip. This dynamic anterior shift, depicted by trunk flexion, was merely balanced by the large base of support of the walker and may not be caused by it, as initially thought. Nevertheless, since a walker is less likely to promote an erect posture, a unilateral support like a cane and a lumbo-pelvic stability program may reduce trunk flexion by re-aligning GRF vector posterior to the hip and further balance foot loading.

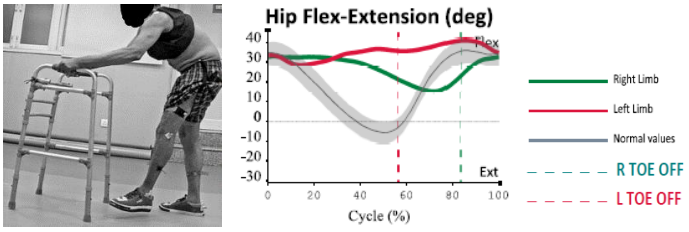

Figure 1: (Left) Sagittal view of patient freeze-framed in right stance phase; (Right) Hip kinematics in sagittal plane with legend.

Table 1: Trunk flexion in sagittal plane of gait cycle

Trunk tilt (degrees)	Lab reference	Pelvis reference
Maximum value	28.4	34.35
Minimum value	17.8	23.8
Total excursion	10.6	10.55
Average value	23.19 ± 3.4	29.17± 3.4

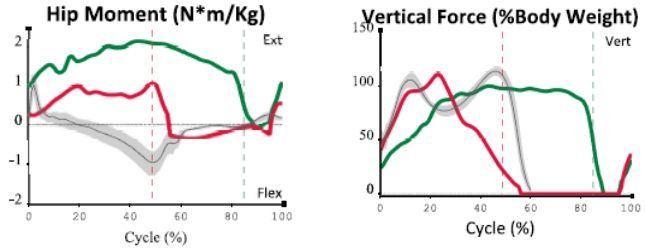

Figure 2: (Left) Hip internal moment in sagittal plane and (Right) vertical GRF (Ground reaction force) with shoe-raise

Hence, gait changes in an arthrodesed joint are not limited to limb-length discrepancy. Analysis of proximal joints, including trunk and pelvis, may be crucial for treatment goal-setting and a positive impact on the final recovery of such patients.

Significance

This is the first study using gait analysis in an elderly knee arthrodesis patient to improve function. This shows that independent ambulation may not be a part of the natural history of knee arthrodesis and early emphasis on associated joints may minimize long-term inefficient gait compensations and avoid a complicated function-restoring surgery in future. This may also lead to improved exercise protocol after joint fusion resulting in better outcomes to bring this less-preferred surgery at par with other limb salvage procedures [1] especially in a developing country where it is still a cost-effective choice without the need for extensive post-operative rehabilitation, like after amputation.

Acknowledgments

We thank Dr. Venkatesan S. Kumar for his support and guidance in data interpretation.

References

1. Lucas Eric M et al. *SpringerPlus* **5**,1606, 2016
2. Watanbe K et al. *Mod Rheumatol* **2**: 243–249, 2014
3. Makhdom AsimM et al. *JBone Joint Surg Am*101:650-60, 2019
4. Kadaba MP et al. *J Orthop Res* ***8,*** 383-392, 1990.
5. Crosbie J. *JOSPT* **20**, 186-192, 1994

A COMPARISON OF CYCLIC AND DISCRETE TASKS FOR ASSESSING AVOIDANCE BEHAVIOUR DURING REACHING

Alexander T. Peebles[1*], Susanne Van Der Veen, Alexander Stamenkovic[2], and James S. Thomas
[1]Motor Control Laboratory, Virginia Commonwealth University, Richmond VA
email: *peeblesat@vcu.edu

Introduction

Low back pain (LBP) is the most common source of chronic pain among middle- and older-aged adults, and results in significant financial burden [1]. The fear-avoidance model suggests that LBP patients who exhibit signs of avoidance behavior during functional tasks (e.g., forward reaching) have an increased risk of symptom recurrence [2,3]. Prior work has investigated lumbar motion during discrete forward reaching (i.e., where there is a defined period of quiet posture before and after movement execution), and cyclic forward reaching (i.e., where participants repeatedly reach between a target and their starting posture without a clearly defined pause). Despite evidence suggesting that discrete and cyclic movement behaviors are controlled through distinct motor primitives, with cyclic movements requiring significantly less cortical and more sub-cortical involvement than discrete movements [4], a direct comparison of reaching regularity is not currently available in LBP patients. Considering that changes in central nervous system structure and function in LBP that are primarily supraspinal (e.g., decreased cortical excitability [5]; altered sensory processing [6]; altered motor planning [7]; heightened kinesiophobia [2,3]), we would expect to see more pronounced movement deficits during discrete reaching tasks that are known to require more supraspinal involvement [4]. Thus, the purpose of the present study was to determine the effect of reaching regularity (i.e. discrete versus cyclic), biological sex, and prior history of LBP on coordination between the pelvis and lumbar spine. Our first hypothesis is that patients with a history of LBP will have altered reaching coordination, relative to matched uninjured control participants. Our second hypothesis is that there will be a group by task interaction, with greater between-group differences being observed during discrete tasks relative to cyclic tasks.

Methods

Twenty patients with chronic LBP (defined as recurring LBP for at least 3 months) and twenty-one uninjured control participants signed University Institutional Review Board approved informed consent and participated in the present study. All participants completed both discrete and cyclic reaching to an anthropometrically-matched target in the mid-sagittal plane. Whole-body kinematics were collected in three-dimensions at 100 Hz during movement testing using a seven-camera motion capture system (Vicon, Los Angeles, CA). Hip and lumbar joint angles were computed between thigh and pelvis segments and between the pelvis and lumbar segments, respectively. Reach time, total excursion at the lumbar spine and the hips, and the ratio between lumbar spine and hip excursion were computed for each reach and averaged across conditions. Separate repeated measures ANOVAs were computed to determine the main effects of and interactions between reaching condition (discrete vs cyclic), biological sex (male vs female), and group (patients with chronic LBP vs uninjured controls) for each reaching outcome. All data analysis was performed using SPSS (Version 24, IBM, Chicago, IL), and significance was set at 0.017 to account for multiple comparisons.

Results and Discussion

A main effect of group was observed for lumbar-hip ratio, where the lumbar-hip ratio was reduced in patients with LBP relative to matched controls ($p = 0.015$, Figure 1). However, isolated lumbar and hip flexion excursion were similar between groups. These findings expand upon prior literature which observed reduced lumbar-hip ratios during the maximum forward bend test, which quantifies limits of motion between segments [8-10]. As forward reaching involves kinematic redundancy, it is a better suited task for assessing avoidance behavior. Future work should explore whether lumbar-hip ratios during reaching are associated with kinesiophobia and pain recurrence. However, the large variance in lumbar-hip ratios among the control group warrants further investigation into the validity and repeatability of this outcome.

The cyclic task resulted in reduced lumbar-hip ratios, reduced lumbar excursion, and reduced reaching time, relative to the discrete task (all $p < 0.001$). As lumbar motion decreased and hip motion remained consistent during cyclic reaching, motion likely increased at other joints (e.g. knee flexion), reflecting a change in motor strategy. However, as reaching time was not consistent between the two tasks, it is unclear if this observed change in reaching strategy was due to movement regularity. No significant interactions were observed, which indicates that motor deficits in LBP patients are consistent between cyclic and discrete reaching.

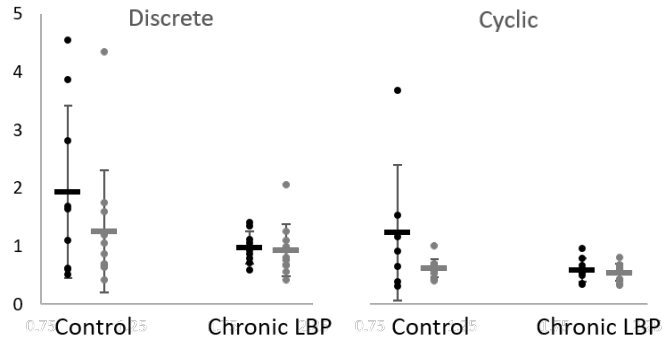

Figure 1: Lumbar-hip ratios compared across group, reaching condition, and sex.

Significance

Reductions in the lumbar-hip ratio during reaching may be an indicator of avoidance behaviour in LBP patients. While there are differences between cyclic and discrete reaching, differences are consistent between persons with and without prior LBP. Therefore, this study suggests that both cyclic and discrete tasks are sufficient for assessing avoidance behaviour in LBP patients.

References

[1] Henschke et al., Mayo Clin. Proc. (2015); [2] Thomas and France, Spine (2007); [3] Thomas et al., J. Pain. (2016); [4] Hogan and Sternad, Exp. Brain Res. (2007); [5] Parker et al., Brain Stimul. (2016); [6] Roussel et al., Clin. J. Pain. (2013); [7] Jacobs et al., Clin. Neurophysiol. (2010); [8] Porter et al., Spine (1997); [9] Shojaei et al., J. Biomech. (2017); [10] Larivière et al., Clin. Biomech. (2000).

ROM IN KNEE, ANKLE, HIP CONTRIBUTE MOST TO LANDING VARIABILITY ACCORDING TO PCA

Kayt E. Frisch[1,2], Robin Dorociak[1,3]

[1]George Fox University [2]Mechanical, Civil & Biomedical Engineering, [3]Physical Therapy
email: kfrisch@georgefox.edu

Introduction

Jump landing is a common cause of knee injury in athletes and different "landing strategies" for absorbing the impact (at the knee vs. ankle vs. hip) may explain the variation between individuals [1-2]. In this study we used Principal Components Analysis (PCA) to explore causes of variability and the presence of these groupings in a large data set of drop vertical jumps.

PCA is a linear algebra based statistical dimension reduction technique to determine which variables in a data set contribute the most to the variability in the data set by creating new variables in the directions of greatest variance (Fig 1). These new variables are "recipes" combining old variables with the goal of having a few variables that explain most of the data variability. For a more detailed introduction to PCA see [3]. In this study, we hypothesized that performing a PCA on jump landing data would reveal clusters associated with the different landing strategies.

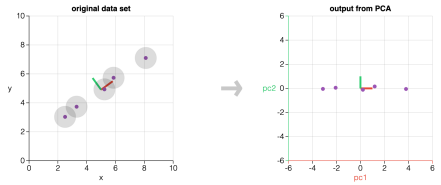

Figure 1: PCA creates a new variable, PC1 that aligns with the greatest amount of variability in the data [4].

Methods

Drop vertical jumps were performed by 145 collegiate NCAA D3 athletes (85 female, 59 male; box height: females - 60.7 cm, males - 76.2 cm) wearing a bilateral lower body marker set with feet on separate force plates. Marker and force data were collected simultaneously (11 Qualisys cameras, 100Hz; 2 AMTI force plates, 1000 Hz) and Visual3D was used to calculate kinematics and kinetics. A 4th order Butterworth low pass filter was applied to the trajectories (f_c= 12 Hz) and forces (f_c= 20 Hz). Key parameters from the landing phase (initial contact to max knee flexion) were extracted bilaterally for the hip, knee and ankle using Matlab: ROM, max moment, energy stored, max GRF (28 parameters total). PCA was performed on the 145 samples with 28 variables using Matlab's pca algorithm.

Results and Discussion

The scree plot (Fig 2) indicates that the first two principal components (PCs) account for 80% and 10% of the variability in the data respectively, for a total of 90% of variability accounted for in the first wo PCs. This suggests that PCA may be a reasonable lens through which to consider the data.

The biplot (Fig 3) shows that ROM at the ankle, knee, and hip are the primary contributors to variability in the data set (the contribution magnitudes of all other variables are inside the inset box). most of the variability between individuals appears to occur in the knee and the hip, as PC1 describes 80% of the variability in the data set and ankle ROM has approximately a zero score on the PC 1 axis.

The individual data points (Fig 3, red dots) show a wide range of values (particularly along PC1, as expected). However, there is no apparent clustering visible in the biplot (Fig 3), which suggests that landing strategies are not immediately apparent from the kinematic and kinetic variables analysed.

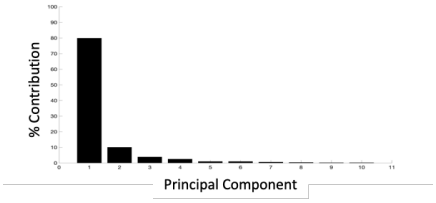

Figure 2: Scree Plot showing contributions of PCs to variability

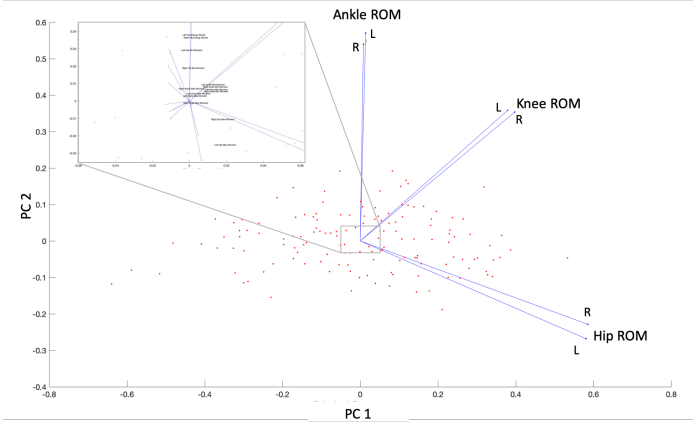

Figure 3: A biplot displaying the first two PCs (90% of variance). PC1 and PC2 scores for individual athletes (red dots) display a relatively large range, especially on the PC1 axis, but do not form clusters or groups. Blue lines represent the contribution of original variables with ROM in the ankle, knee and hip being primary drivers of variability. The inset box shows the relative magnitudes of the other variables.

PCA may be a valid way to consider variability in this data set. Most of the variability between subjects appears in the knee and hip ROM, however, with the variables used, the data does not appear to cluster into landing strategy groups.

Significance

These results support the idea that joint ROM are key variables when considering the motion of individuals, however they do not seem to support the notion that individuals can be grouped into simple "landing strategy" groups. Further work should explore other parameters that may influence variability in jump landing.

Acknowledgments

Thank you to ENGM 420 (Fall 2020) for piloting this analysis and GFU Physical Therapy for sharing their data set.

References

[1] Malinzak, et. al. *Clin. Biomech.* 16 (2001) 438-445
[2] Hansberger, et. al. *J. Athl. Train.* (2018) 53.4
[3] Brems (2017) https://towardsdatascience.com/a-one-stop-shop-for-principal-component-analysis-5582fb7e0a9c (Acs 20 Jan 2021)
[4] Powell (N.D.) https://setosa.io/ev/principal-component-analysis/ (Acs 25 Jan 2021)

ALLOMETRIC SCALING FOR KNEE ADDUCTION MOMENT

Samantha Andrews[1], E. Parke[2], and C. Stickley3
[1]Straub Medical Center, Honolulu, HI, USA
email: samantha.andrews@straub.net

Introduction

Joint kinetics during running are commonly used to evaluate the influence of pathology or fatigue. Specially, differences in external knee adduction moment (KAM) between groups can indicate the presence of pathology and/or increased joint loading within the medial compartment. While highly correlated with patient specific anthropometrics [1,2], such as body mass and height, ratio scaling kinetics by these variables commonly results in an overcorrection or a negative correlation [3]. Allometric scaling has previously been evaluated in biomechanical studies, with varying recommendations for its use [2,4]. This study, therefore, evaluated (1) the relationship between KAM and anthropometric variables and (2) the effectiveness of allometric scaling KAM to remove the influence of body mass (BM) and height (HT).

Methods

Eighty-four males (age: 23 ± 5 years; HT: 178 ± 7.9 cm; BM: 77.6 ± 12.4 kg) and forty-seven females (age: 26 ±7 years; HT: 164.4 ± 7.8 cm; BM: 62.5 ± 9.1) were recruited from a university population. Participants underwent a one-time data collection, during which biomechanical data were collected for three running trials at a prescribed velocity (4.0m/s ± 10%), while 17 Vicon motion capture cameras (Vicon, Inc., Centennial, CO) collected data from 27 retroreflective markers placed on the lower extremities and trunk. Kinetic data, from one force plate (Advanced Mechanical Technology Incorporated, Boston, MA), were collected at 960 Hz and time synchronized with the kinematic data, collected at 240 Hz. Log- linear regression was used to develop gender specific allometric exponent for BM and HT and a log-multilinear regression was used to develop exponents for BM and HT together, both in an attempt to remove the influence of these variables on KAM [5]. Pearson product-moment correlations were performed for raw, ratio and allometrically scaled KAM to evaluate the effectiveness of each scaling procedure.

Results and Discussion

The correlations for each scaling method are presented in Table 1. Raw KAM was correlated with BM for males and HT for females, suggesting the primary anthropometric influence on KAM may be different between genders. Ratio scaling by BM did not remove the influence of HT for males and overcorrected for females, while ratio scaling for BM*HT was unable to remove the influence of HT for both males and females. The shortcomings in these commonly used ratio scaling techniques is cause for concern, as the majority of research evaluating KAM provides clinical recommendations from data that may be influenced by anthropometrics even after scaling. Raw KAM was allometrically scaled for BM (1) and HT (2), independently, as well as BM and HT together (3), resulting in the following equations:

$$(1)\ \text{Raw KAM}/(BM^{exp}) \qquad (2)\ \text{Raw KAM}/(HT^{exp})$$

$$(3)\ \text{Raw KAM}/((BM^{exp})*(HT^{exp}))$$

The derived exponents for the independent influence of BM and HT were 0.723 and 1.511 for males and 0.668 and 4.316 for females, respectively. The derived exponent for the combined influence of BM and HT were 0.725/-0.012 for males and 0.042/4.258 for females. The influence of BM and HT were best removed by allometric scaling for BM in males and by HT in females. Due to the complexity of the multilinear regression, there appears to be no added benefit to allometric scaling for BM and HT. The difference in gender specific scaling recommendations provide further evidence that generalized ratio scaling for BM or BM*HT may be inappropriate.

Significance

While previous evaluations of KAM commonly ratio scale by BM or BM*HT, the results of this study indicate that KAM scaled by these methods may be inappropriate for removing the influence of anthropometrics. By evaluating the effectiveness of scaling, both the influence of BM and HT were accurately identified and removed from KAM for both genders. Allometric scaling should continue to be evaluated to determine the feasibility and external validity across a variety of cohorts and pathologies.

References

1) Moisio, KC, et al. J. Biomech 36(4), 599-603, 2003
2) Mulineaux, DR, et al. J. Appl. Biomech 22((3), 230-233, 2006
3) Winter, E. Pediatr. Excerc. Sci. 4, 296-301, 1992
4) Stikely, CD, et al. J. Biomech 77, 55-61, 2018
5) Vanderburgh, PM, et al. *Med Sci Sports Exerc* 66(1), 80-84, 1995

Table 1. Correlations between raw and scaled knee adduction moment and anthropometrics - r (p-value)

		Male		Female	
Anthropometric		Body Mass	Height	Body Mass	Height
Raw Data		**0.357 (0.001)**	0.196 (0.074)	0.206 (0.175)	**0.587 (0.000)**
Ratio Scaled by:	BM	-0.105 (0.340)	**0.291 (0.007)**	-0.156 (0.306)	0.165 (0.280)
	HT	-0.074 (0.504)	0.072 (0.515)	**0.430 (0.003)**	**0.487 (0.001)**
	BM/HT	-0.105 (0.341)	**0.263 (0.016)**	-0.027 (0.858)	0.265 (0.079)
Allo Scaled by:	BM	0.033 (0.764)	0.007 (0.946)	-0.038 (0.804)	**0.489 (0.001)**
	HT	**0.255 (0.019)**	0.007 (0.950)	-0.039 (0.798)	-0.032 (0.836)
	BM/HT	0.033 (0.764)	0.009 (0.939)	-0.054 (0.725)	-0.030 (0.842)

HT = height; BM = body mass; BMHT = BM*HT; BM/HT = body mass and height; Allo = allometric

AGE-RELATED DIFFERENCES IN CALF MUSCLE RECRUITMENT STRATEGIES IN THE TIME-FREQUENCY DOMAIN DURING WALKING AS A FUNCTION OF TASK DEMAND

Hoon Kim[1] and Jason R. Franz[1]
[1]Joint Department of Biomedical Engineering, University of North Carolina at Chapel Hill and North Carolina State University, Chapel Hill, NC, USA
email: hoonkim@email.unc.edu

Introduction

Conventional analysis of plantar flexor EMG magnitudes has provided critical information about how these muscles contribute to accelerating the body's center of mass during the push-off phase of walking in older adults.[1] Unfortunately, EMG magnitudes alone are unable to fully characterize motor unit recruitment. The frequency content inherent to EMG recordings can also vary in complex ways due to age and/or task demand due to changes in muscle morphology (e.g., active fiber types) and neural signaling (i.e., nerve conduction velocity).[2] Despite known changes in muscle morphology and neural signaling between older and young adults, no study to our knowledge has quantified age-related differences in the time-frequency content of plantar flexor EMG recordings during walking. Thus, the aim of this study was to quantify plantar flexor muscle activation differences in the time-frequency domain between young and older adults during walking across a range of speeds and with and without horizontal aiding and impeding forces, the latter designed to augment demands for push-off intensity. We first hypothesized that older adults would exhibit lower intensities at faster frequencies and a shift to slower frequencies compared to young adults during walking. We also hypothesized that those age-related differences would increase with task demand (i.e., walking faster or with horizontal impeding forces).

Methods

Ten healthy young (24.0 ± 3.4 year) and older adults (73.7 ±3.9 year) walked at three different speeds (0.8 m/s, 1.2 m/s, and 1.6 m/s) and walked at 1.2 m/s with a 5% BW horizontal aiding and impeding force while we recorded the 3D positions of skin markers and muscle activations of soleus (SOL) and gastrocnemius (GAS).[3] We analyzed EMG data from SOL and GAS over nine consecutive strides using a wavelet transform with 11 non-linearly scaled Morlet wavelets to decompose muscle activations in the time-frequency domain.[4] We then used principal component analysis to extract principal components (PCs) for each muscle (e.g., SOL, GAS) and each set of conditions (*i.e.*, walking speeds and horizontal forces) using a variance account for (VAF) criterion of ≥5%. Separate mixed factorial ANOVAs identified significant main effects of and interactions between age and either walking speed or horizontal forces on SOL and GAS PC scores.

Results and Discussion

PC2 mainly captured variation in GAS intensity timing (10% VAF) and showed a main effect of age ($p = 0.035$, $\eta_p^2 = 0.235$). Specifically, compared to young adults, older adults exhibited greater GAS intensity in slower frequencies during early stance but lower GAS intensity in almost all frequency ranges during midstance and low to middle frequency ranges during push-off. PC3 captured variation both in frequency and timing of GAS intensity (7% VAF). A significant age × walking speed interaction ($p = 0.033$, $\eta_p^2 = 0.221$) showed that older adults exhibited larger PC3 scores with faster walking speed while young adults exhibited smaller PC3 scores with faster walking speed. Specifically, compared to young adults, older adults exhibited higher GAS intensity at slower frequencies ranges during early to midstance but lower GAS intensity across all frequency ranges during push-off with faster walking speed. Conversely, we found no main effect or interaction involving age for SOL. In partial support of our hypotheses, we show that GAS motor unit recruitment strategies in older versus young adults: 1) shift to slower frequencies with earlier timing as walking speed increases and 2) decrease GAS intensity across all frequency ranges during midstance and low to middle frequency ranges during push-off independent of walking speed.

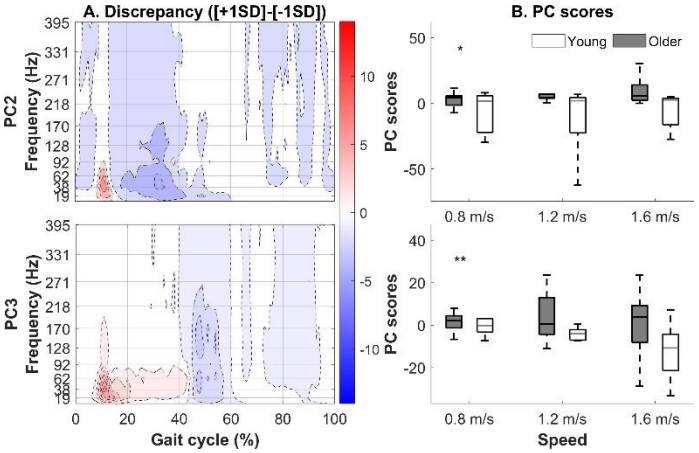

Figure 1: Variation in EMG intensity captured by PC2 and PC3 for GAS as a function of age and walking speed. A. Discrepancy of +1SD and -1SD, B. Boxplots of PC scores for PC2, and PC3. ** and * represents significant age × speed interaction and age main effect, respectively.

Significance

Our results implicate GAS time-frequency content, and its morphological and neural origins, as a potential determinant of hallmark ankle push-off deficits due to aging, particularly at faster walking speeds. Rehabilitation specialists may attempt to restore GAS intensity across all frequency ranges during mid to late stance while avoiding disproportionate increases in slower frequencies during early stance.

Acknowledgments

We thank William H. Clark for data collection. Supported by a grant from the National Institutes of Health (R01AG058615).

References

[1]Van Criekinge et al (2018), *J Electromyogr Kinesiol* 41:124-131
[2]Wakeling (2004), *J Exp Biol* 207:3883-3890
[3]Clark et al (2020), *Ann Biomed Eng* 1-13
[4]Cohen (2019), *Neuroimage* 199:81-86

EFFECT ON THE CENTER OF PRESSURE OF VISION, FLOOR CONDITION, AND THE HEIGHT OF CENTER OF MASS DURING QUIET STANDING

Seungsu Kim[1], Kitaek Lim[1], Woochol Joseph Choi[1]
[1]Injury Prevention and Biomechanics Laboratory, Dept of Physical Therapy, Yonsei University, South Korea
email: wcjchoi@yonsei.ac.kr

Introduction

Theoretically, balance is affected by the height of center of mass (COM) during quiet standing. While efforts have been made to understand this in humans [1], no one systematically examined this in humans from biomechanical perspectives. We have conducted balance experiment to measure the trajectory of the center of pressure (COP) during quiet standing, in order to examine how the COP measures were affected by the height of COM, vision, floor conditions, and gender.

Methods

Twenty young healthy individuals stood still with feet together and arms at sides for 30 seconds on a force plate. Prior to data collection, we have determined the height of COM using a reaction board method (Figure 1a~c) [2]. Trials were acquired with three COM heights adjusted by a weight belt: 1% increased or decreased, and not changed. Trials were also acquired with two vision conditions: eyes closed (EC) and eyes open (EO), and with two floor conditions: unstable (foam pad) and stable (force plate) floor (Figure 1d~f). Outcome variables were computed from COP data, and included the mean distance, root mean square distance, total excursion, mean velocity, and 95% confidence circle area.

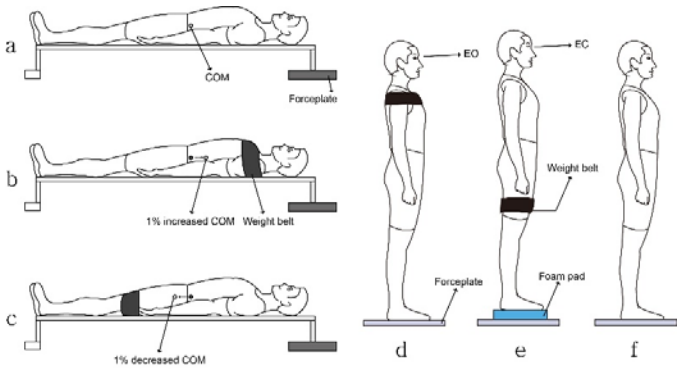

Figure 1: Participants lay on a reaction board to determine (a) the height of COM, and positions of a weight belt (5% of body weight) so the height of COM (b) increased or (c) decreased 1% with respect to the original height of COM. Then, participants stood still with different standing conditions. Sample schematics of quiet standing tasks with (d) eyes open, COM raised, and stable floor condition, (e) eyes closed, COM lowered, and unstable floor condition, and (f) eyes open, COM not changed, and stable floor condition.

Results and Discussion

All outcome variables were associated with the COM height ($p < 0.0005$), vision ($p < 0.0005$), and floor condition ($p < 0.003$). The mean velocity and 95% confidence circle area were 5.7% and 21.8% greater, respectively, in raised COM than in lowered COM (24.6 versus 23.2 mm/s; 1013.4 versus 832.3 mm^2), 85.5% and 101.2% greater, respectively, in eyes closed than in eyes open (31.5 versus 17.0 mm/s; 1241.9 versus 617.1 mm^2), and 129.6% and 216.5% greater, respectively, in unstable than in stable floor condition (33.7 versus 14.7 mm/s; 1412.6 versus 446.3 mm^2) (Figure 2). However, there were no interactions between the COM height and vision condition ($p > 0.096$), and between the COM height and floor condition ($p > 0.183$) for all outcome variables. Furthermore, there was no difference between male and female participants for all outcome variables ($p > 0.186$).

Our results suggest that individuals swayed more over greater area with greater velocity when the height of COM increased, and this agrees well with a model prediction. Our results also suggest that the three environmental conditions (COM height, vision, floor) affect balance independently and not influence each other, indicating no combined effects among conditions.

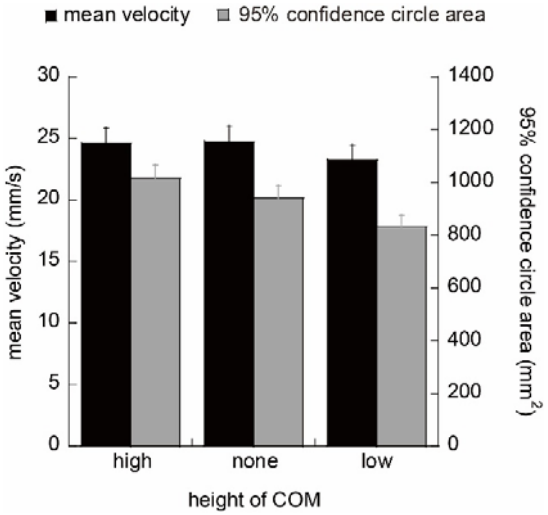

Figure 2: Effects of the height of COM on COP measures during quiet standing. Individuals swayed more over greater area with greater velocity when the COM height increased.

Significance

The change of COM height with a weight belt successfully created a challenging environment, under which the outcome of balance training can be better. Furthermore, in balance training, one may want to change the level of difficulty depending on individuals' status (i.e., patients in early rehab stage or elite athletes) by combining several environmental conditions (i.e., balancing on the unstable floor with eyes closed while wearing a weight belt above waist). However, our results suggest that such strategy provides no additional benefits in the outcome of training.

Acknowledgments

This study was supported, in part, by the "Brain Korea 21 FOUR Project", the Korean Research Foundation for Department of Physical Therapy in the Graduate School of Yonsei University.

References

[1] Phan et al., 2020, Physical Therapy Korea, 27(2):155-161
[2] Ozakya et al., 2012, New York, Springer, 3rd ed:53-54

MUSCLE MECHANICS ARE ALTERED IN PERIPHERAL ARTERY DISEASE AFTER SUPERVISED EXERCISE

Cody Anderson[1], Hafizur Rahman[1], Iraklis Pipinos[2,3], Jason Johanning[2,3], and Sara Myers[1,2]
[1]Department of Biomechanics, University of Nebraska at Omaha, Omaha, NE, USA
[2]Department of Surgery, Omaha VA Medical Center, Omaha, NE, USA
[3]Department of Surgery, University of Nebraska Medical Center, Omaha, NE, USA

email: codypanderson@unomaha.edu

Introduction

Peripheral Artery Disease (PAD) is characterized by atherosclerotic plaques in the conduit arteries. Previous work shows that gait in patients with PAD is altered, particularly posterior chain mechanics, which are important for propelling the body forward. A common, non-invasive, treatment for PAD is supervised exercise training [1]. However, for reasons that have not been elucidated, gait is not fully restored following supervised exercise training (SET) [2]. Musculoskeletal simulation with OpenSim may provide insight into how muscle activation changes following SET.

Methods

Kinematic and kinetic data from overground walking of patients with PAD (n=12), before and after a 6-month exercise intervention, was used as input for musculoskeletal modeling (OpenSim). The subjects in our sample were subdivided based on whether they reported an attenuation of ischemic thigh pain, due to SET, on the San Diego Claudication Questionnaire. Virtual models were scaled to match the anthropometry of the subjects before muscle parameters were derived. Muscle activation was analyzed across the stance phase of gait and the output was analyzed across subjects and conditions.

Results and Discussion

The subset of subjects that reported an attenuation of thigh pain as a result of SET (pain-free, n=4) showed a significant increase in late-stance knee-flexor force compared to baseline (Figure 1), whereas the group that experienced no difference in thigh pain following SET (pain, n=8) did not demonstrate a significant change in knee-flexor force compared to baseline. Additionally, compared to controls, the subjects with PAD (n=12) demonstrated significantly attenuated peak knee-flexor force at baseline (Figure 2), however, peak knee-flexor force was not significantly different among subjects with PAD and controls after SET. On further analysis, the most significant contributors to the increase in peak knee-flexor force was the subset of PAD subjects that reported an attenuation of thigh pain as a result of SET (pain-free, n=4). These results indicate that SET may be capable of improving posterior chain mechanics in those with PAD.

Significance

This study has given unique insight into the potential mechanisms underlying alterations to gait in PAD after SET. This study has shown that posterior chain mechanics converge to values similar to healthy control subjects as a result of SET, which may improve push-off. This is the first study to examine the gait mechanics of PAD with the OpenSim simulator.

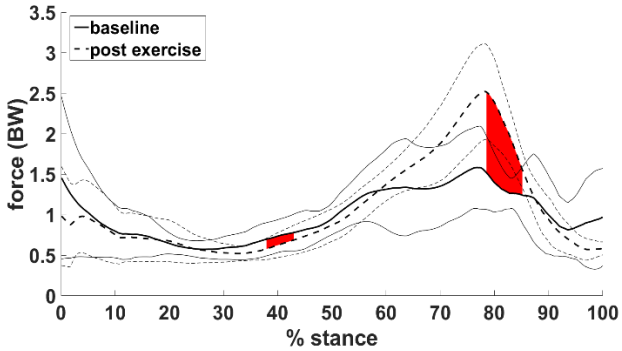

Figure 1: Knee-flexor force (no-pain, n=4). The red regions indicate significant differences in group means across highlighted data points ($p<0.05$).

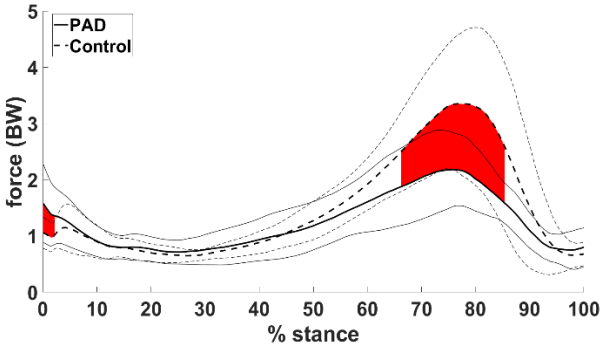

Figure 2: Knee-flexor force (n=12). The red regions indicate significant differences in group means across highlighted data points ($p<0.05$).

Acknowledgments

This study was supported by NIH grants (R01AG034995, R01HD090333, R01AG049868) and VA RR&D grant (I01RX000604, I01RX003266).

References

[1] N. M. Hamburg and M. A. Creager, "Pathophysiology of intermittent claudication in peripheral artery disease," Circ. J., vol. 81, no. 3, pp. 281–289, 2017, doi: 10.1253/circj.CJ-16-1286.
[2] Schieber MN, Pipinos II, Johanning JM, Casale GP, Williams MA, DeSpiegelaere HK, Senderling B, Myers SA. "Supervised walking exercise therapy improves gait biomechanics in patients with peripheral artery disease," J Vasc Surg. 2020 Feb;71(2):575-583. doi: 10.1016/j.jvs.2019.05.044.

FEATURE EXTRACTION AND EVALUATION FOR CLASSIFICATION MODELS OF INJURIOUS FALLS BASED ON SURFACE ELECTROMYOGRAPHY

Kitaek Lim, Woochol Joseph Choi[1]
[1]Injury Prevention and Biomechanics Laboratory, Dept of Physical Therapy, Yonsei University, South Korea
email: wcjchoi@yonsei.ac.kr

Introduction

Only 2% of falls in older adults result in serious injuries (i.e., hip fracture) [1]. Therefore, it is important to differentiate injurious versus non-injurious falls, which is critical to develop effective interventions for injury prevention. The purpose of this study was to a. extract the best features of surface electromyography (sEMG) for classification of injurious falls, and b. find a best model provided by data mining techniques using the extracted features.

Methods

Twenty young adults self-initiated falls and landed sideways. Falling trials were consisted of three initial fall directions (forward, sideways, or backward) and three knee positions at the time of hip impact (the impacting-side knee contacted the other knee ("KT: knee together") or the mat ("KOM: knee on mat"), or neither the other knee nor the mat was contacted by the impacting-side knee ("KF: knee free")) (Figure 1). Falls involved "backward initial fall direction" or "free knee" were defined as "injurious falls" as suggested from previous studies [2,3]. Nine features were extracted from sEMG signals of four hip muscles during a fall, including Integral of Absolute Value (IAV), Wilson Amplitude (WAMP), Zero Crossing (ZC), Number of turns (NT), Mean of amplitude (MA), Root mean square (RMS), Average amplitude change (AAC), Difference Absolute Standard Deviation Value (DASDV). The decision tree (DT) and support vector machine (SVM) were used to classify the injurious falls (DT1: entropy index was used; DT2: Gini index; SVM1: $c=10^{(-5:1)}$, $\gamma=10^{(0:2)}$; SVM2: $c= 2^{(-3:3)}$, $\gamma=2^{(-3:3)}$).

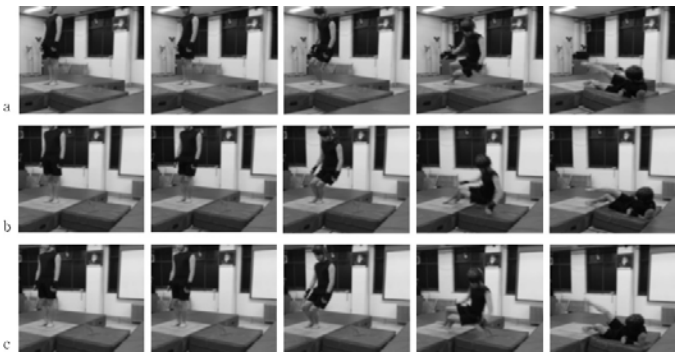

Figure 1: Sample snapshots of falls initiated sideways and landed sideways in a particular participant, where (a) the impacting-side knee contacted the mat, (b) the impacting-side knee contacted the contralateral knee, and (c) neither the impacting-knee nor the mat contacted the impacting-side knee at the time of hip impact during a fall.

Results and Discussion

Classification model for fall direction

Total 540 trials were collected in three fall directions. After removing 282 trials that did not show a pre-defined onset time for muscle contraction, 258 trials remained for forward falls (78 trials), sideways falls (97 trials), and backward falls (83 trials). Total 234 trials were selected by under-sampling for model construction. For the initial fall direction, accuracy of the best model (SVM1 with a DASDV feature) was 48%, and the worst model (DT2 with a MA feature) was 22% (Figure 2a). There was no model which has sensitivity and specificity of 80% or greater.

Classification model for knee position

After removing inappropriate data, 258 falling trials remained for KOM (82 trials), KT (84 trials), and KF (83 trials). Total 246 trials were selected by under-sampling. For the knee position, accuracy of the best model (SVM1 with an AAC feature) was 49% and the worst model (SVM1 with an IAV feature) was 29% (Figure 2b). There was no model which has sensitivity and specificity of 80% or greater.

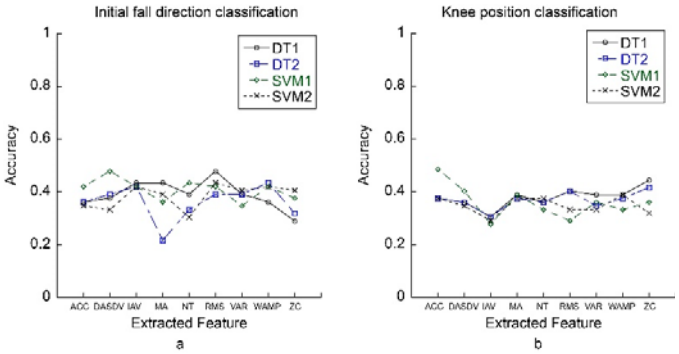

Figure 2: Accuracy of classification model that used various sEMG features of hip muscles. Accuracy was less than 50% across all features.

Significance

Classification of initial fall direction through sEMG of hip muscles was not promising, and the accuracy of the best model was less than 50%. Moreover, classification of knee position at the time of hip impact was not encouraging, either, and the best model provided 49% of accuracy at most. Future studies should consider other muscle groups (i.e., trunk muscles) along with different data mining techniques to generate the best model for classification of injurious versus non-injurious falls using sEMG data during a fall.

Acknowledgments

This study was supported by the "Brain Korea 21 FOUR Project", the Korean Research Foundation for Department of Physical Therapy in the Graduate School of Yonsei University.

References

[1] Sattin, *Annu Rev Public Health*, 1992.
[2] Lim and Choi, *Osteoporos Int*, 2020.
[3] Yang et al., *J Bone Miner Res*, 2020

CHARACTERIZING VISCOELASTIC PROPERTY OF SOFT TISSUE OVER THE HIP AS A RISK FACTOR OF PRESSURE ULCER

Kitaek Lim[1], Seungsu Kim[1], Woochol Joseph Choi[1],
[1]Injury Prevention and Biomechanics Laboratory, Dept of Physical Therapy, Yonsei University, South Korea
email: wcjchoi@yonsei.ac.kr

Introduction

A pressure ulcer is common in soft tissue over the greater trochanter (GT) in side-lying position, and sustained tissue deformation induced by the prolonged external force is a primary cause [1]. While the degree of tissue deformation depends on viscoelastic properties (i.e., stress relaxation, creep response) of soft tissue, limited information exists on the viscoelastic properties of the trochanteric soft tissue. Using an automated hand-held indentation device, we measured the viscoelastic properties of soft tissue over the hip area, in order to examine how the properties are affected by site with respect to the GT.

Methods

20 participants (15 males and 5 females) who aged from 21 to 32 were participated. An automated hand-held indentation device was used to measure the stress relaxation time and creep response (a ratio of "stress relaxation time" to "time to cause maximum deformation") (MyotonPRO, Myoton AS, Tallinn, Estonia). Trials were acquired for three different locations with respect to the GT (i.e., right over the GT, 6 cm anterior or posterior to the GT) (Figure 1a). For each location, five trials were acquired and averaged for data analyses.

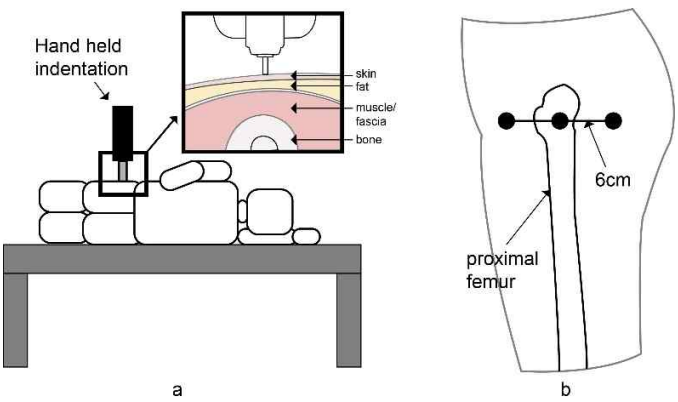

Figure 1: a. experimental setup, b. measurement sites with respect to the greater trochanter.

Results and Discussion

Stress relaxation was associated with site ($F = 23.98$, $p < 0.005$). The stress relaxation time differed across three sites with respect to the GT, being greatest (19.2 ± 2.49 ms) at the posterior gluteal region and least (14.4 ± 3.18 ms) at right over the GT (Figure 2a).

Similar trends were observed for creep response, and creep response was associated with site ($F = 24.09$, $p < 0.005$). The creep response differed across three sites over the hip region, being greatest (1.16 ± 0.14) at the posterior gluteal region and least (0.89 ± 0.18) at right over the GT (Figure 2b).

Our results indicates that the gluteal soft tissue is more resistant to tissue deformation induced by the prolonged external force when compared to the trochanteric soft tissue, suggesting that a risk of pressure ulcer over the GT may decrease with slightly posteriorly rotated side-lying position. This finding supports the repositioning guidelines for the individuals who are bedridden [2]. The guidelines suggest side-lying position with body rotation 30 degrees posterior would reduce the incidence of pressure ulcer in hospitalized patients when compared to side-lying position with a pelvis perpendicular to the horizontal line, where the GT contacts the bed directly [3].

A potential reason why the viscoelastic properties differed across sites might be explained, in part, by varying properties and composition of soft tissue over the hip area. The soft tissue may include skin, fat, muscle and fascia, and each tissue layer has different viscoelastic properties (i.e., muscle is more viscoelastic than fat). Furthermore, distribution (thickness) of each layer depends on site with respect to the GT (more muscle and adipose tissue in posterior (gluteal) region than in anterior or right over the GT). This variability results in changes in soft tissue properties over the hip area.

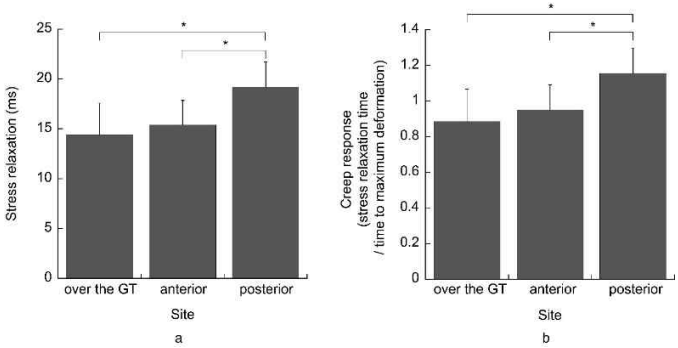

Figure 2: Effect of site on the stress relaxation (a) and creep response (b) over the hip area

Significance

The stress relaxation time and creep response were greatest at the posterior gluteal region and least right over the GT, indicating that the gluteal soft tissue is more resistant to tissue deformation induced by the prolonged external load, when compared to the trochanteric soft tissue. The results suggest that a risk of pressure ulcer over the GT may decrease with slightly posteriorly rotated side-lying position.

Acknowledgments

This study was supported by the "Brain Korea 21 FOUR Project", the Korean Research Foundation for Department of Physical Therapy in the Graduate School of Yonsei University.

References

[1] Zeller et al., *JAMA*, 2006
[2] Haesler, *Cambridge Midiea*, 2014
[3] Moore et al., *J Clin Nurs*, 2011

Stochastic Resonance and Heaviness Perception of an Occluded Object

Alli Grunkemeyer[1], Aaron D. Likens[1]
[1]Department of Biomechanics, University of Nebraska at Omaha, Omaha, NE USA
Email: agrunkemeyer@unomaha.edu

Introduction

Heaviness perception is the ability to use haptic feedback from effortful touch to determine the weight of a wielded object [1]. The perception of an object being wielded does not rely solely on the object's mass, but muscular effort as well. When an object is wielded, torques and moments of inertia are produced. The inertia tensor contains those moments and provides information about how mass is distributed in a rigid body. The corresponding eigenvalues and eigenvectors of the inertia tensor have been related to an object's perceived magnitudes (e.g., weight) and directions (e.g., orientation with respect to hand), respectively (**Figure 1a)** [2]. The inertia tensor can be visualized as an ellipsoid, as seen in **Figure 1b**, which is produced in effect from the constraints related to the position of the limb. In this study, we will manipulate the eigenvectors associated with an object in relation to the limb.

Recent studies have also provided evidence that adding noise to a weak stimulus can enhance a person's ability to detect it [2]. Introducing a subthreshold (vibrational) stimulus embedded with noise may, in some cases, improve sensations gained from limb movements [1]. We hypothesize that adding vibrotactile noise of various forms will improve accuracy in perceiving heaviness of a wielded object (**Figure 2)**.

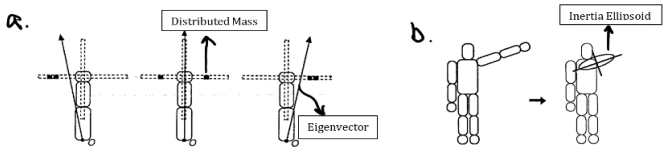

Figure 1. (a) Effect of varying mass loads on eigenvectors. **(b)** Inertia ellipsoid of upper **limb.**

Methods

Ten adults (18-45 years of age) will be seated for the duration of the trial with a BM3C tactor fastened to the humerus of the subject as seen in **Figure 2.**

Vibrational stimuli will be introduced via the tactor with different signals of colored noise, or signals produced by stochastic processes varying in power spectral slope. Noise (3) × mass (6) combinations will be presented. Each condition of noise and mass will be introduced randomly. Subjects will rate the heaviness of the object by stating their perceived proportion of mass added on a scale of 1-10.

Expected Results and Discussion

We expect that the embedded pink noise signal will produce the highest level of accuracy regarding heaviness perception compared to the alternative condition as seen in the projected outcomes in **Figure 3**.

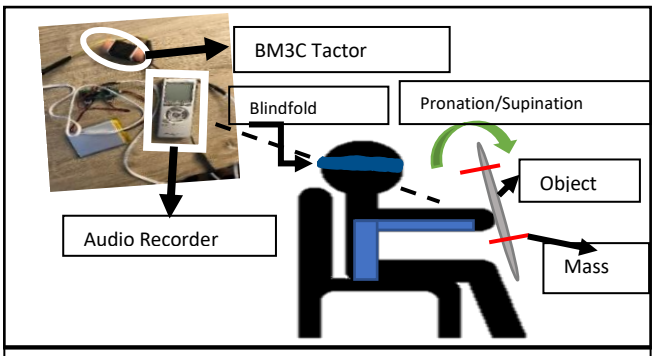

Figure 2. Proposed experimental set up. Object has been 3D printed via Ultimaker 2 Plus with incremental masses added pertaining to desired condition. The participant will be blindfolded to ensure proper occlusion of the wielded object. The BM3C tactor will be fastened to the humerus where vibrational stimuli embedded with a noise signal will be applied.

Conclusions

Introducing a noise as a subthreshold vibration is hypothesized to improve the heaviness accuracy of a given wielded object. Pink noise is expected to display the highest level of accuracy considering the exploratory patterns conveying fractal properties the subjects will exert. These fractal properties are common in most biological systems, therefore producing a more accurate identification of weight.

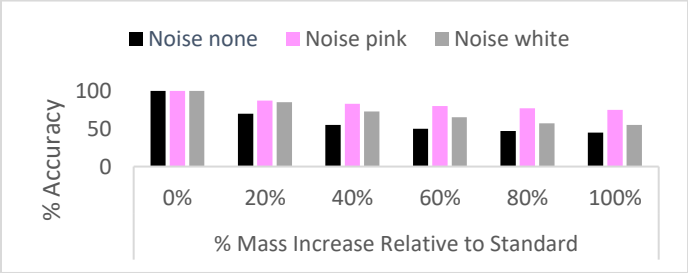

Figure 3. Expected outcomes of accuracy for given incremental masses with respective embedded noise signals for proposed experimental design.

Significance

We are investigating a novel means to enhance haptic perception of wielded objects.

This research project, if successful, would contribute new theoretical knowledge about the role and structure of neuromuscular noise in the perception of wielded objects. Stochastic resonance is a newly introduced phenomenon and when applied to perception it can advance the theoretical literature in this topic and apply it to human movement variability.

References

[1] Pagano et al. *Journal of Applied Biomechanics,* ***14****: 331-359, 1998.*
[2] Nozaki et al. *Physical Review Letters,* **82:** 2402-2405, 1999.

Modeling Spatial Asymmetry in Visuomotor Coordination

Kolby Brink, Nicholas Stergiou, and Aaron Likens
[1]Department of Biomechanics, University of Nebraska at Omaha, Omaha, NE USA
email: kolbybrink@unomaha.edu
Presentation Preference: **Podium**

INTRODUCTION

Coordinated movement, addressed mathematically, portrays a complex process when accounting for all possible degrees of freedom. One model, however, has garnered attention through its simplicity while still predicting and measuring several movement behaviors. The Haken-Kelso-Bunz (HKB)[1] predicts changes in relative phase between two oscillators according to the following equation: $\dot{\phi} = \Delta\omega - a\sin(\phi) - 2b\sin(2\phi) - \sqrt{Q}\zeta_t$.

$\Delta\omega$ quantifies differences in natural periods between the oscillators. The ratio, b/a, models the collective frequency of coordinated oscillation. $\sqrt{Q}\zeta_t$ is a noise term with strength Q. $\Delta\omega$ is an 'imperfection parameter' that predicts deviations in relative phase, ϕ, due to timing differences in oscillators. Deviations of ϕ might also result from asymmetries in spatial alignment of oscillators, such as in visual motor coordination. We propose two possible mechanisms for modeling asymmetry based on a modified HKB model: $\dot{\phi} = \Delta\omega + \Delta s - a\sin(\phi - \eta) - 2b\sin(2\phi) - \sqrt{Q}\zeta_t$.

Δs and η are potential terms to model the effects of spatial asymmetries of oscillators. Both predict shifts in mean relative phase, $\bar{\phi}$, away from stable fixed points. Only Δs predicts a shift in $SD_{\bar{\phi}}$, a decrease in the stability of coordination. This study was which parameter best models spatial asymmetry.

METHODS

Participants were 10 healthy adults (26.4 ± 6.87 years, 7 M, 3 F). A 6-camera system (Optotrak, NDI) measured upper body movement at 100 Hz. Participants coordinated their arm movements with a visually displayed sinusoidally oscillating stimulus (S_{Sine}). Forearm movements pivoted about the elbow which rested on a rotating platform. A user controlled visual stimulus (S_{RA}) was displayed on the screen that oscillated due to elbow rotation. Figure 1A shows a display in which the horizontal centers of oscillation of S_{Sine} and S_{RA} are manipulated. Given horizontal screen coordinates (x) and amplitude of oscillation (A) of S_{Sine}, we scaled this offset parameter as ρ = x_{shift}/A (Figure 1C). Figure 1B depicts the relative positions of S_{Sine} and S_{RA} for ρ = -2.0 over several cycles. We hypothesized that certain spatial offsets will be preferred. To test this hypothesis, we studied preferences for particular spatial arrangements of S_{Sine} and S_{RA} that arise from initial arrangements of ρ = -3, -2, -1, 0, 1, 2 or 3. Participants were free to move the location of S_{RA} as long as they could comfortably perform anti-phase and in-phase coordination. Subjects performed 3 trials for each phase (in-phase, anti-phase) × ρ pair, each lasting 60 seconds. 3 practice trials were given at ρ = 0 to familiarize subjects with the task.

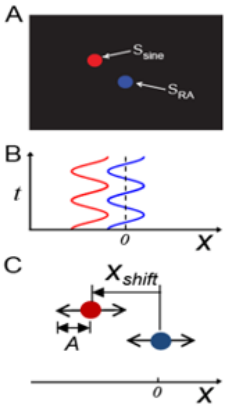

Figure 1. See Text

Analysis Strategy. We computed instantaneous relative phase between S_{Sine} and S_{RA} for all trials, along with circular means and standard deviations.[2] We then modeled $\bar{\phi}$ and $SD_{\bar{\phi}}$ as a function of ρ and phase (inphase/antiphase) in separate Bayesian multilevel models developed specifically for circular/directional dependent variables.[3]

RESULTS AND DISCUSSION

Estimates in Table 1 replicate well known differences between required phases because the 95% credible intervals defined by LB and UB do not overlap. Modeling results in Table 2 show that most slope estimates indicate that a one unit change in ρ predicts a negative change in $\bar{\phi}$ because credible intervals do not contain 0. Models relating ρ and $SD_{\bar{\phi}}$ (not reported to due to space) found no evidence of such a relationship, implying that Δs may not be useful in modeling asymmetry effects.

Table 1. Estimated circular descriptive statistics for $\bar{\phi}$ as a function of required phase. Estimates are in radians.

	Mean	Mode	SD	LB	UB
Anti-phase	-2.82	-2.87	0.13	-2.98	-2.59
In-phase	0.14	0.12	0.03	0.08	0.21

Table 2. Slope estimates for ρ predicting $\bar{\phi}$

Slopes	Mean	SD	Mode	LB	UB
β_c	-0.18	-0.22	0.23	-0.31	0.14
AS	-0.08	-0.08	0.15	-0.22	-0.02
SAM	-0.08	-0.09	0.06	-0.20	-0.02

Note: β_c = Slope at inflection point, AS = Average Slope, SAM = Slope at Grand Mean, LB/UB = Upper and lower bounds of 95 % credible interval from Bayesian estimates.

CONCLUSIONS

Results suggest that, in the current context, spatial asymmetries may best be modeled via the η parameter in the modified HKB model. Future work will investigate the extent to which this modification transfers to other conditions of asymmetry.

REFERENCES

1. Kelso, J., *MIT PRESS,* (1995).
2. Lamb, P.F., et al. *Clinical Biomech.,* (2014) ***29(5),*** *484-493.*
3. Cremers, J. et al, *Frontiers in psychology* (1994). **9**, 2040.

ACKNOWLEDGEMENTS

This work was supported by NIH P20GM10909 awarded to N. Stergiou and a Pilot Project Award to A. Likens from the Center for Research in Human Movement Variability and the NIH.

ACUTE EFFECTS OF VIBRATION FEEDBACK ON REDUCING MECHANICAL JOINT LOADING IN INDIVIDUALS WITH CHRONIC ANKLE INSTABILITY

Jaeho Jang[1], Kimmery Migel[1], Hoon Kim[1], and Erik. A Wikstrom[1]
[1]University of North Carolina Chapel Hill, NC, USA
email: jaeho@live.unc.edu

Introduction

Lateral ankle sprains are the most common musculoskeletal injury within the US. About 40% of individuals with lateral ankle sprains develop chronic ankle instability (CAI), a condition characterized by recurrent sprains and altered gait neuromechanics such as a more laterally shifted center of pressure and a more inverted foot position during walking [1]. The recurrent trauma and neuromechanical alterations have been linked with altered loading of cartilage as well as talar cartilage degeneration [2].

Excessive compressive loads multiplied by thousands of steps over time are thought to be the contributing factors of cartilaginous degeneration. Compressive loads on the articular cartilage can be estimated by the magnitude of compressive joint contact forces (JCF). Multiple knee JCF variables (e.g. peak JCF, JCF impulse, and JCF loading rate) have been associated with the development of knee osteoarthritis [3].

Gait retraining with vibration feedback was shown to reduce the lateral center of pressure shift in those with CAI during walking [4]. However, is it unknown if this novel gait retraining strategy also reduces joint loading at the ankle. Therefore, the purpose of this secondary study was to determine if vibration feedback gait retraining acutely reduces ankle JCF variables in those with CAI.

Methods

Ten physically active individuals with CAI were randomly pulled from a larger database of those who underwent vibration feedback gait retraining (age= 23.20±4.19 years, weight= 68.54±12.03 kg, height= 168.69±12.00 cm). CAI inclusion criteria were in accordance with the International Ankle Consortium guidelines. A battery powered customized vibration feedback tool (0.57kg) was secured to the shoe and lower leg (Figure1). In-shoe pressure was detected by a force sensing resistor under the fifth metatarsal head. The lowest individualized threshold was determined such that standing on the involved limb triggered the vibration stimuli but standing on both limbs did not [4]. When pressure exceeded the threshold, the device turned on and provided a continuous vibration stimulus (200Hz) until pressure on the force sensing resistor fell below the threshold.

Kinematic (120Hz) and kinetic data (1200Hz) were collected during walking on an instrumental treadmill with two force plates embedded in it. Participants walked at their self-selected walking speed. After familiarization, participants walked a 2 min baseline assessment (no vibration). Participants then walked for another 10 min while receiving feedback. Data was captured during an early (min 1-2) and late (min 9-10) adaptation period. Opensim 4.0 calculated ankle JCF variables during stance phase via a full-body musculoskeletal model (gait2392). Scaling, inverse kinematic, residual reduction algorithm, static optimization, and joint reduction analysis were conducted in sequence. The peak, impulse, and loading rates of ankle JCF were compared between 1) baseline and the early adaptation phase and 2) baseline and late adaptation phase using paired sample *t*-tests. Statistical significance was set at p=0.05.

Results and Discussion

At the early adaptation phase, peak ankle JCF, ankle JCF impulse, and ankle JCF loading rate were significantly reduced compared to baseline (p≤0.027). At the late adaptation phase, ankle JCF impulse was significantly reduced compared to baseline (p=0.004). Group means and standard deviations can be seen in Figure 2.

The results suggest that vibration feedback could reduce compressive loads in those with CAI. The mechanism underlying the observed changes remains unknown, as feedback gait retraining studies have focused on treatment efficacy (i.e. shifting the center of pressure) to date. However, it could be due to the reduced activation of triceps surae muscles as it accounts for a large portion of ankle JCF [5]. Regardless of the mechanism, reduced JCF could contribute to slowing early cartilage degeneration in those with CAI after a prolonged intervention protocol.

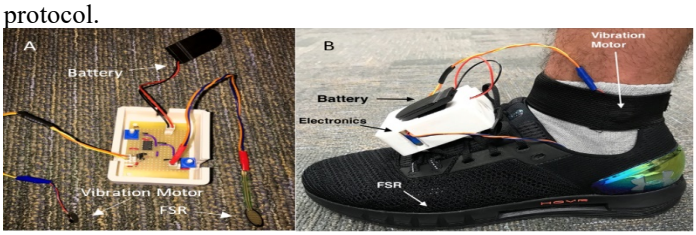

Figure 1. A: Feedback tool with component parts. B: Feedback tool placement on foot. FSR = Force sensing resistor.

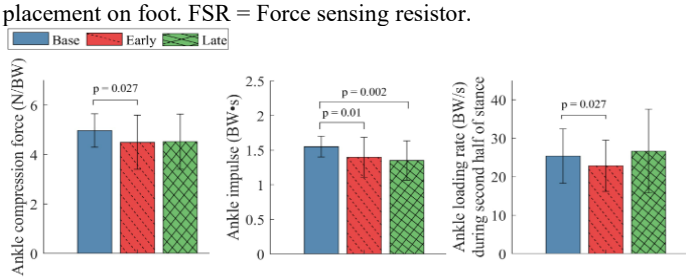

Figure 2. Mean±SD of the compression force, impulse, and loading rate of the ankle joint in individuals with chronic ankle instability in the involved limb during the stance phase.

Significance

The results provide additional evidence that vibration based feedback gait retraining can be beneficial to those with CAI. More specifically, the results illustrate that vibration feedback gait retraining reduces the ankle JCF and the compressive loads imparted onto the talar cartilage.

Acknowledgments

This work was supported in part by a Promotion of Doctoral Studies Scholarship from the Foundation for Physical Therapy Research.

References

[1] Moisan et al. (2017). *G&P*, 52, 381-399.
[2] Song&Wikstrom (2019). *Phys and SpoMed*. 47(3) 275-283.
[3] Miller et al. (2017). *PeerJ*. 5 e2960-e2960.
[4] Migel&Wikstrom (2021). *G&P*, 85, 238-24
[5] Prinold et al. (2016), Ann of Biomed Engine, 44(1), 247-257

IMU-DERIVED ERGONOMIC METRICS MEASURED DURING DAILY LIFE MAY DIFFERENTIATE MANUAL WHEELCHAIR USERS WITH SPINAL CORD INJURY WITH AND WITHOUT ROTATOR CUFF PATHOLOGY PROGRESSION

Omid Jahanian [1], Meegan G. Van Straaten [1], Brianna M. Goodwin[1], Stephen M. Cain[2], Jonathan D. Barlow[1], Naveen S. Murthy[1], and Melissa M. B. Morrow[1]
[1]Mayo Clinic, Rochester, MN, USA; [2]University of Michigan, Ann Arbor, MI, USA
email: morrow.melissa@mayo.edu

Introduction

Manual wheelchair (MWC) users with spinal cord injury (SCI) are at higher risk of incidence and progression of rotator cuff disease than the general population [1]. This is theorized to be due to arm overuse during activities of daily living including MWC use. The purpose of this study was to investigate the ability of risk and recovery metrics of arm use, inspired from ergonomics literature on risk factors in industrial manual handling [2], to differentiate between MWC users with and without rotator cuff pathology progression over one year.

Methods

Under Mayo Clinic IRB approval, 16 MWC users (14 males, age (SD): 41(12) years, injury level: C6–L1, median years of MWC use (IQR): 6(4, 12) years) were recruited. IMUs were worn on the upper arms and chest for one or two days in the free-living environment and humeral elevation and static/dynamic periods were calculated across the day(s) [3]. Periods that may represent risk (humeral elevation > 60°) and recovery (static ≥5 seconds & humeral elevation <40°) were then defined for each 10-minute period. Risk and recovery metrics as well as risk to recovery ratio were calculated for each participant (Table 1). Two separate magnetic resonance imaging (MRI) studies were completed (before and after IMU data collection) approximately one year apart [4]. MRI abnormalities of rotator cuff tendons, including tendinopathy and tendon tears, were graded using a novel scoring system, wherein more points were given to higher grades of pathology from mild tendinopathy through full thickness tear. The differences between the scores at the two time points were calculated for each rotator cuff tendon (supraspinatus, infraspinatus, subscapularis, and teres minor). Any positive difference in the tendinopathy or tear score on each shoulder was defined as progression of rotator cuff pathology for that shoulder. Differences between the MWC users with and without progression of pathology were compared using Mann-Whitney U tests for the risk and recovery metrics ($\alpha = 0.05$).

Table 1. Risk and recovery metrics.

Metric	Calculation
Duration of risk/recovery events	Average summated duration of risk/recovery events for each 10-minute within a day.
Frequency of risk/recovery events	Average frequency of risk/recovery events for each 10-minute period within a day across all periods with at least one risk event.
Risk to recovery ratio	Average natural log of the ratio of summated duration of risk events to summated duration of recovery events for each 10-minute period within a day.

Results and Discussion

The MRI findings indicated that five participants experienced progression of rotator cuff tendon pathology (progression in tear or tendinopathy score) on their dominant shoulder. MWC users with pathology progression experienced a longer duration of risk events (Figure 1, A; P = 0.047), had higher frequency of risk events (P = 0.027), experienced shorter duration of recovery events (P = 0.036), had lower frequency of recovery events (P = 0.047), and had larger risk to recovery ratio (Figure 1, B; P = 0.02) than the MWC users without pathology progression. These results indicate that the risk and recovery metrics in this study have the potential to differentiate between the MWC users who exhibited rotator cuff pathology progression over one year from MWC users without pathology progression.

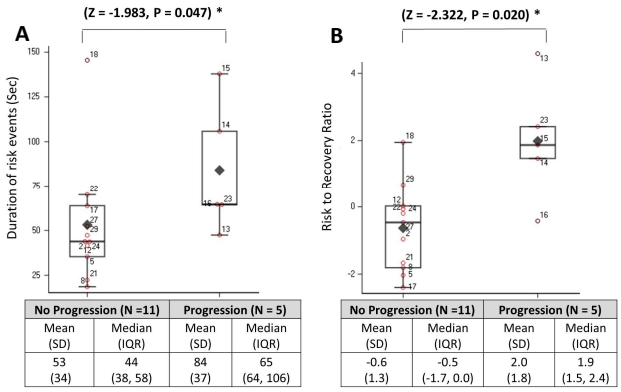

	No Progression (N =11)		Progression (N = 5)	
	Mean (SD)	Median (IQR)	Mean (SD)	Median (IQR)
A	53 (34)	44 (38, 58)	84 (37)	65 (64, 106)
B	-0.6 (1.3)	-0.5 (-1.7, 0.0)	2.0 (1.8)	1.9 (1.5, 2.4)

Figure1: Box plots and data points for the dominant side duration of risk event and risk to recovery ratio for the MWC users with and without progression of rotator cuff pathology. Group mean, standard deviation (SD), median, and inter quartile range (IQR) for each metric are reported in the tables below the box plots. The statistical results for each metric are reported on top of the box plots. *, indicates statistical significance

Significance

Free-living IMU data collected from the upper arm may be able to assess potential risk factors for rotator cuff pathology progression. Specifically, metrics quantifying arm use at postures >60° and the risk to recovery ratio may provide clinically relevant interventional targets. Ongoing investigation of other time periods where work was done at lower elevations is also informative in understanding risky and beneficial arm use to the rotator cuff. Additional data collections with larger sample size and longer follow-up are warranted to confirm the findings of this study and fully validate definitions of risk and recovery.

Acknowledgments

This research was supported by NIH Grants R01 HD84423 and NCATS UL1 TR002377.

References: [1] Akbar et al. (2010). *JBJS (Am),* 92(1):23-30. [2] Lind et al. (2020). *Ergonomics*, 63(4):477-504. [3] Goodwin et al. (2021). *Sensors*, *21*(4), 1236. [4] Jahanian et al. (2020). *J Spinal Cord Med: 1-11.*

Prediction of Lower Limb Incapacitation as a Result of Cross-sectional Muscle Tissue Loss

*Morgan J. Dalman[1], Matthew Berno[1], Mikael Koeneke[1], Kerry A. Danelson[2], Katherine R. Saul[1]
[1]Department of Mechanical and Aerospace Engineering, North Carolina State University, Raleigh, NC, USA
[2]Department of Orthopaedic Surgery, Wake Forest University Health Sciences, Winston-Salem, NC, USA
Email: *mdalman2@ncsu.edu

Introduction

Injuries to the extremities are common among military combat casualties and can limit mobility. From 2005-2009, 82% of musculoskeletal wounds from combat casualties were explosion related [1]. From 2000-2009, 4,693 service members had sustained a gunshot wound related to combat [2], and 73% of gunshot wounds affected the extremities, potentially limiting mobility [3]. Despite the frequency of these injuries, the level of resulting incapacitation that can be expected is not yet clear. Blast and penetrating wound injuries cause volumetric loss of muscle tissue, which inherently reduces the mechanical capacity of muscle due to loss of contractile material. While other factors - such as blood loss, neurological injury, bone fracture and pain - can additionally impact function, the mechanical deficits can provide an estimate of functional deficits expected from wounds of a particular size. Using computational musculoskeletal modeling, this study evaluates potential incapacitation experienced by an individual as a result of cross-sectional muscle tissue loss in the lower extremity.

Methods

Five typical functional tasks - pedal pushing, sit to stand, squatting, walking (declined, level, inclined), and running (declined, level, inclined) - were established as a baseline for evaluating lower limb incapacitation. The range of required joint moments for performance of each lower extremity functional task was obtained from prior literature [4-9]. An existing lower limb computational musculoskeletal model representing a 50th percentile male [10] was used to simulate effects of muscle loss using OpenSim (v3.3) [11] and Matlab (r2020b) (The Mathworks, Natick, MA). We systematically decreased muscle cross-sectional area from 0-100% (10% increments) for functional muscle groups and the individual muscles comprising them (e.g. **Fig 1**). Simulated joint moments were calculated for the hip, knee, and ankle joints.

Results and Discussion

The simulations suggest that isolated injury to most single muscles at the hip, knee, or ankle (**Fig. 1a-c**) is unlikely to directly limit functional performance, but more significant injury to a functional group, as is common in these types of penetrating or blast injuries, may limit ability to perform important mobility tasks when as little as 40% of cross sectional area is disrupted. This is consistent with prior work observing that gait can become impaired when lower limb muscles are weakened by ~40% of maximum force-generating capacity [12]. However, injury to soleus in isolation results in a more marked deficit than that associated with other muscles.

Limitations of the current work include that we have initially considered effects of cross-sectional muscle loss in isolation and injury to single muscles and functional groups rather than more complex patterns of injury or concomitant factors such as nerve or bone injury; these will be addressed in future work. In addition, an individual's nominal anthropometry, age, and strength will also affect outcomes. Future work will consider these limitations and extend analysis to the upper limb.

Significance

These simulations provide insight into whether functional deficits for lower limb functional tasks are likely to occur following injury causing volumetric muscle loss, based on the mechanical consequences of lost contractile material.

Acknowledgments

This work was funded under a US Army contract by DEVCOM DAC in support of the Operational Requirements-based Casualty Assessment (ORCA) project.

References

[1] Belmont, et al. (2013). *J Orthop Trauma*. **27**: 107-113.
[2] Walker, et al. (2012). *Int J Surgery* **10**: 140-143.
[3] Laughlin, et al. (2017). *Int J Surgery **48***: 286-290.
[4] Huang et al. (2020). *J Biomech.* **108:** epub ahead of print.
[5] Karimi et al. (2013). *The Knee*. 526-531.
[6] Ferber et al. (2002). *Clin Biomech.* **17**: 274-285.
[7] Silder et al. (2012). *J Biomech.* **45**: 1842-1849.
[8] Orendurff et al. (2018). *J Biomech*. **71**: 167-175.
[9] Xu et al. (2017). *Musculoskelet Disord*. **18**: 1-12.
[10] Rajagopal, et al. (2016). *IEEE Trans Biomed Eng.* **63**: 2068-2079.
[11] Delp, S.L. et al. (2007). *IEEE Trans Biomed Eng*, **55**: 1940-1950.
[12] van der Krogt, et al. (2012). *Gait Posture.* **36**:113–119.

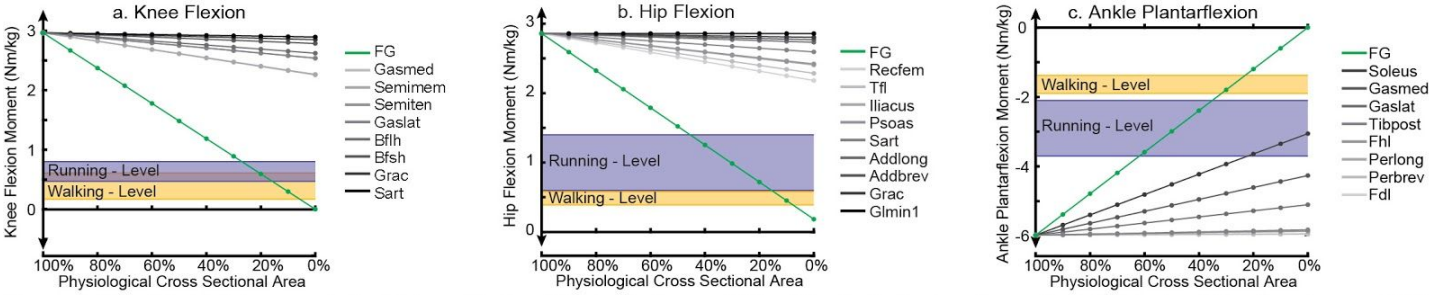

Figure 1. Simulated joint moments for (**a**) knee flexion, (**b**) hip flexion, and (**c**) ankle plantarflexion shown for individual and functional group (FG) muscle conditions. Muscles listed in descending order of influence on total moment. Physiological cross sectional area represents intact area capable of force production relative to nominal muscle.

Is This Safe for Baby? Using Biomechanics to Explore Safety of Inclined Sleepers

[1,2]Erin M. Mannen, [2]Junsig Wang, [1,2]Safeer Siddicky, [2]John Carroll, [2]Brien Rabenhorst, [2]David Bumpass, [2]Brandi Whitaker
[1]Boise State University, Boise, ID [2]University of Arkansas for Medical Sciences, Little Rock, AR
Email: ErinMannen@BoiseState.edu

Introduction

Over 450 adverse incidents have been reported in infant inclined sleep products over the past 12 years, with many infants found dead in the prone position having apparently rolled from supine to prone in the product[1]. The inclined sleep products may have suffocation hazards related to their unique designs. However, no research has investigated how inclined sleep products impact infant's muscle activity and ability to move in the context of a safe infant sleep environment. Therefore, the purpose of this study was to assess muscle activity and movement of normal healthy infants when placed on different inclined sleep products compared to a flat crib mattress during prone positioning.

Method

Fifteen healthy full-term infants (age: 17.7±4.9 weeks; 8M, 7F; length: 61.5±4.1 cm; weight: 6.5±1.0 kg) were recruited for this IRB-approved study. Four conditions were tested: three inclined sleep products with unique features, representative of different designs (*sleepers a, b,* and *c*; Figure 1), and one control condition (0° baseline, a flat crib mattress). Surface electromyography (Delsys Inc., Natick, MA; 1000Hz) was recorded from infants' cervical paraspinal, abdominal, and lumbar erector spinae muscles while motion analysis system with 10 high-resolution cameras (Vicon Nexus, Oxford, UK; 100 Hz) was used to collect three-dimensional kinematic data during each prone-lying testing condition. Filtered and rectified mean EMG was normalized to the flat crib mattress. Sagittal plane ranges of motions (ROMs) of neck and trunk as well as the number of neck and trunk angle peaks were calculated. Paired t-tests and Wilcoxon signed-rank tests were performed to compare each inclined sleeper to a flat crib mattress (0° baseline condition). Due to missing trials and small samples for the sleeper product conditions, we were not able to compare between the inclined sleep products.

Figure 1. Three inclined sleep products (*sleepers a, b,* and *c*).

Results and Discussion

Increased neck and trunk ROMs were found for *sleeper b* compared to the flat crib mattress (p=0.014, p=0.003; Table 1). In addition, the number of trunk angle peaks were increased for *sleepers b* and *c* compared to the flat crib mattress (p=0.047, p=0.039). Erector spinae muscle activity decreased by 21%, 36%, and 48% respectively for *sleepers a, b,* and *c* compared to the flat mattress (p=0.050, p=0.029, p=0.003; Figure 2). Conversely, abdominal muscle activity increased by 75%, 39%, and 93% respectively for *sleepers a, b,* and *c* compared to the flat mattress (p=0.024, p=0.029, p=0.033; Figure 2). Inclined sleep products resulted in different neck and trunk movement patterns, compared to a flat crib mattress. *Sleeper b* with no plastic surface and narrow width at the shoulder required greater postural changes evidenced by neck and trunk ROMs to maintain a safe position. Products without any plastic surface support (*sleepers b and c*) caused babies to move more often as evidenced by increased peaks as they worked against the pliant surface to move their bodies compared to the firm and flat crib mattress.

Table 1. Effect of sleep product design on kinematic variables. * p <0.05

Variable	*flat mattress*	*sleeper a*	*sleeper b*	*sleeper c*
neck ROM °	41±16	44±18	**44±10***	44±18
trunk ROM °	29±14	44±25	**42±19***	41±19
# of neck peaks per 10s	1.7±0.8	1.8±1.1	2.5±1.5	2.2±1.3
# of trunk peaks per 10s	0.9±0.8	1.4±1.0	**1.7±1.0***	**2.0±1.3***

Products with thick padding (*sleepers a* and *c*) exhibited abdominal muscle activity of 175% and 193%, respectively, compared the flat crib mattress condition. One product without plastic molding (*sleeper b*) showed 139% of abdominal muscle activity compared to the flat crib mattress condition. These findings may indicate that the lack of firmness and/or the presence of extra padding in the sleep surface alters a baby's ability to move into a safe breathing position, which could contribute to the increased risk of suffocation[2]. The combination of incline angle and product design requires infants to use significantly more core effort (abdominal strength) to maintain a prone position compared to lying on a flat surface, which adds to the abdominal effort required for normal breathing.

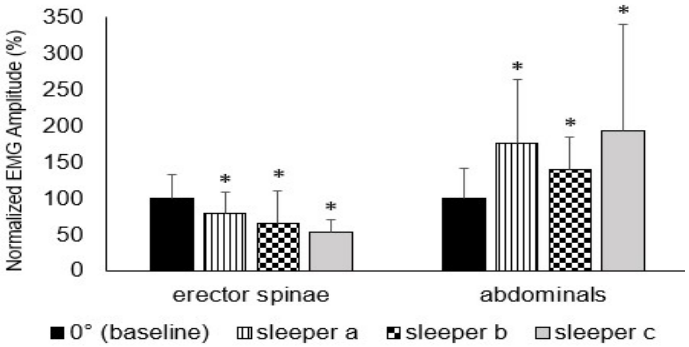

Figure 2. EMG activity during prone positioning in sleepers normalized to flat crib mattress (0° baseline). * p < 0.05

Significance

Inclined sleep products resulted in significantly higher abdominal muscle activity and trunk movement, which may exacerbate fatigue and contribute to suffocation if an infant finds themselves in a prone position in the product. This novel study serves as the basis for future work aimed at understanding movement-related suffocation risk factors associated with infant products.

Acknowledgments

This project has been funded with federal funds from the United States Consumer Product Safety Commission under contract number 61320618P. The content of this publication does not necessarily reflect the views of the Commission, nor does it mention of trade names, commercial products, or organizations imply endorsement by the Commission.

References: 1. CPSC, Federal Register. (2019) Safety Standard for Infant Sleep Products; 2. Thach et al, J. Pediatr. (2007) 151, 271-274.

‘OPTIMUM’ FOOT PARAMETERS FOR MAXIMAL VERTICAL JUMPS

Daniel J. Davis and J. Challis
The Biomechanics Laboratory, The Pennsylvania State University, State College, PA 16803
email: djd426@psu.edu

Introduction

The human foot can act as both a lever and a spring. Where the stiffness of the foot lies on a continuum from compliant to rigid may influence the performance of the foot for a given task. For example, the foot’s arch functions like a spring during steady state running [1], but a compliant arch may waste valuable mechanical energy if the moment produced by ankle plantar flexors is not efficiently transferred to the ground. It may be that a foot that is best for saving energy during submaximal effort steady-state tasks is different from one that is best for explosive maximal effort tasks, and vice versa. The present analysis, therefore, aimed to examine the extent to which foot joint stiffness influences maximal vertical jumping.

Methods

Two-dimensional direct dynamics models of the lower limb were created in OpenSim (v4.0) based on a simplified set of muscles and joints. The baseline model had joints at the hip, knee, ankle, midfoot, and metatarsophalangeal (MTP) joints (Figure 1). Midfoot and MTP joint passive stiffnesses were modelled as torsional spring dampers (Figure 1). The model had muscles representing the gluteus maximus, biceps femoris long head, rectus femoris, vastii, gastrocnemius, soleus, and flexor hallucis longus muscles. Muscle strengths were manually adjusted to approximate torque-angle relations of more complex models [3].

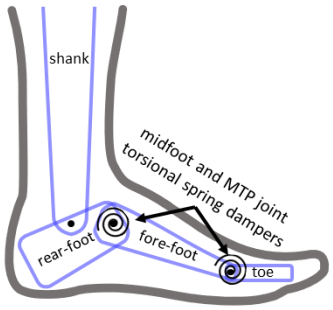

Figure 1: Rigid body foot model with torsional springs at the midfoot and metatarsophalangeal (MTP) joints.

An optimal control problem was solved as a direct collocation problem using OpenSim Moco [v0.4.0; 4] to maximize jump height from an initial quarter-squat position. The muscle excitation time-histories were optimized to maximize the sum of squared pelvis vertical velocity and position while minimizing the reserve actuator controls throughout the jumping motion. Jump height as a function of both midfoot and MTP joint spring stiffnesses were measured across a wide range of stiffnesses. Stiffness values were chosen to approximate joint ranges of motion expected from very compliant to very stiff feet or feet in very stiff shoes.

Results and Discussion

Midfoot joint stiffness had a much larger influence on jump height than MTP joint stiffness (Figure 2). For example, a change from 100 Nm/rad to 1,500 Nm/rad of midfoot torsional stiffness with MTP joint stiffness at a constant 0 Nm/rad increased jump height by 1.56 cm (11.5%). When MTP joint stiffness was then increased to 150 Nm/rad, jump height increased by 0.29 cm (1.3% increase).

Differences in jump height were in part due to muscle dynamics, in that for a given MTP joint stiffness, a stiffer midfoot joint lead to decreased muscle fiber shortening velocity for the plantar flexors, which in turn resulted in greater fiber forces. The negative work from the midfoot joint torsional spring as a function of both spring stiffnesses followed a similar pattern to jump height, however the positive work performed by each of the joint torsional springs was relatively constant across the range of spring stiffnesses (Figure 2). This finding indicates that for the range of stiffnesses tested, reducing midfoot joint negative work was the primary determinant of jump performance, more so than generating positive work at either joint. Indeed, a model with both foot joints welded in place demonstrated the highest jump height. The ‘springiness’ of the human foot arch may therefore be less beneficial than its rigidity for maximal jumping even when the foot’s arch is compressing and recoiling.

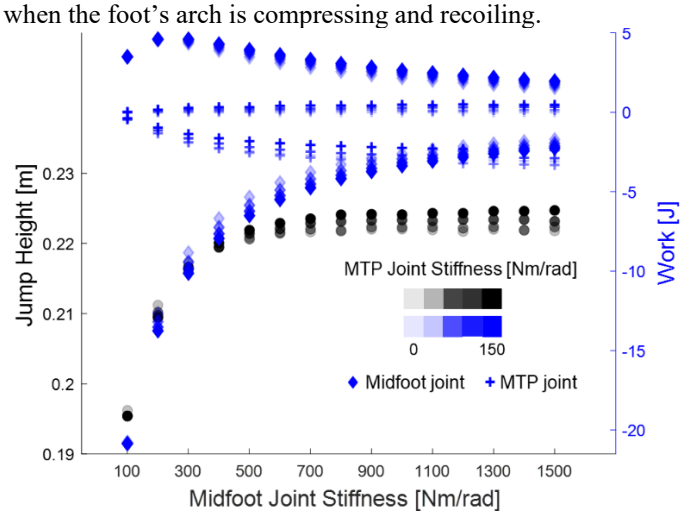

Figure 2: Jump height and torsional spring work as a function of midfoot and MTP joint stiffness.

Significance

Determining the extent to which the foot’s lever and spring functions coexist can shed light on the human foot’s unique evolution. Perhaps a foot ‘optimized’ or evolved for sub-maximal tasks like steady-state running would be more compliant than one ‘optimized’ for maximal sprinting or jumping. Conversely, a foot that can accomplish both tasks at least moderately well would allow for a broader range of activities without sacrificing effort or efficiency. Lastly, researchers should carefully consider how feet are modelled when performing simulations of jumping as foot deformation and stiffness impacted task performance.

References

[1] Stearne et al. (2016). *Scientific Reports*, 6(1), 1-10.
[2] Delp et al. (2007). *IEEE Trans Biomed Eng,* 54(11), 1945-1950.
[3] Arnold et al. (2010). *Ann Biomed Eng*, 38(2), 269-279.
[4] Dembia et al. (2019). *PLoS Comput Biol*, 16(12), e1008493.

TIBIAL BONE STRUCTURAL PROPERTIES IN AMBULATORY CHILDREN WITH CEREBRAL PALSY

Tishya A. L. Wren[1], Adriana Conrad-Forrest[1], and Robert M. Kay[1]
[1]Children's Orthopaedic Center, Children's Hospital Los Angeles, Los Angeles, CA, USA
email: twren@chla.usc.edu

Introduction

Fractures of the lower extremity long bones are common in patients with cerebral palsy (CP) and may be due, at least in part, to compromised bone structural properties associated with smaller bone size and/or reduced bone density. We have previously shown that children with CP who require assistive devices to walk have lower bone properties in the tibia diaphysis and proximal metaphysis than independently ambulatory children with CP [1]. However, it could not be determined whether the independently ambulatory children with CP had lower bone properties than typically developing children due to lack of data from a control group without disability. Such data is now available, and the purpose of the current study was to compare tibial bone properties between children with CP with varying levels of disability and typically developing children.

Methods

Thirty-three ambulatory children with CP (24 male) and 177 typically developing controls (95 male) ages 6-16 years underwent quantitative computed tomography (QCT) imaging of the tibias on a clinical CT scanner (Gemini GXL, Philips Medical Systems Inc., Cleveland, OH, USA) using a low-dose protocol (contiguous 1 mm slices acquired at 90 kVp, 32 mA, 1 sec rotation time; effective radiation dose <0.05 mSv) with a solid mineral reference phantom for density calibration (Model 3 CT Calibration Phantom, Mindways Software, Inc., Austin, TX, USA). Bone geometric properties (cortical bone area, cross-sectional area, cortical thickness, and moments of inertia) were measured at the mid-diaphysis (50% of bone length); cross-sectional area, cancellous density, and density-weighted area were measured in the proximal (13% of bone length) and distal (90% of bone length) metaphyses [2]. The children with CP were grouped by Gross Motor Function Classification System (GMFCS) level, where GMFCS I (n=16) is independently ambulatory on all surfaces, GMFCS II (n=14) is independently ambulatory with difficulty on uneven terrain, and GMFCS III (n=3) is ambulatory with assistive devices (walker or crutches) [3]. Bone properties were compared among each GMFCS level and controls using linear mixed effects models with sex and age as covariates.

Results and Discussion

In the diaphysis, cortical bone area and moments of inertia were lower in all CP groups compared with controls ($p \leq 0.04$, Fig. 1). Cortical thickness was also lower in the CP groups, but the difference was statistically significant for GMFCS II and III only ($p \leq 0.004$). In the proximal metaphysis, density-weighted area was lower in all CP groups compared with controls ($p \leq 0.08$) due to smaller cross-sectional area in all groups ($p \leq 0.05$) and lower cancellous density in GMFCS II and III ($p=0.02$). However, in the distal metaphysis only GMFCS III had lower density-weighted area than controls ($p=0.04$), primarily due to reduced cancellous density ($p=0.02$). Thus, most bone properties were reduced in ambulatory children with CP, even at GMFCS levels I and II, although bone deficits were greatest at GMFCS level III.

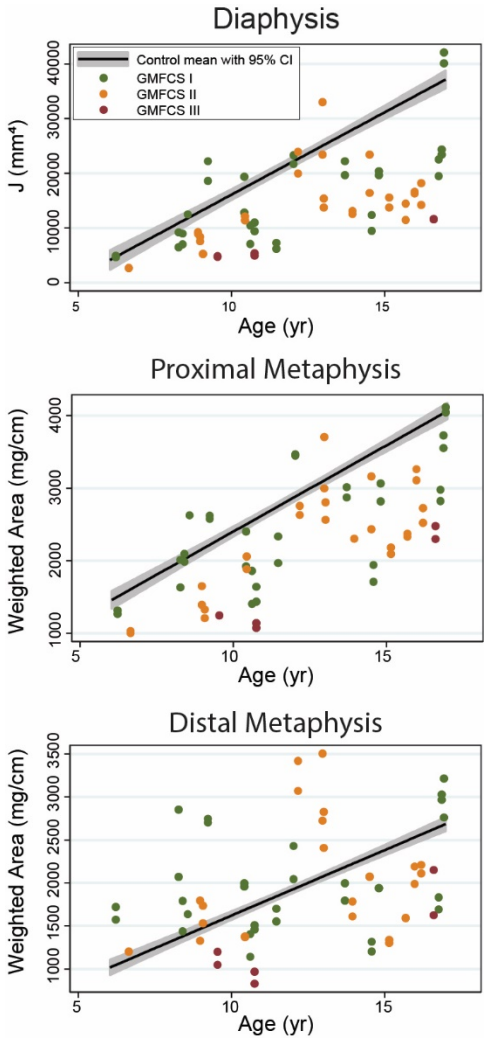

Figure 1: Comparison of groups for select bone properties. Black line and grey band indicate mean and 95% confidence interval for controls.

Significance

Our results indicate that even the most functional children with CP have reduced bone properties in the tibial diaphysis and proximal metaphysis, which may contribute to increased fracture risk. As expected, bone deficits are greater in less functional children. Children in GMFCS level III had reduced bone properties at all sites examined.

Acknowledgments

Funding provided by NIH-NICHD grants 5R01HD059826 and 1R01HD095456.

References

[1] Wren et al. Dev. Med. Child Neurol. (2011) 53: 137-41.
[2] Wren et al. J Bone Mineral Plus (2020) 4: e10427.
[3] Palisano et al. Dev. Med. Child Neurol. (2008) 50: 744-50.

REPEATED MEASURES CORRELATION BETWEEN ELBOW MOMENTS AND TORSO ANGLES IN YOUTH PITCHERS

Kristof Kipp[1], J. Howenstein, and M.B. Sabick
[1]Department of Physical Therapy – Program in Exercise Science, Marquette University, Milwaukee, WI, USA
E-mail: kristof.kipp@marquette.edu

Introduction

Elbow injuries are common in elite baseball players but are also becoming more common in youth players. To mitigate injuries, biomechanists often use correlational approaches to identify modifiable movement strategies that could decrease joint loading (2, 4). Baseball research has focused on the role of trunk motion in relation to upper body loading (3). However, most of this research averaged biomechanical variables across trials and used statistical methods focused on group-average comparisons, which may mask individual movement strategies in relation to elbow loading. The purpose of this study was to use repeated measures correlations to investigate the player-specific associations between torso angles and external elbow valgus net joint moments across repeated pitching trials.

Methods

Twenty-three little league players (range: 9-13 years, height: 1.55±0.12 m, body mass: 46.0±11.9 kg) were recruited and asked to throw up to 15 fastball pitches (22.9±3.2 $m \cdot s^{-1}$) at a strike zone 14 m away. Players wore 32 markers and 7 marker clusters while kinematic data were collected at 250 Hz (2). Two in-ground force plates recorded kinetic data at 1000 Hz. Kinematic and kinetic data were filtered with a 4th order zero-lag low-pass Butterworth filters at 14 and 300 Hz, respectively. Global torso angles were calculated from the thorax segment in accordance with best practice recommendations (5). An inverse dynamics procedure was used to calculate external net joint moments (NJM) at the elbow joint. NJM were normalized to body mass. Global torso angles around each of the cardinal axes were extracted at the instant of ball release. Peak external elbow valgus NJM were also extracted. Between eight and 15 trials from each pitcher were used for the analysis.

The associations between torso angles and elbow valgus NJM were investigated with repeated measures correlation (1), where the independent variables were torso flexion, lateral rotation, and axial rotation and the dependent variable was external elbow valgus NJM.

Results and Discussion

The repeated measures correlation analysis indicated that elbow valgus NJM was significantly correlated with torso flexion and lateral rotation angles at ball release (Table 1), which indicated that greater forward torso flexion and lateral rotation away from the throwing arm at ball release were both associated with greater elbow valgus NJM. Oyama et al. (3) noted that high school pitchers with excessive lateral torso rotation at ball release also exhibited greater elbow loading.

Table 1: Repeated measures correlation data for associations between absolute torso angles at instant of fastball pitch release and external elbow valgus net joint moment.

	r	95% CI	*p*-value
Flexion	-0.353	-0.454, -0.242	0.001
Lateral Rotation	-0.123	-0.241, -0.002	0.046
Axial Rotation	-0.029	-0.150, -0.093	0.641

Significance

Two of the three global torso angles at ball release were associated with elbow valgus NJM. Importantly, these associations were consistent across pitching trials of individual players, which provides strong evidence that torso position at ball release may be an important determinant of elbow loading in youth players. Future research should investigate if instruction to alter torso angles attenuates elbow loading.

References

1. Bakdash JZ & Marusich LR. *Front Psych* **8**, 456, 2017.
2. Howenstein J et al. *Med Sci Sports Exerc* **51**, 523-531, 2019.
3. Oyama S et al. *Am J Sports Med* **41**, 2430-2438, 2013.
4. Sabick MB et al. *J Should Elb Surg* **13**, 349-355, 2004.
5. Wu et al. *J Biomech* **38**, 981-922, 2005.

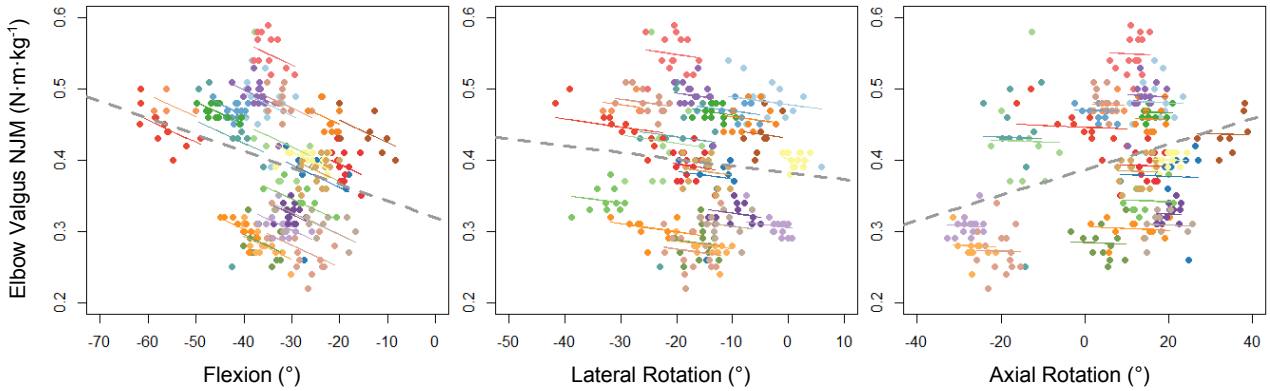

Figure 1: Repeated measures correlations between absolute torso angles (°) at instant of ball release and external elbow valgus net joint moment (NJM: $N \cdot m \cdot kg^{-1}$) for 24 little league players.

ASSESSMENT OF DYNAMIC STRENGTH INDEX IN ELITE PARA-ATHLETES

April L. McPherson[1], L. Benson[1,2], S. Gardner[1], K. Wittman[1], and D. Taylor[1]
[1]United States Olympic and Paralympic Committee, Colorado Springs, CO
email: April.mcpherson@usoc.org

Introduction

Dynamic strength index (DSI), also referred to as the dynamic strength deficit, is a method used by strength and conditioning staff to provide greater insight into an athlete's training status and ability to express force production. This is calculated as a ratio of ballistic peak force (PF), most commonly from a countermovement jump (CMJ) or squat jump (SJ) compared to PF during an isometric mid-thigh pull (IMTP). With high reliability and low variability, this assessment provides a unique method to understand and prescribe individualized training plans. It has been suggested that training should focus on ballistic and plyometric force production when DSI is low (<0.6), and maximal strength production when DSI is high (>0.8).[1]

Previous investigation of DSI in healthy athletes demonstrated that DSI-CMJ was a more reliable measure than DSI-SJ, but the ratios were similar.[2] However, it is unknown how neural impairment affects the nature of this ratio and the relationship between the two calculation methods. Therefore, the purpose of this preliminary analysis was to determine if the DSI ratio calculated using CMJ and SJ were similar in para-athletes with neurological impairments. It was hypothesized that DSI-CMJ would be less than DSI-SJ due to the presence of neurological impairment and the inability to express dynamic force.

Methods

Two para-athletes with neurological impairments completed force plate testing, which included IMTP, CMJ, and SJ tasks. The IMTP was performed on two in-ground force plates (AMTI; Watertown, MA). For IMTP testing, a standard 20 kg weightlifting bar was affixed on a squat rack with pins positioned and locked consistently between trials. The athletes assumed a self-selected position where the stationary bar was aligned with their mid-thigh, with knee angle between 125-145° and hip angle 140-150°. Athletes were instructed to pull the bar against the pins as hard as possible and hold for five seconds. Two trials were completed. For CMJ testing, athletes stood on the force plates and were instructed to squat and immediately jump as high as possible. For SJ testing, athletes were instructed to hold the bottom of a squat position for three seconds before jumping as high as possible. Three repetitions were performed for each jump task.

Raw force-time data were analyzed using both Noraxon (Noraxon, U.S.A., Inc., Scottsdale, AZ) and custom software. Peak force during each trial was obtained, and maximum PF between all trials for each test day was used for analysis. One athlete had three test days and the other athlete had two test days.

Results and Discussion

Similar to previous studies, PF was higher for IMTP than during jump movements (**Table 1**). Interestingly, for four of the five test days PF was higher for SJ than CMJ, which was unexpected due to the stretch-shortening cycle involved with CMJ. Despite the trend toward greater DSI-SJ values than DSI-CMJ, in accordance with previous research the ratios were similar between the two methods of calculation, R^2=0.933 (**Fig. 1**).

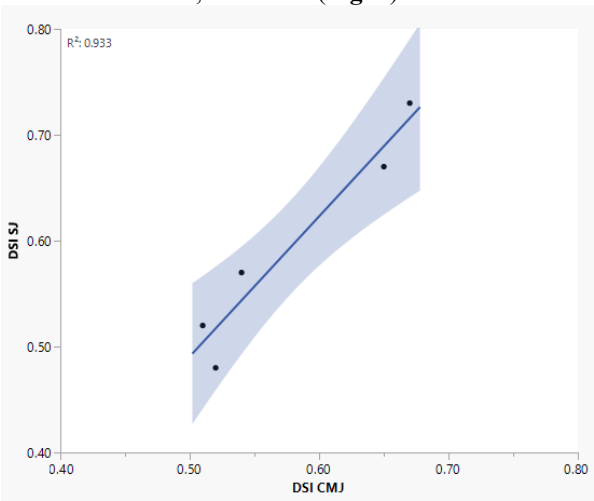

Figure 1: Relationship between DSI-CMJ and DSI-SJ.

Practical individualized training plan recommendations (i.e., focus on strength training when DSI >0.8 or ballistic training when DSI <0.6) did not differ between jump types for either athlete on any of the testing dates.

Significance

This study begins to explore if a neurological impairment affects training recommendations based on DSI. Future work could assess if different impairment types (e.g., visual, neurological, amputation) influence DSI calculated by different methods. Use of the DSI may help to inform coaches and clinicians who work with para-athletes assess their dynamic force production capabilities in a sport-specific manner and assess training adaptations.

References

[1] Sheppard, J. (2011) *J Aus Str & Cond*. **19(2):** 4-10.
[2] Comfort, P. (2018) *Int J Sports Phsyiol and Perf.* **13(3)**: 320-325.

Table 1: Maximum Peak Force Values (N), and Resultant Dynamic Strength Index ratios

Athlete	Test Day	SJ PF (N)	CMJ PF (N)	IMTP PF (N)		DSI SJ	DSI CMJ
1	1	1730	1666	2565		0.67	0.65
1	2	1925	1765	2622		0.73	0.67
1	3	1767	1904	3661		0.48	0.52
2	1	1933	1914	3738		0.52	0.51
2	2	1981	1880	3502		0.57	0.54

TRUNK KINEMATICS AND LOWER EXTREMITY MUSCLE ACTIVATION EFFECTS ON POSTURAL STABILITY DURING STAND-TO-SIT IN YOUNGER AND OLDER ADULTS

Woohyoung Jeon*[1], Jill Whitall[1], and Lisa Griffin[2], and Kelly Westlake[1]
[1]Department of Physical Therapy & Rehabilitation Science, University of Maryland School of Medicine, Baltimore, MD, USA
[2]Department of Kinesiology and Health Education, University of Texas at Austin, Austin, TX, USA
Email: *wjeon@som.umaryland.edu

Introduction

Stand-to-sit (StandTS) movement is an important functional daily activity. Performing a StandTS task can be challenging for older adults due to age-related changes in neuromotor control [1]. Although trunk flexion and eccentric contraction of the rectus femoris (RF) muscle are important during StandTS, the effects of aging on these and related outcomes are not well studied. Thus, the purpose of this study was to investigate the differences in trunk flexion, RF muscle activation pattern, and postural stability between young and older adults, and to identify the relationship between trunk flexion and eccentric RF muscle activation with postural stability.

Methods

Ten younger and ten older healthy adults were compared during three StandTS trials performed at a self-selected speed. Outcomes included peak amplitude, peak timing, and burst duration of electromyography (EMG) activity of the RF muscle, trunk flexion angle and angular velocity, whole body center of mass (CoM) displacement, center of pressure (CoP) velocity, and ground reaction force (GRF).

Results and Discussion

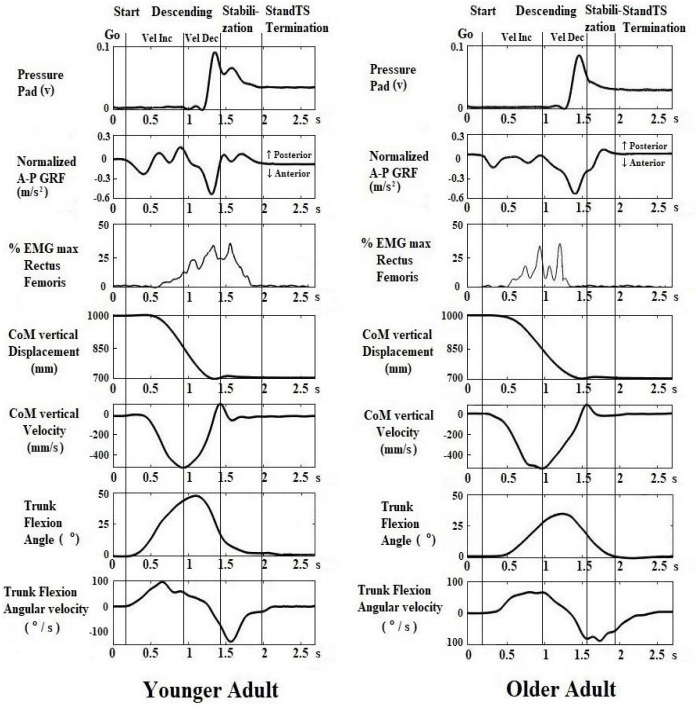

Figure 1 : Trunk and whole body CoM kinematics and normalized EMG activity of the RF muscle from a representative younger and older adult during StandTS. "0 s" represents "Go" signal. Vel Inc / Dec : Vertical CoM velocity increment / decrement. v:voltage, s:second

Compared to young adults, older adults demonstrated shorter RF EMG burst duration and reduced trunk flexion (**Figure 1**). Older adults also demonstrated reduced stability as indicated by a longer duration in which CoM was maintained beyond the posterior limit of the base of support (BoS), greater mean anterior-posterior CoP velocity and larger standard deviation of CoM vertical acceleration during StandTS with smaller vertical GRF before the StandTS termination.

A significant correlation of trunk flexion angle and EMG burst duration of the RF muscle with the duration in which the CoM stayed within the BoS was also found (**Figure 2**). There were no age-related differences in weight-bearing symmetry, StandTS speed, and trunk flexion angular velocity.

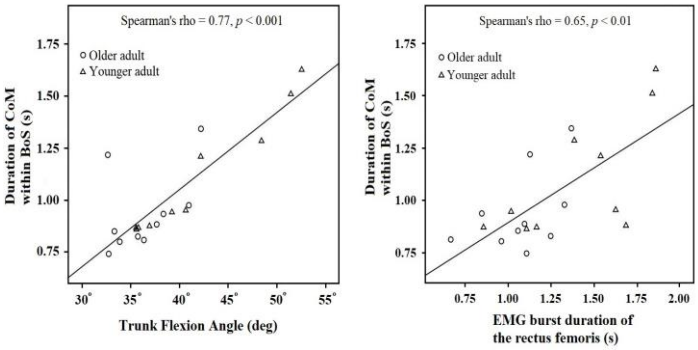

Figure 2 : Correlation between maximum trunk flexion angle (left) / EMG burst duration of RF (right) and duration in which CoM remained within the BoS during StandTS.

With greater trunk flexion, the CoM moves towards the anterior border of the BoS at the start of StandTS, which enables the CoM to maintain its position longer in the BoS area throughout StandTS. Reduced eccentric RF burst duration in older adults leads to a lack of descending control and reduced postural stability in combination with their decreased trunk flexion.

Significance

In older adults, StandTS assessments and training that focused on trunk flexion and maintaining eccentric RF control should be part of a comprehensive balance intervention. Currently, timed Sit-to-Stand assessments neglect the importance of a controlled StandTS to improve accuracy and safety.

Acknowledgements

Woohyoung Jeon is supported by the University of Maryland Advanced Neuromotor Rehabilitation Research Training (UMANRRT) post-doctoral program (NIDILRR 90AR5028).

Reference

[1] S.R. Chang, R. Kobetic, R.J. Triolo, Understanding stand-to-sit maneuver: Implications for motor system neuroprostheses after paralysis, J. Rehabil. Res. Dev. 51 (2014) 1339 - 1352

BIOMECHANICAL VARIABLES SHOULD BE INCLUDED IN ANALYSES OF ARTHROPLASTY REGISTRY DATA

Richard E. Hughes, Huiyong Zheng, Brian R. Hallstrom
[1]University of Michigan
email: rehughes@umich.edu

Introduction

Arthroplasty registries are important sources of knowledge about implant revision risk in elective total hip replacement (THA). Many registries release annual report that report risk of revision by implant name, allowing surgeons and patients to make informed decision about implant selection. Most report raw cumulative percent revision (CPR) post-operatively, but some also report age and sex-adjusted hazard ratios based on Cox proportional-hazards modeling. In the last thirty years, investigators in epidemiology and biostatistics [1] have developed analytical tools for selecting covariates to include in statistical models to enhance causal inference. While these methods do not solve the problem of gaining causal knowledge from observational data, they can substantially reduce bias of the statistical estimates of model parameters. Greenland *et al*. [1] propose the concept of a "sufficient set adjustment variables" that is required given a specified causal model.

The purpose of this project was to use modern methods in causal inference to determine if adjustment for age and sex is sufficient to estimate the relationship between implant and revision without bias. We hypothesize that age and sex are an insufficient adjustment set given current knowledge of the biomechanical causes of revision, and additional biomechanical variables must also be included in registry analyses of THA revision risk.

Methods

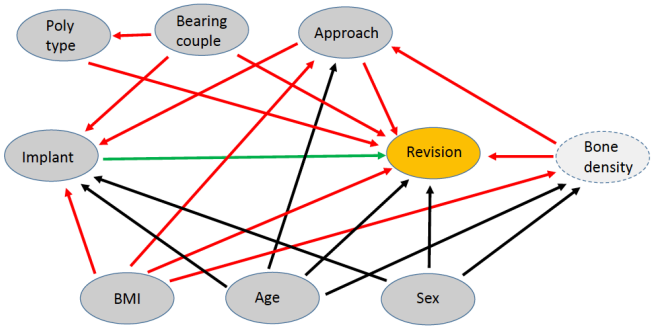

Figure 1: Directed acyclic graph (DAG) showing the unblocked backdoor paths with only *Age* and *Sex* are included as adjustment variables. Open paths are depicted in red. The direct causal relationship to be estimated is in green.

Causal inference methods require creating a causal model relating exposure to outcome and representing that model as a directed acyclic graph (DAG). Each node in the DAG represents a variable (indicated in *italics*), and each directed edge indicates a causal relationship between two variables. Absence of an edge represents statistical independence. Figure 1 shows a DAG created based on biomechanical and clinical knowledge. The exposure is the choice of *Implant* and the outcome is *Revision*. Note *Bone density* is a latent variable (i.e. shown in lighter gray) because it is not typically recorded in arthroplasty registries.

The requirement for unbiased estimation of the parameter representing the true causal relationship between *Implant* and *Revision* is that all "backdoor" paths from exposure to outcome are blocked by a variable in the adjustment set. A backdoor path is an undirected path connecting the exposure to outcome AND has an edge directed into the exposure. For example, the path *Implant*←*Age* → *Revision* is a backdoor path. Adding *Age* to the adjustment set blocks that path. DAGitty software was used to conduct the analysis of open and closed backdoor paths given adjustment sets.

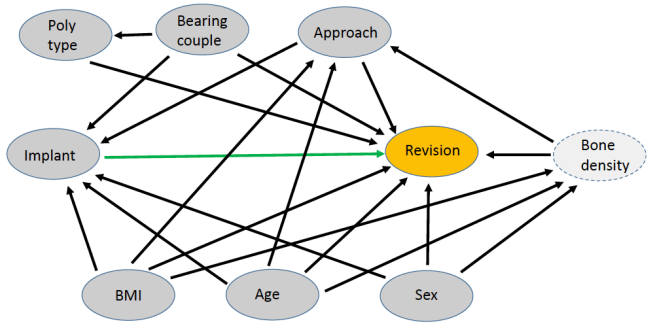

Figure 2: Directed acyclic graph shows all backdoor paths are blocked when *BMI*, *Sex*, *Age*, *Approach*, and *Bearing Couple* are included as adjustment variables.

Results and Discussion

The analysis showed that adjusting for only age and sex leaves many backdoor paths open (Figure 1). Adding *Approach*, *BMI*, and *Bearing Couple* closes all backdoor paths (Figure 2). A very notable property of Figure 2 is that all backdoor paths passing through *Bone density* are also closed by this adjustment set. This means that *Bone density* does not have to be in the adjustment set, which is very fortunate because it is not typically collected by arthroplasty registries.

Significance

This analysis indicates the sufficient set of adjustment variables for analysing the effect of implant on revision should include biomechanical variables, *Bearing Couple and BMI*, in addition to *Age*, *Sex*, and *Approach*.

Acknowledgements

Financial support was received from the Value Partnerships Program of Blue Cross Blue Shield of Michigan/Blue Care Network.

References

1. Greenland, S., J. Pearl, and J.M. Robins, *Causal diagrams for epidemiologic research.* Epidemiology, 1999. **10**(1): p. 37-48.

ROTATIONAL INERTIA AND PRINCIPAL AXES OF ROTATION DURING DANCE PIROUETTES

Melanie B. Lott
Denison University, Department of Physics & Astronomy, Granville, Ohio
email: *lottm@denison.edu

Introduction

Distribution of body mass around axes of rotation (rotational inertia) affects the kinematics and dynamics of turns, including those performed in dance.[1] When rotation is around a principal axis (e.g., the symmetry axis of a top), the angular momentum and angular velocity vectors are parallel, and the rotating mass system is considered to be dynamically balanced in mechanics. Otherwise, the rotation axis experiences a "wobble" effect. For asymmetric objects (e.g., dancers), a principal axis may not extend through the point of support and center of mass (CoM), so static and dynamic balance conditions might not be met simultaneously. Principal moments of inertia and principal axes have yet to be studied with respect to balance during dance turns.

This study investigated two hypotheses: (1) Two of the three principal moments of inertia are equal during ballet pirouettes as predicted by a prior theoretical analysis,[2] and (2) Successful pirouettes have closer alignment between the spin principal axis, CoM, and point of support than unsuccessful pirouettes.

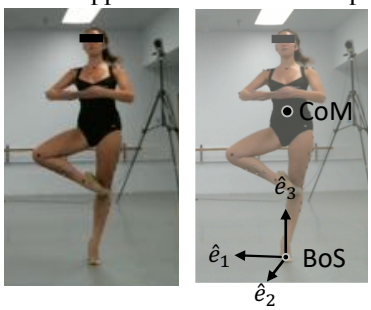

Figure 1: Dancer performing a pirouette in retiré position. Principal axes ($\hat{e}_1, \hat{e}_2, \hat{e}_3$) are defined with their origin at the base of support center.

Methods

Six advanced, injury-free, female dancers (age: 20 ± 5 yr; mass: 54 ± 3 kg; height: 164 ± 6 cm; dance training: 17 ± 5 yr) gave informed consent and performed triple-turn, en dehors ballet pirouettes in the IRB approved study (Fig.1). A 6-camera, Qualisys motion capture system (100 Hz) tracked a full body reflective marker set to determine positions and orientations of fourteen body segments. De Leva's segment inertial properties[3] were used to compute the CoM and whole-body inertia tensor relative to an origin at the base of support (BoS). The centroid of the BoS was found using three markers: the first metatarsus head, fifth metatarsus head, and great toe distal phalanx. Eigenvalues and eigenvectors of the inertia tensor determined the principal moments of inertia (I_1, I_2, I_3), the principal axes of rotation ($\hat{e}_1$, $\hat{e}_2$, $\hat{e}_3$), and their evolution throughout the pirouettes. The angle (θ) between the spin principal axis ($\hat{e}_3$) and the vertical ($\hat{z}$) were found from the scalar product: $\cos\theta = \hat{e}_3 \cdot \hat{z}$. The scalar product was also used to determine the angle between the vertical and a vector extending from the BoS centroid to the CoM.

Results and Discussion

While pirouette position (retiré) is not bilaterally symmetric, I_1 and I_2 ("topple" moments of inertia) were equal as hypothesized and as expected for rotationally symmetric objects (Table 1).

Table 1: Average moments of inertia (all in kg-m^2) around the three principal axes, $\hat{e}_1$, $\hat{e}_2$, and $\hat{e}_3$.

Dancer	I_1	I_2	I_3
A	49.8 ± 1.5	49.8 ± 1.5	1.32 ± 0.05
B	59.0 ± 0.3	59.0 ± 0.3	1.39 ± 0.03
C	60.5 ± 0.2	60.4 ± 0.2	1.51 ± 0.02
D	61.6 ± 0.2	61.6 ± 0.2	1.49 ± 0.03
E	62.2 ± 1.7	62.1 ± 1.7	1.44 ± 0.05
F	63.1 ± 0.4	63.0 ± 0.4	1.50 ± 0.04

Dynamic variations in inertia were measured, consistent with subtle body position adjustments during pirouettes,[4] and I_1 and I_2 remained equal as their values fluctuated over time.

The "spin" moment of inertia (I_3) often decreased slightly with time, consistent with a tightening mass distribution around the spin axis during pirouettes. The third principal axis ($\hat{e}_3$) was aligned closely with the BoS-CoM line, and its direction varied with respect to the vertical throughout the turns. Figure 2 shows that the angles between $\hat{e}_3$ and the vertical and between the BoS-CoM line and the vertical were nearly equal for all dancers and trials, refuting the second hypothesis that successful pirouettes would have closer alignment between $\hat{e}_3$ and the BoS-CoM line than unsuccessful pirouettes. These results indicate that the mass distribution in pirouette retiré position is conducive to meeting both the static and dynamic balance conditions simultaneously.

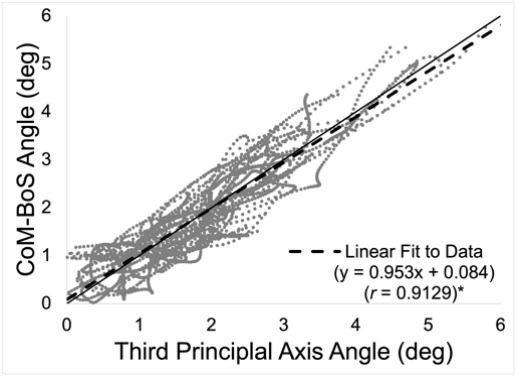

Figure 2: Highly significant (*p < .001) positive correlation between CoM-BoS and $\hat{e}_3$ angles (with respect to the vertical), and slope close to 1 (solid line shows y = x). Data include all dancers, trials, and times.

Significance

The "topple" inertia results ($I_1 = I_2$) indicate a certain symmetry or lack of preferred direction of topple in pirouettes; however, this analysis based on body configuration does not consider other essential factors such as how the pirouette's initiation or muscle strength imbalances may affect direction of topple. Turns in other body configurations (e.g., arabesque, à la seconde) may not have as close alignment between $\hat{e}_3$ and the BoS-CoM line, which may lead to pedagogical implications distinguishing how static balance versus dynamic balance in those positions are taught.

References

[1] Kim, et al. (2014), *Sports Biomech* **13**, 215-229.
[2] Lott & Laws (2012), *J Dance Med Sci* **16**, 167-174.
[3] De Leva (1996), *J Biomech* **29**, 1223-1230.
[4] Lott & Xu (2020), *J Appl Biomech* **36**, 103-112.

GAIT EFFECT ASSESMENT OF ORTHOTIC SHOES ON DIABETIC PERIPHERAL NEUROPATHY PATIENTS

Phuoc Nguyen, Mary C. Spires, James Leonard, and Lauro V. Ojeda*
The University of Michigan
email: *lojeda@umich.edu

Introduction

Type II diabetes is a widespread disorder affecting many people in the United States. One of the most common complications of this disorder is distal symmetric diabetic peripheral polyneuropathy (DPN) commonly involving the feet of patients [1]. This complication can result in severe symptoms including numbness or loss of sensation and pain in the feet. DPN frequently results in altered foot posture and mechanics leading to gait alteration from abnormal pressures placed on the foot tissues. DPN also places the diabetic patient at much higher risk of foot ulcer development. Extra-depth (orthopedic) shoes and use of custom orthotic insoles have been traditionally used as a preventive measure and a treatment reducing foot complications associated with DPN [2-3], however their effectiveness at mobility improvement have not been quantitatively addressed. By using inertial measurement units (IMUs), this research aims to quantitatively study the immediate effects of orthotic interventions on the mobility of DPN patients. We hypothesized that the two orthotic interventions employed, that is extra depth shoes and extra depth shoes with custom insert, might increase the stride length and speed compared to the patients' preferred shoes during self-selected normal walking. We also expected that the use of extra-depth shoes together with custom fabricated insoles for each subject would outperform the use of the extra-depth shoes only.

Methods

Seven participants (1F, 6M, age 68.1/2.3 years mean/std) who were diagnosed with Type II diabetes mellitus (≥2 years), DPN (≥1 year), and BMI of 24-30 kg/m^2. None of them had a history of previous use of prescription orthotic footwear. The University of Michigan IRB approved the study and all subjects provided informed consent. Participants were tested in clinic wearing their preferred (regular daily) shoes and with each of the footwear interventions. During our tests, participants were asked to walk a 75-foot hallway 10 times at comfortable (normal, self-selected) speed. During these tests, we collected IMU sensor data (accelerations and angular rates) using data loggers (GT9X, ActiGraph) attached to their shoes. We collected data with the participants wearing their normal shoes (regular daily), prescribed extra-depth shoes and extra-depth shoes fitted with custom insoles. For the prescription shoes, we collected data a week after participants wore the shoes for a week (break in or adjustment period). Estimated foot trajectories and timing were derived from the IMU sensor data using a previously validated method [4]. Using the foot trajectories, we determined individual stride and timing information and computed stride speed and length [5]. In addition, we analyzed the left and right foot strides assuming they were symmetric. For each participant, a two-sample t-test was used to determine statistically significant difference between the means of the interested parameter across the three different shoe options.

Results and Discussion

The clearest outcome shows that participants walked faster (statistically significant difference) (Fig. 1-left) when wearing extra-depth shoes (6 out of 7, 5.0 cm/s or 4.1% mean increase), or the custom insert (5 out of 7, 7.5 cm/s or 6.4% mean increase), compared to their normal shoes. When comparing extra-depth shoes and the use of custom insoles, the results are not that obvious since some patients exhibited higher speed when wearing custom insoles while others saw the opposite effect (4 out of 7, 3.2 cm/s or 2.5% mean increase; 2 out of 7, 5.8 cm/s or 4.5% mean decrease). Analysis of stride length (Fig. 1-right) showed a similar trend as the case of speed. Most patients exhibited longer strides when wearing extra-depth shoes (5 out of 7, 4.5 cm or 3.9% mean increase), and to a lesser degree using the custom insert (4 out of 7, 7.3 cm or 6.2% mean increase). As in the case of the stride length, the outcome is not conclusive when comparing extra-depth shoes against custom insoles (4 out of 7, 2.8 cm or 2.2% mean increase; 2 out of 7, 4.4 cm or 3.0% mean decrease).

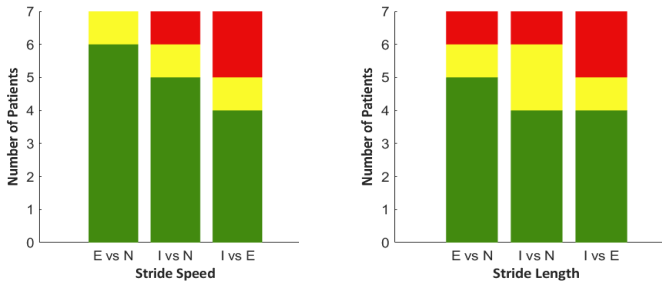

Figure 1: Comparison of stride speed (left), stride length (right). Results indicate statistical significance difference across the three types of shoe options (N=normal, E=extra-depth, I=extra-depth and custom insert). Color codes indicate direction change (green=increase, yellow=no change, red=decrease).

As we have predicted we observed an increase of the stride length and speed of patients with either orthotic intervention or shoe interventions, yet the use of custom-made inserts did not seem to outperform the use of commercial extra depth shoes in any parameters. We also must acknowledge that it is possible that patients overexert themselves when walking in new shoes under the psychological influence that these shoes can help their problems or their desire to perform well to please the researchers. Improved or better ambulation in a clinic setting as opposed to that in the everyday "real" world is an observed and well recognized phenomenon seen in patients in the clinic by practicing clinicians. Thus, these results must be further tested and verified under a longer period of testing and more importantly with a larger sample size.

Acknowledgments

This research was supported by the BCBSM Foundation under Grant# 002195.II

References

1. Alavi et al., J Am Acad Dermatol, 70(1): 1.e1-18, 2013.
2. Lázaro-Martínez et al., Int J Low Ext W, 13(4): 294-319, 2014.
3. Mayfield et al., Diabetes Care, 21(12), 2161-2177,1998
4. Ojeda and Borenstein, J of Nav, 60(3): 391-407, 2007.
5. Rebula et al., Gait Posture, 38(4): 974-980, 2013

CLASSIFICATION OF COUNTERMOVEMENT JUMP EFFORT FROM GROUND REACTION FORCE TIME-SERIES DATA

Michael H. Haischer[1], T. Smith[2], M. Smith[2], and K. Kipp[1]
[1]Department of Physical Therapy – Program in Exercise Science, Marquette University, Milwaukee, WI
[2]Department of Intercollegiate Athletics, Marquette University, Milwaukee, WI
email: michael.haischer@marquette.edu

Introduction

The countermovement jump (CMJ) is one of the most common tests used to monitor neuromuscular status among athletes[1]. However, ensuring that athletes are producing maximal effort during testing can present a challenge. CMJ assessments often use force plates to record ground reaction force (GRF) time-series data. Classification of effort level during CMJ may be possible with machine learning methods, such as artificial neural networks (ANN). The purpose of this study was to investigate the ability of an ANN to classify three different CMJ effort levels based on GRF time-series data.

Methods

Twenty NCAA Division I basketball players (8 males, 12 females) performed up to three CMJ trials at three different perceived levels of effort (i.e., low, medium, high). GRF data were collected from two force plates at 1000 Hz, and filtered with a cut-off frequency of 50 Hz, which was based on residual analyses. Right and left GRF data were summed into a single vector, and time-normalized to 101 data points (Figure 1).

A classification ANN was constructed with the pattern recognition app in the MATLAB neural network toolbox. The data set included 170 jumps, and the input to the ANN was therefore a 170x101 matrix. The target data consisted of 170x3 matrix that represented the three different effort levels. The ANN included one hidden layer with five neurons and was trained with scaled conjugate gradient backpropagation. The ANN was trained with data from nineteen randomly chosen athletes and tested with data from one athlete (Table 1). Performance of the ANN was assessed via classification accuracy and cross-entropy.

Table 1: Mean ± SD CMJ height (cm) across efforts.

	Low	Medium	High
Training Data	25.1 ± 5.4	30.0 ± 5.1	35.8 ± 5.8
Testing Data	23.5 ± 10.3	34.4 ± 4.0	48.3 ± 0.4

Results and Discussion

The trained ANN classified CMJ trials with 99.4% accuracy (cross-entropy error = 0.07). Data from the hold-out test subject was classified with 88.9% accuracy (cross-entropy error = 14.70). Specifically, all three of the test subject's high effort CMJ were correctly classified, and no medium or low effort jumps were incorrectly classified as high effort. However, one of the test subject's medium effort jumps was misclassified as low effort.

The results of this study indicate that the trained ANN can accurately distinguish between maximal and submaximal effort levels of the CMJ. Although there was one misclassification, it should be noted that it is more important that all high effort jumps are correctly classified, and that no sub-maximal effort jumps were misclassified as high effort, since both would be reasons for concern as the major goal is to be able to identify whether a specific CMJ trial reflects maximal effort during testing. An explanation for the misclassification among the sub-maximal effort CMJ may be that the CMJ height during the medium and low effort trials was not explicitly controlled. This lack of control may also indicate that athletes had problems consistently producing medium and low efforts. Thus, the ANN may have difficulty classifying CMJ trials among these two categories.

The GRF curves of high effort CMJ are characterized by greater rate of force development, an earlier GRF peak, and a more sustained GRF plateau (Figure 1). It is questionable if CMJ effort level could be distinguished based solely on discrete peak GRF. While it remains to be determined how classification accuracy changes over time, with more varied input data, or with athlete-specific changes (e.g., with fatigue), the current findings hold promise to be useful to practitioners who regularly monitor CMJ and are interested in ensuring a consistent effort across test sessions. Classification of CMJ in the context of within-athlete or case-study designs warrants consideration in future research as between-athlete differences in jump strategies[2-4] may limit the predictive capabilities of ANN trained on more heterogeneous groups as in the current study.

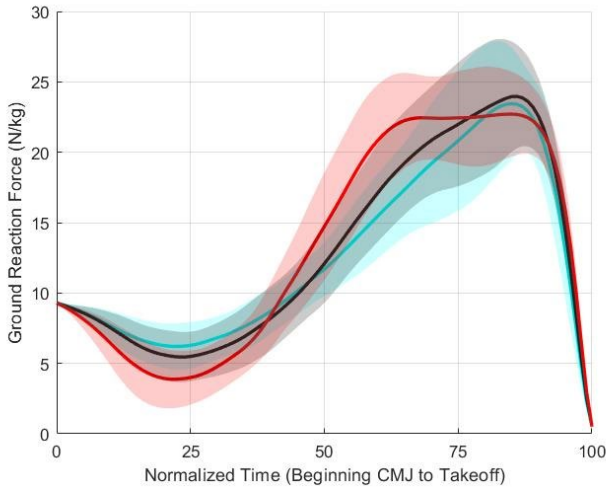

Figure 1: Ensemble mean and standard deviation time-normalized ground reaction force time-series data for three efforts of countermovement jump (Blue: Low, Black: Medium, Red: High).

Significance

Classification of GRF data based on effort would be useful to ensure consistent effort in testing. We showed that a trained ANN is capable of this type of classification and demonstrated its efficacy across three CMJ effort levels in collegiate basketball players. The outlined approach may have broad applications in sports science testing and research where time-series GRF data often reflect key performance indicators of sporting activities.

References

[1]Claudino et al., 2017. J Sci Med Sport 20: 397–402.
[2]Cormie et al, 2009. J Strength Cond Res 23: 177–186.
[3]Kipp et al., 2020. J Sports Sci 38: 652–657.
[4]Wu et al., 2019. PLoS One 14: e0219295.

TARGETED HAMSTRINGS TRAINING EFFECTS ON MUSCLE STIFFNESS IN YOUNG BASKETBALL ATHLETES

Nathaniel A. Bates[1], Takashi Nagai[1], Luca Rigamonti[1], Ryo Ueno[1], Nathan D. Schilaty[1]
[1]Department of Orthopedic Surgery, Mayo Clinic, Rochester, MN, USA
email: batesna@gmail.com

Introduction

Targeted neuromuscular training (TNMT) has been shown to effectively reduce non-contact musculoskeletal injuries [1]. Hamstrings muscle (HAM) strains are prevalent non-contact injuries among basketball athletes [2]. Recently, ultrasound shear wave elastography (SWE) technology has been developed that noninvasively assesses stiffness of soft tissues [3]. Accordingly, the objective of this abstract was to use SWE to assess differences in HAM stiffness before and after TNMT.

Methods

206 lower extremities from 103 high school basketball athletes were examined through pre- and post-season SWE imaging over a 3-year period. Athletes were assigned to Control (22, year 1) or TNMT groups (81, years 2 & 3) based on year of accrual. The TNMT group completed a 15-minute warm-up twice a week for the duration of their basketball season. This warm-up incorporated bodyweight activities designed to activate the HAM musculature, including acceleration tasks, reverse HAM curls, and plyometrics. The Control group received no additional training to their normal basketball activities. Before and after the season, each subject was maneuvered through a range of passive lower extremity flexion by a clinician. A GE Logiq E9 ultrasound was used to assess SWE stiffness of the HAM at three points along their flexibility pathway (80%, 60%, and 40% of maximal 90/90 extension orientation). Three SWE images were taken at each location and averaged into a subject mean. A 2x2 ANOVA of Intervention (TNMT, Control) vs. Time (Pre-, Post-Season) was used to assess for statistical differences. Individual differences within groups were assessed via Student's t-test. Significance was set at $\alpha < 0.05$.

Results and Discussion

HAM stiffness was greater at 60% and 80% of peak flexibility than at 40%. This indicates that the athletes place greater stress on their HAM musculature as they approach the boundaries of their passive flexibility.

Intervention was a significant factor at the 80% and 60% flexibility orientation ($p \leq 0.01$), but not at the 40% orientation ($p = 0.12$). Time was not a significant factor for the whole dataset ($p \geq 0.28$). However, within the TNMT group, Time was significant for the 80% and 60% orientation ($p \leq 0.05$) and approached significance for the 40% orientation ($p = 0.09$). In all cases, the TNMT exhibited a decrease in HAM stiffness from pre-season to post-season testing (Table 1, Figure 1). Pre-season HAM stiffness was higher in TNMT subjects than Controls. However, as no training had been enacted prior to the season, the rationale for this baseline difference remains to be determined.

Table 1: SWE stiffness of HAM (mean ± std) by Intervention and Time

Flexibility	TNMT		Control	
	Pre	Post	Pre	Post
80%	69.4 ± 35.4	62.0 ± 33.4	43.3 ± 31.4	45.5 ± 29.4
60%	67.7 ± 32.4	60.2 ± 33.4	54.3 ± 31.3	53.5 ± 34.4
40%	56.1 ± 29.4	50.8 ± 27.3	48.8 ± 25.7	47.9 ± 25.9

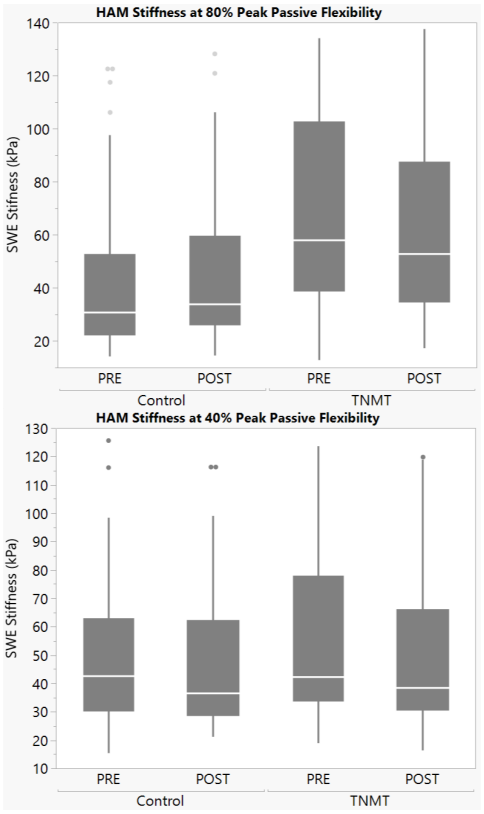

Figure 1: HAM stiffness at 80% of peak passive flexion (top) and 40% of peak passive flexion (bottom). TNMT reduced HAM stiffness at the 80% orientation, but exhibited no effect at 40%.

The present data indicates that a TNMT HAM warm-up program is likely to decrease HAM stiffness in lower extremity orientations associated with elevated HAM stress. As such, dynamic warm-ups targeted to specific muscle groups may prove efficacious to soft-tissue injury prevention during athletic participation. This entire project witnessed 225 Control athletes suffer 3 HAM injuries, while 96 TNMT athletes suffered 0 HAM injuries. Decreased passive HAM stiffness may be associated with decreased risk of HAM strain.

Significance

HAM injuries are prevalent in basketball. TNMT can reduce HAM muscle stiffness across a basketball season and therefore, is likely efficacious in muscular injury prevention of. These concepts can be extrapolated across sports and muscle groups to target prevention toward sport-specific injury mechanisms.

Acknowledgments

NBA / GE Collaborative Grant; NIH NIAMS R01-AR055563 & L30-AR070273; NIH NICHD K12-HD065987; Foderaro-Quattrone Grant for AI Innovation in Orthopedic Surgery

References

[1] Hewett TE, et al. Am J Sports Med. 2017;45(9):2142-7
[2] Dalton SL, et al. Am J Sports Med. 2015;43(11):2671-9
[3] McPherson AL, et al. Skeletal Radiol. 2020;49(8):1231-7

IMPACT OF INDUCED GAIT ASYMMETRY ON KNEE JOINT REACTION FORCES

*Emily M McCain[1], Michael D Lewek[2], and Gregory S Sawicki[3], Katherine R Saul[1]
[1]Department of Mechanical Engineering, North Carolina State University, Raleigh, NC, USA
[2]Division of Physical Therapy, University of North Carolina at Chapel Hill, Chapel Hill, NC, USA
[3]George W. Woodruff School of Mechanical Engineering, Georgia Institute of Technology, Atlanta, GA, USA
email: *emmccain@ncsu.edu

Introduction

Chronic injury- or disease-induced asymmetric gait deviations are metabolically costly and may precipitate changes in joint loading associated with joint pain and osteoarthritis [1]. Therefore, interventions often target restored gait symmetry to minimize harmful consequences of gait deviations. In many clinical populations, neurological and/or anatomical changes make isolating the impact of any specific gait deviation difficult. Our previous work employed ankle and knee bracing to impose limitations on joint range of motion (ROM) and induce asymmetric gait in unimpaired participants [2]. Here, we extend this work by conducting musculoskeletal simulations driven with experimental kinetics and kinematics and constrained by electromyography (EMG) to determine the interaction between induced asymmetry and knee joint reaction forces (KJRF). Our hypotheses are that (h1) asymmetric restrictions will result in increased KJRF loading rate and peak value on the ipsilateral (due to reduced knee compliance) and contralateral (due to asymmetric propulsion) limb when compared to unrestricted walking and (h2) changes in propulsive asymmetry will correlate with changes in contralateral KJRF loading rate.

Methods

Data were recorded on 8 (4M/4F) healthy controls walking at 0.8 ms^{-1} while a 3D printed ankle stays and knee bracing (DonJoy T-ROM) were used to restrict the ankle (r-ank), knee (r-knee), and combined ankle and knee (r-a+k) ROM; trials were compared to unrestricted (unr) walking where bracing was worn without restriction (T-ROM unlocked). We recorded ground reaction forces, kinematics, and EMG of 6 lower limb muscles bilaterally. Recorded marker locations were used to scale a lower limb adaptation of a full-body model to each participant [3]. Personalized models, experimentally determined kinematics, and GRFs were used with the computed muscle control (CMC) tool to determine simulated muscle activations guided by EMG-driven timing constraints [4]. A joint force analysis probe calculated KJRF along the long axis of the tibia. We normalized KJRF by body weight and averaged values across ten stance phases for each participant. The 1st peak KJRF was found as the maximum in the first 50% on stance phase, the KJRF loading rate was defined as the median gradient between heel strike and 1st Peak KJRF timing. Propulsive asymmetry was determined as the ratio of the max to the sum of peak anteriorly directed GRFs. A one-way repeated measures ANOVA performed in SAS was used to determine whether restriction type (unr, r-ank, r-knee, r-a+k) significantly affected outcomes. Post-hoc analysis t-tests with Bonferroni corrections for multiple comparisons were performed for significant factor levels. We determined significance of Pearson's linear correlations for comparisons with Δpropulsive asymmetry using a custom MATLAB script.

Results and Discussion

Our EMG-informed CMC simulations produced subject averaged KJRF profiles over stance phase (Fig 1a,b) within the range of values reported in literature [1]. We reject h1 because KJRF peak values and loading rates do not significantly *increase* on either limb when compared to the unr condition. Specifically, peak contralateral KJRF were not significantly affected, and ipsilateral peak KJRF values (Fig 1c) were significantly *reduced* in the r-ank condition when compared to the unr ($p=0.008$) and r-knee ($p=0.041$) conditions. While not significant ($p=0.2$), ipsilateral KJRF loading rate (Fig. 1d) tended to decrease with restriction in contrast to our hypothesis that reduced knee compliance would lead to increased KJRF. While ROM restriction did not significantly affect contralateral KJRF loading rate (Fig 1e), it tended to increase with knee restriction (r-knee, r-a+k) when compared to ankle restriction. Lastly, we observed a weak relationship between the ΔKJRF loading rate and Δpropulsive asymmetry ($r^2=0.25$; $p=0.01$) indicating additional factors may drive increases in KJRF load rate contralaterally.

Significance

Musculoskeletal simulations offer an opportunity for further decoupling of the interaction between gait deviations and the resulting changes in JRFs. Future work should investigate the impact of joint restriction on the hip and consider whether additional factors such as the limitation of compensatory degrees of freedom may explain the variance in the KJRF data.

Acknowledgments

NIH grant F31 HD097872-01 to EMM

References

[1] Nejad, I et al. (2020). Ann Biomed Eng 48 p1430-1440.
[2] McCain, E et al. (2021) JNeurEng & Rehab **18** p1-18.
[3] Rajagopal et al. (2016). IEEE T Biomed Eng. 63: 2068-2067.
[4] McFarland et al.(2019) J Biomech Eng 141

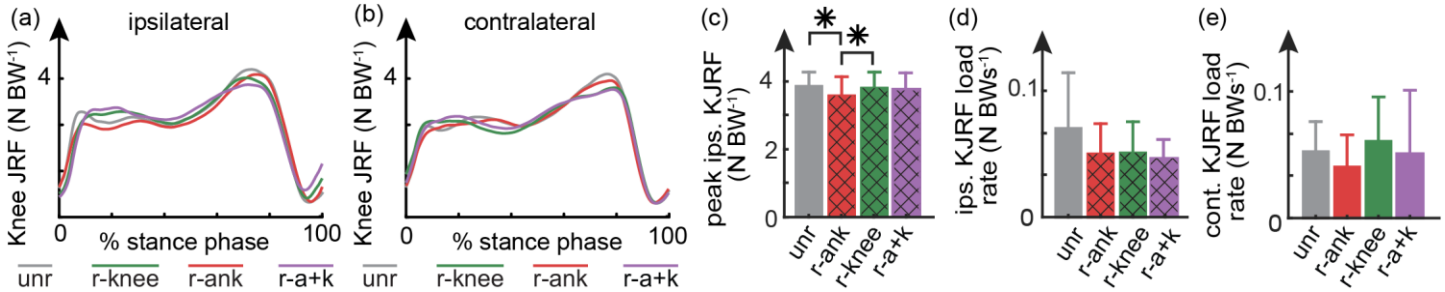

Figure 1. Subject averaged KJRF on the (a) ipsilateral and (b)contralateral limbs plotted over stance phase. Ipsilateral (c) peak KJRF and (d) loading rate and contralateral (e) KJRF loading rate are illustrated (mean ± st. dev). Hatched patterns indicate a joint restriction on plotted limb.

LOW BACK PAIN INFLUENCES COORDINATION DURING STANDING BALANCE IN PERSONS WITH LIMB LOSS

Courtney M. Butowicz[1], A. Yoder[2], B. Mazzone[2], S. Farrokhi[2], and B.D. Hendershot[1,3]
[1]DoD-Extremity Amputation and Trauma Center of Excellence; Walter Reed National Military Medical Center
email: courtney.m.butowicz.civ@mail.mil

Introduction

Standing balance is maintained via multi-joint coordination of postural responses, wherein joint torques – typically at the ankle and/or hip – help keep the body's center of mass (COM) within the base of support. Low back pain (LBP) alters posture and muscular responses that shift toward hip-dominant coordination strategies associated with poor balance control [1]. Moreover, persons with lower limb loss often demonstrate altered coordination (e.g., increased out of phase trunk-pelvis coordination, increased hip and knee mechanical work) and impaired balance control [2,3]; it is possible that these coordination strategies are associated with the development and/or recurrence of LBP, particularly given the high prevalence rates (52-89%) of LBP in this population [4]. Though recent work in persons without limb loss suggests that COM motion control is tri-modal, including the ankle, knee, and hip [5], the role of the knee in COM control is less clear in persons with limb loss. Further, the extent to which trunk-lower extremity coordination patterns impact COM dynamics during standing balance among persons with limb loss, particularly those with LBP, is unknown. The aim of this study was to determine the influence of COM-lower limb joint coordination on COM dynamics during standing balance among persons with lower limb loss, with and without LBP. We hypothesized that combinations of trunk-lower limb coordination patterns would predict COM dynamics in persons with limb loss; specifically, trunk-hip coordination would be the predominant pairing predicting COM dynamics among those with LBP.

Methods

Forty participants with unilateral lower limb loss, 17 without LBP (6F/11M, 13 transtibial, 4 transfemoral, 34.1±8.1 yrs, 174.5±8.9 cm, 83.7±17.8 kg) and 23 with LBP (10F/13M, 16 transtibial, 7 transfemoral, 35.3±9.1 yrs, 174.8±8.3 cm, 83.5±19.6 kg), stood quietly for 30s on a firm surface, with eyes open (EO) and eyes closed (EC), while wearing accelerometers on the sacrum (surrogate for COM), and bilaterally on the thigh, shank, and foot (128Hz, Opal Gen2, APDM Inc, Portland, OR). A state-space model with a causal Kalman filter calculated hip, knee, and ankle joint flexion-extension angles on the intact and prosthetic limbs. Fuzzy entropy (FE; m=2, r=0.2, n=2) assessed COM dynamics using the sacral angular velocity variability [6]. Normalized cross-correlation functions identified trunk-lower limb joint coordination patterns (trunk-hip, trunk-knee, trunk-ankle). Peak positive and negative cross-correlation values were used for statistical analyses. Multiple linear regression predicted COM dynamics from cross-correlation values for each pattern, with BMI and amputation level as covariates, and limbs analyzed independently (p<0.05).

Results and Discussion

Among persons with limb loss and LBP, with EC, the intact limb regression ($F_{(7,22)}$=3.70, p=0.02, R=0.81) explained 66% of the variance with a positive trunk-hip coordination strategy contributing significantly to the model (β=0.33, p=0.02). The prosthetic limb regression ($F_{(7,22)}$= 3.54, p=0.02, R=0.79) explained 62% of the variance with a negative trunk-hip strategy contributing significantly to the model (β=0.45, p=0.03). The models were not significant (p>0.17) for either group with EO (Figure 1), nor for the no LBP group with EC (p>0.54).

Persons with limb loss and LBP demonstrate opposing coordination strategies between the lower limbs and COM, wherein the flexion/flexion coordination pattern of the intact hip and extension/flexion coordination strategy of the prosthetic side hip may create a rotational torque about the COM, particularly when vision is removed. This strategy explains a large proportion of the variance in postural dynamics (i.e., regularity in COM angular velocity) and may identify a mechanism associated with LBP recurrence. The lack of significant findings with EO, yet with at least a third of the variance explained, could indicate an increased reliance on vision, which is typical [2], to control postural dynamics rather than coordination.

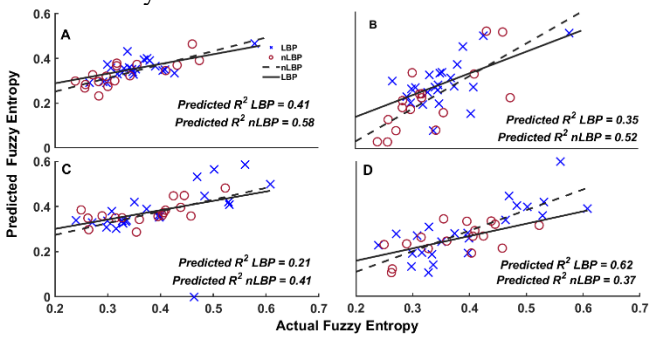

Figure 1: Regression model predicted values vs. actual values of fuzzy entropy by group: A) Eyes open, intact limb; B) Eyes open, prosthetic limb; C) Eyes closed, intact limb; D) Eyes closed, prosthetic limb. LBP: low back pain group; nLBP: no low back pain group.

Significance

Given the unique interplay between lower limb joints and the altered somatosensory afferents after limb loss, evaluating the relationships between joint coordination, postural dynamics, and LBP will assist in the understanding of how coordination strategies influence balance control during functional activities (e.g., standing, walking), and help mitigate the adoption of deleterious mechanics to improve longer-term outcomes (e.g., reduce development or recurrence of LBP).

Acknowledgments

This work was supported by the DoD-VA EACE. The views expressed herein are those of the authors and do not reflect the official policy of the U.S. Department of the Army/Navy/Air Force, Department of Defense, nor the U.S. Government.

References

[1] Mok N. (2004) *Spine* **29(6)**: E107-12.
[2] Ku P. (2014) *Gait & Posture* **39**: 672-82.
[3] Butowicz CM. (2019) *Gait & Posture* **73**: 8-13.
[4] Ehde D. (2001) *Arch Phys Med Rehabil* **82**: 731-4.
[5] Yamamoto A. (2015) *Gait & Posture* **41**:291-94.
[6] Caballero C. (2019) *Gait & Posture* **70**: 1-5.

Kinematic Changes are Associated with Improved Outcomes Following Superior Capsular Reconstruction

Clarissa LeVasseur[1], Gillian Kane[1], Jonathan D. Hughes[1], Adam Popchak[1], James Irrgang[1], Albert Lin[1], and William Anderst[1]
[1]Department of Orthopaedic Surgery, University of Pittsburgh
Email: cll100@pitt.edu

Introduction

Patients with irreparable rotator cuff tears (RCT) exhibit functional limitations while performing activities of daily living such as combing their hair. One viable treatment is superior capsular reconstruction (SCR). SCR has been shown to restore stability of the glenohumeral (GH) joint in cadavers[1], but its effect on *in vivo* scapular and humeral motion is unknown. The aims of this study were to determine the effect of SCR on *in vivo* scapular and humeral kinematics during a functional hand to head motion and to identify associations between shoulder kinematics and patient-reported outcomes (PROs). We hypothesized that moving the hand to the back of the head would be accomplished by using more GH based movement including rotation and abduction, and less scapular motion after SCR, and there would be a positive correlation between these kinematics changes and improved PROs

Methods

Ten patients (8M, 2F, age 63 ± 7 years) with irreparable RCT provided informed consent to participate in this prospective IRB-approved study. American Shoulder and Elbow Surgeon (ASES), Disability of the Arm Shoulder and Hand (DASH), and Western Ontario Rotator Cuff Index (WORC) surveys were completed before (PRE) and 1-year after (1YR-POST) SCR. PRE and 1YR-POST, participants were seated and instructed to move their hand from their lap to the back of their head while synchronized biplane radiographs of the shoulder were collected at 50 images/s for 3 separate trials. Six degree of freedom GH and scapular kinematics were determined with sub-millimeter accuracy by matching subject-specific CT-based bone models of the humerus and scapula to the synchronized radiographs using a validated volumetric tracking technique[3]. The contributions of humeral abduction, plane of elevation and internal/external (I/E) rotation relative to the scapula, as well as scapular upward rotation, protraction, and tilt, were calculated for each subject PRE and 1YR-POST for the entire motion. PRE to 1YR-POST differences in end range rotational positions and the total contribution of each rotation were evaluated using a paired t-test. Among-subject variability in rotational contributions to the motion was calculated as the absolute differences from the group mean for each test day. Differences in variability were analyzed using a paired t-test. Correlations between rotation contributions and PROs were evaluated with Pearson's correlation coefficients. Significance was set at $p < 0.05$ for all tests.

Results and Discussion

End-position I/E rotation was 12° lower 1YR-POST compared to PRE ($p = 0.03$, Figure 1), while end-position scapular protraction was 6° degrees higher 1YR-POST compared to PRE ($p = 0.01$, Figure 1). No differences in the total contribution of each rotational component were identified from PRE to 1YR-POST (Figure 2), but inter-subject variability decreased 4.0% in GH abduction and 2.6% in GH I/E rotation ($p = 0.047$, and $p = 0.005$, respectively, Figure 2). The PRE to 1YR POST increase in contribution from GH abduction was positively correlated to the increase in contribution from GH I/E rotation ($R = 0.8$, $p = 0.001$) and negatively correlated to the change in contribution from scapular protraction ($R = -0.94$, $p = 0.001$). Decreased contributions of glenohumeral rotation and abduction were offset by increased scapular protraction, while end-range I/E rotation decreased and scapular protraction increased, which contradicts our first hypothesis.

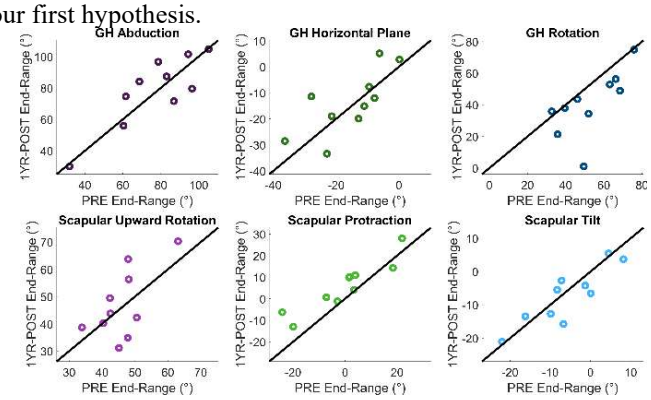

Figure 1. End-position rotation for the three GH rotations and three scapular rotations during a hand-to-head motion. Dots above the solid black lines indicate a higher end-position rotation 1YR-POST while dots below the solid black lines indicate a higher end-position PRE.

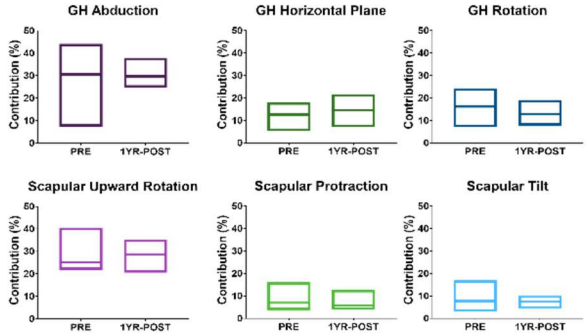

Figure 2. Percent contributions of each of the 6 rotations PRE and 1YR-POST with boxes indicating the range of contributions and the middle line indicating the group mean contribution.

Improvements in ASES scores were also positively correlated with increased plane of elevation contribution ($R = 0.635$, $p = 0.048$). This supports our second hypothesis, and may correspond with improved glenohumeral kinematics and efficiency of movement during a functional task following SCR. Future work will investigate GH and scapular kinematics in healthy individuals performing the hand to head movement to determine if movement strategy after SCR is closer to healthy.

Significance

Changes in scapular and GH kinematics following SCR suggest a convergence towards a more similar and potentially more efficient movement pattern following SCR. Focusing on restoring horizontal plane motion may lead to improved clinical outcomes after SCR.

References

[1] Mihata et al, (2012). *AJSM.* [2] Sochaki et al. (2019). *J Arthroscopy.* [3] Bey et al. (2006) *J Biomech*.

SUPER NEWTONIAN STRATEGIES ADOPTED BY CHILDREN WITH AUTISM SPECTRUM DISORDER

Alyssa N. Olivas[1], Emily A. Chavez[2], Jeffrey D. Eggleston[2,3]
[1]Department of Biomedical Engineering, The University of Texas at El Paso, El Paso, TX, USA
[2] Interdisciplinary Health Sciences Doctoral Program, The University of Texas at El Paso, El Paso, TX, USA
[3]Department of Kinesiology, The University of Texas at El Paso, El Paso, TX, USA
Email : anolivas4@miners.utep.edu

Introduction

Load accommodation strategies are responses to an external stressor, such as external mass, while performing a movement [1]. Several load accommodation strategies have been identified, including a Newtonian strategy, where an increase in vertical ground reaction force (vGRF) is linearly related to the increase in the external weight and occurs at an equal rate [1]. Past load accommodation strategy studies have focused on healthy adults, and there is little research in strategies children with Autism Spectrum Disorder (ASD) may adopt. ASD is a neurodevelopment disorder with socio-behavioral deficits, though, recent evidence demonstrates that motor deficits may be a core symptom of ASD [2]. Weighted vests (WV) are a common treatment modality used to decrease hyper-reactivity and sensory defensiveness in this population [3], however, the impacts of WVs on motor deficits and gait have proved beneficial as they have increased the center of mass smoothness [4]. Therefore, a WV may be a suitable external stressor to use in load accommodation strategy studies for children with ASD to further understand how they move. Therefore, the purpose is to evaluate load accommodation strategies by analyzing the vGRF during walking with a WV with 5% body mass in children with ASD. It is hypothesized that children with ASD will demonstrate a non-Newtonian response, due to past literature suggesting possible instabilities in the stance phase causing difficulty supporting body weight [5].

Methods

3 children (1 female, 2 males) with a clinical diagnosis of ASD (10.67±0.58 years; 1.56±0.03 m; 54.63±6.65 kg) and 3 age-and-sex matched neurotypical (NT) children (10.67±0.58 years; 1.48±0.03 m; 43.35±10.55 kg) participated. Participants walked 9 m over-ground, for 10 trials at a self-selected velocity without a WV (baseline) and with a WV with 5% body mass evenly distributed posteriorly and anteriorly. Force data were collected with 3 AMTI force platforms mounted flush with the floor (1000 Hz, Advanced Mechanical Technology Inc., MA, USA) and exported to Visual 3D (C-Motion, Inc., Germantown, MD, USA) for analysis. Data were smoothed using a low-pass Butterworth digital filter with a cut-off frequency of 25 Hz. vGRFs were normalized to body mass. The first peak of vGRF during walking was chosen for analysis and averaged for each participant. Limbs were collapsed after a paired samples t-test (α=0.05) yielded no significant difference between limbs (p = 0.73). A 2x2 (group x condition) factorial analysis of variance (ANOVA; α=0.05) was conducted. Percent change in vGRF was used to quantify which strategy was adopted between groups and individuals in both conditions.

Results and Discussion

Analysis revealed no statistically significant interaction between the effects of group and condition $F(1,12) = 0.06$, p = 0.81, η^2=0.01. There was no group main effect (p=0.90) and no condition main effect (p=0.32). However, the percent change in vGRF revealed both groups displayed a Super Newtonian response to the load **(Figures 1 and 2)**. Some individuals displayed responses different from the group response, suggesting that load accommodation strategies may be individualistic among children. However, both groups demonstrated a Super Newtonian response, indicating that a neuromuscular strategy was adopted resulting in larger increase in vGRF than the mass in the vest. While additional participants are needed to confirm these results, children with ASD may adopt a similar strategy to their neurotypical peers.

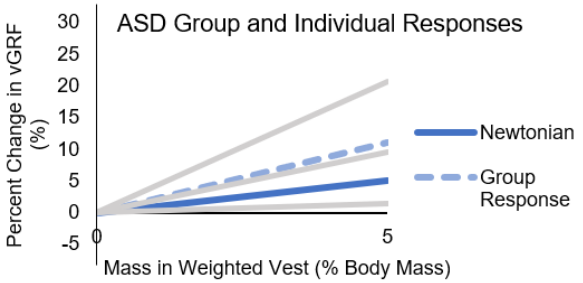

Figure 1: Strategies demonstrated by the ASD group and the individuals (gray lines) compared to the Newtonian strategy.

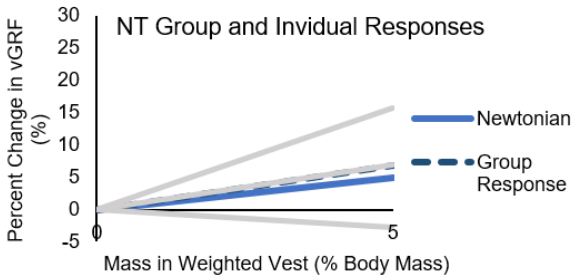

Figure 2: Strategies demonstrated by the NT group and the individuals (gray lines) compared to the Newtonian strategy.

Significance

There is little research the effects of external stressors have in children with ASD during gait. It is important to understand the biomechanical strategies children with ASD use to further distinguish the motor deficits that are present in this population. The use of load accommodation strategies with an external stressor that is a common treatment among this population, may allow for the possibility of identifying those differences.

Acknowledgments

This research was supported by the University of Texas at El Paso University Research Institute Grant.

References

[1] James et al. (2003). *Jrl Appl. Biomech.*, **19(2)**, 106-118.
[2] Floris et al. (2016), *Mlclr Autism*, **7(1)**, 35.
[3] Olson et al. (2004). *Phys. Occup. Ther. Pedia.,***24**, 45–60.
[4] Harry et al. (2019). *Trans. Jrl. ACSM*, ***4*(10),** 64-73.
[5] Hasan et al. (2018). *Int. Jrl. Eng.,* ***31*(5)**, 705.

HAMSTRING STIFFNESS INCREASES WITH COMPETITIVE LEVEL BUT NOT AGE IN BASKETBALL ATHLETES

Nathaniel A. Bates[1], Takashi Nagai[1], Luca Rigamonti[1], Ryo Ueno[1], Nathan D. Schilaty[1]
[1]Department of Orthopedic Surgery, Mayo Clinic, Rochester, MN, USA
email: batesna@gmail.com

Introduction

Application of ultrasound shear wave elastography (SWE) in sports medicine biomechanics has expanded [1]. While literature has established that males exhibit greater hamstrings muscle (HAM) stiffness than females [2], HAM stiffness progression relative to age remains unexplored. Accordingly, the objective of this abstract was to establish the correlation between SWE stiffness and age in basketball athletes. It was hypothesized that HAM stiffness would increase with age in high school basketball athletes. It was further hypothesized that collegiate athletes would have greater HAM stiffness than high school athletes.

Methods

571 lower extremities from 236 high school basketball athletes (163F:73M) were examined for HAM stiffness prior to the start of their competitive season. In addition, each subject's lower extremities were individually articulated through a passive range of flexion motion with the knee in an extended position. A GE LogiqE9 ultrasound was used to capture SWE images of the HAM at three subject-specific orientations (80%, 60%, and 40% of the peak range of motion). Three SWE images were taken of the biceps femoris midsubstance at each orientation. Custom MATLAB code was used to extract SWE stiffness (kPa) these values were averaged into a subject mean. Data were separated by sex and a one-way ANOVA was used to assess differences between ages (14-18 years). Individual differences within age pairs were assessed via Student's t-test. Pearson correlations were used to assess association between age and stiffness at each orientation. Significance was set at $\alpha < 0.05$.

Results and Discussion

Age was a significant factor for HAM stiffness in females at all three orientations ($p \leq 0.03$) and in males at the 60% orientation ($p < 0.01$). However, there was no significant linear correlation between age and HAM stiffness for either sex at any orientation ($r^2 \leq 0.08$). Instead, in females HAM stiffness peaked at ages 15 & 16 for the 80% orientation and age 15 for the 60% and 40% orientations (Table 1). In males, HAM stiffness decreased by age 17 relative to 14 & 15 in the 80% and 60% orientations (Table 1). Based on this data, HAM stiffness does not appear to be directly associated with development. Accordingly, the hypothesis was rejected.

Collegiate status was significant to HAM stiffness for females at all orientations and for males at the 80% and 60% orientations. In each of these orientations, the collegiate athletes had significantly greater HAM stiffness than their high school counterparts (Figure 1). This outcome directly supports the hypothesis. Despite this significance, further investigation is warranted to determine if these differences are related to age and development as opposed to alterations in training regimens between collegiate and high school sports. Further, as musculoskeletal injuries increase dramatically between high school and collegiate levels, further investigation is also warranted relative to the role of tissue stiffness in injury prevention.

Table 1: Mean (std) female HAM stiffness by age and limb orientation

	Age (Years)	80% Orientation	60% Orientation	40% Orientation
Females	14	37.0 (26.3)	43.4 (28.2)	37.0 (20.7)
	15	52.4 (35.7)	58.5 (35.8)	50.0 (28.8)
	16	53.5 (38.8)	52.2 (32.0)	44.2 (26.5)
	17	35.8 (22.9)	44.3 (30.2)	43.2 (26.7)
	18	46.5 (38.3)	45.0 (27.7)	44.3 (28.9)
Males	14	71.3 (37.3)	73.1 (39.2)	55.3 (33.0)
	15	71.6 (38.4)	80.3 (37.7)	59.5 (32.2)
	16	63.0 (39.5)	60.1 (34.0)	47.1 (27.3)
	17	53.9 (33.1)	52.6 (31.0)	50.8 (29.7)
	18	64.9 (37.6)	69.8 (37.6)	62.4 (31.7)

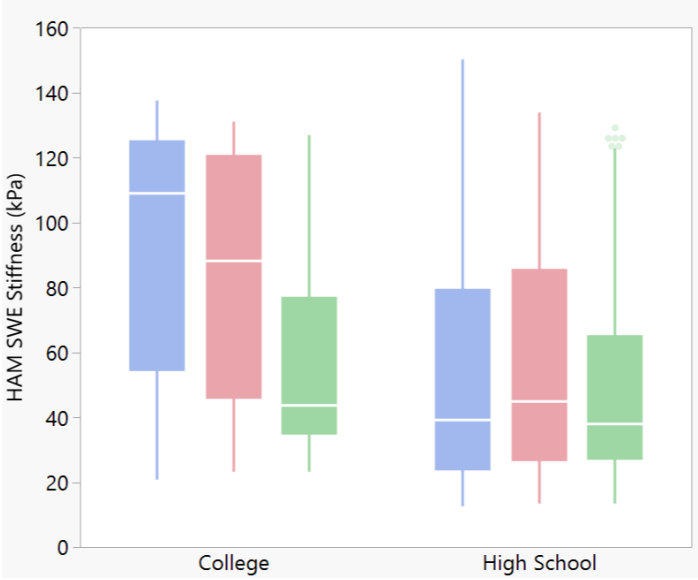

Figure 1: HAM stiffness as recorded by SWE at orientations of 80% (blue), 60% (red), and 40% (green) of peak passive flexion. At the 80% and 60% position, collegiate basketball players have significantly increased HAM stiffness relative to their high school counterparts.

Significance

HAM stiffness does not directly associate with age in young athletes but alters dramatically between the high school and collegiate levels. As such, there may be potential to utilize SWE stiffness as a surrogate for injury risk between levels of competition; however, further study is necessary to substantiate such claims.

Acknowledgments

NBA / GE Collaborative Grant; NIH NIAMS R01-AR055563 & L30-AR070273; NIH NICHD K12-HD065987; Foderaro-Quattrone Grant for AI Innovation in Orthopedic Surgery

References

[1] McPherson AL, et al. BMC Muscu Disord. 2020;21(1):320.
[2] McPherson AL, et al. Skeletal Radiol. 2020;49(8):1231-7

The Effects of Ankle Exoskeleton Assistance on Metabolic Efficiency of Incline Walking and Stair Ascent in Cerebral Palsy

Ying Fang.[1], Orekhov Grigoriy[1], and Zachary F. Lerner. [1,2]
[1]Department of Mechanical Engineering, Northern Arizona University, Flagstaff, AZ 86011, USA
[2]Department of Orthopedics, the University of Arizona College of Medicine-Phoenix, Phoenix, AZ 85004
Email: *yf82@nau.edu

Introduction

Inclines and stairs are common terrains encountered during daily life that pose challenges to mobility in people with impaired walking abilities, such as those with cerebral palsy (CP) [1,2]. We previously demonstrated that ankle exoskeleton assistance can improve level ground walking economy and gait mechanics in individuals with CP [3,4]. Working towards our long-term goal of augmenting mobility in free-living settings, the **purpose** of this study was to investigate the effects of ankle exoskeleton assistance on metabolic power and muscle activity during incline walking and stair ascent in CP.

Methods

Seven participants with CP (Table 1) completed 6-minute walking trials on a treadmill (Bertec) at 5° incline and 5-minute stair stepping trials (Stairmaster). For both activities, participants walked while wearing shoes (Shod) and while wearing a battery-powered ankle exoskeleton (Exo) (Fig. 1, [3]) in a randomized order.

Figure 1: Experimental setup.

We collected metabolic data and muscle activity of the tibialis anterior (TA), soleus, and vastus lateralis (VL). Net metabolic power was calculated by subtracting the standing metabolic rate from the gross metabolic power of each condition, and normalizing by body mass. Average integrated electromyography (iEMG) data were calculated for the stance phase, swing phase, and a complete gait cycle, averaged by all gait cycles and between limbs for each trial. All parameters were compared using paired two-tailed t-tests between Shod and Exo conditions ($\alpha \leq 0.05$).

Table 1. Participant characteristics.

	Age (Years)	Sex	Height (m)	Mass (kg)	GMFCS
P1	33	M	1.7	71.4	II
P2	11	M	1.5	48.4	I
P3	15	M	1.65	57.2	I
P4	25	F	1.47	47.4	III
P5	14	M	1.48	39.5	II
P6	12	M	1.41	37.7	II
P7	14	M	1.65	55.8	II

GMFCS: Gross Motor Function Classification System.

Results and Discussion

Walking with ankle assistance reduced net metabolic power by 13.2% and 15.4% during incline walking and stair climbing, respectively, compared to walking wearing shoes (Fig. 2). Compared to the Shod condition, walking with exoskeleton reduced soleus iEMG by 12.1% and 22.2% during incline walking and stair climbing, respectively, and reduced VL iEMG by 10.8% and 18.6% during incline walking and stair climbing, respectively (Fig. 3). During incline walking, stance phase muscle activity was reduced by 12.4% for the soleus and 9.8% for VL, respectively, and swing phase iEMG was reduced by 17.7% for TA, in Exo condition compared to Shod.

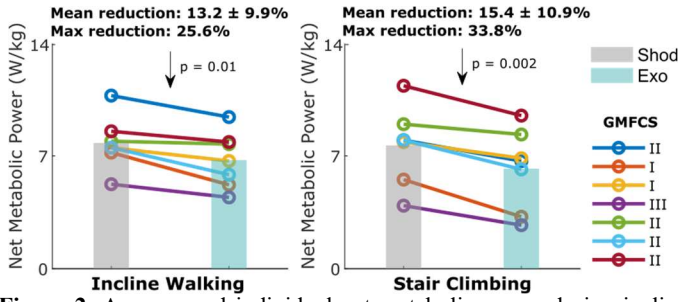

Figure 2: Average and individual net metabolic power during incline walking and stair climbing when walking wearing shoes (Shod) and ankle exoskeleton (Exo). GMFCS: Gross Motor Function Classification System.

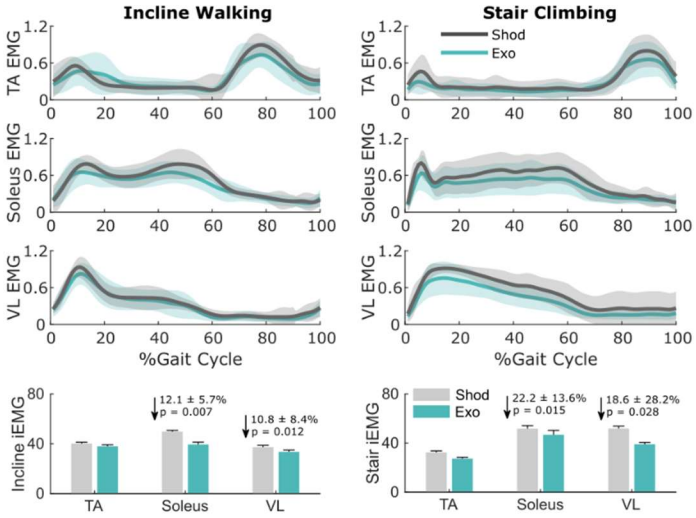

Figure 3: Normalized muscle activity of a gait cycle and integrated eletromyography (iEMG) for the tibialis anterior (TA), soleus, and VL (vastus lateralis) when walking with shoes (Shod) and exoskeleton (Exo) on inclines and stairs. Error bars indicate standard error. Shading depicts mean ± standard deviation.

Significance

To the best of our knowledge, this is the first study to demonstrate that battery-powered ankle exoskeleton assistance can improve metabolic efficiency during incline and stair ambulation in people with CP. These findings motivate future research of ankle exoskeleton assistance to improve mobility free-living settings.

Acknowledgments

This project was partially supported by the National Institutes of Health under Award Numbers 1R15HD099664 and 1R44HD104328.

References

[1] Ma et al. *Appl Bionics Biomech*, 2019. [2] Gillett et al. *APMR*, 99, 2018. [3] Orekhov et al. *IEEE Trans Neural Syst Rehabil Eng*, 1, 2020. [4] Lerner et al. *Ann Biomed Eng*, 47, 2019.

JOINT-SPECIFIC CONTRIBUTIONS TO HORIZONTAL GROUND REACTION FORCES DURING A JUMPING TASK

Nayun Ahn and Kristof Kipp
Department of Physical Therapy, Marquette University, WI, USA
mail: nayun.ahn@marquette.edu

Introduction

Deleterious landing biomechanics during sporting tasks are associated with non-contact lower extremity injuries, such as anterior cruciate ligament (ACL) tears [1, 2]. Previous literature demonstrated that women are more susceptible to ACL injuries than men, and that women with higher ground reaction forces (GRF) during landing showed greater injury risk [2]. Posterior GRF in particular are strongly associated with risk factors of ACL injuries because they are linked with greater peak anterior tibial shear forces and knee extension moments [1].

Although studies have identified sex-specific differences in joint kinetics and kinematics during landing tasks, little is known about joint-specific contributions to posterior GRF in either males or females. Induced acceleration analysis (IAA) can calculate the direct contributions of lower limb net joint moments (NJM) to posterior GRF during landing tasks and therefore quantify joint-specific contributions to a known ACL injury factor [3]. The purpose of this study was to investigate sex-specific contributions of ankle, knee, and hip NJM to posterior GRF during forward drop vertical jump task.

Methods

Eight male and eight female NCAA Division 1 basketball players performed three forward drop vertical jump trials (DJ-LESS) [2]. Kinematic data of 26 markers were collected with a motion capture system at 100Hz. Kinetic data were collected with two force plates at 1000 Hz. All data were filtered with a fourth-order low pass filter at a cut off frequency of 16 Hz. An inverse dynamics analysis was used to calculate the NJM at the ankle, knee, and hip joints. An IAA module was then used to calculate the sagittal plane contributions of these NJM to the horizontal GRF. These contributions were calculated for the entire ground contact phase, which was based on a vertical GRF threshold of 10 N (Figure 1). All data were time-normalized (e.g., 0-100%) and averaged across the three trials from each participant. NJM and GRF were normalized by body mass.

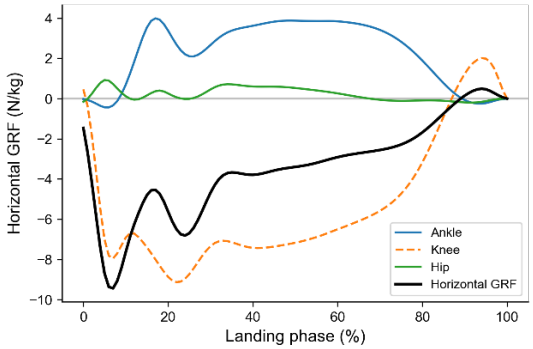

Figure 1: Joint-specific contributions to horizontal GRF.

All statistical comparisons of joint-specific IAA-based NJM contributions between males and females were made with the "spm1d" package in Python [4]. Specifically, an SPM independent *t*-test was used to compare data between males and females during the first 50% of the DJ-LESS ground contact phase ($\alpha = 0.05$).

Results and Discussion

The SPM analysis did not identify any significant sex differences in NJM contributions to the horizontal GRF during the first half of the ground contact phase of the DJ-LESS. However, marked individual differences among players were noted for ankle and hip NJM contributions, which appeared to capture trade-offs between these joint's contribution to horizontal GRF (Figure 2).

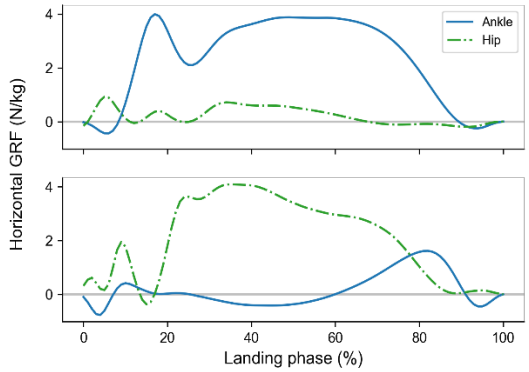

Figure 2: Exemplary NJM contributions to horizontal GRF for players with ankle (top) and hip (bottom) dominant strategies.

Previous literature found time-varying trade-offs in peak ankle and hip kinetics such that peak vertical and posterior GRF or extensor NJM did not differ between males and females [1, 5]. These trade-offs showed that females used knee extensor and ankle plantarflexor strategy, whereas males used the knee and hip extensors strategy to decelerate the body during landing [5].

Greater posterior GRF, which are commonly associated with greater risk of ACL injuries, are the result of knee extensor NJM. Basketball players appear to use highly individualized ankle or hip extensor strategies to mitigate excessive posterior GRF. Inconsistent with previous studies, our analyses showed that ankle and hip NJM trade-offs during initial half phase of DJ-LESS do not depend on the sex of the participants.

Significance

This study highlighted that investigating subject-specific trade-offs between ankle and hip extensors strategy to mitigate posterior GRF and risk of ACL injury may be more important than the subject's sex.

References

[1] Yu B et al. *Clin Biomech* 21: 297-305, 2006.
[2] Peebles AT et al. *J Biomech* 105: 109818, 2020.
[3] João F et al. *Hum Mov Sci* 33: 312-320, 2014.
[4] Pataky TC et al. *PeerJ* 4: e2652, 2016.
[5] Decker et al. *Clin Biomech* 18: 662-669, 2003.

COORDINATION BETWEEN VERTICAL GROUND REACTION FORCES DURING DOUBLE SUPPORT IS DIFFERENT FOR STAIR ASCENT VS. DESCENT

Chuyi Cui[1], Z. Yang[2], S. Rietdyk[1], and S. Ambike[1]
[1] Department of Health and Kinesiology, Purdue University, West Lafayette, IN, USA
[2] School of Biomedical Engineering, Capital Medical University, Beijing, CHINA
email: cui111@purdue.edu

Introduction

Regulation of whole-body angular momentum (WBAM) during stair negotiation is essential to prevent falling, and WBAM is regulated more tightly during stair descent compared to ascent [1]. However, the mechanisms employed for this control are poorly understood. The ground reaction forces and moments significantly influence WBAM. Therefore, we examined the coordination between the vertical ground reaction forces (GRFs) under the feet during the double support phase to identify their role in regulating WBAM about the medio-lateral (ML) axis during stair ascent and descent.

During double support, vertical GRFs beneath the feet could covary negatively, thus stabilizing their sum and thereby the vertical translation of the centre of mass (COM). Conversely, the GRFs could covary positively, thus stabilizing their difference. Since these GRFs create opposing moments about the COM (Fig. 1A), positive covariation will result in the stabilization of the WBAM. We recently demonstrated negative covariation in the GRFs while ascending, but no covariation while descending a curb [2]. Here, we quantify the covariation in the GRFs on three consecutive steps of a staircase during ascent and descent. We expect that the GRF sum will be stabilized during ascent and the difference will be stabilized during descent for all steps.

Methods

Eight healthy males (24±1.4 yrs) ascended and descended a five-step staircase (17 cm rise, 26 cm tread) 20 times, and stopped at the top and bottom of the staircase after each ascent and descent, respectively (Fig. 1B). The number of steps were the same in ascent and descent. The vertical GRFs were measured with force plates (Kistler, 1000Hz) for the middle three steps (bottom, middle, top; Fig. 1B).

We quantified the covariance between GRFs using the uncontrolled manifold (UCM) analysis at each percentage of the time-normalized double support phase. The working hypothesis was that the sum of GRFs is stabilized. We partitioned the across-trial variance in GRFs into a component along the UCM that maintains the GRF sum (V_{UCM}), and a component orthogonal to the UCM that changes it (V_{ORT}). We computed the normalized difference between V_{UCM} and V_{ORT}, z-transformed it to obtain the *synergy index* (ΔVz), and averaged ΔVz over the double support phase. Student's two-tailed t-test was conducted to compare ΔVz to zero. ΔVz > 0 supports the working hypothesis; ΔVz < 0 indicates that the force difference is stabilized instead of the sum [2]; ΔVz = 0 indicates no stabilization. We conducted *Step* (top, middle, bottom) × *Direction* (ascent, descent) repeated-measures ANOVA on ΔVz, and conducted post-hoc comparisons with Tukey adjustments.

Results and Discussion

ΔVz for the bottom step during stair descent was not different from zero. ΔVz for all other steps were significantly greater than zero, indicating that the sum of the GRFs was stabilized ($p<.05$).

We observed a significant *Step* × *Direction* interaction ($F_{2,35}=4.47$; $p=.019$). ΔVz for the bottom step during descent was significantly smaller than that for all other steps during ascent and descent ($p\leq.04$; Fig. 1C).

Overall, the vertical GRFs beneath the feet are coordinated to regulate the vertical motion of the COM. However, there is a shift from stabilizing the force sum toward stabilizing the force difference, which indicates a shift towards regulation of the ML WBAM while descending compared to ascending stairs, consistent with our result on curb crossing [2]. Furthermore, this shift is observed after descending the middle step. It is likely that WBAM tends to increase while descending multiple steps, as the body rotates forward about the stance ankle to descend each step. The decline in ΔVz is a compensatory mechanism to regulate the WBAM magnitude. Alternatively, the decline in ΔVz may be preparation for transitioning from a stair-descending gait to quiet standing at the end of the staircase, which requires almost zero WBAM. However, we did not see similar preparation for the gait-to-standing transition for ascent. Note that the vertical GRFs influence the ML WBAM, but do not determine it, since the anterior-posterior GRFs also contribute to the ML WBAM.

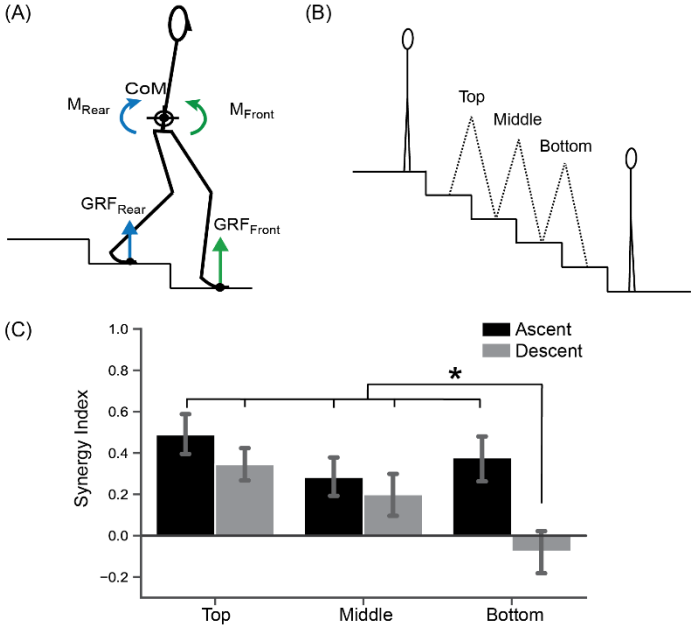

Figure 1: (A) Forces and moments acting at whole body COM (B) The five-step staircase (C) Mean ± SE of synergy index for each step and walking direction. The horizontal line indicates no stabilization.

Significance

Clarifying the between-foot GRF coordination during stair negotiation will (1) help understand why more falls occur while descending stairs [1], and (2) assist in the design and control of powered lower-limb prostheses, which are typically not designed for negotiating stairs, which, in turn, limits their utility [3].

References

[1] Silverman et al. *Gait & Posture,* 2014, 39: 1109–1114
[2] Cui et al. *J Biomech*, 2020, 106: 109837
[3] Pickle et al. *J Biomech*, 2014, 47: 3380–3389

THE RELIABILITY AND MINIMUM DETECTABLE CHANGE OF THE MARGIN OF STABILITY

Michael Christensen[1], James Tracy[1], and Jeremy Crenshaw[1]
[1]University of Delaware
email: *crenshaw@udel.edu

Introduction

The margin of stability (*MoS*) is a commonly used measure of dynamic gait stability. It accounts for the position and scaled velocity of the whole-body center of mass, i.e. the extrapolated center of mass (*xCOM*), relative to the edge of the base of support [1]. This measure has both clinical validity, as it is changed in populations at a greater risk of falling [2], and mechanical validity, as it is proportional to the impulse required to cause a loss of stability [1]. Although the *MoS* appears to be a valid metric of stability, there is little evidence to support its reliability [3]. The purpose of this study was to evaluate the test-retest reliability of the *MoS* during overground walking.

Methods

Fifteen unimpaired participants (6M/9F, mean (SD) Age: 21.0 (3.2) years; BMI: 21.3 (2.5) kg/m^2) were recruited to walk over ground at self-selected preferred and fast walking speeds [4]. The *xCOM*, as defined in Equation 1, and the *MoS* across each stance phase were then calculated.

$$EQ1: xCOM = COM + \frac{vCOM}{\sqrt{g/l}}$$

Equation 1: The extrapolated center of mass is defined by this equation where *vCOM* is the velocity of the center of mass, *g* is gravity, and *l* is the length of the pendulum.

The minimum lateral *MoS* ($MOS_{ML\text{-}Min}$) was defined as the minimum lateral distance from the stance toe to the x*COM*, with positive values indicating an *xCOM* medial to the toe. The anterior *MoS* at midswing ($MoS_{AP\text{-}Midsw}$) was also calculated, with positive values indicating an *xCOM* that was posterior to the stance toe. $MOS_{ML\text{-}Min}$ and $MoS_{AP\text{-}Midsw}$ were each averaged across limbs. This protocol was repeated at a second visit (Time Between Visits: 24.9 (15.4) days).

To assess reliability, intraclass correlations ($ICC_{2,1}$) and Bland-Altman Plots (mean [limits of agreement]) were determined between visits. Calculated ICC values were used to estimate minimum detectable changes (MDC) [5].

Results and Discussion

At both preferred and fast walking speeds, $MOS_{ML\text{-}Min}$ showed good agreement (ICC = 0.78 & ICC = 0.75, Fig. 1A & Fig. 1B). The MDC was 0.68 cm and 0.80 cm for each speed, respectively.

In the anterior direction, $MoS_{AP\text{-}Midsw}$ showed excellent agreement at each walking speed (ICC = 0.87 & ICC = 0.97, Fig. 1C & Fig. 1D). The MDC was 2.62 cm. and 1.07 cm. for each speed, respectively.

These results suggest that the *MoS* has sufficient test-retest reliability for research purposes, and outlines the minimum values necessary to show meaningful differences in stability maintenance. In the anterior direction, *MoS* values showed stronger agreement than that of those calculated in the mediolateral direction. These results are somewhat unexpected, as we expected that within-subject variation in gait speeds (Preferred: ICC = 0.79 & Fast: ICC = 0.96), an aspect that directly influences anteroposterior stability, would contribute to weaker agreement of $MoS_{AP\text{-}MidSW}$.

Future work will be directed towards determining how gait kinematics (e.g. step width or step frequency) and data collection factors (e.g. marker placement and instructed walking path) may underlie the moderately limited reliability of the lateral stability measure. A weak correlation between inter-visit differences in gait speed and inter-visit differences in $MOS_{ML\text{-}Min}$ at each walking speed (Preferred: r = 0.41 & Fast: r = 0.34) suggest that gait speed is not a factor that, if controlled more precisely, would improve lateral stability reliability.

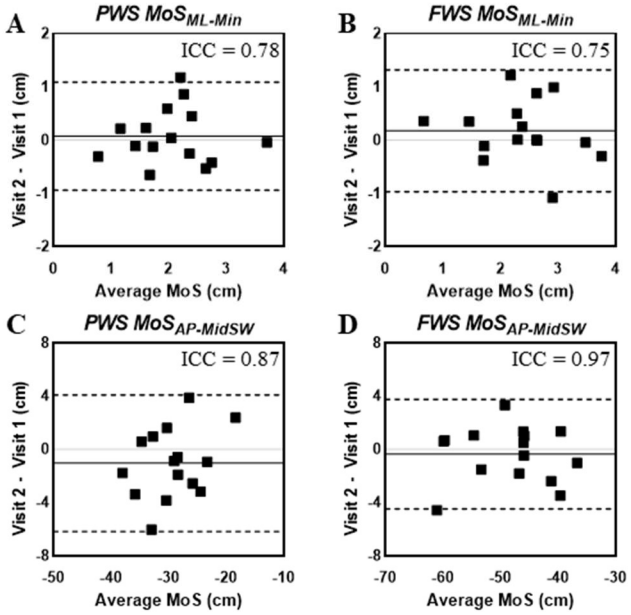

Figure 1: Bland Altman Plots showing limits of agreement for $MoS_{ML\text{-}Min}$ (A & B) and $MoS_{AP\text{-}MidSW}$ (C & D) at self-selected preferred (A & C) and fast (B & C) walking speeds.

Significance

To our knowledge, this is the first evidence that the MoS represents not only a valid, but *reliable* metric of gait stability. This information can inform the planning of studies aimed at evaluating the effects of experimental manipulation, intervention, or the natural course of impairment or development on this measure. This reliability may be specific to our MoS measures, not representative of other approaches (i.e. taken in different orientations or gait phases) and treadmill walking. This reliability also may not be representative of pathological gait, which could be characterized by greater within- and between-subject variance.

References

[1] Hof et al. (2005). *J Biomech*, **38:** 1-8
[2] Tracy et al. (2019). *Gait Posture*, **72**: 182-187
[3] Bruijn et al. (2013). *J R Soc Interface*, **10** 20120999
[4] Dempster. (1995). *WADC,* 55-159
[5] Haley et al. (2006). *Phys Ther.* **86(5)**: 735-43

TRICEPS SURAE MUSCLE AND TENDON MORPHOLOGY ASSOCIATED WITH FUNCTIONAL PERFORMANCE IN PATIENTS WITH ACHILLES TENDINOPATHY

Kayla D. Seymore[1,2], Haraldur B. Sigurðsson[1], Karin Grävare Silbernagel[1]
[1]Dept. of Physical Therapy, University of Delaware, Newark, DE, USA
[2]Biomechanics and Movement Science Program, University of Delaware, Newark, DE, USA
email: seymorek@udel.edu

Introduction

Achilles tendinopathy exercise treatment programs have been shown to alter calf muscle strength and tendon morphology [1], but do not always return patients to full functional performance [2]. While the contribution of triceps surae muscle and tendon morphology to lower limb function has been established in healthy populations [3,4], triceps surae attributes that relate to functional outcomes in the Achilles tendinopathy population are not well understood [1]. Therefore, the purpose of this investigation was to determine the relationship between triceps surae muscle size and tendon material properties and the functional performance of patients with Achilles tendinopathy. Establishing the relationship between triceps surae morphology and lower limb functional performance for patients with Achilles tendinopathy could aid in the refinement of clinical rehabilitation protocols to improve functional performance.

Methods

Ninety-one (46 F, 47.6 ± 11.6 yrs) patients with clinically confirmed mid-portion Achilles tendinopathy were included in the study. Triceps surae size was measured, via ultrasound, as cross-sectional area (CSA) of the medial (MG) and lateral (LG) gastrocnemius muscle, as well as thickness of the soleus (SOL) muscle, according to previously published protocol [5]. Achilles tendon material properties of shear modulus and viscosity were obtained with continuous shear wave elastography (cSWE) [6].

A test battery was then used to assess lower limb functional performance [7]. Total repetitions and work for a maximum endurance single-leg heel-rise test were measured using a linear encoder affixed to the heel. Hop frequency was calculated for the middle 20 hops (out of 25) during a single-leg hopping test using a light-mat, which triggered a timer when disrupted. The maximum drop counter-movement jump (drop CMJ) height from 3 single-leg drop CMJs was also measured with the light-mat.

Independent variables of triceps surae muscle size and tendon material properties and dependent variables of heel rise, hopping, and drop CMJ tests were analyzed with a two-way multivariate analysis of covariance to determine the relationship between triceps surae muscle and tendon morphology and functional performance, while controlling for sex, limb, age, weight, and physical activity level, measured with the Physical Activity Scale questionnaire [8]. Alpha was set *a prior* at 0.05.

Results and Discussion

Functional performance of the test battery was associated with MG ($p=0.031$) but not LG ($p=0.635$) or SOL ($p=0.184$) muscle size, nor tendon shear modulus ($p=0.064$) or viscosity ($p=0.171$). Triceps surae muscle size and tendon material properties correlated to heel rise repetitions ($p<0.001$, $R^2=0.279$), heel rise work ($p<0.001$, $R^2=0.296$), hopping frequency ($p=0.006$, $R^2=0.185$), and drop CMJ height ($p<0.001$, $R^2=0.478$), after controlling for sex, limb, age, weight, and physical activity level. However, large differences in triceps surae morphology were required for appreciable change to functional performance (Table 1). There were significant effects of sex, age, weight, and physical activity level ($p<0.05$), with no effect of limb nor interaction of sex and limb on functional performance.

The current study supported the presence of a relationship between triceps surae muscle and tendon morphology and functional performance in patients with Achilles tendinopathy. Smaller medial gastrocnemius muscle size and greater Achilles tendon shear modulus was related to improved heel rise and hopping performance, respectively.

Significance

There is sufficient evidence that triceps surae morphology strongly impacts functional performance [3,4]. The weak relationships reported for patients with Achilles tendinopathy suggest that this pathology may disrupt the neuromuscular mechanisms that typically link morphology and performance [1], potentially through pain interference. Conjunctively, calf muscle CSA may be an insufficient proxy for muscle volume, as it relates to strength and functional performance [4]. Future research is needed to investigate the impact of activity-induced pain and volumetric calf muscle measurements on the relationship between triceps surae morphology and functional performance in the Achilles tendinopathy population.

References

[1] Murphy M et al. (2018). *Int J Sports Phys Ther*, **13**:537-551.
[2] Silbernagel KG et al. (2007). *Br J Sports Med*, **41**:276-280.
[3] Monte A and Zamparo P. (2019). *PLoS One*, **14**:e0213347.
[4] Bellinger P et al. (2021). *Med Sci Sports Exerc*, doi: 10.1249/MSS.0000000000002605.
[5] Zellers JA et al. (2019). *J Orthop Res*, **37**:933-941.
[6] Cortes DH et al. (2015). *Ultrasound Med Biol*, **41**:1518-1529.
[7] Silbernagel KG et al. (2006). *Knee Surg Sports Traumatol Arthrosc*, **14**:1207-1217.
[8] Grimby G. (1986) *Acta Med Scand Suppl*, **711**:233-237.

Table 1: Regression coefficient estimates (β), 95% confidence intervals (CI), and p-values for the fit model.

	Heel Rise Repetitions			Heel Rise Work			Hop Frequency			Drop CMJ Height		
	β	95% CI	p-value	β	95% CI	p-value	β	95% CI	p-value	β	95% CI	p-value
MG CSA	-0.673	(-1.326, 0.020)	0.043	2.283	(-46.138, 50.703)	0.926	-0.021	(-0.048, 0.007)	0.137	-0.018	(-0.228, 0.192)	0.868
Shear Modulus	0.030	(-0.048, 0.107)	0.450	4.018	(-1.705, 9.741)	0.167	0.004	(0.000, 0.007)	0.027	-0.010	(-0.035, 0.015)	0.415

AGE-RELATED CHANGES TO TRICEPS SURAE MUSCLE-SUBTENDON INTERACTION DYNAMICS DURING WALKING

William H. Clark[1*] and Jason R. Franz[2]
[1]Department of Ecology and Evolutionary Biology, Brown University, Providence, RI, USA
[2]Joint Department of Biomedical Engineering, UNC Chapel Hill and NC State University, Chapel Hill, NC, USA
*email: william_clark@brown.edu

Introduction

Push-off intensity is largely governed by the forces generated by the triceps surae muscles (gastrocnemius-GAS, soleus-SOL). Despite sharing a common tendon, the triceps surae muscles undergo different fascicle kinematics and contribute differently to biomechanical subtasks during walking [1]. These differences may be facilitated by the Achilles tendon (AT), which is comprised of subtendons that originate from the triceps surae muscles. We and others have revealed non-uniform displacement patterns within the AT – evidence for sliding between subtendons that may facilitate independent muscle actuation. However, in older adults, we have observed more uniform AT tissue displacements that correlate with reduced push-off intensity [2]. Here, we employed dual-probe ultrasound imaging to investigate differences in GAS vs. SOL muscle behaviour as a determinant of reduced ankle moment generation. First, we hypothesized that, compared to young, older adults would have more uniform AT tissue displacements that would be accompanied by smaller differences between GAS and SOL muscle length-change. Second, we hypothesized that differences between GAS and SOL muscle length-change would correlate with peak ankle moment generation.

Methods

9 young (24±4 yrs, 4F) and 9 older (74±4 yrs, 3F) adults walked on a treadmill for 1 min each at 1.2 m/s with and without: (1) a 5% body weight horizontal aiding force (decrease ankle moment) and (2) a 5% body weight horizontal impeding force (increase ankle moment), as shown in Fig. 1A. A 60 mm ultrasound transducer recorded cine B-mode images through the right medial GAS and SOL at 76 fps. Simultaneously, a 38 mm ultrasound transducer recorded ultrasound radiofrequency data of the right leg free AT at 155 fps enabling synchronized assessment of two equally sized tendon depths – corresponding to superficial (GAS) and deep (SOL) subtendon tissue. We secured the second ultrasound probe approximately 6 cm distal to the SOL muscle-tendon junction. Post collection, we quantified time series of GAS and SOL fascicle lengths [3] and subtendon displacements [4], averaged across 2 strides per condition. We report stance-phase differences in longitudinal muscle length change (i.e., GAS-SOL) and AT non-uniformity (i.e., superficial-deep). Mixed factorial ANOVAs tested for the effect of age and condition (1.2 m/s, aiding, and impeding) on peak ankle moment, GAS-SOL longitudinal muscle length change, and AT non-uniformity.

Results and Discussion

In support of our hypotheses, older adults walked with 49% more uniform AT tissue displacements ($P < 0.05$) that were accompanied by 17% smaller differences between GAS and SOL muscle length-change ($P < 0.05$). Only young adult muscle-level behavior correlated with AT non-uniformity and peak ankle moment generation (Fig. 1B-C). Moreover, we add that older adult muscle- and tendon-level behavior were significantly less sensitive to changes in horizontal force, as evidenced by significant age×condition interaction effects ($P < 0.05$). We interpret these cumulative findings to suggest that the Achilles tendon facilitates independent triceps surae muscle actuation in young adults and restricts that actuation in older adults – likely through decreased capacity for sliding between adjacent subtendons. Indeed, compared to younger tendons, older tendons present with a proliferation of interfascicle adhesions which may underly prominent reductions in the capacity for sliding between adjacent subtendons [5].

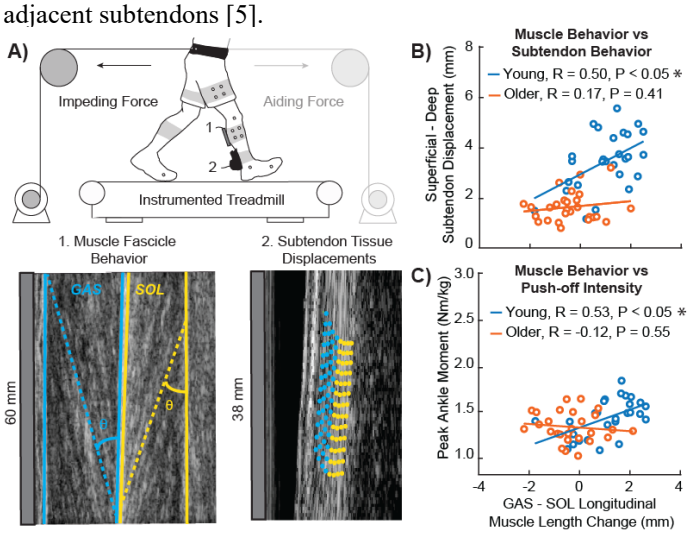

Figure 1: (A) Depiction of experimental protocol. Differences in triceps surae muscle behavior correlated with Achilles subtendon behavior (B) and peak ankle moment (C) in young (blue), but not older (orange) adults. *significant ($P \leq 0.05$) correlation.

Significance

Our findings suggest that the capacity for sliding between subtendons facilitates independent triceps surae muscle actuation in young adults but restricts that actuation in older adults. The resultant disruption in muscle contractile behaviour may contribute at least in part to hallmark reductions in push-off intensity (e.g., ankle moment) during walking in older adults.

Acknowledgments

We thank Nathan Lehr for his help with data collection. This study was funded by NIH (R01AG051748, F31AG060675).

References

[1] Fukashiro S, et al. (2006). J Appl Biomech, **22**: 131-47.
[2] Franz JR, et al. (2015). J Appl Physiol (1985), **119**: 242-9.
[3] Farris DJ, et al. (2016). Comput Methods Programs Biomed, **128**: 111-8.
[4] Chernak Slane L, et al. (2014). J Biomech, **47**: 750-4.
[5] Thorpe CT, et al. (2013). Eur Cell Mater, **25**: 48-60.

AGREEMENT BETWEEN HIP KINEMATICS USING TWO PELVIS TRACKING MARKER METHODS

*Kevin D. Moore, Ashley L. Hawke, Robert E. Carey, John Z. Wu, Scott P. Breloff
National Institute for Occupational Safety and Health, Morgantown, WV, USA
email : *qcp5@cdc.gov

Introduction

Optical marker-based motion capture systems are a common tool used to study human movements. Reflective markers are placed on anatomical landmarks of human subjects and are often accompanied by tracking markers, which are then used to model body segments and calculate kinematic data. The pelvis segment is predisposed to anatomical marker occlusions particularly with overweight participants and during tasks which require larger trunk/hip flexion [1]. Due to this difficulty, tracking markers are commonly used in addition to the anatomical markers on the pelvis. Variances in marker locations, number of markers, and maker cluster types are associated with differences in kinematic data, which can be problematic when comparing various publications or collaborating with other researchers [2,3]. The purpose of this investigation was to examine the agreement of kinematic data obtained using two different pelvis tracking methods during two dynamic roofing tasks.

Methods

Five healthy males (age: 26.4±8.3 yrs, height: 1.81±0.09 m, weight: 87.8±9.6 kg) participated in this study and completed a roofing task under two conditions: level platform while standing (SC) & kneeling on a 15° roof segment (KC) (3 trials per condition) [4]. Marker trajectories were captured by a 14-Camera system (Vicon Inc.) at a sampling rate of 100 Hz.

The marker trajectories were processed in Visual 3D (C-Motion Inc.). The anatomical pelvis was created with the CODA model (Charnwood Dynamics Ltd.) and two tracking methods for the CODA pelvis were compared. One— the trochanter tracking method (TTM)—used the right posterior superior iliac spine (RPIS), left posterior superior iliac spine (LPIS), the right trochanter, and left trochanter markers. Two —virtual pelvis tracking method (VPTM)—created two CODA pelvises. The VPTM used the virtual hip joint centers created by the second CODA pelvis (kinematic only) as tracking markers in addition to the RPIS and LPIS. Hip joint angle rotations for the same trials were computed for both tracking methods.

Mean absolute differences (MAD) were calculated for the hip joint angles between the two tracking methods using a one tailed t-test between the absolute differences and zero to determine significance ($p < 0.01$). Bland-Altman plots were used to assess the agreement between the two methods.

Results and Discussion

There were statistically significant differences in MAD for SC left hip (LH) flexion/extension (Fl/Ex) (10.8°) ($p < 0.001$), SC LH abduction/adduction (Abd/Add) (8.9°) ($p < 0.001$), SC LH external/internal rotation (E/I Rot) (3.8°) ($p < 0.001$), SC right hip (RH) Fl/Ex (13.7°) ($p < 0.001$), SC RH Abd/Add (4.5°) ($p < 0.001$), SC RH E/I Rot (3.2°) ($p < 0.001$), KC LH Fl/Ex (7.1°) ($p < 0.001$), KC LH Abd/Add (3.8°) ($p < 0.001$), KC LH E/I Rot (2.9°) ($p < 0.001$), KC RH Fl/Ex (7.6°) ($p < 0.001$), KC RH Abd/Add (2.5°) ($p < 0.001$), and KC RH E/I Rot (1.8°) ($p < 0.001$). The overall average MAD is 9.8° for hip Fl/Ex, 4.9° for hip Abd/Add, and 2.9° for hip E/I Rot. The differences in this study are similar but larger than those found during gait, demonstrating that each task can differ in agreement [5]. The agreement between maximum hip joint angles (Fig. 1) ranged from poor to moderate with the SC demonstrating less agreement than the KC (Fig. 1). The max hip joint angles showed a larger difference overall compared to the MAD of the entire dataset, indicating that more dynamic tasks show less agreement.

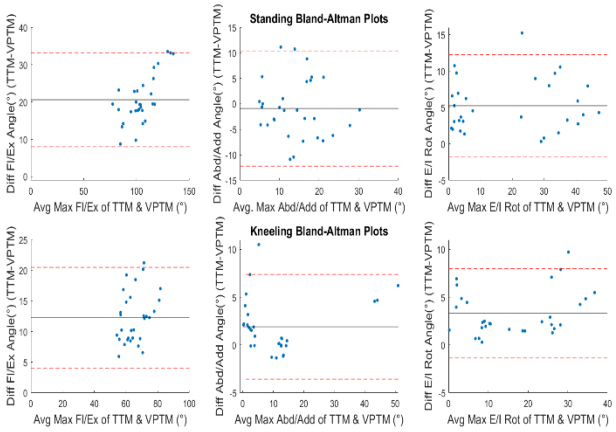

Figure 1: : Bland-Altman plots indicating the difference (y-axis) and the mean (x-axis) of the maximum hip angles between the two pelvis tracking methods. The solid black line represents the mean difference and the red dashed lines represents the mean difference ± 1.96 standard deviation. The top row is standing, the bottom row is kneeling, and left to right is flexion/extension, abduction/adduction, and external/internal rotation, respectively.

Significance

These results indicate that there are significant differences in the hip joint angles calculated from the two different pelvis tracking methods. Agreement between maximum joint angles was poor when compared to the MAD of the whole dataset, suggesting that the use of different tracking methods may be of greatest concern in the most dynamic tasks. For tasks with smaller ranges of motion, or in cases where a few degrees of difference are acceptable, either tracking method may be useful as they are both within a single variation range of the MAD. These results support previous findings that the pelvis tracking method should be consistent when comparing datasets or collaborating among research teams [3].

Disclaimer

The findings and conclusions in this report are those of the authors and do not necessarily represent the official position of the National Institute for Occupational Safety and Health, Centers for Disease Control and Prevention.

References

[1]McClelland et al. (2010) *Gait Posture 31(4)*, 415-419
[2]Barré et al. (2015) *J. Biomechanics 48(10)*, 1965-1971
[3]Gorton et al. (2009) *Gait Posture 29(3)*, 398-402
[4]Dutta et al. (2020) *J. Const Eng & Management 146(3)*
[5]Langley et al. (2019) *Gait Posture 71,*

PRINCIPAL FEATURES OF POSTURAL SWAY IN PERSONS WITH LOWER EXTREMITY AMPUTATION

Adam J. Yoder[1,2], Courtney Butowicz[1,3,4], Brad D. Hendershot[1,3,4], Brittney Mazzone[1,2], Shawn Farrokhi[1,2]
[1]DoD-VA Extremity Trauma and Amputation Center of Excellence, USA
[2]Naval Medical Center, San Diego, CA, USA, [3]Walter Reed National Military Medical Center, Bethesda, MD, USA
Email: adam.j.yoder.civ@mail.mil

Introduction

Instrumented sway assessments have proven useful to detect degraded postural control in a variety of clinical populations (e.g. Parkinson's, elderly, orthopaedic conditions) [1]. Persons with lower extremity amputation (LEA) typically have postural control deficits, yet sway assessments are uncommon in clinical practice [2]. One barrier may be the ever-increasing array of parameters proposed to best characterize sway, which can quickly confound interpretation [1,3]. To this end, dimensionality reduction has been used to identify concise, non-redundant sway parameter sets for uninjured persons [4], and for persons with neurodegenerative conditions [1], but not yet for persons with LEA. An added barrier to broader use may be the space and cost burden of platform-based sway systems, although efficient wearable sensors with comparable specificity and sensitivity exist, and may be more clinic-friendly [3]. This study aimed to identify principal features of postural sway in persons with unilateral LEA, measured using a single wearable sensor.

Methods

Participants with unilateral LEA (N=49, 29/20 male/female, 34/15 transtibial/transfemoral, 35±9 years of age, 8.5±9.1 years with LEA,) stood quietly on firm ground while wearing an accelerometer mounted over the sacrum (128Hz, Opal Gen2, APDM Inc, Portland, OR). Two 30-second trials were recorded: eyes open, and eyes closed. Triaxial accelerations were transformed to inertial medial-lateral (ML) and anterior-posterior (AP) components, on which the following were computed [3]: 95% fit ellipse area (AREA), ellipse rotation (ROT, assesses ML versus AP directed sway), mean velocity (VEL), root-mean-square (RMS), range (RNG), jerk (JERK, assess amount of underlying regulatory corrections), centroidal frequency (FC) and frequency dispersion (FD). A principal component (PC) analysis was then applied to reduce dimensionality of the correlated, 14-parameter set (MATLAB 2019a). Each parameter was centered, scaled by variance, and analyzed independently for eyes open versus closed [1,4]. PCs describing 90% cumulative variance were retained for inspection. Loadings between each PC and each original variable (i.e., correlations) were additionally computed to aid in selection of a reduced, non-redundant set of parameters most associated with the PCs.

Results and Discussion

Six PCs were necessary to describe at least 90% variance, in both eyes open and closed states. PC1 (41-43% variance) was most strongly loaded by AREA (R>.9), $RMS_{AP/ML}$ (R>.75), and $RNG_{AP/ML}$ (R>.7), which collectively measure size of the planar sway trajectory (Figure 1). $JERK_{AP/ML}$ also had strong PC1 loading (.55>R>.86, greatest in ML with eyes closed). JERK has prior shown high test-retest reliability and sensitivity in sway assessment of patients with Parkinson's [3], which alongside our findings, may also support utility in LEA sway assessment.

PC2 (16-24% variance), with eyes open, was most strongly loaded by ellipse ROT and FC_{AP} (R>.75), followed moderately by VEL_{ML}, $JERK_{ML}$, RMS_{ML}, RNG_{ML} (.5>R>.6). In contrast, with eyes closed, PC2 loading of these ML time-distance parameters decreased, shifting to PC1, while spectral parameters FC_{ML} and FD_{ML} increased, shifting from PC1 to PC2. This change is likely associated with increased dependencies on vision to modulate postural control in persons with LEA [2], highlighted here by a more distinct PC1/2 separation of spectral versus time-distance sway parameters in the ML direction.

PC3 (12-13% variance, not shown Figure 1) was exclusively loaded by ROT, FC_{ML}, and FD_{ML} (R>.7) with weak associations across all other parameters (R<.4), and negligible change in constituent parameters, with eye closure. PCs 4-6 were not strongly loaded by any single parameter, and were instead a weak mixture of FC, FD, and JERK (R<.4).

Prior work using a similar PC-informed feature selection approach, recommended RMS, ROT, FC, and FD to characterize sway of uninjured persons [1], and additionally VEL for patients with Parkinson's disease [4]. Considering this and our similar PC1-3 findings, we likewise **recommend RMS, ROT, FC, FD**, and additionally **JERK**, as a concise parameter set which captures principal features of sway in persons with LEA.

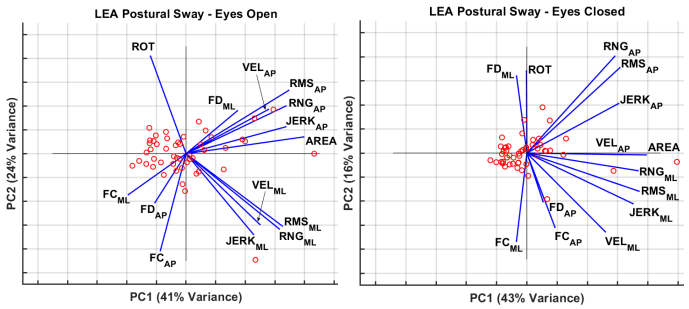

Figure 1: Bi-plots visualizing original variable weights along the first two of six principal components defining postural sway variance in persons with LEA. Length of each vector along each PC axis indicates the strength of association between parameters and PCs (i.e., loading/correlation). Co-directed vectors are positively correlated. Data are participants (**o**) projected into the PC1-2 subspace, which aids in identification of extreme cases.

Significance

Dimensionality reduction identified principal features of standing postural sway in persons with LEA, measured using a single wearable sensor. Continued study will evaluate whether these features can further classify persons with LEA, e.g. those at heightened risk for loss of balance and falls.

Acknowledgments

The views expressed are those of the authors and do not reflect official policy of U.S. Department of Army/Navy, Department of Defense, nor U.S. Government.

References

[1] Rocchi, L (2006) *Nueroscience Letters*. **394**:140-145.
[2] Ku, P. (2014) *Gait & Posture*. **39**:672-82.
[3] Mancini, M. (2012) *J Neuroeng Rehabil*. **9**:1-8.
[4] Rocchi, L (2004) *Med Bio Eng Comp*. **42**:71-79.

STEPPING KINEMATICS INDICATE MINIMAL DISRUPTIONS TO BALANCE CONTROL WHEN LINKING THE ARMS AND LEGS DURING TREADMILL WALKING

Daisey Vega[1*], H. J. Huang[2], and C. J. Arellano[1]
[1]Center for Neuromotor and Biomechanics Research, Dept. of Health and Human Performance, Houston, TX, USA
[2]Dept. of Mechanical and Aerospace Engineering, Orlando, FL, USA
email: *dvega2@cougarnet.uh.edu

Introduction

Coordinating the active use of the arms with the motion of the legs shows promise for gait rehabilitation [1]. In recent work, we physically linked the arms and legs during treadmill walking [2; Fig. 1] which significantly reduced the need for propulsion and the net metabolic power required to walk. However, we observed abnormal arm swing and greater collision forces, which may have disrupted the control of balance from step-to-step. Disrupting balance control could increase fear of falling, hinder walking recovery and/or lead to a direct fall. Therefore, understanding if and to what extent balance control was compromised would help determine if this arm-to-leg assistive approach could feasibly translate to clinical users. As indicators of balance, we quantified step width, step length, step time, and variability. We hypothesized that these indicators of balance control would remain the same when walking normally and when the arms and legs are physically linked during walking.

Methods

Eight young, healthy subjects (3F/5M) participated in the study. Subjects performed two randomized walking trials: (1) Normal and (2) Assisted (walking with the arm-leg pulley system) on a treadmill at 1.25 m/s. A twelve-camera motion capture system recorded the 3-D positions of reflective body markers (100 Hz) during the last 3 min of each 7 min trial. We calculated foot placement from the left and right heel marker positions and used 288 steps as the minimum number of steps for all subjects. We calculated average and standard deviation values for all step parameters. We then normalized step width and length by leg length (LL) and step time by $\sqrt{LL/g}$. Paired sample *t*-test (or the non-parametric Related Samples Wilcoxon Signed Rank test) were performed based on the assumption (or not) of normality.

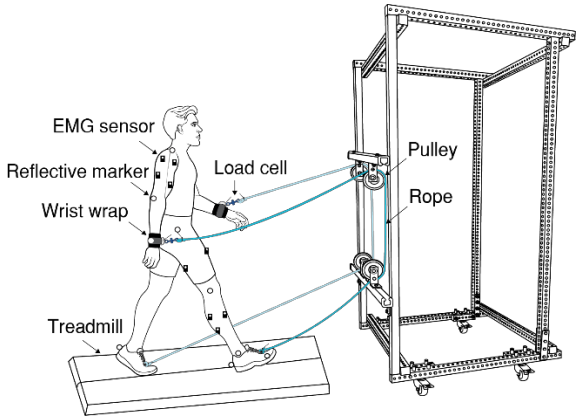

Figure 1: Arm-leg rope pulley system.

Results and Discussion

When compared to normal walking, we found that linking the arms and legs during assisted walking revealed no significant differences in step length and step time ($p > 0.05$). However, subjects increased their step width by 31% ($p = 0.012$, effect size = 0.630, Fig. 2). Despite adjustments in step width, the variability of step width and step length did not differ between conditions ($p > 0.05$). Step time variability, however, increased by 39% ($p = 0.008$, effect size = 0.012, Fig. 2).

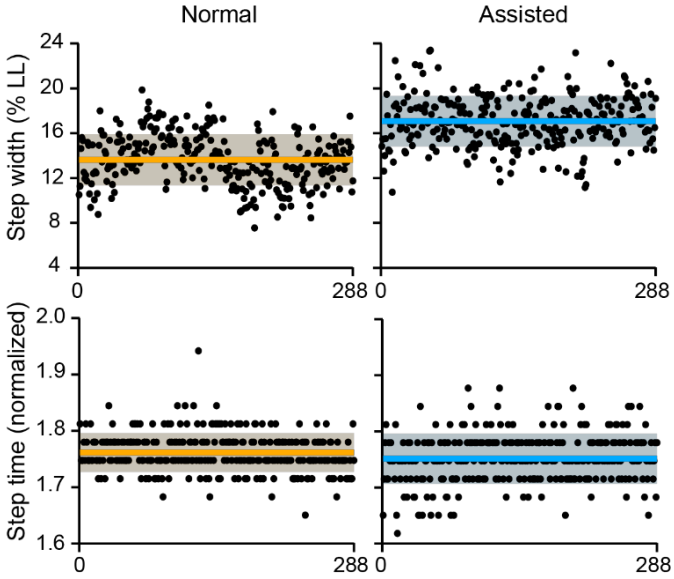

Figure 2: Representative data for both conditions ($n = 1$). Average and SD values shown as solid lines and shaded regions, respectively.

Our results show that linking the arms and legs altered both step width and step time variability. Thus, we reject our hypothesis. While these changes indicate differences at the $p < 0.05$ level, we look to their predictive ability of falling to understand their functional significance. Of all the kinematic variables, step time variability is the strongest predictor of falls in older adults (e.g. see Callisaya et al. 2011). For relative comparisons, the effect size of 0.012 for step time variability is ~39-fold smaller compared to the effect size of 0.47 in older fallers [3]. Therefore, the extent to which balance control was functionally compromised appears minimal. Taken together, these results suggest that linking the arms and legs may be a feasible strategy for gait rehabilitation.

Significance

Our results suggest that physically linking the arms and legs during walking reduces both the mechanical and metabolic demands placed on the legs [2], and it does so in the absence of major disruptions to balance control. These findings have inspired us to understand whether individuals recovering from a spinal cord injury could benefit from using our arm-leg treadmill assistive device during gait rehabilitation.

References

[1] Ferris DP et al. (2006). *Exerc Sport Sci Rev.*, **34**: 113-120.
[2] Vega D and Arellano CJ. (2021). *J Neuroeng Rehabil.,* In review.
[3] Callisaya et al. (2011). *Age and Ageing*., **40**: 481 – 487.

CALCULATING TRAILING LIMB ANGLE: VALIDATING ALTERNATE METHODS

Margo Donlin[1], N. Ray[2], and J. Higginson[1,2]
University of Delaware, Departments of [1]Biomedical and [2]Mechanical Engineering, Newark, DE, USA
Email: donlinm@udel.edu

Introduction

Trailing limb angle (TLA) is the sagittal plane angle between the back leg and the vertical during terminal stance [1]. TLA is commonly used as a surrogate measure of propulsion, which is required to increase walking speed and is therefore correlated with mobility and function in individuals post-stroke [2]. However, calculating TLA requires either motion capture with retroreflective markers or the use of inertial measurement units (IMUs) [3,4]. The current methods are time-consuming or require additional technology that may not be readily available.

Other gait parameters, like step length, can be calculated using the center of pressure (COP) data from force plates. Additionally, the anterior-posterior position of the center of mass (COM) can be estimated using the average of the COPs of both feet [4], while the vertical position can be estimated using a standardized estimate of the height [5]. The **purpose** of this analysis was to determine if estimates of TLA using COP and COM data were comparable to the true values of TLA. We **hypothesized** that the angle between the vertical and a vector joining the COM and the COP of the trailing limb would be equivalent to the true TLA calculated from motion capture.

Methods

Twenty-three young healthy subjects were recruited from the University of Delaware community (10 M/13 F: age 23 ± 4 years; height 1.72 ± 0.11 m; 69.82 ± 10.68 kg). Participants walked for one minute on a fixed-speed treadmill at their comfortable walking speed. Motion capture data (Motion Analysis Corp., CA, USA) and force data from the instrumented split-belt treadmill (Bertec Corp., OH, USA) were collected at 100 Hz and 2000 Hz, respectively. The study was approved by the University of Delaware's Institutional Review Board and all participants signed an informed consent.

TLA was calculated at peak propulsion in V3D (C-Motion Inc., MD, USA) as the angle between the vertical and the vector joining the greater trochanter and the fifth metatarsal head. Alternate TLA calculations, also at peak propulsion, were performed in MATLAB (MathWorks, MA, USA) by creating a vector joining the COP of the trailing limb and the estimated location of the COM. The location of the COM was estimated in two ways: (1) the unweighted average of the anterior-posterior position of the COP of each foot; and (2) the weighted average of the positions of the COP, weighted by the relative proportion of the vertical ground reaction force under each foot.

Distributions of TLA were tested for normality and compared using a one-way ANOVA, blocking for subject, with Tukey post-hoc testing as needed ($\alpha = 0.05$). Linear regressions of TLA on peak propulsive force were also calculated.

Results and Discussion

Both the unweighted calculation (14.4 ± 0.8°) and weighted calculation (10.6 ± 1.8°) significantly underestimated TLA compared to the calculation in V3D (19.0 ± 0.9°) (all $p < 0.001$). Because of these significant differences, the method of estimating TLA based only on force data may not be valid.

However, true TLA is correlated with propulsion ($R^2 = 0.47$, $p = 0.0003$), and the unweighted estimate was more strongly correlated ($R^2 = 0.77$, $p < 0.0001$) (Figure 1). The weighted estimate was also correlated ($R^2 = 0.18$, $p = 0.04$), although the correlation was weak and approaching insignificant.

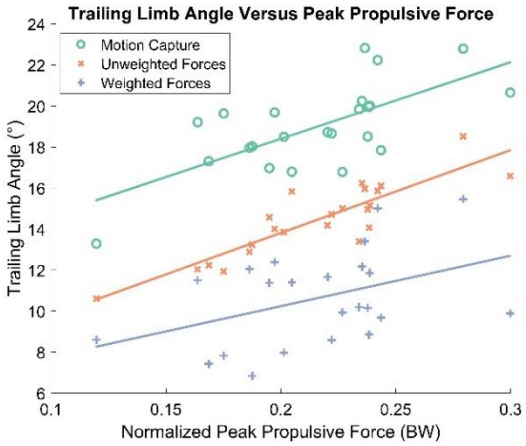

Figure 1: True TLA and estimated TLA versus peak propulsive force normalized to bodyweight (BW).

The slopes of both the V3D regression (40.4°/BW) and unweighted estimate regression (37.3°/BW) were similar, and both were significantly nonzero. The weighted estimate slope (24.6°/BW) was statistically nonzero but may not be useful because of its weak correlation. The unweighted estimate is approximately parallel to the true TLA and appears to preserve the relationship between TLA and propulsion. Although the unweighted calculation may not accurately estimate TLA, it may be responsive to changes in propulsion similar to the true TLA and could be used to indicate changes in gait mechanics.

Estimating the vertical position of the COM with generalized proportions may have introduced error. If the estimated COM was higher than the true COM, the estimated TLA would be less than the true TLA. Additionally, the COPs may not have aligned well with the fifth metatarsal heads, introducing further error into the estimated TLA.

Significance

Estimating TLA using COP and COM may be able to indicate changes in gait mechanics, especially peak propulsive force. The unweighted estimate of TLA may be used as a surrogate indicator of peak propulsion similar to the true value of TLA.

Acknowledgments

NIH P30 GM 103333 and the University of Delaware Helwig Mechanical Engineering Fellowship.

References

[1] Hsiao et al. (2015). *Hum. Mov. Sci.* 39:212-221.
[2] Lewek et al. (2019). *Clin. Biomech.* 67:115-118.
[3] Miyazaki et al. (2019). *Biomed Res. Int.*
[4] Ray et al. (2018). *J. Biomech.* 78:143-149.
[5] Winter (2009). *Biomechanics and Motor Control of Human Movement*.

INCREASED VASTUS LATERALIS ACTIVATION AT FASTER WALKING SPEEDS PRESERVES STRUT-LIKE MUSCLE MECHANICAL BEHAVIOR

Amanda E. Munsch[1], Meaghan E. Quinn[1], Brian Pietrosimone[2], and Jason R. Franz[1]
[1]Joint Department of Biomedical Engineering, UNC Chapel Hill and North Carolina State University, Chapel Hill, NC, USA
[2]MOTION Science Institute, Department of Exercise and Sport Science, UNC Chapel Hill, Chapel Hill, NC, USA
email: aemunsch@live.unc.edu

Introduction

Faster walking speeds associate with better biochemical and radiographic outcomes related to the progression of osteoarthritis in older adults and in individuals with knee injuries. It has been suggested that individuals slow their walking speeds to reduce knee joint loading and that reduced joint loading facilitates cartilage degeneration and osteoarthritis progression [1]. The quadriceps muscles decelerate body mass during the early stance phase of walking (i.e., weight acceptance) and contribute more than any other muscle group to cartilage loading. Quadriceps muscle forces during functional movements cannot be directly measured. Instead, determinants of force production such as muscle activation or knee joint moments are often used as convenient surrogates. However, despite widespread recognition that muscle force is also governed by contractile state (*i.e.*, fascicle length) [2], no study to our knowledge has quantified how walking speed affects quadriceps fascicle length change behavior. Our purpose was to address this gap in the context of more well-documented changes in muscle activation and knee joint moments.We recently reported that the vastus lateralis (VL) operates with isometric to slight concentric action during weight acceptance at preferred walking speed [3]. Here, we hypothesized that the VL in healthy young adults would produce force more eccentrically in early stance at faster walking speeds with concomitant increases in muscle-tendon unit (MTU) lengthening, peak knee extensor moment (pKEM), and activation.

Methods

Ten young participants without knee injury or evidence of osteoarthritis (6 females, age: 24.0 ± 2.6 years) completed 2-minute walking trials at their preferred speed (1.35 ± 0.12 m/s) and at 0.75 m/s and 1.75 m/s. We recorded ground reaction forces (GRFs), 3D motion capture, and the activity of seven muscles spanning the left knee. We normalized muscle activations to the activity during the preferred walking speed trial. We simultaneously used a 60 mm ultrasound transducer to record B-mode images through a longitudinal cross-section of participants' right VL. We calculated joint kinematics and kinetics using inverse dynamics. We manually estimated VL fascicle length at heel-strike and the instant of pKEM using an opensource ultrasound analysis tracking routine [4]. Repeated measures ANOVAs evaluated the effects of walking speed on main outcome variables: pKEM, average VL activation during weight acceptance, VL fascicle length at heel-strike, and change in (i) VL MTU length and (ii) VL fascicle length during weight acceptance, defined as the time between heel-strike and the instant of pKEM.

Results and Discussion

We found a significant main effect of walking speed on pKEM, VL activation, and change in VL MTU length (p-values ≤0.001). Post-hoc comparisons revealed differences between both walking speeds compared to preferred speed for these three variables (Fig. 1 A, C, D). However, contrary to our hypothesis, we found no significant effects of walking speed on change in VL fascicle length (p=0.53) or length at heel-strike (p=0.30, Fig. 1 A-B). We conclude that at faster walking speeds, the quadriceps muscles receive increased activation to meet the greater mechanical demands for weight acceptance and body mass deceleration with each step.

Significance

This study provides a more complete neuromuscular representation of quadriceps force production during walking. Specifically, to increase walking speed, young adults increase quadriceps activation to resist muscle lengthening and maintain nearly strut-light mechanical behavior. As a result, nearly isometric to slight concentric muscle action alludes to a disproportionate role of series elastic tendon lengthening to accommodate increased MTU lengthening at faster walking speeds. This study establishes an important benchmark for comparison to individuals with known quadriceps strength deficits, inhibition, and/or heightened risk for the development of osteoarthritis.

Acknowledgments

Supported by a grant from NIH (R21AR074094).

References

[1] Luc et al (2018). *Clin Biomech*, 60.
[2] Hug et al (2015). *J Orthop Sports Phys*, 45.
[3] Munsch et al (2020). *PeerJ*, 8:e9509.
[4] Farris and Lichtwark (2016). *Comput Methods Programs Biomed*, 128.

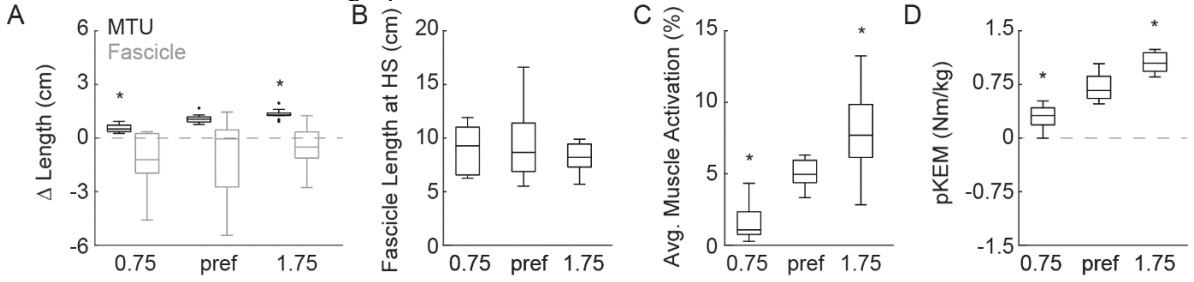

Figure 1: Primary outcomes as a function of walking speed. Asterisks (*) indicate significant pairwise difference from preferred speed (p<0.05). MTU, fascicle, and activation outcomes are reported for the vastus lateralis. HS: heel-strike.

MANIPULATING ADAPTIVE TREADMILL CONTROL TO INCREASE PROPULSIVE IMPULSE

Kayla M. Pariser[1], M. Donlin[2], K. Downer[1], and J. Higginson[1,2]
Departments of [1]Mechanical and [2]Biomedical Engineering, University of Delaware, Newark, DE, USA
email: pariserk@udel.edu

Introduction

Walking speed is strongly correlated to functional ability, independence, and quality of life [1]. Consequently, increasing walking speed is a common goal of rehabilitation following neuromuscular injury or disease onset [2]. Increases in propulsive force are strongly associated with increases in walking speed [3].

Treadmill gait training is a commonly used rehabilitation strategy but exhibits mixed effectiveness, possibly due to the failure to target individual-specific impairments. To address this concern, we have developed a novel adaptive treadmill (ATM) that adjusts belt speed by responding in real-time to changes in step length, propulsive impulse, and center of mass (COM) position [4]. The **objective** of this study is to determine if we can promote increased propulsion by adjusting the relative importance of propulsive impulse in the ATM control function. We **hypothesized** that as the coefficient on propulsive impulse increased relative to the coefficient on step length, propulsive impulse would increase while speed would be maintained.

Methods

Twenty-two adults with no history of neuromusculoskeletal injury or disease (11 male, 24 ± 3 years, 1.72 ± 0.11 m, 76.52 ± 11.29 kg) walked on an instrumented split-belt treadmill (Bertec Corp., OH, USA; 2000 Hz) at their self-selected (SS) walking speed with four conditions of ATM control for one minute each. The ATM controller calculates the belt speed for the subsequent time step (v_{i+1}) via the sum of the weighted intermediate speeds due to user step length ($v_{Avg,SL}$), propulsive impulse ($v_{Avg,PI}$), and COM position ($COM_{Pos}{}^2$):

$$v_{i+1} = v_i + \alpha\left(v_{\mathrm{Avg,SL}}\right) + \gamma\left(v_{\mathrm{Avg,PI}}\right) - \frac{(\alpha+\gamma)}{2}(v_i) \pm \beta\left(COM_{Pos}{}^2\right)$$

where α and γ are unitless coefficients that dictate the importance of step length and propulsive impulse, respectively, on determining the walking speed. The coefficient on the COM term, β, remained unchanged for this study. The four conditions were presented in random order: Baseline (γ=α=1.5), Level 1 (γ=1.25α), Level 2 (γ=1.5α), Level 3 (γ=1.75α). Average walking speed, peak propulsive and braking forces, and propulsive, braking, and net impulses were calculated. If normally distributed, a one-way ANOVA (α=0.05) blocked by subject and post-hoc Tukey HSD tests were used to detect significant differences between conditions.

Results and Discussion

The results support our hypothesis that adjusting the ATM control function could promote increased propulsive impulse without altering walking speed. Participants chose similar walking speeds across all four conditions (Fig 1A). Average propulsive impulse increased significantly from the baseline to Levels 2 and 3, braking impulse was similar across all four conditions, and net impulse trended toward net positive as γ was increased relative to α (Fig 1B). Peak propulsive and braking forces were not significantly different between conditions (not shown). Since propulsive impulse increases but peak propulsive force does not, this suggests that as the coefficient on propulsive impulse, γ, is increased, users spend a greater duration of stance phase in propulsion versus braking to achieve their desired speed. However, the slight decrease in walking speed from Level 1 to Level 3 may imply that there is a threshold at which increases in γ may eventually significantly decrease walking speed. This threshold likely differs between individuals.

To our knowledge this is the first study to demonstrate that coefficients in an ATM control function combining propulsive force, gait parameter, and position-based control can be modified to promote increased propulsive impulse without detrimental effects on speed. Therefore, we anticipate that implementing similar increases in γ during post-stroke gait rehabilitation may promote increased propulsion, improving the efficacy of the ATM as a rehabilitation tool.

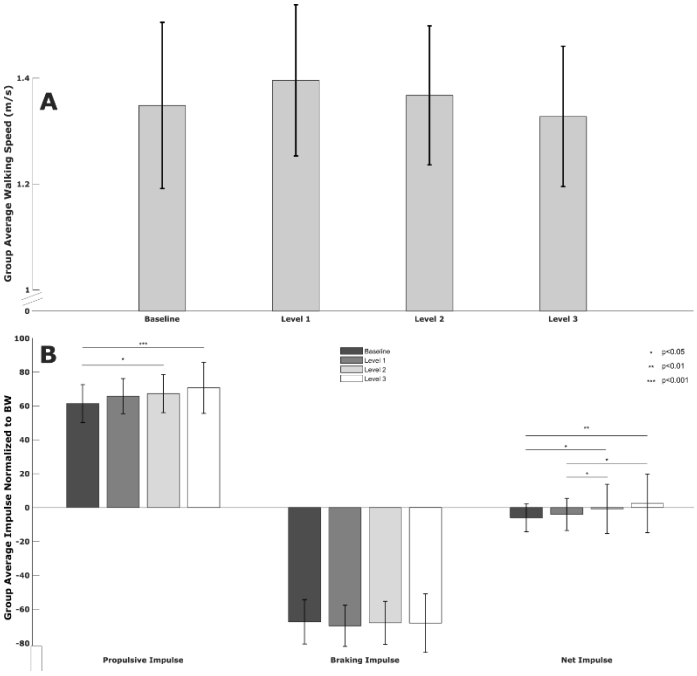

Figure 1: Average ± SD SS walking speed (A) and propulsive, braking, and net ground reaction force impulses with all ATM variations (B).

Significance

The ATM can be modified to encourage users to increase propulsion while maintaining a consistent walking speed. In future work, we will customize the controller to target individual-specific impairments and therapeutic goals for stroke survivors.

Acknowledgments

Funding: NSFGRFP, NIH P30 GM 103333, and University of Delaware Helwig Mechanical Engineering Fellowship.

References

[1] Fritz S., Lusardi M., *J Geriatr Phys Ther.*, 2009.
[2] Abellan Van Kan G et al., *J Nutr Health Aging.,* 2009.
[3] Hsiao H et al., *J Biomech.,* 2016.
[4] Ray NT et al., *J Biomech*., 2018.

FORCE-TIME BASED PERFORMANCE MEASURES IN SPORT CLIMBING

Harald Penasso[1] & Alena M. Grabowski[1,2]
[1]University of Colorado Boulder, Boulder, CO, USA, [2]VA Eastern Colorado Healthcare System, Denver, CO, USA
email: harald.penasso@colorado.edu

Introduction

Characteristics of reaction forces reflect an athlete's ability to move. Sport climbing assessments are typically isometric and upper limb mechanical power output is rarely assessed. While force transmission from the lower to upper body and body position and technique are essential in climbing, performance is often constrained by the physiological limits of the muscles of the arms and shoulders. In an ongoing project we are measuring force during pull-up-dynos and calculating 20 upper body climbing-specific performance measures per test. As a first step, we will select the greatest contributing measures of principal component analysis (PCA) and use correlation analysis to check for multicollinearity. By relating these to competition results in the future, we aim to establish a tool for assessing climbing ability.

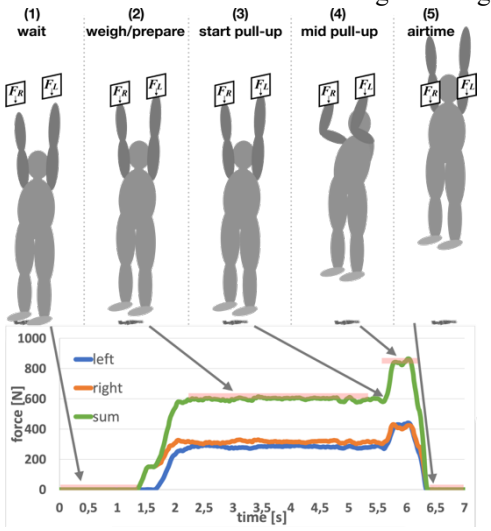

Figure 1: Sketch of the hangboard test (top) and measured left (F_L) and right (F_R) forces (bottom). (1) Initial tare, (2) establish stable position, measure bodyweight, (3) initiate pull-up, (4) dyno as high as possible, (5) contact to holds lost. Measures calculated from phase (4).

Methods

Force-time data were obtained from 2 youth (14–18 yrs) training sessions (22 elite climbers; tests from 21 M, 8 F). Each subject performed a pull-up-dyno test, which is a movement similar to a maximum-effort pull-up that transitions into reaching, where the athlete aims to "jump"/dyno as high as possible (Fig. 1). We used a custom-built split hang-board with rectangular 2 cm deep crimp wood-holds that were screwed onto plates connected to loadcells (HLC A1 C3 220 kg). Left and right forces were recorded at 91.5 ± 22.7 Hz, resampled to 200 Hz, and filtered with a Butterworth low pass 20 Hz cut-off filter. We summed left and right forces to calculate pull-up height (gained during contact period), velocity (maximum [max], mean, take-off), force/kg (F_{max}, F_{mean}), rate of force development (RFD; mean 0–50 ms, mean dF/dt, median dF/dt, max dF/dt), max power/kg, impulse/kg (acceleration phase, total), work/kg (acceleration phase, total), time series signal complexity, and a smoothness factor "parabola vs. force" [1]. We compared left to right forces to calculate symmetry index, complexity of left vs. right signals, and mean absolute difference (Python 3.8.5). We used PCA, Pearson correlation, and linear models for data analysis (R 4.0.3).

Results and Discussion

Ten measures contribute most to the first 5 principal components (PCs), which explain 87% of the dataset variance. The measures of PC1 and PC2 that contribute most are based on force-time integrals and contain similar information (Table 1).

	var.	main measure(s)	cos^2	contr.	corr.
PC1	52.7%	max velocity	0.97	9 % *each*	$r \geq 0.99$ $p \leq 0.01$
		acceleration phase impulse/kg	0.96		
		max. power/kg	0.96		
PC2	12.5%	pull-up height	0.49	19 % *each*	$r > 0.99$ $p \leq 0.01$
		total work	0.47		
PC3	7.8%	RFD 50 ms	0.35	22 % *each*	$r = 0.12$ $p = 0.55$
		RFD max dF/dt	0.33		
PC4	7.6%	smoothness factor	0.54	35 %	–
PC5	5.9%	left/right complexity	0.39	33 %	$r = 0.09$ $p = 0.66$
		symmetry index	0.27	23 %	

Table 1: First 5 principal components (PCs), variance explained (var.), most prominent measure(s), quality of representation (cos^2), contribution (contr.), and mean correlation (corr.) between PC measures.

Using the most contributing measure of the first 5 PCs in a linear model explained 54% of the dataset variance ($r^2_{adj} = 0.43$, $p \leq 0.01$), while combining those of the first 3 PCs explained 49% of the variance ($r^2_{adj} = 0.42$, $p \leq 0.01$). To represent as much of the data from the dyno test, one measure of the first 3 PCs should be included in climbing ability assessments. Force-time curve shape (PC4) and left/right force comparison (PC5) add symmetry and coordination information which is relevant for movement quality and injury prevention [2] but do not explain much more variance.

Figure 2: Correlation (r) matrix shows uncorrelated key features.

Significance

Impulse generation capacity, RFD, coordination of force production, and left vs. right force symmetry are the key components of this set of performance measures (Fig. 2). Relating these features to performance and monitoring changes during the season will help coaches and athletes to improve the effectiveness of training.

Acknowledgments

Team ABC Boulder CO; BlocHouse Graz AUT; Dr. B. Lechner

References

[1] Fuss & Niegl. *Sports Tech.* 1(6), 301–303, 2008.
[2] Mersmann, Bohm & Arampatzis. *Front Phys*. 8(987). 2017.

IMU-CAMERA FUSION FOR ESTIMATING KNEE ADDUCTION AND FLEXION MOMENTS

Tian Tan[1]*, Dianxin Wang[1], Peter B. Shull[1], Eni Halilaj[2]
[1]School of Mechanical Engineering, Shanghai Jiao Tong University, Shanghai, China
[2]Department of Mechanical Engineering, Carnegie Mellon University, Pittsburgh, USA
email: * alantantian@sjtu.edu.cn

Introduction

The knee adduction moment (KAM) and knee flexion moment (KFM) are important gait parameters for a variety of biomechanical applications, including knee osteoarthritis. Assessment of KAM and KFM are traditionally performed with force plates and optical motion capture (OMC) systems in specialized laboratories. Wearable sensors and computer vision can potentially advance the assessment of KAM and KFM from laboratories to natural environments, but new algorithms are still needed to extract meaningful outcomes from these new modalities. In this study, we aimed to build new deep learning models for estimating KAM and KFM from fusion of wearable inertial measurement units (IMUs) and smartphone cameras.

Methods

Seventeen subjects (all male; age: 23.2±1.1; height: 1.76±0.06m; mass: 67.3±8.3kg;) wore eight IMUs (SageMotion, USA) at the trunk, pelvis, both thighs, both shanks, and both feet to collect data at 100 Hz. Two smartphone cameras (iPhone 11, Apple Inc., USA) were placed vertically on the back and right side of the subject to record video at 120 Hz. Ground-truth KAM and KFM were computed using marker data collected by an OMC system (Vicon, UK) and ground reaction force (GRF) data collected by an instrumented treadmill (Bertec, USA). KAM and KFM were normalized by body weight (BW) times height (BH). Subjects performed a baseline trial and then three subsequent trials with modification of foot progression angle, step width, and trunk sway angle.

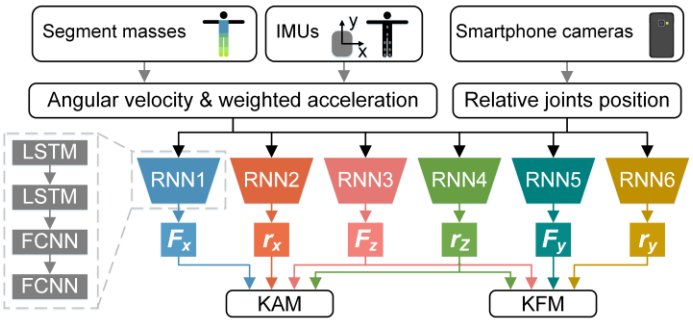

Figure 1: Architecture of KAM and KFM Estimation Model. Features were extracted from raw data and fed into six RNNs to estimate knee moment components. KAM and KFM were then computed via the cross-product approach [2].

A generalizable model (Figure 1) was developed to estimate KAM and KFM based on three steps: 1) extraction of angular velocity and weighted acceleration from IMU data and shoulder, hip, knee, and ankle joint positions from camera data using OpenPose [1], 2) estimation of GRF and lever arm components from six deep recurrent neural networks (RNNs), and 3) computation of KAM and KFM via the cross-product approach [2]. Each RNN consisted of two bi-directional long short-term memory (LSTM) layers and two fully-connected (FCNN) layers. Apart from the proposed model, an IMU-based model and a camera-based model were built for comparison. Repeated measures analyses of variance (RM-ANOVA) were used to determine if fusion was significantly ($p<0.05$) more accurate than IMUs alone or cameras alone.

Results and Discussion

The RMSE, rRMSE, and correlation coefficient of the IMU-camera fusion model across all walking trials were 0.52%BW·BH, 7.0%, and 0.91 for KAM estimation and 0.68%BW·BH, 5.8%, and 0.94 for KFM estimation. For both KAM and KFM estimation, IMU-camera fusion was significantly more accurate than either IMUs or cameras alone (Figure 2). For KFM estimation, IMUs alone was significantly more accurate than cameras alone (Figure 2).

One possible reason for IMU-camera fusion being more accurate is that the complementary nature of IMU and camera provided more comprehensive kinematic information for kinetic estimation. Comparing these two sensing approaches, IMU might be less accurate in estimating body segment pose due to drift, while camera might be less accurate in tracking movement direction and speed due to small pixel differences between consecutive frames.

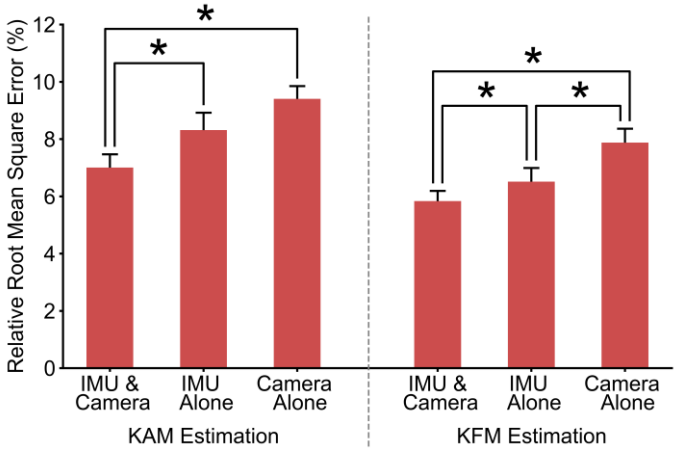

Figure 2: Model Performance by Data Source. IMU and camera fusion significantly (*) improved KAM and KFM estimation accuracy.

Significance

IMU and camera fusion can enable more accurate estimation of KAM and KFM during walking. The code and trained models are available on GitHub (https://github.com/TheOne-1/KAM_and_KFM_Estimation). Users can download and implement our models to enable knee moment estimation in various environments outside of traditional motion capture biomechanics labs such as clinics, homes, or gymnasiums.

Acknowledgments

This work was supported by the National Natural Science Foundation of China under grant 51875347.

References

[1] Z Cao et al. (2019). *IEEE PAMI*, **43(1)**: 172-186.
[2] DJ Rutherford et al. (2018). *J. Biom.*, **78**:150-154.

PROLONGED LOAD CARRIAGE IMPACTS MAGNITUDE AND VELOCITY OF KNEE ADDUCTION BIOMECHANICS

Salverda, G.J., Drew, M.D., Krammer, S.M. and Brown, T.N.
Center for Orthopaedic and Biomechanics Research, Dept. of Kinesiology, Boise State University, Boise ID USA
email: gaervynsalverda@u.boisestate.edu

Introduction

Service members are greater than twice as likely to develop premature knee osteoarthritis (OA) than the general population. This elevated OA risk may be attributed to increases in knee adduction biomechanics adopted during load carriage that are implicated in the disease pathogenesis[1]. Although the magnitude of knee adduction angle and moment increase during prolonged load carriage task[2], it is unknown whether service members exhibit similar increases in knee adduction velocity, a potential knee OA risk factor, as it encompasses both speed and direction, when walking with body borne load. Both knee varus alignment and varus thrust, i.e., rapid lateral (i.e., adduction) motion during the first 16% of stance[3], may be precursors to knee biomechanics related to joint OA. But it is currently unknown if knee adduction velocity increases during prolonged load carriage, a common military task, or whether knee varus alignment or varus thrust are related to increases in velocity. We hypothesized that velocity of knee adduction velocity would increase with body borne load and walk duration, and participants that present varus alignment or thrust would exhibit greater increases in knee adduction velocity.

Methods

Seventeen (11 male/6 female) participants (23.2 ± 2.9 yrs, 1.8 ± 9.4 m, 71.0 ± 12.1 kg) had knee adduction biomechanics quantified during a prolonged walk task with three body borne loads (0 kg, 15 kg, and 30 kg). Participants wore a weighted vest that was systematically adjusted for each load, while they walked 1.3 m/s ± 5% for 60 minutes. During the walk task, three trials of dominant limb biomechanical data were collected at minutes 0, 30, and 60. At each time point, knee adduction angle and moment were calculated in Visual 3D (C-Motion, Rockville, MD) from filtered (12 hz) ground reaction force and marker data.

Custom MATLAB code (Mathworks, Natick, MA) was used to calculate velocity (average and maximum) of knee adduction angle (KAA) and moment (KAM), and varus thrust. Specifically, average velocity was the change in adduction magnitude from initial contact to peak of stance (or first 16% of stance) divided by the corresponding change in time. Static knee alignment was also calculated as the joint frontal plane projection angle (ab-adduction) with participants in anatomical position.

For statistical analysis, participants were defined as varus thrust (VT, n=8), those that exhibited 2.5 degrees or more of varus thrust at minute 0 with the 0 kg load, or control (CON, n=9). Each knee adduction variable was submitted to a repeated measures ANCOVA to test the main effect and interaction between body borne load (*0 kg, 15 kg, and 30 kg*), time (*minutes 0, 30, and 60*), and group (*VT and CON*). Static alignment was considered a covariate. A Bonferroni correction was applied to significant pairwise comparisons, and all statistical analysis were performed in SPSS (IMB, Armonk, NY), with alpha $p < 0.05$.

Results and Discussion

In partial support of our hypothesis, the VT group exhibited larger and faster knee adduction, and potentially greater knee OA risk than the CON group. Specifically, the VT group had greater maximum KAA velocity, and magnitude and average velocity of varus thrust than the CON group, but only with 0 and 15 kg loads ($p<0.05$). Although the VT group exhibited knee adduction biomechanics related to knee OA with the light body borne loads, similar group differences were not observed with the heavy, 30 kg load ($p<0.05$). In fact, with the 30 kg load, the VT group decreased magnitude and velocity of knee adduction, while the CON group increased knee adduction.

The addition of body borne load led to larger and faster KAM (**Fig. 1**), while walk duration increased varus thrust. Magnitude and maximum velocity of KAM were greater with the 15 kg ($p=0.002$; $p=0.014$) and 30 kg ($p=0.02$; $p=0.012$) loads compared to the 0 kg condition. Considering KAM is a correlate for loading of the medial knee joint compartment, walking with heavy body borne load may increase impact forces transmitted to the joint and possibly elevate knee OA risk. Prolonged walking led to increases in the abrupt lateral knee motion related to OA development at the joint, as varus thrust magnitude was greater at minutes 30 ($p=0.038$) and 60 ($p=0.050$) compared to minute 0.

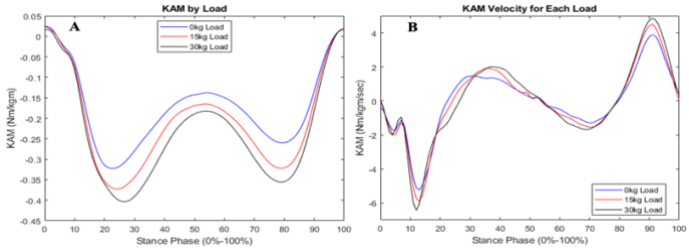

Figure 1: Depicts mean magnitude (A) and velocity (B) of knee adduction joint moment during stance (0-100%) for each load.

In conclusion, prolonged load carriage increases knee adduction biomechanics related to knee OA, and those with varus thrust may be at greater risk – particularly when walking with light loads. But, walking with heavy loads may increase knee adduction for all participants. Static knee alignment, however, did not currently impact knee adduction biomechanics during the prolonged load carriage task.

Significance

Prolonged load carriage, particularly with the heavy, 30 kg load, increased knee adduction velocity and magnitude, potentially elevated risk of knee OA development among service members. Screening service members for varus thrust may lead to a reduction in the risk for premature knee OA among military populations, but training protocols that decrease knee adduction during load carriage for all service members are needed.

Acknowledgments

Funding was provided by MW CTR-IN/NIGMS (Award #2U54GM104944)

References

1. Mahmoudian, A. *et al. Gait Posture* **57**, (2017).
2. Drew, M. D. *et al. Gait Posture* **84**, (2021).
3. Chang, A. H. *et al. Osteoarthr. Cartil.* **21**, (2013)

EFFECT OF UNILATERAL LOADING ON GAIT PATTERNS OF TREADMILL WALKING IN ADULTS

Haneol Kim[1], Matthew Beerse[2], & Jianhua Wu[1]
[1]Georgia State University
[2]University of Dayton
email: *hkim162@student.gsu.edu

Introduction

Walking is a complex locomotion regulated by the human locomotor control system. A typical gait requires appropriate muscle activation and joint coordination [1]. External ankle load increases the moment of inertia of the lower extremities and has been used to study gait adaptations to manipulated mechanical properties. Specifically, the use of unilateral loading allows examining the asymmetry between the loaded and unloaded sides during walking.

This study aimed to investigate the effect of unilateral ankle loading on the kinetic and spatiotemporal parameters between male and female adults during treadmill walking. We hypothesized that both male and female adults display similar kinetic and spatiotemporal parameters such that the loaded side will show a longer step length and swing time and a higher impulse, particularly during push-off, than the unloaded side [2].

Methods

Twenty healthy young adults (aged 18 to 35 years, ten males and ten females) participated in this study. The male subjects had a higher body mass, height, and leg length than the female subjects. A Vicon motion capture system and a Zebris FDMT-S instrumented treadmill were used to collect kinematic and kinetic data, respectively, during treadmill walking. Participants first walked overground at their self-selected speed three times, and the average speed was used for treadmill walking. Participants completed a 5-minute treadmill walking trial at each of four load conditions in a random order: A0, A25, A50, and A75, representing no load and ankle load equal to 0.8%, 1.6%, and 2.4% of body weight, respectively. Spatiotemporal variables included step length normalized by leg length and swing time. Kinetic variables included braking and propulsive impulses normalized by body weight. A three-way (2 group × 4 load × 2 side) mixed ANOVA was conducted at a significance level of α=0.05. Post-hoc pairwise comparisons with Bonferroni adjustments were performed when necessary.

Results and Discussion

Both the males and females tended to increase normalized step length and swing time with ankle load (Fig. 1). The loaded side demonstrated the longer normalized step length than the unloaded side for both groups. Statistical analysis revealed that there was a load effect (p=0.006) and a side effect (p=0.003), but not a group effect in normalized step length. While swing time increased with ankle load on the loaded side, it maintained similar values on the unloaded side across the load conditions. There was a load by side interaction but not a group effect in swing time (p<0.001). These results indicate that external ankle load did not induce gender differences in the selected spatiotemporal parameters during walking.

Normalized braking and propulsive impulses showed similar values across load conditions; however, the male subjects had smaller braking and propulsive impulses than the female subjects. Statistical analysis revealed a group effect in both impulse variables (p<0.001) and a side effect in normalized propulsive impulse (p=0.012). Note that the average walking speed was 1.34 m/s in the males and 1.19 m/s in the females. These impulse results suggest that the smaller impulse values may be due to a faster walking speed in the males than the females. In addition, both the males and females showed asymmetry between the loaded and unloaded sides only in the propulsive phase but not the braking phase of walking, suggesting different propulsive needs between the two sides during push off.

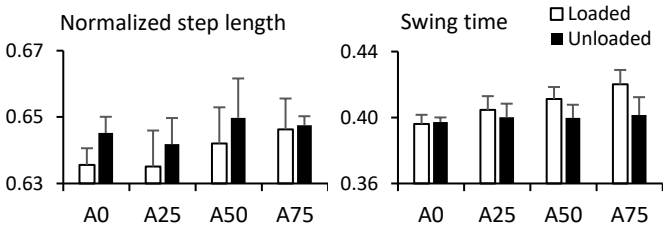

Figure 1: Mean and SD of normalized step length and swing time (in second) at different loading conditions

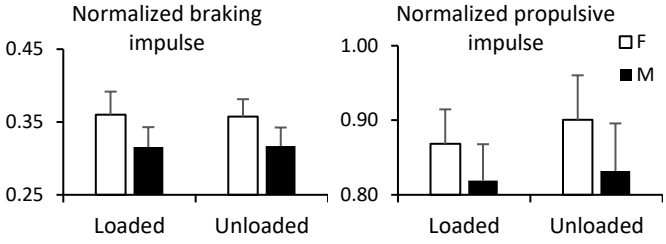

Figure 2: Mean and SD of normalized braking impulse and propulsive impulses between males and females across four loading conditions

Significance

This study demonstrated that external load affects spatiotemporal and kinetic variables as expected. However, manipulating ankle load induced different kinetic patterns but similar spatiotemporal variables between male and female adults. It will be interesting to investigate if muscle activation shows similar trends between males and females. Our findings provide essential information to understand the effect of physical rehabilitation with different loads on gait outcomes, which can help improve the rehabilitation effectiveness. Clinicians may use our findings to develop and implement an intervention protocol with ankle load to improve the locomotor function of people with disabilities such as limb length discrepancy or amputation.

Acknowledgments

We are grateful to all the participants for their participation.

References

1. Noble and Prentice. (2006). Exp Brain Res, 169(4), 482-495.
2. Wu and Ajisafe. (2014). Gait Posture, 39(1), 241-246.

Effect of Changes in Estimated Pelvic Tilt on Hip Joint Forces

[1]Karim Ismail, [2]Cara L Lewis
[1]Department of Biomedical Engineering, Boston University, Boston, MA, USA
[2]Department of Physical Therapy & Athletic Training, College of Health & Rehabilitation Sciences: Sargent College, Boston University, Boston, MA, USA
Email: kismail@bu.edu Web: http://sites.bu.edu/movement/

Introduction

Femoroacetabular impingement syndrome (FAIS) is a disorder characterized by specific bony morphology of the femur and/or acetabulum, which may lead to hip pain. People with FAIS walk with more anterior pelvic tilt [1], and their pain may result from excessive anteriorly-directed joint forces from the femur onto the acetabulum [2]. Previous approaches using musculoskeletal modeling to calculate joint forces, however, may inaccurately assume that each participant stands in a neutral position when stationary. In turn, information on parameters that affect joint forces (such as pelvic tilt) is lost in kinematic data used to estimate joint loading. As a proof of concept, we computationally altered the pelvic tilt of six healthy individuals to observe its effect on hip joint forces.

Methods

Motion (100Hz) and force (1000Hz) gait data were collected and processed using Vicon (Vicon Motion Systems Ltd, Centennial, CO). These data were processed in Visual3D (C-Motion, Inc, Rockville, MD), which scaled anatomical segments based on marker locations and tracked joint motion. Each participant's pelvic orientation was adjusted by ±5 degrees and ±10 degrees of tilt at all time points. Five analyses were performed per individual: neutral tilt, two posterior (positive) tilts, and two anterior (negative) tilts. Force and gait data of each orientation were imported into OpenSim 3.2 [3], and a generic musculoskeletal model was scaled. To calculate joint moments and muscle activation, the Residual Reduction and Computed Muscle Control tools were used. These results were used to estimate forces from the femur to the acetabulum in the anterior, superior, and medial directions in the pelvic reference frame. Data were normalized from heel-strike to ipsilateral heel-strike and adjusted for bodyweight in MATLAB. Forces of both limbs were averaged, and statistical parametric mapping software [4] was used to determine if the differences in joint loads were significant between pelvic orientations.

Results and Discussion

A more anterior pelvic tilt led to a reduction in anterior hip joint forces (Figure 1A) at all points in the gait cycle ($p < 0.001$). In the superior direction, there was a small increase in joint forces in the terminal swing phase with a 10-degree anterior tilt ($p = 0.05$). In the medial direction (Figure 1C), there was an increase in joint forces throughout most of the stance phase ($p < 0.001$) in both anterior orientations. A 10-degree anterior tilt slightly increased the resultant forces (Figure 1D) in the terminal swing phase ($p = 0.036$). Those differences were not as prominent in the femoral reference frame; although the muscle orientations change to the same extent in both frames, the perspective is also altered when tilt is adjusted in the pelvic frame. Our findings suggest that altering pelvic tilt affects force in different ways; despite the decrease in anteriorly-directed forces with anterior tilt, there was a simultaneous increase in the superior and medial directions. A more anterior pelvic orientation may reduce pain in people with FAIS, although further research is needed to test this hypothesis. Thus, our approach will help simulate different conditions in OpenSim, and allow for more realistic comparisons between groups.

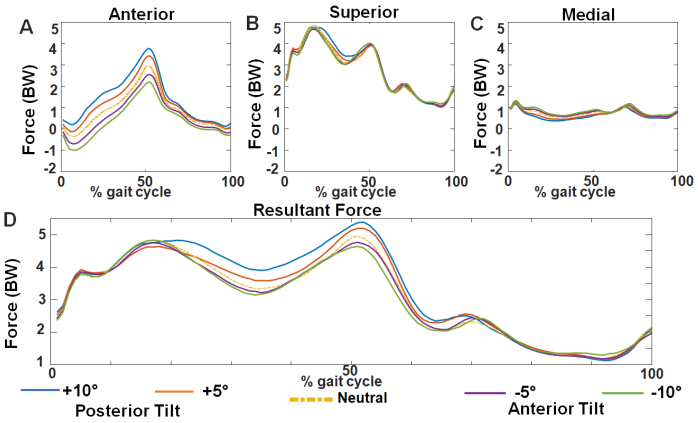

Figure 1: Joint forces in the A) anterior, B) superior, C) medial directions in the pelvic reference frame. D) Resultant (net) forces.

Significance

Computational changes in pelvic tilt should be considered in future analyses to observe how bodily orientations can alleviate or exacerbate conditions such as FAIS. These findings can be applied in future studies that compare the joint forces of healthy individuals to those of people with FAIS. Such studies can inform researchers on gait alteration strategies or the design of assistive devices to manage the onset of FAIS.

Acknowledgments

Data were collected and analyzed with the assistance of members of the Boston University Human Adaptation Laboratory. Research reported in this publication was supported by NIH NIAMS (R21 AR061690 and K23 AR063235).

References

1. Lewis et al. *J Orthop Sports Phys Ther*. **48(8)**, 649-658. 2018.
2. Lewis et al. *J Biomech*. **48(1)**, 181-185. 2015.
3. Delp et al. *IEEE Trans Biomed Eng*. Nov. **54(11)**, 1940-50. 2018.
4. Pataky. *J Biomech*. **43**, 1976-1982. 2010.

QUANTIFYING EFFECTS OF KNEE SAVERS ON KNEE JOINT LOADING IN DEEP SQUATTING POSTURES

John Z. Wu*, Kevin Moore, Robert E. Carey, Ashley Hawke, Liying Zheng, Christopher M. Warren, Scott P. Breloff
National Institute for Occupational Safety and Health, Morgantown, WV, USA. *Email: jwu@cdc.gov

Introduction

During some occupation activities, workers need to perform deep squatting tasks. Epidemiological studies indicate that these unfavourable knee postures are associated with knee osteoarthritis (OA) [1]. Foam knee savers have been used to alleviate knee loading for repetitive deep squatting in sports [2] and in occupational activities [3]. The goal of the current study was to analyse the effects of the knee saver on the musculoskeletal loading at the knee for deep squatting postures.

Methods

One healthy male subject (body mass = 78.8 kg; height = 1.82 m) participated in the study. The subject completed two rounds of five continuous deep squats: 1) without wearing knee savers and 2) with wearing knee savers, with a rest period of three minutes between sets. The deep squatting tasks were performed at self-selected pace, with the heels always in contact with the ground. A pair of off-the-shelf foam knee savers (Easton, AliMed) were used in the study. The human subject test protocol was approved by the IRB of the National Institute for Occupational Safety and Health. The kinematics of the human body were measured by using a motion capturing system, which was identical to our previous studies [3,4]. A 14-camera system (Vicon Nexus, Oxford Metrics Ltd.) was used to capture the marker trajectories at 100 Hz. The data of the ground reaction forces were collected at 1,200 Hz via two force plates (Model OR6-6-2000, Advanced Mechanical Technology Inc.). The interface contact pressures between the posterior thigh and shank were measured using a pressure sensor film (Model 5101, TekScan). The inverse dynamical model (Fig. 1a) was based on an existing model in AnyBody (AMMR.v2.0) [5]. The kinematics of the body segments and the contact forces on the shanks and thighs were used as the model inputs. The forces in each of the muscles across the knee joint, the forces in the tibiofemoral (TF) and patellofemoral (PF) joints, and the ground reaction forces were calculated. The comparison of the predicted ground reaction forces with those measured experimentally served as a model validation.

Results and Discussion

For both squatting conditions, without and with wearing knee savers, the contact forces on the thighs and legs, and the muscle forces in the quadriceps and hamstring are plotted as a function of knee flexion, as in Fig. 1b. Wearing the knee savers restricted the knee flexion motion (i.e., maximal knee flexion angle reduced from 124^0 to 110^0) and increased the contact forces between thigh and leg by approximately 59%. The mean peak muscle force in the quadriceps was reduced by approximately 20% and the knee flexion angle position for the occurrence of the peak muscle force was reduced from 107^0 to 86^0, due to the knee savers. However, wearing the knee savers had little effect on the muscle forces in the hamstrings. A previous study [6] indicated that the contact force in the PF joint is linearly related to the quadriceps tendon force for given knee flexion angle. Therefore, a 20% reduction of the muscle force in the quadriceps, as obtained the current study, will result in a reduction of approximately 20% in PF contact force. The biomechanical modelling was validated indirectly by comparing the predicted time histories of the ground reaction forces with the experimental measurements (results not shown). The ground reaction forces were found to fluctuate around the body weight in squatting tasks, which was caused by the dynamic mass inertial effects of the body segments and by the muscular forces that were needed to maintain the dynamic balance during the squatting tasks.

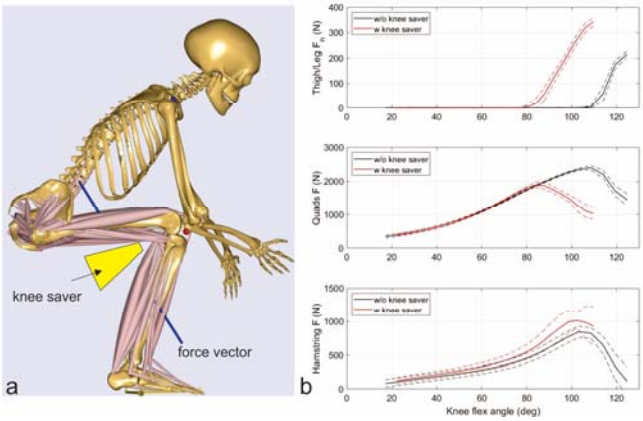

Figure 1: Inverse dynamic model **(a)** and model predictions **(b)**. The whole-body inverse dynamic model was developed using AnyBody system. The thigh/leg contact forces were measured experimentally, whereas the muscle forces in quadriceps and hamstrings were calculated via inverse dynamic analysis.

Significance

The current study demonstrated via the biomechanical modelling that wearing knee savers during deep squatting postures helped reduce the quadriceps tendon force, which is linearly proportional to the PF joint contact force, by about 20%. Since the PF joint is known to be a common source of knee pain [1], wearing knee savers may help reduce the risks of the knee OA for workers who need perform deep squatting tasks for extended time.

Disclaimer

The findings and conclusions in this report are those of the authors and do not necessarily represent the official position of the National Institute for Occupational Safety and Health, Centers for Disease Control and Prevention.

References

[1] Coggon, D, Croft, P, Kellingray, S., Barrett, D, McLaren, M, and Cooper, C. *Arthritis Rheum. 2000. 43(7):1443-9.*
[2] Dooley, E, Carr, J, Carson, E, Russell, S. *J Biomech. 2019. 82:164-170.*
[3] Breloff SP, Dutta A, Sinsel EW, Carey RE, Warren CM, Dai F, Ning S, Wu JZ. *Int J Ind Ergon. 2019. 74:10.1016.*
[4] Breloff SP, Dutta A, Dai F, Sinsel EW, Warren CM, Ning X, Wu JZ. *Appl Ergon. 2019. 81:102901.*
[5] Wu JZ, Sinsel EW, Carey RE, Zheng L, Warren CM, Breloff SP. *J Biomech. 2019. 96:109333.*
[6] Reilly, DT and Martens, M. *Acta Orthop Scand 1972. 43 (2), 126–37.*

Evidence for the use of Dynamic Maximum Normalization Method of Muscle Activation During Weighted Back Squats

Eva U. Maddox[1], Hunter J. Bennett[1], Joshua T. Weinhandl[2]
[1]Neuromechanics Laboratory, Human Movement Sciences, Old Dominion University, Virginia, USA
[2]Department of Kinesiology, Recreation and Sports Studies, The University of Tennessee Knoxville, Tennessee, USA
Email: hjbennet@odu.edu

Introduction

Muscle activation is typically reported as a normalized electromyography (EMG) signal. In weighted exercises, EMG is most often normalized as a percentage of a maximum voluntary isometric contraction (MVIC). However, EMG can also be normalized to the peak EMG signal of the dynamic task being performed (DMVC)[1]. Maximal loading is required for full activation of muscles in order to complete the back squat[2], which suggests the use of a DMVC could be a more applicable normalization for EMG signals during weighted exercise movements[3]. The back squat presents a unique opportunity to simultaneously evaluate intra (normalization method) and inter (group) subject effects due to 1) the similarity in joint angles during the squat and MVIC setup and 2) the presence of back squats in nearly all exercise programs for all persons (i.e., males and females). Currently there is no universally adopted method for normalization of muscle activation during weighted exercises, likely due to the mixed results from previous comparisons between each scheme.

Methods

Muscle activation patterns were collected at 2000 Hz using a Delsys Trigno Wireless EMG system (Delsys, Inc.), of 18 participants. MVICs of each muscle were recorded for 10 seconds. The rectus femoris (RF) and vastus medialis (VM) were performed seated with the knees flexed 60º [4,5]. The biceps femoris (BF) was performed prone with the knee flexed to 30º [4,5]. Participants performed a 5-minute warm-up of their choice, followed by the NSCA 1RM back squat testing protocol[6]. Squats were performed with a shoulder-width stance to full depth (contact between posterior thigh and shank). Recorded muscle activations from MVIC, 1RM (DMVC) and 80% 1RM (submax) trials were imported into Matlab (R2019b, The MathWorks, Natick, MA). EMG waveforms during the concentric phase (full depth to standing upright) were used for analysis[7]. Peak activation from the DMVC and MVIC were extracted and used for normalization[3]. All submax trials were normalized to the MVIC and DMVC. Inter-participant variability for both normalization techniques was assessed with coefficient of variation (CV) and variance rations (VR)[8]. Test-retest reliability was assessed by intraclass correlation coefficient (ICC)[1]. Mixed-model analyses of variance (MMANOVAs) were performed to determine if significant normalization (within-subjects; n=2) by sex (between-subjects; n=2) interactions existed for each muscle.

Results and Discussion

The results of this study suggest the use of DMVC as a more reliable and superior normalization technique than MVIC for analyzing the squat exercise. The DMVC normalization method demonstrated greater specificity (reduced inter-subject variability), with peak CV and mean CV for all muscles reduced by 24%, 48%, and 56% in DMVC compared to MVIC, respectively (Figure 1). The current study found BF activation was more sensitive to normalization methods in females than males. A significant normalization method by sex interaction was found for both peak and mean BF activation levels (p=0.005 and p=0.007, respectively).

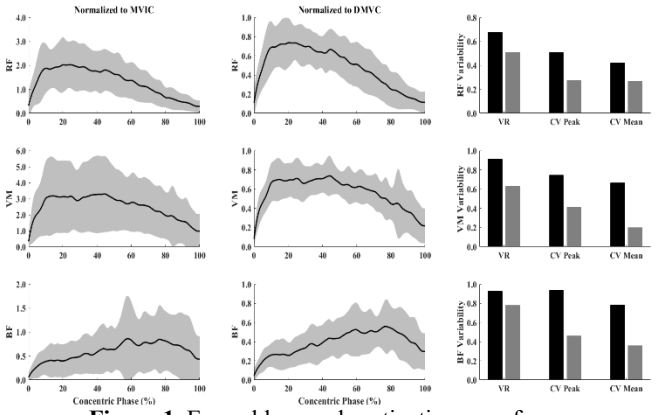

Figure 1. Ensemble muscle activation waveforms

Significance

One-repetition maximums are tests to establish baseline numbers for training percentages and testing baselines. In many high-performance and tactical settings, coaches and researchers employ EMGs to measure muscle imbalances during dynamic movements. The combination of these assessment techniques is an important step for ensuring athletes' peak readiness. Here, we provide evidence for the use of the peak muscle activation measured during the 1RM test as the denominator when normalizing/assessing submaximal tests of the same movement. Although these findings hold for both sexes, outcomes of muscle activations in females were more susceptible to normalization method compared to males. As such, this study clearly illustrates the need for exercising caution when considering results from multiple studies that implement different normalization schemes. Therefore, caution should be used when interpreting measures of muscle activation in the literature.

References

[1] Balshaw TG and Hunter AM (2012) JEK, **22**: 308-319.
[2] Yavus HU et al. (2015) J Spo Sci, **33**: 1058-1066.
[3] Besomi M et al. (2020) JEK, **53**: 102438.
[4] Barbero M et al. (2012) Atlas of muscle innervation zones; Springer.
[5] Konrad P (2006) ABC of EMG; Noraxon, Inc.
[6] Haff GG and Triplett NT (2016) Essentials of strength training and conditioning; Human Kinetics.
[7] Maddox EU et al. (2020) J Biomech, **106**: 109830.
[8] Yang JF and Winter DA (1984) Arch Phys Med Rehabil, **65**: 517-521.

EFFECT OF CENTER OF MASS ON ADAPTIVE TREADMILL CONTROL

Kaitlyn E. Downer[1], K. Pariser[1], M. Donlin[2], and J. Higginson[1,2]
[1]Department of Mechanical Engineering, University of Delaware, Newark, DE, USA
[2]Department of Biomedical Engineering, University of Delaware, Newark, DE, USA
email: kdowner@udel.edu

Introduction

Adaptive treadmills designed to change speed in real time to match the user's walking speed are increasingly being used in gait research [1]. While there are various adaptive control schemes being used by research groups around the world, many are controlled primarily by user position and spatiotemporal parameters [2]. These controllers ignore measures of forward propulsion, such as anterior ground reaction forces, that are known to linearly correlate with walking speed [3]. To address this limitation, we developed a novel adaptive treadmill (ATM) controller where speed changes with position, spatiotemporal parameters, and forward propulsion [4].

The study **objective** was to determine the effect of adjusting the weight on the center of mass position term in the ATM control function on propulsion mechanics. We **hypothesized** that adjusting the weight on the position term would not significantly alter walking speed, average peak anterior or posterior ground reaction forces, or anterior, posterior, or net impulses.

Methods

Eighteen healthy adults (10 male, 24 ± 3 yrs., 1.72 ± 0.11 m, 76.56 ± 12.13 kg) walked at their self-selected walking speed on a split-belt instrumented treadmill (Bertec Corp., OH, USA; 2000 Hz) under four modifications of ATM control. Participants walked on each modification for one minute in random order. In the treadmill control, beta is the weight function on the center of mass (COM) position term. To test the impact of the position control on propulsion mechanics, β was varied for each modification: $\beta = 0.001$, $\beta = 0.25$, $\beta = 0.5$, $\beta = 2$. Average walking speed, peak anterior (propulsive) and posterior (braking) ground reaction forces, and anterior, posterior, and net ground reaction force impulses were computed with a custom MATLAB code (MathWorks, MA, USA). A one-way ANOVA ($\alpha = 0.05$) blocked by subject and post-hoc Tukey HSD tests were run to determine if any significant differences were present between trials.

Results and Discussion

As hypothesized, subjects chose similar walking speeds across all four modifications. Peak anterior and posterior ground reaction forces as well as anterior and posterior impulses were also not significantly different between trials. However, there was a significant difference between net impulse values on the $\beta = 0.001$ modification compared to $\beta = 0.5$ and $\beta = 2$ modifications (Fig 1). While differences were not observed between anterior and posterior impulse values individually, the combination of average increased propulsive impulse and decreased braking impulse with a smaller beta suggests that decreasing the weight function on the position term may promote increased propulsion.

The results of this study suggest that removing the COM position term in the ATM controller causes the user to rely on other gait mechanics, specifically propulsive impulse to achieve and maintain their desired self-selected walking speed. However, many subjects commented that it became more challenging to achieve and maintain their desired walking speed as reliance on position-based control decreased. In addition, we observe that as beta decreased subjects tended to use a light touch on the handrails to assist with stability and allow them to increase their propulsion to reach their desired walking speed. With that being said, individuals more experienced with ATM walking did not require the use of the handrails. We anticipate that through training on an ATM without position-based control, individuals would become more comfortable and no longer use the handrails. Thus, removing or minimizing the importance of position-based control may improve the effectiveness of ATM-based gait training programs at increasing propulsion.

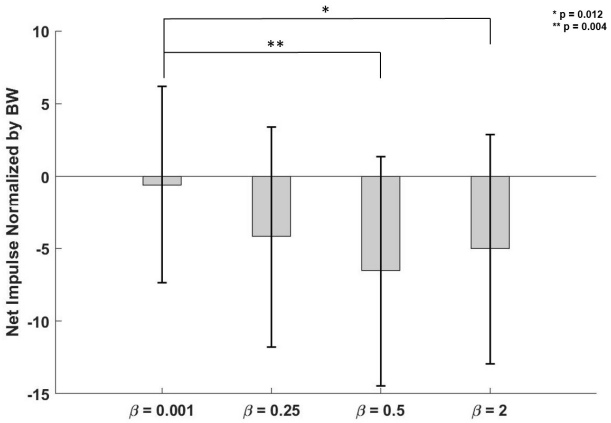

Figure 1: Group average ± standard deviation net impulse for each modification.

Significance

Decreasing the importance of position-based control in an ATM controller can encourage users to shift closer to a net zero ground reaction force impulse by increasing propulsive and decreasing braking impulses. This suggests that ATM controllers based on spatiotemporal and propulsion mechanics may be more suited to target increased propulsion than solely position-based control, improving the efficacy of ATM gait rehabilitation. Future work will seek to understand how spatiotemporal parameters varied between these modifications and determine baseline factors that may promote participants to rely more heavily on either spatiotemporal or propulsive-based control in the absence of position-based control.

Acknowledgments

Funding was provided by the NSFGRFP, the University of Delaware Helwig Mechanical Engineering Fellowship, NIH U54-GM104940, and University of Delaware Summer Scholars.

References

[1] Castano C., Huang H., *bioRxiv.,*2021.
[2] Sloot LH et al., *Gait Posture*., 2013.
[3] Hsiao H et al., *J Biomech.,* 2016.
[4] Ray NT et al., *J Biomech.,* 2018.

An Exoskeleton Controller Design Using Soleus Adenosine Triphosphate Hydrolysis Rate

Paul Stegall[1*] and Leia Stirling[2]
[1] Department of Aeronautics and Astronautics, Massachusetts Institute of Technology, corresponding email: *stegall@mit.edu
[2] Department of Industrial and Operations Engineering, Robotics Institute, University of Michigan

Introduction

There are two common strategies that support metabolic cost reduction using ankle exoskeletons: mimicking the ankle positive power [1] or using a human-in-the-loop (HITL) optimization with a parameterized trajectory [2-4]. The positive power approach can generalize across walking and running, but applies torque over a smaller portion of the gait cycle; where the HITL method applies torque over a larger portion of the gait cycle, but is constrained by the selected parametrization. The physiological factors that contribute to effective actuation profile shape are unknown. We present a method for generating the actuation profile using an estimate of the soleus adenosine triphosphate (ATP) hydrolysis rate that is applicable from walking through running speeds. This approach is expected to improve energy cost reduction over traditional power methods as it applies torque over a larger portion of the stance phase. It is simpler than HITL methods as it is generalizable over locomotion speed without a long optimization process.

Methods

We digitized soleus muscle and tendon dynamics data for both walking and running, which were recorded using ultrasound [5]. The human muscle fiber ATP hydrolysis rate based on fascicle velocity in isometric contractions [6] was extended, $h(V_{CE})$.

$$h(V_{CE}) = max\left(\frac{M + D*max\left(\left|\frac{V_{CE}}{l_0}\right| - \left|\frac{V_{CE}^{TVMax}}{l_0}\right|, 0\right)}{1 + D*max\left(\left|\frac{V_{CE}}{l_0}\right| - \left|\frac{V_{CE}^{TVMax}}{l_0}\right|, 0\right)} - M, 0\right) \quad (1)$$

Where M and D are parameters of a hyperbola that were fit [6] for type I (slow) and IIA (fast) fibers, V_{CE} is the fascicle velocity, and l_0 is the fascicle resting length during static standing. A dead-band threshold was applied to the fascicle velocity to allow for the small contractions used for tendon tensioning, defined as the fascicle velocity value when the tendon reached its peak lengthening velocity, V_{CE}^{TVMax}. The ATP hydrolysis rate during static contraction was removed. The contributions based on muscle composition of both fast ($R_f = 0.2$) and slow ($R_{sl} = 0.8$) [7] twitch fibers was used to estimate the net ATP hydrolysis rate of the soleus (Eq. 2), with a correction for eccentric contractions (1/2.7) applied [8]. The resulting curve was scaled by C_D so it had the same peak value as the HITL profile.

$$h_{net}(V_{CE}) = \begin{cases} 0 & If\ F < 0 \\ C_D\left(R_{sl}h_{sl}(V_{CE}) + R_f h_f(V_{CE})\right) & If\ V_{CE} \le 0 \\ \frac{C_D}{2.7}\left(R_{sl}h_{sl}(V_{CE}) + R_f h_f(V_{CE})\right) & Otherwise \end{cases} \quad (2)$$

Results and Discussion

The proposed method supports creating generalized control strategies based on biological phenomenon that require no specific knowledge of the activity. For walking h_{net} has a shape similar to a linear ramp (Fig. 1a). It is unknown if this shape is more or less effective than the HITL profile, as the profile used for the HITL optimization was predefined to reduce the number of parameters. These two methods operate over the same region of the gait cycle. The h_{net} profile has similar timing and shape to the running HITL profile (Fig. 1b). This ATP-based approach considers localized information without accounting for changes in full body motion that may arise in response to externally applied torques. The approach presented only used fascicle velocity as an input, meaning it may not translate to static tasks. Extensions to the model could account for both muscle force and fascicle velocity. The results presented had inputs without the exoskeleton intervention applied. External torques may impact the shape and timing of the estimated profiles due to changes in fascicle velocity. Further studies are needed to quantify these effects and compare performance to other task-invariant controllers, such as energy shaping methods [9].

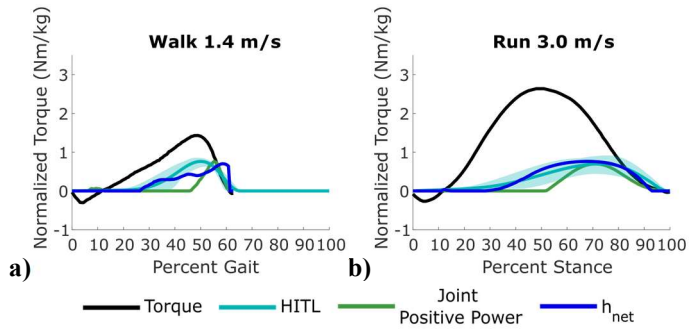

Figure 1: The torque is the ankle torque reported by Lai et al. for the speed presented. Because only stance time was reported, for walking the last point was set to the mean offset time reported by Zhang et al. [2]. The HITL profile is the mean profile reported for walking at 1.25 m/s by Zhang et al., and for running at 3.0 m/s reported by Witte et al. [4]. The shaded region is the range of reported curves.

Significance

A controller that generalizes across tasks extends the capabilities of an individual exoskeleton. We have presented an initial exploration of a muscle ATP model to generate exoskeleton torque profiles. This approach has the potential to generalize to tasks where the behaviour is not well defined, e.g. non-cyclic gait tasks, and can be applied to any muscle of interest.

Acknowledgments

DISTRIBUTION STATEMENT A. Approved for public release. Distribution is unlimited. This material is based upon work supported by the United States Air Force under Air Force Contract No. FA8702-15-D-0001. Any opinions, findings, conclusions or recommendations expressed in this material are those of the author(s) and do not necessarily reflect the views of the United States Air Force.

References

[1] L. M. Mooney et al., *J of NeuroEng Rehabil,* 11(1):1-11, 2014
[2] J. Zhang et al., *Science,* 356(6344):1280-1284, 2017
[3] Y. Ding et al., *Sci Robot,* 3(15), 2018
[4] K. A. Witte et al., *Sci Robot,* 4(40), 2020
[5] A. Lai et al., *J of Appl Physiol,* 118(10):1266-1275, 2015
[6] Z.-H. He et al., *Biophys J,* 79(2):945-961, 2000
[7] B. R. Umberger et al., *Comput Method Biomec,* 6(2):99-111, 2003
[8] D. Hawkins, P. Molé, *Ann Biomed Eng,*25(5):822-830, 1997
[9] J. Lin et al., *IEEE Control Syst. Lett.*, 5(5):1711-1716 2020

Effect of Changing Stability Conditions on Approximate Entropy of Center of Pressure During Quiet Standing

Natalie Tipton[1], Gordon Alderink[2], Samhita Rhodes[1],
[1]School of Engineering, Grand Valley State University, Grand Rapids, MI, USA
[2]Department of Physical Therapy, Grand Valley State University, Grand Rapids, MI, USA
Email: tiptonna@mail.gvsu.edu

Introduction

The physiological processes involved with keeping a human upright are complex and dynamic. A metric commonly used to quantitatively analyze postural control is center of pressure (COP). In order to maintain balance during quiet standing, this factor follows a general oscillatory pattern where it sways about the center of mass (COM) to counteract a potential fall that could otherwise be caused by the COM moving beyond the base of support [1]. The primary objective of this research was to determine whether approximate entropy (ApEn), which quantifies the regularity of a signal [2], could be capable of quantifying changes in stability in typical individuals when implemented on COP signals during quiet standing under increasing levels of instability. We hypothesized that as stability decreased ApEn would increase, indicating less predictability in the postural control mechanism.

Methods

Six healthy individuals (4 females; 24.8±3.3 yrs; 170.8±10.5 cm; 71.0±13.5 kg) participated. Approval was obtained from the Grand Valley State University Human Research Review Committee (#18-246-H). A Full-Body Plug-in-Gait model was utilized in conjunction with 16 Vicon MX cameras (120 Hz) and Nexus motion capture software v2.9.2 (Oxford Metrics) to track anatomical marker trajectories, which were filtered with a 15 Hz Woltring filter. Ground reaction forces were collected using floor-embedded AMTI (Advanced Mechanical Technology Inc.) force plates (1200 Hz) and were filtered with a 6 Hz Butterworth filter. Data were collected for 30 seconds over 5 trials with participants standing with arms flexed, hands touching shoulders, on two force plates under six conditions, from most to least stable: 1) eyes open feet together (EOFT), 2) eyes closed feet together (ECFT), 3) eyes open dominant foot on rear plate (EODB), 4) eyes closed dominant foot on rear plate (ECDB), 5) eyes open dominant foot on fore plate (EODF), and 6) eyes closed dominant foot on fore plate (ECDF). Participants were asked to stand with knees extended, while maintaining equal distribution of weight on each force plate for tandem foot stances. Custom Python code (Python Software Foundation) was used to determine the combined (from the rear and fore force plates) COP location [1]. ApEn was used to quantify changes in stability in antero-posterior (AP) and medio-lateral (ML) directions. Estimation of ApEn requires carefully choosing the parameters m (data length) and r (filter or tolerance level). We selected m = 2, as suggested by Pincus [2]. However, the choice of r largely depends on the data itself and so is less standardized. We chose r = 10 based on empirical observation.

Results and Discussion

Five of the six subjects showed a significant difference ($p<0.01$) in ApEn between one or more stability conditions. For all of these subjects, a 2-sided Dunnett's post-hoc test showed that every tandem foot position was significantly different from the most stable, EOFT condition in both ML and AP directions (Figure 1), which is supported by previous research [3,4]. ApEn was also able to determine significant differences between eyes open and eyes closed variants of the feet together position on multiple occasions. This suggests that ApEn can be used as a sensitive indicator of stability in postural control. Changes in ApEn between stability conditions did not appear to differ significantly between the AP and ML directions.

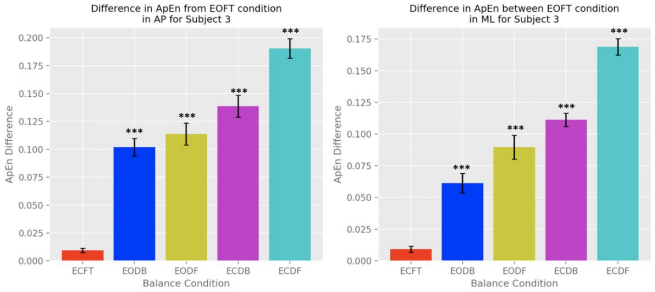

Figure 1. Difference in approximate entropy for each stability condition from most stable, eyes open feet together, position where *** denotes a significance of $p<0.001$, for representative subject.

Significance

It is known that postural control is affected by injuries to the brain [5,6]. Additional information gained from ApEn on the COP provides insight into patterns and indices that are characteristic of a typical brain and how it works to maintain balance. Understanding how an uninjured brain works to keep a person upright during different stability conditions is invaluable for future research with subjects that have suffered from a traumatic brain injury such as a concussion. Our data suggest that ApEn is a metric that can distinguish less stable postural control in healthy individuals. These findings will allow for comparison between the way a typical brain and a damaged brain react to the same quiet standing conditions, and may lead to eventual conclusive testing for concussion diagnosis.

References

[1] Winter, D. (1995), *Gait Posture*, 3, pp. 193–214.
[2] Pincus, S. (1995), *Chaos Interdiscip. J. Nonlinear Sci.*, 5, pp. 110–117.
[3] Cavanaugh, J. et al. (2007), *J. NeuroEng. Rehabil.*, 4, p. 42
[4] Sabatini, A. M. (2000), *Med. Biol. Eng. Comput.*, 38, pp. 617-624
[5] Rochefort, C et al. (2017), *Orthop. J. Sports Med.*, 5.
[6] Catena, R.D. et al. (2009), *J. NeuroEng. Rehabil.*, 6, p. 25.

Center of Pressure Velocity Distinguishes Differences in Stability in Quiet Standing Positions

Natalie Tipton[1], Gordon Alderink[2], Samhita Rhodes[1],
[1]School of Engineering, Grand Valley State University, Grand Rapids, MI, USA, [2]Department of Physical Therapy, Grand Valley State University, Grand Rapids, MI, USA, Email: tiptonna@mail.gvsu.edu

Introduction

The physiological processes involved with keeping a human upright are complex and dynamic. A metric commonly used to quantitatively analyze postural control is center of pressure (COP). The COP follows a general oscillatory pattern where it sways about the center of mass (COM) to counteract a potential fall that could be caused by the COM moving beyond the base of support [1]. The primary objective of this research was to determine whether the velocity of COP oscillations would be capable of quantifying changes in stability in typical individuals during quiet standing under increasing levels of instability. We hypothesized that as stability decreased, COP velocity would increase, indicating the body's need for more rapid adjustments to maintain balance.

Methods

Six healthy individuals (4 females; 24.8±3.3 yrs.; 170.8±10.5 cm; 71.0±13.5 kg) participated. Approval was obtained from the Grand Valley State University Human Research Review Committee (#18-246-H). A full-body Plug-in-Gait model was utilized in conjunction with 16 Vicon MX cameras (120 Hz) and Nexus motion capture software v2.9.2 (Oxford Metrics) to track anatomical marker trajectories, which were filtered with a 15 Hz Woltring filter. Ground reaction forces were collected using floor-embedded AMTI (Advanced Mechanical Technology Inc.) force plates (1200 Hz) and were filtered with a 6 Hz Butterworth filter. Data were collected for 30 seconds over 5 trials with participants standing on two force plates under six conditions: 1) eyes open feet together (EOFT), 2) eyes closed feet together (ECFT), 3) eyes open dominant foot on rear plate (EODB), 4) eyes closed dominant foot on rear plate (ECDB), 5) eyes open dominant foot on fore plate (EODF), and 6) eyes closed dominant foot on fore plate (ECDF). Custom Python code (Python Software Foundation) was used to determine the combined (from the rear and fore force plates) COP location [1]. Velocity was used to quantify changes in stability in antero-posterior (AP) and medio-lateral (ML) directions (Equation 1), where x is the COP signal, t is the time vector, and i is the index pointing to each COP location.

$$V(i) = \frac{x(i+1) - x(i)}{t(i+1) - t(i)} \quad \ldots\ldots\ldots (1)$$

The application of this equation resulted in a velocity signal that was equal in length to the COP signal. The magnitudes of each velocity value were averaged together to create a single average velocity to represent each trial, respectively.

Results and Discussion

Five out of six subjects showed a significant difference ($p<0.05$) in velocity magnitude between one or more stability conditions. For four subjects, a 2-sided Dunnett's post-hoc test showed a significant increase in velocity between, at least, the most stable (EOFT) and one of the least stable (ECDF, ECDB) conditions in both ML and AP directions (Figure 1). This is supported by previous research as well as a systematic review assessing similar techniques [3,4]. These results indicate that velocity magnitude could be used to differentiate between large differences in stability levels in postural control. However, these results also suggest that velocity magnitude may not be the best choice for identifying minute differences in stability in postural control.

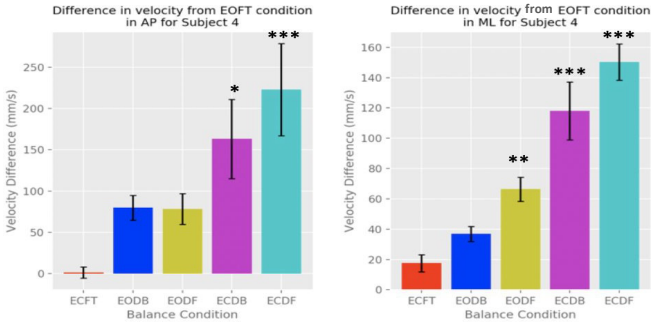

Figure 1. Difference in velocity for each stability condition from most stable, eyes open feet together, position where *** denotes a significance of $p<0.001$, ** denotes $p<0.005$, and * denotes $p<0.05$, for a representative subject.

Significance

Although it is known that postural control is affected by injuries to the brain [3,5], the degree to which it is affected is not as clear. Information gained from COP velocity provides insight into characteristics that typify how a healthy brain works to maintain balance. Our data suggest that velocity is a metric that can distinguish large differences between stable and less stable quiet standing positions. We believe that the COP velocity could be a useful metric in clinical decision making with regard to return-to-play for concussed athletes. In a parallel study, approximate entropy (ApEn) was investigated as another metric that could characterize instability in postural control. While ApEn was more sensitive to changing stability than velocity, computational expense was very high. The ease of analyzing velocity of COP makes this an attractive method.

References

[1] Winter, D. (1995), *Gait Posture*, 3, pp. 193–214.
[2] Pincus, S. (1995), *Chaos Interdiscip. J. Nonlinear Sci.*, 5, pp. 110–117.
[3] Rochefort, C. et al. (2017), *Orthop. J. Sports Med.*, 5.
[4] Roman-Liu, Danuta. (2018), *Archives of Gerontology and Geriatrics,* 77, pp. 68-80.
[5] Catena, R.D. et al. (2009), *J. NeuroEng Rehabil.,* 6, p. 25.

EVERESTING: THE OPTIMAL SLOPE TO CYCLE OR RUN UP THE TALLEST MOUNTAIN ON EARTH

Wannes Swinnen[1], Emily Laughlin[2], and Wouter Hoogkamer[2]
[1]Department of Movement Sciences, KU Leuven, Belgium
[2]Department of Kinesiology, University of Massachusetts Amherst, USA
email: wannes.swinnen@kuleuven.be

Introduction

With the worldwide COVID-19 pandemic in 2020, many cyclists and runners saw most of their races cancelled or postponed. For athletes still wanting to test their fitness Everesting became a popular challenge: cycling or running up an elevation equivalent to Mt. Everest (8,848m or 29,029ft). During Everesting, athletes are free to pick any hill and repeat it as many times until they have reached the accumulated elevation. With an almost infinitely number of different hills, the question arises what is the most optimal hill for Everesting and whether this hill is different for cycling and running. While there are several factors determining the optimal hill, in this abstract we will focus on the optimal slope for cycling and running.

Methods

To determine the optimal slope, we modelled cycling and running across slopes with an assumed constant metabolic power of 15 W/kg during both cycling and running.

In cycling, mechanical power output is a reliable surrogate for metabolic power, and equals the power necessary to overcome rolling resistance, air resistance and work against gravity:

$$P_{mech} = P_{roll} + P_{air} + P_{gravity}$$

Each term in the equation can be estimated:

$$P_{mech} = C_r * m * g * cos\left[tan^{-1}\left(\frac{slope}{100}\right)\right] * v_c + 0.5 * \rho_{air} * C_d * A * {v_{c+w}}^2 * v_c + m * g * sin\left[tan^{-1}\left(\frac{slope}{100}\right)\right] * v_c$$

With C_r the coefficient for rolling resistance, m the combined mass of cyclist and equipment, g the gravitational acceleration, v_c the cycling velocity, ρ_{air} the density of air, $C_d$the coefficient of aerodynamic drag, A the cyclist's frontal area and v_{c+w} the combined speed of the cyclist and the wind. From our initial assumption of metabolic power (15 W/kg), we calculated the metabolic power (cyclist body mass = 70 kg) and combined with an estimated gross efficiency of 22.7%[1] we calculated the mechanical power output (238.4 W). Making several more assumptions ($m = 70 + 8\ kg$; $C_r = 0.005$; $\rho_{air} = 1.22\ kg/m^3$; $C_dA = 0.48\ m^2$ and $v_w = 0$), we calculated the cycling velocity as a function of the slope and, subsequently, calculated the time needed to gain 8,848m of elevation.

In contrast to cycling, in running metabolic power is not related to mechanical power. Yet, several studies have investigated the relationship between metabolic power and slope for uphill running and walking. Applying those equations allows us to calculated the optimal slope[2–4].

Results and Discussion

To minimize the ascending time in cycling a cyclist wants to use most of his mechanical (and hence metabolic) power to overcome gravity. Given the general equation, a steeper slope will reduce the cycling speed and thus the related air resistance, making steeper slopes theoretically faster (Figure 1). Nevertheless, the increases in performance (i.e. reduced ascending time) diminishes once the slope exceeds 15% (Figure 1). Moreover, slopes exceeding 20% are often too steep to climb with a traditional road bike and gearing ratio.

In contrast to cycling, for running not all the equations suggest that steeper is faster. Only the equation by Hoogkamer et al. (2014)[3] demonstrates that with increasing slope ascending time reduces. The other equations indicate an optimum, although this optimum is highly different between studies (Figure 1). Minetti et al. (2002)[2] found an optimum around 20-30%, while Giovanelli et al. (2016)[4], who experimentally measured the steepest slopes (up to 81.6%), found an optimal range between 40 and 70%. Interestingly, the authors found that walking was metabolically cheaper than running.

As one would expect for slopes under 12% cycling is faster, but at steeper slopes – depending on the equation used – uphill running becomes faster than cycling. These results are in line with previous research demonstrating that cycling is faster at slopes below 10-15%[5]. Note that we only modelled the uphill section, downhill cycling is much faster and metabolically cheaper compared to downhill running.

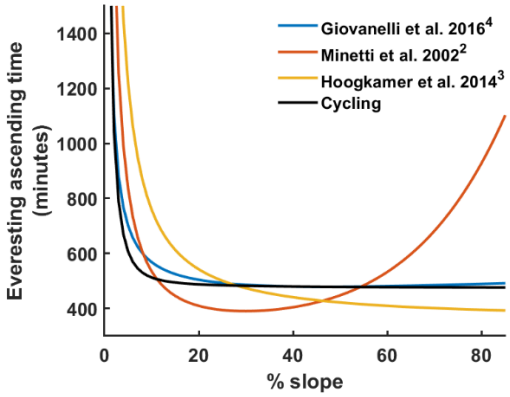

Figure 1: Ascending time during an Everesting attempt with an assumed 15 W/kg metabolic power for cycling (black) and running, differently colored lines represent different equations.

Significance

Although the current Everesting records for cycling are faster than running (Male 7 vs 11h; Female 9 vs 13h), our results indicate that uphill running is potentially almost as fast as cycling, if not faster, when running up steep slopes. Future research can expand our work to other factors determining the optimal hill for Everesting, such as the number of repetitions, fuelling, effect of altitude and downhill running.

Acknowledgments

WS obtained a PhD fellowship from the Research Foundation Flanders (11E3919N).

References

1. Millet et al. (2002) *Med Sci Sports Exerc,* **34**:1645-1652.
2. Minetti et al. (2002) *J Appl Physiol,* **93**:1039-1046.
3. Hoogkamer et al. (2014) *PeerJ,* 10.7717/peerj.482.
4. Giovanelli et al. (2016) *J Appl Physiol,* **120**:370-375.
5. Ardigo et al. (2003) *Eur J Appl Physiol*, **90**:365-371.

ISOMETRIC SHOULDER STRENGTH IN HEALTHY COLLEGIATE PITCHERS

Aaron Trunt, M.S.[1,2], and Lisa MacFadden, Ph.D.[1,2]
[1]University of South Dakota Department of Biomedical Engineering, Sioux Falls, SD
[2]Sanford Sports Science Institute, Sanford Health, Sioux Falls, SD
Email: aaron.trunt@coyotes.usd.edu

Introduction

Overuse injuries to the shoulder joint are common in athletes who participate in overhead sports such as baseball. Rehabilitation and pre-season screening for these injuries involve measurements of shoulder range of motion and strength. However, there are a limited number of reliable and clinically relevant tests available to measure the strength of an athlete's shoulder complex[1].

The Athletic Shoulder (ASH) test has been proposed as a novel and reliable method for measuring isometric strength of the shoulder girdle through a range of abduction[2]. Normative values have yet to be provided for baseball players performing the ASH test. Further, ASH test measures have never been linked to sport performance in this population. Therefore, the purpose of this study was to investigate ASH test performance in a group of collegiate baseball pitchers. It was hypothesized that isometric strength of the dominant arm would be significantly greater than that of the non-dominant arm. Additionally, it was hypothesized that ASH test performance would be related to fastball velocity.

Methods

This study was approved by the Sanford Health Institutional Review Board. Twenty one (n=21) healthy NCAA Division II collegiate baseball pitchers participated in the study.

The ASH Test was conducted as part of a clinical evaluation where subject height, weight, arm length, and isometric strength were collected. The ASH test was performed with subjects prone on the floor with the forehead resting on a towel for support with the testing limb in a pre-determined amount of shoulder abduction with the full hand resting on a portable force plate (Figure 1). After a brief warmup, subjects were familiarized with the testing protocol and the testing arm was determined randomly. For each test position (0, 90, 135, and 180° of shoulder abduction), subjects performed three maximal effort trials. Subjects were instructed to push as hard and fast as possible to generate maximal force for three seconds. If any compensatory strategies such as excessive trunk rotation were observed, the trial was discarded and a new trial was recorded. The same protocol was then followed for the opposite limb. Peak force was obtained for each trial and averaged across the three trials for each test position. Force data was normalized to bodyweight prior to analysis.

Figure 1: Example of ASH test setup (135° abduction pictured).

Subjects returned approximately two weeks later for a bullpen session in a biomechanics lab. After a warmup, each pitcher threw 10 fastballs from an artificial mound at a simulated strike zone 45 feet from the rubber. Fastball velocity was recorded with a radar gun. The five fastest pitches thrown for strikes were averaged and used for analysis.

Isometric strength differences were assessed bilaterally using paired T-tests. Pearson correlations were used to assess the relationship between dominant arm isometric strength and fastball velocity ($\alpha = 0.05$).

Results and Discussion

Dominant arm isometric peak force was greater than the non-dominant side at each level of shoulder abduction. The test position where the arm was abducted to 180° was shown to provide the highest force outputs for both the dominant and non-dominant arms. Isometric peak force at 90° abduction was significantly greater in the dominant side (Table 1). This test position was also where the lowest peak force outputs were observed bilaterally. Results from the Pearson correlations showed no significant relationships between isometric peak force and fastball velocity.

Table 1. Isometric peak force (Mean ± SD)

	0°	90°	135°	180°
D	13.4 ± 2.7	**11.9 ± 2.3**	13.0 ± 2.9	15.8 ± 3.8
ND	12.8 ± 3.2	**10.9 ± 2.3**	12.3 ± 2.5	15.2 ± 3.8
p-value	0.18	**<0.01**	0.09	0.35

Peak force expressed in % bodyweight. D=Dominant; ND=Non-Dominant

Results from the ASH test showed that baseball players present stronger isometric shoulder strength in the throwing arm compared to the non-throwing arm. Bilateral differences were between 4-9% depending on shoulder abduction angle with the greatest difference being observed at 90°. These normative values can be used as a benchmark for shoulder strength as part of the rehabilitation process or for pre-season screening of overhead athletes. However, caution should be taken when using the ASH test for prediction of sport performance in pitchers.

Significance

Normative values for the ASH test did not exist previously for healthy pitchers. The isometric strength profile of the healthy collegiate pitcher has been provided. Based on these results, it is recommended that peak isometric strength of the throwing arm be at least 10% of a player's bodyweight and ≥90% of the non-throwing arm. Clinicians using the ASH test as an outcome measure for rehabilitation of overhead athletes should evaluate the isometric strength of the shoulder girdle bilaterally at least at 90 and 180° abduction since these positions were shown to provide the end ranges of force production.

References

1. *Borms & Cools*. Int J Sports Med. 2018 Jun;39(6):433-441
2. *Ashworth et al*. BMJ Open Sport Exerc Med. 2018 Jul;4(1)

BETWEEN-GROUP DIFFERENCES IN GAIT STABILITY OF CHILDREN WITH AND WITHOUT CEREBRAL PALSY PERSIST WHEN EVALUATED RELATIVE TO PELVIC ORIENTATION

James B. Tracy[1], Michael S. Christensen, Drew A. Petersen, Jamie Pigman, Benjamin C. Conner, Henry G. Wright, Christopher M. Modlesky, Freeman Miller, Curtis L. Johnson, and Jeremy R. Crenshaw[1]*
[1]University of Delaware, Newark, DE, USA; email: *crenshaw@udel.edu

Introduction

Cerebral palsy (CP) is associated with a high risk and rate of falling, with 55% of falls occurring during walking [1]. Our previous analysis of the margin of stability (MOS) [2] during walking determined that children with CP had more lateral stability during stance on their non-dominant limb, but no between-group differences in anterior stability [3]. We recently validated a new method of determining lateral and anteroposterior stability relative to the pelvic orientation [4], a useful method in evaluating stability relative to anatomical orientations and in contexts when the walking trajectory is not clearly defined. We do not know, however, how the pelvic-oriented MOS alters conclusions in a clinical study. Our purpose was to determine how the between-group conclusions of a cross-sectional study, comparing the dynamic stability of children with and without CP, were altered when using a traditional global reference frame and a pelvic-oriented reference frame.

Methods

Participants included 13 children with CP *(6 boys/7 girls, age 9.2 (2.1) years, BMI 16.5 (1.4) kg·m^{-2}, 10 GMFCS Level I, 3 Level II, 8 di- & 5 hemiplegic)* and 13 children with typical development *(TD, 6 boys/7 girls, age 9.4 (2.4) years, BMI 16.9 (2.6) kg·m^{-2})*. Using motion capture technology *(120 Hz)*, the over-ground gait of all participants was recorded at preferred (*mean (SD) stat·s^{-1}; CP: 1.34 (0.28), TD: 1.27 (0.25); p=0.49*) and fast speeds (*CP: 2.07 (0.46), TD: 2.14 (0.45); p=0.70*). The MOS (*minimum lateral, anterior at mid-swing, and anterior at foot strike*) was calculated in the global [3] and pelvic reference frames [4]. Mixed factorial ANOVAs were used to evaluate the main effects and interactions of GROUP *(CP/TD)*, LIMB *(dominant/non-dominant)*, SPEED *(preferred/fast)*, and METHOD *(global/pelvic)*.

Results and Discussion

In our previous study that evaluated the MOS in the global reference frame, we found between group differences in lateral stability when bearing weight on the non-dominant limb [3]. These results generally persisted when assessed using the novel pelvic-oriented method (Figure 1). We observed a significant LIMBxGROUP interaction for the lateral minimum MOS with large between-group effects on the non-dominant limb ($p=0.02$, $\eta^2=0.20$). There were no significant interactions containing GROUP or METHOD ($p>0.14$, $\eta^2<0.09$), suggesting that the selected reference frame did not alter between-group effects on stability.

In our previous study, we did not observe between-group differences in anterior MOS measures. This conclusion persisted regardless of the used reference frame, as shown by no significant interactions or main effects containing GROUP ($p>0.18$, $\eta^2<0.08$).

For all MOS measures, there was a significant METHODxSPEED interaction ($p<0.01$, $\eta^2>0.50$), suggesting that the between-method differences in MOS were amplified at faster walking speeds (Figure 1). Generally, at preferred speeds, the pelvic-oriented measures were less stable laterally and anteriorly at mid-swing, but more stable anteriorly at foot strike. We suggest that the interaction of speed and method is due to pelvic rotation in the transverse plane [5], an aspect that causes forward gait velocity to increase the extrapolated center of mass lateral position in the pelvic-oriented reference frame.

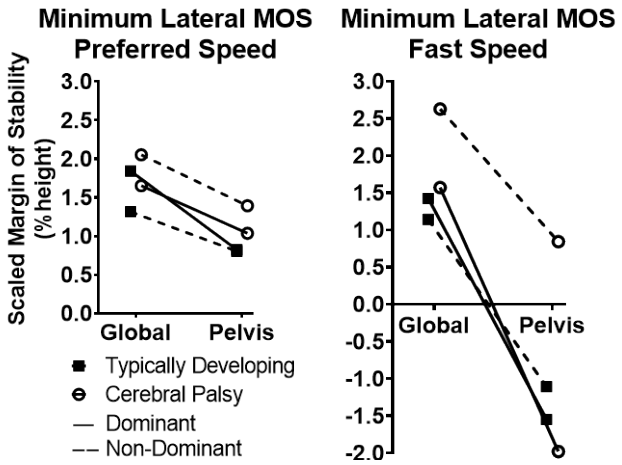

Figure 1: Height-scaled lateral MOS at preferred and fast walking for global and pelvis-oriented reference frames. Although the stability values were altered with the transition to a pelvic-oriented MOS calculation, the between-group differences when bearing weight on the non-dominant limb (dashed lines) persisted across methods.

Significance

A pelvic-oriented MOS has two advantages over that determined in the global reference frame. First, the pelvic-oriented measure quantifies stability with anatomically relevant context. With regards to pelvic orientation, anteroposterior and lateral balance control strategies and capacities are different [6], so it is reasonable to evaluate stability in these two directions separately and with reference to the pelvis. Second, a pelvic-oriented MOS calculation does not require assumptions of a known walking trajectory. So, it is a relevant stability measure when the prescribed trajectory is not known, is variable, or is not followed as instructed. This is the first clinical application of the pelvic-oriented MOS. We concluded that the new approach altered MOS values, but did not alter the between-group effects when comparing children with and without CP. Therefore, the pelvic-oriented MOS maintains construct validity as an indicator of altered gait stability.

Acknowledgments

DE INBRE (NIGMS P20-GM103446) and 1R01HD090126.

References

1. Morgan et al. *Rehab Research Practice*. 196395, 2015.
2. Hof et al. *J Biomech*. **38**:1-8, 2005.
3. Tracy et al. *Gait Posture*. **72**:182-187, 2019.
4. Christensen et al. *Am & Int Soc Biomech*, 2019.
5. Taylor et al. *Gait Posture*. **9**:88-94, 1999.
6. Winter. *Gait Posture*. **3**:193-214, 1995.

LOPSIDED LEG STRENGTH MAY LEAVE ONE LACKING FOLLOWING LIMB LOSS

Wyatt D. Ihmels[1,2], Michael E. Cobb, Jr[1,2], Elizabeth Russell Esposito[1,3,4]
[1]Center for Limb Loss and MoBility, VA Puget Sound, Seattle, WA
[2]Henry M. Jackson Foundation, Bethesda, Maryland
[3]DoD-VA Extremity Trauma and Amputation Center of Excellence, JBSA Ft. Sam Houston, TX
[4]University of Washington, Department of Mechanical Engineering, Seattle, WA
email: wihmels@hjfresearch.org

Introduction

Individuals with unilateral transtibial amputation (TTA) exhibit significantly less knee flexion and extension strength on their residual limb compared to their sound limb [1]. This strength asymmetry may contribute performance impairments during ambulation. Predictive optimization techniques showed strength loss of 10% in the residual limb musculature can significantly increase the metabolic cost of walking from pre to post amputation [3]. It is currently unknown however, if these findings appear congruent with measurements on live humans. Thus, our study examined how knee strength asymmetries between residual and intact limbs affected walking energetics across speeds in individuals with TTA.

Methods

Seven participants with unilateral TTA have been recruited for this study (height: 1.75 ± 0.06 m, mass: 101.3 ± 16.7 kg, age: 50 ± 8 years). Participants walked on the treadmill for six minutes at slow, medium, and fast Froude speeds based on leg length while their heart rate and oxygen consumption were collected using indirect calorimetry (K5, Cosmed, Inc., Rome, Italy). Rating of perceived exertion (RPE) was recorded following the completion of each walking speed using the Borg scale. Participants also performed three maximum isokinetic knee flexion and extension contractions at 30°/sec on both the sound and residual limb (Biodex Medical Systems, Shirley, NY). Participants rested at least 30 seconds between tests.

Metabolic cost and heart rate were averaged over one minute of steady state walking. Metabolic cost was scaled to the biological mass of the participant, excluding the prosthesis mass. Each participant's peak knee flexion and extension torque were averaged from the three isokinetic strength repetitions for both the sound and residual limb. Similar to [2], the average value was used to calculate an asymmetry index (ASI) score, where a positive (+) value indicated greater strength in the sound limb. A linear regression determined the relationship between bilateral strength ASI and walking economy dependent measures.

Results and Discussion

Greater knee extension strength asymmetry was significantly associated with an increase in metabolic cost (p=0.029) at faster walking speeds. RPE scores were also correlated to knee extension strength ASI during moderate (p=0.038) and fast (p=0.050) walking speeds (Table 1; Fig. 1). These results relate to prior work that has also shown greater bilateral knee strength asymmetry can negatively impact functional outcomes [3, 5].

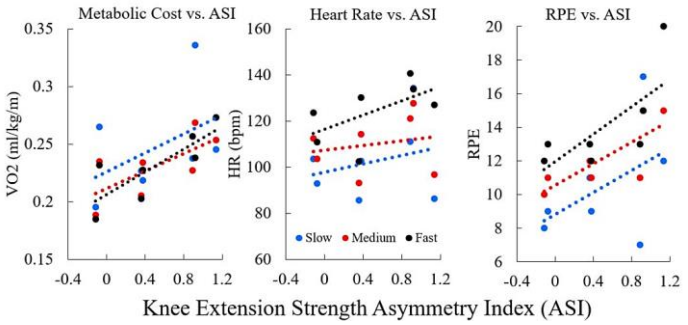

Fig 1: Association between knee extension strength ASI and metabolic rate (A), heart rate (B), and RPE (C).

However, knee flexion strength asymmetry was not significantly correlated to any economy measure across speeds (p<0.05).
Prior *in silico* modelling and simulation work highlighted that maintaing both knee flexion and extension strength in the residual limb could mitigate the increase in metabolic cost commonly found after amputation [3]. However, when evaluating this *in vivo*, the present study only found a significant relationship with knee extension strength. This relationship was also found in perceptions of the task being more taxing in those with assumed greater residual limb strength loss.

Significance

Data collection is ongoing, but these significant preliminary results provide further evidence of the importance of strength retention, specifically in knee extension musculature of the residual limb, in order to improve outcomes in individuals with TTA. Future research should look to include a clinical evaluation of knee extensor strength as an important part of any studies investigating metabolic cost post-amputation.

Disclosure

The views expressed herein are those of the authors and do not reflect the official policy or position of the US Army Medical Department, the US Army Office of the Surgeon General, Department of the Army, Department of Defense, Department of Veteran's Affairs or the US Government.

References

[1] Hewson et al. (2020). *Pros. & Ortho. Int.,* **44**: 323-40.
[2] Kaufman et al. (2012). *Clin. Biomch.* **27**: 460-65.
[3] Russell Esposito & Miller (2018). *PloS ONE,* **13**: 1-19.
[4] Chehab et al. (2014). *Osteoarthritis Cartilage,* **11**: 1833-39.
[5] Eagle et. Al. (2010). *J. Strength & Cond.,* **33**: 89-94.

Table 1: Knee extension strength ASI correlation at Froude 2, 3, and 4 walking speeds. * denotes statistical significance (p<0.05)

	Metabolic Cost (ml/kg/m)	Heart Rate	RPE
FR2	[R^2 = 0.204, p = 0.308]	[R^2 = 0.084, p = 0.529]	[R^2 = 0.234, p = 0.271]
FR3	[R^2 = 0.476, p = 0.086]	[R^2 = 0.049, p = 0.632]	**[R^2 = 0.604, p = 0.040]***
FR4	**[R^2 = 0.650, p = 0.029]***	[R^2 = 0.370, p = 0.148]	[R^2 = 0.514, p = 0.070]

COMPARISON OF METHODS FOR EVALUATING ANKLE-FOOT ORTHOSIS STIFFNESS

B.R. Shuman[1,2,3], D. Totah[4], D.H. Gates[4], and *E. Russell Esposito[1,2]
[1]RR&D Center for Limb Loss and Mobility (CLiMB), VA Puget Sound Health Care System, Seattle, WA, U.S.A.
[2] DOD-VA Extremity Trauma and Amputation Center of Excellence (EACE)
[3] The Henry M. Jackson Foundation for the Advancement of Military Medicine, Bethesda, MD
[4] Rehabilitation Biomechanics Laboratory, School of Kinesiology, University of Michigan, Ann Arbor, MI
email: * elizabeth.m.russell34.civ@mail.mil

Introduction

Ankle-foot orthoses (AFOs) are frequently prescribed to stabilize and restore function in the lower limb. The impact of an AFO on a user's gait is determined in part by the AFO's mechanical properties. Thus, AFO stiffness is important to characterize for appropriate device prescription (1). However, methods for determining stiffness vary in the literature. Here, we compare results from three methods for determining sagittal plane AFO stiffness.

Methods

We calculated the rotational stiffness of four commercially available carbon composite AFOs using three approaches (Fig. 1). The same AFO specimens were used in each approach. All AFOs were non-articulated, non-modular, size U.S. 10.5 and incorporated an anterior tibial shell.

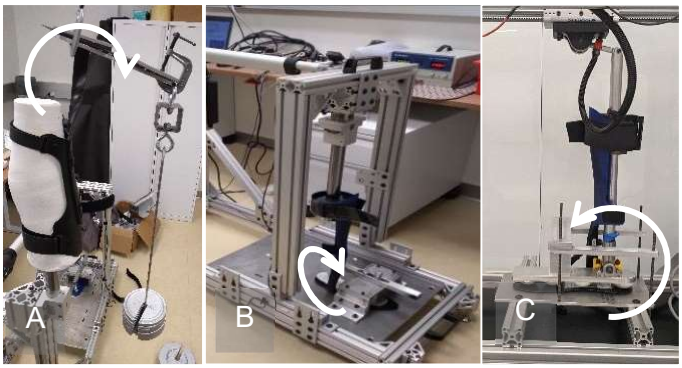

Figure 1: Methods for testing AFO stiffnesses. A) Hanging weights B) CLiMB Stiffness Apparatus C) SMApp.

Method 1, Hanging Weights (Fig 1A): Each AFO was strapped upside down to a molded shank and an aluminum plate was clamped to the front and back of the footplate, constraining deflection to the AFO strut. The initial footplate angle and the moment arm between the center of the surrogate shank and the AFO toe were measured. Weights were hung from the toe of the AFO and incrementally increased through a minimum of five increments.

Method 2, CLiMB Stiffness Apparatus (Fig 1B): A custom designed test fixture was constructed to automatically rotate an AFO in the sagittal plane about a defined ankle axis from 0° to 20° of dorsiflexion at 0.9°/s (2). Deflection was constrained to the AFO strut by clamping the footplate to the fixture base and securing the tibial cuff to a surrogate shank. The fixture was calibrated to account for the fixture weight on the loadcell throughout the range of motion and data filtered at 1 Hz.

Method 3, Stiffness Measurement Apparatus (SMApp) (Fig 1C): Each AFO's footplate was clamped into a previously-validated custom apparatus and its tibial cuff was secured around a custom ring with a linear bearing, to allow movement along the surrogate shank (3). The SMApp loaded the AFO in the sagittal plane at the same range of motion and speed tested in Method 2. We subtracted the fixture dynamics from the measured torque at each deflection angle in post-processing, then transformed the angle data to match the rotation axis used in Method 2.

For all methods, stiffness was calculated by fitting a line to the angle-moment data during dorsiflexion loading. We compared the stiffnesses obtained across methods.

Results and Discussion

AFO sagittal plane stiffness for the tested AFOs differed across testing methods by 12% (Blue Rocker) to 73% (SpryStep) of the maximum stiffness value. Stiffnesses measured by the CLiMB and SMApp were more similar to each other, varying by a maximum of 0.27 Nm/° or 14%. The AFO stiffnesses calculated from hanging weights were an average of 29% lower than those calculated from either custom fixture.

Both custom test fixtures constrained the motion of the AFO to rotation about a single axis, while the hanging weights method also allowed for both translation and rotation in additional planes. The lack of constraints resulted in a lower measured stiffness by hanging weights compared to both fixtures. Only the ToeOFF stiffness measured by hanging weights was higher than a custom test fixture.

Table 1: Measured stiffnesses of AFOs across test methods.

Method \ AFO	Sagittal Stiffness (Nm/°)			
	Blue Rocker	ToeOFF	SpryStep	Matrix
Hanging Weights	3.29	1.73	0.39	0.41
CLiMB Tester	3.74	1.96	1.42	0.63
SMApp	3.58	1.69	1.22	0.55

Significance

This research demonstrates that different testing methods used to determine AFO mechanical properties do not necessarily yield comparable results, reinforcing the need for standardized testing practices. Establishing gold standard methodology for evaluating AFO mechanical properties is important for optimizing device prescription and comparing across manufacturers.

Acknowledgments

This work was supported by an Extremity Trauma and Amputation Center of Excellence (EACE) Rehabilitation Technology Development Fellowship.

References

1. Totah, D. et al. Gait & Posture. 69 101-111, 2019
2. Parham, K.R. US Army Natick Research 1992.
3. Totah, D. et al. Mechatronics. 2020 (accepted)

PILOT TESTS OF A ROBOTIC PROSTHETIC ANKLE WITH PARALLEL ELASTICITY AND OFFBOARD ACTUATION

Anthony Anderson[1,2], Y. Hudak[1,2], C. Richburg[2], and P. Aubin[1,2]
[1]Department of Mechanical Engineering, University of Washington, Seattle, WA
[2]Center for Limb Loss and Mobility (CLiMB), VA Puget Sound Health Care System, Seattle WA
email: ajanders@uw.edu

Introduction

Research in lower-limb prosthetic devices has been improved by high-performance mechatronic testbeds. These laboratory-based testbeds pair stationary actuation and control platforms with simple and lightweight prostheses through flexible actuation tethers [1]. These systems allow scientists to quickly test new hypotheses relating prosthesis performance to gait biomechanics, user preference, and other relevant outcomes without building complex and heavy robotic devices for each new experiment. Existing systems are limited in their ability to emulate healthy biomechanics in early stance because the dorsiflexion moment behaviour is set in hardware with cantilever springs. This means different dorsiflexion moments cannot be programmatically rendered by the device during walking.

This work introduces a novel robotic ankle prosthesis with offboard actuation and control. The prosthesis pairs a Bowden cable actuator with a parallel torsion spring, allowing for active control of both plantarflexion and dorsiflexion moments. Results are presented from one healthy subject walking on the device with prosthesis simulator boots. These tests were conducted to confirm the electro- and biomechanical behaviour of the prosthesis and control system.

Methods

The offboard actuation and control system is comprised of a Kollmorgen AKM74L servomotor, a National Instruments PXI real-time controller, and a desktop PC that operates as an experimenter interface. The motor torques are transmitted to the prosthesis via a custom transmission consisting of a drive shaft, pulley, and Bowden cable.

The ankle prosthesis consists of a custom rotary joint and aluminium structure. The prosthesis attaches to a standard composite footplate and pyramid adapter. Plantarflexion moments are provided by the Bowden cable while dorsiflexion moments are provided by a custom parallel torsion spring. Joint angles and prosthesis moments are measured with compact wearable sensors. The prosthesis mass is 1.3 kg and total range of motion is 46 degrees.

For this experiment, the prosthesis joint torque controller was programmed to make the joint emulate a virtual torsion spring. The prosthesis controller contains a data-driven model of the parallel torsion spring, allowing the total joint torque to be controlled by the actuator.

One healthy subject (M, 28, 75.1 kg) was recruited under an IRB approved protocol to walk on the device with prosthesis adapter boots. Five plantarflexion quasi-stiffnesses from [2] were tested while the subject walked at a self-selected pace of 0.75 m/s. Ankle kinematics and kinetics were computed from wearable prosthesis cable force and ankle angle sensors.

Results and Discussion

The robotic ankle prosthesis and offboard actuation system successfully rendered five quasi-stiffnesses during walking. Sagittal plane joint biomechanics are shown for seven steps from each quasi-stiffness condition in Figure 1.

The peak plantarflexion and dorsiflexion torques provided by the prosthesis during the experiment were 86.5 Nm and 18.26 Nm, respectively. The average RMS torque tracking error across all conditions was 12.68 Nm.

As the prosthesis quasi-stiffness increased, the prosthesis range of motion decreased and the total joint moments remained mostly invariant, which is consistent findings from other studies [3]. The prosthesis moments and powers were lower than those reported in healthy subjects, but this was due to our subject's relatively slow self-selected walking speed and lack of training with the novel device rather than limitations with the hardware or control system.

This pilot experiment showed that our novel prosthesis is capable of rendering a range of human-like ankle behaviours during walking and is ready for experimental studies with lower-limb amputees.

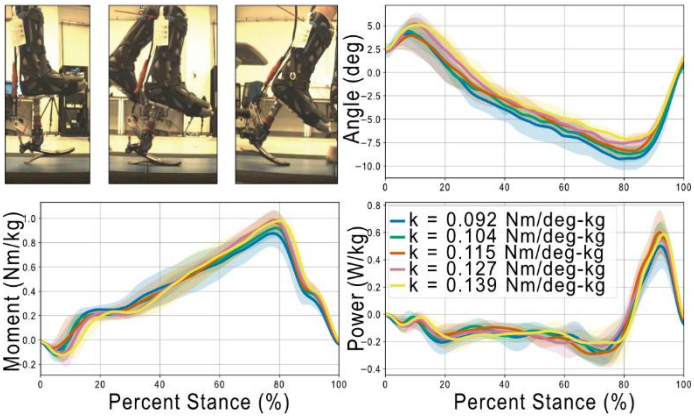

Figure 1: Top-left: images of the prosthesis at heel-strike, midstance, and toe-off. Top-right: prosthetic ankle angle. Bottom-left: Mass normalized ankle-moment. Bottom right: Mass normalized ankle power. Positive direction indicates plantarflexion for both moments and angles.

Significance

Our robotic ankle prosthesis differs from other Bowden-cable driven prostheses in several ways. The device uses a standard prosthesis footplate and will fit inside of a cosmesis and shoe. The parallel torsion spring allows the dorsiflexion moment of the prosthesis to be set on a software level. More high-quality off-board actuation systems and prostheses with unique designs will ultimately make the field of active lower-limb prostheses more robust.

Acknowledgments

This work was funded in part by VA RR&D grants A9243C, RX002357, and RX002130.

References

[1] Caputo and Collins, *IEEE ICRA*, 2013
[2] Hedrick et al. *Journal of NeuroEng. & Rehabil.*, 2019
[3] Clites et al. *IEEE BioRob*, 2020

SOFT HINGE CORRECTION FOR IMU-BASED HIP JOINT ANGLE ESTIMATES FOR ARBITRARY GAIT

Michael V. Potter[1], Stephen M. Cain[1], Lauro V. Ojeda[1], Reed D. Gurchiek[2], Ryan S. McGinnis[2], and Noel C. Perkins[1]
[1]Department of Mechanical Engineering, University of Michigan, Ann Arbor, MI, USA
[2]M-Sense Research Group, University of Vermont, Burlington, VT, USA
email: mvpotter@umich.edu

Introduction

Inertial measurement units (IMUs) are an attractive option for estimating human kinematics without traditional laboratory constraints. However, accurate estimation of joint angles from body-worn IMUs must overcome several challenges, including integration drift errors (caused by the integration of noisy IMU signals). Thus, kinematic estimation methods must leverage additional constraints or measurements to correct such integration drift errors.

Correcting integration drift errors can be particularly challenging for estimating internal/external rotation (IE) of joints because of the relatively low signal-to-noise ratio about the IE axis and because these errors often cannot be observed from measured gravitational acceleration. While magnetometers are commonly used for this purpose, magnetometer-based corrections may be unreliable where magnetic interference is present (e.g., indoors). Other approaches leverage known kinematic constraints or states (e.g., knee acting as an approximate hinge) to correct relative orientation errors (especially IE) between segments [1]. Similar approaches for the hip are more challenging because the hip exhibits three degrees of rotational freedom; however, there still exist limits for anatomically reasonable hip joint angles. We leverage these limits to propose a novel "soft" hinge measurement correction for the hip to improve estimates of IE within an IMU-based lower-limb kinematic estimation method without degrading estimates of flexion/extension (FE) and abduction/adduction (AbAd). We also evaluate the success of the method compared to MOCAP.

Methods

An error-state Kalman filter [2] method is utilized to estimate lower-limb kinematics from an array of seven IMUs (one on each foot, shank, thigh, and pelvis). The measurement model (to correct integration drift errors) comprises gravitational tilt corrections, zero velocity updates for the feet, joint center corrections, and hinge axis corrections for the knee. Within the measurement model, we add a "soft" hinge measurement for the hip. The measurement assumes the FE axes of the thigh and pelvis are approximately aligned in the world frame at all times. A high measurement standard deviation (57 deg., hence a "soft" hinge) corrects anatomically unrealistic hip angles (especially IE) while maintaining accurate estimation of FE and AbAd angles.

To evaluate the proposed measurement correction, we evaluate hip joint angle estimates with and without the correction in comparison to MOCAP. From data for a larger study, we evaluate the method on five subjects performing six one-minute walking trials with different walking gaits for each trial. The walking gaits are forward walking at three speeds (Normal, Fast, and Slow), Backwards walking (Back), and lateral shuffles to the left (Left) and right (Right). Subjects wear IMUs on each major lower-body segment, with three reflective markers on each IMU. Assuming rigidity between respective IMUs and anatomical frames, marker trajectories are used to obtain MOCAP estimates of the hip joint angles and the error-state Kalman filter method is used to obtain IMU-based estimates.

Results and Discussion

For each hip and trial, we calculate RMS differences between IMU and MOCAP-based estimates of the hip joint angles. Mean RMS differences (IMU-MOCAP) across the ten hips are reported for each gait type with the "soft" hinge correction (Tab. 1) and without the correction (Tab. 2). Comparison of these tables reveals that the "soft" hinge measurement correction decreases mean RMS differences in IE estimates across all gait types by an average of 10%. Importantly, these improvements in IE estimation present without any apparent degradation in FE and AbAd estimates. Importantly, RMS differences in FE and AbAd estimates are also similar across all gait types evaluated (Tab. 1).

These results demonstrate that the novel "soft" hinge measurement correction is indeed successful in correcting integration drift errors in IE estimates of the hip without degrading estimates of FE and AbAd. Significantly, this correction achieves these goals even for gaits where the hip is not primarily acting like a hinge in FE (e.g., Left and Right gaits).

Table 1: Mean RMS difference (IMU-MOCAP) in hip joint angle estimates *with* "soft" hinge correction. All values in degrees.

	Normal	Fast	Slow	Back	Left	Right
FE	2.71	2.44	2.73	2.60	2.95	2.99
IE	5.70	4.53	8.22	8.08	7.13	7.46
AbAd	3.09	2.54	3.18	3.02	2.86	3.56

Table 2: Mean RMS difference (IMU-MOCAP) in hip joint angle estimates *without* "soft" hinge correction. All values in degrees.

	Normal	Fast	Slow	Back	Left	Right
FE	2.70	2.44	2.73	2.60	2.96	3.00
IE	6.73	5.17	9.26	9.97	7.32	7.57
AbAd	3.22	2.64	3.26	3.33	2.86	3.58

Significance

For IMU-based kinematic estimation to prove valuable in broad biomechanical contexts, methods must remove restrictive assumptions about environment (e.g., level ground) and/or type of movement. The success of the "soft" hinge measurement correction for the hip over a variety of gaits demonstrates that this correction effectively reduces integration drift errors (especially in IE) without such assumptions. Thus, this novel correction likely remains valid for use in broad biomechanical contexts including those focused on pathological gait.

Acknowledgments

This research is supported by the US Army Contracting Command APG, Natick Contracting Division, under contract W911QY15-C-0053 and by the NSF Graduate Research Fellowship Program under Grant DGE 1256260. Any opinions, findings, conclusions, or recommendations are those of the authors and do not necessarily reflect the views of the sponsors.

References

[1] Vitali, et al. "Method for estimating..", *Sensors*, 2017.
[2] Sola. "Quaternion kinematics...", arXiv:1711.02508, 2017.

KINEMATIC CHANGES PRIOR TO AND FOLLOWING WALKING SPEED TRANSITIONS

Francesca Wade[1,2], G. Roque[1], G. Kellaher[1], S. Baudendistel[1], S. Pesquera[2], D. Clark[2,3], D. Ferris[4], R. D. Seidler[1,6], T. Manini[3], and C. Hass[1,6]

[1]Department of Applied Physiology & Kinesiology, University of Florida
[2]Brain Rehabilitation Research Center, Malcom Randall VA Medical Center [3]Department of Aging and Geriatric Research, University of Florida [4]J. Crayton Pruitt Family Department of Biomedical Engineering, University of Florida [5]Institute on Aging, University of Florida [6]Norman Fixel Institute for Neurological Diseases, University of Florida email: fwade21@ufl.edu

Introduction

Walking in the community requires individuals to acutely speed up or slow down based on task-related demands and environmental constraints. Transitioning speed is a form of gait adaptability, and reduced adaptability can lead to reduced community mobility. Understanding how young individuals produce gait speed changes provides a baseline for future work investigating age-related changes in these processes that might affect community mobility.

It is well-reported that gait biomechanics are dependent on velocity [1]. However, much less is known about the transition between velocities. To our knowledge, no one has investigated the kinematic changes prior to and following a speed transition within walking.

We studied the kinematics of the transition between preferred walking speed to faster or slower walking. We hypothesized that the change kinematics following the speed transition would be consistent with the established velocity-dependent changes [1].

Methods

Healthy adults (n = 10, mean ± SE age: 24.6 ± 1.50 y; height: 1.71 ± 0.04 m; mass: 70.98 ± 4.69 kg) provided written informed consent prior to data collection.

Reflective markers, placed according to the Plug-In Gait marker set, were recorded at 100 Hz in Nexus (Vicon, Oxford Metrics Inc.). Individuals were instructed to "*begin walking at your typical pace. When I tell you* slow, *walk at the slowest possible speed that still feels natural. When I say* go, *walk at your fastest safe speed."* 5 trials of each speed transition were obtained on a 10 m long walkway.

Forward center of mass (CoM) velocity was calculated and plotted in Matlab (Mathworks Inc.). Within a user-selected range, the transition point was defined mathematically as the point when CoM velocity only increased (for faster walking) or decreased (for slower walking) following either a peak or a trough. The step prior to and the step immediately following the transition point were identified and spatiotemporal gait variables and stance limb peak joint angles were computed. The number of steps taken to reach mean CoM velocity following the transition was found.

A two-way repeated measures MANOVA with Dunn-Bonferroni corrections for multiple comparisons was run to investigate the influence of transition speed (to 1. faster 2. Slower walking) and time (1. pre- 2. post-transition) on CoM velocity, step length, step width, peak hip extension angle, peak hip flexion angle, peak knee flexion angle, peak plantarflexion and peak dorsiflexion of the stance limb.

Results and Discussion

Group mean CoM forward velocity increased by 0.58 m/s ($p < 0.001$) and decreased by 0.34 m/s ($p < 0.001$) for faster and slower transitions respectively. However, there was no significant change in velocity at the step prior or step immediately following either transition ($p = 0.054$); it took an average of 0.8 steps to increase and 0.92 steps to decrease speed. Step length increased after a faster transition when compared with the step length prior (Figure 1, $p < 0.001$). The opposite was true for slower speed transitions – step length reduced ($p < 0.001$). Statistically, step width decreased transitioning to faster walking ($p = 0.033$), but not when transitioning to slower walking ($p = 0.076$). This is in agreement with what we hypothesized based on the literature [1].

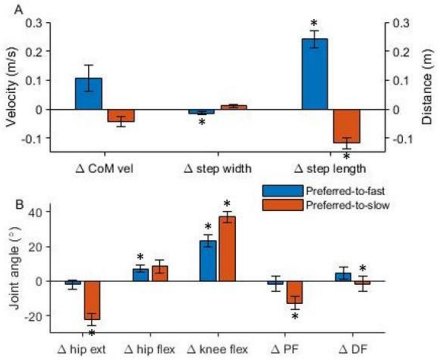

Figure 1: Mean ± SE post-pre transition change (Δ) in **A** center of mass velocity, step width, and step length **B** peak stance hip extension, hip flexion, knee flexion, plantarflexion, and dorsiflexion transitioning from preferred-to-faster speed (blue) and preferred-to-slower speed (orange). *p<0.05 when comparing post-transition value to pre-transition value

There was increased hip extension following the transition to slower walking ($p < 0.001$) as the hip remained flexed prior to the transition. This may explain why hip flexion was not affected ($p = 0.057$). Conversely, hip extension was not affected by transitioning to faster walking ($p = 0.486$) but hip flexion increased ($p = 0.009$). Knee flexion increased following the transition to both faster ($p < 0.001$) and slower walking ($p < 0.001$). There was increased dorsiflexion ($p = 0.018$) and reduced plantarflexion ($p = 0.012$) transitioning to slower walking, but not when transitioning to faster walking ($p \geq 0.257$). This suggests joint kinematics are altered during speed changes, and explorations of the muscular activity would give further insight into the strategy being utilized. Investigations have seen how surface EMG readings vary with speed [e.g., 2], but have not looked at the transitions themselves.

Significance

Here, we outline how healthy adults may initiate a change in walking speed by altering step length, hip extension, and knee flexion. This provides a baseline for comparison with older adults who may have more limited community mobility.

Acknowledgments

This project is supported by NIH U01AG061389.

References

[1] Fukuchi et al. 2019. Systematic Reviews (8), 153.
[2] den Otter et al., 2004. Gait and Posture (19), 270-278.

CHANGES IN REARFOOT KINEMATICS WITH INCREASING STEP RATE

Kathryn A. Farina[1*] and Michael E. Hahn[1]
[1]Bowerman Sports Science Center, Department of Human Physiology, University of Oregon, Eugene, OR, USA
e-mail : * kfarina@uoregon.edu

Introduction

Increased pronation, the combined actions of dorsiflexion, eversion, and abduction, occurring partly at the subtalar joint (STJ), has been implicated as a factor in running related injuries (RRIs) [1]. The STJ axis passes through the talus and calcaneus, and due to inabilities to place markers on the talus, motion at the rearfoot, or calcaneus, has been used as a measure of STJ motion [1]. Attempts to control or alter STJ motion have focused on orthotic and shoe interventions [2], but these efforts do not correct underlying weaknesses that may be responsible for excessive STJ motion. Increasing step rate (SR) during running has become a popular method in gait retraining for injury prevention and recovery, and has been shown to alter kinematics and kinetics at the hip, knee, and ankle joints [3,4]. The focus of this study was specifically to evaluate changes in rearfoot kinematics as a result of increasing step rate, and to visualize these changes in multiple planes of motion.

Methods

Twenty runners (11 male, 9 female; 24.9 ± 8.7 years old; 173.7 ± 9.8 cm; 64.7 ± 11.3 kg; 34.5 ± 17.1 miles per week) gave informed consent to participate in this IRB-approved study. Participants had to run at least 15 miles per week, and be pain free at the time of testing. Participants ran on a force-instrumented treadmill (Bertec, Columbus, OH) while marker position data (Motion Analysis Corp., Rohnert Park, CA) were collected (f_s = 1000 and 200 Hz, respectively) under three conditions while wearing standardized, neutral shoes (Brooks Launch). Participants ran at their preferred running pace (3.33 ± 0.4 m/s) at preferred SR, +5%, and +10% of preferred SR for three minutes each. Participants were cued by metronome set to the goal SR for each of the increased SR conditions. Twenty strides were recorded during the final minute of each condition. Data were analyzed using a custom MATLAB script (The MathWorks, Natick, MA). Marker coordinate and force data were filtered with a 4th order lowpass Butterworth filter at 20 Hz. Sagittal and frontal plane angles for the rearfoot segment were calculated with respect to the shank, averaged across 20-foot strikes, and ensemble averaged across participants for each condition. Discrete values at peak angle, initial contact (IC), and toe-off (TO) were extracted. A repeated measures ANOVA was used to evaluate differences in discrete variables across conditions.

Results and Discussion

Significant differences were observed between SR conditions, with the preferred SR (175 ± 7 steps/min) being significantly lower than the +5% (185 ± 9) and +10% (192 ± 9) conditions ($p < 0.001$), confirming the SR protocol was effective. Repeated measures ANOVA revealed significant differences in peak and TO angles in the sagittal plane, and peak angle in the frontal plane (Table 1). Plotting sagittal and frontal plane rearfoot angles together, it was observed that peak rearfoot eversion occurred earlier in stance than peak dorsiflexion across conditions (Figure 1).

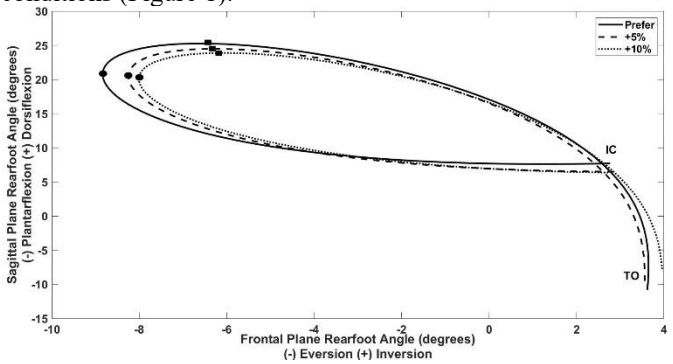

Figure 1. Sagittal and frontal plane motion of the rearfoot segment for step rate conditions. Black squares = peak dorsiflexion angle. Black circles = peak eversion angle. IC = initial contact. TO = toe-off.

Kinematic values at IC between conditions appeared to be similar, with differences between conditions being observed in the timing of peak dorsiflexion. At TO, there was a significantly decreased plantarflexion angle in the +10% condition. Slight differences were observed in frontal plane rearfoot angles between conditions. It appears the primary method of change in the rearfoot due to step rate alteration occurred in the sagittal plane, with some significant changes in the frontal plane. Previous studies have reported decreases in peak dorsiflexion angle of around 2 degrees with a 10% increase in step rate, similar to the results seen in the present study [4].

Significance

The results from this study add to the growing evidence that increasing step rate affects motion at the rearfoot. These results indicate that despite the interconnected motion of pronation at the STJ, planes of motion may be affected differently by gait retraining interventions.

References

[1] McClay, I and Manal, K. (1998). *Clin Biomech,* **13** (3)
[2] Clement, D and Taunton, J (1980). *Can Fam Physician*, **26**
[3] Heiderscheit, B. et al. (2011). *Med Sci Sports Exerc*, **43** (2)
[4] Lenhart, R. et al. (2014). *Med Sci Sports Exerc*, **46** (3)

Table 1. Rearfoot sagittal and frontal plane angles (degrees) at peak, initial contact (IC), and toe-off (TO). Negative values correspond to plantarflexion and eversion. * = sig. diff from preferred step rate (SR); # = sig. diff from +5% SR

	Preferred SR	+5% SR	+10% SR
Peak Sagittal Plane Angle	25.85 ± 9.28	24.94 ± 9.60 *	24.27 ± 9.53 *#
Peak Frontal Plane Angle	-8.97 ± 5.15	-8.40 ± 5.44*	-8.18 ± 5.52*
IC Sagittal Plane Angle	7.72 ± 11.94	6.50 ± 11.74	6.37 ± 11.40
IC Frontal Plane Angle	2.77 ± 6.22	2.85 ± 5.47	2.73 ± 5.79
TO Sagittal Plane Angle	-10.79 ± 10.69	-9.48 ± 10.34*	-7.94 ± 10.64 *#
TO Frontal Plane Angle	3.62 ± 7.00	3.56 ± 6.02	3.96 ± 6.16

TIBIAL COMPRESSION DURING SUSTAINED WALKING WITH BODY BORNE LOAD

Elijah M. Walker, M. Nelson, M.D. Drew, S.M. Krammer, and T.N. Brown
Center for Orthopaedic and Biomechanics Research, Biomedical Engineering Program, Boise State University, Boise ID USA
email: eliwalker@u.boisestate.edu

Introduction

Military personnel routinely carry heavy body borne loads for prolonged periods of time. Walking with heavy body borne load is reported to increase vertical GRFs approximately 10%[1], which may abnormally compress the distal tibia, leading to bone microdamage that characterizes stress fracture. Both magnitude and rate of vertical GRFs are reported to increase every 15 minutes of sustained walking with body borne load[2], and may further elevate tibial stress fracture risk. Considering GRF is the strongest predictor of stress fracture development among military personnel, it is imperative to determine how routine military tasks lead to tibial bone loading and stress fracture.[1] This study determined whether body borne load and duration of walking increase tibial bone load, and whether these increases are related to vertical GRFs. It was hypothesized that both body borne load and walk duration would lead to significant increases in tibial bone load, but increases in vertical GRFs would not have a strong linear relation to larger tibial bone loads.

Methods

Thirteen participants (9 male/4 female: 23.8 ± 2.8 years, 1.8 ± 0.1 m, 72.0 ± 12.6 kg) had vertical GRFs and tibial bone load quantified during a 60-minute walk task with three body borne loads (0 kg, 15 kg and 30 kg). For each load, participants wore a weighted vest (V-MAX, WeightVest.com, Rexburg, ID, USA) that was systematically adjusted to apply necessary load. For the walk task, participants walked continuously at 1.3 m/s ± 5% and had three trials of biomechanics data recorded every 5 minutes throughout the task. Synchronous 3D marker trajectories and GRF data were collected using eight high-speed optical cameras (MXF20, Vicon Motion Systems LTD, Oxford, UK) and a single force platform (2400 Hz, OR6, AMTI, Watertown, MA) for each trial. For each trial, marker and GRF data were lowpass filtered (12 Hz, 4th order Butterworth), and then ankle rotations, 3D ankle joint forces and moments were calculated using Visual3D (C-Motion, Rockville, MD). Custom MATLAB (Mathworks, Natick, MA) code quantified tibial compression (maximum and impulse), calculated as the summation of external net force on the ankle (estimated as the 3D GRF projected on the long tibia axis) and internal muscle force contributions (estimated as sagittal ankle moment divided by Achilles tendon moment arm)[3], and GRF metrics (peak, impact peak, impulse and loading rate).

For statistical analysis, tibial compression and GRF metrics were submitted to a RM ANOVA to test the main effects and interaction between load (*0, 15 and 30* kg) and time (*minute 0, 30 and* 60), and correlation analyses determined the relation between tibial compression metrics and vertical GRF measures for each load and time. All analysis was performed in SPSS (v26, IBM, Armonk, NY) and alpha level was $p < 0.05$.

Results and Discussion

In agreement with our hypotheses, each tibial compression and GRF measure increased with the addition of body borne load (all: $p<0.001$) (**Fig. 1A**), and may place greater stress on the tibia, increasing injury risk. Although both tibial compression and vertical GRFs increased with load, the vertical GRF measures exhibited negligible to weak (r: -0.37 to 0.35), and weak to moderate (r: -0.62 to 0.59) relation with maximum and impulse of tibial compression with each body borne load. The discrepancy between vertical GRFs and tibial compression may stem from the muscle force necessary to walk with body borne load. Yet, despite large increases in gastrocnemius force when walking with body borne load, future research is needed to determine how these muscle forces increases tibial stress fracture risk.

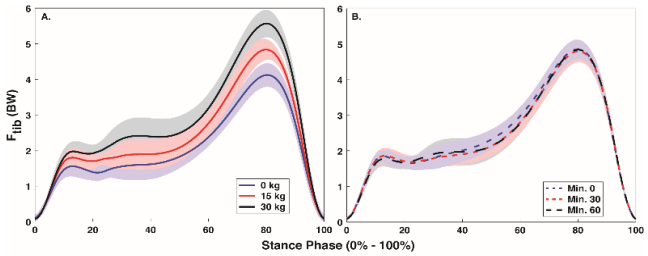

Figure 1. Mean ± SD stance phase (0% - 100%) tibial compression with each load (0, 15, and 30 kg) (**A**) and time point (min. 0, 30 and 60) (**B**).

In partial agreement with our hypotheses, walk time increased GRF impact peak ($p=0.034$) and loading rate ($p=0.017$) of GRFs, but no other GRF or tibial compression measure ($p>0.05$) (**Fig. 1B**). Although sustained load carriage led to faster GRF loading on the musculoskeletal system and potential injury risk, a similar increase in tibial compression was not observed throughout the walk task. Additionally, at each time point, the vertical GRF measures exhibited negligible to weak (r: -0.39 to 0.27), and weak to moderate (r: -0.53 to 0.65) relation with maximum and impulse of tibial compression, respectively. As such, sustained load carriage may lead to faster GRF loading on the musculoskeletal system, but may not further increase tibial compressive force.

In conclusion, the addition of body borne load resulted in a 20% increase in maximum tibial compressive forces, and may accelerate tibia bone microdamage that characterize stress fracture. Although sustained load carriage increases the rate of GRF loading on the musculoskeletal system, this did not produce a concurrent increase in tibial compressive force.

Significance

Walking with body borne load increased tibial compression that may elevate stress fracture risk. But, increased tibial compression did not stem from concurrent increases in vertical GRFs. Future work is needed to determine the muscular contributions to tibial bone loads during load carriage and whether they elevate injury risk for military personnel.

Acknowledgments

Funding was provided by MW CTR-IN/NIGMS (Award # 2U54GM104944).

References

1. Birrell, S.A., et al., *Gait Posture* **26**, 611–614, 2007.
2. Lidstone, D.E., et al., *J. Appl. Biomech.* **33**, 248-255, 2017.
3. Matijevich, E.S., et al., *PLoS One* **14**, e0210000, 2019.

BACK LOADS ARE INSENSITIVE TO INTRA-ABDOMINAL PRESSURE IN WALKING SIMULATIONS

Jordan T. Sturdy[1], Pinata H. Sessoms[2], and Anne K. Silverman[1]
[1]Department of Mechanical Engineering, Colorado School of Mines, Golden, CO
[2]Warfighter Performance Department, Naval Health Research Center, San Diego, CA
email: sturdy@mines.edu

Introduction

Full body musculoskeletal models with detailed lumbar spine regions are useful to investigate forces in intervertebral discs for dynamic activities. While there is debate regarding the influence of intra-abdominal pressure (IAP) on spinal loads, this pressure contributes to a lumbar extension moment through interaction with the diaphragm. IAP has previously been modeled as a constant force applied to the torso anterior to the T12 vertebral body for musculoskeletal simulations [1]. During walking, IAP follows a variable pattern that closely matches net ground reaction force [2]. However, the importance of this IAP variation in estimating lumbar spine joint contact forces is unknown.

Methods

We developed simulations in OpenSim v3.3 (NCSRR, San Jose, CA) of five participants (5M, 27.2±4.4 years, 26.7±1.9 BMI) using kinematic (120 Hz) and ground reaction force (1200 Hz) data during walking at their self-selected speeds [3]. Three IAP conditions were simulated: (1) no IAP, (2) constant IAP, and (3) variable IAP. IAP was modeled as an external force applied upward on the torso approximately 4 cm anterior to T12 [1] and downward on the pelvis at the pelvis center of mass. For the variable IAP implementation, left and right ground reaction forces were summed and scaled to the range 4.4–9.0 kPa. During the constant condition, IAP was 6.7 kPa to represent the average pressure during the variable condition. Force due to IAP was calculated using a diaphragm area of 210 cm^2 [4] that was scaled by each participant's torso scale factor.

Walking kinematics and ground reaction forces were identical for all conditions. We used a static optimization to solve for muscle forces, which were used to compute compressive L4L5 joint contact forces. Maximum and minimum joint contact and IAP forces were normalized to body weight (BW) and compared across conditions using one-way analyses of variance with post hoc comparisons in MATLAB (MathWorks, Inc.) (α=0.05).

Results and Discussion

Applied force due to variable IAP was 4.57% BW greater and 4.87% BW less at the extrema compared with the constant IAP condition ($p<.001$). Maximum L4L5 joint contact force (Figure 1) was on average 16.70% BW less during constant and 18.85% BW less during variable compared with no IAP, which approached a significant main effect ($p=.052$). Minimum L4L5 force had a significant main effect ($p<.001$), which was 12.17% BW less in constant and 8.59% BW less in variable IAP conditions compared with no IAP. There were no differences between constant and variable IAP conditions for either maximum or minimum L4L5 force. In addition, the difference in joint contact force was less than the difference in applied force due to IAP between constant and variable conditions, which suggests differences in torso muscle force requirements.

Modeling IAP to produce a net extension moment on the torso did not significantly affect L4L5 joint contact force. However, the magnitude difference in peak force on average (>15% BW) may be important to consider for injury risk and may be further explored. This study assumed a high peak IAP value, which is applicable to lifting or carrying weight [1]. However, peak IAP during walking has been measured to be as low as 2.67 kPa [2] and 4.95 kPa [5], and smaller differences between all conditions would be expected if these values were implemented in the walking simulations.

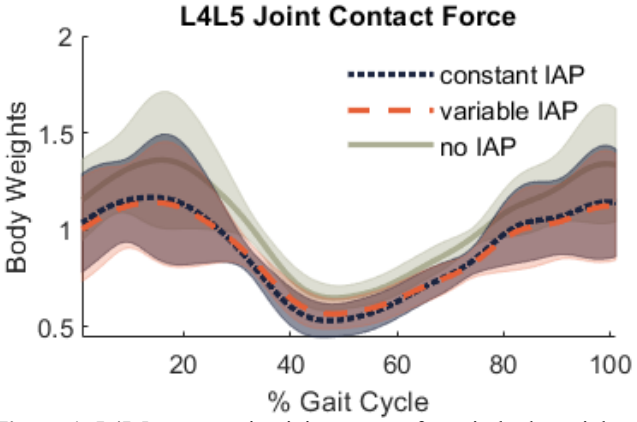

Figure 1: L4L5 compressive joint contact force in body weights from each IAP condition averaged across all participants. Mean values are plotted in the *dotted dark blue* line for *constant* IAP, *dashed orange* line for *variable* IAP, and *solid green* line for *no* IAP. Shaded regions show the mean±1 standard deviation for each condition.

Significance

The difference in peak L4L5 joint contact force due to IAP implementation was less than 3% BW, which suggests that potential benefit in a variable IAP implementation is less important than the average IAP during walking. In addition, IAP did not significantly affect maximum L4L5 loads in either implementation and may not be critical to include in walking simulations. However, results should be interpreted with caution as validation of IAP magnitudes and spinal loading is needed.

References

[1] Arjmand and Shirazi-Adl. *Eur Spine J* 2006;15(8):1265–1275.
[2] Grillner et al. *Acta Physiol Scand* 1978;103:275–283.
[3] Sturdy et al. *Appl Ergon* 2021;90:103277.
[4] Daggfeldt and Thorstensson. *J Biomech.* 2003;36(6):815–825.
[5] Coleman et al. *Int Urogynecol J* 2015;26(7):967–974.

Disclaimer: I am a military service member or employee of the U.S. Government. This work was prepared as part of my official duties. Title 17, U.S.C. §105 provides that copyright protection under this title is not available for any work of the U.S. Government. Title 17, U.S.C. §101 defines a U.S. Government work as work prepared by a military service member or employee of the U.S. Government as part of that person's official duties. This work was supported by the U.S. Defense Health Agency under work unit no. N1814. The views expressed in this abstract are those of the authors and do not necessarily reflect the official policy or position of the Department of the Navy, Department of Defense, nor the U.S. Government. The study protocol was approved by the Naval Health Research Center Institutional Review Board in compliance with all applicable federal regulations governing the protection of human subjects. Research data were derived from an approved Naval Health Research Center Institutional Review Board protocol number NHRC.2013.002

BALANCE EFFORT AND COMPENSATORY MECHANISMS IN COMMON DEGENERATIVE SPINAL PATHOLOGIES

Ram Haddas, PhD; Thomas Kosztowski, MD; Damon Mar, PhD; Akwasi Boah, MD; Isador H. Lieberman, MD
Texas Back Institute, Plano, TX, USA | email: rhaddas@texasback.com

Introduction

Balance changes are common in individuals with spinal disorders and may cause falls. Aging, vestibular deficits, poor vision, spinal disorders that cause changes in posture, and weak core and leg musculature all predispose an individual to postural instability.[1] Balance efficiency is the ability of a person to maintain their center of gravity with minimal neuromuscular energy expenditure, oftentimes referred to as Cone of Economy (CoE).[2] CoE balance is defined by two sets of measures taken from the center of mass (CoM) and o head: 1) the range-of-sway (RoS) in the coronal and sagittal planes, and 2) the overall sway distance.[3] This allows spine caregivers to assess the severity of a patient's balance, balance pattern, and dynamic posture and record the changes following surgical intervention. Maintenance of balance requires coordination between the central nervous and musculoskeletal systems.[4] The purpose of this study was to discern differences in balance effort values between common degenerative spinal pathologies and a healthy control group.

Methods

Three-hundred and forty patients with degenerative spinal pathologies: cervical spondylotic myelopathy (CSM), adult degenerative scoliosis (ADS), sacroiliac dysfunction (SIJD), degenerative lumbar spondylolisthesis (DLS), single-level lumbar degeneration (LD), and failed back syndrome (FBS), and 40 healthy controls were recruited. Each patient was tested one week before surgical treatment for their underlying spinal pathology. Healthy subjects were tested on a date convenient for the subject. Each patient was fitted with a full-body external reflective marker set for three-dimensional (3D) balance analysis. Markers being used to track primary joints of the trunk and extremities. Each patient performed a Romberg's test which they were asked to stand erect with feet together and eyes open in their self-perceived balanced and natural position for a full minute. Three-dimensional kinematic data was recorded at 100Hz using a 10-camera system (Vicon, Oxford, UK) and was low-pass filtered using a 4th-order Butterworth filter at a 6Hz cut-off frequency. Multiple one-way ANOVAs were used to test for significant changes between the degenerative spinal pathologies cohorts to the healthy group.

Results and Discussion

Balance effort and compensatory mechanisms were found to be significantly greater in degenerative spinal pathologies patients compared to controls. Head and Center of Mass (CoM) overall sway ranged from 65.22-92.78 cm ($p<0.004$) and 35.77-53.31 cm ($p<0.001$), respectively in degenerative spinal pathologies patients and in comparison to controls (Head: 44.52 cm, CoM: 22.24 cm; Figure 1). Patients with degenerative spinal pathologies presented with greater trunk (1.61-2.98°, $p<0.038$), hip (4.25-5.87°, $p<0.049$), and knee (4.55-6.09°, $p<0.036$) excursion when compared to controls (trunk: 0.95°, hip: 2.97°, and knee: 2.43°).

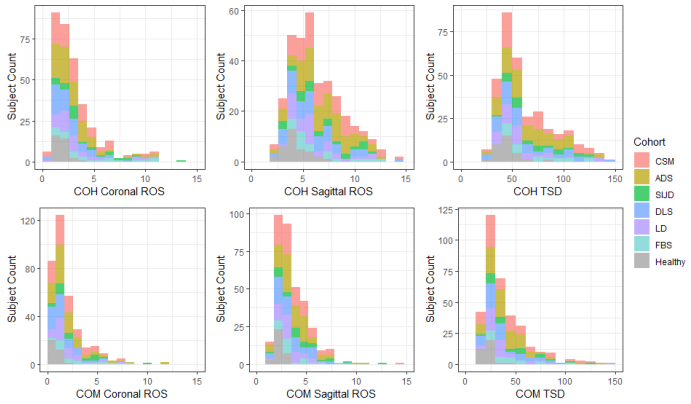

Figure 1. Histogram plots showing the head range and total sway by cohort.

The results of this study indicate that patients with degenerative spinal pathologies exhibit markedly diminished balance (and compensatory mechanisms) as indicated by increased sway on a Romberg test and larger CoE. Balance effort, as measured by overall sway, was found to be approximately double in patients with degenerative spinal pathologies in comparison to healthy matched controls. CoE dimensions were found to be significantly greater in common degenerative spinal pathologies in comparison to controls. This may be due to a variety of reasons including direct inhibition of sensory/proprioceptive feedback (CSM), overcompensation to restore sagittal/coronal balance (ASD), pain mechanisms causing altered posture (SIJD/FBS/LD), and habitual postural changes due to chronicity of symptoms. Conscious and unconscious proprioceptive mechanisms (vestibulospinal tracts, spinocerebellar tracts, dorsal columns) require unimpeded pathways for optimal function.[5] Their alteration, as per our data, reliably demonstrates quantifiable alterations in CoM as well as head sway (overall, sagittal, coronal).

Significance

The results of this study indicate that patients from a wide variety of degenerative spinal pathologies similarly exhibit markedly diminished balance (and compensatory mechanisms) as indicated by increased sway on a Romberg test and a larger CoE as compared to healthy controls. Balance effort, as measured by overall sway, was found to be approximately double in patients with degenerative spinal pathologies compared to healthy matched controls. The clinical importance of these measurements allows spine caregivers to assess the severity of a patient's balance, balance pattern, and dynamic posture and record the changes following surgical intervention.

References

1. Ten T, et al. *J Appl Biomech,* 32, 316-23, 2016.
2. Dubousset J, *Ped Spine*, 479-96, 1994.
3. Haddas R, et al. *Euro Spine J*, 29(9), 2319-2328, 2020.
4. Wall PD et al. *Brain*, 100(4), 641-53, 1977.
5. Johnson EO et al. *J Surg Orthop Adv,* 17, 159-64, 2008.

MUSCLE MODELLING USING MACHINE LEARNING AND OPTIMAL FILTERING OF SEMG SIGNALS

Ali Nasr[1*], Jiayuan He[2], Ning Jiang[2], and John McPhee[1]
[1]Motion Research Group, University of Waterloo, Canada
[2]Waterloo Engineering Bionics Lab, University of Waterloo, Canada
email: *a.nasr@uwaterloo.ca

Introduction

Muscle models have many uses, including musculoskeletal simulations, post-rehabilitation analysis, and biomechatronic device control. Developing a machine learning muscle model that maps surface electromyography (sEMG) signals to muscle activation torque is critically dependent on signal quality. By optimizing the structure and cut-off frequencies of the sEMG signal processing algorithm, the muscle model accuracy can be maximized. This study proposes a novel filtering-and-mapping evaluation algorithm, which considers different topologies and cut-off frequencies for the filtering steps, for maximizing the accuracy of sEMG mapping to muscle activation torque. The algorithm is inspired by training methods for convolutional neural networks: finding the minimum error for filtering (convolutional layers) and mapping (fully connected layers).

Methods

First, a model for assessing the mapping accuracy of filtered sEMG to activation torque is necessary for this evaluation. This is achieved by combining machine learning with a mathematical muscle model, using the steps: (i) Kinematic data of a human joint (using Vicon Motion Systems, Oxford, U.K.) along with sEMG signals from N electrodes (using TeleMyo, Noraxon Inc, Arizona, USA) should be collected. (ii) The joint torque has been calculated using an inverse dynamic model of the human skeletal body. (iii) The joint torque has been converted into an activation torque τ_a using a muscle torque generator model [1] or a control-oriented muscle torque model [2]. (iv) A feed-forward artificial neural network with wide and shallow layers (ANN MuscleNET) has been used to map the filtered sEMG to τ_a [3].

Secondly, for finding the optimum cut-off frequency and filtering combinations for minimum mapping error, the method illustrated in Fig.1 has been proposed. The pool of possible steps includes a low-pass filter, high-pass filter, normalization to the maximum value of signals, rectifying step, and white step (a non-filtering step). We have drawn from the pool with the following conditions: (1) The minimum and maximum number of steps selected from the pool should be one and four, respectively; (2) All steps except the white one have one chance of being chosen; (3) The white step can only be at the end of the previous steps; (4) If the filtering steps of high-pass or low-pass are selected, they may have 10, 40, 70, 100, 200, or 500 Hz cut-off frequency. After drawing from the pool, the filtering and manipulation steps construct 1504 possible unique methods, categorized into 63 unique steps without considering the cut-off frequency. The particle swarm method has been used to infer the cut-off frequency from the mentioned range for minimizing the mapping error cost function. Each permutation and cut-off frequency has been used to filter the raw sEMG channels and produced filtered sEMG signals. Then ANN MuscleNET has been trained using the filtered sEMG (input) and the activation torque (output). The cost function of optimization is mean squared normalized error (MSE) calculated by ANN MuscleNET output $\hat{\tau}_a$, activation torque τ_a, start time t_s, and finish time t_f of the task. The task performed by seventeen healthy right-handed young individuals was grasping an object from a desk, lifting it to an upper target, and lowering it back to the desk, all in the sagittal plane.

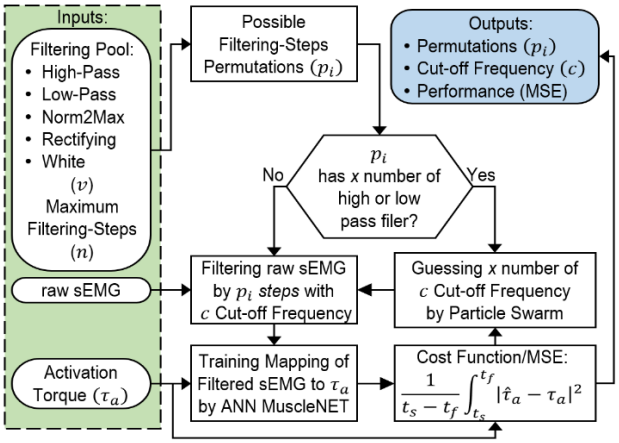

Figure 1: Schematic to evaluate all possible permutations of filtering pool with optimal cut-off frequency for ANN MuscleNET

Results and Discussion

The algorithm tested 1504 input groups in the training procedure of ANN MuscleNET with the same training conditions and saved the best MSE for each unique step. After evaluating the MSE of the steps, we found that 5 of them had the least MSE (Table 1), and the rest had considerably higher MSE. One of the interesting results of this evaluation was that the low-pass filtering step appeared after the rectifying step in all seven best steps. Furthermore, the 10 Hz low-pass filter had a better result than all other (higher) cut-off frequencies.

Table 1: The top 5 filtering combinations with the lowest MSE. H: High-Pass, L: Low-Pass, R: Rectifying, N: Norm2Maximum

#	Combination and Cut-off Frequency	MSE %
1	70 Hz H > R > 10Hz L	7.95
2	500 Hz H > R > 10 Hz L > N	7.96
3	N > 10 Hz H > R > 10 Hz L	8.33
4	R > N > 10 Hz L	8.50
5	10 Hz H > R > N > 10 Hz L	8.58

Significance

By using three filtering steps of 70 Hz High-Pass > Rectifying > 10 Hz Low-Pass, the key sEMG information is preserved for a machine learning muscle model; additional filtering steps or different filtering frequencies are not needed for the object manipulation task. Combining the optimized filtering algorithm with the ANN MuscleNET model, one obtains an accurate sEMG to torque mapping that can replace traditional muscle models.

Acknowledgments

This work was funded by the Canada Research Chairs program.

References

[1] Inkol et al., *Multibody Syst Dyn* **50**, 435–452, 2020.
[2] Nasr et al., In *Proceedings of CDSR*, 144, 2020.
[3] Nasr & McPhee, In *Proceedings of CDSR*, 146, 2020.

EFFECT OF WHOLE-BODY VIBRATION ON KNEE JOINT KINEMATICS AND MUSCLE ACTIVITY IN CHILDREN WITH DOWN SYNDROME DURING THE PENDULUM TEST: A SERIES OF CASE STUDIES

Diego M. Ferreira[1], Gena Priest[2], Haneol Kim[3], and Jianhua Wu[3]
[1]Department of Exercise Science, Lebanon Valley College, Annville, PA, USA
[2]Department of Physical Therapy, Georgia State University, Atlanta, GA, USA
[3]Department of Kinesiology and Health, Georgia State University, Atlanta, GA, USA
Email: ferreira@lvc.edu

Introduction

The Wartenberg pendulum test has been shown to detect increased passive stiffness of the knee in children with Down syndrome (DS) compared to their typically developing (TD) counterparts [1]. This increased passive stiffness is due to increased joint laxity and consequently increased muscle activity in the quadriceps, which provides a protective mechanism during high acceleration activities [2].

Whole-body vibration (WBV) has been used to elicit motor benefits and increase muscle strength across multiple populations. However, the use of WBV in individuals with DS has been limited to improve body composition and balance. Therefore, the purpose of this study was to investigate the acute effects of WBV on knee joint kinematics and muscle activity in children with DS during the pendulum test. We hypothesized that WBV would reduce muscle activity of the quadriceps and increase the passive motion of the lower leg.

Methods

Four children (3F/1M, 11.08±2.8 years) with DS sat in a 45-degree incline angle on a table with their legs hanging over the edge of the table. Their dominant leg was raised so that the knee was in an extended position. Subjects were instructed to relax their leg. The leg was released allowing it to swing freely until it came to a stop. Subjects completed 5 trials before and after one session of WBV, in which subjects completed 10 bouts of 30 seconds of standing on a Galileo side-alternating vibrating platform with one minute of rest between bouts. The frequency and amplitude of the vibration was set to 25 Hz and 2 mm, respectively. An 8-camera Vicon motion capture system was used to collect kinematic data of the knee (Fig. 1). Electromyography (EMG) was collected using Delsys wireless surface electrodes on the rectus femoris (RF), vastus lateralis (VL), and vastus medialis (VM).

Kinematic variables included: first knee flexion excursion (A1), a relaxation index (RI), number of swing cycles (#cycles), and peak velocity in the first knee flexion [2]. The EMG data integrated over the first flexion excursion was calculated for the RF, VL, and VM.

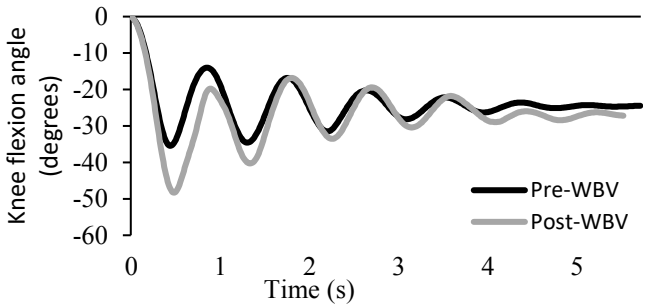

Fig. 1: Sagittal knee kinematics during the pendulum test from a subject.

Results and Discussion

Subjects 1 and 4 completed all 10 bouts of WBV while Subject 2 & 3 were only able to complete 5 bouts due to skin irritation. While Subjects 2 and 3 demonstrated improvements following WBV, Subjects 4 did not demonstrate a clear response and Subject 1 worsened following vibration (Table 1).

The EMG data showed similar integrated areas before and after WBV for all the muscles. This suggests that WBV may reduce the passive stiffness of soft tissues but not the muscles. It is interesting to note that the two subjects who only completed 5 bouts of WBV responded more positively. Additional data is warranted to determine if the observed kinematic pattern maintains and if muscle activity is affected by WBV.

Significance

The preliminary results of this study indicate that WBV may be used as therapy modality to reduce passive stiffness in the DS population. There is a need to collect further data in this population to determine if the improvements seen in some of the subjects can be seen in a larger group. There is also a need to determine if there is an optimal dosage of vibration to elicit the greatest benefits.

References

[1] Ferreira D, et al., Gait & Posture. 76: 311-317, 2020.
[2] Casabona A, et al. *J Appl Physiol*. 113: 1747-1755, 2012.

Table 1: Mean of the kinematic variables.

Variable	Subject 1		Subject 2		Subject 3		Subject 4	
	Pre	Post	Pre	Post	Pre	Post	Pre	Post
A1	43.93	34.81	44.39	49.27	35.24	48.45	25.73	24.69
RI	1.58	1.28	1.59	1.68	1.43	1.87	1.11	1.14
# Cycles	5.4	2.8	6.6	7.2	4	4.8	1.5	2.33
Peak velocity (°/s)	-145.73	-116.66	-138.28	-154.48	-129.54	-162.4	-90.66	-90.82

EFFECT OF BODY POSITION AND EXTERNAL LOAD ON KNEE JOINT KINEMATICS AND MUSCLE ACTIVITY IN CHILDREN WITH DOWN SYNDORME DURING THE PENDULUM TEST: A PRELIMINARY STUDY

Diego M. Ferreira[1], Gena Priest[2], Robert Zeid[3], and Jianhua Wu[3]
[1]Department of Exercise Science, Lebanon Valley College, Annville, PA, USA
[2]Department of Physical Therapy, Georgia State University, Atlanta, GA, USA
[3]Department of Kinesiology and Health, Georgia State University, Atlanta, GA, USA
Email: ferreira@lvc.edu

Introduction

The Wartenberg pendulum test has been used in different populations to assess passive stiffness of the knee. We previously found that body position did not affect the pendulum test in healthy young adults and typically developing children. Additionally, using an ankle load increased the passive motion of the lower leg in children during the pendulum test [1]. However, there has been no investigation into the effect of body position and ankle load in children with Down syndrome (DS). Therefore, the purpose of this study was to investigate the extent to which body position and ankle load affects the knee kinematic performance and muscle activity in children with DS. We hypothesized that ankle load but not body position would affect the kinematic variables and muscular response.

Methods

Five children (3F/2M, 11.08±2.8 years) with DS sat on a table with their legs hanging over the edge of the table. Their dominant leg was raised so that the knee was in an extended position. Subjects were instructed to relax their leg. The leg was released allowing it to swing freely until it came to a stop. Three body positions included: sitting upright, sitting reclined at 45 degrees, and lying supine. Two loading conditions included: no load (NL) and ankle load (AL) equal to 6% of body mass. An 8-camera Vicon motion capture system was used to collect kinematic data of the knee (Fig. 1). Electromyography (EMG) was collected using Delsys wireless surface electrodes on the rectus femoris (RF), vastus lateralis (VL), and vastus medialis (VM).

Kinematic variables included: the first flexion excursion (A1), a relaxation index (RI), number of swing cycles (#Cycles), and peak velocity during the first flexion excursion [2]. The EMG data was normalized by the maximal amplitude for each muscle and integrated over the first flexion excursion.

Results and Discussion

Body position did not affect the kinematic variables of the knee (Table 1) nor the muscle activity across the body positions (Table 2). Ankle load increased the amount of passive motion of the knee. There was an increase in A1, RI, and number of cycles, but not peak velocity (Table 1). However, the ankle load did not elicit an increase in the muscle activity.

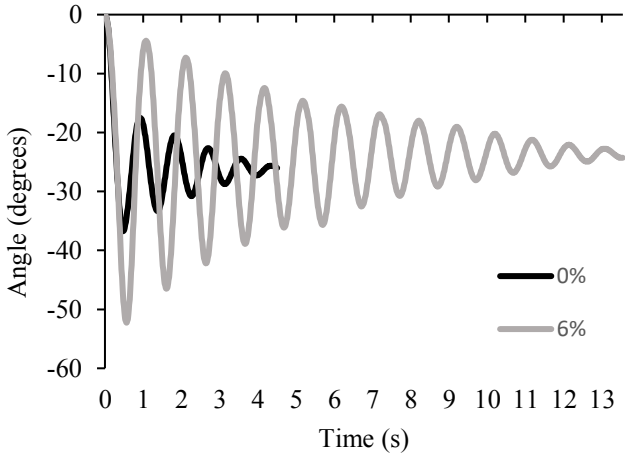

Fig. 1: Sagittal knee kinematics during the pendulum test.

Table 2. Mean (SD) of the integrated area of muscle activity across the body positions.

Variable	NL	AL
RF	27.61 (21.13)	31.6 (27.62)
VL	62.15 (28.74)	71.01 (27.02)
VM	615.12 (1256.18)	635.57 (1132.07)

Significance

The preliminary results of this study indicate that an ankle load can be used to increase passive motion of the knee in children with DS. Neither body positions nor ankle load changed muscular activity. Additional data will verify if these trends remain for a larger group of children with DS. This knowledge will provide a foundation for designing a therapy tool to decrease passive stiffness of the knee in this population.

References

[1] Ferreira D, et al., Gait & Posture. 76: 311-317, 2020.
[2] Casabona A, et al. *J Appl Physiol*. 113: 1747-1755, 2012.

Table 1: Mean (SD) of the kinematic variables.

	NL			AL		
Variable	Supine	Incline	Upright	Supine	Incline	Upright
A1	42.93 (11.01)	42.21 (9.3)	40.77 (11.25)	48.85 (8.15)	48.3 (8.68)	43.5 (5.06)
RI	1.56 (0.28)	1.54 (0.26)	1.45 (0.33)	1.87 (0.26)	1.9 (0.3)	1.77 (0.36)
#Cycles	5.09 (1.53)	4.84 (1.96)	4.61 (1.12)	9.92 (2.9)	8.63 (3.67)	10.56 (3.7)
Peak velocity (º/s)	-146.7 (45.53)	-146.02 (41.12)	-145.52 (43.46)	-145.51 (28.49)	-150.23 (41.6)	-132.69 (30.19)

SHORT- AND LONG-TERM EFFECT OF SURGICAL INTERVENTION ON STATIC AND DYNAMIC BALANCE, GAIT AND PAIN LEVEL

Ram Haddas, PhD; Jakub Sikora-Klak, MD; Damon E Mar, PhD; Andrew Block, PhD; Isador Lieberman, MD
Texas Back Institute, Plano, TX, USA | email: rhaddas@texasback.com

Introduction

In the diagnosis and treatment of adult spinal deformities, static radiographic measurements in the sagittal and coronal anatomical planes and patient-reported outcome measures (PROMs) serve as the gold standard for assessment of spinal alignment and deformity.[1] However, there is a lack of published literature on their relation to objective functional outcome measures (FOMs) among patients afflicted with adult spinal deformity. Adult spinal deformity (ASD) is due to degeneration, functional decline is partly due to loss of postural stability and neuromuscular capacity and coordination.[2] Objective functional measures (e.g. static standing and walking alignment) cover more information than just radiographic alignment in the ASD population.[3] Gait and dynamic balance analysis can reveal functional compensatory alignment changes where static imaging is limited.[1,3] The purpose of this study was to determine the one-year effects of spinal alignment on function in ADS patients following surgical treatment using radiographic parameters, 3D gait and balance analysis, PROMs, and psychological tests and compared to healthy control.

Methods

43 symptomatic ASD patients performed dynamic balance and gait evaluations before surgery (Pre) and at 3 months (Post3), and 12 months (Post12) postoperatively, and were compared to 24 non-scoliotic controls. Full-Body kinematic data was collected at 100Hz using a Vicon 3D motion capture system (Vicon, Oxford, UK). Kinematic data was filtered with a 4th-order Butterworth low-pass filter at a 6 Hz cut-off frequency. Each patient underwent full-length, head-to-toe, micro-dose x-rays (EOS imaging, Paris, Franch) to generate coronal and sagittal views of the spine, pelvis, and lower extremities at Pre, Post3, and Post12. During each clinical evaluation, patients first completed PROMs including the Visual analog scale (VAS) for back and leg pain, Oswestry Disability Index (ODI), and SRS22r. Repeated measurement analysis of variance (ANOVA) was used to determine differences in radiographic, dynamic balance, gait, and PROMs parameters before and after surgical intervention. One-way ANOVA was used to compare dynamic balance and gait surgical data to the non-scoliotic control group.

Results and Discussion

Significant improvements in radiographic alignment were found in Cobb angle ($p<0.001$), sagittal ($p<0.009$) and coronal ($p<0.003$) vertical axes, and pelvic incidence-lumbar lordosis mismatch ($p<0.001$) at Post3 and Post12. There were significant improvements in all PROMs after surgery (VAS, ODI, and SRS: $p<0.050$). Surgical intervention resulted in a significant decrease in balance effort (head: $p<0.017$ and center of mass: $p<0.042$) and Cone of Economy dimensions (sagittal: $p<0.004$; and coronal: $p=0.029$). Gait was also enhanced after surgery as seen with a faster walking speed ($p<0.024$) and longer stride length ($p<0.024$). There may be no procedure that places larger stress on the human skeleton than reconstruction of an adult scoliotic deformity, and much of the prior research focuses on whether the risks and costs are worth the undertaking. The baseline radiographic and PROM improvements provide a foundational trajectory upon which functional measures can be concurrently considered in relation to overall treatment success. It is important to note that from the initial 3-month to the 12-month postoperative follow-up, these radiographic parameters did not significantly change, validating the stability of the construct. However, the result of this study shows that surgical technical success is only one dimension in the patients' post-surgical prognosis, and a multidisciplinary approach using FOMs, PROMs, and pain factors provides more detailed prognosis information.

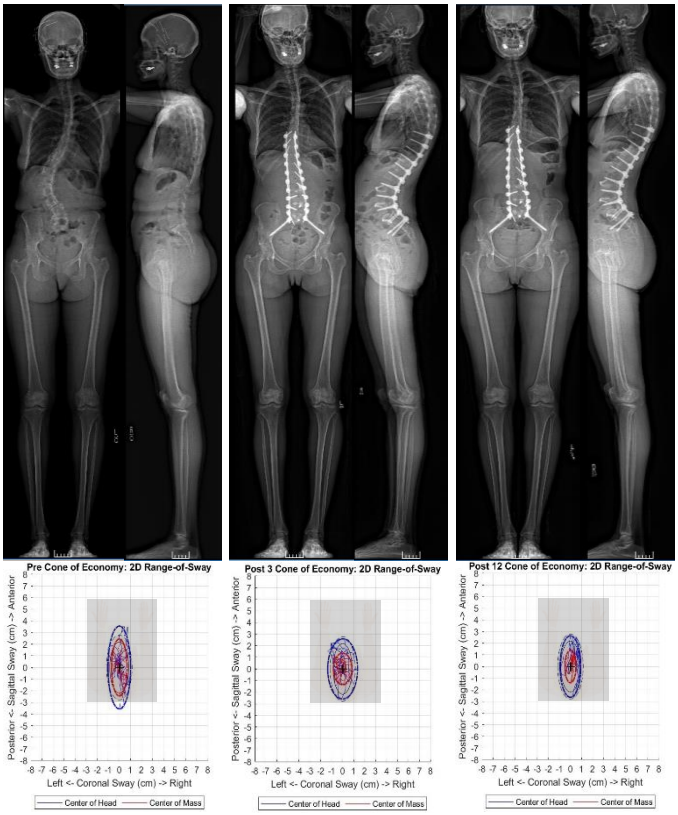

Figure 1. Example ASD patient one week before (Left), three- (Middle), and twelve- (Right) months after realignment surgery.

Significance

Balance effort and CoE limits improved at all time points post-operatively and ultimately matched the controls at 12 months. Similar to the significant improvement in static and dynamic balance in these patient groups, gait parameters also improved Post3 and Post12 to closely resemble the control group and continued to improve over time. Our findings present a more comprehensive set of outcome metrics, which, once combined, provide a more detailed and sensitive assessment of overall treatment outcomes.

References

1. Diebo BG, et al. *JBJS Rev,* 6(7), E3, 2018
2. Yagi M et al. *Spine,* 42(10):E584-91, 2017
3. Haddas Gait *Euro Spine J*, 27(8), 1712-23, 2018.

IMPACT MITIGATION OF WOMEN'S LACROSSE HEADGEAR AT HIGH IMPACT SPEEDS

Grant M. Baker[1], Lorraine Nichols[1], Amanda O. Esquivel[1]
[1]University of Michigan – Dearborn Department of Mechanical Engineering
email: aoe@umich.edu

Introduction

Due to its recent growth in participation, safety concerns for women's lacrosse players are on the rise. However, since the rules of the sport prohibit any player-to-player contact or shot-blocking, helmet use is not mandatory, although head injuries do occur.

There are two commercially available headgear for female lacrosse athletes, the Hummingbird (v1 and v2) (Hummingbird Sports; Holmdel, NJ) and the Cascade LX (Cascade; Liverpool, NY). Recent studies have examined the headgears' abilities to mitigate lower speed women's lacrosse related impacts by measuring peak resultant linear acceleration (PLA) and peak resultant rotational acceleration (PRA) [1, 2]. However, these studies failed to incorporate higher impact speeds and did not consider rotational velocity, which is the kinematic metric most closely correlated with brain injury [3]. Therefore, the purpose of this study was to determine impact mitigation of women's lacrosse headgear at a higher impact speed and to incorporate peak rotational velocity (PRV) metrics in the analysis.

Methods

A 50th percentile male Hybrid III headform (Humanetics; Farmington Hills, MI) instrumented with tri-axial accelerometers and gyroscopes and attached to a Hybrid III neck was struck by a lateral linear impactor (Cadex; St-Jean-sur-Richelieu, Quebec). The impact speed was set to 5.0 m/s to simulate body-to-head impacts based on the analogous high-speed running of female soccer players [3]. The headform was struck with no headgear, with the Hummingbird v2, and with the Cascade LX at a frontal, front boss, and side location since most female lacrosse head injuries occur at the front and side of the head [3].

For all three trials of each impact condition and location, resultant PLA and resultant PRV were determined. Head injury criterion (HIC) and brain injury criterion (BrIC) were calculated using PLA and axis-dependent rotational velocity, respectively. Results were compared between headgear at each impact location using a one-way ANOVA to determine statistical significance ($p < 0.05$).

Results and Discussion

Impact testing results and their statistical significance are shown in **Figure 1**. These results depict that both headgear significantly reduced all four metrics at each impact location besides PRV and BrIC for the Cascade LX at the frontal location.

The Hummingbird's ability to reduce PLA and HIC at the frontal location more than the Cascade LX is consistent with previous studies at lower impact velocities [1, 2]. However, these studies also reported a significantly higher reduction in PLA and HIC for the Hummingbird at the front boss location compared to the Cascade LX, which was not seen in this study.

Literature suggests that a HIC value of 381 is associated with concussion [4] and that a rotational velocity of 27.43 rad/s and BrIC of 0.50 are associated with a 50% probability of concussion [5]. According to the HIC threshold and our results, both headgear were capable of mitigating a potentially concussive impact to a sub-concussive one at all impact locations. However, according to the BrIC and PRV thresholds, the Hummingbird v2 and the Cascade LX were only able to mitigate impacts to a sub-concussive level at the frontal and side locations, respectively.

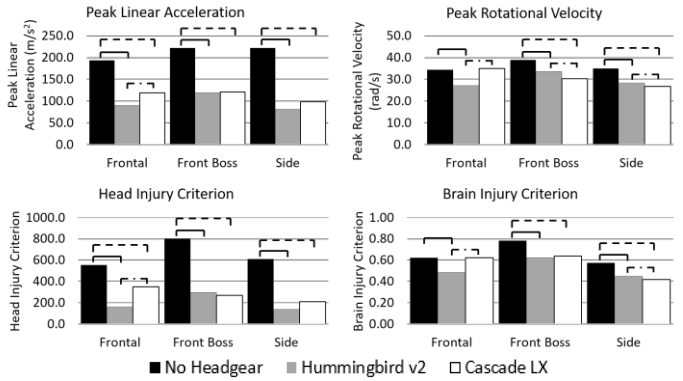

Figure 1: Impact testing results. For the lines above the bars, a solid line indicates significant difference between no headgear and Hummingbird v2, a dashed line indicates significant difference between no headgear and Cascade LX, and a solid line with a dot in the middle indicates significant difference between the Hummingbird v2 and Cascade LX.

Significance

The findings of this study suggest that (1) higher impact velocity may result in different impact mitigation capabilities of women's lacrosse headgear compared to lower velocity impacts and that (2) conclusions on concussion preventiveness may depend on which metrics are considered.

Acknowledgments

This material is based upon work supported by the National Science Foundation under grant no 1919416.

References

[1] McIver, Kevin G., et al. "Impact Attenuation of Male and Female Lacrosse Helmets using a Modal Impulse Hammer." Journal of Biomechanics, vol. 95, 2019, pp. 109313-109313.

[2] Bowman, Thomas G., et al. "Impact Mitigation Properties of Women's Lacrosse Headgear." Annals of Biomedical Engineering, vol. 48, no. 5, 2020, pp. 1491-1498

[3] Gabler, Lee F., Jeff R. Crandall, and Matthew B. Panzer. "Assessment of Kinematic Brain Injury Metrics for Predicting Strain Responses in Diverse Automotive Impact Conditions." Annals of Biomedical Engineering, vol. 44, no. 12, 2016, pp. 3705-3718

[4] Funk, James R., et al. "Validation of Concussion Risk Curves for Collegiate Football Players Derived from HITS Data." Annals of Biomedical Engineering, vol. 40, no. 1, 2012, pp. 79-89

[5] Takhounts, Erik G., et al. "Development of Brain Injury Criteria (BrIC)." Stapp Car Crash Journal, vol. 57, pp. 243-26

THE IMPACT OF GRIP STRENGTH RECOVERY ON GRIP FORCE ACCURACY IN CHRONIC STROKE

Tasnuva Alam[1], Prakruti Patel[2,3], and Neha Lodha[2,3]
[1]Kinesiology & Health, Georgia State University, Atlanta, GA, USA
[2] Health & Exercise Science, Colorado State University, Fort Collins, CO, USA
[3]Biomedical Engineering, Colorado State University, Fort Collins, CO, USA
email: talam5@student.gsu.edu

Introduction

Decreased grip force accuracy and grip strength are two well-documented grip impairments that impede upper extremity function after stroke. Grip force accuracy is essential to perform precise motor actions in everyday life. Further, grip strength represents the ability to produce maximal grip force in a short duration of time and constitutes a hallmark of upper extremity recovery in chronic stroke. Adequate grip strength and grip force accuracy are both critical for regaining motor function after stroke. Despite this, no study has investigated whether the recovery of grip strength influences improvements in force accuracy. Therefore, the purpose of the study was to investigate the impact of grip strength recovery on grip force accuracy in chronic stroke patients.

Methods

We recruited two distinct stroke groups with low (less than 60%) and high (60% or more) grip strength recovery. The grip strength recovery was computed as the percent of paretic grip strength relative to nonparetic grip. A total of thirty-three participants, eleven in the low strength recovery group, eleven in the high strength recovery group, and eleven age-matched controls, participated in the study. To examine the impact of grip strength recovery on grip force accuracy, all participants performed two tasks, a) maximum voluntary contraction (MVC) and b) dynamic force tracking task, using each hand. We quantified grip strength as the maximum force produced in the MVC task. Further, we assessed force accuracy by measuring root mean square error relative to the absolute target force.

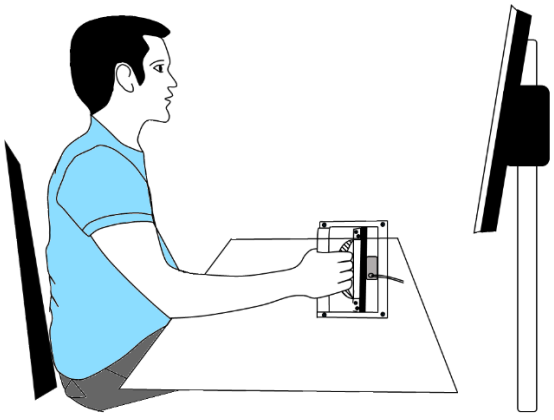

Figure 1: Experimental setup for the grip strength (MVC) and grip force tracking task. Participants were seated in an upright chair in front of a computer screen and performed the grip MVC and the dynamic grip force tracking tasks holding the customized grip device in one hand at a time. In the MVC task, participants exerted maximum grip force. In the force tracking task, participants tracked a trapezoid trajectory as accurately as possible.

Results and Discussion

The low strength recovery stroke group showed decreased grip strength recovery and decreased force accuracy compared to the high strength recovery group. Further, the high strength recovery stroke group exhibits grip strength recovery comparable to the control group, yet decreased force accuracy compared with the control group. Our study provides novel evidence that despite near-normal grip strength recovery, the grip force accuracy may still be impaired in chronic stroke individuals.

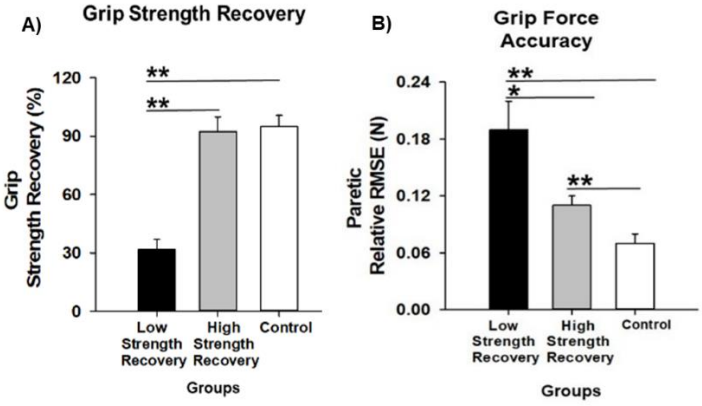

Figure 2: A) Grip strength recovery, B) Paretic grip force accuracy of low and high strength recovery and control groups.

Significance

The precise application of grip forces according to the task requirement is crucial to perform activities of daily living. We found that grip force accuracy varies between the low and high strength recovery groups. Although strength recovery was comparable to the healthy controls, force accuracy continued to be impaired in the high strength recovery group. The interventions and rehabilitation strategies targeting strength recovery alone might not be sufficient. In stroke survivors, following improvements in strength, additional interventions to train force accuracy may be beneficial to allow individuals to apply regained strength more meaningfully.

References

1. Lodha N, Patel P, Casamento-Moran A, Hays E, Poisson SN, Christou EA. Strength or Motor Control: What Matters in High-Functioning Stroke? *Front Neurol.* 2019; 9:1160-1160.
2. Sosnoff JJ, Newell KM. Are age-related increases in force variability due to decrements in strength? *Experimental brain research.* 2006;174(1):86.
3. Xu J, Ejaz N, Hertler B, et al. Separable systems for recovery of finger strength and control after stroke. J Neurophysiol. 2017;118(2):1151-1163.

CHILD GAIT PREDICTION USING MUSCULOSKELETAL AND NEUROMUSCULOSKELETAL MODELS: INVESTIGATION OF DIFFERENT COST FUNCTIONS

Mahdokht Ezati and John McPhee
Systems Design Engineering, University of Waterloo, Waterloo, Ontario, Canada
email: mezati@uwaterloo.ca

Introduction

Recent predictive gait simulations used an anatomically-detailed muscle model (i.e., Hill-type muscle model) to simulate the muscles. However, it is challenging to fit an anatomically-detailed muscle model to specific subjects due to computational and modeling challenges. Muscle torque generators (MTGs) allow researchers to develop simplified but accurate muscle models that fit specific subjects more easily than the anatomically-detailed muscle models [1]. In this research, we used MTGs to generate computationally-efficient musculoskeletal (MSK) and neuromusculoskeletal (NMSK) models that best fit child gait. We developed a wide range of child natural-gait simulations, ranging from fully-data-tracking to fully-predictive, to evaluate the effect of different cost terms on the accuracy of the predicted results.

Methods

We developed a 2-dimensional 11-degree-of-freedom (11-DOF) child model in contact with the ground through a 3-dimensional (3D) ellipsoidal volumetric foot-ground contact model [2]. The model includes 3-DOF HAT-to-ground joint (HAT: head-arms-trunk segment), 1-DOF hip joints, 1-DOF knee joints, 1-DOF ankle joints, and 1-DOF metatarsal joints. The metatarsal joints are torque-driven, and the hip, knee, and ankle joints are actuated by pairs of agonist and antagonist MTGs proposed by [1]. The parameters of the MTGs were fitted to our child gait model using a parameter identification done by direct collocation optimal control in which the mean experimental gait motion data of 20 healthy children were tracked. The subjects were 9 males and 11 females with an age of 10.8±3.2 years, a mass of 41.4±15.5 kg, and a height of 1.47±0.2 m [3].

To investigate different gait simulations, ranging from fully-tracking to fully-predictive, we developed two separate direct collocation optimal controls: "*MSK-model optimization*" and "*NMSK-model optimization*". In the MSK-model optimization, the musculoskeletal geometry and muscle contraction dynamics were represented by MTGs and the control inputs are 12 MTG activations, considering 6 MTGs for each leg. In the NMSK-model optimization, the MSK model along with muscle activation dynamics were used and the control inputs are 16 muscle excitations, considering 8 muscles for each leg.

For each model's optimization, we investigated eight cost functions composed of a wide range of cost terms, including dynamic-based (DYN), stability-based (STB), human-criteria-based (HC), and data-tracking (DT) cost terms (Table 1). The dynamic-based cost term minimizes joint jerks and residual loads and solves motion dynamics implicitly. The stability-based cost term controls the position and orientation of the center of mass. The human-criteria-based cost term minimizes MTG activations for the MSK model, and muscle activations and metabolic energy consumption for the NMSK model. The data-tracking cost terms track experimental joint angles (Ang), joint torques (Trq), and ground-reaction forces (GRF).

The cost terms, specified by a checkmark in each row of Table 1, were first multiplied by weighting factors and then summed together to form the cost function named at the beginning of the row. In cost function #1, fully-data-tracking (FDT), all three DT cost terms were used. In cost functions #2-4, semi-data-tracking (SDT), two of the DT cost terms were used and in cost functions #5-7, semi-predictive (SP), only one of the DT cost terms was used. In cost function #8, fully-predictive (FP), there is no DT cost term.

Table 1: The configurations of cost functions

#	cost function	cost term					
		DYN	STB	HC	DT		
					Trq	Ang	GRF
1	FDT	✓	✓	✓	✓	✓	✓
2	SDT1	✓	✓	✓	-	✓	✓
3	SDT2	✓	✓	✓	✓	-	✓
4	SDT3	✓	✓	✓	✓	✓	-
5	SP1	✓	✓	✓	-	-	✓
6	SP2	✓	✓	✓	-	✓	-
7	SP3	✓	✓	✓	✓	-	-
8	FP	✓	✓	✓	-	-	-

Results and Discussion

The NMSK-model optimizations converged roughly 2.5 times faster than MSK-model optimizations since the control inputs of the NMSK-model optimizations were muscle excitations, the initial guess of which were set to EMG data. However, if experimental data are available to compose DT cost terms, and the muscle excitations and cost of transport (COT) are not required to be calculated, MSK-model optimization is more efficient since it has simpler equations than the NMSK-model optimization. The NMSK-model optimization with the SDT3 cost function predicted the most accurate muscle excitations. With the FP cost function, the NMSK-model optimization predicted angles, torques, tangential, and normal GRFs with root-mean-square errors (RMSEs) of 5.8 degree, 7.5 N.m, 15.8 N, and 62 N, respectively, which are 20%, 16%, 10%, and 8% more accurate than the MSK-model optimization's results. The NMSK-model optimization with the FP cost function predicted muscle excitations with an RMSE of 0.06, 12% more accurate than NMSK-model optimization's muscle excitations with the FDT cost function.

Significance

The proposed MTG-based NMSK-model predicted angles, torques, GRFs, and muscle excitations comparable with experimental data and estimated COT (1.53 $Jkg^{-1}m^{-1}$) for child gait without using an anatomically-detailed muscle model.

Acknowledgments

This research was funded by the Natural Sciences and Engineering Research Council of Canada (NSERC) and the Canada Research Chairs (CRC) program.

References

[1] M. Millard et al. 2019. doi: 10.1016/j.jbiomech.2019.04.004.
[2] M. Ezati et al. 2020. doi: 10.1007/s11044-020-09731-3.
[3] G. Bovi et al. 2011. doi: 10.1016/j.gaitpost.2010.08.009.

SEMI-PREDICTIVE MUSCULOSKELETAL AND NEUROMUSCULOSKELETAL MODELS FOR SIMULATION OF SLOW AND FAST GAITS OF CHILDREN

Mahdokht Ezati and John McPhee
Systems Design Engineering, University of Waterloo, Waterloo, Ontario, Canada
email: mezati@uwaterloo.ca

Introduction

Most of the recent predictive gait simulations focused on adults and older people, but clinical centers working on treatments of child gait disorders prefer to rely more on pediatric gait simulations than adult gait simulations. In this research, we used muscle torque generators (MTGs) to develop semi-predictive musculoskeletal (MSK) and neuromusculoskeletal (NMSK) models that predict child slow and fast gaits, without tracking the experimental data of the corresponding slow and fast gaits.

Methods

We developed a 2-dimensional 11-degree-of-freedom (11-DOF) child model in contact with the ground through a 3-dimensional (3D) ellipsoidal volumetric foot-ground contact model [1]. The model includes 3-DOF HAT-to-ground joint (HAT: head-arms-trunk segment), 1-DOF hip joints, 1-DOF knee joints, 1-DOF ankle joints, and 1-DOF metatarsal joints. The metatarsal joints are torque-driven, and the hip, knee, and ankle joints are actuated by pairs of agonist and antagonist MTGs [2]. The parameters of the MTGs were fitted to our child natural-speed gait model using a parameter identification in which the experimental gait motion data of 20 healthy children were tracked. The subjects were 9 males and 11 females with an age of 10.8±3.2 years, a mass of 41.4±15.5 kg, and a height of 1.47±0.2 m [3]. To generate semi-predictive slow-gait and fast-gait simulations, we used two separate direct collocation optimal controls: "*MSK-model optimization*" and "*NMSK-model optimization*". In the MSK-model optimization, the musculoskeletal geometry and muscle contraction dynamics were represented by MTGs and the control inputs are 12 MTG activations, considering 6 MTGs for each leg. In the NMSK-model optimization, the MSK model along with muscle activation dynamics were used and the control inputs are 16 muscle excitations, considering 8 muscles for each leg. We used the MSK-model and NMSK-model optimizations to predict four different-speed gaits, including very slow walking at 0.9 m/s (XS), slow walking at 1.09 m/s (S), fast walking at 1.29 m/s (L), and very fast walking at 1.58 m/s (XL). The final times of the optimizations and the bounds on the states and control inputs were defined based on the experimental data of the corresponding slow and fast gaits extracted from [3]. The cost function consists of: (1) a dynamic-based cost term, minimizing joint jerks and residual loads and solving motion dynamics implicitly, (2) a stability-based cost term, controlling the motion of the center of mass, (3) a human-criteria-based cost term, minimizing MTG activations for the MSK model, and muscle activations and metabolic energy consumption for the NMSK model, and (4) a data-tracking cost term, tracking the experimental joint angles, torques, and ground reaction forces (GRFs) of the natural-speed gait at 1.26 m/s (M) scaled (stretched/shrank) with respect to the cycle times of the slow and fast gaits.

Results and Discussion

We concluded that the larger the gap between the speed of slow or fast gaits and the speed of natural gait, the longer the computational time and the less accurate the results for slow-gait or fast-gait simulations. The MSK-model and NMSK-model optimizations predicted physiologically-realistic torques, motions, and GRFs for child slow and fast gaits. The NMSK-model predicted the joint torques for the XS, S, L, and XL gaits with normalized-root-mean-square errors (NRMSEs) of 0.10, 0.07, 0.07, and 0.10, respectively, that are 17%, 12%, 10%, and 2% more accurate than the MSK-model's resultant torques. The NRMSEs were calculated given the experimental inverse dynamic torques of child slow and fast gaits. The NMSK-model optimization also predicted muscle excitations (Figure 1-a) and cost of transport (COT) for the different-speed gaits (Figure 1-b). Most of the resultant muscle excitations were in agreement with the experimental EMG data (gray plots in Figure 1-a). The COT plot in Figure 1-b follows the expected 'U'-shaped curve, where the minimum occurs at the natural speed.

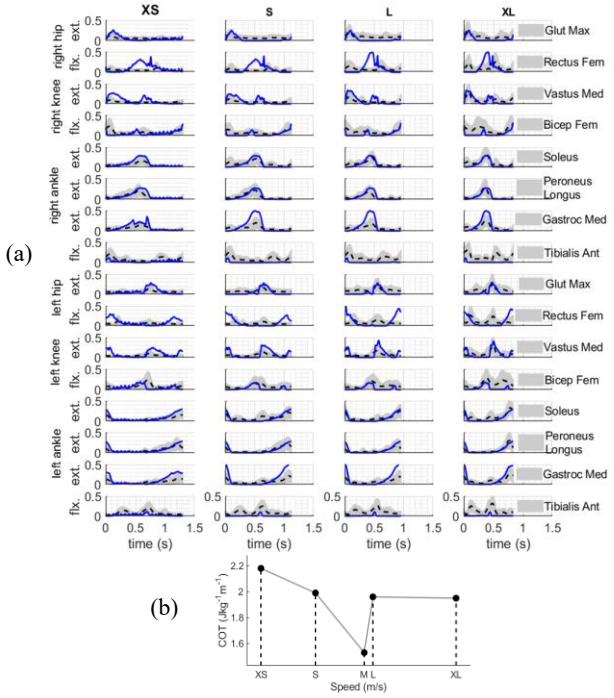

Figure 1: The predicted (a) muscle excitations and (b) COT.

Significance

The proposed MSK-model and NMSK-model optimizations minimized the reliance of simulations on experiments and predicted dynamically-consistent and physically-realistic slow and fast gaits for children by tracking the scaled experimental data of natural-speed gait.

Acknowledgments

This research was funded by the Natural Sciences and Engineering Research Council of Canada (NSERC) and the Canada Research Chairs (CRC) program.

References

[1] M. Ezati et al. 2020. doi: 10.1007/s11044-020-09731-3.
[2] M. Millard et al. 2019. doi: 10.1016/j.jbiomech.2019.04.004.
[3] G. Bovi et al. 2011. doi: 10.1016/j.gaitpost.2010.08.009.

GAIT CHANGES VS. TISSUE CHANGES IN DIABETIC PLANTAR PRESSURE

A. Henderson[1], J. Egbert[2], D. Bruening[2]
[1]Biomechanics and Movement Science Program, University of Delaware, Newark, DE
[2]Exercise Sciences Department, Brigham Young University, Provo, UT
email: ahendo@udel.edu

Introduction

It is widely reported that altered plantar pressures lead to tissue breakdown and potential ulcer formation in individuals with diabetic peripheral polyneuropathy (DPN).[1, 2] Factors that affect plantar pressure can be grouped into two main categories: those that affect the amount of force under the foot and those that affect the contact area of the foot. Changes to the amount of force under the foot primarily come from differences in body weight or walking speed, yet the majority of research done on DPN plantar pressure has not yet controlled for both these variables. Changes to contact area under the foot could be the result of foot deformities or other soft tissue changes. The primary aim in orthosis prescription is to increase the overall contact area under the foot while simultaneously off-loading certain high-risk areas. To our knowledge, no studies have yet attempted to identify which changes in plantar pressure might be the result of mechanistic changes (force and contact area changes) and which are more likely the result of tissue changes.

The purpose of this study is to identify potential mechanistic explanations for changes in plantar pressure between subjects with DPN and healthy matched controls while walking at a controlled speed.

Methods

Twenty-eight participants, 14 with DPN and 14 age, height and weight matched controls, were asked to walk in the lab at a controlled speed (1 m/s). Participants practiced with a motor-driven pulley system which was used during trials to help maintain the desired walking speed.[3] Participants then walked over a pressure sensing mat (HR Mat, Tekscan inc., Boston MA, USA) for a minimum of three trials at the desired speed. Tekscan software was first used to normalize pressure data to the subject's body mass and map the foot into six separate sections for each trial (hallux, lateral toes, medial forefoot, lateral forefoot, midfoot and hindfoot). Peak plantar pressure (PPP), pressure-time integral (PTI), length of contact time (CT) and contact area (CA) were calculated for each foot region while peak pressure gradient (PPG) was calculated for only the hallux, medial forefoot and hindfoot sections. Pressure data for the medial forefoot and hindfoot were then normalized to stance time. Time to each section's start and end of contact was calculated. Student t-tests compared subject groups for all variables at all foot sections. A Benjamini Hochberg correction was used with a false discovery rate of 0.1 in order to account for the multiple tests.

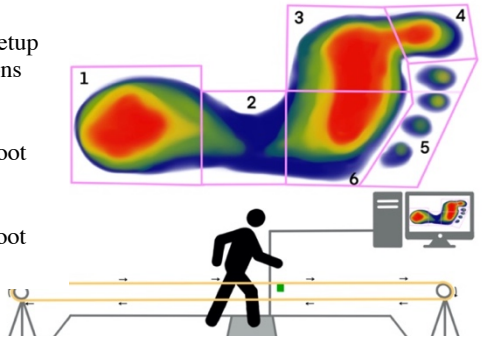

Figure 1: Lab setup with foot sections
1. Hindfoot
2. Midfoot
3. Medial forefoot
4. Hallux
5. Lateral toes
6. Lateral forefoot

Results and Discussion

The hindfoot also showed a significant increase in PTI and CT. Interestingly, it did not have a significant change in PPP suggesting that the change in PTI is primarily due to the increased length of contact. Similar to the medial forefoot, the hindfoot also presented with a significant delay in unloading ($p=0.002$) which can be interpreted as a delayed hindfoot rise.

The medial forefoot saw a significant increase in PPP, PTI, CT and PPG for subjects with DPN. There were no mechanical explanations found for the increased PPP or PPG suggesting that tissue changes may be responsible and should be a primary area of concern for clinicians for off-loading via orthoses in order to avoid skin breakdown. The significant increase in PTI is a result of increases in both pressure and contact time. Upon closer examination, the increased contact time was due to a significant delay in unloading of the medial forefoot ($p<0.001$). These changes were significant between groups despite the controlled walking speed.

The purpose of this study was to evaluate common measures of pressure under a controlled gait speed in individuals with DPN. Controlling the walking speed typically results in similar gait mechanics between individuals. However, despite this provision, there were still multiple differences found in the hindfoot and medial forefoot. The increases in hindfoot PTI, hindfoot CT, medial forefoot PTI, and medial forefoot CT seem to be related to mechanistic changes in the gait of subjects with DPN, namely the delay of hindfoot and medial forefoot segment unloading. There were no mechanical explanations found for medial forefoot PPP or PPG and may instead be linked to tissue changes.

Significance

Ulcer development is a prime area of concern for clinicians and patients with DPN. This study suggests that that off-loading the medial forefoot along with targeted gait training to minimize the unloading delay in both the hindfoot and medial forefoot may benefit patients with DPN and help prevent future tissue breakdown.

References

1. Patry, J., et al. J Am Pod Med Assoc, 2013. 103(4): 322-332.
2. Fernando, M., et al. Clin Biomech, 2013. 28(8): 831-845.
3. Henderson, A., et al. J Diab Research, 2019. 4512501.

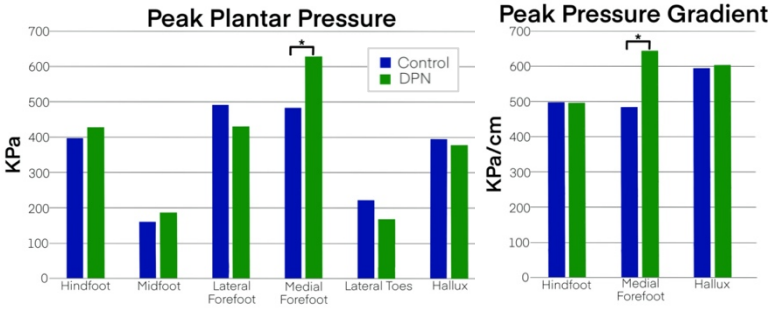

Figure 1: Group differences in PPP and PPG. * denotes significance after Benjamini Hochberg correction

HOW MANY JUMPS ARE NEEDED TO ESTIMATE AN ATHLETE'S TRUE ASYMMETRY?

Lauren C. Benson[1,2,3], A. McPherson[1,2], D. Taylor[1,2], K. Sainani[4], and D. Nabhan[5]
[1]United States Olympic and Paralympic Committee, Colorado Springs, CO
email: lauren.benson@usopc.org

Introduction

Force plates are used to quantify the force generated during different phases of take-off for maximal jumps [1]. Between leg asymmetries are calculated to monitor rehabilitation progress when there is a strength deficit in one leg [2]. Force plate sampling rates allow for multiple sensitive measures, however, often make it challenging for clinicians to detect signal amongst the noise as high variability blurs practitioners' capacity to make insights. Currently, it is not clear how the number of jumps influences variability in estimates of an athlete's true asymmetry. The purpose of this analysis was to facilitate clinician decision-making, identifying the number of jumps necessary to reduce the range of true asymmetry estimated from recorded asymmetry.

Methods

197 (117 F, 80 M) Olympic athletes performed squat and countermovement jumps on dual force plates during their typical performance and rehabilitation testing. A total of 1233 maximal squat jumps were executed over 258 different testing sessions (average: 4.8 jumps/session), and 1276 maximal countermovement jumps were executed over 263 sessions (average: 4.9 jumps/session). Kinetic asymmetry indices were calculated for the first and second half (phase 1 and 2) of take-off during the squat jump and the eccentric and concentric phases of take-off during the countermovement jump [1].

For each jump and phase, a simulated dataset of 100,000 jump sessions was generated. First, we calculated the absolute value of the median asymmetry for each specific athlete over their repeated trials. Second, for each decile of median asymmetry, a linear mixed-effects model was fit to all recorded individual jumps to identify the between- and within-athlete variance of jump asymmetry. Then, for each decile we simulated 10,000 true asymmetry values based on between-athlete variance, and for each simulated true asymmetry value, the asymmetry for 1-10 jumps was simulated based on within-athlete variance. The result was 100,000 simulated jump sessions, each with 10 jumps based on a theoretical true asymmetry.

The simulated datasets were used to estimate the theoretical range of true asymmetry values for each recorded jump session. For example, if an athlete had a median asymmetry of 9.5% over 5 jumps, then we used the simulated datasets to find the range of true asymmetry values that could have generated the observed data. We did this for each recorded session by identifying similar sessions in the simulated dataset: all simulated jump sessions that had a median asymmetry within ±1% of the median asymmetry for the recorded session over the same number of jumps. The interquartile range of true asymmetry values from the similar sessions in the simulated dataset was the estimated range of true asymmetry for the recorded jump session. Two-way ANOVA was used to identify differences in the range of true asymmetry values based on median asymmetry (high or low) and number of jumps (high [6-10], medium [4-5], or low [1-3]).

Results and Discussion

The smallest estimated range of true asymmetry values (mean 1.63%, SD 0.33%) was for squat jump phase 2 with low median asymmetry and high number of jumps, and the largest estimated range of true asymmetry values (mean 6.83%, SD 0.30%) was for countermovement jump eccentric phase with high median asymmetry and low number of jumps.

There were significant main effects of median asymmetry and number of jumps for squat jump phase 1, and a significant interaction between median asymmetry and number of jumps for squat jump phase 2 and both countermovement jump phases (Figure 1). In all cases, regardless of the number of jumps, the estimated range of true asymmetry was significantly greater for high median asymmetry than low median asymmetry. In most cases, regardless of the median asymmetry, the range of true asymmetry was significantly greater for a low number of jumps than a medium or high number of jumps, and the range of true asymmetry was significantly greater for a medium number of jumps than a high number of jumps. Exceptions were for squat jump phase 2 and for countermovement jump concentric phase where there was no effect of number of jumps when the median asymmetry was low.

Athletes with a greater median asymmetry have a larger range of estimated true asymmetry values. The range of estimated true asymmetry can be reduced by increasing the number of jumps.

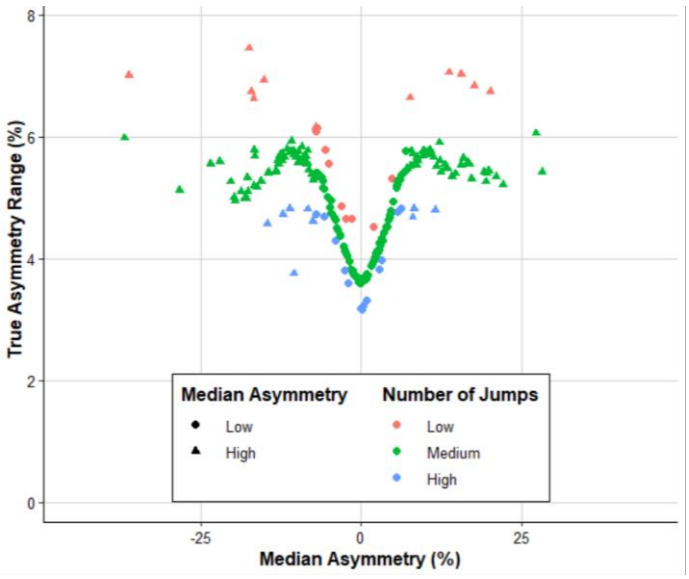

Figure 1: The true asymmetry range is plotted against the median asymmetry for each session. Jump sessions are classified by median asymmetry (high or low) and number of jumps (high [6-10], medium [4-5], or low [1-3]). This plot of countermovement jump eccentric phase is representative of all jumps and phases.

Significance

Knowledge of reduced variability can improve clinician confidence in their inferences as they monitor an athlete's rehabilitation progress.

References

[1] Jordan, MJ. (2015) *Scand J Med Sci Sport.* **25(3)**: e301-e309.
[2] Impellizzeri, FM. (2007) *Med Sci Sports Exerc.* **39(11)**: 2044-2050.

ESTIMATION OF HUMAN UPPER LIMB MECHANICAL IMPEDANCE: A COMPUTATIONAL APPROACH

Morteza Asgari [a*], Dustin L. Crouch [a]
[a] Department of Mechanical, Aerospace, and Biomedical Engineering, University of Tennessee, Knoxville
[*]sasgari@vols.utk.edu

Introduction

The mechanical impedance of the human upper limb describes the limb's ability to resist moving when it is displaced from an equilibrium position [1]. The human neuro-musculoskeletal system regulates limb impedance both passively (i.e., posture) and actively (i.e., muscle contraction) to maintain stability while manipulating objects and interacting with the environment [2, 3]. The ability to regulate limb impedance may be impaired by common orthopaedic (e.g., rotator cuff tear) or neurological (e.g., stroke) injuries, partly contributing to the resulting functional disability [4].

Impedance can be characterized by physical parameters stiffness, viscosity, and inertia. These parameters are usually identified by relating experimental hand restoring forces to displacements to build a second-order linear model [3]. However, the experimental data is usually confined to a few able-bodied subjects, trials, and limb postures, limiting our understanding of underlying mechanisms for impedance modulation in healthy and impaired individuals. To overcome experiment limitations, we aimed to develop a computational modeling and simulation framework to estimate the hand impedance and compare the results with experimental data.

Methods

Our strategy in this preliminary study was to replicate a typical experiment set-up [3]. We added a planar two-joint manipulandum to an existing upper limb musculoskeletal model implemented in OpenSim (version 3.3). The manipulandum consisted of two rigid cylindrical links and massless torque actuators that apply torques to those links about the *z-axis* (Fig. 1(B)). The manipulandum included a handle (i.e., end-effector) whose centroid point along the *z-axis* was fixed at the model's shoulder level. We used contact modeling to attach the handle to the model's hand. A linear PD controller placed the handle in any desired position across the limb's reachable workspace and applied external perturbations to the hand in eight different directions in the *x-y* (i.e., axial) plane (Fig. 1(A)).

We evaluated the endpoint stiffness at six hand locations lateral to the shoulder joint; all were approximately 33 *cm* anterior to and ranged from 0 to 40 *cm* to the right of the glenohumeral joint. During perturbations, forearm pronation-supination, wrist flexion-extension, and radial-ulnar deviation were locked to constrain arm movements to the horizontal plane and mimic typical bracing used in experiments. We set the perturbation amplitude and time to 8 *mm* and 1.2 *s*, respectively. To simulate the experimental scenario of a 'relaxed' limb that is fully supported against gravity, muscle excitations and gravitational acceleration were set to 0.001 and zero, respectively. Handle displacements and restoring forces (i.e., contact forces) were recorded during simulations. To compute the hand impedance parameters, we regressed a second-order linear model to the simulated force field [3, 4]. The estimated hand stiffness, viscosity, and inertia matrices were presented as graphical ellipses whose profiles represent the root locus of restoring force for hand perturbations in every direction by order of one unit (e.g., 1 m displacement for the stiffness).

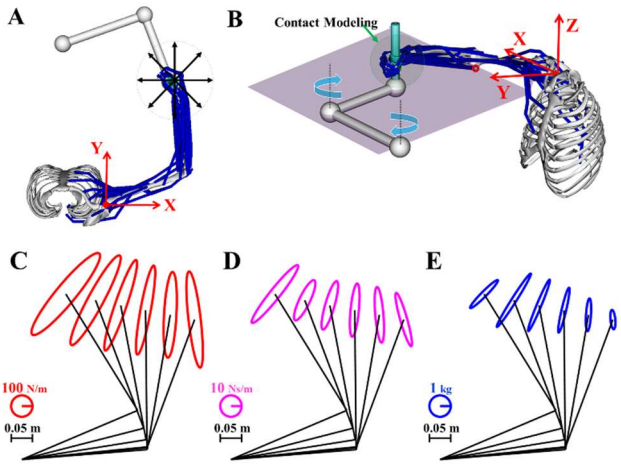

Figure 1: Musculoskeletal-manipulandum model. (A) The arrows show the eight directions of perturbations applied to the hand. (B) Handle was connected to the model's hand using elastic foundation for contact modeling. (C) Estimated Stiffness, (D) Viscosity, and (E) Inertia ellipses for different medial/lateral hand locations.

Results and Discussion

For more medial hand locations, the stiffness ellipses had lower eccentricity and major axis oriented towards the shoulder joint (Fig. 1(C)). These observations agree with the experimental results reported in [2, 3]. However, the size of our stiffness ellipses is larger than the values reported in those studies. Since muscle excitations were virtually zero, the observed spatial pattern for the stiffness ellipses was likely due to the passive forces of biarticular muscles as their involvement grows with increase in shoulder adduction and elbow flexion. With change in shoulder and elbow angles, the muscles' moment arms, fiber lengths, and tendon lengths change, affecting passive muscle forces. The spatial pattern of the viscosity and inertia ellipses across hand locations was similar to that of the stiffness ellipses (Fig. 1(D), (E)). Although the viscosity ellipses matched well with experimental data [3], the shape and orientation of inertia ellipses did not. These differences may be due to unmodelled muscle co-contractions and stretch reflexes, oversimplification of muscles and ligaments in the model, and missing passive human body components such as skin, veins, and cartilage.

Significance

Our preliminary results suggest that computational modeling and simulations can be used to estimate the arm impedance properties to complement and overcome the limitations of experiments. In future studies we will (1) refine the computational approach to predict experimental data more accurately and (2) identify how anatomical and biomechanical features influence upper limb impedance.

References

[1] N. Hogan, *Biol. Cybern.*, vol. 52, no. 5, pp. 315-331.
[2] F. A. Mussa-Ivaldi et al., *J. Neurosci.*, vol. 5, no. 10, pp. 2732-2743, 1985.
[3] T. Tsuji et al., *Biol. Cybern.*, vol. 72, no. 6, pp. 475-485, 1995
[4] D. B. Lipps et al., *Ann. Biomed. Eng.*, pp. 1-16, 2020.

AN OPEN-SOURCE AND WEARABLE SYSTEM FOR ESTIMATING 3D HUMAN MOTION IN REAL-TIME

Patrick Slade[1*], Ayman Habib, Jennifer L. Hicks, and Scott L. Delp
[1] Department of Mechanical Engineering, Stanford University
email: *patslade@stanford.edu

Introduction

Analysing the kinematics of human motion is essential for diagnosing movement disorders and guiding rehabilitation interventions for conditions such as osteoarthritis, stroke, and Parkinson's disease. Optical motion capture systems are the current standard for estimating kinematics but require expensive equipment in a predefined space. While wearable sensor systems can estimate kinematics in any environment, existing systems are generally less accurate than optical motion capture [2]. Further, many wearable sensor systems require a computer in close proximity and rely on proprietary software that is difficult to extend to new applications. Here, we present OpenSenseRT, an open-source and wearable system that estimates upper and lower extremity kinematics in real time by using inertial measurement units and a portable microcontroller.

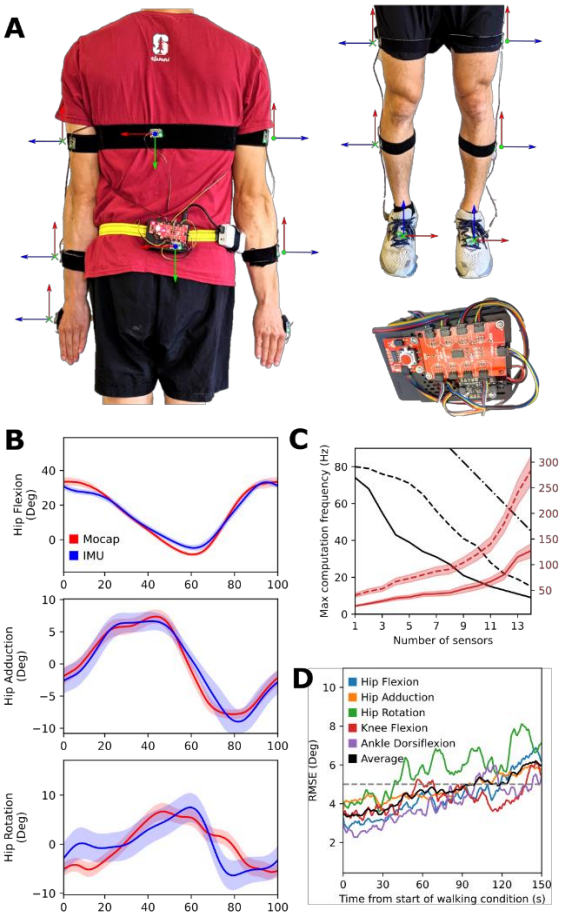

Figure 1: The OpenSenseRT system and performance. (A) The components and default IMU orientations of the OpenSenseRT System. (B) Lower-limb joint kinematics computed with the OpenSenseRT system compared to optical motion capture for five subjects during walking at 1.25 m/s. The error bands represent one standard deviation of the RMSE across all subjects. (C) The maximum sampling rate and associated average delay depends on the number of sensors attached to the system and the mode of computation. (D) RMSEs for joint kinematics computed with the IMU system compared to optical motion capture over time for walking.

Methods

The system uses off-the-shelf parts costing approximately $100 USD plus $20 for each tracked segment (Figure 1A). The open-source software and hardware are scalable, tracking up to 14 body segments with one sensor per segment. Kinematics are estimated in real-time using a musculoskeletal model and inverse kinematics solver [2], with the maximum computation frequency depending on the number of tracked segments (Figure 1C). Motion capture was used a ground truth reference for comparing kinematic estimates.

Results and Discussion

We compared the OpenSenseRT system to optical motion capture and found an average RMSE of 4.4 degrees across 5 lower-limb joint angles during three minutes of walking (n = 5) (Figure 1B) and an average RMSE of 5.6 degrees across 8 upper extremity joint angles during a Fugl-Meyer task (n = 5). The error increased at approximately one degree per minute due to drift in the sensor measurements (Figure 1D).

OpenSenseRT is an open-source, low-cost, easy-to-assemble, and customizable system for computing real-time kinematics. We have documented and openly shared all hardware and software to allow other researchers to use the system in a wide range of new applications that leverage the biomechanics software tools included in OpenSim. We have validated that the system's accuracy meets clinical standards for several common use cases in biomechanics and rehabilitation research.

Significance

This system will enable researchers to translate biomechanics, rehabilitation, and sports performance research that rely on kinematics into real-world solutions. For example, wearable and real-time joint kinematics will allow research to test biofeedback for gait retraining or sports performance outside of the lab, and the low cost could enable large-scale and longitudinal collection of free-living biomechanics data. The accessibility of this technology could also reduce the financial and technological barriers to perform state-of-the-art quantitative biomechanical analysis in low-income or developing countries with limited access to laboratory equipment, offering tools to improve musculoskeletal health on a global scale.

Acknowledgments

This work was supported by the National Science Foundation Graduate Research Fellowship Program Grant DGE-1656518 and the NIH through Grants P41EB027060 and P2CHD101913.

References

1. Mohammad, A et al. "Inertial measurement units for clinical movement analysis: Reliability and concurrent validity", *Sensors*.
2. Seth, A et al. "OpenSim: Simulating musculoskeletal dynamics and neuromuscular control to study human and animal movement", *PLoS computational biology*.

ASSESSING GAIT VARIABILITY AND STABILITY IN CHEMOTHERAPY-INDUCED PERIPHERAL NEUROPATHY

Gu Eon Kang[1,2,*], and Bijan Najafi[1,2,**]
[1]Interdisciplinary Consortium on Advanced Motion Performance, Department of Surgery, Baylor College of Medicine, Houston, TX
[2]Michael E. DeBakey Veterans Affairs Medical Center, Houston, TX
*Email: GuEon.Kang@bcm.edu **Email: Bijan.Najafi@bcm.edu

Introduction

Chemotherapy-induced peripheral neuropathy (CIPN), often presenting as foot numbness due to chemotherapeutic agents, affects more than half of cancer survivors in the long-term [1], and increases the risk for falls in the affected individuals [2]. Impairments in dynamic balance control during locomotor tasks such as gait are major indicators of the increase risk of falls [3] and quantifying these impairments could potentially provide useful implications about target measures for balance interventions for cancer survivors with CIPN [4]. However, to date, only limited information regarding has been documented in cancer survivors with CIPN [5]. Accordingly, we aimed to assess gait variability and stability during a habitual condition and a cognitively demanding condition (i.e., dual-task condition) in cancer survivors with CIPN and compared them to normal controls. We hypothesized that cancer survivors with CIPN would have poorer gait variability and stability for both walking conditions than normal controls.

Methods

We analyzed data from 14 cancer survivors with CIPN (CIPN group; age = 65.3 ± 8.6 years; 5 women; body-mass index = 30.98 ± 4.26 kg/m^2) and 16 normal controls (control group; age = 74.9 ± 5.8 years; 13 women; body-mass index = 26.07 ± 4.99 kg/m^2). Both groups had no history or evidence of a neurological condition such as Parkinson's disease, stroke and mild cognitive impairment. Additionally, the control group had no history of a cardiovascular condition. We confirmed foot numbness of the CIPN group based on vibration perception using a Biothesiometer (Bio-Medical Instrument, Newbury, OH; 26.64 ± 14.95 volts).

In addition to the demographic information, for all subjects, we assessed fear of falling severity using the Falls Efficacy Scale-International (FES-I) [6], and psychological distress using the Center for Epidemiology Studies Depression (CESD) [7].

We assessed habitual walking and dual-task walking using previously validated inertial measurement units (IMUs) (100 Hz; BioSensics, Newton, MA). Specifically, five IMUs were attached on the shanks, thighs and lower back. Subjects were asked to walk over 10 meters at their normal pace (habitual walking) and while counting backward from a random number (dual-task walking). Data were analyzed using a commercial software (LEGSys, BioSensics, Newton, MA) [8,9]. The primary measures were gait speed, gait speed variability (gait variability) and medio-lateral (ML) center-of-mass (CoM) sway (gait stability) for both walking conditions. We compared FES-I, gait speed, gait speed variability and ML CoM sway using independent t-tests (i.e., parametric measures), and compared CESD using a Mann-Whitney test (non-parametric measure).

Results and Discussion

FES-I score was higher in the CIPN group (24.4 ± 8.5) than in the control group (19.2 ± 2.5) ($p < .05$), but CESD score was similar between the CIPN (10.3 ± 10.6) and control (8.5 ± 9.7) groups ($p > .05$). Table 1 shows results for gait variability and stability. Overall, we found significant difference for parameters for gait variability and stability between the two groups.

Table 1. Mean ± standard deviation for gait speed (m/s), gait speed variability (%) and ML CoM sway (degree) across all subjects in each group.

Variables	CIPN	Control	P-value
Habitual walking			
Gait speed	0.99 ± 0.17	1.14 ± 0.16	0.020*
Gait speed variability	7.19 ± 3.59	4.05 ± 3.01	0.013*
ML CoM sway	7.61 ± 3.92	5.16 ± 1.81	0.047*
Dual-task walking			
Gait speed	0.89 ± 0.20	1.02 ± 0.20	0.079
Gait speed variability	6.93 ± 2.53	4.78 ± 2.46	0.023*
ML CoM sway	7.08 ± 2.82	5.21 ± 1.88	0.036*

Significance

Our study demonstrates poorer gait variability and stability in cancer survivors with CIPN. Our results may be useful to determine target outcomes for mobility interventions for cancer survivors with CIPN.

Acknowledgments

This study was partially funded by the National Heart, Lung, and Blood Institute (5T32HL139430) and the National Institutes of Health/National Cancer Institute (1R21CA190933).

References

[1] Ward et al. J Geriatr Oncol. 2014;5:57-64.
[2] Winters-Stone et al. J Clin Oncol. 2017;35:2604-12.
[3] Lamoth et al. J Neuroeng Rehabil. 2011;8:2.
[4] Schwenk et al. Gerongology. 2016;62:553-63.
[5] Zahiri et al. J Geriatr Oncol. 2019;10:960-7
[6] Delbaere et al. Age Ageing. 2010;39:210-16.
[7] Redloff. Appl Psychol Meas. 1977;1:385-401.
[8] Kang et al. Clin Biomech. 2020;72:155-60.
[9] Kang et al. Sensors. 2020;20:5.

GENERATION OF THE BALL VELOCITY AT RELEASE IN SHORT AND LONG MISSES IN THE BASKETBALL JUMP SHOT

Casey Wiens[1], Jill L. McNitt-Gray[1,2]
Departments of [1]Biological Sciences and [2]Biomedical Engineering, University of Southern California, Los Angeles, CA, USA
email: cwiens@usc.edu

Introduction

When developing basketball shot mechanics, a goal is to generate a ball flight trajectory with the ball entering the hoop. The ball velocity magnitude and direction at ball release determine the ball's trajectory during flight. The shooter's center of mass (CM) velocity and contributions by the arms will affect the ball velocity at release[1]. If the ball velocity magnitude at release is too low, it will likely result in a short miss. If ball velocity magnitude at release is too high, it will likely result in a long miss. Characterizing a shooter's tendencies when performing a missed shot is important since between shot differences in ball velocity at release may be multi-factorial and individual specific[2,3]. For example, the CM velocity contributions to the ball velocity at release can be influenced by both the impulse generated during the shot preparation and the time in the air before ball release[3].

In this study, we hypothesized that differences in the arm and the CM contributions to the ball velocity at release would be different between shot makes and misses, and the source of these differences would be player-specific.

Methods

Seven recreational basketball players (4 female and 3 male, university club and recreational league players) provided informed consent in accordance with the university's institutional review board. A minimum of 10 shots was attempted by each participant from 4.57 m (free throw line) and 6.02 m (American high school three-point line). The participant received a chest pass from the passer located underneath the hoop and performed a shot "as if you were in a game."

Successful shots ("make") were those that entered through the hoop without touching the rim or only touching the inside of the rim before entering. Unsuccessful shots that were to the left or right of the hoop were excluded from analysis, leaving only shots that were aligned with the hoop but fell short ("miss – short") or long ("miss – long").

Two portable force plates (Kistler, 1200Hz) measured ground reaction forces generated by each leg. The CM velocity was calculated using the net impulse generated from shot initiation to ground departure and the time in the air before ball release. The resultant CM velocity was calculated in the sagittal plane (anteroposterior and vertical components). The velocity contribution by the arms at release was calculated using the equation by Hay (1985): the CM resultant velocity is subtracted from the resultant ball velocity at ball release.

The lower and upper quartiles defined low and high, respectively, CM resultant velocity and the resultant velocity contributed by the arms. The quartiles were calculated within-participant and at each shot distance.

Results and Discussion

Twenty of the 118 shots analyzed missed short (12) or long (8). Across players, 9 of the 12 short misses were characterized by the CM or arm contributions to ball velocity at release in the lower quartile. All eight long misses across players were characterized by the CM or arm contributions to ball velocity at release in the upper quartile. Within player, reasons for the misses varied across distances (Figure 1). For example, for Participant 1, the miss from the free throw line (4.57 m; gold) was due to a reduction in both the CM and arm contributions to the ball velocity at release as compared to the makes; however, the misses by the same player from the 3-point line (6.02 m; purple) resulted from either a reduction in arm or CM velocity contributions to the resultant ball velocity at release. In contrast, for Participant 2, 2 of the 3 long misses from the free throw line (gold triangles) resulted from greater velocity contribution by the arms than in the makes.

While shot makes and misses may have different resultant ball velocities at release, these preliminary results indicate that the source of these differences may result from between shot differences in the CM or arm contributions. The sources of these differences were also found to be player-specific and varied with shot distance from the hoop. By identifying the factors contributing to between-shot variability in ball velocity at release, we can better understand how an individual player regulates ball velocity at release from different positions on the court.

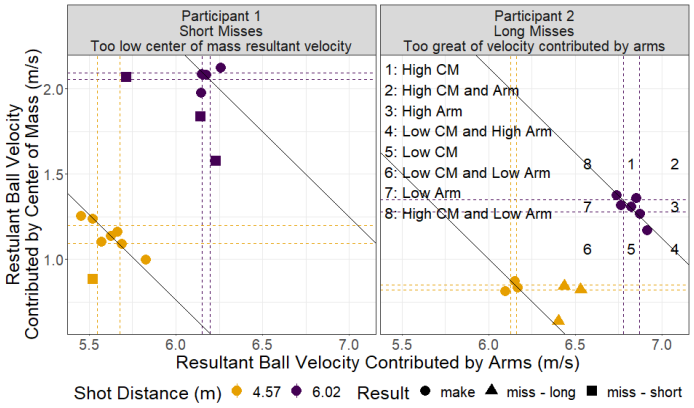

Figure 1: Exemplar data for two participants with short or long misses. Dashed lines represent each variable's lower and upper quartiles to highlight differences in the CM and arm contributions between makes and misses from each distance (color). Solid lines represent the identity line for a constant resultant ball velocity at release.

Significance

Differences in the CM and arm contributions to the ball velocity at release between makes and short and long misses are unique to each player. Future research will increase the sample size, and compare makes and misses with a defender at various distances from the hoop. Characterizing a player's tendencies in different contexts has the potential to provide meaningful insights to inform training and personalize feedback during practice.

References

[1] Hay JG. (1985). Biomechanics Sport Tech; Prentice-Hall.
[2] Coves A. et al. (2020). *Int J of Performance Analysis in Sport*
[3] Wiens C., McNitt-Gray JL. (2021). Submitted to ISB 2021.

RELATIONSHIP BETWEEN ISOKINETIC KNEE TORQUE AND VERTICAL JUMP MEASURES

Ben W. Meyer[1]
[1]Shippensburg University, Shippensburg, PA, USA
email: bwmeyer@ship.edu

Introduction

The purpose of this project was to examine the relationship between participants' isokinetic knee torques and vertical jump heights and maximum power values in healthy college-aged participants. In a study of elite female basketball players, the peak isokinetic knee torque at 240 deg/sec and vertical jump height was found to be strongly related [1]. The relationship is weak at smaller testing velocities, as peak angular velocities at the knee joint during countermovement vertical jumps of 500 deg/sec have been noted [2]. Although peak knee angular velocities of 500 deg/sec can occur during jumps, when the net knee joint torque starts to decrease about 150 ms before toe-off, the knee joint angular velocity is about 280 deg/sec [3]. Thus a dynamometer angular velocity of 240 deg/sec probably captures explosive strength better than smaller or larger testing velocities.

A recent study using high school basketball players provided evidence that the countermovement vertical jump could be used as a surrogate assessment to dynamometer testing [4]. When power increases in a vertical jump, the peak knee torques a person can produce in an isokinetic assessment also increase. Practitioners who do not have access to costly isokinetic equipment could analyze lower extremity variables using simple vertical jump tests if the relationship between isokinetic measures and vertical jump measures is strong and reliable.

It was hypothesized that the relationship between peak isokinetic knee torque and vertical jump measures (peak height and maximum power) would be stronger at dynamometer testing speeds of 180 and 300 deg/sec than at 60 deg/sec.

Methods

Eighteen males and twelve females (age = 22 ± 2 yrs; mass = 77 ± 17 kg; height = 1.72 ± 0.10 m) participated in the study. Each participant performed isokinetic knee extensions and flexions on both right and left legs using a Biodex Isokinetic Dynamometer. Three speeds were tested on the dynamometer: 60, 180, and 300 degrees per second. The dynamometer recorded peak extension and flexion torques at each speed. Participants also performed three countermovement vertical jumps for maximum height on an AMTI force plate that measured maximum power during the jump. The peak extension torque from the participants' preferred jumping take-off leg, the peak power during the best jump and the peak jump height were used for data analysis. The relationships between the peak torques and vertical jump heights, as well as the peak torques and vertical jump maximum powers, were assessed using correlation coefficients (r) and linear regression analyses. Statistical significance was set at $\alpha = 0.05$.

Results and Discussion

The relationships between peak extension torques and vertical jump height shown in Figure 1 were weak at all testing speeds (Table 1). Maximum power during the vertical jump was not strongly related to peak extension torque (Table 2).

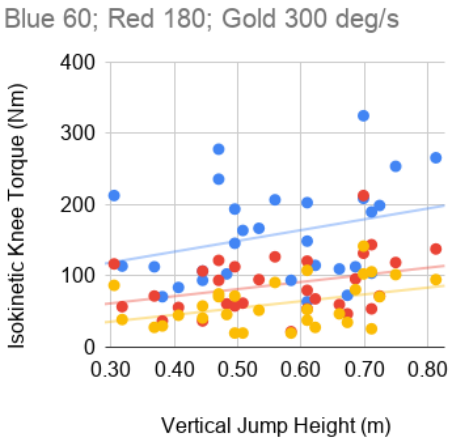

Figure 1: Relationships between peak extension torques and vertical jump height.

Table 1. Relationships between vertical jump height and peak isokinetic torque across angular velocities.

Velocity	Slope	Intercept	r	P
60 deg/sec	152.0	73.6	0.30	>0.05
180 deg/sec	99.9	31.8	0.33	>0.05
300 deg/sec	95.5	7.37	0.40	>0.05

Table 2. Relationships between vertical jump maximum power and peak isokinetic torque across angular velocities.

Velocity	Slope	Intercept	r	P
60 deg/sec	9.36	2818	0.37	>0.05
180 deg/sec	19.3	2606	0.46	>0.05
300 deg/sec	26.6	2680	0.49	>0.05

Although the relationships between vertical jump and dynamometer measures were weak, they were stronger at the 180 and 300 deg/sec speeds than they were at the 60 deg/sec speed (for the maximum power tests), in support of the initial hypothesis. The same trend was observed for jump height and peak torque, also supporting the hypothesis.

Significance

The results of this study do not show strong support for the use of a vertical jump test as a surrogate for isokinetic testing of the lower extremity. Although previous studies had shown correlations as strong as r = 0.88 [1], the present study's correlation values were all less than 0.50. As the countermovement vertical jump is a multi-joint motion, practitioners should use caution when trying to extrapolate the results of an isokinetic test performed at only one joint to more complex multi-joint movements.

References

[1] Rouis M et al. (2015). *J Sp Med Phys Fit,* **55:** 1-7.
[2] Saliba L et al. (2001). *J Sci Med Sport*, **4:** 336-347.
[3] Bobbert MF et al. (1988). *J Biomech,* **21:** 249-262.
[4] Hale R et al. (2019). *Proc ISB/ASB 2019*, 247.

SLOWING DOWN TO PRESERVE BALANCE IN THE PRESENCE OF OPTICAL FLOW PERTURBATIONS

Andrew D. Shelton[1], Ellora M. Mctaggart[1], Jessica L. Allen[2], Vicki S. Mercer[3], Jason R. Franz[1]
[1]Applied Biomechanics Lab, Joint Dept. of BME, UNC Chapel Hill and NC State University, USA
[2]Dept. of Chemical and Biomedical Engineering, West Virginia University, USA
[3]Division of Physical Therapy, UNC Chapel Hill, USA
Email: adshelt@email.unc.edu

Introduction

We commonly presume that an individual faced with a balance challenge during walking would slow down to improve capacity for corrective motor adjustments and balance control, thereby mitigating risk of falls. However, the one study to our knowledge to investigate this cause-and-effect relation found no significant changes in self-selected walking speed in the presence of mediolateral treadmill surface translations [1]. Because walking speed is governed via internal neural circuitry under the influence of complex sensorimotor integration, we believe that sensory perturbations prescribed through the visual perception of lateral instability may elicit a more pronounced effect. Our first hypothesis was that young adults would slow down at the onset of mediolateral optical flow perturbations. Our second hypothesis was that if young adults slowed down, they would do so with improved metrics of walking balance compared to the same perturbations at a fixed walking speed.

Methods

13 young adults (23 ± 4.61 yrs, 8F) completed four 5-minute treadmill walking trials in a randomized order. Subjects wore headphones playing pink noise to block the sound of treadmill speed changes during all trials. Two of these trials were completed using a fixed-speed treadmill controller at the subjects' preferred overground walking speed. The two other trials were completed using a self-paced treadmill controller that varied in response to the subject's instantaneous anterior-posterior position. Then, with each of these treadmill speed controllers, subjects walked while watching a speed-matched virtual hallway with and without mediolateral optical flow perturbations at a nominal amplitude of 35 cm. Instantaneous treadmill speed was collected via a custom MATLAB interface throughout the trials. Subjects wore 36 motion capture markers on their trunk, pelvis, and legs which provided the 3D position data we used to calculate a series of walking balance metrics, including step width and its variability, margin of stability and its variability, and local dynamic stability via maximum divergence exponents. Specifically, we averaged walking speed and balance metrics over the last three minutes of each walking trial. A two-way (speed x perturbation) repeated measures ANOVA detected differences in average walking speed and balance metrics. We excluded two subjects from our analysis due to difficulties acclimating to self-paced treadmill control.

Results and Discussion

In contrast to prior work using treadmill surface translations [1] but consistent with hypothesis 1, the 11/13 analyzed subjects in this study walked 5.4% slower when responding to optical flow perturbations using the self-paced treadmill controller ($p=0.005$) (Fig. 1A). The onset of perturbations when walking at a fixed speed elicited wider step widths, larger margins of stability, and greater local dynamic instability. In support of hypothesis 2, we observed none of these changes in response to optical flow perturbations when using the self-paced treadmill controller (Fig.1B-D). However, we did find that perturbations elicited increases in step width variability and margin of stability variability that were relatively indistinguishable between fixed and self-paced treadmill controllers. Finally, we found no significant differences in balance outcomes in the absence of perturbations between the fixed and self-paced treadmill controllers. This finding suggests that the use of a self-paced treadmill controller does not itself influence walking balance in young subjects.

Significance

The results of this study suggest that sensory perturbations, such as those via the visual perception of instability, have an effect on the selection of walking speed as a strategy to preserve balance. We would expect to see even more pronounced decreases in walking speed in individuals who are more susceptible to mediolateral optical flow perturbations, such as older adults or those with neurodegenerative disease.

Acknowledgments

We thank Dr. Brian Knarr for his assistance with the self-paced treadmill controller. Supported by NIH 1R21AG067388

References

[1] Hak L, et al. (2012) *Gait & Posture,* **36:** 260-264

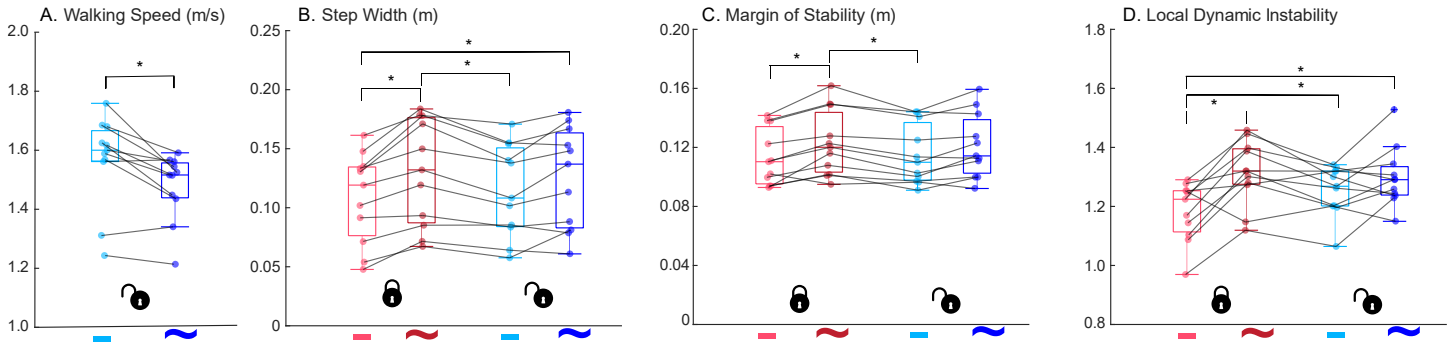

Figure 1. (A) Self-paced walking speed, (B) Step width, (C) Margin of Stability, and (D) Local Dynamic Instability. Asterisks (*) indicate significant ($p \leq 0.05$) pairwise difference. Locked padlock is fixed speed. Unlocked padlock is self-paced. "-" is unperturbed. "~" is perturbed

DESIGN OF A LASER-GUIDED PRECISION STEPPING SYSTEM FOR GAIT AND BALANCE RESEARCH

Andrew D. Shelton[1] and Jason R. Franz[1]
[1]Applied Biomechanics Lab, Joint Dept. of BME, UNC Chapel Hill and NC State University, USA
Email: adshelt@email.unc.edu

Introduction

Falls among older adults continue to be a significant public health challenge, with one-third of individuals over the age of 65 experience a fall annually [1]. Moreover, despite considerable investment and scientific interest, the rate of falls resulting in injury is outpacing the growth in our older adult population [2]. We suspect that this discrepancy arises from a relatively incomplete understanding of balance control during walking tasks in which most of these falls occur [3]. The accurate and appropriately timed-control of lateral foot placement plays a key role in walking balance integrity [4], and deficits therein due to age or disease are implicated in balance impairment and falls. To probe this mechanism, we recently used a precision stepping paradigm based on projected targets during treadmill walking and discovered preliminary evidence that older adults exhibit larger foot placement errors (Fig. 1A) and delayed swing limb adjustments compared to younger adults [5]. However, commercial treadmill-based projection systems for the mechanistic or translational study of precision stepping and balance during walking may be cost prohibitive. Thus, we aim to introduce a simple and cost-effective system to streamline and accelerate the design and implementation of studies seeking to investigate lateral precision stepping as a determinant of walking balance and falls risk.

System Design

At its core, our system uses a stepper motor and laser line generator to provide location and target on a split belt instrumented treadmill (Fig. 1B). Our design uses vertical ground reaction force to trigger both movement of the stepper motor and the laser, but because foot strike timing is all that is required, we envision simplified controllers based on pressure sensitive insoles. This allows for more accurate triggering at specific moments in the gait cycle. The stepper motor (NEMA 23, Openbuilds) drives a linear slide actuator (V-Slot Linear Actuator, Openbuilds) to which the laser line generator is secured using a custom 3D printed mount (model file will be made freely available). We have evaluated the actuation at a nominal velocity of 1.42 m/s and a nominal acceleration of 9.5 m/s^2. These specifications allow the actuator to cover the full 1.0 m treadmill width in 0.87 seconds, or a typical step width of 0.12 m in 0.22 seconds. This latter observation suggests that this simple system with nominal settings could be implemented to prescribe lateral foot placements on a step-by-step basis in future research studies, for example to augment step width sample entropy or as a precision stepping training tool. In addition, we designed the system with the intent to be easily adaptable for future research needs. Changes in target location and timing (i.e., % gait cycle) are easily implemented with the available control algorithms we intend to make freely available to the scientific community. Moreover, while currently used to objectively investigate lateral precision stepping, the system is also easily adapted to provide anterior foot placement targeting as well. A two-axis system could also coordinate lateral and anterior targeting for 2-dimensional precision stepping. The majority of the system parts are off the shelf products with only minor in-house manufacturing required in the form of cutting 11 sections of aluminum 80/20 for the base and 3D printing the laser line generator mount. We plan to make our design and bill of materials fully open source with components, construction instructions, and controls algorithms freely available to the field at the time of publication.

Acknowledgments

This work was funded by NIH grant 1R21AG067388.

References

[1] Tromp, A.M., et al., J of Clin Epidemiol, 2001. 54(8): p. 837-4
[2] Web-based injury statistics query and reporting system (WISQARS), N.C.f.I.P.a.C. Centers for Disease Control and Prevention, Editor.
[3] Tinetti, M.E. et al., N Engl J Med, 1988. 319(26): p. 1701-7.
[4] Kuo, A, 1999. J of International Robotics Research 18 (9), 917–930.
[5] Selgrade, B., el al., J of Biomechanics, 2020. 104

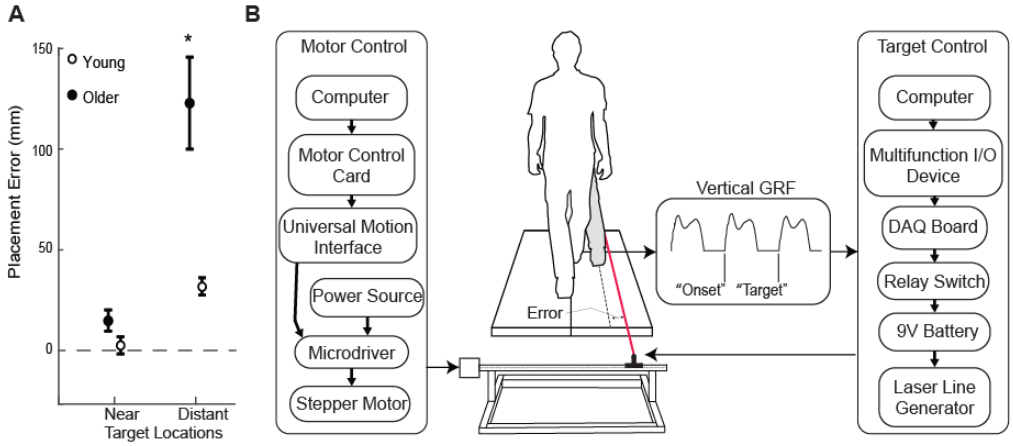

Figure 1. (A) Pilot data show that, compared to those in young adults, lateral foot placement errors during walking are larger in older adults at distant target locations. Asterisks (*) indicate significant ($p \leq 0.05$) pairwise difference. (B) Precision stepping system outline shows order of operations for one measurement cycle beginning with linear slide actuator control and finishing with laser targeting. We cue laser onset at the instant of heel-strike and quantify precision stepping behavior during the subsequent step.

CHRONIC NECK PAIN REDUCES UPPER TRAPEZIUS MUSCLE ACTIVITY DURING FUNCTIONAL REACHING

Whitney L. Wolff[1] and David B. Lipps[1]
[1]School of Kinesiology, University of Michigan, Ann Arbor, MI
Email: wolffw@umich.edu

Introduction

Neck pain affects 65% of all adults at some point in their life, with 1/3rd of these adults reporting difficulty performing activities of daily living due to pain [1]. Chronic neck pain (CNP) (lasting >3 months) affects the neuromuscular drive to the neck and shoulder muscles. Experimental muscle pain in the sternocleidomastoid (SCM) leads to increased neural drive to that painful muscle [2]. Sufferers of CNP often describe the sensation of muscle stiffness in their neck and upper trapezius muscle (UT) [3]. An increase in muscle activation due to neck pain would likely increase muscle stiffness and inhibit the proper function of the muscle [4]. Ultrasound shear wave elastography (SWE) provides a reliable and non-invasive measurement estimate of muscle stiffness by measuring the velocity of shear waves (SWV) propagating through the muscle of interest. It is currently unclear how neck pain affects the stiffness of shared neck-shoulder musculature during activities of daily living such as reaching tasks. The purpose of this study was to compare SWV and muscle activity in the SCM and UT during functional reaching tasks between people with chronic neck pain and healthy individuals. We hypothesized that mean SWV and muscle activity for the SCM and UT would be significantly greater for those with CNP when compared to healthy controls.

Methods

The Neck Disability Index (NDI) was used to identify participants for this study. Increasing NDI scores indicate greater impairment due to CNP. Ten adults with mild CNP (4M, 6F, NDI 5-14) and seven age, height, and weight-matched controls (3M, 4F, NDI 0-4) (mean: age: 34 years, height: 1.7 m, weight: 72.6 kg). During reaching conditions, surface electromyography (EMG) (Trigno, Delsys) and SWE images (Supersonic, Aixplorer) were obtained from the SCM and UT 2-cm distal to the midpoint of the belly of each muscle. Maximal voluntary contractions (MVC) in neck flexion/extension, right/left lateral bending, and shoulder elevation were completed at the beginning of the experiment.

The participants performed three tasks: Task 1) unilateral forward reach to a head-high shelf, Task 2) bilateral reach to a head-high shelf, and Task 3) unilateral upward reach to a lightbulb 4 inches above head-height. Each task required them to reach toward a small object and hold their arm at the top of their natural movement without picking up the object. The participants completed each task four times. SWE images were taken from the SCM and UT muscles while EMG was recorded simultaneously. The mean SWV and normalized EMG RMS (%MVC) of the SCM and UT were compared using an ANOVA. Group (CNP, healthy), muscle side (left, right), and the reaching arm (Aim 2 only) were fixed factors in the model. Significance was set at α=0.05.

Results and Discussion

There was a significant main effect of group on UT EMG for Task 1 ($p=0.012$), Task 2 ($p<0.000$), and Task 3 ($p<0.000$) (**Figure 1**). For all tasks, the CNP group exhibited lower UT EMG amplitude when compared to healthy controls. There was a significant main effect of group on SCM EMG for Task 2 ($p=0.029$), with SCM EMG lower for the CNP group. There was no main effect of group for Task 1 or Task 3(both $p>0.071$). This suggests that individuals with CNP exhibit inhibited SCM activation during bilateral reaches and inhibited UT activation during both bilateral head-high reaches and unilateral reaches. There was no main effect of muscle side or reach arm for the UT or SCM EMG (all $p>0.109$). There were no significant main effects of group, muscle side, or reach arm on SCM SWV or UT SWV during Task 1, 2, or 3 (all $p>0.150$).

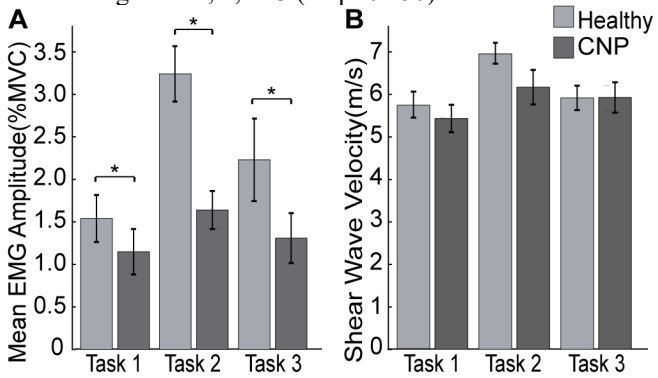

Figure 1: Normalized mean EMG (**A**) and SWV (**B**) for the UT during Task 1, 2, and 3 for healthy individuals compared to people with CNP.

Our findings suggest individuals with CNP exhibit a decrease in SCM and UT muscle activity during functional reaching activities. The pain adaptation model suggests the response to chronic pain differs for agonist and antagonist muscles, with activation of the agonist inhibited [5]. The UT acts as an agonist for the performed reaching tasks and is therefore more likely to be inhibited by the central nervous system during reaching for individuals with CNP. We did not find any significant differences in the SWV data during the active conditions. However, our power analysis suggests our sample size needs to be doubled to more robustly assess SWE in this population. With greater participant numbers, we posit that SWV data will mirror the muscle activity data for the UT during forward reaching. It is also possible that differences in muscle stiffness between the healthy and mild chronic neck pain group were not large enough to be detected with SWE. Future work will also evaluate muscle stiffness in individuals with CNP categorized with moderate pain or above on the NDI scale.

Significance

The results of this study support the need for motor retraining during physical rehabilitation for CNP, specifically during bilateral and unilateral reaches. Following data collection on more participants, our findings may also enhance diagnostic options for those with CNP.

References

[1] Tsang, S., et al. *Euro J Appl Phys*. 118 (2018).
[2] Ashton-Miller, J., et al. *Spine.* 15 (1990).
[3] Dieterich, A.V., et al. *J Ortho Sport Phys Ther*. 50 (2020).
[4] Taş, S., et al. *J Manip Phys Ther.* 41 (2018).
[5] Lund, J.P., et al. *Can J Phys Pharmacol.* 69 (1991).

EFFECT OF COGNITIVE TASK ON STEPPING PARAMETERS DURING EXPECTED TERMINATION

Ashwini Kulkarni[1], Cui[1], Rietdyk[1], Ambike[1], Barbieri[2]
[1]Department of Health and Kinesiology, Purdue University, West Lafayette, IN, USA
[2]Department of Physical Education, São Paulo State University (UNESP), Bauru, São Paulo, Brazil
Email : *kulkar50@purdue.edu

Introduction

Curb negotiation is a challenging activity for older adults. Approximately 15% of falls in this population occur during stepping down the curb [1]. The likelihood of falling increases when older people are required to terminate gait quickly. This rapid gait termination requires the complete interruption of forward momentum and precise foot placements during the transition to standing [2]. Furthermore, in everyday life, it is common to perform two or more tasks concurrently, which imposes demands on attentional resources. Older adults have reduced attentional capacity [3]. Therefore, stepping down a curb and stopping while performing a cognitive task may affect the stepping behavior. We investigated the effect of a concurrent cognitive task on stepping parameters during expected gait termination in young and older adults.

Methods

Ten young (22.6±3.6 years) and eight older adults (67.8±3.8 years) performed ten trials (five trials each for gait termination with and without cognitive task). Participants walked on an 8 m walkway and stepped down a curb (15 cm height) and stopped as quickly as possible with the feet aligned. Participants knew they were going to have to stop. For the cognitive task, subjects listened to a number sequence and counted the number of times a specified number was played in a pre-recorded sequence.

We quantified horizontal and vertical distances of heel and toe from the curb edge during the last stride (Fig. 1). We conducted a 2 x 2 age by task ANOVA on vertical lead heel and trail toe clearances.

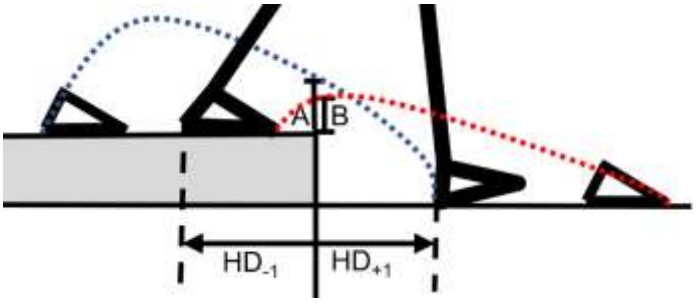

Figure 1. Figure shows the horizontal distances of heel from the curb edge (HD_{-1} and HD_{+1}); vertical lead heel clearance (A) and vertical trail toe clearance (B) when heel and toe were above the curb edge.

Results and Discussion

Interaction effects of age by task revealed that vertical heel clearance of the lead foot was lower in older adults during the dual-task condition ($p<0.02$; Fig. 2A). Main effects of age included the following: Older adults placed their back foot (HD_{-1}) farther away from the curb edge ($p<0.01$). Older adults had lower vertical toe clearance of the trail foot ($p<0.02$; Fig. 2B). Only older adults were at greater risk of contact during the dual task. The reduced lead heel clearance in older adults during dual-tasking can be explained as a result of increased attentional demands. The increase in attentional demand may be attributed to sharing of brain structures, particularly pre-frontal areas [4], which is involved in decision making and the controlling and planning of complex cognitive behavior. Further, the farther placement of the back foot (HD_{-1}) in older adults may have following implications during gait termination: (1) Greater risk of contacting the hazard edge with the heel of front foot as it is lowered during late swing phase, (2) inability to reduce the whole body angular momentum that may in turn increase the time to termination [3]. Longer HD_{-1} in older adults may also explain the reduced vertical toe clearance of trail foot.

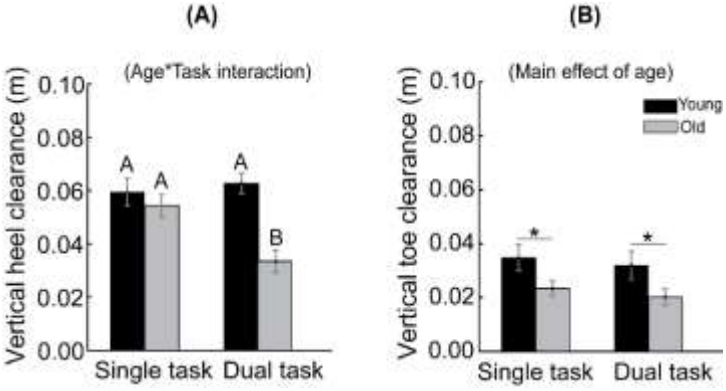

Figure 2. (A) Mean ± SE of vertical heel clearance. Different letters denote significant differences; (B) Vertical toe clearance.

Significance

In everyday life, the ability to perform two tasks concurrently enables people to communicate with others, use mobile phones, transport objects, and respond to environmental stimuli when walking. We demonstrated that altered foot placements in older adults may pose higher risk of falls in the situations where cognitive demands are high such as talking to a friend while stopping to cross street. Extending these findings to people with pathologies would be beneficial in understanding the etiology of falls during complex interaction with environments.

Acknowledgments

Fulbright Scholar program for Dr. Fabio Barbieri

References

[1] Jacobs, J. V. (2016). *Gait & Posture*, *49*, 159–167.
[2] Menant et al. (2009). *Gait & Posture, 30*, 65-70.
[3] Sparrow, W. (2002). *Hum Mov Sci*, *21*, 961-972.
[4] Sparrow & Tirosh (2005). *Gait & Posture, 22*, 362-371.

DETECTION OF DIFFERENT FALL TYPES IN HEALTHY YOUNG ADULTS

Lindsey K. Lewallen[1], Corey A. Pew[2], Shane R. Wurdeman[3], and Richard R. Neptune[1]
[1]Walker Department of Mechanical Engineering, The University of Texas at Austin, Austin, TX
[2]Department of Mechanical and Industrial Engineering, Montana State University, Bozeman, MT
[3]Department of Clinical and Scientific Affairs, Hanger Clinic, Austin, TX
email: lindsey.lewallen@utexas.edu

Introduction

Individuals with a lower-limb amputation are at an increased risk of falling compared to young healthy adults. Approximately 50% of individuals with unilateral amputation report at least one fall annually.[1,2] Falls are dangerous, occasionally leading to injury, hospitalization or death.[3] Fortunately, individuals who obtain aid within 1 hour of a fall have a 50% increased survival rate compared to individuals who obtain aid after 72 hours.[4] Thus, devices that have the ability to detect falls and alert proper personnel could serve to help lower the consequences of falling for individuals with a lower-limb amputation.

A number of studies have developed body worn sensors that can detect fall events. These devices primarily use inertial measurement units (IMUs) to record signals from 3-axis accelerometers, gyroscopes, and/or magnetometers. Individuals with a lower-limb amputation utilize a prosthesis that allows for fall detection sensors to be conveniently integrated within the prosthesis (e.g., directly attached to the pylon). However, it is not clear if such sensors are able to detect a wide range of fall types. Therefore, the purpose of this study was to investigate the accuracy of detecting different fall types with an IMU placed on an individual's shank in preparation for application and validation on individuals with a lower limb amputation.

Methods

IMU sensors (XSens, Enschede, Netherlands) were placed on both shanks of 15 healthy young adults in positions analogous to the pylon of a prosthesis distal to the knee. Tri-axis accelerometer and gyroscope data were recorded from these devices at 100-Hz while subjects completed an overground course with simulated falls and near-falls. The course was designed to simulate activities of daily living (ADL: walking/running in a straight line at a self-selected pace, navigating turns, sitting and rising from a chair, laying down and getting up from a bed, picking up an object on the floor, and ascending/descending stairs/slopes). Subjects performed 4 types of simulated falls: forward/backward trips (i.e., subjects walked forward/backward until they impacted a fall pad and fell) and left/right lateral falls (i.e., subjects stood with their left/right side adjacent to the fall pad while a lab technician pushed them until they lost balance and fell onto the fall pad). For the simulated near falls, subjects walked until their left/right foot struck the fall pad and then recovered from the stumble.

Raw data were analysed using the MATLAB Classification Learner Toolbox. First, data were split into two categories: ADL or Fall. Data were divided into 0.5 second windows with a 0.25 second overlap. During these 0.5 second windows, a total of 40 features were computed (Table 1). Data were randomly split into training (80%) and model verification (20%) sets for each subject and each category. Three different classification algorithms were used for activity classification and validated with 5-fold cross validation: support vector machine with a cubic kernel (SVM), K nearest neighbor with weighted dimensions (kNN), and a bagged decision tree ensemble (Tree).[5]

Table 1: Features extracted for each 0.5 s window for each accelerometer (accel) and gyroscope (gyro).

Vector resultant (r_{accel}, r_{gyro})	Median, Mean, Standard Deviation, Skewness, Kurtosis, IQR, Minimum, Maximum
Each axis (x_{accel}, y_{accel}, z_{accel}, x_{gyro}, y_{gyro}, z_{gyro})	Mean, Max, Min, IQR

To determine algorithm accuracy, a simple control scheme was created. First, models were implemented on the verification data set. A fall was identified if at least two adjacent windows contained a label associated with a fall. If this occurred within the duration of the fall (~1s), a correct fall classification was made. Falls were labelled by type: forward/backward trips and lateral falls with the sensor placed on the inside/outside leg. Finally, fall detection accuracy was calculated, defined as the number of correct classifications divided by total number of falls (Table 2).

Results and Discussion

Forward falls had the lowest detection accuracy for each algorithm. When falling forward, participants can more easily protect their body with their hands and knees, acting to reduce the acceleration on impact. On average, inside falls had the highest detection accuracy. The inside shank is often the first part of the body that impacts the ground during lateral falls, possibly contributing to the higher accuracy. This is in contrast to previous work that noted highest classification accuracy with backward falls when an IMU sensor is placed on the waist of each participant.[6]

Significance

This study highlighted that fall detection accuracy is not the same across fall types and classification algorithms. Future work should seek to improve detection of forward falls (e.g., placing sensors in different locations, implementing different classification algorithms such as threshold algorithms,[7] and exploring different features) and validate these results on individuals with a lower limb amputation.

Acknowledgments

This work was supported by CDMRP W81XWH2010164.

References

[1]Miller WC, et al. *Arch Phys Med Rehabil.* 2001. [2]Kulkarni J, et al. *Physiotherapy.* 1996. [3]Rubenstein LZ, et al. *Age Ageing*. 2006. [4]Gurley RJ, et al. *N Engl J Med.* 1996. [5]Pew C, et al. *IEEE.* 2018. [6]Hwang SY, et al. *Int Conf on CS and Tech.* 2012.

Table 2: Accuracy for each type of fall and algorithm

	Type of Fall				
	Forward	**Backward**	**Outside**	**Inside**	**All Falls**
SVM	76.7%	93.3%	100%	100.0%	92.5%
kNN	73.3%	90.0%	90.0%	100.0%	88.3%
Tree	76.7%	86.7%	93.3%	93.3%	87.5%

COMBINED MUSCULOSKELETAL AND FINITE ELEMENT MODELING TO OBTAIN TIBIAL LOADING DURING COUNTERMOVEMENT JUMPING AND LANDING

Merwa Al-Rasheed, T. Willett, and J. McPhee
Systems Design Engineering at the University of Waterloo, ON, Canada
email: m7alrash@uwaterloo.ca

Introduction

Several sports, including basketball and volleyball, involve jumping and landing motions that are associated with a high prevalence of injuries in the lower extremities [1]. A significant percentage of these injuries take place in the tibial bone [1]. Countermovement jumping, also referred to as squat jumping from a standing position, can impose high loadings on the body at a very high speed, which can be correlated to injuries in sports [2]. A thorough study of the full jumping-landing motion is needed to understand how and where injuries take place. The purpose of this work is to study the impact dynamics of a countermovement jump (CMJ) to obtain loading on the tibial bone. This procedure can provide loading conditions to examine the behavior of the bone, rather than the current approach of using approximate forces related to the bodyweight of the subject [3].

Methods

Position and ground reaction force (GRF) data were collected from a healthy male subject (age 23 years, mass 80 kg, and height 1.78 m), who performed three trials of countermovement jumping to a maximum height with hands placed on the waist. Inverse kinematics was performed on the data to obtain joint angles in MATLAB (Mathworks, Natick, MA). A 2D subject-specific sagittal model of the body was constructed in MapleSim (MapleSoft, Canada). The model consisted of 4 rigid bodies (HAT, thigh, shank, and foot), 3 revolute joints (hip, knee, and ankle), and 19 muscles of the lower extremity. Anthropometric properties of segments were obtained from Winter [4]. Inverse dynamics was used to compute joint moments at the hip, knee, and ankle. To solve the problem of redundancy in obtaining muscle forces, a static optimization approach was used to minimize muscle stress with maximized energy expenditure.

For finite element (FE) analysis, a model generated from CT scans of the leg of a male subject was utilized [5]. Joint contact forces obtained from the musculoskeletal model and muscle forces obtained from static optimization were used as loads in the tibia-fibula FE model. Bone was modeled as an inhomogeneous, orthotropic material. As a boundary condition, the distal tibia is pinned to only allow axial rotation. The finite element model was used to examine stresses and deformations of the tibia. The overall process is illustrated in Figure 1.

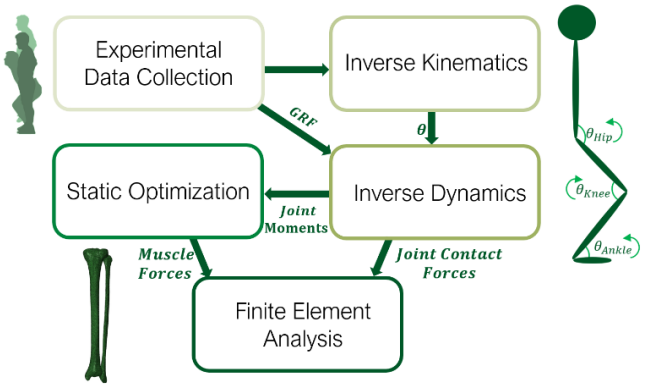

Figure 1: Modeling Pipeline to obtain realistic stresses and deformation in the human tibia during countermovement jumping and landing.

Results and Discussion

During countermovement jumps, the maximum GRF obtained during jumping was 2.4 ± 0.15 BW, while the maximum GRF obtained during landing was 5.60 ± 0.61 BW, which are consistent with existing literature. Inverse dynamics with intersegmental angles and GRFs as inputs provided joint moments throughout the motion. The moments about the hip, knee, and ankle joints are shown in Figure 2, phases of a countermovement jump are labelled respectively. Overall, the moments are larger in magnitude during the landing phase than the propulsion phase due to higher ground reaction forces. Peak moments resulted in peak forces in specific muscles (soleus, vastus muscles, rectus femoris). Preliminary FE results indicated that the higher loads led to a higher strain in the tibia, as expected, and identified regions of highest stresses in the bone.

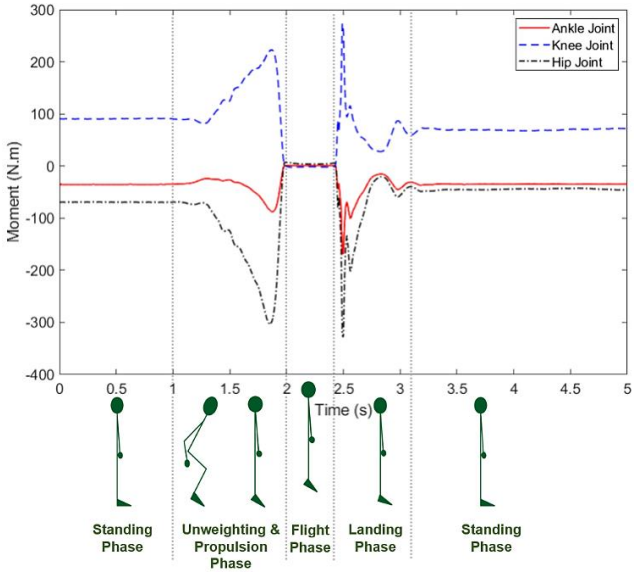

Figure *2*: Hip, knee, and ankle joint moments from inverse dynamics during countermovement jumping and landing

Significance

This study utilizes a computational approach, using both a musculoskeletal multibody model and a finite element model, to obtain realistic loads on the tibia for the full countermovement jump. This allows for the investigation of various injuries, such as stress fractures, that take place with high impact forces.

Acknowledgments

We would like to thank Natasha Ivanochko and Dr. Ifaz T. Haider for providing the data and the FEM used in this work, respectively. This research was funded by the Natural Sciences and Engineering Research Council of Canada (NSERC).

References

[1] Bleecker, C., et al., *Sports Med*, 50(8), 1515-1532, 2020.
[2] Alptekin, A., et al., *J Sports Sci*, 8(3), 58-71, 2017.
[3] Hadid, A., et al., *Med Sci Sports Exerc,* 50(9), 2018.
[4] Winter, D. A., *John Wiley & Sons.*, 2009.
[5] Haider, I., et al., *J Biomech Eng*, 142(2), 2019.

Phantom-less calibration methods for vertebral fracture properties estimation using QCT-based FEA

Maria Prado[1], Sundeep Khosla [2], Christopher Chaput [3], and Hugo Giambini*[1]
[1]Department of Biomedical Engineering and Chemical Engineering, University of Texas at San Antonio, San Antonio, TX, USA.
[2]Kogod Center on Aging and Division of Endocrinology, Mayo Clinic College of Medicine, Mayo Clinic, Rochester, MN, USA.
[3]Department of Orthopedics, The University of Texas Health Science Center at San Antonio, San Antonio, TX, USA
e-mail: *hugo.giambini@utsa.edu

Introduction

Vertebrae are the second most common affected bones with osteoporosis presenting a fracture incidence exceeding 1.4 million annual cases in the U.S. [1]. Quantitative computed tomography (QCT) combined with finite element analysis (FEA) has shown significant improvements in predicting fracture properties [2]. To obtain QCT/FEA subject-specific estimates of fracture properties, Hounsfield unit (HU) values from the CT images are converted to bone mineral density (BMD) using a calibration phantom. These BMD values are then converted to Young's modulus and assigned as material properties to the model. This process is inconvenient as it requires a calibration phantom during CT scanning. Alternative approaches would implement patient-specific phantom-less calibration techniques considering the patient's own tissues, as the calibrating reference materials, to convert HU to BMD. The purpose of this study was to develop robust and novel phantom-less calibration methods, using subject-specific tissues, which could be applied prospectively and retrospectively to databases of CT scans to obtain fracture properties estimations using QCT/FEA.

Methods

Data: DXA and QCT scans from 111 subjects. 80 QCT scans were used to obtain subject-specific parameters using a phantom-specific approach and for the development of phantom-less equations. 31 CT scans were used for validation.

Phantom-specific calibration: QCT images from 80 subjects were imported into Mimics software, the L3 vertebra identified, and a region of interest (ROI) placed at a mid-slice to obtain a mean HU value for trabecular bone (***Fig. 1***). HU values were then converted to equivalent BMD using the calibration phantom.

Phantom-less calibration: HUs were measured from various regions at the same mid-slice: air (A), fat (F), psoas muscle (M), and subject perimeter (P) (***Fig. 1***). Using multiple regression analyses and the calculated trabecular BMD, equations were developed using combinations of these ROIs to estimate vertebral BMD from soft tissue measurements in the CT image.

QCT/FEA: Voxel models of the L3 vertebrae were created from the CT images of 31 subjects using Mimics and previously validated techniques. Each voxel was assigned an HU value corresponding to the CT voxel in the image. HUs were converted to BMD using 6 phantom-less and1 phantom-specific equations. QCT/FEA fracture loads were estimated as a function of predicted stiffness (K) and height (H) of the vertebra: $F_{FE} = 0.0068 K_{FE} H$ [3].

Statistical analyses: Predicted fracture loads from the 31 subjects and from all 7 equations were correlated with aBMD from DXA. Correlations were also obtained between all phantom-less and phantom-specific equations. Level of significance was $p<0.05$.

Results and Discussion

The proposed phantom-less methods can successfully be used

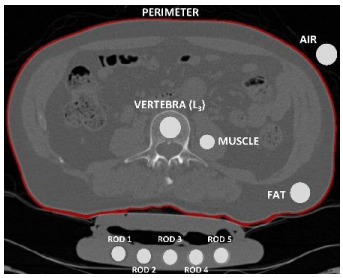

Figure 1: Mean HU values were collected from the various ROIs on the L3 vertebra, psoas muscle (M), fat (F), air (A).

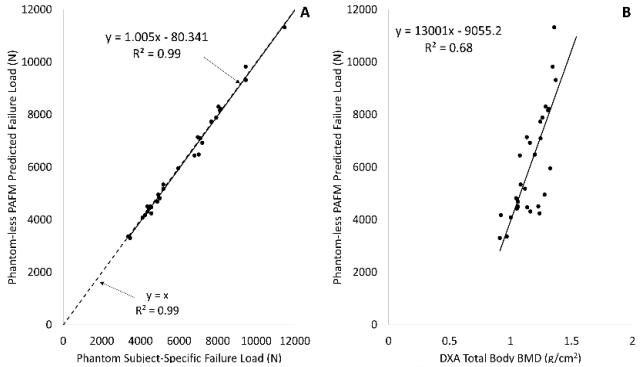

Figure 2. Correlation outcomes between **A)** predicted failure loads using a phantom-less (**PAFM**; sample equation) and phantom-specific equations; **B)** predicted failure loads using PAFM and aBMD.

in QCT/FEA to estimate vertebral failure loads that are highly accurate and correlate with fracture loads obtained using the traditional phantom calibration method. Equations using the perimeter of the patient highly correlated with outcomes using the calibration phantom ($\widetilde{R}^2$ of 0.99). In order to validate and evaluate the precision of the predicted fracture load outcomes, aBMD values from DXA were correlated to QCT/FEA predictions showing moderate correlations (68%).

Significance

The phantom-less approach presented in this study can be used for osteoporosis diagnosis and QCT/FEA fracture risk assessment using images previously acquired for other purposes, or prospectively without the use of a calibration phantom, minimizing logistic controls and reproducibility errors associated with external reference phantoms.

Acknowledgments

This study was supported by the University of Texas at San Antonio (HG) and in part by NIH grant AR027065 (SK)

References [1]Johannesdottir F et al. (2018); [2] Giambini H et al. (2016); [3] Crawford RP et al. (2003)

INFLUENCE OF PAIN ON FUNCTIONAL DEMAND AND JOINT COORDINATION IN KNEE OSTEOARTHRITIS

Skylar C. Holmes[1], Erica Casto[1], Ethan Steiner[1], and Katherine Boyer[1]
[1]University of Massachusetts, Amherst
email: scholmes@umass.edu

Introduction

Knee extensor (KE) function is important for locomotion, joint stability, and load attenuation during such tasks as walking and stair climbing [1]. KE weakness is commonly exhibited in individuals with knee osteoarthritis (KOA) [2] and may contribute to increased disability in this population. Pain, a primary symptom in KOA, has been linked to KE dysfunction. Previous research has shown that while habitual exercise has a beneficial effect on KOA pain, individual bouts of exercise can result in acute pain exacerbations [3]. The impact of acute pain on KE muscle function and physical performance in OA is not well characterized. Quantifying the KE functional demand (FD) is one way to assess the impact of pain related changes KE muscle function on physical performance in KOA. Muscle FD is defined as the percentage of maximal strength that is used during a task. KE dysfunction and acute pain-related changes may increase the FD as compared to healthy individuals and contribute compensatory gait strategies and disability in KOA. The compensatory gait strategies could include a change in the distribution of joint power and mechanical work. Therefore, the purpose of this study was to investigate the impact of exercise-induced pain on KE functional demand and joint coordination in individuals with KOA.

Methods

Fourteen adults with symptomatic KOA (Age: 65.2±5.2 years, BMI: 25.2±3.7 kg/m^2, KOOS pain:68.9±16.2) participated in this study after completing informed consent approved by the University's IRB. Participants completed three maximal isometric KE contractions on an isokinetic dynamometer (Biodex System 4 Pro, Shirley, NY) set at 60° of knee flexion before and after a 20min treadmill walk (20MTW) previously shown to increase pain in KOA [4]. Perceived pain was evaluated on an 11-point verbal numeric rating scale (vNRS) every two minutes throughout the 20MTW. The pain scores in the first and final 2 min of the 20MTW were used to evaluate change in pain in response to exercise. Participants also completed 5 overground walking trials at a faster than preferred pace before and after the 20MTW. Functional demand was determined at the time of the peak knee flexion moment (KFM) and was calculated as the ratio of the peak knee joint moment and the maximum KE isometric muscle torque at that peak and is expressed as a percentage. Joint powers were calculated as the product of the joint moments and angular velocities. Total limb power was calculated as the sum of individual joint power values at the hip, knee, and ankle. The relative contribution for each joint to total limb power was calculated by dividing the power at a joint by the total limb power and is expressed as a percentage. Joint powers were extracted from the stance phase while the peak KFM was extracted from the first 50% of stance. Paired samples t-tests were used to compare FD, joint coordination, and pain variables between pre and post 20MTW (α= .05). We hypothesized that there would be an increase in pain, FD, and ankle power post 20MTW.

Results and Discussion

Our hypotheses were partially supported. There was a significant increase pre to post walk in pain t(13)= -3.267, p=.003. However, we found no differences pre to post 20MTW in FD, or joint coordination (all p>0.05). When compared to an older reference group, individuals with KOA had higher FD, indicating they are more impaired [5]. Despite the increase in pain, we saw no differences in relative joint powers or peak KE torque between pre to post 20MTW. Walking at a speed greater than preferred may require reliance on weaker muscles to maintain gait speed. This strategy to maintain gait speed may interfere or preclude a pain related adaptation to reduce FD and off load the joint by changing joint coordination.

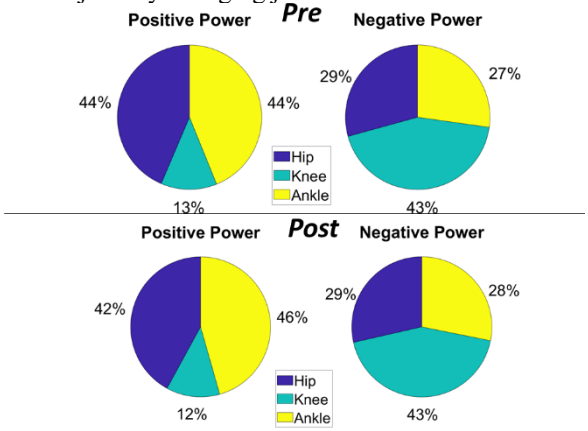

Figure 1. Distribution of relative positive and negative joint powers pre and post 20MTW

Significance

Higher pain is thought to stimulate a change in gait mechanics to offload the joint. The lack of a change in coordination and FD in response to pain suggests acute increases in pain do not impair KE function to the extent that it impairs mobility.

Acknowledgments

Funding provided by a University of Massachusetts-Amherst hMRC Pilot Grant

References

[1] Bennell KL, et al. Rhe Dis Clin North Am. 2013;39:145-76.
[2] Lewek MD, et al. J Orthop Res. 2004;22:110-5.
[3] Focht BC, et al. Ann Behav Med. 2002;24:201-10.
[4] Boyer KA, et al. BMC Musc Disord. 2019;20(1):107
[5] Hafer, JF et al. J Appl Biomech. 2020;1-8.

	KE Peak Torque (Nm)	Functional Demand (%)	Knee Flexion Moment (%Bw*ht)	Pain
Pre20MTW	111± 50.6	49.9±16.1	52.1± 2.0.5	1.21±1.53
Post20MTW	117± 63.2	52.0±25.6	51.7± 20.5	3.07±1.82*

Shoulder Internal Rotation Deficit and Total Rotational Motion Deficit of the Throwing Arm Are Not Related to Injuries and Surgeries in Collegiate Baseball Pitchers

Marc Duemmler[1], Hannah L. Stokes[1], Koco Eaton[2], Nigel Zheng[1]
[1]Department of Mechanical Engineering and Engineering Science, University of North Carolina at Charlotte, NC, USA
[2]Tampa Bay Rays and University of South Florida, FL, USA
Email: nzheng@uncc.edu

Introduction

Both glenohumeral internal rotation deficit (GIRD) and total rotational motion (TRM) deficit are related to shoulder injuries [1]. GIRD and TRM deficit are defined as the loss of greater than 20° and 5° of rotation, respectively, compared to the contralateral shoulder (i.e., non-throwing arm) [2]. Pitchers who have both GIRD and TRM deficit are defined as having pathological GIRD [2]. GIRD and TRM deficit are commonly assessed qualitatively by team clinicians. The purpose of this study is to quantitatively investigate how shoulder rotational properties are related to injuries and surgeries in collegiate baseball pitchers. This connection could allow for intervention and ultimately reduce the number of injuries and surgeries. We hypothesized that shoulder rotational properties would have no statistically significant relationship to injury or surgery occurrence.

Methods

The study included 109 college baseball pitchers (height: 186±8 cm and weight: 85±9 kg). The study was approved by an institutional review board and all pitchers gave informed consent. All pitchers were healthy during testing. The injury questionnaire reports if the pitcher has had a surgery or injury that resulted in loss of playing time within the previous year. Pitchers included in this study were followed for at least one year after testing. The shoulder rotational test measured the rotational end-point-angle (EPA) under a force of 40 N applied using a custom-made wireless device during physical exam[3]. Both internal and external rotation of both the throwing and non-throwing arm were examined. Total range of motion (tROM) is defined as internal rotation EPA (IR-EPA) plus external rotation EPA.

This study utilized IR-EPA deficit and tROM deficit, which are related to GIRD and TRM deficits, respectively, with the same thresholds as defined in literature. Four deficit groups were defined: both IR-EPA and tROM deficit, tROM deficit only, IR-EPA deficit only, and neither deficit. The pitchers separated into three categories: healthy, had injury/surgery before testing, and had injury/surgery after testing (Table 1). Eight pitchers had injury/surgery before and after testing. One-way ANOVA and Chi-squared tests were performed using SPSS with an alpha set to 0.05.

Table 1: Distribution of pitchers in deficit groups for each categorical group. (S/I: surgery/injury)

	Both	tROM	IR-EPA	Neither
Healthy	8	**13**	0	**20**
S/I After	5	6	3	**19**
S/I Before	6	**13**	2	**22**

Results and Discussion

The bilateral differences of tROM and IR-EPA had no significant relationship between the categorical groups (Table 2). The Chi-squared test showed that there were no significant relationships between the deficit groups to the categorical groups (p-value = 0.46). These findings indicate that there are more factors than just tROM and internal rotation EPA deficits that influence injury and surgery occurrence.

Table 2: Mean ± SD for Bilateral differences of tROM and IR-EPA for each categorical group. (S/I: surgery/injury)

	N	tROM	IR EPA
Healthy	41	-3.05 ± 12.9	-11.67 ± 10.81
S/I After	33	0.04 ± 13.48	-9.45 ± 13.17
S/I Before	43	-1.71 ± 15.48	-9.18 ± 13.23

Wilk et al found that there was an increase of risk of injury and surgery in professional baseball pitchers who had GIRD, TRM deficits, and flexion deficits, but that there were no significant differences [4]. Our study has similar findings in collegiate baseball pitchers, in that there were no significant relationships. Future studies can focus on finding additional categories that might have a significant relationship with injury or surgery occurrence. Additionally, a larger sample size could lead to better understanding of causes of injuries.

Significance

There are no significant relationships between IR-EPA and tROM deficits to injury or surgery. While IR-EPA and tROM deficits can play a role in injury and surgery occurrence, there are more factors to consider than just those two deficits. If these other factors can be determined, interventions can be designed to lower the overall occurrence of injury and surgery in collegiate baseball pitchers.

Acknowledgments

This study is funded by a Clinical Research Grant from Major League Baseball.

References

[1] Wilk K et al. (2011). *Am J Sports Med,* **39**: 329-335.
[2] Rose M and Noonan T. (2018). *Open Access J Sports Med,***9**: 69-78.
[3] Zheng N. (2011). *Int J Sports Med*, **33**: 463-468.
[4] Wilk K et al (2015). *Am J Sports Med,* **43**(10): 2379-2385.

VERTICAL GROUND REACTION FORCE RECORDED USING ZEBRIS TREADMILL DURING WALKING DECLINES OVER TIME

Prabhat Pathak[1] and Jooeun Ahn[1,2*]
[1]Department of Physical Education, Seoul National University, South Korea
[2]Institute of Sport Science, Seoul National University, South Korea
email: *ahnjooeun@snu.ac.kr

Introduction

Vertical ground reaction force (VGRF) is an important biomechanical indicator of human walking, so an accurate and reliable VGRF measurement is essential [1]. To achieve this goal with a relatively less expensive cost, treadmills embedded with capacitive pressure sensors, particularly Zebris treadmills, are extensively used to measure VGRF during walking. Previous studies have shown the reliability of a Zebris treadmill between trials and days when the treadmill measures peak VGRF of walking for a short period of time, ranging from 20 seconds to 2 minutes [2,3]. However, several other studies have reported that capacitive pressure sensors show a decline in the measured plantar force [4,5]. To address this discrepancy, we aim to evaluate long-term temporal changes in VGRF while walking on a Zebris treadmill.

Methods

Twenty healthy adults (16 males and 4 females) between the ages of 20 and 40 participated in the study. Participants performed two walking trials, 10 minutes per trial, on a Zebris treadmill (Model Gait analysis FDM-TDSL-3i, Zebris Inc®, Germany) at their preferred walking speed. VGRF was recorded at a sampling frequency of 50 Hz. Participants rested for 10 minutes between trials. We extracted the VGRF values of three typical extrema during each step: VGRF at load response, mid stance, and push off. We averaged each of the three VGRF extrema over every one-minute interval, separately for left and right foot.

Results and Discussion

Figure 1 shows the mean and standard error of the measured VGRFs for 20 participants at the three time points (load response, mid stance, and push off) over every one-minute interval for the both feet and two trials. There was a general decline in the mean VGRF over time for all three time points, and the mean VGRF for the first trial is always larger than that for the second trial. Considering the participants are walking at the same preferred walking speed and body weight can hardly change over 10 minutes of walking, VGRF should remain almost constant. Hence, the results conclude that a Zebris treadmill is not reliable for VGRF measurement during walking for a long period of time.

Significance

Zebris treadmills are widely used to record VGRF by researchers in the field of human movement science worldwide. Considering a significant decline in the VGRF measured using the Zebris treadmill over time and trials, we recommend taking caution while recording VGRF for a long time period using the Zebris treadmill during locomotion to avoid an erroneous interpretation.

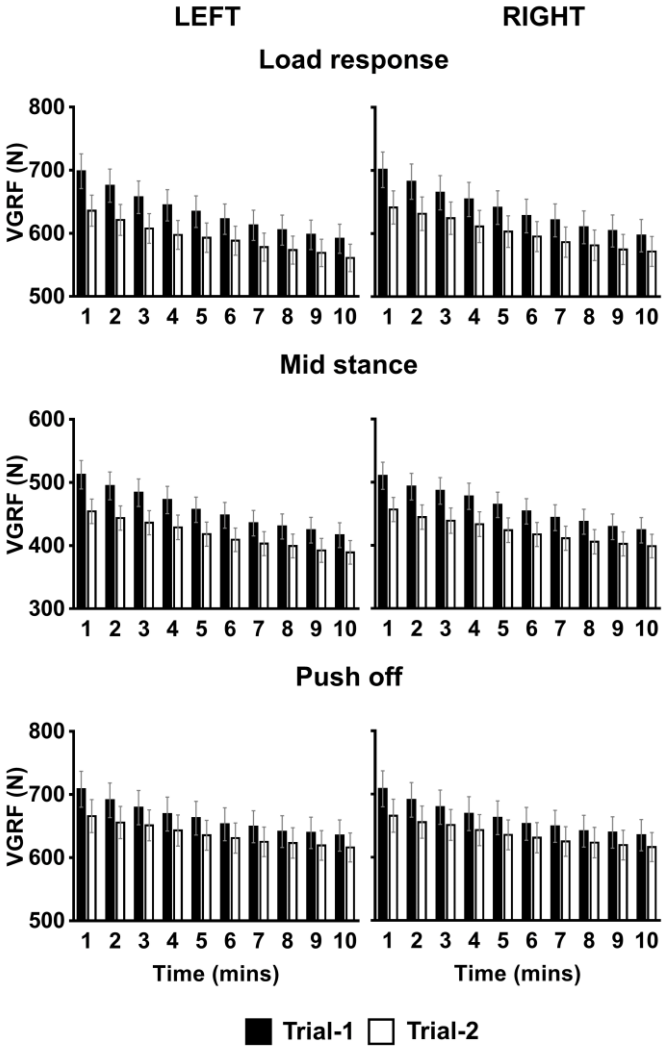

Figure 1. Mean and standard error of the three typical extrema VGRF values for 20 participants over time and trials

Acknowledgments

This work was supported in part by the National Research Foundation of Korea (NRF) Grants funded by the Korean Government (MSIT) (No. NRF-2016R1A5A1938472, and No. NRF-2018R1C1B5046957).

References

[1] Creaby MW et al. 2013. *Clin Biomech*
[2] Nüesch C et al. 2018. *Gait Posture*
[3] Item-Glatthorn JF et al. 2016. *Gait Posture*
[4] Miyazaki S & Ishida A. 1984. *Med Biol Eng Comput*
[5] Sorrentino I et al. 2020. *Sensors*

Auditory Cues can Elicit Anticipatory Ajustments for Posterior Perturbations after Short Training

Huaqing Liang[1], Tippawan Kaewmanee[2], and Alexander S. Aruin[2]
1. School of Physical Therapy, Marshall University, WV, USA, liangh@marshall.edu
2. Department of Physical Therapy, University of Illinois at Chicago, USA

Introduction

The central nervous system employs anticipatory postural adjustments (APAs) as an effective feedforward mechanism to minimize the postural disturbance caused by external perturbations. Strong APAs could reduce the demands for compensatory postural adjustments (CPAs) after the impact [1]. However, the generation of APAs majorly relies on visual information, and is optimized through past experience. Hence, external perturbations from the back would cause more postural disturbance and increased risks of fall when such protective mechanism is unavailable. Our previous work showed that an auditory cue could facilitate the generation of APAs for a front perturbation [2]. The purpose of this study was to evaluate the effectiveness of an auditory cue in generation of APAs for an unexpected external perturbation coming from the back.

Methods

Ten young adults (mean age 31.6±3.1 years) were recruited for this study. A swinging pendulum with an additional weight (3% of the body weight) was used to create the external perturbation by hitting the participants' shoulders bilaterally from the back. An accelerometer attached on the pendulum was used to identify the moment of impact (T0).

The participants were instructed to stand on a force plate, look forward and be prepared for the impact. First, they received perturbations with no cues provided (baseline, BL, 5 trials). Then they received training (Tr, 50 trials) when an auditory cue signaling the moment of the pendulum release was provided via headphones. After 5 minutes rest, they received perturbations with the same auditory cue (Test, 5 trials).

Muscle activities were recorded from the right tibialis anterior (TA), medial gastrocnemius (MG), rectus femoris (RF), biceps femoris (BF), rectus abdominus (RA), and erector spinae (ES). EMG integrals were calculated during the APA phase (-250 to +49ms) and CPA phase (+50 to +349ms), and were normalized [2]. The COP displacements in the AP direction at T0 and its peak value after T0 were identified.

Data were organized into 5-trial blocks. Data from the BL, one block from the beginning (Tr1), middle (Tr5), and the end (Tr10) of training, and the Test were used for further analysis. A series of one-way repeated measures ANOVAs were conducted. Statistical significance was set at $\alpha = 0.05$.

Results and Discussion

In the BL condition, minimum muscle activation was observed in the APA phase and the COP displacement at T0 was close to zero. Consequently, the demands for muscle activation and the COP peak displacement were large during the CPA phase. These results suggest that no APAs were generated for an unexpected perturbation from the back and such perturbation caused large postural disturbance. Throughout the training, there was a gradual increase of muscle activation and a slight anterior shift of the COP during the APA phase; at the same time, we observed a gradual decrease of muscle activation and a decrease of peak COP displacement during the CPA phase.

Statistical analysis showed condition effect for BF integral during the APA phase; MG, RF, and BF integrals during the CPA phase, and COP displacement at T0 and its peak value (all $p<0.05$). Changes in integrals for a representative muscle (BF) across the conditions are shown in Figure 1, and changes in the COP displacement are shown in Figure 2. In Figure 1 and 2, * and ^ denote a significant difference compared to the the BL and Tr1 condition, respectively.

In foreseeable front perturbations, an effective APA pattern would be the activation of frontal muscles and inhibition of dorsal muscles [3]. In this study when the perturbation was coming from behind, we observed more prominent changes in the activations of dorsal muscles, implying a different muscle activation pattern as the APA strategy.

Figure 1

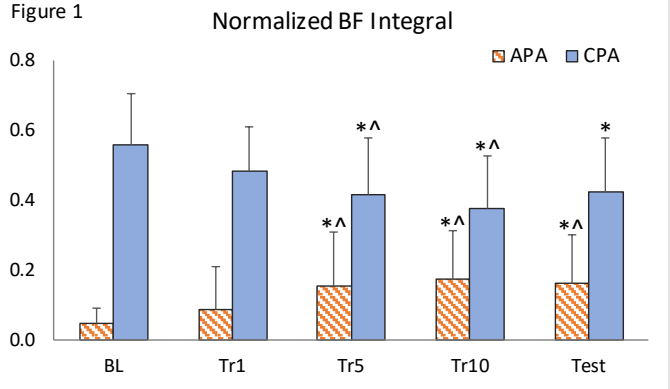

Figure 2

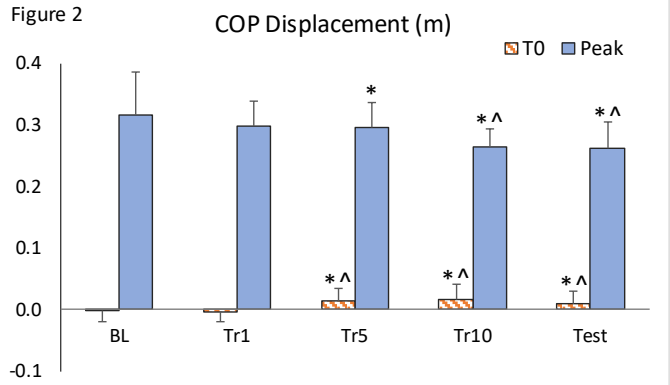

Significance

After a short training, young adults could learn to generate new APA patterns relying on an auditory cue for an otherwise unpredictable postural perturbation. Further study will explore the feasibility of implementing such training in more dynamic settings in indivudals with balance problems.

References

[1] Santos et al. J Electormyogr Kinesiol 20:398-405, 2010b.
[2] Liang et al. Exp Brain Res 238(3):631-641, 2020.
[3] Massion. Prog Neurobiol 38:35-36, 1992.

Role of Auditory Cues on Anticipatory Adjustments to Perturbations Might be Directional Specific

Huaqing Liang[1], Tippawan Kaewmanee[2], and Alexander S. Aruin[2]
1. School of Physical Therapy, Marshall University, WV, USA, liangh@marshall.edu
2. Department of Physical Therapy, University of Illinois at Chicago, USA

Introduction

Anticipatory postural adjustment (APA) is an effective feedforward mechanism to help us maintain balance in the events of external postural perturbations. With the generation of strong APAs, the postural disturbance caused by the perturbation is diminished, which is confirmed by reduced compensatory postural adjustments (CPAs) [1]. The generation of optimal APAs relies majorly on visual information and past experience. However, our previous work showed that an auditory cue could elicit the generation of APAs for an otherwise unexpected external perturbation [2]. The aim of this study was to explore if this learned pattern of APA generation using an auditory cue is directional specific and whether people could elicit appropriate APAs for perturbation coming from another direction relying on the same auditory cue.

Methods

Ten young adults (mean age 31.6±3.1 years) participated in this study. A swinging pendulum with an additional weight (5% of the body weight) was used to hit the participants' shoulder laterally and induce an external perturbation in the medial-lateral (ML) direction. Participants were instructed to stand on a force plate with either their left or right side facing the pendulum, look forward and be prepared for the impact. First, they received perturbations with no cues provided while facing one of the two directions (BL_R and BL_L, each condition included 5 trials). Then they received perturbations to the right side (training, 50 trials) when an auditory cue signaling the moment of the pendulum release was provided via headphones. After 5 minutes rest, they received perturbations with the same auditory cue while facing one of the two directions (Test_R and Test_L, each included 5 trials).

An accelerometer was used to identify the moment of impact (T0). EMGs were recorded from bilateral tibialis anterior (TA), medial gastrocnemius (MG), rectus femoris (RF), biceps femoris (BF), gluteus maximus (GM), external obliques (EO), rectus abdominus (RA), and erector spinae (ES). EMG integrals were calculated during the APA phase (-250 to +49ms) and CPA phase (+50 to +349ms), and were normalized [2]. The COP displacements in the ML direction at T0 and its peak value after T0 were identified.

Data from the BL_R, Test_R, BL_L, and Test_L conditions were averaged for further analysis. A series of t-tests were conducted. Statistical significance was set at $\alpha = 0.05$.

Results and Discussion

When perturbations came from both directions unexpectedly in BL_R and BL_L conditions, small muscle activation was observed in the APA phase and the COP displacement at T0 was close to zero. Consequently, the demands for muscle activation and the COP peak displacement were large during the CPA phase. When the participants received perturbations on the right side after the training period, there was an increase of ipsilateral (IPS) muscle activation and a slight shift of the COP to the left side during the APA phase; we also observed a decrease of muscle activation on both sides of the body during the CPA phase. However, the magnitudes of muscle activation seem to be unchanged when the pendulum hitting their left side.

When comparing BL_R and Test_R conditions, significant differences were observed for ipsilateral MG, BF, and GM integrals during the APA phase, for ipsilateral TA, RF, EO, ES integrals and contralateral (CON) MG, RF, BF, and EO integrals during the CPA phase, and COP displacements at T0 (all $p<0.05$). There was no difference between BL_L and Test_L conditions. Integrals for a representative muscle (MG) are shown in Figure 1, and COP displacements in Figure 2.

It is also interesting to note that when the perturbation hitting participants laterally, the mucle activation patterns in the distal muscles (TA-MG pair) were side specific: co-contraction was seen on the contralateral (CON) side and reciprocal activation on the ipsilateral (IPS) side.

Figure 1

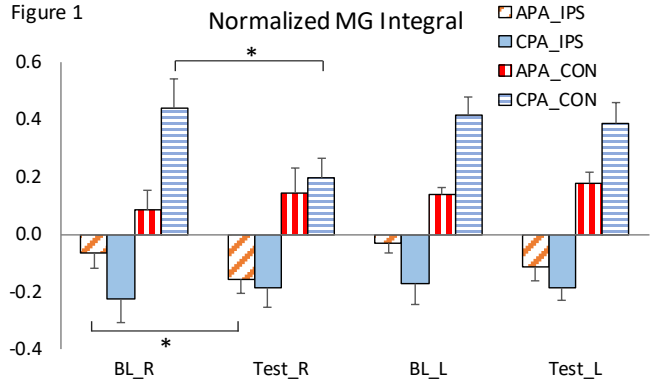

Figure 2

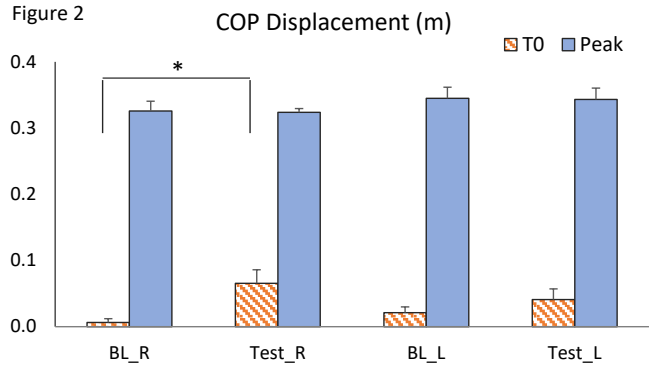

Significance

Young adults could learn to generate APA patterns relying on an auditory cue in response to an unpredictable lateral perturbation after a short training. However, this training effect is directional specific. Further study will explore the feasibility of implementing perturbations from all directions into a training program using auditory cues.

References

[1] Santos et al. J Electormyogr Kinesiol 20:398-405, 2010b.
[2] Liang et al. Exp Brain Res 238(3):631-641, 2020.

FUNCTIONAL MOVEMENT IN A RAT MODEL OF BRACHIAL PLEXUS BIRTH INJURY

Raveena M. Doshi[1], Monique Y. Reid[2], Nikhil N. Dixit[1], Emily B. Fawcett[2], Jacqueline H. Cole[2], Katherine R. Saul[1]
[1]Department of Mechanical and Aerospace Engineering, NC State University, Raleigh, NC
[2]Joint Department of Biomedical Engineering, UNC, Chapel Hill, NC and NC State University, Raleigh, NC
email: ksaul@ncsu.edu

Introduction

Brachial plexus birth injury (BPBI), the most common nerve injury among children,[1] involves damage to C5-C6 nerve roots with shoulder internal rotation and elbow flexion contracture as frequent sequelae.[2] More severe contractures present with nerve root ruptures distal to the ganglion (postganglionic),[3] while avulsion injuries proximal to the ganglion (preganglionic) typically present as paralysis without contracture.[4]

The effect of BPBI on passive movement has been well-documented in rodent models,[3,5,6] as surgically induced BPBI reproduces similar musculoskeletal deformities.[7] The effect on functional movement, however, remains underexplored. Given that treatment of BPBI typically focuses on passive functionality,[8] insight into the impact of BPBI on functional movement could better inform intervention and highlight mechanisms responsible for neuromusculoskeletal deficits.

We developed a non-invasive framework integrating gait analysis with musculoskeletal modeling to elucidate the effect of injury location on functional movement. We hypothesized that injury location would affect functional movement outcomes, and that passive range of motion (ROM) would be a good predictor of functional shoulder movement.

Methods

We studied 18 Sprague Dawley rat pups that underwent unilateral surgical intervention (preganglionic neurectomy, postganglionic neurectomy, or sham surgery) 3-5 days postnatally as part of larger, prior studies.[6,9] After 8 weeks, rats were assessed for passive shoulder external rotation ROM and with treadmill gait analysis, then sacrificed for muscle architecture measurements.

Shoulder protraction and elbow flexion angles were extracted using virtual markers. Time spent on the stance limb (quantified by duty factor) was calculated based on heel-strike and toe-off timing. The effect of injury location on duty factor was assessed using one-way ANOVA. The relationship between functional and passive ROM was assessed with linear regression.

We developed 18 musculoskeletal models of the rat forelimb in OpenSim[10] using a generic skeletal structure[11] and animal-specific muscle parameters. Fourteen Hill-type muscle-tendon actuators represented 10 shoulder muscles. Animal-specific kinematic trajectories were used to simulate gait in corresponding models. Muscle fiber lengths were extracted and normalized by optimal length to calculate excursion. Effects of injury group and passivity on excursion were assessed using two-way ANOVA.

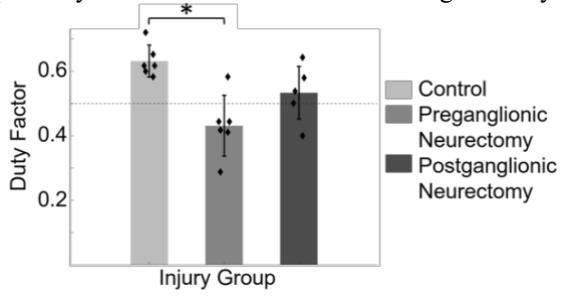

Figure 1. Mean duty factor by injury group. In able-bodied gait, walking should have a duty factor above 0.5 (dotted line). * $p<0.05$.

Results and Discussion

The preganglionic group had less shoulder protraction and elbow flexion than other groups, primarily during late-stance and early-swing when limb loads are highest. Compared to control, duty factor was significantly lower ($p=0.0012$) in the preganglionic group but not the postganglionic group (**Fig. 1**).

Reduced functional elbow flexion during walking following preganglionic neurectomy is consistent with passive elbow contracture seen in a mouse model of BPBI.[5] However, functional shoulder movement was not significantly correlated with experimental passive shoulder ROM within injury groups or across animals ($r^2=0.061$, $p=0.32$). Between functional and passive movements, excursions differed significantly for 11 actuators ($p<0.0009$ for nine; $p<0.02$ for two) (**Fig. 2**).

We conclude that passive external rotation shoulder ROM is not an effective predictor of functional shoulder protraction performance in rat models of BPBI. The functional outcomes we observed during gait likely result from a combination of altered muscle architecture and compensatory motor control strategy to manage limb loading following BPBI.

Significance

Our results suggest that restoring passive functionality in a BPBI patient may not always translate to improved functional performance. Differences in fiber excursion indicate that muscles may undergo significantly different use under passive and functional joint rotation. Given that functional ROM determines joint loading and development, our findings suggest inclusion of functional movement analysis in clinical treatment of BPBI.

Acknowledgments

This work was supported by the NIH grant R21 HD088893.

References

[1] Foad. 2008. *J Bone Joint Surg Am* 90:1258; [2] Pearl. 2009. *J Am Acad Orthop Surg* 17:242; [3] Nikolaou. 2015. *J Hand Surg Am* 40:2007; [4] Al-Qattan. 2003. *Ann Plast Surg* 51:257; [5] Nikolaou. 2011. *J Bone Joint Surg Am* 93:461; [6] Dixit. 2020. *J Hand Surg Am*. [Epub]; [7] Soldado. 2012. *J Brachial Plex Peripher Nerve Inj* 7:9; [8] Hale. 2010. *J Hand Surg Am* 35:322; [9] Dixit. 2018. ORS Annual Meeting; [10] Delp. 2007. *IEEE Trans Biomed Eng* 54:1940; [11] Bonnan. 2016. *PLoS One* 11:1. [12] Murray. 2000. *J Biomech* 33:943.

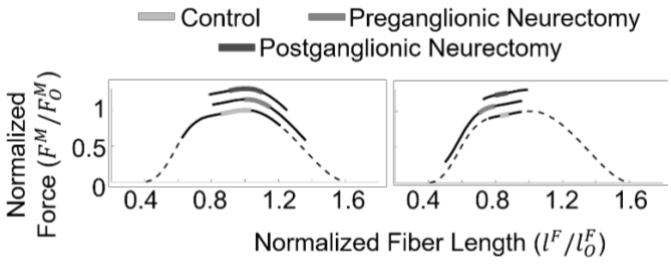

Figure 2. Normalized biceps short head fiber excursions for functional (left) and passive (right) shoulder movement superimposed on a normalized force-length curve.[12]

FUSION OF WEARABLE METRICS TO ESTIMATE STEP-BY-STEP TRICEPS SURAE WORK DURING OUTDOOR LOCOMOTION ON SLOPES

Sara E. Harper[1,2], D. Schmitz[2], P. Adamczyk[2,1], and D. Thelen[2,1]
[1]Department of Biomedical Engineering, University of Wisconsin-Madison, Madison, WI, USA
[2]Department of Mechanical Engineering, University of Wisconsin-Madison, Madison, WI, USA
email: *seharper@wisc.edu

Introduction

Wearable tensiometry has been recently introduced as a means of characterizing tendon loading during outdoor locomotion.[1] The coupling of tensiometry and inertial measurement units (IMUs) could enable a mobile motion analysis system. For example, wearable measures of tendon kinetics and movement kinematics could be fused to characterize power and work production of muscle-tendon units.[2] This study aimed to 1) establish a wearable system which enables simultaneous kinematic and tendon kinetic measurements, and 2) investigate step-by-step triceps surae work production during outdoor locomotion on varying slopes.

Methods

The tensiometry unit consisted of a piezoelectric tapper and miniature accelerometers embedded in silicone. Accelerometry data were recorded on a custom battery-powered data logger, comprised of a Raspberry Pi 4B and an IEPE Measurement HAT (MCC 172, Measurement Computing Corporation). Taps were delivered at 100 Hz, each providing a measure of tendon wave speed.[1,2] IMUs (MTw Awinda, XSens Gmbh) synchronously recorded subject position, knee flexion, and ankle plantarflexion.

Twelve healthy young adults (23.3 ± 2.4 years, 6F/6M) were tested, of whom one is analyzed to-date. The tensiometer was placed over one Achilles tendon, chosen at random. Following acclimation, subjects completed a calibration task that enabled tendon force to be estimated from wave speed.[2] Each subject then walked at self-selected speeds along an outdoor 800 m course including varied slopes from -10° to 10° (Fig. 1). Slope of the course was assessed with an IMU secured to a bicycle which was pushed along the course.[1] Slope of each step was then extracted from a lookup table by knowing the subject position and terrain slope. Work against gravity per step was calculated as 50% of the product of each stride length and the tangent of its incline.

Knee and ankle angles were used in conjunction with average moment arm relationships to calculate soleus and gastrocnemius excursions.[2,3] Calibrated tendon force was normalized to body mass and apportioned to soleus and gastrocnemius forces based on average physiological cross-sectional area, 65% and 35%, respectively.[4] Net muscle-tendon work per step was then calculated from muscle force and length ($W = \int_{t_0}^{t_1} \vec{F} * \left(\frac{d}{dt} L\right) dt$) from early stance to push-off. To test how muscle-tendon work about the ankle changes with terrain slope, nonlinear regression was performed to fit a logistic curve between net work and incline angle of each step for both the soleus and gastrocnemius.

Results and Discussion

This subject demonstrated net soleus and gastrocnemius work per step on level slopes (0.09 J/kg and 0.10 J/kg, respectively) that compare well to recent laboratory-based results.[2] Congruence to prior findings provides further validation for use of the tensiometry-based wearable system.[1,2,5]

Net soleus and gastrocnemius work per step modulated significantly with slope ($p<0.00001$) (Fig. 2). Soleus work production increased at a higher rate than the gastrocnemius over small slopes (0.031 vs 0.009 J/kg/deg), but then tended to saturate at the steepest inclines (0.36 J/kg) and declines (-0.06 J/kg). This behavior may reflect a slope-dependent shift in work production to the knee and hip at steeper inclines, as reflected by the greater work against gravity.[6] Further analysis of more subjects will investigate consistency of these trends, universality of the plateau in work at steep slopes, and commonality of the angle at which work transitions from negative to positive.

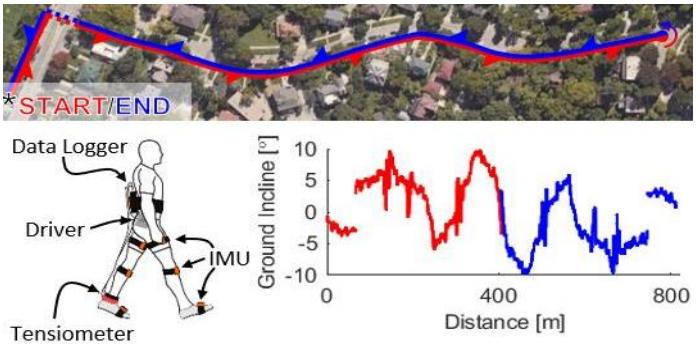

Figure 1: Schematic of instrumentation during outdoor trials as well as ground incline along the outdoor course.[1]

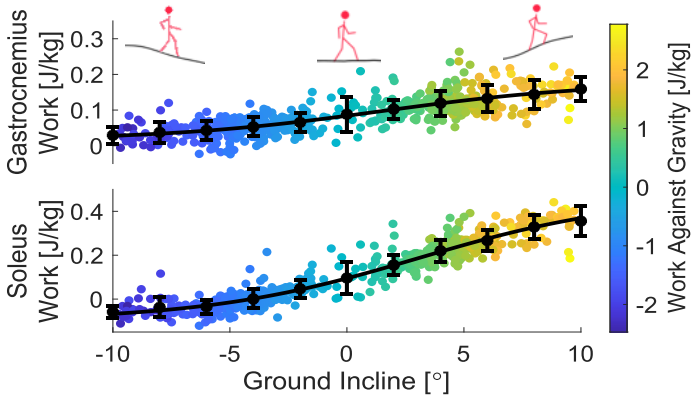

Figure 2: Work about the ankle for each step increased with slope for one subject (24 years, F), with mean and standard deviation for each bin.

Significance

This work fuses wearable tensiometry and IMU measures to simultaneously assess muscle-tendon kinematics, kinetics, and work production during outdoor locomotion. The wearable motion analysis system could enable exciting new applications beyond the traditional laboratory setting.

Acknowledgments

Funding provided by WARF Accelerator Program, NIH (STTR AR074897; TL1TR002375), and NSF GRFP (DGE-1747503).

References

[1] Harper, SE+, *Sensors*, 2020; [2] Ebrahimi, A+, *Front Sports Act Living*, 2020; [3] Buford, WL+, *IEEE Trans Rehabil Eng*, 1997; [4] Handsfield, GG+, *J Biomech*, 2014; [5] McIntosh, AS+, *J Biomech*, 2006; [6] Montgomery, JR+, *R Soc Open Sci*, 2018.

LEG STIFFNESS IS AFFECTED BY DEPRESSION SYMPTOMS AND SEX DURING DROP JUMPS WITH COGNITIVE LOAD

Hillary H Holmes[1], Jaimie A Roper[1]
[1]Auburn University, Auburn, AL, USA
Email: hhholmes@auburn.edu

Introduction

Psychological well-being is a risk factor for musculoskeletal injuries.[1,6,8] Psychological stressors, like anxiety and depression, have potential to diminish cognition, and thus alter neuromuscular control during dynamic tasks.[1,6] Considering neuromuscular control and psychological well-being during tasks of higher cognitive load may add insight to injury risk.

Increasing the cognitive load of dynamic tasks, like drop jumps, has been shown to alter neuromuscular control.[2,3,5,7] Thus, our purpose was to use multilevel modelling to determine if increasing the cognitive load of drop jumps, by adding decision-making, would influence leg stiffness, and if psychological well-being further affected the relationship between drop jump conditions and leg stiffness. Because sex differences are reported in relationships among drop jump mechanics, psychological well-being, and injury, we also tested interactions of sex with psychological well-being and drop jump conditions on stiffness using sex as a random intercept.[2,6] We hypothesized decision-making conditions and psychological well-being to influence leg stiffness, with psychological well-being to interacting with drop jump conditions and sex.

Methods

Thirty-three healthy, active young adults (males=13, females = 20, age=21 yr ± 2 yr, height=1.71 m ± 0.81 m, mass=70.5 kg±10.6 kg) completed the Beck Anxiety and Depression Inventories (BAI and BDI-II) and a drop jump protocol with four decision-making conditions. The choice condition had participants choose between drop jumps or lands. Visual and auditory conditions had participants react to visual or auditory cues presented while the participant was in mid-air. The standard condition involved asking participants to perform a drop jump or a drop land. Leg stiffness was normalized to body mass, equaling the ratio of peak vertical ground reaction force and change in leg length between foot strike and minimum leg length. Leg length equaled the height of the greater trochanter to the floor.

Multilevel modelling was performed in R (The R Foundation for Statistical Computing, Vienna, Austria). We fitted a model predicting leg stiffness by condition, sex, BDI-II and BAI scores, and interactions among condition, sex, BAI, and BDI-II on leg stiffness. This model included sex as a random intercept, as it is known that mechanics and psychological well-being have reported sex differences.[2,6]

Results and Discussion

Our model identified a significant three-way interaction among sex, choice condition and BDI-II scores (p=0.00641). Specifically, males did not present the same relationship between worse BDI-II scores and increased leg stiffness during the choice condition compared to females. Significant main effects existed in BDI (p=0.0345) and BAI scores (p=0.0475), with 1-point increases on the BDI and BAI scores indicating an increase and decrease in stiffness by 7.74N/mkg and 4.20N/mkg, respectively.

Our results indicate males present different relationships between depressive symptoms and leg stiffness when tasked with volitional decision-making compared to other decision-making and females. Increased injury rates have been reported in male athletes with depression symptoms.[6] Although we analyzed leg stiffness and not injury, increased or sub-optimal leg stiffness may indicate injury risk.[4,7] However, larger leg stiffness also enhances athletic performance, allowing for multiple interpretations of this result. For males, volitional choices of movements may minimize excessive leg stiffness, but also decrease performance if leg stiffness is less than optimal for the task. More research is needed on mental health, sex, and biomechanics for a comprehensive understanding of injury and performance.

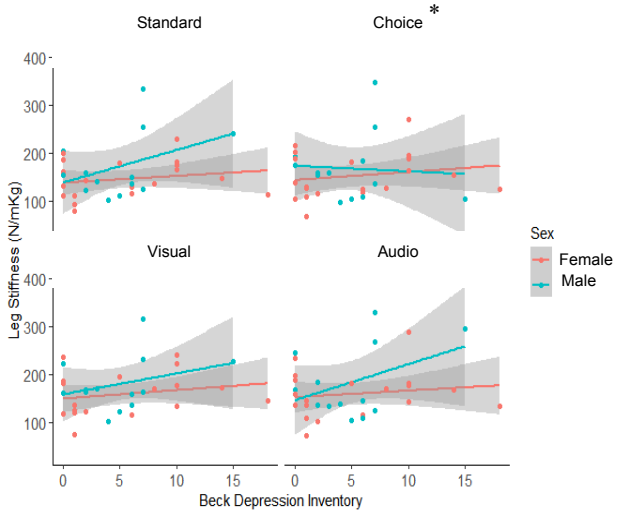

Figure 1: Relationships between leg stiffness and BDI-II scores in males and females during drop jumps with different decision-making demands. *p<0.05

Significance

This novel investigation used multilevel modelling to identify relationships among leg stiffness, psychological well-being, and sex during a dynamic task. Drop jumps are accessible and reliable to screen for injury and test athletic performance. Considering sex and depression symptoms can influence leg stiffness provides rationale to consider psychological well-being in athlete testing and injury prevention.

Acknowledgments

Undergraduate research fellowship, College of Education.

References

1. Anderson & Williams 1998. *J Appl Sport Psychol*
2. Bruton et al., 2013. *J Electromyogr Kinesiol*
3. Herman & Barth 2016. *Am J Sports Med*
4. Leppänen et al. 2017. *Am J Sports Med*
5. Leukel et al., 2012. *Hum Mov Sci*
6. Li et al., 2017. *Am J Sports Med*
7. Swanik 2015. *J Athl Train*
8. Yang et al., 2014. *Res Sports Med*

INCREASED AGE IS ASSOCIATED WITH DECREASED ANKLE AND KNEE EXCURSION IN FEMALE RUNNERS

Heather M. Hamilton, DPT,[1] Rumit Singh Kakar, PT, PhD.[1]
[1]Old Dominion University, Norfolk, VA, USA
Email: hmcco006@odu.edu

Introduction

Older runners present with differences in running biomechanics compared to younger runners. Specifically, older runners demonstrate decreased ankle and knee joint range of motion during running [1-4]. Evidence suggests that females' physical function declines more rapidly than males' during middle-age, which may be due to physiological effects of menopause [5]. Postmenopausal women demonstrate decreased muscle strength and power compared to premenopausal women [5], and it is therefore important to include separate-sex analyses when studying the effects of age on sport biomechanics.

To the authors' knowledge, there are no studies evaluating the relationship between age and sagittal plane kinematics specifically in female runners. Additionally, few studies consider the effect of a maximum running speed, though this may be more sensitive to age-related changes in running biomechanics. The purpose of this study was to determine the relationship between age and lower extremity kinematics at self-selected jogging and maximal running speeds specifically in female runners.

Methods

Forty-six female participants (18-65 years) ran at a self-selected long distance pace (JOG) and maximal running pace (MAX) on a treadmill. Lower extremity kinematic data were collected using 34 lower extremity reflective markers and 3D motion capture (Vicon®). Linear regression was used to determine the association between age and sagittal plane peak ankle, knee, and hip angles of the right limb in stance for both JOG and MAX speeds. Speed was controlled for in the first block of the regression model. Independent t-tests were used to determine differences in peak angles between the youngest (ages 18-28, n = 13) and the oldest runners (ages 50-65, n = 11) amongst all participants.

Results and Discussion

Mean JOG speed was 2.66 ± .30 m/s, and MAX speed was 3.80 ± .61 m/s. After controlling for speed, age was significantly negatively correlated to peak dorsiflexion and knee flexion for both JOG and MAX (Table 1, Figure 1). Age was not related to hip flexion at initial contact or hip extension at toe-off (Table 1). The oldest runners demonstrated significantly lower peak dorsiflexion and peak knee flexion compared to the youngest runners for both JOG ($p < .001$) and MAX ($p < .001$) speeds.

These results are consistent with literature reporting decreased ankle and knee joint excursion in aging runners, with no significant change in hip excursion [1-4]. Devita et al [1] predict an 11% decrease in peak knee flexion between a 20 and 60 year old runner, based on a sample of mixed-sex participants. In our sample of female participants, there was a 28.3% (JOG) and 28.7% (MAX) decrease in peak knee flexion between the youngest and oldest runners, suggesting that female runners may experience a more dramatic decrease in peak knee angles during running with age. Although kinetics were not measured in this study, decreased joint excursion suggests a decreased range in which power can be generated [2], and aging runners demonstrate decreased peak ankle and knee positive work [3]. Decreased joint excursion, along with decreased muscle strength and power that postmenopausal women demonstrate, may negatively affect running biomechanics in the older female runner.

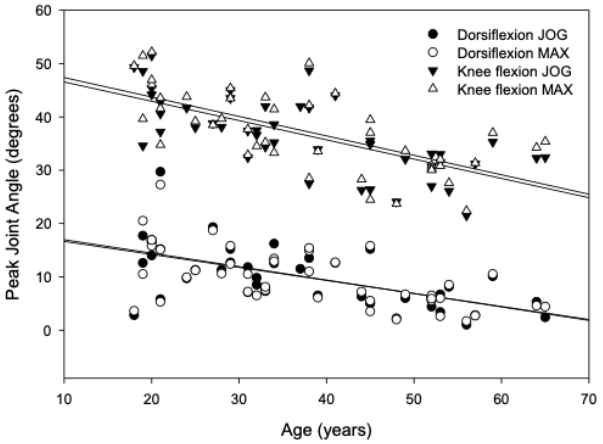

Figure 1. Relationship between age and peak dorsiflexion and knee flexion.

Significance

Older runners, and particularly female runners over the age of 50, are at risk for running-related injury (RRI) [6,7]. Female runners face unique physiological changes during the aging process due to the effects of menopause, and it is therefore important to study the effects of age specifically in this population. Results suggest that training targeting improved distal joint excursion, and subsequently joint power, may be beneficial for aging runners. Further exploration is needed to understand the relationship between running biomechanics and RRI in aging runners, specifically in the master female runner.

References

1. Devita et al. (2016). *Med Sci Sports Exerc*, **48**: 98-106.
2. Bus. (2003). *Med Sci Sports Exerc*, **35**: 1167-1175.
3. Fukuchi RK et al. (2014). *Clin Biomech*, **29**: 304-310.
4. Fukuchi RK and Duarte M (2008). *J Sports Sci*, **26**: 1447-1454.
5. Bondarev et al. (2018). *Menopause*, **25**: 1432-1441.
6. Nielsen et al. (2013). *Orthop J Sports Med,* **1**: 1-7.
7. Taunton et al. (2003). *Br J Sports Med*, **37**: 239-244.

Table 1: Linear regression results for relationship between age and kinematic variables for JOG and MAX speeds. IC = initial contact, TO = toe-off. * denotes $p < .05$.

	JOG		MAX	
	Mean (SD)	R^2(p-value)	Mean (SD)	R^2(p-value)
Peak dorsiflexion (º)	10.1 (5.7)	.46 (< .001)*	9.91 (5.6)	.36 (< .001)*
Peak knee flexion (º)	36.6 (7.1)	.48 (< .001)*	37.3 (7.5)	.46 (< .001)*
Hip flexion IC (º)	31.9 (8.2)	.001 (.980)	33.9 (9.2)	.002 (.962)
Hip extension TO (º)	5.8 (7.9)	.11 (.084)	7.8 (8.4)	.01 (.777)

DIRECTION DEPENDENT FAILURE STRENGTH OF THE PORCINE THORACIC AORTA

Manoj Myneni[1*], Raghuveer L. Sridhar[1], K. R. Rajagopal[1], and Chandler C. Benjamin[1]
[1]Department of Mechanical Engineering, Texas A&M University, College Station, TX, USA
email: *manojmyneni@tamu.edu

Introduction

Aorta is a mixture of cells, elastin, collagen, GAGs, water, and several chemicals. It also contains small blood vessels called vasa vasorum. The aorta is inelastic, anisotropic, and inhomogeneous. It responds to external stimuli by modifying its microstructure through continuous addition and removal of its constituents. Yet it is often modelled as an elastic and homogeneous body, and is generally regarded to have an orthotropic material symmetry with respect to the circumferential-axial-radial planes [1] (Note: Refer to [2] for a review of the inadequacies of existing constitutive models, almost all of which assume artery as an elastic solid). Owing to this assumption, most studies in literature restrict their testing, although inadequate, to the specimens oriented along the circumferential and the axial directions [3]. Studying the rupture of the aorta in a diseased state like an aneurysm or a dissection requires the knowledge of the failure properties, not just in the circumferential and the axial directions. Even the constitutive models (and the failure criteria) that are intended to represent failure under controlled testing conditions require the evaluation of failure properties in multiple directions and should have the ability to replicate these experimental results.

Methods

Fresh porcine aortas (n=10) were collected from the Rosenthal meat center on the Texas A&M University campus. Connective tissue was carefully removed using forceps and a scalpel. The segment of the aorta between the end of the aortic arch and the third branching arteries was separated and stored in 0.01M Phosphate Buffer Saline (PBS) solution at -20ºC. Before the day of the experiments, the aortas were thawed overnight. The aorta was cut open longitudinally and dumbbell-shaped specimens (Total length ~30mm, gauge length ~10mm, gauge width ~3mm, width of the wider portion of the specimen ~6mm) were punched out at 0º, 30º, 45º, 60º, 90º with respect to the circumferential direction. Images of the specimens were taken to measure the width and the thickness of the specimens. A preload less than 0.05N was applied to straighten the specimens. Eight preconditioning cycles were applied by stretching the specimen to a nominal stretch of 1.5 at a stretch rate of 2% s^{-1}. Following these preconditioning cycles, the specimen was stretched until failure (complete tearing) at 2% s^{-1} stretch rate. Images of the sample taken during the experiment were used to perform DIC analysis using Ncorr [4]. The average Green strain (**E**) is calculated over a 1.5mm x 1.5mm region near the center of the specimen. The load is divided by the area of the specimen to obtain nominal stress.

Results and Discussion

Figure 1a shows the variation of nominal stress with nominal stretch for 45º specimens. Specimens from remaining angles show a similar characteristic response with a softer response at smaller stretch values and a stiffer response at larger nominal stretches. Figures 1b, 1c show the variation of E_{xx} vs. nominal stretch, and E_{xy} vs. E_{xx} for 45º specimens. E_{xy} vs. E_{xx} shows a crescent-shaped response with the slope change around an E_{xx} of 0.5, indicating the effect of straightening of the collagen fibers as the specimen is stretched. Figure 1d shows a 45º specimen after failure, with the failure surface oriented at an angle to the direction along which the specimen is uniaxially stretched. Table 1 shows the nominal stress before failure for different directions with the highest strength along the circumferential direction and the least along the axial direction.

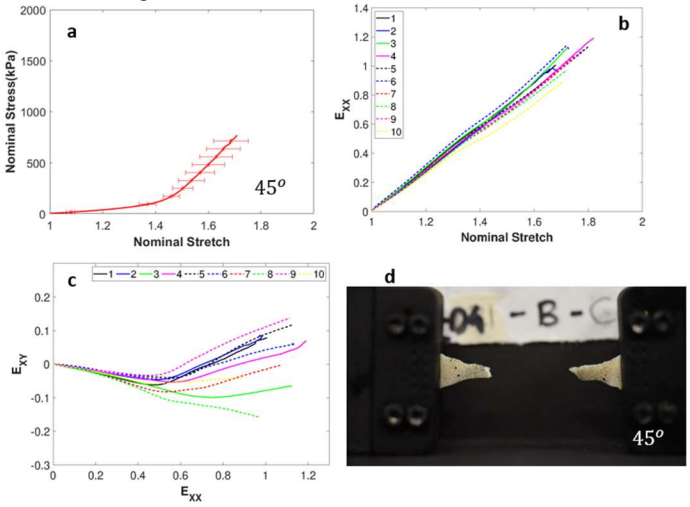

Figure 1: (a) Mean nominal stress vs. nominal stretch for 45º specimens (95% confidence intervals shown using error bars), (b) Exx vs. nominal stretch (c) Exy vs. Exx, (d) A 45º specimen after failure.

Table 1: Failure stress in different directions.

Measured in MPa	0º	30º	45º	60º	90º
Mean failure stress	2.34	1.51	1.04	0.86	0.73
Standard deviation	0.40	0.23	0.16	0.17	0.15

Significance

Very few of the previous studies ([5], [6]) examine the failure characteristics of the aorta along non-circumferential and non-axial directions. Even these studies are limited in terms of either the number of specimens they examined or incomplete deformation measurement (E_{xy}, E_{yy} not measured). Results presented here provide more comprehensive information than previous studies regarding the deformation the specimens experience during a uniaxial test to failure, and will aid the development (or evaluation) of a failure criterion for the aorta.

Acknowledgments

We would like to thank Dr. Michael Moreno[1], for providing the lab facilities to conduct the experiments.

References

[1] Chuong et al. (1986). *J. Biomech. Eng.* **108(2)**: 189-192.
[2] Rajagopal et al. (2020). Aorta, **8**(4): 91–97.
[3] Teng et al. (1986). *J. Biomech. Eng.* **43(11)**: 189-192.
[4] Blaber et al. (2015). *Exp. Mech.* **55**: 1105-1122.
[5] Korenczuk et al. (2017). *J. Biomech. Eng.* **139(7)**: 071008.
[6] Liu et al. (2020). *J. Biomech. Eng.* **142(11)**: 111002

SPRINTING WITH PROSTHETIC VERSUS BIOLOGICAL LEGS: AN UNFAIR ADVANTAGE?

Owen N. Beck[1*], Paolo Taboga[2], & Alena M. Grabowski[3,4]
[1]Schools of Mechanical Engineering & Biological Sciences, Georgia Institute of Technology, Atlanta, GA
[2]Dept. of Kinesiology, California State University, Sacramento, CA
[3]Dept. of Integrative Physiology, University of Colorado, Boulder, CO
[4]Dept. of Veterans Affairs, Eastern Colorado Healthcare System, Denver, CO
Email: *obeck3@gatech.edu

Introduction

Exceptional athletes with bilateral prosthetic legs have run 400m faster than the Olympic track and field qualifying standard. Yet, the potential for these athletes to race alongside non-amputee Olympians has been stifled by policymakers who assume that running-prostheses provide users an overall advantage versus non-amputees. This assumption has not been well-informed by the scientific literature, as there is no consensus regarding the *net effect* of running with prosthetic versus biological legs. Accordingly, we sought to determine whether athletes with bilateral prosthetic legs have inherent advantages versus non-amputees during 400m races by comparing athlete 400m performance metrics: initial race acceleration, maximum straightaway velocity, maximum curve running velocity, velocity at aerobic capacity ($v\dot{V}o_{2max}$), and sprint endurance. We reasoned that if an athlete with prosthetic legs exhibits a superior 400m performance metric to that achieved by elite non-amputees, prosthetic legs likely confer specific advantages to their users versus athletes with biological legs.

Methods

We quantified 400m performance metrics from the fastest male athlete with bilateral prosthetic legs following his competitive season where he ran a season best 400m time of 44.42 s. We compared the respective athlete's 400m performance metrics to those of other athletes with bilateral leg amputations using running-prostheses, including the 2nd fastest such 400m athlete in history [1]. Subsequently, we compared the value of the best 400m performance metric achieved across all athletes with prosthetic legs to those of non-amputees. Statistically, we deemed there to be differences in a 400m performance metric if an athlete with prosthetic legs achieved a value outside the non-amputee range, and/or when our statistical tests revealed ≥95% confidence that their best 400m performance metric was different from the average of the non-amputee cohort ($p<0.05$).

Results and Discussion

The fastest initial acceleration out of the starting blocks through 20m from an athlete with prosthetic legs was 40% slower (>59 SDs) than the average of elite non-amputees (Fig. 1A) [2]. Mechanistically, the athlete with prosthetic legs had slower 20m performance than elite non-amputees due to 31% lower mass-specific horizontal ground reaction force, which resulted in a 32% slower horizontal velocity exiting the starting blocks compared to elite non-amputees [2]. The fastest treadmill-running velocity achieved by an athlete with prosthetic legs (11.4 m/s) was similar to, but not faster than that achieved by a non-amputee athlete (11.72 m/s). Notably, at a mutual running velocity (10 m/s), the fastest athlete with prosthetic legs exhibited similar ground reaction forces and stride kinematics as non-amputees (<8% and <2 SDs) [1]. Further, the maximum running velocity of the fastest athlete with prosthetic legs was 6% slower on a regulation outdoor track curve radius (lane 1) than on a straightaway, whereas the maximum velocity of non-amputees is 3-4.7% slower on a similar curve radius compared to a straightaway [3]. The fastest $v\dot{V}o_{2max}$ from an athlete with prosthetic legs (5.0 m/s) is nearly identical to that of non-amputee athletes (400m personal record (PR): ≤48.03 s; Avg $v\dot{V}o_{2max}$: 4.9 m/s) [1] and 19% (>3 SDs) slower than that of non-amputee distance-runners (10km PR: <32 min) [4]. Additionally, the lowest metabolic cost of transport recorded from an athlete with prosthetic legs (160 ml o_2/kg/km) was 19% better (>8 SDs) and non-different (<1 SD) from non-amputee 400m athletes and distance-runners, respectively [5]. Lastly, the sprint endurance profiles of the two fastest athletes with prosthetic legs were both similar to those of non-amputees (<3% & <1 SD; Fig. 1B) [1].

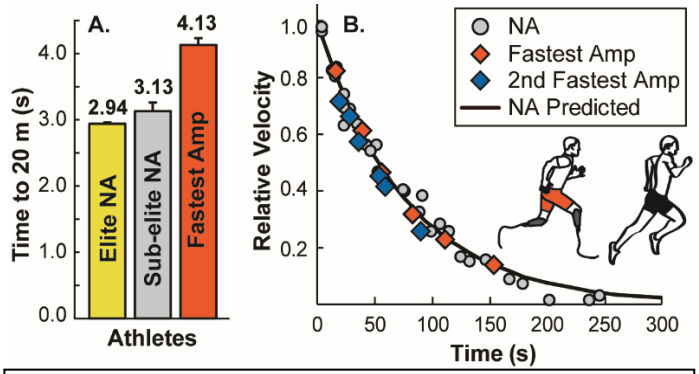

Figure 1. **A.** Avg ± SD time to sprint from the starting blocks to 20m for elite non-amputees (NA) [1], sub-elite NA [1], and the fastest athlete with prosthetic legs (AMP). **B.** The time that NA [1] and two fastest AMP athletes could sustain a treadmill running velocity relative to their maximum velocity and $v\dot{V}o_{2max}$ [1].

Significance

Currently, no athlete with bilateral leg amputations using running-prostheses, including the fastest such athletes, has ever been reported to have a lab-tested 400m performance metric superior to that achieved by non-amputees. We acknowledge that it is uncertain exactly how fast an athlete with prosthetic legs could run 400m if they were a non-amputee athlete with biological legs using footwear (or vice-versa). Nonetheless, based on all the available empirical data, athletes with bilateral leg amputations using passive running-prostheses cannot be unequivocally considered to have an advantage over non-amputee athletes during 400m competitions.

References

1. Weyand et al. (2009). *J Appl Physiol* **107**: 903-11.
2. Rabita et al. (2015). *Scand J Med Sci Sports* **25**: 583-94.
3. Churchill et al. (2015) *Sports Biomech* **14**: 106-12.
4. Kipp et al. (2018) *J Exp Biol* **221**: jeb184218.
5. Svedenhag & Sjödin (1984) *Int J Sports Med* **5**: 255-61.

COMPARISON OF JOINT ANGLES DERIVED FROM MARKERS AND IMUS USING OPENSIM

Jocelyn F. Hafer[1], Andrew J. Hunt[1], Julien A. Mihy[1], and Russell T. Johnson[2]
[1]University of Delaware, [2]University of Southern California
email: jfhafer@udel.edu

Introduction

Gait analysis is a useful tool for examining the mechanisms that contribute to musculoskeletal impairments such as knee osteoarthritis. Short, intermittent (or once-in-a-lifetime) lab-based gait analyses may not fully describe the impact of long-term, daily gait on knee osteoarthritis incidence and progression because in-lab gait may not accurately reflect the gait patterns of life outside of a lab [1,2]. Advances in inertial measurement units (IMUs) enable the collection of movement data outside of a lab. However, the calculation of familiar, anatomically referenced biomechanical outcomes remains challenging.

Combining IMU data with common musculoskeletal modeling techniques that constrain degrees of freedom between body segments may ease the estimation of gait biomechanics with IMUs. Musculoskeletal modeling in combination with predictive optimization may also provide a pipeline for estimating joint kinetics from purely kinematic IMU data. The validity of kinetics estimated via predictive optimization will critically depend on reliable kinematics. Thus, as a first step towards estimating joint kinetics using IMU data and predictive optimization, we sought to evaluate joint kinematics calculated using IMU data and publicly available software. In this preliminary work our aim was to determine whether sagittal hip, knee, and ankle angles differed when estimated using IMU- or marker-derived data. Because our long-term goal is to use these methods to study knee osteoarthritis progression, we also aimed to determine whether the estimation of kinematics using IMUs or markers differed between young adults, older asymptomatic adults, and older adults with knee osteoarthritis.

Methods

We used a unilateral standard 6DOF lower extremity marker set and IMUs (Opal v2, APDM Inc) placed on the pelvis and one thigh, shank, and foot. The participants in the current analyses include 6 young adults (26±4 years, 3 female), 4 older adults (72±3 years, 2 female), and 4 older adults with knee osteoarthritis (71±6 years, 2 female). For each participant's marker data, we scaled the gait2354 model using a static trial in OpenSim [3]. For each participant's IMU data, we used a static frame of data from the start of each walking trial to align virtual IMU axes to the axes of body segments in the gait2354 model using OpenSim OpenSense algorithms. These algorithms align IMU data to anatomical axes assuming a known posture. For both marker and IMU data, we then used the OpenSim inverse kinematics tool to estimate lower extremity kinematics for each stride of data.

We compared sagittal hip, knee, and ankle angles between marker and IMU data and between groups using a continuous 2-way repeated measures ANOVA (statistical parametric mapping). This is a secondary analysis of a larger study [4].

Results and Discussion

There were significant differences between IMU- and marker-derived knee and ankle angles (Figure 1) but no significant differences in hip angles, significant interactions between tool (IMU v marker) and group or significant main differences between groups. Ankle angles estimated with IMUs were significantly more plantar flexed than those estimated from marker data from 25-95% of the gait cycle ($p<0.001$). Knee angle estimated with IMUs was significantly more extended than those estimated from marker data from 8-27 and 57-88% of the gait cycle (both $p<0.001$).

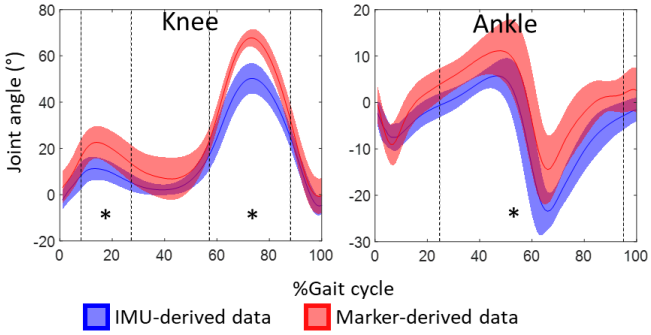

Figure 1. Average sagittal knee and ankle angles (with shaded SD). Positive angles are flexion for knee, dorsiflexion for ankle. * between vertical dashed lines indicate regions where angles were significantly different between IMU and marker data.

While IMU-derived joint kinematics replicate the overall shape of marker-derived kinematics, knee and ankle angles were 5-17° different on average during large portions of the gait cycle. These differences are likely largely due to a mismatch between assumed and actual alignment of IMUs relative to anatomical reference frames. The extent of these tool-based kinematic differences on predicted kinetics remains to be seen.

The differences found in knee and ankle angles in this study are likely a result of differences between the alignment of the IMU sensor axes and body segment anatomical axes. The current approach assumes alignment between sensor and body axes, and differences in assumed alignment could contribute to an offset in angles, among other errors. Our results indicate that additional calibration data, such as the joint angles of the calibration posture, may be needed to obtain realistic knee and ankle angles.

Significance

Despite significant differences in knee and ankle kinematics, inverse kinematics derived from IMU data using OpenSense may still be able to identify important between-group differences in kinematics. Including all participants from our original study (where between-group differences were found [4]) will allow us to verify whether IMU-derived kinematics detect group differences. If our preliminary findings are supported, OpenSense may be an accessible tool for studying between-group differences in joint kinematics using IMU data.

Acknowledgments

Data were collected at the University of Michigan.

References

1. Foucher et al., *Arch Phys Med Rehabil* 2010; 91(9):1390
2. Carcreff et al., *Sci Rep* 2020; 10(1):2091
3. Seth et al., *PLoS Comput Biol.* 2018;14(7)
4. Hafer et al., *J Biomech* 2020; 99:109567

WEEKLY EXERCISE AMOUNT AFFECTS GAIT ADAPTATION IN HEALTHY YOUNG ADULTS

Sarah A. Brinkerhoff[1], Natalia Sánchez[2], and Jaimie A. Roper[1]
[1]Auburn University, Auburn, AL, USA
[2]University of Southern California, Los Angeles, CA, USA
email: sbrinkerhoff@auburn.edu

Introduction

The American College of Sports Medicine recommends at least 150 minutes/week of exercise, based on the numerous health benefits of regular physical activity (1). While many benefits of exercise are understood, it is currently unknown if the recommended weekly exercise amount affects people's ability to adjust their movements to meet the demands of different environments. The purpose of this study was to determine the effect of the recommended weekly amount of exercise on gait adaptation in healthy young adults. We hypothesized that the active young adults would adapt to the perturbation of the split-belt treadmill faster compared to sedentary young adults.

Methods

Gait adaptation is typically studied on a split-belt treadmill and can be quantified by step length asymmetry (SLA). Thirty-three young adults walked on a split-belt treadmill with the belt speeds at a 2:1 ratio for ten minutes. Participants filled out surveys on their exercise activity over the past three months and were grouped by Sedentary (less than 150 minutes/week exercise) or Active (at least 150 minutes/week exercise). Exercise modalities in this sample were: running, cycling, swimming, dancing, tennis, and basketball.

In typical healthy populations, we expect a large SLA that initially adjusts quickly and then plateaus over time. Because of the exponential shape of SLA data, we fit two nonlinear mixed effect models to the data. Recent split-belt work provides evidence for a two-exponent model (2-5) (figure 1). The two models were: 1) two-exponent model without a fixed effect of group, allowing random effects of SLA plateau for individual participants, and 2) two-exponent model with a fixed effect of group, allowing random effects of SLA plateau for individual participants. Statistical differences in the mixed effects models were compared by AIC difference (a lower AIC is a better fit of the data), weight of evidence (probability being best-fitting model), and the evidence ratio (odds ratio between the best-fitting model and other models).

$$SLA = c + a_f * e^{-step*r_f} + a_s * e^{-step*r_s}$$

Figure 1. Equation for the two-exponent model, where c is the SLA plateau, a_f and a_s are the fast- and slow-adapting curve intercepts, and r_f and r_s are the fast- and slow-adapting curve growth rates, respectively.

Results and Discussion

Weekly exercise ranged from 0 to 750 minutes, with a mean (SD) of 180 (169) minutes. The Sedentary group exercised for 38 (44) [range: 0-120] minutes/week, and the Active group exercised for 268 (152) [range: 150-750] minutes/week.

Model 2, the two-exponent model with a fixed effect of group, best estimated SLA adaptation compared the two-exponent model without an effect of group (AIC difference = 720.08; weight of evidence = 1.0 probability; evidence ratio = 1:2.3×10^{156} odds). Initial SLA for the slow-adapting curve, a_s, was significantly more negative for Active young adults, and the growth rate for the fast-adapting curve was significantly higher for Active young adults. This resulted in differences in the overall two-exponent curve (figure 2). Specifically, Active young adults finish the steep, early portion of SLA adaptation by 40 steps, whereas Sedentary young adults require 100 steps.

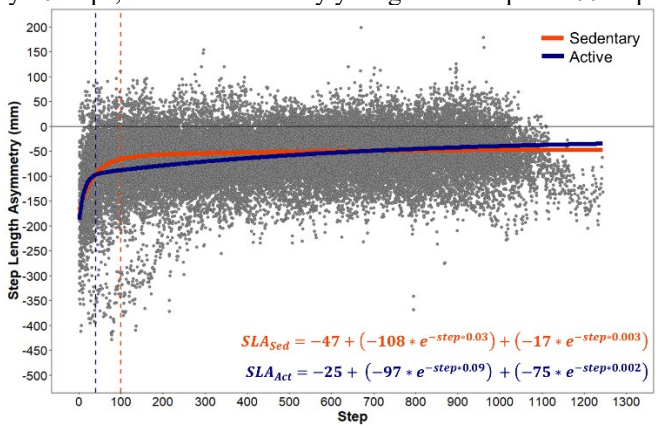

Figure 2: The SLA curves estimated by model 2. The orange curve indicates the Sedentary group and blue curve indicates the Active group. The vertical dashed lines indicate the step at which the fast-adapting curve plateaued, for each group. The equations are those for the two-exponent curves for each group.

Significance

Exercise of at least 150 minutes/week has resounding multi-system benefits. The results of this study provide further evidence of the benefits of exercise, specifically during a response to sustained gait perturbations. Our findings show that individual differences in activity influence adaptation to perturbations. Quicker responses are advantageous to respond to real-world perturbations like terrain change or unstable surfaces. Therefore, being active may help populations with mobility disabilities more quickly respond to real-world perturbations.

Acknowledgments

This study was funded by an Auburn University seed grant. SAB is funded by an AU Presidential Graduate Research Fellowship.

References

1. Piercy, et. al., 2018, *JAMA*
2. Sánchez et al., 2021, *J Neurophysiol*
3. Darmohray et. al., 2019, *Neuron*
4. Mawase et. al., 2013, *J Neurophysiol*
5. Roemmich et. al., 2016, *Curr Biol*

WALKING SPEED IS MORE STRONGLY ASSOCIATED WITH KNEE RATE OF MOMENT DEVELOPMENT IN THE UNINVOLVED THAN THE INVOLVED KNEE AFTER ANTERIOR CRUCIATE LIGAMEN RECONSTRUCTION

Naoaki Ito[1], Elanna K. Arhos[1], Jacob J. Capin[2], Sarah E. Hall[1], Thomas S. Buchanan[1], Lynn Snyder-Mackler[1]
[1]University of Delaware, Newark, DE [2]University of Colorado Anschutz Medical Campus, Aurora, CO
email: nito@udel.edu

Introduction

Patients after anterior cruciate ligament reconstruction (ACLR) walk with aberrant gait mechanics.[1,2] Manipulating gait speeds may be one approach to improve sagittal plane gait mechanics[3], and prevent the onset of post-traumatic knee osteoarthritis (OA).[4,5] Faster walking is associated with higher peak external knee flexion moments[3], but this association is not as strong after ACLR[6]. Quantifying the rate at which the knees are loaded during gait may assist in understanding the underlying mechanism behind altered peak knee moments. The sagittal plane knee rate of moment development (RMD) during gait in comparison to gait speeds, however, has not been studied. The purpose of this study was to establish the relationship between gait speed and RMD during the weight-acceptance phase of gait in the involved and uninvolved knees of athletes six months after ACLR.

Methods

Sixty-nine athletes (Sex: 32 Women / 37 Men, Age: 22.1 ± 7.9 years, BMI: 26.1 ± 3.2 Kg/m^2) 5.6 ± 1.9 months after ACLR walked overground in a motion capture setting at self-selected speeds (1.5 ± 0.1 m/s). Kinetics were derived via inverse dynamics and normalized to body mass and height. The time of peak knee flexion moment from initial contact was established, and the mean rate of moment development (or the slope of the knee moment curve against time, Nm/Kg/s) during the last 50 milliseconds (ms), and between 50 to 100ms prior to peak knee flexion moment were calculated and reported as RMD_{50ms} and RMD_{100ms}. Peak instantaneous RMD between initial contact and peak knee flexion moment were also calculated (RMD_{peak}). Simple linear regressions ($\alpha = 0.05$) were performed between gait speed and the three variables of interest in both the involved and uninvolved knees.

Results and Discussion

Walking speed was positively associated with RMD_{peak} and RMD_{50ms} in both knees (**Figures 1 and 2**). RMD_{100ms} was positively associated with gait speed in the uninvolved knees ($p < 0.001$*, $R^2 = 0.197$) but not in the involved knees ($p = 0.057$, $R^2 = 0.053$). All associations were weaker in the involved compared to uninvolved knees.

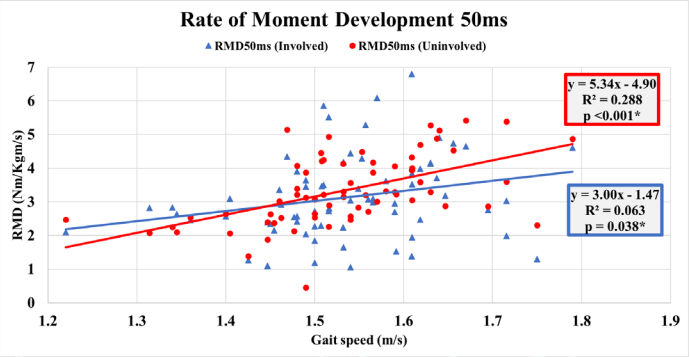

Figure 1. Walking speed was positively associated with RMD_{50ms} in both knees. The association was weaker in the involved ($R^2 = 0.063$) versus uninvolved ($R^2 = 0.288$) knees.

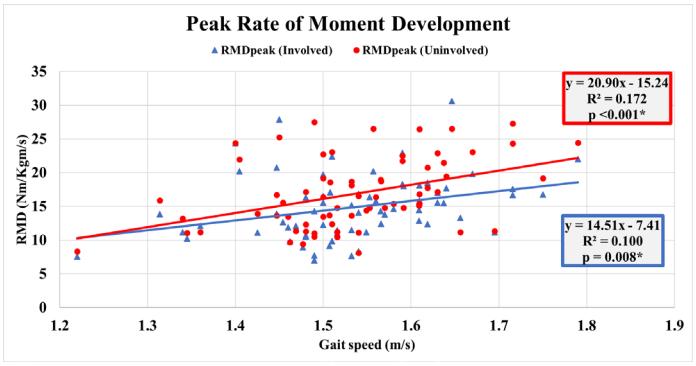

Figure 2. Walking speed was positively associated with RMD_{peak} in both knees. The association was weaker in the involved ($R^2 = 0.100$) versus uninvolved ($R^2 = 0.172$) knees.

Athletes who walked faster also walked with faster RMD in both knees during the weight-acceptance phase of gait six months after ACLR. The association between gait speed and RMD, however, was weaker in the involved knees compared to the uninvolved knees during all three time-intervals. The differences in these associations between involved and uninvolved knees were largest immediately before reaching peak knee flexion moment (**Figure 1**), and most similar between knees early after initial contact (**Figure 2**). These findings may be due to fear avoidance behaviors or learned non-use[7] demonstrated near peak knee flexion moment to avoid fully loading the knee.[8] Conversely, immediately after initial contact, the RMD may reflect a more implicit portion of the gait cycle with less volitional control. This evidence suggests that neuromuscular adaptations may depend on time and phase of gait, and therefore may require different approaches to address following ACLR. While our current literature on gait mechanics and OA following ACLR focuses primarily on the peak magnitude of kinetics and kinematics, the mechanics surrounding these peaks may also have to be considered. The RMD metrics introduced in this study are parameters that are unique to specific intervals during the early phases of gait, and may be targeted in future interventions addressing aberrant gait mechanics after ACLR.

Significance

Altering gait speed alone may not be sufficient as an intervention targeting aberrant gait mechanics after ACLR as there may be a differential effect of speed on the two limbs. RMD during different time-intervals early in stance may have to be considered for targeting gait interventions after ACLR.

Acknowledgments

This work was funded by NIH R37-HD037985, R01-AR048212, R01-HD087459, F30-HD096830, F32-AG066274, P30-GM103333, and U54-GM104941.

References

1. Slater et al., JAT, 2017 2. Kaur et al., Sport Med, 2016 3. Lelas et al., Gait Posture, 2003 4. Khandha et al., JOR, 2017 5. Capin et al., JOR, 2020 6. Knobel et al., IJSPT, 2020 7. Chan et al., MSSE, 2019 8. Zarzycki et al., JOSPT, 2018

THE EFFECT OF A HIGH INTENSITY RUN TO VOLITIONAL FATIGUE ON DROP JUMP PERFORMANCE

Caden Gatlin[1], Nickolai J. P. Martonick[1], Lukas Krumpl[1], Youngmin Chun[1], and Joshua P. Bailey[1]
Department of Movement Sciences, University of Idaho, Moscow, ID, USA
Email: *gatl8917@vandals.uidaho.edu

Introduction

The effect of fatigue elicited from running on factors of jumping performance is currently not well understood. Recently, researchers have demonstrated the potential to improve acute counter movement jump (CMJ) performance following running fatigue protocols through a post activation potentiation (PAP) mechanism [2,4]. The PAP effect is defined as an acute enhancement of muscular performance following maximal or submaximal muscle stimulus [3]. It is thought that eccentric actions activate the elastic components through the stretch shortening cycle and increase passive force production in subsequent actions [1,3]. Although researchers have shown acute enhancements in CMJ performance following running fatigue protocols [2,4], it is not known whether the PAP mechanism might modify performance factors related to a drop jump (DJ). Therefore, we investigated whether factors of jump performance (i.e. jump height [JH], vertical impulse [VI], foot contact time [FCT], amortization time [AmT], and vertical stiffness [VS]) were modified following a running fatigue protocol. We hypothesized that increased potentiation of eccentric muscle action would maintain, or elevate JH, VI, and VS while reducing or maintaining FCT and AmT.

Methods

Twelve recreational runners who reported running at least 5 miles per week (age = 36.3 ± 13.9, ht = 1.72 ± 1.04m, mass = 67.5kg ± 8.2) Participants were asked to perform a standardized 5-minute warmup on the treadmill at a self-determined speed prior to collecting their baseline jumping data. Five DJs were then performed from a box (height = 30 cm) placed half of the participant's leg length from the center of the force platforms (AMTI) and recorded with 3d motion capture (Vicon) at 250 Hz. Upon landing, participants were instructed to jump as quickly and as high as possible. Following baseline DJs participants performed a run to exhaustion at their pre-identified speed at 90% ventilatory threshold (3.62 ± 0.64 m/s, 19.6 ± 6.5 min). This was determined during a graded exercise test session at least 24 hours prior. Within two minutes of finishing their run, participants performed five additional successful DJs. The FCT was identified using a 20N threshold for vertical ground reaction force (VGRF) data from initial contact (IC) to TO. The participant's JH was defined as the difference between height of the COM at toe off (TO) and the peak height of the COM. To identify VI, we normalized the peak VGRF to body weight (BW) and calculated the area under the curve relative to COM displacement. We defined the AmT as the time at which COM position was within 1cm of the local minimum. Vertical stiffness was calculated using peak VGRF ($VGRF/BW \cdot \Delta COM$). Pre and post measures were compared with paired t-tests. Cohen's *d* was also calculated.

Results and Discussion

The results of the present study indicate no significant changes for DJ performance between the pre- and post-treadmill run. Additionally, no significant differences were found pre- and post-run in JH, VS, AmT, FCT, and VI (Table 1).

Table 1. Drop Jump Performance Metrics (Means ± SD)

Variable	Pre-Run	Post-Run	P-value	ES
JH	28.6 ± 1.2	27.8 ± 0.8	0.71	0.11
VS	12.7 ± 4.4	12.5 ± 3.5	0.92	0.03
AmT	0.10 ± 0.03	0.11 ± 0.04	0.29	0.33
FCT	0.61 ± 0.12	0.62 ± 0.15	0.84	0.06
VI	186.7 ± 33.4	187.7 ± 34.1	0.89	0.04

*Note. JH = Jump Height (cm), VS = Vertical Stiffness (BW/m), AmT = Amortization time (s), FCT = Foot Contact Time (s), VI = Vertical Impulse (N*s), ES = Effect Size (Cohen's d)*

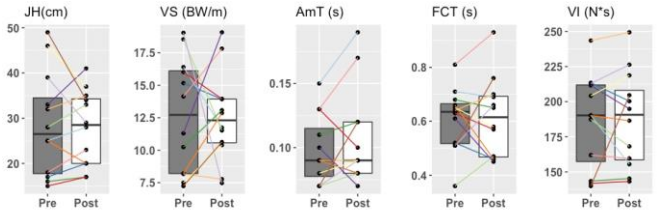

Figure 1: Box plots with medians and upper/lower quartiles are presented for each variable. Individual responses are represented by a line with a specific color connecting their data points.

Based on the results of our study, we may accept part of our hypothesis. While we did not see significant increase in performance, runners maintained pre-exhaustion levels. However, we may not have seen an increase in JH because our protocol was not task specific enough (i.e. running vs. bipedal jumping), was performed below maximum running velocity, or recreational runners do not receive maximal benefits from PAP. For example, Hughes et al. [1], demonstrated CMJ performance can be enhanced by depth drops from a 60cm box. Further, researchers who demonstrated an increase in CMJ height following running protocols either had their participants run at maximum velocity or examined elite runners [1,4]. Thus, we suggest that running velocity, training status, and task specificity plays a role in eliciting the PAP response.

Significance

Although we did not observe a statistical group increase in DJ performance, the majority of our participants increased JH, and few decreased (Figure 1). Future research should examine the biomechanical strategies used by individuals who run to volitional exhaustion and do not see a decrease in JH. Understanding the underlying strategies of runners who increase or maintain JH following a run to volitional exhaustion would provide further evidence for the PAP mechanism.

Acknowledgments

The authors would like to thank Jennifer Sheasley and Christopher Alfiero for their assistance in data collections.

References

1. Hughes et al. (2016). J Str and Cond R, 30(12), 3450-3455
2. Pinillos et al. (2015). Sports Biomechanics, 15(2), 103-115
3. Timon et al. (2019). J Human Kinetics. 69, 271-281
4.Vuorimaa et al. (2006). J App Phys 96, 282-291

EFFECTS OF SENSORY DISRUPTIONS ON RATES OF LOCOMOTOR ADAPTATION

Daniel Kuhman[1], A. Moll[1], N. Rosenblatt[2], and C. Hurt[1]
[1]University of Alabama at Birmingham, Birmingham AL USA
email: *dkuhman@uab.edu

Introduction

Human locomotion often occurs through complex environments involving both internal (e.g., accuracy of visual input) and external (e.g., variation in terrain) constraints. These environments require individuals to accurately sense and appropriately respond to such constraints – a process known as locomotor adaptation. Adaptation is underpinned by processes of the higher central nervous system such as sensorimotor integration [1]. Behavioural probes of adaptation (e.g., split-belt treadmill walking (SBTW)) can therefore provide important information regarding the health of the nervous system. One important feature of sensorimotor integration is the ability to reweight sources of sensory information, placing more importance on reliable input and less importance on unreliable input. We can assess this feature by quantifying the extent to which adaptation is altered when individuals perform a locomotor adaptation task under reliable and unreliable sensory conditions.

The purpose of this study was to assess the effects of reduced visual and proprioceptive feedback on rates of locomotor adaptation to SBTW. We hypothesized that individuals would maintain normal rates of adaptation in sensory disrupted environments via appropriate reweighting of sensory information.

Methods

16 healthy adults (age: 24.4 ± 2.9 years) completed four 8-minute SBTW trials with the following structure: 2-min. tied at 0.7 ms^{-1}, 5-min. split (right: 1 ms^{-1}, left: 0.4 ms^{-1}), 1-min. tied at 0.7 ms^{-1}. Each participant completed the first two trials under normal sensory conditions (Normal 1, Normal 2), a trial with reduced peripheral vision (via visually constricting goggles; Vision), and a trial with reduced proprioception (via 30% bodyweight support; BWS). We enforced ≥ 5-min. of overground walking between trials to limit trial-to-trial "carry-over."

We captured step lengths, defined as the anteroposterior distance between the two heels at foot strike of the leading leg, and calculated step length symmetry (SL_{sym}) throughout each trial:

$$SL_{sym} = \frac{(SL_{fast} - SL_{slow})}{SL_{fast} + SL_{slow}}$$

Where SL_{fast} and SL_{slow} refer to SL calculated when the leading leg is on the faster (right) and slower (left) moving belt, respectively. SL_{sym} during the split phase of each trial was fit with a single exponential function and the time constant (t) was used to quantify adaptation rate (similar to [2]):

$$ae^{(-\frac{x}{t})} + c$$

Adaptation rates were compared across all trial conditions (Normal 1, Normal 2, Vision, BWS) using a one-way repeated measures ANOVA. Statistical significance was determined at $p < 0.05$.

Results and Discussion

In support of our hypothesis, we observed no significant effect of condition on the rate of locomotor adaptation to SBTW ($p = 0.09$).

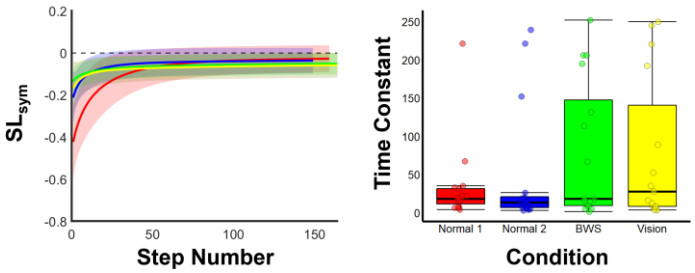

Figure 1: Average exponential model fits (left panel) and time constants (right panel) for each condition. The exponential function was applied to each trial of each participant and the time constant is used to quantify rate of locomotor adaptation. In the left panel, shaded regions represent standard deviation across participant fits in each condition. Results from the repeated measures ANOVA indicated no significant differences in adaptation rates between conditions.

These results suggest that healthy young adults are able to reweight sensory information to maintain locomotor adaptation to SBTW. When peripheral visual feedback was blocked, individuals were able to maintain a normal rate of adaptation, likely by increasing the weight of importance placed on other, more reliable sources of feedback (e.g., proprioception). Similarly, reduced proprioceptive feedback via BWS did not negatively affect adaptation rate, likely because individuals were able to rely more on other sources of feedback (e.g., vision). Qualitatively, there are clear differences in between-subject variation in time constants across conditions (Figure 1, right panel), with much larger variation in the two sensory disrupted trials compared to the two normal trials. A larger sample may be needed to more adequately test our hypothesis.

Significance

Our results support the hypothesis that healthy individuals reweight sensory information to maintain locomotor adaptation during walking, likely due to well-functioning sensorimotor integration. Populations with dysfunctional sensorimotor integration – for example, Parkinson's disease [3] – may be disproportionately more affected by sensory disruptions and would therefore be less able to maintain adaptability. These findings add to our collective understanding of human locomotion – particularly adaptability – and provide a non-invasive experimental framework that can be used to probe processes of the higher central nervous system.

References

1. Torres-Oviedo et al., 2011. *Prog in Brain Research*.
2. Malone et al., 2011. *J Neurosci*.
3. Lewis & Byblow, 2002. *Brai*

Limited Maximum Walking Speed on a Treadmill is related to Dynamic Stability, Balance Confidence, and State anxiety

Jutaluk Kongsuk[1]; Christopher P. Hurt[1]
[1]University of Alabama at Birmingham, Birmingham, AL, U.S.A.
email: jutalukk@uab.edu

Introduction

Walking in the community often requires both a wide range and constant modification of walking speed[1]. Walking at increasing speeds may reflect to human walking behavior. Previously we have used a walking protocol that allowed us to separate older individuals into those completed all walking trials and those that did not[2]. Previous research has shown that dynamic stability, balance confidence, and state anxiety are all factors that relate with a decline in walking speed. The purpose of this study was to investigate whether physical and/or psychological factors result in limiting walking performance using our walking protocol among clinical populations.

Methods

Sixteen young healthy individuals (aged 31±5.85 years), 16 community-dwelling older adults (aged 69±3.10 years), and 10 people with Parkinson's disease (PD) (aged 69±8.83 years) were included. Participants were asked to walk with a range of walking speeds start at 0.4 m/s until they elected to not attempt a fastest speed or they completed the fastest speed at 2.0 m/s[2]. Prior to increasing each treadmill speed, participants were asked if they wanted to attempt a faster speed and to rate their balance confidence (BC) and state anxiety (SA) using a custom scale we have previously validated. These measures provided more dynamic measures compared to the traditional measures. Kinematic data was collected and a measure of gait stability, the margin of stability in the anterior direction at heel strike (MOS_{AP}) was quantified, to assess dynamic stability[3]. Older adults and participants with PD were grouped based on their ability to complete all walking trials. The primary outcomes assessed were MOS_{AP}, BC, and SA at the fastest speed attempted (FSA), and the quantified slope of the line of the last 3 values in MOS_{AP}, BC, and SA. Comparisons between groups were made with One-way Analysis of Variance or Kruskal-Wallis analysis. Correlations between the limited FSA and physical/psychosocial variables were examined with Spearman's rank correlation.

Results and Discussion

Ranges of MOSAP, BC, and SA while performing the scaled treadmill speeds between groups are presented in Figure 1. All young adults completed all trials. Older participants and those with PD were grouped by whether they could (n=11; 66±7.88 years) or could not (n=15, 68±4.67 years) complete all walking trials. Significant differences were detected in the FSA, MOS_{AP} at FSA between non-completers/completers and young controls ($p<0.05$ for all comparisons). A significant difference was detected in the SA between completers and non-completers as well as the slope of the last 3 values of SA ($p=0.005$, and $p=0.014$, respectively). Additionally, significant differences were detected in the slopes of the last 3 values of MOS_{AP} and BC between non-completers/completers and young controls ($p<0.05$). The FSA was significantly correlated with MOS_{AP} (rho=-0.80, $p<0.001$), BC (rho=0.43, $p=0.029$), and SA (rho=-0.55, $p=0.004$), as shown in Figure 2.

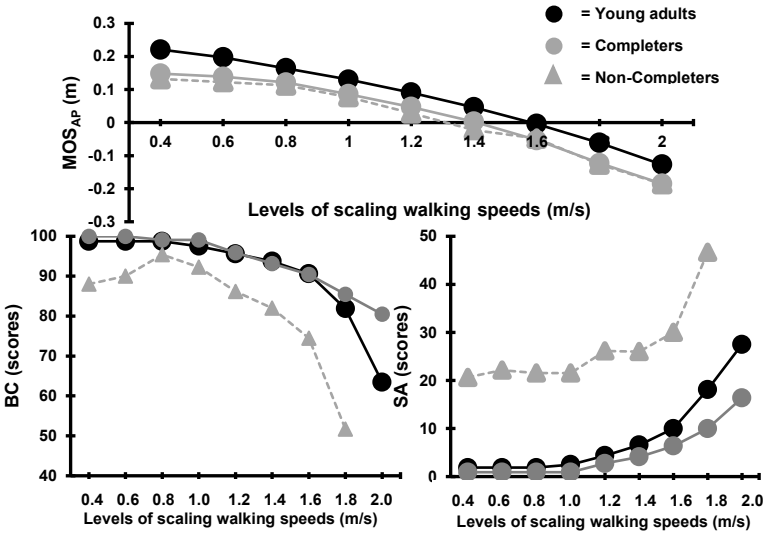

Figure 1: Walking speeds vs a) MOS_{AP} b) BC and c) SA (n= 15 at 0.4 m/s, 14 at 0.6 m/s, 13 at 0.8 m/s, 13 at 1.0 m/s, 13 at 1.2 m/s, 10 at 1.4 m/s, 7 at 1.6 m/s, and 6 at 1.8 m/s for non-completers.

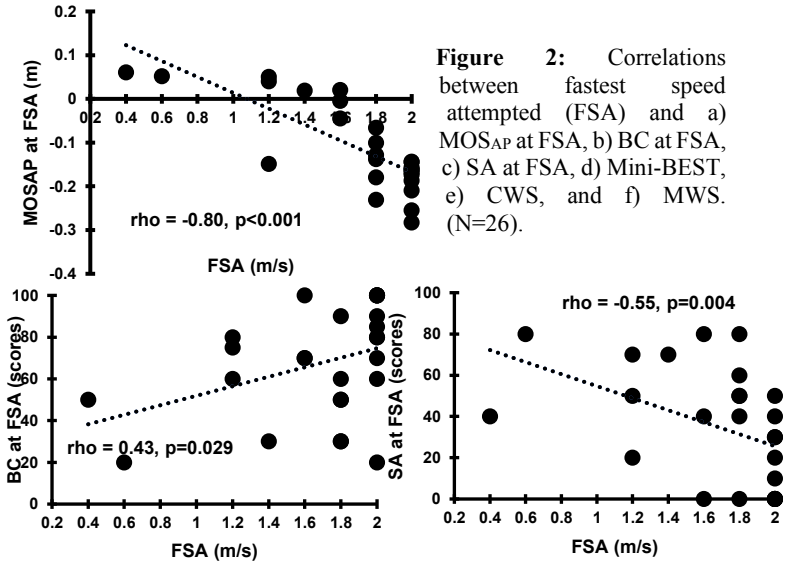

Figure 2: Correlations between fastest speed attempted (FSA) and a) MOS_{AP} at FSA, b) BC at FSA, c) SA at FSA, d) Mini-BEST, e) CWS, and f) MWS. (N=26).

Significance

In this investigation we highlight that individuals were grouped by their ability to complete all walking trials and not by their disease status. This walking protocol can reflect the walking capacity of an individual. Fyrther our study suggestes that evaluations of both physical and psychological factors should be incorporated into assessment of mobility limitation in clinical populations.

References

1. Bohannon RW. Age Ageing. 1997;26(1):15-9. **2.** Kongsuk J, Brown DA, Hurt CP. Gait Posture. 2019;73:86-92. **3.**Hof A, Gazendam MG, Sinke WE. J Biomech. 2005;38:1-8.

THE EFFECTS OF A NEUROMUSCULAR KNEE SLEEVE ON MUSCULOSKELETAL INJURY RISK: A PILOT STUDY

Cody A. Reed[1*], Justin R. Brown[2], and Lisa N. MacFadden[1, 2]
[1]Sanford Orthopedics & Sports Medicine Research, Sanford Health, Sioux Falls, SD
[2]Sanford School of Medicine, University of South Dakota, Vermillion, SD
email: *cody.reed@sanfordhealth.org

Introduction

In the United States, almost 50 million people run on a regular basis. While running is associated with numerous health benefits, up to 70% of runners develop an overuse injury within any 1-year period [1]**.** Novice runners are at a higher risk than experienced runners [2]. Numerous factors have been related to running related injuries (RRIs) including lack of running experience, injury history, training distance, and biomechanical risk factors [3]. A higher rate of loading (ROL) is a specific biomechanical risk factor related to musculoskeletal injury.

The Topical Gear T25 neuromuscular knee sleeve utilizes pressure pads that sit on top of the medial hamstrings and vastus medialis. By adding pressure to these muscles, they aim to promote better neuromuscular control patterns during movement, particularly in novice runners with untrained activation patterns. This study observed the biomechanics of runners wearing the T25 knee sleeve, including ROL and foot-strike patterns.

Methods

Data was collected as part of a product evaluation. The Sanford IRB determined the following analysis is not human subject research. One experienced and two novice runners (83.5 ± 12.3 kg, 1.76 ± 0.16 m, 1 m/2 f) had their running kinetics assessed with and without wearing the T25 knee sleeves. Ground reaction force (GRF) data was recorded using a Bertec instrumented treadmill, and 2-D video was also captured. Participants ran at self-selected speeds for at least 30-seconds at a time. Participants ran at their same speeds for both conditions. ROL was calculated as the slope of the GRF curve between 20% and 80% of the way to impact peak and compared across knee sleeve conditions. ROL was calculated for left and right limbs, individually, and averaged across all strides within a trial. One participant also underwent cadence manipulation. For their self-selected speed of 7.5 mph, the participant ran without wearing the T25 knee sleeves but with 5.6% increased cadence from their preferred cadence. To achieve the increased cadence, the participant was instructed to match each foot-strike to an audible metronome.

Results and Discussion

With the T25 knee sleeves, novice runners demonstrated a reduced ROL across various speeds, while the experienced runner showed no difference (**Figure 1**). Additionally, 2-D video analysis and GRF curves indicated improved foot-strike patterns and reduced impact peaks in one novice runner (**Figure 2**). Without the sleeve, this participant landed with a heel strike, but while wearing the T25 knee sleeve, they demonstrated a midfoot strike. Interestingly, this midfoot strike was also present under cadence manipulation without the T25 knee sleeve. These results demonstrate the potential utility of the T25 knee sleeves as an injury prevention tool. With higher rates of loading linked to increased risk of RRIs, this pilot study sets the groundwork for finding an avenue to protect novice runners [3].

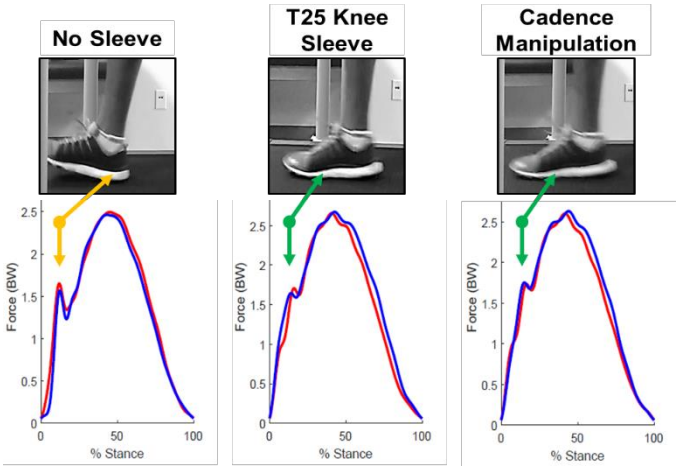

Figure 2: Foot-strike patterns and GRF curves for all conditions.

Significance

This pilot study suggests the T25 knee sleeve can potentially induce neuromuscular patterns to reduce musculoskeletal injury risk. The present gold standard for running injury prevention is training targeted at improving neuromuscular control, which requires professional intervention. This pilot study suggests the T25, a low-cost knee sleeve, may reduce RRIs in novice runners, through changes in ROL and foot-strike patterns. For rural or underprivileged areas, the impact of these sleeves on runner's health could be immeasurable, where access to professional intervention is limited.

Acknowledgments

Steadfast Solutions Inc. for donating the T25 knee sleeves.

References

1. Hreljac, *Med & Science in Sports & Exercise*, 2004, 36(5).
2. Tonoli et al., *Sport en Geneeskunde*, 2010, 43(5).
3. Van Gent et al., *British J Sports Med,* 2007, 41(8).

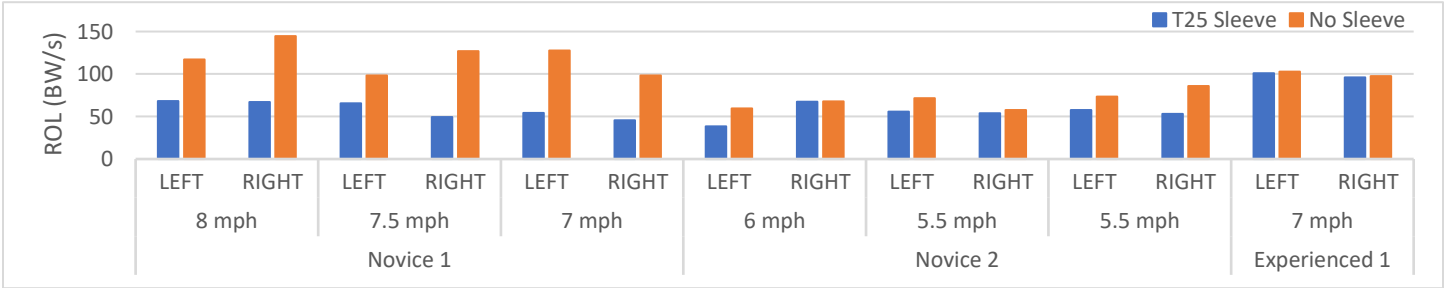

Figure 1: ROL pilot data for each runner at various speeds.

CONTEXTUALIZING WALKING BOUTS IN THE FREE-LIVING ENVIRONMENT

[1]Loubna Baroudi, [1]Xinghui Yan, [1]Mark Newman, [2]Elizabeth Jackson, [1]Kira Barton, [1]K. Alex Shorter, and [1]Stephen M. Cain
[1]University of Michigan, Ann Arbor, MI, USA and [2]University of Alabama, Birmingham, AL, USA
email: lbaroudi@umich.edu

Introduction

Parameters extracted from data collected during walking are often used during clinical assessments to help describe locomotor capacity. In particular, walking speed can be a powerful predictor of overall health [1]. However, walking as assessed in a clinical setting may not be representative of how people move in their daily lives. To address this gap, wearable sensing technologies can be used to complement in-lab assessments to gain new insight into walking in unconstrained environments. These technologies are used during extended periods of persistent monitoring, and often require the identification of walking bouts from a limited set of measurements. Thus, there is often no information on the context in which a walk takes place, limiting the interpretation of the data. In this work, we used an accelerometer-based sensor secured on the thigh to collect multi-week data in the free-living environment. A novel framework was used to identify and cluster walking periods based on duration and continuity. Data from these clusters were then used to investigate how walking speed estimates varied between the clusters.

Methods

We collected 14 days of uninterrupted measurements using a lightweight (20 grams) compact accelerometer (activPAL) secured to the thigh using an adhesive bandage tape from a single participant. Periods of sitting, standing, and stepping (e.g., walking, running) were first identified using the built-in activPAL classification algorithms. A decision tree was created using acceleration features related to gait to isolate walking bouts from data classified as stepping. This method was refined using expertly labeled data points. Then, these ambulatory walking bouts were regrouped into walking periods that contained both bouts of consecutive steps and standing (<1min) between bouts. Periods were bounded by extended standing (>1min) or the transition to another state (e.g., sitting). Within a period, walking was quantified as followed:

$$Walking\ Percentage = \frac{t_p - t_r}{t_p} \quad \text{(Eq. 1)}$$

Where t_p is the period duration and t_r is the total standing time within a period. Walking percentage reflects the continuity of a period, with a low value corresponding to frequent pauses within a walk. We define walking contextualization as the classification of walking periods into distinct modes based on their walking percentage and their duration. Seven modes were identified, using 5 and 10 minutes as the transition times for t_p, and 80% as the transition for t_r. Walking periods that exhibited 100% walking percentage were grouped in a mode as well. Finally, we calculated estimates of stride speed using stride frequency extracted from the activPAL for each walking mode using a subject-specific model [2]. Values were averaged for three consecutive strides to decrease errors.

Results and Discussion

Over 10,000 strides were recorded during 230 periods of walking over the two weeks. Fig. 1-a presents the classification of the periods into seven walking modes. Mode 1 corresponds to short and discontinuous modes of walking, while mode 7 corresponds to long and continuous periods of walking. We observed that 49% of the walking periods belonged to mode 1, which suggests that most of the observed walking was short and punctuated by frequent pauses. For periods longer than 5 minutes, we observed that as the period duration increased, walking percentage also increased. This could indicate that the purpose of the activity is the walk itself (e.g., exercise in the park). Estimates of stride speed for each walking mode were statistically different ($p < 0.01$), and a post-hoc test revealed that estimates of walking speed for mode 1 were significantly lower ($p < 0.05$) than for mode 5, Fig. 1-b. Additionally, mode 5 (n = 858, M = 1.45, SD = 0.08) and mode 7 (n = 1093, M = 1.37, SD = 0.08) contained the largest percentage of total walking steps (21.8% and 27.8% respectively) with the least variability, resulting in more precise estimates of stride speed. Data from these modes were grouped and used to estimate a preferred walking speed of 1.40 ± 4e-2 $m.s^{-1}$. The average walking speed calculated from this subset differed by as much as 0.15 $m.s^{-1}$ from the other modes, highlighting the importance of data selection when calculating this parameter.

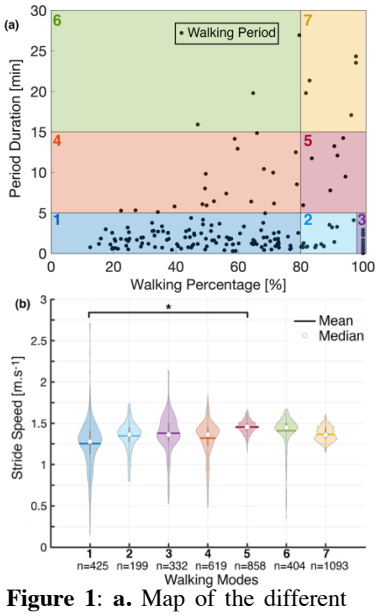

Figure 1: **a.** Map of the different walking modes. Each point represents a walking period, containing several strides. **b.** Distribution of stride speed over the different walking modes. One value of stride speed corresponds to the average of three strides. * $p < 0.05$

Significance

Datasets collected in the real-world enable an investigation into the impact of environmental variability on walking behavior and the development of methods to group data based on context. Here, we present an approach to group data based on walking period characteristics and show that the calculation of a key gait parameter, walking speed, is sensitive to this grouping. Future work to identify what environmental or behavioral factors result in these groupings will be important to better understand how to contextualize free-living walking data [3].

Acknowledgments

This research was funded by the Precision Health Investigators Award of the University of Michigan.

References

1. Fritz S, et al. *J of geriatric physical therapy* 32, p 2-5, 2009
2. Baroudi L, et al. *Frontiers in Sports & Active Living* 2, 2020
3. Montufar J, et al. *Transport. research rec*, no1 90-97, 2007

ANKLE PROPRIOCEPTION CONTRIBUTES TO CONSCIOUS PERCEPTION LOCOMOTOR DISTURBANCES

Daniel J. Liss[1], Jessica L. Allen[1]
[1]West Virginia University, Morgantown, WV
Email: djl0024@mix.wvu.edu

Introduction

We previously found young adults were able to consciously perceive very small slip- and trip-like locomotor disturbances [1]. Which sensory modalities contribute to such precise perception (e.g., visual, vestibular, proprioceptive, and/or somatosensory) remains an open question. As a first step to answering this question, the purpose of this study was to identify perturbation-induced deviations in gait kinematics that could explain the ability of young adults to perceive small locomotor disturbances.

Methods

8 young adults (4M, 22.4±2.6yrs) walked on a split-belt instrumented treadmill (Bertec, Inc.) at self-selected walking speed while experiencing balance disturbances every 8-12 strides. Disturbances were imposed through short duration decreases in treadmill belt velocity (dV) triggered at heel-strike, where dV was 0, 0.02, 0.05, 0.1, 0.15, 0.2, 0.3, 0.4 m/s. Disturbances were randomized and repeated 5 times on the dominant leg with nondominant leg disturbances interspersed to reduce learning effects. After each disturbance, subjects were asked if they perceived a balance disturbance and responded "yes" or "no". Subjects wore noise cancelling headphones to prevent auditory feedback. The conscious perception threshold was determined by fitting a psychometric curve to the proportion correct responses for each dV.

We then analyzed perturbation-induced deviations in head angle (visual analogue), head angular velocity (vestibular analogue), sagittal hip, knee, and ankle angles (proprioceptive analogue), and anterior-posterior center-of-pressure (COP, somatosensation analogue) in response to the two perturbation levels nearest each subject's perception threshold. For each variable, the deviation between the perturbed gait cycle and the five gait cycles immediately preceding the perturbation was calculated as $(x_i - \bar{x}_i)/SD_i$, where i is gait cycle %, x is the perturbed gait cycle, and $\bar{x}$ and SD are the average and standard deviation of the pre-perturbation gait cycles. We then averaged over 20-60% of the gait cycle to estimate mid-to-late stance phase deviations. Because head angle and head angular velocity varied quite substantially even during pre-perturbation steps, we focused our analyses on joint angle and COP deviations.

We first used a rank-sum test to compare the perturbation-induced deviations to determine which variables differed between perceived and non-perceived perturbations, with Bonferroni corrections to account for multiple comparisons (α=0.05/4). We then used logistical mixed effects models to examine the extent to which each perturbation-induced deviation could explain whether a perturbation was perceived. A separate model was created for each variable, with the variable of interest treated as a fixed effect and subject as a random effect.

Results and Discussion

Young adults perceived very small locomotor disturbances of 0.08±0.03 m/s. Ten perturbations were analyzed per subject, with the median number of perceived perturbations across subjects equal to 5 (range: 3-7, avg: 4.8).

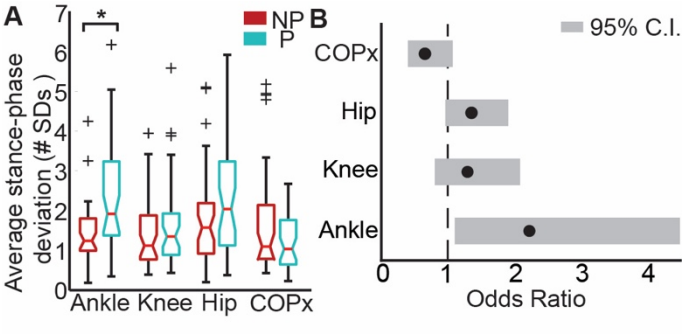

Figure 1: A) Ranked sums test compared perceived (P) to not perceived (NP) disturbances. B) Odds ratio on the ability of each variable to predict whether a disturbance was perceived.

Perturbation-induced ankle deviation was the only variable that significantly differed between perceived and non-perceived perturbations (p=0.001, Fig. 1A). Ankle angle deviation was also the only variable whose 95% confidence interval on the odds ratio did not cross one, with an estimated odds ratio of 2.22. This means that for every 1 SD increase in ankle angle deviation from normal unperturbed walking, a subject was twice as likely to consciously perceive that a perturbation has occurred.

Sensing small ankle joint deviations requires healthy mechanoreceptors in muscle spindles and Golgi tendon organs that are sensitive to muscle length and tension changes. Reduced mechanoreceptor sensitivity that can occur with aging or disease may decrease the ability to consciously perceive locomotor disturbances, contributing to an increased risk of falls. Moreover, degradations in distal musculature with age (e.g., increased tendon compliance [2]) may further reduce the ability to sense locomotor disturbances using ankle proprioception. As such, hip proprioception may become more important for sensing locomotor disturbances with age.

In summary, our results suggest that ankle proprioception was the primary contributor to young adult's ability to perceive small locomotor disturbances. We expect that the sensorimotor mechanisms contributing to disturbance perception are altered with aging, contributing to increased fall risk in older adults.

Significance

These results suggest that sensing changes in ankle motion plays an important role in perceiving subtle slips and trips during walking. Understanding the ability to perceive locomotor disturbances, the sensorimotor contributions to this perception, and changes due to aging and disease may provide targets for rehabilitation aimed at improving locomotor balance.

Acknowledgments

This research was supported by NIH NIGMS under Award Numbers 5U54GM104942-04 and T32GM133369.

References

1. Liss et al. *44th Annual ASB Meeting,* 2020.
2. Stenroth et al. *J Appl Physiol,* 113, 1537–1544. 2012.

HIP JOINT FORCES IN INDIVIDUALS WITH FEMOROACETABULAR IMPINGEMENT SYNDROME

Karim K Ismail[1], Cara L Lewis, Ph.D.[2]
[1]Department of Biomedical Engineering, Boston University, Boston, MA, USA
[2]Department of Physical Therapy & Athletic Training, Sargent College, Boston University, Boston, MA, USA
Email: kismail@bu.edu Web: http://sites.bu.edu/movement/

Introduction

Femoroacetabular impingement syndrome (FAIS) is a clinical disorder characterized by specific bony morphology of the femur and/or acetabulum, which may lead to hip pain. This pain may result from excessive anterior joint forces from the femur onto the acetabulum [1]. In a pilot study, we noted that computationally altering pelvic tilt affects hip joint forces and can help simulate more realistic FAIS and control conditions. However, previous musculoskeletal modeling approaches used to calculate joint forces may inaccurately assume that each participant stands in a neutral pelvic position when stationary. Since people with FAIS walk with more anterior pelvic tilt [2], the purpose of this study was to compare the hip joint loads of patients with FAIS to those of individuals without pain while accounting for each individual's pelvic orientation.

Methods

Motion (100Hz) and force (1000Hz) gait data were collected and processed using Vicon (Vicon Motion Systems Ltd, Centennial, CO) for 22 people with cam FAIS and 22 people without pain. All participants walked at a speed of 1.25 m/s. These data were processed in Visual3D (C-Motion, Inc, Rockville, MD), which scaled anatomical segments based on marker locations and tracked joint motion. Each participant's pelvic orientation was adjusted at all time points, based on the static pelvic angle obtained from Visual3D. Force and gait data of each individual were then imported into OpenSim 3.2 [3], and a generic musculoskeletal model was scaled. To calculate joint moments and muscle activation, the Residual Reduction and Computed Muscle Control tools were used. These results were used to estimate forces from the femur to the acetabulum in the anterior, superior, and medial directions in the pelvic reference frame. All data were normalized from heel-strike to ipsilateral heel-strike and adjusted for body weight in MATLAB. FAIS data were split into more and less painful limbs, and compared to the average of both limbs of the control group. Statistical parametric mapping software [4] helped determine if the differences in joint loads were significant between both FAIS limbs, and between groups.

Results and Discussion

We did not note significant differences between the forces of the control group and the more painful limb, or between the more and less painful limbs in FAIS patients. This may be due to the use of the same musculoskeletal model for both the control and FAIS groups despite their different hip morphologies. The FAIS group had a more anterior pelvic tilt than that of the control group, although the differences were not significant. Since our pilot study showed that pelvic tilt affects joint forces, it was expected that they would aid in observing group differences.

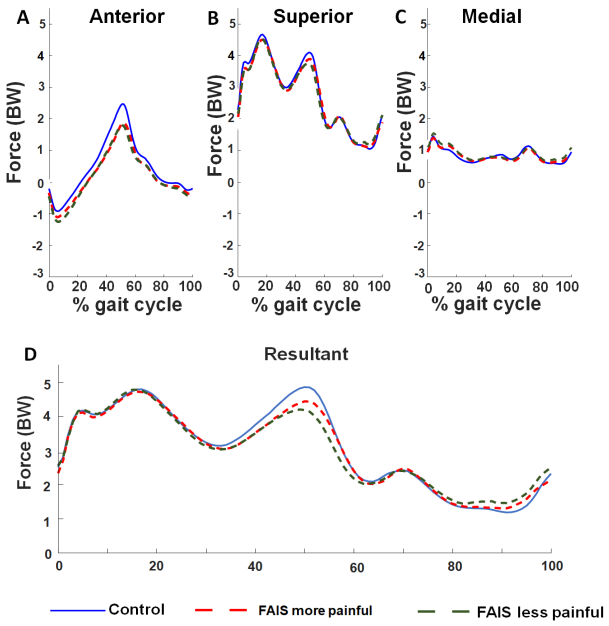

Figure 1: A) Anterior, B) superior, C) medial, and D) resultant (net) forces of the more and less painful limbs of people with FAIS and individuals without pain.

Significance

This is the first study to estimate joint forces of people with FAIS during a full gait cycle (i.e. during stance and swing), and while they walk at the same speed. Despite accounting for pelvic tilt, other underlying assumptions need to be addressed during musculoskeletal modeling in order to accurately compare different conditions. In turn, future studies comparing pathological and healthy joint loads can help researchers determine gait alteration strategies, design assistive devices, and use finite-element simulations to model bone shapes over time.

Acknowledgments

Data were collected and analyzed with the assistance of members of the Boston University Human Adaptation Laboratory. Research reported in this publication was supported by NIH NIAMS (R21 AR061690 and K23 AR063235).

References

1. Lewis et al. *J Biomech*. **48(1)**, 181-185. 2015.
2. Lewis et al. *J Orthop Sports Phys Ther*. **48(8)**, 649-658. 2018.
3. Delp et al. *IEEE Trans Biomed Eng*. Nov. **54(11)**, 1940-50. 2018.
4. Pataky. *J Biomech*. **43**, 1976-1982. 2010

SHOULDER POSITION AND CLIMBING SPECIFIC GRIP FORCE PRODUCTION

Stephanie Huang[1], Shawn Wood[1], Johnathon Crawley[1], Emily Higgins[1],
Claire Lorbiecki[1], Lena Parker[1], Kevin Cowell[2], Erika Nelson-Wong[1]
[1]Regis University School of Physical Therapy
[2]The Climb Clinic
email: shuang@regis.edu

Introduction

Rock climbing has grown expansively in its popularity and participation levels in the last twenty years. As the sport continues to grow professionally and recreationally, it is important for participants to quantify the unique demands of the sport and create targeted training strategies to improve performance and reduce risk of injury. Central to a rock climber's ability to compete and ascend walls is their ability to produce sufficient force to grasp holds. Additionally, rock climbing requires the participant to grip holds in varied arm positions that may affect grip force production. Baláš et. al. [1] sought to quantify the effect of shoulder and elbow angle position on crimp grip force production. The findings suggested that upper extremity position could alter grip force production.

The methodology used by Baláš et. al. [1], limited degrees of freedom with a fixed joint angle apparatus when assessing grip forces. This apparatus added environmental constraints to their analysis that are not present in the activity of rock climbing. To create effective sport-specific testing protocols, environmental demands of the sport should be considered, therefore shoulder positioning should be evaluated in non-fixed positions [2].

The aim of this study is to determine the effect of shoulder position on grip force production with varying upper extremity positioning. We hypothesize that shoulder position will have a significant impact on climbing specific grip force production.

Methods

13 participants (8 female, 5 male) between the ages of 19 and 33 have participated in this study at time of abstract submission. The study protocol was approved by the Regis University IRB and informed consent was obtained from all participants. Skill and experience level were documented via questionnaire. After a standardized warm up, participants were placed in a seated position under the testing apparatus that consisted of a climbing hold (Tension, The Block, Denver, CO, USA) with a 20 mm lip attached to a load cell (Exsurgo gStrength, Sterling, VA, USA) with force data sampled at 250 Hz. Participants had a fixed steel bar positioned above their thighs to restrict upward body translation during pulls (Figure 1).

The participants were asked to pull with 2 grip types; an open-hand drag, pulling with 2nd-4th digits with distal interphalangeal (DIP) and proximal interphalangeal (PIP) joints at an angle greater than 90º, and a half-crimp, where the 2nd-5th digits are used with a 90º bend in the PIP joint. Different shoulder angles were also tested by positioning the participant with a shoulder flexion angle at either 90º or 120º, confirmed with a goniometer.

Participants were asked to gradually "ramp up" to maximal isometric pull and then hold for 3-5 seconds. Each combination of grip type and shoulder flexion angle were performed two times on each arm for a total of sixteen trials. The order of hand and shoulder positions were randomized for each participant with two-minute rest intervals between each pull. Rate of perceived exertion (RPE) using the modified Borg scale was taken after each pull.

Pulls correlated with a self-reported RPE of ≤ 7 were excluded from data analysis. Left/right, and between-trial data for each participant were examined for differences with paired t-tests. No left/right or between-trial differences were detected; therefore, these values were averaged to yield a single force variable per participant for each shoulder/hand position as a data reduction measure. Force data were normalized to body weight and expressed as % BW. Maximum values were extracted for each trial and entered into paired t-tests to explore differences in force output between shoulder angles for each of the 2 hand positions.

Figure 1: Experimental configuration of testing apparatus.

Results and Discussion

No significant differences were found between shoulder angles for either open hand (52.19 ± 11.49 % BW for 90° shoulder flexion vs. 52.56 ± 11.42 % BW for 120° shoulder flexion, $p = .81$) or half-crimp (57.71 ± 12.82 %BW for 90° shoulder flexion vs. 58.18 ± 11.72 %BW for 120° shoulder flexion, $p = .56$) positions. These findings do not support our hypothesis and they also contradict existing research which shows that upper extremity position influences climbing grip strength [1]. These findings suggest testing climbing grip force production in a variety of arm positions is not likely to alter a climber's ability to generate force at their fingers. These preliminary findings are from an ongoing study with continuing data collection. As sample size increases, interactions between shoulder and hand position as well the influence of sex, climbing experience and anthropometrics on climbing-specific grip strength will be explored.

Significance

Early evidence suggests that shoulder position does not need to be considered when testing rock climbing specific grip strength. Caution should be taken with these findings as they may change with increased sample size.

References

1. Balas J. et. al., The role of arm position during finger flexor strength measurement in sport climbers. Int J Perform Anal Sport. 2014;14.
2. Michailov ML et. al., Reliability and validity of finger strength and endurance measurements in rock climbing. Res Q Exerc Sport. 2018;89(2):246-254.

KINEMATICS AND SPATIOTEMPORAL GAIT CHARACTERISTICS DURING THE SIX MINUTE WALK IN PARTICIPANTS WITH HIP OSTEOARTHRITIS

Hope Davis-Wilson[1,2], Rashelle Hoffman[1,2], Victor Cheuy[3], Dana Judd[1,2], Jennifer Stevens-Lapsley[1,2], and Cory Christiansen[1,2]
[1]Geriatric Research Education and Clinical Center, VA Eastern Colorado Healthcare System, Denver, CO
[2]Department of Physical Medicine and Rehabilitation, University of Colorado Aurora, CO
[3]Department of Physical Therapy and Rehabilitation Science, University of California, San Francisco, San Francisco, CA
email: hope.davis-wilson@cuanschutz.edu

Introduction

Individuals with end-stage hip osteoarthritis (HOA) walk 28% less during a 6-min walk test (6MWT) compared to healthy controls,[1] which is linked to neuromuscular compensations observable in faulty movement patterns. Studies have shown participants with HOA ambulate with aberrant trunk, hip, and knee kinematics and spatiotemporal characteristics.[2,3] Yet it is not well understood how kinematics and spatiotemporal characteristics of the involved and uninvolved limbs progress over prolonged bouts of walking (e.g., the 6MWT). Most overground walking studies measure gait pattern characteristics over a few steps recorded in a laboratory setting. However, inertial measurement units (IMU) make it possible to evaluate gait during prolonged walking bouts in clinical settings. The purpose of the study was to evaluate joint and segmental kinematics and spatiotemporal characteristics between limbs (involved vs. uninvolved) and between early and late time points of the 6MWT in participants with end-stage HOA. We hypothesized participants would demonstrate kinematic and spatiotemporal differences between limbs and between time-points.

Methods

Sagittal trunk, hip, and knee kinematics and spatiotemporal variables (speed, stride length, and step rate) were recorded using an 8-sensor full-body IMU system (Xsens Technologies). Each stance phase of the first and final minute of the 6MWT was defined using foot velocity in the anteroposterior direction using a custom MATLAB script. Turns were excluded from the analysis due to high variability of stepping characteristics during turning. Peak kinematic and spatiotemporal variables were calculated for each stance phase and averaged over the number of stance phases within the first or final minute. We conducted paired t-tests to determine differences in kinematics and spatiotemporal variables between limbs and between the first and final minute of the 6MWT.

Results and Discussion

Eleven participants (4 female, age: 65± 7yrs, BMI: 28±5 kg/m^2) with end-stage HOA participated. During the first and final minute of the 6MWT, the involved limb demonstrated decreases in peak hip flexion (first: t=-5.57, P<.001; final: t=-5.41, P<.001), peak hip extension (first: t=3.36, P=.007; final: t=3.56, P=.005), trunk flexion (first: t=-3.35, P=.007; final: t=-3.04, P=.013), and peak knee flexion (first: t=-5.41, P<.001; final: t=-6.27, P<.001) compared to the uninvolved limb (Figure 1). Participants demonstrated no kinematic differences between time-points and no spatiotemporal differences between limbs or between time-points (P>.05). In agreement with our hypothesis and previous literature,[2,3] trunk and involved limb hip and knee motion was reduced. However, relative between-limb differences did not change between the 6MWT first and last minute, indicating persistent asymmetrical movement compensations that are not exaggerated with prolonged walking.

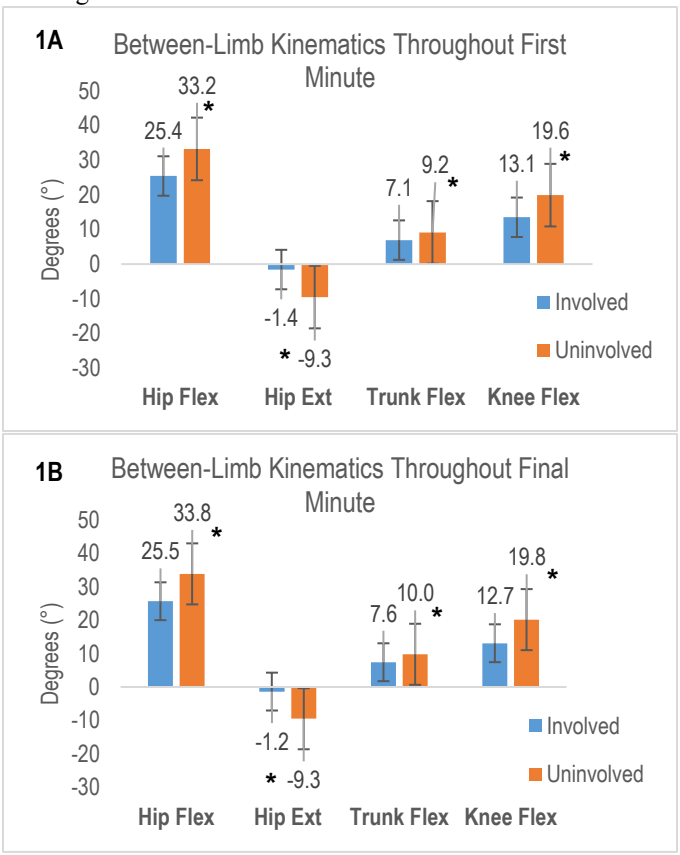

Figure 1. Peak kinematics throughout the first minute (1A) and final minute (1B) of the 6MWT. Hip Flex: Peak hip flexion during stance phase; Hip Ext: Peak hip extension during stance phase; Trunk Flex: Peak trunk flexion during stance phase; Knee Flex: Peak knee flexion during stance phase; * significantly different between limbs (P<.05)

Significance

Sagittal trunk, hip, and knee kinematic asymmetries are associated with HOA progression,[4] and IMUs may allow for their feasible assessment in a clinical setting.

Acknowledgements

Supported by VA RR&D (5I01RX002251-05)

References

1. Judd et al. 2014. *Disabil Rehabil*. 36(4):307-212.
2. Ismailidis et al. 2020. *J Orthop Res.* Online ahead of print.
3. Zeni et al. 2015. *J Orthop Res*. 33(3):382-389.
4. Farkas et al. 2019. *Hip Int*. 29(2):209-21

Measuring Mechanical Support of Semi-Rigid Ankle Braces: Test-Retest Reliability

Adam J. Yoder[1,2], Yingjun Zhao[3,5], Han Joo Lee[4], Kenneth J. Loh[3,4], Shawn Farrokhi[1,2]
[1]DoD-VA Extremity Trauma and Amputation Center of Excellence, [2]Naval Medical Center San Diego,
[3]University of California San Diego, Dept of Structural Engineering, [4]University of California San Diego, Dept of Material Science and Engineering, [5]Oak Ridge Institute for Science and Education
Email: adam.j.yoder.civ@mail.mil

Introduction

Semi-rigid ankle braces (*e.g.*, lace-up, stirrup) are recommended for sprain prevention in high-risk activities [1]. Standardized tests have been developed to measure mechanical properties of limb prosthetics [2] and of rigid ankle-foot orthoses [3,4], but not for semi-rigid braces. Such procedures are needed to compare existing braces and to guide design iterations for next-generation braces. This report presents methods and reliability for a simple test procedure to measure mechanical support of semi-rigid ankle braces.

Methods

Requirements for the test procedure were defined as: easily replicated in other labs (*no custom load frames, cadaveric specimen*); allow load-displacements representative of high-risk activity (*versus quasi-static*); avoid human subjects (*due to physiologic variance, testing to injury*); excellent test-retest reliability ($ICC > 0.9$).

A common physical rehabilitation dynamometer was selected (System Pro 4, Biodex Inc, New York; max eccentric speed 300 deg/sec, torque 544 Nm). An ankle-foot replica was designed by 3D scanning a volunteer's limb and incorporating a 2-degree-of-freedom saddle joint at the functional joint center measured with optical motion capture. The adjusted model was printed with thermoplastic polyurethane (100% fill, NinjaTek NinjaFlex 3mm 85A, LulzBot, Cura).

Test-retest reliability was measured across the following factors: three braces (*i.e.*, no brace; lace-up, *Med Spec ASO*; and stirrup, *3M Futuro*), two operators (non-clinicians), three velocities (5, 60, and 300°/s), three repetitions; yielding 54 total tests. For each test, the foot replica was mounted for ankle inversion/eversion (removed/replaced completely between each trial) and run through a pre-configured sequence of five passive isokinetic cycles spanning ±40°.

Brace torque-angle stiffness was parameterized with a linear best fit, and input to a two-way mixed-effects model for calculation of intraclass correlation coefficients (ICC(2,1), SPSS v25), standard error of measurement (SEM=$SD\sqrt{1-ICC}$), and smallest detectable difference (SDD$SEM * 1.96 * \sqrt{2}$) Supplementary ANOVA's were executed to test the hypotheses, that stiffness would differ across braced conditions, but not across operators or test velocity ($\alpha<0.05$).

Results and Discussion

Stiffness differed across the three brace conditions: unbraced 0.04±0.02 Nm/°, lace-up 0.16±0.01 Nm/°, and stirrup 0.21±0.02 Nm/° ($p<0.001$, Fig. 1); in agreement with a report that compared similar semi-rigid brace designs on cadaveric specimen at quasi-static speeds [5]. Some inherent stiffness of the foot replica should be expected; the unbraced magnitudes measured indicate a low and fixed response which can be subtracted to isolate stiffness due only to worn braces. Stiffness was not influenced by test velocity, which could have occurred with fixture instabilities or unanticipated damping. This supports use of the test procedure to characterize prototype braces with designed, velocity-responsive behavior (up to 300°/s).

Both inter- and intra-operator reliability were excellent (ICC=0.94, 0.97), with high measurement resolution (SEM=0.02 Nm/°, SDD=0.05 Nm/°). Similar test-retest reliability has been reported for test procedures developed to measure plantar/dorsiflexion stiffness of rigid ankle-foot orthoses, but which employed more cumbersome custom-built load frames, limited to quasi-static speeds [3,4].

Significance

The test procedure addresses an apparent gap in standardized testing of semi-rigid ankle braces. The 3D-printed ankle-foot can be easily shared and re-produced for ~$75 USD, which could facilitate inter-laboratory consistency (*file available upon request*), along with the common dynamometer.

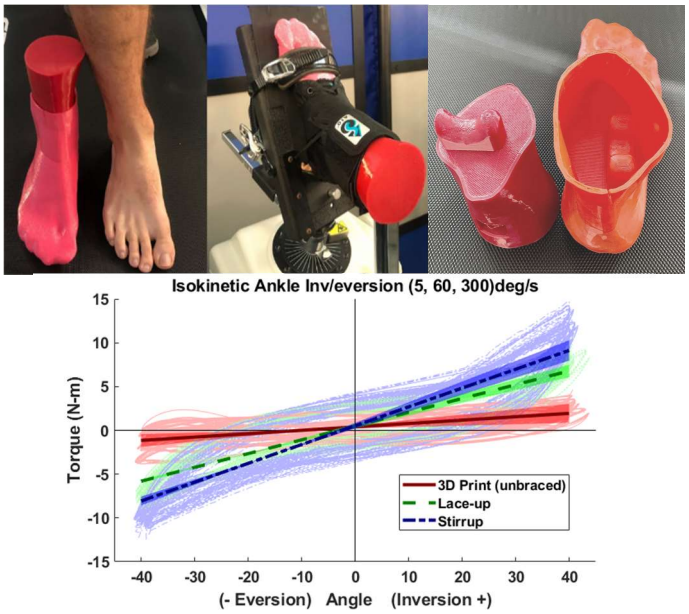

Figure *1*: Rotational stiffness of the 3D printed ankle-foot replica, reinforced with lace-up and stirrup semi-rigid braces. Ensemble mean (±1 SD) linear trends are shown across all scenarios per brace (18 tests: 2 raters, 3 velocities, 3 repetitions).

Acknowledgments

The views expressed are those of the authors and do not reflect official policy of U.S. Department of Army/Navy, Department of Defense, nor U.S. Government.

References

[1] Newman T. (2017). *Mil Med*. **182**: 1596–602.
[2] Prosthetics & Orthotics. *ISO*. Tech Committee **168**.
[3] Ielapi A. (2018). *BMC Research Notes*. **11**:1-7.
[4] Bregman D. (2009). Gait & Posture. **30**: 144-9.
[5] Benca E. (2019) *Sc J Med Sci Sport*. **29**:1174-80

WEEKLY EXERCISE DOES NOT INFLUENCE OVERGROUND TRANSFER OF A NEW WALKING PATTERN

Eric B. Finley[1], Sarah A. Brinkerhoff [1] , Jaimie A. Roper[1]
[1]Auburn University, Auburn, AL
Email: ezf0016@auburn.edu

Introduction

Previous research has examined the ability of healthy and neurologically impaired adult populations to transfer a newly learned walking pattern to overground walking.[1,2] No research has examined the influence of factors that may be specific to an individual such as activity level on transfer ability. Active individuals have demonstrated better control of gait while performing tasks that require more coordination and while navigating challenging environments compared to non-active individuals.[3,4] Recognizing the impact of activity level on the ability to transfer gait patterns could be crucial for understanding mechanisms of gait rehabilitation.

The purpose of this study was to compare the transfer of a novel split-belt treadmill walking pattern to overground walking between sedentary and active young adults. We hypothesized that active individuals would have a faster return to their baseline walking pattern from split-belt treadmill to overground walking.

Methods

Two groups of healthy young adults participated in this study: 12 sedentary, and 19 active individuals. Individuals who exercised less than 150 minutes per week for the past three months were assigned to the sedentary group; individuals who exercised aerobically at least 150 minutes per week were assigned to the active group.

Participants walked overground, then completed a typical 2:1 ratio split-belt treadmill adaptation paradigm: 3-minute baseline tied-belt walking, 10-minute split-belt walking, 3-minute deadaptation, and 3-minute readaptation. Following readaptation, participants walked overground. Step length asymmetry (SLA), a common measure of gait adaptation and learning, was measured during all steps of baseline overground walking and baseline treadmill walking, during the first four steps of deadaptation, and during the first four steps of overground transfer walking. Average overground and treadmill baseline SLA were subtracted from each of the first four steps of overground transfer and deadaptation SLA, respectively. To determine the effect of group on the transfer of SLA from split-belt treadmill walking to overground walking, we analyzed linear mixed effect models predicting SLA at each of the first four steps of overground transfer. Fixed effects were added in one at a time and models were compared for fit to the data using an *a priori* alpha of 0.05. The fixed effects entered, in order, were: step number (linear), average SLA during the first 4 steps of deadapt, and group. All models contained a random intercept on participant to account for variance in SLA due to individuals.

Results and Discussion

Minutes of exercise per week ranged from 0 to 750 minutes, with a mean and (SD) of 179 (169) minutes. The Sedentary group exercised for 37 (45) [0,120] minutes/week, and the Active group exercised for 269 (156) [150,750] minutes per week. Only two steps of SLA could be obtained for seven participants in the Active group, while four steps were obtained for all other participants. The removal of these seven participants did not alter the statistical results; therefore, all participants were included in the analysis.

Neither group returned to baseline SLA during the first four steps of overground transfer walking (Figure 1A). The linear mixed effects models revealed a significant intercept and significant linear effect of step. SLA during the first step of overground transfer was significantly different from zero (52.52 mm, $p < 0.001$), indicating that young adults transfer the new pattern to overground walking. SLA decreased with each step of overground walking (-3.96 mm/step, $p = 0.020$), indicating that young adults begin to return toward baseline SLA within the first four steps. The magnitude of SLA during treadmill deadaptation does not affect overground transfer. After accounting for the linear effect of step, 78% of the remaining variability in SLA during overground transfer was due to individual differences (Figure 1B). Our study shows that the source of these individual differences is not current exercise amount. Further research is needed to determine the source of variability in amount of SLA transferred from split-belt walking to overground walking.

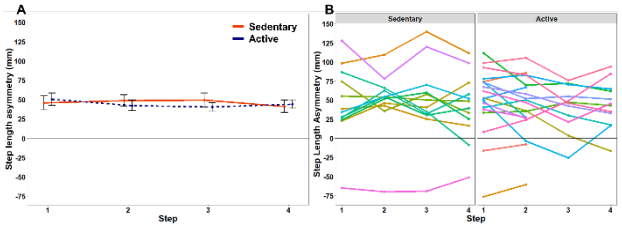

Figure 1A. SLA during overground transfer walking for groups. Zero indicates baseline SLA. Error bars indicate standard error. There was no difference in overground transfer between groups but there was a linear effect of step number. **Figure 1B**. SLA during overground transfer walking for each of the 31 participants, separated by group.

Significance

Our findings provide insight into the mechanisms of rehabilitation that target transfer of a new locomotor pattern. Specifically, future research should focus on better understanding how individual factors influence the transfer of a new walking pattern to a different environment.

Acknowledgments

This study was funded by an Auburn University seed grant. E.B.F and S.A.B are each funded by Auburn University Presidential Graduate Fellowships.

References

1. Reisman, et al. 2009.
2. Torres-Oviedo, et al. 2010.
3. Gérin-Lajoie, M., et al. 2007.
4. Cristina-Elena, M., et al. 2014.

EFFECT OF PROSTHETIC ANKLE PUSH-OFF POWER AND FOOT STIFFNESS ON BIOMECHANICAL SYMMETRY

Joshua Tacca[1], Zane Colvin[2], Alena M. Grabowski[2,3]
[1]Department of Mechanical Engineering & [2]Department of Integrative Physiology, University of Colorado Boulder, Boulder, CO
[3]Department of Veterans Affairs, Eastern Colorado Healthcare System, Denver, CO
email: Joshua.tacca@colorado.edu

Introduction

Many people with unilateral transtibial amputation (TTA) use passive-elastic prosthetic feet to walk. Such prostheses cannot provide the peak mechanical power typically generated by biological calf muscles during walking [1]. Thus, people with TTA compensate and walk with biomechanical asymmetry such as greater loading on the unaffected (UL) compared to affected leg (AL) [2]. Biomechanical asymmetry may increase risk of joint pain and osteoarthritis compared to non-amputees [2].

Powered ankle-foot prostheses such as the BiOM (Ottobock, Duderstadt, Germany) provide stance-phase, battery-powered ankle torque. People with TTA using the BiOM normalize biomechanics during walking compared to non-amputees by increasing positive AL work [3]. But the relationship between BiOM power setting and asymmetry is not known. Moreover, the BiOM attaches to a passive-elastic prosthetic foot with manufacturer-defined stiffness that may affect biomechanical asymmetry. A previous modelling study found that use of a stiffer prosthetic foot minimizes UL knee joint loading [4]; however, the effect of prosthetic stiffness may also depend on the power setting of the BiOM. We hypothesized that increasing prosthetic power and stiffness would reduce biomechanical asymmetry and the relationship would depend on walking speed.

Methods

2 subjects (1M, 1F; 28±6 yrs.; 63.4±5 kg; 1.70±0.06 m) with TTA walked at 0.75–1.75 m/s on a dual-belt force treadmill (Bertec, Columbus, OH) using the low-profile (LP) Variflex (Össur, Reykjavik, Iceland) foot at the recommended stiffness category (Rec Cat), one Cat more stiff (+1), one Cat less stiff (-1), and two Cat less stiff (-2). One subject walked at 0.75–1.75 m/s using the BiOM tuned so that the subject's net positive prosthetic ankle work was within 2 SD of average non-amputee net positive ankle work [3]. The subject used the BiOM with the recommended power (Rec Pow) from tuning, 10% greater power (+10%), and 20% greater power (+20%) with each prosthetic Cat.

We measured vertical ground reaction forces (GRFs) at 1000 Hz, filtered them using a 4th-order low-pass Butterworth filter with a 30 Hz cut-off and used a 20 N GRF threshold to calculate contact time (t_c). We determined 1st and 2nd peak vertical GRFs (F_1 and F_2, respectively) of the UL and AL from 6 strides (Matlab, Mathworks, Natick, MA). We also calculated symmetry index (SI) for each variable, which is the percent difference between the UL and AL where a positive SI means UL > AL, negative SI means AL > UL, and 0% is perfect symmetry.

Results and Discussion

t_c SI averaged across all speeds and stiffness Cat was 5.62%, 1.63%, 1.57%, and 1.90% for passive (LP), and Rec, +10%, and +20% Pow, respectively (Fig. 1a). Across all speeds, using the BiOM reduced t_c SI compared to the LP. However, there was no trend for t_c SI across BiOM power setting. t_c SI averaged across all speeds and power was 2.62%, 3.02%, 3.71%, and 3.73% for -2, -1, Rec, and +1 Cat, respectively (Fig. 1b). Decreased stiffness reduced t_c SI at 0.75, 1.00, and 1.75 m/s. F_1 SI averaged across all speeds and stiffness Cat was 5.57%, -1.39%, -3.10%, and -2.98% for LP, and Rec, +10%, and +20% Pow, respectively (Fig. 1c); however, there was no trend between conditions at 0.75, 1.00, and 1.25 m/s and increased power increased F_1 asymmetry at 1.50 and 1.75 m/s. F_1 SI averaged across all speeds and power was -0.27%, 1.36%, 1.15%, and 0.70% for -2, -1, Rec, and +1 Cat, respectively (Fig. 1d), and at 1.75 m/s increased stiffness reduced F_1 asymmetry. F_2 SI averaged across all speeds and stiffness Cat was 7.15%, 6.22%, 6.59%, and -0.09% for LP, and Rec, +10%, and +20% Pow, respectively (Fig. 1e); use of the +20% Pow increased F_2 asymmetry at 0.75, 1.00, and 1.25 m/s perhaps because the prosthesis was overpowered. F_2 SI averaged across all speeds and power was 5.07%, 6.65%, 4.31%, and 5.58% for -2, -1, Rec, and +1 Cat, respectively (Fig. 1f), and there was no trend for F_2 SI with prosthetic stiffness at each speed.

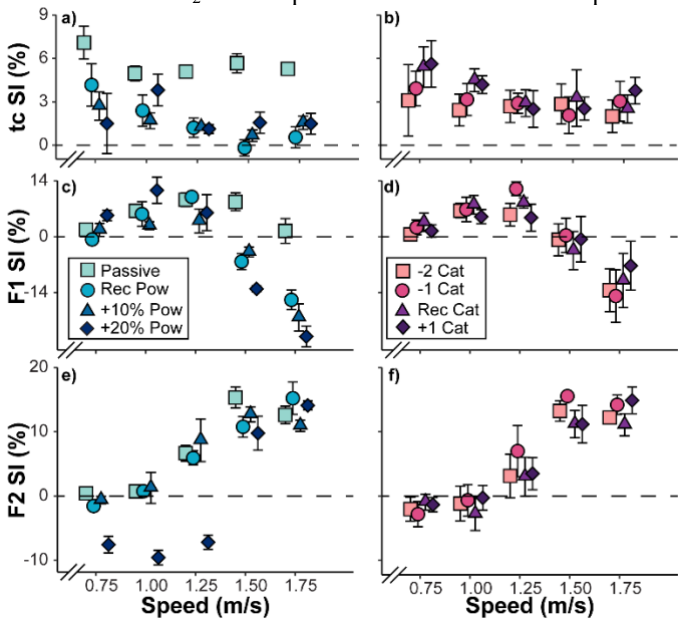

Figure 1: t_c (a, b), F_1 (c, d), and F_2 (e, f) SI across walking speeds. Left panels (a, c, e) averaged across stiffness categories (Cat) for each prosthetic power setting (Pow) and right panels (b, d, f) averaged across Pow for each Cat. Error bars are SEM. Symbols are offset for clarity.

Significance

Use of the BiOM compared to passive prosthesis decreased t_c SI. But increased prosthetic power did not affect t_c SI, and increased F_1 and F_2 asymmetry at 1.50–1.75 m/s and 0.75–1.25 m/s, respectively. Increased prosthetic foot stiffness decreased F_1 asymmetry at 1.75 m/s, increased t_c asymmetry at 0.75, 1.00, and 1.75 m/s and did not affect F_2 asymmetry. The effects of prosthetic power and stiffness on asymmetry depended on speed. Our results inform prosthetic prescription and design, which could reduce injury risk for people with TTA.

Acknowledgments

This study was funded by the Department of Veterans Affairs.

References

[1] Zmitrewicz et al. (2007). *J. Biomech,* **40:** 1824-1831
[2] Morgenroth et al. (2012). *PM&R,* **4:** S20-S27
[3] Herr & Grabowski (2012). *Proc. Royal Soc. B,* **279:** 457-464
[4] Fey et al. (2012). *J. Biomech Eng,* **134:** 111005

THE METABOLIC COST OF WALKING BALANCE CONTROL AND ADAPTION IN YOUNG ADULTS

Shawn Ahuja[1] and Jason R. Franz[2]
[1]School of Medicine, University of North Carolina, Chapel Hill, NC, USA
[2]Joint Department of Biomedical Engineering, UNC Chapel Hill and NC State University, Chapel Hill, NC, USA
Email: shawn_ahuja@med.unc.edu

Introduction

Older adults consume oxygen at a faster rate during walking than young adults, accelerating fatigue and reducing independence. Despite its importance in governing independence and quality of life, the mechanisms responsible for this increased metabolic energy cost remain elusive. O'Connor et al. found that the metabolic cost of walking increases in the presence of optical flow perturbations designed to challenge balance via the visual perception of instability [1]. These data suggest that the act of preserving balance during walking exacts a metabolic penalty. However, prior work has focused on average outcomes after several minutes of responding to perturbations. We have shown that young and older adults respond to the onset of optical flow balance perturbations with generalized anticipatory control (i.e., shorter and wider steps [2,3]. This gives way to task-specific reactive control with prolonged exposure, in which step width and length return to baseline values despite persistent increases in step-to-step variability to orchestrate balance corrections. This adaption may be governed in part by metabolic costs associated with generalized anticipatory versus task-specific reactive control. Our aim was to quantify the role of metabolic energy cost in governing neuromuscular adaption to prolonged exposure to optical flow perturbations during walking in young adults. We first hypothesized that metabolic cost would increase at the onset of balance perturbations in a manner consistent with wider and shorter steps and increased step-to-step variability. We also hypothesized that metabolic cost would decrease with prolonged exposure in a manner consistent with a return of step width and step length to values seen during normal, unperturbed walking.

Methods

18 healthy young adults (age: 23.3 ± 2.7, 10M/8F) walked for a total of 20 min at 1.2 m/s while watching a speed-matched virtual hallway projected on a semi-circular curved screen positioned in front of the treadmill. A the 5-min mark, we added side-to-side oscillations to the virtual hallway, prescribed as a summation of sine waves with a nominal amplitude of 0.35 m. After 10 minutes of responding to optical flow perturbations, subjects walked for 5 min without perturbations. We used three-dimensional motion capture to record the trajectories of markers placed on subjects' trunk, pelvis, and right and left legs. These were used to extract step kinematics, including step width, step length, and their respective variabilities. We also measured subjects' rates of oxygen consumption and carbon dioxide production using a portable indirect calorimetry system (Cosmed K5). We used standard procedures to estimate net metabolic power, reporting in W/kg. For all outcome measures, we computed average values during the following four time periods of interest: Pre (minutes 3-5), Early Perturbation (minutes 5-7), Late Perturbation (minutes 13-15), and Post (minutes 15-17). A repeated measures ANOVA tested for main effects of time, following by post-hoc pairwise comparisons.

Results and Discussion

With the onset of perturbations, participants walked with 3% shorter, 17% wider, and 53-73% more variable steps (p-values≤0.001) (Fig. 1). As hypothesized, these changes were accompanied by a significant 12% increase in net metabolic power compared to walking normally (p=0.001). With prolonged exposure to perturbations, we found that step width and step length tended toward values seen during normal, unperturbed walking. Specifically, compared to those measured at the onset of perturbations, participants increased step length by 2% and decreased step width by 8% (p-values ≤0.004) following prolonged exposure. Consistent with our previous work[2,3], these changes occurred despite continued or even modest increases in step width variability. We interpret those cumulative findings to suggest that participants responded to the onset of perturbations using generalized anticipatory control, but deprioritized that strategy in favor of task-specific, reactive control following prolonged exposure. As the most significant novel contribution of this study, we add here that these changes were accompanied by and may thereby be orchestrated to permit a statistically significant 5% reduction in net metabolic power compared to that at the onset of perturbations (p=0.005).

Significance

Our findings suggest that metabolic energy cost may shape the strategies we use to regulate and adapt walking balance in response to perturbations. Planned studies will compare the metabolic cost of balance control and adaption between younger and older adults. Our findings may have important implications for the interaction between higher metabolic cost of walking, increased fatigability, and increased risk of falls in older adults.

Acknowledgments

NIH R21AG067388 and the UNC Medical Alumni Fund.

References

1. O'Connor SM et al. Gait Posture 2012.
2. Thompson JD et al. Clin Biomech 2018.
3. Richards JT et al. J Neuroeng Rehabil 2019.

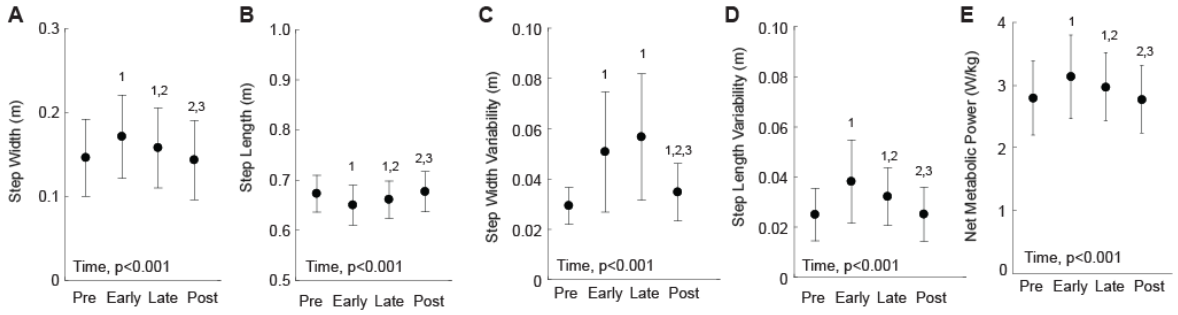

Figure 1. Primary outcomes as a function of time. [1]significant versus Pre, [2]significantly versus Early, [3]significantly versus Late.

Combining an Artificial Gastrocnemius and Powered Ankle Prosthesis: Effects on Transtibial Prosthesis User Gait

David M. Ziemnicki[1], Joshua M. Caputo[2], Kirsty A. McDonald[3], and Karl E. Zelik[1]
[1]Department of Mechanical Engineering, Vanderbilt University, Nashville, TN, United States
Email : david.m.ziemnicki@vanderbilt.edu

Introduction

Powered prosthetic ankles can restore the monoarticular function of the soleus muscle during walking, which provides a burst of push-off power in late stance. However, the benefits observed from powered ankles (e.g., magnitude of metabolic cost reduction) have often been less than those theorized/expected [1], [2].

One potential explanation is that powered ankles do not restore the biarticular function of the gastrocnemius muscle, which provides a mechanical coupling across the ankle and knee and assists in initiating leg swing. Indeed, simulation [3] and experimental [4] studies provide preliminary evidence that restoring the gastrocnemius ankle-knee coupling to transtibial prosthetic device users (PDU) may improve walking performance above and beyond restoring soleus function alone. For instance, PDU demonstrated reductions in prosthesis-side hip and knee joint torques when gastrocnemius function was restored in combination with a powered ankle [4]. However, it is unclear if restoring the gastrocnemius function is only important for prosthetic ankles that generate sufficiently high magnitudes of push-off power, or whether the gastrocnemius behavior itself (e.g., gastrocnemius stiffness) should to be tuned differently based on the powered ankle behavior. This knowledge gap remains because benefits of an artificial gastrocnemius (AG) have not yet been compared across various levels of powered prosthetic ankle push-off.

The objective of this study is therefore to emulate gastrocnemius-like ankle-knee coupling in PDU, and to characterize its effect on whole-body gait biomechanics across various levels of prosthetic ankle push-off power and across various levels of gastrocnemius stiffness. We predict that kinematic and kinetic effects of the artificial gastrocnemius will be larger for higher levels of prosthetic ankle push-off power.

Methods

To study the role of the gastrocnemius we are using a robotic emulation system (HuMoTech) that we customized to include: a soleus actuator (to emulate the powered ankle prosthesis), a separate gastrocnemius actuator (to vary behavior of the ankle-knee coupling), a soft conformal leg interface (which attaches to the user's thigh to provide an anchor point for the gastrocnemius), and a foot prosthesis (a modified version of HuMoTech's standard prosthetic hardware, Fig. 1). We have developed a controller that can command the artificial soleus and gastrocnemius in a repeatable, accurate, and precise manner. As subjects walk, we can independently manipulate the dynamics of the soleus and gastrocnemius, in order to systematically analyze how different parameters affect gait.

Otherwise healthy PDU (N=5) attended an initial familiarization session. Participants then returned for a second session, during which the artificial ankle (soleus) push-off power and the artificial gastrocnemius stiffnesses were systematically varied as participants walked at 1.1 $m \cdot s^{-1}$. Ground reaction forces (Bertec), kinematic marker data (Vicon), and electromyography signals (Delsys) were recorded. It is expected that a more complete (e.g., N=8) dataset will be presented at ASB.

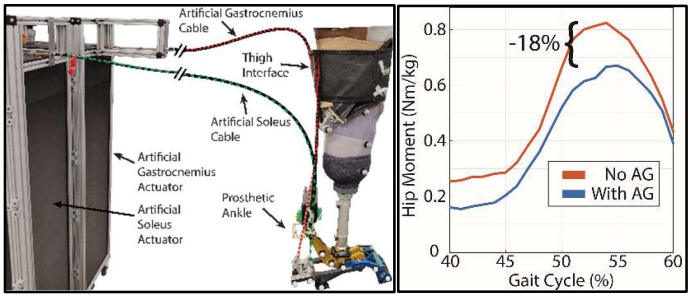

Figure 1: Experimental Set-up (left), Example of Prosthetic Side Hip Torque with vs. without the AG (right).

Results and Discussion

We have verified the controller's ability to emulate different gastrocnemius spring stiffness profiles during walking as well as its ability to provide various levels of ankle (soleus) push-off power while working in tandem with the artificial gastrocnemius. We are partway through our data collection and will continue to test unilateral, transtibial PDU while we sweep across a range of stiffness values for a passive artificial gastrocnemius, and also sweep across different ankle prosthesis push-off powers.

Preliminary results confirm that walking with an artificial gastrocnemius has a considerable effect on gait biomechanics, including reducing prosthesis-side hip moments during push-off (Fig. 1). Comparison of how the artificial gastrocnemius affects gait kinematics and kinetics for higher vs. lower magntiudes of prosthetic ankle (soleus) push-off power is presently underway, and the newest results will be presented at ASB.

Significance

The results from this study will provide deeper understanding of the role of the gastrocnemius and how it interplays with soleus behavior during walking, as well as inform how to improve the benefits PDUs received from powered prosthetic ankles.

Acknowledgments

We thank Dr. Gerasimos Bastas, Dr. Michael Goldfarb and Dr. Steve Collins for their input and advice, and funding from NSF grant 1705714.

References

[1] Herr et al. (2012). Proc. R. Soc. B Biol. Sci.
[2] Quesada et al. (2016). J. Biomech.
[3] Wilson et al. (2015). NW Biomech. Symposium.
[4] Eilenberg et al. (2018). J Robotics.

DYSKINESIA DETECTION IN PEOPLE WITH PARKINSON'S DISEASE USING ACCELEROMETRY

Carolin Curtze[1], Jenny Anne Maun[1], Fay B. Horak[2], and John G. Nutt[2]
[1]Department of Biomechanics, University of Nebraska at Omaha, Omaha, NE
[2]Department of Neurology, Oregon Health and Science University, Portland, OR
email: ccurtze@unomaha.edu

Introduction

Parkinson's disease (PD) is a progressive neurodegenerative disorder, with patient numbers projected to double to 12 million in the next 20 years. While dopamine replacement therapy and dopamine agonists are standard of care and most effective in treating the slowness of movement in PD, side effects can occur. Levodopa-induced dyskinesia is a major problem associated with the long-term use of levodopa for symptomatic treatment of PD. These involuntary hyperkinetic movements can become disabling and may interfere with quality of life. Our prior research showed PD with levodopa-induced dyskinesia were less stable while standing (i.e., increased postural sway) and had a higher incidence of falls [1]. While postural sway increased, the relative contribution of each segment to this overall increase of sway is unclear. The aim of this study is to characterize the relative contribution of these abnormal, involuntary movements to the overall postural sway in people with PD using accelerometry.

Methods

Individuals with idiopathic PD (n = 26; 14 showed clinical signs of dyskinesia) performed 30 seconds of postural sway under two conditions: (1) a single task: standing quietly with arms along their sides, and (2) a cognitive dual task: standing while performing a serial subtraction task. Individuals were tested in their OFF state (i.e., after withholding their anti-parkinsonian medication for at least 12 hours) and ON state (i.e., about 1 hour after intake of a levodopa challenge dose, approximately 1.25x their regular medication dosage). Postural sway was collected using 9 inertial sensors (Opals V1, APDM) attached to specific body segments (Figure 1). The root-mean-square (RMS) sway were calculated from the head, sternum, and lumbar accelerations. Additionally, sway ratios were determined as the superior segment's sway relative to the inferior segment's sway [2]. To determine which measures best differentiate individuals with and without levodopa-induced dyskinesia, we first calculate Receiver Operating Characteristic (ROC) curves and computed the Area Under the ROC Curve (AUC).

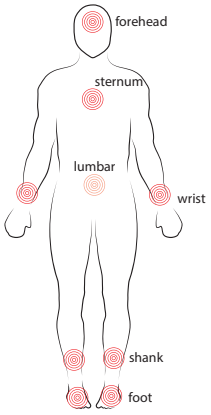

Figure 1: Placement of inertial sensors

Results and Discussion

Our findings confirm that postural sway increases with medication in people with dyskinesia, but not in people without dyskinesia (Figure 2). This increase in postural sway is amplified in the cognitive dual task condition.

Accuracy of classification strongly improved with the use of a cognitive dual task known to provoke dyskinesia (Table 1). The sensor attached to the head was most accurate at differentiating people with dyskinesia and without dyskinesia under the single and dual tasks condition.

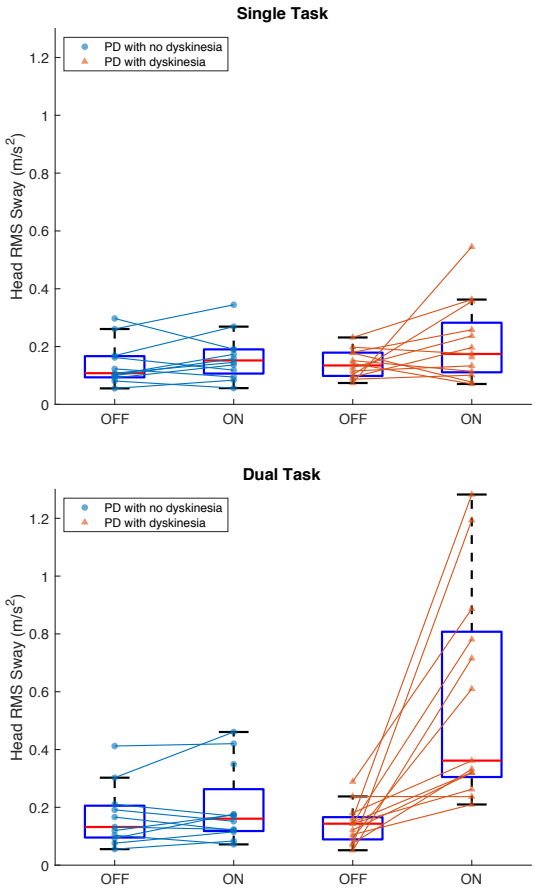

Figure 2: Effect of medication on head RMS sway during single (top) and dual task (bottom) in PD with and without dyskinesia

Table 1: Area under the ROC Curve (AUC)

	Single Task	Dual Task
RMS Sway Head	0.606	0.944
RMS Sway Sternum	0.591	0.713
RMS Sway Lumbar	0.523	0.853
Sway Ratio Head/Sternum	0.485	0.888
Sway Ratio Head/Lumbar	0.530	0.769

Significance

Our findings show that a single sensor is sufficient to accurately classify patients with and without dyskinesia in a supervised setting during a cognitive dual task.

Acknowledgments

This research was supported by the Medical Research Foundation of Oregon and NIH P20 GM109090.

References

[1] Curtze C, et al. Movement Disorders 30, 1361-1370, 2015.
[2] Fino P, et al. J Biomech 112, 110045, 2020.

BIOMECHANICS OF THE INSIDE AND OUTSIDE LEG WHEN SPRINTING ALONG FLAT CURVES

Ryan Alcantara[1] & Alena M. Grabowski[1]
[1]Applied Biomechanics Lab, University of Colorado Boulder, CO, USA
email: ryan.alcantara@colorado.edu

Introduction

For outdoor track events such as the 200 and 400 m sprint, over half the race is completed along a flat curve. Curve sprinting requires an athlete to produce vertical and centripetal ground reaction forces (GRF) to support body weight and accelerate the body towards the inside of the curve [1]. Specifically, curve sprinting maximum velocity (v_{max}) can be described by $mv^2r^{-1} = GRF_c$, where v is a function of an athlete's mass (m), curve radius (r), and centripetal GRF (GRF_c).

Track athletes navigate different curve radii depending on lane assignment and track design, but previous studies have investigated leg-specific (inside vs. outside) GRFs on flat curves with radii smaller than those experienced by track athletes (1-6 m) [2] or only one curve radius [3]. Additionally, leg-specific GRFs may change with curve radius, as the inside leg produces greater GRF_c than the outside leg on a 37.72 m radius curve [3] but smaller GRF_c than the outside leg on 1-6 m radii curves [1]. Determining leg-specific GRFs when sprinting on curve radii typical for track athletes may also provide opportunities to improve curve sprinting performance.

We measured centripetal and vertical GRFs of the inside and outside leg during counterclockwise (CCW) and clockwise (CW) sprinting on curves with 17.2 m and 36.5 m radii, representative of the innermost lanes for a 200 m and 400 m athletics track. We hypothesized that: 1) v_{max} would decrease by ~5% from a 36.5 m to 17.2 m curve radius according to Greene [4], 2) the inside leg would produce greater GRF_c than the outside leg for both curve radii, and 3) the outside leg would produce greater vertical GRF than the inside leg for both curve radii.

Methods

9 experienced sprinters (8 M, 1 F; 200 m Personal Best (PB): 22.60 ± 2.39 s, 400 m PB: 47.76 ± 1.49 s; 74.6 ± 9.5 kg; 1.83 ± 0.10 m; 21 ± 1 yr) completed a randomized series of 40 m sprints on a flat indoor track. Athletes were instructed to perform maximal effort sprints CCW and CW along curves with radii of 17.2 m and 36.5 m. Athletes sprinted over two force plates embedded in the ground and covered with an indoor track surface that was level with the surrounding surface. Force plates and motion capture cameras were located halfway along the curve and athletes adjusted their starting position backwards to allow them to reach v_{max} in the capture volume.

We measured lower body 3D kinematics (200 Hz) and calculated v_{max} using markers on the pelvis and averaged over the capture volume (5 m). We measured 3D GRFs (1000 Hz) and transformed them so that the mediolateral axis was oriented relative to the athlete to determine GRF_c. We combined data from CCW and CW directions and calculated stance-average centripetal and vertical GRF of the inside and outside leg for both curve radii. We applied the Bonferroni correction method to each family of comparisons and set statistical significance at $\alpha = 0.05$.

Results and Discussion

On average, athlete v_{max} decreased by 7.2 ± 2.4% (0.66 ± 0.05 m/s) from the 36.5 m to 17.2 m radii curve ($p<0.01$), which was significantly different ($p<0.01$) than the 5.0 ± 0.8% change predicted by Greene [4]. The inside leg produced greater stance-average GRF_c than the outside leg on the 36.5 m radius curve ($p<0.01$), but not on the 17.2 m radius curve (Fig. 1A). Previous research suggests the inside leg produces less GRF_c than the outside leg when running on curves with a small (1-6 m) radius [1], but the opposite occurs on curves with a larger (37.72 m) radius [3]. We found a significant interaction ($p=0.03$) between curve radius and GRF_c produced by each leg, indicating that the inside and outside leg are affected differently by curve radius. v_{max} may decrease with curve radius due to the inside leg's inability to meet the increased GRF_c requirement.

The outside leg produced greater stance-average vertical GRF than the inside leg on 36.5 m and 17.2 m radii curves (both $p<0.01$; Fig. 1B). These findings indicate the inside leg may be responsible for redirecting the body's center of mass to the inside of the curve and the outside leg may be responsible for generating vertical GRF during curved sprinting. However, we found a significant interaction ($p<0.01$) between curve radius and stance-average vertical GRF for each leg, where the difference between legs increased as radius decreased from 36.5 m to 17.2 m.

Changes in the ankle's frontal plane kinematics and plantarflexor moment generation may be responsible for changes in centripetal and vertical GRF production during maximal effort sprinting [2]. We intend to investigate the ankle's frontal plane kinematics as a potential mechanism that modulates the ability of plantarflexors to produce the necessary centripetal and vertical GRF during curve sprinting.

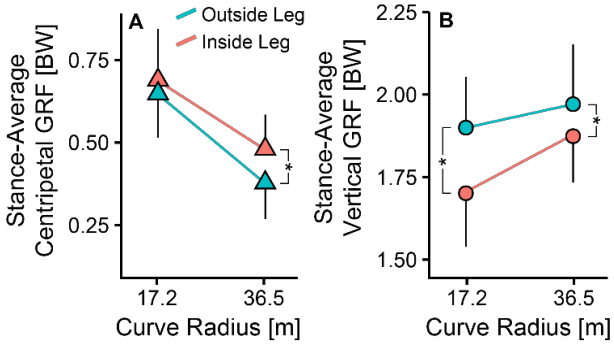

Figure 1. A) The inside leg had greater stance-average centripetal ground reaction force (GRF) on the 36.5 m radius curve (*$p < 0.01$), but not on the 17.2 m radius curve ($p = 0.3572$) compared to the outside leg. B) The outside leg had greater stance-average vertical GRF for both curve radii compared to the inside leg (*$p < 0.01$).

Significance

The inside and outside legs exhibit different biomechanics when sprinting at v_{max} along curve radii typical for track athletes. Considering the relationship between centripetal GRF and curve v_{max}, athletes could improve performance by increasing the inside leg's centripetal GRF and the outside leg's vertical GRF on a flat curve. This could be accomplished by strengthening the plantarflexors under various degrees of ankle eversion/inversion.

References

[1] Luo & Stefanyshyn (2012). *J Biomech,* **45**: 2763-8.
[2] Chang & Kram (2007). *J Exp Biol,* **210**: 971-82.
[3] Churchill et al. (2016). *Scand J Med Sci Sport,* **26**: 1171-9.
[4] Greene (1985). *Biomech Eng,* **107**: 96-103.

REAL-TIME ANKLE PLANTARFLEXOR MOMENT ESTIMATION ACROSS SLOPED WALKING AND UNEVEN TERRAIN

Safoura Sadegh Pour Aji Bishe[1], and Zachary F. Lerner[1]
[1]Department of Mechanical Engineering, Northern Arizona University, Flagstaff, AZ, USA
email: SafouraSadeghpour@nau.edu

Introduction

The ankle joint plays an important role in human walking and locomotion [1], with the ankle plantar flexors contributing to vertical support and forward progression of the body [2], [3]. As such, the ankle is a frequent target for wearable robotic intervention. Seeking to meet the need for adaptive ankle exoskeleton control strategies, the primary goal of this study was to validate a practical approach for estimating the ankle joint in real-time across varied terrain.

Methods

We applied an inverse dynamics approach to estimate the ankle moment (A_m), as following:

$$A_m = I\alpha - \left(GRF_t \times MR_{GRF_t}\right) - \left(GRF_n \times MR_{GRF_n}\right) \quad (1)$$

where I is the mass moment of inertia of the foot, α is the angular acceleration of the foot, GRF_t and GRF_n are the tangential and normal ground reaction forces, respectively, and MR represents the moment arm of ground reaction forces.

First, we analyzed the primary contributions to the external biological ankle moment during walking from gait biomechanics data collected during level treadmill walking in 1 unimpaired individual. The moment contributed by GRF_n predicted the biological ankle moment with 97% accuracy during level and incline walking up to 15°, and more than 92% to the ankle moment during decline walking up to 15°; over the stance phase, the contribution from GRF_t was < 3%, while the contribution from the foot's inertial properties (Iα) was <0.001% (Fig. 1). The primary concentration of foot-ground contact occurs beneath the forefoot and heel because the arch of the foot prevents mid-foot force localization [4], [5]. Similar to computing the moment about one of two supports of a beam, the moment contribution produced by the total normal ground reaction force and average center of pressure can be computed as in Equation (2):

Figure 1. Contributions to the biological ankle moment during A) level walking, B) incline 15°, and C) decline 15°.

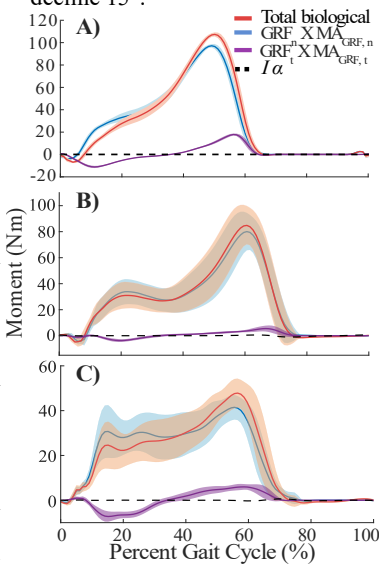

$$A_{m,est} = GRF_{n,forefoot} \times MR_{GRF_{n,forefoot}} \quad (2)$$

where $GRF_{n,forefoot}$ forefoot is the vertical normal ground reaction force applied to the forefoot and $MR_{GRF_{n,forefoot}}$ forefoot is the tangential distance between the forefoot and ankle.

We computed the relative estimated ankle moment ($A_{m,rel}$) as follow:

$$A_{m,rel} = GRF_{n,forefoot,ins} / GRF_{n,forefoot,peak} \quad (3)$$

where $GRF_{n,forefoot,ins}$ is the instantaneous normal ground reaction force applied to the forefoot during any ambulatory task and $GRF_{n,forefoot,peak}$ is the peak normal ground reaction force applied to the forefoot during walking at preferred speed.

We tested the ability of our model to appropriately adjust plantarflexion torque for level, incline, and decline with 5°, 10°, and 15° slope, as well as walking on soft (foam) and hard (2 cm tall board) uneven surfaces. Online measurements from force sensitive resistors (FSR, Tekscan) placed under each forefoot were used as inputs into a body-worn microcontroller that estimated the relative ankle moment in real-time via Eqn. 3. We recorded the kinematic and kinetic data needed to calculate biological joint moments using motion capture cameras and a split-belt treadmill. We computed the biological ankle joint moment using inverse dynamics in OpenSim for comparison to the estimated ankle plantarflexion moment.

Results and Discussion

We assessed the accuracy of our online ankle joint moment estimation model by calculating the average and peak root-mean-squared-error (RMSE) between the estimated and measured biological ankle moment across the stance phase.

The average accuracy of estimated ankle plantarflexion moment relative to the biological ankle moment was 92.7 ± 0.2% across all of the validation conditions (Table 1). There was also a very strong relationship (R = 0.97 ± 0.01) across all of the validation conditions. Our results from the validation experiment suggest that the foot-sensor-based ankle estimation model was effective for estimating the desired moment during level, 5°, 10°, and 15° incline/decline, and walking on uneven terrain.

Table *1.* VALIDATION RESULTS

Walking Condition		Prediction Accuracy (%)	Correlation Coefficient (R)
Incline	15°	97.6±0.1	0.99±0.01
	10°	96.9±0.6	0.99±0.01
	5°	96.6±0.6	0.99±0.01
Decline	15°	92.0±0.3	0.97±0.01
	10°	92.3±0.6	0.97±0.01
	5°	93.0±0.2	0.98±0.01
Foot on foam		88.2±2.5	0.95±0.02
Heel on board		89.9±7.0	0.95±0.06
Toe on board		91.5±2.5	0.97±0.02
Average		92.7±0.2	0.97±0.00

Significance

This online ankle moment estimation scheme has potential to be used in control of exoskeletons to assist individuals with neuromuscular disorders in real-time across varied terrines.

References

[1] R. Jiménez-Fabián et al, *Med. Eng. Phys,* 2012. [2] R. R. Neptune et al, *J. Biomech,* 2001. [3] S. Nadeau et al, *Clin. Biomech,* 1999. [4]A. P. Hills et al, *Int. J. Obes. Relat. Metab. Disord. J. Int. Assoc. Study Obes,* 2001. [5] E. J. Luger et al, *J. Bone Joint Surg. Br,* 1999.

TELEROBOTIC GESTURE CONTROL TO QUANTIFY BALANCE TRAINING PERFORMANCE

Ava D. Segal[1*], P.G. Adamczyk[2], A.J. Petruska[1], and A.K. Silverman[1]
[1] Dept. Mech. Engr., Colorado School of Mines, Golden, CO, USA; [2]Dept. Mech. Engr., University of WI, Madison, WI, USA
email: *asegal@mines.edu

Introduction

Dynamic balance training with a wobble board (WB) is effective for treating ankle instability and balance deficits [1,2]. However, treatment efficacy is contingent on long-term adherence to therapy programs, which remains challenging [3]. To address this problem, instrumented WB therapy with 2D feedback [2] is a goal-directed approach involving continuous, voluntary postural adjustments to actively shift attention to the movement outcome. However, instrumented therapy devices often do not easily translate to the home [4]. Affordable, uncumbersome sensors that reliably quantify balance performance could facilitate at-home rehabilitation. Although instrumented WB and force plate center of pressure (COP) velocities during static standing are strongly correlated [5], balance performance during standard dynamic WB training [1] is less established. While 2D game interfaces are promising for at-home rehabilitation, excessive screen time may be detrimental [6]. Alternatively, telerobotic biofeedback from a physical robot's movement may provide intuitive and engaging gesture-controlled therapy [7]. We explored quantifying balance training performance with gesture-controlled signals by comparing foot-mounted inertial measurement unit (IMU) sway angle and velocity to two gold-standard motion capture laboratory measurements: COP and WB angle.

Methods

Two healthy adults (21.5±0.7 yrs) provided informed consent to participate in this approved study. The gesture controller (**Fig 1A**, [8]) was secured to the dorsal side of the non-dominant foot with zero-offsets established during quiet standing on a stable surface to accommodate differences in foot mounting location. Euler angles from the IMU (pitch/roll) were calculated and transmitted wirelessly at 100 Hz. Three-dimensional motion analysis was performed with a seven-camera motion capture system (150 Hz) and COP was collected with a concealed force plate (1500 Hz). Four markers each were placed on the WB and car platform.

Telerobotic gesture control was developed by mapping IMU angle (pitch/roll) to car velocity (linear (v)/angular (ω)). The telerobotic platform (**Fig 1B**) included a robot kit (Zumo 32U4, Pololu) and dual motor drive system with quadrature encoders (12 counts/rev) for closed-loop proportional-integral speed control of each wheel. A microcomputer (Raspberry Pi 3B+) performed high level processing and IMU data acquisition.

After being instructed on system controls, participants performed two-minutes of structured practice driving the car using WB tilting motion. Next, they navigated the telerobot through a figure-eight maze for three repeated trials (**Fig 1C**).

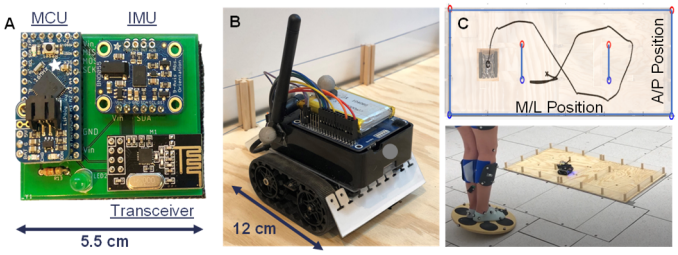

Figure 1: (A) IMU-based gesture controller (B) Telerobot (C) Car trajectory (top-down view) of a maze trial (upper) and experimental setup (lower).

This paradigm was repeated for three challenge levels in the following order: (1) with foam under the board and slow car speed response (2) no foam and slow car speed response, and (3) no foam and fast car speed response, to study the effect of varied conditions on signal validity. All trials were performed barefoot with the medial borders of the feet touching and aligned with the WB reference frame.

All data were de-meaned, filtered (4th-order Butterworth, f_c=10 Hz), and normalized by the peak of the rectified signal per trial. COP trajectories were rotated into the WB reference frame. Sway velocity was also calculated using a first order finite difference. COP and WB signals were down-sampled to the IMU sampling rate. Pearson correlation coefficients (r) were calculated for COP (X/Y), WB (mocap, pitch/roll) and IMU (gesture controller, pitch/roll) sways and velocities to assess agreement between signal pairs: IMU-COP, IMU-WB, WB-COP.

Results and Discussion

All signals were strongly correlated (**Fig 2**), with mean (±SD) sway correlations across trials and participants highest for WB-COP (r=0.93±0.08) compared to IMU-WB (r=0.92±0.08) and IMU-COP (r=0.89±0.09, all p<0.001). Velocity signals were also strongly correlated (r=0.80±0.2), albeit less strongly and more variably than sway. Correlations were similar (<3% difference) on the pitch and roll axes and across all challenge levels. The weaker correlation for IMU-COP may be related to subtle foot motion that is not reflected in COP and WB angle. Mounting the IMU directly to the WB may increase signal congruency and reduce inter-subject variation.

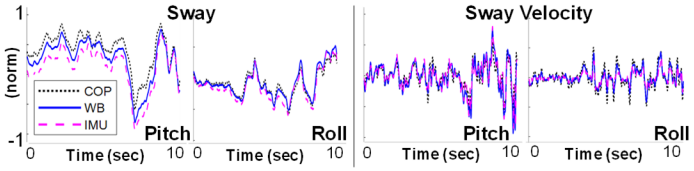

Figure 2: Representative COP, IMU and WB pitch and roll trajectories normalized to the peak rectified value per trial for the no foam fast condition.

Significance

An engaging alternative to balance therapy using gesture-control sensors with lab-level monitoring performance has potential to track remote training progress for customized at-home therapy. This approach could reduce therapy time and cost, promoting long-term adherence and efficacy.

Acknowledgments

NSF GRFP (Grant No. DGE-1646713) funded this research.

References

[1] Wester, J.U. et al, *J Orthop Sport Phys Ther,* 1996. 23(5): 332-6.
[2] Kosse, N.M. et al, *J Cyber Ther Rehabil,* 2011. 4(3): 399-407.
[3] Schneider, J.K. et al, *J Gerontol Nurs*, 2003. 29(9): 21-31.
[4] Balasubramanian, S. *Am J Phys Med Rehabil*, 2012. 91(11): S255-69.
[5] Bizovska, L. Med Eng Phys, 2017. 50: 29-34.
[6] Barlett, N.D. et al, *J Child Media*, 2012. 6(1): 37-50.
[7] Gamecho, B. et al, *J Med Syst*, 2015. 39(11): 1-11.
[8] Segal, A.D. et al, Sensors, 2020. 20(4269): 1-18.

INFLUENCE OF COGNITIVE PERTURBATIONS ON TRANSIENT CHARACTERISTICS OF BALANCE CONTROL

Cody A. Reed[1, 2] and Scott Monfort[2]
[1]Sanford Orthopedics & Sports Medicine Research, Sanford Health
[2]Department of Mechanical & Industrial Engineering, Montana State University
email: scott.monfort@montana.edu

Introduction

Initial, transient periods of destabilization following sensory transitions (e.g., closing eyes) have been reported during quiet stance balance control, which has spurred their potential association with sensory reweighting [1]. However, these transient characteristics have also been reported during eyes open stance when no sensory transition was present (**Figure 1**). It was speculated that the persisting transient behavior during eyes open stance (i.e., without a sensory transition) may be due to a cognitive perturbation that resulted from participants counting down aloud to initiate trials ("3-2-1-Go") [1].

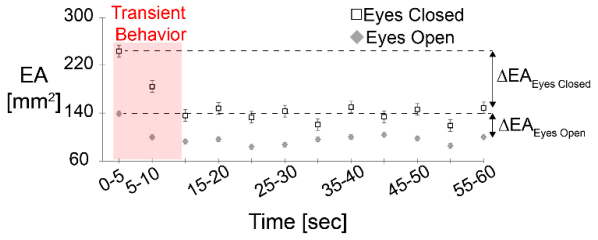

Figure 1: Ellipse area (EA) data over 60-second quiet stance trials immediately following eyes closure or keeping eyes open [1].

To better understand the utility of transient characteristics for assessing balance control, research is needed to elucidate driving factors for non-sensory aspects of transient behavior during quiet stance. Therefore, the purpose of this study was to investigate the influence of cognitive perturbations on transient characteristics of balance control. We hypothesized that cognitive perturbations would introduce transient behavior during quiet stance compared to no cognitive perturbation.

Methods

Twenty healthy, younger adults (22.4 ± 2.1 years, 72.2 ± 10.7 kg, 1.80 ± 0.15 m, 13 males/7 females) had their postural control assessed during eyes open quiet stance. Center of pressure was recorded using a Bertec balance plate for a total of 100 seconds per trial. The initial 40 seconds was used to introduce a cognitive perturbation of three different levels. Specifically, participants first stood quietly for 30 seconds and then had a period of 10 seconds of either 1) no cognitive perturbation present (**NO**), 2) did serial subtraction by ones (**LO**), or 3) did serial subtraction by sevens (**HI**). Upon completion of the 10-second period, participants stood quietly for 60 seconds, which was the period of focus for the CoP analysis. Three trials were completed for each condition, with the order of conditions block randomized.

95% confidence ellipse area (EA) was calculated for 5-second epochs throughout the trial [1]. EA epoch estimates were transformed by taking their natural logarithm to obtain normally distributed statistical model residuals. The difference in EA from the first epoch following the cognitive perturbation to the last epoch of the trial (i.e., 55-60 seconds after perturbation) was used to characterize transient postural control behavior. This transient measure (**ΔEA**) was used as the dependent variable for statistical analyses. A general linear model was used to test for relative differences in ΔEA between NO, LO, and HI conditions. 'Condition' and 'Trial Number' were considered fixed effects. Cohen's d effect sizes (ES) were also calculated.

Results and Discussion

The general linear model demonstrated a significant 'Condition' effect for ΔEA (p=0.006). Tukey post-hoc tests identified significant pairwise differences between both cognitive perturbation conditions relative to the NO condition, but not a significant difference between the LO and HI conditions [NO vs. LO: ES=0.44 **(p=0.047);** NO vs. HI: ES=0.58 **(p=0.007)**; LO vs. HI: ES=0.13 (p=0.771)]. These results suggest that intentional and/or unintentional cognitive tasks that are used to initiate balance trials (e.g., participants counting down) can introduce transient effects into quiet stance balance trials.

Additional insight is gained by comparing the ΔEA measure across several populations and perturbations from this and previous work (**Figure 2**) [1]. Cognitive tasks (i.e., counting) elicited a significant transient response. A sensory perturbation of closing one's eyes in addition to a counting task was associated with larger transient effects. Notably, these transient effects were more pronounced in older adults (83.5±8.4 years) than in young adults (24.9±3.9 years) [1]. Collectively, existing data support the utility of transient measures for detecting differences in how individuals initially adapt to changing sensory [1], cognitive, and stance conditions [2]. Notably, the transient measures have consistently been largely unrelated to traditional whole-trial estimates [1, 2], which supports their ability to provide unique information in assessing an individual's balance control.

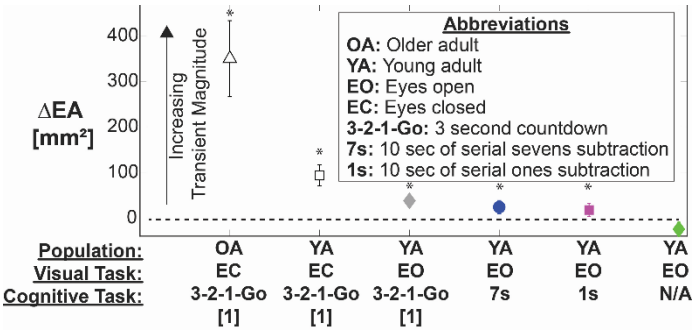

Figure 2: Magnitudes of transient effects (indicated by ΔEA) across populations, visual conditions, and cognitive conditions.

Significance

Our findings suggest cognitive perturbations are a plausible explanation for the remnant transient behavior observed during quiet stance without sensory perturbations. These findings are significant because they 1) demonstrate the utility for transient measures to quantify responses to cognitive perturbations, and 2) provide methodological guidance for researchers to be aware of the confounding role that (un)intended cognitive tasks can have on transient characteristics of balance control.

References

[1] Reed et al., *PLOS ONE,* 2020. 15(8):e0237246.
[2] Žiga et al., *J Biomech*, 2020. 110195

SEASONAL EFFECTS ON GAIT AND POSTURE IN WILDLAND FIREFIGHTERS

Lukas Krumpl[1], Samantha Brooks[1], Ann Brown[1], Christopher Alfiero[1], Youngmin Chun[1], Nickolai Martonick[1], and Joshua P. Bailey[1]
[1]Department of Movement Sciences, University of Idaho, Moscow, ID, USA
email: *lkrumpl@uidaho.edu

Introduction

Wildland firefighters (WLFFs) experience extreme weather, temperature, and terrain conditions at work. During their time on duty, WLFFS are exposed to uneven, steep terrain and heavy equipment strapped to their backs [5]. Injuries among WLFFs commonly occur due to falls, slips, and trips and to the lower extremities [3]. Thus, research in WLFFs has focused on fatalities due to accidents, rather than biomechanical factors as injury causes [2]. Meanwhile, greater trunk inclination in response to graded walking and carrying a load, common in WLFF, has been a well-established adaptive mechanism [1]. However, increased trunk flexion may lead to muscular strain in the shoulders and lower back [1]. With a WLFF season lasting up to nine months, repetitive stress on the back may lead to chronic issues. Gait analyses using 3D motion capture could provide valuable insight into kinematic adaptations of WLFFs in response to their season demands. Yet, biomechanical studies investigating potential mechanical injury risk factors and prevalence in this population are rare, specifically across an entire season, including post-season and off-season. Thus, the purpose of the present study was to evaluate whether the season can influence gait kinematics and posture in wildland firefighters.

Methods

Three laboratory sessions were structured around a WLFF season (pre-season, post-season, off-season). Fifteen healthy male WLFFs participated in the present study (25.9 yrs (±5.5), 179.4 cm (±6.6), 88.3 kg (±16.0)). No significant differences in body mass were found between data collection sessions. Participants were instrumented with a full-body reflective marker set. A fire-line gear backpack (mass = 58 lbs) was placed on the individuals and secured around their midriff with a buckle clip. Participants then completed two 5-minute walking trials at 5% and 10% grade on a motorized treadmill set at 1.34 m/s. Motion capture data were collected at 250Hz using an 8-Vantage camera system (VICON). Two 20-second trials, separated by two minutes, were collected for each grade condition. Motion capture data were imported to Visual3D for further processing. A 6 Hz low-pass Butterworth filter cut-off was applied to the marker trajectory data. For each session and grade condition, data were reduced to five consecutive strides of the right limb and then extracted. Right foot strikes were visually identified by the same researchers. Dependent variables (stride length and stride frequency for gait; trunk inclination at foot strike for posture) were analysed with two-way repeated measures ANOVA. Alpha level was set at .05. All statistical analyses were completed via SPSS version 25.0 (IBM, Armonk, NY).

Results and Discussion

The main finding of the present study was that a WLFF season did not have an effect on gait or posture. There were no significant differences in stride length and stride frequency, or trunk inclination between each of the visits for both grade conditions (Table 1).

Table 1. Gait and posture data by grade at each session (means ± SD)

	Pre	Post	Off
5% Grade			
Trunk inclinations mean (°)	25.9 ± 5.2	22.4 ± 4.1	28.4 ± 11.0
Trunk inclination peak (°)	29. 4± 5.5	25.9 ± 4.4	31.4 ± 10.4
Stride length (m)	1.5 ± 0.1	1.5 ± 0.1	1.5 ± 0.1
Stride frequency (spm)	54.1 ± 2.7	54.0 ± 2.5	53.6 ± 3.2
10% Grade			
Trunk inclination mean (°)	33.2 ± 6.7	29.0 ± 5.5	32.3 ± 8.0
Trunk inclination peak (°)	37.8 ± 7.3	33.2 ± 5.9	36.8 ± 9.0
Stride length (m)	1.5 ± 0.1	1.5 ± 0.1	1.5 ± 0.1
Stride frequency (spm)	54.7 ± 3.3	54.7 ± 3.6	54.4 ± 3.8

°= degrees of trunk flexion, m= meters, spm= strides per minute

However, grade had a significant effect on both stride length ($p<0.001$) and stride frequency ($p=0.002$), as well as mean and peak trunk inclination at foot strike ($p<0.001$ & $p<0.001$, respectively) regardless of WLFF season and participant visit (Table 2).

Table 2. Collective gait and posture data at each grade (means ± SD)

	5% Grade	10% Grade
Trunk inclination mean (°)	25.5 ± 7.7	31.5 ± 6.9†
Trunk inclination peak (°)	28.8 ± 7.5	36.0 ± 7.6†
Stride length (m)	1.5 ± 0.1	1.4 ± 0.1†
Stride frequency (spm)	53.9 ± 2.7	54.6 ± 3.5†

†$p<0.05$ shows significant difference between the two conditions
°= degrees of trunk flexion, m= meters, spm= strides per minute

A trend to increased trunk flexion was found at the post-season visit compared to pre-season. However, as WLFFs may be exposed to continuous biomechanical stress throughout their season, this implies that any sustained detrimental effects on posture or gait were short-lasting or merely did not occur. Participants adapted to the 10% grade by taking shorter and more frequent strides, yet it was reported that longer steps and a lower step frequency at graded walking may be beneficial for WLFFs to decrease metabolic cost [4]. Whether these adaptations, both in terms of stride and posture, happen on the field as well as in the lab has yet to be observed.

Significance

This study was the first to evaluate the impact of a fire-line gear pack on WLFF walking posture and gait throughout a season. Findings suggest that WLFFs respond to changes in grade with expected gait and postural adaptations [1]. However, long-term effects on injury risk of these responses remain unidentified. Thus, future research should focus on the occurrence of lower extremity and low back injuries due to kinematic and postural adaptations in response to changes in grade.

References

[1] Attwells et al. (2006). Ergonomics, 49(14), 1527-1537.
[2] Britton et al. (2013). Am J Emergency Med 31(2), 339-345.
[3] Moody et al. (2019). Int J Wildland Fire, 28(6), 412-419.
[4] Shannon (2013). CSU Fullerton.
[5] Strang et al. (2018). Scholar Works UMT.

KINEMATIC ASSESSMENT OF STAGES OF A GRADED EXERCISE TEST

Lukas Krumpl[1], Youngmin Chun[1], Nickolai Martonick[1], and Joshua P. Bailey[1]
[1]Department of Movement Sciences, University of Idaho, Moscow, ID, USA
email: *lkrumpl@uidaho.edu

Introduction

The use of treadmills in research provides the ability to control both speed and grade. Thus, studies have focused on evaluating biomechanical differences and similarities of various speeds and grades [3]. However, most studies investigating the effects of different speeds and grades on running biomechanics included separate trials, allowing for breaks and adjustments between conditions [2]. A graded exercise test (GXT), commonly used to evaluate cardiorespiratory fitness, does not allow for breaks between stages, and is accompanied by changes in speed and/or grade. Thus, an individual is tasked with adapting to these changes quickly, and, as the test progresses, make these adaptations in a state of perceived fatigue. Not much is known about changes in gait mechanics during a continuous GXT. Thus, the purpose of the present study was to observe mechanical gait parameters during consecutive stages of a continuous GXT.

Methods

Ten healthy males, running a minimum of 5 miles per week, participated in the present study (33.6 yrs (±11.2), 179.5 cm (±6.0), 70.0 kg (±6.4)). Participants were instrumented with a full body reflective marker set. Following a 5-min self-selected warm-up, the participants started the GXT on a motorized treadmill (Woodway). The GXT was comprised of 3-min running stages at progressively higher speeds. The initial grade was set to 1% to mimic over-ground running and the speed was set between 2.235 and 2.681 m/s, depending on past racing performances. Speed then increased by 0.447 m/s per stage until a speed of 5.36 m/s (max. speed) or ventilatory threshold 2 (VT^2) was observed, at which point the grade was increased by 2%. Metabolic data were used to identify VT^2. VT^2 was indicated by a concomitant increase in VE/VO_2 and VE/VCO_2. Participants continued running until volitional fatigue. Motion capture data (250 Hz) were collected using an 8-Vantage camera system (VICON) and analysed via Visual3D, using a 6 Hz low-pass Butterworth filter. Runners who completed 5 GXT stages (increase in speed at stages 1-4 and grade at stage 5) were included in the analysis. For each GXT stage, right ankle, knee, and hip flexion/extension angles were computed at three different running gait cycle events (Foot strike [FS], Mid stance [MS], and Toe Off [TO]). All events were visually identified by the same researcher. Dependent variables (joint angles at each event) were then analysed with multiple repeated measures ANOVA. Significant main effects were further investigated with pairwise comparisons (Bonferroni). Alpha level was set at .05. Statistical analyses were completed via SPSS (v. 25.0).

Results and Discussion

Statistical analyses revealed significant main effects across all stages for hip flexion at FS, MS, hip extension at TO (both $p < .05$), and ankle plantarflexion at TO ($p < .01$). Hip flexion at FS and MS, hip extension at TO, and ankle plantarflexion at TO significantly increased as the GXT progressed. Significant main effects and individual (per stage) post-hoc analysis results are displayed in Figure 1.

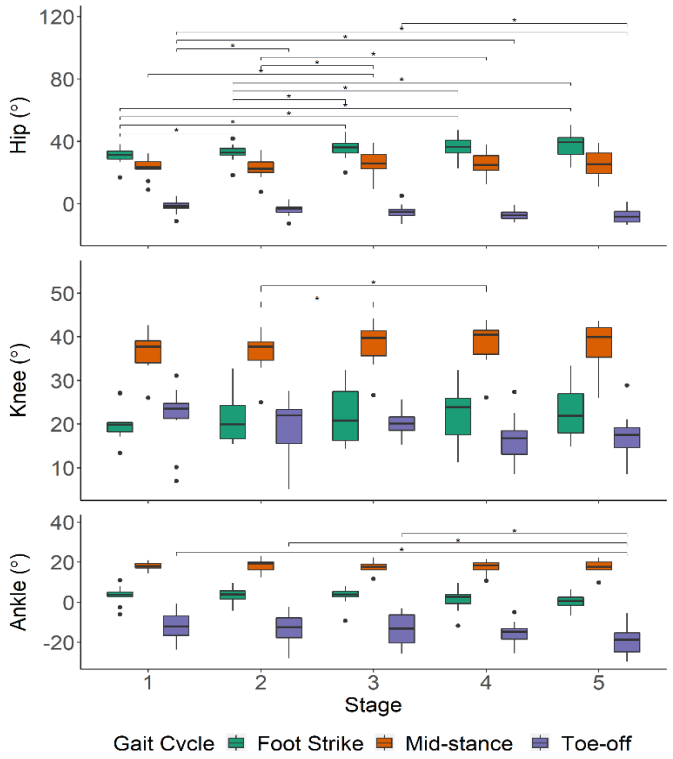

Figure 1. Hip and knee flexion and extension, and ankle plantarflexion (-) and dorsiflexion (+) angles (in degrees) at each stage of the GXT, separated by running gait events. Boxplots display range and median values. Significant differences ($p < .05$) are marked with a line and outliers are represented by dots.

To adapt to changes in speed (stages 1-4) and grade (stage 5), participants primarily adjusted their hip flexion and extension, and plantarflexion angles. These gait strategies and angle values align with data collected in trials evaluating the kinematic effects of different treadmill speeds and grades [1,2]. This finding suggests that habitual runners adapt to changes in speed and grade in a state of perceived fatigue, just as much as individuals who received breaks and acclimatization time between trials.

Significance

To the knowledge of the authors, the present study was the first to assess running gait kinematics during a continuous GXT. The observations from each joint at each specific gait event add valuable data to the body of running gait literature and may be used as reference values for future investigations regarding kinematic analyses of a GXT. However, additional research is required to evaluate whether gait adaptations in response to consistent increases in running speed or grade are biomechanically beneficial strategies to maximize treadmill running economy and performance.

References

[1] Khassetarash (2020). S J Med & Sc in Sp, 30(9), 1642-1654.
[2] Swanson (2000). Med & Sc in Sp & Ex, 32(6), 1146-1155.
[3] Van Hooren (2020). Sports Med, 50(4), 785-813.

HUMAN-IN-THE-LOOP OPTIMIZATION OF A VARIABLE DAMPING CONTROLLER FOR ENHANCED PHYSICAL HUMAN-ROBOT INTERACTION

Fatemeh Zahedi, and Hyunglae Lee*
School for Engineering of Matter, Transport and Energy, Arizona State University
email: *hyunglae.lee@asu.edu

Introduction

Addressing the trade-off between stability and performance (agility and user-effort) has been an important issue in physical human-robot interaction (pHRI). Previously, we developed a variable damping controller (VDC) that manipulates the damping component of an impedance/admittance controller based on the human user's intent of movement. The study showed that the VDC could significantly enhance the trade-off in pHRI [1].

Here, we present a human-in-the-loop optimization of the VDC using Bayesian optimization with Gaussian processes to reduce the lengthy tuning process by adjusting a key parameter of the VDC based on real-time evaluation of human performance.

Methods

The VDC changes robotic damping (b_r) from negative (energy injection) to positive (energy dissipation) based on the user's intent of motion. When the user intends to initiate and accelerate the motion, lower b_r is desirable to enhance agility; conversely, when the user intends to decelerate and end the motion, higher b_r is desirable to assist stabilization.

One of the most important parameters in the VDC is the lower bound of the robotic damping (b_{lb}). Overall performance of the coupled human-robot system is highly sensitive to the selection of b_{lb}, and thus it is important to carefully select this key parameter. Previously, this parameter was determined after running a separate tuning process, which was a lengthy experimental procedure requiring hundreds of trials [2]. Further, the tuning process only considered stability and neither agility nor user effort were considered. To overcome this limitation, we proposed a human-in-the-loop optimization of the VDC using Bayesian optimization with Gaussian processes.

In the Bayesian optimization approach, the optimal b_{lb} is determined based on real-time evaluation of human performance that integrates stability, agility, and user effort metrics. Stabilization time, defined as the duration to complete the reaching task after first hitting the target, was used to quantify the stability. Mean speed and mean root-mean-squared interaction force were calculated to quantify agility and user effort, respectively. The optimization was initiated with 5 iterations with different values of b_{lb} in the range of [-50, -5] Ns/m. After the initialization, the objective function ($f(x)$), defined by the linear combination of the three performance metrics, was evaluated using Gaussian processes, where $x = b_{lb}$. Given the calculated $f(x)$, the next sample of b_{lb} was selected by maximizing its expected improvement. With the new sample b_{lb} added to the existing data set, the $f(x)$ was refined to select the next sample of b_{lb}. This process was repeated until b_{lb} did not change for at least 5 consecutive iterations. Gaussian process was represented by mean and covariance functions, and their hyperparameters were determined at each iteration by maximizing log marginal likelihood of the collected data $\{x, f(x)\}$.

Three young, healthy subjects (2 males, 1 female, age: 21-30, weight: 50-75 kg) participated in this study, which was approved by the Institutional Review Board of Arizona State University.

Subjects completed a typical target reaching task in seated while holding the handle connected to the end-effector of the robotic arm (LBR iiwa R820, KUKA, Germany). The target reaching task was constrained in the horizontal plane in this pilot study. Each subject performed repeated target reaching trials until the optimal b_{lb} for the VDC was determined based on the Bayesian optimization with Gaussian process explained above. Each iteration consisted of 10 reaching trials.

Results and Discussion

For each subject, the optimal parameter b_{lb}, balancing the performance metrics of stability, agility, and user effort, was found in less than 6 iterations. With 5 iterations of initialization, it took less than 11 iterations (110 trials). In comparison, the previous study required 240 trials just for the separate tuning session to find the fixed b_{lb} [2]. In this study, the optimal value for b_{lb} ranged from -15 to -5 Ns/m (Table I).

The proposed Bayesian optimization approach was effective in enhancing the overall performance of pHRI in all tested subjects. Compared to the previous study using the fixed b_{lb} [1], determined by the separate lengthy tuning process [2], each subject showed significant improvement in the stability and user effort (i.e., stabilization time and mean interaction force, respectively). While a slight decrease in agility (mean speed) was observed, it was not substantial (-3.5% when averaged across the 3 subjects) (Table I). When all three performance metrics were averaged, each subject showed at least about 22% of improvement with the proposed approach compared to the previous results [1, 2].

Table I. Optimal b_{lb} and percentage improvement of each performance metric with the Bayesian optimization approach compared to the previous study [1, 2].

	Optimal b_{lb} (Ns/m)	***Stabilization Time***	***Mean Speed***	***Mean RMS Interaction Force***
Subject 1	-5.0	98.2%	-0.2%	14.4%
Subject 2	-10.0	72.7%	-7.2%	15.0%
Subject 3	-15.0	50.6%	-3.0%	18.1%

Significance

The proposed human-in-the-loop optimization approach could optimize the trade-off between stability, agility and user-effort while minimizing the experimental procedure. Its extension to multi-dimensional variable impedance/admittance controllers will significantly enhance the overall performance of the human-robot systems in many pHRI applications including robot-aided biomechanics and motor control studies, robotic assistance and rehabilitation.

Acknowledgments

Research supported by NSF awards #1846885 and #1925110.

References

[1] T. Bitz, et al, "Variable Damping Control of a Robotic Arm to Improve Trade-off between Agility and Stability and Reduce User Effort," *IEEE Int'l Conf. Robotics and Automation (ICRA)*, Paris, France, 2020.

[2] F. Zahedi, et al., "Regulation of 2D Arm Stability against Unstable, Damping-Defined Environments in Physical Human-Robot Interaction," *IEEE/RSJ Int'l Conf. Intelligent Robots and Systems (IROS)*, Las Vegas, 2020

PREDICTION OF GROUND CONDITIONS DURING POSTURAL BALANCE USING DEEP LEARNING

Vu Phan[1], Hyunglae Lee[1]
[1]School for Engineering of Matter, Transport and Energy, Arizona State University, Tempe, AZ USA
Email: Hyunglae.Lee@asu.edu

Introduction

Recent years have witnessed an increasing number of studies applying machine learning (ML) to predict/diagnose balance impairment caused by neuromuscular diseases, such as Parkinson's disease or multiple sclerosis [1, 2]. Meanwhile, the prediction of dynamically challenging ground conditions, such as those are compliant and unstable, during postural balance is also critical. The reason is that (1) those ground conditions are common in daily life, and (2) even healthy individuals' balance can also be severely suffered. However, little is known if ML can be applied for such a goal. Moreover, different to the diagnosis purpose, in the context of standing on challenging grounds, the prediction often demands not only high accuracy but also quick response to changes of environments, bringing a huge challenge to traditional ML models. This is because these models normally utilize stability measures as features to learn while these measures were not developed to characterize postural stability behaviors observed from short-time periods.

Therefore, the primary purpose of this study is to prove that deep learning (DL) can overcome this difficulty by learning more efficient features by itself. We hypothesized that DL could outperform traditional ML with small segmented data.

Methods

Fourteen young healthy subjects provided informed consent before participating in this ASU IRB approved study. A dual-axis robotic platform [3] was utilized to simulate different challenging ground conditions, namely rigid, compliant, and highly compliant. Each subject was asked to perform 45-second trials of quiet stance on the robotic platform with eyes-open. A force plate placed on top of the robotic platform recorded the subjects' center-of-pressure (COP) during each trial.

The COP data were then segmented with 0.5-, 1-, 2.5-, and 5-second window sizes and labelled based on the compliant ground undergone by the subjects, producing different datasets. This is aimed to determine the optimal window size for the classification performance of the DL model. A convolutional neural network (CNN), containing 1D convolution layers, were trained to learn predicting the ground conditions to which the subjects were exposed. For comparison, traditional ML models, including multi-layer perceptron (MLP), support vector machine (SVM), and decision tree (DT) were also trained with seven common stability features extracted from the dataset with the optimal window size. Those seven features included anterior-posterior/medio-lateral displacements, COP path length, time-to-boundary (TTB), and sway area. For performance evaluation, the datasets were divided into 80% for training and 20% for testing. One-way ANOVA with the Turkey post-hoc test was used to find statistical significances of training and testing performances.

Results and Discussion

The results revealed that the DL performance was improved significantly as the window size was increased from 0.5 to 2.5 seconds ($p < 0.001$) but not from 2.5 to 5 seconds ($p = 0.972$ for training and 0.679 for testing), see Figure 1.

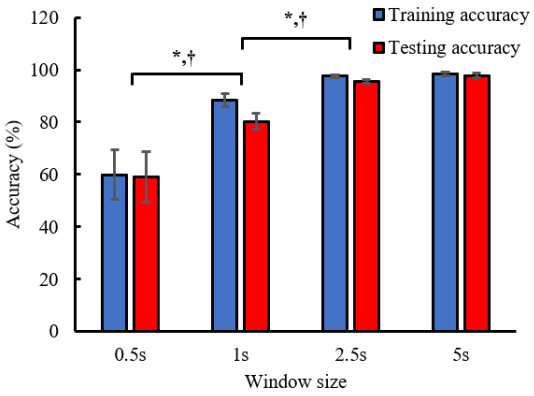

Figure 1: Classification performance of the CNN model according to different window sizes. Of note, * and † shows statistical significances found in training and testing accuracy, respectively.

Table 1: Classification performance, represented by mean (standard deviation), of different models using the 2.5-second window size dataset.

Accuracy	CNN	MLP	SVM	DT
Training (%)	97.56% (0.63%)	92.04% (1.26%)	90.25% (2.36%)	86.00% (1.41%)
Testing (%)	95.54% (0.79%)	73.80% (2.45%)	76.67% (2.80%)	63.70% (3.16%)

Besides, as hypothesized, the CNN model outperforms the others in both training and testing ($p < 0.001$), given the optimal window size of only 2.5 seconds, see Table 1. This may be due to its capability of efficiently learning highly non-linear features of the COP dynamics, which cannot be achieved by common stability measures used in assessments of postural balance. It should be noticed that, for those measures to capably characterize human postural stability under compliant grounds, Haibach et. al. [4] recorded COP data up to 1 minute of standing for each trial. This explained the poor performance of the common ML models as the window size was drastically reduced to only 2.5 seconds.

Significance

This study presented the possibility of deploying DL to predict challenging ground conditions during postural balance rapidly and accurately. Further, it suggested that complex features extracted by hidden layers of the DL model could also be used as a novel effective stability measure for multiple purposes of postural stability assessment. Future work should assess the performance of DL on data from wearable devices.

Acknowledgments

This work is funded by the Global Sport Institute of the adidas and Arizona State University (ASU) Global Sport Alliance.

References

[1] Y. Li, et. al. J. Biomech., 113, 110073, 2020.
[2] R. Sun, et. al. Sci. Rep., 9, 16154, 2019.
[3] V. Nalam, et. al. IEEE ASME TMECH, 24, 459 - 470, 2019.
[4] P. S. Haibach, et. al. Exp. Brain Res., 177, 471-482, 200

STANDING POSTURAL BALANCE UNDER MULTI-DIRECTIONAL PERTURBATIONS

Vu Phan[1], Lauren Berrett[1], and Hyunglae Lee[1]
[1]School for Engineering of Matter, Transport and Energy, Arizona State University, Tempe, AZ USA
Email: Hyunglae.Lee@asu.edu

Introduction

It is not uncommon that, in daily activities, individuals experience challenging environments, such as those are compliant or oscillatory, which may lead to falls and harmful consequences. Hence, it is critical to understand how perturbations caused by those environments affect postural balance. Based on that, the development of therapeutic training and assistive devices could be advanced to avoid fall risks. Given that importance, several studies investigated postural balance under compliant grounds using foam surfaces [1] or under oscillatory environments simulated by moving platforms [2]. However, those replicated environments were solely available for assessments of postural balance in one direction (1D), i.e., vertical in [1] and anterior-posterior (AP) or medio-lateral (ML) in [2]. Yet perturbations commonly happen in multiple directions in real life, and their effects on postural balance remain unknown.

Therefore, the main purpose of this study is to investigate the impacts of compliant and oscillatory environments simulated in multiple directions (i.e., both AP and ML at the same time) using our developed platform. We hypothesize that human postural balance is severely worsened as the compliance or oscillatory frequency/amplitude of the ground increase.

Methods

Following the ASU IRB approval, sixteen and fourteen young healthy subjects, under 30, were recruited for the passive and active perturbation study, respectively. A dual-axis robotic platform [3] was utilized to simulate perturbations. Regarding the passive perturbation study, the platform was set up to simulate different compliant grounds, namely rigid, compliant, and highly compliant. For the active perturbation study, sinusoidal oscillations with varying frequencies (i.e., 0.5, 1, and 1.5 Hz with a constant amplitude of 1 degree) and varying amplitudes (i.e., 0.5, 1, and 1.5 degrees with a constant frequency of 1 Hz) were simulated. The perturbations were generated in AP and ML directions simultaneously (i.e., 2D perturbations). All subjects were required to perform quiet stance trials with eyes-open. Center-of-pressure (COP) displacements of subjects were measured by a force plate located on top of the platform.

The COP data were then low pass filtered with a cutoff frequency of 10 Hz. A relatively new stability measure, named virtual time-to-contact (VTC) was adopted for the postural balance assessment [1]. VTC predicts the average amount of time needed for the COP to reach the base of support. Thus, a reduction in VTC indicates an increase in postural instability. A Friedman test was used to determine the impacts of the perturbations, followed by a Wilcoxon signed-rank test for pair-wise comparisons.

Results and Discussion

Our results highlighted that an increase of the ground compliance significantly degraded postural standing balance ($p < 0.001$). This is consistent with Haibach et. al. [1] although different compliant environments were simulated. Statistical significances were also found in all pair-wise comparisons between compliant grounds, see Figure 1A. Regarding the active perturbation study, both varying frequencies and amplitudes were found to cause a significant deterioration in postural standing stability, represented by decreases in VTC as the oscillatory frequency or amplitude increased ($p < 0.001$). Similar results were observed by Nawayseh et. al. [2] but with the 1D oscillatory perturbation. Moreover, all pair-wise comparisons were significantly different, see Figure 1B and C. Together, we concluded that both active and passive perturbations have negative effects on postural standing stability regardless of perturbation directions.

Significance

This study illustrated that 2D perturbations have severe impacts on human postural balance. It also suggested that VTC can be an effective stability measure to assess postural standing stability under challenging environments, like ones with ground compliance or oscillation presented in this study. Future study should include more subjects and evaluate benefits of balance assistive devices on postural stability under those environments.

Acknowledgments

This work is funded by the Global Sport Institute of the adidas and Arizona State University (ASU) Global Sport Alliance.

References

[1] P. S. Haibach et. al., Exp. Brain Res., 177, 471-482, 2007.
[2] N. Nawayseh et. al., JSV, 298, 725-754, 2006.
[3] V. Nalam, et. al. IEEE ASME TMECH, 24, 459 - 470, 2019.

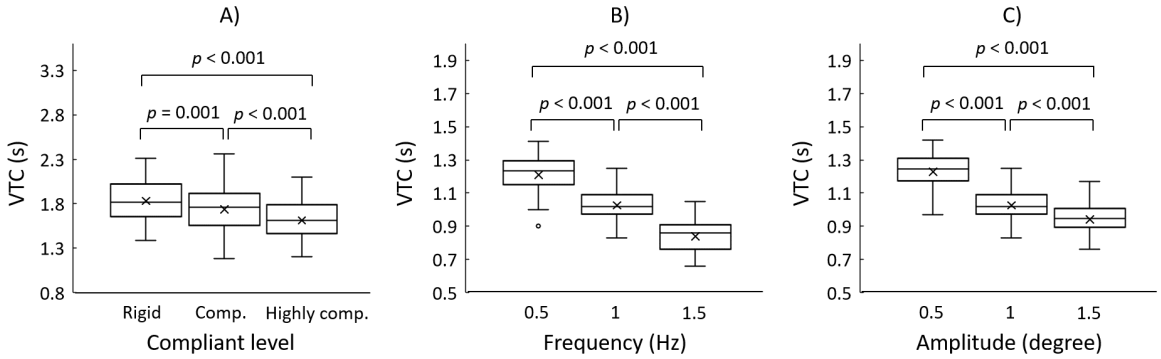

Figure 1: ***Passive perturbation study*** *(i.e., compliant ground)*: A) Impacts of 2D compliant environments on VTC. ***Active perturbation study*** *(i.e., oscillatory ground)*: Impacts of 2D oscillatory perturbations with B) varying frequencies and C) varying amplitudes on VTC.

INTERMITTENT SWITCHING RATE AS A MEASURE TO ASSESS IMPACTS OF PARKINSON'S DISEASE AND A SECONDARY COGNITIVE TASK ON POSTURAL BALANCE

Vu Phan[1], Daniel S. Peterson[2,3], and Hyunglae Lee[1]
[1]School for Engineering of Matter, Transport and Energy, Arizona State University, Tempe, AZ USA
[2]College of Health Solutions, Arizona State University, Phoenix, AZ USA
[3]Phoenix VA Medical Center, Phoenix, AZ USA
Email: Hyunglae.Lee@asu.edu

Introduction

The balance impairment of people with Parkinson's disease (PwPD) has been known as a major cause of their chronic disability, costing a vast amount of money for treatment, and permanently affecting not only their life but also their family's. Hence, studying postural balance control of PwPD is necessary to understand and prevent fall risks in this population.

Recently, stability measures derived from underlying human control systems have been explored. These measures enable explanation of postural stability linked to brain function [1, 2], facilitating us to gain deeper insights into human postural control. One study conducted by Perera et. al. [2] utilized the intermittent switching rate (ISR) of postural sway and observed a noticeable reduction of ISR in severe PD compared to healthy people. However, it remains unknown if ISR will retain the same performance with the mild-to-moderate PD population. Besides, it is ubiquitous that individuals, including PwPD, do a cognitive task while standing in daily activities. Completing both tasks simultaneously often worsen the performance of at least one. However, little is known about how that situation impacts ISR.

In this study, we investigated the impact of PD and dual tasking effects on ISR of postural sway. We hypothesized that this measure can capably examine the effects of mild-to-moderate PD as well as the secondary cognitive task.

Methods

Following ASU IRB approval, fourteen PD and thirteen healthy control (HC) subjects, over 55 years old, were recruited. The PD subjects had no injuries or neurological diseases other than mild-to-moderate balance impairment caused by PD. All subjects were asked to perform single-task (i.e., quiet stance), followed by dual-task trials (i.e., quiet stance with a cognitive task) on an instrumented treadmill. The auditory Stroop task was chosen as the secondary cognitive task. Each trial lasted 50 seconds and separated from others by a short break.

The center-of-pressure (COP) data were low pass filtered at 10 Hz. The resultant distance (RD) time series, defined in [3], was then computed. Afterwards, the wavelet-frequency analysis developed by Nema et. al. [1] was applied to obtain IS behaviors of subjects from both groups, see Figure 1A and B. Prominent peaks larger than a pre-defined threshold, determined based on our sensitivity analysis, were counted to yield ISR of each trial per subject. A mixed ANOVA was then utilized to examine the group (PD or HC) and task (i.e., single or dual) effects. Moreover, an independent t-test was also performed to compare the performance of PD subjects under single and dual tasking.

Results and Discussion

The results can be seen on Figure 1C. No interaction between group and task effects was found ($p = 0.054$). As hypothesized, the statistical significance was observed regarding the group effect ($p = 0.001$), such that PwPD were lower (worse) than HC. The reduction in ISR in PwPD may be due to the degradation of the sensorimotor system which has been presumed to be the root of the motor intermittency. Our result is consistent with Perera et. al. [2], and extend this work to show that mild-to-moderate PwPD also show deficits in ISR. Interestingly, the secondary cognitive task only has a modest effect on ISR of postural sway ($p = 0.437$). The pre-planned across time t-test showed a subtle and non-significant effect of dual tasking on ISR in PwPD ($p = 0.159$). This may indicate a subtle intervention of the cognitive task on sensorimotor processing of PD subjects during postural control. This should be investigated further with larger cohorts.

Significance

This study suggested that ISR could be used to examine the impact of PD but not dual tasking on postural balance. Future work should investigate other approaches to extract information from the IS behavior to efficiently characterize cognitive effects. It is also worth testing the applicability of ISR on other neurological disease populations such as multiple sclerosis.

Acknowledgments

This work was funded by ASU-Mayo Seed Grant.

References

[1] S. Nema et. al., 51, 27-40, Hum. Mov. Sci., 2017.
[2] T. Perera et. al., 141, 3009-3022, Brain, 2018.
[3] T. E. Prieto et. al., 43, 9, 956-966, IEEE TBME, 1996.

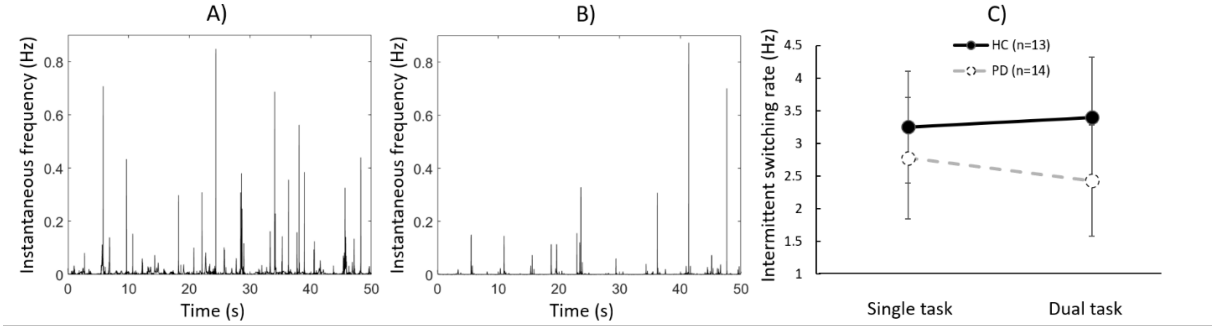

Figure 1: Intermittent switching behaviors (i.e., discontinuities) plotted in the time-frequency domain of a representative A) HC subject, and B) PD subject. C) Impact of PD a secondary cognitive task on the intermittent switching rate of postural sway.

Does Arch Height Influence Lateral Jumping?

Wendi H. Weimar[1], Brandi E. Decoux[2], Portia T. Williams[3], Randy T. Fawcett[4], and Christopher M. Wilburn[1]

[1]Auburn University, Auburn, AL
[2] Bridgewater State University, Bridgewater, MA
[3]North Carolina A&T State University, Greensboro, NC
[4]Virginia State University, Blacksburg, VA
Email: weimawh@auburn.edu

Introduction

Propulsion is an essential component of bipedalism that enables the body to progress in a directionally-specific manner. A major component in the process of propulsion surrounds utilizing the active and passive components development mechanisms that accelerate the body forward, while adapting to any changes within the terrain [1-2]. Extensive investigations have displayed that deviations from healthy MLA structural alignment produce dysfunctional and accessory motions during the propulsive phase of locomotive tasks [3-5]. However, these biomechanical differences may produce propulsive mechanisms that are beneficial for directionally-specific task. Therefore, the purpose of this study was to examine the influence of arch height on lower extremity propulsive mechanics during a lateral jumping task.

Methods

Twenty-four healthy Division I collegiate athletes (height: 1.84± 0. 06 m; mass: 91.66 ± 18.39 kg) were recruited to participate in the study (12 normal arch height, 12 low arch height). Upon obtaining foot anthropometrics to classify specific arch classifications, participants were instructed to complete a lateral jumping task [6]. The task consisted of jumping in a rhythmic sequence: jumping from the dominant leg to the non-dominant leg, non-dominant leg to dominant leg, and dominant leg to non-dominant leg (Figure 1).

Lower extremity kinematics and kinetics were analyzed during the propulsive phase of the task. Specifically, retro-reflective markers were placed bilaterally to analyze sagittal ($ankle_{sagittal}$) and frontal ankle ($ankle_{frontal}$) kinematic, sagittal plane knee kinematics($knee_{sagittal}$), and mediolateral estimated center of mass displacement (eCOM). Additionally, peak mediolateral ground reaction forces (mGRFs) were averaged and normalized to body weight.

Figure 1: Phases of the lateral jumping task. Dominant to non-dominant to dominant.
https://www.acefitness.org/education-and-resources/professional/expert-articles/5869/explosive-plyometric-workout/.

Results and Discussion

The results of a series of one-way ANOVAs presented significant differences in eCOM, and mGRFs. Results associated the lower extremity kinematic and kinetic are presented in the table below.

	Normal Arch Height *M (SD)*	Low Arch Height *M (SD)*	*df*	df_{error}	*F*	*p*
Ankle						
Plantarflexion (°)	88.55 (3.39)	90.24 (3.55)	1	23	4.67	.242
Eversion (°)	-13.96 (6.88)	-9.73 (8.59)	1	23	4.42	.688
Knee						
Flexion (°)	-63.80 (5.74)	-61.08 (8.86)	1	23	2.31	.370
Estimated Center of Mass	.17 (.03)*	.09 (.09)*	1	23	11.30	.035*
Mediolateral Ground Reaction Forces	-4.57 (4.08)*	-22.84 (16.64)*	1	23	4.47	.048*

These findings indicate that the individuals with lower arch height develop larger mediolateral forces than those with normal arches. Furthermore, individuals with lower arches also performed these tasks with less center of mass translation during stance. This suggests that the center of mass stays more in the direction of the next motion during stance, in low arched individuals.

Significance

These findings suggest a new interpretation of the efficacy of lower arches. While the collapse of the medial longitudinal arch has long been suggested as a dysfunction, these data suggest that the dysfunction may be advantageous in lateral movements. It is interesting to note the finding of larger mGRFs in individuals with lower arches, with no significant difference in plantar flexion or eversion range of motion, This combination of findings suggests that individuals with lower arches maybe able to apply a lateral force through plantarflexion and not through excessive eversion. Further research is needed to ensure that the already everted foot of individuals of lower arches is gaining lateral force from the everted calcaneus and not from an advantageous muscle length.

References

[1] Exerc. Sport Sci. Rev. 2005; 33 (2) 88-97
[2] J.Ant (1954) 88.Pt 1. 25
[3]Gait Posture. 2009; 30(3): 334–349.
[4] Gait Posture. 2008; 28(1): 29-37.
[5] Gait Posture. 2013; 38(3): 363-372
[6] JAPMA. 2008. 98(2), 102-106

PLANTAR FLEXION RESISTANCE DURING GAIT CAN ALTER H-REFLEX MODULATION IN HEALTHY ADULTS

Benjamin C. Conner[1]*, Safoura Sadegh Pour Aji Bishe[2], Brittany A. Bolusan[3], Trevor A. Irion[3], Sequoia J. LaVoy[3], Pamela R. Bosch[3], and Zachary F. Lerner[1,2]
[1]College of Medicine – Phoenix, University of Arizona, Phoenix, AZ
[2]Department of Mechanical Engineering, Northern Arizona University, Flagstaff, AZ
[3]Department of Physical Therapy, Northern Arizona University, Phoenix, AZ
email: *benjaminconner@email.arizona.edu

Introduction

Locomotion in humans involves a dynamic interplay between spinal reflexes and supraspinal modulation of those reflexes based on sensorimotor input to align with a specific task [1]. An example of this spinal reflex modulation that has been heavily studied in both healthy individuals and those with neurological injury is the Hoffman (H-) reflex. It is well known that the soleus H-reflex is highly modulated during dynamic tasks, such as walking, whereby reflex magnitudes will change in accordance with specific phases of gait [2]. Given the importance of an intact neurological system for proper reflexes, it is not surprising that there are deficits in task-dependent modulation of the soleus H-reflex for individuals with neurological injury, with many patient populations displaying exaggerated reflex responses [3-5], which likely relates to deficits in motor function.

Increased task complexity has been shown to reduce H-reflex excitability [6]. Recently, we developed an exoskeleton device that is able to provide resistance to plantar flexion during walking that is proportional to a user's real-time, estimated ankle moment. Walking with resistance necessitates increased neuromuscular engagement [7], increasing the complexity of this task. The goal of this study was to determine if walking with resistance could alter H-reflex modulation in healthy adults, which may have significant implications for improving function in those with neurological conditions.

Methods

Ten healthy adults with no known neurological conditions were recruited for participation in this study. Stimulating electrodes (Ag-AgCl) were placed in the popliteal fossa of the dominant leg for an effective stimulation of the posterior tibial nerve. Wireless surface EMG sensors were placed over the soleus for recording reflex responses. Standing H-reflex and M-wave curves were collected for each participant through delivery of 1-ms, square wave pulses at increasingly higher stimulation levels until a maximal motor response (M_{max}) was achieved (Fig. 1A).

Each participant was outfitted with an untethered, battery-powered ankle exoskeleton device that could deliver plantar flexion resistance while walking, the details of which can be found in [7]. Soleus H-reflexes were then measured during the stance phase of gait under two conditions while walking at 1.25 m/s: 1) wearing the device with no delivery of plantar flexion resistance (i.e., baseline condition), and 2) wearing the device with delivery of plantar flexion resistance (i.e., resistance condition). During the resistance condition, participants walked at a resistance level of 0.15 Nm/kg, which represents the level of resistance delivered during a user's peak estimated plantar flexor moment. Prior to H-reflex measurements, participants were given 15 minutes to acclimate to the resistance condition.

To account for the movement of stimulating electrodes on the skin relative to the underlying nerve while walking, the M-wave was monitored, and only those stimulations that resulted in an M-wave of 25 ± 10% of M_{max} were accepted. Ten reflex responses meeting this criteria were collected for each condition. H-reflex amplitudes were measured as the peak-to-peak amplitude of the raw EMG signal. To reduce inter-subject variability, mean amplitudes of each phase were normalized to M_{max} (Fig. 1C).

Results and Discussion

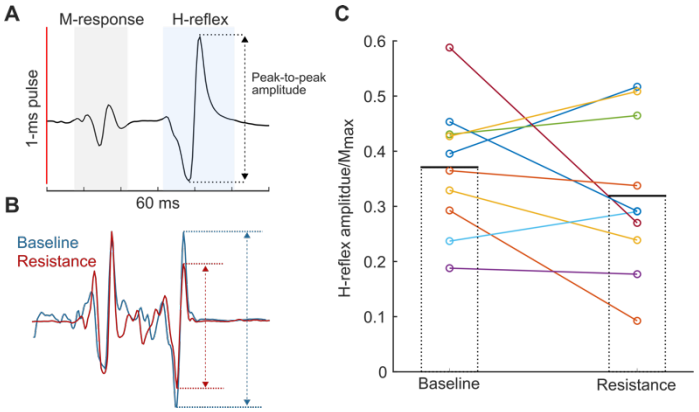

Figure 1: Representative standing (A) and stance phase (B) reflex responses; C) Group-level changes in normalized stance phase H-reflex.

Responses to plantar flexion resistance varied, with the majority (6/10) of participants displaying a decrease in stance phase H-reflex amplitude (Figs. 1B,C). While this suggests the ability of this novel device to alter H-reflex modulation, more work is necessary to determine why some participants responded differently than others. One potential explanation is the level of engagement with resistance, which may not have been uniform due to the short-term exposure and lack of acclimation to this condition. Future work will repeat these measurements after users have had ample time to acclimate to the device.

Significance

Modulation of one's reflexes during a functional task is essential for effective coordination of the nervous system. If a device could train the nervous system to better modulate one's reflexes within the functional task of walking, it could have significant implications for patient populations who lack appropriate modulation and have subsequent deficits in function.

Acknowledgments

This research was supported in part by NICHD of the NIH under Award Number 1R15HD099664. The content is solely the responsibility of the authors and does not necessarily represent the official views of the NIH.

References

[1] Rossignol et al 2006 *Physiol Rev* **86** [2] Capaday et al 1986 *J Neurosci* **6** [3] Knikou et al 2009 *Exp Brain Res* **193** [4] Hodapp et al 2007 *J Neurophysiol* **98** [5] Huang et al 2006 *J Electromyogr Kinesiol* **16** [6] Pinar et al 2010 *J Electromyogr Kinesiol* **20** [7] Conner et al 2020 *Ann Biomed Eng* **48**

REACTIVE POSTURAL RESPONSES PREDICT MUSCULOSKELETAL INJURY IN COLLEGIATE ATHLETES

Peter C. Fino[1], Amanda Morris[1], Nora F. Fino[2], Ryan Pelo[3], Daniel M. Cushman[4], Nicholas E. Monson[5], Trevor Jameson[6], and Leland E. Dibble[3]
[1]Department of Health & Kinesiology, [2]Division of Epidemiology, [3]Department of Physical Therapy & Athletic Training, [4]Division of Physical Medicine and Rehabilitation, [5]Department of Orthopaedic Surgery, [6]Department of Athletics, University of Utah
email: peter.fino@utah.edu

Introduction

The association between musculoskeletal (MSK) injuries and the *neuro*muscular system has gained attention, highlighted by a two-fold greater risk of MSK injuries in athletes after concussion compared with non-concussed teammates.[1] While the precise relationship between MSK injuries and concussions remains unknown, reactive postural responses hold promise for predicting MSK injuries in general. [2] These responses consist of short-, medium-, and long-latency components from spinal, brainstem, and cortical networks. [3] Delayed or imprecise responses may indicate an inability to prime motor patterns, integrate sensory information, and respond to disturbances. However, quantifying reactive postural responses often requires instrumentation common to biomechanics laboratories, but prohibitive in athletic training clinic settings.

Our objective was to quantify reactive postural responses in an athletic training clinic setting using inertial measurement units (IMUs), and to characterize associations between reactive postural responses and prospective MSK injuries in collegiate athletes. We hypothesized that impaired postural responses would be associated with a shorter time to MSK injury. [2]

Methods

Reactive postural responses were assessed in 182 collegiate athletes (54 % female) at the beginning of their 2019-2020 athletic season. All athletes provided informed written consent and protocols were approved by the IRB. Each athlete completed a modified version of the instrumented Push and Release (P&R) in forward, backward, left, and right directions [2]. Participants closed their eyes when in the final supported position, but could open their eyes upon release. Participants completed the P&R without (ST) and with (DT) a cognitive dual-task.

Step latency, step length, and time to stability were determined from acceleration and angular velocity data sampled at 128 Hz by IMUs (Opal, APDM Inc.) placed on the feet and lumbar spine of the participant. (Fig. 1). [2]

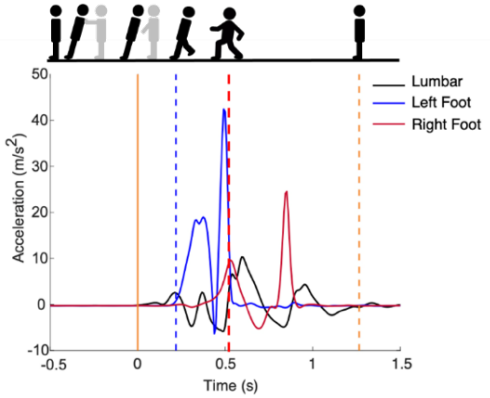

Figure 1: Example of IMU data from a single subject. The black and grey figures represent the participant and administrator, respectively. Support was released at time 0 (solid orange). Step latency (blue dashed line), zero velocity instant of first step (red dashed line) and time to stability (orange dashed line) are marked.

One IMU was also placed on the administrator's hand to determine the time of release. The four lean directions were consolidated using the median step length, median time to stability and maximum step latency.

Acute MSK injuries of the lower extremities, pelvis, lumbar spine, or abdomen were prospectively recorded. Cox proportional hazards models were constructed to determine if each reactive step outcome was associated with faster times to injury from the date of first team activity. Time to stability was the primary outcome [2]. Models were adjusted for previous MSK injury in the past two years, history of concussion, age, gender, and contact/non-contact sport. The follow-up period spanned the first official team activity to March 14, 2020, when athletic activities were halted due to COVID-19.

Results and Discussion

Forty-four athletes (24%) suffered a MSK injury over an average follow-up of 199 days. A 250 ms increase in DT time to stability was associated with a 37% increased risk of MSK injury (p = 0.023). There were also notable, but non-significant, associations between slower ST but faster DT step latencies with MSK injuries (Table 1).

The results support the notion that the ability to rapidly integrate sensory information and execute a precise response, particularly under cognitive loads, is critical to minimizing injury risk. [4] Further, these results confirm the clinical importance of longer stabilization times during the DT P&R. Future research in at-risk populations (e.g., concussed athletes) is warranted.

Table 1: Adjusted hazard ratios (HR) and confidence intervals (CI).

Outcome		HR	95% CI
Time to Stability	ST	1.29	(0.94, 1.78)
(per 250 ms)	DT	**1.37**	**(1.05, 1.79)**
Step Latency	ST	1.06	(0.99, 1.13)
(per 100 ms)	DT	0.96	(0.91, 1.02)
Step Length	ST	1.01	(0.99, 1.01)
(per 25 cm)	DT	1.01	(0.99, 1.02)

Significance

A clinically-attainable, objective measure of reactive postural response predicts future MSK injuries in collegiate athletes. Reactive recovery of balance, particularly under DT conditions, should be considered in assessments of MSK injury risk and as a potential rehabilitation target.

Acknowledgments

Funding from the Pac-12 Conference's Student-Athlete Health and Well-Being Initiative (PI: Fino, Dibble) and the National Center for Research Resources NCATS / NIH UL1TR002538.

References

[1] McPherson et al. (2019). *Am J Sports Med*. 47(7):1754-1762.
[2] Morris et al. (2020). *Front Sports Act Living*. 29;2:574848.
[3] Jacobs et al. (20006). *J Neurol.* 253(11):1404-13.
[4] Swanik (2015). *J Athl Train.* 50 (10): 1100–1102.

ALTERED LANDING STRATEGIES BY BOX HEIGHT AND ITS EFFECTS ON DROP JUMP PERFORMANCE

Youngmin Chun[1], Nickolai Martonick[1], Lukas Krumpl[1], Joshua P. Bailey[1]
[1]Department of Movement Sciences, University of Idaho, Moscow, ID, USA
email: *ychun@uidaho.edu

Introduction

During dynamic athletic activities, the human body continuously reacts to and accommodates external loads which can be increased during actions such as landing from a higher jump or running at a faster velocity. From the physics perspective, an object typically increases its reaction, such as deformation in response to the increased external load linearly. However, the human body does not show this linear relationship due to actively manipulating the response. Researchers [1,2] have classified 5 landing strategies for impact accommodation in response to manipulating landing height or adding additional mass. These strategies identify the loading phase of simple tasks (i.e., drop landings) related to injury risk factors. However, the effect of changes in landing strategies on the performance of the subsequent task (i.e. jumping) has not been examined despite the possibility of altered lower-extremity contribution to the performance of the task. Thus, the purpose of this study was to examine the changes in landing strategies in response to the increased landing height and its effect on the subsequent jump performance.

Methods

A total of 30 healthy and active college students participated in this study (15 males: age = 25.8 ± 6.6 yrs, ht = 1.82 ± 0.04 m, mass = 82.4 ± 12.1 kg; 15 females: age = 25.2 ± 9.2 yrs, ht = 1.71 ± 0.09 m, mass = 64.5 ± 11.2 kg). Participants were instructed to perform 15 trials of drop jumps from each 30 and 60 cm box positioned at the distance of a half of participant's height away from the force platforms. The jumps were captured by 3D motion capture system (250 Hz) synchronized with two embedded force platforms (1000 Hz). The initial contact time (IC) was determined by the moment of vertical GRF (vGRF) exceeding 20 N, and the end of eccentric phase was identified when the center of mass (COM) located at the lowest position. The resultant velocity of COM right before IC was used to calculate the kinetic energy (K) of each jump. The resultant work (W) of COM was identified by the area under the GRF-COM displacement curve from IC to lowest COM position. The K-W ratio was calculated to indicate how drop jumps from two box heights have different landing strategies from each other based on the work-energy theorem. The impact force (IF) was obtained by the averaged vGRF during the eccentric phase. The lower extremity joint stiffnesses were calculated for each subdivided eccentric phase, the loading and absorption phase by the first peak of vGRF, using the 2nd order polynomial regression model [3]. Multiple paired *t*-tests were performed to identify changes in landing mechanics and jump performance by the box height. The significance level was set at .05. To indicate the magnitude of differences, Cohen's *d* effect size (ES) was also reported.

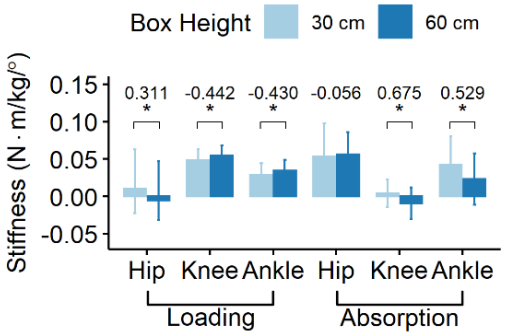

Figure 1: Changes in lower extremity joint stiffness during loading and absorption phases in response to the increased drop jump height. Numbers indicate the Cohen's *d*. * indicates significant differences between drop jumps from 30 cm and 60 cm boxes (p <.05).

Results and Discussion

Although the drop jump W-K ratio was significantly reduced by increasing the box height, no change was observed in the subsequent jump height (Table 1). Both factors that affect Work, IF and ΔCOM, were also significantly increased in 60 cm box. Interestingly, while participants manipulated their landing strategies by increasing ΔCOM in response to the increased IF, the knee and ankle joint stiffness during the loading phase were significantly increased whereas the hip joint stiffness was significantly reduced. Also, both knee and ankle joint stiffness were significantly decreased during the absorption phase (Figure 1). It can be considered that the distal joints (i.e., knee and ankle) contribute more to accommodate the increased impact force during the landing phase and the same jump height may be attributed to strain energy lost by decreased stiffness in the distal joint during the absorption phase.

Significance

This study provides a better understanding of how the body manipulates landing strategies to accommodate the external load when the stressor increases, as well as how joint stiffness contributes to the changes in the strategies when the landing was combined with other activities. Also, it will aid to outline the training protocol to enhance the subsequent jump performance by understanding the effects of altered landing strategy on the jump performance.

References

[1] James et al. (2003) *Journal of Applied Biomechanics*, Vol **19**, 108 – 118
[2] Nordin et al. (2017) *Journal of Sports Sciences*, Vol **35(18)**, 1858 – 1863
[3] Chun & Bailey (2020) *Virtual American Society of Biomechanics*, 632

Table 1: mean ± SD of kinetic variables, vertical displacement of COM, and jump heights of drop jump from each 30 and 60 cm box.

	W-K ratio*	K (J)*	W (J)*	IF (N/kg)*	ΔCOM (m)*	Jump Height (m)
30 cm	1.735 ± 0.321	256.2 ± 60.7	457.9 ± 131.7	20.1 ± 3.3	0.353 ± 0.104	0.270 ± 0.093
60 cm	1.583 ± 0.209	412.3 ± 87.4	650.1 ± 152.8	22.7 ± 3.7	0.417 ± 0.101	0.270 ± 0.093
ES	0.557	-1.955	-1.348	-0.746	-0.628	-0.001

* indicates significant differences between box heights (p < .001).

FOOT-ANKLE MECHANICAL WORK IN A CARBON FIBER PLATE RACING SHOE COMPARED TO A MINIMAL SHOE

Li Jin[1], Luisa Westley[1], and JJ Hannigan[1-2]
[1]San Jose State University, San Jose, CA 95192
[2]Oregon State University – Cascades, Bend, OR 97701
email:*li.jin@sjsu.edu

Introduction

The advent of road racing shoes with an embedded carbon fiber plate, novel midsole material, and maximally designed stack height has led to significant improvements in long-distance racing performances over the past five years, including breaking the 2-hour marathon barrier. Early research has suggested these performance improvements may be related to a reduced energetic cost of running [1], due in-part to changes in running biomechanics at the foot and ankle, specifically in positive and negative joint work [2].

While many shoes now exist in this category, the Nike ZoomX Vaporfly line of shoes remains the most popular and widely studied. However, studies to date have either looked at a Nike prototype or the Nike 4%, with no published data on the more recently released Nike NEXT%. Therefore, the purpose of this study was to compare mechanical work at the foot, ankle and foot-ankle system between the Nike NEXT% and a common minimal shoe. It was hypothesized that the NEXT% would reduce foot-ankle negative work and increase positive work during stance, without any changes in the active peak of the vertical ground reaction force or running speed.

Methods

Twenty-one reflective markers and six marker clusters were placed on twelve healthy competitive distance runners (age: 21.0 ± 2.5 yrs; height: 174.8 ± 10.9 cm; mass: 62.2 ± 7.4 kg) who ran overground in the lab at their marathon pace wearing the a) Nike Vaporfly NEXT% (NP) and b) New Balance Minimus (NB) shoes in random order. Five successful running trials for each shoe were collected at 100 Hz with a 16-camera 3D motion capture system (Vicon Motion Systems, Oxford UK). Two force plates collected ground reaction forces at 1000 Hz (Kistler Instrument Corp., Novi, MI).

Kinematics and kinetics (previously reported at ASB 2020) were calculated using Visual3D software (C-Motion, Germantown, MD). Distal foot segment power ($P_{UD-foot}$) was calculated based on the unified deformable (UD) model [3]. Ankle joint power (P_{ankle}) was calculated as the sum of ankle linear and angular power profiles [3]. Foot-ankle system total power ($P_{foot-ankle}$) was calculated as the sum of $P_{UD-foot}$ and P_{ankle} [3]. Negative and positive work for the foot (W_{foot}), ankle (W_{ankle}), and foot-ankle system ($W_{foot-ankle}$) were calculated from positive and negative $P_{UD-foot}$, P_{ankle}, and $P_{foot-ankle}$ integrated over time, respectively [3]. Average running speed and the overall peak vertical ground reaction force (vGRF) were also calculated. All outcome variables were compared using paired t-tests with the alpha-level set to 0.05.

Results and Discussion

Positive and negative ankle joint work were significantly lower in the NP shoe (W^{+}_{ankle}, $p < 0.001$; W^{-}_{ankle}, $p = 0.012$). However, positive and negative foot segment work were significantly higher in the NP shoe (W^{+}_{foot}, $p < 0.001$; W^{-}_{foot}, $p = 0.006$). Foot-ankle system positive and negative work were not significantly different between the shoes (Fig. 1). No significant differences were found between shoes for the average running speed and the active peak of the vGRF ($p > 0.05$).

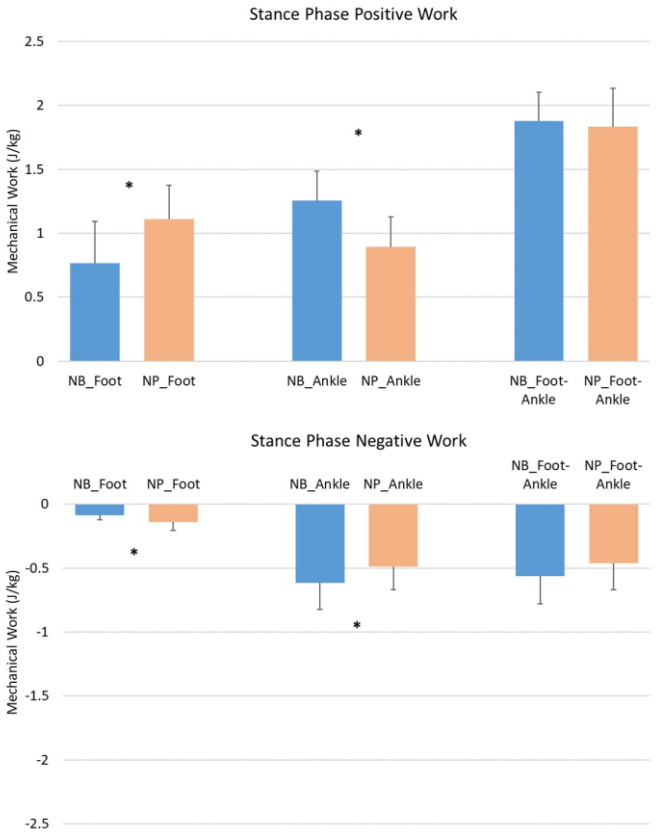

Figure 1: Group average (n = 12) stance phase foot segment, ankle joint and foot-ankle system positive work (above) and negative work (below) between the two shoes (NB & NP).

Significance

While previous research has also reported reduced positive and negative ankle joint work in carbon-fiber plate racing shoes [2], this study suggests that positive and negative work of the foot-ankle system may not be different between shoes. This supports the conservation of energy hypothesis [3]: when footwear insole mechanical properties change, ankle positive work will compensate for the reduced foot mechanical work to maintain a relatively consistent overall foot-ankle system work output. This study did not investigate MTP joint work, which may contribute to the perceived metabolic savings in the NP shoe [2] and should be included in future research.

Acknowledgments

The authors would like to acknowledge Junko Griffith for her assistance in data collection.

References

[1] Hoogkamer et al., Sports Med 48(4), 2018.
[2] Hoogkamer et al., Sports Med 49(1), 2019.
[3] Arch et al., J Appl Biomech 32(6), 2016.

META-ANALYSIS: HIGH PEAK KNEE ADDUCTION MOMENT PROGRESSES MEDIAL KNEE OSTEOARTHRITIS

Ross H. Miller[1]
[1]Department of Kinesiology, University of Maryland, College Park, MD, USA
email: rosshm@umd.edu

Introduction

Articular cartilage explants typically fail in fatigue testing after a number of loading cycles relevant to the human lifespan (Weightman et al., 1978), motivating a causal role for mechanical loading in the development and progression of osteoarthritis. Explant testing lacks the important element of biology in osteoarthritis, but prospective studies on human subjects suggest *in vivo* joint loading is a major factor in knee osteoarthritis disease progression. Miyazaki et al. (2002) was the first to distinguish between progressive vs. non-progressive severity of medial knee osteoarthritis using the peak knee adduction moment (KAM), which correlates well with medial joint loading during the early stance phase of gait (Kutzner et al., 2013). However, only one of the three prospective studies over the next decade replicated this finding. A meta-analysis of these four studies concluded there is limited, low-quality evidence supporting a causal link between medial knee joint loading and structural progression of medial knee osteoarthritis (Henriksen et al., 2014).

The review by Henriksen et al. (2014) preceded numerous prospective studies on baseline knee mechanics during walking and medial knee osteoarthritis. Therefore, the purpose of this study was to provide an update on the relationship between peak KAM at baseline and the initiation or progression of medial knee osteoarthritis. Most recent studies have had positive effects, so a positive meta-effect was anticipated.

Methods

Google Scholar was searched for "knee adduction moment osteoarthritis" and results were reviewed manually by the author to locate studies on the peak KAM at baseline and the initiation or progression of medial knee osteoarthritis over a follow-up period. The same review was performed on studies citing Miyazaki et al. (2002). Studies were included if Cohen's *d* effect size and its 95% confidence interval could be determined. Correlation coefficients and odds ratios were converted to effect sizes using standard methods (Borenstein et al., 2009).

Studies were classified as "initiation" studies if the participants had no diagnosis of knee osteoarthritis at baseline, and as "progression" studies otherwise. Meta-analytic effect sizes were calculated as the weighted average of the effect sizes in the different studies, weighted by the inverse of their variance and assuming the random-effects model, which allows that the population-level effects of the studies may have different means.

Results and Discussion

Twenty studies were located: 17 publications, two conference abstracts, and one dissertation. The total sample size was 1,336. Six were classified as initiation and 14 as progression. The meta-effect for all studies was 0.57 (Fig. 1). Confidence intervals on meta-effects were [0.31, 0.83] for all studies, [0.27, 0.88] for progression, and [-0.01, 1.22] for initiation. Lower bounds on confidence intervals of meta-odds ratios were 1.76 for all studies, 1.64 for progression, and 0.97 for initiation. There were 11 significant positive effects and no significant negative effects.

The results suggest peak KAM when walking is an important risk factor for medial knee osteoarthritis progression, within the limitations of these observational studies. The result for initiation is inconclusive. The progression effect was robust to exclusion of the unusually large, heavy-weight effect from Miyazaki et al. (2002). Increasing the peak medial knee load by an effect size of 0.57 increased the probability of knee osteoarthritis at age 55 from 13-36% to 25-49% in a computer model of knee contact mechanics and cartilage damage (Miller & Krupenevich, 2020).

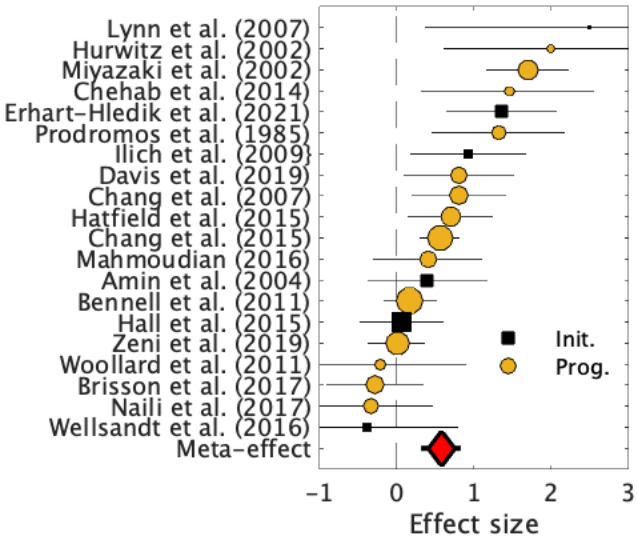

Figure 1: Effect sizes and 95% confidence intervals for baseline peak KAM and medial knee osteoarthritis initiation (squares) or progression (circles). Larger symbols had more weight in the meta-effect. Positive effects indicate KAM was prospectively damaging.

The studies included a wide range of demographics, follow-up times, and protocols such as walking speed, and different diagnostic criteria using structural, clinical, or symptomatic outcomes. These differences could be viewed as confounders, but also as strengths: peak KAM appears as a consistent risk factor for many populations and definitions of osteoarthritis.

Wellsandt et al. (2016), with the largest negative effect, is an important exception as the only included study on post-traumatic osteoarthritis. Load-related disease mechanisms may differ between idiopathic and post-traumatic osteoarthritis.

Significance

High peak KAM at baseline may indicate risk for progression of medial knee osteoarthritis for a variety of disease definitions. Prospective studies on gait mechanics and knee osteoarthritis initiation or progression should report peak KAM data. Effect sizes well above ~0.5 appear to be meaningful.

References

Borenstein M et al. (2009): 10.1002/9780470743386.ch7
Henriksen M et al. (2014): 10.1136/bmjopen-2014-005368
Kutzner I et al. (2013): 10.1371/journal.pone.0081036
Miller RH, Krupenevich RL (2021): 10.7717/peerj.9676
Miyazaki T et al. (2002): 10.1136/ard.61.7.617
Seedhom BB (2006): 10.1093/rheumatology/kei197
Weightman B et al. (1978): 10.1136/ard.37.1.58
Wellsandt E et al. (2016): 10.1136/bmjopen-2014-0053

RUNNING STRIDE-TO-STRIDE FLUCTUATIONS ARE NOT AFFECTED BY PHYSIOLOGICAL INTENSITY

Stefanie Brzezinski[1], Nelson Cortes[1], João S. Gomes[2], Joana F. Reis[2], Nick Stergiou[3], João R. Vaz[2]
[1] George Mason University, VA, USA
[2] Faculty of Human Kinetics, University of Lisbon, Portugal
[3] Department of Biomechanics, University of Nebraska at Omaha, NE, USA
email: ncortes@gmu.edu

Introduction

Nonlinear analysis of the gait cycle provides valuable feedback regarding its adaptability to changing conditions. Fractal patterns have been identified in both walking and running stride intervals. Speed appears to play a critical role in the strength of these patterns in walking, however, there is an ongoing debate in terms of what these patterns represent in running. Some authors have reported that speeds above and below preferred running speeds lead to more fractal-like patterns[1,2] while others have shown a breakdown of these patterns toward randomness as speed increases,[3] or no changes at all.[4,5] Furthermore, fatigue appears to influence fractal-patterns where experienced runners show lower fractal-patterns in their stride-to-stride fluctuations,[4,6] but in the presence of fatigue they exhibit more fractal-like patterns compared to unexperienced runners.[7] In practice, running performance is often determined via physiological data rather than the metabolic demand of a self-preferred speed. Therefore, the purpose of the current study is to investigate how running at physiologically defined speeds alters stride-to-stride fluctuations. We hypothesize that fractal scaling within stride-to-stride fluctuations will remain unaltered during different submaximal running intensities.

Methods

Thirteen male subjects participated in this study. Participants completed an incremental test to exhaustion to determine maximal oxygen uptake (VO2max), maximal aerobic speed (MAS), and the first ventilatory threshold (VT1). These values were used to determine running intensity for the experimental session. In the experimental trials, participants ran in a moderate-intensity domain (80% of VT1) and a heavy intensity domain (20 % Δ (VT1 + 0.20 x [MAS - VT1])) with a 45-minute rest period between trials. A miniaturized triaxial accelerometer (Bioplux, Plux, Portugal), placed at the external malleoli, was used to determine gait events. Metabolic data was calculated as the mean value from the last minute of VO_2 and ventilation (VE) data for each condition. A custom MATLAB code was used to determine inter-stride intervals (ISI). Detrended fluctuation analysis (DFA) was used to determine the fractal-scaling exponent (α) for the ISI time series. Statistical analyses were performed using R (R Core Team; Vienna, Austria) with the level of significance set a priori to 0.05. To study concomitant changes between conditions, repeated measures analysis of variance was used to determine if differences existed in participants' mean values across conditions.

Results and Discussion

Participants exhibited higher VO_2 during the heavy intensity domain (42.26 ± 2.46 mL/kg/min) than the moderate-intensity domain (31.26 ± 2.20 mL/kg/min, $p<0.001$). Participants also exhibited higher VE during the heavy intensity (76.40 ± 12.18 L/min) than the moderate intensity (50.91 ± 7.82 L/min, $p<0.001$). No significant difference was found for αISI (0.90 ± 0.12 and 0.91 ± 0.14) for moderate and heavy intensities, respectively - Figure 1). These results indicate despite different physiological demands, running stride-to-stride fluctuations present fractal properties that remained unchanged between running intensities.

Figure 1: Violin plots generated for data distribution of αISI for each intensity: Moderate (green) and High (orange). It represents the boxplots with interquartile range and the distribution of the data.

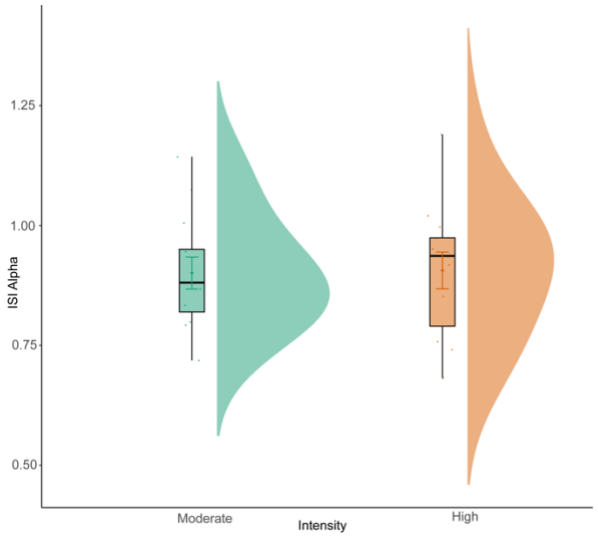

Significance

The results from this study support our hypothesis that fractal scaling within stride-to-stride fluctuations would remain unaltered during different submaximal running intensities. The present study's findings suggest the regulation of stride-to-stride fluctuations is independent of physiological stress during running. It suggests a higher level of flexibility of the locomotor system by presenting fractal-patterns at different physiological intensities, determined here by different treadmill speeds. We strongly believe our contradictory findings compared to others showing the effect of running speed on the fractal properties of running are mostly explained by our methodological approach. The treadmill speeds differed between participants considering individual and objective measures of physiological profiles, compared to the typically subjective approach using the self-selected speed method.

References

[1] Jordan et al. (2006). Gait & Posture, 24, 120-125
[2] Jordan et al. (2007). Human Movement, 26, 87-102
[3] Mann et al. (2015). Scand J Med Sci Sports, 25
[4] Nakayama et al. (2010). Gait & Posture, 31, 331-335
[5] Fuller et al. (2016). Gait & Posture, 44, 137–142
[6] Agresta et al. (2019). Gait & Posture, 70, 376–382
[7] Mo & Chow (2018). Gait & Posture 64, 7–11

Acknowledgements

NS was supported by the NIH (P20GM109090 and R01NS114283)

INFLUENCES OF PASSIVE AND POWERED ARTICULATING PROSTHETIC FEET ON TRUNK MOTION AMONGST SERVICE MEMBERS AND VETERANS WITH TRANSTIBIAL LIMB LOSS

Jonathan R. Gladish[1,2], J. Chomack[3], M. Poppo[3], A.D. Knight[2,4], J. Maikos[3], and B.D. Hendershot[2,4]

[1]Henry M. Jackson Foundation, [2]Walter Reed National Military Medical Center
email: jonathan.r.gladish.ctr@mail.mil

Introduction

Fifty-two to eighty-nine percent of persons with lower limb loss (LL) report experiencing persistent, bothersome low back pain [1,2]. While it is difficult to isolate risk factors for the onset/recurrence of low back pain, particularly among persons with LL [3], compensational movement strategies likely play a more substantial role in this population. Specifically, persons with versus without LL demonstrate larger and asymmetric trunk-pelvic motions [4] associated with elevated spinal loads [5]; these altered movement and loading patterns are influenced by level of LL and walking speed, but the specific influences of prosthesis type/features remain unclear.

Ankle-foot prostheses are often broadly sorted into three categories: non-articulating Energy Storing and Returning (ESR), articulating ESR (ART), and articulating powered (POW). Compared to ESR feet, the biomimicry of POW and ART feet improve lower-body biomechanical outcomes [6]; however, there is still a knowledge gap in terms of the residual effects on trunk mechanics. The aim of this analysis was therefore to compare trunk movement patterns during over-ground walking amongst persons with unilateral transtibial LL wearing three different ankle-foot prostheses (ESR, ART, and POW). We hypothesized that, compared to ESR prostheses, ART and POW prostheses would be associated with reduced sagittal lean, lateral trunk range of motion (ROM), and peak lateral flexion on the affected side. An auxiliary aim was to evaluate the influences of walking speed on trunk motion across these three foot types.

Methods

Seventeen persons (15 M/2 F) with unilateral transtibial LL were recruited to participate; six of which were classified as K3, eleven as K4, on the Medicare Functional Classification Level, as determined by the Amputee Mobility Predictor. Participants were randomly assigned an ART and POW foot, and utilized their personal ESR foot (or were prescribed one by a study prosthetist). In a random order, participants sequentially wore each foot for one week prior to biomechanical testing, consisting of walking at three forced speeds (1.0, 1.3, and 1.5 m/s). Trunk kinematics were collected (120Hz) using an optical motion capture system (Qualisys), and trunk segment angles were calculated using Visual3D (C-Motion) relative to the lab coordinate system with a Cardan sequence of X-Y-Z. K3 and K4 data were analyzed separately with a two-way (or three-way; for lateral flexion peaks) repeated measures ANOVA using R (p<0.05).

Results and Discussion

Anterior sagittal lean was greater at increasing speeds for K3 (p<0.01); sagittal ROM was greater at 1.5m/s compared to both 1.3m/s (p=0.01) and 1.0m/s (p<0.01). Walking speed did not affect sagittal lean or ROM for K4. Speed did not affect peak trunk lateral flexion in prosthetic or intact stance (Figure 1) for K3, but these peaks were greater with increasing speed for K4 (all p<0.01). For K3, sagittal ROM was greater in POW than ART (p<0.01) and ESR (p=0.02); however, foot type had no effect for K4. Foot type did not affect sagittal lean or lateral flexion for either K3 or K4. Peak lateral flexion was greater in prosthetic stance for both K3 (Δ=5.9°, p<0.01) and K4 (Δ=2.9°, p<0.01).

The results did not support the hypothesis that POW and/or ART prostheses would reduce trunk motions. Amongst K3, sagittal ROM increased with the use of the POW prosthesis. Apart from influences of walking speed, trunk motions amongst K4 were similar across all three feet. These results reinforce that walking speed generally influences trunk mechanics, even for highly functional persons with LL. However, while prosthetic ankle-foot type clearly influences overall gait outcomes [6], the effects on overall trunk motion are not as readily apparent.

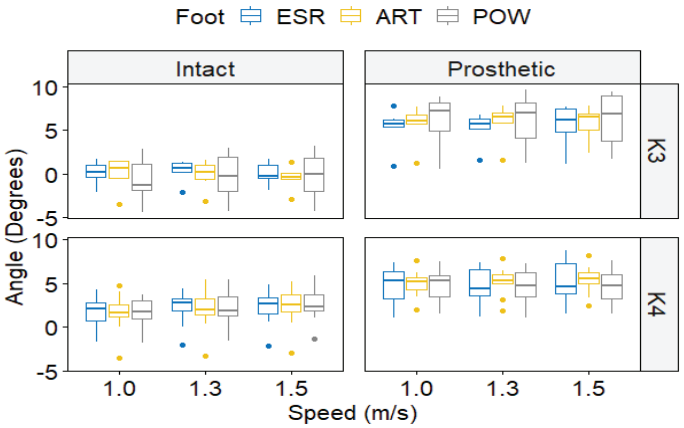

Figure 1: Box plots of peak trunk lateral flexion angles during intact and prosthetic limb stance, by walking speed, for K3 and K4 participants. Positive values indicate flexion in the direction of the denoted limb.

Significance

The lack of discernible differences in trunk motions across feet might suggest the need for advanced analyses examining internal joint contributions which may offset each other holistically (e.g., induced acceleration analyses). Although we distinguished three categories of device type, a wide variety of devices were ultimately used; further subcategorization may identify specific devices or features which influence trunk motion and, subsequently, risk for low back pain. Furthermore, the wide range of functional level of these cohorts illustrates that presumed effects may not be generalizable to the entire LL population (i.e., specific to persons below a K3 level).

Acknowledgments

Supported by DoD Award W81XWH-17-2-0014. The views expressed are those of the authors, and do not reflect the official policy of HJF, USU, the U.S. Departments of the Army/Navy/Air Force, Veterans Affairs, Defense, nor the U.S. Government.

References

[1] Dougherty. (2001) *JBSA* 89(3), 383-389
[2] Farrokhi, et. al. (2018) *Arch Phys Med Rehab* 99, 348-354
[3] Farrokhi, et.al. (2017) *Med Hypotheses* 108, 1-9
[4] Sagawa Jr, et. al. (2011) *Gait & Posture* 33(4), 511, 526
[5] Hendershot, et. al. (2018) *J Biomech* 70, 249-254
[6] Müller, et. al. (2019) *PloS One* 14(11)

HUMAN EXPOSURE TO HAND-ARM VIBRATION FROM A SURGICAL DRILL DURING SPINE SURGERY

Stacy R. Loushin[1], Courtney A. Pendleton[2], Robert J. Spinner[2], Kenton R. Kaufman[1]
[1]Motion Analysis Lab, Department of Orthopedic Surgery, Mayo Clinic, Rochester, MN, USA
[2]Department of Neurologic Surgery, Mayo Clinic, Rochester, MN, USA
email : Loushin.Stacy@mayo.edu

Introduction

Increased exposure to vibration can result in neurological, vascular, and musculoskeletal impairments. These symptoms commonly include carpal tunnel syndrome and Raynaud's phenomenon [1]. To reduce these risks, occupational health standards have been implemented to limit exposure levels. Hand-Arm Vibration (HAV) has been well characterized in occupations involving frequent exposure to vibrations using handheld equipment. Both the exposure action value (EAV) and exposure limit value (ELV) establish vibration exposure limits that require the worker to monitor vibration and ultimately stop equipment usage if the limit is exceeded over an 8-hour workday.

During spine surgery, surgeons are exposed to vibrations from surgical drills. The prevalence of carpal tunnel syndrome in surgeons is significantly higher than in the general population, indicating that the vibration exposure may exceed safe limits. However, the vibration exposure in this occupation has not been characterized. Therefore, the purpose of this study is to quantify human exposure to hand-arm vibration from a surgical drill during a common spine procedure and determine if this exposure exceeds occupational health standard limits.

Methods

Five neurosurgery residents were evaluated. Each subject performed three 30 second lumbar hemilaminectomies on fresh frozen cadaver torso specimens using a standard surgical drill (Midas Rex Electric High-Speed Drill, Medtronic, Minneapolis, MN). Vibration measurements were acquired using a tri-axial piezoelectric accelerometer (Type 8766A, Kistler, Novi, MI) affixed to the surgical drill in accordance with ISO 5349-2 [2]. The placement of the accelerometer did not interfere with the surgeon's grip. The accelerometer was attached to a charge amplifier (Type 5165A, Kistler, Novi, MI), and the data was acquired continuously at 1000 Hz (NI-USB-6225, National Instruments, Austin Texas).

The root mean square (rms) frequency-weighted acceleration values were calculated for the x, y, and z axes in accordance with ISO 5349-1 [4]. The daily vibration exposure for the three drills, expressed in terms of an 8-hour energy equivalent frequency-weighted vibration total value (A(8)), was also calculated. Based on the A(8) value, the time to reach 2.5 m/s^2 A(8) (EAV) and 5 m/s^2 A(8) (ELV) were determined.

Results and Discussion

The time to reach the EAV and ELV values while using a surgical drill varied between subjects, with the shortest times being 5.4 min and 21.8 min, respectively (Table 1). Four of the five subjects had similar EAV and ELV values (mean ± std dev, 6.7±1.7 min and 26.7 ± 6.8 min, respectively). Subject 2 had the highest EAV and ELV values (13.0±1.3 min and 52.0±5.2 min respectively), indicating a differing drilling technique. These ELV values are comparable to a study of orthopedic surgeons using a sagittal saw, where surgeons reached ELV limits at 23 minutes [4].

The EAV and ELV values are established by the Control of Vibration at Work Regulations and represent the maximum amount of time a surgeon should be exposed at the measured vibration level. This includes the combined exposure throughout the day. With the EAV value being as low as 5 minutes and equipment termination being reached in 21 minutes, a surgeon may reach the EAV limit within a single surgery. Because of this, drill usage times become critical. While elimination of these tools is not possible, other strategies to reduce exposure should be explored including grip technique and vibration dampening materials on the drill handle. Further investigation is needed to determine the total vibration exposure over a day, specifically in surgeons who perform multiple surgeries within a single workday.

Significance

This study quantifies the hand-arm vibration in surgeons using a surgical drill commonly used during spine procedures. The results demonstrate that a common surgical drill transmits hand-arm vibration levels approaching the EAV and ELV over short periods of use. Quantifying vibration exposure in surgeons will enable protective measures to be implemented which should reduce the high prevalence of carpal tunnel syndrome.

References

[1] Heaver, C. (2011) *J Hand Surg Eur*. **36(5):** 354-363.
[2] ISO 5349-1. (2011)
[3] ISO 5439-2 (2011)
[4] Mahmood, F. (2017) *Occ Med Lond.* **67(9)**: 715-715.

Table 1: Vibration measurements over three 30 second trials while performing lumbar hemilaminectomies

Subject	Weighted RMS Value (m/s^2)	A(8) value (m/s^2)	EAV >2.5 m/s^2 (min)	ELV >5 m/s^2 (min)
1	22.9±1.1	1.1	5.7±0.6	22.3±2.1
2	15.2±0.8	0.7	13.0±1.3	52.0±5.2
3	21.3±1.9	1.0	6.7±1.2	26.7±4.5
4	23.9±3.6	1.1	5.4±1.5	21.8±5.8
5	18.6±1.5	0.9	8.8±1.3	35.3±5.4

Values are expressed as Mean±SD.

JOINT LOADING IS AFFECTED BY ROTATOR CUFF TEAR SEVERITY AND DYNAMIC TASK PERFORMANCE

Joshua Pataky[1], V. Seelam[1], L. Engle[1], S. Khandare[1], and M. E. Vidt[1,2]
[1]Biomedical Engineering, Pennsylvania State University, University Park, PA, USA
[2]Physical Medicine & Rehabilitation, Penn State College of Medicine, Hershey, PA, USA
email: jjp6192@psu.edu

Introduction

Rotator cuff tears (RCT) are common in older adults, negatively affecting mobility and function[1]. RCT severity ranges from a partial thickness supraspinatus tear to a massive 3-tendon tear including the supraspinatus, infraspinatus, and subscapularis. Results of simulation-based studies have shown that with increased RCT severity glenohumeral joint contact force (JCF) is relatively consistent for static tasks, but changes with posture[2]. These outcomes suggest that dynamic tasks may require postures that alter glenohumeral JCF in ways that could lead to development of secondary injuries. Our objective was to determine how glenohumeral JCF magnitude and orientation change with increased RCT severity during dynamic task performance to identify tasks and tear severities that may place an individual at increased risk of secondary injury.

Methods

A computational model of the upper limb[3] was developed in OpenSim (v.3.3)[4], representing mean muscle force-generating characteristics of healthy older adult males[5]. Eight different models, representing increasing RCT severity, were developed by systematically reducing peak isometric forces of supraspinatus, infraspinatus, and subscapularis muscle actuators. Kinematics for functional upper extremity tasks, including forward reach, functional pull, axilla wash, and upward reach to 90° and 105° humeral elevation, were measured from 9 older adults with RCT and 9 healthy age-, sex-matched controls in a prior study[6], with notable differences between groups. Computational simulations were performed with each RCT severity model and task kinematics (n=144 simulations per task) using Computed Muscle Control[7] and Joint Force Analysis tools in OpenSim. Magnitude and orientation of peak glenohumeral JCF was determined using a custom Matlab (The MathWorks, Natick, MA) program and compared across tear severity and task using two-way ANOVA with Tukey post hoc tests in SAS (v9.4, SAS Institute, Inc., Cary, NC, USA), with significance at $p<0.05$.

Results and Discussion

Projecting the resultant peak JCF vector onto the glenoid fossa revealed that the JCF was oriented more superiorly with greater RCT severity (Fig. 1), but the force remained within the glenoid rim for all tear severities and motions. The peak glenohumeral JCF magnitude decreased for all motions as tear severity progressed. The JCF plateaued for tears involving 3 tendons, which was a trend observed across all tasks, despite the difference in postures used in each task. Although RCT and control groups had different task kinematics, no differences between groups were observed for JCF magnitude.

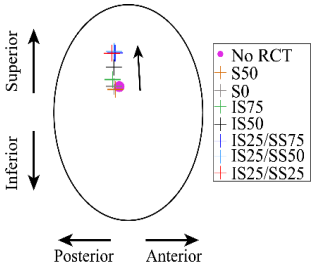

Figure 1: Joint contact force (JCF) vector across increasing tear severity for forward reach task projected onto the glenoid fossa. Arrow indicates trend of JCF location change with increased tear severity.

Main effects of tear severity and task were observed. JCF magnitudes across tear severity were not different for upward reach 105° (Fig. 2), although the task was different compared to all other tasks ($p<0.05$). On average, JCF magnitude decreased

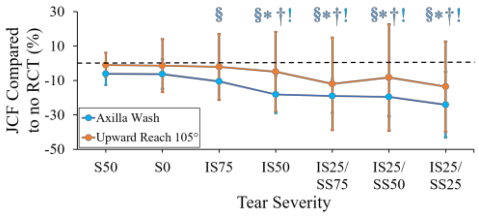

Figure 2: Percent change of peak glenohumeral JCF magnitude from no RCT for increasing RCT severity for axilla wash and upward reach 105° tasks. $p<0.05$ is indicated by: § for comparison with no RCT model; * for comparison with S50 model; † for comparison with S0 model; ! for comparison with IS75 model.

by 13.6% for the greatest tear severity versus no RCT. Within tasks, predicted JCF decreased by an average 22.5% (all $p<0.05$) for the greatest tear severity compared to no RCT for forward reach, functional pull, axilla wash (Fig. 2), and upward reach 90°. There was a significant JCF decrease in the most severe tear severity compared to partial (S50; 19.8% ($p<0.05$)) and full (S0; 18.5% ($p<0.05$)) supraspinatus tendon tears for forward reach, axilla wash, and upward reach 90°. The decreased JCF magnitude and superior trend of JCF orientation are consistent with expectations, as fewer intact muscles contribute to overall force distribution across the joint, enabling superiorly oriented resultant forces that suggest increased risk for secondary injury.

Significance

At the greatest tear severity, JCF is significantly decreased compared to the no RCT model, and partial and full supraspinatus tendon tear models. Differences in peak JCF between upward reach 105° and other tasks could be due to uninvolved shoulder muscle compensation. Dynamic tasks using different postures and increased RCT severity affected JCF. The JCF changes identified here are consistent with clinical studies of increased secondary injury risk,[8] highlighting the need for balanced force distribution across the joint. Ongoing work explores associated muscle compensation strategies with increased RCT severity.

Acknowledgments

Penn State start-up funds (Vidt)

References

1. Lin JC. et al. J. Am. Med. Dir. Assoc. 2008;9(9):626-632.
2. Khandare S. et al. J. Electromyogr. Kinesiol. 2019;(18):30516-9.
3. Saul KR. et al. Comput. Methods Biomech. Biomed. Eng. 2015;18(13):1445-58.
4. Delp SL. et al. IEEE Trans Biomed Eng. 2007;54(11):1940-50.
5. Vidt ME. et al. J. Biomech. 2012;45(2):334-341.
6. Vidt ME. et al. J. Biomech. 2016;49:611-617.
7. Thelen DG. et al. J. Biomech. 2003;36(3):321-328.
8. Hsu HC. et al. Acta Orthop. Scand. 2003;74(1)89-9

QUADRICEPS TORQUE COMPLEXITY BEFORE AND AFTER ACL RECONSTRUCTION

Alexa K. Johnson[1], Kazandra M. Rodriguez[1], Riann M. Palmieri-Smith [1,2]
[1]School of Kinesiology, University of Michigan, Ann Arbor, MI
[2] Department of Orthopedic Surgery, University of Michigan, Ann Arbor, MI
email: akjohns@umich.edu

Introduction

Following anterior cruciate ligament injury and reconstruction (ACLR), individuals present with substantial quadriceps dysfunction [1]. Quadriceps dysfunction has primarily been quantified by examining the maximal torque output of the quadriceps muscle. This allows for an understanding of the magnitude of force the quadriceps can produce but does not provide information about the quality of the muscle contraction. The ability to produce precise and controlled muscle contractions is important for smooth, fluid movements during physical activity and thus should be considered an important component of quadriceps function after ACLR.

One way to assess the quality of a muscle contraction is to examine torque complexity. Torque complexity establishes the predictability of the torque signal between successive data points by quantifying the variability of the torque signal during a contraction. Torque complexity is thought to affect overall coordination and motor task performance [2] and thus it is important to understand if it is affected after ACLR. Therefore, the purpose of this study was to determine if patients who undergo ACLR have altered torque complexity. We hypothesized that those with ACLR will demonstrate increased torque complexity in the involved limb compared to the uninvolved limb, and that torque complexity will not return to pre-surgical levels by the time of return to activity.

Methods

A total of 34 individuals (19F, 15M, Age=16.5±2.6yrs; Mass=75.4±18.5kgs) scheduled to undergo ACLR were recruited for this study. Individuals completed quadriceps strength testing at three time points, prior to surgery (PRE), five months post-surgery (MID; 5.0±0.5 months), and at time of return to activity (RTA; 9.4±1.7months).

Bilateral maximal isometric quadriceps torque was sampled at 2000 Hz with the individual seated in an isokinetic dynamometer with their knee flexed to 90°. Individuals were instructed to perform 3 maximal effort isometric contractions, lasting approximately 5 seconds each. The maximum voluntary isometric contraction trial with the largest peak was used for sample entropy calculations. Sample entropy was calculated as SampEn(m, r, N)=-ln(A/B). Where, m (set to 2 for clinical data) is the number of data points in which the distance between data points was compared to fit within r, which is the similarity criterion, set to 0.2 times the standard deviation, N is the total window of data, in our case 4000 data points of the isometric torque plateau, A represents the number of sequential data points ($m+1$) that fall within r, and B is the number of sequential data points (m) that fall within r [3]. A time series with similar distances between data points indicates predictability and results in lower sample entropy values, while large differences between data points indicate complexity, resulting in greater entropy values. A two-way repeated measures ANOVA was used to determine differences between limbs and times in peak quadriceps torque and quadriceps torque complexity. Univariate F tests and Bonferroni multiple comparison procedures were used post hoc in the case of significant interactions. Significance was set a priori at $p < 0.05$.

Results and Discussion

A limb x time interaction was found for quadriceps peak torque ($p<0.001$; Fig. 1) and torque complexity ($p<0.001$; Fig. 1). Peak quadriceps torque was lower in the involved limb when compared to the uninvolved limb at every time point ($p<0.001$). Further, quadriceps torque of the involved limb was lower at MID compared to PRE ($p=0.023$) and RTA ($p=0.041$), with no differences between PRE and RTA ($p=0.865$). In regard to torque complexity, entropy values were higher in the involved limb compared to the uninvolved limb at MID ($p<0.001$) and RTA ($p<0.001$), indicating greater complexity. Additionally, the involved limb demonstrated an increase in torque complexity following surgery from PRE to MID ($p=0.023$), but not PRE to RTA ($p=0.169$) or MID to RTA ($p=0.541$). The uninvolved limb had significantly less complexity from PRE to RTA ($p=0.003$), but no differences between PRE and MID ($p=0.085$), or MID and RTA ($p=1.000$).

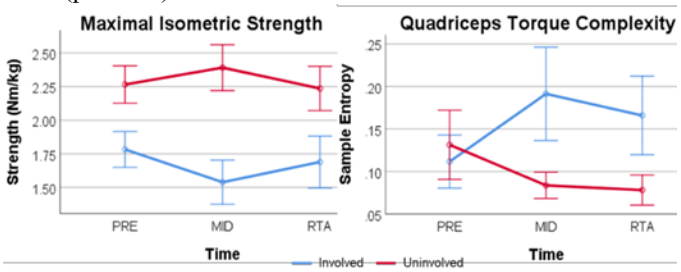

Figure 1: Mean and 95% confidence intervals of maximal isometric quadriceps strength and torque complexity between limbs, and time points before and following ACLR.

Increases in torque complexity in the involved limb after ACLR could be attributed to altered corticospinal control resulting in inefficiencies in the coordination of quadriceps contractions. The decreased complexity that manifests in the uninvolved limb may occur to compensate for the impaired quadriceps function in the ACLR limb.

Significance

The increased torque complexity in the ACLR limb may promote uncoordinated quadriceps contractions thereby altering biomechanics during movement. These effects could have devastating outcomes, such as increased risk for secondary injury and the development of post-traumatic osteoarthritis.

Acknowledgments

The authors would like to thank Mike Curran for his assistance with data collection.

References

1. Palmieri-Smith et al. (2008). *Clin Sports Med*, 27(3)
2. Pethick, Jamie, et al. (2019). *Exp Physiol*, 104(1)
3. Richman, & Moorman. (2000). *Am J of Physio-Heart and Circ Physiol.*
4. Cortes et al. (2014). *Gait & Posture,* 39(3)

DOES PUSH-OFF INTENSITY MEDIATE THE EFFECTS OF TENDON STIFFNESS ON WALKING METABOLISM?

Ricky Pimentel and Jason R. Franz
Joint Dept. of Biomedical Engineering, UNC Chapel Hill and NC State University, Chapel Hill, USA
Email: rickypim@live.unc.edu

Introduction

In vivo imaging studies demonstrate that age-related increases in series elastic tendon stiffness associate with reduced walking performance in older adults.[1] Using musculoskeletal models, we[2] and others[1,3] revealed that the potential mechanism underlying this association is that decreased tendon stiffness elicits shorter muscle fiber lengths, requiring higher activations and thus higher metabolic costs to meet the task demands of walking. We suspect the neuromechanical cascade elicited by decreased tendon stiffness may contribute to higher metabolic costs during walking due to aging, potentially coinciding with older adults' tendencies to walk with smaller peak propulsive forces and diminished ankle push-off compared to young adults. However, prior studies have only augmented Achilles' tendon stiffness (rather than all model tendons), and there is little experimental data to suggest that age-related decreases in tendon stiffness are limited to muscle-tendon units spanning the ankle. It is also unclear whether push-off intensity mediates the effect of tendon stiffness on walking metabolic cost. Thus, our purpose was to quantify the effects of altered tendon stiffness on muscle mechanics and metabolic costs in young adults walking normally and with different magnitudes of push-off intensity prescribed using biofeedback.

Methods

We iterated musculoskeletal simulations to estimate individual muscle mechanics and metabolic energy costs[4,5] driven by experimental data from 12 participants (age: 23.3±3.1 years; 7 female) who walked normally and using biofeedback designed to prescribe changes in push-off intensity at a fixed speed. We scaled a gait2392 model and used computed muscle control with default tendon strains at max isometric force (ε_o: 3.3%) and repeated simulations after changing ε_o values to 2, 4, 6, and 8% (2% = most stiff, 8% = least stiff) for all model tendons. Statistical parametric mapping repeated measures ANOVA tested for main effects of compliance on metabolic cost, activation level, and muscle fiber length (α=0.01).

Results and Discussion

While we continue to iterate simulations across all targeted push-off conditions, we present a preliminary analysis on modifying all model tendon stiffnesses during normal walking (Fig. 1). On average, estimated whole-body metabolic cost increased 3-5% as tendon stiffness decreased due to higher costs to operate the hamstrings and quadriceps during early stance and the plantar flexors during mid-to-late stance. Increasing tendon compliance shifted the metabolic cost of push-off earlier in the gait cycle. At the individual muscle level, we reveal that with decreased tendon stiffness, the gastrocnemius activated earlier, consuming significantly more metabolic energy during midstance but less during late stance, compared to the model default tendon stiffness. This change in timing seems to favor relatively isometric activity but likely disrupts the natural catapult action of plantar flexor muscle-tendon units during mid to late stance. At the ankle, changing tendon stiffness disproportionately affected the gastrocnemius which, given its prominent role in regulating forward propulsion, will be a focus of our future simulations at targeted push-off intensities.

Significance

Normal walking simulations suggest that varying tendon stiffness fundamentally changes individual muscle mechanics and activation dynamics during walking. These changes, in part, sum to increase the metabolic cost of walking, even in a young adult walking model while maintaining similar net joint dynamics. Our future task-dependent simulations seek to reveal the extent to which emulating age-related reductions in ankle push-off intensity mediate these effects of tendon stiffness on walking metabolism.

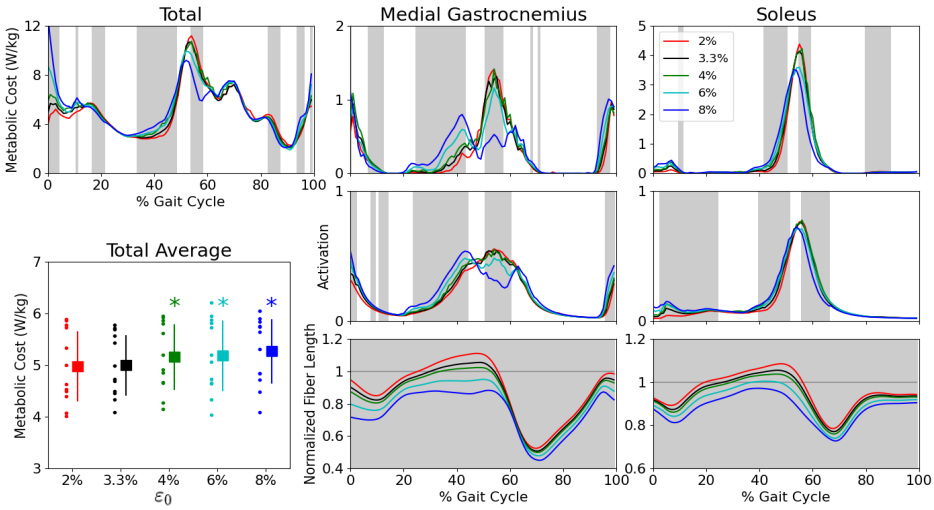

Figure 1. Simulated whole body metabolic cost during normal walking varies between tendon stiffness levels during weight acceptance in early stance and during push-off in mid-to-late stance (top left). Increased tendon compliance yields shorter plantar flexor lengths and disrupts the natural catapult action of the medial gastrocnemius, yielding higher metabolic costs during midstance. Shaded areas indicate significant repeated measures ANOVA result using statistical parametric mapping.

Acknowledgments

We thank our participants for volunteering their time and acknowledge the NIH for funding this work (R01AG058615).

References

1. Delabastita T et al. *J. Aging Phys. Act.* 27, 116–127 (2018).
2. Orselli, MIV et al. *J. Biomech.* 60, 227–231 (2017).
3. Delabastita T et al. *bioRxiv.* (2020) doi:10.1101/2020.02.10.941591.
4. Umberger BR. *J. R. Soc. Interface.* 7, 1329–1340 (2010).
5. Bhargava LJ et al. *J. Biomech.* 37, 81–88 (2004).

TEST-RETEST RELIABILITY OF TRUNK EXTENSOR MUSCLE FORCE MODULATION

John R. Gilliam[1], A.J. Jacobs[1], and S.P. Silfies[1]
[1]University of South Carolina, Arnold School of Public Health, Department of Exercise Science
email: JRG15@email.sc.edu

Introduction

Low back pain (LBP) is the most common chronic pain in the United States.[1] Impairments in trunk muscles of individuals with LBP include decreased strength and endurance (muscle capacity) and altered motor planning and activation patterns (neuromuscular control).[2] One aspect of neuromuscular control that has limited investigation as an underlying mechanism of movement impairment in individuals with LBP is voluntary muscle force modulation. Muscle force modulation requires sensorimotor integration and is defined as the capacity of the neuromuscular system to generate coordinated, accurate and/or smooth force output.[3,4] The ability of the trunk musculature to modulate force is a unique muscle performance characteristic. Thus, the purpose of this study was to establish reliable methods to assess sub-maximal trunk extensor force modulation. Three protocols were assessed that progressively challenge the rate of voluntary muscle force modulation.

Methods

Twenty-nine healthy participants were tested (15 males, mean age of 24.5 years) using three dynamic force matching paradigms. Participants were positioned in a modified kneeling position with their pelvis stabilized and fitted with a harness around their shoulders that was attached to a tension load cell mounted in front of the participant (Fig. 1, left).

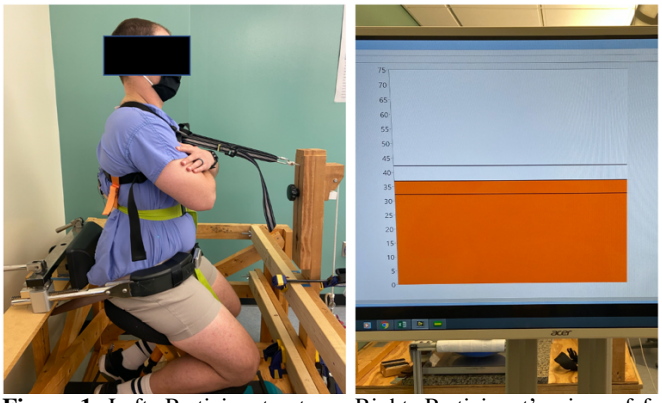

Figure 1: Left: Participant set up. Right: Participant's view of force target (black lines) and feedback of extensor force (orange) during force modulation protocols. Target lines moved in a submaximal force range based on a sine wave function.

Two trials of maximum voluntary isometric force (MVF) of back extensors were performed by extending the trunk to neutral from a position of ≈15 degrees of trunk flexion. The participants MVF (N) was used to calculate their submaximal dynamic target force range (20-50% MVF). The three protocols challenged the participant's ability to accurately match increasing and decreasing force targets using visual feedback (Fig. 1, right). The dynamic target force protocols were controlled by a sine wave function of varied frequency (number of cycles over 45 and 60 s) at .083, .167, .222 Hz. Each protocol was performed twice and then repeated to measure within-day reliability. Subjects performed a second session within 7 days repeating the same protocols. The accuracy of the subjects' voluntary sub-maximal force modulation capabilities was calculated as the root mean square error (RMSE) between the dynamic target force and subject generated force (Fig 2). Mean RMSE values were used to determine the within- and between-day reliability by calculating the ICC (Intraclass correlation coefficient) and minimal detectable difference with a 90% confidence interval (MDD_{90}).

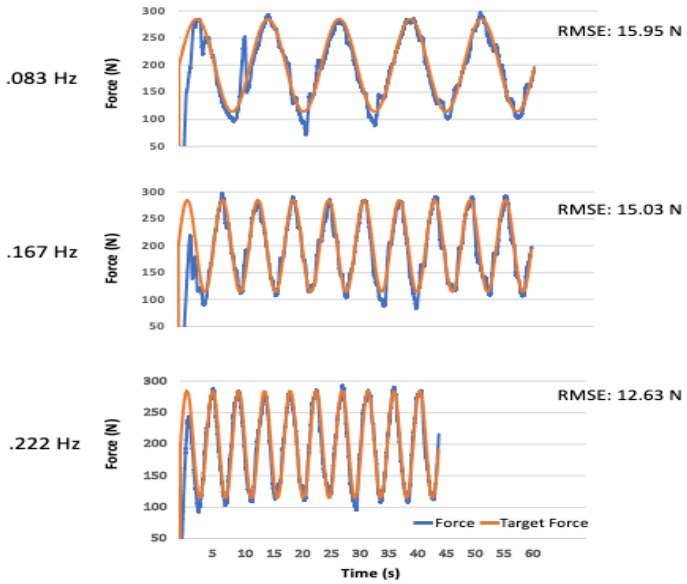

Figure 2: Examples of dynamic force matching trials and RMSE for the three prototocls using a sine wave function at varied frequency.

Results and Discussion

Within-day reliability across the three protocols ranged from .77 to .95 $ICC_{(2,2)}$ with MDD_{90} ranging from 4.0 to 5.9 N. Test-retest reliability ranged from .71 to .96 $ICC_{(3,2)}$ with MDD_{90} ranging from 3.6 to 5.7 N. The lowest ICCs were calculated for the slowest rate of force modulation. Results indicate these protocols demonstrate moderate to excellent within-day and between-day reliability. An RMSE difference >3.6 to 5.7 N would need to be observed for between-day changes in order to confidently attribute differences in performance on these protocols to something other than measurement error.

Significance

Moderate to excellent reliability of these dynamic force modulation protocols indicates that they could be used in future research. These protocols could be deployed to investigate the role of sensorimotor integration impairments that are linked to trunk extensor muscle dysfunction and altered control of movement in persons with LBP.

References

1. Pizzo et al. (2011) *Relieving Pain in America*.
2. Hodges et al. (2019) *JOSPT*, **49(6):** 464-476.
3. Enoka et al. (2002) *Neuromechanics of Human Movement*.
4. Laine et al. (2016) *Front. Comput. Neurosci*. **10(86)**: 1-14.

LOWER LIMB MUSCLE ACTIVITY PATTERNS DURING HEAVY LOAD CARRIAGE

Michelle A. Aube[1,2], Nathaniel I. Smith[1,2], Victoria G. Bode[1,2], Peter N. Frykman[2], Joseph F. Seay[2], Rebecca E. Fellin[2]
[1]Oak Ridge Institute for Science and Education
[2]United States Army Research Institute of Environmental Medicine
email: michelle.a.aube.ctr@mail.mil

Introduction

Load carriage is required in military training. Heavy load carriage can influence the kinematic and spatiotemporal parameters during gait (Seay et al., 2014). Following a prolonged hike with loads up to 40% of body weight, muscle activity increased (Simpson et al. 2011) presumably as a way to aid in shock absorption and maintain lower limb stability. Increases in muscle activity have been shown while carrying loads up to 30% of body weight while walking at a self-selected pace set across load conditions, yet the effects of a self-selected pace that varies across loads have not been widely explored (Silder et al., 2013). There is little research exploring the effect of heavy loads, greater than 40% bodyweight, on the muscle activity of the lower limb.

The purpose of this study was to examine the effects of heavy load carriage, greater than 40% bodyweight, on the muscle activity of the lower limb while walking at a self-selected pace.

Methods

16 Soldiers (8 male, 8 female) participated in this study (height: 1.7±0.13m, mass: 75.9±14.3kg). For each participant, preferred speed on an outdoor level course was determined while wearing 25kg and 55kg vest borne loads, as well as unloaded. Speed was measured using the SPORTident (SPORTident, Germany) tracking system.

During motion capture, participants were instrumented with electromyography (EMG) on the medial and lateral gastrocnemius muscles (MG, LG), the medial and lateral hamstrings (MH, LH), and the soleus (SOL) muscle (MotionLab Systems, Baton Rouge, LA, USA). Participants completed 3 successful trials walking across a 15m runway for each of the three load conditions. For each load condition, participants were walked at their predetermined walking speed, within ±5%.

EMG data were analysed and processed in Visual 3D (C-Motion Inc., Rockville, MD). Data passed through a high pass and low pass filter followed by a moving root mean square (RMS). Data were normalized to the maximum value from a maximum vertical jump trial. A period of 100ms of inactivity for each muscle per trial was used to determine the threshold for muscle onset and offset times. A muscle was considered active when the signal exceeded twice the standard deviation of the inactive period. Onset was determined relative to heel strike. Muscle activity duration was determined by subtracting muscle onset from muscle offset. Repeated measures ANOVAs were conducted in SPSS ($p<0.05$) to analyze muscle onset time, duration, speed, and stance time.

Results and Discussion

Table 1 summarizes the results. Stance time significantly increased as load increased. Speed significantly decreased as load increased. No significant differences were found for muscle onset or muscle duration time for the LG, MG, and LH. The MH displayed later onset times relative to heel strike at 25kg and 55kg loads compared to unloaded, contradicting results from Silder et al 2013. This difference may be due to the freely chosen speeds for each load in the present study.

Variable	Walk	Ruck25	Ruck55
LG Onset (s)	0.035	0.058	0.035
LG Duration (s)	0.505	0.538	0.548
MG Onset (s)	0.084	0.062	0.037
MG Duration (s)	0.509	0.513	0.544
LH Onset (s)	0.293	0.193	0.195
LH Duration (s)	0.130	0.202	0.267
SOL Onset (s)	0.078	0.094	0.062
SOL Duration (s)	0.545	0.579	0.615*
MH Onset (s)	0.200	0.217*	-0.154*
MH Duration (s)	0.228	0.197	0.199
Speed (m/s)	1.717	1.623*	1.490*^
Stance Time (s)	0.583	0.611*	0.650*^

Table 1: Mean EMG and spatiotemporal parameters for load conditions. For load conditions: *significant difference from walk; ^significant difference from 25kg.

The duration time of the SOL was significantly longer during the 55kg condition compared to the unloaded walk, similar to the results by Silder et al., who saw increased activity of the SOL muscle with a load 30% body weight. The increase in SOL duration with increase in load may be acting to increase the magnitude of force needed to propel the body forward during the late stance phase, as seen by Silder et al.

Significance

When Soldiers walked at their preferred speeds during prolonged loaded marches, different muscle activity patterns were observed compared to previous studies in which speed was held constant across load conditions. Using preferred speeds for each walk and load carriage condition may more accurately reflect how a Soldier's body responds in a field setting.

References

[1] Seay JF, Fellin RE, Sauer SG, Frykman PN, Bensel CK. Mil Med. 2014 Jan;179(1):85-91.
[2] Silder A, Delp SL, Besier T. J Biomech. 2013 Sep 27;46(14):2522-8.
[3] Simpson KM, Munro BJ, Steele JR.J Electromyogr Kinesiol.2011 Oct;21(5):782-8.

Disclaimer

The views expressed in this abstract are those of the authors and do not reflect the official policy of the Department of Army, Department of Defense, or the U.S. Government.

NOVEL CLAMP PROTOCOL EXAMINES CAUSE-EFFECT RELATIONS BETWEEN PROPULSIVE FORCE, WALKING SPEED, AND COST OF TRANSPORT

Richard E. Pimentel[1], Jordan N. Feldman[1], Michael D. Lewek[2], Jason R. Franz[1]
[1]Joint Dept. of BME, UNC Chapel Hill and NC State University, USA [2]Division of Physical Therapy, UNC Chapel Hill, USA
Email: rickypim@live.unc.edu

Introduction

Walking speed serves as a simple surrogate for human health status and ambulatory function. The selection of walking speed in healthy young adults is often attributed to minimizing the metabolic cost of transport (CoT). However, declines in walking speed due to age or disease are frequently accompanied by smaller propulsive forces (F_P) during push-off. Thus, F_P is considered a biomechanical determinant of walking speed. However, no study to our knowledge has established empirical cause-and-effect relations between F_P, walking speed, and CoT, even in healthy young adults. Our purpose was to: (1) investigate if F_P governs the selection of walking speed using real-time targeted biofeedback and self-pacing treadmill control, and (2) quantify how metabolic energy cost shapes the relation between F_P and walking speed. We ultimately aim to better understand the time course of gait changes due to age or disease and to inform targeted rehabilitative interventions.

Methods

Fourteen young unimpaired adults have thus far participated (6F/8M; age: 25.0±5.3 years, typical overground walking speed: 1.41±0.10 m/s, typical F_P: 21.8±2.3 %BW). We first determined participants' typical overground walking speed (4 passes of 30 m). Next, participants completed five 5-minute trials on a dual-belt instrumented treadmill at a fixed speed. We recorded participants' average peak F_P at their typical speed as well as at ±10% and ±20% of that speed in randomized order (speed clamp). Participants then walked for 5 minutes each on the same treadmill in a self-paced mode while responding to a visual biofeedback paradigm to target their average peak F_P from each of the fixed-speed trials (F_P clamp). The self-pace mode adjusted speed in real-time based on subjects' anterior-posterior position on the treadmill. We measured rates of oxygen consumption and carbon dioxide production, which were averaged over the final 2 minutes of each trial to calculate net metabolic CoT using standard procedures. We averaged speed and F_P over the same time period. A two-way repeated measures ANOVA analyzed differences in walking speed, F_P, and CoT between clamp types (prescribed speed vs. prescribed F_P) and condition intensity.

Results and Discussion

Participants increased and decreased F_P and CoT in response to faster and slower walking speeds; participants also increased and decreased walking speed and CoT in response to larger and smaller F_P, respectively (p-values<0.05, Figure 1). Significant condition × clamp interaction effects revealed several unanticipated differences between the F_P and speed clamp conditions. First, when increasing condition intensity, participants exerted smaller F_P during the F_P clamp despite walking at an identical speed. Conversely, when decreasing intensity, participants walked at faster speeds during the F_P clamp, despite exerting similar F_P. Finally, while walking at low-to-normal condition intensities, participants chose to walk with a higher CoT during the F_P clamp compared to the speed clamp. This higher cost may be due to continued exploration of walking speeds and gait patterns to optimize CoT during F_P targeting.

Significance

Walking with larger and smaller F_P yields faster and slower walking speeds paralleled by changes in CoT in young adults. However, these cause-effect relations are more complex than previously appreciated and may not always be governed by minimizing metabolic cost of transport.

Acknowledgments

Thank you to the participants for donating their time to participate in this study funded by NIH (R01AG058615).

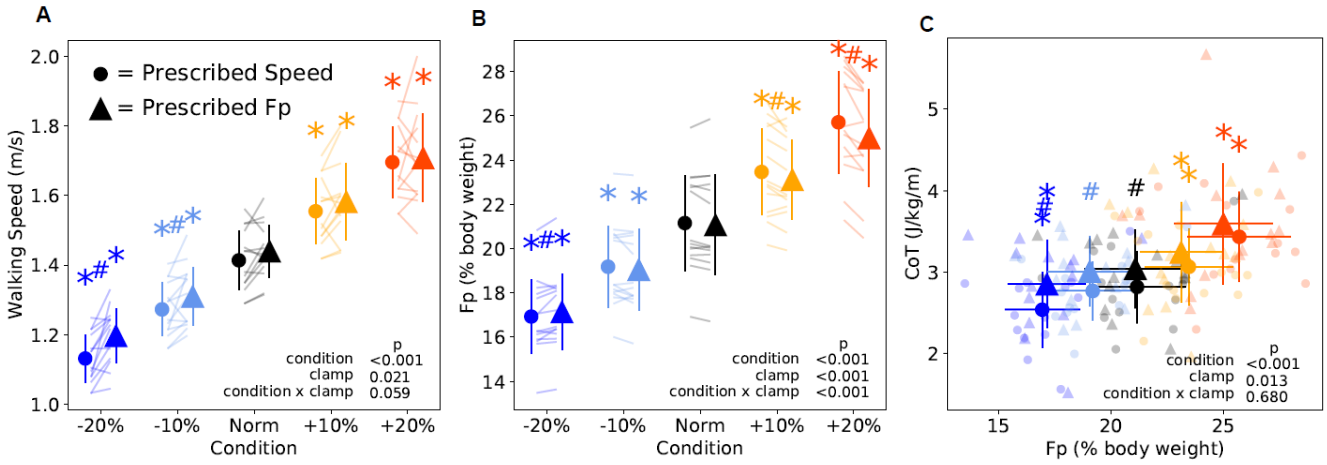

Figure 1: Speed (A) and F_P (B) across condition intensities for each clamp type (prescribed speed vs prescribed F_P) and resultant changes in metabolic cost of transport (C). Asterisks (*) indicate a significant (p<0.05) pairwise difference versus preferred condition (Norm). Hashtags (#) indicate a significant (p<0.05) pairwise difference between clamp types.

EVALUATION OF ANKLE RANGE OF MOTION AND DYNAMIC STIFFNESS FOR HUMAN FOOT-ANKLE SURROGATE DESIGN

Julia-Grace Polich[1,4], Michael B. Tegtmeyer[2], John H Bolte IV[3], Aaron Scott, MD[4], Paula Gangopadhyay, DPM[5], Per Kristian Moerk, DPT[6], and Kerry A. Danelson[1,4]

[1]Wake Forest School of Medicine, Biomedical Engineering
[2]US Army Research Laboratory
[3]Ohio State University, Injury Biomechanics Research Center
[4]Wake Forest School of Medicine, Orthopedic Surgery
[5]Wake Forest Baptist Health, Foot and Ankle Surgery
[6]Wake Forest Baptist Health, Physical Therapy
Email: jpolich@wakehealth.edu

Introduction

Lateral ankle sprains (LAS) and overuse injuries account for 73.6% and 31% of reported lower-limb injuries, respectively, during military fitness training programs.[1-3] Repetitive exposure to this injury damages the lateral ligamentous support of the ankle joint and leads to chronic ankle instability in 70% of individuals with history of LAS.[4-6] In 2019, overuse injuries cost the Army more than 8 million duty days. Residual symptoms after LAS can limit the activity of military personnel from 6 weeks to 18 months.[5-7] Military combat boots are tested in a variety of configurations to determine slip resistance, tolerance to heat and cold, sole flexion, and toe compression. However, the current footwear evaluation methodology lacks any lateral stability assessment. There are existing anthropometric testing devices (ATDs) developed to predict lower limb injury to humans during high-load vertical blast or frontal impacts. These ATDs, however, have not been validated for assessing lower-velocity scenarios observed in LAS and overuse injuries (<120°/s). A human foot-ankle surrogate with the correct ankle joint mechanics and anatomy similar to the human leg would provide an objective measure of the interface between the foot-ankle complex and military issued footwear.

Methods

Fifty healthy volunteers (25m/25f) with no pre-existing ankle problems were recruited for this study. All subjects were 18-25 years old to be representative of the age of incoming service members. Each subject's ankle range of motion was quantified in plantar flexion, dorsiflexion, inversion, and eversion using a Biodex isokinetic dynamometer (Biodex Medical Systems, Inc.). Bilateral dynamic stiffness measurements in plantar flexion, dorsiflexion, inversion and eversion were taken at 5°/s and 60°/s within subject-specific range of motion. The same tests were performed with the THOR ATD leg, a device designed for automotive crash injury assessment. The human subject data was used to define a response corridor for average ankle stiffness and to validate the use of the THOR ATD leg in footwear ankle-stability testing methodology.

Results and Discussion

The results from this study demonstrate that the THOR ATD leg yields a stiffer response than the human foot-ankle in plantar flexion, eversion, and inversion. These data indicate that the THOR leg does not appropriately model the response of the human foot-ankle under low-velocity lateral loads, and a more biofidelic foot-ankle surrogate should be designed and validated for use in ankle stability-testing methodology appropriate for evaluating footwear.

Table 1: Left Ankle peak average stiffness response ± SD (Nm/°) at 5°/s.

	Plantarflexion	Dorsiflexion	Inversion	Eversion
Male	0.78 ± 0.5	1.29 ± 0.6	0.39 ± 0.2	0.49 ± 0.2
Female	0.31 ± 0.1	0.62 ± 0.3	0.27 ± 0.2	0.34 ± 0.2
THOR	1.30	1.46	1.20	0.91

Significance

This study quantifies the human ankle response in low-velocity loading scenarios and evaluates the biofidelity of the THOR ATD leg in ankle-stability testing. These results will contribute to the development of a novel methodology to assess military footwear in lateral bending. Since no lateral-bending assessments currently exist for military footwear, the expected outcomes are innovative and will further the understanding of how the combat boot design may reduce risk of LAS and overuse ankle injuries.

Acknowledgments

This research was sponsored by the Army Research Laboratory. The views and conclusions contained in this document should not be interpreted as representing the official policies of the Army Research Laboratory or the US Government.

References

1. Kucera KL et al. (2016). *Med Sci Sports Exerc.* 48:1053-61.
2. Waterman BRC et al. (2010). *J Bone Jt Surg - Ser A.* 92:2279-84.
3. Kaminski TW et al. (2001). *J Sport Rehab.* 10:205-220.
4. Gribble PA et al. (2019). *J Athl Train.* 54:617-627.
5. Hertel J et al. (2002). *J Athl Train.* 37:364-375.
6. Herzog MM et al. (2019). *J Athl Train.* 54:603-610.
7. Orr JD et al. (2014). *Clin Sport Med.*33:675-692.

IMMEDIATE SENSORIMOTOR EFFECTS FROM A 15-MIN POSTURAL INTERVENTION

Nathan D. Schilaty[1], Nathaniel A. Bates[1], Luca Rigamonti[1], Takashi Nagai[1]

[1]Mayo Clinic, Department of Orthopedic Surgery
Email: schilaty.nathan@mayo.edu

Introduction

Posture is one of the foundations of human movement and plays an integral part of human neuromuscular physiology, psychology, and overall health.[1,2] With increased screen-time usage, posture can be negatively affected[3] and lead to decreased sensorimotor function. The objective of this study was to evaluate the *immediate effects* of a 15-min postural intervention on the general population, specifically sensorimotor control via leg extension force steadiness. It was hypothesized that the postural intervention would demonstrate immediate effects on force steadiness with decreased error and increased force from the target.

Methods

To evaluate the immediate effect of the 15-min postural intervention, 40 subjects were recruited [Age: 33.4 (12.5) yrs; Sex: 15M:25F]. All subjects had 6 trials of quadriceps force steadiness evaluated [3 eyes open (EO); 3 eyes closed (EC)] alternating between EO and EC conditions. The EC condition allowed the participants to utilize their sensorimotor awareness of the prior EO task to reconstruct it. The subjects were instructed to trace a trapezoidal waveform for 21 seconds with a 50 N threshold target (**Fig. 1**) and were allowed as much practice as desired prior to data collection. During EO condition, the subjects were instructed to 'remember the effort' at the threshold so that they could duplicate it in the EC condition.

A Delsys Trigno wireless system collected load cell (MLP-500) data at 2 kHz and was low-pass filtered with a zero-lag 4th order Butterworth at 10 Hz. Data was then smoothed with a median filter and assessed in the steady (7-14 sec) phase. All post-processing was performed in customized LabVIEW code to fit lines for each phase and extract discrete values of mean force steadiness, % target, slope, coefficient of variation (CoV), and root mean square error (RMSE).

Discrete data was assessed with Student's t-tests comparing EO and EC conditions both pre- and post-intervention. With the EC condition, only the right limb was assessed as it solely had post-intervention data. RMSE was log transformed to improve normalcy for mean statistics. Significance was set at $\alpha < 0.05$.

Table 1. Summary statistics. (EO = eyes open; EC = eyes closed)

	Pre-Intervention		Post-Intervention	
	EO	EC	EO	EC
Mean (N)	49.2	53.0	49.8	61.5
% target	98.4	106.0	99.6	123.0
Slope	0.02	0.06	0.09	-0.26
CoV	0.14	0.04	0.02	0.04
Log RMSE	-0.08	0.06	0.00	0.21

Results and Discussion

With the EO condition, there were significant differences for mean force steadiness (p=0.001), % target (p=0.001), slope (p=0.023). However, as these assessments compare the EO condition, there is a very narrow window of error and thus the statistics likely demonstrate the 'learning effect' of the task and are likely not clinically relevant.

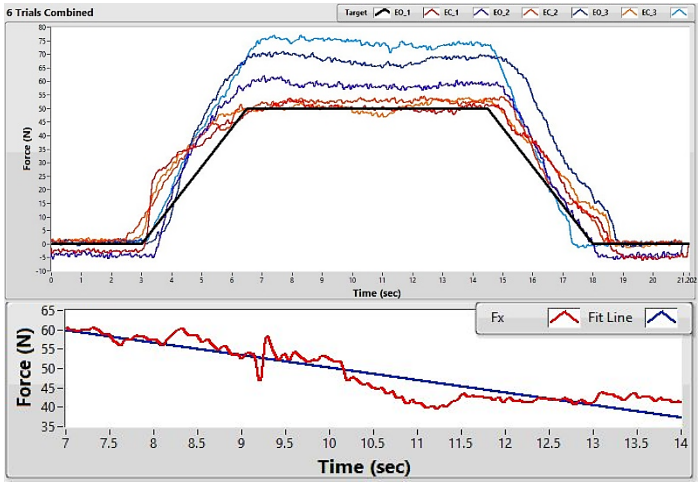

Figure 1: Representative Force Steadiness Trials. *Top*: Subjects were instructed to trace the black trapezoid as steady as possible and be aware of their effort / force output to reproduce without visual feedback. Red/orange = eyes open (EO); Blue/Light Blue = eyes closed (EC). *Bottom*: example of a fitted line to the 'steady' state data.

The EC condition mean force steadiness demonstrated an increase from pre- to post-intervention (p<0.001, **Table 1**). There was no significant change of CoV, however, there was an increase of RMSE post-intervention (p=0.040). Interestingly, there was a change in the slope post-intervention (p=0.014) with the slope negative vs slightly positive (**Table 1**). This data confirmed the hypotheses for increased force but rejects the hypothesis for decreased error.

As the 15-min postural intervention stretches and activates musculature, there is a possibility of post-activation potentiation which would result in an increase of force output and error without immediate sensorimotor awareness. This potentiation could also potentially explain the decrease of slope due to the stretched / activated muscle being more compliant. It is not clear whether these short-term effects demonstrated herein would persist with long-term intervention and should be further explored.

Significance

A 15-min postural intervention does have immediate effects on force steadiness, with an increase force output, change in slope, and an additional increase of error. These immediate effects demonstrate that a long-term evaluation of the postural intervention is warranted to determine long-term sensorimotor effects.

Acknowledgments

NCMIC Foundation; Foderaro-Quattrone Grant for AI Innovation in Orthopedic Surgery; NIAMS L30-AR070273

References

1. Grasso et al. *J Neurophysiol*; 2000; 83(1):288-300.
2. Granata et al. *Clin Biomech*, 2001;16(8):650-659.
3. Park et al. *Physiother Theory Pract*. 2017;33(8):661-669.

ACHILLES TENDON SHEAR WAVE SPEEDS EXHIBIT GUIDED WAVE DISPERSION DURING WALKING

Stephanie G. Cone[1], D. Schmitz[1], and D. Thelen[1]
[1]Department of Mechanical Engineering, University of Wisconsin – Madison
email: sgcone@wisc.edu

Introduction

Tendon kinetics play an important role in both healthy and pathological musculoskeletal function with implications in postural control, transmission of force, and elastic energy storage [1,2]. Current estimates of tendon kinetics during dynamic movement are limited to indirect measurement methods based on inverse kinematics, inverse dynamics and static optimization. In turn, these measurements require assumptions to resolve musculoskeletal redundancies.

Shear wave tensiometry is a noninvasive method to assess tendon loads by exciting and measuring shear wave propagation [3]. A tensiometer consists of a piezo-electric tapper that excites the shear wave and two accelerometers to record the wave arrival downstream. Wave speed modulates with tensile load via a constitutive relationship based on a tensioned beam model. Our work to date has measured transient wave speed in response to impulsive taps. This approach has been shown to delineate changes in tendon loading between conditions for a given subject. However, variability in wave speed magnitudes occurs between subjects. One possible explanation is dispersion, or the dependence of wave speed frequency. Dispersion could arise due to guided wave effects, viscosity and the influence of adjacent layered structures. To better our understanding of dispersion effects, the objective of this work was to explore how frequency content of the excitation can affect measured wave speeds.

Methods

With IRB approval, a shear wave tensiometer was secured on the right Achilles tendon of 16 subjects (8F/8M, 23.5 ± 3.9 years, 71.8 ± 11.2 kg, 1.75 ± 0.1 m) (Fig. 1). Each subject walked continuously at 1.34 m/s with a warm-up period and 10 second intervals of various excitations at 7 order-randomized frequencies (range: 250 to 1450 Hz) in triplicate (Fig. 1).

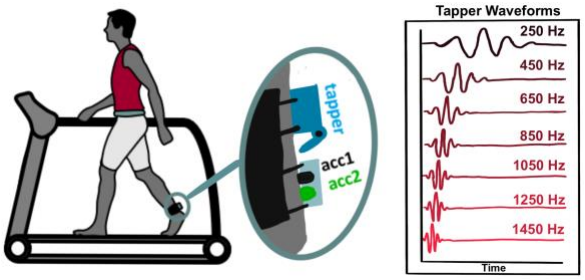

Figure 1: Shear wave tensiometry was performed with various inputs.

Shear wave speed was calculated as described previously [3]. Wave speeds were ensemble averaged over all strides per frequency. Minimum wave speed in stance and early swing and maximum wave speed in push-off and late swing were extracted. Effects of excitation frequency on wave speed maxima and minima were assessed using repeated measures ANOVA.

Results and Discussion

Wave excitation frequency had a significant effect on the shear wave speeds measured in the Achilles tendon during walking ($p<0.05$). Peak wave speed during push-off generally decreased in magnitude with increasing excitation frequency ($p<0.05$), with a nearly two-fold difference in reported shear wave speeds across frequencies (Table 1). Frequency-dependent differences were smaller in magnitude across other phases of stance and swing but were still significant ($p<0.05$). Additionally, the measured stride-to-stride variability was frequency dependent ($p<0.05$).

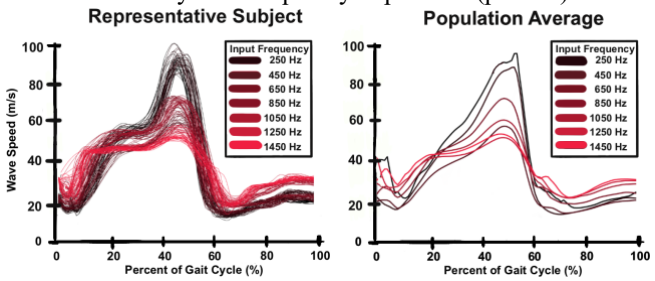

Figure 2: Excitation frequency has a significant effect on wave speed in a single subject (left, strides) and averaged across subjects (right, mean).

Qualitatively, different excitation frequencies affected the shape of the wave speed curve in mid- to late-stance (Fig. 2). This, along with prior reports using impulsive taps of varied duty cycles [4], suggests that observed variability in transient wave speed magnitudes plausibly arise from dispersive effects that are present in intact tendons.

Significance

Shear wave tensiometry is a promising addition to traditional motion analysis. Tensiometry allows for noninvasive measurement of tendon loading and is readily adaptable as a wearable [3]. However, the use of tensiometry to assess absolute tendon loads requires an understanding of dispersive effects that have been observed in this study. Moving forward, we hope to develop an analytical model of dispersion arising from guided wave behavior and establish best practices for measuring shear wave speeds in tendons with high repeatability and sensitivity to load variation.

Acknowledgments

This work was funded by the NIH (NIAMS: F32 AR076276), Stryker-ORS Fellowship, and NSF GRFP (DGE-1747503).

References

[1] Baker, R, J, Neuroeng Rehab, 2006; [2] Roberts, M +, Phys Ther Rehabil, 2017; [3] Martin, JA +, Nat Comm, 2018; [4] Cone, SC+, SB3C Annual Meeting, 2021.

Table 2: Shear wave speeds (mean ± standard deviation) at points of interest in gait.

Frequency	250 Hz	450 Hz	650 Hz	850 Hz	1050 Hz	1250 Hz	1450 Hz
Stance Minimum	18.0±3.7	15.0±1.7	15.0±2.2	17.7±3.0	22.9±6.7	24.5±5.9	28.1±8.2
Stance Maximum	93.4±30.6	87.5±24.3	57.6±15.3	74.4±50.4	61.9±17.3	53.0±10.2	56.7±13.9
Swing Minimum	15.6±4.3	13.4±1.4	15.6±3.8	19.9±6.0	20.7±4.6	21.8±5.3	22.4±5.7
Swing Maximum	23.9±4.3	22.5±2.7	20.9±2.2	24.8±2.9	29.0±5.7	31.2±4.7	31.8±4.4

GLENOHUMERAL RANGE OF MOTION BETWEEN DIVISION I MALE OVERHEAD ATHLETES

Oliver A Silverson[1], Emily Aaron[2], Aleah Fine[3], Chelsea Gruber[4], Fanchon Ohlrogge[5], and Justin L Staker[6]
[1,6]Department of Rehabilitation Medicine, University of Minnesota
[2-6]Department of Intercollegiate Athletics, University of Minnesota
email: *silve567@umn.edu

Introduction

Alterations in glenohumeral (GH) joint movement characteristics are prevalent in competitive overhead athletes.[1] Adaptations occur as a result of the increased physiological demands placed on the associated structures.[2] Increased GH external rotation (ER) and decreased internal rotation (IR) range of motion (ROM) have been observed in swimmers and throwers.[2,3]

The current body of literature evaluating the GH ROM characteristics between various overhead sports is limited by heterogeneous samples.[3] Differences in demographic characteristics and competitive level limit the interpretation of many published comparisons. Therefore, the purpose of this analysis was to compare the GH ROM characteristics between similar samples of overhead athletes. We hypothesized that baseball pitchers would have the greatest amount of ER compared to other male overhead athletes.

Methods

This analysis included healthy male athletes from the University Division I baseball, gymnastics, and swim teams. GH ROM was measured on all participants during a pre-season physical assessment. Passive ER and IR values were recorded with a standard goniometer to the nearest degree. An ER to IR ratio (ER:IR Ratio) was calculated for each individual by dividing each participant's ER by their IR value.

Descriptive statistics were used to summarize the sample. Each ROM characteristic (ER, IR, ER:IR Ratio) was compared between the three sports. Data variance was evaluated with a Levene's Test. Data with equal variance was evaluated with a one-way ANOVA. Data with unequal variance was evaluated with a Kruskal-Wallis rank sum test. Alpha ($p<0.05$) was set *a priori* and adjusted with a Bonferroni correction ($p<0.016$). For the purpose of comparing ROM characteristics to baseball pitchers, only the dominant arm data were included in each comparison.

Results and Discussion

A descriptive summary of the variables included in each comparison are presented in the Table.

Table: Summary of dominant arm GH ROM

	Age (yrs)	ER (º)	IR (º)	ER:IR Ratio
Gymnasts (n=9)	20.1 (1.1)	91 (11.8)	61.4 (9.8)	1.5 (0.3)
Pitchers (n=6)	20.7 (1.2)	92.8 (8.9)	32 (13.1)*	3.3 (1.4)*
Swimmers (n=14)	19.7 (1.3)	100.9 (9.5)	47.9 (13.0)	2.2 (0.6)*

All cell values represent mean (standard deviation). *Significantly different than gymnasts ($p<0.016$).

There were significant differences in IR between sports ($F(2,26) = 10.74$, $p<0.001$). A Tukey post hoc test indicated pitchers had significantly less IR than gymnasts ($p<0.01$) and a trend towards significantly less IR than swimmers ($p=0.03$). Additionally, there were significant differences in ER:IR Ratio between sports ($x^2 = 14.9$, $p<0.01$). A pairwise Wilcoxon rank sum post hoc comparison indicated gymnasts had a significantly smaller ratio than pitchers ($p<0.01$) and swimmers ($p<0.01$). There was not a significant difference in ER:IR Ratio between pitchers and swimmers ($p=0.27$). (Figure) There were no significant differences in ER between sports ($F(2,26) = 3.0$, $p=0.07$).

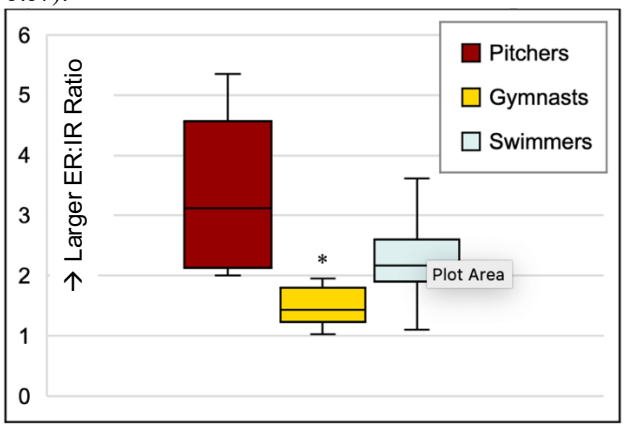

Figure: *Boxplots representing the interquartile range of ER:IR Ratio for each sport. The * indicates a significantly different value compared to pitchers and swimmers.*

Though not statistically different, our results suggest that swimmers have the largest ER compared to gymnasts and pitchers. This result does not support our hypothesis. Competitive swimmers may possess increased ER because of increased GH joint laxity, a physiological adaptation to the GH joint due to the swim stroke. All sports had less IR than ER in our sample. However, pitchers and swimmers had significantly less IR than gymnasts. This resulted in significantly larger ER:IR Ratios for both pitchers and swimmers, respectively, when compared to gymnasts. The loss of IR in pitchers and swimmers could be caused by the repetitive nature of each sport.

Significance

Gymnasts do not exhibit the GH ROM profile typically seen in overhead athletes.[1] This is likely caused by the diversity of gymnastics movements. Loss of IR ROM is a major risk factor for injury in overhead athletes.[1,3] Repetitive overhead movements may predispose pitchers and swimmers to future shoulder injury.

Acknowledgments

We would like to acknowledge the University of Minnesota Department of Intercollegiate Athletics.

References

1.Wilk et al. Shoulder injuries in the overhead athlete. *JOSPT*. 2009.
2. Tate et al. Changes in clinical measures and tissue adaptations in collegiate swimmers across a competitive season. *JSES*. 2020.
3. Tooth et al. Risk Factors of Overuse Shoulder Injuries in overhead Athletes: A Systematic Review. *Sports Health*. 2020.

MODULATION OF SPINAL STRETCH REFLEXES IN THE LOWER EXTREMITY WITH REPEATED POSTURAL PERTURBATIONS

[1]Dong Jae Park, [1]Tyler Wood, [2]Samuel J. Wilson, [3]Harish Chander, [1]Christopher M. Hill*
[1]Northern Illinois University, DeKalb, IL, 60115, United States
[2] Georgia Southern University, Statesboro, GA 30460, United States
[3] Mississippi State University, Mississippi State, MS 39762, United States
Email: chill8@niu.edu*

Introduction

Rapid adaptation of the neuromuscular system's reactive and anticipatory mechanisms to novel perturbations decreases the possibility of falls [1]. Proper neuromuscular response to these disruptions, requires sensory afferents to stimulate spinal stretch reflex (SSR) arcs to contract and relax lower extremity musculature in accordance with the disruption's direction. Muscular co-contraction decreases with repeated exposure to balance perturbations suggesting adaptation of feedforward control after initial exposure [2, 3]. However, this effect seems to be short-lived [3]. The collective evidence suggests that SSRs are modulated through feedforward control mechanisms when repeated exposed to balance disruptions, however, this possibility has yet to be tested. Thus, the purpose of this study is to examine alterations to SSR arcs after multiple exposures to the same postural disruption over the course of several days.

Methods

Seventeen young healthy adults (8 males, 9 females) with no physical abnormalities that affect postural control, participated in this study. Platform translations were delivered with the Neurocom® EquiTest's Motor Control Test (MCT) and translations in the anterior direction (Figure 1A) (large, FWL; medium, FWM; small, FWS) were selected for analysis. Participants performed five fully randomized MCTs over six testing sessions, which they were not given knowledge of the direction or magnitude of the perturbations. The first five sessions occurred on consecutive days, with the sixth occurring two days after the fifth. Muscle activity was collected on medial gastrocnemius (MG), tibialis anterior (TA), vastus medialis (Q) and semitendinosus (H) using the Noraxon TelemyoTM T2400 G2 wireless surface EMG system at 1500 Hz. Raw EMG data was band-passed filtered at 20-250Hz, normalized to peak, and full wave rectified. To quantify SSR, mean muscle activity was taken 30-55ms after perturbation onset, a window based on H-reflex latency [4]. The first trial of a perturbation on each testing day was analyzed using a 1 x 6 (Days) repeated measures ANOVA.

Results and Discussion

SSR activity changed across testing days for both distal and proximal musculature of the lower extremity. Significant differences were noted for Q [$F(5,80)=2.656$, $p=0.028$] and H $F(5,80)=3.681$, $p=0.005$] during the FWM perturbation. A significant decrease in SSR activity from Day 5 to 6 ($p=0.03$). Pairwise comparisons for H revealed a significant decrease in SSR activity from Day 1 compared to Day 4 ($p<0.01$), Day 5 ($p<0.01$), and Day 6 ($p<0.01$). No differences were detected between Day 5 and Day 6 ($p=0.99$) in H. No significant differences were detected across days for Q and H for FWL and FWS. A significant difference was found for MG in FWM [$F(5, 80) =2.656$, $p< 0.001$]. A significant decrease in SSR activity from Day 1 compared to Day 2 ($p<0.01$), Day 3 ($p<0.01$), Day 4 ($p<0.01$), Day 5 ($p<0.01$), but not Day 6 ($p=0.051$) (Figure 1B). No significant differences were found for TA across all perturbation types.

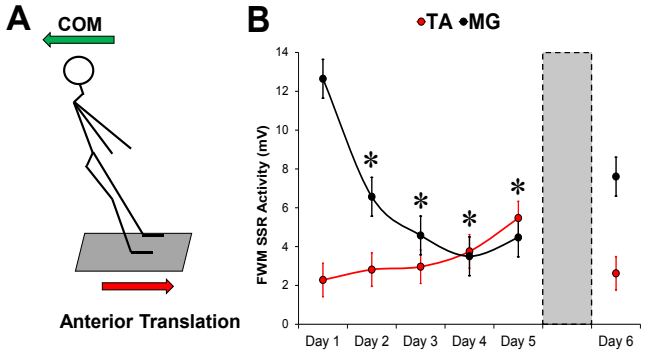

Figure 1: A. Representation of an anterior platform translation. COM= Center of Mass **B.** TA and G SSR activity during the FWM balance perturbation across the six testing sessions. Shaded region represents the two-day retention phase. * represents a significant difference from Day 1 for MG.

Previous studies documented changes to lower extremity muscle activity after exposure to the same postural disruptions [2, 3]. This study provides evidence that SSR arcs are modified when exposed to the same balance distributions over the course of several days. Specifically, the posterior musculature decrease SSR activity as the participants were exposed to the perturbation, suggesting that upright standing is maintained through inhibition of muscle spindle activity in heteronymous muscle to the balance perturbation. This inhibition could result from a decrease in gamma motor neuron activation through anticipatory balance mechanisms [1]. Confirming previous findings [3], this modification is not maintained after the two-day retention period, suggesting that the fixed support balance strategies used to maintain balance are situational and decay when not in use.

Conclusion

Spinal stretch reflex arcs are modified after repeated balance perturbation exposure, but these changes are not maintained over small retention periods. These findings provide insight into how reflexive responses tune fixed support balance strategies to meet environmental demands.

References

1/ Woollacott M. et al. *Gait & Posture*, 1-14. 2002
2/ Welch, T. & Ting., *PloS One*, 1-18, 2014
3/ Hill, C.M. et al., *J of Electomy Kin*, 96-102, 2018
4/ Weiler J. et al., *Nat Neurosci,* 529-533, 2019

ASSESSMENT OF FEMORAL HEAD TRANSLATION TO DIAGNOSE HIP MICROINSTABILITY

Ethan Ruh[1], Camille Johnson, Naomi Frankston, Shaquille Charles, William Anderst, Michael McClincy

[1]Department of Orthopaedic Surgery, University of Pittsburgh, Pittsburgh, PA

Email of presenting author: ruher@upmc.edu

Introduction

Hip microinstability is a hip dysfunction in which extraphysiological motion of the hip causes pain and may contribute to the development of osteoarthritis[1]. Pain associated with microinstability is believed to be caused by excess translation of the femoral head[2,3]. Hence, evaluation of femoral head translation may be clinically relevant for quantifying the severity of hip instability. Previously, it was found that femoral head translation could be reliably measured during a supine clinical exam using dynamic ultrasonography[4], however, the amount of femoral head translation that occurs during a more functional standing position and typical side-to-side differences (SSD) in healthy individuals remains unknown. Additionally, the typical amount of bilateral asymmetry that exists in native, uninjured hip kinematics is necessary to provide context for assessing symptomatic patients and for evaluating the restoration of hip kinematics after injury, surgery and/or rehabilitation. The purpose of this study was to characterize femoral head translation and bilateral symmetry in hip kinematics during a static standing pivot in healthy young adults.

Methods

Eighteen adults (6 male, 12 female; age: 21.8±2.1 years; BMI: 22.6±2.0 kg/m^2) with no history of hip surgery or pathology participated in this study. Synchronized biplane radiographs were collected during a static standing trial (neutral stance, one trial per hip) and during a standing static pivot position where the participant extended, rotated and abducted at their back hip (one trial per hip) (Figure 1). During the static pivot position, participants were instructed to stand with their feet split in the anterior-posterior direction and pivot as far as they could towards their contralateral side. Femur and pelvis position were determined by matching subject-specific CT bone models to the biplane radiographs using a validated volumetric model-based tracking technique (precision: 0.8˚, 0.3 mm)[5].Femoral head translations were calculated as displacement of the center of the femoral head relative to the center of the acetabulum along each anatomical axis[6]. Anatomical coordinate systems were established on each hemi-pelvis[7] and mirrored to each side to produce identical coordinate systems for each hip. Femoral head translation, and rotation of the femur relative to the pelvis in the pivot position, were normalized to the static standing posture. Bilateral symmetry in hip kinematics was assessed by calculating absolute side-to-side differences (SSD_A) for each participant and averaged to obtain overall SSD for the cohort.

Figure 1: Imaging of the right hip during the pivot motion.

Results and Discussion

Average normalized translation magnitude of the femoral head was less than 0.4 mm during the pivot (Table 1). The pivot motion induced combined external rotation, adduction and extension at the hip (Table 1). Average SSD_A in the kinematics when moving from standing to the pivot position were 1.1 mm or less in translation and 7.2° or less in rotation (Table 1).

The primary finding of this study was that single side and SSD_A translation of the femur head relative to the acetabulum during a pivot relative motion from standing was less than 1.1 mm. This finding suggests that translational asymmetries greater than 1.1 mm during a standing pivot may be indicative of dysplastic hip pathologies.

Significance

Previously, d'Hemecourt et al. reported femoral head translation values ranging from 1.06 to 2.2 mm using ultrasound[4]. Those values are not comparable to the values we found, as they measured femoral head translation as the space between the femoral head and the acetabulum during a supine twisting motion, where we measured translation based upon coordinate systems centered at the femur head and acetabulum. Further research on symptomatic patients is required to determine the threshold at which femoral head translation becomes painful and to assess the ability of conservative and surgical intervention to restore native symmetry.

References

1) Woodward et al. *Skel Rad.* 2020 2) Akiyama et al. *Osteoarthr Cartil.* 2011 3) Safran. *JAAOS-J Am Acad Orthop Surg.* 2019 4) d'Hemecourt et al. *Clin Orthop Relat Res.* 2019. 5) Martin et al. *J Arthroplasty.* 2011. 6) Wu et al. *JBiomech.* 2002. 7) Pataky, *JBiomech.* 2014.

Table 1. Average position and orientation of the femur relative to the acetabulum during standing and pivot positions, and relative motion from standing to pivoting. Absolute side-to-side differences (SSD) for each position and SSD in relative motion is also shown (mean ± SD). For average kinematic values, positive directions are anterior, superior and medial.

	Translations (mm)								**Rotations (degrees)**					
	Anterior-Posterior		Superior-Inferior		Medial-Lateral		Magnitude		Flexion		External Rotation		Abduction	
	Avg.	SSD	Avg.	SSD	Avg.	SSD	Avg.	SSD	Avg.	SSD	Avg.	SDD	Avg.	SSD
Stand	1.7±1.3	0.9±06	-2.1±1.2	1.0±0.6	-4.3±2.1	1.4±1.2	3.2±2.1	1.4±1.1	-1.5±6.4	4.5±2.4	-11.3±9.8	7.6±7.8	2.8±3.1	1.4±3.8
Pivot	2.1±1.4	1.4±1.2	-2.1±1.4	0.9±0.8	-4.4±2.1	1.3±0.8	5.7±2.0	5.1±0.8	-0.6±8.8	5.1±3.1	11.3±12.3	7.0±4.3	2.9±3.8	4.2±3.4
Relative	0.4±1.0	1.1±0.8	0.0±0.7	0.8±0.5	-0.1±6.2	0.7±0.7	0.4±0.8	1.0±0.8	0.9±6.2	4.4±2.9	22.7±12.0	7.2±6.8	5.7±4.5	5.4±4.3

PREDICTION OF KNEE ADDUCTION MOMENTS USING INSTRUMENTED INSOLE AND NEURAL NETWORKS

Samantha J. Snyder[1], Edward Chu[1], Jumyung Um[2], Yun Jung Heo[3], Ross H. Miller[1,4], and Jae Kun Shim[1,3,4,5]
[1]Department of Kinesiology, University of Maryland, College Park, MD, USA
[2]Department of Industrial & Management Systems Engineering, Kyung Hee University, Yongin-Si, Gyeonggi-do, South Korea
[3]Department of Mechanical Engineering, Kyung Hee University, Yongin-Si, Gyeonggi-do, South Korea
[4]Neuroscience and Cognitive Science Program, University of Maryland, College Park, MD, USA
[5]Fischell Department of Bioengineering, University of Maryland, College Park, MD, USA
email: jkshim@umd.edu

Introduction

Knee osteoarthritis (KOA) is a widespread, complex chronic disease that is difficult to detect and prevent. Because KOA is characterized by a gradual loss of cartilage, knee joint loading is a suspected factor in the disease, and previous studies have shown that higher peak and impulse of the knee adduction moment (KAM) during walking is associated with KOA [1-4]. Although KAM is considered a biomechanical risk factor of KOA, standard data collection is expensive, time consuming, and requires a gait lab, motivating alternative methods to simplify KAM measurement and its "real-world" assessment. Previous studies used artificial neural networks in conjunction with wearable sensors to predict gait characteristics from different sensor configurations [5,6]. While these studies apply basic feed-forward neural networks (FFNN) to predict gait characteristics, other models such as convolutional (CNN) and recurrent neural networks (RNN) intended for time-series data could have greater success predicting KAM [7]. Shoe-based wearable sensors are desirable for convenient data collection because they are typically non-invasive, require minimal setup, and can feasibly be translated to outside-the-lab applications. Therefore, the purpose of this study is to apply CNN, RNN, and FFNN and a custom-made insole embedded with multiple thin 3-axis force sensors to predict KAM during walking. Given previous research, it was hypothesized that the neural networks will predict peak and total KAM with high accuracy; however, performance between the structures will differ [5,6].

Methods

Nine healthy young female subjects (23±3 y; 164.6±2.5cm; 61.4±6.1kg) participated. Each subject walked across 10 force plates for 8 trials at self-selected "slow" to "fast" speeds in random order. Motion capture and ground reaction force data were collected, and KAM was calculated through inverse dynamics modeling. Insole sensor data were synchronously collected through five 3-axis piezoresistive force sensors located at big toe, medial ball, central ball, lateral ball, and heel. Each stance phase of data was scaled to 1024-time intervals to facilitate application of the neural networks to all trials. The insole sensor data were input to CNN, RNN, and FFNN models and leave-one group out cross validation was applied [8]. This method reduces prediction bias by allowing individual subject data to be in either the test or the training set. First peak and second peaks of KAM and the overall KAM time series were compared to corresponding predictions from each neural network. Spearman's correlation coefficient (r) and root mean squared error (RMSE) were used to determine the prediction accuracy.

Results and Discussion

All three models estimated KAM with RMSE ranging from 0.6-1.2% (Table 1), which is well within the typical accuracy and reliability of inverse dynamics calculations. Each model also predicted KAM with strong correlation coefficients greater than 0.72. CNN resulted in the highest correlation coefficients (r > 0.89) and lowest RMSE (RMSE < 0.8%) followed by the RNN and FFNN.

Table 1. Accuracy of models calculated as Spearman's rank correlation coefficient (r) and root-mean-squared error (RMSE) of each outcome variable

	Total KAM		Peak 1		Peak 2	
Model Type	r	RMSE [%]	r	RMSE [%]	r	RMSE [%]
FFNN	0.84	1.0	0.77	1.2	0.72	1.2
RNN	0.91	0.8	0.86	0.9	0.79	0.9
CNN	0.95	0.6	0.89	0.8	0.93	0.8

The present study demonstrated that instrumented insole-based wearable sensors could allow KAM to be assessed without lab-based motion and force data. Furthermore, the study demonstrated that predicting the stance phase KAM with neural networks intended for time series data was a successful method. CNN had the strongest correlation coefficients and lowest RMSE compared to other models for first peak, second peak and total KAM. The successful prediction of first peak, second peak and total KAM demonstrates a great potential for a simplified KAM calculation that can be applied outside of laboratory settings.

Significance

This study was the first to apply multiple artificial neural networks to predict KAM-related variables from the wearable instrumented insole. The concise technique presented in this study is expected to allow for clinical uses and promote future research studies on the effects of reduced KAM on KOA severity and progression. In future research, this method can be used to provide instantaneous KAM prediction, which can be used to reduce KAM, and eventually KOA, using smartphone-based biofeedback to KOA patients.

Acknowledgments

The authors appreciate Hyun Ji Lee for her contribution to data collection.

References

[1] Bennell et al. (2011). *Ann. Rheum. Dis.*, **70**: 1770-1774.
[2] Brisson et al. (2017). *J. Orthop. Res.,* **11**: 2476-2483.
[3] Chang et al. (2015). *Osteoarthr. Cartil.*, **23**: 1099-1106.
[4] Chehab et al. (2014). *Osteoarthr. Cartil.*, **22**: 1833-1839.
[5] Stetter et al. (2020). *Front. Bioeng. Biotechnol.*, **8**: 9.
[6] He et al. (2019). *Gait Posture*, **70**: 408-413.
[7] Ismail Fawaz et al. (2019), *Data Min. Knowl. Discov.*, **33**: 917-963.
[8] Halilaj et al. (2018), *J. Biomech.*, **81**: 1-11

A META-ANALYSIS OF VIBRATION TRAINING ALTERING QUALITY OF LIFE IN OLDER ADULTS

Rebekah Buehler, OTR/L, MHS[1] and Feng Yang, PhD[1]
[1]Department of Kinesiology and Health Georgia State University, Atlanta, GA 30303, USA
Email : rbuehler2@student.gsu.edu

Introduction

Older adults often experience reduced quality of life (QOL).[1] Although physical activity could improve QOL among older adults, many are unable to participate in recommended levels of physical activity.[2] Vibration training is a low-intensity exercise with the potential to improve strength, sensation, balance, and flexibility for older adults.[3] It may benefit those unable to tolerate higher activity demands, and has been applied to older adults to improve their QOL.[4] However, findings from previous studies are inconsistent. This preliminary systematic review and meta-analysis sought to summarize and clarify the effects of vibration training in altering the eight domains of QOL, as listed by the Short Form-36 (SF-36) among older adults, based on randomized controlled trial (RCT).

Methods

A systematic literature search was performed in Web of Science, PubMed, APA PsychInfo, and Cochrane Library databases were searched for relevant articles up to August 2020. The MeSH terms used to conduct the search were: "quality of life", "health related quality of life", "whole body vibration", and "older adults." The initial search yielded 86 studies for consideration with the following criteria: 1) conducted among older adults (mean age of 60 years or over); 2) a RCT, in that one group of participants underwent vibration training and at least another group received placebo, or alternate treatment, assessed QOL outcomes; and 3) was published in English. To reduce the heterogeneity in outcome measurements among studies, only studies which adopted the SF-36 as the QOL outcome measures were included. Four RCTs qualified for our inclusion criteria. The four included RCTs enrolled 178 participants.[5-8] One of the four studies utilized three different vibration training frequencies. The three groups were considered and analyzed separately.[6] Therefore, *six* comparisons based on the four studies were made. Quality of all four studies was obtained from checking the Physiotherapy Evidence Database (PEDro) scale.

Information about the article (author(s), publication year), the participants (sex and age) and interventions (vibration frequency, amplitude, duration and number of bouts of each training session, number of sessions weekly, and training duration) were collected per study. Values from each of the eight QOL health domains were extracted in the form of means and standard deviations (SD),[5-8] and sample size for both vibration training and non-vibration (or control) groups at pre-and post-training assessments. The standardized mean difference (SMD) was calculated as the effect size measurement, and a significance level of $p < 0.05$ was used. Meta-analyses were completed for each of the eight SF-36 domains using a fixed-effects model from the four studies within RevMan 5.3 (Denmark).

Results and Discussion

The average PEDro score for the four studies was 5.25 ± 1.71 out of 10. The average age of the participants ranged from 66.4 to 84.5 years. The training sessions repeated one to three times per week over six to 35 weeks. The vibration frequency and amplitude varied from 10 to 35 Hz and from 0.5 to 7 mm, respectively. Vibration training showed a low attrition rate of 7.9%. Relative to controls, vibration training is more effective for older adults in improving three QOL domains: physical function (SMD = 0.54, p = 0.0002, Figure 1), physical role limitations (SMD = 0.31, p = 0.03), and vitality (SMD = 0.33, p = 0.02). Vibration training may not lead to greater improvements for the other five QOL domains (social function, emotional role limitations, mental health, bodily pain, and general health perceptions, SMD = 0.02 - 0.27, p-values = 0.06 - 0.88) than controls.

Vibration training can be well accepted by older adults. Compared to controls, vibration training may provide greater benefits to improve the SF-36 domains of physical function, vitality, and physical role limitations. This could be explained by the fact that vibration training can improve strength, power, sensation, and flexibility for older adults, which are related to the physical functions of older adults. Although our results showed non-significant effect sizes for vibration training improving other five SF-36 domains relative to controls, it is premature to definitively conclude that vibration training is not more effective than controls due to the small sample size included in this meta-analysis. More well-controlled RCTs are needed to further examine the effects of vibration training on improving QOL among older adults.

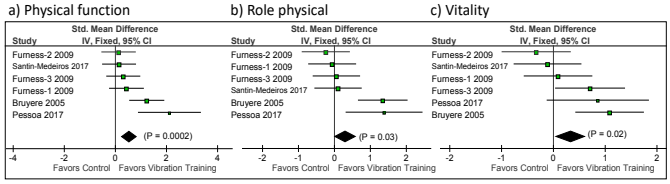

Figure 1: Forest plots of effect sizes (SMD) for a) physical function, b) role physical, and c) vitality summarized from four studies that assessed effects of vibration training on QOL (as quantified by SF-36). Studies labeled as Furness-1, -2, and -3 correspond to the once through thrice weekly sessions of vibration training received by these groups.[6]

Significance

The findings from this meta-analysis are significant as healthcare to older adults is increasingly focused not only on factors which positively influence physical health measures, such as balance, mobility, and strength, but on improving QOL especially among older adults. Our findings indicate that vibration training could be an encouraging alternative for older adults, especially those who lack necessary physical capacity to undertake traditional exercise-based training programs, to improve QOL.

References

1 Álvarez-Barbosa, *Maturitas,* 2014, 79(4), 456-63.
2 Lam, *Int. J. Geriatr. Psychiatry*, 2018, 33(1), 21-30.
3 Yang, *J. Biomech.*, 2015, 48, 3206-12.
4 Pessoa, *Whole Body Vibrations*, CRC Press, 2018, 101-14.
5 Bruyere, *Arch. Phys. Med. Rehabil.*, 2005, 86(2), 303-7.
6 Furness, *J. Strength Cond. Res.*, 2009, 23(5), 1508-13.
7 Pessoa, Brandão, *J. Gerontol.,* 2017, 72(5), 683-8.
8 Santin-Medeiros, *Res. S. Med.*, 2017, 25(1), 101-7.

BODY-WEIGHT SUPPORT DISRUPTS STEPPING COORDINATION

Andrew Dragunas[1,2], Keith E. Gordon[1,3]
[1]Physical Therapy and Human Movement Sciences, Northwestern University, Chicago, IL, USA
[2]Department of Biomedical Engineering, Northwestern University, Chicago, IL, USA
[3]Edward Hines Jr. VA Hospital, Hines, IL, USA
email: *andrew.dragunas@northwestern.edu

Introduction

Many populations with neuromuscular impairments are at a significant risk of falling due to deficits in control of locomotor stability. Specifically, in people post-stroke a primary mechanism to maintain lateral stability during gait – the modulation of step-by-step lateral foot placement relative to ongoing center of mass (COM) state – is impaired [1]. Body-weight support (BWS) systems are frequently used during rehabilitation to facilitate gait training with the goal to develop coordinated stepping movements. While BWS systems are a safe and effective tool for reducing limb load during gait, the forces applied to the body alter normal COM dynamics [2] and result in increases in step width [3]. Thus, the use of BWS systems during gait training may have an unintended and undesirable effect of limiting practice of coordinated stepping. Understanding how BWS affects the coordination of lateral foot placement is important for clinical decision-making regarding how and when to utilize this rehabilitation tool.

Based on our previous observations, we hypothesize that BWS will reduce the coordination between lateral foot placement and lateral COM state during steady-state walking.

Methods

We recorded lower body kinematics and ground reaction forces from nine healthy participants as they walked at their preferred speed on an instrumented split-belt treadmill with varying levels of BWS. Participants walked with three levels of BWS: 0%, 30%, and 60% provided by an overhead system (ZeroG, Aretech). We repeated each condition twice and collected data during the last 2 minutes of each 4-minute walking trial.

For each condition, we calculated the correlation between lateral foot placement position and lateral COM state (position and velocity) over the swing phase. This data was then used to create a time-series R^2 trajectory showing the percentage of variability in lateral foot placement position explained by lateral COM state.

Results and Discussion

We found that the correlation between lateral COM state and lateral foot placement position decreased as the percentage of BWS increased. There was a significant main effect of BWS level ($F(2,16) = 6.528$, $p < 0.001$). Post hoc analysis identified that R^2 correlations at 0% BWS were stronger than either 30% BWS ($p < 0.001$) or 60% BWS ($p < 0.001$) for the entire swing phase. R^2 correlations at 30% BWS were significantly stronger than 60% BWS ($p < 0.001$).

Our hypothesis was supported. As BWS increased, lateral COM state became less predictive of lateral foot placement. Maintenance of lateral stability requires coordination between the COM and subsequent foot placement. At 0% BWS, COM state becomes increasingly predictive of lateral foot placement as swing progresses, ultimately explaining ~80% of the variance in foot placement position. In contrast, at 60% BWS, COM state explains less than 50% of the variance (Figure 1).

We suspect that the changes to COM dynamics induced by BWS leads to this discoordination of lateral stepping. When walking in reduced gravity the passive dynamics of the COM and lower extremities change. The altered passive dynamics may conflict with an individual's internal model used to create coordinated foot placement in normal gravity. While BWS systems facilitate gait training, they encourage lateral stepping behavior that is less correlated with the COM.

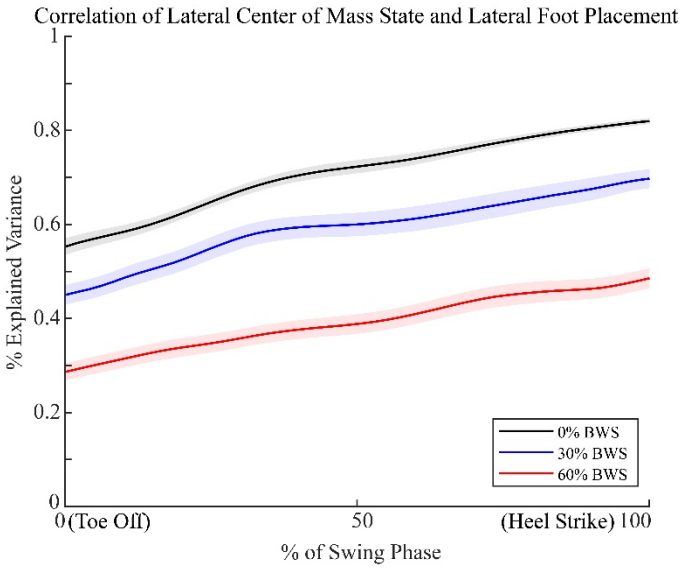

Figure 1: Mean ± standard error (shaded region) of R^2 time-series showing the percentage of variability in lateral foot placement position that can be explained by COM state (position and velocity) at different levels of body-weight support.

Significance

BWS training is a common rehabilitation tool used during gait training. This tool is excellent at facilitating stepping for individuals who could not do so otherwise, but BWS does impact lateral foot placement coordination. Clinicians who utilize these systems should consider augmenting BWS training with interventions that may improve regulation of lateral foot placement, such as targeted stepping. Although future studies investigating the training effects BWS in specific impaired populations are needed to fully understand the interaction between BWS and stepping coordination, the results of the current study provide a framework for clinical decision-making.

Acknowledgments

This work was supported in part by the NIH training grant #T32EB009406-10 and the US Department of Veteran Affairs, Rehabilitation Research and Development Services, Merit Review Award # I01RX001979.

References

[1] Dragunas AC, et al. *IEEE Trans Neur Sys Rehab Engr*, 2021.
[2] Aaslund MK, et al. *Gait & Posture* **28**, 303-308, 2008.
[3] Dragunas AC, et al. *J. Biomech* **49**, 2662-2668, 2016.

DYNAMIIC STABILITY DURING A CHALLENGING LOCOMOTOR TASK IS NOT AFFECTED BY WEEKLY EXERCISE DURATION

Patrick G. Monaghan[1], Sarah A. Brinkerhoff[1], and Jaimie A. Roper[1]
[1]Auburn University
email: pmonaghan@auburn.edu

Introduction

Balance control is fundamental in daily life to safely perform many movements, while most falls occur in dynamic conditions.[1] Active individuals have enhanced physical function and mobility compared to sedentary individuals[2], yet how activity levels impact dynamic stability in different environments is unclear. Examination of this relationship and the relationship between overground gait measures and measures of dynamic stability is crucial. Greater understanding may lead to enhanced and targeted rehabilitation approaches with the potential to reduce fall risk. The purpose of our study was to 1) examine changes in dynamic stability between active and sedentary individuals during overground walking and walking on a balance beam, and 2) assess the relationship between overground spatiotemporal parameters of gait and dynamic stability measures during balance beam walking in active and sedentary individuals.

Methods

Two groups of healthy young adults participated in this study: 13 participants in the sedentary group and 24 participants in the active group. Participants were classified as active if they participated in at least one hundred and fifty minutes per week of exercise for at least three months. Participants first completed overground walking during which they walked across the flat ground at their typical speed. The participants then completed a heel-to-toe walk on a nonplanar balance beam. The beam was placed on the flat ground, measured 2.44 meters long, 8.89cm wide, and 3.81cm.

Step length, time, and width were analyzed from the overground walking trials. The coefficient of variation (CoV) of these outcome measures was also derived as measures of variability. The mediolateral margin of stability (ML-MoS) was used to quantify dynamic balance.[3] The ML-MoS was calculated during both overground walking and beam walking. The ML-MoS was defined as the minimum difference between the extrapolated center of mass (XCoM) and base of support at heel-strike for each step. The lateral malleolus marker defined the lateral boundary of the base of support. The XCoM and MoS were calculated using:

$$XCoM = CoM + \frac{Vcom}{\sqrt{g/l}} \quad (1)$$

$$MoS = BoS - XCoM \quad (2)$$

Figure 1. Equations for the extrapolated center of mass (1) Margin of Stability (2). XCoM = extrapolated center of mass, CoM = position of center of mass, VCoM = velocity of center of mass, g = gravity, l= leg length.

A two-way repeated-measures ANOVA was conducted to compare the effect of condition (overground or beam) and group (sedentary or active) on ML-MoS. Multivariate regressions were conducted to determine whether spatiotemporal parameters of overground gait could predict dynamic balance measures during beam walking in active and sedentary individuals. The regressions were calculated separately for sedentary and active individuals.

Results and Discussion

A significant main effect of condition on ML-MoS was observed; $F(1,33) = 75.811$, $p < .001$. ML-MoS significantly decreased during beam walking ($M = 6.09$, $SD = 1.56$) compared to overground walking ($M = 8.67$, $SD = 1.05$). On average, ML-MoS decreased by 2.56cm during the beam walk (**Figure 2**). These results indicate that beam walking provided sufficient challenge to stability in the frontal plane, resulting in a marked decrease in ML-MoS. No significant effect of group was reported; $F(1,33) = .032$, $p = .86$. Similarly, there was no significant interaction between group and condition; $F(1,33) = 1.464$, $p = .235$. Overground spatiotemporal parameters of gait did not predict ML-MoS during beam walking in either group. While the relationship between dynamic stability control and sport-specific athletic performance has been established,[4] our results indicate that simply meeting the recommended dosage of activity per week was not sensitive to detect differences in dynamic stability.

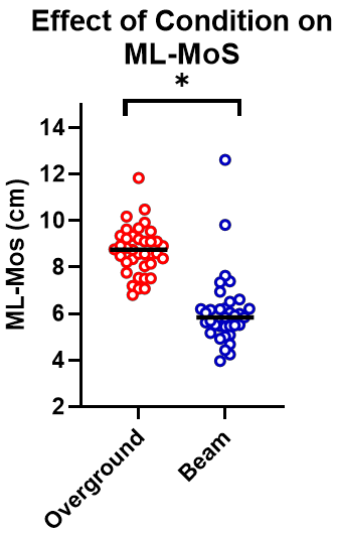

Figure 2: ML-MoS significantly decreased between overground and beam walking. Horizontal bar indicates mean, *indicates p <.001.

Significance

Beam walking is an effective task for altering dynamic stability compared to overground walking in young adults. Active and sedentary young adults did not display differences in dynamic stability during a challenging locomotor task. However, we only measured the volume of exercise and did not investigate the type of activity/sport our participants were partaking in, which may influence our results. For example, investigating this question in a population of gymnasts versus swimmers may yield different findings. Further, our study was in young adults; future work is needed in older adults to understand the impact of general exercise amount and dynamic balance performance.

References

[1]Rubenstein, L. Z. (2006). *Age and Ageing*.
[2]Morie et al., (2010). *Journal of American Geriatrics Society*
[3]Hof et al., (2005). *Journal of Biomechanics*.
[4]Hrysomallis, C. (2011). *Sports Medicine*.

IMPAIRED QUADRICEPS FUNCTION AND KNEE MECHANICS IN ACTIVE FEMALES WITH LOW BACK PAIN

Joshua D. Winters[1], Kristen M. McTernan[2], Matthew C. Hoch[1], Cale A. Jacobs[3], Nicholas R. Heebner[1], John P. Abt[4] and Alexa K. Johnson[5]

[1]College of Health Sciences, University of Kentucky, Lexington, KY

email: *joshua.winters@uky.edu

Introduction

Chronic low back pain (LBP) is one of the most widely experienced musculoskeletal disorders in the general population and is becoming increasingly common in an active population [1,2]. Athletes with LBP have demonstrated poorer quadriceps function compared to those without LBP [3]. Female athletes with LBP are more likely to present with deficits in lower extremity strength compared to male athletes with LBP [2]. During running, load is dissipated throughout the kinetic chain as the quadriceps attenuate shock and eccentrically control the knee. Deficits in quadriceps function have been linked to altered knee biomechanics during running. Specifically, individuals with LBP present with reduced knee flexion, or an increased knee joint stiffness, during stance phase [4].

A lack of quadriceps function, in active females with LBP, may contribute to less knee flexion and altered knee moments, influencing loading patterns experienced at the knee, increasing the risk of a lower extremity injury. Therefore, the purpose of this study was to determine if females who suffer from LBP have asymmetrical quadriceps strength and inefficient running mechanics compared to healthy females. We hypothesized that females with LBP would present with lower quadriceps strength, increased quadriceps strength asymmetry, stiffer knee flexion and increased ground reaction forces during running.

Methods

Twenty females with LBP (Age=23.8±3.5yrs; Mass=66.9±8.2 kgs; Height=1.7±0.05m; Duration of Pain=4.6±3.7 years; Oswestry Disability Index=15.8±3.7%) and 20 healthy female controls (CTRL; Age=23.6±3.7yrs; Mass=67.1±8.9kgs; Height=1.7±0.04m) completed this study. Individuals were included in the study if they scored a minimum of five on the Tegner physical activity scale, had no history of a previous lower extremity surgery, or a lower extremity injury within the last year. Individuals in the LBP group reported experiencing LBP for a minimum of four months, while those in the CTRL group had no reported history of LBP.

Dominant and Non-Dominant quadriceps strength was assessed as isometric torque recorded on an isokinetic dynamometer with the knee flexed to 60°. Individuals completed three maximal effort isometric quadriceps contractions, in which peak torque was averaged across the three trials and normalized to body mass. A three-dimensional motion analysis and in-ground force plate system was used to assess over ground running mechanics. Euler angles were used to calculate bilateral lower extremity kinematic variables. Inverse dynamics were used to calculate bilateral lower extremity kinetics, along with peak vertical ground reaction forces, and loading rate (from initial ground contact to peak vertical force). A 2x2 (group x limb) repeated measures analysis of variance with post-hoc t-tests were used to assess group and limb differences in peak quadriceps strength, knee flexion angle at initial ground contact, peak knee flexion angle, peak internal knee extension moment, peak vertical ground reaction force, and average loading rate. Significance was set a priori at $p < 0.05$.

Results and Discussion

There was a significant main effect between groups in quadriceps strength and peak knee flexion (Figure 1) and between limb in quadriceps strength, average loading rate, peak knee flexion, and peak knee extension moment. The CTRL group had greater quadriceps strength compared to the LBP group in the dominant ($p=0.040$) and non-dominant limbs ($p=0.015$). Both groups had greater dominant limb strength compared to the non-dominant limb (CTRL: $p=0.004$; LBP: $p=0.015$). Additionally, the CTRL group exhibited greater peak knee flexion during stance phase of both limbs compared to the LBP group (dominant: $p=0.033$, non-dominant: $p=0.009$). Those in the LBP group also had asymmetrical peak knee extension moments ($p=0.014$) and loading rates (0.015). There were no differences in peak vertical ground reaction force or knee flexion angle at initial contact.

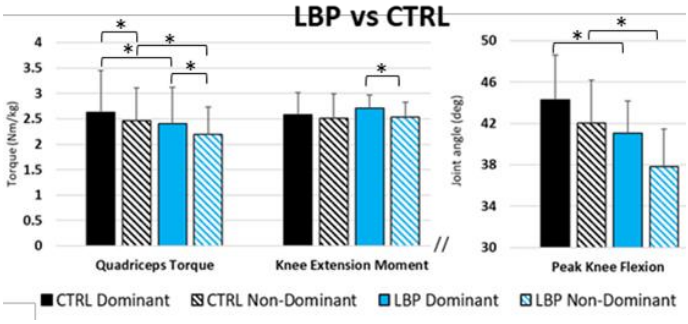

Figure 1: Bar graph of quadriceps torque and running mechanics comparing dominant to non-dominant limb in healthy control subjects (CTRL) and those with chronic low back pain (LBP).

Significance

Subjects with LBP demonstrated impaired quadriceps function, lower knee flexion angles, asymmetrical knee joint loading, and asymmetrical loading rates during running. These findings likely have a significant impact on the occurrence or onset and recovery from pain, the risk of developing secondary musculoskeletal injuries, and the progression of LBP severity throughout the individual's lifetime.

Further research is needed to better understand the relationships between the strength deficits, altered mechanics, and asymmetrical loading patterns identified within this study. These relationships will contribute to the development of more effective evidence-based low back injury/pain prevention and rehabilitation strategies.

Acknowledgments

This research was supported by the American Society of Biomechanics Student Grant-in-Aid. Content is the responsibility of the authors and does not represent the views of ASB.

References

1. Taunton et al. 2003. *Br J Sports Med.* 36(2).
2. Nadler at al. 1998. *Spine.* (23)7.
3. Hart et al. 2010. *Clin Biomech.* 25(8).
4. Hamil et al. 2009. *Res Sports Med.* 17(4)

SEX AND RACE DIFFERENCES IN CENTER OF PRESSURE TRAJECTORIES DURING SHOD GAIT

Cherice N. Hill[1], Daniel Schmitt[2], Matthew McCullough[3], and Robin M. Queen[4]
[1]Clemson University – Medical University of South Carolina Bioengineering Program, Charleston, SC, USA
[2]Department of Anthropology, Duke University, Durham, NC, USA
[3]Department of Chemical, Biological, and Bioengineering, North Carolina A&T State University, Greensboro, NC, USA
[4]Department of Biomedical Engineering and Mechanics, Virginia Tech, Blacksburg, VA, USA
email: hughesch@musc.edu

Introduction

The progression of the center of pressure (COP) is essential for normal locomotion. COP trajectories have been used to describe functional foot behavior, movement performance, efficiency, and balance control during gait[1-3]. Although normal COP motion has been well defined, little is known about sex and race COP trajectory differences in healthy young adults.

Therefore, the purpose of this study was to test the hypothesis that COP trajectories during gait would differ between sexes (male, female) and racial groups (African American: AA, white American: WA) in young adults.

Methods

92 participants equally divided by sex and race were recruited. Ground reaction force data was recorded during 7 shod gait trials at a set speed (1.35m/s) across a force plate walkway. COP time series trajectories were normalized to stance and exported from Visual 3D for the dominant limb (limb used to kick a soccer ball).

The following discrete COP outcomes were extracted: initial (I-Loc) and final (F-Loc) proximo-distal locations and total proximo-distal excursion (PDE) as a percentage of shoe length, peak lateral (P-L-Loc) and medial (P-M-Loc) COP locations as a percentage of shoe width, as a percentage of shoe length. Main and interaction effects of sex and race on discrete measures were evaluated with a multivariate ANOVA (α=0.05), and partial eta squared (η^2) effect sizes were computed.

Continuous COP trajectories were analyzed to assess differences throughout the stance phase. Statistical parametric mapping (SPM) was used to perform paired Hotelling's T^2 tests including both COP components for sex and race. Post hoc SPM t-tests were performed, when appropriate, to evaluate proximo-distal and medio-lateral components separately (α=0.05).

Results and Discussion

Only sex was significant in the discrete MANOVA model ($p<0.001$, $\eta^2=0.322$). Corrected models for P-L-Loc and P-M-Loc were not significant, so only sex effects for I-Loc, F-Loc, and PDE are reported from the discrete analysis. COP excursion was greater in females compared to males, and the COP trajectory began more proximally and ending more distally (Table 1).

Table 1: Discrete COP measures ($p<0.05$) between sexes. †medium effect size, ‡large effect size.

Variable (%)	Males	Females	Sex Effect
I-Loc	3.9 ± 3.9	2.2 ± 2.6	$p=0.015$, $\eta^2=0.065$†
F-Loc	95.0 ± 2.2	97.2 ± 2.3	$p<0.001$, $\eta^2=0.203$‡
PDE	92.5 ± 3.6	96.0 ± 3.5	$p<0.001$, $\eta^2=0.208$‡

Sex differences were observed throughout stance using SPM (Figure 1). While COP trajectories varied between sexes in the medio-lateral direction for a brief portion of terminal stance, the majority of observed sex differences were in the proximo-distal direction. While no racial differences were observed with discrete analysis, SPM identified a region of racial difference in the medio-lateral direction during early stance.

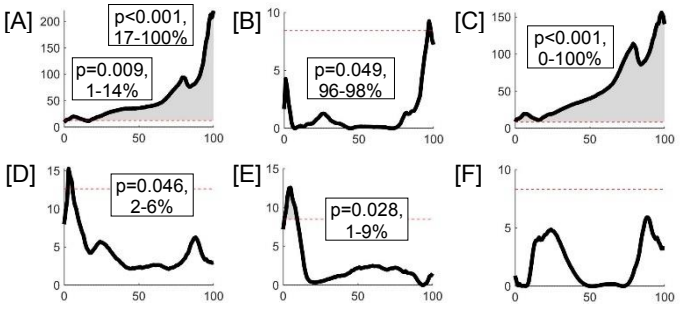

Figure 1: Paired Hotelling's T^2 [A,D] and post hoc medio-lateral [B,E] and proximo-distal [C,F] SPM results for sex [A-C] and race [D-F] effects. Regions of significant difference (gray) and details shown.

Relevant prior literature in healthy young adults is limited. Greater COP excursion in young females was previously reported with the use of an unstable shoe [4], which aligns with our findings. Interestingly, smaller COP excursion was found in middle aged and older females compared to males[5], suggesting that sex differences may be dependent on age. The ratio between foot length and overall height is also smaller in females [6], which may be related to utilization of greater COP excursion; this possibility should be investigated in future studies.

Racial differences in COP motion have not been previously reported and are essential to investigate given racial disparities in fall risk[7] and other chronic conditions such as diabetes[8]. COP is an indicator of postural control and balance stability, so racial differences in COP displacement may be related to this health disparity. Racial differences in medio-lateral COP motion may be explained by foot type, of which pes planus is more common in AA[9], or foot flexibility, which should be further explored.

Significance

Consideration of differences in COP trajectory displacement between sexes and racial groups is essential to inform risk analysis, intervention planning, and rehabilitation protocol development in diverse populations. This study identified distinct sex and race differences in COP trajectories during healthy gait, which reinforces the importance of considering such factors in research and clinical care.

Acknowledgments

The Howard Hughes Medical Institute Gilliam Fellowship and the Institute for Society, Culture, and the Environment at Virginia Tech provided funding during data collection.

References

[1]Zeininger(2020) *JOR*. [2]Li(2020) *JLeatherSciEng*. [3]Huang(2017) *PloS ONE* **12**(1). [4]Nigg(2010) *ClinBiomech* **25**(10):1047-52. [5]Hagedorn (2013) *JFootAnkleRes* **6**(18). [6]Fessler (2005) *Ann HumBiol* **32**(1):44-59. [7]Nicklett(2014) *JAgingHealth* **26**(6): 1060-75. [8]McBean(2004) Diabetes Care **27**(10): 2317-2324. [9]Golightly (2012) *ArthritisCareRes* **64**(11): 1756-59.

INTERACTION BETWEEN SOLEUS AND PLANTAR INTRINSIC MUSCLE LENGTH POINTS TO A STRUCTURAL TRANSMISSION BETWEEN THE HUMAN FOOT AND ANKLE

Rebecca L. Krupenevich[1], Kota Z. Takahashi[2], Howard E. Kashefsky[3], and Jason R. Franz[1]
[1]Joint Department of Biomedical Engineering, UNC Chapel Hill and NC State University, Chapel Hill, NC
[2]Department of Biomechanics, University of Nebraska Omaha, Omaha, NE
[3]Department of Surgery, UNC School of Medicine, Chapel Hill, NC

email: rlkrup@email.unc.edu

Introduction

The plantar aponeurosis (PA) is a highly elastic structure that contributes to the foot's ability to function as a stiff lever for push-off and elastic energy storage and return system for economical locomotion. In combination with the PA, the plantar intrinsic muscles actively regulate foot stiffness in response to task demand [1]. Anatomical studies reveal structural connections between the PA and Achilles that may facilitate force transfer to enhance the ankle-foot interaction [2]. The extent to which these connections influence muscle contractile dynamics is unclear. Thus, the purpose of this study was to characterize the independent and combined effects of ankle and metatarsophalangeal (MTP) joint angles on soleus (SOL) and abductor hallucis (ABDH) fascicle lengths and maximal force capacities. ABDH was selected due to its role in stiffening the longitudinal arch. We hypothesized that SOL fascicle length would increase and maximal voluntary isometric ankle moment would decrease with MTP extension. Further, there is no direct structural connection between the ABDH and Achilles. As such, we hypothesized ABDH fascicle length and maximum voluntary isometric MTP moment would be independent of ankle angle.

Methods

Thus far, 9 young adults (age: 24±5 yrs, 5M/4F) have performed a series of ankle plantarflexion (*i.e.*, -20, 0, and 20°) and MTP flexion (*i.e.*, 0, 30, and 60°) maximum voluntary isometric contractions (MVIC). Cine B-mode ultrasound images of the SOL were recorded during ankle plantarflexor MVICs across all combinations of joint angles prescribed using a Biodex dynamometer. We developed and used a custom foot dynamometer to measure MTP flexion MVICs across all combinations of joint angles while simultaneously recording cine B-mode ultrasound images from both SOL and ABDH. We quantified fascicle lengths using Ultratrack [3]. A two-factor repeated measures ANOVA compared SOL and ABDH fascicle lengths and MVIC moments across all joint angles (p<0.05).

Results and Discussion

During ankle plantarflexion MVICs, SOL fascicle length increased with MTP extension at neutral and dorsiflexed ankle joint angles (Fig. 1A). When the ankle was plantarflexed, ankle MVIC moments were larger at 60° MTP extension (46±18 Nm) than at 0° (43±14 Nm, p=0.04) or 30 ° MTP extension (43±19 Nm, p=0.05). Ankle MVIC moment was not different between MTP extension angles when the ankle was neutral or in dorsiflexed. During MTP flexion MVICs, SOL length was affected by ankle joint angle (Fig. 1B), but neither ABDH length (Fig 1C) nor MTP MVIC moments were affected by ankle joint angle, and MTP MVIC moments were not affected by MTP angle (all p>0.05). Increased SOL fascicle length at greater MTP angles may suggest a structural transmission between the Achilles tendon and PA. We interpret our findings such that as the PA stretches with increasing MTP extension, the Achilles stretches, yielding longer SOL fascicle operating lengths. Fascicles that operate closer to optimal length are advantageous for force generation. Individuals with reduced foot mobility may not benefit from this ankle-foot interaction. The lack of dependence of ABDH lengths on ankle joint angle supports this theory as the ABDH does not directly connect to the Achilles tendon. More work is needed to confirm these preliminary results.

Significance

We propose that a structural transmission between the human foot and ankle enables MTP joint extension, a surrogate for passive foot stiffness, to increase SOL operating length and thereby force-generating capacity. Individuals with reduced PA stiffness may fail to capitalize on this structural transmission with functional consequences that warrant continued study.

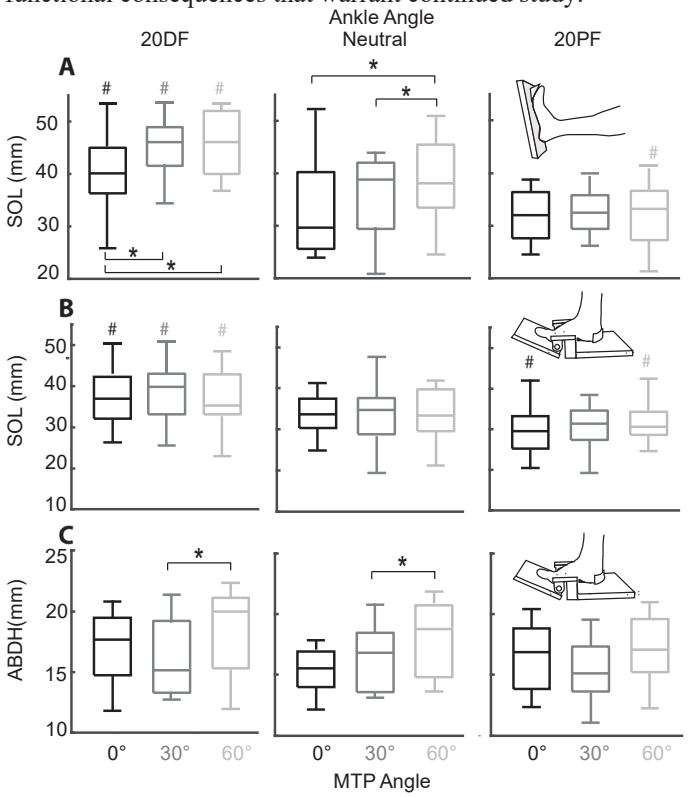

Figure 1. (A) SOL fascicle length during plantarflexor MVICs, and (B-C) SOL and ABDH fascicle lengths during MTP flexion MVICs. *indicates significant pairwise difference across MTP angles and #indicates significantly different from neutral ankle angle. Inset figures illustrate experimental setup during (A) ankle and (B-C) MTP MVICs.

Acknowledgments

This work was supported by an NIH grant (F32AG067675)

References

[1] Kelly et al. (2014). *J R Soc Interface.* 12(102)
[2] Snow et al. (1995). *Foot Ankle Int.* 16(7): 418-21
[3] Farris and Lichtwark (2016). *CMPB.*128, 111-118.

CLUTCH-BASED QUASI-PASSIVE KNEE BRACE TO REDUCE TIBIOFEMORAL CONTACT FORCES

Ericber Jiménez Francisco, Katherine A. Boyer, and Frank C. Sup IV
University of Massachusetts Amherst, Amherst, MA, USA
email: ejimenezfran@umass.edu

Introduction

Knee osteoarthritis (OA) is a degenerative disease affecting over 240 million people around the world, with joint pain, stiffness, and reduced functionality as the most disabling symptoms [1]. Pain and disease progression have been associated with tibiofemoral alignment due to its association with knee loading. As an intervention, valgisation knee braces have been developed to correct joint alignment but have no direct effect on knee OA progression, tibiofemoral contact forces [2], or mobility. As an innovative alternative, this work aimed to determine the effects of clutch-based knee bracing on tibiofemoral contact forces during daily life activities.

After identifying the specific assistance requirements, we designed and prototyped a clutch-based assistive knee brace for daily life activities, capable of delivering higher torques, compared to weight and power consumption, than previous exoskeletons in the literature [3,4].

Methods

We developed an assistive knee brace capable of storing energy, and then releasing it at another desired state of knee flexion during activity (Fig. 1). The device operated by activating two electromagnetic brakes that engaged or disengaged an elastic band. It was controlled via force sensing for estimation of assistive torque, and a 3-axis inertial measurement unit (IMU) used in a finite state machine controller.

Beyond device characterization, one subject was selected to perform multiple repetitions of Stair Ascent (SA), Stair Descent (SD), Stand-to-Sit-to-Stand (STS), and Level Walking (W) at No Assistance, Low Assistance, and High Assistance. The level of assistance was determined by the stiffness and preload of the elastic band. Kinematics and external forces were recorded in synchronization with the assistive knee brace. Tibiofemoral contact forces (KCF) were estimated through musculoskeletal simulation in Opensim. A one-way ANOVA was implemented for SA, SD, and STS, and a paired t-test was applied to the W condition.

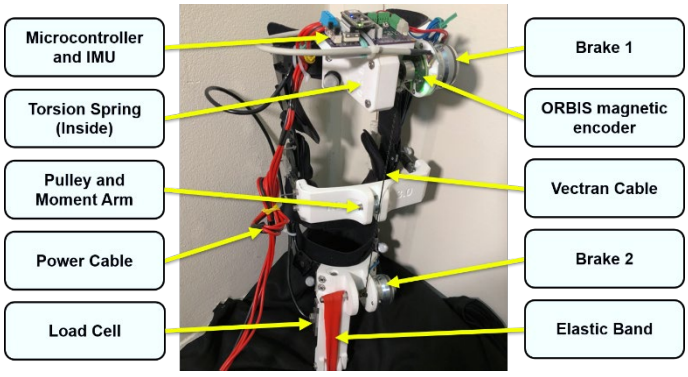

Figure 1: Fully assembled clutch-based knee brace for storing and releasing energy at different knee flexion states.

Results and Discussion

The total weight of our device (2.58kg) was comparable to knee exoskeletons in the literature, the maximum torque achieved (23 Nm) was greater, and the power consumption (19.9 W) was significantly lower than some comparable active exoskeletons [3,4]. The maximum engagement/disengagement frequency achieved was 11.8 Hz, this dynamic range is sufficient for completing daily living activities. Our novel design is a suitable low-power, moderate-to-high torque alternative for knee assistive devices. Moreover, considering that it was a prototype, and some components were above the required capacity, the design can be optimized to further reduce the total weight.

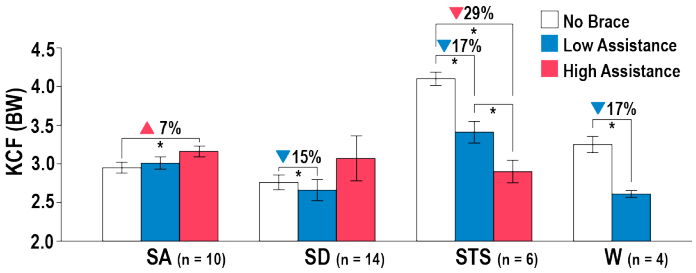

Figure 2: Peak medial tibiofemoral contact force for each task and level of assistance.

Our musculoskeletal simulations showed a significant reduction in peak tibiofemoral contact forces for three different physical tasks. The knee brace was most effective under the STS task (Fig.2), presumably due to the amount of eccentric contraction involved, which implies a high potential for energy absorption and storage as elastic potential energy by the knee brace. Our post-hoc analysis revealed a possible direct relationship between the stiffness of the elastic element used to store energy and the magnitude of medial KCF reduction for this task. However, it is necessary to investigate this effect on a wider range of assistance values and tasks, since for SD only the low assistance level elicited a medial KCF reduction. This indicates the possible existence of an assistance level threshold, beyond which the benefits of external assistance are diminished. While a statistically significant reduction of 17% was observed for the W task, further experimentation is warranted due to the small sample size. Our work demonstrates the capacity of quasi-passive assistive knee bracing to reduce tibiofemoral contact forces and its potential to be extrapolated as a non-invasive treatment to slow down the disease progression in knee OA patients.

Significance

This is the first time, to our knowledge, that this type of quasi-passive assistive device has been evaluated under four daily living tasks. We identified the potential of clutched external knee assistance as an intervention to reduce knee joint loading, especially during the STS task. This approach can potentially serve as the basis for the development of novel hybrid assistive devices for OA patients and other musculoskeletal pathologies.

References

[1] Shimura, Y., et al. *Osteoarthritis and Cartilage* 21 (2013): S262.
[2] Steadman, J., et al. *Knee Surgery, Sports Traumatology, Arthroscopy* 24.1 (2016): 42-50.
[3] Liao, Y., et al. *IEEE Int Conf on Industrial Tech* (2015).
[4] Dollar, A. and Herr, H *IEEE/RSJ Int Conf on Intelligent Robots and Systems*. (2008).

MODELING THE LEAN RELEASE, LEAN RELEASE WITH SURFACE TRANSLATION AND SURFACE TRANSLATION PERTURBATIONS WITH AN INVERTED PENDULUM ON A SKID FOR FORWARD, SIDEWAYS AND BACKWARD LOSS OF BALANCE DIRECTIONS

Gaspard Diotalevi and Cécile Smeesters
Research Centre on Aging, Sherbrooke QC, Canada
Department of Mechanical Engineering, Université de Sherbrooke, Sherbrooke QC, Canada
email: Cecile.Smeesters@USherbrooke.ca

Introduction

The perturbation threshold line method has predicted the outcome (fall or recovery) of different forward postural perturbations (lean releases, waist pulls, surface translations and their combinations) in different age groups.[1] It is defined as the linear regression between the angular positions and velocities of participants at reaction time for the maximum amplitude postural perturbations. It has also been accurately simulated using the same inverted pendulum on a skid model for all of these forward postural perturbations and age groups. This study will determine if the same model could accurately simulate the outcome of lean releases (LR), lean releases with surface translations (LR+ST) and surface translations (ST) for forward (FW), sideways (SW) and backward (BW) loss of balance directions.

Methods

Experimental procedure: The angular position and velocity of 10 younger adults (18-41yrs, 50% ♀) were measured from onset of perturbation (OP) to onset of response (OR) for FW, SW and BW maximum LR, LR+ST and ST from a recent experimental study.[2]

Theoretical procedure: These maximum postural perturbations were simulated in Matlab using the inverted pendulum on a skid model, setting the waist pull force F_1=0.[1] The inputs were the mass (m), height (h) and reaction time (RT) of the participant, skid mass (M), rubber sheet pull force $F_2=(M+m)a$ modelled as a step, rubber sheet on floor coefficient of friction (μ=0.74), gravity (g=9.81m/s^2) and ankle torque (τ=0). For LR $M=\infty$ and a=0, while for ST M=25.6kg and a=25m/s^2 for $\delta t = v_{ST}/a$ and x_{max}=0.7m. The outputs were the angular and translational position (θ and x), velocity (ω and v) and acceleration (α and a) from OP to OR. The initial conditions were θ_o, $\omega_o \approx 0$, x_o=0 and v_o=0 for LR and LR+ST, and θ_o=0, ω_o=0, x_o=0 and v_o=0 for ST.

Data analysis: For trials at the maximum lean angles or translation velocities, both the RMS error from OP to OR and the error at RT were calculated between the experimental and theoretical angular positions ($\delta\theta$) and velocities ($\delta\omega$).

Results and Discussion

Considering all directions together, all RMS errors and errors at RT were significantly different from zero ($p \leq 0.005$, single sample t-tests), except for $\delta\theta_{RT}$ and $\delta\omega_{RT}$ for ST ($p \geq 0.053$). Several errors were also significantly affected by both direction (p_D) and perturbation (p_P), with significant interactions (p_{DxP}, Table 1, two-way rm-ANOVA). However, all $\delta\theta$ and $\delta\omega$ were smaller than 2% (0.7°) and 5% (10°/s), which is smaller than the experimental perturbation threshold line standard deviations of 15% (5.3°) and 15% (32°/s), respectively.

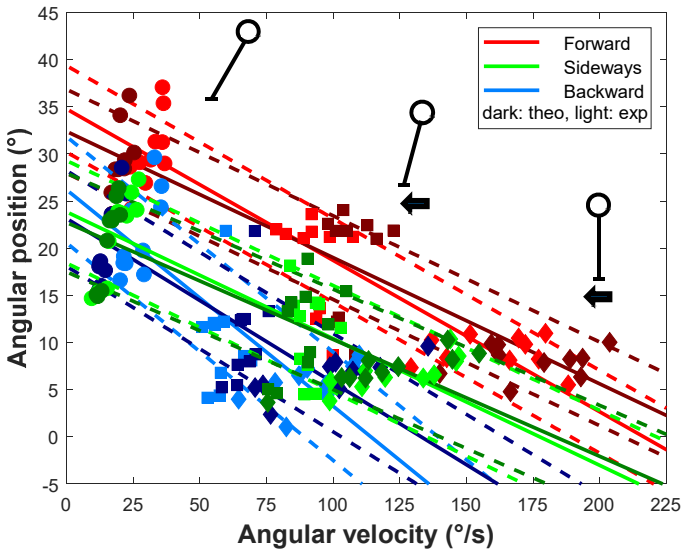

Figure 1: The experimental and theoretical perturbation threshold lines for maximum LR (circles), LR+ST (squares) and ST (diamonds).

More importantly, the experimental (pseudo$R^2 \geq 0.826$) and theoretical (pseudo$R^2 \geq 0.856$) angular positions and velocities of participants at RT for trials at the maximum lean angles and translation velocities formed very similar perturbation threshold lines separating falls from recoveries (Figure 1, unconditional growth linear regressions). Finally, these perturbation threshold lines moved toward the origin if the loss of balance direction changed from FW to SW or FW to BW.

Significance

The same inverted pendulum on a skid model can thus accurately simulate the outcome of LR, LR+ST and ST, not only in different age groups,[1] but also in different loss of balance directions, an important risk factor for fall-related fractures. This reduces the need for expensive, time consuming, fatiguing, and dangerous experiments, especially if large postural perturbations are used and avoiding a fall is not always possible.

Acknowledgments

The Université de Sherbrooke for its financial support.

References

1. Pierre M and Smeesters C. 40th Annu Meet Am Soc Biomech, Raleigh NC, Aug 2-5 2016.
2. Chebbi A and Smeesters C. XXVIIth Congr Int Soc Biomech, Calgary AB, Jul 31 - Aug 4 2019.

Table 1: Errors (mean±SD) expressed as a percentage of the experimental FW perturbation threshold line intercepts (θ_i=34.6°; ω_i= 216°/s)

All directions	RMS errors from OP to OR						Errors at RT					
	LR	LR+ST	ST	p_D	p_P	p_{DxP}	LR	LR+ST	ST	p_D	p_P	p_{DxP}
δθ	1±1%	1±0%	2±1%	0.911	**0.024**	0.117	2±1%	-1±1%	0±1%	**0.000**	**0.001**	**0.000**
δω	4±2%	4±1%	5±1%	**0.008**	0.512	**0.000**	4±2%	-3±3%	-3±4%	**0.002**	**0.000**	**0.002**

Significant effects are **bolded**.

The Unexplored Milestone: Kinematics and Muscle Utilization of How Babies Roll

Danielle N. Siegel[1], Wyatt D. Davis[1], Abby Prow[2], Olivia Scholes[2], Erin M. Mannen[1] and Safeer F. Siddicky[1]
[1]Mechanical and Biomedical Engineering, Boise State University, Boise, ID. [2]Idaho College of Osteopathic Medicine, Meridian, ID.
Email : daniellesiegel@u.boisestate.edu

Introduction

Achieving a roll is a key motor skill and an important developmental milestone for infants. To initiate and complete a roll, infants must use whole-body, goal-oriented movements that take them from a supine to prone position [1]. Rolling allows infants to interact with their external environment in daily life. Infant biomechanics studies, particularly in rolling, are sparse. A previous study by Kobayashi et al. established six qualitative categories of limb coordination, related to the synchronicity of stationary and moving limbs, when infants roll [2]. However, no studies have explored muscle utilization and kinematics to understand how infants achieve a roll. The purpose of this study is to determine muscle utilization during various movement mechanisms of infants rolling from supine to prone.

Methods

Five healthy infants (6.7 ± 0.8 months, 4M, 1F) participated in this ongoing IRB-approved study. The infants lay supine on a flat play mat until a roll was achieved. Surface EMG electrodes (Delsys, 2000Hz) recorded muscle activity from the triceps (TRI), abdominals (ABS) quadriceps (QUAD), hamstrings (HAM), and gluteus maximus (GM). Marker-based motion capture (Vicon, 100Hz) tracked infant kinematics using custom rigid bodies on the torso, and pelvis. A video camera (GoPro) recorded all trials. A medical-grade pulse oximeter monitored infants' SpO_2 levels to ensure safety. Mean filtered EMG signal [3], and ranges of motion (ROM) of the Eulerian rotational angles between the trunk and pelvis rigid bodies, were calculated using MATLAB for eight half-rolls.

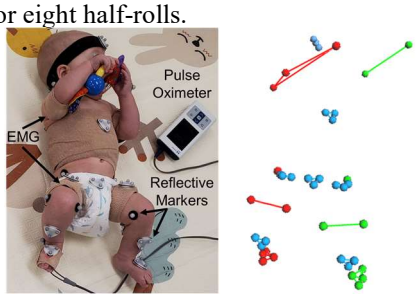

Figure 1: Experimental setup (L) and labeled motion capture data (R).

Results and Discussion

Five rolling limb coordination categories according to Kobayashi's criterion [2] were observed in our data (Figure 2). The limbs are codified as ipsilateral arm (IA) and leg (IL), and contralateral arm (CA) and leg (CL) in the direction of the roll, and the filtered EMG is normalized as percentage (%) of ipsilateral limb. When only the IA is stationary, with the other limbs moving synchronously (Figure 2A), the arm and "pelvic tuck" movements are supported by the high trunk-pelvis ROM in all rotational directions, and the TRI and higher contralateral ABS and QUAD EMG. When the CA is moving and the CL following, with the IA and IL stationary (Figure 2B), the across-body arm movement and trailing CL are supported by the higher trunk lateral bending and contralateral TRI and ABS EMG activity. The higher ipsilateral HAM and QUAD activity may indicate a push off mechanism with the IL. When the IA and IL are stationary with the CA and CL moving synchronously (Figure 2C), the synchronous movement allows for the higher pelvis-trunk rotation with higher contralateral TRI and GM EMG activity. The higher ipsilateral HAM and QUAD EMG likely indicates a push-off mechanism during the roll. When all four limbs are moving synchronously (Figure 2D), most of the ROM is in trunk-pelvis flexion, with higher contralateral EMG activity in the TRI and QUAD and higher ipsilateral EMG activity in the ABS and GM. When the IL and CA are moving synchronously, with the CL following and IA stationary (Figure 2E), the trunk-pelvis movement is similar to Figure 2D, but the contribution of the IL is apparent from the high ipsilateral HAM EMG activity.

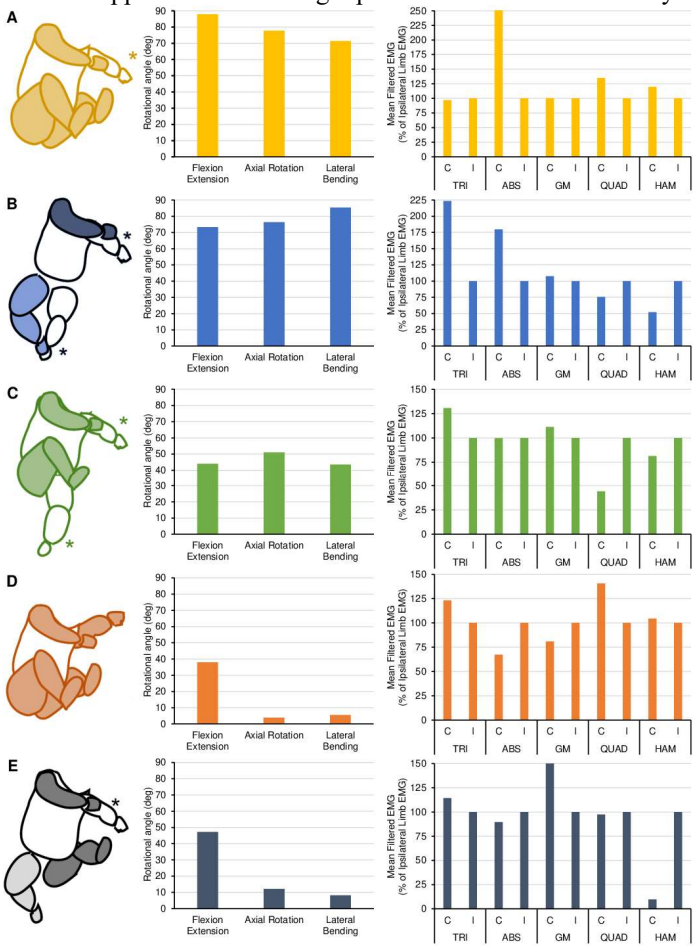

Figure 2: Trunk-pelvis angular ROM and normalized EMG of observed roll categories (illustrations adapted from [2], * stationary limb)

These preliminary results indicate a promising approach towards quantifying the movement patterns of infant rolls using a combination of video, motion capture, and EMG. Future studies exploring full rolls and head and lower body kinematics may help provide a more holistic understanding of the movement and muscle utilization of how infants roll.

Significance

Understanding the movement biomechanics of rolling infants can provide crucial insight into their motor development and strategies to self-correct from inadvertent suffocation scenarios.

References

[1] Richter RR, et al. *Phys. Ther.*, 1989. [2] Kobyashi Y, et al. *Exp Brain Res*, 2016. [3] Siddicky S, et al. *J. Biomech, 2020.*

EFFECT OF HANDHELD DEVICE USAGE ON NECK STRESSES, POSTURE, AND PAIN IN YOUNG ADULTS SUFFERING FROM RECURRENT CERVICAL PAIN AND HEALTHY CONTROLS

Ram Haddas, PhD; Sheena Bhuva, MD; Nayan Patel, MD; Craig Lankford, MD; Peter Derman, MD, MBA
Texas Back Institute, Plano, TX, USA | email: rhaddas@texasback.com

Introduction

Text neck syndrome is a repetitive stress injury caused by excessive texting and overuse of handheld electronic devices.[1] Cell phone ownership in North America is reported to be 92% with 81% of owners using mobile phones for texting.[1] According to recent research, smartphone users spend an average of two to four hours a day with their heads dropped down.[2] This results in 700 to 1,400 hours a year of excess stress on the cervical spine. Flexing the head forward to use a smartphone directly affects the spine (Figure 1).[1,2] Frequent forward flexion can cause changes in the cervical curvature, supporting ligaments, tendons, and musculature, as well as the bony segments, commonly causing postural changes.[3,4] Text neck symptoms may include pain in the neck, upper back, and/or shoulders, forward head posture and rounded shoulders, reduced mobility, headache, and increased pain with neck flexion. Recently, spine specialists are noticing an increase in patients with neck and upper back pain, likely related to poor posture during prolonged smartphone use.[1] The purpose of this study was to explore the effect of handheld device usage on cervical spine neuromuscular control, biomechanics, and pain level in patients with recurrent cervical pain.

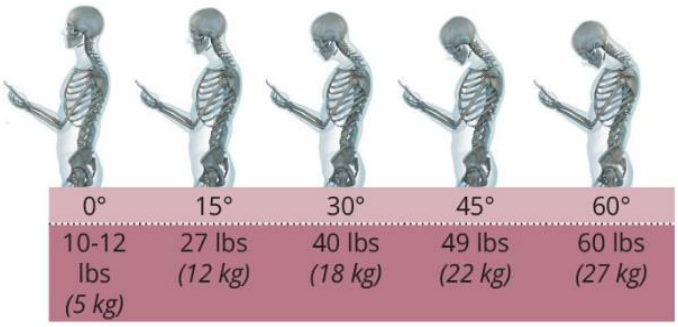

Figure 1. Weight of head when flexing the neck at varying degrees.

Methods

This study was a non-randomized, prospective, concurrent control cohort study. Fifteen recurrent cervical pain patients and 15 controls completed the following functional outcome measurements: 1- and 5-minutes standing and 1-minute sitting and walking without (NP) and with (P) using their phone in a texting-type posture. Each patient was fitted with a full-body external reflective marker set (Vicon, Oxford, UK) along with neck and upper extremity dynamic surface EMG (Delsys, Boston, MA). Neck RoM and neuromuscular activity were calculated during the standing, sitting, and walking tests. Moreover, three-dimensional Cone of Economy (CoE) boundaries were determined during the functional balance tests. A custom algorithm was used to determine the sagittal, coronal, and vertical range of sway (RoS) for the center of mass (CoM) and the head. Outcome measures included neck RoM, balance effort, and limits of the CoE as measured by total sway and range of sway (RoS), neuromuscular activity, and neck and arm visual analog scale (VAS) and neck disability index (NDI). Repeated measurements and one-way analysis of variance (ANOVA) were used to analyze data. Statistical analyses were conducted using SPSS, Version 23.0 (IBM, Armonk, NY, USA).

Results and Discussion

Using the phone produced increased neck flexion angle during standing (NP: 15.3 vs. P:48.3°; $p<0.001$), seating (NP: 8.4 vs. P: 42.7°; $p<0.001$), and walking (NP: 18.3 vs. P: 39.8°; $p=0.031$). Increase in balance effort was observed with greater total sway during standing (NP: 55.3 vs. P: 69.6 cm; $p=0.008$) and sitting (NP: 28.3 vs. P: 37.2 cm; $p=0.045$) and larger CoE dimensions when using a phone ($P<0.050$). There was significantly more neuromuscular activity in the bilateral upper trapezius and middle deltoid muscles with phone use during sitting and standing ($p<0.050$). Use of the phone during walking was associated with a slower walking speed (NP: 1.02 vs. P: 0.89 m/s; $p=0.013$), longer stride time (NP: 1.10 vs. P: 1.19 s; $p=0.022$) and widther step width (NP: 0.10 vs. P: 0.14 m; $p=0.019$). No significant differences were found in pain level when using the phone in comparison to the NP condition.

Despite the utility of smartphones and other handheld devices, their potentially deleterious impact on long-term health is important to consider. Increasing neck RoM, neuromuscular activity, and balance effort are observed with handheld device use and may predispose patients to cervical spondylosis and myofascial pain. While these devices have become an integral part of modern life, individuals should make an effort to maintain a neutral spine during use and to avoid extended hours on such devices. Spine caregivers should promote awareness, prevention, and treatment of text neck. Long-term studies are needed to definitively establish a connection between text neck and cervical spine pathology.

Significance

Increasing neck range of motion (RoM), neuromuscular activity, and balance effort were observed with handheld device use and may predispose patients to cervical spondylosis and myofascial pain.

References

1. Cuellar JM, et al. *Spine J,* 17(6): 901-2, 2017
2. Barrett JM, et al. *Ergonomics,* 63(1), 101-8, 2020
3. Correia IMT, et al. *Spine,* 6(7), E3, 2021
4. Filho, NM, et al. *Spine J,* 18(4), 714-5, 2018

FUNCTIONAL ALIGNMENT REDUCES PLACEMENT-INDUCED ERROR IN IMU-DERIVED METRICS

Julien A. Mihy[1], Mayumi Wagatsuma[1], Stephen M. Cain[2], Jocelyn F. Hafer[1]
[1]University of Delaware, [2] University of Michigan
Email: jmihy@udel.edu

Introduction

Inertial measurement units (IMUs) allow us to collect gait data outside the lab. However, if we want to collect gait data over multiple days outside of researcher observation, participants may place sensors in slightly variable, non-standard locations. Changes in IMU location on a body segment and participant placement irregularities have been shown to influence outcome measures [1,2]. Functional alignment methods exist to align IMU data to recognizable reference frames [3], but the extent to which these methods minimize the effects of sensor malalignment on calculated metrics has not been demonstrated. Therefore, the purpose of this study was to determine the extent to which a functional alignment method minimizes the effect of differences in IMU placement on gait calculations.

Methods

Four healthy adults (3 male, 29±5 years) were recruited. Thigh, shank, and foot linear accelerations and angular velocities were collected with IMUs as individuals walked across an overground runway. Static and functional trials (straight walk and toe touches) were collected to orient one axis of IMU data to approximately sagittal [4]. Participants performed roughly 20 walking trials at a preferred pace. We extracted steady state strides for analysis. Sagittal thigh and shank angular excursions were calculated by integrating thigh and shank angular velocity about a *functionally-aligned* medial-lateral axis and about an axis *assumed to be aligned* with the anatomical medial-lateral axis. All data were normalized to 100% of the gait cycle.

To determine the effects of functional alignment and different IMU placements, 3 sensors were placed on the thigh (Fig 1): one in our typical location, midway between the hip and knee on the lateral thigh (T1), one proximal to typical (T2), and one on the anterior thigh (T3). Data from all sensors were oriented to 2 reference frames: functionally aligned (F) and assumed alignment (A). Sagittal knee angular excursions were averaged across all strides. Root mean squared difference (RMSD) was calculated between the functionally aligned typical sensor data (FT1) and the other functional and assumed alignment data for all thigh sensors.

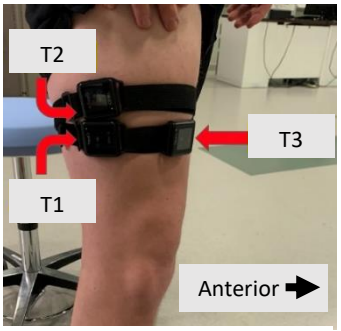

Figure 1. IMU placement for thigh sensors.

Knee sagittal angular excursion was determined between each thigh sensor placement and alignment method and functionally aligned shank data from a sensor placed in a standard location (i.e., 3 thigh sensors, 2 alignment conditions: functional (F) and assumed (A), against 1 standard shank sensor). Knee range of motion (ROM) was the maximum minus the minimum knee excursion.

Results and Discussion

The functional alignment minimized differences in thigh angular excursion between different sensor placements. The functional alignment was more robust for correcting distal/proximal (FT1 vs FT2, average RMSD 0.7±0.2°) than anterior/posterior (FT1 vs FT3, average RMSD 5.8±1.0°) differences in IMU placement. Although anterior placement of the sensor increased error, both sensors in non-standard locations had lower RMSD and standard deviations for functionally aligned data than from assumed alignment data (average RMSD vs. FT1: AT1 = 8.0±2.7°, AT2 = 7.2±2.5°, AT3 = 9.3±2.5°). Functional alignment reduced the error in knee ROM by up to 20.7 (Fig 2). Using assumed alignment procedures on thigh segment IMU data could lead to large and unpredictable differences in knee ROM.

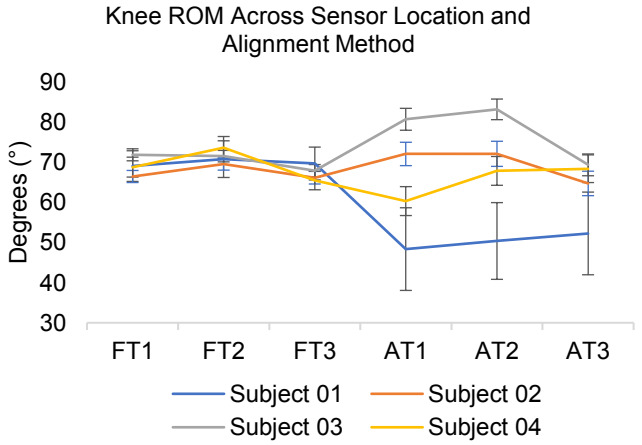

Figure 2. Knee range of motion (mean and SD) calculated from each sensor and alignment strategy. F = Functional alignment, A = Assumed alignment, T1 = Standard thigh placement, T2 = Proximal offset, T3 = Anterior offset.

Significance

Differences in segment angular excursion due to varied sensor placement can be reduced with functional alignment. Functional alignment may improve data reliability in cases where participants place and replace their own IMU sensors. This advancement allows for repeatable and consistent measures of gait variables and furthers our ability to reliably measure real world gait mechanics using IMUs.

References

1. Cresswell et al., *Sensors* (2017) 17, 466
2. Rispens et al. *Gait & Posture* 40 (2014) 187–192
3. Vitali et al., *Journal of Biomechanics* 106 (2020) 109832
4. Cain et al., *Gait & Posture* 43 (2016) 65-69

DYNAMIC VERIFICATION OF A LINEAR MODEL APPROACH TO ESTIMATE SCAPULAR KINEMATICS DURING BASEBALL PITCHING

Benjamin Lerch[1], Kristen F. Nicholson[2], and R. Tyler Richardson[1]
[1]Pennsylvania State University Harrisburg, Middletown, PA, USA
[2]Wake Forest School of Medicine, Winston-Salem, NC, USA
email: rtr12@psu.edu

Introduction

Biomechanical analyses of pitching possess limitations in accurately measuring scapular kinematics and distinguishing between glenohumeral (GH) and scapulothoracic (ST) contributions to shoulder motion[1]. An individualized linear model (LM) approach using measurable humerothoracic (HT) orientation to estimate ST orientation has been validated for static postures within a pitching motion[2], but dynamic HT external rotation angles exceed static HT limits used for LM creation potentially resulting in non-physiological estimates of ST orientation. Dynamic validation is needed but is not feasible as dynamic gold standard references either prohibit a natural throwing motion (bone pins) or have inadequate sampling rates for a dynamic pitch (fluoroscopy). In lieu of a gold standard dynamic validation, LM estimated ST kinematics during a pitch can still be evaluated to provide insights beyond those of a static validation[3]. This study provides a dynamic verification of the LM by assessing its ability to estimate ST kinematics throughout a full speed pitch. We hypothesized that LM estimated ST kinematics would be within physiological ST ROM limits.

Methods

Trunk and upper extremity segment orientations of 14 NCAA Division III collegiate pitchers were measured with motion capture during a pitch. Each subject's arm was placed in six calibration positions nearly representing the extremes of HT orientations within his pitching motion while ST orientations were determined by palpation. The LM used multiple linear regression on the static position data to create equations that estimate ST angles from HT angle inputs[2]. The LM was applied to predict ST kinematics for a second pitch (mean velocity: 75 mph). LM estimated ST kinematics were compared against ST ROM limits established in a non-pitching biplane fluoroscopy study involving various functional arm movements[4].

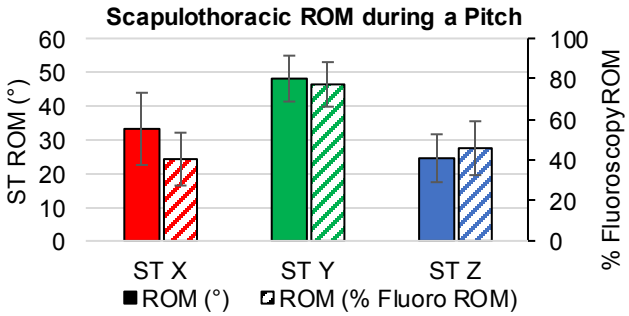

Figure 1: LM estimated ST ROM during pitching (mean±2 SD). ROM expressed in degrees and as a % of ST ROM limits from fluoroscopy[4]. ST X=up./down. rot., ST Y=int./ext. rot., ST Z=ant./post. tilt.

Results and Discussion

The LM estimated ROMs on ST upward/downward rotation and anterior/posterior tilt were less than the ROM observed in the fluoroscopy study on these ST axes for all subjects (**Fig. 1**). All LM estimated ST angles on these axes were also within the max./min. fluoroscopy values for all subjects. Thus, the hypothesis is accepted for these ST axes as the LM produced estimates that were within established physiological limits.

Despite the total ROM being less than the fluoroscopy ROM (**Fig. 1**), LM estimated ST internal/external rotation kinematics occasionally went beyond fluoroscopy max./min. bounds. One subject achieved ST internal rotation that was 0.4° beyond the max. fluoroscopy value. Six subjects reported ST external rotation angles beyond the max. fluoroscopy value; the largest exceeded by 16.8°. The fluoroscopy study, however, did not measure arm postures that specifically targeted HT horizontal adduction/abduction which elicit substantial ST internal/external, respectively. While the hypothesis is rejected for this ST axis, even the most extreme LM reported values on ST internal (76.6°) and external (-2.8°) rotation seem plausible given the substantial shoulder motion involved with pitching (**Fig. 2**).

These results provide a rudimentary dynamic verification of the LM during pitching by showing that LM estimated ST kinematics during pitching are largely physiologically plausible, if not entirely possible.

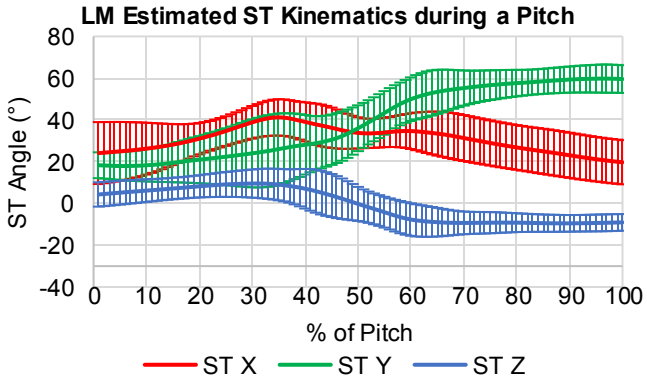

Figure 2: LM estimated ST kinematics during pitching (mean±1 SD). ST X=up./down. rot., ST Y=int./ext. rot., ST Z=ant./post. tilt. Pitch began at max. HT horizontal abduction in stride phase (0%) and ended at max. HT horizontal adduction in follow-through phase (100%).

Significance

The results of both the published static validation of the LM[2] and this dynamic verification suggest that the LM is a viable approach for accurately estimating ST kinematics throughout a full speed pitch. Future applications to dynamic pitching may provide previously unknown joint-specific information to facilitate an understanding of how ST and GH function relate to injury risks, rehabilitation, and performance.

Acknowledgments

Thank you to Jesse Donahue, Alyssa Knisley, and Brandon Hoover for their assistance with data collection.

References

1. Thompson et al. (2018), Sports Health, 10:133-140.
2. Richardson (2021), J Biomech, 114:110160.
3. Oliver et al. (2015), J Human Kinetics, 49:47-54.
4. Nicholson et al. (2017), J Biomech, 54:101-105.

OUT-OF-LAB GAIT VARIABLES DIFFER BASED ON STRIDE SELECTION CRITERIA

Mayumi Wagatsuma[1], Julien A. Mihy[1], Stephen M. Cain[2], and Jocelyn F. Hafer[1]
[1]University of Delaware, [2]University of Michigan
email: mayumiw@udel.edu

Introduction

Inertial measurement units (IMUs) can be used to calculate kinematic and spatiotemporal gait parameters with a reliable level of accuracy. Measuring gait outside the lab could provide a more in-depth understanding of real-world gait patterns for the general population, elderly population, and people with disabilities. Even though IMUs are dependable sensors for measuring gait, limited studies have been done using IMUs to analyze gait characteristics in out-of-lab settings. Previous studies have shown that gait characteristics differ between inside lab and outside lab settings [1,2]. However, there is currently no standardized method to select what out-of-lab data to include in gait analyses. Prior studies selected data based on walking times or the number of strides [1,2]. It has been shown that people walk slower on average outside the lab compared to inside the lab [3]. Thus, comparing gait outside of the lab may lead to different results depending on how matched lab speed are selected. No previous studies have explored different approaches of data extraction based on speed from inside and outside of the lab. Therefore, the purpose of this study was to compare the effects of different speed selection methodologies on the resulting IMU-derived gait parameters for out-of-lab walking.

Methods

A total of four young adults (28.8±4.8yrs) were recruited to participate in this study. Seven IMUs were attached to each participant: one on the pelvis and one each on both thighs, shanks, and feet. Participants were asked to perform straight-line walking trials at their comfortable speed inside the lab followed by a supervised walk at self-selected speed outside of the lab. Spatiotemporal variables were calculated from foot-mounted IMU data using a zero velocity update algorithm [4]. Thigh and shank data were oriented to roughly align one axis to sagittal using a functional alignment procedure. Walking velocity, stride length, and knee angular excursion (ROM) were calculated for all strides that were level and did not include a turn. Variables were compared between in-lab data and out-of-lab data selected using different speed thresholds. The three out-of-lab data selection methods were 1) lab speed ± 5%, 2) lab speed ± 25%, and 3) all out-of-lab strides.

Results and Discussion

With the inclusion of more data from outside of the lab setting, mean gait speed and stride length decreased whereas mean knee range of motion (ROM) was unaffected (Inlab: 84±20strides, ±5% speed: 130±64strides, ±25% speed: 231±75strides, All speed: 427±37strides). Compared to in-lab, speed was 0.01±0.01 m/s, 0.09±0.07m/s, and 0.2±0.08m/s lower for ±5%, ±25%, and all speed out-of-lab data conditions (Fig. 1A). Similarly, out-of-lab stride length decreased 0.01±0.02m, 0.07±0.04m, and 0.19±0.06m across conditions when compared to in the lab (Fig. 1B). Finally, the Knee ROM changed less than 0.6±1.4° compared to inside lab speed across all speed data selections (Fig. 1C). While we did find a trend in spatiotemporal variables, we did not identify any changes in our joint kinematic variable. Our data agree with previous findings that people tend to walk more slowly and with shorter stride lengths outside of the lab [3].

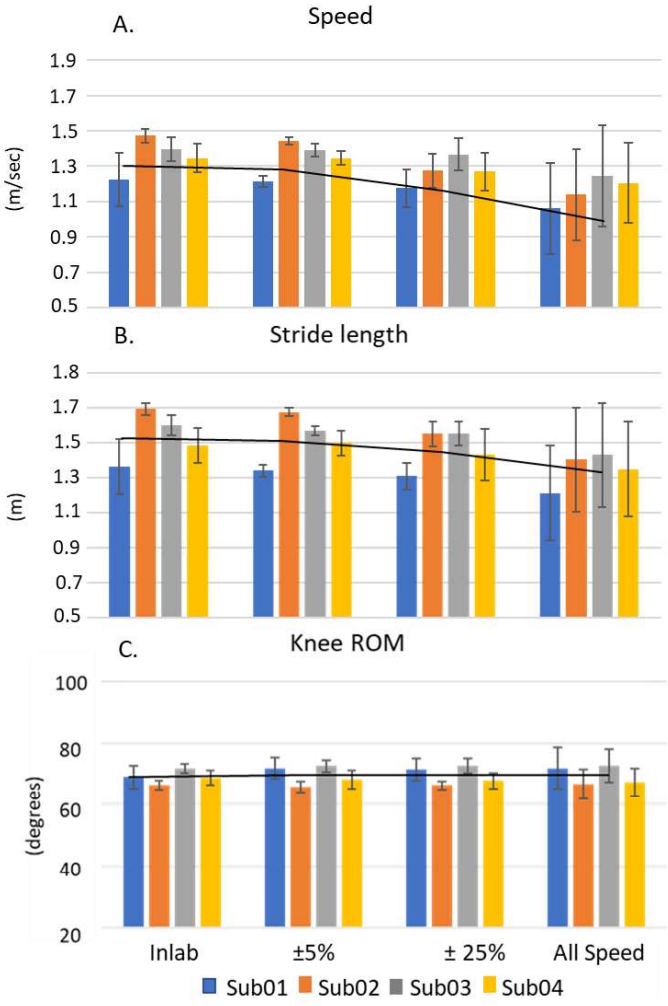

Figure 1: A. Speed, B. stride length, and C. knee ROM for each participant (mean and SD); ± 5%, 25%, & All speed are from out-of-lab; Solid lines represent the average of each condition.

Significance

As new technologies such as IMUs make it possible to quantify human gait outside of the lab, it is important to understand how to use these data to make decisions and how these data relate to traditional, in-lab analyses of gait. To our knowledge, this is the first study to compare the effects of different speed selection methodologies on the resulting IMU-derived gait parameters for out-of-lab walking. Our findings demonstrate that data selection is important and should be carefully considered depending on the specific aims of out-of-lab gait analyses.

References

1. Carcreff, L et al., *Scientific reports* 2020, 10(1), 2091
2. Del Din, S et al., *J Neuroeng Rehabil* 2016, 13(1):46
3. Renggli D et al., *Front Physiol* 2020, 11, 90
4. Rebula, JR et al., *Gait & Posture* 2013, 38, 974-980.

TRUNK AND PELVIS MOTION BEFORE AND AFTER OSSEINTEGRATION IN SERVICE MEMBERS WITH TRANSFEMORAL LIMB LOSS

Caitlin Mahon[1,2], Courtney Butowicz[1,2], Brad D. Hendershot[1,2], Christopher L. Dearth[1,2], Benjamin K. Potter[2], Jonathan A. Forsberg[2]
[1]DoD-VA Extremity Trauma and Amputation Center of Excellence [2]Walter Reed National Military Medical Center
email: caitlin.e.mahon.civ@mail.mil

Introduction

Low back pain (LBP) is a common musculoskeletal condition secondary to lower limb loss,[1] and may be related to larger spinal loads associated with altered trunk-pelvis movements while walking with a prosthetic device(s)[2]. Trunk-pelvis continuous relative phase (CRP), a measure of intersegemental coordination, has been used to examine spinal motion in persons with LBP. More rigid and less variable trunk-pelvis coordination, in addition to larger trunk-pelvis motion, have been shown to positively correlate with greater (chronic) LBP disability[3]. Osseointegration (OI), a surgical approach for direct skeletal attachment of the prosthesis, aims to eliminate socket complications and overall improve outcomes, perhaps thereby mitigating risk for secondary musculoskeletal conditions (e.g., LBP). The purpose of this analysis is to compare trunk-pelvis range of motion (ROM), CRP, and CRP variability while walking among a cohort of Service members with transfemoral (TF) limb loss, directly before and 12-months after OI. It was hypothesized Service members would demonstrate lesser trunk-pelvis ROM, with greater CRP and CRP variability (i.e., less rigid and more flexible coordination) after OI.

Methods

Fifteen Service members (mean±SD age: 39±11 yrs, stature: 178±4.2 cm, mass: 98±18 kg) with lower limb loss (8 unilateral TF, 4 bilateral TF with bilateral OI, 1 bilateral TF with unilateral OI, 2 bilateral TF/transtibial) walked at a self-selected walking velocity over ground, using an assistive device, if required, before and 12-months after OI. Trunk-pelvis ROM, mean CRP, and CRP variability were computed. Mean CRP was determined for each stride[4] and expressed in absolute value for purposes of interpretation; 0-90º indicates in-phase (more rigid) movement, while 90-180º indicates out-of-phase movement. Participants also completed questionnaires to characterize chronic LBP, with chronicity defined as LBP being a problem for at least half the days in the past 6 months, using the NIH Minimal Data Set. Pairwise t-tests ($p<0.05$) compared self-selected walking velocity, ROM and CRP outcomes between time points.

Results and Discussion

Self-selected walking velocity decreased ($p=0.03$) between baseline (mean±SD: 1.07±0.24 m/s) and 12-month (1.02±0.23 m/s) time points. Over time, there were no changes in sagittal ($p=0.14$), frontal ($p=0.38$), or transverse ($p=0.13$) trunk ROM, nor sagittal ($p=0.09$), frontal ($p=0.30$), or transverse ($p=0.21$) pelvis ROM (Figure 1a and 1b, respectively). Additionally, there were no changes in sagittal ($p=0.60$), frontal ($p=0.31$), or transverse ($p=0.60$) mean CRP, nor sagittal ($p=0.26$), frontal ($p=0.62$) or transverse ($p=0.67$) CRP variability (Figure 2a and 2b, respectively). Mean CRP remained in-phase (more rigid) both before and 12 months after OI. While sagittal and frontal CRP values here are similar in magnitude to those reported for persons after 1 year of independent ambulation following TF limb loss (with traditional sockets),[5] transverse CRP is more in-phase. Therefore, optimal axial coordination may require greater accommodation time following OI. Of note, subjective reports of chronic LBP decreased from baseline to 12-months, in a subset of subjects (i.e., of 8 Service members reporting chronic LBP at baseline, only 4 continued to report chronic LBP at 12 months). These results collectively suggest unique subject responses to OI, likely dependent on numerous factors beyond merely trunk-pelvic biomechanical outcomes.

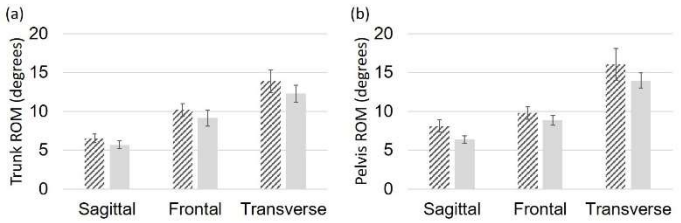

Figure 1: Mean (standard error) tri-planar **(a)** trunk and **(b)** pelvis ROM before (dashed) and 12-months after (solid) OI.

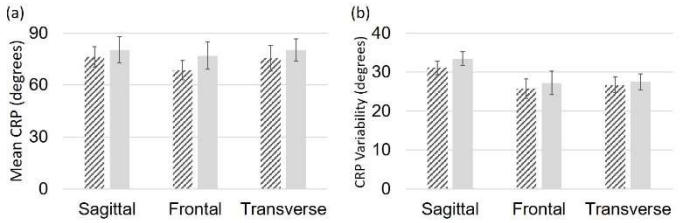

Figure 2: Mean (standard error) tri-planar **(a)** mean CRP and **(b)** CRP variability before (dashed) and 12-months after (solid) OI**.**

Significance

Within this preliminary analysis, trunk-pelvis motion and coordination did not change 12 months after OI (despite a decreasing prevalence of chronic LBP in a subset of the sample). In combination with a comprehensive suite of outcomes, continued follow-up will further characterize longer-term biomechanical changes among Service members with TF limb loss receiving OI, to more broadly realize the functional and psychosocial effects of OI and facilitate widespread adoption within the Military Health System.

Acknowledgments

This work was supported by Award W81XWH-17-2-0060 and the Extremity Trauma and Amputation Center of Excellence. The authors also acknowledge the support of the DoD OI Program, as well as those specifically supporting the functional outcomes assessments (MLT, BK, HSM, JCA, JME, and JRG). The views expressed herein are those of the authors and do not to reflect the views of the Department of Defense, Departments of the Army/Navy/Air Force, nor the U.S. Government.

References

1. Butowicz, et al. 2017. Adv Wound Care **6**(8):269-78
2. Hendershot, et al. 2018. J Biomech **70**: 249-54
3. Ebrahimi, et al. 2018. J Biomed Phys Eng **8**(2):193-202
4. Hamill et al. 1999. Clin Biomech **14**(5): 297-308
5. Mahon, et al. 2019. Arch Phys Med Rehabil **101**(3): 426-33

NECK POSTURE IN INDIVIDUALS WITH AND WITHOUT ENLARGED EXTERNAL OCCIPITAL PROTUBERANCES

Caleb C. Burruss[1], Anita Vasavada[2], Claire E. Terhune[1], and Kaitlin M. Gallagher[1]
[1]University of Arkansas, Fayetteville, AR, USA [2] Washington State University, Pullman, WA, USA
Email: *kmg014@uark.edu

Introduction

Recent research has shown that 41% of young adults present with an enlarged external occipital protuberance (EEOP)[1]. These EEOPs have been shown to cause tenderness/pain in the occipital region and can even require surgery[2-3]; however, the origin of the EEOP and subsequent postural changes due to their development are unknown. Therefore, the purpose of this study was to use radiographic measurements to investigate how neck posture differed between those with and without an EEOP.

Methods

This was a retrospective study of 50 neutral posture sagittal plane radiographs (25 females, 25 males) from two different studies[4-5]. An EOP was classified as enlarged if it exceeded 10 mm[1] **(Figure 1).** Landmarking was performed in ImageJ (Rasband, W.S., ImageJ, US National Institute of Health, Bethesda, Maryland, USA). EOP length, C2-C7 intervertebral angles, and gravitational moment arm of the neck (horizontal distance between the center of C7 to External Auditory Meatus) were calculated in Microsoft Excel using the landmarks. Two-way ANOVAs with between factors of EOP group (enlarged vs. normal) and sex and a covariate of height were run on each variable. Height was included since previous work has shown that anthropometrics may influence neck posture[6]. Tukey post-hoc tests were run on any significant main effects. Simple effects were run on significant interactions. Significance was set a $p<0.05$.

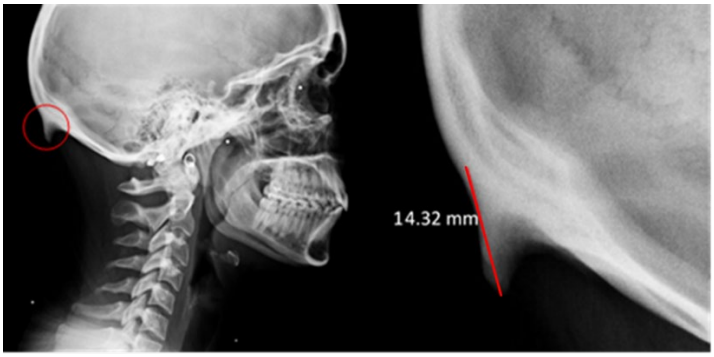

Figure 1: Example of an EEOP (left) and the EOP length measurement (right)

Results and Discussion

Twenty percent (10/50) of our participants presented with an EEOP. Twenty-five percent (9/36) of young adults (18-30 years of age) presented with an EEOP and 2.5% (1/8) in older adults. A high prevalence of EEOPs in younger adults is consistent with previous literature[1,] but the percentage of young adults is much smaller (41% in previous work[1]).

The only significant difference for the intervertebral joint angles was at the C3-C4 level ($p<.001$) (**Table 1**). The C3-C4 angle was more extended in those with EEOPs. The C3-C4 joint is at the apex of the lordotic curve of the cervical spine. We hypothesize that this difference may be due to differences in the size and strength of neck muscles. Stronger muscles could lead to an extended cervical spine and stress the ligamentum nuchae, which puts stress on the EOP, leading to an EEOP.

In summary, our study found that EEOPS were more prevalent in young adults, which is consistent with previous research. We also found that those with EEOPs present with more extended C3-C4 intervertebral angles.

Variable	Enlarged EOP (n=10)	Normal EOP (n=40)
EOP Length* (mm)	13.6 ± 2.38	3.31 ± 3.64
Moment Arm (mm)	10.75 ± 9.42	19.83 ± 9.52
C2-C3 Angle	7.52 ± 7.70	7.20 ± 4.28
C3-C4 Angle*	6.09 ± 5.14	3.10 ± 4.71
C4-C5 Angle	3.87 ± 4.58	0.85 ± 4.17
C5-C6 Angle	3.46 ± 3.61	0.43 ± 4.54
C6-C7 Angle	7.21 ± 4.49	5.43 ± 4.41

Table 1: Mean and standard deviations for each variable. For angles, negative = flexion and positive = extension. Note: * indicates significance at $p<0.05$.

Significance

The C3-C4 intervertebral angle was the only significantly different variable between our two groups, indicating a possible relationship with the lordotic curve of the cervical vertebrae. An abnormally extended curve may lead to the potential of pain due to increased facet spinous process interaction and should be investigated further. Tubercle growth has been shown to be reliant on the pull/force of muscle[7]. Our continued work will explore the relationship between muscle strength and EOP size.

Acknowledgments

This work was supported by the National Science Foundation's REU program under grant number 1658845, a University of Arkansas Collaborative Faculty Development Grant, and an Arkansas Student Undergraduate Research Fellowship.

References

1. Shahar, D., & Sayers, M. G. L. (2016). Journal of Anatomy DOI:10.1111/joa.12466
2. Zubiaur, G. A. et al, (2019). Actas Dermo-Sifiliográficas, DOI:10.1016/j.adengl.2019.06.001
3. Marshall, R. C. et al., (2015). Journal of Plastic, Reconstructive & Aesthetic Surgery, DOI:10.1016/j.bjps.2015.06.013
4. Vasavada, A. N. et al, (2015). Ergonomics. DOI: 10.1080/00140139.2015.1005166
5. Douglas, E. C., & Gallagher, K. M. (2018). Applied Ergonomics, DOI:10.1016/j.apergo.2018.02.020
6. Yoakum, C. B. et al., (2019). Clinical Anatomy http://doi.org/10.1002/ca.23440
7. Rudnicki, M. A. et al, (1993). Cell (Cambridge). DOI:10.1016/0092-8674(93)90621-v

REACHABLE WORKSPACE WITH REAL-TIME MOTION CAPTURE FEEDBACK TO QUANTIFY UPPER EXTREMITY FUNCTION

R. Tyler Richardson[1], Stephanie A. Russo[2], Ross S. Chafetz[2], Spencer Warshauer[2], Emily Nice[2], Scott H. Kozin[2], Dan A. Zlotolow[2], James G. Richards[3]
[1]Pennsylvania State University Harrisburg, Middletown, PA, USA
email: rtr12@psu.edu

Introduction

Clinical upper extremity (UE) functional assessments have been criticized for being insensitive to certain meaningful differences in UE function[1]. More precise motion capture measures are typically constrained to a set of static postures and/or limited motions relevant to the patient population[2] and may provide an incomplete assessment of a patient's UE functionality. Like clinical assessments, motion capture analyses are also reliant on patient compliance with traditional task-based data collections, which can be challenging to collect on younger patients.

Assessing UE functionality by utilizing a less prescriptive and more game-like environment may provide the opportunity to obtain precise measures of UE function on young children[3]. The measurement of reachable workspace can be obtained in such an environment. Reachable workspace provides a precise numerical and visual assessment of global UE function by quantifying the regions in space that a patient can reach with his/her hand[4]. Incorporating real-time (RT) visual feedback with motion capture into current UE workspace measures can provide an innovative way to engage patients[3] while also ensuring acquisition of the patient's entire available workspace.

This study provides an evaluation of a new clinical tool that incorporates RT visual feedback with motion capture to quantify UE reachable workspace. It was hypothesized that 1) the use of RT feedback would result in greater workspace and 2) workspace on the affected/injured limb would be less than that of the unaffected/healthy limb.

Methods

Trunk and UE segment orientations of 10 children with brachial plexus birth injuries (4-10 years) were measured using motion capture. An array of virtual targets surrounding each participant was created using spherical coordinates. Custom LabVIEW software displayed virtual targets with RT feedback from motion capture. Movements of a virtual cursor were controlled in RT based on the position of the hand marker relative to the trunk. Once the cursor moved within a threshold of a virtual target, that target would disappear. Targets throughout the spherical space were displayed sequentially by octant (e.g., upper hemisphere, right side, anterior) until all targets were completed or until the subject was unable to reach any more. Subjects completed trials on their affected and unaffected limbs under two conditions – with and without RT feedback. For the trials without RT feedback, guidance like that given during clinical functional assessments was provided by the researcher to help ensure that the participants attempted to reach all regions of their workspace. The workspace trials without RT feedback would end once the researcher had the participant move through all regions to the best of their ability. Reachable workspace space was calculated for each octant as the points reached by the hand expressed as a percentage of the potential reachable points along the outer surface area. The upper and lower posterior octants on the contralateral side of the limb being measured were not analysed due to the minimal of reachable space available in these regions.

Results and Discussion

The use of RT feedback resulted in significantly greater workspace on both the affected (3/6 octants) and unaffected (6/6 octants) limbs (**Fig. 1**). We accept hypothesis 1 as RT feedback increased workspace reported for each limb.

The affected limb had significantly less workspace than the unaffected limb for 4/6 octants when using RT feedback (**Fig. 1**). Without RT feedback the difference between limbs was significant for only 1/6 octants (**Fig. 1**). We accept hypothesis 2 given that workspace analysis with and without RT feedback was able detect interlimb differences in workspace but conclude that the use of workspace analysis with RT feedback was more sensitive for detecting the functional deficits on the affected limb.

This assessment demonstrates the viability of a reachable workspace tool with RT feedback to facilitate data collection and provide a more complete measure of global UE function that is capable of illustrating areas of impairment.

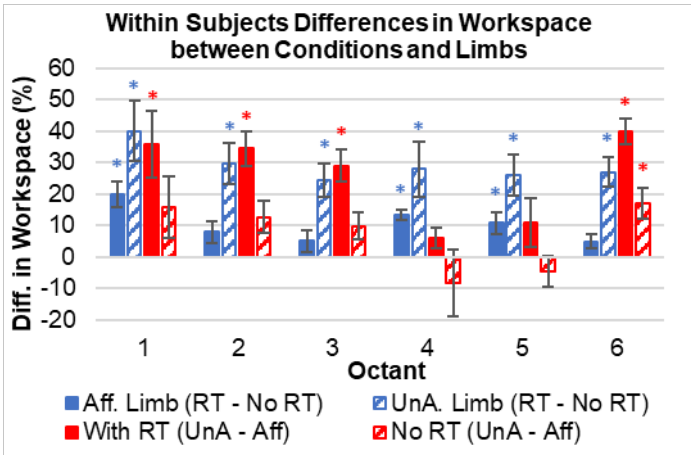

Figure 1: Blue columns: differences between real-time feedback conditions on the affected (Aff.) and unaffected (UnA.) limbs. Red columns: differences between limbs with (RT) and without (No RT) RT feedback. * indicates statistical significance ($p<0.05$). Octants: 1=up./ant./ipsil., 2=up./ant./contra., 3=up./post./ipsil., 4=low./ant./ipsil., 5=low./ant./contra., 6=low./post./ipsil.

Significance

A reachable workspace tool with RT feedback provides a more complete measure of global UE function, may facilitate testing in younger patients to obtain previously unavailable pre-operative data, and offers a highly visual and intuitive depiction of patient function for clinicians, patients, and caretakers.

Acknowledgments

2019 Shriners Hospitals for Children Developmental Research Grant (70901-PHI-19).

References

1. Hogendoorn (2010) J of Bone and Joint Surg, 92(4):935-942.
2. Russo (2014) J of Shoulder and Elbow Surg, 23(3):327-338.
3. Parsons et al. (2014) Develop Neurorehab, 12(4): 224-238.
4. Abdel-Malk (2004) Ergonomics, 47(13):1386-1405.

EFFECTS OF MATURATION ON WHOLE-BODY METABOLIC RATE IN FEMALE SOCCER PLAYERS

Lauren E. Schroeder[1], Kevin R. Ford[2], Audrey E. Westbrook[2], Jeffrey B. Taylor[2], Anh-Dung Nguyen[2,3], Joshua T. Weinhandl[1]
[1]Department of Kinesiology, Recreation, and Sport Studies, The University of Tennessee, Knoxville, Knoxville, TN, USA
[2]Department of Physical Therapy, High Point University, High Point, NC, USA
[3]Division of Athletic Training, West Virginia University, Morgantown, WV, USA
Email: lschroe1@vols.utk.edu

Introduction

Human motion is driven to be both efficient and cost effective (i.e., maximize energy intake and minimize energy use). Frequent decelerations and accelerations, commonly seen in change of direction movements in soccer, require high levels of metabolic work. Assessing the workloads needed to complete common soccer movements is vital in understanding the mechanical demand needed for these injury-prone movements.

Musculoskeletal modelling makes it possible to predict the metabolic cost of muscle actions in human movement. However, limited research exists that examines the metabolic cost in athletic movements. Therefore, the purpose of this study was to compare gross average whole-body metabolic rate between maturation groups in young female soccer players. It was hypothesized that more mature females would exhibit decreased gross average metabolic rate compared to less mature females.

Methods

Motion capture data from 15 adolescent female soccer players completing unanticipated 90° side cutting trials (CUT) off the dominant leg were used. Participants were classified into three maturation groups based on their predicted adult stature percentage [1]: prepubertal (PRE: n = 5, age: 9.9±0.3 yrs, height: 1.34±0.05m, mass: 34.27±2.32kg), pubertal (PUB: n = 5, age: 12.1±1.0 yrs, height: 1.60±0.03m, mass: 46.40±6.41kg), and post-pubertal (POST: n = 5, age: 14.3±1.5 yrs, height: 1.70±0.02m, mass: 55.0±2.66kg).

Musculoskeletal simulations of the CUT trials were done in OpenSim (v3.3, http://simtk.org). Inverse kinematics and inverse dynamics were used to calculate joint angles and moments from a subject-specific scaled musculoskeletal model [2]. Residual Reduction Algorithm (RRA) was used to reduce the residual forces and moments (applied to the pelvis) resulting from dynamic inconsistencies between measured kinematics and ground reaction forces. The resulting RRA-adjusted model was then used in the Computed Muscle Control tool to generate a set of muscle excitations that produced a coordinated muscle-driven simulation of the CUT trials. To estimate metabolic energy consumption, the Umberger2010MuscleMetabolicsProbe with some modifications was used [3,4].

Gross average whole-body metabolic rate was calculated according to Dembia et al. [5]. Briefly, total rate of energy consumption from all lower extremity muscles (normalized to body mass), with a basal rate of 1.2 W/kg added to account for the upper extremity, was integrated over the stance phase, and then divided by the duration of the stance phase. A one-way ANOVA, with effect sizes, was performed on average metabolic rate between the three maturation groups (SPSS, $\alpha = 0.05$).

Results and Discussion

Our hypothesis was not supported, as there were no significant differences between maturation groups: $F(2,12) = 3.351$, $p = 0.070$, $\eta^2_p = 0.358$. However, a large effect size was detected. Gross average metabolic rate was largest in the PRE group (39.21 W/kg), indicating more metabolic energy was consumed in less mature female soccer players. This also suggests an inefficient movement strategy was used in the PRE group during the CUT task. Interestingly, the PUB group exhibited the lowest gross average metabolic rate, suggesting this maturation group uses an effective movement strategy that reduces metabolic cost during this highly dynamic task.

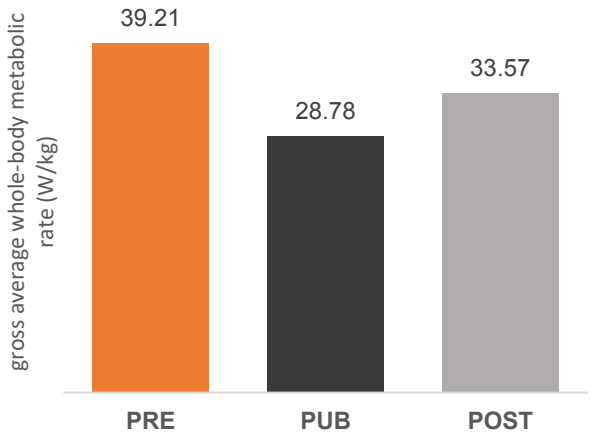

Figure 1: Gross average whole-body metabolic rate between prepubertal (PRE), pubertal (PUB), and post-pubertal (POST) maturation groups.

Significance

Results from this preliminary work indicate that less mature adolescent female soccer players require greater energy consumption to complete an unanticipated sidecut task compared to more mature females. Additionally, the POST group exhibited greater energy consumption compared to the PUB group. Identifying why greater energy consumption is needed in the POST group may aid in determining why this age group is prone to season-ending injuries, such as ACL injuries.

Acknowledgments

This work was supported by the International Society of Biomechanics Dissertation Grant.

References

[1] Westbrook AE et al. (2020) *PLoS One*, **15**: e0233701.
[2] Lai AM, et al. (2017). *Ann Biomed Eng.* **45**: 2762-74.
[3] Umberger, et al. (2003). *Comp Methods Biomech Biomed Eng.* **6**: 99-111.
[4] Uchida, et al. (2016). *PLoS ONE*. **11**: e0150378.
[5] Dembia, et al. (2017). *PLoS ONE*. **12**: e0180320

THE RELATIONSHIP BETWEEN LOAD AND TASK DEMAND IN INDIVIDUALS WITH AND WITHOUT UNILATERAL TRANSTIBIAL AMPUTATION

Sarah C. Moudy[1,2*], Neale A. Tillin[1], Amy R. Sibley[1,3], Siobhan Strike[1]
[1]University of Roehampton, London, UK, [2]University of North Texas Health Science Center, Fort Worth, TX, USA, [3]London South Bank University, London, UK; Email: *sarah.moudy@unthsc.edu

Introduction

Active community mobility and exercise for health involve a range of activities including walking, step negotiation and running. The magnitudes of the peak vertical ground reaction force (vGRF) and knee moments in early stance are related to the activity and the more dynamic the task the higher the load. During early stance, the large vertical deceleration (loading) in these locomotor activities has been associated with the development of knee pain and degenerative conditions [1]. Potentially, for individuals with unilateral transtibial amputations (ITTAs), the load response to increased task demand may explain the increased intact side musculoskeletal comorbidities. **The purpose of this study was to examine the relationship between load and task demand in individuals with and without transtibial amputation.**

Methods

Eight recreationally active ITTAs and 21 age and activity-level matched controls performed five movement tasks: habitual walking, fast walking, single step-descent, jog, and run. Habitual walking represented everyday walking pace, while fast walking was the pace required if "running late to a meeting". Single-step descent, representative of stepping off a curb, was performed by walking the length of a 5 m platform, stepping down from a 14 cm height, and continuing to walk. Jog pace was determined by the participant as the typical pace they would run to complete a 10K whereas the run pace was for a 5K.

Task demand was defined by the vertical velocity at initial contact (VIC). The following loading measures were extracted from early stance phase of each movement: peak vGRF and peak knee external adduction and flexor moments (KAM and KFM). Data were extracted for the intact limb of ITTAs and a control limb. Simple linear regressions were performed with VIC as the predictor, and vGRF, KAM, and KFM as the dependent variables individually for ITTAs and controls. Independent *t*-tests were run on the regression slopes to determine if the relationship between load and task demand differed between ITTAs and controls.

Results and Discussion

No significant differences were found in the regression slopes for vGRF ($t(141) = 1.75$, $p = 0.082$) or KFM ($t(141) = 1.19$, $p = 0.235$). A significantly different regression slope was found between ITTAs and controls for KAM ($t(141) = 2.38$, $\boldsymbol{p = 0.019}$). KAM in the intact limb responds differently to increases in task demand than a control limb. However, the low adjusted R^2 values may indicate underfitting in the KAM and KFM models and that other factors, outside increasing task demand, are involved. As KAM is a marker strongly associated with the progression of knee osteoarthritis, further research is needed to understand the relationship between intact limb load and task demand that could better inform daily and exercise activity options that minimize high intact limb load and gain the health benefits of activity.

Future directions: Develop a multiple regression model, which includes 1) horizontal velocity as the predictor to represent changes in deceleration by task, 2) movement mechanics, and 3) muscular strength measures. Further, examine the relationship between load and task demand using a higher-order polynomial and a greater range of tasks.

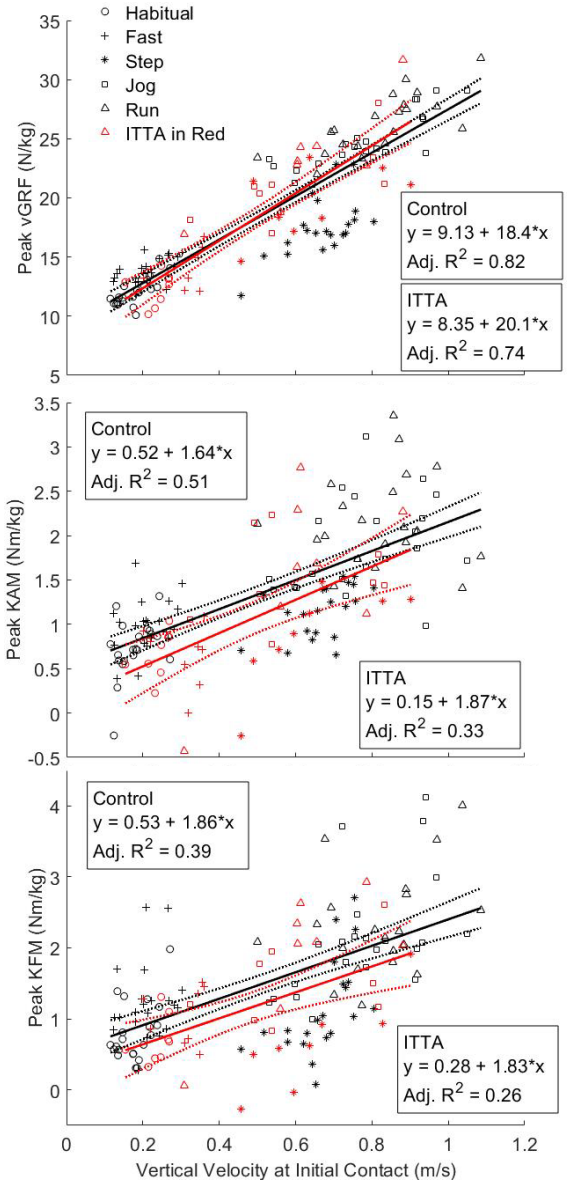

Figure 1. Linear regression lines of best fit (solid) with 95% confidence intervals (dotted)

Significance

Increases in ITTA intact knee load is not fully explained by task demand. Thus, load magnitude compared to control limbs may not be the mechanism of increased knee pain and degenerative diseases. This is consistent with recent previous research [2-3]. Rather, between-limb load symmetry may be a better predictor.

References

[1] Struyf et al. 2009. *Arch Phys Med Rehabil.* 90: 440-446.
[2] Strike et al. 2018. *Gait Posture.* 62: 327-332
[3] Moudy et al. 2021. *Clin Biomech*. 82(2): 105279

THE EFFECTS OF FATIGUE ON LOWER EXTREMITY MECHANICS IN HEALTHY AND ACL-RECONSTRUCTED FEMALES: A STATISTICAL NON-PARAMETRIC MAPPING APPROACH

Shelby A. Peel[1,2], J. Melaro[1], J. Reinbolt[1], S. Zhang[1], L. Schneider[1], J. Sorochan[1], J. T. Weinhandl[1]
[1]University of Tennessee, Knoxville, TN, USA, [2]High Point University, High Point, NC, USA
Email: speel@highpoint.edu

Introduction

Muscular fatigue is a controversial lower extremity injury risk factor, in part due to its complexity. It is thought that when an individual becomes fatigued, the musculature's ability to absorb energy is reduced, leading to decreases in neuromuscular control and altered lower extremity mechanics [1,2]. Few studies have observed the effects of fatigue on lower extremity mechanics in healthy and ACL-reconstructed (ACL-R) females, which have yielded conflicting results. Because fatigue in athletics is unavoidable, a better understanding of its influence on lower extremity mechanics is warranted.

Therefore, the purpose of this study was to determine the effects of muscular fatigue on lower extremity kinematics and kinetics in healthy and ACL-R females using a laboratory-based fatigue protocol. We hypothesized that lower extremity kinematics and kinetics would be different pre- to post-fatigue.

Methods

Seven healthy (23.0 ± 2.6 yrs, 69.2 ± 6.9 kg; 1.66 ± 0.6 m) and four ACL-R (21.8 ± 2.1 yrs, 67.3 ± 4.8 kg; 1.68 ± 0.6 m) recreationally active females volunteered to participate in this study. Participants completed a 5-minute self-selected warm-up, followed by five box land-and-cut trials from a 30 cm box placed ½ their height from the force plates. The box land-and-cut task required participants to jump off the box with their left foot, land on the force plate with their right foot and make a 45° cut to the left. Then, they completed a laboratory-based fatigue protocol, before returning to the laboratory and performing five additional box land-and-cut trials. Briefly, the fatigue protocol consisted of running to 4 different exercise stations and performing various types of body weight exercises. Participants were asked to complete as many rounds as possible, and the protocol stopped when participant maximal jump and reach height decreased 25% during two consecutive jumps.

A 12-camera motion capture system (200Hz, Vicon) and a force platform (2000Hz, AMTI) were used to collect marker coordinate and GRF data, respectively. Visual3D (C-Motion) was used to process and analyze all data. Marker coordinate and GRF data were filtered using fourth-order Butterworth low-pass filters with cut-off frequency of 12 Hz. 3D lower extremity joint kinematics were calculated using a joint coordinate system approach. 3D internal joint moments were expressed in the joint coordinate system and normalized to body mass. Pre- and post-fatigue lower extremity mechanics were compared across the landing phase with one-dimensional statisticial non-parametric mapping F-tests (SnPM{F}). If a group x fatigue interaction was found, *post-hoc* SnPM *t*-tests (SnPM{t} were conducted on each pairwise comparison separately. Significance for all tests were *a priori* set at $p < 0.05$.

Results and Discussion

The only group × fatigue interaction found was hip flexion angle (Figure 1). ACL-R females had an average of 18.7° more hip flexion pre-fatigue (23 – 70% stance phase) and 15.3° more hip flexion post-fatigue (62 – 79% stance phase) compared to healthy females (Figure 1). Significant group main effects included hip flexion, abduction, and rotation angles ($p < 0.05$). Significant fatigue main effects included hip flexion and knee abduction angles, as well as hip rotation moment ($p < 0.05$). No other significant supra-threshold clusters were found.

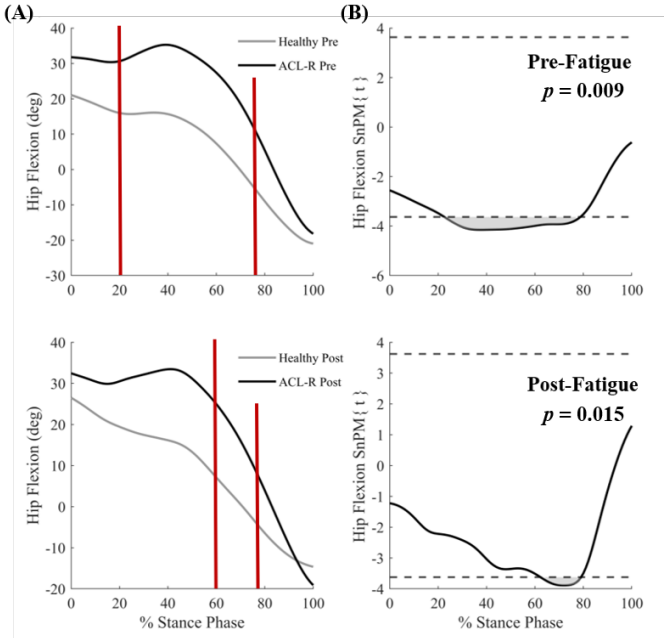

Figure 1: Mean ensemble curves for healthy and ACL-R hip flexion angles pre-fatigue and post-fatigue (A) with their respective SnPM{t} output from 0 to 100% of stance phase (B). Red vertical lines represent the % stance phase that was indicated significant by the respective SnPM{t}.

Significance

Our results indicate that muscular fatigue and previous ACL-R may play a role in influencing hip mechanics kinetics in ACL-R females. It has been shown that ACL-R females may be prone to poor neuromuscular control of the trunk [3], thus increasing hip flexion and potentially risk of injury. However, it appears that prior ACL-R may play a larger role in differences found in hip flexion than fatigue, given that compared to healthy females, ACL-R females had greater hip flexion pre-fatigue over a larger period of stance phase compared to post-fatigue. This may be indicative to clinicians and coaches that muscular strength and endurance of the hip musculature is vital in rehabilitative and injury prevention protocols for ACL-R females.

References

1. Borotikar et al. (2008) *Clin Biomech,* Vol **23**, 81-92.
2. Mair et al. (1996) *A J Sports Med,* Vol **24**, 137-43.
3. Clark et al. (2015) *Med Sci Sports Exerc,* Vol **47**, 120-27.

HIP JOINT CONTACT FORCES DURING SIT-TO-STAND IN PEOPLE WITH A TRANSTIBIAL AMPUTATION

Luis A. Nolasco[1], Anne K. Silverman[2], and Deanna H. Gates[1]
[1]School of Kinesiology, University of Michigan, Ann Arbor, MI
[2]Department of Mechanical Engineering, Colorado School of Mines, Golden, CO
email: *lnolasco@umich.edu

Introduction

People with a transtibial amputation (TTA) have higher rates of bilateral hip[1] and intact leg knee osteoarthritis compared to non-amputees[2]. A greater risk of osteoarthritis is attributed at least in part to high and asymmetric joint loads[2]. At the hip, considering contributions from muscles in joint loading computations is important given the many muscles surrounding this joint and documented bilateral hip muscle compensations in people with TTA[1]. In people with TTA, it is unclear whether the intact or amputated leg hip is more at risk. For example, no differences in hip joint contact force were found during walking between the intact leg and non-amputees[3], while greater intact leg hip contact forces were found during the stance phase of running compared to the amputated leg[4]. As the development of osteoarthritis likely occurs due to the cumulative loading across different tasks over time, understanding how the hip joint is loaded during different tasks can provide insight on loading strategies and may help predict joint degradation in people with TTA. One important functional task is sit-to-stand (STS), which is performed ~50 times per day by people with TTA[5]. As STS requires large hip muscle forces for hip extension and postural stabilization[6], it is important to quantify hip joint contact forces during this task. Therefore, the purpose of this study was to investigate hip joint contact forces during STS in people with TTA.

Methods

One person with TTA (M, 56 yrs, 1.7 m, 99.6 kg) and one person without an amputation (M; 52 yrs; 1.7 m, 69.6 kg) were selected from a larger study where participants performed five self-paced STS trials[7]. Participants began seated with hips, knees, and ankles flexed at 90°, feet hip-width apart on separate force plates recording at 1200 Hz. Kinematics were collected at 120 Hz using a full-body marker set.

Marker positions and ground reaction forces (GRFs) were low-pass filtered using a 4th-order Butterworth filter with cut-off frequencies of 6 Hz and 10 Hz, respectively. An 8-segment model was created in Visual3D and used to determine the inverse kinematics solution from seat-off to standing (body center of mass velocity reaches zero) using a least squares optimization approach for all five trials for each participant. The inverse kinematics solutions were input with a musculoskeletal model (gait2392) to OpenSim 4.1. We performed a residual reduction algorithm to ensure dynamic consistency between the inverse kinematics solutions and GRFs. Individual muscle forces were then determined using a computed muscle control algorithm (CMC) to minimize the sum of squared muscle controls, which reproduced the STS motion. The individual muscle forces were then used to calculate the vector magnitude of the hip joint contact force during STS.

Hip joint contact forces were low-pass filtered using a 4th-order Butterworth filter with a 6 Hz cut-off frequency and normalized by body weight. We then calculated peak hip joint contact force asymmetry between legs as a percent difference. We also calculated the difference between intact and amputated legs relative to the non-amputee participant.

Results and Discussion

Peak hip joint contact force occurred just after seat off and was 19% greater on the intact leg compared to the amputated leg and 22% greater than the non-amputee participant. Peak force on the amputated side was similar to the non-amputee participant (0.4% difference). These preliminary results suggest that people with TTA have asymmetric hip joint contact force between legs during STS due to large intact leg hip joint forces, which may negatively affect hip joint health. However, further analyses with a larger sample size are needed.

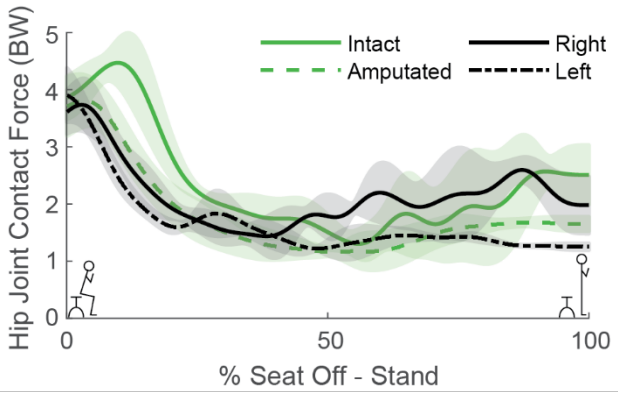

Figure 1: Hip joint contact forces in body-weights (BW) from seat-off to standing for one person with (green) and without (black) TTA.

Significance

Our preliminary analysis suggests that the asymmetry in hip joint contact forces during STS is higher in people with TTA compared to people without TTA. This asymmetry may contribute to a greater risk of developing osteoarthritis in the intact hip compared to the amputated leg and non-amputees. As people with TTA generally have asymmetric weight-bearing during STS and asymmetric hip muscle strength, these results highlight the clinical need for improving weight-bearing symmetry and strengthening amputated leg hip muscles in this population. Quantifying joint contact forces during tasks of daily living is useful in understanding long term joint health. In addition, insights on cumulative joint loading of different tasks over time may help with designing rehabilitation protocols for people with TTA aimed at promoting joint health and mobility.

Acknowledgments

Thanks to Kelsey Ebbs and Jay Kim for help with data collection and Jordan Sturdy for help with simulations.

References

1. Kulkarni, J, et al. 1998. Clin Rehab, 12, 348-353.
2. Gailey, R, et al. 2008. J Rehab Res Dev, 45, 15-29.
3. Karimi, M, et al. 2017. Gait & Pos, 58, 246-251.
4. Sepp, L, et al. 2021. J Biomech Eng, 143, 031012.
5. Bussmann, J, et al. 2008. Arch Phys Med Rehab, 89, 430-434.
6. Jeon, W, et al. 2021. J Biomech, 117, 110251.
7. Nolasco L, et al. 2020. J Biomech, 109, 109926.

Effects of lower limb joint powers and kinesiophobia on physical activity in people with knee osteoarthritis

Burcu Aydemir, Chun-Hao Huang, and Kharma C. Foucher
Department of Kinesiology and Nutrition, University of Illinois at Chicago, IL, USA
email: baydem2@uic.edu

INTRODUCTION

Lacking regular participation in physical activity is a prevalent risk factor for functional limitations in people with knee osteoarthritis (OA) [1]. Loss of mobility with OA can lead to disability and changes in gait. Joint power profiles differ significantly in people with knee OA compared to healthy adults [2]. Additionally, psychological factors such as kinesiophobia or fear of movement have been linked to activity limitations in people with knee OA [3]. However, to our knowledge, no studies have explored the collected effects of both psychological and biomechanical factors on physical activity in people with knee OA. The primary aim of our study was to explore the combined effects of generative (propulsive) lower limb joint powers (ankle, knee, and hip) and kinesiophobia on self-reported physical activity in people with knee OA. We *hypothesized* that generative joint powers during walking gait and fear of movement (kinesiophobia) would together predict physical activity level in people with knee osteoarthritis.

METHODS

Thirty-seven participants (F 21 | M 10; age 57.2 ± 9.2 years; BMI 34.7 ± 7.2 kg/m^2) with doctor-diagnosed uni- or bilateral knee OA consented to participate in this cross-sectional study. Physical activity level and kinesiophobia were assessed by self-report using the UCLA activity score (scale 1-10, inactive to regular participation in impact sports) and Tampa Scale for Kinesiophobia (TSK; scale 17-68, no fear to extreme fear of movement), respectively. Kinematic (120 Hz) and synchronized kinetic data (1200 Hz) were collected as subjects walked at their preferred walking speed on a split-belt treadmill. Passive reflective markers were placed bilaterally over selected bony landmarks using standard methods. The following peak generative mechanical joint powers of the lower limb during late stance were calculated using Visual 3D software (C-Motion, Inc., Germantown, MD): hip power generation (H_{POWER}), knee peak power generation (K_{POWER}), peak ankle power generation at push off (A_{POWER}). Joint powers were normalized to body weight Watt/kg (W/kg). Only the affected/most affected limb was used for statistical analysis. We performed a multiple linear regression analysis to test our hypothesis. Alpha was set at $p < 0.05$ for all analyses. Prior to parametric analysis, data were transformed when necessary, using square root or logarithmic transformations. Data were analyzed with SPSS, version 27. Under these conditions a sample size of 37 subjects provides 80% power for detecting a small $f^2 = 0.41$ ($R^2 = 0.291$).

RESULTS AND DISCUSSION

In support of our hypothesis, peak power generation at the ankle, hip, and TSK score all significantly predicted UCLA score or physical activity (5.14 ± 2.14), however, peak power generation at the knee was not a significant predictor (Table 1). Approximately 55.3% of the variance in physical activity was accounted for by all predictors (adjusted $R^2 = .497$, $p < .001$). However, after accounting for treadmill gait speed (0.58 ± 0.22 m/s) as a covariate in our model, only peak power generation at the hip ($p = .003$), TSK score ($p = .001$), and gait speed ($p < .001$) were significant predictors of physical activity (Figure 1). During late stance, people that use more propulsive hip generation are less active regardless of propulsive generation at distal joints, kinesiophobia, and gait speed. Increased hip flexor power during late stance is thought to be a compensation for reductions in plantarflexor power in older adults [4,5]. It is possible that this compensatory mechanism during regular activities of daily living could lead to quicker fatigue, potentially explaining the reduced activity levels seen in this population. Additionally, greater kinesiophobia (fear of movement) was still a significant predictor of physical activity even after accounting for the other variables, highlighting the import role psychological factors play on physical activity in this population.

Table 1.

	b	SE b	BCa 95% CI Lower	BCa 95% CI Upper	*p*
H_{POWER}	-0.443	0.235	-0.950	-0.156	**.033**
K_{POWER}	-0.025	0.069	-0.172	0.120	.719
A_{POWER}	0.639	0.254	0.167	1.153	**.014**
TSK	-0.023	-0.375	-0.042	-0.005	**.019**

Note. BCa—bias corrected and accelerated confidence interval and SE—standard error were based on 10,000 bootstrap samples. b—unstandardized regression coefficient.

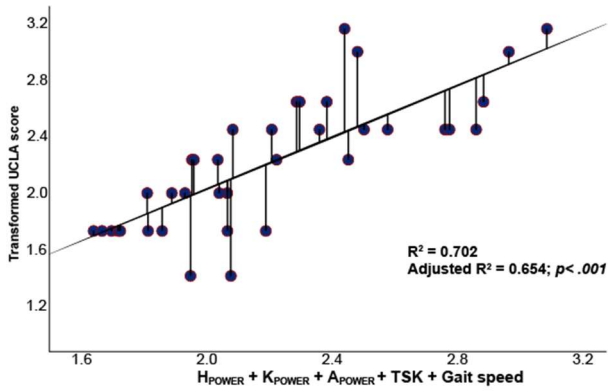

Figure 1. UCLA vs. regression adjusted predicted value of full model.

SIGNIFICANCE

Interventions aimed at improving participation in exercises, such as walking, should consider the combined effects of behavioral and biomechanical factors.

ACKNOWLEDGMENTS

Funded by UIC, CCTS (UL1TR002003) Pilot Grant (KCF)

REFERENCES

[1] Dunlop et al. (2010) Arch Phys Med Rehabil, 91: 714-21
[2] McGibbon & Krebs (2002) J Rheumatol, 29: 2410-9
[3] Heuts et al. (2004) Pain, 110:228-35
[4] McGibbon et al. (2001) Clin Biomech, 16: 324-33
[5] Judge et al. (1996) J Gerontol, 51: M303-M312

Compartmental Knee Contact Forces in Patients with Unilateral Total Knee Arthroplasty during Stationary Cycling

Songning Zhang[1], Erik Hummer[2], Tanner Thorsen[1], Joshua T. Weinhandl[1], Jeffrey A. Reinbolt[1], Harold E. Cates[3]
[1]University of Tennessee, Knoxville, TN, USA
[2]Kessler Foundation, West Orange, NJ, USA
[3]Tennessee Orthopaedic Clinic, Knoxville, TN, USA
Email: szhang@utk.edu

Introduction

Total knee arthroplasty (TKA) is the surgical solution for people with end-stage knee osteoarthritis. Patients of TKA often experience deficit of knee extension moment in their replaced limbs during gait [3] and more recently during stationary cycling [1]. Information on knee joint contact force during cycling in TKA is very limited in literature. Such information is valuable for clinical as well as research applications. Therefore, the purpose of this study was to use musculoskeletal modeling to examine inter-limb differences of total (TCF), medial (MCF), and lateral (LCF) tibiofemoral contact forces for patients of TKA across different workrates during stationary cycling.

Methods

Fifteen unilateral patients of TKA (64.3 ± 8.2 yrs, 94.1 ± 20.4 kg, 1.74 ± 0.1 m, 8.6 ± 2.4 months post-op, cruciate retaining = 14, bi-cruciate stabilizing = 1) were recruited from a local orthopedic clinic and were operated by the same orthopedic surgeon. Participants cycled on a stationary cycle ergometer (Excalibur Sport, Lode) in two randomized workrates (80 and 100 Watt) at a cadence of 80 RPM for one-minute in each test condition. During the final 10 seconds, 3D motion capture (240 Hz, Vicon Motion Inc.) and pedal reaction force data (1200 Hz, Kistler) were collected simultaneously and filtered at 6 Hz with a 4th order low-pass filter.

A generic musculoskeletal model with 23 degrees-of-freedom and 92 musculotendon actuators was used in OpenSim (3.2, Stanford University) with a modified knee joint with medial and lateral tibiofemoral compartments [2] to simulate TCF, MCF and LCF. Static optimization was used to estimate muscle forces using experimental data and joint reaction analysis was used to compute TCF, MCF and LCF. A 2×2 (limb × workrate) and a 2 × 2 (compartment × limb) repeated measure ANOVA were run on the selected variables.

Results and Discussion

The results of the limb×workrate ANOVA showed that peak TCF and LCF did not exhibit any significant interaction, limb or workrate main effect (Table 1). Peak MCF displayed a significant limb main effect (p = 0.028). The post hoc comparison found that peak MCF was greater in the non-replaced compared to replaced limb.

The results of the compartment×limb ANOVA showed at 80 W, the interaction for peak MCF was significant (p = 0.001). Post-hoc analysis indicated that peak MCF in the non-replaced limbs was greater than peak MCF for the replaced limbs (p = 0.003, Figure 1), and was greater than peak LCF in the non-replaced limbs (p < 0.001). At 100 W, MCF was greater than LCF(p=0.017).

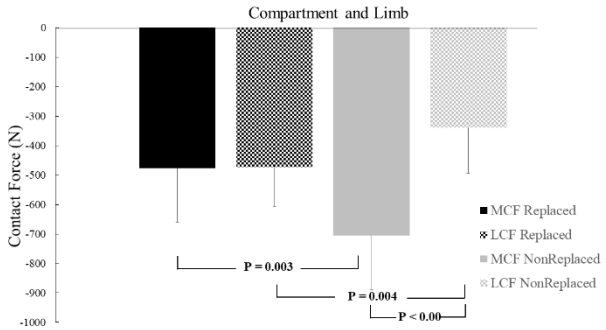

Figure 1. Comparison of MCF and LCF (Mean ± STD) for both the replaced and non-replaced limb at 80 W.

Significance

The lack of limb difference of TCF is contrary to the results found using inverse dynamics in the same subject group in cycling [1]. The magnitude of tibiofemoral joint loading for cycling is much lower than walking, which might have led to the inability to detect the difference for peak TCF between the replaced and non-replaced knees. Further studies are necessary to confirm these findings. Although TCF did not increase significantly from 80 – 100 W, MCF showed greater increases relatively to LCF and TCF, suggesting it would be safer to cycle at the lower worktate at 80 W for patients with TKA.

Acknowledgements

Funding for this study was provided by the International Society of Biomechanics Matching Dissertation Grant to EH.

References

1. Hummer, E., et al. (2021). *J Biomech,* **115**, 110111.
2. Lerner, Z. F., et al. (2015). *J Biomech,* **48**, 644-650.
3. Wen, C., et al. (2019). *J Biomech,* **89**, 40-47.

Table 1. Peak knee contact forces (N) and knee extensor and flexor group muscle forces (N): mean ± STD.

	80 Watts		100 Watts		p (η^2_p)		
	Replaced	Non-Replaced	Replaced	Non-Replaced	Inter	Limb	Workrate
TCF	-918.6±253.4	-1021.4±212.7	-952.5±208.6	-1024.7±276.2	0.556 (0.03)	0.181 (0.16)	0.577 (0.16)
MCF	-477.4±182.7	-705.2±183.2	-597.2±296.7	-699.0±213.9	0.219 (0.13)	**0.028** (0.37)	0.233 (0.13)
LCF	-472.2±133.7	-339.8±154.5	-411.9±238.9	-399.3±212.5	0.179 (0.16)	0.255 (0.12)	0.994 (0.00)
Extensor	876.1±263.7	910.0±214.4	901.6±234.9	894.4±271.3	0.224 (0.13)	0.846 (0.00)	0.875 (0.00)
Flexor	230.5±101.4	242.3±80.2	255.9±141.1	267.8±117.1	0.997 (0.00)	0.633 (0.02)	0.159 (0.17)

η^2_p: partial eta squared.

REGIONAL PECTORALIS MAJOR ACTIVATION INDICATES FUNCTIONAL DIVERSITY IN HEALTHY FEMALES

Tea Lulic-Kuryllo[1], F. Negro[2], N. Jiang[3], and C.R. Dickerson[1]
[1]Department of Kinesiology, University of Waterloo, Waterloo, ON
[2]Department of Clinical and Experimental Sciences, Universita degli Studi di Brescia, Brescia, Italy
[3]Depatment of Systems Design Engineering, University of Waterloo, Waterloo, ON
Email: *tlulic@uwaterloo.ca

Introduction

Pectoralis major (PM) activation aids performance of daily, occupational, and exercise tasks. While documented regional pectoralis major activation in males exists [1-3], the same is unknown in healthy females. Damage to the pectoralis major is disproportionately greater in females, particularly following breast reconstruction surgery or radiotherapy treatment to eradicate breast cancer [4,5]. Thus, documented pectoralis major activation in healthy females is critical to distinguish between atypical and typical regional pectoralis major activation. This data can help develop targeted exercise or rehabilitation interventions in compromised female populations.

Methods

PM activation was explored via two experiments. Experiments 1 and 2 consisted of 20 (22.4 ± 2.2 years) and 9 (24.5 ± 3.1 years) healthy young females. Activation data was acquired via 64-channel high-density surface electromyography (EMGUSB2+, OTBioelecttronica, Torino, Italy) in monopolar mode at 2048 Hz (bandpass: 10-500 Hz). Participants performed submaximal trapezoidal ramp-and-hold isometric contractions for four tasks in Exp. 1: adduction at 60°and 90°; internal rotation at 60°; and adduction at 90° of arm elevation and external rotation; and Exp. 2: extension, flexion, horizontal adduction, and internal rotation at 90° of elevation and 20° of internal rotation. All submaximal trials were scaled to 15%, 25%, 50%, or 75% of the posture-specific maximal voluntary force (MVF).

Raw EMG signals were bandpass filtered with a 3rd order Butterworth filter (20-500 Hz), followed by differential derivation and RMS quantification for each channel. All RMS values were normalized to channel-specific maximum obtained in maximal contractions. The resultant force was used as a reference to analyze first half of the hold to avoid drift or fatigue effects. Channels were grouped based on anatomical data [6], yielding a clavicular and two sternocostal regions. A 2-way repeated-measures ANOVA was performed with within-subject factor Effort (E; 15, 25, 50%, or 75% MVF) and Region (R; clavicular, superior, and middle sternal). Significance was set to $p < 0.05$. If significant interactions existed, planned comparisons with a post-hoc Bonferonni correction were performed.

Results and Discussion

The middle sternocostal activated more than the clavicular and the superior sternocostal region in extension (~2 times greater; RxE: $F_{(1.77,14.1)}$=12.6, p=0.001), adduction with external rotation (~12-42%; RxE: $F_{(1.8,32.7)}$= 4.1, p=0.028), adduction 90° (RxE: $F_{(2.4,43.9)}$ =3.6, p=0.027), and internal rotation 90° (~14-24%; R:$F_{(2,16)}$=166, p<0.0001). These findings reflect observations in healthy males [1-3]. In internal rotation 60° (RxE: $F_{(2.5,43.1)}$ = 4.77, p=0.008) and adduction 60° (RxE:$F_{(2.4,41.2)}$ = 10.09, p<0.0001), the clavicular and the middle sternocostal regions activated more than the superior sternocostal region (Figs. 1A and B). In horizontal adduction and flexion, all regions activated similarly across efforts (Fig. 1C; RxE: $F_{(6,48)}$ = 28.4, p<0.0001, Fig. 1D; RxE: $F_{(1.7,14.1)}$=12.2, p=0.001), except 25% MVF flexion, where the clavicular region activated more than the superior sternocostal region. These results contrast with those reported in healthy males [1-3].

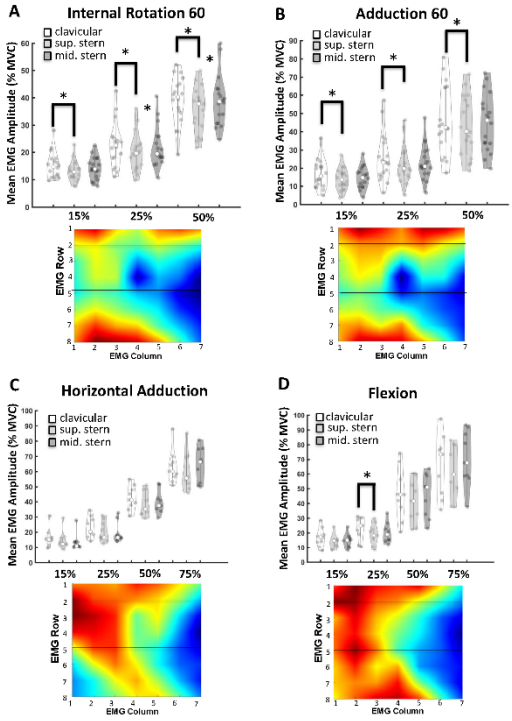

Fig. 1: Mean regional PM activation (%MVC) across efforts for internal rotation 60 (A), adduction 60 (B), horizontal adduction (C), and flexion (D) with group-averaged spatial maps. High activation is denoted in red and low activation in blue in spatial maps. Asterisks (*) denote significant differences between regions.

Significance

Female PM activation is distinct from males [1-3] across various tasks. These differences may be indicative of divergent sex-related architectural and neural properties and should be probed further in future studies. Further, the high activation of the sternal regions in adduction, extension, and internal rotation indicates an important functional role of these regions in these tasks, as previously reported in males [1-3]. Injuries to these regions may alter PM neuromuscular control, as observed following subpectoral breast reconstructions [5]. The results can aid future interventions in compromised female populations.

References

[1]Paton et al. (1994). J Electromyogr Kinesiol. 4; p.161-9.
[2] Brown et al. (2007). J Electromyogr Kinesiol.17; p. 57-73.
[3] Wickham et al. (2004). J Musckuloskel Res. 8; 57-73.
[4] Lipps et al. (2017). Radiother Oncol. 122; p. 431-436.
[5] Leonardis et al. (2019). J Orthop Res. 37; p. 1610-1619.
[6] Fung et al. (2009). Clinical Anatomy. 22; p. 500-508.

MUSCLE ACTIVITY OF THE LUMBOPELVIC-HIP COMPLEX DURING VARIOUS CORE STABILITY EXERCISES

Erika Zambarano[1], A Murray[1]
[1]The University of Toledo, Toledo, OH
email: *erika.zambarano@rockets.utoledo.edu

Introduction

The lumbopelvic-hip complex (LPHC) includes muscles of the lower back, abdomen, pelvic floor, and hip that form the center of the kinetic chain. The LPHC includes deep muscles responsible for local stability and superficial muscles that help with global stability and act as prime movers. Muscles of the LPHC activate in a feed-forward mechanism starting with deep, proximal muscles then moving to more superficial and distal muscles. Appropriate activation of the LPHC is important for providing stability and generating optimal force during athletic movement. Therefore, LPHC function is often assessed clinically and targeted for musculoskeletal injury prevention and treatment.

The LPHC is commonly assessed clinically and treated using a variety of core stability exercises aimed at activating the deep and superficial muscles of the LPHC. Activation patterns of superficial muscles of the LPHC during core stability exercises have been described, but less is known about activity of the deep, stabilizing muscles during these activities. Deep muscle activity is traditionally assessed using indwelling electromyography (EMG), making assessment of deep muscles in the LPHC difficult. Investigating activity of both local and global stabilizers during core stability exercises would provide clinicians more accurate information regarding function of the LPHC and allow for more effective treatment prescription. Our purpose was to assess deep and superficial LPHC muscle activity through combination of musculoskeletal ultrasound (MSK-US), a non-invasive method to investigate the activity of deep muscles, and surface EMG (sEMG) during various core stability exercises.

Methods

This descriptive laboratory study included 13 healthy, active adults (11 females; 22.4±1.4yrs; 170.1±8.4cm; 72.9±12.1kg). Participants performed a battery of core stability exercises including a seated trunk control test, prone plank, side plank, unilateral hip bridge, and trunk flexion test. We assessed activity of the transverse abdominis (TrA), internal oblique (IO), and external oblique (EO) during each exercise using M-mode of MSK-US, which records video of muscle thickness changes. We normalized muscle thickness to a resting measure, creating an activation ratio, with a ratio greater than 1.0 indicating the muscle was activated. The sEMG measured activity of upper rectus abdominis (URA), lower rectus abdominis (LRA), gluteus medius (GMed), and erector spinae (ES). Mean EMG amplitude during each exercise was normalized to supine resting activity. Repeated measures ANOVA with pairwise comparisons evaluated differences in muscle activity during each exercise, $p \leq .05$. For descriptive purposes, the percentage of participants with an MSK-US activation ratio greater than 1.0 was calculated.

Results and Discussion

The IO, URA, GMed, and ES activity differed significantly depending on the exercise (Table 1). The seated trunk control test elicited lower activity of GMed and ES and was the only exercise where 100% of participants activated the TrA. This exercise may be better for targeting the deep muscles with minimal influence of the superficial muscles. The prone plank elicited higher activity from URA and LRA. The side plank elicited greater IO, GMed, and ES activity and had a higher percentage of individuals achieving EO activation. Planking tasks are often used as core stability exercises, but the prone and side plank only elicited TrA activation from 54% and 62% of participants respectively. This could be due to higher activity of the superficial muscles, making planking tasks a better measure of global stability than local stability. The unilateral hip bridge showed high levels of IO and ES activity with low levels of URA activity. The unilateral hip bridge could provide insight into how the ES is contributing to LPHC function. The trunk flexion test did not show higher activity for any muscles, likely due to involvement of hip flexor muscles.

Significance

No single exercise elicited the greatest muscle activity for every muscle, indicating that a battery of multiple core stability exercises should be used when evaluating LPHC function. Clinicians should consider these findings when deciding how to assess and treat muscles of the LPHC based on patient performance on certain core stability exercises.

References

1. Kibler WB, Press J, Sciascia A. *Sports Med*. 2006.
2. Hodges PW and CA Richardson. *Phys Ther.* 1997.
3. Mangum LC, et al. *J Ultrasound Med.* 2018.

Table 1: Average muscle activity for each task (normalized to resting measures)

	Seated Trunk Control		Prone Plank		Side Plank		Unilateral Hip Bridge		Trunk Flexion	
	Mean (SD)	% Active	Mean (SD)	% Active	Mean (SD)	% Active	Mean (SD)	% Active	Mean (SD)	% Active
Transverse abdominis	1.4 (0.1)	100	1.1 (0.1)	54	1.1 (0.1)	62	1.3 (0.1)	85	1.3 (0.2)	62
Internal oblique	1.0 (0.1)	70	**0.9 (0.1)[a,b]**	46	**1.3 (0.1)[a]**	77	**1.2 (0.1)[b]**	69	0.7 (0.1)	31
External oblique	1.2 (0.1)	77	1.0 (0.1)	39	1.3 (0.1)	77	0.9 (0.1)	23	1.4 (0.2)	54
Upper rectus abdominis.	4.4 (0.8)		**23.4 (5.9)[c]**		12.1 (2.7)		**3.2 (0.3)[c]**		5.9 (1.4)	
Lower rectus abdominis.	5.7 (1.2)		30.5 (8.2)		16.6 (3.7)		4.4 (0.6)		9.8 (2.9)	
Gluteus medius	**2.6 (0.4)[d]**		**3.3 (0.4)[e]**		**18.9 (3.9)[d,e,f]**		5.9 (1.3)		**2.7 (0.3)[f]**	
Erector spinae	**3.4 (0.7)[g]**		**4.2 (1.4)[h]**		**13.9 (2.4)[g,h,i]**		**20.1 (2.4)[g,h,i]**		**1.5 (0.2)[i]**	

[a-i] Bolded values are significantly different ($p \leq .05$) from those for the same muscle in the other tasks that have a matching superscript.

SIMULATION OF THE ROLE OF THE SUBSCAPULARIS DURING REVERSE SHOULDER ARTHROPLASTY

Morgan C. Everly[1*], O. Anakwenze[2], and K. R. Saul[1]
[1]Mechancial and Aerospace Engineering, North Carolina State University, Raleigh, NC 27695, USA
[2]Orthopedics, Duke University, Durham, NC, 27708, USA
*mceverly@ncsu.edu

Introduction

Reverse shoulder arthroplasty (RSA), a type of joint replacement surgery, is commonly used to treat glenohumeral arthritis in patients with rotator cuff tears. RSA has an associated risk of instability and weakening in internal rotation (IR) but the underlying biomechanics driving this are unclear. One clinical hypothesis is that lack of intact subscapularis muscle post-RSA contributes to IR weakness due to its function as an internal rotator [1]. However, some studies report no significant differences between RSA with and without subscapularis repair for complication rates, range of motion [2] or IR strength [3]. In contrast, other work suggests that success of RSA with subscapularis repair may depend on placement of the joint center of rotation (COR) during RSA; specifically, that subscapularis repair with RSA that places the COR in a lateral position nearer to the native COR may have negative outcomes [1]. The goal of this simulation study is to examine whether subscapularis functional IR capacity is affected by COR after RSA.

Methods

Simulations were performed using an existing computational shoulder model [4], implemented in OpenSim. To simulate COR placement after RSA, glenohumeral COR was translated according to clinical reports of COR location post-RSA [5]; it was translated medially from the native COR position 10mm (representing lateralized RSA technique), 20mm, and 30mm (medialized RSA) along the scapular spine axis. Subscapularis moment-generating capacity, moment arm, force-generating capacity, and muscle-tendon length were computed over -40° to 40° shoulder axial rotation (internal rotation: positive) in neutral abduction (the range of axial rotation postures in which most daily activities occur) [6]. Moment-generating capacity, a measure of strength, is the product of moment arm and force.

Results and Discussion

Subscapularis moment-generating capacity after simulated RSA decreased with IR, as in an intact shoulder (**Figure 1A**). Moment-generating capacity was affected by COR >10mm medial displacement, with larger decreases as COR medialized from native COR. Subscapularis moment arm was minimally affected in medial COR locations; peak moment arm was only 0.7mm higher for the 30mm medial COR compared to the intact shoulder (**Figure 1B**). However, the posture in which the peak moment arm occurred shifted +6° for every 10mm of medialization. Subscapularis muscle-tendon force decreased markedly with more medial COR. The 10mm, 20mm and 30mm COR positions exhibited decreased mean forces of 144N, 412N and 565N from native, respectively (**Figure 1C**). Subscapularis muscle-tendon length decreased with medialized COR. Changes were most notable with increased IR (**Figure 1D**).

The minimal effect on moment-generating capacity with lateral COR is consistent with a cadaver study [3] of 4 RSA configurations which reported that IR and ER are not significantly affected in a lateral placement. However, a prior clinical study reported declines in American Shoulder and Elbow Surgeons (ASES) score 2 years post-RSA with a lateralized repair when subscapularis repair is also performed [1]; ASES scores reflect measures including shoulder strength and pain [7]. Thus, other consequences of lateralization on subscapularis, such as potential changes to joint reaction force direction and stability, or concomitant consequences of shoulder injury, such as altered muscle architecture, should be explored to further explain clinical observations of post-RSA outcomes.

Significance

Medial shoulder COR drives moderately reduced subscapularis moment-generating capacity in medialized RSA locations, primarily driven by slackened subscapularis in accordance with force-length behavior of muscle. This work provides biomechanical underpinning for decisions about RSA placement. Results suggest COR has limited effects on subscapularis moment in lateralized RSA, and reduced moment with medialized placement may be moderated by tensioning of subscapularis during repair.

References

1. Saltzman et al. JSES 19, 1028-1033. 2010.
2. Friedman et al. JSES 26, 662-668. 2017.
3. Giles et al. JSES 25, 1592-1600. 2016.
4. Werner et al. J Am Acad Orthop Surg 26, e114-e119. 2018.
5. Saul et al. Comput Methods Biomech Biomed Eng 18(13), 1445-1458. 2015.
6. Roy et al. The Open Orthopedics Journal 4, 157-163. 2010.
7. Vidt et al. J EMG and Kinesiology 29, 90:99. 2015.

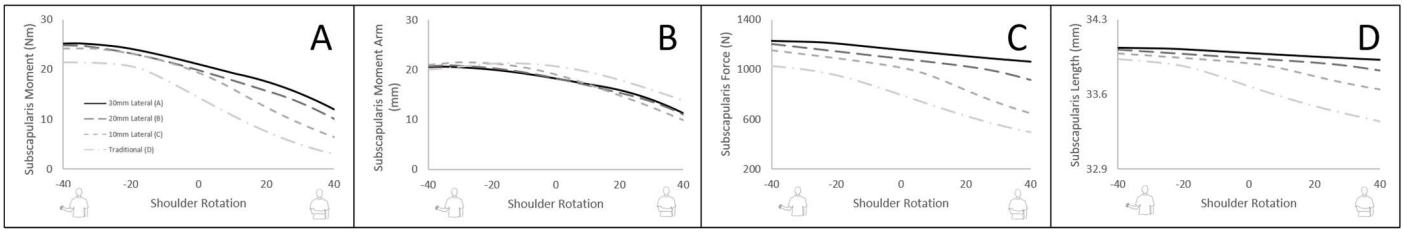

Figure1. Subscapularis moment (**A**), moment arm (**B**), musculotendon force (**C**), and musculotendon length (**D**) vs. shoulder rotation.

Evaluating Anthropometric Scaling of a Generic Adult Model to Represent Pediatric Strength

*Morgan J. Dalman[1], Ashlee Liao[1], Katherine R. Saul[1]
[1]Department of Mechanical and Aerospace Engineering, North Carolina State University, Raleigh, NC, USA
Email: *mdalman2@ncsu.edu

Introduction

The developing musculoskeletal system during childhood and adolescence influences tissue loading and function [1]. Youth participation in sports and reports of musculoskeletal pain and injury are increasing [2,3]. Shoulder injuries in pediatric athletes (e.g. physeal fractures) are increased due to strength imbalance between bones and surrounding soft tissue and during developmental events [4]. Limited data is available on upper limb muscle architecture and joint moments of pediatric patients, which are critical factors for understanding expected loading. Work by Im *et al* [5] suggests pediatric muscle volume distribution in the shoulder is consistent with adults; thus, some aspects of shoulder musculoskeletal structure may be easily scaled from adults. However, other factors such as differences in limb proportion and coordination may also affect pediatric strength profiles. Using computational musculoskeletal modeling, this study evaluates whether anthropometric scaling of a generic adult upper limb model to represent the pediatric upper limb is able to accurately capture shoulder strength of a pediatric individual.

Methods

An existing upper limb computational musculoskeletal model representing an adult male [6] was scaled to represent the pediatric limb using OpenSim (v3.3) [7] and Matlab. First, we determined scaling rules based on reported limb length and shoulder muscle volumes in children. We performed linear regression for males and females for forearm lengths vs. heights of 366 children and adolescents from Neu *et al* [1] (**Fig. 1a**). All model length dimensions were thus scaled for a child of a given height using a *length scale factor,* defined as the ratio of estimated forearm length to adult model forearm length. We also performed linear regression for males and females identified as normal weight from *Im et al* [5] for body weight vs. total shoulder muscle volume (**Fig. 1b**). Individual muscle volumes were defined to have the same relative proportion of volume as in the adult model. *Max isometric force* (MIF) for each shoulder muscle actuator in the scaled model was calculated using:

$$F^{M}_{0,muscle} = \frac{v_{muscle} \bullet \sigma}{l^{M}_{0}} \qquad (1)$$

where v_{muscle} is the individual muscle volume, σ is a constant specific tension, and l^{M}_{0} is optimal fiber length, obtained from the model post length scaling. A *MIF scale factor* was determined by taking the average ratio of calculated force and corresponding peak isometric force from the nominal adult model for each individual muscle. To evaluate performance of the scaling rules, individual pediatric models for 6 children (7-18yrs, 3M/3F) were developed based on their height, weight, and sex reported by Im *et al* [5]. The models were used to calculate predicted isometric shoulder moment in flexion/extension, internal/external rotation, and ad/abduction assuming full excitation of the relevant functional group of muscles. Predicted moments were compared to measured maximum voluntary joint moments for the same children [5].

Results and Discussion

Predicted moments from scaled models were significantly correlated to measured moments ($p<0.04$, $r^2 > 0.7$) (**Fig. 1e**). The predicted moments tended to underestimate measured values, with shoulder external rotation being most accurate (slope: 0.7332) and shoulder adduction being most underestimated (slope: 0.4623).

Limitations include the small sample size available in literature upon which regressions were based. Forearm length was not reported for the 6 participants, so estimated length could not be verified. Other potential factors may affect musculoskeletal function in children such as differences in limb proportion and coordination and may account for discrepancies in predicted moment; additional data describing these factors is needed and should be considered in the future.

Significance

This work provides an initial basis by which pediatric upper limb models can be generated by scaling an adult model using a child's height and weight, predicting moments highly correlated with their measured moment-generating capacity.

References

[1] Neu et al. (2002). *Am J Physiol Endocrinol Metab.* **283**: E103-E107.
[2] Kamper et al. (2016). *Braz J Phys Ther.* **20**(3): 275-284.
[3] Patel et al. (2017). *Translational Pediatrics*. **6**(3): 160-166.
[4] Delgado et al. (2016). *Radiographics*. **36**(6): 1672-1687.
[5] Im et al. (2014). *J. Biomech.***47**: 2730-2737.
[6] Saul et al. (2015). *Comput Methods Biomech Biomed Engin.* ***18*** : 1445-1458.
[7] Delp, S.L. et al. (2007). *IEEE Trans Biomed Eng*. **55**: 1940-1950.

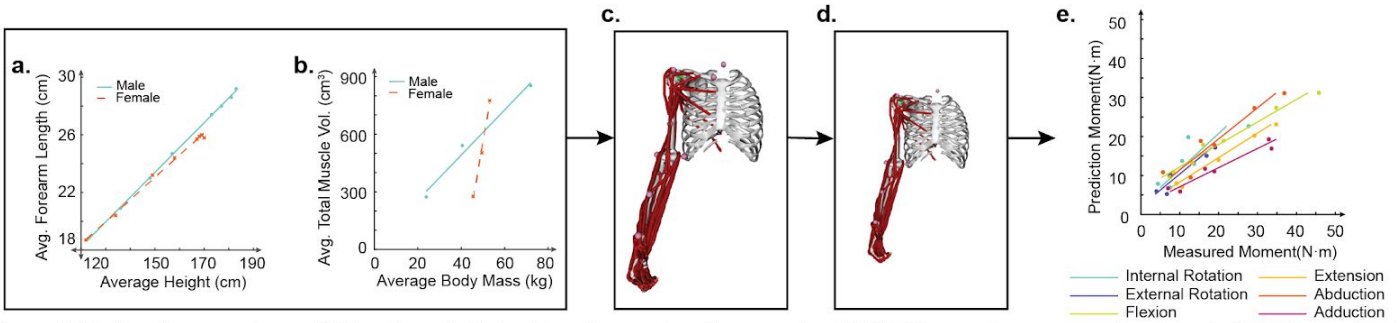

Figure 1. Scaling framework uses (a) length scale factor from forearm length regression (b) MIF from volume regression to scale the (c) generic adult model into a (d) pediatric model. We used the scaled models to compare (e) predicted shoulder moments to measured shoulder moments.

ALTERATIONS IN KNEE QUASI-STIFFNESS DURING EARLY AND MIDSTANCE AFTER ACL RECONSTRUCTION

Steven A. Garcia, Alexa K. Johnson, Scott R. Brown, Edward P. Washabaugh, Chandramouli Krishnan, Riann M. Palmieri-Smith
[1]School of Kinesiology, University of Michigan-Ann Arbor,
email: stevenag@umich.edu

Introduction

Gait alterations are ubiquitous following anterior cruciate ligament (ACL) reconstruction and do not resolve with standard-of-care rehabilitation [1, 2]. For instance, many studies have reported truncated sagittal plane knee excursions and reduced sagittal plane moments during early stance in the surgical limb which many consider reflective of "stiff-knee" gait [2-4]. Unfortunately, most studies have focused on gait alterations in early phases of stance and thus, less data is available detailing abnormal mechanics (i.e., stiff-knee gait patterns) in mid/late stance phases. Stiffened knee mechanics are common in osteoarthritic (OA) gait [5] and may impair one's ability to attenuate shock leading to elevated loads about the articular tissues. Knee quasi-stiffness can be measured dynamically by evaluating the concurrent interaction between knee flexion excursions and the change in joint moment[5]. Given the associations between higher sagittal plane knee quasi-stiffness and patellofemoral OA progression [6], characterizing alterations in knee quasi-stiffness after ACL-reconstruction may provide insight into targets for gait intervention strategies. Therefore, we aimed to evaluate sagittal plane knee quasi-stiffness in the involved and uninvolved limbs in individuals with ACL-reconstruction during early stance and midstance.

Methods

Twenty-six individuals with ACL-reconstruction (Age: 20.2±5.1 yrs., Body mass index: 23.9±3.3, Time post-op: 7.2±0.9 mo., self-selected speed: 1.4±0.2 m/s) were recruited as part of a larger clinical study. Gait biomechanics were assessed overground at a self-selected pace using a Vicon Motion Capture system (120 Hz) and two AMTI force platforms (2400 Hz). Raw marker position and force data were imported into Visual 3D and filtered using a low-pass fourth order Butterworth filter at 12 Hz. Angles were calculated relative to static standing posture. Standard inverse dynamics procedures were used, and moments were resolved in the proximal segment and reported internal. Knee quasi-stiffness (Nm/°) was calculated as the slope of the regression line between early stance (Figure 1: blue dots) and midstance (Figure 1: maize dots) data points obtained by plotting the sagittal plane knee angle versus knee moment curve. Early stance knee quasi-stiffness was calculated between peak internal flexion moment to the peak internal knee extensor moment (KEM). Midstance knee quasi-stiffness was calculated between the peak KEM and the minimum midstance knee moment (Figure 1).

For descriptive comparisons, peak knee flexion excursion during loading response, knee extension excursion during midstance, and the peak KEM and midstance knee moment were also calculated. The average of seven trials was used for further analysis. All gait outcomes were compared using paired t-tests with a Bonferroni correction to adjust for multiple comparisons (corrected α =0.008).

Results and Discussion

We found greater knee quasi-stiffness in the involved relative to uninvolved limb in both early- (7.3 Nm/° vs. 6.1 Nm/°) and midstance (7.3 Nm/° vs. 5.7 Nm/°) (p <0.01). The involved limb exhibited lesser knee flexion excursion (13.1° vs. 17.5°) and extension excursions (9.4° vs. 13.6°) but greater midstance knee moments (7.3 Nm vs. -6.3 Nm) relative to the uninvolved limb (p<0.01). Peak KEM was not different between limbs (p>0.05).

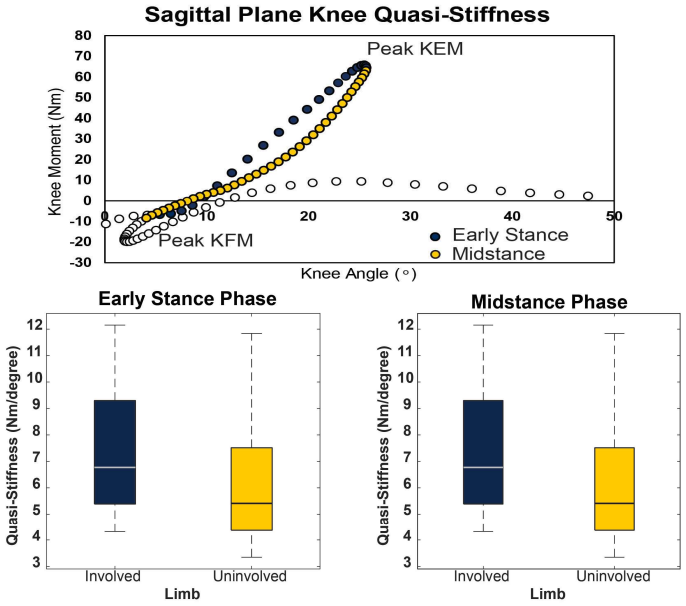

Figure 1: Representative angle-moment plot for knee quasi-stiffness measures. Boxplots show stiffness comparisons for early/midstance.

Our results suggest individuals with ACL reconstruction walk with greater knee quasi-stiffness in the involved limb. Greater knee quasi-stiffness during early stance has been similarly shown in OA gait [6] and reduced knee extension excursion have been reported after ACL-reconstruction [4]. Importantly, increased knee stiffness was observed despite the involved limb reaching similar peak KEM. Thus, the reduced knee excursions in both early- and mid-stance may be driving the increased knee quasi-stiffness in the involved limb. Greater knee quasi-stiffness has been shown to predict patellofemoral OA progression [6] and the reduced knee excursions observed in our cohort may reflect loading applied about a smaller region of cartilage relative to the contralateral limb. Future research should evaluate the link between knee quasi-stiffness in early/midstance and cartilage health after ACL reconstruction.

Significance

Individuals with ACL-reconstruction walk with a stiffer knee in both early and midstance. Evaluating gait through the entirety of stance may be beneficial as kinematic and loading alterations across stance may influence joint health outcomes.

References

1. Davis-Wilson, H.C., et al., Med Sci Sports Exerc, 2019.
2. Kaur, M., et al., Sports Med, 2016.
3. Roewer, B.D., et al., Biomech, 2011.
4. Capin, J.J., et al.,. Clin Orthop Relat Res, 2017.
5. Dixon, S.J., et al., Arthritis Care Res (Hoboken), 2010.
6. Chang, A.H., et al., Osteoarthritis Cartilage, 2017.

Machine Learning Optimization Tool for Classification of Human Movement Data

Mojtaba Mohasel[1] Corey Pew[1]
[1]Department of Mechanical and Industrial Engineering, Montana State University, Bozeman, MT
Email:*Corey.Pew@montana.edu

Introduction

Classification and prediction of human movement has become an important research topic in the field of biomechanics and health.[1] Quantitative interpretation of an individual's motions in real-time is necessary for the control of robotic prosthetics, orthotics, and exoskeletons and is useful for clinical identification of abnormal gait or adverse events such as falling.[2,3] Body-worn sensors are often used to collect data used to classify human movement, however, the interpretation of data varies considerably among researchers.

Two main hurdles exist when processing sensor data: 1) feature selection and 2) machine learning algorithm selection. First, when processing sensor information, features of the data (such as mean, max, standard deviation, etc.) are analyzed. In addition, these features are often analyzed over time using sliding windows, where the size and overlap of the windows can affect feature usefulness.[4] Second, the processed data is analyzed with machine learning techniques to relate data patterns to varying activity classifications. With a multitude of combinations between feature selection and machine learning methods the same data set can be analyzed in different ways with varying results.[2,4] Finally, machine learning analysis of body worn sensor data lacks standardization in the biomechanics field. This makes it difficult to evaluate and replicate results from other researchers, ensure that proper techniques are being used, and share data sets between labs.

The objective of this project was to create a stand-alone software application to provide a standardized framework to automate processing and optimization of data from body worn sensors to accurately classify human movement.

Methods

The stand-alone application has been initially implemented in MATLAB. The user provides the application a raw dataset by inputting a table with labeled predictor and response variables. Default values for window size and overlap are suggested, or the user has the option to initially indicate minimum and maximum time ranges and overlap. The user then indicates which machine learning algorithms they would like to consider for the analysis. The software begins with a feature extraction module to extract ten features from each predictor variable (mean absolute value, mean absolute value slope, slope sign change, wavelength, variance, min, max, skewness, kurtosis and inter quartile range) which have been shown to important for analyzing biomechanics data.[5] The features are calculated over time using sliding windows where the size and overlap of the windows can affect the feature usefulness. A genetic algorithm is utilized to iteratively determine optimal values for window size and overlap.[6] During the iterations it also evaluates which features positively impact classifier accuracy and suggests feature sets that are most useful. Machine learning algorithm accuracy is calculated at each iteration using five-fold cross validation. The optimization terminates searching if no improvement in algorithm accuracy is found after five subsequent iterations.

Initial evaluation of the application utilized pre-existing data used to classify turning in lower limb amputees.[2] In the previous study, we looked at data from five amputee subjects and classified whether they were turning or walking straight using data from a single inertial measurement unit. The initial testing compared the efficacy of using support vector machine (SVM), K-nearest neighbor (KNN), and decision tree ensemble (Ensemble) algorithms on algorithm accuracy for each participant individually and all participant data pooled together.

Table1: Comparison of classification accuracy results. Original is previous data, New is optimized outcome.

subject	SVM		KNN		Ensemble	
	Original	New	Original	New	Original	New
A01	96.2	99.0	96.5	99.2	96.2	99.7
A02	95.2	98.3	94.9	99.4	94.8	99.7
A03	90.7	94.9	90.4	99.3	90.3	99.1
A04	92.7	98.3	92.6	99.4	92.1	99.2
A05	93.0	97.4	94.4	99.0	93.8	99.4
Pooled	90.5	93.8	91.2	98.0	90.5	99.2

Results and Discussion

Results from the previous study compared to the new analysis are shown in **Table 1**. We found that the new application was able to attain higher classification accuracies than our original analysis. Both KNN and Ensemble could consistently achieve high level accuracy (near 99%) not only for individuals but also for pooled data. It was also found that the specific set of features needed for highest accuracy differed by individual as well as by algorithm. The SVM algorithm often required fewer features as compared to KNN and Ensemble. Furthermore, window length and overlap varied between the individual participants. This indicates that individuals may benefit from customized algorithms. Lastly, the in the original study, iterative adjustments to improve accuracy were competed manually, requiring weeks of work. Our new method ran in approximately two hours for each algorithm type and participant combination. These results indicate that higher classification accuracies are attainable in far less time using this automated method as compared to manual analysis.

Significance

This work further highlights that reported classification outcomes using machine learning to predict human motion from body worn sensors are highly variable depending on the method of analysis. Each user is unique and generalized control may not provide adequate results as compared to user specific control. This initial application establishes a framework for machine learning optimization and future work will expand the application's functionality and user interaction.

References

1) Yang et al., Sensors, 2010, 10(8), 7772-88; 2) Pew, et al., IEEE Trans. Bio. Eng., 2017, 65(4), 789-96; 3) Porciuncula, et al., Phys. Med. Rehab., 2018, 10(9), S220-32; 4) Shell, et al., PloS One, 2018, 13(2), 1-17; 5) Miller, et al.,IEEE Trans. Bio. Eng., 2013, 2745-2750; 6) Goldberg, Addison-Wesley, 1989.

TRUNK AND LOWER EXTREMITY RUNNING KINEMATICS AND KINETICS IN PREGNANT FEMALES DIFFER FROM FEMALES WHO HAVE NEVER BEEN PREGNANT

Jennifer J. Bagwell[1], N. Reynolds[2], M. Walaszek[3], H. Runez[4], K. Lam[5], J.A. Smith[6], D. Katsavelis[7]

[1] Department of Physical Therapy, California State University Long Beach, 1250 Bellflower Blvd, Long Beach, CA 90840, USA
Email: *jenny.bagwell@csulb.edu

Introduction

Half of pregnant and postpartum females report low back or pelvic pain [1]. While physical activity during pregnancy is important to the health of the mother and baby, pain during pregnancy may interfere with achieving the recommended amount of activity. Additionally, pain during pregnancy is associated with reduced quality of life [2]. Understanding changes in joint demand during pregnancy is an important step toward identifying potentially modifiable factors contributing to pain to inform development of interventions or prevention strategies. While biomechanical gait changes during pregnancy have been studied [3-5], there is a lack of evidence regarding more demanding tasks such as running. Therefore, the purpose of this study was to compare joint kinematics and kinetics during running between pregnant females and matched control females.

Methods

Fourteen pregnant and 14 matched females (age within 3 years and body mass index within 2 kg/m2 of pre-pregnancy body mass index) without history of pregnancy participated. Pregnant participants completed testing second trimester (2T) and the same participants were tested third trimester (3T). Matched control participants were tested on one occasion. Participants completed seven successful self-selected pace running trials. Kinematics and ground reaction force data were calculated using an 8-camera motion capture system and force plates. Data from seven stance phases of running were averaged to calculate peak trunk versus laboratory, pelvis, and lower extremity kinematics, lower extremity moments, work normalized to pre-pregnancy body mass, and work distribution across hip, knee, and ankle. Independent t-tests were used to compare running velocity at both time points and kinematic and kinetic variables of interest were corrected for running velocity and compared between groups using linear regression.

Results and Discussion

Running velocity during 2T did not significantly differ from non-pregnant females (2.81 ± 0.36 vs. 3.04 ± 0.37 m/s; p=0.107), however, running velocity was slower 3T (2.59 ± 0.39 vs. 3.04 ± 0.37 m/s; p=0.004). After controlling for running velocity, trunk contralateral rotation was smaller 2T and 3T compared to controls (2T 11.1 ± 4.0º, 3T 9.8 ± 2.6º, Control 14.9 ± 4.1º, p=0.032 and p=0.003, respectively). During 2T, pregnant females as compared to controls demonstrated greater percent contribution of the ankle to negative work (p=0.031) and smaller percent contribution of the hip to negative and total work (p=0.012 and p=0.034; **Figure 1**). No other variables or time points assessed differed significantly between groups after controlling for running velocity.

During 2T and 3T, pregnant females exhibited reduced trunk rotation away during the stance leg. During 2T increased utilization of the ankle and decreased utilization of the hip was demonstrated by the greater percent negative ankle work and smaller percent negative and total work at the hip.

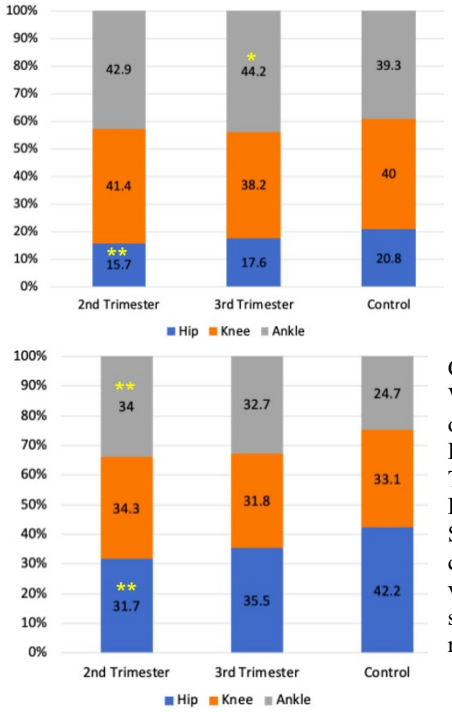

Figure 1: **Top:** Percent Contribution to Negative Work During Stance Phase of Running. **Bottom:** Percent Contribution to Total Work During Stance Phase of Running. * Significant prior to controlling for running velocity. ** Remained significant controlled for running velocity.

Significance

Current findings of smaller trunk rotation during running are consistent with altered trunk rotation in pregnant females during gait [5] and with previously reported postpartum running kinematics [6]. It is possible that lesser trunk rotation could contribute to load distribution over a smaller area of the spine and pelvis, however, attenuated trunk motion could also reflect a stabilization strategy. The greater relative ankle contribution and smaller hip contribution to work is consistent with previously reported pregnancy gait kinetics [3]. Because the hip is a low back and pelvic girdle stabilizer, decreased hip utilization during dynamic activity could contribute to lumbopelvic pain. Further research should examine how kinetic and kinematic changes relate to orthopedic conditions during pregnancy and if increasing hip strength or utilization may benefit this population.

Acknowledgments

This work was supported by the American Physical Therapy Association Orthopaedic Section grant and the Creighton University Health Sciences Strategic Investment Fund Faculty Development Grant. We acknowledge the support of Esther Baek, Chelsea Bendebel, Shawna Berk, Kiana Cupples, Jonathan Hong, and Rachel O'Hara for assistance with data analysis.

References

1. Wu, et al. *Eur Spine J*. 2004.
2. Olsson, et al. *Acta Obstet Gynecol Scand*, 2004.
3. Bagwell, et al. *Gait Posture*, 2020.
4. Foti, et al. *J Bone Joint Surg Am*, 2000.
5. Eldeeb, et al. *Acta Bioeng Biomech*, 2016.
6. Provenzano, et al. *J Womens Health Phys Ther*, 2019.

CAN FOOT'S MECHANICAL ENERGY DURING WALKING BE DISSIPATED AS HEAT?

Nikolaos Papachatzis[1], Dustin R. Slivka[2], Iraklis I. Pipinos[3], & Kota Z. Takahashi[1]
[1]Department of Biomechanics, University of Nebraska at Omaha, Omaha, NE, USA
[2]School of Health and Kinesiology, University of Nebraska at Omaha, Omaha, NE, USA
[3]Department of Surgery, University of Nebraska Medical Center, Omaha, NE, USA
email: npapachatzis@unomaha.edu.

Introduction

During human walking, the leading limb collides with the ground and performs negative work [1]. It is now well established that a large portion of this collision work is performed by the foot, particularly the heel[2,3]. Energy absorption (or dissipation) maybe be beneficial as a protective mechanism to minimize trauma or injuries[4]. However, it is currently unclear where the foot's energy goes or how the body absorbs or dissipates this energy. One possibility is that the heels' energy is dissipated as heat. The thermodynamics laws state that the dissipated energy may increase the heels' thermal energy (i.e., increase temperature), potentially explaining the increases in heel temperature during walking[5]. Currently, it is unclear whether the heel's mechanical energy can induce thermodynamic responses. Understanding the relationship between biomechanics and temperature regulation may be valuable for improving diagnoses for foot complications, such as the formation of diabetic foot ulcers that are thought to arise due to impaired ability to dissipate heat[6]. Here, we used walking with added mass to increase the heel's negative work[3] and investigated its effect on thermodynamic responses. We hypothesized that the heel's temperature would increase when walking with added mass. We also hypothesized that the increase in temperature is related to increased energy absorbed (i.e., negative work) and energy dissipated (i.e., net negative work) by the heel.

Methods

A total of 20 healthy young adults (5 females, 15 males; age: 24.4±2.8 yrs; height: 1.74.61±0.07 m; mass: 83.6±21.2 kg; means± s.d.) walked over-ground on force plates and for 10 minutes on a treadmill (both at 1.25 m/s). Participants carried (via weight vest) three different levels of symmetrical loads: 0%; no added body mass, 15%, and 30% of their body mass. The over-ground walking conditions were used to collect foot mechanics data (kinematic & kinetic), whereas the treadmill conditions were used to measure the foot temperature data. We quantified the mechanical power and work done by the foot using a unified-deformable analysis[7]. To isolate the heel contribution, we computed the work when the center-of-pressure was underneath the heel segment during the early stance phase[3,8]. An estimate of the total work over the 10 minutes of treadmill walking was calculated by multiplying the average work per step measured in over-ground trials by the number of steps taken in 10 minutes of treadmill walking. Temperature measurements were taken immediately before and after each treadmill condition at the bottom of the right foot, including the heel pad. We computed the change in temperature of the heel before and after each walking condition. A one-factor repeated-measures ANOVA was used to determine the effect of the added mass on the dependent variables. When a significant main effect was found, a Bonferroni post hoc analysis was conducted for pair-wise comparisons. We used a linear mixed models test to examine the relationship between foot temperature changes (before and after walking) and foot energy dissipation. The significance level was set to $\alpha = 0.05$ for all the statistical tests.

Results and Discussion

Our hypotheses were not supported as there was no significant increase in heel temperature between added mass walking conditions (p=0.138, Figure 1), despite a significant increase in the magnitude of heel's negative and net work (p=0.002 & p=0.003; respectively, Figure 1). Neither the negative nor the heel's net work was associated with increased heel temperature (p=0.535 & p=0.661, respectively).

It is possible that the heel's mechanical work was dissipated as sound and not heat – although a direct measure of sound is needed to verify this conclusion. Additionally, we are currently investigating alternative hypotheses to determine whether other factors could explain increases in foot temperature, such as shear force and increased blood flow.

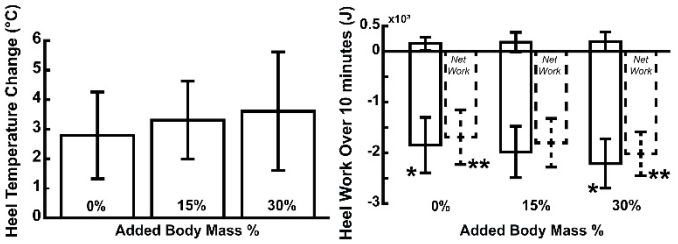

Figure 1: **(Left side)** The heel's temperature increased after 10min. of walking, but there was no significant effect of added mass on change in temperature (p=0.138). **(Right side)** The added mass significantly increased the magnitude of the heel's negative (p=0.002) and net (p=0.003) work over 10 minutes of treadmill walking, but not the positive work (p=0.265). The asterisks indicate significance (*: negative work; **: net work) (N=20).

Significance

Energy dissipation in the foot may lead to temperatures which damage soft tissue in individuals with diabetes. If we want to help these patients, we must first learn how healthy feet regulate temperature daily. Our comparison of mechanical energy loss at the foot in healthy subjects has found no strong relationship between foot-work and plantar temperature changes. Our results are likely related to agile temperature control by the healthy function of the vascular system (e.g., blood flow & tissue oxygenation) of the normal leg and the excellent control of the shear forces by the plantar structures of the foot. In different diseases, the ability of the vascular and musculoskeletal systems to control the temperature in the foot is significantly decreased, therefore producing a closer association between negative work and heat dissipation. Future studies are needed to uncover further the mechanisms of temperature responses, which may lead to novel insights for understanding the causes of foot complications such as diabetic ulcers[6].

References

1. Kuo AD., et al. *Exercise and sport sciences reviews,* **33**(2), 88-97, 2005.
2. Honert EC & Zelik KE. *Human movement science*,**64**, 191-202, 2019
3. Papachatzis N, et al. *Journal of Experimental Biology*, **223**, 12, 2020.
4. Wearing S., et al. *Medicine and science in sports and exercise*, (**46**),8, 1588-1594, 2014.
5. Reddy PN., et al. *Gait & posture*, **52**, 272-279, 2017
6. Armstrong DG., et al. *The American journal of medicine*, **120**(12), 1042-1046, 2007
7. Takahashi KZ., et al. *Journal of biomechanics*, **45**(15), 2662-2667, 2012
8. Bruening DA & Takahashi KZ., *Gait & posture*, **62**, 111-116, 2018

SARCOMERE STRAIN RATHER THAN WHOLE MUSCLE STRAIN PREDICTS PASSIVE MUSCLE TENSION

Lomas S. Persad[1], Benjamin I. Binder-Markey[3], Alexander Y. Shin[1], Kenton R. Kaufman[1], and Richard L. Lieber[2]
[1]Department of Orthopedic Surgery, Mayo Clinic, Rochester, MN
[2]Shirley Ryan AbilityLab, Chicago, IL
[3]Drexel University, Philadelphia, PA
Email: rlieber@sralab.org

Introduction

Passive tension in muscle develops exponentially when it is stretched beyond its resting length. This provides a resistive force that is necessary for joint stability and defines muscle physiological operating range. Significant alterations in this property can result in increased resistance to movement, impairing function. Therefore, it is important to understand and define the passive mechanical property of muscle to fully describe its function.

The passive elastic property of human skeletal muscle is attributed to both the intracellular protein titin and the parallel complex connective tissues that make up the extracellular matrix (ECM). To quantify the relative contribution of intra- and extracellular structures to passive tension, muscles are mechanically tested at different scales—single fibers (where titin is the dominant load bearing structure) or bundle of fibers and whole muscle (where the ECM is the major load bearing structure) [1, 2]. Analogous to this relationship between passive load bearing structure and scale, strain, which is used to predict passive tension, can be quantified at the whole muscle or sarcomere scale. Therefore, the aim of this study was to determine whether strain measured at the whole muscle or sarcomere scale is better at predicting gracilis passive tension.

Methods

In situ gracilis muscle-tendon unit (MTU) length (measured intraoperatively), sarcomere length (measured from clamped biopsies) and passive tension (measured with a buckle transducer) were measured from nine patients undergoing a gracilis muscle transfer surgery. All measurements were measured at four joint configurations (JC) designed to gradually lengthen the gracilis muscle. MTU length was measured by holding one end of a suture proximally at the muscle's origin then threading the suture parallel to the MTU and marking the MTU insertion location on the suture using surgical clips. Muscle tissue samples were clamped and excised at three of the four JC that corresponded to a knee flexion angle of 130°, 90° and 0°, a hip abduction of 45°, 45° and 60° with hip flexion fixed at 60°. Samples were fixed in 10% buffered Formalin within the clamp to allow sarcomere length determination at each JC via laser diffraction. *In vivo* passive tension was measured using a buckle force transducer (BFT) placed on the distal gracilis external tendon. The BFT signal was recorded using a custom LabVIEW program with a sampling frequency of 1 kHz. After the MTU was harvested, it was weighed then spread along a sterile surgical towel adjacent to a ruler and photographed. Muscle slack length was measured from this image when the muscle was at true slack length with zero passive tension. Muscle length at each JC was calculated by subtracting external tendon length from the measured MTU length. A natural exponential curve, traditional for muscle passive tension [3], was fitted to the data for comparison.

Results and Discussion

The exponential model fit the observed normalized force-sarcomere strain data (r^2=0.69; Fig. 1B) better than the normalized force-muscle strain data (r^2=0.37; Fig. 1A). These results demonstrate that, for the human gracilis muscle, muscle strain was a poor indicator of the passive tension in the MTU even though muscle strain was measured with respect to true slack length.

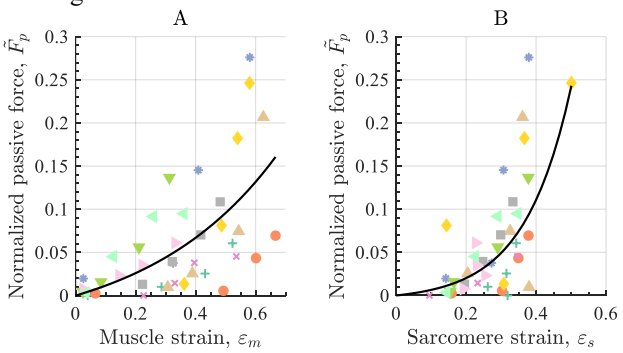

Figure 1: Gracilis passive force-strain data and natural exponential function [3] fit. (A) Normalized passive force *versus* muscle strain (r^2=0.37). Muscle strain was calculated relative to the resting length of the muscle measured from the slack, harvested MTU. Passive force was normalized to muscle physiological cross-sectional area x 22.5 N-cm^{-2}. (B) Normalized passive force-sarcomere strain data (r^2=0.69). Sarcomere strain was calculated relative to an optimal length of 2.7 μm. Individual subject data are shown by each symbol and color pair.

These data demonstrate that passive mechanical properties of the human gracilis are closely defined by sarcomere length as the important reference for tissue strain. This suggests that it is important to measure (or know) sarcomere length in future studies. In contrast, relying only on whole muscle data, even at a very precise level using direct measurements, resulted in a poor passive force-length model which failed to accurately predict gracilis passive tension. Also, generic passive force-length models are non-dimensional and are scaled by optimal fiber length which is a function of optimal sarcomere length. These models describe passive tension as a function of optimal fiber strain. For the first time, we quantified this passive force-length relationship for the human gracilis using whole muscle and sarcomere length.

Significance

These results show that the main determinant of passive tension in the gracilis MTU is sarcomere strain rather than whole muscle strain.

Acknowledgments

Supported by VA grants I01 RX002462 and IK6 RX003351.

References

[1] Meyer, G.A. and R.L. Lieber, (2011). *J. Biomech.*, **44**: p. 771-773.
[2] Ward, S.R., et al., (2020). *Front. Physiol.*, **11**: p. 1-9.
[3] Magid, A. and D.J. Law, (1985). *Science.*, **230**: p. 1280-1282.

CHANGES IN STEPPING BIOMECHANICS AFTER 6-WEEK PERTURBATION-INDUCED WEIGHT TRANSFER TRAINING POST-STROKE

Keng-Hung Shen[1], James Borrelli[2], Vicki Gray[2], Kelly P. Westlake[2], Mark W. Rogers[2], Hao-Yuan Hsiao[1]
[1]*Department of Kinesiology and Health Education, University of Texas at Austin, Austin, TX, USA*
[2] *Department of Physical Therapy and Rehabilitation Science, University of Maryland Baltimore, Baltimore, MD, USA*
Email : kenghung.shen@utexas.edu

Introduction

Stroke is a leading cause of disability worldwide[1]. Decreased speed and amplitude of body weight transfer towards the paretic leg during voluntary movement is commonly observed in individuals post-stroke. Abnormalities in weight transfer may deteriorate weight bearing symmetry between legs and affect postural stability[2] and forward progression[3]. Thus, improving weight transfer ability is an important goal.

Emerging evidence showed promising improvements in balance control in people with Parkinson's disease and chronic stroke following standing-perturbation-based training[5,6]. Because timely and sufficient lower limb loading ability is required for functional weight transfer, we developed a perturbation-induced lateral weight transfer training program that targets paretic limb loading ability. The primary purpose of this study was to determine the changes in functional stepping outcomes and biomechanical characteristics during voluntary stepping after 6 weeks of perturbation-induced weight transfer training. We hypothesized that reduced weight transfer time and increased Step Test score will be observed following training. In addition, peak paretic stance limb loading and knee extension torque will be increased from pre- to post-training.

Methods

Eight individuals with chronic stroke completed the training program to date. The training program consisted of 3 sessions per week for 6 weeks. Each session included 50 unilateral support surface lowering perturbations *(Fig.1a)* delivered to the paretic limb. Step Test and Choice Reaction Stepping assessment were performed before and after training. Step Test examined the participants' ability to place their foot on and off a 7.5-cm-high step as many times as possible within 15 seconds. During the Choice Reaction Stepping assessment, participants were instructed to react as soon as possible to the light cue indicating the instant and limb used to take a forward step. Five steps with each leg were performed with randomized time and limb selection. Kinetic and kinematic data were collected during stepping assessment via a 10-camera motion analysis system (Vicon, UK) and a force platform beneath each foot (AMTI, US). Vertical ground reaction forces (vGRF) were normalized to each participant's body weight. Following the light cue, weight transfer time was defined from the instant of minimum vGRF beneath the stance limb to the instant when vGRF beneath stance limb exceeded step limb[3] *(Fig.1b)*. Knee extension torque was calculated at the instant of maximum vGRF beneath the stance limb. Data with the non-paretic limb stepping were analysed and averaged across trials. Two-tailed paired t-tests were used to compare pre and post training data.

Results and Discussion

Preliminary results for 6 individuals post-stroke were analyzed to date (63±7.9yrs, 3 females, time since stroke 12.5±8.5yrs). We observed a trend of 1.6% increment in paretic stance limb peak vGRF, 13.4% reduction in weight transfer time, and 18.9% increment in knee extension torque post-training (*Fig. 2*). Improved paretic limb loading and knee joint support function may contribute to more efficient stepping as demonstrated by a ST score that improved by 18.1% following training (*Fig. 2*). These preliminary results expanded from previous perturbation studies and showed that the perturbation-based training that targets paretic limb loading can enhance voluntary weight transfer toward the paretic limb in individuals post-stroke.

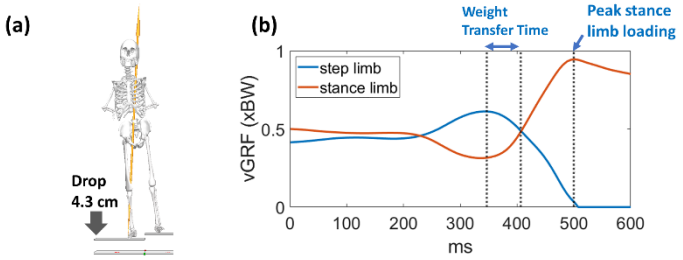

Figure 1: (a) The schematic diagram of the perturbation-induced weight transfer training. (b) A representative trial of step initiation process

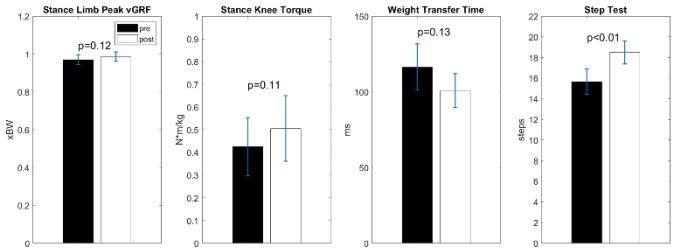

Figure 2: Comparisons of weight transfer measurements pre- and post-training.

Significance

Perturbation-induced paretic limb loading training appeared to be effective to restore weight transfer ability after stroke. Based on our preliminary results, we anticipate that these trends will achieve statistical significance with ten more subjects. Future work will determine the efficacy of this training by comparing the outcomes against conventional therapy. Upon completion, the study will advance current knowledge of perturbation-based rehabilitation program in the chronic stroke population, and positive outcomes will endorse the development of a portable training system in the future.

Acknowledgments

[1] NIH 1R21AG060034-01to VLG, KPW, and MWR
[2] Texas New Scholar Recruitment Fellowship to K-H S

References

[1] Campbelt al., (2019 *Nat Rev Dis Primers* **5(1):**70
[2] de Haart et al. (2005) *Arch Phys Med Rehabil* **86(4):**755-62
[3] Hsiao et al. (2017) *J Biomech* **60:**72-78
[4] Sheikh et al. (2016) *Clin Rehabil* **30(11):**1088-1096
[5] Mansfield et al. (2015) *Phys Ther* **95(5):**700-9
[6] Mansfield et al. (2017) *J Stroke Cerebrovasc Dis* **26(10)**:2174-80

IMMEDIATE EFFECTS OF GAIT METRICS FROM A 15-MINUTE POSTURAL INTERVENTION

Nathan D. Schilaty[1], Nathaniel A. Bates[1], Luca Rigamonti[1], Takashi Nagai[1]
[1] Mayo Clinic, Department of Orthopedic Surgery
Email: schilaty.nathan@mayo.edu

Introduction

Posture is one of the foundations of human movement and plays an integral part of human neuromuscular physiology, psychology, and overall health.[1,2] With increased screen-time usage, posture can be negatively affected[3] and lead to decreased sensorimotor function. The objective of this study was to evaluate the *immediate effects* of a 15-min postural intervention on the general population, specifically gait characteristics as the common mode of locomotion. It was hypothesized that the 15-min postural intervention would demonstrate immediate and positive effects on various gait metrics.

Methods

To evaluate the immediate effects of the 15-min postural intervention, 40 subjects were recruited [Age: 33.4 (12.5) yrs; Sex: 15M:25F]. Three *APDM Opal* inertial motion unit sensors (IMUs) were placed on the lumbar spine and dorsum of each foot, respectively. Subjects were requested to walk a 4-meter distance at their usual walking pace, turn around, and return to the start.

The IMUs exported discrete values of anticipatory postural adjustment (APA), cadence, gait cycle duration, gait speed, foot elevation at mid-swing, lateral step variability, leg circumduction, foot strike angle, toe-off angle, stance asymmetry, stride length, step duration, and range of motion (ROM) in all three planes. These metrics were assessed with either Student's t-test or Wilcoxon Rank Sum to determine differences between pre- and post-intervention differences. Significance was set at $\alpha < 0.05$.

Results and Discussion

For gait metrics of cadence, gait cycle duration, gait speed, leg circumduction, toe-off angle, stance asymmetry, stride length, step duration, and range of motion in all three planes, there were no significant differences between the pre- and post-intervention measurements (**Table 1**).

For anticipatory postural adjustment (ROM), there was an increase in ROM of 1.7° (p=0.053) and a decreased amount of variation from pre-intervention. Elevation at mid-swing was increased (0.20 cm) for the left limb (p=0.002) with no change for the right limb. Lateral step variability increased (0.54 cm) for the right limb (p=0.031) with no change for the left limb. Lastly, foot strike angle increased (1.1°) for the left foot (p=0.026) with no change for the right foot.

These results demonstrate that a 15-min postural intervention can have a short-term effect on gait mechanics, likely due to the improved function and adaptability of the musculature with light stretching and body awareness. The results were typically more localized to the left side which is likely the non-dominant side of the participants.[4] Even though some metrics did not demonstrate statistical significance, there were directional improvements in many metrics that could reach significance provided either more intervention time or population sample size. This project will continue with evaluation of long-term effects of a postural intervention on a larger and more diverse population to improve generalizability.

Table 1: Summary of Gait Metrics Pre- and Post-Intervention. Values in **bold** are significant.

Gait Metric	Pre	Post	*p*-value
APA duration (s)	0.43	0.44	0.512
APA first step duration (s)	0.48	0.46	*0.053*
APA first step ROM (°)	23.0	24.7	0.258
Forward APA peak (m/s^2)	0.51	0.55	0.439
Lateral APA peak (m/s^2)	0.48	0.49	0.917
L Cadence (steps/min)	115.4	116.1	0.580
R Cadence (steps/min)	115.1	116.0	0.520
L Gait cycle duration (s)	1.05	1.04	0.684
R Gait cycle duration (s)	1.05	1.04	0.583
L Gait speed (m/s)	1.18	1.19	0.625
R Gait speed (m/s)	1.16	1.17	0.516
L Mid-swing foot elevation (cm)	0.55	0.75	**0.002**
R Mid-swing foot elevation (cm)	0.61	0.65	0.510
L Lateral step variability (cm)	3.49	3.68	0.372
R Lateral step variability (cm)	3.45	3.97	**0.031**
L Leg circumduction (°)	2.52	2.44	0.661
R Leg circumduction (°)	2.68	2.49	0.219
L Foot strike angle (°)	18.3	19.4	**0.026**
R Foot strike angle (°)	18.5	17.9	0.247
L Toe-off angle (°)	37.5	38.1	0.354
R Toe-off angle (°)	38.0	38.2	0.657
Stance Asymmetry (% diff)	-0.15	-0.06	0.736
L Stride length (m)	1.22	1.22	0.773
R Stride length (m)	1.20	1.21	0.750
L Step duration (s)	0.52	0.52	0.757
R Step duration (s)	0.52	0.52	0.477
Coronal Lumbar ROM (°)	7.82	7.37	0.112
Sagittal Lumbar ROM (°)	5.73	5.59	0.587
Transverse Lumbar ROM (°)	10.3	10.3	0.883

Significance

These results demonstrate the *immediate* effects of a 15-minute postural intervention on gait metrics. A longer-term intervention would likely further improve many of these metrics and provide a long-lasting effect on overall health with the extended amount of time that one spends in gait during the day. In addition, improved gait metrics may provide additional motivation for one to remain active.

Acknowledgments

NCMIC Foundation; Foderaro-Quattrone Grant for AI Innovation in Orthopedic Surgery; L30-AR070273

References

1. Grasso et al. *J Neurophysiol*; 2000; 83(1):288-300.
2. Granata et al. *Clin Biomech*, 2001; 16(8):650-659.
3. Park et al. *Physiother Theory Pract*. 2017; 33(8):661-669.
4. Melick et al. *PLoS ONE*. 2017; 12(2):e0189876.

IMU FILTER SETTINGS FOR HIGH INTENSITY ACTIVITIES

Emily J. Miller[1], Riley C. Sheehan[2,3], and Kenton R. Kaufman[1]
[1]Mayo Clinic, [2]Center for the Intrepid-Brooke Army Medical Center,
[3]Henry M. Jackson Foundation for the Advancement of Military Medicine
email: miller.emily@mayo.edu

Introduction

A filter is used to remove noise from the signal in biomechanics research. There is a paucity of recommendations for the filter cut-off frequency when using inertial measurement units (IMU) for data collection of high intensity activities. Authors either don't report cut-off frequency values, default to values used for maker-based motion analysis [1], or make recommendations using low intensity self-selected waking speed trials [2,3]. Therefore, the purpose of this study was to determine the IMU cut-off frequency filter settings for high intensity activities.

Methods

Ten healthy young adults had an IMU (OPAL, APDM, INC., Portland, OR) placed on their sternum to estimate trunk kinematics during controlled postural perturbation using a microprocessor-controlled treadmill [4]. The three most energetic (trip inducing) trials in both the forward and reverse directions were selected from each participant. The cut-off frequency was calculated for trunk angle, angular velocity and linear acceleration about the flexion-extension axis using 99 percent of the energy spectrum (E99) and residual analysis (RA) [2].

Results and Discussion

Sixty trials were analyzed. The cut-off frequencies converged on the same value for the angular velocity (E99: 25±6, RA: 22±35), but not for the angle (E99: 2±1, RA: 18±2) and acceleration (E99: 31±8, RA: 23±3) (Fig. 1).

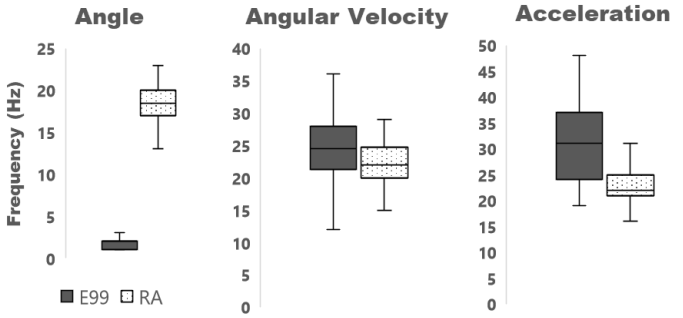

Figure 1: Cut-off frequency quartiles, with variability outside lower and upper quartiles, for trunk angle, angular velocity and acceleration about the flexion-extension axis using the E99 (solid) and RA (dotted) methods.

For this analysis, post-processing filtering was not applied to the data. The angular velocity data obtained directly from the IMU's gyroscope and acceleration data obtained directly from the IMU's accelerometer were purely raw signals. The angle data was calculated from the orientation matrix obtained from the fusion of the IMU's magnetometer, gyroscope, and accelerometer using a proprietary Kalman filter. This may explain the lack of convergence between the two methods for the angle data. While the range for the angle cut-off frequency was larger than the other two variables, the current study range (2-18 Hz) included cut-off frequency values (6 Hz) [1] typically used for IMU angle data and cut-off frequency ranges (4.5-9 Hz) previously used for marker-based trunk angles during treadmill induced disturbances [5].

The calculated cut-off frequencies converged on 24 Hz for trunk sagittal angular velocity. A previous study using self-selected waking trials recommended cut-off frequencies greater than 10 Hz for angular velocity [2]. The calculated cut-off frequencies for the trunk acceleration ranged from 23 Hz (RA) to 31 Hz (E99). For a healthy subject population in a previous study, for accelerations about the flexion-extension axis, mean cut-off frequencies were 18 Hz (RA) and 24 Hz (E99) [3].

The recommended filter cut-off frequency for trunk sagittal angular velocity and accelerations, due to the more energetic activity, were higher than values previously reported. For the angular velocity, the specific values were consistent using two independent methods. For acceleration, the relative difference between the two methods for this study and previously reported results were similar. The two methods produced a range of recommended cut-off frequencies for the trunk sagittal angle, which included previously recommended values.

Significance

High intensity activities yielded higher cut-off frequencies than low intensity activities for the same variables of interest. For an able-bodied population, the E99 and RA methods returned different cut-off frequencies. Selection of cut-off frequency should be based on the data variable, origin of signal, and the activity of interest.

Acknowledgments

Funded by Department of Defense Grant No. W81XWH-15-2-0071. The view(s) expressed herein are those of the author(s) and do not reflect the official policy or position of Brooke Army Medical Center, the U.S. Army Medical Department, the U.S. Army Office of the Surgeon General, the Department of the Air Force, the Department of the Army, Department of the Navy, or the Department of Defense, The Henry Jackson Foundation, or the U.S. Government.

References

1. Morrow et al. J App Biom, 33 (2017) 227-232.
2. Allseits et al. IEEE Sensors, 19 (2019) 4115-4122.
3. Fazlali et al. G&P, 80 (2020) 217-222.
4. Miller & Kaufman. Med Eng & Phys, 70 (2019) 51-54.
5. Pavol et al. J. Gerent, 57A (2002) M496-M503.

Effects of Prosthetic Stiffness and Added Mass on Metabolic Cost and Symmetry in Female Runners with a Leg Amputation.

Kara Ashcraft[1] & Alena M. Grabowski[1,2]
[1]University of Colorado, Boulder, CO, USA; [2]Dept. of Veterans Affairs, Eastern Colorado Healthcare System, Denver, CO, USA
Email: Kara.Ashcraft@colorado.edu

Introduction

To run, people with a transtibial amputation (TTA) require use of running-specific prostheses (RSPs), which are comprised of carbon fiber and act mechanically as passive-elastic springs in-series with the residual limb. RSPs store and return elastic energy during the stance phase of running, similar to tendons and ligaments in biological limbs,[1] and in some instances allow the user to run with similar metabolic energy expenditure as those with two biological limbs.[2]

During running, athletes with a TTA using an RSP have asymmetric biomechanics; they generate 9% lower stance-average vertical ground-reaction forces ($vGRF_{avg}$) in their affected leg (AL) than their unaffected leg (UL) across a range of speeds.[1] This difference in $vGRF_{avg}$ is likely due to the inability of an RSP to generate net positive work and power.[1] Prior work has found that a 10% decrease in peak vGRF asymmetry correlated to a 1.9% decrease in net metabolic power in runners with TTA, and that using lighter-weight RSPs had no effect on biomechanical asymmetry.[3] However, these findings neglect the effect of gender on running biomechanics.

Females with TTA represent only 23% of all subjects previously studied in research that has analyzed the effects of using RSPs. Thus, to better understand how RSP configuration specifically effects women with TTA, we measured metabolic power and kinetics while female runners used RSPs with different stiffness categories, and with and without mass added to the RSP. We hypothesized that use of a less-stiff RSP without added mass would result in the lowest net metabolic power and $vGRF_{avg}$ asymmetry compared to a more-stiff RSP and added mass.

Methods

2 female athletes (mean: 67 kg) with unilateral TTA participated. On day 1 a prosthetist fit and aligned an RSP with the athlete's manufacturer recommended (Rec) stiffness category (Cat), based on their body mass, one Cat less stiff, and two Cat less stiff than Rec. On day 2, subjects ran at 2.5 m/s on a force-measuring treadmill (1000 Hz; Treadmetrix, Park City, UT) for 5 minutes using the Rec Cat, -1 Cat, and -2 Cat RSPs.

We measured rates of oxygen consumption and carbon dioxide production throughout each trial (ParvoMedics TrueOne 2400, Sandy, UT). We calculated average steady-state metabolic power (W) from minutes 3-5 of each trial[4], normalized to body mass including the RSP, and subtracted standing metabolic power. We then added 100g, 200g and 300g 10 cm from the distal end of the RSP Cat that resulted in the lowest metabolic power. Athletes also ran for 5-minutes with each added mass condition while we measured metabolic rates and GRFs. We calculated $vGRF_{avg}$ symmetry index (SI) between the AL and UL for all conditions.[5] We used independent one-tailed *t-tests* to compare net metabolic power and $vGRF_{avg}$ SI between conditions using R-Studio software (Boston, MA), with $p = 0.05$.

Results and Discussion

On average, net metabolic power decreased by 12% when using a -1 Cat RSP ($p = 0.07$) and 8.6% when using a -2 Cat RSP ($p = 0.11$) compared to the Rec Cat. When subjects used the -1 Cat RSP, net metabolic power increased 7.6%, 5.8% and 7.1% when adding 100g, 200g and 300g, respectively, compared to no added mass ($p>0.10$ Fig.1A).

$vGRF_{avg}$ SI decreased from 7.1% to 4.9% when using -1 Cat compared to the Rec Cat ($p=0.30$) and increased from 7.1% to 9.2% when using -2 Cat ($p=0.42$) compared to the Rec Cat. The most symmetric $vGRF_{avg}$ occurred with 200g added (SI = 2.09 %, $p = 0.06$) but increased 3-fold with 100g added and 2-fold with 300g added, on average ($p<0.30$ Fig.1B-D).

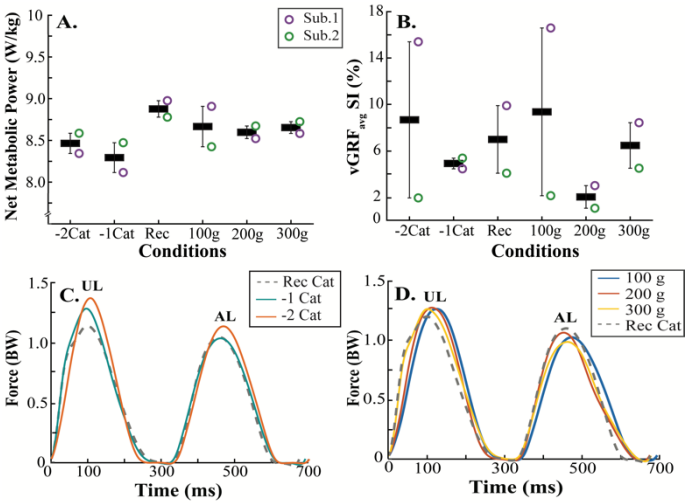

Figure 1. **A.** Net metabolic power for different RSP stiffness categories (Cat) compared to recommended (Rec) and added mass conditions. **B.** Stance average vertical ground reaction force symmetry index ($vGRF_{avg}$ SI) for different stiffness Cat compared to Rec and added mass conditions. **C-D.** Representative vGRF of the unaffected (UL) and affected legs (AL) for **C.** -1 Cat and -2 Cat compared to Rec Cat (grey dotted line) and **D.** added mass compared to the -1 Cat with no added mass (grey dotted line).

Conclusion

From these preliminary results we accept our hypothesis that decreasing RSP stiffness without adding mass decreases net metabolic power during running in women with TTA. Moreover, women with TTA reduce $vGRF_{avg}$ asymmetry by using a less-stiff RSP with 200g added to the distal end. Thus, there is an apparent trade-off between minimizing metabolic power and asymmetry during running due to different RSP stiffness and added mass conditions. Our results inform RSP design and prescription for women with TTA.

References

1. Grabowski, A. M. *et al*. *Biol. Lett.* **6**, 201–204 (2010).
2. Beck, O. N. *et al*. *Exerc. Sport Sci. Rev.* **47**, 15–21 (2019).
3. Alcantara, R. S. *et al*. *Eur. J. Appl. Physiol.* **120**, 1449–1456 (2020).
4. Brockway, J. M. *Hum. Nutr. Clin. Nutr.* **41**, 463–471 (1987).
5. Robinson, R. O. *et al. J. Manipulative Physiol. Ther.* **10**, 172–176 (1987).

Acknowledgment

Views expressed do not reflect the view or policy of the Dept. of the Navy, DOD, DHA, or US Govt. CDMRPL-17-0-DMI170709

DORSAL SUBLUXATION AS A PROGNOSTIC METRIC OF PROGRESSIVE THUMB CARPOMETACARPAL OSTEOARTHRITIS

Amy M. Morton[1], Janine D. Molino[1], Douglas C. Moore[1], Amy L. Ladd[2], Arnold-Peter C. Weiss[1], Joseph J. Crisco[1]
[1]Department of Orthopaedics, Brown University and Rhode Island Hospital, Providence, RI, USA.
[2]Department of Orthopaedic Surgery, Stanford University School of Medicine, Stanford, CA, USA
email: amy_morton1@brown.edu

Introduction

Osteoarthritis (OA) of the first Carpometacarpal (CMC) joint is a complex disease of bone, cartilage and surrounding tissue[1], characterized by pain at the base of the thumb and functional impairment. Postulated causes of the disease include combinations of mechanical stress[2], ligament laxity, incongruent loading[3] and biochemical changes. The complex multi-factor etiology and symptomology of CMC OA make it challenging to establish metrics that might predict disease progression.

Using a dataset of patients followed for six years at the outset of their thumb CMC OA disease, we have identified an association between osteophyte (OP) volumes and dorsal subluxation (DS) of the first metacarpal. Thus, the aim of this study was to determine if dorsal subluxation (DS defined as a % of articular width) could predict progression of OA disease severity.

Methods

Following IRB approval, 86 patients with early thumb CMC OA (self-reported pain and radiographic Eaton 0/1 grading) and 22 age-matched asymptomatic heathy volunteers were recruited into an NIH-funded thumb CMC OA biomechanics study.

At enrolment (baseline) and 1.5, 3, 4.5 and 6-year follow-up visits, data were collected for each OA patient; healthy volunteers returned for only a 6-year follow-up visit. At each visit, CT scans of the affected (patient) or dominant (healthy) wrists were acquired in 11 range-of-motion and task-related positions[4]. Digital surface models of the trapeziae (TPM) and first metacarpals (MC1) were segmented from CT data. For each day 0 model, coordinate systems (CS) were calculated from manually delineated TMC articular facets[5].

OP volumes were computed using dissimilarity excluding Procrustes[6] registration and Boolean subtraction of a healthy control from each OA bone. Patients were categorized into stable or advanced OA groups, based on a previously presented OP volume threshold-based classifier[7]. Subluxation was defined as the position of the MC1 CS, resolved along the dorsal-volar axis of the TPM CS, scaled by facet area. Linear mixed effects models (LMEM) with random slope and intercept were used to examine DS over the study for each category and pose.

The computed c-statistics from logistic regression and receiver operating characteristic (ROC) curve analysis were then used to quantify the power of the DS value at each thumb pose, and its rate of change, to predict classification of disease progression (advanced OA vs stable OA vs healthy). Individual poses with a c-statistic ≥ 0.70 were examined further to see whether a combination of poses would yield higher classification power. Once the pose with the highest classification power was identified, ROC curves were estimated to identify cut-off values for diagnosing progressive OA. Youden's J statistic was used to identify the cut-off value that provided the best trade-off between sensitivity and specificity. Lastly, sensitivity, specificity, negative predictive values, and positive predictive values were calculated to assess the performance of diagnostic tests using the computed cut-off values.

Results and Discussion

Examining baseline DS data, thumb flexion and hand-on-jar-lid (jar) poses had the best ability to differentiate stable and advanced OA (c-statistic 0.7), with cut-off values of 2% *volar* and 15% DS, respectively. The greatest rate of change in thumb CMC DS in advanced OA patients also occurred during thumb flexion (2.9%/year). Using the rate of DS change in flexion, a 1.94%/year cut-off threshold maximized sensitivity and specificity. All three cut-off values yielded diagnostic tests with high positive predictive values (PPV of 0.8 to 0.94), meaning that in those who have a positive screening test, the probability of OA progression is high. The sensitivity, specificity, and negative predictive values for the diagnostic tests based on the baseline flexion and jar poses were low, with values ranging from 0.54 to 0.72. The diagnostic test based on the subluxation rate of change in the flexion pose had a low specificity (0.52). However, it had high sensitivity and negative predictive values (0.88 and 0.87, respectively). By assessing DS during flexion at multiple timepoints among those who exhibit OA symptoms, there was a high ability to predict the likelihood of further progression versus disease stability.

Significance

This study examined dorsal subluxation (DS) as a metric to predict worsening disease in patients with evidence of early thumb CMC OA. The promising prognostic statistics reveal that DS of the MC1 on the TPM during flexion or jar have clinical diagnostic potential. The *volar* baseline MC1 cut-off threshold in flexion and near-zero values for control and stable groups suggest that thumb flexion may be a position of congruency for the thumb CMC joint, but it dorsally subluxated with OA disease. Examining DS in thumb poses independently allowed distinction between kinematic induced DS (positions in which the CMC joint dorsally subluxated regardless of disease) from disease-correlated DS observed in thumb flexion. The ability to predict a patient whose OA is likely to progress based on the magnitude and rate of change in subluxation during thumb flexion provides the foundation for a powerful clinical screening mechanism.

Acknowledgments

This research was supported in part by funding from NIH AR059185

References

1. Loeser, 2012. doi:10.1002/art.34453 2. Eaton and Littler, 1973. PMID: 4804988 3. Pellegrini, 2005. doi.org/10.1016/0363-5023(93)90354-6
4. Halilaj, 2014. doi:10.1109/EMBC.2014.6944588 5. Halilaj, 2013. doi:10.1016/j.jbiomech.2012.12.002 6. Morton, 2019. doi:10.1002/jor.24569 7. Morton ASB '20 #104

Wearables-Only EMG-Driven Simulation of Muscle Contraction During Gait

Reed D. Gurchiek[1,2], Nicole Donahue[1], Niccolo M. Fiorentino[1,2], and Ryan S. McGinnis[1,2]
[1]Dept. of Electrical and Biomedical Engineering, University of Vermont
[2]Dept. of Mechanical Engineering, University of Vermont
Email: reed.gurchiek@uvm.edu

Introduction

Continuous monitoring of joint and muscle loading in free-living conditions would facilitate novel insight into musculoskeletal disease etiology and comprehensive patient characterization. This has motivated recent developments in wearables-based biomechanical analysis that enable estimation of clinically relevant variables including joint moment and individual muscle force [1,2]. However, the number of required sensors (e.g., 17 [1], 7 [2]) is often a barrier to translation. Machine learning techniques have been proposed to overcome this problem, but they do not characterize relevant internal state variables (e.g., muscle force) as in physics-based techniques. This work presents a novel hybrid approach which combines both physics-based simulation and machine learning in a complementary fashion in order to reduce sensor array complexity. Herein, preliminary validation results are presented for the proposed technique in estimating knee extension moment (KEM), ankle plantarflexion moment (PFM), and muscle work during the stance phase of gait.

Methods

A single healthy female performed 10 overground walking trials at a self-selected normal speed. Marker positions and force plate data for a single stance phase in each trial were used to compute KEM and PFM via inverse-dynamics (ID). Muscle excitations were computed as in [3] from electromyograms (EMG) recorded from 10 muscles: vastus medialis (VM), vastus lateralis (VL), rectus femoris, long head of the biceps femoris (BFL), semitendinosus (ST), medial gastrocnemius (MG), lateral gastrocnemius (LG), peroneus longus (PL), soleus, and tibialis anterior. Muscle contraction was simulated for thirteen Hill-type muscles including all 10 muscles instrumented with EMG as well as the vastus intermedius (excitation assumed equal to the average of VM and VL), semimembranosus (excitation assumed equal to ST), and the short head of the biceps femoris (excitation assumed equal to BFL) using an implicit solver [4]. Outputs from the simulation were used to estimate KEM, PFM, and muscle work (referred to as the reference EMG-driven analysis). Seven of the ten walking trials were used to tune muscle-specific parameters via Bayesian optimization. The remaining three trials were used only for validation of the proposed technique.

The proposed technique is to use EMG-driven simulation of muscle contraction to estimate KEM, PFM, and muscle work as described above. This requires muscle-tendon unit (MTU) length (following inverse-kinematics) and muscle excitation for each MTU. To reduce the number of required EMG sensors, the proposed technique informs a full set of muscle excitations from a measured subset (VM, MG, LG, PL) using Gaussian process synergy functions [3] and the inverse-kinematics were solved (and hence MTU length) using inertial sensor data from thigh- and shank-worn inertial sensors. Shank kinematics were solved for via direct integration. Thigh kinematics were given from the shank kinematics and an estimate of the knee flexion angle [5]. Pelvis orientation was assumed null except that the heading angle was equal to the average shank heading during the stance phase. Foot kinematics were assumed to lie in the sagittal plane only during the stance phase and were based off of a foot-ground contact model with two contact points (below the heel and toe).

Estimates of KEM and PFM from the proposed technique were compared to both the ID and reference EMG-driven analyses using root mean square error (RMSE, units in Nm and as a percentage of the product of body weight and height) and Pearson's correlation coefficient (r). Correlation analysis was used to compare estimates of muscle work from the proposed technique to the reference EMG-driven analysis. Muscle work was considered only for the type of contraction (concentric or eccentric) in which each muscle did the most work.

Results and Discussion

Compared to the ground truth ID analysis, the proposed technique estimated KEM to within 13.6 Nm (1.2%) RMSE with $r = 0.90$ and PFM to within 15.2 Nm (1.3%) RMSE with $r = 0.95$. These results are comparable to other wearables-based techniques [1,2], but with a significant reduction in sensor array complexity (e.g, sensors placed on 7 to 17 segments vs. 2 in the proposed technique). Notably, the peak KEM, an important biomarker in early knee osteoarthritis, was estimated with less than 3.0 Nm mean absolute error across the three test trials. Joint moment estimates from the proposed technique compared well with the reference EMG-driven analysis for both KEM ($r = 0.98$, RMSE = 5.3 Nm, 0.5%), PFM ($r = 0.99$, RMSE = 5.0 Nm, 0.4%), and muscle work ($r = 0.87$). These results suggest the proposed technique is a valid alternative for EMG-driven simulation.

This work presents the first wearables-only EMG-driven simulation of muscle contraction that uses machine learning only to map a subset of excitations to a full set. The preliminary findings of this work demonstrate the feasibility of the proposed approach for characterizing joint and muscle tissue loading and may be generalized for analysis of other muscles and joints.

Significance

The proposed technique requires four sensors at locations very near the knee joint that could be built into a knee brace. A mechanism of this sort may allow non-invasive monitoring of joint and muscle loading in patients recovering from knee surgery without any additional burden beyond what is normally prescribed (e.g., a knee brace).

Acknowledgments

This work was supported in part by the Vermont Space Grant Consortium through the NASA Cooperative Agreement under Grant NNX15AP86H.

References

[1] Karatsidis, et al. (2019), *Med Eng Phys*, 65:68-77.
[2] Dorschky, et al. (2019), *J Biomech*, 95:109378.
[3] Gurchiek, et al. (2020), *IEEE TNSRE*, 28(11):2478-87.
[4] van den Bogert, et al. (2011), *Procedia IUTAM*, 2:297-316.
[5] Seel, et al. (2014), *Sensors*, 14(4):6891-909.

The Effects of Cognitive Load on Local Dynamic Stability During a Fatigue Jump

Jacob Larson[1], William Taylor[1], Abigail Jacobs[1], Michael Zabala, Ph.D[1]
[1]Department of Mechanical Engineering, Auburn University, Auburn, AL, USA

Email: jsl0043@auburn.edu

Introduction

Previous studies in the field of biomechanics suggest that neurocognitive deficits can result in a higher risk of noncontact lower extremity injury [1]. Similarly, many studies have correlated local dynamic stability (LDS) with injury risk by quantifying instability throughout various movement tasks [2]. Although both previously cited studies effectively identify subjects with injury risk, not much is known about the interaction between LDS and cognitive load. To better understand the relationship between LDS and mental load, this study had subjects perform repetitive movements while performing a semantic fluency task. The authors hypothesized that the LDS will decrease during the semantic fluency task, suggesting that subjects will not be able to spend as much cognitive effort on completing a proper movement.

Methods

This study was performed on five male Auburn University club sports athletes (age = 19.40 ± 0.55yrs, weight = 154.80 ± 14.58lbs, height = 5.85 ± 0.29ft). Subjects were asked to complete a vertical jumping task in place for 30 seconds. They were then asked to repeat the jumping task while also performing a semantic fluency task, simulating cognitive load. The semantic fluency task required subjects to name as many words as possible from the following preselected letters of the same approximate recall difficulty: H, D, M, W, A, B, F, P, T, C, and S [3]. Letters were randomly chosen at the beginning of each test, and the semantic fluency task was performed while simultaneously performing the 30 second jumping task. All subjects signed informed consent forms approved by the Auburn University Internal Review Board. LDS for the both the control and dual task trials was calculated for all angles at the ankle, knee, and hip. A paired *t*-test was used to compare the LDS during the control fatigue jump to that of the corresponding dual task fatigue jump.

Results

Table 1 shows the results of the paired t-test, as well as the average LDS difference and standard deviation of difference between the control and semantic fluency task. Ankle internal rotation LDS was found to be significantly different between tasks (p=0.015), and the differences in this variable are further shown in Figure 1.

Discussion

Although ankle internal rotation LDS was the only significant difference between the control and semantic fluency task, it appears that there was a consistent trend for LDS to decrease during the semantic fluency task. Decreasing LDS is commonly associated with increased "stability", and typically results in more repetitive and rigid movements. This finding is generally supported by the hypothesis of this study, and would suggest that increased cognitive load causes subjects to use less complex movement patterns in order to accomplish their cognitive task. Additionally, the trend towards decreased LDS under cognitive load shows that an individual may have difficulty adapting to changing conditions in stressful situations.

Table 1: Percentage change in LDS before and after a semantic fluency task. Here, a negative percentage change indicates a decrease in LDS.

	Avg LDS Diff	Avg LDS % Diff	p
Knee Flexion LDS	-0.003 ± 0.019	-5%	0.670
Knee Abduction LDS	0.006 ± 0.028	5%	0.512
Knee Internal Rotation LDS	-0.012 ± 0.029	-21%	0.222
Ankle Flexion LDS	-0.012 ± 0.026	-11%	0.169
Ankle Abduction LDS	0.020 ± 0.049	22%	0.228
Ankle Internal Rotation LDS	**-0.027 ± 0.029**	**-25%**	**0.016**
Hip Flexion LDS	-0.012 ± 0.023	-17%	0.118
Hip Abduction LDS	-0.014 ± 0.033	-10%	0.201
Hip Internal Rotation LDS	-0.012 ± 0.027	-13%	0.196

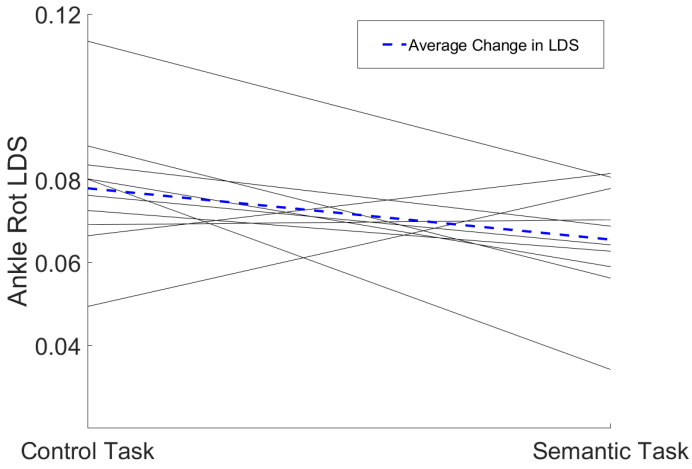

Figure 1: Difference in LDS Values between Control and Semantic jumping trial (**p=0.0164**)

Significance

This study is important to the field of biomechanics because it helps researchers better understand how LDS changes under different cognitive conditions. The knowledge that the LDS is correlated to neurocognitive load could allow researchers to explore using cognitive training to better control LDS.

References

[1] Swanik C, et. al, *The American Journal of Sports Medicine.* 2007; 35 (6): 943-948.
[2] Marcel J.P.Toebesa, Marco J.M.Hoozemans, *Gait & Posture.* 2012; 36 (3): 527-531
[3] Tombaugh T, et. al, *Archives of Clinical Neuropsychology.* 1999; 14(2): 167-177

PROSTHETIC MODEL INFLUENCE ON POWER AND WORK DURING SUBMAXIMAL RUNNING

Tatiana Djafar[1], J. Collins[1,2], and T. Kingsbury[1]
[1]Clinical Biomechanics Laboratory, Navy Medicine Readiness and Training Command San Diego, San Diego, CA, USA
[2]BIOMS, University of Delaware, Newark, DE, USA
email: tatiana.e.djafar.ctr@mail.mil

Introduction

Carbon fiber running-specific prostheses (RSPs) have facilitated the return to high-level functional activities, such as running, for patients with transtibial amputation (TTA). Available RSP models are generally C-shaped or J-shaped. Previous work has demonstrated that this prosthetic geometry affects both metabolic cost and maximum running velocity, but not much is known about the RSP models' mechanical influence [1,2]. Thus, the purpose of this study is to evaluate the effect of RSP model on power and work during submaximal running.

Methods

Eleven subjects with unilateral TTA provided informed consent under a research study approved by the Naval Medical Center San Diego Institutional Review Board (CIP# NMCSD-2013.0109). All subjects had been medically cleared for high-level activity by their providers and were clinically prescribed an Össur® Flex-Run™ (C, 5 subjects) or Össur® Cheetah Xtend™ (J, 6 subjects) RSP by their prosthetist.

The subjects were outfitted with a modified 6 degrees of freedom (6DoF) marker set from the pelvis down and instructed to run through the capture volume of an overground mobile motion capture system at $3.5 m \cdot s^{-1}$ ± 5% during data collection. The Unified Deformable (UD) segment model was applied to calculate power and work for structures distal to the knee, while a Constituent Lower Extremity Work (CLEW) approach was used to calculate mechanical Cost of Transport (CoT) defined as the total burden of work for each limb over a full stride [3,4].

A 2x2 (C/J RSP model x affected/unaffected limbs) ANOVA with Tukey-adjusted post-hoc analysis was run to determine statistical differences between the following dependent variables: minimum and maximum power, positive and negative work, work-ratio and CoT. Additionally, a t-test was run between RSP model groups to compare prosthetic transport reliance within the affected limb (aff-PTR), defined as the RSP work contribution to the affected limbs' CoT. Significance for all tests was set at $\alpha = 0.05$.

Results and Discussion

Results are displayed in Table 1. Limb main effects were found for maximum power ($p = 0.013$) and positive work ($p = 0.027$). Regardless of RSP model used, the musculature of the unaffected, intact limbs allows for increased power generation and, thus, positive work done as compared to the affected limbs, which are limited by the mechanical properties of the carbon fiber RSP donned.

RSP model and limb main effects were found for CoT ($p \leq 0.014$). CoT comparisons between all model and limb combinations differed from each other except between the two unaffected limbs groups ($p = 0.934$). Affected limbs donning the C RSP experienced a lower CoT than the J RSP affected limbs, and both had a lower total burden of work than the unaffected limbs. Additionally, aff-PTR was larger in the C affected limb compared to the J affected limb ($p = 0.050$). RSP model did not influence work done by the unaffected limb but did appear to impact work in the affected limb. With both a lower CoT and higher aff-PTR, use of the C RSP suggests an increased reliance on the mechanical properties of the device for energy generation and absorption during running rather than the musculature of the rest of the affected limb compared to use of the J RSP. Additionally, use of the C RSP resulted in a lower mechanical CoT while a previous study showed use of a J RSP resulted in lower metabolic cost of transport, suggesting multiple measures should be used to evaluate how a device interfaces with a patient [1].

This study is limited by low subject numbers and relatively large data variability to elicit clinically meaningful statistics; however, as the data is presented, RSP model appears to play a role in total work done by the affected limb as well as muscle recruitment in the affected limb during submaximal running.

Significance

Different RSP geometry correspond to different activities according to manufacturers (e.g. C-shaped RSPs are generally recommended for distance running, while J-shaped RSPs are recommended for sprinting); however, other factors can contribute to the clinical prescription of a certain RSP, such as residual limb length or even financial burden. Understanding the different mechanical influences these devices have on patients with amputation can help their clinical care providers to better address their musculoskeletal health through rehabilitation, training, and beyond.

Acknowledgments and Disclosure

Thanks to General Dynamics Information Technology and NMRTC-SD CBL staff, past and present. The views expressed herein do not necessarily reflect those of the Department of the Navy, Department of Defense, Defense Health Agency, or U.S. Government.

References

[1] Beck ON et al. (2017), *J Appl Physiol*, **123**: 38-48.
[2] Taboga P et al. (2020), *Sci Rep*, **10**: 1783.
[3] Takahashi KZ et al. (2012). *J Biomechanics*, **45**: 2662-7.
[4] Ebrahimi A et al. (2017). *Gait Posture*, **56**: 49-53.

Table 1: Mean and standard deviation of power and work variables. ♦ - limb main effect, • - RSP model main effect

	Max Power (W/kg) ♦	Min Power (W/kg)	Positive Work (J/kg) ♦	Negative Work (J/kg)	Work-Ratio	CoT (J/kg/m) ♦•	aff-PTR (%)•
C, Affected	10.0 ± 2.3	-13.6 ± 3.0	0.71 ± 0.18	-0.81 ± 0.19	0.88 ± 0.0	1.15 ± 0.23	57.7 ± 17.0
C, Unaffected	13.8 ± 1.6	-16.4 ± 7.0	0.91 ± 0.12	-0.89 ± 0.22	1.06 ± 0.2	1.98 ± 0.15	
J, Affected	11.2 ± 3.3	-10.9 ± 2.4	0.71 ± 0.18	-0.80 ± 0.18	0.88 ± 0.0	1.59 ± 0.06	39.9 ± 8.5
J, Unaffected	13.3 ± 2.2	-14.7 ± 3.9	0.85 ± 0.16	-0.90 ± 0.13	0.97 ± 0.2	2.06 ± 0.34	

THE EFFECT OF MINIMALIST FOOTWEAR TYPES ON STATIC POSTURAL STABILITY

Sachini N. K. Kodithuwakku Arachchige, Harish Chander, Adam C. Knight, Alana J. Turner
Neuromechanics Laboratory, Department of Kinesiology, Mississippi State University
Email: snk128@msstate.edu

Introduction

According to the National Health Statistics Report 2016, in 2011-2014, 8.6 million sports and recreation-related injuries have been reported. Such injuries were more prevalent in young males (~ 61%), and falls have been identified as a major causative factor of those injuries (~ 28%)[1]. A fall could occur following a slip, trip, and loss of balance, with a greater incidence reported with the latter. Except for minimizing falls, maintaining optimal postural stability is crucial for better performance in sports[2].

Human postural control has multiple impactful factors. Among those, the type and the nature of footwear worn are shown to be critical. Footwear with minimalistic features (less weight, low heel-to-toe drop, low sole height, etc.) and footwear with thin, hard soles are known to elicit better postural stability[3]. Due to the minimalist nature, the ability to mimic barefoot conditions, and the exact contour of human feet, Vibram™ five fingers shoes (VFF) are favored by many individuals currently. Thus, the present study incorporated two types of VFF, Vibram™ Bikila (VB) and Vibram™ Trek ascent (VT), which have unique design characteristics (Table 1). The purpose of this study was to study the impact of minimalist footwear on static postural stability in young, healthy males.

	VB	VT
Mass (g)	168.4	173.5
Sole thickness (mm)	3.35	6.73
Heel height (cm)	2.1	3.2
Midsole hardness (Shore A durometer units)	74.7	63.45

Table 1: Footwear design characteristics of Vibram™ Bikila (VB) and Vibram™ Trek ascent (VT).

Methods

Twenty-four recreationally active, healthy males (age 21.38 ± 2.50 years, height 1.74 ± 0.06 m, mass 71.24 ± 10.37 kg) were recruited. Their static postural stability was measured using a force platform (AMTI AccuGait, Watertown, MA) in stable and unstable surfaces (foam), bipedal (BL), and unipedal (UL) stances, and eyes open (EO) and eyes closed (EC) conditions. Each participant's static stability in the barefoot (BF) condition was measured first, followed by the counterbalanced shod conditions (VB and VT) on a single day.

Each postural sway variable of interest [center of pressure average in the anteroposterior direction (COP-AP average), center of pressure average in the medial-lateral direction (COP-ML average), average radial displacement (RD), and center of pressure length (COP-L)] was analyzed using a one-way repeated-measures ANOVA for each testing condition. Significant main effects were followed up with the Bonferroni correction factor. The alpha level was set for 0.05.

Results and Discussion

The analysis revealed significant footwear main effects in COP-ML average [$F(2,46) = 3.437$, $p = 0.041$, $\eta_p^2 = 0.130$] and COP-AP average [$F(2,46) = 3.684$, $p = 0.033$, $\eta_p^2 = 0.138$] in the unstable BL EO condition. Follow up tests showed a significant difference between BF and VB with higher sway values for VB. COP-AP average in the unstable BL EC [$F(2,46) = 5.052$, $p = 0.010$, $\eta_p^2 = 0.180$] condition demonstrated significant differences between BF and VB as well as BF and VT (Figure 1). Average radial displacement [$F(2,46) = 3.319$, $p = 0.045$, $\eta_p^2 = 0.126$] and COP-L [$F(2,46) = 4.074$, $p = 0.034$, $\eta_p^2 = 0.150$] showed significant footwear differences in unstable BL EC condition.

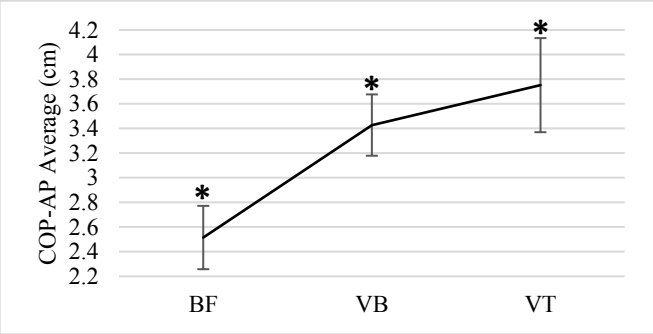

Figure 1: Center of pressure average in the anteroposterior direction (COP-AP) in barefoot (BF), Vibram™ Bikila (VB), and Vibram™ Trek ascent (VT) conditions. ✱ represents significant footwear differences.

The participants demonstrated superior postural stability in the BF condition compared to the shod conditions. This could be explained with the greater somatosensory feedback in the BF condition due to no obliteration from a shoe sole. Although no significant differences were observed between VFF types, the VT demonstrated higher postural sway values, suggesting poor postural stability compared to VB. Having no significant differences in the stable condition suggests that the participants could maintain satisfactory postural stability with any footwear condition when the standing surface was firm. However, this was not possible on the unstable surface due to the affected somatosensory feedback on a foam.

Significance

Although the participants demonstrated superior postural stability in BF, being barefooted during sports or recreational activities may not be practical. Thus, the individuals must choose a footwear that causes fewer balance decrements to minimize falls during sports. Thus, VB appears to be a better solution compared to VT, which could be attributed to its design characteristics such as lesser weight, sole thickness, heel height, and greater sole hardness. The absence of significance between the shod conditions could be due to the use of a young healthy population. The results could be different among the geriatric or clinical populations.

References

1. Yahtyng, S., & Li-Hui, H. H. (2016). Sports- and recreation related injury episodes in the USA, 2011–2014. National Health Statistics.
2. Hrysomallis, C. (2011). Balance ability and athletic performance. Sports Medicine, 41(3), 221–232.
3. Chander, H., Knight, A. C., Garner, J. C., Wade, C., Carruth, D., Wilson, S. J., Gdovin, J. R., & Williams, C. C. (2019). Impact of military type footwear and load carrying workload on postural stability. Ergonomics, 62(1), 103–114.

DECOUPLING VISUAL CONSTRAINT FROM UNANTICIPATED DIRECTIONAL CUES IN A JUMP-LANDING TASK

Patrick D. Fischer[1], K. Hutchison[2], J. Becker[3], and S. Monfort[1]
[1]Department of Mechanical and Industrial Engineering, Montana State University, Bozeman, MT USA
[2]Department of Psychology, Montana State University, Bozeman, MT USA
[3]Department of Health and Human Development, Montana State University, Bozeman, MT USA
email : *patrick.fischer2@student.montana.edu

Introduction

Unanticipated movements are used in lab-based biomechanical studies to simulate sport-specific tasks [1]. However, tasks that fixate the participant's visual gaze away from the intended path of travel, whether they be unanticipated [1] or pre-planned [2], have demonstrated effects on movement performance. Because unanticipated conditions have been administered with visual stimuli (e.g,, a light, arrow, simulated defender), decoupling the effects of visual constraints from those of unanticipated task requirements is necessary to understand to what extent each factor plays in influencing movement performance.

The purpose of this study was to elucidate the individual and combined effects of constrained gaze and unanticipated cues on landing mechanics. We hypothesized that combined effects of constrained gaze and unanticipated cues on early-stance landing mechanics would be greater than individual effects of either task requirement.

Methods

Twenty-two recreationally active young adults (8F/14M; 19.9±1.1yr; 1.8±0.1m, 73.3±8.5kg) provided IRB-approved informed consent. Participants scored 12+ on the Marx activity scale [3], were free of lower-extremity surgeries, and had not suffered a concussion within six months of participating or lower extremity injuries within three months of study participation.

Participants completed a previously established jump-landing task [4], under a baseline (**Base**) and four dual-task conditions: auditory unanticipated without visual constraint (**Aud**), auditory unanticipated with visual constraint (**Aud_Fix**), visual unanticipated (**Vis**), and anticipated with visual constraint (**Fix**). Auditory directional cues were pre-recorded commands stating "Up", "Left", or "Right". Visual directional cues were images of arrows pointing up, left, or right. Directional cues were presented ~250 ms prior to initial contact with the force plates. The visual fixation used for **Aud_Fix** and **Fix** was a large, black cross.

Motion capture and ground reaction force data were collected, and kinematic and kinetic data were calculated using an inverse kinematics model in Visual 3D. Joint moments are externally defined and normalized to participant height and weight. Peak knee flexion angle (pKFA) and abduction angle (pKAbA) and moment (pKAbM) were identified within a 50 ms window following initial contact [5]. Only the straight-up condition was analyzed for this study.

Linear mixed models were used to test for a main effect of trial type on pKFA, pKAbA, and pKAbM; 'subject' was defined as a random effect. Where a main effect was found, post-hoc pairwise comparisons were done using Tukey HSD tests. Significance was set at $\alpha = 0.05$.

Results and Discussion

There was a main effect of condition on pKFA ($F=12.98$, $p<.001$) and pKAbM ($F=3.08$, $p=.023$; **Table 1**). Post-hoc comparisons indicated that participants completed the **Aud, Aud_Fix**, and **Vis** conditions with less pKFA than the **Base**. Participants completed the **Aud** and **Aud_Fix** conditions with less pKFA than the **Fix** condition. Participants also completed the **Vis** condition with greater pKAbM than the **Base**. There was no main effect of condition on pKAbA ($F=0.19$, $p=.945$; **Table 1**).

Preliminary results suggest that constrained gaze, by itself, may not appreciably influence movement performance, as no differences in landing mechanics were observed between the **Base** and **Fix** conditions. All three unanticipated conditions were associated with some form of adversely-affected landing mechanics (e.g., less pKFA, greater pKAbM) when compared to both the **Base** and **Fix**, corroborating previous assumptions that detrimental effects from unanticipated conditions are primarily driven by the inability to pre-plan movement rather than the visual constraint that is often present with how the tasks are presented. The lack of difference between auditory and visual unanticipated conditions suggest that removal of the ability to pre-plan the secondary movement may dominate the changes seen in landing mechanics. Current results should be interpreted with caution, as an *a priori* power analysis found that a sample size of 35 or more participants is needed to maintain statistical power of 80%. Study enrolment is ongoing.

Significance

Competitive sport places a large demand on an athlete's visual system to provide key information for navigating their environment. However, the effects of visual constraints used in a lab setting have yet to be systematically decoupled from common unanticipated testing paradigms. This study seeks to delineate the contributions of visual constraints and unanticipated movements to adverse changes in injury-relevant knee mechanics.

Acknowledgments

This material is based upon work supported by the NSF Graduate Research Fellowship under Grant No. W7834.

References

1. Almonroeder *et al* (2018), *JOSPT*, **48**(5): 381-7
2. Ford *et al* (2005), *J Strength Cond Res*, **19**(2): 394-9
3. Marx *et al* (2001), *Am J Sports Med*, **29**(2): 213-8
4. Herman and Barth (2016), *Am J Sports Med*, **44**(9): 2347-53
5. Krosshaug *et al* (2007), *Am J Sports Med*, **35**(3): 359-67

Table 1: Kinematic and kinetic values for jump-landing mechanics (*Indicates p<.05 compared to Base, $^{+}$indicates p<.05 compared to Fix)

	Base	Fix	Aud	Aud_Fix	Vis
pKFA (°)	60.3 ± 6.4	59.3 ± 6.3	**57.1 ± 5.4*$^{+}$**	**56.8 ± 5.1*$^{+}$**	**57.8 ± 5.9*$^{+}$**
pKAbA (°)	11.1 ± 4.9	11.0 ± 5.1	11.1 ± 4.2	11.1 ± 4.6	11.4 ± 4.1
pKAbM (%BW*Height)	4.8 ± 2.2	5.7 ± 3.0	5.4 ± 2.9	5.6 ± 2.8	**6.1 ± 3.9***

HOW VISUAL AND AUDITORY COGNITIVE PERFORMANCE RELATE TO LANDING MECHANICS

Patrick D. Fischer[1], K. Hutchison[1], J. Becker[1], and S. Monfort[1]
[1]Montana State University, Bozeman, MT USA
email: *patrick.fischer2@student.montana.edu

Introduction

Cognitive performance is an important facet of anterior cruciate ligament (ACL) injury research [1] for two key reasons. Cognitive ability is related to ACL injury rates [2], and baseline cognitive performance can explain athlete-specific differences in knee mechanics during injury-relevant movements [3]. Understanding how baseline cognitive ability contributes to the change in knee mechanics elicited by secondary tasks may inform novel advances in multifaceted ACL injury risk screening.

The purpose of this study is to investigate the relationships between visual- and auditory-based measures of cognitive ability and dual-task jump-landings. We hypothesize that poorer cognitive performance will be associated with greater dual-task changes in early-stance peak knee abduction angle (pKAbA) and moment (pKAbM) and peak knee flexion angle (pKFA).

Methods

22 healthy young adults (8F/14M; 19.9±1.1yr; 1.8±0.1m; 73.3±8.5kg) have participated in the study. All scored 12+ on the Marx activity scale [4] and had no lower-extremity surgeries or recent history of lower-extremity injury or concussion.

Participants completed cognitive assessments of visual and auditory simple reaction time and attentional control. Simple reaction time tests required that participants perform a button-press after seeing or hearing a stimulus. Accuracy and reaction times were collected from attentional control tests (visual and auditory Stroop) [5]. Cognitive results were normalized into z-scores for simple reaction time (**VisRT, AudRT**), attentional control reaction time (**StroopRT**), and attentional control accuracy (**Stroop_accuracy**). Participants also completed jump-landings [4] for a baseline (**Base**) and four dual-task conditions: visual unanticipated (**VisUn**), auditory unanticipated with no visual constraint (**AudUn)** and with visual constraint (**AudUn_Fix**), and anticipated with visual constraint (**Fix**). Direction cues appeared ~250 ms before initial contact. The visual constraint for **AudUn_Fix** and **Fix** was a cross. Auditory direction cues were audio files stating "Up", "Left", or "Right". Visual direction cues were arrows pointing up, left, or right.

Motion capture and ground reaction force data were collected, and kinematic and kinetic variables were calculated using an inverse kinematics model in Visual3D. Straight-up jumps were analyzed. External joint moments were normalized to participant height and weight. pKFA, pKAbA, and pKAbM were identified within 50 ms following initial contact [6]. Dual-task costs (DTC) were calculated as a percent change in pKFA, pKAbA, or pKAbM from baseline. Stepwise linear regression examined relationships between cognitive z-scores and DTC for each dual-task condition and biomechanical variable. Significance was $\alpha = 0.05$.

Results and Discussion

Stroop_accuracy and **StroopRT** associated with pKFA DTC for the **Fix** condition. Greater attentional control associated with smaller pKFA changes during **Fix** (R^2_{adj}=42.91%, p=.004). **AudRT** and **VisRT** associated with pKAbA dual-task cost for **AudUn** (R^2_{adj}=42.34%, p=.004). Faster auditory simple reaction times associated with less pKAbA change (p=.022; **Figure 1**). Faster visual simple reaction times associated with more pKAbA change (p=.022). **AudRT** and **StroopRT** associated with pKAbA DTC for **VisUn** (R^2_{adj}=47.67%, p=.002). Faster auditory simple reaction times associated with less pKAbA change (p=.005). Greater attentional control associated with more pKAbA change (p=.039). No significant relationships were observed between cognitive z-scores and pKAbM DTC.

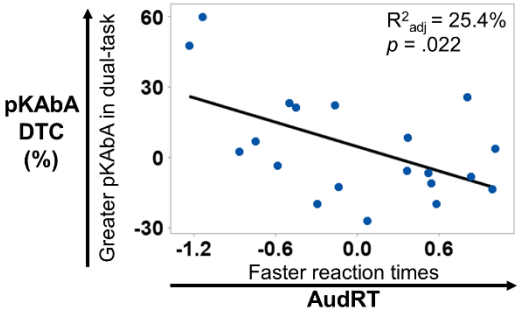

Figure 1: Faster auditory reaction times associated with less dual-task effect of auditory unanticipated condition on pKAbA.

The findings in **Figure 1** suggest that, for a purely auditory secondary task, improved ability to quickly process auditory information necessitates smaller adaptations in early-stance landing strategy. The current findings support that attentional control has a task-specific role in cognitive-motor function. Better overall attentional control performance had a 'protective' role regarding pKFA for **Fix** condition, but **Stroop_RT** had the opposite relationship for pKAbA during **VisUn**. Taken together, these results tentatively suggest that attentional control abilities may not sufficiently mitigate dual-task effects past a certain threshold of cognitive demand. Study enrolment is ongoing; findings will be updated when the full n=35 dataset is available.

Significance

Determining the most salient cognitive processes for predicting athlete-specific cognitive-motor function may provide a more comprehensive approach for injury risk screening. This ongoing project aims to contribute to this larger goal by elucidating the relevance of facets of reaction time and attentional control for jump landings with simultaneous visual and auditory challenges.

Acknowledgments

This material is based upon work supported by the NSF Graduate Research Fellowship under Grant No. W7834.

References

1. Shultz *et al.* (2019), *J Athl Train*, **54**(9): 970-84
2. Swanik *et al.* (2007) *Am J Sports Med,*, **35**(6): 943-8
3. Herman and Barth (2016), *Am J Sports Med*, **44**(9): 2347-53
4. Marx *et al* (2001), *Am J Sports Med*, **29**(2): 213-8
5. Stroop (1935), *J Exp Psychol*, **18**(6): 643-62
6. Krosshaug *et al* (2007), *Am J Sports Med*, **35**(3): 359-67

LOWER EXTREMITY NET JOINT MOMENT AND FORCE CONTRIBUTIONS IN RELATION TO DROP JUMP PERFORMANCE

Jessica Julian, Nayun Ahn, and Kristof Kipp
Department of Physical Therapy, Marquette University, WI, USA
email: jessica.julian@marquette.edu

Introduction

Jumping performance is an important performance aspect for high-level basketball players. Repeated jumping, in particular, is important in several situations (e.g., rebounding), and depends on effective use of the stretch-shortening cycle (SSC). Performance of the SSC, in turn, depends in part on the peak ground reaction forces (GRF) produced during jumping tasks [1,2]. From a sports performance and training perspective, knowledge about the joint-specific contributions to peak GRF could help identify specific targets for training interventions that aim to optimize SSC function and maximize jumping performance [3].

The vertical drop jump (DJ) is a task often used to test SSC performance as it requires an athlete to optimize muscle pre-activation in preparation for landing as well as during the eccentric phase as they get ready to immediately reverse movement directions and propel themselves upwards again [2,5]. In addition to identifying joint-specific contributions to peak GRF during the drop jump in basketball players, comparing these contributions between players who exhibit higher and lower DJ performance may further help improve training strategies to optimize muscle-specific SSC function and improve jump performance. The purpose of this study was to compare hip, knee, and ankle biomechanics at the instant of peak GRF during the drop jump in male and female athletes with different jumping abilities.

Methods

Eight male and eight female NCAA Division 1 basketball players performed three DJ from a height of 30.5 cm. Kinematic data from 26 lower body and torso markers were collected with a motion capture system at 100 Hz. Kinetic data were collected at 1000 Hz from two force plates. All data were filtered with a fourth-order low pass filter at a cut off frequency of 13 Hz. An inverse dynamics analysis was used to calculate sagittal plane net joint moments (NJM) at the ankle, knee, and hip joints. Sagittal plane contributions from each NJM to the vertical GRF were calculated with an induced acceleration analysis (IAA) [4]. The NJM and IAA-based contributions at the instant of peak vertical GRF were extracted for analysis (Figure 1). Peak GRF, NJM and IAA-based contributions were normalized to body mass. The jump height during the DJ was calculated from the vertical velocity of the center of mass at take-off. All data were averaged across the three trials from each player.

Data from the four male and female players with the greatest and lowest DJ heights in regard to their sex were allocated into groups of high (HPJ) and low (LPJ) performance jumpers (HPJ), respectively. DJ height, peak GRF, NJM, and IAA-based contributions of the HPJ and LPJ groups were then compared.

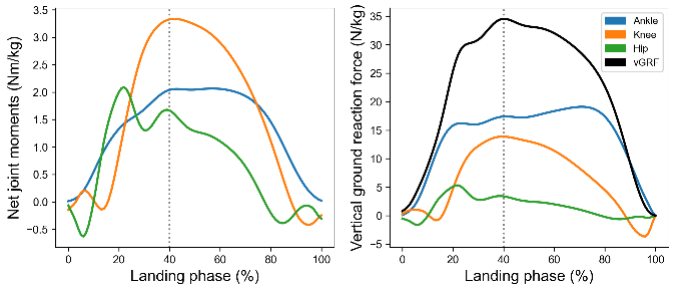

Figure 1: (Left) Net joint moments and (right) vertical ground reaction force (vGRF) and net joint moment contributions to vGRF. Note: dotted vertical line indicates instant of peak vGRF.

Results and Discussion

DJ heights were statistically significant different between the two groups (Table 1). In addition, the players in the HPJ group exhibited greater knee NJM at the instant of peak GRF than players in the LPJ group.

The observed group differences suggest that male and female basketball players who generate greater knee extensor NJM at the instant of peak GRF are also able to jump higher. Interestingly, despite the greater observed knee extensor NJM in the HPJ group, the relative contributions of the knee extensor NJM to peak GRF did not differ from the LPJ group. This discrepancy may highlight important differences between the roles of absolute magnitudes of the NJM and their IAA-based contributions to GRF with respect to functional performance, especially since peak GRF did not differ between groups,

Since greater knee extensor NJM are also purported to be a risk factor for some musculoskeletal injuries (e.g., ACL injuries), further studies may need to evaluate the associations between NJM and jump performance in the context of these injuries.

Significance

Male and female basketball players who generate greater knee extensor NJM at the instant of peak GRF exhibit greater DJ heights, which may be relevant for sports science or sports conditioning specialists.

References

[1] Bosco et al. (1982). *Acta Phys Scand* 111, 135-140.
[2] Barker et al. (2018). *J Strength Cond Res* 32, 248-254.
[3] Ford et al. (2009). *J Strength Cond Res* 23, 1327-1331.
[4] Joao et al. (2013). *J Mech Med Biol* 13, 1350027.
[5] Pedley et al. (2017). *Strength Cond J* 39, 36-44.

Table 1: Drop jump (DJ) height (m), peak vertical ground reaction forces (N/kg), lower extremity net joint moments (NJM – N·m/kg) at peak vertical GRF, and induced acceleration (IAA) based contributions (%) to peak vertical GRF for high (HPJ) and low performance jumpers (LPJ).

	DJ Height	Peak GRF	Ankle NJM	Hip NJM	Knee NJM	Ankle – IAA	Hip – IAA	Knee – IAA
HPJ	0.338 ± 0.048	37.9 ± 11.5	2.24 ± 1.01	2.31 ± 0.60	2.57 ± 0.78	64 ± 12	11 ± 10	25 ± 8
LPJ	0.258 ± 0.062	33.2 ± 5.2	1.60 ± 0.74	2.62 ± 1.21	1.70 ± 0.84	61 ± 14	17 ± 15	22 ± 6
p-value	**0.012**	0.319	0.167	0.531	**0.045**	0.698	0.402	0.418

Effects of Tolerance Value on Sample Entropy for Postural Control in Military Populations

Emma San Martin[1], Christian Witkop[1], Scott Monfort[2], Nathan Henry[1], Donald Goss[3], and Gregory Freisinger[1]
[1]United States Military Academy – West Point; [2]Montana State University; [3]High Point University
Email: gregory.freisinger@westpoint.edu

Introduction

To make timely decisions in training and combat, it is critical to develop methods for rapidly assessing the health and readiness of soldiers. However, military readiness is difficult to quantify, and it is not well understood which signals or metrics are both measurable and relevant to performance. Previous studies have found that, in combination, linear and nonlinear metrics calculated from center-of-pressure (COP) data during static postural control may provide a relevant estimate of neuro-muscular function [1]. However, no study has used nonlinear metrics to assess postural control in military populations.

Sample entropy (SampEn) reflects the regularity of a time-varying data set, in our case providing insight into COP data measured during standing balance. Lower SampEn values may reflect "over-management" of balance, indicating a degradation in neuromuscular function [2]. The tolerance value, *r*, used to determine the window size for vector matching may significantly distort output SampEn and interpretation of results [3]. However, the lack of a normative set of SampEn, calculated with a selection of *r*-values, has left the effect of this parameter on analyses of military population data sets unsettled.

Thus, the objective of this study is twofold: (1) to establish a normative set of SampEn values across a range of *r*-values during balance conditions in a healthy military population, and (2) to observe the effect of changing *r*-value on calculation of SampEn.

Methods

242 individuals (176 male:66 female, 18.8±2.4yrs;1.8±0.2m; 75.6±9.5kg) participated in the IRB-approved protocol. COP position data were collected during a Sensory Organization Test (SOT) with six conditions on a NeuroCom Balance Master [Natus, Pleasanton, CA], each a combination of platform fixed/sway-referenced, visual surround fixed/sway referenced, and eyes open/closed. COP position data were collected at 100 Hz for three twenty-second trials for each condition and downsampled to 50 Hz [2].

After removal of incomplete tests, 4459 trials were analyzed. SampEn of unfiltered data for the increment of the resultant COP position for each condition was calculated four times, at r=0.1, 0.2, 0.3, and 0.4. SampEn was averaged across trials for each participant and aggregated by condition number. The template length (m) was set to m=3 for all scenarios, representing the length of each vector to be compared for similarity within the given tolerance [2][3]. The time series were demeaned and normalized to unit variance prior to the SampEn calculation.

Results and Discussion

Mean and standard deviation for each condition and tolerance are summarized in Table 1. Histograms for SOT Condition 1 (eyes open; fixed platform and surround) are shown in Figure 1.

As *r* increases, both mean value and standard deviation of SampEn tend to decrease. The same trend was observed for SOT Conditions 2-6, which have been omitted here due to space. This result parallels observations by Yentes et al. 2021, who discuss how altering the size of the tolerance window by adjusting *r* can affect the number of matches found during vector comparison, altering the output SampEn. As *r* decreases, the window size grows smaller, lowering the probability of a vector match, and thus increasing SampEn [3].

Table 1: Sample entropy means and standard deviations for SOT Conditions 1-6 at four different tolerance values

	r = 0.1	*r* = 0. 2	*r* = 0.3	*r* = 0.4
	Mean ± STD	Mean ± STD	Mean ± STD	Mean ± STD
Cond. 1	2.65 ± 0.23	1.96 ± 0.10	1.59 ± 0.08	1.33 ± 0.07
Cond. 2	2.59 ± 0.23	1.94 ± 0.12	1.56 ± 0.10	1.29 ± 0.10
Cond. 3	2.54 ± 0.24	1.91 ± 0.14	1.53 ± 0.12	1.26 ± 0.12
Cond. 4	2.38 ± 0.24	1.73 ± 0.18	1.35 ± 0.17	1.09 ± 0.15
Cond. 5	2.12 ± 0.22	1.46 ± 0.19	1.09 ± 0.17	0.85 ± 0.16
Cond. 6	2.16 ± 0.24	1.52 ± 0.21	1.14 ± 0.19	0.90 ± 0.17

Significance

This is the first study to establish a normative dataset of SampEn during an SOT for a military population. This work identifies the effect of varying tolerance on calculated values, and provides a baseline for comparison to future datasets using the same protocol. This allows for more precise examination of the effect of prolonged physical activity on SampEn. Because SampEn depends on a number of factors, including *r*, it is important to use a consistent *r*-value when calculating SampEn for comparison between different data sets, and report this value along with findings. A limitation of this study is that all participants were cadets at the United States Military Academy and these results may not accurately represent other populations.

Acknowledgments

No funding to disclose.

References

[1] Ashtiani et al. (2017) Acta Neurobiol Exp 77 (1): 168-175
[2] Roerdink et al. (2011) Hum Mov Sci 30: 203-212
[3] Yentes et al. (2021) Annals of Biomed. Eng. 49: 979-990

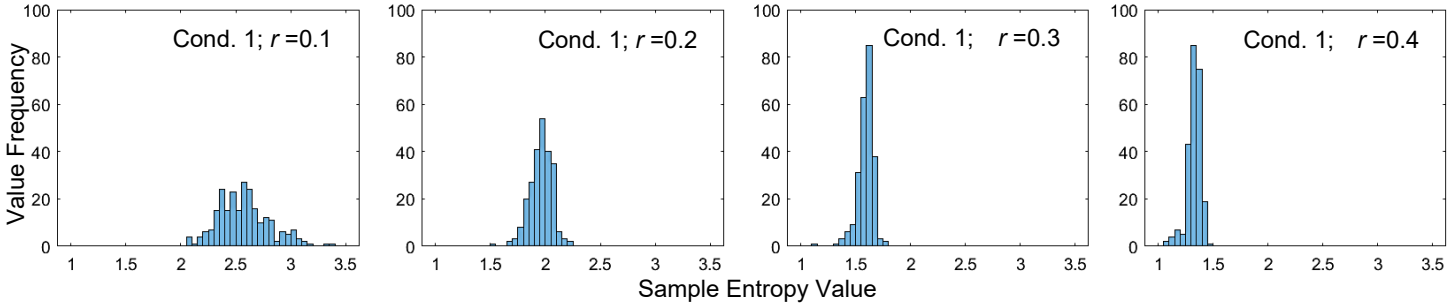

Figure 2: Histograms for sample entropy values for SOT Condition 1, as calculated using graduated tolerance values (0.1, 0.2, 0.3, 0.4). Both the variance and the mean value decrease as the tolerance increases.

WHY I PARTICIPATE IN NATIONAL BIOMECHANICS DAY

Paul DeVita[1], J. Aeles[2], B. Row Lazzarini[3], T. Darkenwald[1], A. Zaferiou[4], and S. Landry[5]
[1]Dept. of Kinesiology, East Carolina Univ., [2]Univ. of Nantes, [3]Willamette Univ., [4]Stevens Institute of Technology, [5]Acadia Univ.
email: devitap@ecu.edu

Introduction

Biomechanics creates our understanding of biology in the physical world, the physical nature of life (1). One could reasonably argue there is not a more valuable scientific endeavor. Yet, despite this significance, Biomechanics remains in a nascent state. It has yet to fully break through into our society's consciousness. Indeed, we are often neglected in STEM despite the fact that Biomechanics is the combination of all things STEM. This predicament is at least partially due to the fact that Biomechanics is poorly positioned in the world of education. Biomechanics is largely shuttered within post-graduate programs that remain unknown to most people.

National Biomechanics Day (NBD) was created in 2016 to counteract this situation and to increase the influence and impact of Biomechanics on our society by expanding the awareness of Biomechanics among young people. Over the past 5 years and through the participation of over 900 biomechanics faculty and students, NBD has with great enthusiasm and fun, introduced biomechanics to nearly 30,000 high school students around the world. Here we describe why biomechanists participate in NBD through the stories of 5 faculty members in 3 countries.

Jeroen Aeles

In only a handful of years since its inauguration, NBD has expanded globally and taken the biomechanics world by storm. NBD raises awareness of biomechanics through outreach events for high school students inspiring young minds to pursue an education and a career in any biomechanics-related field. While holding true to its original goal, NBD has grown to so much more and it has great potential to break through barriers, educating and motivating teenagers of any sex, color, and social class. By being a free event in locations worldwide, by a truly diverse and motivated group of scientists, its reach has gone far beyond typical stand-alone science outreach events. In a time that could one day be described as pivotal in fighting social injustice, raising racial and gender awareness, and prioritizing inclusiveness, NBD becomes more important than ever to showcase education and career opportunities in biomechanics and STEM for *all*. NBD provides a fun, informative tool to inspire the next generation of scientific leaders. Let's take every effort to make sure they are in Biomechanics.

Brandi Row Lazzarini

I participate in NBD because it inspires my students, our visitors and me! I usually invite schools in the region that traditionally do not have access to our college campus, including the Oregon School for the Deaf and students from local low-income schools. My students demonstrate various biomechanics measurement activities, and I see in them a new spring in their step as a result of being trusted with this leadership role. I've made a pandemic adjustment this year that has become quite meaningful. My students met on Zoom with a local high school class to generate ideas for lab projects and are now creating videos demonstrating how to address their curiosities about human movement using biomechanical methods. Our high school partners now see a career path in an exciting and growing scientific field. My students are inspired by having this audience provide a real-life purpose for their projects. This approach will remain a feature in my future, in-person NBDs, where we can all enjoy everyone's smiles.

Teal Darkenwald & Antonia Zaferiou

NBD has become more than a day to celebrate all that is biomechanics. It is a day that brings people together from around the world and highlights many facets of the field including growing areas such as dance biomechanics. NBD enables undergraduate and high school dance students to engage each other and opening their eyes to the possibilities in the field of dance science. This serves as an important educational moment, broadening the scope of careers beyond graduation. Many dance students have expressed interest in pursuing careers in dance science as a result of these engaging events. We highlight the technologies used in biomechanics through interactive displays using motion capture, surface electromyography (e.g., Triceps and Biceps student choreography challenges) and force sensors. Through these experiences, we encourage students to imagine how these technologies can be used for creative and scientific purposes. It is the interdisciplinary nature of these events that prove to be most effective because it allows dancers to view themselves as scientists opening a new world of study. Enjoy this dance science video and these NBD dance-science materials.

Scott Landry

I participate in NBD to introduce young students to the fascinating world of biomechanics and to the sophisticated yet "fun" technologies we use to study human movement and also to share relatable stories about the impactful work being carried out by colleagues and friends throughout Canada and beyond. I am inspired to see how inquisitive young students are about the application of biomechanics in developing footwear, for example or about the technologies used to study joint replacement or osteoarthritis, a debilitating disease many of these students see in their parents or grandparents. Each visiting student can relate some aspect of their life to biomechanics, eg, a previous injury or how their muscles produce the movements required for their favorite activities. Fun competitions are important aspects of our NBDs and we enjoy seeing youngsters competing with each other and their teachers in activities quantifiable with our instruments. NBD is a very important initiative that not only introduces young students to the wide breadth of research in our field, but just as importantly, introduces these students to the strong sense of family and community that has been established within our societies worldwide over the years.

Everyone

Through our and everyone's efforts, we are all moving Biomechanics to become the Breakthrough Science of the 21st Century!

References

1. 1) Why National Biomechanics Day? JoB, 2018, 1-3.

The Effect of Cognative Loading on Landing Mechanics in Division II Collegiate Female Basketball Players

Erin Schneider, Issac Fisher, Sara Teske, Morgan Frank, and Mostafa A. Hegazy
Southwest Minnesota State University
email: Mostafa.hegazy@smsu.edu

Introduction

Typical landing mechanics studies involve stepping off a box in laboratory settings. Stepping off a box has been shown to be different than landing from a jump (Afifi & Hinrichs, 2012). Thus, more researchers are now investigating landing from countermovement jumps. However, when investigating landing mechanics experienced by certain athletes, such as basketball players, a laboratory setting may still not be ideal. Being in a laboratory setting, participants' cognitive load is different from those during game situations for two reasons:1) Real game conditions are absent. 2) The need to land on a force plate creates its own task specific cognitive load.

With the introduction of insole force sensors, landing mechanics can be studied in real game situations. A first step would be to study landing kinetics on the court during basketball tasks, prior to introducing a real game situation.

Methods

Fourteen right-handed female NCAA DII collegiate basketball players (age: 20.97±0.98 yr.; mass: 74.94±7.4 kg; and height: 174±6.13 cm) participated in this study. Loadsol insoles (Novel, Munich, Germany) were inserted into participants' shoes to measure ground reaction forces during landing. Participants shot three-point shots under 3 shooting conditions: No defender (ND), Simulated defender (an object set to their reach height, D), Simulated defender after receiving a pass (PD). Participants performed 3 shots for each condition, from three different spots (right corner, left corner, top of key) making up a total of 27 shots.

Two-way ANOVA with repeated measures compared peak ground reaction force (GRF) and peak loading rates with condition and position as the independent variables.

Results and Discussion

Participants experienced greater right peak ground reaction forces for PD compared to ND ($p<0.05$; Figure 1). They also experienced greater right peak load rate for PD and SD compared to ND ($p<0.05$; Figure 2). Altered mechanics caused by cognitive load may lead to increased injury risk resulting from higher ground reaction forces and loading rates (Schnittjer et al., 2021). The more complex the cognitive load, the greater the change (Schnittjer et al., 2021).

In our original design of the study, participants would have taken shots in the presents of a defender as well as shots during an actual game. However, due to Covid-19 restrictions, the protocol was changed to use a simulated defender. Despite these changes, an increase in cognitive load led to an increase in peak GRF and peak loading rates on the right side. The more complex the cognitive element, the great the increase in both dependent variables. In a real game situation, players are not only concerned with the shot but also rapid changes in their surroundings, including the presents of a mobile defender. Thus, we can hypothesize that adding these elements would only lead to an increase in the kinetic variables. In addition to studying real game situations, future studies should also investigate the differences in other populations, such as males, who are known to experience less injuries than females as well as different levels of women sports. Higher levels such as DI or professional basketball would increase the cognitive element, however, there would also be an increase in the level of performers.

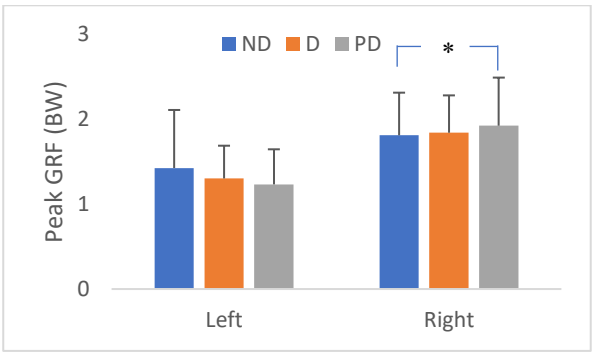

Figure 1: Peak ground reaction force without a defender, with simulated defender, and pass with simulated defender. * indicates $p<0.05$.

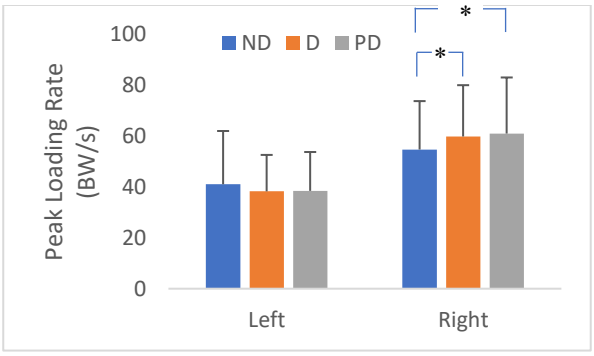

Figure 2: Peak loading rate without a defender, with simulated defender, and pass with simulated defender. * indicates $p<0.05$.

Significance

With the increase in number of female athletes participating in basketball, there is also an increase in the number of injuries associated with jump landing. Thus, many teams participate in different injury prevention programs. However, most prevention programs are focused on strength, balance, coordination, and controlling the core without considering the cognitive element (Swanik et al., 2007). It is possible that adding a cognitive element to injury prevention programs may improve their efficacy, however, this should be further investigated.

Acknowledgments

We would like to thank the Southwest Minnesota State University Women's Basketball Team for participating in our study.

References

Afifi, M., & Hinrichs, R. N. (2012). *J. Appl. Biomech*, 28(1), 1-9.

Schnittjer, A. et al. (2021). *Int. J. Sports Med*, 42(01), 90-95.

Swanik, C. B. et al. (2007). Am J Sports Med, 35(6), 943-948.

DOES THE MUSCLE OR THE TENDON DICTATE ANKLE STIFFNESS DURING MOVEMENT?

Kristen L. Jakubowski[1], Daniel Ludvig[1], Sabrina S.M. Lee, and Eric J. Perreault[1]
[1]Department of Biomedical Engineering, Northwestern University
Email: kristen.jakubowski@northwestern.edu

Introduction

Appropriate regulation of muscle and tendon impedance is central to safe and economical ambulation as they are the primary determinants of ankle impedance. Joint impedance decreases during movement compared to postural conditions [1]. However, it remains unknown how changes in muscle and tendon impedance contribute to this decrease. Filling this gap is important for understanding the respective roles of muscle and tendon impedance in safe and efficient locomotion. Therefore, this study aimed to determine how muscle and tendon contribute to ankle impedance between posture and movement. Tendon impedance is proportional to force, and to our knowledge, there are no data suggesting that it would vary between force-matched posture and movement conditions. In contrast, muscle impedance differs not only between posture and movement, but also between concentric and eccentric contractions [2]. Thus, we hypothesize that the decrease in ankle impedance during movement is driven by decreased muscle impedance.

Methods

Four healthy young adults were seated with their right foot rigidly secured to a rotary motor, which was instrumented to measure ankle torque and displacement. Participants completed two different tasks: a torque-matched task where the force on the tendon is matched since tendon impedance depends on force; and an EMG-matched task where activation in ankle plantarflexors is matched since muscle impedance is sensitive to activation. Participants produced voluntary plantarflexion torque or plantarflexor EMG at 15% of their maximum with the aid of real-time visual feedback. Plantarflexor EMG feedback was the normalized mean of the EMG from the medial and lateral gastrocnemius and soleus. Visual feedback of the tibialis anterior EMG was provided to prevent co-contraction. The motor moved the subject's ankle through a 20-degree sinusoidal motion at 0.5 Hz to create periods of concentric and eccentric contractions. The sinusoidal ankle motion is similar to ankle kinematics during walking [3]. Four isometric angle-matched conditions were also tested (Fig 1a). Small stochastic perturbations were superimposed on the large sinusoidal movement and isometric conditions to quantify ankle impedance [4]. B-mode ultrasound of the medial gastrocnemius muscle-tendon junction was used to track muscle and tendon displacement. We estimated ankle, muscle, and tendon impedance from the collected data using time-varying system identification [4, 5]. Here we present the stiffness component of these impedances. Linear mixed-effects models were used for all statistical analyses.

Results and Discussion

Across all angles, during the torque-matched task, the average ankle stiffness decreased by 44% during movement compared to the isometric contractions ($p=0.005$; Fig 1b). Similarly, during movement, the average muscle stiffness decreased by 61% compared to isometric contractions ($p=0.007$; Fig 1c). Surprisingly, we also observed a decrease in the average tendon stiffness of 23% during movement compared to isometric contractions ($p=0.002$; Fig 1d). During the torque-matched task, muscle activation differed between isometric and movement conditions, which may be contributing to the observed differences in stiffness. To control for this confounding factor, participants completed the EMG-matched task. During the EMG-matched task, we observed similar decreases in ankle, muscle, and tendon stiffness between posture and movement. The muscle was 2.8x and 3x stiffer than the tendon during isometric contractions for both torque- and EMG-matched tasks, respectively. The large decrease in muscle stiffness during movement decreased this ratio. Muscle was 1.4x and 1.7x stiffer than the tendon during each task, respectively. Since the more compliant component limits ankle stiffness, these results indicate that the tendon determines ankle mechanics during posture, but the muscle and tendon contribute more evenly during movement.

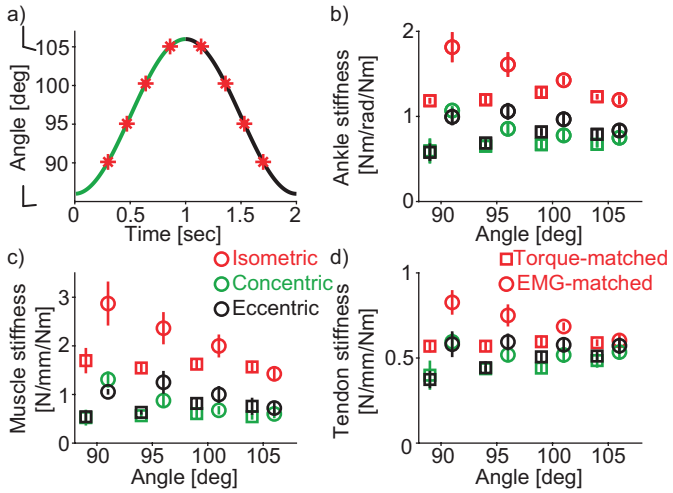

Figure 1: (a) During the movement condition, ankle angle was varied to produce concentric (green) and eccentric (black) contractions. Isometric contractions at matched angles were performed (red *). Comparisons between ankle (b), muscle (c), and tendon (d) stiffness during the concentric, eccentric, and isometric contractions for both the torque feedback (□) and the EMG feedback (o) tasks. The tasks are offset for ease of viewing. The error bars are the standard error across subjects.

Significance

These data are the first *in vivo* measurements on how muscle and tendon individually contribute to ankle impedance between posture and movement. We demonstrate that the respective roles of the muscle and tendon differ between posture and movement and that these differences cannot be attributed to differences in torque or muscle activation. These results must be considered when examining how the muscle and tendon dictate ankle impedance to enable safe and efficient locomotion.

Acknowledgments

Supported by NIH F31AG069412 and ASB GIA

References

[1] Ludvig et al (2017) *Exp Brain Res* **235**: 2959-2970.
[2] Ettema and Huijing (1995) *J. Biomech.* **27**: 1316-1368.
[3] Kadaba et al (1990) *J. Orthopaed. Res.* **8**: 383-392.
[4] Ludvig et al (2012) *IEEE Trans Biomed Eng* **59**: 3541-3549.
[5] Jakubowski et al (2020) *Eng. Med. Biol. Soc. Ann.* 4819-4822.

COORDINATION VARIABILITY PREDICTS PEAK PATELLOFEMORAL LOADING DURING RUNNING

Allison J. Hoffee[1], Scott Monfort[2], and James Becker[1]
[1]Department of Health and Human Development, [2]Department of Mechanical and Industrial Engineering, Montana State University, Bozeman, MT, USA
Email: james.becker4@montana.edu

Introduction

While running is one of the most popular forms of physical activity in the world, it is plagued with high rates of overuse injuries like patellofemoral (PF) pain. This pain is often attributed to increased PF joint stress [1]. However, the mechanism of injury associated with PF joint stress has yet to be resolved. Some hypothesize that a reduction in coordination variability (CV) may help to explain this mechanism [2]. This theory suggests that reduced CV may increase loading imposed on specific tissues over time, leading to injury. Contrary to this, recent studies have shown that injured populations display greater CV rather than reduced CV [3]. These discrepancies in literature press for the discernment of CV and tissue loading due to their relationships with injury. Therefore, the purpose of this study was to establish the relationship between PF loads and CV during running. It was hypothesized that runners with smaller amounts of CV would also display greater PF loads.

Methods

Sixty-four healthy individuals ran for five minutes on an instrumented treadmill while kinematics and kinetics were recorded. Twenty consecutive gait cycles were extracted for analysis. Data were smoothed, filtered, and normalized to 100% of stance. Knee flexion, shank internal rotation, and rearfoot eversion were then calculated. CV was calculated for each coupling as the orientation of a vector between two time points from the right horizontal for knee-shank, shank-rearfoot, and knee-rearfoot couplings [3]. Mean CV over stance for each coupling was determined. Six PF metrics were calculated using previously described musculoskeletal models that account for co-contraction of the knee flexors with custom MATLAB code [4] (Table 1). A principle component analysis was performed for PF metrics and factor loadings were interpreted to create surrogate variables. Multiple regressions were performed to determine whether CV determined PF loading surrogates.

Table 1. Mean (± standard deviation) coordination variability (CV) metrics (K-S: knee-shank, K-R: knee-rearfoot, S-R: shank-rearfoot) and patellofemoral (PF) metrics (KE: knee extensor, Imp: impulse).

CV Metrics (°)		PF Metrics	
K-S	5.42 ± 1.40	KE Moment (Nm/kg)	1.07 ± 0.33
K-R	5.10 ± 1.54	Contact Force (BW)	4.21 ± 1.34
S-R	9.03 ± 2.84	Joint Stress (MPa)	5.82 ± 1.43
		Loading Rate (MPa/s)	145.24 ± 70.86
		Imp (MPa*s)	0.56 ± 0.15
		Imp per km (MPa*s/km)	253.20 ± 71.45

Results and Discussion

Descriptive statistics for CV and PF metrics are shown in Table 1. Two principle components were extracted for PF: 1) a peak loading component and 1) a cumulative loading component. A model containing knee-shank and knee-rearfoot CV predicted peak PF loading ($R^2 = 0.285$, $p < 0.001$). For every one-degree increase in knee-shank CV, peak PF loading decreased by 4.15 units after accounting for knee-rearfoot CV ($p = 0.016$, 95% CI -7.5 – -0.8, Figure 1a). For every one-degree increase in knee-rearfoot CV, peak PF loading decreased by 4.79 units after accounting for knee-shank CV ($p = 0.003$, 95% CI -7.9 – -1.7, Figure 1b). No CV metrics predicted cumulative PF loading.

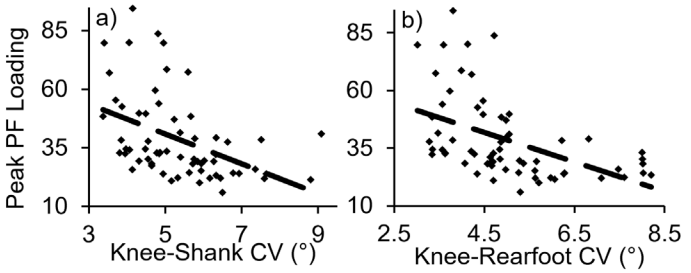

Figure 1. Peak patellofemoral (PF) loading surrogate values with respect to **(a)** knee-shank CV (°) and **(b)** knee-rearfoot CV (°).

The hypothesis was partially supported as individuals with reduced CV displayed greater peak PF loading. However, CV did not predict cumulative PF loads, which contests previous theories. This may be explained by injury thresholds. Overuse injuries may develop from small amounts of load accumulating over a large amount of time or large loads in short amounts of time [5]. With reduced CV, tissues are repeatedly loaded in a similar manner. In other words, the frequency of loading within the tissue increases. Therefore, the combination of high loads and high frequency due to reduced CV may be of more consequence to the development of overuse injuries than CV leading to increased cumulative loading. Additionally, the driving factor of CV was the knee, where both couplings including the knee predicted peak loading. This amplifies the importance of relative motion, as discrete kinematic measures like peak knee flexion or peak rearfoot eversion may not be adequate when assessing overuse injuries.

Significance

This is the first study that directly assesses the relationship between CV and internal loading during running. While it does not support the theory that reduced CV leads to increased cumulative loading, it does support the idea that reduced CV may lead to increased injury risk due to the relationship to high peak PF loads.

Acknowledgments

This project was funded by the Ellen Kreighbaum Movement Science Laboratory Endowment at Montana State University.

References

1. Farrokhi, S. (2011). *Osteoarthr Cartil* **19**(3):287-94.
2. Hamill, J. (2012). *Sport Med Arthrosc Rehabil Ther Technol* **4**(1):45.
3. Desai, G. (2020). *J Sports Sci* **39**(1):38-47.
4. Willy, R. (2016). *J Ortho Sport Phys* **46**(8):664-74.
5. Hreljac, A. (2005). *Phys Med Rehabil Clin N Am* **16**(3):651-67.

LOWER EXTREMITY STIFFNESS IN PREVIOUSLY INJURED VS. UNINJURED FEMALE ATHLETES

Abigail Jacobs[1], Jacob Larson[1], Michael Zabala[1]
[1]Department of Mechanical Engineering, Auburn University, Auburn, AL, USA
Email: zabalme@auburn.edu

Introduction

Many of the injuries sustained by athletes in contact sports are noncontact soft tissue injuries. These injuries primarily occur during deceleration and change of direction movements, such as cutting or landing [1]. Leg stiffness is important to understanding deceleration during these events and why injury may occur. This is because an individual's leg stiffness contributes to both performance and risk of injury, with an optimal stiffness value being associated with greater athletic performance and too little stiffness being indicative of risk of future soft tissue injury [2]. This study evaluated data which characterized lower limb stiffness during tests designed to resemble potential noncontact injury events, with the aim of determining whether stiffness differences existed between previously injured and uninjured subjects. The hypothesis of this study was that previously injured subjects would demonstrate different knee stiffness than uninjured subjects during both a cutting and jump landing task.

Methods

This study analyzed the kinematics of run to cut (RTC) and LESS jumps from fifteen female subjects who participated in D1 soccer, D1 basketball, or club soccer teams at Auburn University (170.4 ± 7.4 cm, 66.4 ± 7.6 kg, 19.9 ± 1.7 yrs). All subjects were cleared to participate in their respective sport at the time of data collection. Out of the 15 athletes, six had previously repaired knee injuries, and nine did not have any previous knee injuries. Each subject signed informed consent forms approved by the Auburn University Internal Review Board. For all subjects, both legs were grouped as injured or uninjured based on the subject injury designation. Knee and hip height were calculated using the virtual joint centers as provided by Visual3D. Change in knee and hip joint height was calculated as the difference between height at peak vertical ground reaction force (VGRF) during the task and during a passive standing trial. Leg stiffness was evaluated as the peak VGRF divided by the change in hip height [3]. Injured and uninjured subjects were compared using paired t-tests using SAS software version 9.4.

Results and Discussion

The results of this study failed to confirm the hypothesis in that there was no significant difference in stiffness between previously injured and uninjured subjects for either task (Table 1). However, there was a trend of greater limb stiffness in the uninjured group during the RTC (p=0.09). During RTC, the injured population was found to have a significantly reduced change in knee height and significantly reduced ankle dorsiflexion, consistent with the trend towards increased stiffness. Conversely, during LESS jumps the injured population exhibited a greater change in knee height, reduced knee flexion, and greater ankle dorsiflexion compared to the uninjured population.

Table 1. Comparison of stiffness components between injured and uninjured groups in RTC and LESS tasks, where the differences are calculated as (previously injured – uninjured metric).

	RTC		LESS	
	Mean Diff	p	Mean Diff	p
Stiffness (N/m)	2454.1	0.09	-4494.4	0.16
Hip Height Δ (m)	-0.021	0.23	0.031	0.077
Knee Height Δ (m)	**-0.044**	**0.001**	**0.027**	**0.008**
Knee Flexion (º)	0.559	0.89	**-11.68**	**0.024**
Ankle Dorsiflexion (º)	**-12.2**	**0.03**	**10.93**	**0.021**
GRF Zmax (N)	64.72	0.50	-85.30	0.520

One of the most noticeable findings in this study is that while previously injured subjects show a reduced change in knee height and reduced ankle dorsiflexion during a cutting motion, they reversed these tendencies during a jump landing. Also, although previously injured subjects showed reduced knee flexion during LESS, they demonstrated a greater change in knee height, likely due to the increased dorsiflexion.

Significance

As this study is cross-sectional in nature, it is impossible to determine whether these differences in stiffness and kinematics between previously injured and uninjured subjects are responsible for knee injury or were developed as a result of injury. However, these results do suggest that future studies should continue to evaluate stiffness component contributions during dynamic movements to explore whether the differing strategies for the previously injured group are linked to the well-documented increased risk of re-injury.

References

[1]Gabbett TJ, 2010; **24**:2593-2603. *J.Strength & Conditioning Research.*
[2] Butler RJ, Crowell HP III, & Davis IM, 2003; **18**:511-517. *Clinical Biomechanics*
[3] Lorimer AV, Keogh JWL, & Hume PA, 2018; *PeerJ* 6:e5845

BIOMECHANICAL EFFECTS OF FOOT PLACEMENT DURING BASEBALL PITCHING

Jonathan S. Slowik[1], Alek Z. Diffendaffer[1], Ryan L. Crotin[2], Megan S. Stewart[1], Karen Hart[1], and Glenn S. Fleisig[1]
[1]The American Sports Medicine Institute (ASMI), Birmingham, Alabama and [2]The Los Angeles Angels, Anaheim, California
email: jons@asmi.org

Introduction

Rear and front foot placement may be among the easiest baseball pitching parameters to modify through coaching, as previous research has shown that it is easier to modify mechanics near the beginning of the delivery than near ball release [1]. Coaches commonly target foot placement to improve pitch accuracy, ball movement, and velocity, but it is unknown how changing foot position affects the rest of the pitcher's biomechanics [e.g., 2]. Therefore, the purpose of this study was to determine the effect of rear and front foot placement on pitching biomechanics. We hypothesized that differences in foot placement would affect (1) kinematics, especially those related to the rotation of the pelvis and trunk; and (2) elbow and shoulder kinetics. In particular, we expected a 'cross-bodied' (3B-Closed group, defined below) or 'excessively open' (1B-Open) would have higher kinetics than deliveries with foot placement directed more towards home plate (i.e., 1B-Closed and 3B-Open).

Methods

This was a retrospective review of biomechanical data of 325 healthy right-handed collegiate and professional baseball pitchers collected and processed at ASMI between 2013 and 2020 using methods previously described [e.g., 3]. The global coordinate system was located at the center of the pitching rubber, with a vertical Z-axis, X-axis pointing toward home plate, and Y-axis a cross-product of Z and X. Rear foot position (RFP) was defined as the Y-position of the rear ankle at the time of maximum front knee height; thus, a positive/negative value denoted a pitcher on the 1B/3B side of the rubber. Front foot position (FFP) was defined as the foot's Y-position at foot contact, relative to the RFP (i.e., the Y-difference). A positive/negative value denoted a closed/open foot position.

The pitchers were sorted into three RFP groups: 1B, 3B, and a middle-rubber buffer group that was discarded. The two remaining groups (1B and 3B) were each divided into three FFP subgroups: open, closed, and a middle buffer group (discarded). This resulted in four groups of 36 pitchers each: first base open (1B-Open), first base closed (1B-Closed), third base open (3B-Open), and third base closed (3B-Closed).

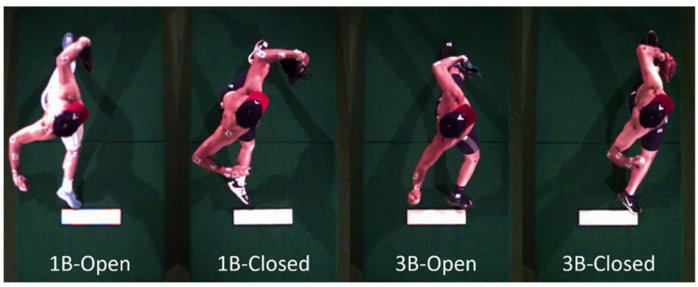

Figure 1: Example pitchers illustrating the four groups in this study.

To determine if foot placement affected pitching biomechanics variables, a 2x2 statistical design (1B vs. 3B; Open vs. Closed) was employed. An ANOVA was used for normally-distributed data, while the closest non-parametric equivalent (Scheirer–Ray–Hare) was used otherwise. In the case of a significant interaction effect, pairwise comparisons were performed using t-tests (parametric) or Mann-Whitney U tests (non-parametric) with a Bonferroni adjustment for multiple comparisons ($\alpha = 0.05$). Clinical significance was evaluated using effect size $r = Z/\sqrt{N}$, where Z is the statistical test's Z-score, and N is the total sample size, and categorized as trivial ($r<0.2$), small ($0.2\leq r<0.5$), moderate ($0.5\leq r<0.8$) or large ($r\geq 0.8$).

Results and Discussion

Pitchers with an open front foot position had less shoulder abduction at the time of ball release ($p<0.001$, $r=0.252$) and greater maximum shoulder internal rotation velocity in comparison with closed pitchers ($p=0.017$, $r=0.209$). Open FFP pitchers also had less forearm pronation at the time of ball release ($p=0.012$, $r=0.197$) and greater maximum elbow extension velocity ($p=0.025$, $r=0.186$), although those two results were categorized as trivial, not quite reaching the small effect threshold. Additional statistically significant results were found; however, extremely low effect sizes ($r\leq 0.13$) cast doubt on their clinical significance.

The hypothesis that foot placement would lead to differences in pitching kinematic parameters, especially those related to the rotation of the pelvis and trunk, was partially supported. While we found kinematic variables with statistically significant findings, only two of them (trunk separation and upper trunk tilt at the time of foot contact) were related to the pelvis and trunk, and both of those had trivial effect size values.

The hypothesis that differences in foot placement would be related to kinetic differences was not supported by our results, as the only two statistically significant results found in the kinetic variables were interaction effects with trivial effect sizes. This lack of significant main effects or pairwise comparisons for any of our kinetic variables was surprising, as a previous study [4] found that open pitchers had higher shoulder anterior force, and we expected that kinetics would be affected by rear foot placement as well. Consequently, despite our expectations, we cannot suggest that any particular placement of either the rear foot or front foot may be more stressful than others.

Significance

Overall, the results of this study suggest that while differences in foot placement between groups of pitchers affect pitching kinematics, the clinical significance of these differences are small or trivial. Furthermore, this study did not support the concept that foot placement affects injury risk, as differences in elbow and shoulder kinetics were few and trivial. It should be noted that this study compared four different groups of pitchers categorized by their self-selected foot placement, which they may have instinctively optimized over years of pitching experience. Future research should use a within-pitcher design to examine the effects of intentional modifications to self-selected foot placement.

References

1. Fleisig GS, et al. *Sports Biomechanics* **17**, 314–321 (2017).
2. Davis JT et al. *AJSM* **37**, 1484–1491 (2009).
3. Escamilla RF et al. *J Applied Biomech*, **34**, 377–385 (2018).
4. Fleisig GS. *The biomechanics of baseball pitching* (Doctoral dissertation-UAB, 1994).

REAL-TIME GAIT PREDICTION WITH TWO SENSORS FOR SEMI-ACTIVE PROSTHESIS CONTROL

J. Liu[1], P. Adamczyk[2]
University of Wisconsin–Madison
email: [1] jliu798@wisc.edu [2] peter.adamczyk@wisc.edu

Introduction

The human lower limb behaves differently under various types of locomotion. It is vital for a prosthesis to adjust accordingly for best performance. Existing research includes real-time classification of falls and detection of gait phase[1,2] and of gait mode for control of transfemoral prostheses using prosthesis sensors and electromyographic signals[3,4]. For semi-active prostheses, early prediction of gait mode (e.g. level, ramps, stairs) is important so the device can pre-adapt to the impending stance phase. Here we demonstrate an algorithm to predict gait mode among level ground, up ramp, down ramp, up stairs and down stairs at the end of the first half of the swing phase.

Methods

Experiment: Four subjects with unilateral transtibial amputation walked with a variable-stiffness prosthesis[5] in each of three stiffness settings over an indoor course containing the five types of terrain, all hard smooth surfaces in an academic building. Subjects wore a suite of inertial measurement units (IMUs; XSens MVN Biomech) with sensors on the pelvis and on both thighs, shanks, and feet. The system recorded movement data at 60-100 Hz and its built-in gait reconstruction was used to compute orientation of every sensor; further analysis used custom processing code. One subject's data are the basis for this abstract, with other processing to follow.

Prediction: Data from the low-stiffness condition were used to train a gait mode prediction algorithm, which was then tested on data from the high-stiffness condition. Support vector machine (SVM) was selected as the classification algorithm in this project and the training data comes from sensors on the right foot and right shank. To make the training set, we first separated the data into strides. For each stride, we took the first half of swing phase and computed the three-dimensional velocities and positions of all three directions with respect to the prior footfall using strapdown integration of IMU data [5]. We also calculated pitch and roll from the orientation information, but excluded yaw (heading) to eliminate inappropriate world-frame information. We formed a training data sample for one stride as ten consecutive samples of acceleration, velocity, position, roll and pitch yielding 50 features. Each swing-phase sample was associated with the terrain of the following stance phase, so the classifier would be useful for real-time prediction. We trained a model with SVM for each direction (x, y and z) of each sensor (shank and foot) so there are six classifiers in total. Since the training data are not linear, a cubic kernel function is applied to foot data and a quadratic kernel function is applied to shank data. The predictors were subjected to 5-fold cross-validation with the training set, shown in Table 1.

Table1: 5-fold cross validation (CV) result for all data sets.

Sensor	Direction	Kernel Function	CV accuracy
Foot	x	Cubic	87.0%
Foot	y	Cubic	94.4%
Foot	z	Cubic	96.0%
Shank	x	Quadratic	88.9%
Shank	y	Quadratic	93.0%
Shank	z	Quadratic	97.0%

In the testing phase, the acceleration data are first put into a buffer to detect the beginning of a new swing phase. Once it detects, the collected data are pushed to the classifiers. To reduce the effects of false prediction, if at least two classifiers for foot and shank predict a level ground motion, the prediction of this sample would be level ground; otherwise it will be the most-predicted motion type among all sensors. Within one step, the locomotion is determined by the most classified type within all samples in the swing phase. The whole prediction uses a fixed number of samples from the start of swing phase so a prothesis responding to it would have time to adjust before the next stance.

Results and Discussion

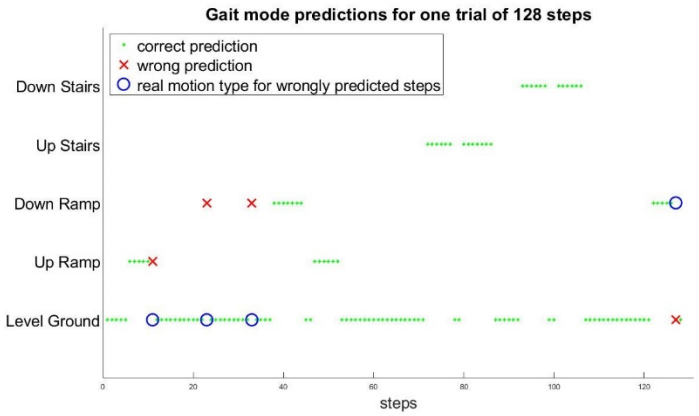

Fig 1: Gait mode predictions for one trial of 128 strides.

The result of one test (128 strides) is shown in Fig 1. Generally, the overall accuracy is 96.8% (124/128). The accuracy of prediction in transition steps is 87.5% (14/16). For both stair motions, the accuracy is 100%. All misprediction occurs in ramp motions and there are no consecutive mispredictions. Because of the different prosthesis stiffness condition in the testing set vs. the training set, the accuracy in real practice could be even higher. An alternative classification using only the foot IMU also gives 124/128 correct predictions with all errors at transitions; classification with only the shank is much worse.

Significance

The result demonstrates that a reliable prediction of locomotion can be generated in real-time while the person is walking. With this information, the prosthesis can adjust automatically and does not need user input. Compared with other motion classification method, it can have a valid result earlier. Also, two sensors are used, which means it does not require a complicated sensing system. This technique could be applied to any assistive device that has periodic leg motion and needs to change configuration under different circumstances.

References

[1] Vu et al 2020 *Sensors* [2] Altun et al 2010 *Patt Rec* [3] Huang et al 2011 *IEEE TBME* [4] Young et al 2013 *IEEE TNSRE* [4] Ojeda et al 2007 *J Nav* [5] Glanzer et al 2018 *IEEE TNSRE*

KNEE BIOMECHANICS WHILE DISRTACTED WHEN NEGOTIATING A SLICK STAIR

Nicholas L. Hunt, Amy E. Holcomb, Christina M. Geisler, Clare K. Fitzpatrick, and Tyler N Brown
Center for Orthopaedic and Biomechanics Research, Dept. of Kinesiology, Boise State University, Boise ID USA
Email : nichunt@u.boisestate.edu

Introduction

An accidental fall often has a significant economic and physical burden for individuals 65 years and older. Up to 40% of older adults fall annually during activities of daily living, such as stair negotiation, often resulting in serious musculoskeletal injury.[1] Older adults fall risk may be attributed to the gait strategies they adopt to compensate for the reductions in strength, balance, and vitality that occur with age. Negotiating stairs requires greater muscle strength and knee joint range of motion compared to level walking, and may further increase older adult fall risk from age-related physical decline.[2] Additionally, if an older adult has to negotiate a slick stair or is distracted from carrying objects (i.e., dual-tasking) it may further exasperate their fall risk.[3] Yet, it is unclear if negotiating slick stairs while distracted results in compensatory changes for older adults. We hypothesized, to stabilize the lower limb and reduce fall risk, that older adults will exhibit a greater change in knee joint biomechanics while distracted on a slick stair compared to young adults.

Methods

Eighteen adults (10 young: ages 18-25 years; 8 older: over 65 years, with at least one accidental fall in the past 12 months) participated. Each participant performed a stair ascent task on a slick surface with and without cognitive distraction task. For the stair ascent, each participant performed three trials at a self-selected pace, where they stepped up a set of stairs (18.5 cm rise). For the slick surface, a low-friction surface was fixed to the top of the stairs and participants wore booties over their shoes. For the cognitive distraction, each participant performed a serial subtraction task, i.e., counted backwards by 3 from a random number provided at the beginning of each stair ascent trial.

During the stair ascent, synchronous 3D marker trajectories and GRF data were collected using ten high-speed optical cameras (240 Hz, Vantage, Vicon Motion Systems LTD, Oxford, UK) and a single force platform (2400 Hz, OR6, AMTI, Watertown, MA). For each trial, the marker and GRF data were lowpass filtered (12 Hz, 4th order Butterworth), and then processed in Visual 3D (C-Motion, Rockville, MD) to obtain 3D stance phase knee joint angles and moments.

For statistical analysis, peak stance (0%-100%) knee flexion and adduction joint angle and moment were submitted to a two-way RM ANOVA to test the main effects and interaction between distraction (undistracted vs distracted) and age (young vs old). For significant pairwise comparisons a Bonferroni correction was used and all statistical analysis was performed in SPSS (v25, IBM, Armonk, NY). Alpha level was $p < 0.05$.

Results and Discussion

Significant distraction by age interactions for peak knee flexion ($p = 0.023$) and adduction ($p = 0.029$) joint moment were observed (Fig. 1). But, no significant effect of distraction or age was evident for peak knee flexion or adduction angle ($p > 0.05$).

In contradiction to our hypothesis, the young adults exhibited a significant 5% reduction in peak knee flexion moment when distracted ($p = 0.009$), whereas, the older adults exhibited non-significant 2% increase in peak knee flexion moment when distracted. Although older adults may increase knee flexion moment to prevent a fall when distracted, the young adults may possess the neuromuscular function to reduce fall risk when ascending slick stairs, regardless of distraction, as their peak knee flexion moment was between 8-16% larger than the older adults. However, this increase was not significant ($p > 0.05$).

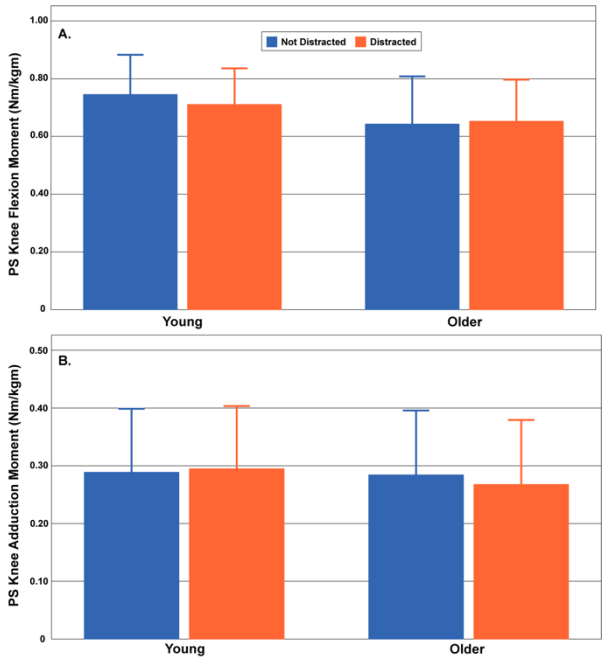

Figure 1: Mean ± SD peak stance knee flexion (**A**) and adduction (**B**) moments (N.m/kg.m) with and without distraction for both young and older adults during the stair ascent.

In partial support of our hypothesis, the distraction task led to a significant 6% reduction in older adults' peak knee adduction moment ($p = 0.031$), but no significant change for young adults ($p = 0.358$). When ascending a slick stair, older adults may adopt cautious gait biomechanics and reduce knee adduction moments to protect the knee from injury.

Significance

Negotiating stairs is a routine activity of daily living that may lead to an accidental fall when individuals have compromised neuromuscular function. Older adults may adopt knee biomechanics to prevent a fall or reduce risk of injury when distracted, while young adults may possess neuromuscular function that reduces fall risk when ascending slick stairs, regardless of distraction.

Acknowledgments

This study was supported by an award from NIH National Institute on Aging (R15AG059655).

References

1. Ambrose et al., *Maturitas* **75**, 2013.
2. Tiedemann et al., *J. of Gerontology: Med Sci* **62**, 2007.
3. Vallabhajosula et al. *J. Biomech* **48**, 2015.

IN VIVO KINEMATICS OF TOTAL WRIST ARTHROPLASTY

Bardiya Akhbari[1], Kalpit Shah[2], Amy Morton[2], Douglas Moore[2], Arnold-Peter Weiss[2], Scott Wolfe[3], and Joseph Crisco[1,2]
[1]Brown University, Providence, RI, [2]Rhode Island Hospital, Providence, RI, [3]Hospital for Special Surgery, New York, NY
email: bardiya_akhbari@brown.edu

Introduction

Total Wrist Arthroplasty (TWA) is a surgical solution for severe wrist arthritis, reducing pain while maintaining some of the function of the joint. However, TWA designs suffer from high complication rates. Currently, there is little, if any, data available on TWA functional kinematics *in vivo*. Much is known about the kinematics of healthy wrists, which have motion envelopes oriented obliquely to the standard anatomical axes. It is unknown if the TWA designs maintain this oblique axis *in vivo*.

The goal of this study was to determine the kinematics of a single TWA design (Freedom®) in patients. Because the Freedom® arthroplasty has an ellipsoidal joint design, we anticipated that its motion would be optimized along its geometric axes. A previous study by Singh has demonstrated that the orientation of the functional axis of a TWA is less oblique compared to the healthy wrist (12 ± 4° compared to 25 ± 15°) by studying the previous generation of Freedom® implants [1]; thus, we hypothesized the functional axis of the TWA design is significantly different from the healthy wrist.

Methods

6 TWA subjects (74.7 ± 5.6 yrs, 2 females) with >6 months follow up (average 22 ± 12 months), and 10 controls (57.0 ± 5.2 yrs, 8 females) provided informed consent. A CT scan (80 kVp and 80mA; 0.39mm × 0.39mm × 0.625mm image resolution) of each studied wrist was acquired to generate three-dimensional models for motion analysis. Both groups were asked to perform wrist flexion-extension, radial-ulnar deviation, and circumduction. Biplanar videoradiography (BVR) was used to capture the 3rd metacarpal, radius, carpal component, and radial component motion at 200 Hz (65-75 kV and 80 mA; continuous). Each task was performed for 2 seconds resulting in 6 seconds of total capture or 1,200 biplane radiographs per subject. The wrist motion was reported as the motion of the 3rd metacarpal with respect to the radius. The detailed description of data acquisition procedure, guidelines for each task, and data processing has been reported in previous works [2].

A 2D-histogram was used to depict all possible wrist motions for both groups (**Figure 1**).

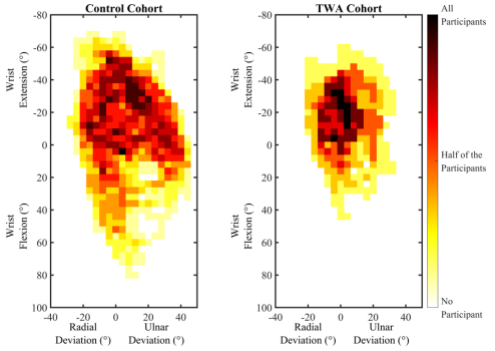

Figure 1: Summary kinematics of the wrist motion of all subjects

To evaluate the overall behavior, the main direction of motion of the anatomical tasks was calculated using principal component analysis (PCA). Pure axis of flexion-extension was set at 0°, and pure radial-ulnar deviation was set as 90°. The orientation and area of the circumduction's envelope were calculated by fitting the best ellipse to the envelope using the least-squares criterion. One-way ANOVA was used (α=0.05) to evaluate the differences between the functional axis' orientation for both groups.

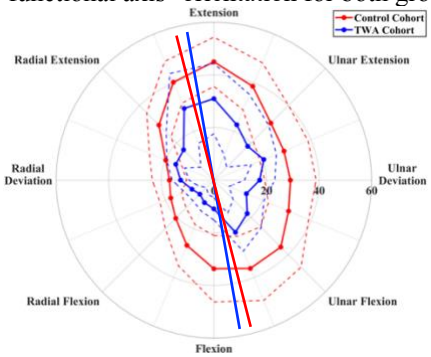

Figure 2: The envelope of circumduction task.

Results and Discussion

The direction of the flexion-extension axis (-4.0 ± 9.3 vs. -7.8 ± 8.3, $p<0.44$) was not different between the groups nor the 0° assigned for the pure axis of flexion-extension. However, the principal axis of motion for the radial-ulnar deviation was significantly different between the two groups (65.2 ± 8.1 vs. 48.2 ± 15.0, $p=0.01$), and compared to the 90° pure radial-ulnar deviation ($p<0.001$).

The orientation of the envelope of the circumduction task (18.8 ± 9.8 vs. 13.0 ± 10.3, $p>0.99$) was not significantly different between the controls and the TWA patients (**Figure 2**). When comparing the principal axes of motion during the circumduction task, which has been used in the past to describe the principal axis of motion for the wrist, both the controls and the TWA patients were significantly oblique (18.8 ± 10.2 and 13.0 ± 10.3 vs 0°; $p<0.05$ for both). The controls' oblique axis of motion was not significantly different to the finding presented in a previous robotics study that described a 26.6° orientation [3]. Lastly, the TWA group demonstrated an approximately 65% reduced area of circumduction compared to the controls ($p<0.05$).

Our study indicates that the orientation of the circumduction's envelope is oblique to the anatomic directions and the implant's axes. This is surprising given more-recent TWAs are designed to optimize motion along the orthogonal axis of flexion-extension and radial-ulnar deviation. The mismatch between the design and behavior may lead to high stress in certain portions of the implant. More subjects and implant designs have to be studied to assure this behavior is universal among all designs.

Significance

The data we provide shows a need for a TWA device that is designed for optimizing and maintaining the wrist's functional axis. This data can also be used to derive future robotics studies.

Acknowledgments

This research was funded by NIH P30-GM122732 and AFSH.

References

[1] Singh, 2017. *doi:* 10.1177/1753193417690472.
[2] Akhbari, 2021. *doi:* 10.3791/62102.
[3] Crisco, 2011. *doi:* 10.2106/JBJS.I.01222.

LEARNING-BASED 3D HUMAN BODY RECONSTRUCTION FROM MULTI-VIEW CAMERAS

Soyong Shin[1]* and Eni Halilaj[1,2,3]
[1]Department of Mechanical Engineering, Carnegie Mellon University, Pittsburgh, PA, USA
[2]Department of Biomedical Engineering, Carnegie Mellon University, Pittsburgh, PA, USA
[3]Robotics Institute, Carnegie Mellon University, Pittsburgh, PA, USA
email: *soyongs@andrew.cmu.edu

Introduction

Computer vision approaches present a promising alternative to marker-based motion capture, which is laborious, requires expensive equipment, and constrains capture to laboratory environments. Single-view algorithms for two-dimensional (2-D) joint center detection, such as OpenPose [1], are starting to be translated to biomechanics applications, but they suffer from occlusions and inability to reconstruct 3-D kinematics. Multi-view methods use geometric triangulation to reconstruct 3-D pose from multi-view cameras, but accuracy is highly dependent on the number of cameras. To improve the accuracy of these approaches, we propose to combine geometric triangulation with learning from ground truth 3-D pose data. Leveraging a parametric body model [2] and features learned from multiple views, our framework resolves both rotation ambiguity and occlusion, surpassing prior vision-based 3-D pose and shape estimation algorithms.

Methods

Meshed Statistical Body Model. To reconstruct 3-D pose, we used a parameterized 3-D human body model—SMPL—which is a body mesh represented by a differentiable function, $\mathcal{M}(\theta,\beta)$, that maps pose $\theta \in \mathbb{R}^{24\times3}$ and shape $\beta \in \mathbb{R}^{10}$ parameters to a triangulated body mesh $M \in R^{6890\times3}$ [2]. The pose parameters include 24 joints, while the shape parameters represent the 10 dimensions of greatest variability in human body shape, learned from large body-scan data.

Algorithm Overview. First, we encoded multi-view images I_i, $(i = 1,\cdots,4)$ into 2-D feature maps, f_i^{2D}, using 2-D convolutional neural networks (CNN). Second, we generated empty 3-D grids, V_i, in a global coordinate system and filled each grid with the 2-D feature map from the same view using a back-projection algorithm. Then, a softmax operation was used to aggregate 3-D grids into a single volume, V_{aggr}, that contains information from all the views. The aggregated volume was then fed into a 3-D CNN and final fully connected layers to estimate SMPL parameters $\Theta^{\text{reg}} = \{\theta^{reg}, \beta^{reg}\}$. Finally, the 3-D human body was reconstructed using the SMPL function: $M^{reg} = \mathcal{M}(\theta^{reg}, \beta^{reg})$. The reconstructed body mesh can be mapped to 3-D joint centers X^{reg}. The entire network was trained by comparing it against ground-truth joint centers X^{gt} (Fig. 1).

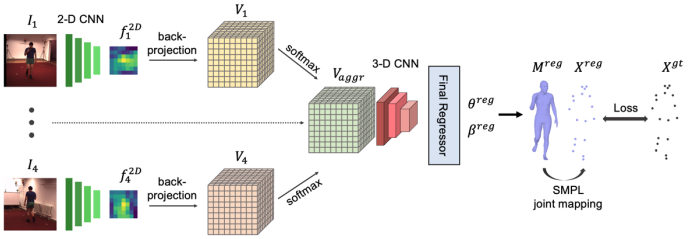

Figure 1. **Algorithm Overview.** Images from calibrated cameras are encoded by a 2-D CNN, and the encoded features are aggregated into a single volume using back-projection. The 3-D human body is reconstructed using a 3-D CNN and a final regressor network to estimates the SMPL (meshed body model) parameters.

We report a quantitative evaluation of our model against marker-based motion capture data using a canonical dataset—Human3.6M [3], with *Mean Per Joint Position Error* (MPJPE) as an evaluation metric. We compare our algorithm to the prior state-of-the-art in multi-view algorithms using 4 cameras.

Results and Discussion

Our model improves the prior state-of-the-art performance by nearly 10% across joints. The MPJPE was 35.2 *mm* for the ankle, 31.5 *mm* for the knee, and 27.6 *mm* for the hip. A qualitative evaluation of the same 3D human body reconstructed using a single part-occluded image and 4 cameras illustrates the advantages of multi-view algorithms (Fig. 2).

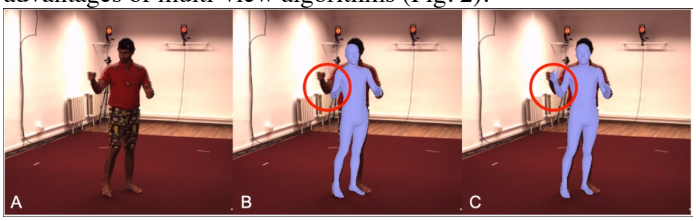

Figure 2: **Qualitative Evaluation.** A) Input image for the single-view model, B) prediction from the single-view model, C) prediction from the multi-view model. Red circles show how the multi-view model benefits from different views.

Significance

By leveraging a statistical body model, our model can estimate not only joint centers but also 3-D kinematics of the human body. As 3-D joint kinematics are important in the context of disease progression or recovery, our approach is more appropriate for biomechanics application than methods that focus only on estimation of joint centers (e.g., simple triangulation of OpenPose). Our method resolves occlusion by using learning-based feature triangulation, which effectively fuses view-dependent information. Currently our model is trained on ground-truth joint center locations, however, not joint angles. The output joint angle is only constrained by a prior distribution obtained from large-scale motion capture datasets, such as the CMU MoCap Dataset. For this reason, the model possibly lacks physiological relevance, although the output is seemingly plausible. Our future work will focus on learning from ground truth joint angles and joint centers simultaneously, enriching pose prior datasets to be more generalizable across patients, and evaluating algorithm accuracy in the context of joint angles. Further, physics-based approaches can also be used to improve the plausibility of vision-based approaches.

References

[1] Cao et al., "OpenPose: Realtime multi-person 2D pose estimation using part affinity fields"
[2] Loper et al., "SMPL: A skinned multi-person linear model."
[3] Sminchisescu et al., "Latent structured models for human pose estimation."

ASSESSMENT OF STATIC POSTURAL STABILITY USING STABILOGRAM DIFFUSION ANALYSIS IN ACL RECONSTRUCTED INDIVIDUALS

Nathan J. Robey[1] K. Otto Buchholz[2], Shane P. Murphy[3], and Gary D. Heise[4]
[1]Western Washington University, Bellingham, WA, [2]Eastern Washington University, Cheney, WA,
[3]University of Montana, Missoula, MT, [4]University of Northern Colorado, Greeley, CO
Email: robeyn@wwu.edu

Introduction

Athletes seeking a return to sport (RTS) typically undergo ACL reconstruction (ACLR). Despite both surgical and rehabilitation interventions, the likelood of sustaining a second ACL injury on either limb remains high [1]. The increased risk of contralateral injury and the common non-contact mechanism support the hypothesis that an ACL injury may not be a simple musculoskeletal injury but rather a more complex neurological injury [2]. While ACLR restores mechanical stability, somatosensory deficits resulting from the injury may still exist even after rehabilitation and RTS [3].

Traditional center-of-pressure (COP) measures have been previously used to indicate an athlete's knee function and readiness to RTS [4]. The evaluation of COP measures provides information on general spatial-temporal measures of static postural stability but provides limited physiological meaning. Collins and De Luca proposed the stabilogram diffusion analysis (SDA) as a method to offer more physiologically meaningful results [5]. The SDA offers a unique insight into the neuromuscular control (i.e., open- and closed-loop control) system during postural stability tasks [5]. Therefore, this study aimed to evaluate differences between ACLR and healthy control (HC) individuals using SDA.

Methods

Twelve ACLR (F=7, 19.8±1.2 years, 1.71±0.09 m, 76.0±8.3 kg, 28.0±10.12 months since surgery) individuals volunteered for this study and were age and sex-matched with recreationally active HC (F=7, 21±2.3 years, 1.69±0.08 m, 68.1±12.3 kg). During each trial, participants were asked to stand barefoot in a single-limb stance with their eyes open on an AMTI force plate (Watertown, MA, USA). Ground reaction forces were captured at 1000 Hz for 30 seconds and filtered using a 4th order, Butterworth low-pass filter with a cut-off frequency of 20 Hz. SDA calculations for dependent variables were based on previous work [5]. For group comparisons, the ACLR injured limb was compared to the dominant limb of the HC group. A one-way MANOVA ($\alpha = 0.05$) was performed to identify any significant effects between groups on SDA measures (SPSS 26, IBM, USA). Significant main effects were evaluated using pairwise comparisons with Bonferroni correction.

Results and Discussion

No significant main effect between ACLR and HC groups was observed for any SDA outcome measure ($p = .424$) (Table 1). These findings were surprising as SDA has previously demonstrated group differences between HC and pathological conditions [6].

While not significant, some unique findings can be discussed based on this study's means. ACLR individuals were expected to display a right-shifted behavior similar to the HC on a compliant surface. However, ACLR individuals displayed, an opposing, left-shifted critical point, indicating an earlier transition from open- to closed-loop control. ACLR participants also had lower Δt when compared to the HC in this study, indicating an earlier transition to closed-loop control. The shift in Δt may be a compensatory mechanism for the larger D_S [6]. Previous research has suggested that increased stochastic activity (D_S) over short-term time intervals may result in more unstable behavior, leading to earlier transition times [6]. Similar behavior was observed in a previous study comparing rigid and compliant surfaces. ACLR individuals also demonstrated increased open-loop control mechanisms (H_S) compared to HC. The shifted critical points, increased D_S and H_S displayed by ACLR participants may be a maladaptive response and may decrease postural stability [6].

Significance

The findings of this study indicate no differences in motor control strategies between ACLR and HC individuals. Therefore ACLR individuals with longer times since surgery may have some level of somatosensory recovery. ACLR individuals in this study were on average 28 months post-surgery and, therefore, the somatosensory systems that support posture have been restored to a functional level to support posture demands. These findings may support the hypothesis of delayed RTS in ACLR individuals to allow for increased recovery of neuromuscular systems.

References

[1] Paterno M, et al. (2014). *Am J Sports Med*
[2] Kapreli E, et al. (2009). *Am J Sports Med*
[3] Needle A, et al. (2017). *Sports Med*
[4] Mohammadi F, et al. (2012). *Knee Surg Sports Traumatol Athrosc*
[5] Collins and De Luca (1993). *Exp Brain Res*
[6] Wuehr M, et al. (2013). *J Neurol*

Table 1. Mean and standard deviation of the SDA outcome variables

Measure	CritR2	CritDeltaT	D_S	D_L	H_S	H_L
ACLR	185.16 ± 114.84	1.22 ± 1.70	116.76 ± 64.10	5.27 ± 4.78	0.61 ± 0.10	0.14 ± 0.09
HC	174.41 ± 105.49	1.39 ± 0.92	80.69 ± 59.50	5.05 ± 5.53	0.53 ± 0.10	0.13 ± 0.08
[Robey(a)]	134	1.23	171.39	3.71	0.60	0.07
[Robey(b)]	297	1.14	71.83	4.01	0.58	0.12
[Collins(a)]	13	1.03	6.74	1.76	0.76	0.28
[Collins(b)]	19	0.92	11.21	3.05	0.76	0.34

Note: Mean values from [Collins] represent two different groups (a = 30 trials, n = 10, b = 10 trials, n = 15), mean values from [Robey] are from two different surface types (a = compliant, n = 19; b = rigid, n = 19)

EFFECT OF TRUNK AND SHANK POSITION ON HIP-TO-KNEE MOMENT RATIO

Anne L. Halverstadt, Kerri A. Graber, PT, DPT, Simone V. Gill, PhD, OT, OTR, and Cara L. Lewis, PT, PhD
College of Health and Rehabilitation Sciences: Sargent College, Boston University, Boston, MA, USA
Email: annehalv@bu.edu Web: http://sites.bu.edu/movement/

Introduction

The bilateral squat (BLS) is commonly used for both strengthening and assessing movement[1]. The best way to perform the squat has been debated with opinions ranging from a 'hip dominant' squat, through 'neutral', to a 'knee dominant' squat. A 'hip dominant' squat has a higher hip extensor moment and a lower knee extensor moment, while a 'knee dominant' squat has the reverse. The majority of the literature focuses on knee position and its effect on joint moments; however, trunk angle may also affect the distribution of moments between the hip and knee during the squat. The purpose of our study was to investigate how sagittal plane trunk angle and knee position, measured by shank angle, affect hip and knee extensor moments with regards to 'hip dominant' versus 'knee dominant' positioning. We hypothesized that increased trunk flexion would redistribute the moment from the knees to the hips, and that trunk flexion would have a greater impact on joint moments than shank angle.

Methods

As part of a larger study, BLS data were collected from 101 individuals with and without hip pain (65 female, 36 male, mean age, 25.5 ± 8.1 years, mean height 1.71 ± 0.1 m, mean weight 68.7 ± 13.0 kg). Participants were instructed to stand with feet shoulder width apart and arms out in front of them, squat down until their thighs were horizontal with the floor, and then to return to standing. No instructions were given on trunk or knee positioning.

Motion (100Hz) and force data (1000Hz) were collected. Segment angles of the trunk and shank, and joint moments for the hip and knee were calculated using Visual3D (C-Motion, Inc., Germantown, MD). A multivariate stepwise linear regression was used to predict the ratio between the hip and knee moments (hip-to-knee moment ratio) from the sagittal plane trunk and shank angle. The analysis was performed in 10° increments between 60° and 110° of knee flexion and at peak knee flexion separately.

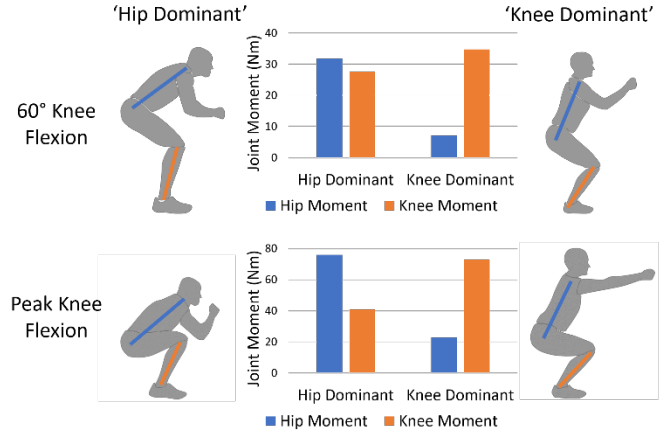

Figure 1 'Hip Dominant' squat and 'Knee Dominant' squat movement patterns and their associated distribution of hip and knee extensor moments for representative participants.

	60°	70°	80°	90°	100°	110°	PKF
TRUNK	3%	5%	**38%**	**41%**	**37%**	**35%**	**39%**
SHANK	**35%**	**40%**	6%	7%	8%	10%	12%
TOTAL	38%	45%	44%	48%	45%	45%	51%

Table 1 Variance in hip-to-knee moment ratio explained by trunk angle and shank angle at 60-110° of knee flexion and at peak knee flexion (PKF). Bold numbers represent the explained variance of the specified segment at each analysis point while non-bolded numbers represent the additional variance contributed by the other segment.

Results and Discussion

At all points of analysis, trunk angle and shank angle each contributed to the prediction of the hip-to-knee moment ratio ($p<.001$). At 60° and 70° of knee flexion, the shank angle had a greater influence on the hip-to-knee moment ratio, with shank explaining 35% and 40% of the variance respectively. Between 80° and 110° of knee flexion, the trunk had a greater influence on the hip-to-knee moment ratio, with the explained variance ranging from 35% to 41%. Mean ± SD peak knee flexion was 107° ± 16°; therefore, we only analysed points up to 110°.

These findings indicate that the influence of the trunk and shank position change over the course of the squat, with the trunk angle becoming more important as the participant nears their maximum depth. This supports the idea that trunk position may have a greater impact on hip and knee moments than originally thought, while also acknowledging the influence of shank angle and knee position on the moment ratio.

Significance

The bilateral squat is commonly used as an intervention in rehabilitation and in strength and conditioning settings. Presently, many clinicians and coaches use a cue regarding knee position to alter hip and knee joint moments. Our findings reveal that cueing individuals on their trunk position may accomplish the same goal, especially at knee flexion angles greater than 80°. This provides clinicians and coaches with greater, and potentially more effective, options for cueing and instructing their patients and clients.

Acknowledgments

Data were collected and analyzed with the assistance of members of the Human Adaptation Laboratory. Research reported in this publication was supported by the Peter Paul Career Development Professorship, the Dudley Allen Sargent Research Fund, and the National Institute of Arthritis and Musculoskeletal and Skin Diseases of the National Institutes of Health under Award Numbers R21 AR061690 and K23 AR063235.

References

1. Kritz M, Cronin J, Hume P. The bodyweight squat: A movement screen for the squat pattern. *Strength & Conditioning Journal*. 2009;31(1):76-85.

HYBRID VOLITIONAL CONTROL AS A FRAMEWORK FOR LOWER-LIMB PROSTHETIC CONTROL

Ryan R. Posh[1], J. Schmiedeler[1], P. Wensing[1]
[1]Department of Aerospace and Mechanical Engineering, University of Notre Dame, Notre Dame, Indiana
email: *rposh@nd.edu

Introduction

Realizing the potential of active lower-limb prostheses to help users increase their mobility and efficiency requires safe, reliable, stable, and intuitive control strategies. The two prevailing classes of lower-limb prosthesis control can be categorized as volitional and non-volitional. Volitional control strategies (VCs) directly sense the user's intentions, but this generally intuitive approach can be quite demanding of users, leading to fatigue and misactivation of the device. Non-volitional control strategies (NVCs) sense the state of the system instead, often taking advantage of the cyclic nature of the gait cycle to produce robust and reliable outputs. NVCs, however, do not give the user freedom to realize non-standard movements. This work proposes and analyzes a Hybrid Volitional Control (HVC) approach that operates across the entire gait cycle and seeks to balance the reliability, safety, and low demand of NVCs with the freedom and intuitive control associated with VCs.

Methods

In general, the output torque generated by an HVC is equal to the sum of the torque generated by a VC component and that generated by an NV base component [1]. The additive nature of this combination ensures that the HVC can operate independent of user input signals since any NVC, by definition, is not a function of volitional parameters. In the HVC formulation herein, the volitional control input for the HVC is thresholded in a way that freely allows volitional inputs during certain phases of the gait cycle and discourages them during others. The modular nature of HVC is explored by combining an idealized proportional VC with either a finite-state machine (FSM) impedance NVC from [2] or a continuous phase-based trajectory NVC from [3]. HVC was analyzed using an OpenSIM model of an individual with an active transtibial prosthesis, where the individual was assumed able to produce ideal volitional control inputs. Results are compared for the two configurations of HVC, the two NVCs, and the one VC, all aiming to match the able-bodied ankle torque profiles for level-ground walking from [4]. Activity modes of descending a 2.5-degree ramp, walking on level ground, and ascending a 5-degree ramp were assessed.

Results and Discussion

HVC shows an opportunity to reduce the torque error from an able-bodied reference in both cases compared to the two NVCs and to reduce the volitional demand in both cases compared to a pure VC. Compared to an NVC, HVC could reduce the RMS torque error by as much as 94%. Similarly, compared to a pure VC, HVC could reduce the volitional demands by as much as 91%. The implementation of HVC with an FSM impedance NV base controller applied across an entire gait cycle at the ankle joint is shown in Fig. 1. As the NV base controller better approximates the desired torque profile, the volitional demands from the user are reduced. Conversely, if the NV base controller does not match the desired torque well, the user would be required to provide a larger volitional input to match the desired torque. Reducing the volitional demand offers additional benefits when sensor noise is considered, since typical volition signals, such as from EMG, exhibit noise in proportion to their magnitude, requiring filtering and contributing to control delay.

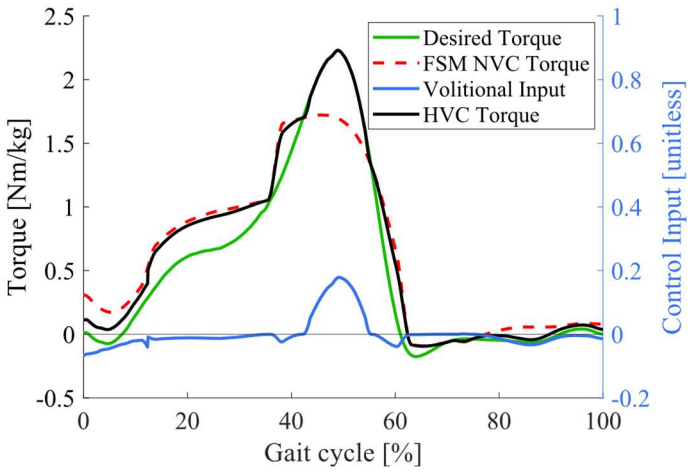

Figure 1: Idealized HVC output ankle torque for 5-degree ramp ascent using a finite-state impedance NV base controller. Volitional input is plotted on right-hand vertical axis, and desired able-bodied torque, FSM NVC torque (also representative of NV base controller), and resulting HVC torque are plotted on left-hand vertical axis. Positive/negative torques and inputs represent plantar- and dorsiflexion, respectively.

Significance

HVC has great potential to supersede the limitations of both purely non-volitional and volitional control strategies. It could allow users to ambulate reliably throughout the community with minimal volitional input, while still having continuous freedom to significantly alter the device dynamics to achieve desired unique motions. In this way, HVC could enable individuals with transtibial amputation to participate in a wider range of activities, including those that deviate from basic gait dynamics, such as marching in a marching band, standing or walking on tip-toes, and reacting quickly to the environment, which are not reliably achievable today. By safely and reliably returning the freedom of limb control to users, HVC could further erase the distinction between ability and disability from amputation.

Acknowledgments

This work is funded by National Science Foundation (NSF) grant DGE-1841556 awarded to Ryan Posh.

References

[1] R. Posh, et al., “Hybrid volitional control as a framework for lower-limb prosthetic control”, submitted to *IROS,* 2021.
[2] F. Sup, et al., “Upslope walking with a powered knee and ankle prosthesis: initial results with an amputee subject”, *IEEE Trans. Neural Syst. 19.1*, pp. 71-78. 2010.
[3] D. Quintero, et al., "Continuous-phase control of a powered knee–ankle prosthesis: Amputee experiments across speeds and inclines." *IEEE Trans. Robot. 34.3*, pp. 686-701, 2018.
[4] K. Embry, et al., "Modeling the kinematics of human locomotion over continuously varying speeds and inclines." *IEEE Trans. Neural Syst. 26.12,* pp. 2342-2350, 2018.

TOWARD TASK-LEVEL CONTROL OF POWERED LOWER-LIMB PROSTHESES

David J. Kelly, P. Wensing
email: dkelly7@nd.edu

Introduction

Ambulation is an underlying function of many activities in everyday life. Individuals with lower-limb amputations face a decreased ability to locomote in their surroundings, which can lead to a lower quality of life and the potential for secondary injuries from gait asymmetry and load compensation. Passive lower-limb prostheses help restore some mobility to users, however the inability to provide positive work for activities like climbing stairs, or actively react to perturbations prevents passive devices from fully restoring function. Powered devices have actuated joints that can provide positive work throughout the gait cycle and have the potential to react to perturbations and gait changes. Most current control schemes for powered prostheses use joint impedance control, which senses joint kinematics to set desired joint-torque commands throughout the gait cycle. However, this approach limits synergy between user and device since control actions are set from feedback isolated to the device itself.

Task-level control looks to address the disconnect between a user and their prosthesis by incorporating center of mass (COM) kinematics and angular momentum into the control scheme. Balance is a key aspect of stable walking and can be a consistent concern for prosthesis users. Previous work [1] suggested that the body's long latency response to perturbations used task-level variables for balance feedback. The use of template models offers the possibility to capture these task-level characteristics to track a person's balance while addressing the inherent complexity of human dynamics. Template models are low-dimensional systems that capture the salient aspects of real-world complex systems. Establishing a means for tracking task-level variables may open the door to understanding how desired task-level goals evolve throughout the gait cycle.

This work focuses on establishing the framework of template models for capturing task-level trajectories using able-bodied walking data. Future work will look to incorporate the framework into controllers for powered prostheses, using task-level tracking to create an explicit connection between a user and their prosthesis, promoting positive Human Robot Interaction (HRI).

Methods

COM kinematic data is collected using an XSENS MVN motion capture suit, which features 17 inertial measurement unit (IMU) sensors that are fused to generate estimates of the wearer's COM and body segment orientation. The data is collected throughout the wearer's gait cycle for a full picture of task-level evolution while walking. Initial trials focus on able bodied data to obtain a reference of desired trajectories.

The collected experimental data is used for analyzing the capabilities of task-level trajectory tracking with template models. The COM kinematic data is streamed into MATLAB for fitting with template models that are optimized using IPOPT and the CasADi framework. For human walking (Fig. 1), the template models that will be considered are the bipedal spring loaded inverted pendulum (B-SLIP) [2] and the bipedal trunk SLIP with virtual pivot point (VPP).

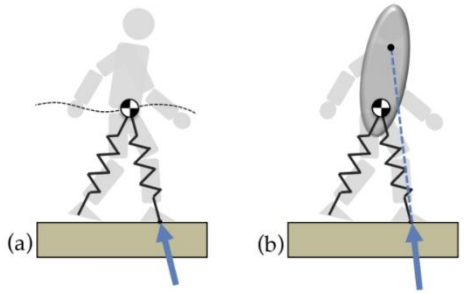

Figure 1: Template models of walking; (a) bipedal SLIP model; and (b) the bipedal trunk SLIP using the Virtual Pivot Point (VPP).

Results and Discussion

For this work in progress, able bodied data has been collected from the XSENS suit. An initial B-SLIP optimization model has been programmed in MATLAB that demonstrates the feasibility of the model without data assimilation. The XSENS data will be introduced to the model with an objective to minimize the disagreement in COM kinematics between the template model and the XSENS data. This will illustrate the ability of the B-SLIP model to capture the desired salient features of human walking.

The same process will be conducted for the VPP model. This will provide insight into whether the regulation of the upper body's angular momentum may play a role as a task-level goal throughout the gait cycle. Development of the optimized models with regard to the captured XSENS data will provide a reference point for a desired task-level trajectory.

Significance

Work done towards task-level control looks to address how incorporating COM kinematics and angular momentum into the control scheme impacts the overall stability and balance during walking. The ability of the template models to capture the trajectory of task-level goals throughout the gait cycle provides a low-dimensional reference for desired human walking. Longer term, this reference will be incorporated into the controller of a powered prosthesis [3] to reduce fall risk in a way a joint impedance controller cannot.

Acknowledgments

The authors would like to acknowledge the National Science Foundation for funding this project (NSF Grant #1943703).

References

[1] S. A. Safavynia and L. H. Ting. Long-latency muscle activity reflects continuous, delayed sensorimotor feedback of task-level and not joint-level error. *Journal of Neurophysiology*, 2013.

[2] R. Blickhan. The spring-mass model for running and hopping. *Journal of Biomechanics*, 1989.

[3] A. F. Azocar, L. M. Mooney, L. J. Hargrove, and E. J. Rouse. Design and characterization of an open-source robotic leg prosthesis. In *IEEE International Conference on Biomedical Robotics and Biomechatronics*, 2018.

LATERAL CENTER OF MASS SWAY ON SELF-PACED AND FIXED SPEED TREADMILLS IN AGING

Troilyn A. Jackson[1], Sheridan M. Parker[2], Erica A. Hedrick[2], Brian A. Knarr[2], Hao-Yuan Hsiao[1]
[1]Department of Kinesiology & Health Education, The University of Texas at Austin
[2]Department of Biomechanics, University of Nebraska at Omaha
email: troilynaj@utexas.edu

Introduction

Falls contribute to injuries and reduced level of physical activity in older adults, occurring most often during whole-body movements like walking.[1] Thus, identifying approaches that improve balance control during walking in older adults is an important goal.

Gait training using treadmills has been a safe and effective way to assist older adults who deal with ambulation deficiencies.[2] However, conventional treadmill conditions oftentimes do not resemble overground walking, and therefore may limit the ability to translate training gains to daily life walking; for example, treadmill gait trainings, which are typically performed at fixed speed (FS). Imposing a constant speed can constrain movements[3], and humans commonly show speed variations during overground walking. Recent development of self-paced (SP) treadmill controller allows variations in walking speed and offers the opportunity to better emulate overground walking while on a treadmill. During the SP condition, older adults increased their walking speeds compared to FS[4], indicating altered forward progression characteristics during SP condition. To date, how a SP treadmill affects lateral balance stability during walking remains unclear. The primary purpose of this study was to compare body center of mass (COM) lateral sway during SP versus FS treadmill conditions. In addition, we determined whether changes in lateral COM sway between treadmill conditions were coupled with changes in gait characteristics in the anterior-posterior direction.

Methods

Seventeen healthy older adults (70.24 +/- 5.25 yrs) completed two treadmill walking conditions, FS and SP, which were randomized in order. Kinematic and kinetic data were collected using a 14-camera motion capture system and an instrumented split-belt treadmill. During SP, the adaptive speed controller adjusted the belt speed in response to the force impulse, step length and duration, and the participant's position relative to the treadmill.[4] Standard deviation of whole-body COM accelerations in the medial-lateral (ML) and anterior-posterior (AP) directions were calculated to characterize lateral sway and forward/backward variability, respectively. Peak anterior ground reaction force for each gait cycle was calculated and averaged across gait cycle to characterize propulsive force. Changes across conditions were calculated by subtracting values in FS from the SP condition (Δ = SP – FS). Paired T-test was used to determine differences in COM lateral sway between conditions. Coefficient of determination (R^2) was used to determine the relationships between changes in COM lateral sway, changes in AP COM variability, and changes in peak propulsive force from FS to SP conditions.

Results and Discussion

Compared to FS, COM lateral sway was increased during SP ($p=0.02$, Fig.1). Changes in AP COM variability explained 23% of the variances in changes in COM lateral sway across conditions ($p<0.05$, Fig.2A). In addition, changes in peak propulsive force explained 48% of the variance in changes in COM lateral sway across conditions ($p<0.01$, Fig.2B). These results agree with previous literatures that reported multi-planar trunk control[5] by demonstrating that modifying treadmill conditions from FS to SP increased COM lateral sway that were coupled with COM movement and force production characteristics in the AP direction.

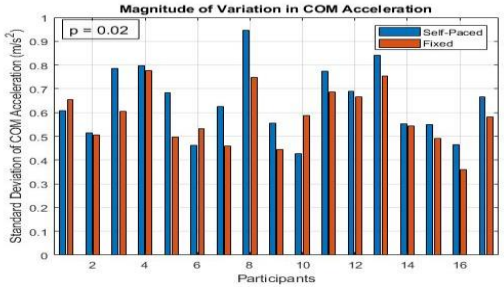

Figure 1. COM lateral sway during FS and SP conditions across all participants ($p=0.02$).

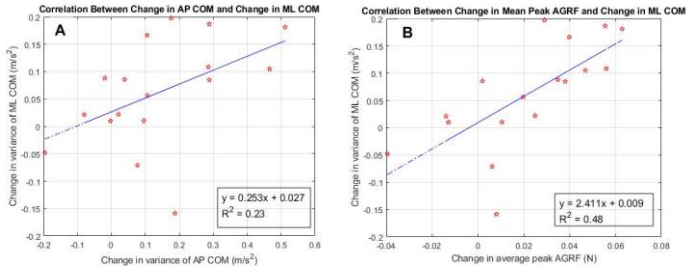

Figure 2. (A) Relationship between changes in COM lateral sway and changes in the variance of AP COM ($p<0.05$). **(B)** Relationship between changes in COM lateral sway and the changes in peak propulsive force ($p<0.01$).

Significance

Our results suggested that balance stability control in the frontal plane was affected by sagittal plane constraints. Findings warrant future investigations to determine whether additional lateral COM variances could be beneficial for gait training in older adults. Future work identifying other variables that contribute to the observed changes in variance of ML COM could also provide valuable insight on how forward progression and control of lateral balance stability are coupled during locomotion

Acknowledgments

NIH R21-AG060034, P20-GM109090, R15-HD094194, and R01-NS114282.

References

[1] Talbot, L. A. et al. (2005). *BMC Public Health*, **5**:86, 1-9.
[2] Gerards, M. H. G. et al. (2017). *Geriatr Gerontol Int*, **17**, 2294-2303.
[3] Terrier, P., Dériaz, O. (2011). *J Neuroeng Rehab*, **8**:12, 1-13.
[4] Hedrick, E. A. et al. (2021). *J Biomech*, **115**, 1-8.
[5] Shih, H.-J. S. et al. (2021). *J Biomech*, **114**, 1-9.

STEP TIME ASYMMETRY DOES NOT IMPACT METABOLIC COST IN MODELS WITH UNILATERAL WEAKNESS

Russell T. Johnson[1], Nicolas A. Bianco[2], James M. Finley[1]
[1]University of Southern California, [2]Stanford University
email: rtjohnso@usc.edu

Introduction

Many neuromuscular impairments occur after an individual has a stroke, such as muscle weakness, spasticity, overactivity, and paresis, and these impairments primarily affect one side of the body more than the other. These impairments can impact gait performance, as people post-stroke tend to walk slower than controls and display spatiotemporal and kinematic asymmetries [1,2]. However, since various combinations of these neuromuscular impairments are often present in people post-stroke, it is difficult to determine their respective contributions to gait performance. Musculoskeletal modeling and predictive simulation provide an opportunity to investigate how specific neuromuscular impairments affect gait performance.

Our aim was to quantify the spatiotemporal asymmetries and changes in metabolic cost that emerge when muscle strength is unilaterally reduced in a musculoskeletal model via predictive simulations. We also determined how the forced adoption of gaits with symmetric step times impacted the metabolic cost of walking in "healthy" gait models and models with unilateral muscle weakness. This study will allow us to better understand how muscle strength impairments affect gait asymmetry and metabolic cost, independent of other neuromuscular confounding changes that occur post-stroke.

Methods

We used a 2-D musculoskeletal model with 11 degrees-of-freedom and actuated by 24 muscle-tendon units within OpenSim and Moco [3]. The base model was then modified by uniformly reducing the peak isometric muscle force in all muscles on the left limb of the model by 20, 40, and 60 percent. This unilateral reduction in muscle strength is representative of the between-limb asymmetry in force generation often measured in people post-stroke [4].

Optimal control simulations of walking were generated at 1.25 m/s with the four different strength models for the nominal results. The objective of the optimizations was to minimize the sum of the cubed muscle excitations across all muscles divided by stride length, chosen based on its proxy to muscle fatigue [5]. After the nominal optimizations, we then added a term to the objective function that minimized the model's step time symmetry to study the effects of step time symmetry on the weakness models.

Outcome measures included asymmetry indices (Asym) for step time, stance time, and step length, and were calculated as follows:

$$Asym = \frac{X_{NW} - X_W}{(|X_{NW}| + |X_W|)}$$

Where X_{NW} is the variable for the right/non-weak limb, and X_W is the variable for the left/weak limb. Positive values of Asym indicate greater values on the right/non-weak than the left/weak side. Additionally, we estimated metabolic rate using the Umberger 2010 probe built into OpenSim. The metabolic rate was calculated while holding muscle mass constant throughout the muscle weakness model conditions.

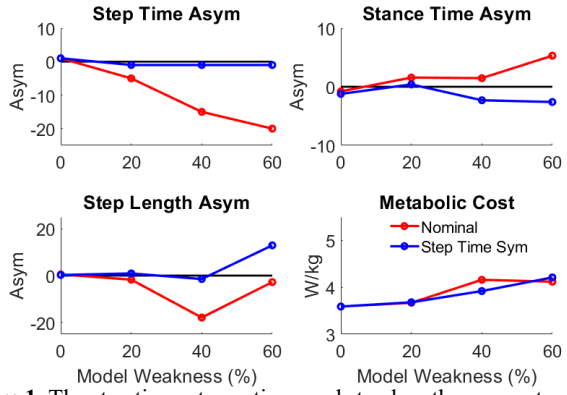

Figure 1: The step time, stance time, and step length asymmetry (Asym) and predicted metabolic rate (W/kg) for each of the model weakness conditions (0 is the base model, then 20%, 40%, and 60% left limb weakness). The red lines show results for the nominal conditions, and the blue lines show results for the symmetric step time goal.

Results and Discussion

In the nominal conditions, as the unilateral weakness was increased, the optimal solutions had greater negative step time asymmetry (greater left/weak-side step time) and greater positive stance time asymmetry. The step length asymmetry was -18% for the 40% weakness model, but the 60% weakness model had an asymmetry index of -3%. The metabolic rate gradually increased with greater muscle weakness, from 3.6 W/kg in the base model to 4.2 W/kg in the 60% weakness model.

The addition of the step time symmetry goal effectively reduced the step time asymmetry from the nominal conditions, resulting in an asymmetry index of -1% for each of the weakness model conditions. The reduction in step time asymmetry resulted in changes in stance time and step length asymmetry indices, notably changing the direction of the stance time asymmetry index from positive (greater stance time with right/non-weak limb) to negative. However, the metabolic rate followed the same pattern as the nominal conditions, gradually increasing with greater muscle weakness.

Significance

Reducing the step time asymmetry for the asymmetrical gait models had no effect on the magnitude of the predicted metabolic rate, however it resulted in different spatiotemporal asymmetries from the nominal conditions. This indicates there may be several different gait strategies that result in similar metabolic cost for individuals with unilateral muscle weakness.

Acknowledgments

Funding: NIH NCMRR R01HD091184

References

1. Olney SJ & Richards C, Gait Posture. 4, 136-148, 1996.
2. Finley JM & Bastian AJ, Neurorehab Neural Re. 31, 2. 2017.
3. Dembia CL et al., PLoS Comput. Biol. 16, 12. 2021.
4. Sanchez N et al., Neurorehab Neural Re. 31, 9. 2017.
5. Crowninshield RD & Brand RA, J Biomech. 14, 11. 1981

LONGITUDINAL EVALUATION OF WRIST JOINT KINEMATICS IN PEDIATRIC MANUAL WHEELCHAIR USERS

Samantha R. Schwartz[1], Alyssa J. Schnorenberg[1], Lawrence C. Vogel[2], and Brooke A. Slavens[1],
[1] Occupational Science and Technology, University of Wisconsin-Milwaukee, Milwaukee, WI, USA
[2]Shriners Hospitals for Children-Chicago, Chicago, IL, USA
email: slavens@uwm.edu

Introduction

Wrist pain and pathology have been directly connected to overuse injuries in manual wheelchair users with spinal cord injury (SCI). More than one third of adult manual wheelchair users report wrist pain (1). It has been found that increased time since injury is directly related to the increasing severity of carpal tunnel syndrome (CTS) (2). Though recommendations have been developed for preventing pain and pathology in adults (3), they are outdated, and there is a void in recommendations specifically for children. Children are fundamentally different than adults, both in musculoskeletal development and time spent in a wheelchair over a lifetime. Longitudinal evaluations may provide valuable insights into timing of interventions for preventing wrist pain and pathology in pediatric manual wheelchair users as they age. Therefore, this study investigated changes in wrist joint kinematics over time during pediatric manual wheelchair propulsion.

Methods

Six pediatric manual wheelchair users with spinal cord injury participated in two data collections approximately one year apart. Participants ranged from 8.6 to 19.9 years of age at the first visit and 9.4 to 21.3 years at the second visit. ASIA scores ranged from A to C with injury levels from C6 to T11. Twenty-seven passive retro-reflective markers were placed on the participant following our team's established marker set (4). A 14-camera Vicon MX motion capture system using Vicon Nexus software (Vicon Motion Systems, Oxford, UK) collected 3D kinematic data as the participant propelled their personal manual wheelchair along a 15m tile walkway at a self-selected speed and stroke pattern. Multiple trials of data were processed and filtered before applying our custom MATLAB (The MathWorks Inc., Natick, MA) inverse dynamics model to calculate and characterize wrist joint angles at two visits (4).

Results and Discussion

Wrist joint kinematics were determined for all six participants. Four of the participants increased their coronal and sagittal plane ranges of motion. The three eldest participants showed relatively large changes between visit one and visit two in the wrist coronal and sagittal plane ranges of motion (ROM), with average increases of 15.5˚ and 31.8˚, respectively, compared to 0.9˚ and 0.6˚, respectively, in the three youngest.

Studies have demonstrated that peak wrist extension greater than 33˚ and peak ulnar deviation greater than 14.5˚ elicits pressure in the carpal tunnel beyond the critical pressure threshold, indicating the potential of nerve damage that could lead to CTS (5). During the first visit, all participants were above 33˚ of extension. At the second visit, only two participants were under 33˚ of extension by an average of 2.4˚, while the remaining four exceeded this threshold by an average of 10.7˚. While none of the participants exceed the critical position for ulnar deviation at their first evaluation, four of the six exceeded it by an average of 7.4˚ at the second visit (Figure 1). These findings will likely continue to rise as the participants age and may be indicative of a high prevalence of wrist pain and pathology in pediatric manual wheelchair users.

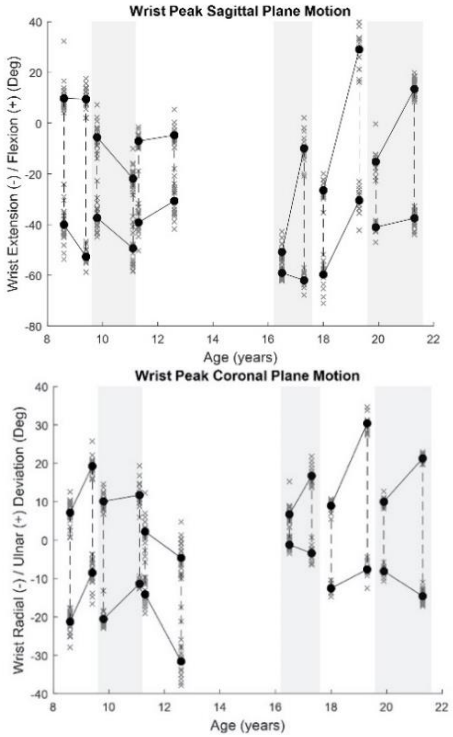

Figure 1: Each participant's average peak flexion and extension angles (top) and peak ulnar and radial deviation angles (bottom) are each represented by solid black circles for each visit, plotted by age. Average peak values within a visit are connected by a vertical dashed black line, indicating average ROM. Average peak values between visits are connected by solid black lines indicating the change in that metric. Diverging solid black lines indicate an increased ROM, while converging lines indicate a decreased ROM.

Significance

This work successfully quantified changes in wrist joint kinematics between two visits in children approximately one year apart. By investigating the changes in wrist kinematics over time in pediatric manual wheelchair users, future research may be able to help predict, intervene early, and ultimately prevent the development of wrist pain and pathology.

Acknowledgments

This work was supported by the Eunice Kennedy Shriver National Institute of Child Health and Human Development (NICHD) of the NIH (1R01HD098698) and the National Institute on Disability, Independent Living, and Rehabilitation Research (90RE5006-01-00).

References

1. Akbar et al., J Hand Surg, 39(2):132-138, 2014.
2. M. Asheghan et al., J Spinal Cord Med, 39(3):265-271, 2016.
3. Consortium for Spinal Cord Medicine, 2005.
4. A. J. Schnorenberg, et al., J Biomech, 47:269-276, 2014.
5. P. Keir et al., Hum Factors, 49(1):88-99, 2007.

LOWER EXTREMITY MUSCLE ADAPTATION TO WALKING WITH A POWERED ANKLE EXOSKELETON

C. A. Haynes[1], C. S. Poindexter[1], A. K. McGough[1,2], and J. C. Bradford[1]
[1]U.S. ARMY DEVCOM Army Research Laboratory, Human Research and Engineering Directorate
[2]DCS Contracting, Inc
email: courtney.a.haynes2.civ@mail.mil

Introduction

Locomotion is a critical task for warfighters that may benefit from augmentation, such as when walking long distances carrying heavy loads. Physical augmentation devices have been shown to augment locomotion by reducing metabolic energy consumption during locomotor tasks (Mooney and Herr 2016, Galle et al., 2013). While metabolic energy consumption is often used to determine the effectiveness of these devices, it is also critical to understand other metrics of adaptation and performance such as comfort, cognitive fit, fatigue, injury risk, movement speed, balance, and skill (Ferris and Schlink, 2017, Stirling et al., 2018). In this study we used mobile brain and body imaging to examine physiological responses while users learned to walk with a bilateral, active, ankle augmentation device. We measured electroencephalography (EEG), electromyography (EMG), kinematics, and kinetics while subjects walked on a treadmill. We hypothesized that users would modify their neuromuscular strategy as they adapted to walking with the device, and we present preliminary EMG results here.

Methods

Participants included twenty-two healthy, active adults aged 18-50 with no current or chronic musculoskeletal injuries nor neuropathies affecting the lower extremities. Participants donned bilateral, active ankle exoskeletons (exos) and were equipped with 128-channel EEG, 10 channels of surface EMG, and motion capture markers on the head, trunk, and lower extremities. Bipolar surface EMG electrodes (HEX Dual 2.0 cm, Ag/AgCL, Noraxon USA, Inc., Scottsdale, AZ) were applied bilaterally over the rectus femoris (RF), lateral biceps femoris (BF), lateral gastrocnemius (GS), soleus (SOL), and tibialis anterior (TA) muscles.

Participants completed a series of walking trials on an instrumented treadmill at a speed of 1.2 m/s. Participants walked for a duration of 5 min each with the exos powered off ("off") and powered on ("on"). Following these initial baseline trials, participants performed 3 walking trials of approximately 15-min duration during which power to the exos was cycled on and off without warning. Participants then completed two final 5-min walking trials for the off and on conditions ("off post" and "on post", respectively). EEG, EMG, and kinematic data were collected synchronously for all trials. EMG data was collected wirelessly at a rate of 1500 Hz using myoMotion software and Noraxon DTS wireless sensors (Noraxon USA, Inc., Scottsdale, AZ). EMG data were bandpass-filtered (10-500 Hz, 4th-order, zero lag Butterworth), full-waved rectified, and smoothed using a 20 Hz low-pass filter to create a linear envelope. Individual gait cycles were downsampled to 101 data points using linear interpolation and normalized to the mean signal maximum during the initial off trial.

Results and Discussion

Preliminary analyses (n = 5) compared EMG signals obtained during the off, on, off post, and on post trials. Mean EMG profiles were generated by averaging the ~250 normalized gait cycles for each muscle and each leg. Sample graphs are shown in Figure 1.

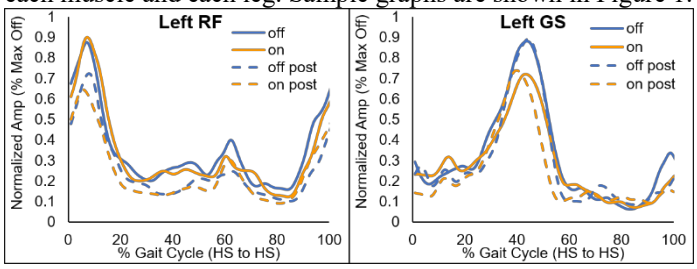

Figure 1. Mean EMG amplitude (Amp) for the left RF and GS muscles normalized to max during the initial off trial (% Max Off). Stride time is presented as 0-100% of gait cycle from heel strike (HS) to HS.

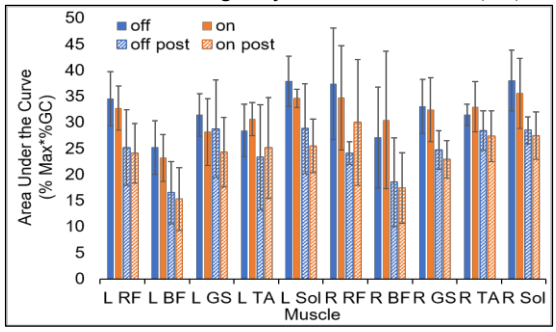

Figure 2. Mean & SD of area under the curve for normalized EMG signals. (L = left, R = right).

Bilaterally, RF and BF muscles demonstrated similar magnitudes and timing for the on and off trials, but EMG signals remained suppressed for off post and on post trials. GS muscles demonstrated reduced peak EMG at toe-off (~60% gait cycle) for the on compared to the off trials. Area under the curve analyses suggests that the muscles exhibited decreased activation for both post conditions. Future analyses will evaluate signal amplitudes, onset timing, burst duration, and co-contraction indices for off and on trials as well as for the various power cycle transitions during the 15-min walking trials.

Significance

As exoskeletons and intelligent agents are being developed for use by warfighters, it is essential that we gain a greater understanding of the neurological and behavioral adaptation to these systems. Identifying metrics indicative of adaptation as well as understanding the time scales for adaptation can help us monitor user progress, identify when sufficient system training has occurred, and optimize human-system performance.

Acknowledgments

The authors would like to acknowledge Ms. Seongmi Song for her intellectual contributions and continued support of this work.

References

Mooney, L. & Herr, H. M. (2016). *J Neuroeng Rehabil*, 13(1), 1-12.
Galle, S., et al. (2013). *Gait Posture*, 38(3), 495-499.
Ferris, D. P., & Schlink, B. R. (2017). *Kinesiol Rev*, 6(1), 70-77.
Stirling, L., et al. (2018). *IEEE Systems Journal*. *13*(1), 1072-1083.

MODELING THE EFFECT OF FEMORAL ANTEVERSION ON GAIT DYNAMICS

Benjamin B Wheatley[1*], Mark A Seeley[2]
[1]Bucknell University, Department of Mechanical Engineering [2]Geisinger Musculoskeletal Institute
email: *b.wheatley@bucknell.edu

Introduction

Increased femoral anteversion can cause joint malalignment, impaired gait, and lower limb joint pain [1]. However, treatment remains a challenge due to morphological, kinematic, and clinical presentation variability. Musculoskeletal modelling provides a cost-effective and non-invasive approach to studying the interactions between femoral anteversion and joint mechanics. The goal of this work was to develop a modeling workflow to simulate the changes in lower limb joint kinematics and joint moments during gait due to increased femoral anteversion.

Methods

A validated musculoskeletal model developed to simulate human walking was implemented along with freely available marker and ground reaction force data [2]. All muscles were removed and replaced with linear joint actuators. Lower limb degrees of freedom included hip flexion/adduction/rotation, knee flexion, ankle plantar flexion, and subtalar inversion. Four modified femoral anteversion models were created by transecting the distal femur and rotating the remaining child geometry inward by 10, 20, 30, or 40 degrees [3] (Figure 1).

The open-source optimal control software Moco was used for all inverse kinematics and tracking problems [4]. Kinematics for the typically developing case were generated by marker tracking of freely available data [2]. Dynamics for each model were generated by optimal control tracking of a weighted combination of the typically developing joint angles and the marker trajectories, producing distinct kinematics and joint moment for each model were thus distinct from each other.

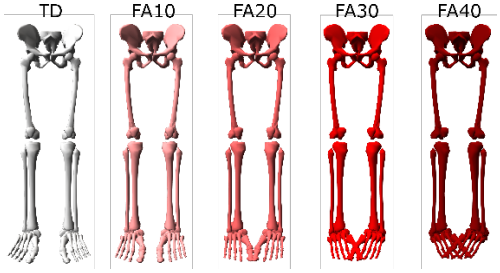

Figure 1: Lower limb musculoskeletal model geometry, ranging from typically developing (TD) to an increase in femoral anteversion of 40 degrees (FA40).

Results and Discussion

Some simulated lower limb dynamics showed distinct dependences on femoral anteversion (Figure 2). In particular, hip rotation and subtalar eversion exhibited noticeable changes in kinematics, with hip rotation decreasing and subtalar increasing with increases in femoral anteversion. Thus, our results suggest that kinematic adjustments from increased femoral anteversion are distributed between hip rotation, subtalar inversion, and foot progression angle. Dynamic tracking results indicate that increases in femoral anteversion may alter hip, knee flexion, and subtalar inversion moments. Specifically, we found decreases in hip flexion, hip rotation and knee flexion moments and increases in subtalar inversion moments (Figure 2).

Our kinematic and joint moment results agree well with published experimental findings in subjects with increased femoral anteversion, namely changes to hip rotation angles, subtalar inversion, and knee flexion moment [5]. Thus, this work presents a method to simulate the effect of lower limb torsion on gait kinematics and joint dynamics. Future efforts to leverage this modeling workflow to investigate joint loads and muscle force contributions would strengthen clinical applications of this work.

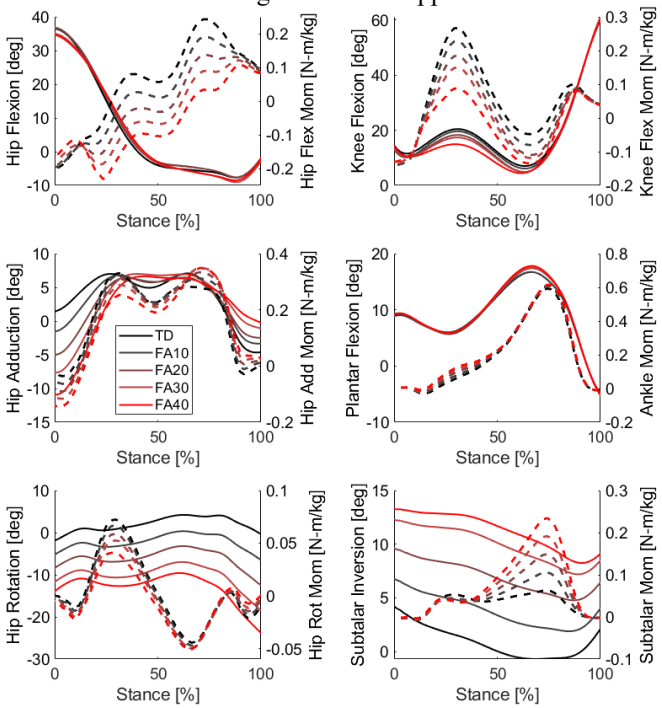

Figure 2: Simulation kinematic and joint moment results. Plots are presented for each joint degree of freedom, with the kinematics denoted as solid curves and the moments denoted as dashed curves.

Significance

While the results presented here are representative of a generalized case only, they provide insight into the potential changes to joint moments due to lower limb torsion. Such variations in joint moments – and thus joint loads – may play an important role in the prevention or development of joint pain. For example, while increased femoral anteversion exacerbates patellofemoral joint malalignment, this could be "offset" by decreased joint moments in some individuals. This modeling workflow could be implemented for such investigations, but requires further development and validation to experimental data.

Acknowledgments

Authors would like to acknowledge funding by the Bucknell-Geisinger Research Initiative and training through the NCSRR at Stanford funded through NIH grant P2C HD065690.

References

[1] Scorcelletti et al, doi: 10.1111/joa.13249.
[2] Rajagopal et al, doi: 10.1109/TBME.2016.2586891
[3] Pitto et al, doi: 10.3389/fnbot.2019.00054
[4] Dembia et al, doi: 10.1101/839381
[5] Mackay et al, doi: 10.1016/j.gaitpost.2021.03.004

CERVICAL SPINE BIOMECHANICS AFTER FUSION AND ARTIFICIAL DISC DURING PILOT EJECTION

Muzammil Mumtaz [1], Casey W. Pirnstill [2], Timothy Dewitt [2], Amey Kelkar [1], Justin Mendoza [1], Sudharshan Tripathi [1], V. K. Goel [1]
[1] Department of Biomedical Engineering, University of Toledo
[2] Airman Biosciences Division, Wright-Patterson Air Force Base
Email: vijay.goel@utoledo.edu

Disclaimer: The views expressed in this paper represent the personal views of the author and are not necessarily the views of the Department of Defense or of the Department of the Air Force

Introduction

The United States Air Force (USAF) has experienced ongoing issues with chronic neck pain with its high-performance flight aircrew. To meet force readiness targets, the USAF has introduced a pilot waiver program to permit pilots to continue to fly after corrective cervical spine surgeries such as cervical fusions and/or cervical arthroplasty. The risk of injury to the pilots who have undergone these types of surgeries during high loading events, such as aircraft ejection, remains unknown. Thus, the objective of this study was to investigate the risk of injury among pilots who have undergone these procedures and compare to those who have not undergone any corrective procedures in similar loading events.

Methods

A validated osseo-ligamentous model from Head-T1 was used in this study. The model was validated under both quasi-static loading and dynamic loading. The anterior cervical discectomy and fusion (ACDF) and total disc replacement (TDR) surgery was simulated at the C5-C6 segment. For the ACDF surgery, a lordotic PEEK cage with Ti-alloy screw-plate system was used, and *Prodisc-C* (Centinel Spine, West Chester, PA) was used in the TDR surgery. The model was subjected to the vertical ejection acceleration of up to 10G [1]. The data for range of motion (ROM), intradiscal pressure (IDP), and endplate stresses were computed for the intact, ACDF and TDR model.

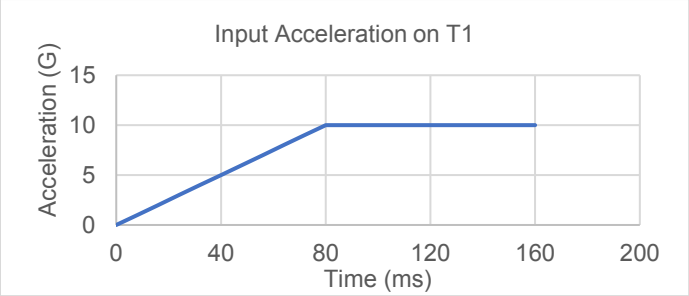

Figure 1:Vertical ejection acceleration applied on the bottom of T1.

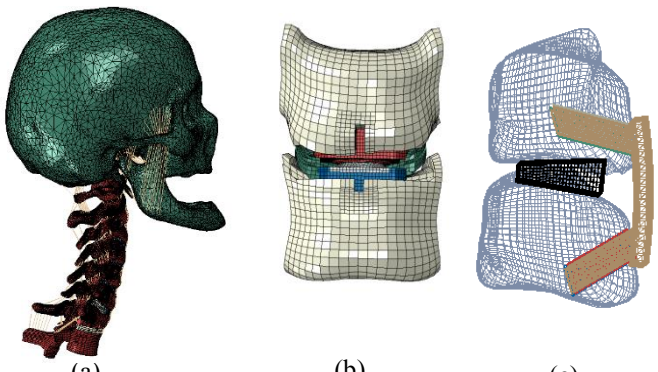

Figure 2: a) C0-T1 FE model, b) C5-C6 segment with *Prodisc-C*, and c) C5-C6 segment with cage and screw-plate system.

Results and Discussion

The ROM at the index segment decreased by 7.84° (-85.5%) in the ACDF model and increased by 3° (+33%) in the TDR model. The ROM at the cranial adjacent segment increased by 8.5° (+104%) in the ACDF model and decreased by 0.68° (-8%) in the TDR model. At the caudal adjacent segment, ROM decreased by 6.2° (-85.5%) in the ACDF model and decreased by 1.16° (-16%) in the TDR model. The IDP at the cranial adjacent segment was 10.7 MPa (+395%) and 1.1 MPa (-48.8%) in the ACDF and the TDR model, respectively. The IDP at the caudal segment was 0.28 MPa (-84%) and 1.5 MPa (-10.5%) in the ACDF and the TDR model, respectively. The maximum von Mises stress on C5-inferior endplate was 31.5 MPa (+95%) and 46 MPa (+187%) in ACDF and TDR model, respectively. The maximum von Mises stress experienced by C6-superior endplate was 9.9 MPa (-21%) and 84 MPa (+168%) in ACDF and TDR model, respectively. The maximum von Mises stress in the ACDF construct was located at the C5 left screw with a magnitude of 4572 MPa and in *Prodisc-C* implant was observed on the top endplate of the implant with a magnitude of 1616 MPa.

Thus, it can be concluded that the TDR model shows kinematics similar to the intact model, but the ACDF model does not. However, the TDR model shows that pilots with arthroplasty may be prone to injury at the endplates of the index segment. Contrastingly, the ACDF model predicts that the maximum load exerted on the cervical spine is carried by the implants, and therefore, pilots with ACDF may experience implant failure. Additionally, ACDF minimizes motion at the index segment leading to excessive motion on the cranial adjacent segment. Thus, the ACDF model predicts that pilots with cervical fusion may have a higher risk of injury at the cranial adjacent intervertebral disc or have the potential of developing adjacent segment pathologies in future.

Significance

This is the first FE study to assess the risk of injury to the pilots sustaining ejection acceleration who have undegone cervical fusion/arthroplasty. Currently, pilots with cervical fusion are able to return to service via the USAF pilot waiver process. However, our results suggest that pilots with TDR are less prone to injury compared to pilots with ACDF -- except for injury to the index segment endplates. However, additional research is needed to make a definitive recommendation for pilots with TDR to return to service and fill the shortage of USAF pilots.

Acknowledgments

The work was supported in part by NSF Industry/University Cooperative Research Center at The University of California at San Francisco, San Francisco, CA, The University of Toledo, Toledo, Ohio, The Ohio State University, Columbus, Ohio and Northeastern University, Boston, Massachusetts (www.nsfcdmi.org), Wright-Patterson Airforce Base and by an allocation from the Ohio Supercomputer Center.

References

[1] Teo et al. *J Muscul Research* 8.04 (2004):155-16

UPPER BODY EXOSKELETON ASSESSMENT DURING CONSTRUCTION IN THE ALASKA WHITTIER TUNNEL

Jason C. Gillette[1*], Shekoofe Saadat[1], and Terry Butler[2]
[1]Department of Kinesiology, Iowa State University
[2]Lean Steps Consulting
email: *gillette@iastate.edu

Introduction

In 2019, occupational shoulder injuries resulted in a median of 22 missed days of work for private industry in the USA [1]. Shoulder injury risk increases with increased work cycle percent in elevated arm postures and with hand-held tool usage [2]. Threshold limit values (TLVs) for upper limb fatigue provide a relationship between duty cycle and percent maximal voluntary contraction (%MVC) [3].

The Levitate Airframe is a passive upper body exoskeleton that provides shoulder support during elevated arm postures. Field studies at John Deere and Toyota manufacturing sites indicated that an exoskeleton may reduce deltoid fatigue [4, 5]. Our purpose was to expand exoskeleton field studies to elevated arm postures during construction in the Whittier Tunnel, Alaska. We hypothesized that the exoskeleton would reduce deltoid EMG amplitude and predicted fatigue for these construction tasks.

Methods

Four construction workers involved in the Whittier Tunnel water mitigation project participated in this study. Six job tasks were performed by each worker: 1) cut excess rods, 2) drill in rods, 3) hanging pans, 4) installing levelling nuts, 5) installing pans, and 6) stuff grout in holes. Approximately ten minutes of EMG data per job task were collected with and without the exoskeleton during four overnight work shifts.

EMG sensors were placed bilaterally on the anterior deltoid, biceps brachii, upper trapezius, and lumbar erector spinae. Postures for MVCs included 90° shoulder flexion, 90° shoulder abduction, 90° elbow flexion, and prone spinal extension. Mean active EMG amplitudes (muscle active when >5 %MVC) and duty cycles (percent time muscle was active) were calculated. Fatigue TLVs were calculated using duty cycles [3] and compared to mean EMG amplitudes to predict fatigue risk [4].

Results and Discussion

Across jobs, anterior deltoid EMG amplitude ($p=0.02$) and fatigue risk ($p=0.01$) were significantly reduced when wearing the exoskeleton (Figure 1). Biceps brachii, upper trapezius, and lumbar erector spinae EMG amplitudes and fatigue risk were not significantly different ($p>0.05$).

Anterior deltoid EMG amplitude and fatigue risk were reduced for all six jobs when wearing the exoskeleton (Figure 1). Job #1 was above the fatigue TLV (positive fatigue risk) both without and with the exoskeleton. Jobs #2-#5 were above the fatigue TLV without the exoskeleton and below the fatigue TLV (negative fatigue risk) with the exoskeleton. Job #6 was below the fatigue TLV both without and with the exoskeleton.

An exoskeleton may be beneficial for job #1, but additional controls are needed to shift below the fatigue TLV. Job #1 involved the entire duty cycle in elevated arm postures (often 135° shoulder flexion) and the highest loads. An exoskeleton appears to be an effective match for jobs #2-#5, shifting from above to below the fatigue TLV. Jobs #2 - #5 involved nearly the entire duty cycle in elevated arm postures (often 60°-90° shoulder flexion) and moderate loads. An exoskeleton may be lower priority for job #6 since it falls below the fatigue TLV. Job #6 involved half the duty cycle in elevated arm postures (often 60° shoulder flexion) and moderate load requirements.

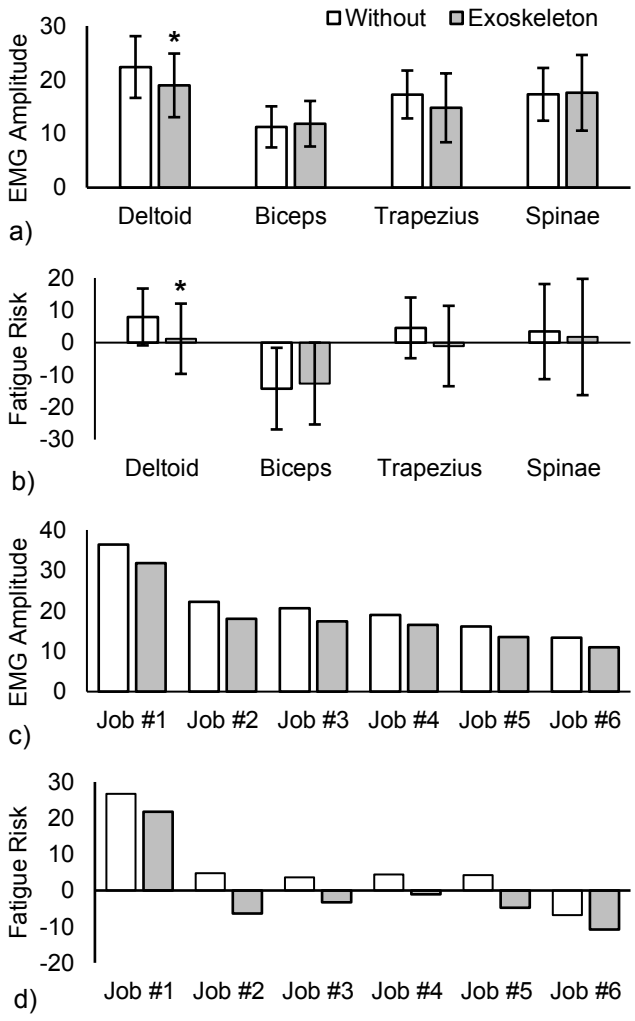

Figure 1: a) EMG amplitudes and b) fatigue risk values across job tasks (%MVC, mean ± SD, *$p < 0.05$), c) EMG amplitudes and d) fatigue risk values as a function of job task (%MVC).

Significance

Upper body exoskeleton usage may be effective for reducing shoulder fatigue during construction if carefully matched for range of support and support level requirements of the job tasks.

Acknowledgments

Levitate Technologies supported this study as a fee-for-service.

References

[1] Bureau of Labor Statistics (2020)
[2] Punnett et al. (2000) *Scan J Work Environ Health* 26:283-291
[3] ACGIH (2016) Upper limb localized fatigue
[4] Gillette & Stephenson (2019) *IISE TOEHF* 7:302-310
[5] Gillette & Stephenson (2018) *ASB Annual Conference*

Are Gait Biomechanics Related to Physical Activity Engagement? An Examination of Adolescents with ASD.

Hunter J. Bennett, Stacie I. Ringleb, Jonna Bobzien, Justin A. Haegele
Old Dominion University, Norfolk, Virginia, USA
Email: hjbennet@odu.edu

Introduction

Persons with autism spectrum disorder (ASD) tend not to engage in health-enhancing levels of physical activity (PA) [1]. Walking, the most common mode of PA amongst humans, is considered a low-load, mechanically and physiologically efficient form of light PA. Despite its widespread favor and ease of implementation (can be performed nearly anywhere), those with ASD tend to spend most of their leisure-time engaged in various sedentary activities (e.g., using personal computers, watching television) [2]. Although research has evaluated the PA engagement of individuals with ASD, less is known about what factors influence these behaviors in this population.

Research on gait biomechanics in persons with ASD have found significant deviations from the "typical" patterns found in control groups. Specifically, persons with ASD choose to walk at slower self-selected speeds, with shorter stride lengths, greater step widths, reduced lower extremity kinematics, and increased frontal plane loading [3-5]. Although engagement in PA is multifactorial (range from socioeconomic to motivational barriers), it is possible that altered gait mechanics and energetics could present an additional, yet to be considered, barriers. Previous literature has found spatiotemporal characteristics of walking are significantly related to PA in healthy/fall-prone adults and persons with a visual impairment [6-7]. It is possible that gait efficiency (i.e., mechanical energy/work) could be related to engagement of this mode of PA, where greater efficiency is demonstrated in the more active [8].

Therefore, the purpose of this study was to determine if gait biomechanics variables of total body mechanical work, speed, and/or stride length are significantly related to engagement in moderate to vigorous (MVPA) and total PA.

Methods

Three-dimensional motion capture and ground reaction forces were recorded while twenty-five adolescents (13-18 years) with a confirmed diagnosis of ASD walked at self-selected speeds. Inverse dynamics were calculated using bilateral upper arm, trunk, pelvis, and bilateral lower extremity kinematics and ground reaction forces during the full stride. Positive and negative work were calculated as the integral of the positive and negative power curves for each joint (shoulder, hip, knee, ankles, and lower back) and the trunk segment. Total body mechanical work was derived as the sum of the absolute value of the positive and negative mechanical works. Mechanical work was normalized to body mass times stride length. Speed and stride length were normalized using leg length and are unitless.

Physical activity engagement was measured off-site using triaxial accelerometers worn on the participant's waist for a seven-day period. The cutoff criteria included light (101-2,295 counts per minute), moderate (2,296-4011 CPM), and vigorous (4,012+CPM) PA. Light and MVPA were summed for total PA. Linear regression analyses were performed to determine if work, speed, and/or stride length were significantly ($p<0.02$) related to average total physical activity and MVPA per day (measured in mins).

Results and Discussion

Suprisingly, mechanical work was not a significant predictor of either MVPA or total PA (both $p>0.500$, $r^2=0.02$). Therefore, mechanical efficiency in walking is not likely a barrier for PA engagement in healthy persons with ASD. It is possible that the multifaceted nature of work (derived from full-body movement patterns and joint loading) negatively impacts its generalizability to the similarly multifaceted variable PA. In agreement with previous results, self-selected walking speed and stride lengths explained greater than 20% of the variance in MVPA and total PA (Table). Although we cannot answer the "chicken or the egg" question regarding spatiotemporal characterstics and PA, the significance of the current study and the previous litearture is that speed and stride length are strong markers of physical and mental health across several populations [6-7].

Table. Regression statistics.

	SPEED		STRIDE LENGTH	
	Total PA	MVPA	Total PA	MVPA
P-value	0.009	0.010	0.002	0.009
R^2	0.269	0.265	0.357	0.286

Significance

Persons with ASD tend to not meet PA guidelines and not reap associated health benefits of PA. Thus, it is important to ascertain what barriers are negatively impacting their engagement. This study adds to the support of walking speed as an indicator of physical/functional health and engagement in PA. Educational/rehabilitation programming for adolescents with ASD should consider focusing on increasing comfort with their environment and confidence during walking by increasing speeds and stride lengths.

Acknowledgements

This study was funded by the Thomas F. and Kate Miller Jeffress Memorial Trust.

References

[1] Healy, S, et al. (2017) J Aut Dev Dis **47:** 48-57
[2] Mazurek, M, et al. (2013) J Aut Dev Dis **43:** 1258-1271
[3] Calhoun, M, et al. (2011) Clin Biomech **26(2):** 200-206
[4] Eggleston, J, et al. (2017) Gait Posture **55:** 162-166.
[5] Bennett, H, et al. (2020) J Biomech, **119** [epub]
[6] Rogge, A, et al. (2021) Exp Brain Res [epub]
[7] Brach, J, et al. (2007) J Gerontol **62A(9):** 983-988
[8] Van de Walle, P, et al. (2012) Gait Posture **35(2)**: 231-237

SENSITIVITY OF ACETABULAR CONTACT PRESSURE TO HIP MOTIONS IN FEMOROACETABULAR IMPINGEMENT: A FINITE ELEMENT ANALYSIS

Jordan Cannon, Christopher M. Powers
Division of Biokinesiology and Physical Therapy, University of Southern California, Los Angeles, CA
Email: cannonjo@usc.edu

Introduction

Femoroacetabular impingement syndrome (FAIS) is a motion-related clinical disorder resulting from abnormal hip joint morphology [1]. Mechanical impingement, in which the aspherical femoral head (cam morphology) abuts with the acetabular rim, is created with simultaneous hip flexion, adduction, and internal rotation. The area of impingement on the anterior-superior acetabulum corresponds with the location of intra-articular joint damage in FAIS [2], which is hypothesized to initiate pain and further progression of the syndrome [3]. During tasks that require high degrees of hip flexion, such as squatting, it is unknown how frontal and transverse plane motion influences acetabular loading associated with impingement. Understanding the influence of frontal and transverse plane motion on acetabular contact pressure may inform conservative care aimed at modifying movement to reduce symptoms in FAIS.

The purpose of this pilot study was to investigate the sensitivity of acetabular contact pressure to isolated and combined frontal and transverse plane rotations during a simulated squat task at 90º hip flexion.

Methods

A 3D finite element (FE) model of the hip joint was developed from a male with a diagnosis of cam FAIS (32 years, 1.79 m, 70.9 kg, axial alpha angle = 59º). Subject-specific bony geometry was obtained from CT scans of the pelvis and proximal femur to create a 3D model of the symptomatic (left) hip. The acetabulum and femur were modelled using homogeneous, isotropic, triangular continuum shell elements with an elastic modulus of 17.0 MPa and a Poisson ratio of 0.30. Quasi-static loading simulations were performed using a nonlinear FE solver in Abaqus using a hard contact algorithm, with a surface-to-surface, finite sliding contact, and a surface coefficient of friction of 0.02.

Peak acetabular contact pressure was evaluated across a range of isolated and combined frontal and transverse plane rotations with the hip at 90º of flexion. From a neutral position, the femur was rotated in the frontal and transverse planes in 3º increments (range: -15º – 15º). For the combined conditions, adduction and internal rotation as well as abduction and external rotation were evaluated. A resultant bone-on-bone contact force of 1109 N was applied over a group of nodes representing the articulating surface of the femoral head. This force was held constant across all model simulations and was representative of the participant's natural squat.

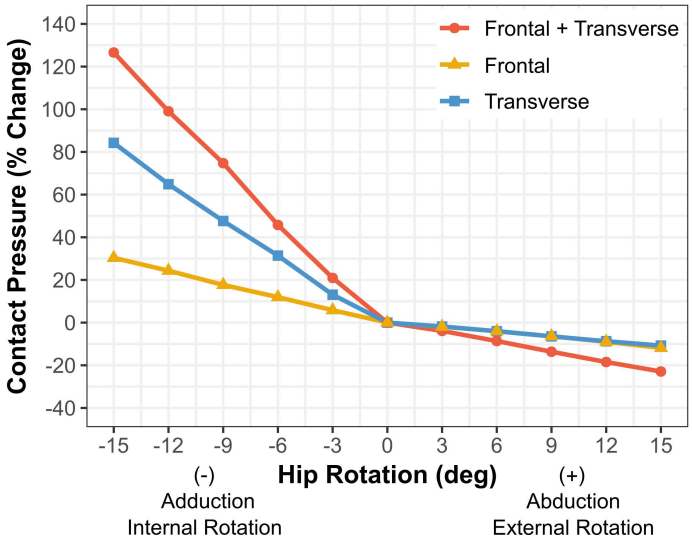

Figure 1: Percent change in contact pressure from 90º hip flexion with isolated and combined rotations in the frontal and transverse plane.

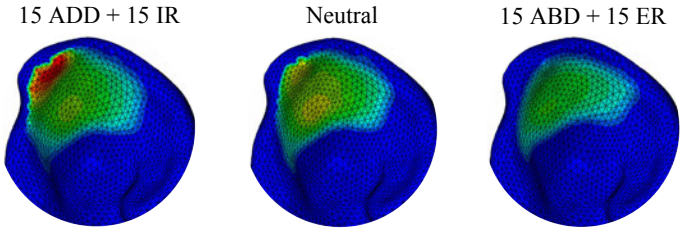

Figure 2: Left acetabular contact pressure at: 15º adduction + 15º internal rotation, neutral (no frontal or transverse plane rotation), and 15º abduction + 15º external rotation. Peak acetabular contact pressure is located at the anterior-superior acetabular rim. (left = ant., top = sup.)

Results and Discussion

The isolated motions of hip adduction and internal rotation resulted in a linear increase in peak acetabular contact pressure. (Figure 1). However, peak contact pressure appeared to be more sensitive to internal rotation than adduction. The combined motions of hip adduction and internal rotation had a greater influence on peak acetabular contact pressure compared to either of the isolated motions. In contrast, the combined motions of 15º abduction and 15º external rotation reduced contact pressure by 23% (Figure 1).

During tasks that demand high degrees of hip flexion, such as squatting, the motions of adduction and internal rotation can result in an increase in peak acetabular contact pressure on the anterior-superior acetabulum (Figure 2) and may contribute to symptomatic impingement. The combined motions of abduction and external rotation may provide a strategy to minimize peak acetabular contact pressure on the anterior-superior rim during squatting in persons with FAIS (Figure 2).

Significance

These initial results highlight the importance of minimizing hip adduction and internal rotation in FAIS during activities that require high degrees of hip flexion. In particular, minimizing hip internal rotation motion appears to be most important.

Acknowledgments

We acknowledge the financial support provided by the International Society of Biomechanics Matching Dissertation Grant and USC Division of Biokinesiology & Physical Therapy.

References

[1] Griffin, DR et al (2016). *BJSM*, **50**(19): 1169-1176.
[2] Tannast et al (2008). *Clin. Orth. Rel. Res.*, **466**(2): 273-280.
[3] Cannon et al (2020). *Physical Therapy,* **100**(5): 788-79.

Simulating Walking for Developing Metabolic Estimation Methods

Alex Dzewaltowski[1], Seungmoon Song[2], Philippe Malcolm[1]
[1]Department of Biomechanics, University of Nebraska at Omaha, Omaha, NE, USA
[2]Department of Mechanical Engineering, Stanford University, Stanford, CA, USA
email: adzewaltowski@unomaha.edu, web: cobre.unomaha.edu

Introduction

Attainable reduction in metabolic rate is one of the main performance indicators for assistive devices, but there are many challenges associated with metabolic cost measurement. While respiratory measurements are the gold standard, their usefulness is greatly diminished by various clinical populations' inability to exercise for sufficient durations to obtain steady-state measurements. In this abstract, we investigate if an existing predictive model can estimate changes in metabolic rate from an assistive device, thereby eliminating the need for exposing clinical populations to strenuous tests.

Our lab has reported reductions in metabolic rate during walking with assistive forces at the center of mass (COM) [1]. Assistance was provided with 35 different force conditions by utilizing a tether connection at the subject's waist. We have applied these experimental force conditions to the COM of a neuromuscular model from Song and Geyer (MATLAB-Simulink) [2]. The neuromuscular model utilizes a muscle reflex system coupled with a series of constraints consistent with a human range of motion where this model is capable of discovering strategies for walking. By combining the muscle behaviour predicted by the model with standard equations for estimating the muscle-metabolic cost, we can predict metabolic rate without experimental data input. We hypothesize that the model will independently predict experimentally measured reductions in metabolic rate due to assistance at the COM.

Methods

Neuromuscular model

Utilizing the algorithm Covariance Matrix Adaptation – Evolution Strategy (CMA-ES) to optimize the model, the optimization process has achieved an emergent walking pattern consistent with young and elderly walking depending on the physiological input parameters [3]. By applying our experimental force conditions to this model, we can generate muscle data outputs necessary for metabolic rate estimation. The neuromuscular model was constrained to sagittal plane dynamics. Nine muscle groups were implemented in the analysis: gastrocnemius, soleus, tibialis anterior, glutei, lumped hip flexors, vastii, rectus femoris, biceps femoris (short head), and hamstrings. The model optimization process tunes 71 parameters that are separated into ten modules of control. These modules are split evenly between the stance and swing phase of walking.

Metabolic rate

We have chosen the Umberger et al. (2003) equations for estimating the metabolic rate from muscle actions. Data required for metabolic rate prediction from the neuromuscular model are muscle excitation, activation, fiber length, fiber velocity, and fiber force. Equation 1 consists of the components to approximating metabolic rate as the summation of heat rate ($\dot{h_A}$), maintenance heat rate ($\dot{h_M}$), shortening/lengthening heat rate ($\dot{h_{SL}}$), and the mechanical work rate of the contractile element ($\dot{w_{CE}}$) [3].

$$\dot{E} = \dot{h_A} + \dot{h_M} + \dot{h_{SL}} + \dot{w_{CE}} \qquad \textbf{Eq 1.}$$

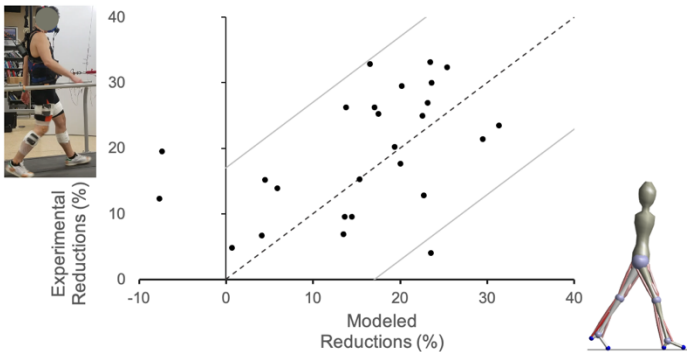

Figure 1: Experimental reductions compared to model predicted reductions in metabolic rate for 26 different force conditions are indicated by positive values. The dashed line indicates a perfect correlation. The two grey parallel lines indicate the average standard deviation across experimental conditions for metabolic rate. Reductions are in respect to measured or simulated unassisted walking values.

Experimental Comparisons

We implemented the force conditions used in our previous experiment onto the neuromuscular model's COM. Each force condition has a set peak force, onset timing, and duration. Onset timing and duration are continually being adjusted to maintain a set percent of stride. **We predicted reductions in metabolic rate from assistive forces at the COM compared to the predicted metabolic rate for unassisted, normal walking. The predicted metabolic reductions were within one standard deviation of the average experimental metabolic reductions for 23 of the 26 successfully optimized conditions.** The nine optimizations that were unsuccessful had encountered a Simulink compiling error.

Results and Discussion

The model has successfully discovered walking while assisted at the COM. The emergent muscle contraction strategies from the model yielded reductions in metabolic rate similar to experimental data for the majority of our assistive conditions. Our results are well within two standard deviations of experimental measurements following previous recommendations for new simulations of walking [4].

Significance

We plan to use this modelling process to advance methods of estimating metabolic cost. This research may inform future assistive device designs or rehabilitation strategies utilizing far fewer preliminary tests and greatly reducing the initial involvement of patients.

Acknowledgements

Original experimental data was collected by Arash M. Gonabadi and Prokopios Antonellis. COBRE P20GM109090

References

[1] Prokopios et al. 2021, Under review
[2] Song S. & Geyer H., 2018, *Journal of Physiology*
[3] Umberger et al., 2003, *Comp.Methods in Bio & Bio Eng.*
[4] Hicks et al., 2015, *Journal of Biomechanical Engineering*

TRIPPING DURING PREGNANCY: FAILURE TO PERCEIVE THE ENVIRONMENT OR THE BODY?

Pegah Jamali, Kameron M. Kinkade, Robert D. Catena
Washington State University
email: robert.catena@wsu.edu

Introduction

Tripping during pregnancy is a primary reason why at least 1 in 4 pregnant women fall [1], yet the root causes are unknown. We have previously shown that all anthropometry combined is only a partial contributor ($r<0.5$) to balance deficits during pregnancy [2]. Understanding the root causes of trips and falls will have clinical impacts on the health of pregnant women, health of the fetus, and help us understand limitations to our bipedal evolution.

Bipedal gestational lumbopelvic change to accommodate fetal growth may predispose the lumbar plexus (at the root) and sciatic nerve (at the root and around sciatic notch) to impingement, degrading lower extremity proprioception. However, there are also accounts that several neurological processes related to vision, including acuity [3] and spatial attention [4], are compromised during pregnancy. As both perception of the environment and of the body provide needed information for successful obstacle avoidance, our goal is to evaluate how the two relate to obstacle avoidance through gestation.

Methods

Eleven pregnant participants, starting at 13 weeks gestation, were tested five times in 6-week intervals, to 37 weeks gestation. First, obstacle perception (**OP**) was tested by asking participants to match their foot heights to the top of a 10% body height obstacle 2.7 m in front of them, relying first on working memory (eyes closed), and then online processing (gaze fixated on the obstacle). Second, joint position senses (**JPS**) were tested by asking participants to actively match their hip and knee angles to a passively created joint angle. Finally, participants walked an obstacle course (**OC**) at a self-selected speed for 2 minutes (Figure 1). Obstacles randomly set to 5%, 7.5%, and 12.5% of each participant's body height served as distractors. Crossing heights only over the two 10% obstacles and minimum distance to the 10% obstacles were measured for trailing and leading foots.

Motion capture marker data were used to calculate obstacle avoidance and joint angles. Linear mixed models were conducted on OP, JPS, and OC measures (DVs) over gestation time (IV). Stepwise regressions identified significant correlations between OP and JPS measures (IVs) and OC measures (DVs).

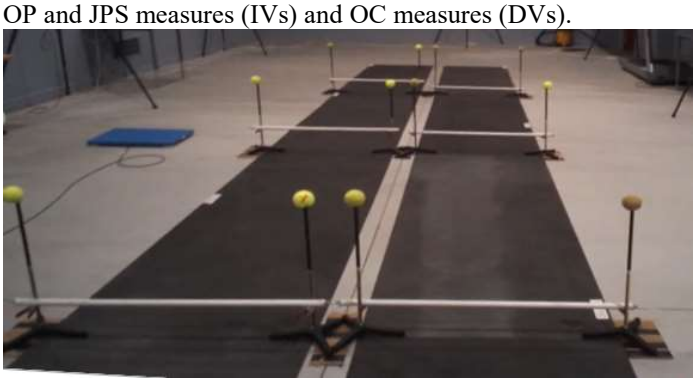

Figure 1: View from the start of the obstacle course. Six obstacles spaced 3 m apart. Participants walk the right side (12 m) to the end of the walkway, come back on the left side, and repeat. During OP, participants stand 0.3 m past the first obstacle and match their foot to the height of the second obstacle 2.7 m away.

Results and Discussion

Regardless of visual information, OP significantly degraded through the second trimester of pregnancy ($p=0.003$). Pregnant women undershot, rather than overshot the obstacle (Figure 2). There were no statistically significant changes in JPS throughout pregnancy ($p>0.194$). OP and JPS findings combined suggest that that visual perception changes, rather than proprioceptive change, may influence trip rates in pregnant women.

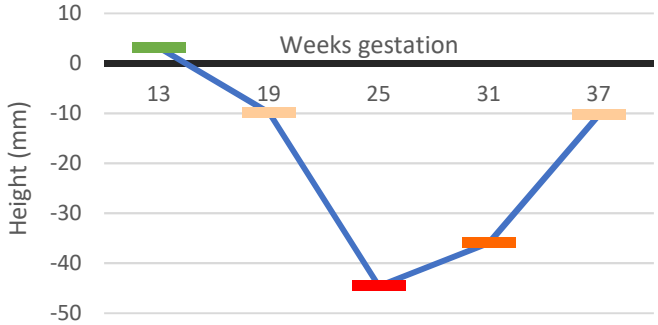

Figure 2: Average height of foot relative to the obstacle during OP at different weeks of gestation. Negative (red spectrum) values indicate the foot lifted to a height below the obstacle (solid black line at 0 mm).

During OC, participants had a 39% reduction in trailing foot crossing height over time ($p=0.009$) and a 33% reduction in the minimum distance of the trailing foot to the obstacle over time ($p=0.045$). OP change, the amount of foot height change over 5 seconds as participants were told to keep their foot matched to the height of the obstacle, was correlated with reduced trailing foot obstacle distance ($\beta=-2.185$, $r=0.572$, $p=0.004$).

These results indicate that increased potential for obstacle contact occurs as a result of inability to properly translate visual spatial information into posture. Our results do not indicate the problem lies within the somatosensory-motor pathway (i.e. no change in JPS throughout pregnancy). The problem is also not in working memory integration, as results were similar between eyes open and eyes closed OP conditions ($p>0.593$). Therefore, the problem is either in early processing of dorsal visual stream information or before this in visual sensory acquisition.

Significance

Increased trip rates during pregnancy seem to be a result of failure to process visual information. The next step is to dissect early visual processes like visual acuity, alertness, and visuospatial orientation. Also, we must uncover why OP improves in the 3rd trimester. This information will help us understand the causes of increased fall rates for pregnant women and understand the link between neurosensory and bipedal evolutions.

Acknowledgments

ASB (Junior Faculty Research Award) funded this research.

References

1. Dunning et al. (2003). *Am J of Industrial Medicine.*
2. Catena et al. (2019). *J Applied Biomechanics.*
3. Naderan (2018). *J Current Ophthalmology.*
4. Plamondon et al. (2015). *Early Human Development*

INFLUENCE OF SAGITTAL CERVICAL ALIGNMENTS ON TOTAL DISC REPLACEMENT SURGERY

Muzammil Mumtaz [1], Amey Kelkar [1], Justin Mendoza [1], Sudharshan Tripathi [1], Ashish Sahai, Nayan Makwana, V. K. Goel [1]
[1] Department of Biomedical Engineering, University of Toledo
Email: vijay.goel@utoledo.edu

Introduction

Recently, total disc replacement (TDR) surgery has gained preference over traditional cervical fusion surgery. Studies report that TDR reduces the occurrence of adjacent segment degeneration (ASD) [1]. However, some studies have shown that the rate of ASD is similar in both cervical fusion and TDR surgery [2]. Additionally, the correlation between cervical alignment and clinical outcome is arguable [3]. We believe that this conflict exists because the parameters that influence the biomechanics of the cervical spine are not well understood -- specifically, the effect of TDR on different cervical alignments.

We hypothesize that the alignment of the cervical spine may influence the outcome of TDR surgery. Thus, the objective of this study is to explore the biomechanics of different cervical alignments and the effect of TDR surgery on each alignment.

Methods

A validated osseo-ligamentous model from C2-C7 was used in this study after validation under quasi-static loading. The C2-C7 cobb angle of the base model was modified to generate three cervical spine models with different sagittal alignments: Lordotic (-10°), Straight (0°) and Kyphotic (+10°) alignments. The TDR surgery was simulated at the C5-C6 segment for all three sagittal alignment models using an implant modeled after the *Mobi-C* TDR device. The base of the C7 vertebra was fixed in all directions, and a 100N follower load was applied to simulate the effect of muscles and weight of the head. A pure moment of 1.5Nm was applied to the uppermost vertebra (C2) to simulate the cervical spine's motion in flexion/extension, left/right bending, and left/right rotation. Range of motion (ROM), intradiscal pressure (IDP), annular stresses, and facet loads were computed for the three sagittal alignment models in both the intact and the TDR configurations.

Figure 1: C2-C7 FE models: a) Lordotic, b) Straight, and c) Kyphotic

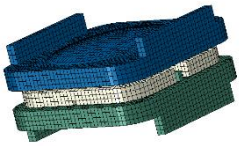

Figure 2: TDR implant

Results and Discussion

Under extension, left/right bending and left/right rotation loading conditions, the intact lordotic model demonstrated the smallest ROM at all levels. Additionally, under all loading conditions, the lordotic model demonstrated the largest facet loads while the kyphotic model demonstrated the highest annular stresses.

When comparing only the TDR models, the IDP values were comparable for all alignments at all levels. However, the lordotic model demonstrated the largest facet loads followed by the straight and kyphotic models. Average facet forces in the lordotic model increased by 67%, 66% and 95% at the index, superior, and inferior levels, respectively, compared to the kyphotic model. Contrastingly, the kyphotic model predicted highest annular stresses followed by the straight and lordotic models. Average annular stress in kyphotic model increased by 38% and 18% at the superior and inferior segment, respectively, compared to the lordotic model.

In conclusion, the lordotic TDR model was associated with the highest facet loads while the kyphotic TDR model was associated with the highest annular stresses. Facet loads increased post-operatively in the lordotic model. It has been clinically observed that cervical TDR surgery is associated with increases in both post-operative lordosis at the index level as well as global cervical spine lordosis [4,5]. Therefore, we recommend that care must be taken in surgical management of patients with pre-existing hyper lordosis of cervical spine as TDR surgery may accelerate facet joint degeneration at the index, superior adjacent, and inferior adjacent levels leading to ASD.

Significance

This study shows that the sagittal alignment of the cervical spine has a noticeable effect on the outcome of TDR surgery. Special care must be taken while operating on patients with lordotic cervical alignments because TDR surgery may degrade facet joints on this patient at higher rates compared to other patients with different sagittal alignments. This study also paves the way for development of new TDR-designs that may be specially designed based on the patient's specific sagittal alignment.

Acknowledgments

The work was supported in part by NSF Industry/University Cooperative Research Center at The University of California at San Francisco, San Francisco, CA, The University of Toledo, Toledo, Ohio, The Ohio State University, Columbus, Ohio and Northeastern University, Boston, Massachusetts (www.nsfcdmi.org), and by an allocation from the Ohio Supercomputer Center.

References

[1] Wang et al. *Orthop Surg*. 12.1 (2020): 16-30
[2] Martino et al. *Eur Spine J*. 24.7 (2015): 810-825
[3] Patel et al. J Spine Surg. 6.1 (2020):106-123
[4] Barrey et al. *Eur Spine J*. 21.08 (2012): 1648-59.
[5] Guerin et al. *J Spinal Disord Tech*. 25.1 (2012): 10

Effect of walking speed on gait stability and joint kinematics in children with and without Down syndrome

Matthew Beerse[1], Tasnuva Alam[2], Kaylee Larsen[1], and Jianhua Wu[2]
[1]University of Dayton, [2]Georgia State University. Email: mbeerse1@udayton.edu

Introduction

Children with Down syndrome (DS) walk at slower speeds, with shorter and wider steps, and greater center-of-mass (COM) variability (1). Previous studies of walking at faster speeds and with ankle load have been shown to improve the spatiotemporal and kinetic aspects of gait (2, 3), particularly by increasing stride length, decreasing stride width (2), and improving general muscular activation (3). However, it is unknown what joint kinematic strategies children with DS adopt to accomplish faster than preferred walking speeds.

Moreover, little work has been done to directly assess individuals with DS's stability during gait; instead, stability is often inferred by step length and width. The margin of stability (MOS) is an innovative measure of dynamic stability that incorporates COM motion and base of support during walking (4). Evaluation of MOS provides insight of fall risk and capacity to increase mobility when increasing gait speed.

This study aimed to assess joint kinematics and MOS of typically developing (TD) children and children with DS while walking at their preferred and faster speeds. We hypothesized that children with DS would show less stable MOS and underdeveloped joint kinematics compared to TD children.

Methods

Twelve children with DS (10M/2F, 8.80 (1.23) years) and twelve age- and sex-matched TD children participated in this study. Subjects walked overground at their self-selected preferred walking speed (*normal*) and at a speed described "as fast as possible without running" (*fast*).

We collected kinematic data using a Vicon motion capture system (Oxford, UK) and a custom full-body marker set. 3D COM position was estimated from 12 body segments. MOS was calculated as the difference between the projected position of the COM and the base of support. MOS was evaluated at discrete gait events (heel-strike and mid-swing) in both the anterior/posterior (AP) and mediolateral (ML) directions, as well as continuously during single-limb support phases. MOS was normalized by body height. Ankle, knee, and hip joint angles were evaluated in the sagittal plane continuously during the gait cycle.

Two-way (2 group x 2 speed) mixed ANOVAs were conducted for each discrete MOS variable. Continuous MOS and joint angle data were evaluated using a two-way (2 group x 2 speed) mixed ANOVAs statistical parametric mapping (SPM1d) approach. Significance level was set at alpha=0.05.

Results and Discussion

Children with DS walked with similar AP MOS at heel-strike and mid-swing as TD children (Fig. 1). In contrast, ML MOS at heel-strike and mid-swing was less stable in children with DS than TD children (Fig. 1). SPM analysis indicated that reduced stability occurred throughout single-limb support and particularly towards the end of this phase. These results further support the classification of reduced ML stability in children with DS. Encouragingly children with DS were able to increase mobility in the AP direction when challenged to walk at the *fast* condition.

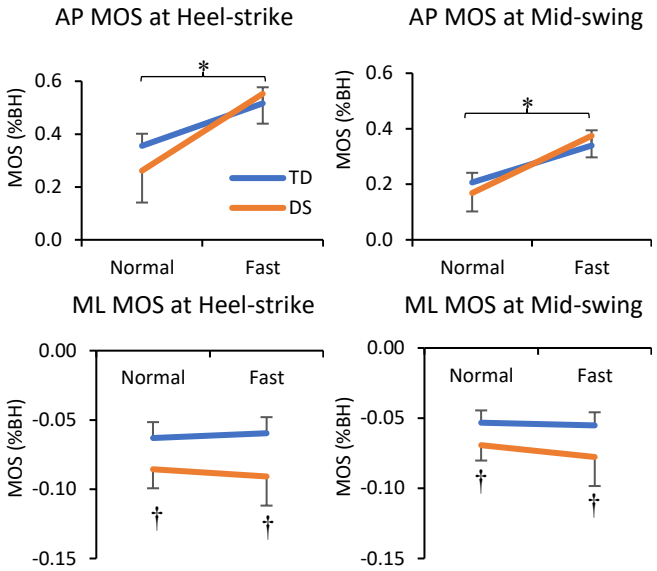

Figure 1: AP and ML MOS at heel-strike and mid-swing. For AP, a positive number indicates projected COM is anterior to the base of support. For ML, a negative number indicates projected COM is outside of the base of support. * indicates speed effect. † indicates group effect.

Children with DS increased walking speed by increasing hip and knee flexion during swing phase and decreasing hip and knee extension during stance phase. In contrast, TD children also increased hip and knee flexion during swing, but without the concurrent decrease in stance phase extension. While children with DS were able to increase their walking speed, they likely used an undesirable strategy by adopting a more crouched gait during stance phase. Therefore, interventions targeting strengthening of the hip and knee extensors might be beneficial for this population.

Significance

This study provides evidence that children with DS have the capacity to increase their mobility in the AP direction when challenged to walk faster than preferred. However, children with DS are less stable in the ML direction during gait, which suggests the common characteristic of increased step width is insufficient to alleviate their instability. In addition, children with DS increase their walking speed by increasing swing phase hip and knee flexion at the detriment of stance phase extension. Rehabilitation might therefore focus on increasing hip and knee extensor muscle strength in this population.

Acknowledgments

We are grateful to the participants and their parents for their contributions to this study.

References

1. Agiovlasitis S et al. 2009. Gait & Posture, 30(3): 345-350.
2. Smith BA et al. 2007. Phy Ther, 87:766-777.
3. Wu J & Ajisafe T. 2014. Gait & Posture, 39:241-246.
4. Tracy JB et al. 2019. Gait & Posture, 72:182-187.

Exploring Novel IMU-Based Strategies for Quantifying Manual Asymmetries During Activities of Daily Living

Athena Prine[1], Tea Lulic[1], Alicia Carmichael[2], Natalie Leonard[2], Andrew Lemmen[2], Maren Wisniewski[2], Stephen Cain[3], David Lipps[1]
[1]School of Kinesiology, [2]Institute for Social Research, [3]Department of Mechanical Engineering
University of Michigan, Ann Arbor, MI USA
Email: aprine@umich.edu

Introduction

Capturing atypical arm movement during the performance of activities of daily living (ADL) has clinical implications in assessing and restoring arm function. Traditionally, position-based approaches are used to measure and analyze arm movement during ADLs [1,2]. However, these approaches are often limited to controlled laboratory environments. Inertial measurement units (IMUs) are wearable sensors that can acquire and examine movement in real-world settings. IMUs do not measure position directly, but instead measure linear acceleration and angular velocity. Therefore, alternative approaches that are independent of position are needed to quantify and understand arm movements acquired during everyday living with IMUs. The current study aims to identify new, IMU-based strategies for characterizing reaching tasks that can be employed in future work to quantify arm function in healthy and clinical populations. In particular, this study developed a novel IMU-based analysis for assessing manual asymmetries during unilateral reaching tasks.

Methods

Four right-handed female subjects (mean±SD age 54±4.3 years) provided written consent to participate in this study at the University of Michigan HomeLab, a fully functional apartment where participants can be observed performing ADLs while simultaneously collecting physiological data. Each participant wore five IMUs (APDM Opal; sampling rate: 128 Hz): one on each wrist, one above each elbow, and one above the sternum. During the experiment, participants performed seven ADLs with either their dominant arm, non-dominant arm, or bilaterally. The current study focused on a single ADL: unilateral shelf reaching. Participants were instructed to reach for a can on a shelf and place it on a counter or lift a can off a counter and place it on a shelf (Figs. 1C and 1D). We calculated the velocity and position of each wrist from the raw IMU data using a ZUPT algorithm [3]. Forearm, upper arm, and thorax elevation angles were estimated from the IMU data [4]. Wrist heights relative to the shoulder joint were calculated from segment elevation angles [5]. We then extracted spatiotemporal metrics to characterize the shape of the angle-angle-position (Fig. 1A) and position trajectories (Fig. 1B). In particular, we focused on the reach trajectory curvature, peak velocity, and timing as our primary measures, and explored how arm dominance influences these measures with dependent t-tests.

Results and Discussion

The left arm's angle-angle-position trajectory had 94% greater mean curvature than the right arm. This trended towards significance despite our low sample size ($p = 0.06$; Figs. 1A and 1E). In comparison, the mean curvature of the wrist position trajectory was 5% greater for the left arm than the right arm, but was not statistically significant ($p = 0.64$; Figs. 1B and F). The peak wrist velocity of the left arm was 2.3% greater than the right arm (Fig. 1G) and the time after peak velocity was 8% longer in the right in comparison to the left arm (Fig. 1H). These findings were not significantly significant ($p > 0.28$), similar to previous studies [6]. Lastly, reaching durations did not differ between the hands ($p = 0.91$), which is consistent with the literature [6]. These preliminary analyses indicate temporal and spatial metrics related to manual asymmetry can be quantified with IMUs, and are consistent with previous controlled laboratory findings [1,2].

Significance

This pilot study provides evidence that data from wireless and wearable IMUs can quantify arm movement during ADLs. Importantly, our approach yields metrics drawn from prior research on manual asymmetries during reaching tasks. These results show that IMUs, when used in tandem with carefully designed algorithms to extract meaningful metrics, have the potential to be deployed to patient's home to assess their arm movements outside a controlled laboratory environment. Future work will determine if this IMU-based strategy can detect impairment and be used to screening patients for rehabilitation.

Acknowledgments

This project was funded by NIH/NICHD R03HD097704 and the U-M School of Kinesiology Marie Hartwig Research Fund.

References

[1] Przybyla, A., et al. *Neurosci Lett.* (2011).
[2] Shabbott, B.A., & Sainburg, R.L. *J Neurophysiol.* (2008)
[3] Rebula, J.R., et al. *Gait & Posture* (2013)
[4] Savage, P.G. *J Guidance, Ctrl, Dyn* (1998).
[5] Laidig, D. & Seel, T. *Current Dir Biomed. Eng.* (2017).
[6] Heath, M. et al. *Laterality* (2002).

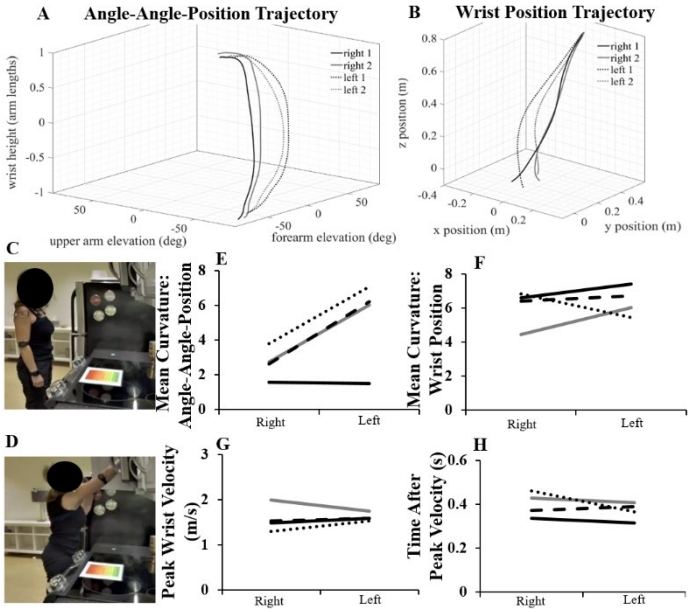

Figure 1. Representative data from one participant (right arm dominant). (A) A novel angle-angle-position plot that reveals manual asymmetry. (B) IMU-derived wrist position trajectory during unilateral reach. (C) The starting/ending posture for each reach. (D) Posture at maximum reach. (E-H) Manual asymmetries between the right and left arm of 4 participants was investigated based on the mean curvature of angle-angle-position trajectory (E), mean curvature of the 3-D position trajectory (F), peak wrist velocity (G) and time after peak velocity (H).

Differences of joint function between children and adults during hopping at different frequencies

Matthew Beerse[1] and Jianhua Wu[2]
[1]University of Dayton, [2]Georgia State University. Email: mbeerse1@udayton.edu

Introduction

Hopping in-place is a fundamental motor skill that follows the spring-mass model, which is generally used to model running and jumping (1). Therefore, evaluation of this skill provides insight to the development of neuromuscular control strategies and sheds light on its implications in play and plyometric interventions. Indeed, developmental differences have indicated that children might coordinate the movement with greater contribution of the knee and hip joints (2). This is in contrast with young adults who modulate hopping frequency primarily through the ankle joint (1).

The joint functional index analysis incorporates both kinematics and kinetics to characterize strut, spring, motor, and damper function of a joint (3). During two-legged hopping in-place, young adults hop with an ankle and knee spring-like function and modified joint functions when increasing hopping frequency (4). However, it is unknown if children show similar functional use of the ankle and knee joints, like adults, during hopping.

This study aimed to characterize the joint function of the ankle and knee joints during single-leg hopping in-place in adults and children across various hopping frequencies.

Methods

Thirteen young adults (5F/8M, 24.54 (3.53) years) and fourteen children (9M/5F, 8.70 (1.81) years) participated in this study. Subjects hopped on their dominant leg continuously for 20-seconds at four frequency conditions: *slow* (80% preferred), *preferred* (self-selected), *moderate* (120% preferred), and *fast* (140% preferred). Each frequency was guided by a metronome. Subjects completed three trials of each frequency and order was randomized across subjects.

We collected kinematic data using a Vicon motion capture system (Oxford, UK) and the Vicon PSIS Lower-Body Plug-In Gait marker set . We collected kinetic data using an AMTI force plate (MA, USA). Ankle, knee, and hip joint moments were estimated using an inverse dynamics approach. We classified joint function during stance phase as strut, spring, motor, and damper (3).

Two-way (2 group x 4 frequency) mixed ANOVA was conducted for each function at each joint. Post-hoc pairwise comparisons with Bonferroni adjustment were completed when necessary. Significance level was set at alpha=0.05.

Results and Discussion

Children hopped with less ankle joint spring function across frequencies than young adults (Fig. 1). When increasing frequency, children illustrated an adult-like pattern by increasing ankle strut function while reducing others. However, this increase might have led to a change in overall function from spring to strut in children as the composition shifted towards greater strut than spring at the *moderate* and *fast* frequencies. In constrast, young adults retained a spring function majority, even at the *fast* frequency (mean of 53%). Our results suggest that children are still developing the capacity to effectively utilize the ankle joint as a spring to increase hopping frequency.

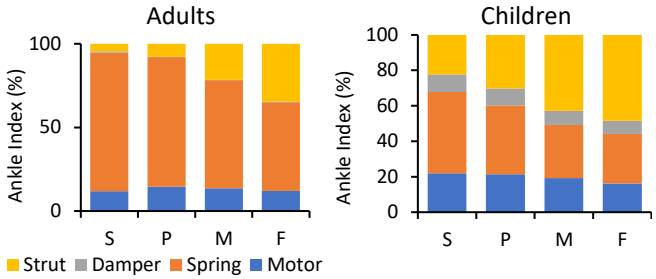

Figure 1: Mean joint functional indices for the ankle joint. S: *slow*; P: *preferred*; M: *moderate*; F: *fast*.

Children hopped with less knee joint spring function, but greater strut function than young adults at the preferred frequency (Fig. 2). Children increased frequency by increasing strut and motor function and decreasing spring and damper, similar to adults. The loss of spring function in children while hopping at faster frequencies might have required more motor function to accommodate lost energy storage.

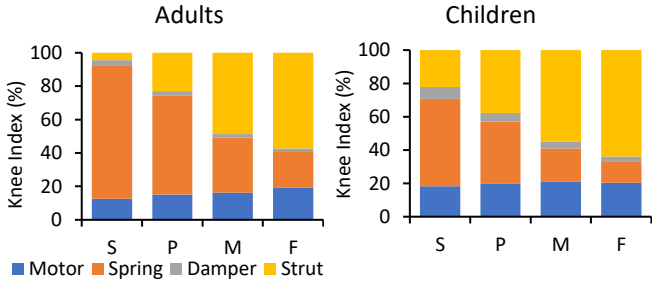

Figure 2: Mean joint functional indices for the knee joint. S: *slow*; P: *preferred*; M: *moderate*; F: *fast*.

Significance

The joint functional index analysis revealed development differences in ankle and knee functions between children and adults during single-leg hopping in-place. Specifically, children relied on more strut-like function at the knee and ankle joints rather than spring-like function. Therefore, previously identified neuromechanical differences between young adults and children might be due to functional disparities at the joint level. These results could inform interventions and serve as a reference when evaluating the development of joint functions in populations with motor disabilities.

References

1. Farley CT & Morgenroth DC. 1999. J Biomech, 32(3):267-273.
2. Beerse M & Wu J. 2021. Gait & Posture, 84:175-181.
3. Mu Q & Jindrich DL. 2016. J Biomech, 49(1):66-72.
4. Monte A et al. 2021. J Biomech, 118.

Preliminary Movement Data of Yucatan Mini Pig

Nicole Arnold[1], Alesa Hughson[1], Galit Pelled[1], PhD, and Tamara Reid Bush[1], PhD
[1]Michigan State University, East Lansing, MI, USA
Email: reidtama@msu.edu, arnoldn5@msu.edu

Introduction

Traumatic brain injuries (TBIs) are one of the leading causes of death and disability among people of every age, race and color [1]. Motor control disorders following TBI often include deficits in locomotion, which affect an individuals' mobility. There has been considerable research on rodent models to understand the pathophysiology of TBIs, but there is a lack of translation between these experiments and clinical outcomes. Large animal models (i.e. pigs) are more commonly used now as there are many similarities between pig and human brains (size, development, ratio of white to gray matter to name a few). Thus, pigs are a preferred model for analyzing the response of mechanical trauma on the brain from a TBI. The goal of this research was to conduct pilot work to confirm gait data of Yucatan mini pigs could be obtained. The long-term goals of this work are to study pigs pre and post TBI to determine if changes in gait parameters can be detected.

Methods

Three-dimensional (3D) kinematic data of a single pig during walking trials were captured with a Qualisys motion capture system. Three rigid marker pods were placed on the spine of the pig (Figure 1). Each pod consisted of three reflective markers arranged in a triangle formation. One pod was placed on the head (covering the base of the skull to the second cervical vertebrae), a second on the shoulders (directly over the third thoracic vertebrae), and a third on the rear (directly over the sixth lumbar vertebrae). Additionally, four single markers were placed on the front and hind limbs distal to the condyle of the humerus and distal to the lateral condyle of the femur, respectively. Initial kinematic analysis of the pig gait trials were performed. Data of each local coordinate system were analyzed of each pod with respect to the fixed reference system (i.e., global coordinate system) and the motions about each axis as shown in Figure 2. This initial analysis included the average linear velocity, along with angle data. Markers used to calculate average linear velocity were aligned with the spine of the pig in the direction of movement (i.e. along the x axis). Angle data were referenced from the neutral position of the head, shoulders and rear which was identified as the position of each at the beginning of the walking trial.

Results and Discussion

Data are reported from a single gait cycle. The average linear velocity of this pig was 1.01 m/s. Data showed lateral tilt (about the x-axis) of the head ranged from neutral with tilting to 12.6° (degrees) on the right side with no significant tilt toward the left side. Additionally, the head flexion-extension or "nodding" motion (about the y-axis) ranged between 1.16° (flexion) and 16.7° (extension), but this movement may have been influenced by food incentives used to entice the pig to walk through the space. Left to right rotation (about the z-axis) of the head ranged from neutral to 30.1° rotation to the left (as the pig moved its head in an attempt to turn) and up to 7.10° on the right. Lateral tilt of the shoulders (about the x-axis) from neutral ranged up to 11.7° and 3.79° on the left side and right sides, respectively. Rotation of the shoulders (about the y-axis) ranged up to 9.35° forward and 9.59° backward throughout the walking trial. Left to right rotation (about the z-axis) of the shoulders ranged up to 15° to the left and 3.07° to the right. Lateral tilt (about the x-axis) of the rear ranged up to 11.6° on the left and 8.98° of rotation on the right. Rotation (about the y-axis) forward of the rear ranged up to 14.2° and with no significant movement measured downward. Lastly, left to right rotation (about the z-axis) of the rear ranged up to 32.0° and 19.6° on the right and left, respectively. This work demonstrates the initial data sets possible with a 3D kinematic gait analysis. In the future we will take rotations of each pod location (head, shoulders, rear) and compare the motions between each whereas the above data are the movement of the pods with respect to a global system. Additionally, future work will use this approach to quantify and compare changes in movement pre and post trauma within and across pigs.

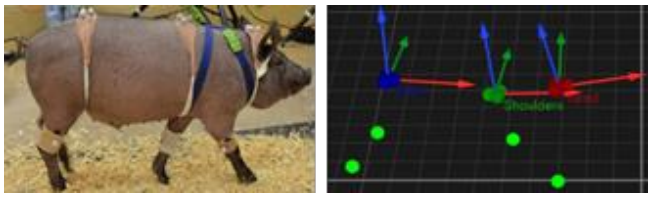

Figure 1: (Left) Pig with reflective markers. (Right) Three rigid pods in Qualisys. Pods were located along the spine (starting on the right: head, shoulders, and rear) with four single markers, one on each leg. Coordinate system is labeled as follows: x-axis in red, y-axis in green, z-axis in blue.

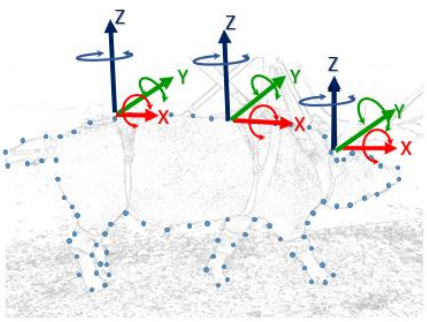

Figure 2: Motion about each axis. Lateral tilt rotation occurs about x-axis (red), flexion-extension motion occurs about y-axis (green) and left-right rotation occurs about the z-axis (blue)

Significance

Research shows that impairments from a TBI can last or go undiagnosed for years [3]. Currently, there are no long-term solutions to enhance the outcomes from TBI related disorders. By understanding the behavior of pigs before and after a TBI, we will be able to identify and quantify changes in motor function potentially leading to new approaches for diagnosis or treatments.

References

1. Taylor CA., MMWR Surveill Summ 2017
2. Bhatti, Z., Thesis, University of Sindh, 2017
3. Rivara FP., Am J Public Health. 2012

GAIT VARIABILITY DURING TREADMILL WALKING IN CHILDREN WITH AUTISM SPECTRUM DISORDER

Emily A. Chavez[1], Alyssa N. Olivas[2], Jeffrey D. Eggleston[1,3]
[1] Department of Interdisciplinary Health Sciences, The University of Texas at El Paso, El Paso, TX, USA
[2] Department of Biomedical Engineering, The University of Texas at El Paso, El Paso, TX, USA
[3]Department of Kinesiology, The University of Texas at El Paso, El Paso, TX, USA
Email : eachavez4@miners.utep.edu

Introduction

Movement pattern variability represents flexibility in the neurological system which allows an individual to accommodate changes to their environment through strategy modifications [1]. In this context, motor disabilities have been described as non-stereotypical or unpredictable [1]. Previously, treadmill-use (TM) resulted in optimally altered gait variability patterns compared to over-ground (OG) gait in those with Parkinson's disease [2]. Individuals with Autism Spectrum Disorder (ASD) display motor impairments where posture and gait have been described as "Parkinsonian-like", due to similar abnormalities observed in the basal ganglia [3]. Past OG gait findings support that children with ASD exhibit different magnitudes of movement pattern variability [4]. It can be posited that children with ASD may not have appropriate flexibility in their system to accommodate external stimuli, possibly due to brain abnormalities. Current literature is lacking in examining gait variability responses in children with ASD on a TM, despite previous benefits found in similar populations. Thus, the purpose of this study is to quantify variability magnitudes during TM gait in children with ASD compared to children with neurotypical (NT) development. It was hypothesized that children with ASD will display decreased variability patterns during TM gait compared to a NT group.

Methods

19 children, 10 with a clinical diagnosis of ASD (11.56±1.39 yrs; 1.57±0.12m) and 9 children with NT (12.13±2.09 yrs; 1.60±0.15m) initially walked OG across 9m for 12 trials at a self-selected velocity. Gait velocity from the OG trials were computed as an aggregate mean value used during the TM condition; shoes were worn throughout. Marker trajectories were obtained using a 10-camera three-dimensional motion capture system (200 Hz, Vicon Motion Systems, Ltd., Oxford, UK). Participants walked for 5-min, continuously, on an ActiveStep TM (Simbex, Lebanon, NH, USA). Data were collected after the first 60s to ensure a homeostatic gait pattern. Raw marker trajectories were exported to Visual 3D (C-Motion, Inc., Germantown, MD, USA) and were smoothed using a low-pass Butterworth digital filter (6Hz). Bilateral continuous relative phase (CRP) angles were computed for the thigh-leg, leg-foot, and thigh-foot segment couples bilaterally [5]. Coordination variability (vCRP) was determined as the standard deviation of CRP angles for each segment couple [6]. Data were normalized to heel strikes were reduced to left and right strides using a velocity-based algorithm [7]. The Model Statistic technique ($\alpha = 0.05$) was used to statistically compare each child with ASD to a collated normative NT group [4] at each gait sub-phase for all segment couples, bilaterally.

Results and Discussion

Analysis revealed on average, children with ASD displayed different magnitudes of variability compared to the NT group at each sub-phase and across each segment couple in response to TM walking. Children with ASD and NT displayed symmetry variability between limbs (**Figure 1A & 1B**), thus, a distinct pattern was undetected, further supporting movement heterogeneity of children with ASD [4]. Additionally, NT displayed symmetry variability across segment couples.

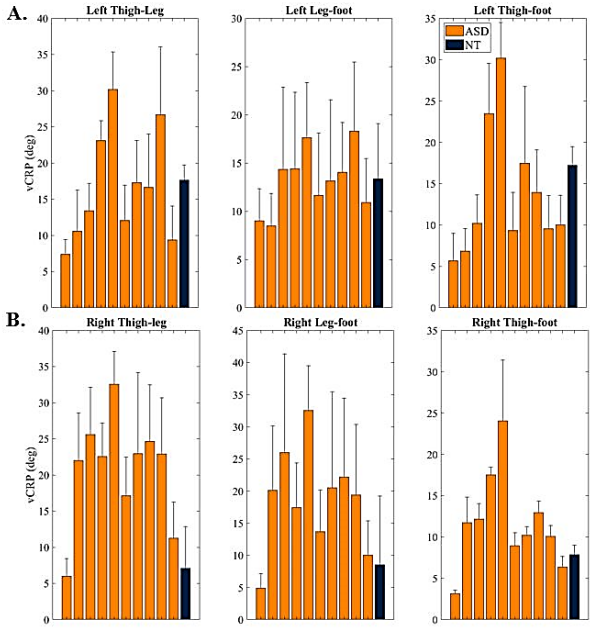

Figure 1: Left limb (A.) and right limb (B.) segment couple mean and standard deviation magnitudes during Initial Swing between individual children with ASD (orange bars) and the NT group (dark blue bar).

Significance

Due to the cyclic nature and repeatability of gait, using TMs may allow researchers to collect greater volumes of gait cycles to optimize ASD movement analysis. This study supports that children with ASD may have varied lower extremity movement patterns. However, an indiscernible pattern poses difficulties in evaluating how children with ASD may adapt their movements to a changing environment which puts locomotor safety at risk. Future research should examine ASD motor impairments individualistically to identify motor-specific characteristics which may prompt clinicians to use more individualized rehabilitation interventions.

Acknowledgments

This research was supported by the University of Texas at El Paso Dodson Research Grant.

References

[1] Stergiou et al. (2006), *J. Neuro. Phys. Ther.,* **30(3)**, 120-129
[2] Bello & Fernandez (2012). *Current Aging Sci.,* **5(1)**, 28-34.
[3] Maurer & Damasio (1982). *J. Aut. Dev. Dis.,* **12(2)**, 195-205.
[4] Dufek et al. (2018). *J. Devel. Phys. Disabi.,* **30(6)**, 793-805.
[5] Miller et al. (2008), *J. of Appl. Biomec.* **24(3)**, 262-270.
[6] Hein et al. (2012), *Hum. Move. Sci.,* **31(3)**, 683-694.
[7] Zeni & Higgins (2008), *Gai. Pos.*, **27(4)**, 710-714.

REPEATABILITY OF A VISUAL ANALOGUE SCALE TO MEASURE COMFORT OF AN EXOSKELETON

Mohammed Mohammed El Husaini[1], Anne E. Martin[1]
[1]Mechanical Engineering, Penn State University Park, State College, PA, USA
Email: mqm5959@psu.edu

Introduction

While important, user-perceived exoskeleton comfort is often ignored, in part because a validated metric does not exist. Visual analogue scales (VAS) are a reliable method to measure comfort in other contexts, such as footwear[1] and acute pain[2]. The primary objective was to quantify the repeatability of an exoskeleton comfort VAS. The secondary objective was to determine if the comfort signal-to-noise ratio was large enough to test predictions.

Methods

Experimental: Two young, adult male subjects walked at 0.50 m/s with a pneumatically powered ankle exoskeleton on their right leg and an identical, unpowered (due to technical difficulties) exoskeleton on their left leg. The exoskeleton torque was $k_P\theta$, where k_P was the virtual stiffness and θ was the ankle angle in degrees. During each experimental session of 8 trials, we tested k_P values of 0 to 0.9 N·m/deg in 0.15 N·m/deg increments plus 1.0 N·m/deg. Thus, we had a total of 16 conditions = 8 k_P levels × 2 subjects since different subjects were expected to have different comfort scores for a given k_P. After each 3 min trial, subjects responded to ten 100mm horizontal VAS questions on a tablet, immediately followed by a new trial with a new k_P. Each subject completed 7 sessions, 5 with randomly varying k_P and 2 staircase sessions where k_P was increased sequentially.

Analysis: This abstract only analyzed the first question: "How comfortable are you?" due to high correlations between question scores. Repeatability was quantified by computing the repeatability coefficient[3] $RC = 2.77\sqrt{MSE}$, where MSE was the within-condition mean square error calculated using a one-way ANOVA. 95% of responses were expected to be within $\pm RC$ of each other for repeated measures of the same condition. Repeatability was also quantified using the error $e = c - \mu_{k_P}$, where c was the comfort score and μ_{k_P} was the corresponding mean comfort for that condition[3]. The 50%, 90%, and 95% error thresholds were ranges of error that contain those percentages of trials respectively. To determine if predictions were possible, we performed quadratic regression since we expected comfort to be highest for moderate k_P. A strictly negative 95% confidence interval (CI) for the quadratic term would suggest a sufficient signal, despite the noise, to confirm the prediction.

Results and Discussion

The range of responses was [0, 73] mm (Fig. 1), with similar ranges between random and staircase sessions and for individual subjects. There was no apparent drift in comfort scores between sessions. Each subject had different k_P ranges that were most comfortable, as expected. RC was 45mm (Fig. 2), which was significantly larger than the 9 to 20mm RC for acute pain[2]. 50% of trials had errors within 10mm, 90% were within 28mm, and 95% were within 36mm, which was consistent with the high RC for comfort. Thus, the repeatability was poor. A quadratic fit using all of the data had a strictly negative 95% CI for the quadratic term, indicating that the fit was concave down as expected (Fig. 1). However, the R^2 value was 0.094, affirming the low repeatability. Despite the noise, this suggests that there was a sufficient signal to test predictions using data from multiple sessions. The comfort scores of individual random sessions did not reliably produce fits with a strictly negative 95% CI for the quadratic term. Conversely, 3 out of the 4 staircase sessions did, indicating that the staircase sessions may have more repeatable comfort scores. Since comfort likely has an aspect of comparison[1], this was not surprising since the staircase trajectory kept Δk_P constant, but the random sessions did not.

Significance

A comfortable exoskeleton may be more acceptable, motivating the creation of a comfort metric. Despite promising results from other fields, using a VAS to measure exoskeleton comfort had poor repeatability, particularly when k_P was tested randomly. It was still possible to find statistically significant regressions given sufficient data, suggesting that there was an underlying true signal. Nevertheless, further work to develop a comfort metric and an appropriate experimental protocol is required.

Acknowledgments

This work was supported by the NSF under Grant No. 1930430.

References

1. Mündermann, et al. *Gait Posture* **16**, 38–45, 2002.
2. Bailey, et al. *Pain* **153**, 839–842, 2012.
3. Bland & Altman, *Stat Methods Med Res* **8**, 135-160, 1999.

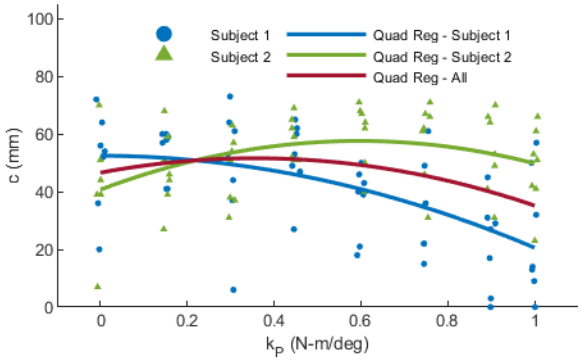

Figure 1: Comfort score c vs. k_P, where c = 0 is very uncomfortable and c = 100 is very comfortable. Despite considerable noise in the data, the quadratic regressions were concave down.

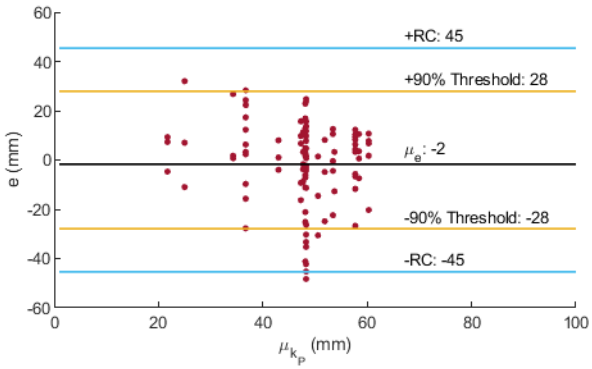

Figure 2: Error vs. mean comfort for that condition. There were significant deviations among responses signifying poor repeatability.

Joint kinematics and work adjustments in adults when learning the kettlebell swing without coaching

Matthew Beerse[1], Cian Callahan[1], Gerry Gallo[1], Joaquin Barrios[1]
[1]University of Dayton. Email: mbeerse1@udayton.edu

Introduction

The kettlebell swing is a contemporary compound exercise involving explosive concentric extension of the ankle, knee, and hip (1). When coached, the kettlebell swing can increase vertical jump height (2) and cardiovascular health (3). However, the kettlebell swing is a complex technical skill and improper hip motion has been found when initially attempting the movement (4), which might limit the aforementioned exercise benefits. Therefore, evaluation of the kinematic and kinetic adjustments young adults make when learning the kettlebell swing would provide pertinent information on the potential effectiveness of implementing a kettlebell training program. Further, recent demand of at-home exercise and remote video instruction necessitate an understanding of self-directed adjustments without individualized external feedback or coaching cues. This evaluation would assist the development of effective and safe video instruction tools, which has become commonplace for commercial exercise equipment.

Therefore, this study aimed to assess the ankle, knee, and hip kinematic and kinetic adjustments with short-term practice, as evaluated by joint angles and joint work, in young adults when practicing the kettlebell swing.

Methods

Twelve young adults (7F/5M, 22.62 (2.04) years) practiced over a one-week period, on five separate days. We collected kinematic data using a Full-Body PIG marker set and Vicon motion capture system (Oxford, UK), as well as kinetic data using a Bertec force plate (OH, USA) on the first and fifth day. On day one, we collected subjects' first attempt at performing the kettlebell swing *no practice* (*NP*). Subjects performed three sets of 20 repetitions. The only instruction was a freely available online video of a skilled individual performing the kettlebell swing and providing verbal instruction. On days two, three, and four, subjects complete five practice sets of 20 repetitions. On day five, we collected data on subjects performing three sets of 20 repetitions, *short-term practice (SP*). Between sets, subjects rested at least three minutes. Subjects received no feedback or cues on their performance, but could rewatch the video. Subjects ≤165 lbs swung 15 lbs and subjects >165 lbs swung 25 lbs.

Ankle, knee, and hip sagittal plane joint angles were time normalized to each kettlebell swing cycle. One cycle started at the catch position followed by extension into a standing position followed by flexion back into the catch position. Ankle, knee, and hip joint moments were estimated using an inverse dynamics approach and joint work was separated into concentric and eccentric portions and summed. In addition, total work in the sagittal plane was estimated as the product of 2D center-of-mass displacement and 2D ground reaction force, also separated into concentric and eccentric periods. Paired t-tests compared joint work between sessions. Statistical parametric mapping was used to compare continuous joint angles between sessions.

Results and Discussion

Young adults made minimal kinematic adjustments of the ankle, knee, and hip joints (Fig. 1). At the catch position (0-10% and 90-100% cycle), the knee and hip joints were less flexed at the *SP* session compared to the *NP* session. This was a partially desirable adjustment. The kettlebell swing is considered a hip-hinge exercise with less knee flexion than a squatting movement (1). Therefore, reducing knee flexion could be considered appropriate, however, reducing hip flexion might indicate a tendency to stay upright rather than hinging forward. These results suggest reminders of hip flexion in an instructional video would be necessary to ensure proper mechanics.

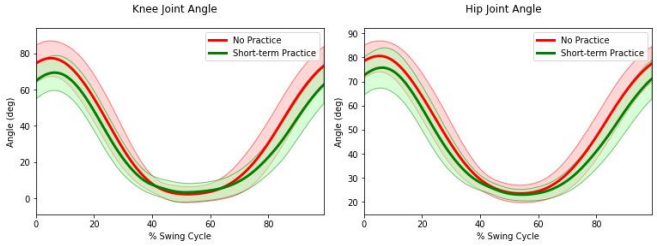

Figure 1: Mean (SD) time normalized knee and hip joint angles during the kettlebell swing.

Total concentric and eccentric work decreased between sessions. In addition, only the hip joint illustrated reduced concentric and eccentric work at the *SP* session. These results suggest that the young adults worked less to complete the kettlebell swing, which could signal a capacity to increase kettlebell load. From a training perspective, this result suggests young adults have a tendency to reduce work without cueing. Therefore, if the kettlebell swing is implemented to increase power (1) specific cueing should be incorporated.

Work	Session	Concentric	Eccentric
Total (J/kg)	NP	354.56 (58.92)	-312.46 (52.89)
	SP	**322.79 (82.52)**	**-271.67 (67.50)**
Ankle (J/kg)	NP	14.27 (5.33)	-14.84 (10.00)
	SP	29.41 (56.14)	-29.88 (65.80)
Knee (J/kg)	NP	18.40 (9.90)	-17.85 (7.15)
	SP	23.38 (62.46)	-34.49 (72.97)
Hip (H/kg)	NP	64.83 (17.02)	-55.73 (12.98)
	SP	**56.58 (18.85)**	**-44.96 (15.73)**

Table 1: Mean (SD) total and joint work. NP: *NP*, SP: *SP*. Bold indicates significantly different from NP at $p<0.05$.

Significance

Our results highlight the general tendencies of young adults to reduce lower body flexion and work when learning a kettlebell swing through self-directed methods. These findings provide guidance to improve the potential effectiveness of instructional videos and suggest coaching cues should focus on the hip joint even if being supplied remotely.

References

1. Meigh NJ et al. 2019. BMC Sprt Sci Med Rehab, 11(1):19.
2. Lake JP & Lauder MA. 2012. J Str & Cond Research, 26(8):2228-2233.
3. Farrar RE et al. 2010. J Str & Cond Research, 24(4):1034-1036.
4. Gelder LHV. 2015. Int J Sprt Phy Ther, 10(6):811-826.

CHANGING SHEAR FORCES AND PRESSURES ON THE BUTTOCKS: IMPLICATIONS FOR PRESSURE INJURIES

Justin Scott[1] and Tamara Reid Bush[1]
[1]Department of Mechanical Engineering, Michigan State University
email: reidtama@msu.edu, scottju5@msu.edu

Introduction

Pressure injuries (PIs) are debilitating injuries that affect up to 47% of wheelchair users with spinal cord injuries [3]. Prevalence of PIs and treatment costs of over $30,000 per incident drive the $27 billion annual expenditure on PI treatment in the US [2,5].

Normal and shear forces are implicated in PI development, and thus PI prevention strategies focus on reducing them, in particular on the buttocks and lower back where PIs are common [4]. Popular strategies include back recline and using specialized cushions to distribute load. Cushions reduce, but don't eliminate PIs, while evidence for the use of recline is inconclusive [1,6].

The goals of this work were to evaluate 1) back recline and seat pan tilt as seated repositioning strategies for the purpose of preventing PIs, and 2) a custom nylon cushion cover's ability to reduce shear force on the buttocks while seated.

Methods

A custom articulating chair with independent back recline and seat pan tilt motions was built for this study. The seat pan, pelvic, and thoracic supports were mounted on six-axis load cells and covered by thin layers of foam. A pressure mat was overlayed on top of the foam, and two interchangeable covers were evaluated over the cushion assembly on the seat pan. One cover consisted of a vinyl fabric and the other a two-layer system of nylon fabric.

20 able-bodied people (10 male, 10 female) volunteered for this study. Participants sat in the chair with it in a neutral position (i.e., with no back recline or seat pan tilt), and with the vinyl cover on the seat pan. The back recline and seat pan tilt were set to 0°, 10°, or 20° and 0°, 15°, or 30°, respectively. The chair was moved to each combination of back recline and seat pan tilt (9 total) in a random order, and interface pressure and force data were collected in each position. The two-layer nylon cover was then placed on the seat pan, and the sitting protocol was repeated.

Pressure measurements were then segmented. Pressures on the posterior half of the mat on the seat pan were considered to be on the buttocks, and pressures on the inferior third of the back pressure mat were considered to be on the lower back. Maximum pressures from both regions were recorded in every position.

Results and Discussion

Maximum pressures in the buttocks and lower back at each recline angle and seat pan tilt are reported in Figure 1. The data indicate recline increased maximum pressures in the buttocks and lower back, while seat pan tilt decreased pressure in both regions.

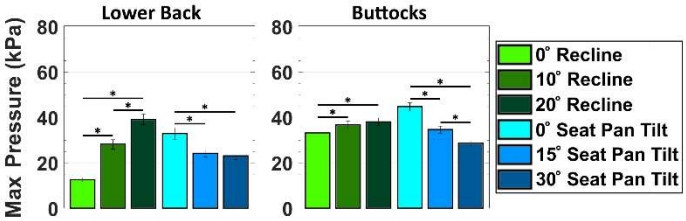

Figure 1: Effects of back recline and seat pan tilt on the maximum pressures in the lower back and buttocks. Recline increased pressures in both regions, while seat pan tilt decreased it, significance indicated by asterisks (*).

Shear forces from the seat pan are reported at all angles of recline for the vinyl and two-layer nylon covers in Figure 3. Recline increased shear force on the seat pan, and the two-layer nylon cover reduced shear force by 10% relative to the vinyl cover.

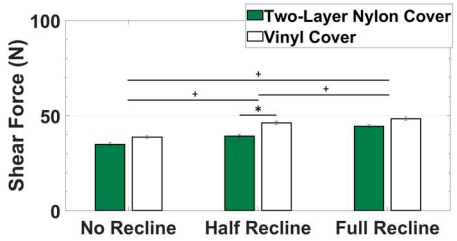

Figure 2: Effects of back recline and two covers on shear forces on the seating surface. The two-layer nylon cover reduced shear forces on the seating surface significantly in the half recline positions (*) and by about 10% across all positions. Recline increased shear forces (+).

The goal of this study was to describe the effects of repositioning and surface cover material on interface loads and pressures while seated. Data showed that back recline, although used to relieve pressure on wheelchair users, increased normal and shear loads on the buttocks, putting them at higher risk of PI development. Our results suggest that back recline be re-evaluated as a pressure relief strategy and that seat pan tilt should instead be considered to reduce PI risk in the buttocks and lower back. The two-layer nylon cover was additionally shown to reduce the shear force on the seat pan by 10% because the layers of nylon slid relative to one another. Seat pan tilt reduced normal pressure on the buttocks and lower back, and the two-layer nylon cover reduced shear force on the buttocks, therefore, both are potential strategies to reduce the risk of PI formation.

Significance

The findings from this study have implications across clinical and computational biomechanics. Clinically, the results of this study assess protocols used to protect patients from PIs. They provide evidence that current practices may need to be re-evaluated. The data from this study are of further use to computational biomechanists. Loading data from the buttocks and lower back can be used as inputs for finite element models that estimate internal stresses related to PI risk. This work advances our understanding of risk factors related to PI formation in wheelchair users.

Acknowledgments

This work was funded by NSF grant CBET-1603646.

References

[1] Brienza et al., *J Am Ger Soc*, 2010.
[2] Chan et al., *J Wound Care*, 2017.
[3] Cowan et al., *Adv Skin and Wound Care*, 2019.
[4] Horn, *J Am Ger Society*, 2002.
[5] Padula and Delarmente, *Int Wound J*, 2019.
[6] Shirogane, et al., *Assist Tech*, 2018.

DEVELOPING A RECIPROCATING GAIT ORTHOSIS THAT TRIGGERS AMBULATION UPON A LATERAL SHIFT IN WEIGHT

Sarah C. Griffin[1], B. Flemming, M. Flynn, O. Bleke, C. Russell, C. Elion., S. Sutphin, Ross Chafetz[2], and Reva Johnson[3]
[1]Department of Bioengineering, University of Pittsburgh, Pittsburgh, PA, USA
[2]Shriners Hospitals for Children—Philadelphia, Philadelphia, PA, USA
[3]Department of Mechanical Engineering and Bioengineering, Valparaiso University, Valparaiso, IN, USA
email: reva.johnson@valpo.edu

Introduction

A Reciprocating Gait Orthosis (RGO) is a bracing system which includes a mechanism that helps the user initiate a gait pattern. Current designs require the patient to use trunk extension to trigger the mechanism and initiate ambulation. This unnatural movement makes the device difficult to use and many patients shuffle their feet instead of utilizing the reciprocating mechanism. To allow for more natural ambulation, this research designed a new mechanism and prototype RGO. The mechanism triggers a reciprocated motion upon a shift in weight to the stance leg. This is a more natural movement since users must shift their weight to one side to allow the swing foot to clear the ground regardless of the mechanism design [1]. We believe this mechanism can revolutionize the RGO, increase patience usage, and restore ambulation to immobile patients.

Methods

A Valparaiso University undergraduate design team completed a design and prototyping process during the 2019-2020 school year. Design requirements were defined in consultation with a pediatric physical therapist. The RGO mechanism was designed in SolidWorks CAD software. A scaled design was 3D printed to confirm that the device moved as planned. Finally, the models were scaled to life-size so that they could be manufactured to fit a healthy test subject. Future testing will outfit a healthy test subject with the RGO to further prove the efficacy of the device.

Results and Discussion

The mechanism consists of rotating hip components attached though a large lever across the back of the individual. Figure 1 depicts mechanism design and the applied forces and corresponding movements of the mechanism. When the user shifts their weight to the stance leg, there is a large upward force on the back of the corresponding hip component. This force propels the stance leg backwards and lowers the lever ipsilaterally. As the back lever rotates towards the stance leg, it pulls upwards on the swing leg, propelling it forward. Once the swing leg has been stepped forward, the user can shift their weight onto that leg. The same process is repeated on the other leg to facilitate a gait cycle.

The 3D printed, scaled mechanism was manually tested to ensure that the device moved as predicted. Future work will require manufacturing and testing of a physical prototype. A full-scale version of the device will be tested with human subjects to confirm the mechanism moves as designed with the desired force pattern and does not require activation of the leg muscles to walk.

This research has developed a novel RGO mechanism to meet patient needs and has provided proof that the mechanism can initiate a gait cycle through a lateral shift in weight rather than trunk extension.

Significance

This project intends to improve mobility and comfort for the thousands of patients who utilize RGOs. Current models are not intuitive and frequently do not improve the user's well-being. This preliminary study proves the feasibility of redesigning the mechanism to improve the user experience and quality of life. A new RGO device will modify therapy practices and can restore mobility to patients.

References

[1] Reciprocating Gait Orthosis Product Manual. Fillauer. 21 Nov. 2011.

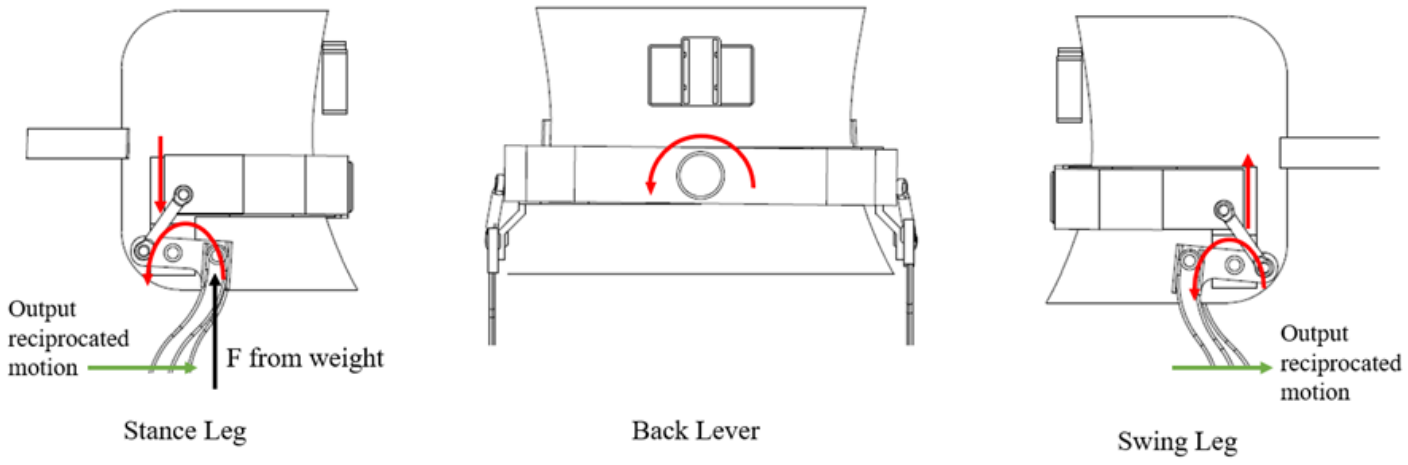

Figure 1. Magnified view of the hip mechanism with arrows indicating how it moves with an applied force. The black arrow indicates the applied force, the red arrows show the subsequent internal movement of the mechanism, and the green arrows show the output reciprocated motion of the device.

Musculoskeletal Demand Influences The Relationship Between Kinematics And Pushrim Efficiency During Pediatric Manual Wheelchair Propulsion

Erik T. Hummer[1,2], N. Oliveira[3], N. Ehrenberg[1], E. S. Suviseshamuthu[1], S. Blochlinger[2], T. Defosse[2] and P. Barrance[1,2]
[1]Center for Mobility and Rehabilitation Engineering Research, Kessler Foundation, West Orange, NJ, USA
[2]Children's Specialized Hospital, New Brunswick, NJ, USA
[3]Faculty of Kinesiology, University of Southern Mississippi, Hattiesburg, MS, USA
Email : ehummer@KesslerFoundation.org

Introduction

Overuse injuries of the upper extremities are common among manual wheelchair users [1]. These concerns are magnified when wheelchair use begins at a young age. Previous work has found that ~50% of push rim force may be wasted, by not being directed towards the forward motion of the wheelchair [2]. Therefore, optimizing push rim kinetic efficiency during propulsion may aid in reducing overuse injury risk. Efficiency of wheelchair propulsion has been previously examined using fractional effective force (FEF) [3]; this is the ratio of the force directed towards forward motion to the total force exerted upon the push rim. Interventions to improve FEF may include modifications to joint kinematics, particularly of the upper extremities and trunk. However, factors independent of kinematics may influence FEF, and to evaluate the potential effectiveness of such interventions it is important to understand the extent to which FEF can be explained or predicted by joint kinematics. Furthermore, it is important to understand how this dependence may vary according to fluctuating propulsive demands, including changes in surface resistance or inclination. To shed light on these questions, the purpose of this study was to examine the extent to which upper extremity and trunk kinematics explain the variance found in FEF while using a manual wheelchair across various surfaces.

Methods

This study further analyzed kinematic and kinetic data collected during a study of twelve adolescent manual wheelchair users [4]. 3D kinematics of the trunk, right shoulder, elbow, and wrist (60 Hz, MVN Biomech, Xsens, NL) were collected synchronously with 3D push rim kinetics (240 Hz, SmartWheel, Out-Front, Mesa, AZ) during three surface conditions (tile, ramp, and mat). Data collected during propulsion of a standard high strength lightweight wheelchair (K4) were analyzed. For "tile", participants traversed a level tiled floor; the "ramp" condition consisted of ascending an ADA compliant ramp, while "mat" consisted of traversing a polyfoam mat to represent grassy terrain. Data from the propulsion phase were extracted and time normalized to 101 points. FEF was calculated for each condition at the same time points.

Partial least squares regressions (PLSR) were run for each surface and wheelchair condition combination using MATLAB (2019a, Mathworks). A n-1 response vector (observations x FEF) and a n-p predictor matrix (observations x kinematic variables) were constructed for each surface. PLSR generated linear combinations of predictor variables (components) which explained the maximum possible cumulative variance in FEF. The dimensionality of the modelled relationship between predictors and response can be reduced by selecting a limited number of components that explains a set percentage of the cumulative variance explained by the full model. As outcome measures, we defined the number of components needed and the cumulative variance predicted at 95% of the full model's cumulative variance (e.g., if a condition had a maximum cumulative variance of 80%, the resulting threshold would be 76%), to define the level at which FEF was predicted by kinematics.

Results and Discussion

Of the three surfaces, the tile condition model required the greatest number of predictor components and explained the lowest cumulative variance in FEF. Propulsion on the tile surface has the lowest musculoskeletal system demand, with the lowest reported push rim forces [4]. The findings are consistent with the proposition that propulsion in the tile condition allows for a wider range of potential kinematic patterns resulting in the same push rim force patterns. Overall, the cumulative variance explained followed a positive relationship with the musculoskeletal demand of the surface condition as quantified by the average tangential force previously reported in tile-ramp-mat ascending order [4]. The relative cost, or detriment, of a low FEF may be considerably lower in low-demand surfaces (tile) but increase with demand. While a wide range of kinematics are viable during low demand conditions, specific kinematics may play a more crucial role in determining FEF when the musculoskeletal demands increase, and wheelchair users may be disadvantaged to a greater extent by a less than optimal FEF.

Significance

The current study found that upper extremity and trunk kinematics explain the cumulative variance in FEF to a greater extent in more demanding surface conditions. To improve push rim efficiency, interventions targeting kinematic patterns may be most beneficial when wheelchair users are propelling in high demand situations.

Acknowledgments

Support for this work was provided by Children's Specialized Hospital, Kessler Foundation, and the Willits Foundation.

References

[1]Ballinger, D. (2000) *Arch Phys Med Rehabil,* **81**: 1575-1581
[2]Boninger M. (1997) *Am J Phys Med Rehabil, 76: 420-6*
[3]Boninger M. (1999) *Arch Phys Med Rehabil,* **80**: 910-15
[4]Oliveira, N. (2017) *Dis & Rehabil: Ass Tech*, **14**(3): 209-1

Table 1. PLSR results for explaining at least 95% of the maximum cumulative variance in FEF by kinematics.

	Tile	Ramp	Mat
# of Components	8	3	3
Variance Explained (%)	59.84	64.32	79.25

TURNING SPATIOTEMPORAL METRICS AND STRATEGIES WITH END-STAGE HIP OSTEOARTHRITIS

Rashelle Hoffman[1,2]*, Hope Davis-Wilson[1,2], Lauren Hinrichs[1,2], Dana Judd[1,2], Jennifer Stevens-Lapsley [1,2], Cory Christiansen[1,2]
[1]Geriatric Research Education and Clinical Center, VA Eastern Colorado Healthcare System, Denver, CO
[2]Physical Therapy Program, Department of Physical Medicine and Rehabilitation, University of Colorado, Aurora, CO
email: *rashelle.hoffman@cuanschutz.edu

Introduction

About 35-50% of steps taken during typical daily activity are turning steps.[1] Poor turn performance (e.g. increased turn duration) in older adults is associated with weak hip abductor strength and increased fall risk.[2, 3] Hip osteoarthritis (OA) is a debilitating condition in older adults that is associated with poor turn performance.[4] However, it is unknown if turn performance differs based on the direction of the turn or changes over prolonged walking. Additionally, it is unknown if turning metrics in older adults with hip OA are related to fall risk. Thus, the purpose of this study was to: 1) compare spatiotemporal stepping metrics based on turn direction for the first and last minute of the 6-min walk test (6MWT), 2) determine if turn performance was related to dynamic balance performance (Functional Gait Assessment (FGA)) in people with unilateral hip OA.

Methods

Thirteen patients with end-stage hip OA awaiting total hip arthroplasty (8 male, 64.8 ± 6.2 y, BMI: 28.1 ± 4.3 kg/m^2) were enrolled. During the 6MWT[5], spatiotemporal stepping metrics (Fig 1A) were recorded using an 8-sensor fully body IMU system (Xsens Technologies) and calculated with a custom MATLAB code. The involved limb was identified as the planned surgical limb. Following the 6MWT, participants completed the FGA [6] and hip abductor isometric muscle strength testing. Percent change was calculated for all turning metrics comparing the last to the first minute of the 6MWT. Spearman rho correlations were used to assess relationships between turning metrics, 6MWT distance, and FGA scores.

Results and Discussion

Four participants consistently self-selected to turn towards the involved limb (IL group), four participants consistently self-selected to turn towards the uninvolved limb (UL group), and five participants self-selected to vary their turn direction (varied direction (VD) group) during the first and last minute of the 6MWT. The UL group had the weakest affected limb hip abductor muscle strength (IL: 21.1 ± 9.0 lbs; UL group: 16.1 ± 10 lbs; VD group: 19.9 ± 6.6 lbs). During the last minute of the 6MWT, the UL group had the largest decrease in turning step duration and the largest increase in number of turning steps followed by the VD group then the IL group (Fig 1A).

Across the sample during the first minute, shorter step duration and a greater number of turning steps were associated with higher FGA scores (Fig 1B & C). This is surprising given that only one of the ten FGA items evaluates turning. Also, longer 6MWT distance was associated with higher FGA scores (Fig 1D). These results suggest that turning performance and 6MWT distance may be related to other domains of balance evaluated by the FGA (e.g., change in walking speed, tandem walking).

Significance

Overall, our findings suggest that assessing turns during the 6MWT using IMUs may provide insight beyond walking endurance, including self-selected turning patterns and dynamic balance performance. The self-selected strategy for turn direction during the 6MWT may be attributed in part to involved hip abductor weakness associated with turning towards the uninvolved limb. Also, the associations between turning metrics and total 6MWT distance with FGA scores warrant larger sample studies to investigate this possible relationship. If larger sample studies support these trends, clinical use of IMUs during the 6MWT may be beneficial to identify physical intervention targets such as turning mechanics and associated balance performance.

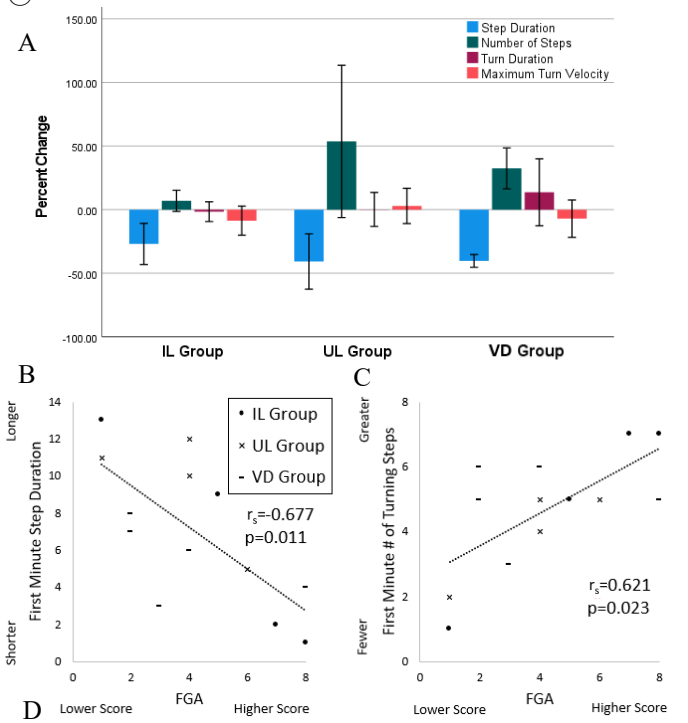

Figure 1. Turn strategies based on group (A). First minute step turn metrics related to FGA (B & C). Total 6MWT distance related to FGA score; VD Group = turns in both directions, UL Group = turn toward uninvolved limb, IL Group = turn towards involved limb, FGA = Functional Gait Assessment

Acknowledgments

This work was supported by a VA Merit Award # RR&D I01 RX002251 from the U.S. Department of Veterans Affairs.

References

1.Glaister, B.C., et al., Gait Posture, 2007. **25**(2): p. 289-94.
2.Greene, B.R., et al., IEEE Trans Biomed Eng, 2010. **57**(12): p. 2918-26.
3.Iijima, H., et al., J Biomech, 2020. **101**: p. 109652.
4.Verlinden, V.J.A., et al., Gait Posture, 2017. **54**: p. 248-254.
5.Kennedy, D.M., et al., BMC Musculoskelet Disord, 2005. **6**: p. 3.
6.Wrisley, D.M. and N.A. Kumar,. Phys Ther, 2010. **90**(5): p. 761-73.

FULL BODY DYNAMIC OPTIMIZATION OF A STANDING POWER THROW

Beau Kewley[1], Manoj Srinivasan[2], and Gregory Freisinger[1]
[1]United States Military Academy – West Point, [2]The Ohio State University
email: gregory.freisinger@westpoint.edu

Introduction

The new Army Combat Fitness Test (ACFT) has brought significant attention to what factors of human anatomy provide advantages or disadvantages in performance. Two anthropometric characteristics of particular interest are individual's height and relative limb length. A dynamic simulation modelling the human body as a four-link pendulum was developed to allow optimization for throwing distance. This simulation is an expansion on previous work with a two-link pendulum that only modelled the upper and lower arm of a participant conducting the SPT. The four-links allowed for a more realistic simulation where the upper and lower leg, torso, and arms are modelled as rigid links working in series to throw a ball overhead for maximum distance. The purpose of conducting this study was to provide a consistent model that analyses the Standing Power Throw (SPT) event of the ACFT and how the limb lengths may impact that performance.

Methods

A dynamic simulation to estimate human motion was developed using MATLAB [Natick, MA]. The differential equations of motion for a four-link pendulum, rotating about a fixed point, were developed. The weight and length proportions were based on research estimating mass moment of inertia for each limb [1]. This simulation utilized the *fmincon* function, which allows for the input of constraints and objectives to satisfy, along with a cost function to optimize our mathematical model [2]. The constraints of the model included the angular range of motion between each link, which were determined by the limits of normal human joint motion during an overhead ball throw. The objectives of the model were defined by initial start and end position of the four links, where the cost function was set to maximize for the translational velocity of the end of the fourth link. This ultimately achieves a maximum throwing distance. The optimization held the release point, segment masses, and maximum allowable joint torque constant throughout each of the trials, therefore allowing us to isolate limb length for estimation.

To investigate the impact of limb length, this optimization scaled lengths for the four links. Each of the proportions for the lower and upper leg, torso, and arms were multiplied by a factor of either 0.5, 1.0, or 2.0 to keep a consistent proportion of limb lengths for each of the trials (Figure 1). The purpose of this study is to compare the results of each iteration with varying limb lengths, not specifically to predict human performance or match experimental data.

Results and Discussion

Optimal solutions for each of scaled link lengths were found, and a positive relationship appeared between the length of limbs and the distance thrown. The percentage changes shown in Figure 1 were compared relative to the 1.0 proportion limb lengths, where. a decrease of 49.26% from 1.0 to 0.5 and increase of 40.78% from 1.0 to 2.0 were recorded. With consistent torques limits being applied to each of the links, larger velocity was possible at the instant of release with longer limbs. This is often seen in throwing sports, such as baseball pitching, where taller individuals can produce a higher velocity at the end effector (hand).

The complexity of the differential equations of motion for a four-link pendulum can lead to lengthy optimizations and sometimes non-intuitive results. However, our simulation was able to converge and reach a maximum for each of the three limb length conditions. While *fmincon* does have terminating criteria that end the simulation when optimization criterion are satisfied, however we cannot be certain that these results are global minima rather than local. Further exploration of initial conditions is required to see if these simulations continue to converge to the values below.

Significance

This study aims to identify the anthropometric differences between individuals that may impact their performance during the standing power throw. The results show that with all other factors held constant, there is a positive trend between length of limbs and distance a ball can be thrown overhead. The ACFT is graded on a single scale, but there may be advantages to performance based upon height. More research should be completed to identify if scoring standards for the ACFT should be normalized by limb lengths. This model also allows for future research on how varied lengths of individual limbs, or their associated torque limits at each joint, may impact an individual's ability to perform in the SPT.

References

[1] Krishnan et al. (2016) *JESTEC*. 11, 166-176
[2] Srinivasan et al. (2006) *Nature*. 439, 72-75

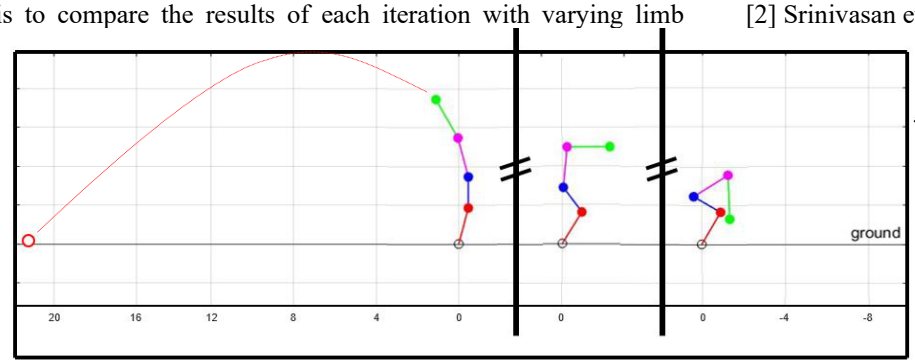

Link Lengths	MATLAB Iterations	Distance Thrown [m]	Percentage Change
0.5* (proportions)	5600	9.93	-49.26
1.0* (proportions)	6000	19.57	N/A
2.0* (proportions)	7500	27.55	+40.78

Figure 1: Time lapse of dynamic simulation with 1.0 proportionate link lengths. (Right to Left) Initial position, Mid-throw, Final position with ball at maximum distance. The table shows the link lengths for the 3 optimizations, number of iterations for *fmincon* to converge on optimal solution, distance of ball thrown, and percent change from link lengths of one.

FOCUSED ULTRASOUND COULD BE AN ALTERNATIVE TO DRY NEEDLING FOR TREATING TENDON INJURIES

Sujata Khandare[1], A. A. Butt[1], M. Smallcomb[2], J. Elliott[2], J. C. Simon[1,2], M. E. Vidt[1,3]
[1]Biomedical Engineering, Pennsylvania State University, University Park, PA, USA
[2]Graduate Program in Acoustics, Pennsylvania State University, University Park, PA, USA
[3]Physical Medicine & Rehabilitation, Penn State College of Medicine, Hershey, PA, USA
Email: uuk72@psu.edu

Introduction

Musculoskeletal conditions are associated with 574 million physician visits, accounting for an annual cost of ~$796.3 billion. Achilles and rotator cuff tendinopathies are the most frequently reported [1]. Injured tendons are mechanically inferior, causing functional impairment. Conservative therapies, like dry needling (DN), involves "peppering" the tendon with a thin filiform needle to create micro damage. However, DN is invasive and has mixed success rates due to high inter-practitioner variability [2]. As tendons are required to withstand high physiological loads, there is a need for treatments that do not diminish tendon mechanical properties while promoting healing. Focused ultrasound (fUS) is an emerging ultrasound therapy that can non-invasively induce thermal and/or mechanical bioeffects in a well-defined focal volume, depending on the choice of ultrasound parameters (e.g. pulse duration, energy) [3]. The objective of this study was to evaluate the effect of DN and 3 different fUS parameter sets, chosen to emphasize mechanical fractionation, on the elastic properties of Achilles and supraspinatus tendons.

Methods

Ex vivo rat Achilles and supraspinatus tendons, 50 each, were divided into sham, DN, fUS-1, fUS-2, and fUS-3 (n=10/group). For DN, a 30G needle (Tai-Chi, Suzhou, Jiangsu, China) was inserted and quickly removed from the central portion of the tendon 5 times over 12s. Tendons were treated with fUS at 1.5MHz with peak +ve and -ve pressure of 89MPa and 26MPa, respectively. The central portion of the tendon was exposed to 1ms pulses @10Hz for 60s for fUS-1, 10ms pulses @1Hz for 15s for fUS-2, and 5ms pulses @1Hz for 60s for fUS-3. Following treatment exposure, tendons were mechanically tested using an MTS 858 Mini Bionix (MTS Systems Corp., Eden Prairie, MN) mechanical testing system, using an established protocol [4]. Tendon elastic properties, including elastic modulus and stiffness, were determined from the stress-strain curve and load-displacement curve, respectively. Group differences in elastic parameters were assessed with two-way (treatment, tendon) ANCOVA, with sex as a covariate, using SAS software (v9.4, SAS Institute, Inc., Cary, NC); significance was set at $p<0.05$.

Results and Discussion

One hundred samples were successfully tested; 6 measures were removed as outliers (>2SD outside mean). There was no significant interaction between the treatments and tendons (Achilles and supraspinatus), but main effects of treatment (p=0.0023) and tendon (p=0.0109) were observed. Modulus of Achilles tendons in sham (p=0.0240) and fUS-1 (p=0.0216) was higher than DN (Fig.1a). Stiffness of Achilles tendons in sham was higher than DN (p=0.0030), fUS-1 (p=0.0002), fUS-2 (p=0.0012), and fUS-3 (p=0.0005) (Fig.1b). Modulus of supraspinatus tendons in sham was higher than DN (p=0.0280), fUS-2 (p=0.0476), and fUS-3 (p=0.0450); modulus of fUS-1 was higher than DN (p=0.0459) (Fig.1c). Stiffness of supraspinatus tendons in sham was higher than DN (p=0.0334); stiffness of fUS-1 was higher than DN (p=0.0045) and fUS-2 (p=0.0136) (Fig.1d).

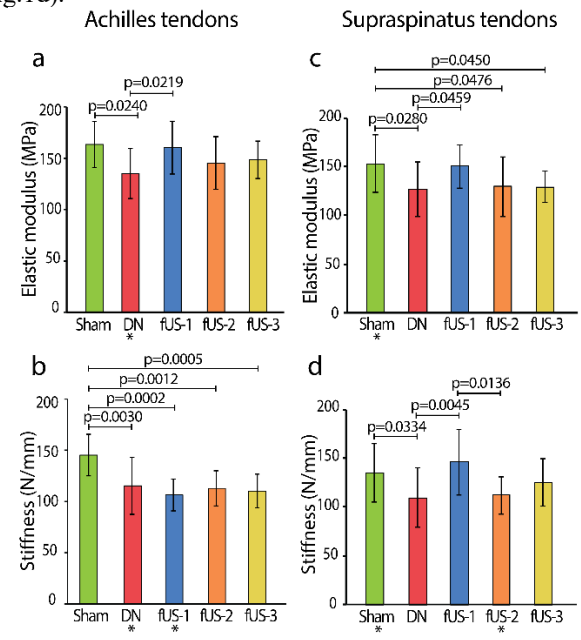

Figure 1: (a) Elastic modulus and (b) stiffness of Achilles tendons and (c) elastic modulus and (D) stiffness of supraspinatus tendons exposed to sham, dry needling (DN), or 3 parameter sets of focused ultrasound (fUS-1; fUS-2; fUS-3). *(n-1) samples due to outlier being removed.

Results suggest that DN causes a decline in elastic properties of both Achilles and supraspinatus tendons. It is possible that repeated needle insertions weaken the tendon and negatively affect the tendon's ability to withstand load. fUS preserved elastic modulus better than DN, with fUS-1 performing better than fUS-2 and fUS-3. The observed differences in mechanical parameters of Achilles and supraspinatus tendons may be driven by the different roles these tendons play *in vivo* and suggests that treatments may need to be tailored to the specific tendon.

Significance

Elastic modulus of both Achilles and supraspinatus tendons in the fUS-1 group was similar to sham, suggesting that fUS-1 does not diminish the tendons' ability to withstand load. Ongoing work involves investigating the *in vivo* mechanical and healing effects of DN and fUS. Understanding the effects of fUS will help evaluate fUS for clinical translation as an alternative, non-invasive treatment for Achilles and supraspinatus tendon injuries.

Acknowledgments

NIH R21EB027886; NSF GRFP DGE1255832 (Smallcomb).

References

[1] Yelin E et al. (2016). *Semin. Arthritis Rheum.* 46; 259–60.
[2] Krey D et al. (2015). *Phys. Sportsmed*. 43; 80–6.
[3] Dubinsky TJ et al. (2008). *AJR* 190; 191-9.
[4] Huang TF et al. (2004). *Ann. Biomed. Eng.* 32; 336–4.

FEMALES WITH FEMOROACETABULAR IMPINGEMENT SYNDROME DEMONSTRATE ALTERED LOWER EXTREMITY KINEMATICS DURING A DROP JUMP TASK COMPARED TO HEALTHY CONTROLS

M. Grosklos[1,2], J. Perry, K. Jochimsen, M. Elwood, and S. Di Stasi
[1]Department of Biomedical Engineering, College of Engineering, The Ohio State University
email: grosklos.2@osu.edu

Introduction

Femoroacetabular impingement syndrome (FAIS) is the most common cause of debilitating hip pain among young, active adults. Morphological variants of the hip associated with FAIS may contribute to motion-related pain, particularly in sports that demand positions of significant hip flexion. Movement patterns in FAIS may be sex-specific[1], which could explain why some studies have reported worse outcomes in females following treatment[2]. This study examined the sex-related differences in sagittal plane mechanics during a drop vertical jump (DVJ), a sports-related task requiring deep hip flexion. The primary hypothesis tested was that kinematics during the DVJ would differ between individuals with FAIS and those without hip pain, and that these differences will be sex-specific.

Methods

37 level I/II athletes (cutting/jumping sports) diagnosed with FAIS and 16 healthy controls (HC) without hip pain underwent 3D motion analysis during a DVJ task. The mean of three successful trials from each participant was used for analysis of sagittal plane hip, knee, and ankle angles at the time of peak hip flexion. General Estimating Equations (GEE) were used to analyse sex by group (FAIS; HC) by limb interactions; significant interactions were followed with group by limb GEE for males and females separately. Post-hoc t-test results were reported if interactions were significant. Main effects were reported if interactions were not significant ($p \leq .05$). Data were reported as mean (95% confidence interval).

Results and Discussion

Age, BMI, and sex distribution were not different between groups ($p \geq .491$). There was an interaction for hip and knee angle such that the involved limb of females with FAIS demonstrated less hip flexion and knee flexion than the dominant limb of female HC (Figure 1). Females with FAIS also demonstrated less ankle dorsiflexion than HC regardless of limb (Table 1). There were no asymmetries in females with FAIS ($p \geq .362$). There were no significant interactions or main effects in males ($p \geq .084$).

In support of our hypothesis, females with FAIS demonstrated different kinematics than their healthy counterparts and this was a sex-specific difference not seen in males. This pattern of decreased hip, knee, and ankle flexion may indicate a pain-avoidant strategy because it circumvents the impingement position that is hypothesized to be problematic for those with FAIS. Our data support recent work indicating sex-specific mechanics in those with FAIS.

	Group	Mean	95% CI	Mean Diff	*p*
Hip	FAIS	77.2°	(72.6, 81.7)	-14.0	<.001
	HC	91.1°	(85.7, 96.6)		
Knee	FAIS	83.8°	(80.6, 87.0)	-12.1	.001
	HC	95.9°	(89.3, 102.4)		
Ankle	FAIS	28.7°	(26.9, 30.4)	-2.84	.037
	HC	31.5°	(29.5, 33.5)		

Table 1: Mean joint flexion for hip, knee, and ankle between the involved versus the dominant limb in females only.

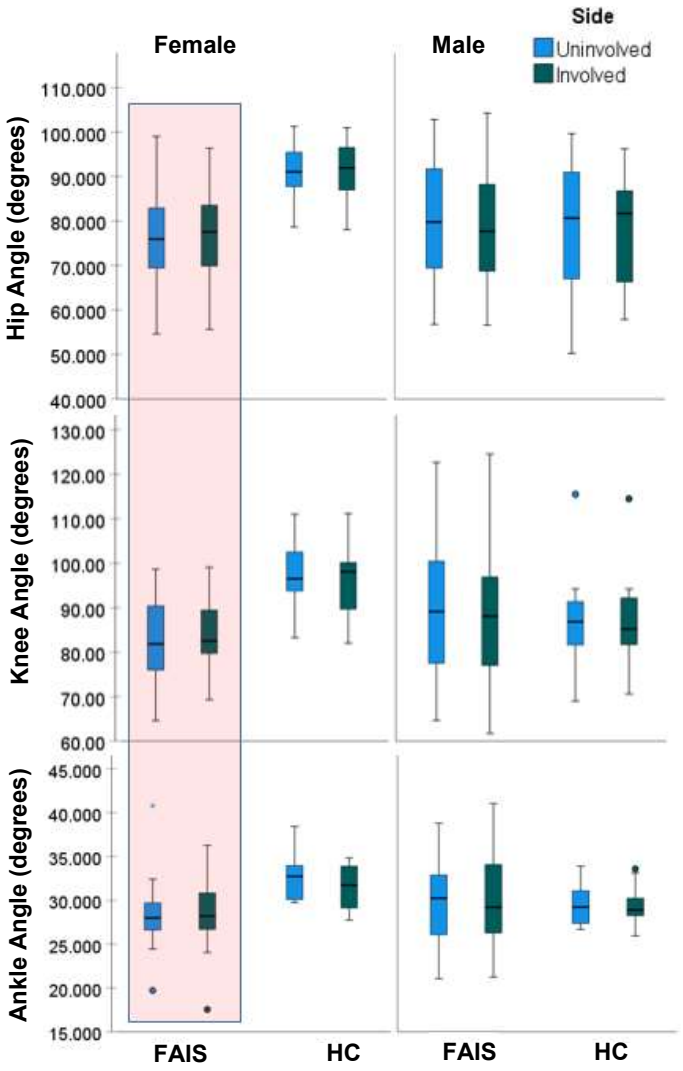

Figure 1: Boxplot of hip, knee, and ankle angles at the point of peak hip flexion. Data in the red box represents females with FAIS, statistically different from their HC counterparts.

Significance

These data indicate that sex-specific interventions and rehabilitation may be warranted for those with FAIS. Sex-specific movement differences in these individuals should be the focus of continued research. Additionally, future research should investigate whether these movement patterns persist post-operatively as this could impact intervention decisions and practices.

Acknowledgments

This work was supported in part by the American Academy of Sports Physical Therapy.

References

[1] Lewis C. *et al.* (2018) JOSPT; 48:649-658
[2] Joseph R. *et al.* (2016) AJSM; 44:54-5

REDISTRIBUTION OF MUSCULAR WORK BY CHILDREN WITH CEREBRAL PALSY WALKING IN CROUCH

Anahid Ebrahimi[1], Michael Schwartz[2], Jack Martin[1], Tom Novacheck[2] & Darryl Thelen[1]
[1]University of Wisconsin-Madison, Madison, WI, USA
[2]Gillette Children's Specialty Healthcare, St. Paul, MN, USA
email: anahide@udel.edu

Introduction

Children with cerebral palsy (CP) often exhibit a crouch gait pattern, characterized by excessive knee flexion in stance, in part due to altered muscle-tendon behavior. Crouch gait often results in the knee and ankle extensors operating at lengths longer than normal [1]. However, it remains challenging to assess the functional force-length behavior of muscles during walking.

Our laboratories are investigating the use of shear wave tensiometry to track tendon loading during walking directly and noninvasively [2]. Tensiometers worn over superficial tendons measure changes in shear wave speed along the tendon during dynamic tasks [3]. The tensile load transmitted by the muscle-tendon is proportional to shear wave speed squared.

Tendon force measures can be fused with muscle-tendon kinematics and EMG data to create a work loop plot [4]. The direction of the loops informs the functional role of the muscle-tendon about the joint. For example, a counter-clockwise loop indicates the muscle-tendon is acting as a motor to generate positive net work, while a curve with minimal/zero net work indicates spring-like behavior of the muscle-tendon. Muscle EMG can be overlaid on the loops to understand the timing of muscle activation. For this study, we investigate work loop plots of the triceps surae (via the Achilles tendon) action about the ankle and quadriceps (via the patellar tendon) action about the knee in children with CP walking in crouch.

Methods

Seven children with CP (2F, 8-16 yrs) and 15 typically developing controls (9F, 8-17 yrs) participated. Children with CP were included if they had spastic diplegia, GMFCS Level I or II status, and evidence of crouch (>20° average stance knee flexion angle) gait. Reflective markers and EMG sensors were placed over the lower limbs. Shear wave tensiometers were secured over the Achilles and patellar tendons. All subjects walked over ground at their preferred speed. A subject-specific calibration procedure was used to estimate muscle-tendon force from shear wave speed squared [2]. The excursions of the muscle-tendon units about the joints were calculated from joint angles and tendon moment arms. Forces were normalized to body weight and excursions to leg length. Work-loop plots were used to evaluate net work of each muscle-tendon group about its joint.

Results and Discussion

Our results show a redistribution of muscular work by the children with CP walking in crouch compared to typically developing controls. Children with CP used their triceps surae as springs (Fig 1), producing minimal net work during walking from foot contact (FC) to foot off (FO) (Table 1). In contrast, controls generally use their triceps surae as a motor to generate positive net work in stance ($p = 0.028$).

The reverse was true at the knee. Controls used their quadriceps as a spring through midstance (from FC to opposite foot contact (OFC)) (Table 1), while children with CP used their quadriceps muscles as motors to generate significantly larger positive net work than controls ($p = 0.002$).

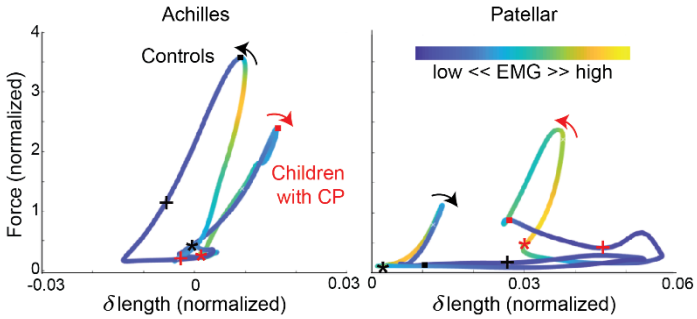

Figure 1: Average work loops show a redistribution of work by children with CP compared to controls. Medial gastrocnemius and Vastus Lateralis EMG is overlaid for triceps surae and quadriceps work loops, respectively, with timing of FC (*), OFC (■), and FO (+) noted.

Table 1. Net work (dimensionless) during relevant portion of stance.

	Controls	Children with CP
Achilles (FC to FO)	0.024 ± 0.010	-0.001 ± 0.005
Patellar (FC to OFC)	-0.002 ± 0.002	0.011 ± 0.013

The spring-like behavior of the controls' quadriceps aligns with previous literature on knee torque-angle curves, where the quadriceps eccentrically control knee flexion during loading response and concentrically extend the knee in midstance [5]. Closer inspection of the timing of force and length for the two groups showed work differences were primarily driven by sustained force production in CP through midstance while the quadriceps were shortening. On average, the children with CP also produced a third less peak Achilles force and double the peak patellar force compared to controls. Overall, the reversal of functional roles of the triceps surae about the ankle and the quadriceps about the knee in children with CP lends greater insight into the mechanics of pathologic gait.

Significance

The work loop approach combines muscle-tendon forces, lengths, and activations to characterize the functional role of the muscle-tendon about the joint. Quantifying quadriceps force in children with CP is clinically relevant, and shear wave tensiometers now provide an opportunity to attain this metric without musculoskeletal modelling estimates [6]. Future work could use the work loop approach to investigate changes in muscle-tendon function pre- and post- crouch gait treatment.

Acknowledgments

Funding provided by NIH HD092697.

References

[1] Gage & Novacheck. *J Ped Ortho Part B* 10 (2001).
[2] Ebrahimi, et al. *Front Sport Act Living* 2 (2020).
[3] Martin, et al. *Nat Commun* 9 (2018).
[4] Dickinson, et al. *Science* 288 (2000).
[5] Frigo, et al. *J Electromyogr Kinesiol* 6 (1996).
[6] Steele, et al. *J Biomech* 45 (2012).

OPTIMIZED STIFFNESS AND POWER OF AN ANKLE-FOOT PROSTHESIS MAY REDUCE METABOLIC POWER DURING WALKING

Zane Colvin[1] & Alena M. Grabowski[1, 2]
[1]University of Colorado Boulder, Boulder, CO
[2]Department of Veterans Affairs Eastern Colorado Healthcare System, Denver, CO
Email: Zane.Colvin@colorado.edu

Introduction

On level ground, people with transtibial amputation (TTA) using a passive-elastic prosthesis require 10-30% more metabolic energy to walk at the same speeds as non-amputees [1]. Use of a less stiff passive-elastic prosthetic foot has reduced metabolic cost in a modelling study [2], but a different experimental study found that prosthetic foot stiffness had no effect on oxygen consumption during level-ground walking at preferred speeds (0.65-1.20m/s) [3]. Prosthetic foot stiffness is prescribed by manufacturers using an individual's body mass and activity level, which may not be optimized to reduce metabolic cost while walking. Moreover, previous studies of people with TTA using a BiOM powered prosthesis during walking have reported conflicting metabolic cost results. Herr and Grabowski found that people with TTA using the BiOM had similar metabolic costs as non-amputees walking at 1.0-1.75 m/s [1]. However, Gardinier et al. reported no difference in metabolic cost for people with TTA walking at 1.31 m/s using the BiOM compared to their passive prosthesis [4]. These conflicting results may be due to different power settings used in the BiOM. Ingraham et al. reported that people with TTA walking at 1.21 m/s using the BiOM reduced metabolic cost 8.8% with a power setting 18-40% greater than what was chosen by a prosthetist using net prosthetic ankle work in relation to normative net ankle work data reported from the BiOM , which indicates that a higher power setting of the BiOM reduces metabolic cost [5].We determined the independent and combined effects of prosthetic stiffness and power on the metabolic cost of people with TTA during walking. We hypothesized that use of a prosthetic foot less stiff than recommended combined with stance-phase power greater than recommended would result in the lowest metabolic power during walking on level ground in people with TTA compared with more stiff and lower power prosthetic settings.

Methods

1 male subject gave informed consent and completed 6 visits. On day 1, a prosthetist fitted the subject with the Össur low-profile Variflex foot (LP) with the manufacturer recommended stiffness category (Rec Cat), one Cat more stiff (+1), one Cat less stiff (-1), and two Cat less stiff (-2) and ensured that affected leg (AL) hip height, foot size, and alignment matched the unaffected leg (UL). The prosthetist also fitted the subject with the BiOM prosthesis with each of the passive LP feet using the same criteria of hip height, foot size, and alignment. The power setting for the BiOM was objectively tuned so that during walking at 1.25 m/s, the subject's AL prosthetic ankle angle, moment, power, and net mechanical work normalized to body mass with the BiOM were within 2 SD of biological ankle data from 20 non-amputees [7]. On subsequent days, the subject completed a total of 16 walking trials using different Cat of the LP (Rec, +1, -1, -2) with and without the BiOM. For trials with the BiOM, we used 3 different power settings, the tuned power (Rec Power), and +10% and +20% more than Rec power. In each trial, the subject walked for 5 min at 1.25 m/s on a dual-belt force-measuring treadmill (Bertec, Columbus, OH) while we collected rates of O_2 consumption and CO_2 production using indirect calorimetry (ParvoMedics, Sandy, UT). Then, we used the Brockway equation [6] to calculate gross metabolic power from the last 2 min of each 5-min trial and normalized to body mass including the respective prosthesis configuration.

Results and Discussion

While using the recommended stiffness Cat and no BiOM, gross metabolic power was 3.82 W/kg. Compared to the other 15 prosthesis configurations, only 1 resulted in a numerically lower gross metabolic power, the BiOM with +1 Cat and +20% power (3.79 W/kg). In agreement with Ingraham et al. [5], using the BiOM with a power setting higher than the Rec results in numerically lower metabolic power than using the BiOM with the same stiffness Cat at Rec power. In contrast to Fey et al. [2], when the subject walked using the LP only at stiffness categories less stiff than Rec, metabolic power was numerically higher.

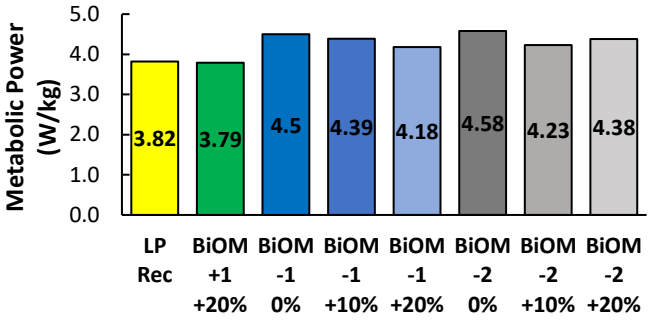

Figure 1: Gross metabolic power (W/kg) of a subject walking at 1.25 m/s with 7 prosthetic foot configurations. LP is the passive-elastic prosthetic foot and BiOM is the powered prosthesis. Rec, +1, -1 and -2 represent the LP prosthetic foot stiffness category. The power setting for the BiOM is 0% for the tuned, and +10%, and +20% power.

Significance

The results of this case study imply that the BiOM prosthetic power setting may be more important for reducing metabolic cost during walking than the stiffness of the prosthetic foot.

Acknowledgments

This study was funded by the Department of Veterans Affairs

References

1. Herr HM, et al. *Proc. Royal Soc. B.* 2012
2. Fey NP, et al. *J. Biomech. Eng-T ASME* 2012
3. Klodd E, et al. *J. Rehabil. Res. Dev.* 2010
4. Gardinier ES, et al. *Clin. Rehabil.* 2018
5. Ingraham KA, et al. *Sci. Rep.* 2018
6. Brockway, JM *Hum. Nutr. Clin. Nutr.* 1987
7. Montgomery JR, et al. *R. Soc. Open Sci.* 2018

USING FOOT MOUNTED IMUS TO ESTIMATE TOE CLEARANCE IN PEOPLE WITH LOWER LIMB AMPUTATION

Jay Kim and Deanna H. Gates
University of Michigan, Ann Arbor, MI, USA
email: jaywoo@umich.edu

Introduction

Individuals with transtibial amputation (TTA) have a higher incidence of trips and falls [1]. One potential contributing factor to increased fall risk is the inability of the prosthetic foot to actively dorsiflex during swing, reducing minimum toe clearance (MTC). Low MTC and high MTC variability are associated with increased fall risk [2]. MTC can be measured experimentally using motion capture systems or foot mounted inertial measurement units (IMU). Both approaches have limitations as motion capture constrains measurement to laboratory environments and current approaches with IMUs rely on prior knowledge of shoe size [3] or assumptions regarding the foot's orientation during swing that may not apply to individuals with TTA [4]. To address these limitations, we developed an estimation approach that calculated MTC by approximating the trajectory of the toe during swing. To validate our approach, we then compared our calculated values of MTC to those from motion capture for an individual with TTA.

Methods

A 39 year old male with unilateral TTA walked on the treadmill at three self-selected slow (0.70 m/s), preferred (1.23 m/s), and fast (1.88 m/s) speeds for at least 2 minutes each. An IMU was affixed to the laces of the shoe on his prosthetic foot. As a "ground truth" reference, an optical motion capture system tracked a reflective marker placed on the distal tip of the shoe on the prosthetic foot.

Using position estimates from a pedestrian dead-reckoning algorithm [5], we calculated relative foot clearance (RFC) as the minimum vertical distance between the IMU's position during swing and its position during foot-flat [3]. In our approach, we constrained the motion of the IMU about a stationary center of rotation (CoR) between foot-flat and toe-off, which approximates the location of the toe. We calculated for the location of the CoR in the IMU reference frame using the following equation,

$$\overrightarrow{{}_s a_s} = \overrightarrow{{}_s a_c} + \frac{d\,\overrightarrow{{}_s \omega_s}}{dt} \times \overrightarrow{{}_s r_c} + \overrightarrow{{}_s \omega_s} \times \left(\overrightarrow{{}_s \omega_s} \times \overrightarrow{{}_s r_c}\right)$$

where ${}_s a_s$ and ${}_s a_c$ are the accelerations of the IMU and the CoR in the sensor frame, ${}_s \omega_s$ is the angular velocity of the IMU, and ${}_s r_c$ is the rotational moment arm about the CoR in the sensor frame. We calculated the ${}_s r_c$ at each point between foot-flat and toe-off where the sensor's pitch angular velocity was greater than 50% of the local maximum then calculated the mean ${}_s r_c$ vector for each speed. At every time point, this vector was rotated to the lab reference frame then subtracted from the IMU position trajectory to calculate the approximate trajectory of the toe. MTC was then calculated as the minimum vertical distance between the CoR during swing and its position during foot-flat (MTC_{CoR}). We used a linear mixed model to test for fixed effects in measurement method and speed and performed paired t-tests between levels.

Results and Discussion

Using the motion capture-based estimate of MTC as reference, MTC_{CoR} had smaller mean absolute differences compared to RFC over the tested walking speeds (Figure 1).

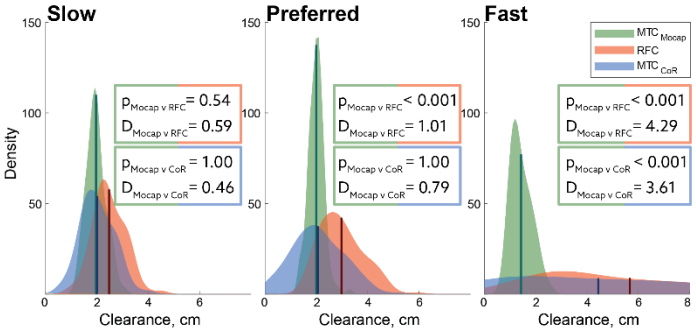

Figure 1: Toe clearance probability density curves for MTC measures Pairwise comparisons and mean average differences (D) between MTC_{Mocap} and RFC/MTC_{CoR}. Vertical lines are distribution means.

The potential advantage of the MTC_{CoR} over the RFC estimate can be attributed to its sensitivity to the foot's pitch angle. RFC is a proxy measure for MTC and assumes the foot's pitch angle during swing is the same as during foot-flat. This assumption cannot be made for individuals with TTA as they typically compensate for the lack of prosthetic dorsiflexion with increased hip and knee flexion. Because the MTC_{CoR} estimate uses the approximate location of the toe to calculate MTC, it is sensitive to the foot's pitch angle during swing.

The within-participant variability of MTC as measured with motion capture were comparable to published values MTC variability [2,6]. IMU-based estimates of MTC had greater variability, which suggests sources of error in calculation rather than variability due to changes in movement. Thus, while our approach may be able to estimate mean MTC given a large enough sample size, it may need to be further refined to yield salient information regarding movement variability. One way to mitigate the signal noise, which propagates into MTC estimate errors, is to affix the IMU more rigidly to the shoe to reduce sensor movement during foot-flat.

Significance

Our MTC estimate is unique for its approximation of the toe's trajectory during swing without prior knowledge of shoe size. Thus, this is a robust approach for long-term MTC measurements outside of the laboratory. This measure may be a useful assessment of fall risk associated with clinical interventions for individuals with TTA.

Acknowledgments

Thank you to Lauro Ojeda, Kelsey White, and Luis Nolasco.

References

[1] Miller, W. Arch Phys Med Rehab, 82, 1031-1037, 2001.
[2] Johnson, L. J Rehab Res & Dev, 3, 429, 2014.
[3] Mariani, B. IEEE Trans Bio Eng, 11, 3162-3168, 2012.
[4] Benoussaad, M. Sensors 16, 12, 2016
[5] Ojeda, L. Sensors 17, 2647, 2017.
[6] De Asha, A. Pros & Ortho 39, 120-125, 2015.

THE BIOMECHANICS INITIATIVE: CREATING OPPORTUNITIES FOR BIOMECHANICS DEVELOPMENT

Lisa N. MacFadden[1], Felipe P. Carpes[1], Ben Hoffman[1], Justin P. Waxman[1], Paul DeVita[1]
[1]The Biomechanics Initiative, Inc, Parent Organization of National Biomechanics Day, Earth
email: lisa.macfadden@sanfordhealth.org

Introduction

National Biomechanics Day (NBD) started in 2016 with the vision of teaching biomechanics in high schools across the U.S. Over the last five years, NBD has grown into a worldwide celebration. Biomechanists have created 394 NBD events across 30 nations, which have reached over 29,000 students and 950 teachers. Since 2016, NBD has connected biomechanics laboratories worldwide through coordinated events, social media, contests, articles in lay and scientific journals, media stories, music playlists, fun and wild graphics, and more. A full explanation of NBD's vision and motivation is explained in Why "National Biomechanics Day"[1]. In 2019, The Biomechanics Initiative, Inc (TBI) was created as the parent organization for NBD. With the success of NBD outreach and support from generous sponsoring organizations, TBI aspired to do more to inspire young people to make an impact on the field of biomechanics. These ambitions led us to create funding opportunities to support NBD events globally and promote outreach to underrepresented groups. We discuss four programs that launched in 2020 and 2021 and their outcomes.

Australia National Biomechanics Day Grant

The Australian NBD Grant and Textbook Program aims to engage Australian high school students with biomechanics through two approaches. First, the grant provides Australian universities financial assistance to deliver an NBD event that facilitates a biomechanics experience for local high school students within a university setting. In the current climate where funding at universities is limited, this grant will assist smaller universities in running an event where they might not otherwise have the capacity to do so. The two recipients of the 2021 grant will be running their first NBD events. Second, the textbook program provides copies of the biomechanics textbook, "A Trail Guide to Movement," from Books of Discovery, to high schools that participate in the NBD events organized by the grant-receiving universities. This provides a resource for the classroom that fosters continuing engagement in biomechanics from both the teacher and the students long after their NBD concluded.

NBD – ASB Black Biomechanists Grant

The Black Biomechanist Outreach Through NBD award was spawned from an enthusiastic affiliation between TBI, the American Society for Biomechanics (ASB), and also with the approval of the newly formed Black Biomechanist Association. Its purpose is to encourage NBD events by Black Biomechanists and their allies. The grants provide funding for NBD events and also pay for one student registration at ASB 2021 per award. In the first year of this grant, TBI received 11 submissions (6 students and 5 professionals) from the United States (10) and Nigeria (1). Of those submissions, five grants were funded (4 students and 1 professional) from both countries. The grant reviewers were all members of the Black Biomechanists Association. Overall, the first year of this program was a success, providing biomechanics opportunities to increase diversity and representation within the field and create awareness for the Black Biomechanist Association on social media and create awareness around the specific needs of this community within the biomechanics field.

Brazilian Biomechanics Experience

The Brazilian Biomechanics Experience encourages the long-term engagement of young students with biomechanics. While there are Brazilian programs funding youngsters enrolled with science and university research groups during high school, it is unclear if the students remain interested in science after the funding ends. In the first year, this initiative promoted an online symposium that combines the importance of science to society and how biomechanics connects with different professions. The online symposium brings together professors and students sharing their experiences and views about biomechanics. To further promote these youngsters' continued enrollment with science and biomechanics, the initiative supports the participation of up to five students in the Brazilian Congress of Biomechanics, the biggest biomechanics event from Latin America. In 2021, there were 134 registrations to join the symposium, and three high school students willing to share their experience during the event.

NBD – ISB Women in Biomechanics Grant

The Women in Biomechanics Grant was created with the International Society of Biomechanics (ISB), and also with the encouragement of the newly formed biomechanics group, International Womxn in Biomechanics. The grants provide funding to host NBD events to diversify biomechanics, specifically groups that are predominantly female, and they provide registration for the ISB 2021 conference. In the first year, we had 20 submissions from 8 countries (Australia, Brazil, Canada, India, New Zealand, Taiwan, United Kingdom, and the United States). Seven grants were funded from five countries (Australia, Canada, New Zealand, Taiwan, and United States). The first year of this program was also a success given the number of applicants, and especially the geographic and cultural diversity represented in the submissions.

Significance

Enthusiasm for National Biomechanics Day has spread across the globe, inspiring future biomechanists and new biomechanics groups. Through these funding awards, we aim to promote opportunities to reach new populations and encourage diversity in the field. TBI & NBD are now able to contribute back to the biomechanics community. Together we will make biomechanics the breakthrough science of the 21st century.

Acknowledgments

We acknowledge the hosts, participants, and sponsors that have made National Biomechanics Day celebrations and TBI grants possible. You inspire us.

References

[1] DeVita, P. (2018). *J Biomech*, **71**:1-3.

Shoulder Muscles with Large Lines of Action Contribute to Glenohumeral Stiffness

Constantine P. Nicolozakes[1-3], J. S. Schmulewitz, D. Ludvig, M. S. Coats-Thomas, E. M. Baillargeon, A. L. Seitz, and E. J. Perreault
[1]Biomedical Engineering and [2]Feinberg School of Medicine, Northwestern University; [3]Shirley Ryan AbilityLab
email: constantine.nicolozakes@northwestern.edu

Introduction

The shoulder is the most commonly dislocated human joint,[1] in part due to its vast mobility and minimal passive tissue constraints. Active stability provided by shoulder muscles is therefore essential to prevent dislocation. Muscles provide active stability by producing forces that compress and center the humeral head within the concave glenoid (concavity compression).[2] An important component of rehabilitation for dislocation is strengthening rotator cuff muscles because they generate compressional forces and are thought to be the primary joint stabilizers. However, rehabilitation outcomes are still suboptimal.[3] Limited understanding of potential active stabilizing mechanisms beyond concavity compression may hinder the success of rehabilitation. Muscles also directly resist humeral head translation when stretched due to their intrinsic stiffness.[4] Intrinsic stiffness increases with muscle activity,[5] but the degree to which intrinsic muscle stiffness actively contributes to keeping the humeral head centered has yet to be explored. Our objective was to determine how shoulder muscles increase glenohumeral stiffness—the resistance to humeral head translation—through concavity compression and intrinsic muscle stiffness mechanisms. We hypothesized that muscles with larger lines of action (i.e., primary shoulder movers) can contribute to glenohumeral stiffness through their own intrinsic muscle stiffness, increasing glenohumeral stiffness overall as much as or more than rotator cuff muscles.

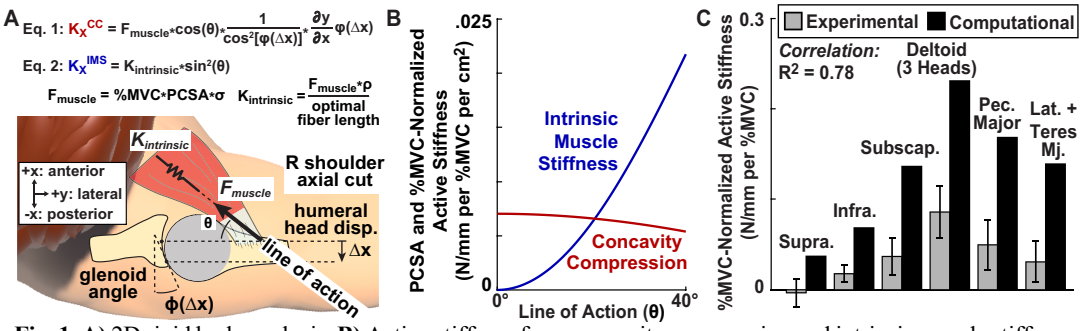

Fig. 1. **A)** 2D rigid body analysis. **B)** Active stiffness from concavity compression and intrinsic muscle stiffness based on line of action. **C)** Comparison of computational and experimental results.

Methods

We created a computational model to estimate active stiffness, defined as the increase in glenohumeral stiffness due to muscle activation beyond the stiffness provided from passive stabilizing structures. The model was derived from a 2D rigid-body analysis (**Fig. 1A**). Active stiffness due to concavity compression ($\mathbf{K_x^{CC}}$; **Eq. 1**) depends on the force a muscle produces ($\mathbf{F_{muscle}}$), its line of action (**θ**), and the glenoid angle at different humeral head displacements (**ϕ(Δx)**). Active stiffness due to intrinsic muscle stiffness ($\mathbf{K_x^{IMS}}$; **Eq. 2**) depends on a muscle's line of action and intrinsic stiffness ($\mathbf{K_{intrinsic}}$).

We compared the model predictions to experimental estimates of active stiffness and recorded muscle activity during shoulder torque generation. Data were collected from 15 healthy adults (8F). Mechanical properties of the shoulder were measured using a linear actuator to apply small, stochastic, anterior-posterior perturbations that translated the humeral head in the glenoid. Measurements were made at 90° abduction, 0° rotation as subjects generated isometric torques. System identification was used to estimate glenohumeral stiffness from the applied forces and measured displacements. Active stiffness was defined as the increase in glenohumeral stiffness during torque generation. EMGs were recorded from 3 rotator cuff muscles (intramuscular) and 6 primary shoulder movers (surface). We used linear mixed effects models to model the experimental relationship between measured EMGs and active stiffness so that we could determine which muscle groups contributed most to increasing the translational stiffness of the glenohumeral joint. We also used our the measured EMGs to predict active stiffness from our computational model to determine how well it accounted for the experimental measures of active stiffness.

Results and Discussion

Shoulder muscles increase active stiffness differently depending on their line of action. For muscles that predominantly produce compressional forces, concavity compression is the dominant stabilizing mechanism (**Fig. 1B**). As the line of action becomes larger, active stiffness provided through intrinsic muscle stiffness increases. A muscle can increase active stiffness through its intrinsic stiffness as much as four times as it can through concavity compression as the line of action approaches 40°. Since active stiffness from both mechanisms scales linearly with muscle force (and PCSA), larger muscles can increase active stiffness more overall than smaller muscles.

Experimentally, EMGs in rotator cuff muscles and primary shoulder movers were positively correlated with active stiffness. EMGs recorded from the primary shoulder movers were a better predictor of active stiffness than EMGs recorded from the rotator cuff muscles (R^2=0.80 vs. R^2=0.56; P<0.001). Active stiffness predicted from our computational model based on experimental EMGs correlated well with, but overestimated, our experimental estimates of active stiffness (R^2=0.78; modeled active stiffness = 2.7x experimental active stiffness; **Fig. 1C**). This overestimation may be due to estimating stiffness of arm soft tissue in series with glenohumeral stiffness.

Significance

Our results suggest that shoulder muscles with large lines of action, like the primary shoulder movers (e.g., *pec. major,* θ=34°), can actively stabilize the glenohumeral joint. The stabilizing potential of the primary shoulder movers should be emphasized in rehabilitation protocols to treat shoulder dislocations in addition to the rotator cuff muscles.

Acknowledgments

Funding: ASB Graduate Student GIA; NIH (F31AR074288, T32GM008152, UL1TR001422); Northwestern University.

References

[1]Kerr. *CJSM.* 2011. [2]Lippitt. *JSES.* 1993. [3]Hurley. *Arthroscopy.* 2020. [4]Debski. *JSES.* 1999. [5]Morgan. *J Physiol.* 1977.

Effects of Lower Extremity Force Variability and Strength on Spatiotemporal Gait Parameters in Healthy Older Adults

Sarah C Powell[1], S. Wait[1], J. Royster[1], B. Ritch[1], and JW. Skinner[1]
[1]Appalachian State University, Department of Health and Exercise Science, Boone, NC.
email: *skinnerjw@appstate.edu

Introduction

Consistent force production of the lower extremities is crucial for motor performance. The unintentional variability in voluntary contractions during daily tasks can be quantified and observed in terms of force control. With age, adults tend to have increased variability values when compared to younger aged adults. An increase in variability has been associated with a decrease in gait function, increase in gait variability and an increased risk of debilitating falls.

Prior research observed an increase in measures of variability in older adults (OA) compared to young adults (YA) during isometric tasks across multiple joints (1,2). The plantarflexors (PF) and the dorsiflexors (DF) have been examined due to the contributions to the performance of almost all activities of daily living, including gait (1). Therefore, the age-associated increase in force variability in the ankle could impair the ability of OA.

This particular study examines how aging effects 1) maximal force and force control during ankle plantarflexion and dorsiflexion, 2) spatiotemporal gait performance, and 3) the relationship between force control and gait performance in healthy O. This analysis tests the presumption that gait variability during over ground walking will have an association with an increased level of force variability in the lower extremities and that OA with higher levels of gait variability will display higher levels of force variability.

Methods

A cross-sectional research design compared force steadiness within the lower extremity and stride-to-stride gait variability of healthy OA. Ten OA:62±7 years and 10 YA: 24±5 years, p <.001) completed ten over-ground walking trials at self-selected speed. Next, participants underwent assessment of maximal force production and submaximal force control (5%,10%,20% MVC) of the ankle dorsiflexors (DF) and plantar flexors (PF). All participants completed Simple Physical Activity Questionnaire (SIMPAQ) prior to beginning the assessments.

Results and Discussion

The results showed that OA had a reduction in joint torque. Maximal isometric force was statistically lower across both the PF and DF muscle groups in OA compared to YA ($P < 0.05$). On average, OA produced 43% less PF force and 28% less DF maximal force. Examination of submaximal PF and DF force control (Figure 1A and B) revealed that the OA produced higher levels of force variability at 5% and 10% MVC compared to YA ($P < 0.05$). No statistically significant difference was noted at 20% MVC.

Gait analysis revealed decreased cadence, lower gait speed, decreased stride length and higher step width in OA. No differences were detected between OA and YA and no significant relationships were present between force control and gait variability in either group. However, physical activity levels, as measured by the SIMPAQ, were found to be related to spatiotemporal variability.

Our research indicates that force control in OA is significantly impaired at lower MVC percentages compared to higher levels, leading to gait variations. We found no relationship between gait variability and force variability Regular physical activity may contribute to this finding. Exercise is associated with improved walking capacity and so physical activity may operate a central mechanism in preserving gait function in older populations and those at a higher risk of falling.

Significance

Loss of lower extremity control and strength due to aging can have negative effects on functional performance. This investigation examines potential underlying mechanisms, their relationship to locomotor dysfunction and the possible aid in preserving functional capacity in OA.

Acknowledgments

None to disclose.

References

1. B. L. Tracy, "Force control is impaired in the ankle plantarflexors of elderly adults," (in eng), *Eur J Appl Physiol,* vol. 101, no. 5, pp. 629-36, Nov 2007, doi: 10.1007/s00421-007-0538-0.
2. A. Gabell and U. S. Nayak, "The effect of age on variability in gait," (in eng), J Gerontol, vol. 39, no. 6, pp. 662-6, Nov 1984.

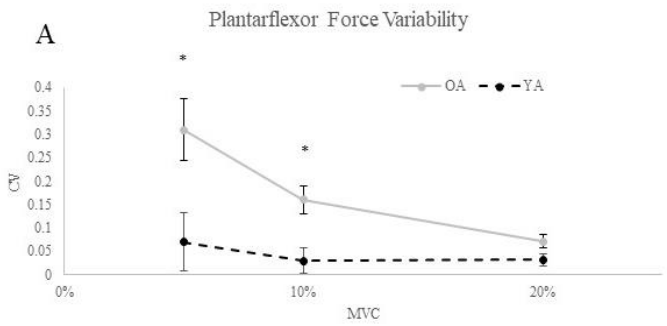

Figure 1A. Plantarflexor Force Variability between OA and YA (* = $p < 0.05$).

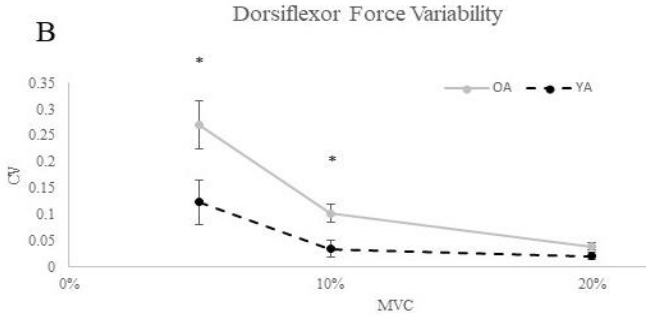

Figure 1B. Dorsiflexor Force Variability for OA and YA (* = $p < 0.05$).

ACCLIMATIZATION OF FORCE PRODUCTION IN INDIVIDUALS WITH PARKINSON'S DISEASE

Marc C. Pappas, Sidney T. Baudendistel, Chris J. Hass
Department of Applied Physiology and Kinesiology, University of Florida, Gainesville, FL
Email: marc.pappas@ufl.edu

Introduction

Parkinson's Disease (PD) is a neurodegenerative disorder that predominantly affects movement, including walking, directly impacting the pace and rhythm of each step[1]. Treadmill walking has been utilized as both an assessment and rehabilitative approach in PD to evaluate and improve spatial-temporal parameters (STP), such as stride length and stride time[2,3]. While treadmill walking is a safe and effective physical intervention, how individuals with PD change and adapt their walking pattern during a single exposure to treadmill walking remains unknown. In comparison, studies have indicated that for optimal gait data collection, in healthy young adult populations, the participant should have at least five minutes of familiarization with the instrumented split-belt treadmill before the collections begin[4]. However, no current studies have investigated the time needed for familiarization with a treadmill in those with PD. Similarly, force production (F_P) changes during walking in the PD population have not been analyzed during treadmill interventions; thus, it is unknown how long is needed for STP changes to occur and how F_P is related to these changes.

Therefore, the purpose of this study is to investigate the changes in STP and F_P in individuals with PD by evaluating them on an instrumented treadmill over a five-minute session. We hypothesized that increases in step length over the duration of the treadmill intervention would be associated with increases in F_P in individuals with PD.

Methods

Twelve individuals with idiopathic PD (9M, 3F, age: 64 ± 7 yrs, disease duration: 9 ± 5 yrs) completed five minutes of treadmill walking at their self-selected, preferred speed. Inclusion criteria required participants to be independently ambulatory and between the ages of 40-80. Exclusion criteria included other diagnoses that may adversely impact gait. Three-dimensional motion capture (Qualisys, Sweden; 120 Hz) was used to compile spatiotemporal measures, while an instrumented treadmill (Bertec Corp., OH, USA; 1200 Hz) collected ground reaction force data. Previous research in clinical populations has suggested that a 50 stride epoch was adequate for comparison over a baseline treadmill session[5]. Thus, we chose to investigate the change in F_P during the first and last 50 strides of the five-minute treadmill intervention.

To determine changes in STP and F_P in individuals with PD, paired t-tests (α=0.05) compared peak force propulsion, peak braking force, stride time, stride length, and double stance time between the first minute and the last minute of walking (first 50 strides of minute one and last 50 strides of minute five).

Results and Discussion

The self-selected walking speed was 1.07 ± 0.27 m/s (range: 0.72-1.57) for the five-minute trial. No significant differences were identified between the first and last 50 strides for the magnitude of both peak propulsive (p=.109) and braking force (p=.263, Table 1). Additionally, the variability measures for peak propulsive (p=.900) and braking (p=.167) force were not statistically different.

Interestingly, for the STP there were significant differences between time points for the magnitude of stride time(p=.045), double stance time (p=.012), and stride length (p=.037). Specifically, individuals took longer, slower strides and spent more time in double stance during the last 50 strides. There was no significant difference between the first and last fifty strides for the STP variability measures (p>.214).

Due to the significant difference between minute one and five for the magnitudes of stride length, stride time, and double stance time—while at a constant belt speed—it is apparent that changes in peak ground reaction force in the anterior-posterior direction may not be the underlying cause for changes in STPs.

To our knowledge, this is the first study analyzing the changes in STP within the familiarization period (between min 1 and 5) to a treadmill in individuals with PD. In only five minutes, the participants' stride length magnitude moved closer to their healthy peers without any change in speed.

Significance

While changes in STP during a single session of treadmill walking have been observed in individuals with PD[6], the underlying kinetic factors for these changes have not been investigated. This study shows that peak ground reaction force is not a primary driver of the observed differences. Further investigation into the change in time-dependent variables could provide a deeper understanding of the changing gait mechanisms of individuals with PD. Additionally, determining the minimum amount of time needed for a significant difference in STP should be identified with further investigation.

Acknowledgments

This work was supported in part by: NIH T32-NS082128, the ASB Graduate Student Grant-in-Aid, and the University of Florida University Scholar's Program.

References

1. Schmitt et al., 2020. Park Dis. ;2020:1-5
2. Bello et al., 2013. Gait Posture. 38(4):590-595.
3. Warlop et al., 2018. Front Physiol. 9:68.
4. Zeni & Higginson, 2010. Clin Biomech. 25(4):383-386.
5. Sombric et al., 2020. J NeuroEngineering Rehabil. 17(1):69.
6. Bello et al., 2008. Movement Disorders. 23(9):1234-1249.

		Peak Propulsive Force (BW)	Peak Braking Force (BW)	Stride Length (m)	Stride Time (s)	Double Stance Time (s)
Mean	*First*	-0.162	0.118	1.059*	1.058*	0.176*
	Last	-0.167	0.123	1.074*	1.073*	0.179*
SD	*First*	0.011	0.015	0.023	0.017	0.010
	Last	0.011	0.016	0.026	0.018	0.009

Table 1. Magnitude (mean) and Variability (standard deviation (SD)) between the first and last 50 strides. *indicates significance

Stretch Reflexes are Elicited in Shoulder Muscles by Translations of the Glenohumeral Joint

Constantine P. Nicolozakes[1-3], M. S. Coats-Thomas, D. Ludvig, A. L. Seitz, and E. J. Perreault
[1]Biomedical Engineering and [2]Feinberg School of Medicine, Northwestern University; [3]Shirley Ryan AbilityLab
email: constantine.nicolozakes@northwestern.edu

Introduction

The glenohumeral joint is the most mobile,[1] yet the most commonly dislocated,[2] joint in the human body. Translational joint stability is maintained by passive structures (e.g., glenohumeral ligaments) and shoulder muscles. Muscles are hypothesized to help maintain active stability through a combination of feedforward and feedback control. Feedforward control is important to protect the glenohumeral joint from harm caused by anticipated external perturbations. However, dislocations are most often caused by unexpected perturbations,[3] and protection from these may instead rely on feedback control. Stretch reflexes elicited by translations at the glenohumeral joint could be an important mechanism for maintaining joint stability, but they have yet to be studied. Our objective was to determine if stretch reflexes are elicited in shoulder muscles by translations of the glenohumeral joint, and to compare the characteristics of reflex responses between different muscles. We hypothesized that the characteristics of stretch reflexes, including the magnitude of their responsiveness and their latencies, would differ between rotator cuff muscles and primary shoulder movers based on the muscles' different lines of action at the glenohumeral joint.

Methods

Data were collected from 15 healthy adults (8F). Stretch reflexes were elicited by a linear actuator which applied small, stochastic, anterior-posterior perturbations that translated the humeral head in the glenoid. Measurements were made at 90° abduction, 0° rotation as subjects generated isometric torque in six directions. EMGs were recorded from three rotator cuff muscles (intramuscular) and six primary shoulder movers (surface). EMGs were segmented, aligned to the onset of each anterior or posterior perturbation, and averaged across a trial for each muscle. Rectified EMGs were averaged 0-40ms prior to the perturbation onset to estimate background activity. The reflex magnitude was calculated as the average change of rectified EMG from background in four windows: S1 (20-40ms after perturbation onset), S2 (40-60ms), L1 (60-80ms), and L2 (80-100ms). We calculated the relationship between reflex magnitude and background activity (gain scaling factor) separately in each muscle and window using a linear mixed effects model. The magnitude of each muscle's reflex responsiveness was evaluated as the root mean square of its gain scaling factors in the four windows across both perturbation directions. We estimated reflex latency for facilitation responses as the time after perturbation onset when the rectified EMG exceeded background by 2 SDs.

Results and Discussion

Stretch reflexes were elicited by translational perturbations in all muscles. Reflexes in four muscles demonstrated consistent facilitation from anterior perturbations: *subscapularis*, *posterior deltoid*, *latissimus dorsi*, *teres major*. Reflexes in four other muscles demonstrated consistent facilitation from posterior perturbations: *supraspinatus*, *infraspinatus*, *anterior delt oid*, *pectoralis major*. Reflexes in the *middle deltoid* demonstrated no clear directionality and appeared to reflect an average of *anterior* and *middle deltoid* reflexes.

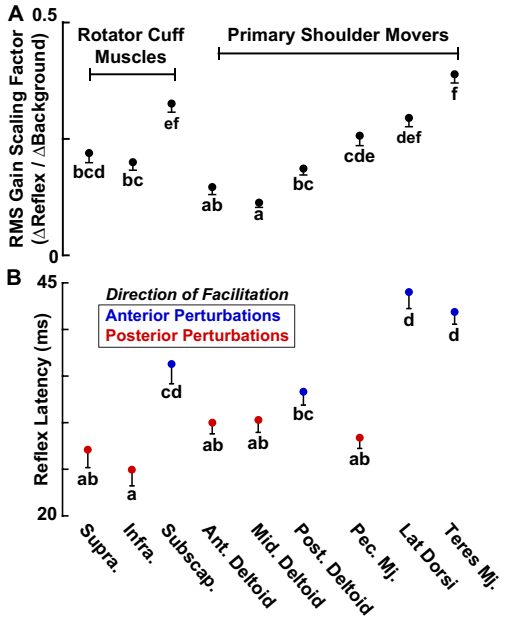

Fig. 1: Reflex responsiveness (**A**) and latency (**B**) in shoulder muscles. Reflex characteristics in each panel that do not share the same letter differed at α=0.05/36.

The overall reflex responsiveness of rotator cuff muscles to translational perturbations did not differ as a whole from the responsiveness of primary shoulder movers (**Fig. 1A**). The responsiveness of the *supraspinatus* and *infraspinatus* was comparable to other primary shoulder movers despite having small, compressional lines of action. The *subscapularis*, which has the largest line of action among rotator cuff muscles, demonstrated increased responsiveness compared to the *supraspinatus* and *infraspinatus*, and was also more responsive than all three heads of the *deltoid*. The three most responsive muscles (*subscapularis*, *latissimus dorsi*, *teres major*) were activated by anterior perturbations.

The shortest latencies were observed in the *supraspinatus* and *infraspinatus*, differing significantly from the *subscapularis*, *teres major*, and *latissimus dorsi* (**Fig. 1B**; all P<0.001). These short latencies reflected a larger trend of shorter latencies in all muscles activated by posterior perturbations (25-30ms) than muscles activated by anterior perturbations (33-43ms).

Significance

Stretch reflexes elicited in all shoulder muscles may contribute to a protective feedback response against dislocations. The decreased latencies in muscles activated by posterior perturbations may indicate more rapid protection from perturbations that can cause posterior dislocations. To fully understand the clinical significance of the observed reflexes, future work is warranted to characterize the relationship between stretch reflexes and translational glenohumeral stability.

Acknowledgments

Funding: ASB Graduate Student GIA; NIH (F31AR074288, T32GM008152, UL1TR001422); Northwestern University.

References

[1]Boone & Azen. *JBJS.* 1979. [2]Kerr. *CJSM.* 2011. [3]Montgomery. *AJSM.* 2019. [4]Day. *Clin Biomech.* 2012. [5]Ackland. *J Anat*. 2009.

EXPECTATION OF GAIT INITIATION ALTERS THE COVARIATION BETWEEN THE HORIZONTAL GROUND REACTION FORCES UNDER THE TWO FEET

Anvesh S. Naik, Paige Thompson, Austin Cooper, and Satyajit Ambike
Department of Health and Kinesiology, Purdue University, West Lafayette, Indiana
Email: naik20@purdue.edu

Introduction

Early postural adjustments (EPAs) are essential, predictive adjustments in muscle activations that unload the stepping foot and generate appropriate body movements to initiate gait. In self-paced stepping tasks, EPAs are preceded by anticipatory synergy adjustments (ASAs) describing the reduction in the stability of performance variables (e.g., center of pressure) that change during the EPAs [1]. Here, we determine whether merely expecting to initiate gait leads to destabilization of the net forces and moments acting on the body. This would constitute a novel kind of ASA, consistent with our recent result in which simply informing participants that they need to alter fingertip force leads to a decline in the stability of the force compared to tasks in which no change is required [2].

During quiet standing, the ground reaction forces (GRFs) under the two feet determine the net force on and the net moment about the whole-body center of mass (COM). The GRFs must covary non-trivially to stabilize body motion. E.g., the anterior-posterior (AP) forces must covary negatively so that their sum, and thereby the AP translation of the COM is stabilized (Fig. 1A). However, since AP forces create opposing moments about the vertical axis through the COM, they must covary positively to stabilize net moment, and thereby the rotation about this axis. Similar tensions exist for GRFs along medio-lateral (ML) and vertical directions [3]. Here, we determine if the expectation to initiate gait alters covariance in the GRFs, thereby destabilizing some aspect of body motion.

Methods

Healthy young adults (N=28, 7 male, 23±3 yrs.) placed their feet on separate force plates (AccuGait, AMTI) shoulder width apart and stood one step-length away from an elevated curb (4 m long, 1 m wide, 15 cm high). A monitor mounted at eye-level and beyond the other end of the curb provided visual cues. In the steady task, participants stood quietly while looking at a square target at the center of the screen. Participants were informed that the target will not move and that they were to remain standing. In the reaction time (RT) task, each trial began like a steady trial, but participants expected the target to jump to the left or the right. Participants had to initiate gait with the corresponding foot by stepping on to the curb as quickly as possible and continue walking on the curb. Both tasks were performed 15 times.

We used the uncontrolled manifold analysis to quantify separately the covariance in the AP, ML and vertical GRFs during the steady task and during the period of the RT task *before* the target jumped. The working hypothesis was that the force sum along each direction is stabilized. We partitioned the across-trial variance in weight-normalized GRFs into a component that maintains the GRF sum, and a component that changes it. We computed the normalized difference between these components and z-transformed it to obtain the *synergy index* (ΔVz). We used two-tailed t-tests to compare ΔVz to zero. ΔVz>0 supports the working hypothesis; ΔVz<0 indicates that the force difference is stabilized instead of the sum [3]; ΔVz=0 indicates no covariation in the force pair. We conducted two-sample t-tests to identify differences in ΔV_z across tasks.

Results and Discussion

ΔVz was greater than zero for all force pairs in both tasks ($p<.01$), indicating that COM translation was stabilized. ΔVz for the AP GRFs ($t_{54}=3.1$, $p<.05$) and ML GRFs ($t_{54}=1.9$, $p<.05$) was higher for the RT task than the steady task, but ΔVz was invariant across tasks for the vertical GRFs ($p=.07$; Fig. 1B).

In the RT tasks, since gait initiation could occur with either leg, maintaining COM position (presumably in the center of the base of support) by controlling more tightly the net AP and ML GRFs would lead to, on average, a more rapid unloading of either limb once the target jump is perceived. Furthermore, increased ΔVz for the RT task in the AP forces also implies that the covariation in the AP forces shifts towards *lower* stabilization of the force *difference*, and hence the moment about the vertical axis. This would facilitate pelvic rotation during gait initiation, if and when gait is initiated. A similar conclusion regarding the ML forces is plausible; however, we do not have the COM position to determine whether the ML forces create opposing moments about the vertical axis. The vertical GRFs support the body weight. This function likely supersedes the preparation for gait initiation, and hence their covariance pattern remains invariant. Finally, individual force pairs contribute to but do not determine net moment about any axis. Therefore, positive ΔVz values in Fig. 1B do not indicate unstable net moments.

In conclusion, covariance in the AP/ML GRFs is altered when individuals expect to initiate gait, likely to facilitate the upcoming movement. Changes in AP GRF covariation is interpreted as a new kind of ASA, similar to that observed in manual tasks [2].

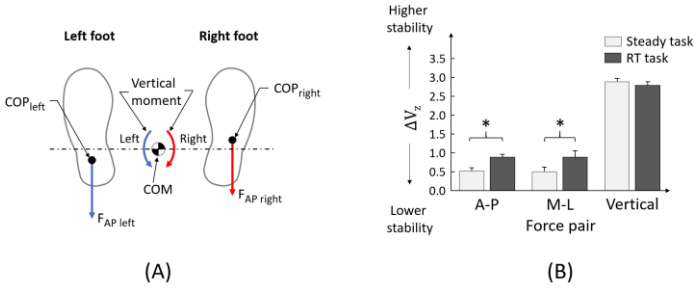

Figure 1: (A) Hypothetical illustration of AP GRFs and corresponding moments about the COM; (B) Mean ± SE of ΔVz for steady and RT tasks for GRFs along AP, ML, and vertical directions.

Significance

Falls in older individuals frequently occur while crossing obstacles [4]. Our results will serve as a baseline for evaluating between-leg coordination in older adults, and assist in identifying mechanisms that lead to falls. These GRF patterns may also assist in creating control policies of powered lower-limb prostheses, especially for detecting the intention to initiate gait [5].

References

[1] Krishnan et al., 2011, *Exp Brain Res*, 212:47-63.
[2] Tillman and Ambike, 2018, *J Neurophysiol*, 119:21-32.
[3] Cui et al., 2020, *J Biomech*, 106:109837.
[4] Berg et al., 1997, *Age Ageing*, 26:261-268.
[5] Wentnik et al., 2013, *Gai and Pos*, 37:223-228.

PREDICTIVE SIMULATIONS TO INVESTIGATE HOW CHANGES IN JOINT TORQUES, STARTING POSITION, AND ASSISTIVE DEVICES CONTRIBUTE TO THE EFFORT OF STANDING WITH ONE LEG

Maria C. DiVita, Robert A. Siston
[1]The Ohio State University
email: *divita.4@buckeyemail.osu.edu

Introduction

Lower extremity weakness caused by advanced age, knee osteoarthritis, stroke, Parkinson's disease, and other disabilities affect a person's ability to rise from a chair [1]. Inability to rise from a seated position can lead to a loss of independence, so several options exist for people who need assistance. Physical therapy may be recommended to increase muscle strength, but strength training may not be effective for all individuals [2]. Assistive external devices can then be helpful in rising from a seated position but can be limited by accessibility and cost [3]. Another method modifies the kinematics of the task by raising the starting position [4], but this approach needs a taller chair when available or the use of a cushion to boost the effective height.

However, the relative effectiveness of these options individually or in combination remains unknown, and such information could help inform decision making strategies to help individual rise from a seated position. As a first step in addressing this problem, we investigated the effects of changes in strength, starting position, and the use of an assistive device on the energetic cost of rising from a squatting position in a simple model with only 1 leg.

Methods

We used Moco (V0.4.0) and a torque-driven model based off of "squatToStand_3dof9musc". The baseline model contained three degrees of freedom at the hip, knee, and ankle with torque actuators of 150, 300, and 150 Nm and a starting position with joint angles of -2, -2, and -0.5 radians at each of the joints, respectively. In the simulation, the model begins at rest in a squat and ends at rest while standing with a straight leg.

We systematically investigated the effects of changes in "strength", starting position, and the use of an assistive device on the energetic cost of the task. We varied the "strength" of the model by changing the magnitudes of the torque actuators to 25%, 50%, and 100% of their baseline torque configurations. We tested the baseline starting position and 2 additional starting positions with the hip and knee joints both at -1.75 and -1.5 radians; the initial ankle position did not change. In each configuration, we added a virtual device to the weakened joint only using a generalized "SpringGeneralizedForce". We tested spring stiffnesses of 0, 10, 20, and 40 Nm on the hip; 0, 10, 20, 40, and 60 Nm on the knee; and 0, -10, -20, and -40 Nm on the ankle. These changes in strength, position, and the device were applied individually and in combination with each other. We solved a total of 117 predictive simulations using direct colocation and calculated "My Effort" for standing, defined as the sum of the squares of activation of the torque actuators.

We analysed the results using stepwise regression with linear, quadratic, and interaction terms, with alpha-to-enter and alpha-to-exit set at 0.15. We analysed the results of all 117 simulations together and the simulations for the weakened joints separately. For the analysis of all 117 simulations, we identified the combination of all factors that minimized the effort of the task. All statistical analyses were performed in Minitab (V17).

Results and Discussion

For the combined data set, energetic cost decreased linearly with decreasing hip angle. There was also a second order relationship that reduced effort with decreased hip device spring stiffness. Increasing all joint strengths quadratically decreased effort until an optimal point and then energetic cost increased. The optimal response included no hip device and a knee with the lowest percent joint strength (Table 1). ($R^2 = 0.794$, $p < .001$).

Table 1: Optimal values of the combined data set.

Angle (rad)		Dev. Spr. Stiff. (Nm)			% Joint Strength		
Hip	Knee	Hip	Knee	Ankle	Hip	Knee	Ankle
-2	-1.5	0	60	-40	91.7%	68.9%	84.8%

With isolated hip weakness, smaller effort was primarily the result of changes in two terms, with increases in the stiffness of the device ($\beta_1 = -0.04 \pm 0.02$) leading to a reduction of effort twice as much as increasing the torque at the hip ($\beta_2 = -0.02 \pm .01$) ($R^2 = 0.730$, $p < 0.001$). With isolated knee weakness, smaller effort was primarily the result of two terms, with increases in the torque at the knee ($\beta_1 = -0.008 \pm 0.005$) leading to a reduction nearly three times as much as the interaction of lowering the starting position and increasing the torque of the knee ($\beta_2 = 0.003 \pm .003$) ($R^2 = 0.814$, $p < 0.001$). With isolated ankle weakness, smaller effort was primarily the result of two terms, with the interaction of lowering the starting position and increasing the device stiffness ($\beta_1 = -0.01 \pm 0.01$) leading to a reduction of 1.27 times as much as the interaction of lowering the starting position and increasing the torque at the ankle ($\beta_2 = 0.009 \pm .004$) ($R^2 = 0.878$, $p < 0.001$).

With such a simple model, the results should be interpreted in their appropriate context. For instance, our findings could be influenced by the lack of interaction with a virtual chair (requiring starting from a static squat) and the requirement of ending the motion standing with a straight leg.

Significance

The choice of changing joint torques, starting position, or device spring stiffness to reduce the effort of rising from a squat depends greatly as to what individual joint is weakened. This study will inform the future research of STS transfer using a muscle-driven model with two legs for simulations to further investigate the optimal combinations of interventions to assist with the task of rising from a seated position.

References

1. Caruthers, et al. *Comp Methods in Biomech and Biomed Eng* 2020 23(11): 765-772. **2.** Janssen, et al. *Phys Ther* 2002 82(9): 866-879. **3.** Rutherford, et al. *Disability and Rehab: Assist Tech* 2014 11(2): 158-165. **4.** Hurley, et al. *Phys Occup Ther Geriatr* 2016 43: 169-15.

IMPACT OF ATHLETIC TRAINER TAPING TABLE HEIGHT ON TRUNK AND SHOULDER ANGLES

Jonathan C. Swain, Kerrie Wilson, and Kaitlin M. Gallagher
[1]Exercise Science Research Center, University of Arkansas, Fayetteville, AR
email: jcswain@uark.edu

Introduction

Athletic trainers (AT) have reported developing work-related musculoskeletal injuries throughout their careers[1,2,3]. In 2018, the incidence rate of AT work-related injuries was estimated as 21.6 per 200,000 hours[3]. Between 2001 and 2011, half of all reported injuries were due to overuse[2]. Moreover, previous literature has indicated a relationship between taping and the development of low back pain and finger injuries[1]. Taping table height has been shown to influence trunk and shoulder muscle activity, though this effect was mediated by participant height[4]. This study investigated the influences of taping table height on trunk and shoulder joint angles. We hypothesized joint angles would differ between the two table heights and would be influenced by a person's height.

Methods

Thirteen AT students (8 female, 5 male) taped a model's right ankle at two table heights – 31" and 36". These heights were chosen as they were the average height of taping surfaces within (36") and outside (31") athletic training clinics[4]. Pelvis, thorax, and left and right upper arm position was tracked during the taping task using a Qualisys motion capture system (100 Hz, Qualisys AB, Gothenburg, Sweden). The participants had a practice trial at each height and then two subsequent trials at each height. Table height order was randomized for participants. Marker data were exported to Visual3D (C-Motion Inc, Germantown, MD, USA), interpolated, and filtered with a 2nd order dual low-pass filter at 6 Hz. Three-dimensional trunk and shoulder angles were then calculated. Trunk angles were defined by the orientation of the thorax to the pelvis and calculated using a ML/AP/Axial rotation sequence. Shoulder angles were expressed as the angle of the trunk to the thorax and calculated using an X/Y/Z rotation sequence[5]. The three-dimensional trunk angles were then entered into an amplitude probability distribution function (APDF) to determine the median (50th percentile) and range (difference between the 90th and 10th percentiles) for the entire taping trial. For the shoulder angles, only the flexion/extension and abduction/adduction angles were processed with the APDF. The medians and ranges were averaged across the two trials for statistical analysis in SPSS. Since the data did not follow a normal distribution, non-parametric paired t-tests were run to compare the variables at the two heights (31" vs. 36"). For the trunk, significance was set at $p < 0.008$ (.05/6 trunk t-tests). For the shoulders, significance was set at $p < 0.0125$ (.05/4 shoulder t-tests per side). A Spearman Rank correlation between participant height and the difference in angles between the two table heights was calculated to determine if a person's height influenced their kinematics at each table height. Significance was set at $p < 0.05$ for these tests.

Results and Discussion

Trunk and shoulder flexion median angles, as well as shoulder abduction angle range of motion, were significantly different between the 31" and 36" table (Table 1). There was more trunk and shoulder flexion with the 31" vs. 36" table height. The difference between left shoulder flexion at the two table heights was positively associated with participant height ($r_s = 0.56$, $p < 0.05$) (Figure 2). There were no other significant differences for the remaining variables or correlations.

In summary, participants had to flex their trunk and shoulders more when taping at 31" height; however, shorter participants had a lower shoulder flexion angle than taller participants to reach the same taping site.

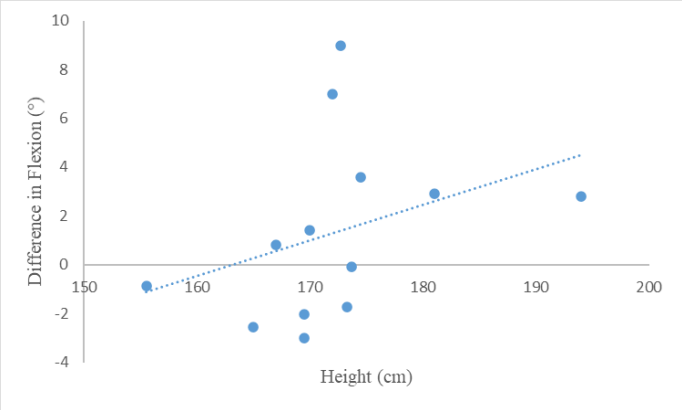

Figure 1. Difference in left shoulder flexion angle between the 36' and 31" tables. Positive indicates shoulder flexion.

Significance

Generally, a taping table height of 36" would reduce the trunk and shoulder flexion angles, as well as the shoulder abduction range of motion required for taping an ankle; however, the extent to which it does this is will be dependent on a person's stature. For adaptability across different situations, ATs should opt for table heights appropriate for their height and task. This can be achieved by using a height adjustable treatment or taping table.

Acknowledgments

An Arkansas student undergraduate research fellowship (SURF) supported this project.

References

1. Ju YY et al. (2011). *J Occup Rehabil*.
2. Kucera KL et al. (2016). *Am J Ind Med*.
3. Kucera KL et al. (2018). *J Athl Train*.
4. Appold A et al. (2019). NATA 2019 Conference.
5. Phadke V et al. (2011). *J Biomech*

	n	31" Median	36" Median.	*Z*	*p-value*
Trunk Median Flexion	12	20.91°	14.64°	78.00	.002
Left Shoulder Median Flexion	13	33.05°	26.78°	3.00	.003
Right Shoulder Median Flexion	13	31.21°	22°	< 0.00	.001
Left Shoulder Abduction Range	13	35.33°	29.52°	6.00	.006

Table 1. Median angles for the 31" and 36" tables and Wilcoxon signed-rank test results. Positive medians indicate flexion.

SHOULDER COMPLEX KINEMATICS IN YOUTHS WITH HYPERMOBILE EHLERS-DANLOS SYNDROME

Joshua M. Leonardis[1], Olivia Wilwert[1], Anahita A. Qashqai[1], Alyssa J. Schnorenberg[1], Michael J. Muriello[2], Donald G. Basel[2], and Brooke A. Slavens[1]
[1] University of Wisconsin-Milwaukee, Milwaukee, WI, USA
[2] Medical College of Wisconsin, Wauwatosa, WI, USA
email: *leonarj@uwm.edu

Introduction

Hypermobile Ehlers-Danlos syndrome (hEDS) is a heterogeneous, autosomal dominant inherited disorder that influences connective tissue. hEDS is characterized by joint pain and the ability to move the joints beyond a normal range of motion (hypermobility). The shoulder complex is at a particularly high risk of both instability and pain. In adults, hypermobility is associated with altered shoulder kinematics and often leads to difficulty performing upper extremity activities of daily living (ADL) [1]. The shoulder kinematics utilized during ADL performance in youths with hEDS is unknown. This pilot study aimed to quantify the independent motion of the sternoclavicular, acromioclavicular, and glenohumeral joints during the execution of common ADLs in youths with hEDS.

Methods

Nine youths with a clinical diagnosis of hEDS (5 females, 4 males; mean (SD) age: 14.0 (2.9) years, height: 1.6 (0.2) m, weight: 57 (14 kg)) participated in a single experimental session. Passive markers were affixed to 27 anatomical landmarks on the torso and upper extremities. Three-dimensional (3D) marker trajectory data were obtained while participants performed four unilateral upper extremity tasks (reach to the opposite shoulder, reach to a back pocket, combing hair, and drinking from a cup). A bilateral upper extremity inverse kinematics model computed 2D sternoclavicular and 3D acromioclavicular and glenohumeral joint kinematics [2].

Results and Discussion

Shoulder complex joint kinematics were largely activity dependent (Figure 1). The sternoclavicular joint operated in both elevation and depression, while maintaining retraction throughout each ADL. Reaching to the opposite shoulder required the greatest sternoclavicular depression (11±4.7º), while reaching to a back pocket required the greatest elevation (8±6.5º). Sternoclavicular retraction was greatest while combing (44±4.4º) and least when drinking from a cup (14±2.9º). The acromioclavicular joint maintained upward rotation, protraction, and posterior tilt regardless of the activity. Drinking from a cup required the least upward rotation (16±4.7º), while combing required the most (56±8.3º). Contrarily, combing required the greatest protraction (62±8.1º), while drinking required the least (29±3.7º). Finally, reaching to a back pocket required the greatest posterior tilt (28±14.3º) and reaching to the opposite shoulder the least (2±5.7º). Reaching to a back pocket necessitated the most glenohumeral adduction (19±6.4º) and extension (46±9.2º). Reaching to the opposite shoulder required the greatest internal rotation (43±8.7º) and flexion (55±9.8º), and combing required the greatest external rotation (91±33º) and abduction (64±11º).

This pilot study is the first to characterize the independent motion of the sternoclavicular, acromioclavicular, and glenohumeral joints during ADLs in youths with hEDS. Our findings largely align with results reported in the literature limited to humerothoracic motion in typically developing children and scapular motion in adults. In typically developing children (mean of 8.3 years old), drinking from a cup required 54º of humerothoracic flexion and 26º of abduction, while reaching toward a back pocket required 52º and 31º of extension and adduction, respectively [3]. The current study found similar results; drinking required a peak of 47.5º of glenohumeral flexion and 35.1º of abduction and reaching behind the back required 45.9º of extension and 19.1º of adduction. In able-bodied adults, eating with a spoon required 25.9º of scapular upward rotation, whereas only 9.5º of upward rotation was required in the current study population when drinking from a cup [4].

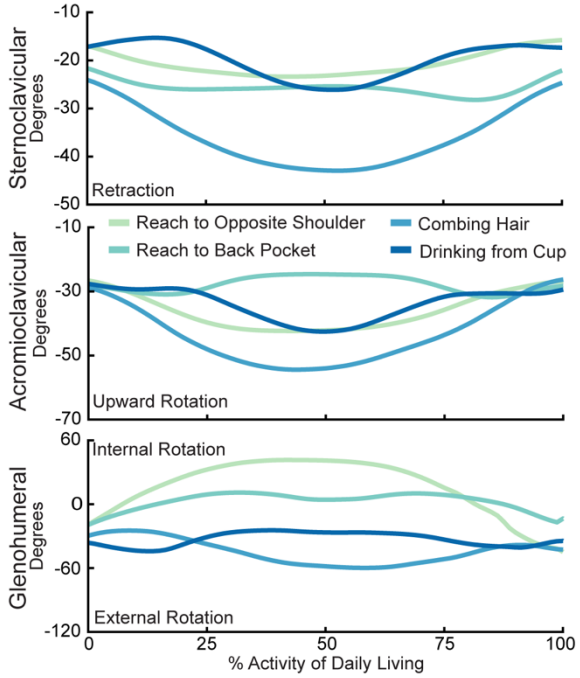

Figure 1: Mean sternoclavicular, acromioclavicular, and glenohumeral joint angles in select planes of motion during the execution of four upper extremity activities of daily living.

Significance

The current pilot study provides the most comprehensive quantitative assessment of shoulder complex kinematics during activities of daily living in youths with hEDS. Although hEDS can significantly disrupt shoulder complex motion, our results suggest that youths with hEDS perform certain ADLs using similar scapular and glenohumeral kinematics to able-bodied children and adults.

References

1. Johannessen, et al., Dis. & Rehab., 38(14), 1382-1390, 2016
2. Schnorenberg, et al., J. Biomech., 41(1), 269-276, 2014
3. Beaudette, et al., J. Med. Bio. Eng., 34(5), 448-454, 2013
4. Magermans, et. al., Clin. Biomech., 20(6), 591-599, 2005

MOTOR ADAPTATION DURING WALKING HAS LIMITED TRANSLATION TO DISCRETE STEPPING IN INCOMPLETE SPINAL CORD INJURY

Tara Cornwell[1]*, Jane Woodward, and Keith E. Gordon
[1]Northwestern University, Physical Therapy and Human Movement Sciences, Chicago, IL, USA
*email: tcornwell@u.northwestern.edu

Introduction

Following an incomplete spinal cord injury (iSCI), a major goal is to improve locomotor stability. It is important that the skills developed in the clinic (e.g., treadmill walking) translate to novel tasks outside the clinic. To this end, research has found that some treadmill-based locomotor adaptations persist during overground walking[1]. We sought to expand our understanding of locomotor translation by exploring if stabilization strategies adapted during treadmill walking will translate to discrete multi-directional stepping movements in individuals with iSCI.

Specifically, participants performed treadmill walking in 3 external force fields (Null, Amplifying, Damping) designed to alter control of lateral stability. The Amplifying field augments lateral center of mass (COM) velocity, while the Damping field opposes lateral COM velocity. These fields have been found to increase (Amplifying) and decrease (Damping) efforts to maintain lateral stability[2,3]. Immediately following walking in each force field, participants performed the Four-Square Step Test (FSST), a clinical test during which individuals step clockwise and then counterclockwise through four squares as quickly as possible. We hypothesized that after steady-state walking in the Amplifying field, participants would exhibit after-effects of greater stabilization effort (slower, more controlled movements) during the discrete stepping within the FSST. We also hypothesized that after walking in the Damping field, participants would exhibit after-effects of reduced stabilization effort (faster, less controlled movements) during the FSST.

Methods

We quantified FSST movements of 12 ambulatory individuals (48 ± 15 years old, 9 males) with iSCI immediately following 3 walking trials in different force fields: *Null, Amplifying,* and *Damping*. In each force field, participants performed 2 minutes of steady-state treadmill walking while a cable-driven robot[4] applied lateral forces to the pelvis that were proportional in magnitude and in the same (Amplifying) or opposite (Damping) direction as the participants' real-time lateral COM velocity.

To characterize overall FSST performance, total test time and movement smoothness were calculated. Smoothness was quantified with normalized COM speed ($\frac{mean\ speed}{peak\ speed}$) and log dimensionless jerk[5]. We also quantified the discrete steps between squares. For steps in the mediolateral and anterior-posterior directions, peak COM excursion and speed were calculated. A linear mixed effects model was fit in SPSS for each metric with "field" as a fixed effect and random intercepts for subjects. Bonferroni-corrected post hoc tests evaluated differences between Null and Amplifying and/or Null and Damping. Significance was set at alpha=0.05.

Results and Discussion

Our two hypotheses were generally not supported. There were no significant differences in FSST time, peak COM excursion, peak COM speed, or log dimensionless jerk between force fields. Only normalized speed changed with field. Normalized speed was significantly greater after walking in Null field than after the Damping field (p=0.040), which suggests FSST movements after walking in the Damping field were less consistent or smooth than after the Null field. Although not significant, there was an interesting trend in mean values of smoothness as quantified by jerk (Fig. 1) between fields (Damping < Null < Amplifying), suggesting, as hypothesized, that movements were more controlled after walking in the Amplifying field and less controlled after walking in the Damping field.

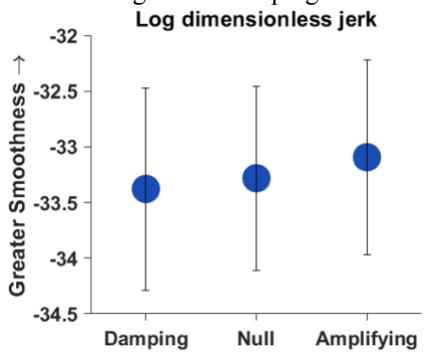

Figure 1: Means and standard errors of log dimensionless jerk during the FSST, which was smoothest after walking in the Amplifying field.

Our previous work has found locomotor adaptations to these force fields during steady-state treadmill walking persist after the field is removed[3] and translate to lateral maneuvers made during treadmill walking[6]. However, the current study did not find significant translation, suggesting that gait stability is controlled differently during steady-state walking versus discrete stepping tasks. Importantly, this study had several limitations, including a small and heterogeneous sample with varying levels of baseline walking ability. Overall, steady-state walking in varying force fields had little effect on discrete multi-directional stepping performance in iSCI. These limited results may indicate an important threshold in locomotor training generalization.

Significance

The locomotor stabilization adaptations made during steady-state treadmill walking did not translate to an overground discrete stepping task. These results suggest that the tasks performed during gait rehabilitation for individuals with iSCI should vary, involving different skills that include both steady-state and dynamic stepping tasks. Future work should continue to evaluate the limits of locomotor adaptation generalization to improve rehabilitation techniques.

Acknowledgments

This study was funded by U.S. Department of Veterans Affairs Merit Award 1 I01RX001979. The authors would like to thank Jonathon Lewis and Tyler Owen for their help in data collection.

References

[1]Reisman et al. 2009. *Neurorehab and Neural Repair*. [2]Wu et al. 2020. *Royal Soc. Open Science*. [3]Wu et al. 2019. *J of NeuroEng and Rehab*. [4]Brown et al. 2017. *IEEE*. [5]Balasubramanian et al. 2011. *IEEE*. [6]Wu et al. 2018. *Dynamic Walking*.

IN-SHOE IMPACT FORCE ON THREE COMMON RUNNING SURFACES

Kurt M DeGoede[1], B. Falk[2], D. Labenberg[1], C. Dunn[1], and J. Tirado[1]
[1]School of Engineering, Mathematics and Computer Science, Elizabethtown College
[2]Athletics Department, Elizabethtown College
email: degoedek@etown.edu

Introduction

Many competitive runners and coaches believe that running on concrete will increase impact forces over running on other surfaces, including asphalt. Runners assume running on the harder surface will produce greater impact forces and higher risk of injury.

However, the ground-shoe-foot interaction involves a stacked series of springs of very different stiffness (or 'hardness'). A typical running shoe might have an elastic modulus on the order of 1 MPa, compared to concrete, the high end of our range, at approximately 5,000 MPa. Our Track surface will have a modulus similar to the shoe, but the rubber is a thin layer laid over asphalt and effectively increase the thickness of the cushioning by a modest amount. With springs in series the 'softest' (least stiff) spring in the series dominates the interaction. Therefore, when running in typical cushioned training shoes the stiffness of the shoe, not the surface, modulates the impact force.

A few limited studies have measured such results experimentally [1], [2], [3], [4]. Investigators have only found significant reductions in impact forces when running in training shoes on natural grass and wood chips. No significant differences have been reported in impact forces for running on concrete, asphalt and traditional spray on rubberized track surfaces. These studies were all conducted at non-competitive training paces (typically no faster than 8 minutes/mile) and running speed did effect impact force [4]. We hypothesize that at a competitive training pace no significant difference in in-shoe peak force or loading rate will be observed between trials on concrete or Mondo.

Methods

Due to COVID restrictions data collection was delayed and when drafting this abstract, we had collected data on 4 of our scheduled 9 subjects. At the meeting, the full dataset will be presented.

Two male and two female competitive distance runners participated in the study (19-21 years old). The right shoe of each subject's preferred distance training shoes was modified to include a thin foam insole on which TekScan™ FlexiForce A201 spot sensors were mounted. Sensors were positioned at the heel, and under the head of the 1st and 5th metatarsals.

All subjects then ran twelve total 100 m intervals at a 20-24 second pace (~6:00/mile): four 100 m trials on each of three surfaces: Concrete, Asphalt, and a Mondo® outdoor track surface. The first and last sets were on Asphalt and the order of the concrete and Mondo were determined by coin flip. All experimental protocols will be approved by the Institutional Review Board.

Data was collected at 500 Hz, on an Arduino and filtered with a 25 Hz digital Butterworth filter in Octave. The sensor with the largest average peak force was identified for each subject. Using that sensor, for each surface we determined an average peak force and an average loading rate, across approximately 200 strides for each surface.

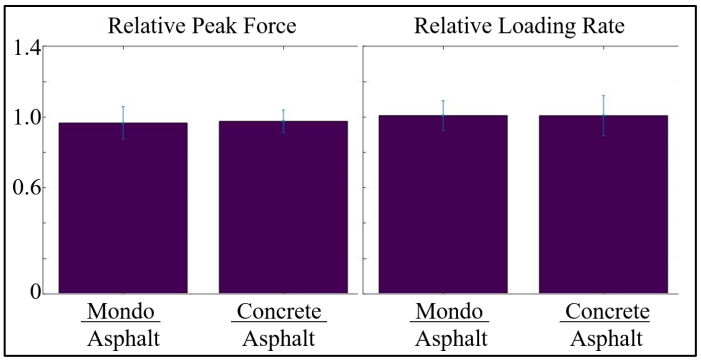

Figure 1: Relative impact force and loading rate for our pilot data, 4 subjects.

The concrete and Mondo data were normalized to each subject's asphalt value.

Results and Discussion

We have expanded on the existing data points in the literature to included competitive speed running (6 minutes/mile) and the Mondo track surface. We measured no significant differences between the normalized Mondo and concrete forces or loading rates (Figure 1). Stride to stride variability was greater than any variability across surfaces.

The data presented here is preliminary, but we will present a full dataset with 9 subjects at the meeting. The A201 spot sensors have a 1 cm diameter sensing area, and subtle shifts in ground contact patterns can have a disproportionate influence on these measures.

Significance

When running in cushioned training shoes, ground surface plays little role in determining impact forces or loading rates. The location for training runs should be decided based on factors other than running surface for surfaces ranging from Mondo to Concrete.

Acknowledgments

This project was funded through an internal collaborative project grants program at Elizabethtown College (CISP). Ryan Fisher assisted with data collection and analysis.

References

[1] V Tessutti, et al, Journal of Science and Medicine in Sport, 13:1, pp. 151-155, 2010.
[2] V Tessutti, et al, Journal of Sports Sciences, 30:14, pp. 1545-1550, 2012.
[3] W Fu, et al, Journal of Sport and Health Science, 4:4, pp. 384-390, 2015.
[4] H Boey, et al, Sports Biomechanics, 16:2, pp. 166-176, 201.

EFFECT OF WALKING SPEED ON COMPENSATORY RESPONSES TO MEDIOLATERAL PERTURBATIONS

Farahnaz Fallahtafti[1], J.M. Yentes[1]
[1]Department of Biomechanics, University of Nebraska at Omaha
Email : ffallahtafti@unomaha.edu

Introduction

Measuring the compensatory responses to a perturbation from an unperturbed condition may be an accurate indicator of the ability to control stability [1,2] (Figure 1). Examining responses to mediolateral movement is of interest as lateral balance requires active control. Lateral balance can be affected by center of mass velocity—and compensated for by appropriate reactive strategies such as foot placement. Further, walking speed is an influential parameter in stability during steady state walking [3], however, during perturbed walking, the speed-related effect of the relative position between the center of mass and the base of support as well as the resistance and flexibility to recover, further complicates the issue of stability in gait. Examining the effect of speed on lateral compensatory responses will better inform about the competing relationship of physical and mechano-sensory reaction parameters associated with stability in perturbed conditions. The aim of this study was to determine the effect of walking speed on compensatory responses to lateral perturbations during walking.

Methods

Eighteen healthy adults (24.33±3.77yrs; 1.75 ±.10m; 68.05± 10.75kg) were asked to walk on a treadmill (Bertec Corp; Columbus, Ohio) at slow, preferred, and fast speed conditions. Preferred speed was estimated as the treadmill operator in(de)creased speed until preferred speed was found. Subjects underwent perturbed and unperturbed walking trials of 45 seconds at each speed. Kinematic marker data (120 Hz) were collected for three trials per speed condition. During perturbed trials, subjects were given a lateral perturbation of 5 cm to the left at the right heel contact, delivered between the 25-35 seconds of each trial. Instantaneous trunk velocity vector (3 angular & 3 linear) was calculated for all timepoints in each trial and used to calculate dependent variables (Figure 1).

Data were inspected for normality. One-way ANOVAs (1x3) were used to compare each variable (τ, β, B, D_{hc}) across walking speed conditions. To assess differences after a lateral perturbation, linear regression models were run with each compensatory response as dependents (τ, β, B, D_{hc}) and the three speeds as independent categorical variables. Statistical significance was set at α=0.05.

Results and Discussion

No differences were found for τ, β, D_{hc}. Maximum distance after perturbation (B) increased as speed decreased ($p<0.0001$). One SD increase in B during slow, led to a 0.37 SD increase during preferred, with all the other variables held constant. Increasing the walking speed allowed the body to resist deviation from the steady state condition—a more stable reaction in response to the lateral perturbations. Increasing momentum during faster walking could be a useful strategy to maintain stability during gait. Increasing the gait speed could increase vertical momentum, which can prevent walking to become unstable as the body progress forward quickly after initial contact [4].

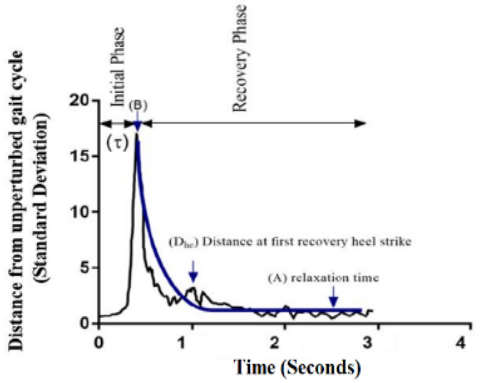

Figure 1: Explanation of compensatory responses. The x-axis denotes time from the onset of perturbation. The y-axis is the standard deviation of the distance between the trunk velocity vector during perturbed and unperturbed gait cycles. B is the maximum deviation from the unperturbed gait cycle after perturbation. Tau, τ, is the time to maximum distance. Beta, β, is the rate of return to the unperturbed gait cycle. D_{hc} is the distance from unperturbed gait cycle of the first recovery heel contact after perturbation. Figure adapted from [2].

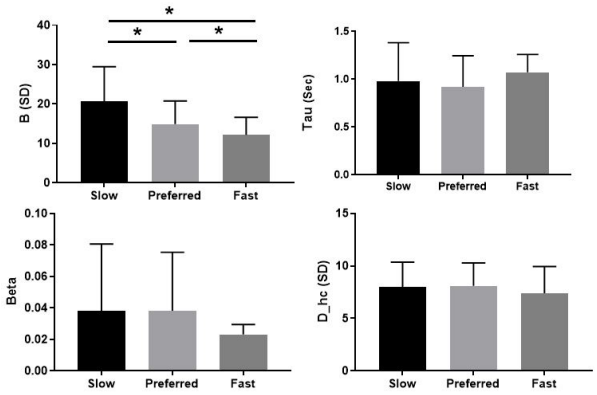

Figure 2: Compensatory response results. Error bars represent standard deviations. (a) Maximum distance from attractor, (B); (b) Time to maximum distance, (τ); (c) Rate of return to the unperturbed gait cycle, beta (β); and (d) Distance to first recovery heel contact, D_{hc}. Asterisks denote post-hoc comparison significance ($p<0.05$).

Significance

Walking speed is a basic factor to manipulate during intervention programs, which can enhance body resistance to deviation during challenging walking conditions. This study also demonstrate that speed can govern mechanical factors associated with stability, which should be considered distinctly in future study designs.

Acknowledgments

Funding provided by NIH (P20 GM109090), Dept of VA (I21RX003294), and UNO GRACA.

References

1. Bruijn et al. J R Soc Interface. 10(83), 2013.
2. Bruijn et al. J Exp Biol, 3945-52, 2010.
3. Fallahtafti et al. Gait Posture, 142-148, 2020.
4. Kaya et al. J Gerontol, 126-34, 1998.

JOINT POWER WHILE HOPPING WITH VARIABLE STIFFNESS, FULL-LEG EXOSKELETONS: A PILOT STUDY

Stephen P. Allen[1] and Alena M. Grabowski[2]
[1]University of Colorado Boulder, Boulder, CO, USA; [2]VA Eastern Colorado Healthcare System, Denver, CO, USA
email: stephen.allen-1@colorado.edu

Introduction

Lower-extremity, passive-elastic exoskeletons (EXOs) can reduce the metabolic power required for two-legged, stationary hopping by providing assistive forces and moments. An ankle-only EXO reduced metabolic power by ~12%, average biological, and mechanical power by 50% at the ankle and 17% at the knee during hopping at 2.5 Hz[1]. Comparatively, a full-leg EXO reduced metabolic power by 18-28% across multiple hopping frequencies[2]. However, the effects of the full-leg EXO on lower-extremity joint kinetics are not known. Moreover, the full-leg EXO spring stiffness type (i.e., profile) affects metabolic power[3], where a degressive (stiff then soft) spring provides the greatest metabolic reduction followed by linear and then progressive (soft then stiff) springs. We determined how the full-leg EXO effects lower-extremity joint kinetics, and biological joint power contributions across all spring stiffness profiles. We hypothesized that hopping with a full-leg EXO reduces metabolic power by decreasing biological joint power at joints where the EXO moment arm is largest, such as the ankle and then the knee[4]. Determining the contribution of biological joint power may provide a mechanist explanation for metabolic power changes due to the spring stiffness profile within a full-leg EXO.

Methods

Two male participants [79 & 84 kg; 175 & 178 cm] hopped in place, on both feet, to the beat of an audible metronome set to 2.4 Hz. Participants hopped normally (NH) and with an EXO using degressive (DG), linear (LN), and progressive (PG) spring stiffness profiles in a randomized order. We used springs that had the same mass-normalized stiffness at 10 cm of displacement[2,3]. Participants hopped with a force platform under each foot (Bertec, Columbus, OH; 1000 Hz). We placed reflective markers bilaterally on the legs and EXO and used 3D motion capture (Vicon, Centennial, CO; 200 Hz) to measure lower-extremity joint kinematics and EXO displacement. The assistive force provided by the EXO was estimated from corresponding force-displacement data measured by a materials testing machine (Instron, Norwood, MA) prior to the test. We performed inverse dynamics calculations (Visual 3D, Germantown, MD) to estimate the total and assistive moments and powers for each lower extremity joint. Biological moments and powers were calculated as the difference between total and EXO moments and powers. Average positive mechanical power was calculated as the sum of positive joint work during the ground contact phase, divided by contact time[1]. We constructed linear mixed effect models (α=0.05) to determine the effect of EXO stiffness profile on average total positive mechanical power normalized to biological mass, as well as average biological positive mechanical power of the ankle, knee, and hip.

Results and Discussion

Average total positive power while hopping with an EXO was not different compared to NH ($p \geq 0.52$; Fig. 1) and average total positive power at the ankle, knee, and hip were not different compared to NH ($p \geq 0.39$) regardless of spring stiffness profile. However, using a DG EXO decreased average biological ankle power by 0.86 W/kg (p=0.05) and knee power by 0.30 W/kg (p=0.04), but did not change average biological power at the hip (p=0.17). Hopping with the LN and PG EXOs did not reduce average biological power at any joint compared to NH ($p \geq 0.08$).

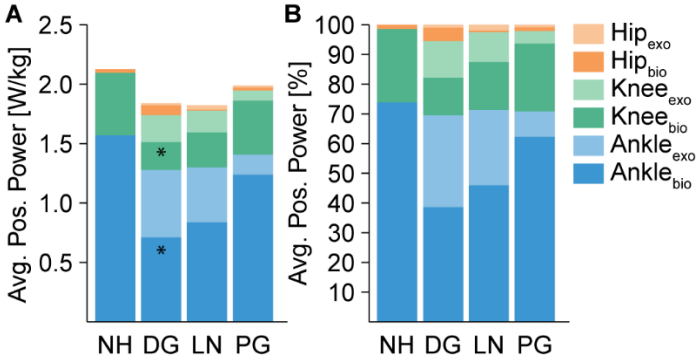

Figure 1 A) Average positive joint power during the contact phase normalized to biological mass and B) relative percentage of total positive joint power. Darker shades represent biological contributions and lighter shades represent EXO contributions. The DG, LN, and PG EXOs were 5.0, 5.8, and 5.5 kg, respectively. * different from average biological joint power in the NH condition.

In the two participants, use of a full-leg EXO with different spring stiffness profiles did not change the total relative percent of positive mechanical power at any joint during two-legged hopping. However, the different spring stiffness profiles reduced average biological ankle power by 21-55% (range of PG to DG) compared to NH. Further, the DG EXO reduced average biological knee power by 56% compared to NH. Our data are in line with previous findings that the hip has negligible contributions to total positive power during hopping[1], and none of the spring stiffness profiles effected average positive hip power. Therefore, use of the DG EXO likely reduces metabolic power more than the LN or PG EXOs due to the greater elastic energy storage and return, and provides positive power at the ankle and knee.

Significance

Hopping with a full-leg EXO elicits greater metabolic reductions (18-28%)[2,3] than joint-specific EXOs (~12%)[1] by reducing average biological joint power at multiple joints. An ankle-only design reduced average biological power at the ankle and knee by 50% and 17%, respectively[1], whereas a full-leg EXO reduces both ankle and knee biological power by up to 55%. Our data show that only the full-leg, DG EXO influences positive power at multiple joints. Future research is planned to increase sample size. Moreover, further research will determine if similar full-leg EXOs and spring stiffness profiles reduce metabolic power and joint power during running when the hip plays a much larger role.

References

1. Ferris & Sawicki. *J Appl Physiol*. 113(12), 2012.
2. Grabowski & Herr. *J Appl Physiol*. 107(3), 2009.
3. Allen & Grabowski. *J Appl Physiol*. 127(2), 2019.
4. Farley & Morgenroth. *J Biomech*. 32(3), 1999.

ASSESSING STRETCH REFLEXES FOLLOWING POSTMASTECTOMY BREAST RECONSTRUCTION

Tea Lulic-Kuryllo[1], Joshua M. Leonardis[1], Adeyiza O. Momoh[2], David B. Lipps[1]
[1]School of Kinesiology, [2]Section of Plastic Surgery, University of Michigan, Ann Arbor, MI
Email: tlulic@umich.edu

Introduction

In the United States, ~63% of breast cancer patients will elect to have a postmastectomy breast reconstruction. The most common breast reconstruction procedures disinsert the pectoralis major from its attachment at the ribs to accommodate an implant underneath the muscle (subpectoral implant; IO) and/or cut the latissimus dorsi muscle to support the implant (LD flap). Alternatively, the breast mound can be recreated by transferring the abdominal tissue to the chest (DIEP) without disinserting the muscles. Breast reconstruction is associated with functional upper extremity deficits, including reduced shoulder joint stiffness [1] and altered stiffness of the pectoralis major's clavicular region [2] during volitional contractions. Muscle stiffness is regulated by short and long-latency stretch reflexes [3], contributing to limb stiffness and acting to increase the musculoskeletal system's stability [4]. This study aimed to quantify stretch reflexes in several shoulder muscles following three commonly performed breast reconstruction procedures. We hypothesized that the breast reconstructions that disinsert the pectoralis major would inhibit shoulder muscle stretch reflexes.

Methods

49 women (age±SD) who underwent postmastectomy breast reconstruction participated: IO (N = 17; 49 ± 10), LD flap (N = 13; 52 ± 9), and DIEP (N = 19; 51 ± 7), and 18 healthy controls (51 ± 6). 61% of the reconstruction patients received either radiation therapy, chemotherapy, or both. Participants had their arm placed in a removable cast that was attached to a computer-controlled servomotor with a six-degree of freedom load cell. Surface electromyography (EMG) was acquired at 2500 Hz from the clavicular and sternal regions of the pectoralis major, anterior, middle, and posterior heads of the deltoid, and the upper trapezius. The participant's arm was perturbed about the glenohumeral center of rotation with small, stochastic perturbations (PRBS, 0.06 rad, 0.15s switch time) for 60 seconds in either vertical or horizontal flexion/extension. During these perturbations, participants were relaxed or maintained net torques scaled to ±10% of their maximum voluntary contractions (MVC).

Raw EMG signals were high-pass filtered with a 30 Hz second-order high pass Butterworth filter, full wave rectified, and normalized to MVC. Stretch reflexes were quantified as the mean rectified EMG between 25-50 ms (short latency reflex; SLR), 50-75 ms (medium latency reflex; MLR), and 75-100 ms (long latency reflex; LLR) after perturbation onset. Mean baseline EMG activity was quantified for the 40 ms prior to perturbation onset and subtracted from the reflex amplitudes to quantify change in the reflex from the background. A one-way mixed-effects ANOVA was performed to examine surgical group differences for each condition, muscle, and reflex window (α = 0.05). Tukey's post-hoc tests were used to determine significant group differences when applicable.

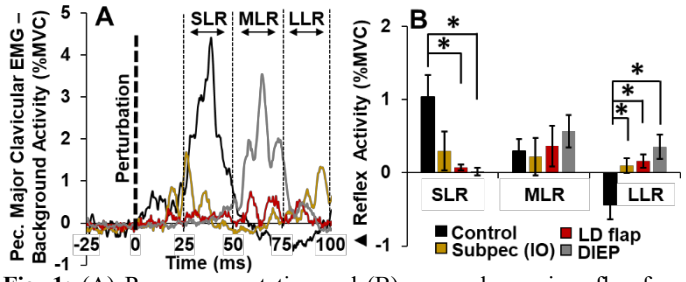

Fig. 1: (A) Raw representative and (B) mean change in reflex from background EMG in the clavicular region of the pectoralis major for SLR, MLR, and LLR in each group during vertical ab/adduction perturbations. Asterisks (*) denotes differences between groups.

Results and Discussion

As participants exerted adduction torque during vertical ad/abduction perturbations, the SLR in the pectoralis major clavicular region was significantly reduced ($F_{3,61}$= 4.5, p = 0.006; Fig. 1) and the LLR was significantly greater in all reconstruction groups than controls ($F_{3,62}$= 5.4, p = 0.002; Fig. 1). Vertical abduction torques produced a greater LLR in the upper trapezius for the IO and DIEP patients than controls ($F_{2,53}$= 6.1, p = 0.004).

As participants held horizontal flexion torque during horizontal flex/extension perturbations, SLR was significantly reduced in the upper trapezius in the IO and DIEP patients than controls ($F_{2,53}$= 10.1, p<0.001). LLR was reduced in the clavicular region in all groups when compared to the controls ($F_{3,64}$= 7.6, p<0.001). Horizontal extension torques produced a reduced SLR in all groups than controls in the clavicular region ($F_{3,64}$=10.4, p<0.001), the posterior deltoid ($F_{3,64}$= 6.9, p<0.001), and the upper trapezius ($F_{2,53}$= 4.6, p = 0.01).

Our findings indicate that the stretch reflex response is inhibited in breast cancer survivors after mastectomy, reconstruction, and radiation/chemotherapy (if necessary). These stretch reflex alterations suggest breast cancer survivors exhibit altered spinal motoneuron (MN) and/or descending cortical input. Neurotoxic effects elicited by the treatments can affect the spinal MN firing [5] or cause muscle fibrosis and nerve damage [6] influencing spinal MN firing, which may explain our findings. Previously, radiation treatment affecting the brachial plexus was found to reduce muscle stretch reflexes in breast cancer patients [7]. Future work is needed to dissociate how radiation or chemotherapy alter these reflex adaptations.

Significance

Altered stretch reflexes indicate that breast reconstruction procedures and breast cancer treatments alter spinal, sensorimotor, and/or brainstem modulation of the shoulder muscles. These findings highlight a previously unexplored mechanism of shoulder morbidity following breast cancer treatment and postmastectomy breast reconstruction procedures that clinicians can target for rehabilitation interventions.

Acknowledgments

This project was funded by NIH/NICHD R03HD097704.

References

[1] Leonardis et al. (2019). *J Orthop Res* 37: 1610-1619.
[2] Leonardis et al. (2019). *Breast Cancer Res Treat* 173: 447-453.
[3] Hoffer et al. (1981). *J Neurophys* 45(2): 267-285.
[4] Shemmell et al. (2010). *Clin Neurophys* 121(10): 168.
[5] Housley et al. (2020). *Exp Neurol* 331: 113354.
[6] Gilette et al. (1995). *Int J Radiat Oncol Biol Phys* 31(5): 1309-18.
[7] Mondrup et al. (1990). *Acta Neurol Scand* 81(2): 153-8.

DYNAMIC STABILITY OF THE SPINE WHEN ASSISTED WITH BACK-SUPPORT EXOSKELETONS

Saman Madinei[1], S. Kim[1], D. Srinivasan[1], and M. A. Nussbaum[1]
[1]Department of Industrial and Systems Engineering, Virginia Tech, Blacksburg, VA
Email : *nussbaum@vt.edu

Introduction

Industrial back-support exoskeletons/exosuits (BSEs) have been introduced as a new intervention to reduce physical demands on the spine. Although growing evidence points to the beneficial effects of BSEs, specifically in reducing low-back physical demands, there is limited understanding of potential unintended consequences of BSE use on neuromuscular control of the trunk during manual material handling (MMH). By providing external structural frames over the trunk and supportive torques about the hip/low back, a BSE may interfere with the active and passive trunk subsystems and their neuromuscular control for effectively maintaining dynamic stability. We explored the impacts of two different passive BSEs (BackX™ model AC, www.suitx.com, and Laevo™ V2.5 www.laevo.nl) on trunk neuromuscular control behavior during repetitive symmetric and asymmetric lifting tasks. A nonlinear dynamical systems analysis approach was used [1]. Based on existing evidence, we expected that trunk dynamic stability would differ when using either BSE, due to changes in active trunk stiffness and postural adaptations when using a BSE. Such changes, however, were expected to vary depending on the specific BSE design and task conditions in which the BSE is used.

Methods

Data used herein were obtained from a prior study, with details of the experimental design, procedures, and simulated tasks previously reported elsewhere [2]. Briefly, a lab-based simulation of repetitive lowering/lifting tasks was designed to examine the effects of two BSEs under three different lifting conditions (two symmetric and one asymmetric). The symmetric conditions included two heights: mid-shank and knee; an asymmetric condition was performed at the knee height from a location 90º to the right of the mid-sagittal plane. Repetitive lowering/lifting trials were performed using a wooden box, the mass of which was set to 10% of individual participant body mass. Participants were instructed to perform freestyle lowering/lifting for four minutes in three different conditions, at a pace of 10 lower/lift cycles per minute (i.e., 40 lower/lift cycles in each trial). Whole-body segmental kinematics were monitored using a wearable inertial motion capture system (MVN Awinda, Xsens Technologies B.V., Netherlands).

Maximum Lyapunov exponents and Floquet multipliers were respectively calculated to quantify the local dynamic and orbital stability of the thorax trajectory during repetitive lifting and lowering. Short-term maximum Lyapunov exponents ($\lambda_{\max-s}$) was determined for the thorax over 0-0.5 lifting cycle, using the algorithm of Rosenstein et al. 1993 [3]. Specifically, a 12D state space was reconstructed from the 3D orientations and angular velocities of the thorax inertial sensor. Orbital stability was determined by computing maximum Floquet multipliers (FM_{max}) using the Poincare section method [4]. The state space was divided into 101 Poincare sections, representing increments from 0 to 100% of the lowering/lifting cycles (0% corresponded to the upright standing posture). FM_{max} is reported at Poincare sections defined at 25, 50, 75, and 100% of the lowering/lifting cycle.

Results and Discussion

Significant effects of BSE use were found on FM_{max} at the 25, 50, and 100% sections, in which using the Laevo™ increased FM_{max} by up to ~10% (Figure 1). No significant effect of BSE use was found on $\lambda_{\max-s}$. The increases in FM_{max} suggest that using the Laevo™ could have compromised the ability of the neuromuscular system to achieve steady-steady motions of the trunk during repetitive lifting, and which may indicate poorer stability in response to small (local) perturbations.

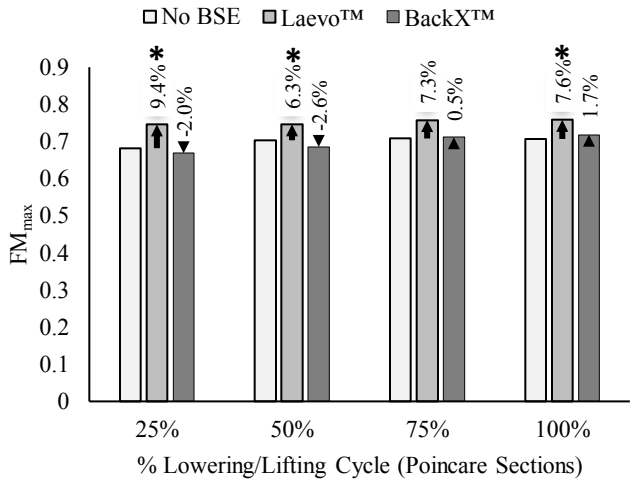

Figure 1: Effects of BSE use on FM_{max} at defined Poincare sections. The asterisks denote significant differences from the Control condition (i.e., no BSE), and arrows and percentage values indicate changes from the Control condition.

Significance

Our results provide new evidence of potential "unintended" consequences of BSE use on neuromuscular behaviors of the trunk when using passive BSEs during repetitive lifting. Specifically, short-term use of a passive BSE might adversely influence trunk dynamic stability. This information can be useful when considering BSE adoption, since reduced trunk stability could pose important safety concerns to users (e.g., making them vulnerable to sustaining or aggravating a low back problem). More research, however, will be needed to assess the generalizability of different BSE design approaches in terms of unintended short-term and long-term effects on the neuromuscular control of the spine.

References

[1] Dingwell & Cusumano (2000). *Chaos,* 10(4), 848-863
[2] Madinei et al. (2020). *Applied Ergonomics*, 88, 103156
[3] Rosenstein et al. (1993). *Physica D: Nonlinear Phenomena*, 65(1-2), 117-134
[4] Hurmuzlu & Basdogan (1994). *J. Biomech. Eng.*, 116(1), 30-36

Moving outside the lab: markerless motion capture accurately quantifies planar kinematics during the vertical jump

William T Phillips[1], John F Drazan, PhD[2], Todd J Hullfish, BSME[2], Josh R Baxter, PhD[2]
[1] Electrical and Computer Engineering, University of Rochester, [2]Department of Orthopaedics, University of Pennsylvania

Introduction

The COVID-19 pandemic has created a need for easy-to-use, socially distanced methods of data collection for biomechanical research. The rise of mature deep learning software packages provides a unique opportunity for a low cost, socially distant, high fidelity alternative to traditional motion capture. One such example of these software packages is DeepLabCut (Mathis, 2020), an open source software developed for pose tracking of laboratory animals. This software has been applied to track human movement, however, there exist concerns about the accuracy of markerless motion capture relative to the marker-based gold standard. The purpose of this study was to evaluate the performance of markerless motion tracking as a method to measure lower limb angles during the vertical jump using a large cohort of subjects from a publically available data set with time synchronized motion capture and video data.

Methods

Data were compiled from the open data set (Ghorbani, 2020). The marker based motion capture data were captured at 120 Hz with a 67-point marker set. Video for markerless tracking was captured on two orthogonal cameras at 30 Hz. We split the data set into a 69 subject training set and a 16 subject test set. To train the model, four people labeled 19 points of interest across 12 frames per subject. Each of these frames were automatically selected via a DeepLabCut clustering algorithm. To test consistency across labelers, a set of five shared subjects were labelled by all four labelers (60 total images). Agreement between labelers was evaluated via the C-1 formulation of the Intraclass Correlation Coefficient (ICC). The data consisted of each of the subjects performing 20 actions. Researchers identified the start and end times of each instance of the subjects' vertical jump and added a one second buffer period to each end of this period. Vertical jump was chosen for further analysis because of its relevance as a common test in sports performance testing. Hip, ankle, and knee angles were extracted from the 1-3 vertical jumps that each subjects performed. The markerless results were compared with the traditional motion tracking results using root mean squared error in addition to coefficient of multiple correlation (CMC) metrics. For both ICC and CMC measurements *r* values above 0.9 indicate "very strong agreement."

Results and Discussion

The level of agreement between labelers was very high across the five shared subjects, with an ICC = 0.998 and RMSE = 4.52 pixels. Results generated from CMC across the whole movement showed very strong agreement between the markerless approach and the traditional motion capture data with a CMC > 0.991 and a RMSE < 3.22°. Across the hip, knee, and ankle angles extracted, the CMC values were similarly high, being 0.970 ± 0.055, 0.963 ± 0.471, and 0.853 ± 0.23 respectively (Figure 1).

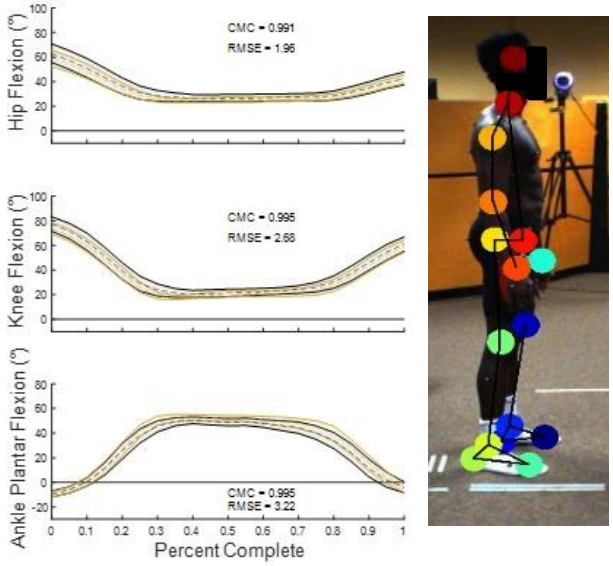

Figure 1. Left) Gold-motion capture, Black-markerless motion tracking. Dashed-means across all subjects and solid-95% confidence intervals. Right) example of tracked frame

The results of the study show that free, easy-to-use, open source markerless tracking is a viable alternative to traditional motion capture technology, especially for data collection outside of traditional laboratory spaces. As the CMC values all indicate strong to very strong agreement between the two methods of motion tracking, this represents a significant development in increasing accessibility to accurate motion tracking technology for human subject research. These findings provide evidence that basic cameras can be used to collect human kinematic data remotely without the need for specialized equipment which provides researchers with the ability to reach historically underrepresented groups that are less likely to participate in studies that take place in a laboratory.

Significance

Markerless motion capture has potential – like other devices including mobile dynamometry, instrumented insoles, tensiometers, and inertial measurement units – to transform biomechanical research away from traditional laboratory settings into venues convenient to populations that are under sampled with present approaches without sacrificing measurement fidelity.

References:

1. Mathis, MW. Nat Neurosci. 2018;21:1281-1289
2. Ghorbani, S. ArXiv, 2020

Acknowledgements: This work was funded in part by NIH K12GM081259 and NIH/NIAMS K01AR075877.

RHEOLOGY OF SKELETAL MUSCLE WORK LOOPS

Khoi D. Nguyen and Madhusudhan Venkadesan
Department of Mechanical Engineering and Materials Science, Yale University, New Haven, CT, USA
email: *khoi.nguyen@yale.edu

Introduction

We develop a hypothesis for the emergence of non-classical perturbation responses in skeletal muscles due to its active and tunable material properties, and test the hypothesis using published datasets and simulations. At the heart of our hypothesis is rheology, the emergent bulk property of how a material deforms under forces. Biology makes extensive use of the tunable rheology of living tissues, but the current toolbox of rheology is devoted to characterizing materials with properties that are fixed during measurement. How do we then understand or characterize skeletal muscles whose motor functionality often arises from its tunability? We bridge this gap by developing a new method to incorporate classical experimental rheological measurements of skeletal muscle into predictions for its response under time-varying stimulus, *i.e.* the work loops it exhibits when phasically stimulated and simultaneously undergoing oscillatory stretches. We test the idea using published datasets and show the rheological origin of work loops in skeletal muscle.

Splicing hypothesis: Skeletal muscle work loops measured under time-varying stimulus are captured by a splicing of loops measured under fixed-stimulus. Namely, for an oscillatory stretch $L(t) = a \sin(\omega t)$, the force response is

$$F(t) = \begin{cases} F_A(t) & \text{for } \phi_A \le \omega t \le \phi_B, \\ F_B(t) & \text{otherwise.} \end{cases}$$

The plots of $F_A(t)$ and $F_B(t)$ versus $L(t)$ are the basis loops measured under fixed-stimuli at activation states A and B, respectively. The time-varying stimulus is a phasic stimulus that switches from B to A at ϕ_A and back to B at ϕ_B, resulting in a work loop that is a splicing of the individual loops at A and B (Fig. 1a). In applying this hypothesis to muscle, we show how isometric twitch data can be used to incorporate excitation-contraction dynamics in predicting the work loop (Fig. 1b).

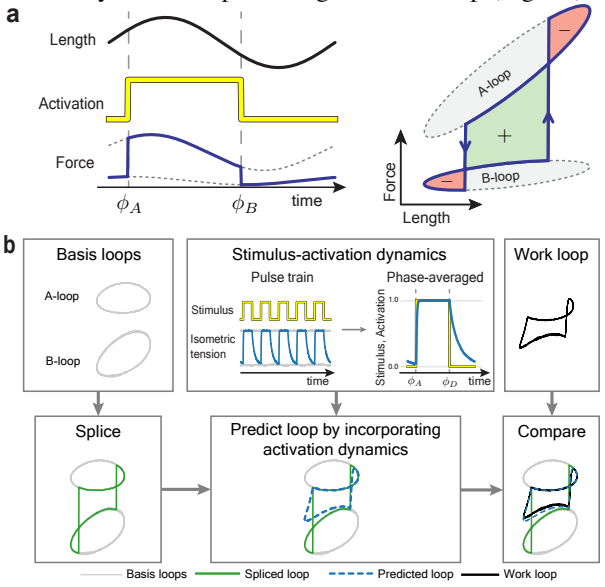

Figure 1: (a) Splicing together fixed-stimulus basis loops at different junctions predicts work loops under a time-varying phasic stimulus. (b) Flow chart to predict work loops from basis loops and to compare with measured work loops. Illustrated with a detailed sarcomere model [2].

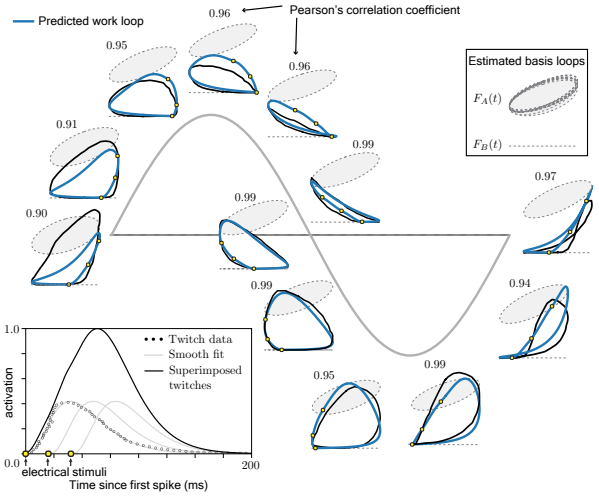

Figure 2: Loops predicted from the splicing hypothesis and twitch dynamics match closely with measured work loops of a sculpin (fish) abdominal muscle [2]. Yellow dots indicate timing of electrical stimuli and loops are roughly positioned on the sinewave according to the timing of the first electrical stimulus relative to the oscillatory stretch.

Results and Discussion

We tested the splicing hypothesis (Fig. 2) with published experimental data [2] on sculpin (fish) skeletal muscle that allowed us to directly test our predictions. Our hypothesis proved quite accurate, with Pearson's correlation coefficients ranging from 0.90--0.99 when compared with measurements. These results are available in a preprint [3].

Our results showed that most of a skeletal muscle's work loop is accounted for by an interpolation between rheological characterizations at fixed stimuli. Where it falls short are muscle phenomena not readily captured by current methods to probe a muscle's rheology. In this manner, the splicing hypothesis is a new tool to study muscle mechanics that expands upon and operates in conjunction with current methods.

Significance

Our work advances the understanding of skeletal muscle mechanics by showing that well-established rheological measurements can be used to predict the response under time-varying stimulation by applying the splicing hypothesis.

Acknowledgments

Funding support from the Raymond and Beverly Sackler Institute for Biological, Physical and Engineering Sciences at Yale, a National Institutes of Health training grant T32EB019941, and the Robert E. Apfel Fellowship awarded by Yale. This material is based upon work supported by the National Science Foundation under Grant No. 1830870.

References

[1] Johnson and Johnston (1991). JEB. 1991; 157(1):409–423.
[2] Walcott (2014). PRE. 2014; 90(4):042717
[3] Nguyen and Venkadesan (2021). arXiv preprint arXiv:2005.07238v2 (2021)

MORPHOLOGY OF HIP DYSPLASIA IN JAPANESE FEMALES: A STATISTICAL SHAPE MODELING STUDY

Joseph D. Mozingo[1], Penny R. Atkins[1], Praful Agrawal[1], Keisuke Uemura[2],
Shireen Y. Elhabian[1], Ross T. Whitaker[1], Andrew E. Anderson[1*]
[1]University of Utah, [2]Nara Institute of Science and Technology
[*]andrew.anderson@hsc.utah.edu

Introduction

Hip dysplasia is a structural pathology characterized by reduced coverage of the femoral head due to a shallowed acetabulum, and results in joint instability, cartilage damage, and osteoarthritis (OA). Other aspects of femur and pelvis shape driving these joint-level changes are not well understood, largely due to the fact that a comprehensive description of 3D hip shape is lacking. Statistical shape modeling (SSM) is an innovative tool gaining traction in orthopaedic applications related to understanding population-level variability in bone shape. The key advantage of this technique is the ability to evaluate shape over the 3D continuum in an objective manner. To date, relatively few efforts have been made to implement a model that encompasses multiple bones, and only the femur has been examined in the context of hip dysplasia. Thus, the purpose of this study was to develop and implement a SSM technique to quantify natural variation in hip anatomy present in individuals with hip dysplasia.

Methods

83 dysplastic hips from 47 Japanese females (age: 37.3±10.2 yrs., BMI: 21.6±2.9) were included in this IRB-approved retrospective study. This cohort was selected due to the high prevalence of hip dysplasia in females of Asian descent. A CT scan of the lower extremity was obtained. The pelvis and femurs were segmented from the images and segmentations were converted to 3D surfaces using Amira v.6.0.1. Surfaces were smoothed, reflected if left-sided, and aligned via the iterative closest point algorithm prior to input to the SSM pipeline. SSM was performed via ShapeWorks 5.3.1 [1]. Briefly, ShapeWorks implements a computational optimization framework to place particles at consistent anatomic sites across input shapes. A two-stage alignment technique was employed to reduce the effect of individual differences in relative bone scale and position to isolate shape differences in the final model [2]. Correspondence particle locations from each input shape were used to quantify mean bone shape and reconstruct surfaces. Principal component analysis determined the modes of variation from the particle locations, and modes that were statistically significant were identified via parallel analysis.

Results and Discussion

The first 11 modes described significant variations in hip shape and accounted for 84.4% of the total variation. Modes 1-3 accounted for 36.0%, 13.5%, and 9.4% of the total variation, respectively, and modes 4-11 each accounted for 5.5% or less. The first three modes represented variation in pelvis height, femoral shaft diameter, and femoral bowing (Fig. 1A); femoral version (Fig. 1B-C), and ilium shape (Fig. 1C). Later modes captured more subtle changes in shape including pelvic version.

The main outcome of this work was quantification of shape and shape variation of hip anatomy in Japanese females with hip dysplasia. Population-level shape differences were present in both the femur and pelvis despite the homogeneous sample of all females having the same ethnicity. Previous SSM efforts have found differences in version at the proximal femur [3] and in femoral head-neck anatomy [4] in individuals with hip dysplasia compared to controls. Similar variations were found herein despite use of a solely dysplastic cohort. Few other studies have quantified morphology in hip dysplasia using an approach that considers the entire 3D anatomy, and none examined the pelvis. Extension of the developed model to include a control group will be a critical next step in identifying which of the observed variations in pelvic anatomy might serve as biomarkers of hip dysplasia.

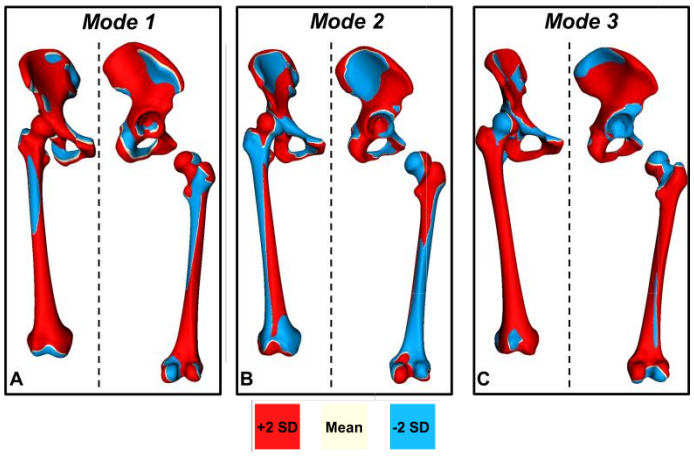

Figure 1: Shape differences present in first 3 modes of variation at ±2 SD from the mean hip. Anterior view of joint (left) and lateral pelvis and exploded posterior femur views (right) are shown for each mode.

Significance

Since our model was developed using a homogeneous cohort, the observed differences may represent anatomic variations associated with disease severity. By analysing a larger cohort incorporating a control group, we will determine which aspects of variation are indeed associated with hip pathoanatomy. From this, we can develop a platform to assess disease staging in patients as part of the standard treatment decision-making process and determine radiographic imaging planes and measurements that better capture the relevant 3D differences. In the future, our technique may be applied to improve diagnostic accuracy.

Acknowledgments

Funding from the NIH (R01EB016701), LS Peery Discovery Program in Musculoskeletal Restoration, the Nakatomi Foundation, and the Nakatani Foundation for Advancement of Measuring Technologies in Biomedical Engineering.

References

[1] Cates J et al. (2017). *Statistical Shape and Deformation Analysis*, 257-98.
[2] Agrawal P et al. (2020). *Lecture Notes in Computer Science*, **12474**:111-21.
[3] Gaffney B et al. (2019) *J Orthop Res*. **37**:665-73.
[4] Mahieu P et al. (2018). *Acta Orthop. Belg*. **84**:307-15.

SEGMENT MASS PROPERTY ERRORS HAVE LESS IMPACT ON ESTIMATED JOINT LOADING IN HUMAN GAIT THAN GROUND REACTION FORCE ERRORS

Todd J. Hullfish[1], J. Drazan[1], and J. Baxter[1]
[1]Department of Orthopaedic Surgery, University of Pennsylvania
email: todd.hullfish@pennmedicine.upenn.edu

Introduction

Estimating joint loading during human movement is a cornerstone of biomechanics research. Traditionally, joint loads are estimated using musculoskeletal models to solve the inverse dynamics problem. Relying on Newton's second law of motion, we sum the external forces acting on a body segment and set that equal to the body segment dynamics [1]. This approach is powerful because it allows researchers to estimate the reaction loads at each joint that are impossible to physically measure without invasive surgeries [2]. However, this approach relies on assumptions and physical measurements that are difficult to quantify and prone to measurement error.

Therefore, the purpose of this study was to evaluate how the accuracy of joint load estimates are impacted by errors in both segment mass properties. To further explore the impact of experimental measurements, we tested the sensitivity to shear ground reaction force errors. We hypothesized that changing the mass properties and shear ground reaction forces would differentially impact estimated joint loading, with the smallest effects on the ankle and the greatest effects on the hip.

Methods

We recruited 8 healthy adults (6 males, 2 females; 30 ± 4 years; BMI, 24.1 ± 3.2 kg / m2) who provided written informed consent. We collected traditional motion capture data during flat ground walking at self-selected speeds and performed inverse dynamics to establish a gold-standard range for sagittal joint load estimates. We then systematically introduced error by manipulating the mass properties of the musculoskeletal model and the magnitude of the externally applied loads. To this end, we scaled both by 0 to 200% in 5% increments, resulting in 1,600 simulations per subject. From this, we compared the peak joint load estimates from each error condition with the gold-standard across the joints in the lower extremities.

Results and Discussion

We found that shear ground reaction force errors had large impacts on joint load estimates while segment mass errors had less of an impact. These joint load estimate errors increased in the more proximal joints. The hip saw changes in mass resulting in around 35% error, changes in shear resulting in 82% error, and a worst-case scenario of 116% error. The knee saw changes in mass resulting in errors of 8%, changes in shear resulting in 140% error, and a worst-case scenario of 147% error. The ankle was least affected, with changes in mass resulting in errors of less than 2%, changes in shear resulting in 17%, and a worst-case scenario of 18%.

These results confirm our hypothesis that the ankle would be least sensitive to changes in mass and shear. This makes sense, as the segments distal to the ankle joint have relatively little inertial force potential compared to the loads experienced by the joint. It was surprising to see that the knee was very sensitive to changes in shear. This is likely due to the ratio of peak joint load to shear force, which in this case is roughly half that of the ankle. Errors in the hip were largely expected as it has the largest distal segment in the lower limbs. In addition to walking, we analyzed other activities of daily living and found that vertical movements like bouncing and heel raises had much smaller errors caused by ground reaction force differences.

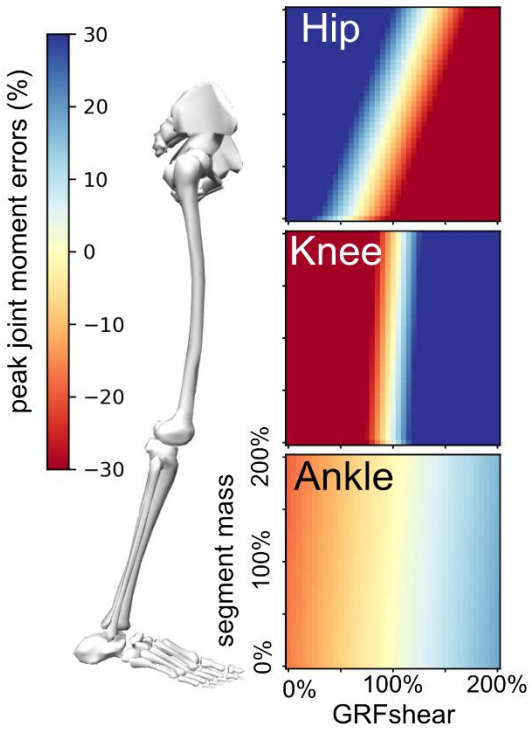

Figure 1: We visualized the precent errors in peak hip, knee, and ankle moments between each error condition and the gold standard measurement through diverging heat maps. Here, blue represents over approximations, red represents under approximations, and light yellow represents accurate approximations of joint moments.

Significance

Our results show that while some research areas such as forward simulation in rehabilitation and tendon transfer simulation might require very high-fidelity measurement techniques, there are many scenarios where faster, more convenient measurement solutions would result in very accurate data. Specifically, the ankle appears to be a largely unaffected by inertial factors and even some errors in shear measurements. These results are encouraging for researchers interested in making measurements outside of the biomechanics lab, both in the clinic and in the field.

Acknowledgments

This work was supported by the PennPORT IRACDA Fellowship Program (NIH grant# K12GM081259) and NIH/NIAMS K01AR075877.

References

1. Seth et al. *Nonlinear Dyn.* 2010; 62: 291-303
2. Bergman et al. *J Biomech.* 2001; 34: 859-71

THE EFFECT OF ASYMMETRIC SHOE HEIGHT ON JOINT KINEMATICS DURING WALKING

Maia Schlechter, Sumire Sato, Wouter Hoogkamer
Department of Kinesiology, University of Massachusetts, Amherst
Email : *mschlechter@umass.edu

Introduction

Asymmetric gait is prevalent in clinical populations with neurological disorders, such as individual's post-stroke [1]. Unilateral deficits can cause gait impairments and between limb kinematic differences. Studies have suggested that joint mechanics adapt to differing conditions and may be the principal factor in peripheral control during gait [2]. It has also been shown hemiparetic patients take longer paretic steps compared to nonparetic [3].

The purpose of this study was to determine if asymmetric shoe heights can be used to induce joint angle and step length asymmetries during walking. We hypothesized that maximum ankle plantar flexion angle at toe off, peak knee flexion angle during stance, and limb angle at heel strike show greater asymmetries during adaptation compared to baseline. We also hypothesized that step length is more asymmetric during adaptation compared to baseline.

Methods

Eleven healthy young adults (21.2 ± 3.09 years) participated in four walking trials on an instrumented treadmill (Bertec, Columbus OH) at 1.3m/s: (1) 5 minutes with equal shoe heights for familiarization, (2) 5 minutes with equal shoe heights for baseline, (3) 10 minutes adaptation with one shoe raised to an asymmetric height (4) 10 minutes post-adaptation phase with equal shoe heights. Shoe height was raised 1 cm for each participant using a shoe insert during the adaptation trial (side with insert = "heightened limb"; shoe without insert = "non-heightened limb"). The side of the shoe insert was randomized between participants (n with right side heightened limb = 6).

We filtered marker data with a fourth-order 8Hz low-pass Butterworth filter and calculated kinematic measures. Between limb asymmetry was quantified [(heightened – non-heightened)/(heightened + non-heightened)] for ankle angle during toe off, knee peak flexion during stance, limb angle during heel strike and step length. Limb angle was defined as the maximum angle between the greater trochanter and fifth metatarsal. A 10-stride average was obtained for baseline, early and late adaptation conditions. We tested for between limb differences using a one-way repeated measured ANOVA and Bonferroni post-hoc tests for each kinematic asymmetry measure. Statistical significance was established with alpha < 0.05.

Results and Discussion

In general, participants did not show differences in limb angle asymmetry, knee peak flexion symmetry, or step length asymmetry, but did show differences between ankle maximum plantar flexion angle symmetry. Limb angle asymmetry was not significantly different between conditions ($F(2,20) = 0.788$, $p = 0.469$). Knee peak flexion was not significantly different between conditions ($F(2,20) = 0.695$, $p = 0.511$). Mauchly's test of sphericity indicated that the assumption of sphericity had been violated ($p = 0.039$) for limb step length asymmetry. A Greenhouse-Geisser correction was run and there was not a step length symmetry difference between conditions ($F(1.322,13,22) = 0.958$, $p = 0.372$).

Ankle plantar flexion asymmetry was significantly different between conditions ($F(2,20) = 8.167$, $p = 0.003$); lower in early adaptation (-0.038 ± 0.108; $p = 0.005$) and late adaptation (-0.033 ± 0.965; $p = 0.010$) compared to baseline (0.025 ± 0.086).

The results showed significant differences in ankle plantar flexion asymmetry, which confirms our hypothesis, but no significant differences in any other measures (knee flexion, limb angle, step length asymmetry) were found, which is not in line with our hypotheses. These results indicate ankle angle adjustments may be the primary kinematic adaptation to brief asymmetric shoe height exposure.

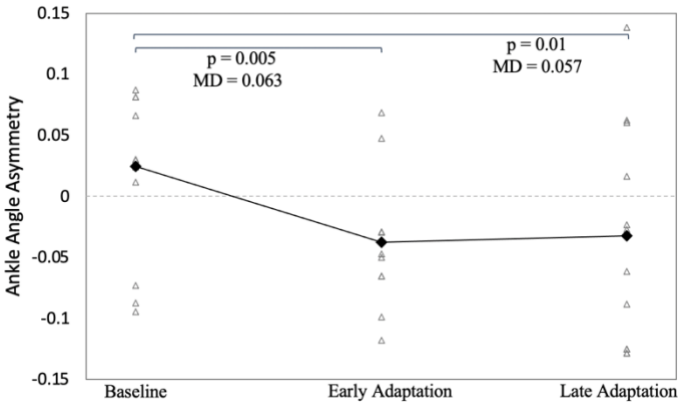

Figure 1: Ankle plantar flexion during toe off was lower in early and late adaptation compared to baseline. Group means for ankle maximum plantar flexion angle during pre-adaptation, early-adaptation, and late-adaptation. Solid diamonds indicate average values. Triangles indicate data for each participant. Dotted line at 0 indicates perfect symmetry

Significance

Asymmetric shoe height may be able to alter ankle joint kinematics during walking. More research should be done with a more pronounced asymmetric footwear height difference to see if that imposes more prominent kinematic adaptations.

Acknowledgments

We would like to thank Calder Robbins, Adam Lee, Yeun Hiroi, Emily Laughlin, Annie Lye, Danielle Zoppo, and our participants.

References

[1] Patterson et al., 2008, *Arch Phys Med Rehabil,* **89**(2):304-310.
[2] McDonald et al., 2019, *J Exp Biol.* **222**(9): jeb195172.
[3] Balasubramanian et al.,2007, *Arch Phys Med Rehabil,* **88**(1):43-49.

ARTIFICIAL TENDON RESTORES BIOMECHANICAL FUNCTION IN THE RABBIT MODEL

Caleb Stubbs[1], Patrick T. Hall[1], Alisha P. Pederson[2], Caroline Bilings[2], Cheryl B. Greenacre[2], Bryce Burton[2], David E. Anderson[2], and Dustin L. Crouch[1]
University of Tennessee-Knoxville (UTK) – [1]Tickle College of Engineering and [2]College of Veterinary Medicine
Email: rstubbs1@vols.utk.edu

Introduction

There are several clinical conditions, such as acute tendon rupture [1], tendinosis [2], and limb amputation, that result in tendon damage or loss too severe to repair surgically. In such cases, artificial tendons could fully replace a damaged or missing biological tendon. One suture-based artificial tendon was recently developed and tested for its mechanical durability and tissue integration in an *in vivo* goat model [3]; however, the effect of the artificial tendon on locomotor function remains unknown.

In this study we replaced select tendons that cross the tarsus with a similar suture-based artificial tendon in 4 healthy New Zealand White (NZW) rabbits to test the tendon's effect on locomotor function. Motion capture and foot-ground pressure data were measured to quantify rabbit hindlimb biomechanics during stance phase at multiple pre- and post-surgery timepoints. We hypothesized that locomotor function would decrease immediately post-surgery but would gradually recover towards pre-surgical levels of function in the following weeks.

Methods

This study was approved by the UTK Institutional Animal Care and Use Committee (IACUC). In this study, we replaced either the Achilles (n=2) or tendinous portion of the Tibialis Cranialis m. (TC) (n=2) with suture-based artificial tendons adapted from Melvin, et al. [3]. The artificial tendons were composed of either six (Achilles) or four (TC) strands of United States Pharmacopeia (USP) size-0 braided polyester suture (Mersilene, Ethicon) and coated with biocompatible silicone (Elkem Silicones). Each artificial tendon was then coated in a lubricating mixture of 50:45:5 distilled water, glycerin, and gelatin, respectively. Lastly, the tendons were washed in an ultrasonic bath, and sterilized using ethylene oxide gas. During surgery we removed either the Achilles or TC insertion tendons by cutting at the muscle-tendon junction. The proximal end of the artificial tendon was sutured into the distal end of the appropriate muscle; the distal end of the artificial tendon was tied to a suture anchor implanted into either the calcaneus (Achilles) or talus (TC) bones.

We measured biomechanics before surgery and at 5 weekly increments post-surgery following a 2-week recovery period. Prior to testing, we shaved the rabbits' hindlimbs and marked the joint centers of the knee, ankle, and metatarsophalangeal (MTP) joints with black ink for motion tracking. The rabbits were coaxed to hop through an acrylic tunnel across a pressure mat (Tekscan, Very HR Walkway 4; South Boston, MA) that recorded vertical ground reaction force (vGRF), contact area, and pressure. This pressure mat data was synchronized with videos recorded from a webcam at 60 Hz; we used a custom MATLAB program to compute foot angles (angle between foot and ground) and ankle angles (angle between shank and foot) from the videos. The rabbits were given pen time as part of an informal rehabilitation program. We qualitatively compared biomechanics among timepoints and experiment groups (Achilles vs TC).

Results and Discussion

In the Achilles group (n=2), foot and ankle angle range of motion (ROM, max-min) during stance were 51.3 and 39.2 degrees lower, respectively, post-surgery than pre-surgery (Fig. 1A,B). Over the next five weeks, ankle ROM recovered (increased) to pre-surgical levels, but foot ROM remained lower. The Achilles group also had lower vGRF and contact area post-surgery that partially returned to pre-surgical levels (Fig. 1C,D). In the TC group, foot and ankle ROM were similar across all timepoints. Following surgery, TC rabbits had lower vGRF and contact area but recovered to pre-surgical levels by the 4-week mark.

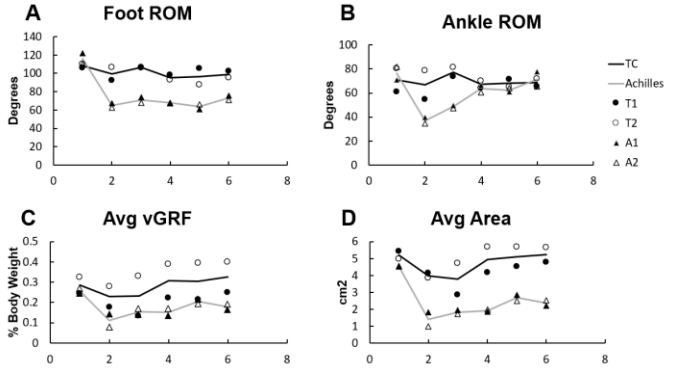

Figure 1: Shows the following changes over a 6-week time period: A. Foot range of motion (ROM). B. Ankle ROM. C. Average vertical ground reaction force. D. Average contact area.

Compared to a healthy control group [4], the Achilles group at 6 weeks post-surgery had similar kinematics at foot strike but increasingly different kinematics as stance phase progressed. From qualitative video analysis, we observed higher-than-normal flexion of the metatarsophalangeal joint in the Achilles group that prevented the midfoot from contacting the ground; this observation potentially explains the lower contact area. The remaining functional impairment in the Achilles group may have been due to tendon laxity (i.e. excessive muscle-tendon length); implanting shorter tendons may prevent laxity. Functional recovery may have been incomplete by 7 weeks post-surgery; future studies will have longer duration and include formal rehabilitation activities to achieve greater functional recovery.

Significance

Rabbits with artificial tendon replacement recovered substantial locomotor function despite functional declines immediately post-surgery, supporting our hypothesis. The TC group had less post-surgery decline and better function at the final timepoint than the Achilles group; this is not surprising since Achilles (plantar flexion) loading is probably higher than TC (dorsiflexion) loading during stance. Despite our small sample size, both rabbits in each group showed similar trends. Our data provides critical information for future studies of the artificial tendon, a potentially valuable clinical device.

Acknowledgments

This work was funded by the NIH (K12HD073945), NSF (CAREER 1944001), and a University of Tennessee Seed Grant.

References

[1] L. Nistor, et al., 1981 JBJS, 63: 3 [2] E. Bass, et al., 2012 IJTMB 5 : 1 [3] A. Melvin, et al., 2010, JOR, 28: 2 [4] Hall, et al., 2020 ASB meeting.

USING SHEAR WAVE TENSIOMETRY IN MECHANICAL PHANTOMS WITH PARTIAL WIDTH DEFECTS

Ruby C. Salbego[1], L. Arant[1], D. Thelen[1,2], S. Cone[2]

[1]Department of Biomedical Engineering, University of Wisconsin-Madison
[2]Department of Mechanical Engineering, University of Wisconsin-Madison
email: rsalbego@wisc.edu

Introduction

Every year in the United States, there are 66 million musculoskeletal injuries, with nearly half involving tendon and ligaments [1]. In many instances, the tissue experiences a partial tear. When this happens, the non-injured portion of the tendon must compensate mechanically for the defect, resulting in higher stress concentrations in the remaining tissue due to a smaller cross-sectional area. Unfortunately, it is challenging to assess mechanical changes in these injured tendons *in vivo*.

Shear wave tensiometry is a recently developed method to non-invasively measure tendon shear wave speeds, which modulate proportionally to the square root of axial stress [2]. While shear wave tensiometry has been validated as a way to measure loading in healthy tendons, it has not yet been applied to injured tendons. Prior to applying this technique to injured tendons, we plan to use mechanical phantoms that emulate tendon behavior to mimic expected changes following partial tears [3]. The objective of this work was to study the effects of partial width defects on the wave speed-stress relationship in mechanical phantoms.

Methods

To create the phantoms, ten strands of yarn were threaded through a custom mold and pretensioned at 10 N. A commercial silicone product was poured into the mold. The mechanical constructs mimic the high axial stiffness and low shear stiffness of tendon [4].

Four phantoms were tested in a uniaxial tensile testing machine (MTS). Each phantom was tested in three defect states: intact, small defect, and large defect (Figure 1). For each trial, the phantom was preconditioned by sinusoidally loading to 200 N over 25 cycles. Then, we applied a ramp load increasing at a rate of 20 N/s from 0 N to 150 N. During the loading, a mechanical tapper was driven by a 10 Hz square wave to excite shear waves in the tendon. Wave speeds were measured on both the intact and defect sides of the tendon using laser Doppler vibrometry (Polytech Inc.). Wave speed was determined using the delay in wave arrival time between two laser measurement points spaced 9 mm apart along the length of the tendon, with the first being 30 mm from the tapper [5].

Linear regressions between tensile load and squared wave speed were created for each trial. A repeated measures ANOVA was used to determine how defects affected peak squared wave speed and the slope of the regression fit, with phantom side and defect level as the main effects.

Results and Discussion

Measurements taken on the intact portion of the phantom exhibited a strong linear relationship between axial tension and squared shear wave speed across defect size (R^2 = [none: 0.756, small: 0.915, large: 0.886]). A 65% increase in peak squared wave speed was observed in large defect phantoms compared to intact phantoms ($p<0.01$). In terms of slope, there was a 106% increase from phantoms without defects to phantoms with large defects, indicating larger wave speed measurements for phantoms with larger defects ($p<0.01$).

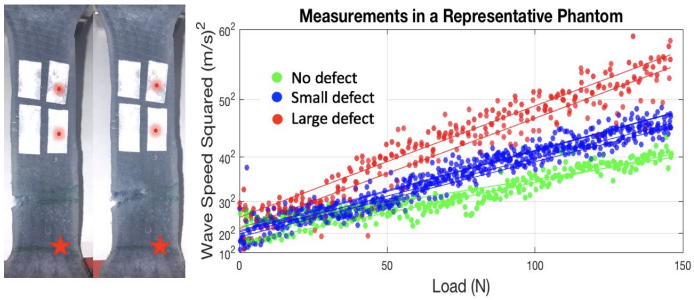

Figure 1: Phantoms with small and large defects, with tapper location indicated by a star (left). Regression lines for measurements taken across load levels and defect sizes in a representative sample with full data included (right).

In contrast, measurements taken on the defect side of phantoms exhibited non-linear relationships between axial tension and squared wave speed as defect size increased. (R^2 = [none: 0.716, small: 0.565, large: 0.039]). The linear model did not hold because the shear wave could not propagate past the defect.

Significance

Our results confirm that phantoms with partial defects experience higher wave speeds than intact phantoms under applied tensile load. The observed 65% increase in wave speed reflects higher stresses due to the decrease in cross-sectional area [5]. Significant differences in wave speed were observed when comparing between intact and large defect phantoms, but not between intact and small defect phantoms, indicating that differences are dependent on the size of the defect. This data exemplifies that shear wave tensiometry holds promise for measuring shear wave propagation in the presence of partial width injuries. In the future, we intend on expanding this research to model more specific ex vivo tendon injuries.
Furthermore, this research is a step forward in the process of eventually integrating shear wave tensiometry into clinical and rehabilitation settings.

Acknowledgments

We gratefully acknowledge the NIH (NIAMS: F32 AR076276).

References

[1] James, R et al., *J. Hand Surg.*, 2008; [2] Blank et al., *J. Mech. Behav. Biomed. Mater.,* 2020; [3] Culjat et al., *Ultrasound Med. Biol.*, 2010; [4] Arant, LR et al., in *ORS*, 2021; [5] Martin, JA et al., *Nat Commun*, 2018

THE EFFECT OF WALKING SPEED, SLOPES, AND STAIRS ON DYNAMIC MEAN ANKLE MOMENT ARM

Katherine Heidi Fehr[1*], Jenny A. Kent[2], Jasmine Nakum[1], Matthew J. Major[2,3], and Peter Gabriel Adamczyk[1]
[1]University of Wisconsin-Madison, Madison WI, USA, [2] Northwestern University Prosthetics-Orthotics Center, Feinberg School of Medicine, Northwestern University, Chicago IL, USA , [3]Jesse Brown VA Medical Center, Chicago, USA
email: *kfehr@wisc.edu

Introduction

Understanding the control mechanism of the human foot-ankle complex can inform the design of novel foot prostheses. To improve the adaptation of these designs to different activities such as ramp and stair descent, it is important to observe the way ankle control changes in a non-impaired human limb. In this study, we observe the changes in dynamic mean ankle moment arm (DMAMA) [1] when performing different activities. DMAMA describes the way the ankle controls the location of force interaction with the ground (moment arm). This summative measure accounts for temporal, spatial, and directional variations in the applied force in a single value. This makes DMAMA a useful target measure for semi-active prostheses that adjust only once per stride.

Methods

Eight unimpaired adults (age: 30±6 years; mass: 65±13 kg; foot length: 28±2 cm; mean ± SD) provided written informed consent to participate in this study. Participants performed at least 8 trials of each of the 7 activities. Walking speeds were self-selected. Kinematics were collected using a 12-camera motion capture system and ground reaction forces using multiple force plates: 6 embedded in a level walkway, 2 in a 5° incline ramp, and a force plate stairway with 3 steps, the last step forming a part of the top platform.

We used Visual3D (C-Motion, Inc.) to filter the force and kinematic data, determine foot contact with force plates, and calculate ankle moment and ground reaction force/moment. We used a custom MATLAB script to determine heel contact (HC) and toe-off (TO) and calculate DMAMA during stance phase according to Equation 1 where M is the ankle moment and F is the sagittal ground reaction force [1]. DMAMA values were subsequently normalized to participant foot length.

$$DMAMA = \frac{\int_{HC}^{TO} M\,dt}{\left\|\int_{HC}^{TO} F\,dt\right\|} = \frac{\bar{M}}{\bar{F}} \quad (1)$$

To assess the difference in DMAMA across different activities, we fit a linear mixed model (LMM) to the means of each subject's DMAMA for each category: speed, slope, and stairs. We included DMAMA as the dependent variable, the activities as the fixed effects and the participant as a random effect. We define sensitivity in table 1 as the regression coefficient from this LMM and each change in activity corresponds to an increment of one (e.g., for speed: slow (-1), normal (0), fast (1)). Critical α was set to $p<0.05$.

Results and Discussion

As walking speed increased, DMAMA decreased as shown in figure 1 and table 1. This result matches previous work by Adamczyk [1], who also found that DMAMA tended to move towards the heel (decrease) as walking speed increased. Higher DMAMA at slower walking speeds may be due to an increased plantar flexor moment attempting to slow the body's progression [2]. We observed an even sharper decrease in DMAMA when participants ascended stairs versus descended them.

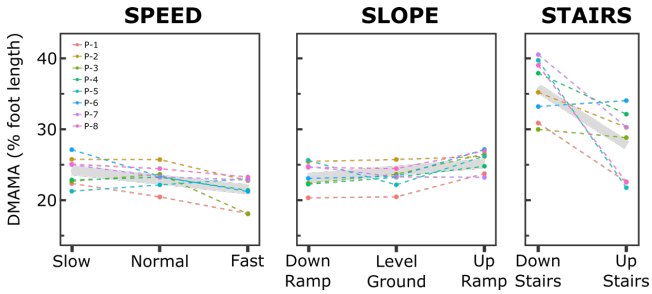

Figure 1: Trends in DMAMA across activities. The thick grey lines show the subject-independent data fit as a result of the linear mixed model. Colored markers connected by dashed lines represent each participant's average in the different categories.

Table 1. Subject-independent regression – LMM

Fixed Effect	*Sensitivity (DMAMA per increment)*	*p-value*	R^2
Walking Speed	-1.34	0.002	0.49
Slope	+1.01	0.010	0.60
Stairs	-8.00	0.003	0.46

Table 2. Mean DMAMA (% foot length) by Activity

Activity	*Mean± SD*	*Activity*	*Mean± SD*
LG Walking:		Down Ramp (-5°)	23.6 ± 2.60
Slow	23.9 ± 2.85	Up Ramp (5°)	25.5 ± 2.20
Normal	23.3 ± 2.28	Up Stairs	27.8 ± 5.48
Fast	21.1 ± 2.54	Down Stairs	35.9 ± 4.99

As the ground incline changed from negative to positive, we observed a significant shift forward in DMAMA. This is consistent with prior work by Leestma et al. [3] who showed a similar increase in DMAMA with increasing ground slope in participants with amputation using an experimental foot-ankle prosthesis. While the sensitivities in table 1 may appear small, DMAMA moving 1-8% foot length per increment, it is important to note that typical DMAMA values fall within a relatively narrow numerical range [1].

Significance

The results of this study can be used to design more biomimetic assistive devices such as prostheses, exoskeletons and orthoses. Using approaches such as varying prosthetic keel stiffness to tune DMAMA, semi-active prostheses can alter the biomechanics of a person's gait [3]. Target DMAMA values, such as the ones presented in this work, could be used to inform the control algorithms of novel prostheses, allowing them to adapt to different activities. DMAMA could also be used as a performance metric in fully robotic devices to evaluate and adjust their continuous ankle torque controllers. Having the ability to adapt to different speeds and terrains may improve the experience of prostheses users, e.g., by reducing maladaptive socket torques.

Acknowledgments

Funding from DOD (W81XWH1920024, W81XWH1710427).

References

[1] Adamczyk, *J. Biomech Eng*. 142, (2020)
[2] Orendurff, et al., *Gait Posture* 27, (2008)
[3] Leestma, et al., *J. Biomech Eng*., (In review)

A TRAINED NEURAL NETWORK MODEL ACCURATELY PREDICTS ACHILLES STRESS FROM SHEAR WAVE PROPAGATION

Jack A. Martin and Darryl G. Thelen
Department of Mechanical Engineering, University of Wisconsin-Madison
email: jamartin8@wisc.edu

Introduction

Quantitative measures of tissue loading have many applications in research and clinical spaces. Shear wave tensiometry can predict stress in superficial tendons based on shear wave propagation speed [1]. The usefulness of the technique will expand further as it transitions into a wearable technology [2]. However, the technique is still limited in that calibration is required if users desire an absolute measure of tissue loading [3]. Calibration can be a time-consuming step that will usually require additional equipment. Here, we present a machine learning approach to generate a model predicting tendon stress directly from skin-mounted accelerometer data. The model performed well on test data, such that it can potentially circumvent the need for calibration on individual subjects.

Methods

Standard shear wave tensiometry involves calculating the speed of an induced shear wave based on tracked wave motion at two downstream accelerometers. Wave speed squared is then calibrated to tendon stress during a simple task [3]. Here, we instead trained neural network models (MATLAB) to predict tendon stress based on all data recorded by the pair of accelerometers. We used data collected during a prior study from the Achilles tendons of 12 subjects walking (1.00, 1.25, 1.50, 1.75, 2.00 m/s) and running (1.50, 2.00, 2.50, 3.00, 3.50 m/s) on an instrumented treadmill. Principal component (PC) analysis was performed on raw accelerometer data from all trials and subjects to reduce the dimensionality of the data. The first 20 PCs accounted for 90% of the variance in the accelerometer data and were retained. PCs, along with calculated wave speed, served as predictors in the models. Models were trained to predict inverse dynamics (ID) estimates of tendon stress using data from stance and early swing. ID stress estimates were made by dividing ID ankle torque estimates by tendon moment arm and cross-sectional area, assuming all torque was produced by triceps surae.

Data from 10 subjects were used for training and validation, and data from the remaining two were held out to test the final trained model. Each of the first ten subjects served as the validation subject once with the nine others being used to train a set of 20 neural network models in each case. This resulted in a total of 120 trained models. The highest performing 80% of these were retained, and contributed to a final ensemble model which averaged their predictions. This process was meant to eliminate bias from individual subject differences and reduce the effects of individual trained models falling into poor local error minima.

The trained ensemble neural network model was used to predict stress from PCs and wave speed for all subjects and trials. For each trial, root-mean-square deviation (RMSD) was calculated between predicted stress and ID stress.

Results and Discussion

The trained model predicted stress accurately for the stance phases in both walking (W) and running (R) trials (Fig. 1; all subjects: $RMSD_W$ =5.9±2.9, $RMSD_R$ =12.3±6.8; test subjects: $RMSD_W$ =4.8±0.6, $RMSD_R$ =12.5±5.4 MPa). Test subject results were as good as training/validation subject results, indicating that the model is not overfitting the data. Model-based predictions compare favorably with published predictions from subject-specific ($RMSD_W$ =8.1 MPa) or group average ($RMSD_W$ =9.4 MPa) dynamometer-based calibration on the same data [3]. Thus, an ensemble neural network model like the one presented here could improve the accuracy of tendon stress predictions, even while eliminating the calibration step.

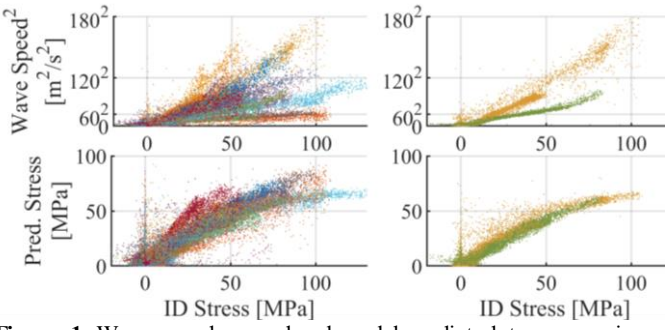

Figure 1: Wave speed squared and model predicted stresses vs. inverse dynamics (ID) derived stresses for all subjects (left) and subjects in the test group (right). Data from each subject appear in a unique color.

The ensemble neural network model under-predicted higher ID stresses during running (Fig. 2). This could indicate a limitation of the approach, or could be due to artificially high ID stresses from experimental measurement error. Interestingly, despite not being trained with swing phase data, the model did predict late swing phase Achilles stresses caused by passive tensioning prior to foot contact.

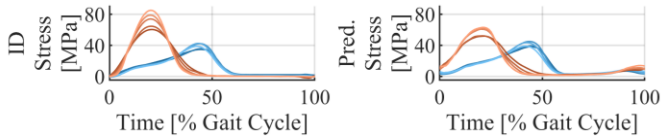

Figure 2: Inverse dynamics (ID) derived stresses and model predicted stresses over the course of walking (blue) and running (orange) gait cycles averaged across subjects for each speed (lighter color = faster).

Significance

A trained neural network model could eliminate the reliance of shear wave tensiometry on calibration and greatly expand its usability, particularly in clinical spaces where there are often tight constraints on the amount of time spent with individual patients. Further, this approach could improve reliability and ease of use, so that training requirements are diminished. Thus, this work represents an important step toward enabling researchers and clinicians alike to use shear wave tensiometry for estimating absolute muscle-tendon loads.

Acknowledgments

Supported by NIH AR074897 and the Wisconsin Alumni Research Foundation. Authors are co-inventors on a related patent (US 10631775).

References

[1] Martin JA, et al. *Nat Commun* 9 (2018). [2] Harper SE, et al. *Sensors* 20 (2020). [3] Keuler EM, et al. *Sci Rep* 9 (2019).

KINEMATIC ADAPTATION OF TREADMILL WALKING WITH ACTIVE EXOSKELETON

C.S. Poindexter[1], C. Haynes[1], AK. McGough [1,2], S. Song[1,3], and J.C. Bradford[1]
[1]US ARMY DEVCOM ARMY RESEARCH LABORATORY
[2]DCS CORP, [3]Texas A&M University
email: csp@udel.edu

Introduction

Lower-extremity physical augmentation devices are typically designed to provide active assistance to the user during a variety of tasks by applying torque across joints. For both rehabilitation and military applications, locomotion remains a critical task that may benefit from augmentation. Metrics such as metabolic cost, movement speed, skill, balance, local fatigue, injury risk, and cognitive metrics may be critical to understanding physical augmentation performance (1, 2). To move the field of physical augmentation forward, it is critical to improve our understanding of how and to what extent humans adapt and interact with these devices (1).

In this study we measured electroencephalography (EEG), electromyography (EMG), kinematics, and kinetics while subjects walked on a treadmill with assistance from an ankle augmentation device. Here we will present our kinematic results to show how study participants adapted their joint movement strategy over time while walking with the augmentation device.

Methods

Six healthy adults walked on an instrumented treadmill (AMTI, MA) at 1.2m/s with bilateral ankle assistance from the Dephy ExoBoot (Dephy Inc, MA), an active, autonomous ankle exoskeleton that gives the user plantarflexion assistance at push-off. We measured EEG, lower extremity EMG, optical motion capture, and ground reaction forces from the treadmill. We recorded data while subjects walked on the treadmill with and without assistance, before, during and after a training period. During the training period, the subject walked on the treadmill for ~45 minutes while the ankle assistance turned on and off at random intervals between 45-70 steps. This resulted in the subject walking with assistance for ~20mins total. While we anticipate interesting comparisons between joint kinematics with/without assistance, and during the training period, for the purpose of this abstract we looked at assisted conditions **before** and **after** the training period.

We collected motion capture data at 120Hz, using 12 infrared cameras (Motion Analysis Corp, CA) and a custom marker set (48 markers). We filtered marker data using a low pass 4th order, zero lag, Butterworth filter (f_c=6Hz). We computed sagittal plane joint angles using Visual 3D (C-Motion, MD). We extracted gait events (heel strike and toe off) using force plate data. We epoched the joint angles using left heel strike events and normalized each gait cycle to have 101 points. We computed average gait cycle joint angle trajectories by averaging across all gait cycles (~250 cycles) for each condition and subject. We also computed range of motion, peak flexion, and peak extension for each gait cycle.

Results and Discussion

We found subjects adapted their ankle joint kinematics (increased ROM) by increasing dorsiflexion, as seen in Table 1. We found that subjects adapted knee kinematics (increased ROM) by increasing knee flexion. We found that subjects adapted hip joint kinematics (increased ROM) by increasing hip flexion.

Table 1: Peak flexion (maximum), Peak extension (minimum), and range of motion (ROM) for all subjects' left side joint angles.

		Max. (degrees)		Min. (degrees)		ROM (degrees)	
		Mean	*Std. Dev.*	*Mean*	*Std. Dev.*	*Mean*	*Std. Dev.*
Ankle	*Before*	5.34	2.77	-19.39	5.11	24.74	4.20
	After	8.90	2.76	-19.44	5.61	28.34	4.48
Knee	*Before*	60.95	5.16	-7.84	3.04	68.79	5.78
	After	64.20	4.04	-8.81	2.37	73.01	4.74
Hip	*Before*	25.78	3.07	-11.54	3.18	37.32	4.98
	After	28.74	3.88	-10.28	3.00	39.02	5.43

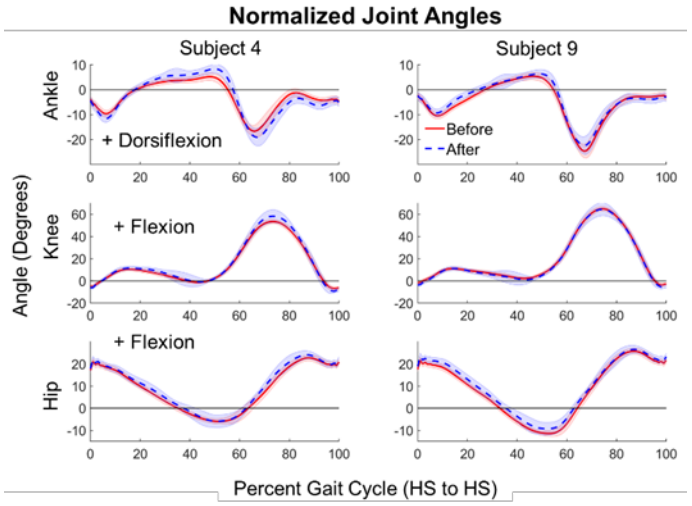

Figure 1: Normalized left side joint angles from two exemplary subjects. Time is normalized for one gait cycle from Left Heel Strike (LHS, 0%) to the subsequent Left Heel Strike (LHS, 100%).

While on average our data shows that subjects adapted their joint kinematics with training, there is inter-subject variability. For example, we have included the data for two exemplary subjects in Fig 1. Subject 4 adapted their ankle and knee kinematics due to training by decreasing peak dorsiflexion and flexion respectively. Comparatively, Subject 9 showed very little adaptation in joint kinematics. In future work we plan to examine how the cortical neural dynamics correspond to adaptation in gait biomechanics.

Significance

Understanding how joint kinematics adapt to active physical augmentation devices can help inform the design of these devices, especially if controllers are based on the user's kinematic variables.

References

[1] Ferris, D. P. (2017). Kinesiology Review, 6(1), 70-77.

[2] Stirling, L. (2018). IEEE Systems Journal, 13(1), 1072-1083.

Sex-Specific Associations Between Body Mass Index and Knee Flexion Characteristics In Individuals With ACL Reconstruction

Derek N. Pamukoff[1], Skylar C. Holmes, Caitlyn E. Heredia, Eric. J. Shumski
[1]Western University, London ON
email: dpamukof@uwo.ca

Introduction

ACL reconstruction (ACLR) contributes to reduced knee flexion during walking and landing, which may influence knee osteoarthritis (OA) development and re-injury risk, respectively.[1] High body mass index (BMI) and female sex are risk factors for knee OA and ACL injury.[2,3] However, there may be unique interactions between sex and BMI on knee mechanics during walking and landing due to differences in regional body fat distribution between males and females.[4]

The purpose of this study was to examine the association between BMI and knee flexion characteristics during gait and landing in a cohort with ACLR. We hypothesized that BMI would be associated with smaller knee flexion angles and external moments, and that the association would be more pronounced in females compared with males.

Methods

Thirty individuals with primary unilateral ACLR participated in this study (14 males, Age=24±4.7 years, BMI = 25.0 ± 5.5, Body Fat % = 21.1 ± 8.6, Gait speed = 1.35 ± 0.10 m·s^{-1}, Time Since ACLR = 80.8 ± 29.6 months; 16 females, Age = 21.5 ± 2.4, BMI = 27.0 ± 5.3, Body Fat % = 29.1 ± 8.3, speed = 1.36 ± 0.17 m·s^{-1}, Time Since ACLR = 65.4 ± 19.7 months).

Body composition was assessed using air displacement plethysmography. All biomechanical data were obtained during a single laboratory session using a 9-camera Qualisys Motion Capture System recording at 240Hz and 2 force plates recording at 2400Hz. Five overground walking trials per limb were performed at a self-selected speed in laboratory standard neutral cushion footwear along a 10m runway, and speed was maintained within ±5%. Bilateral landing biomechanics were obtained during a drop vertical jump using a 30cm box at a distance equivalent to half the participants' height. Marker trajectories and force plate data were low-pass filtered at 6 Hz for gait analyses, and low-pass filtered at 20Hz for landing analyses. All outcomes were extracted bilaterally, but analyses were restricted to the limb with ACLR.

A joint coordinate system was used to obtain knee angles and expressed as motion of the shank relative to thigh segment, and inverse dynamics was used to obtain knee moments resolved in the tibial coordinate system. Gait outcomes included the knee flexion angle at heel contact, the peak knee flexion angle in early stance, and the peak external knee flexion moment. Landing outcomes included the knee flexion angle at ground contact, peak knee flexion angle, and peak external knee flexion moment.

Stepwise linear regression was used to assess the association between BMI (kg/m^2) and gait and landing outcomes after adjusting for body fat (%). We adjusted for body fat percentage because BMI does not consider body composition. We assessed the moderating effect of sex (0=female, 1=male) on the association between mean-centred predictor variables and gait and landing outcomes via the addition of the interaction term (sex x BMI) to the regression model. Where a significant interaction was found, post hoc probing was conducted via an analysis of the conditional slopes within each sex.

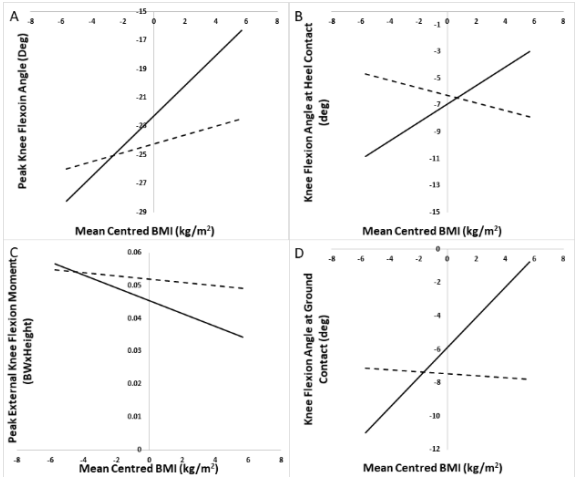

Figure 1: Conditional slopes for each sex where significant interactions were found after adjusting for body fat %. Solid lines represent females, and dashed lines represent males (A: peak knee flexion during gait; B: knee flexion at heel contact during gait; C: peak knee flexion moment during gait; D: knee flexion angle at ground contact during landing).

Results and Discussion

In the ACLR limb, there was a significant interaction between sex and BMI on the knee flexion angle at heel contact (ΔR^2= 0.19, p=0.01), peak knee flexion angle (ΔR^2= 0.11, p=0.04), and peak external knee flexion moment (ΔR^2= 0.10, p=0.05) during gait; and on the knee flexion angle at ground contact during landing (ΔR^2= 0.11, p=0.04). Post hoc probing of the conditional slopes indicated that a higher BMI was associated with a smaller knee flexion angle at heel contact (Effect=0.69, p=0.03), smaller peak knee flexion angle during gait (Effect=1.04, p=0.02), and smaller external knee flexion moment (Effect=-0.002, p=0.01), but only in females. Similarly, a higher BMI was associated with a smaller knee flexion angle at ground contact during landing (Effect=1.06 p=0.03), but only in females.

Significance

Findings indicate that sex influences the association between high BMI and knee flexion characteristics during walking and landing. Females with high BMI may exhibit smaller knee flexion angles and external knee flexion moments, which may exacerbate risk for post-traumatic knee OA and secondary injury. Interestingly, no effects were observed in the contralateral limb. As such, high BMI and sex should be considered when developing rehabilitation programs for individuals with ACLR.

Acknowledgments

This study was supported by the California Program for Research in Biotechnology New Investigator Grant (2017-2018).

References

[1]Lepley AS and Kuenze CM (2018). *Journal of Athletic Training*.
[2]Allen KD and Golightly YM (2015). *Curr Opin Rheumatology*.
[3]Smith HC et al (2012). *Sports Health*.
[4]Power ML and Schulkin (2008). *British Journal of Nutrition*.

OPTICAL FLOW PERTURBATION EFFECTS ON STANDING BALANCE IN PEOPLE WITH MULTIPLE SCLEROSIS

Olivia S. Elie[1], Jason R. Franz[2], and Brian P. Selgrade[1]
[1] Department of Movement Science, Sport and Leisure Studies, Westfield State University, Westfield, MA, USA
[2]Joint Dept. of Biomedical Engineering, UNC-Chapel Hill and NC State University, Chapel Hill, NC, USA
email: *bselgrade@westfield.ma.edu

Introduction

Multiple sclerosis is a progressive, chronic disease that damages nerve fibers and obstructs nerve signal transmission causing balance deficits and falls**.** Mobility and balance deficits fundamentally influence the performance of daily tasks for the 2.5 million multiple sclerosis patients worldwide. In a three-month period, 56% of people with multiple sclerosis (PwMS) reported experiencing falls (Nilsagard et al. 2015). During walking, PwMS are more susceptible to medial-lateral (ML) optical flow perturbations than controls (Selgrade et al. 2020), but we do not know how they respond to these perturbations during standing. Given that direction-dependence differs of balance between walking and standing, the purpose of this study was to examine the effects of optical flow perturbations on standing balance control in PwMS. We first hypothesized that optical flow perturbations would challenge standing balance in PwMS more than control participants. We also hypothesized that, due to a wider base of support laterally, standing balance would be more susceptible to anterior-posterior (AP) perturbations in comparison to ML perturbations in PwMS.

Methods

Fourteen PwMS (38.9±6.6 years, 12 female) participated in this IRB-approved study. Participants stood on a force plate in a virtual reality environment under four 1-minute conditions: eyes closed, eyes open with no perturbation, ML optical flow perturbation, and AP optical flow perturbations. These continuous perturbations elicit the visual perception of instability. We calculated standard deviation, range, velocity, and 95% confidence ellipse area from the center of pressure (CoP) trajectory. A repeated measures ANOVA tested for main effects and interactions between group and condition with post hoc, pairwise comparisons using Bonferroni corrections.

Results and Discussion

Compared to standing with ML perturbations, standing with AP perturbations elicited larger changes in CoP ML range and standard deviation relative to the eyes-open control trial. Our first hypothesis was not supported. Optical flow perturbations did not disproportionately affect standing balance in PwMS compared to age-matched controls. A possible explanation for this would be that the PwMS were relatively fit (average preferred walking speed: 1.29 m/s). Combined with prior research on the same group of subjects, these results suggest that optical flow perturbations better reveal balance deficits in PwMS during walking than during standing (Selgrade et al. 2020). We interpret these findings to suggest that PwMS rely on vision for balance more during walking than during standing. Conversely, our second hypothesis, that balance was more susceptible to AP perturbations, was supported. Compared to standing with ML optical flow perturbations, CoP ML range and standard deviation were higher when standing with AP perturbations. Unexpectedly, neither AP standard deviation nor AP range significantly differed between AP perturbation and any other condition. The base of support is much smaller in the AP direction, and participants may prioritize strategies to limit variability and ensure resilience to perturbations. This effect may explain why AP differences did not reach significance. Neither COP velocity nor 95% confidence ellipse area significantly differed between groups or conditions.

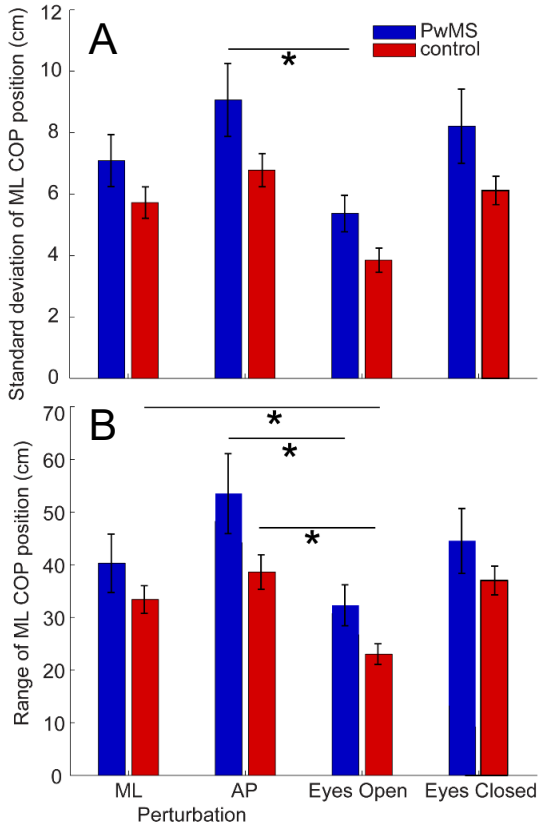

Figure 1: Standard deviation (A) and range (B) of center of pressure position during standing with optical flow perturbations and control conditions in people with multiple sclerosis (PwMS) and age-matched controls. * indicates significant difference ($p<0.05$) between conditions.

Significance

Overall, these findings have implications for clinical screening of PwMS to detect fall risk. This study found that optical flow perturbations affected standing balance similarly in PwMS and age-matched controls. This result, combined with prior research on susceptibility to optical flow perturbations during walking in PwMS, suggests that in clinical settings, perturbed walking may more effectively detect balance deficits and prevent falls in PwMS.

Acknowledgments

The National Institute on Aging (R56AG054797) and a National MS Society Pilot Grant supported this research.

References

1. Y. Nilsagard, H. Gunn, J. Freeman, P. Hoang, S. Lord, R. Mazumder, et al., *Multiple Sclerosis J.* 21 (2015) 92–100.
2. Selgrade, B.P. Meyer, D, Sossnoff, J.J. and Franz, et al. *PLOS One* 15(3):e0230202. 2020.

A PILOT STUDY EVALUATING THE EFFECT OF A NOVEL FOOT OFFLOADING DEVICE ON LOWER EXTREMITY KINEMATICS

Naomi E. Frankston*[1], Milad Zarei[1], Maria A. Munsch[1], Beth Gusenoff[2], Jeffrey Gusenoff[2], William J. Anderst[1]
[1]Department of Orthopaedic Surgery and [2]Plastic Surgery, University of Pittsburgh, Pittsburgh, PA
email: *nef22@pitt.edu

Introduction

Current solutions to offload sensitive areas of the foot may induce compensatory gait and can be uncomfortable, resulting in poor patient compliance. PopSole™ is a novel, fully customizable air-filled insole designed to decrease plantar pressure by deflating localized areas while still providing anatomic support to the foot. The purpose of this pilot study was to compare gait kinematics when walking with the PopSole device, Darco PegAssist device, and neutral running shoes (Figure 1). We hypothesize that lower extremity walking kinematics will be unchanged in PopSole, but will be changed when wearing Darco PegAssist, compared to running shoes.

Methods

10 healthy participants (5F/5M; 28 ± 6.5 years; 23.3 ± 3.0 kg/m^2) with no history of foot injury, surgery, or pathology consented to this IRB-approved study. Participants walked overground at a self-selected pace (1.5 ± 0.2 m/s) for 2 min in three shoe conditions in a randomized order: 1) standard neutral running shoes, 2) PopSole insoles with localized forefoot and heel regions popped, and 3) Darco PegAssist shoes with localized forefoot and heel region pegs removed. Participants completed surveys about footwear comfort and preference. Kinematics were collected using 3D motion capture (12-camera Vicon) at 100 Hz. Joint angles for the hip, knee and ankle during stance were computed in Visual3D. Data were averaged over a mean of 10 ± 3 steps for each shoe condition. A one-way repeated measures ANOVA and post-hoc paired t-tests were run using statistical parametric mapping (SPM)[1] in MATLAB. Ankle kinematics were not available for the Darco shoe and thus SPM paired t-tests were used to evaluate differences in ankle kinematics.

Results and Discussion

The ankle was less abducted and more everted when wearing the PopSole compared to the running shoe (Figure 2AB). This contradicted our hypothesis that PopSole would not change kinematics compared to the running shoe.

Knee and hip flexion/extension and adduction/abduction kinematics waveforms were different among conditions based on the SPM ANOVA. Only hip flexion/extension showed significance post-hoc, with the hip extending less when wearing the Darco compared to running shoes (Figure 2C). This supports our hypothesis that the Darco shoe changes kinematics compared to the running shoe. Knee and hip kinematics were not different between PopSole and running shoes.

All participants preferred PopSole over Darco. 10% of participants reported PopSole affected their hip or knee and 70% felt Darco affected their hip or knee. 90% of participants reported feeling proper leg alignment with Popsole and 0% felt properly aligned with Darco. The PopSole device may therefore improve patient compliance.

Limitations are that ankle kinematic data were not available for the Darco condition, and results are from healthy individuals walking over a flat laboratory walkway.

Significance

PopSole was preferred to and altered hip kinematics less than the Darco PegAssist, suggesting PopSole has potential clinical benefit over the current standard of care.

Acknowledgments

Clarissa Lees for assistance with SPM. Funding from the U of Pittsburgh Clinical and Translational Science Institute.

References

1. Pataky TC *J Biomech,* 2010.

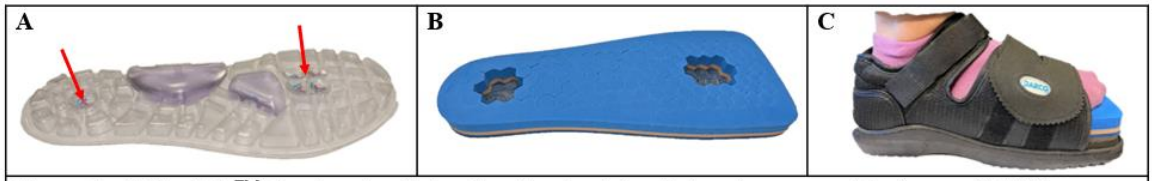

Figure 1: A) PopSole™ shoe insert with localized heel and forefoot regions popped (red arrows), **B)** Darco PegAssist insert with heel and forefoot pegs removed, **C)** Darco shoe with PegAssist insert

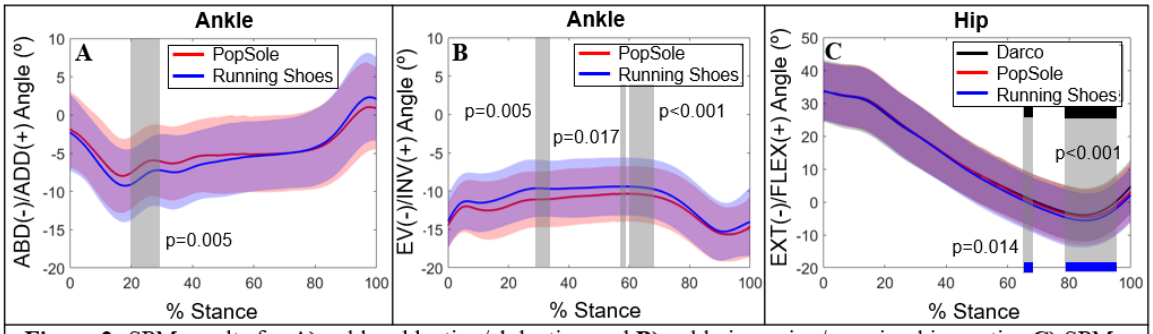

Figure 2: SPM results for **A)** ankle adduction/abduction and **B)** ankle inversion/eversion kinematics **C)** SPM ANOVA results for hip flexion/extension during laboratory walking; grey regions were significant; blue and black bars indicate differences between running shoes and Darco

GEOMETRIC BONE STRENGTH OF METATARSALS IN MALE VERSUS FEMALE RUNNERS

Kyle E. Murdock[1] Adam S. Tenforde[2], and Karen L. Troy[1]
[1]Worcester Polytechnic Institute, Worcester, Massachusetts
[2]Spaulding Hospital, Cambridge, Massachusetts
Corresponding Email: kemurdock@wpi.edu

Introduction

Bone stress reactions are overuse injuries that frequently prevent endurance runners and military recruits from training. Bone stress injuries (BSIs) account for 20% of injuries in sports medicine clinics and up to 10% of all orthopaedic injuries [1]. BSIs, caused by microdamage accumulation from repetitive mechanical loading, are commonly found in the metatarsals of runners. Biological predisposition and biomechanical factors contribute to an individual's risk of developing a BSI. The female athlete triad, more generally regarded as Relative Energy Deficiency in Sport (RED-S), comprise a set of risk factors which are known to predispose athletes to stress injuries [2,3]. Women are 1.5 – 3 times more likely to sustain a BSI than men [4]. However, it is unclear if this stems from triad factors (i.e. menstrual dysfunction, estrogen deficiency) or biomechanical factors. Biomechanical risk factors like poor bone structure and intrinsic foot muscle weakness, have been implicated in BSI risk [5]. We hypothesize that females have weaker bone structure compared to males, even when accounting for body mass.

Methods

This retrospective analysis selected all patients seen by a single sports medicine physician (AST) from 2015 to 2019 with a diagnosis of metatarsal BSI or another foot injury, who also had MRI images of the metatarsals (n=61). Here we report on a subset of 16 patients (9 female, 7 male) whose MRI images were quantitatively analysed. This included three women and four men with a BSI in whom we only analysed the uninjured metatarsals. Sex, weight, and Triad risk factors at the time of diagnosis were obtained from medical records. Coronal T1 images of the metatarsal mid-shafts were manually segmented in Mimics.

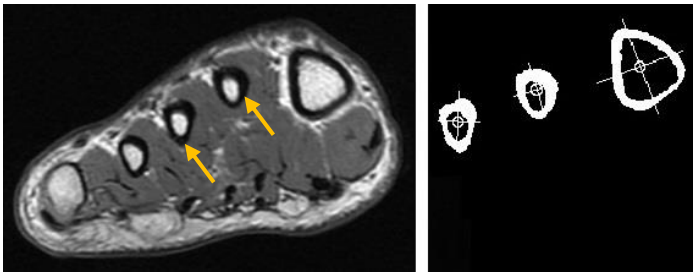

Figure 1. Cross-sections of metatarsals (left) are distinguishable by the cortices' lack of signal (black) in T1-weigthed images (arrow).

The second moment of area (minimum, maximum) were calculated using ImageJ. We compared male vs. female metatarsals using a Mann-Whitney U test, with p-values<0.05 considered significant.

Results and Discussion

There were no differences in age (Male= 30±12, Female= 29±13 years), stratified Triad score (Male = 1.4±1.4, Female = 1.3±1.5), or BMI (Male= 23.4±3.6, Female= 20.6±1.8 kg/m^2) between the two groups. Males had larger metatarsals with thicker cortices. Raw I_{max} and normalized I_{max} are summarized in box-and-whisker plots in Figure 2. The first metatarsal displayed the greatest geometric strength characteristics compared to the lesser metatarsals. Males had stronger 1st (p-value < 0.001), 4th (p-value=0.031), and 5th (p-value = 0.004) metatarsals compared to females; however, these differences were less remarkable when normalizing to body mass (p-value=0.018, p-value=0.11, p-value=0.06, respectively).

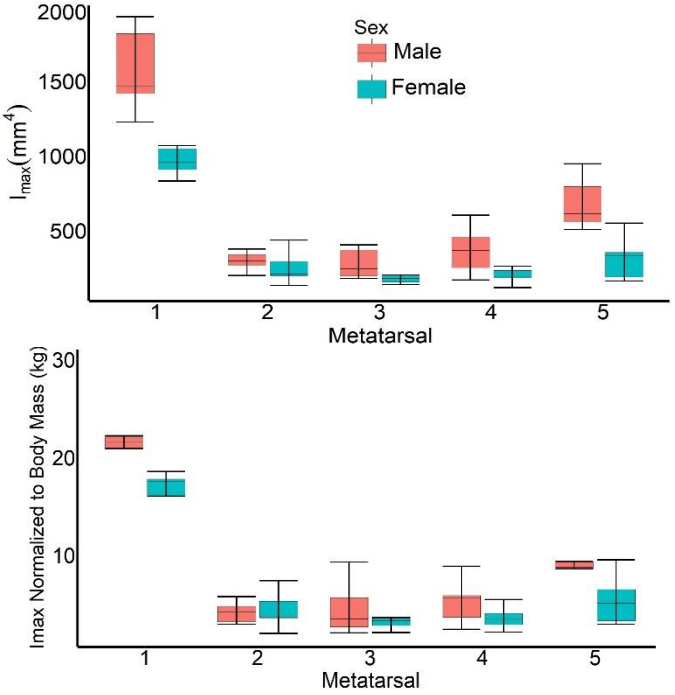

Figure 2. Comparison of raw (top) and body mass-normalized (bottom) I_{max} values for all metatarsals between male and female runners.

Interestingly, metatarsals 2 and 3, which tend to experience BSI most frequently, were not significantly weaker in females (2nd and 3rd metatarsal I_{max}: p-value =0.39, p-value=0.073, $I_{max, Normalized}$: p-value = 0.98, p-value=0.83, respectively).

Significance

The preliminary findings presented here indicate the higher incidence of BSI in female runners may not be explained by metatarsal bone strength alone, though additional comparisons should be made between those with/without BSI. The work performed here is meaningful because its is a first step in identifying imaging biomarkers for assessing relative injury risk. This research study affects the clinical environment by providing practitioners with reference data for metatarsal morphology.

References

[1] Fredericson M et al, *TMRI*. 17:309–25, 2017.
[2] Barrack M et al., *Am J Sports Med*. 42:949-58, 2014.
[3] Tenforde A et al. *Am J Sports Med*. 45:302-310, 2017.
[4] Wentz L et al., *Mil Med*. 176:420-30, 2011.
[5] Fujitaka K et al. *Ortho J Sports Med*. 3: 2325967115603654.

PEDAGOGICAL METHODOLOGY IN DISTANCE LEARNING YOGA TO IMPROVE BALANCE CONTROL

Pranavi L. Depur[1], Belle P. Ponce de Leon[1], Andrew Y. Cho[1], Kimberly G. Hernandez[1], Jacob W. Hinkel-Lipsker[1]
1Move-Learn Lab, Department of Kinesiology, California State University, Northridge, CA USA
Email : pranavi.depur.645@my.csun.edu

Introduction

Yoga is known to have many health benefits and can be learned through many different modalities [1,2]. During the COVID-19 pandemic, many yoga programs transitioned to strictly virtual learning either through live video conference sessions (synchronous) or on-demand video (asynchronous). Although the synchronous group has the benefit of live feedback and the asynchronous group can view content at their own pace, certain disadvantages of both exist, including the availability of the participant or the difficulties in accessing virtual content respectively [3]. While existing research in classroom-based education details the efficacy of incorporating a blend of both methodologies (mixed), the implications of each distance learning paradigm on motor learning parameters in a virtual fitness setting has yet to be explored [3]. Due to a growing proliferation of at-home exercise, determining the most effective method of content delivery in improving yoga-specific skills is of importance. The purpose of this study was to assess the improvements in balance control by asynchronous, synchronous, and mixed learning modalities in novice yoga practitioners over an 8-week virtual yoga program. We hypothesized that, based on a multitude of education research, mixed learning would lead to the greatest improvements in balance control (e.g., reduced center of mass sway and velocity).

Methods

Fifty-three participants between the ages of 18-65 were recruited to participate in a virtual 8-week yoga program. All data was collected over video conferencing and no face-to-face contact was made due to the COVID-19 pandemic. Prior to and following the intervention, participants met with their assigned researcher over video conferencing to conduct a series of balance tests in randomized order as a measure of baseline (pre-intervention) or retention (post-intervention) of balance control ability. These postures were a single leg (SL) stance with eyes closed (to assess generalization of learned balance), eagle pose (for anterior-posterior balance), and tree pose (to test medial-lateral balance). Markers were placed on the participants' estimated center of mass (COM) in the frontal and sagittal planes, and video was recorded during the performance of these postures. Two-dimensional motion analysis software was used to track the COM position during performance of these poses. Marker coordinate data were then used to quantify COM excursion (displacement), velocity, and total distance travelled. Participants were randomly assigned to either the synchronous, asynchronous, or mixed group as a part of the study. During the intervention participants were required to attend classes two times per week depending on the requirements of their group where attendance was recorded. Synchronous participants attended two live yoga sessions offered by trained instructors, while asynchronous participants completed two pre-recorded sessions on their own time. Individuals in the mixed group completed one of each session per week.

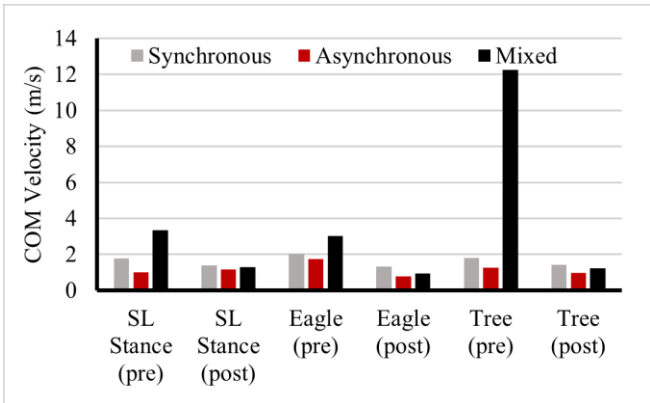

Figure 1: Pre and post-test COM velocity across all three groups for single-leg (SL) stance, eagle, and tree poses.

Results and Discussion

Preliminary results indicate that while all groups improved their balance control abilities, the blended approach was the most effective form of distance learning. Participants within the mixed group exhibited the greatest reduction in their total COM excursion, total distance traveled, and slowed their COM velocity across all poses compared to the other two groups. Improvements in eagle and tree poses indicated increases in sagittal plane and frontal plane balance control, respectively. The SL stance improvements indicated overall balance control. The potency of this type of education may be due to the synergy of real-time instruction, error correction, and feedback gained from the synchronous classes, and the opportunity prescribed to students for reaffirming what they have recently learned and to practice on their own time through the asynchronous classes.

Significance

The purpose of this study was to compare the effects of an 8-week yoga program in participants placed in a synchronous, mixed, and asynchronous group. Due to the COVID-19 pandemic, virtual learning has become a primary means to remain active. Our early findings imply that effective virtual fitness paradigms should incorporate both asynchronous and synchronous components to maximize task-specific motor learning. Future research should focus on special populations such as older adults as this could inform fall injury risk prevention.

Acknowledgments

The research team would like to acknowledge members of the Move Learn Lab who have helped with this study.

References

[1] D. E. Laaksonen, et al. (2002). *Diabetes Care*, vol. 25:1612–1618,
[2] M. D. Tran et al. (2001). *Preventive Cardiology*, vol. 4: 165–170
[3] N.T. Butz, and R.H. Stupinsky (2016). *The Internet and Higher Education,* vol. 28: 85-95

CHANGE IN KNEE CARTILAGE STRESSES FROM 6 TO 24 MONTHS AFTER ACL RECONSTRUCTION: A PRELIMINARY FINITE ELEMENT ANALYSIS

Kelsey Neal[1], Jack R. Williams[1], Ashutosh Khandha[1], Lynn Snyder-Mackler[1], Thomas S. Buchanan[1]
[1]University of Delaware, Newark DE
Email: kaeneal@udel.edu

Introduction

Individuals who undergo ACL reconstruction (ACLR) are at an elevated risk of developing tibiofemoral osteoarthritis (OA). Using neuromusculoskeletal modelling, we found that underloading of the involved limb's medial tibiofemoral compartment 6 months after ACLR is associated with radiographic OA 5 years after surgery[1]. While this modelling approach allows us to estimate medial compartment loading, it does not provide insight into how load is distributed within the joint, and the resultant cartilage stress.

Finite element modelling is one technique that can estimate cartilage stress. Currently, little is known about how stress distribution within knee cartilage changes after ACLR. The purpose of this study was to develop a subject-specific finite element (FE) model of an individual's knee, to assess peak stresses in different regions of the medial tibial cartilage, at 6 and 24 months after ACLR.

Methods

One subject (female; age: 19; $mass_{6Months}$ = 73.6 kg; $mass_{24months}$ = 68.3 kg) who underwent unilateral ACLR (bone-patellar tendon-bone autograft) participated in this exploratory study. Six months after surgery, the subject underwent a sagittal, bilateral knee MRI scan (proton density sequence: repetition time = 4870 ms, echo time = 37 ms, slice thickness = 3 mm, FOV = 150 mm). The subject also completed motion analysis during overground walking. The same subject returned 24 months after surgery to repeat the motion analysis experiment. During motion analyses, kinematic, kinetic, and surface electromyography data were collected bilaterally and used to calculate joint contact forces via a validated EMG-informed neuromusculoskeletal model[2].

To develop a subject-specific FE model, MRI scans were segmented using ScanIP (Synopsys, Inc., Mountain View, USA). Bone geometries were then meshed using triangular shell elements in Hypermesh (HyperWorks, Altair Engineering, Inc, Troy, MI). Cartilage and meniscal structures were meshed using hexahedral elements via an open source software developed by Rodriguez-Vila et. al. 2017[3]. The meshed geometries were then assembled in Abaqus CAE (Dassault Systems Simulia Corp., Providence, USA), where ligamentous structures were modelled as 1D truss elements (Figure 1A).

FE model inputs were applied quasi-statically and included peak knee flexion angle (pKFA), total joint contact force (TCF) at pKFA, and knee adduction moment (KAM) at pKFA. These inputs were applied through a reference point in the femur placed at the midpoint of the transepicondylar line (Table 1, medial compartment force (MCF at pKFA) has also been included for reference). The medial tibial cartilage was divided into five different regions of interest: anterior, central medial, central, central lateral, and posterior (Figure 1B). Peak Von Mises stresses were reported for each region, at each time point (Figure 2).

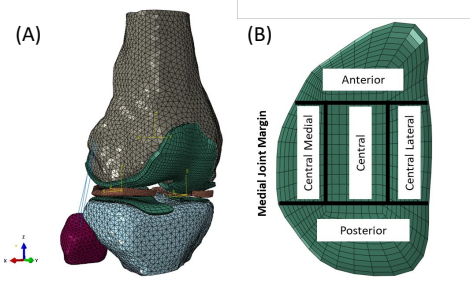

Figure 1: (A) Full FE model and global coordinate system. (B) Regions of interest for medial tibial cartilage.

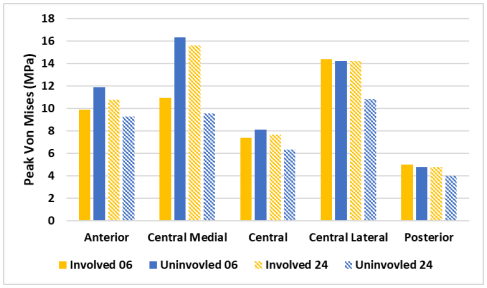

Figure 2: Peak Von Mises stress within the involved (yellow) and uninvolved (blue) limbs medial tibial cartilage at 6 (solid) and 24 (lined) months.

Table 1: FE model inputs applied to the femoral reference point. MCF has also been included for reference.

Time point	Limb	pKFA (°)	KAM (Nm)	TCF (N)	MCF (N)
6 Months	Involved	-20.14	-44.66	-2822	-2139
	Uninvovled	-24.28	-40.08	-3094	-2268
24 Months	Involved	-22.30	-43.04	-2880	-2109
	Uninvovled	-23.82	-29.71	-2506	-2025

Results and Discussion

Six months after ACLR, the involved limb displayed lower peak Von Mises stresses (vs. uninvolved) in 3 of the 5 regions. These lower stresses correspond with less load in the involved limb (vs. uninvolved). Twenty-four months after ACLR, the involved limb displayed higher peak Von Mises stresses (vs. uninvolved) in all 5 regions. However, the reduction in the uninvolved limb's MCF may explain the between limb differences seen at 24 months. The involved limb stresses (like its MCF) remained relatively consistent between times while the uninvolved stresses decreased with time. Interestingly, the notable exception to this occurred in the central medial region, where osteophytes typically develop. Future work should explore a larger sample size.

Significance

This model is the first step towards understanding how stresses change within the knee joint after ACLR, which may provide insight into why OA is developing after this procedure.

Acknowledgments

NIH R01-HD087459

References

[1] Wellsandt 2016 [2] Manal 2013 [3] Rodriguez-Vila 2017.

COUPLING PATTERNS OF THE CERVICAL SPINE: ALTERATIONS ASSOCIATED WITH NECK PAIN

Craig C. Kage, Zachary Eenhuis, Paul Glowacki, Joseph Kagan, Andrew Kezar, Sara Lieven, Arin M. Ellingson
[1]Department of Rehabilitation Medicine, University of Minnesota
email: *ellin224@umn.edu

Introduction

Neck pain is a common musculoskeletal affliction, ranking second only to LBP in annual workers' compensation costs and representing 25% of outpatient physical therapy patients [1]. In the general population, annual prevalence of neck pain is between 30-50% and 67% of people suffer from neck pain at some point in their life [2, 3]. It is currently unknown if abnormal coupling patterns of the cervical spine have a role in creating or contributing to neck pain. This study gives insight into cervical kinematics in individuals with and without neck pain to see if abnormal coupling patterns in the cervical spine are associated with neck pain. The objective of the study was to observe the head-to-torso kinematics and coupling patterns of lateral bending (LB) and axial rotation (AR) of the cervical spine during both LB and AR tasks in individuals with and without mechanical neck pain (MNP).

Methods

After IRB approval and informed consent, 11 participants (6F, 5M) were included; four healthy controls (27.8±3.3 years) and seven individuals with neck pain (28.0±7.6 years) lasting >12 weeks. Head-to-torso kinematics were acquired via optical motion capture (Vicon, UK) and exported using TheMotionMonitor xGen software. Participants completed full range of motion (ROM), left-right-left, of LB and AR in a seated position to the rhythm of a 50 bpm metronome. Three trials were completed for each motion. Coupling ratio and ROM were averaged across the three trials for each motion. The coupling ratio was calculated as a percentage of the maximum/minimum associated component motion relative to primary motion (LB or AR). T-tests were performed in SPSS.

Results and Discussion

The results indicate similar ROM between healthy (LB:85.1±11.8; AR:132.5±7.0) and MNP (LB:96.4±14.9; AR:143.9±15.5) participants, with MNP individuals on average having slightly more ROM. The results also indicate that despite having similar ROM, the MNP group had reduced coupling compared to the healthy individuals – including significantly less extension coupling for both LB and a trend during AR motions.

During AR, AR was coupled with ipsilateral LB and extension. During LB, LB was coupled with ipsilateral AR and extension. These results are displayed in Figure 1.

Symptomatic participants had a tendency to display less coupling than asymptomatic individuals. This observation may be attributed to fear avoidance behaviors in individuals with chronic neck pain, secondary muscle tightness, or aberrant motion. Further studies into coupling motion are needed to investigate this pattern, as treatment for patients with mechanical neck pain typically includes neuromuscular re-education in efficient coupling motion.

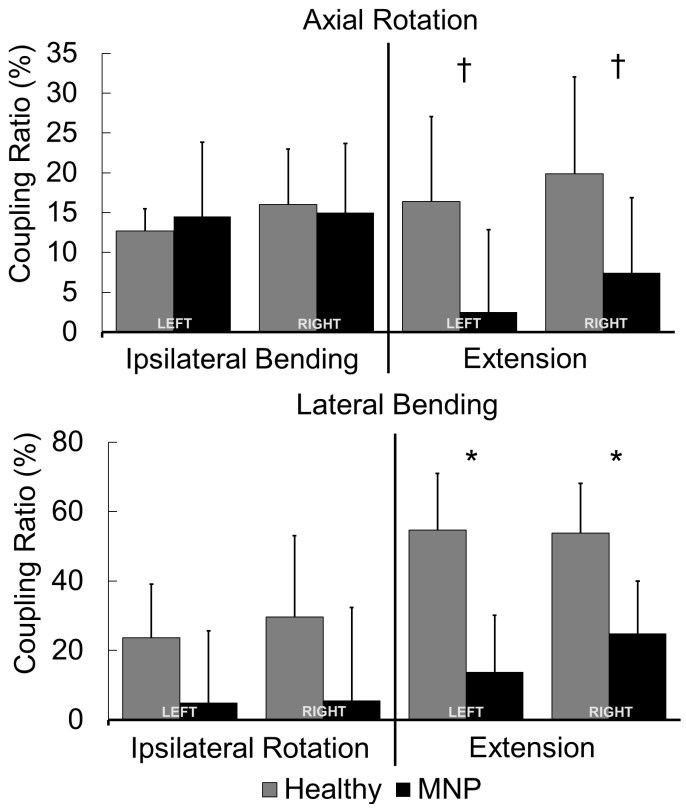

Figure 1: Coupling ratio (percentage) of component motions for Axial Rotation (top) and Lateral Bending (bottom) tasks. (*indicates $p < 0.05$ and † indicates $p < 0.10$)

Significance

It is well known that coupled motion plays a significant role in cervical kinematics; however, it remains unclear as to how these motions are influenced by the presence of cervical neck pain. By further understanding this relationship between coupled motion and cervical neck pain - as supported by the data shown in this study - clinicians may be able to more accurately identify movement strategies of the cervical spine in order to evaluate and diagnose patients without the need for costly, complex medical equipment. Furthermore, this approach focuses on the functional movements of the cervical spine rather than base their interventions around a structural, anatomical approach [4].

Acknowledgments

NIH/NICHD R03HD09771, NIH/NIAMS T32AR050938, and a Promotion of Doctoral Studies (PODS II) Scholarship from the Foundation for Physical Therapy.

References

[1] Jette et al. *Phys Ther* 1994. [2] Haldeman et al. *J Occup Environ Med* 2010. [3] Cote et al. *Pain*. 2004 [4] Van Dillen et al. *J Orthop Sports Phys Ther*. 2003

MOVEMENT CONTROL OF UPPER LIMB PROSTHESIS USERS DURING GOAL-DIRECTED REACHING

Christina Lee[1], Michael A. Gonzalez[1], Matthew B. Mulligan[1], Jiyeon Kang[2], Deanna H. Gates[1]
[1]University of Michigan, Ann Arbor, MI
[2]University at Buffalo, Buffalo, NY
Email: chslee@umich.edu

Introduction

While it is understood that using an upper limb prosthesis can be challenging, only a few studies have experimentally quantified prosthetic movements. One study demonstrated that prosthesis users are able to adapt to force-field perturbations and minimize their peak error while reaching to spatial targets [1]. However, the employed strategy to accomplish these tasks with a prosthesis may differ from that with an anatomical limb. For instance, prosthesis users compensate for the lack of distal joint motion with increased motions of the trunk and shoulder [2]. In goal-directed movements, redundancy in the body allows healthy individuals to perform a task reliably while varying their movements in a way that maintains low variability near the goal. It is unknown whether prosthesis users are able to exploit this variability to the same extent healthy individuals do. With previous studies demonstrating prosthesis users' ability to alter their strategy to accomplish a given task, it is reasonable to expect changes in prosthetic movement variability. These changes likely have important implications on effort towards movement control and overall task performance. Given the lack of degrees of freedom, we expected that prosthesis users will have difficulty exploiting movement variability and make movements with greater errors. Alternatively, they could maintain overall task *performance*: i.e. they could continue to achieve the goal by changing their movement control. The purpose of this study was to examine movement control of upper limb prosthesis users during a repetitive goal-directed reaching task.

Methods

Nine upper limb prosthesis users and eight healthy controls participated. Participants completed constrained and planar goal-directed movements using a custom-built reaching device with a two-link robotic arm. They were harnessed in a chair to reduce trunk motion and instructed to make horizontal excursions with the robotic arm handle to synchronize movement timing with the metronome. These movements were visualized as a circle on the computer screen. Participants completed 300 goal-directed reaches at each of the three target metronome frequencies – 1, 1.5, and 2 Hz. They repeated the experiment with both limbs.

Means and standard deviations of movement distance (D), speed (S), and timing errors (E) were calculated as measures of task performance. E was the time difference between each maximum excursion to its nearest metronome signal. Similar to [3], movement variability was analyzed by recognizing that the primary *goal* of this task was to maintain movement time, which can be achieved by multiple (D, S) combinations, defining the Goal-Equivalent Manifold (GEM) for the task. We decomposed movement variability into those perpendicular (δ_P) and tangent to (δ_T) to the GEM, which represent goal-relevant and goal-irrelevant variability, respectively. We quantified movement control through the scaling component, α, calculated from detrended fluctuation analysis [3]. Lower α values indicate a more tightly controlled process where deviations are more quickly corrected. We compared the mean, variability, and α of outcome measures using a linear mixed model with limb type and frequency as fixed factors and participants as a random factor.

Results and Discussion

Mean and variability (standard deviation) of D, S, or E were not affected by limbs ($p < 0.053$) but were affected by goal frequency ($p < 0.001$). Deviations in S were corrected more quickly (smaller α) for prosthetic limbs than for anatomical limbs ($p = 0.024$). All participants aligned their movements with the GEM such that δ_P was much smaller than δ_T. There were no differences in mean δ_T and δ_P between limbs ($p > 0.191$). There was greater variability of δ_P for prosthetic limbs than anatomical limbs ($p = 0.018$). δ_T was more tightly controlled with prosthetic limbs compared to anatomical limbs ($p = 0.014$).

On average, movements made with prostheses were similar to those made with anatomical limbs. However, participants made more rapid corrections with prostheses than with anatomical limbs. This suggests that prosthesis users had similar performance and chose movement patterns similar to those of healthy controls. However, this required more rapid corrections and may therefore be more effortful.

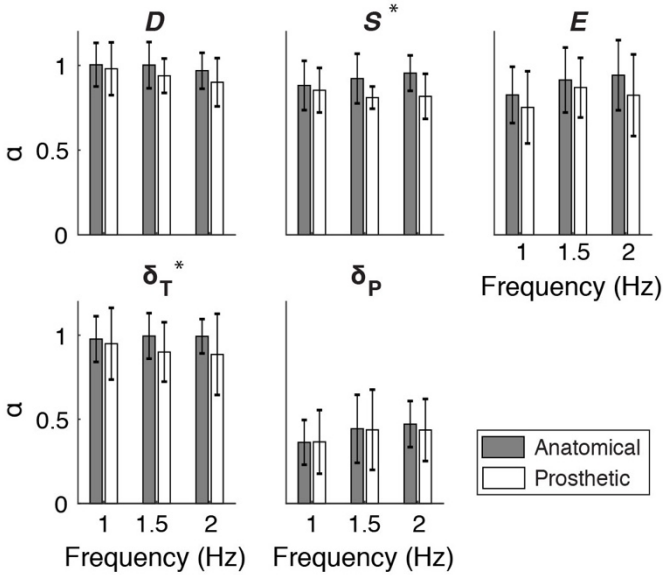

Figure 1: α values of D, S, E, δ_T, and δ_P between anatomical and prosthetic limbs. * denotes statistically significant limb differences.

Significance

Using a prosthesis did not reduce movement variability or affect overall task performance, which required more effortful movement control. Future work should expand on this work with increased sample size to continue to evaluate movement control in upper limb prosthesis users.

Acknowledgments

Thank you to Kelsey Ebbs. This work was supported by CDMRP grant number W81XWH-16-1-0648.

References

[1] Schabowsky et al. (2008). *Exp Brain Res*, **188 :** 589-601.
[2] Major et al. (2014). *J Neuroeng Rehabilitation*,**11**: 1-10.
[3] Gates et al. (2008). *Exp Brain Res*, **187**: 573-585.

SEVEN SEGMENT FOOT MODEL ANATOMICAL LANDMARK CALIBRATION PRECISION

Stephen C. Cobb[1], Mohammed S. Alamri[1], and Chloe R. Glubka[1]
[1]Department of Kinesiology, University of Wisconsin-Milwaukee, Milwaukee, WI, USA
Email: cobbsc@uwm.edu

Introduction

Use of multi-segment foot models to assess foot function during various forms of gait is becoming increasingly common. When using a model, researchers must decide whether to offset the joint angle positions captured to a reference position. If the foot posture of the population being investigated is not typical and/or cannot be positioned in a neutral position, offsetting the reference position may mask important between group gait differences. Precise anatomical landmark location is important with either decision, however, it is especially critical if offsets are not used, and gait will be assessed on more than one occasion and/or by different researchers. A number of studies have investigated the reliability of multi-segment foot model gait patterns [1-3], however, few have investigated foot anatomical landmark precision [4,5]. The purpose of the current study was to investigate the within- and between- tester anatomical landmark precision associated with a seven segment foot model [3].

Methods

Five healthy adults (2 f, 3 m; age: 23.4 ± 8.2 y; BMI: 23.7 ± 8.7 kg/cm^2; US shoe size: 8.1 ± 2.9) provided written inform consent and participated in the study. The foot model includes identification of 21 anatomical landmarks that are used to define seven segments and six functional articulations (rearfoot, medial midfoot, lateral midfoot, medial forefoot, lateral forefoot, first metatarsophalangeal) (Figure 1, Table 1).

To assess between-tester precision, a tester identified all the anatomical landmarks and captured the marker positions during a seated calibration procedure using a 14-camera motion capture system. All skin marker markings were removed and a second tester completed the procedures. To assess within-tester precision, the procedures were repeated on each participant on a separate day.

Within- and between- tester precision was calculated as the root mean square of the deviation between anatomical landmark positions in a trial, and the landmark's mean position within each segment's local coordinate system [4].

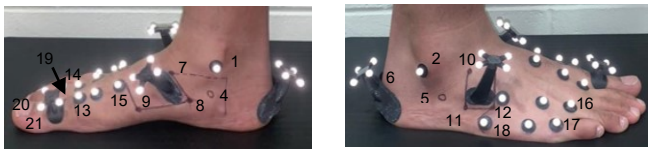

Figure 1: Anatomical landmarks: **Shank** [medial malleolus (1), lateral malleolus (2), tibial tuberosity (3, not pictured)]; **Calcaneus** [sustentaculum tali (4), peroneal tubercle (5), dorsal proximal (6)]; **Navicular** [dorsal proximal (7), plantar proximal (8), plantar distal medial cuneiform (9)]; **Cuboid** [dorsal proximal (10), plantar proximal (11), plantar distal (12)]; **Medial rays** [1st metatarsal head (13), 2nd metatarsal head (14), 1st metatarsal base (15)]; **Lateral rays** [4th metatarsal head (16), 5th metatarsal head (17), 5th styloid process (18)]; **Hallux** [proximal phalanx base (19), distal phalanx head (20), medial aspect (21)].

Results and Discussion

Within- and between- tester precision for most anatomical landmarks was < 2 mm (Table 1). Location was least precise for the shank in general, and the tibial tuberosity specifically. Within- tester precision of landmarks in the current study, that were common to those of a previous study [4], were similar for the shank (malleoli, tibial tuberosity) and improved for the foot (dorsal calcaneus, 1st, 2nd, 5th metatarsal heads). Between-tester precision was generally better in the current study.

Table 1. Mean Anatomical Landmark Precision (mm)

		Within-tester			Between-tester		
Seg	**Landmark[a]**	**x**	**y**	**z**	**x**	**y**	**z**
Shank	Med Mal[b]	1.4	1.9	0.7	1.1	1.9	1.1
	Lat Mal[b]	1.6	2.0	0.7	1.2	1.7	0.8
	Tib Tub[b]	3.0	3.5	0.7	2.3	3.3	1.0
Calc	Sust Tali[c]	0.4	1.2	0.9	0.7	2.8	0.8
	Peron Tub[c]	0.4	0.9	1.1	0.7	1.6	1.1
	Dorsal Prox[b]	0.6	0.7	1.5	0.6	1.3	1.3
Nav	Dorsal Prox[c]	0.3	0.7	0.6	0.3	1.7	1.7
	Plantar Prox[c]	0.5	1.0	0.5	0.4	1.6	0.9
	Distal Prox[c]	0.4	1.1	0.8	0.4	1.6	0.9
Cub	Dorsal Prox[c]	0.6	0.5	0.6	0.6	0.9	0.7
	Plantar Prox[c]	0.3	0.4	0.5	0.3	1.2	0.7
	Plant Dorsal[c]	0.5	0.6	0.5	0.4	0.8	0.5
Medial rays	1Met Head[c]	0.5	1.1	0.3	0.8	1.9	0.1
	2Met Head[c]	0.7	1.2	0.4	1.5	1.0	0.3
	1Met Base[c]	0.4	1.2	0.4	0.7	1.8	0.2
Lateral rays	4Met Head[c]	0.5	1.0	0.3	0.8	1.3	0.1
	5Met Head[c]	0.5	1.0	0.4	0.4	1.3	0.4
	5Met Base[c]	0.8	0.6	0.5	0.7	1.3	0.3
Hallux	Prox Phlx[c]	0.8	0.7	0.6	0.7	1.0	0.4
	Distal Phlx[c]	0.7	0.7	0.5	0.6	1.2	0.4
	Medial Hal[c]	0.3	0.5	0.5	0.8	1.1	0.2

[a] See figure 1 for full segment names
Identified using a 6.4 mm marker [b] or a digitizing pointer [c]

Significance

The anatomical landmarks associated with the seven-segment foot model can be precisely placed and reconstructed within- and between- testers. Even with the high level of landmark precision, between-tester precision of the local coordinate system axis orientations and the calibration position joint angles varied between 0.6 – 7.3° and 1.6 – 8.2°, respectively. This suggests that detailed application procedures and training are critical when using the model.

References

[1] Long, J. et al. 2010. *Gait Posture*, 31 (1): 32–6.
[2] van Hoeve, S. 2015. *Clin Res Foot & Ankle*, 03(02).
[3] Cobb S. et al. 2016. *J Appl Biomech*, 32 (6): 608–613.
[4] della Croce, U. 1999. *Med Biol Eng Comput*, 37(2): 155–61.
[5] Rabuffetti, M. 2002. *Hum Mov Sci*, 21 (4): 439–55.

Excessive Femoral Anteversion Increases Joint Reaction Forces in Dysplastic Hips

Molly Shepherd[1], Brecca M.M. Gaffney[1], Ke Song[1], John C. Clohisy[2], Michael D. Harris[1,2,3]
[1]Program in Physical Therapy, [2]Dept of Orthopaedic Surgery, [3]Dept of Mechanical Engineering and Materials Science
Washington University in St Louis, St Louis, MO, USA
Email: mollycshepherd@wustl.edu

Introduction

Developmental dysplasia of the hip (DDH) causes intra-articular damage, and early development of osteoarthritis.[1] Joint damage is mediated by abnormal bony anatomy and high muscle-induced joint reaction forces (JRF).[2] The main focus on altered mechanics in DDH has been on the consequences of having a shallow acetabulum. Femoral deformities are common in DDH, but their influence on joint biomechanics is poorly understood. We recently found femoral version (FV) to be highly variable in DDH,[3] but its implications for joint loading remain unknown. The objective of this study was to apply probability analysis and musculoskeletal modeling to determine the influence of FV deformities found in DDH on hip JRFs during gait.

Methods

With IRB approval, 15 female patients (aged 16-39, BMI 22.7±2.4 kg/m²) with DDH (lateral center edge angle of the acetabulum <20°) were included.[4] A baseline OpenSim musculoskeletal model was updated with 3D reconstructions of subject-specific pelvis geometries and hip joint centers from MRI,[2,5] and scaled femur geometries with normal femoral version (15° anteversion). A custom joint was added to each femur immediately distal to the lesser trochanter to vary FV within an input range of clinically reported FV deformities from excessive anteversion (35° FV) to retroversion (-5° FV).[6] For each patient, 2,000 Monte Carlo simulations were performed using high throughput computing to assess the influence of FV deformities within the input range on hip JRFs (A/P, S/I, M/L, resultant) during gait.[7] Subject-specific joint angles and ground reaction forces were used from marker-based experimental motion capture data. Muscle and joint reaction forces were calculated during a representative gait cycle on the symptomatic limb using computed muscle control. Sensitivity factors between peak JRF and FV values were calculated using Pearson correlation factors (strong: $r \geq 0.6$)[8] and used to predict the effect of a ±15° change in FV relative to baseline(+ = anteversion, - = retroversion) on hip JRF. 99% confidence bounds were used to establish the range of muscle forces in early (JRF1) and late (JRF2) stance.

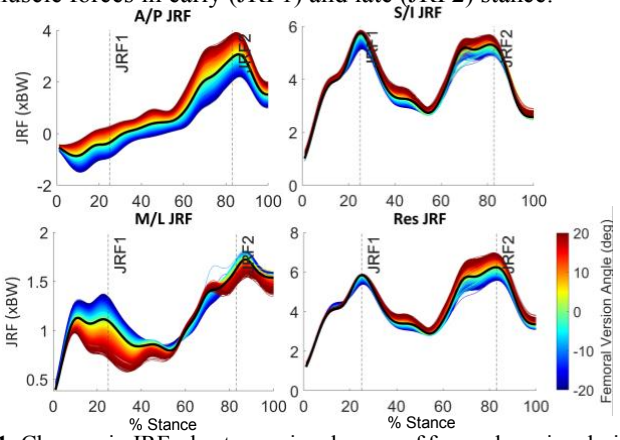

Figure 1: Changes in JRFs due to varying degrees of femoral version during stance phase of gait for a representative subject.

Results and Discussion

All hip JRFs were strongly sensitive to FV variability. A 15° increase in anteversion relative to baseline *increased* the anterior, superior, and resultant JRF components at JRF1 and JRF2, with the largest increase in the anterior component (JRF1: 0.47±0.17xBodyWeight (xBW); JRF2: 0.71 ±0.18) (Fig. 1). Increased anteversion increased the rectus femoris and tensor fascia latae forces at both JRF1 and JRF2 but decreased the anterior gluteus medius relative to baseline at JRF1 (Fig. 2). Increased retroversion had effects opposite to anteversion.

Our results established that increased femoral anteversion increased hip JRFs in early and late stance of gait. The largest change occurred in the anterior direction and during late stance, likely due to larger muscle force contributions from altered hip moment arms. Increased anterior loading could contribute to anterosuperior acetabular cartilage/labral damage common in patients with DDH, and is therefore important to consider when planning surgical treatment for patients with DDH and increased anteversion.[9] Future work will quantify the consequences of surgical intervention for FV in patients with DDH.

Significance

Quantifying the biomechanical influence of femoral deformities, in combination with acetabular deformities, may help explain mechanisms of damage reported in DDH from both sides of the hip joint for improved joint preservation against osteoarthritis.

Acknowledgments

Funding provided through ASB Junior Faculty Research Award and NIH K01AR072072.

References

[1] Murphy SB et al. (1995). *J Bone Jt Surg,* **77**: 985-89. [2] Harris MD et al. (2017). *J Biomech,* **54**: 80-87. [3] Lerch TD et al. (2017). *CORR,* **475**: 1154-68. [4] Gaffney BMM et al. (2019). *J Ortho Res,* **37**: 665-73. [5] Delaunay S et al. (1997). *Skeletal Radio,* **26**: 75-81. [6] Seitlinger G et al. (2016). *Am J. Sport Med,* **44**: 1796-1800. [7] Lai AKM et al. (2017). *Ann Biomed Eng* **45**: 2762-74. [8] Laz PJ et al. (2010). *J Eng Med* **224**: 927-43. [9] Gaffney BMM et al. (2020). *J Biomech* **98**. [10] Tamura S et al. (2013). *Bone Jt J.* **95**: 1320-25.

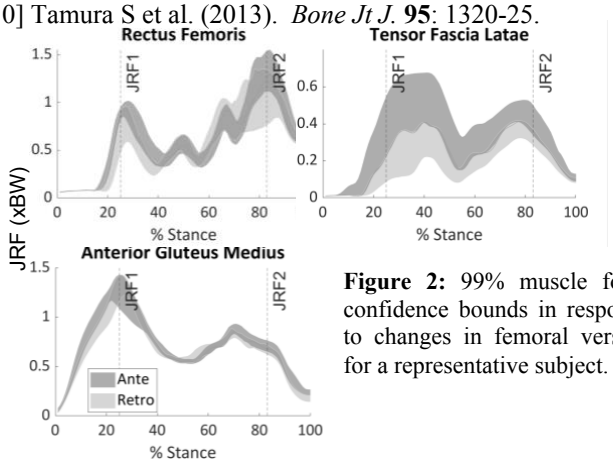

Figure 2: 99% muscle force confidence bounds in response to changes in femoral version for a representative subject.

ROCK CLIMBING SPECIFIC ISOMETRIC GRIP STRENGTH IN TWO HAND POSITIONS

Emily Higgins,[1] Lena Parker,[1] Johnathon Crawley,[1] Stephanie Huang,[1] Claire Lorbiecki[1], Shawnee Wood,[1] Kevin Cowell,[2] Erika Nelson-Wong[1]
[1] Regis University School of Physical Therapy, [2] The Climb Clinic
Mail: ehiggins001@regis.edu

Introduction

In recent years technical rock climbing has become an increasingly popular sport spurred by its introduction into the Olympics, increasing prevalence of indoor rock climbing gyms, and high profile films covering the sport. Rock climbing places unique demands on the finger flexors, tendons, and ligaments of the hands. Climbers must adapt their shoulder, hand and finger positions according to the features of the terrain they are ascending, and occasionally must make decisions about which grip is optimal to use. The two most common grip types are open hand, used for broad holds, and a crimp, which is used for smaller holds.[1]

A number of studies have sought to quantify the grip strength required to rock climb via handheld dynamometry.[2] This poses a problem in that there is a lack of activity specificity in position of grip tested. Handheld dynamometry focuses on a hook or power grip with a standardized arm position, whereas climbing requires various arm positions and sport specific grip choices. Therefore, this measurement tool is limited in its ability to quantify a true measurement of climbing specific grip strength. The development of a climbing-specific rig is critical to obtaining accuracy in quantitative strength measures that will be meaningful for climbers.

The purpose of this study is to observe if there is a difference in force produced between using an open hand grip and a half crimp grip during a maximal isometric pull. We hypothesize that there will be no difference in force between the two grip types.

Methods

Thirteen participants (8 female, 5 male) between the ages of 19 and 33 have participated in this study at time of abstract submission. Study protocol was approved by the Regis University IRB and informed consent obtained from all participants. Climbing skill and experience level were documented via questionnaire. After a standardized warm up, participants completed a maximum pull testing protocol with a test rig consisting of a wood climbing hold (Tension, The Block, Denver, CO, USA) with a 20 mm lip attached to a load cell (Exsurgo gStrength, Sterling, VA, USA) with force data sampled at 250 Hz.

Participants were asked to pull with the two grip types; an open grip, with the 2nd-4th digits of the DIP and PIP joints greater than 90º, and half crimp, where the 2nd-5th digits of the PIP joints are at 90º. Participants were positioned with shoulder flexion at 90º.

Participants were instructed to "ramp up" to maximal isometric pull, and hold 3-5 seconds. The testing protocol was randomized with two-minute rest intervals between each pull. A total of 8 trials (4 for each hand grip, and 2 trials per side) were performed. Paired t-tests revealed no differences between left/right hands or between trials, therefore these data were averaged to yield 1 value for each hand position as a data reduction measure. Peak force measures were normalized to participants' body weight (% BW) and entered into paired t-tests to explore differences between the 2 hand positions.

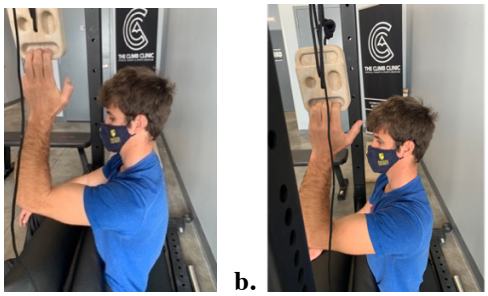

a. **b.**

Figure 1: Participant demonstrating the a) open grip hold, and b) half crimp hold in 90º of shoulder flexion.

Results and Discussion

Based on the preliminary data, there were significant differences in strength between the open hand (51.9 ± 0.12 %BW) and half crimp position (56.9 ± 0.13 %BW). These initial findings show that rock climbers can pull with more force using a half crimp grip than an open hand grip.

These results are consistent with a previous study which found that a crimp style grip generates more flexion force than an open hand grip. This may be explained by the different muscle recruitment patterns of flexor digitorum superficialis (FDS) and profundus (FDP). FDP has been found to be the main flexor used in both grips, with FDS more active in grips similar to the half crimp.[3] In a half crimp grip, FDS is not needed as a PIP stabilizer and therefore, may contribute more effectively to overall force. With more direct contribution from FDS, climbers may be able to generate higher forces with a half crimp versus open hand grip.

Significance

The methodology used in this study closely mimics climbing specific grips, and therefore can more accurately guide clinicians or strength coaches working with rock climbers. It can be implemented into a protocol as a baseline measure of finger flexor strength or used as a measure of change, showing the effectiveness of intervention in both a rehabilitative and strength training setting. These results indicate it will be important to assess both grip positions as they are likely to yield different strength values and these differences may guide future training.

References

1. Cooper C, LaStayo P. A potential classification schema and management approach for individuals with A2 flexor pulley strain. *J Hand Ther* 2020;33(4):598-601.

2. Watts PB. Forearm EMG during rock climbing differs from EMG during handgrip dynamometry. *Int J Exerc Sci*. 2008;1:14–13.

3. Schweizer A, Hudek R. Kinetics of crimp and slope grip in rock climbing. *J Appl Biomech*. 2011;27(2):116-121.

CHANGES IN SHOULDER ACTIVITY AFTER ROTATOR CUFF REPAIR AND ASSOCIATIONS WITH AGE AND TEAR SIZE

Matthew C. Ruder[1], B.J. Diefenbach[1], R. Zauel[1], and M.J. Bey[1]
[1]Bone and Joint Center, Department of Orthopaedic Surgery, Henry Ford Health System, Detroit, MI
email: matthew.ruder@gmail.com

Introduction

Approximately 250,000 rotator cuff repairs are performed in the U.S. each year, but an estimated 20-60% of these repairs fail [1]. Factors that negatively impact repair tissue healing include age, tear size, and fatty degeneration, but these factors do not fully explain the high incidence of failed repairs. Tissue healing is also influenced by mechanical loading, with excessive shoulder activity after repair identified as a risk factor for failed repairs [3]. However, complete removal of loading is also detrimental to healing, suggesting there is an "appropriate" level of activity for optimal healing [4]. Unfortunately, the appropriate level of activity necessary to enhance healing in humans is unknown. Furthermore, the extent to which age and tear size influence post-operative activity levels is not known. Thus, the objectives of this study were to: 1) characterize changes over time in activity levels after rotator cuff repair, and 2) evaluate the extent to which age and tear size are associated with post-operative activity.

Methods

Following IRB approval, 25 patients (6 F, age: 59.1 ± 8.7) who had undergone rotator cuff repair were recruited for this study. Triaxial acceleration data (GENEActiv Original, ActiveInsights) were collected continuously at 10Hz for a week on the patient's ipsilateral wrist of their repaired shoulder. Patients were recruited at one of the following timepoints: 1-2 weeks (n=11), 6-7 weeks (n=13), or 12-13 weeks (n=7) post-surgery; data were collected from five patients at 1-2 weeks and 6-7 weeks. The acceleration data were calibrated to 1 *g* (i.e., acceleration due to gravity) [5], and total acceleration was calculated as the Euclidean norm of the acceleration signals minus 1 *g* [6]. Volume of activity was estimated by calculating mean acceleration and intensity of activity was estimated by calculating the intensity gradient [7]. Associations between shoulder activity (mean acceleration, intensity gradient) and time post-surgery, age, and tear size were assessed independently with linear regression and correlation. Statistical significance was set at $p \leq 0.05$ for all tests.

Results and Discussion

Time post-surgery was significantly associated with mean acceleration (Fig. 1, r=0.61, p<0.001) and intensity gradient (r=0.59, p<0.001). Age was associated with mean acceleration (r=0.84, p<0.001) and intensity gradient (r=0.67, p<0.02), but only at the first post-operative timepoint (weeks 1-2). Tear size was not associated with mean acceleration (p>0.12, Table 1) or intensity gradient (p>0.23, Table 1).

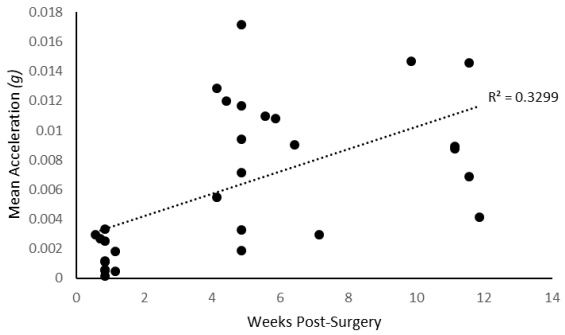

Figure 1: Time post-surgery was associated with the volume of shoulder activity (r=0.61, p<0.001). Each circle represents an individual patient.

These preliminary data demonstrate the feasibility of using a wearable sensor to monitor and detect changes over time in shoulder activity after rotator cuff repair. It was not surprising that the volume and intensity of shoulder activity were associated with time post-surgery (Fig. 1), because post-operative rehabilitation protocols typically prescribe a gradual progression of increasing activity over the first 12 weeks post-surgery. The lack of association between tear size and shoulder activity, coupled with the high variability between patients in shoulder activity at the second (6-7 weeks) and third (12-13 weeks) timepoints, suggests that there may be opportunity to improve outcomes by more carefully calibrating post-operative activity levels to tear size. This on-going study will continue to investigate the relationship between post-operative activity levels and repair tissue healing after rotator cuff repair.

Significance

Quantifying the volume and intensity of shoulder activity after rotator cuff repair and relating these data to measures of repair tissue healing may help identify appropriate levels of activity necessary to optimize healing and reduce failed repairs.

References

[1] Rossi, et al. JBJS Rev 8(1), 2020
[2] Hattrup SJ, JSES 4(2), 95-100, 1995
[3] Chen, et al. AJSM 48(4):931-8, 2020
[4] Killian, et al. JSES 21(2):228-37, 2012
[5] van Hees VT, et al. J Appl Physiol 117(7):738-44, 2014
[6] van Hees VT, et al. PLoS One 8(4), 2013
[7] Rowlands, et al. MSSE 50(6):1323-32, 2018

	Time Post-Surgery		Age						Anterior/Posterior Tear Size					
			Week 1-2 (n=11)		Week 6-7 (n=13)		Week 12-13 (n=7)		Week 1-2 (n=11)		Week 6-7 (n=13)		Week 12-13 (n=7)	
	r	p	r	p	r	p	r	p	r	p	r	p	r	p
Mean Acc.	0.59	*0.001*	0.84	*0.001*	0.52	*0.07*	0.55	0.20	0.49	0.12	0.01	0.96	0.06	0.90
Intensity Grad.	0.84	*0.001*	0.67	*0.02*	0.37	0.22	0.12	0.80	0.39	0.23	0.26	0.38	0.13	0.79

Table 1: Associations between shoulder activity and patient characteristics.

MUSCULOSKELETAL SIMULATION PERFORMANCE IN OPENSIM MOCO USING PARALLEL COMPUTING

Alex N. Denton, and Brian R. Umberger
Locomotion Research Laboratory, School of Kinesiology, University of Michigan, Ann Arbor, MI.
email: umberger@umich.edu

Introduction

Musculoskeletal modeling and computer simulation is a valuable research approach capable of providing novel insights about human movement. The substantial computational cost of musculoskeletal simulation[1] has been reduced, in part, through algorithmic developments such as the direct collocation formulation. OpenSim Moco[3] is a new tool that streamlines the use of direct collocation, facilitating analyses such as bilevel optimization[4] and Monte Carlo methods, where each iteration involves solving a full optimal control problem. In these situations, computational efficiency is a major limiting factor.

OpenSim Moco uses the CasADi[2] library to evaluate the objective and constraint equations in parallel on multicore processors. Processors with dozens of cores are now available in mainstream computers, but come at a financial cost. The potential for parallel computing to reduce execution time is problem-specific. There is overhead in parallelizing a problem, such that using more cores beyond a certain point can lead to no further speedup, or even a reduction in computational performance. Understanding these issues allows computational scientists to select algorithms and computer architectures that best match their simulation problems.

Thus, the purpose of this study was to investigate: 1) the computational performance of generating optimal control simulations of human walking with OpenSim Moco employing different numbers of processor cores in the parallelization, and 2) how the parallel computing performance interacts with the temporal mesh density and the type of initial guess used.

Methods

Tracking simulations of walking (1.3 m/s) were generated using OpenSim Moco with a planar model consisting of 9 segments, 11 degrees of freedom, and 18 musculotendon actuators (nine per limb)[4]. The goal of the objective function was to minimize the tracking error and control effort. A range of processor cores (1, 3, 6, 9, 12, 15, 18) and mesh interval densities (5, 25, 50, 100) were selected to solve the problem. The step duration (0.54 s) was divided into n temporal mesh intervals, resulting in $2n+1$ collocation nodes. The entire process was run using two different types of initial guesses: a dynamically consistent guess (CG) that was not close to the final solution, and a mesh refinement (MR) strategy, whereby the solution at a particular mesh density (e.g., 5) was used as the initial guess for the next mesh density (e.g., 25). Analyses were run on a computer with an Intel 2.2 GHz Xeon 18-core processor and 64 GB of RAM.

Results and Discussion

The CG and MR approaches converged to the same solutions (Fig 1E), which were consistent from 25-100 intervals. The runtime for MR was substantially shorter than CG (Fig 1A & B), though the parallel speed-up was similar (Fig 1C & D). The shorter runtimes for MR were due entirely to fewer iterations (Fig 1F), while the parallel speed-up was due to less time per iteration (being cut almost in half for 18-cores/100 intervals).

There was no benefit to parallel computing for the coarsest mesh (5 intervals, Fig 1C & D). For the finer meshes (25-100 intervals), the parallel speed-up was greatest between 3-9 processor cores, with little or no benefit between 9-18 cores. In fact, most of the improvement was obtained by 3 cores, and the speed-up was far from linear beyond that point. In some cases, computation cost increased beyond 12 processor cores. As an example of how this type of information is useful, for this problem one could obtain essentially the same solution (same objective function value) using MR at 25 mesh intervals with 9 cores as would be obtained using CG at 100 intervals on 1 core, in less than 1/10th of the time.

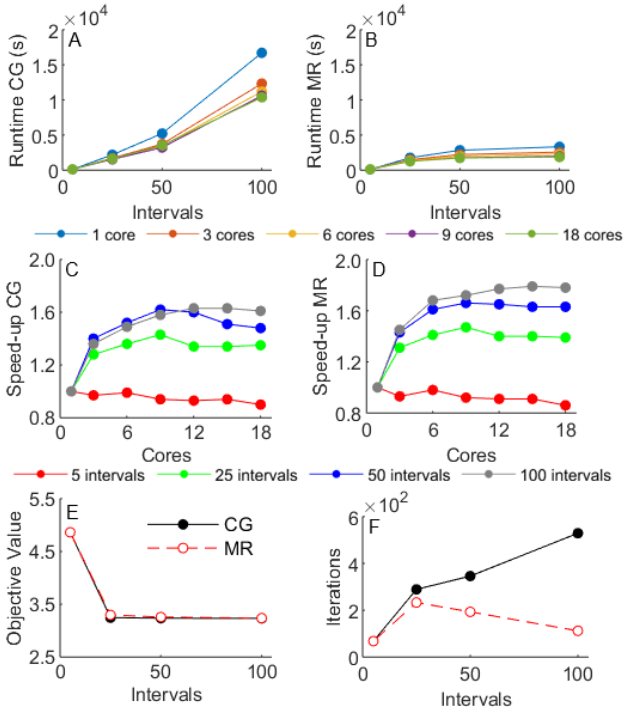

Figure 1: Simulation runtimes across temporal mesh intervals were substantially longer using the CG (A) compared with the MR approach (B). The speed-up factor was similar for CG (C) and MR (D) with little to no benefit beyond 9 processor cores. The objective function value was lower at 25 nodes than 5 nodes, and was consistent between 25-100 nodes (E). The performance advantage of MR over CG was due to fewer iteration, with a greater difference on finer temporal meshes (F).

Significance

Maximizing computational performance requires matching hardware to software algorithms. Given limited financial resources, it would be better to purchase a fast processor with 10 or fewer cores than a slower processor with more cores for the problems considered here. The generality of this conclusion should be evaluated for different movements (e.g., running, jumping, reaching) and using larger-scale models.

References

1. Anderson F, Pandy M. (2001). J. Biom. Eng., 123, 381-390.
2. Andersson JAE et al. (2019). Math. Prog. Comp., 11, 1-36.
3. Dembia, C. et al. (2020). PLoS Comput Biol 16: e1008493.
4. Nguyen V. et al. (2019). IEEE TNSRE, 27, 1426-1435.

RELATIONSHIP BETWEEN FOREARM MUSCLE AND GRIPPING STRENGTH DURING HAND FLEXION-EXTENSION

Rifeng Jin[1*], Mehrdad Javidi[1], and Douglas J. weber[2]
[1]Department of Mechanical Engineering, Carnegie Mellon University, PA, USA
email: *rifengj@andrew.cmu.edu

Introduction

An adequate and comprehensive model is essential in determining dexterous and sophisticated hand activities during the control of motor units such as robot end-effector, assistive exoskeleton, or powered prosthesis. For instance, when operating a remote clinical surgery with the robotic arm, local subtle control of mechanical torque, momentum, and strength is necessary to avoid surgery accidents.

From the natural biomechanical system, hand motion is correlated with muscle activity and joint kinematics. Therefore, the overall control of motion torque, strength, and momentum can be better explained with muscle activity synergy and hand kinematic flexion rather than each of them alone [1].

In this study, Electromyography (EMG) of one hand flexor muscle was recorded during the same hand flexion-extension kinematics when gripping on a soft and hard material or without gripping objects. Clear differences in muscle activity during these simple and similar tasks show that the combination of EMG and force or motion sensors that currently used in robotic design will increase the accuracy of motion prediction models.

Methods

Three healthy volunteers participated in the experiment (three men), aged 24–32 years (median 27 years), and weight 62–98 kg (median 74 kg).

One DELSYS Avanti sensor was placed on Palmaris Longus (PL) muscle to measure EMG at the frequency of 2148 Hz. One short bending flexor sensor was placed on the digit finger to estimate the amount of hand flexion-extension level at the frequency of 159 Hz. Participants initially were asked to perform three maximum isometric contraction tasks under a fixed 20%, 60%, and 80% of hand flexion levels to find the maximum MVC value for each subject. They were then asked to perform 2 trials of 5 flexion-extension cycles for each of three tasks gripped on the strengthened tool, foam cube, or free motion within the same time period. In total, each subject has done 10 flexion-extension cycles for every task. For each flexion-extension cycle, gripping started with the same 0% hand flexion state, then flex to the 80% hand flexion state, and extend back to the original 0% hand flexion state with a total average cycle time period of 8 seconds.

EMG and flexion signals were normalized by MVC and calculated with respect to initial hand posture, respectively. Then, the averages of those parameters were calculated for every single cycle of all tasks from four subjects.

Results and Discussion

The mean±SD of muscle activities of PL muscle for all trials of all three subjects during hand flexion-extension while gripping a strengthened tool (blue), foam cube (green), or freely motion (red) is indicated in Figure 1A. The mean±SD of hand kinematics also is indicated in Figure 1B, which shows similar hand flexion-extension while performing all tasks with low variations.

Although the hand's kinematics is similar for all trials, there are differences in the EMG of muscle. As indicated in Figure 1A,

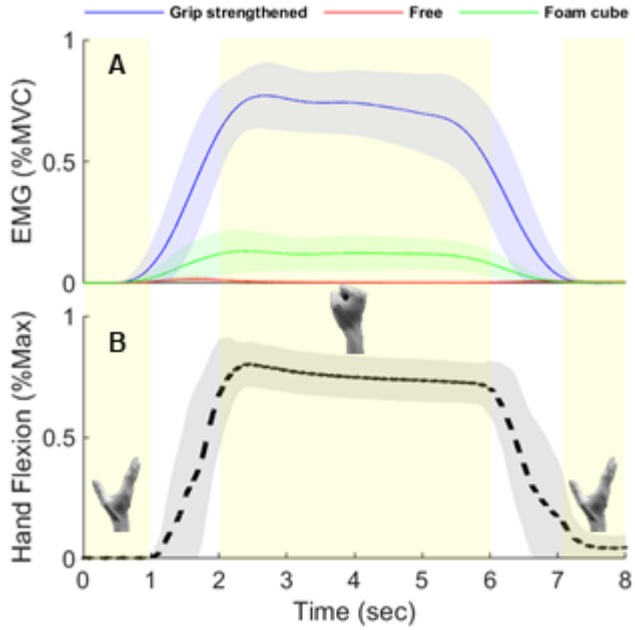

Figure 1: **A:** Mean±SD of EMG of all subjects during squeezing a grip stenghtened (blue) and foam cube (green), and free hand flexion (red). **B:** Mean±SD of hand flexion starts from fully extended, flexed maximally and finally extended to the initial posture.

the muscle activity during hand flex from fully extended posture to fully flexed posture (t=1 sec to 2 sec) is correlated with hand flex from fully flexed posture to fully extended (t=6 sec to 7 sec). Our results indicated that the gripping strength could be predicted independently of the hand kinematics while the operator's hand was in contact with objects and applied force (blue and green curves from t=1sec to t=7 sec). However, EMG activity alone is not able to predict gripping strength in those conditions when the operator performed free motion (red curve from t=1 sec to t=7 sec) or the hand was not in contact with the object to apply force. Thus, using the combination of EMG and kinematics of the hand would be essential for an accurate prediction of the operator's gripping strength while performing a motion.

Significance

High sensitivity force and position sensors combined with a threshold-based model are currently used to predict gripping strength while controlling an end effector. However, the threshold may vary among either subjects or performing tasks. Electromyography (EMG) of the forearm muscle can better refine the end-effector operation quality with sufficient control information since it is highly correlated with gripping strength.

References

[1] Charissou, Camille et al. "Effects of hand configuration on muscle force coordination, co-contraction and concomitant intermuscular coupling during maximal isometric flexion of the fingers" Eur J Appl Physiol (2017) 117:2309–2320

MEDIO-LATERAL COM DISPLACEMENT FOR OLDER ADULTS DURING A STAIR DESCENT ON CHALLENGING SURFACES

Christina M. Geisler, Nicholas L. Hunt, Amy E. Holcomb, Clare K. Fitzpatrick, and Tyler N. Brown
Department of Kinesiology, Boise State University, Boise, ID
email: christinageisler@u.boisestate.edu

Introduction

Falls are the leading cause of hospitalization in older adults (OA: over 65 years of age) and typically occur during activities of daily living, such as stair descent. For OA, descending stairs has one of the highest fall risks and rate of serious injury among daily activities.[1] An OA's compromised neuromuscular function, including decreased muscle strength, balance, and vision, leads them to walk slower with shorter, wider strides and exhibit deficits in postural stability, i.e, inconsistent or rigid COM control, than young adults (YA: 19-25 years of age) during activities of daily living.[2] Although OA present larger compensatory strategies to reduce the likelihood of falling, such as larger, faster and more variable medio-lateral (ML) COM displacement, their reduced neuromuscular function may further compromise their ability to successfully respond to external challenges, such as uneven or slick surfaces, when performing daily activities. Because little is known about how OA respond to challenging surfaces, this study determined the ML COM displacement for both OA and YA during a stair descent on a normal, uneven, and slick surface. We hypothesized that OA would exhibit a larger ML displacement than YA, and OA ML COM displacement would increase on the challenging surfaces.

Methods

Thirteen (6 young / 7 older) participants had ML COM displacement quantified during a stair descent on three surfaces (normal, uneven, and slick). For the stair descent, each participant performed three trials at a self-selected pace, where they walked down stairs (rise of 17.5 cm) onto a force platform. A different surface (normal, uneven or slick) was fixed on top of the force platform. During each trial, filtered (lowpass, 12 Hz, 4th order Butterworth) marker and GRF data were processed in Visual3D (C-Motion, Rockville, MD) to obtain ML COM displacement during stance phase (0% - 100%). The ML COM displacement was calculated as the maximum minus the minimum COM distance from the direction of progression exhibited during stance.[3] The COM was defined as the midpoint between right and left posterior superior iliac spines and direction of progression was defined as the vector connecting the COM position in the first and last frames of the trial, respectively.

For statistical analysis, ML COM displacement measures were submitted to a repeated measures ANOVA to test the main effect and interaction between surface (*normal, uneven, and slick*) and age (*young and older adults*). Bonferroni correction was applied to significant pairwise comparisons, and all analyses were performed in SPSS (v27, IMB, Armonk, NY). Alpha was denoted as $p < 0.05$.

Results and Discussion

Significant surface by age interactions for range ($p = 0.006$) and minimum ($p = 0.004$) ML COM displacement were observed (Fig. 1). But, no significant effect of surface or age was evident for maximum ML COM displacement ($p > 0.05$).

In agreement with our hypothesis, OA exhibited greater range of ML COM displacement than YA on all surfaces, but this difference was only significant on the uneven surface ($p = 0.016$). The OA exhibited a significant increase in ML displacement on the uneven compared to normal ($p = 0.022$) and slick ($p = 0.008$) surface, whereas, surface ($p > 0.05$) had no impact on YA ML displacement. Although OA exhibited a larger range of ML displacement than YA, particularly on the uneven surface, this may not lead to greater fall risk, as the OA did not exhibit a greater maximal ML displacement (COM movement away from the direction progression) than YA ($p = 0.354$).

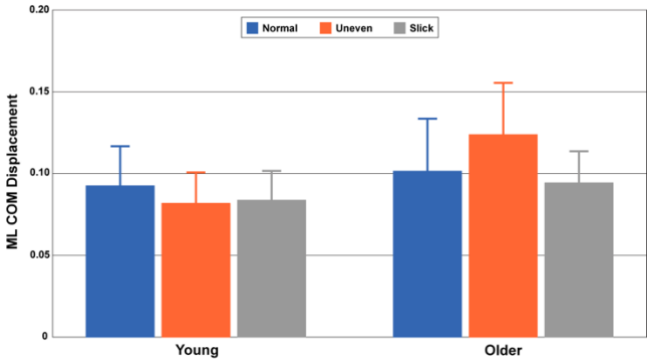

Figure 1: Mean ± SD range ML COM displacement for young and older adults during the stair descent on the normal, uneven and slick surface.

The larger range of ML COM displacement exhibited by the OA participants may stem from differences in minimum ML COM displacement compared to the YA. Specifically, OA exhibited a smaller minimum ML COM distance on the uneven ($p = 0.001$) and slick surfaces ($p = 0.032$), but not normal ($p = 0.372$) compared to YA. To compensate for the challenging surfaces, OA decreased the minimum ML COM displacement during the stair descent, a similar adaptation not exhibited by the YA. Future work is warranted to determine whether this was a compensatory strategy to decrease fall risk or a product of rigid COM control by the OA participants.

In conclusion, descending stairs with challenging surfaces (uneven and slick) led to greater ML COM displacement for OA, but not YA. Future work is needed to determine the impact of the compensatory strategies currently exhibited by OA participants on fall risk.

Significance

Reducing injuries and hospitalizations due to falls is one of the best ways that OA quality of life can be increased. While there are many factors that contribute to fall risk, the current OA participants exhibit ML COM displacement that may alter risk of fall when descending stairs with slick and uneven surfaces.

Acknowledgments

This study was supported by an award from NIH National Institute on Aging (R15AG059655).

References

1. Jacobs et al., *Gait Posture* 49, 2016.
2. Arvin et al., *J. Biomech*, 49, 2016.
3. Conradsson et al., *PLOS One*, 13, 2018.

MEASURING FASCICLE LENGTHS IN EXTRINSIC AND INTRINSIC THUMB MUSCLES USING EXTENDED FIELD-OF-VIEW ULTRASOUND

Taylor R. Rakauskas[1], Tamara Ordonez Diaz[1], and Jennifer A. Nichols[1]
[1]J. Crayton Pruitt Family Department of Biomedical Engineering, University of Florida, Gainesville, FL, United States
email: taylorrakauskas@ufl.edu

Introduction

Measuring muscle fascicle lengths is critical for understanding the force-length and force-velocity properties of muscles [1]. Muscle fascicles are defined as bundles of muscle fibers and can be measured *in vitro* by dissection or *in vivo* using ultrasound or magnetic resonance imaging [2]. Ultrasound is relatively cheap, easy to use [1], and has been accepted as a reliable measurement method for a variety of muscles [1, 3, 4, 5]. However, most prior ultrasound studies have focused on the lower limb, with few studies examining upper limb muscles [5] and no studies, to our knowledge, explicitly measuring thumb muscle fascicles.

Effectively measuring fascicle length of thumb muscles is an important step toward understanding force transmission in the multiarticular muscles of the wrist and hand. Additionally, validated methods for measuring both extrinsic and intrinsic hand muscles *in vivo* could be used to understand how these muscles change with age or pathology. Thus, the objective of this study was to test the reliability and validity of measuring muscle fascicle lengths of extrinsic and intrinsic thumb muscles using extended field of view ultrasound (EFOV-US) imaging.

Methods

Eight healthy adult subjects (4 female, avg. age 21.6 ± 1.3 years, avg. height 175.85 ± 8.26 cm) participated in this IRB-approved study. In each subject, one extrinsic thumb muscle, the flexor pollicis longus (FPL), and one intrinsic thumb muscle, the abductor pollicis brevis (APB) were imaged. Additionally, to enable comparison to prior work [5], the extensor carpi ulnaris (ECU) was imaged. All images were acquired with a SuperSonic Imagine Mach 30 (LH20-6 and L18-5 linear transducers).

Prior to imaging, the path of each muscle was determined and marked. During imaging, the probe was moved distally for the FPL and proximally for the ECU. Images for FPL and APB were acquired with the subject's shoulder at 90° and the forearm in a supine position. For the ECU, subjects sat with both the shoulder and elbow at 90° and hand lightly resting on a hand grip. Subjects were instructed to remain relaxed throughout imaging.

For each subject, 10 images of the ECU, 10 images of the FPL, and 15 images of the APB were recorded. For the ECU and FPL, the best 5 images for each combination of muscle and subject were identified and 2 fascicle length measurements were recorded from each image. For the APB, due to its small size, only one measurement was taken from the 10 best images for each subject. All fascicles were measured from aponeurosis to aponeurosis using the ultrasound machine's built-in measurement software. Averages were calculated for each muscle within each subject and across all subjects. Two-sided t-tests were performed to compare the subject averages with those reported in the literature [5, 6, 7].

Results and Discussion

The EFOV-US method used obtained reliable fascicle length measurements for the ECU (5.12 ± 0.3 cm), FPL (6.15 ± 0.53 cm), and APB (4.0 ± 0.4 cm). EFOV-US measurements for the ECU (p = 0.12) and APB (p = 0.58) were not significantly different than those reported in the literature (Fig.1).

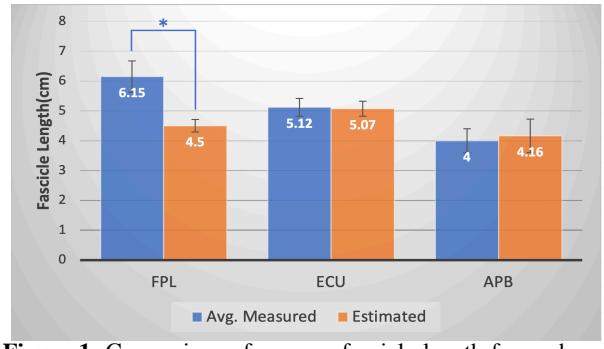

Figure 1: Comparison of average fascicle length for each muscle across all subjects to estimated values found in literature [5, 6, 7]. *p< 0.05

In contrast, FPL measurements were consistently greater ($p < 0.01$) than those reported in the literature (Fig. 1). Potential reasons for this discrepancy include differences in limb posture during measurement. Additionally, prior work measured FPL fascicle lengths in cadaveric specimens. Differences in the age of the specimens versus the subjects of this study as well as differences between living and preserved tissue could account for the reported differences in FPL fascicle lengths.

Interestingly, ECU measurements were strongly correlated with subject height ($r^2 = 0.792$) and forearm length ($r^2 = 0.792$). However, FPL ($r^2 < 0.4$) and APB ($r^2 < 0.1$) measurements were only weakly correlated. This highlights the need to directly measure thumb muscle fascicle lengths, instead of relying upon anthropometric scaling.

Use of EFOV-US to measure fascicle lengths requires images aligned with the fascicle plane. Despite all images being acquired by one trained sonographer, an average of 7.9% of the images were unmeasurable due to lack of visible fascicles. This highlights the need to record multiple images and for research-specific sonography training to ensure high repeatability.

Significance

To our knowledge, this is the first study to measure fascicle lengths of extrinsic and intrinsic thumb muscles using EFOV-US technology. Measuring thumb muscle fascicle lengths *in vivo* will inform our understanding of hand forces and hand pathologies.

Acknowledgments

Thank you to Sarah Barron and Kalyn Kearney for data collection assistance. Funding from NIH NCATS KL2 TROO1429.

References

[1] Arnold et al. *J Exp Bio*, 2013. 216 p. 2150-2160.
[2] Lieber and Ward. *J Appl Physio*, 2011. 366 p. 1466-1476.
[3] Kwah et al. *J Appl Physio*, 2013. 114 p. 761-9.
[4] Noorkoiv et al. *J Appl Physio*, 1985. 109(6) p. 1974-9.
[5] Adkins et al. *J Biomech*, 2017. 63 p. 179-185.
[6] Lieber et al. *J Hand Surg*, 1992. 17(5) p. 787-798.
[7] Jacobson et al. *J Hand Surg*, 1992. 17(5) p. 804-9.

IS PATELLOFEMORAL UNDERLOADING 6 MONTHS AFTER ACL RECONSTRUCTION LEADING TO OSTEOARTHRITIS DEVELOPMENT?

Jack R. Williams[1], Kelsey Neal[1], Abdulmajeed Alfayyadh[1],
Ashutosh Khandha[1], Kurt Manal[1], Lynn Snyder-Mackler[1], Thomas S. Buchanan[1]
[1]University of Delaware, Newark DE
Email: jackrw@udel.edu

Introduction

Tibiofemoral osteoarthritis (OA) after ACL reconstruction (ACLR) is well documented. Underloading of the involved limb's medial compartment 6 months after ACLR is associated with tibiofemoral OA development 5 years after surgery[1]. Recently, patellofemoral OA development after ACLR has been recognized as highly prevalent[2]. However, the mechanisms leading to patellofemoral OA after ACLR are not well understood.

Quantitative magnetic resonance imaging techniques have emerged as a valuable tool to monitor biochemical alterations to knee cartilage. One commonly used technique is T_2 mapping, which can assess the collagen matrix of cartilage. A prolonged T_2 relaxation time is indicative of collagen matrix degradation, one of the earliest signs of knee OA.

The purpose of this study was to determine if there are differences in the biochemical health of patellofemoral knee cartilage 24 months after ACLR in those who underload the patellofemoral compartment versus those that do not, 6 months after ACLR. We hypothesized that: (1) underloaders will display prolonged involved limb T_2 relaxation times (vs. symmetric loaders) and (2) underloaders will have more asymmetric T_2 relaxation times between limbs (involved > uninvolved) compared to symmetric loaders.

Methods

10 participants (5 female, age: 21 ± 5 years) completed motion analysis during overground walking 6 months following unilateral ACLR with a bone-patellar tendon-bone graft. Kinematic, kinetic, and surface electromyography data were collected bilaterally and used as inputs into a subject-specific neuromusculoskeletal model to calculate muscle forces[3]. These muscle forces, in combination with anthropometric and kinematic data, were used to calculate patellofemoral contact forces in each limb, normalized to bodyweight (BW)[4]. Similar methodologies were applied to a group of 12 healthy individuals (5 female, age: 21 ± 3 years). Using the peak patellofemoral contact force (pPCF) from each limb of the healthy population, the minimum interlimb difference (MILD) of pPCF was calculated using similar methodologies established by Gardinier *et. al*.[5]. This MILD value was used as a threshold to determine whether the 10 ACLR participants classified as underloaders (involved limb < uninvolved limb by at least MILD value) or symmetric loaders.

These 10 participants returned 24 months after ACLR and completed a sagittal, bilateral knee MRI featuring a T_2 mapping sequence (echo times: 10-70 ms). For each limb, the centermost slice of the patella was segmented into deep and superficial sub-regions to account for laminar differences in cartilage structure. The average T_2 relaxation time was calculated for each region in each limb. A 1-tailed t-test ($\alpha = 0.05$) was used to compare the involved limb T_2 relaxation times between groups (underloaders vs. symmetric) and between limbs (involved vs. uninvolved).

Results and Discussion

The MILD of pPCF from healthy individuals was calculated to be 0.36 BW. Using this threshold, 4 of the ACLR participants classified as underloaders and 6 classified as symmetric loaders (there were no overloaders). There were no differences in demographic characteristics between groups.

Both of our hypotheses proved correct. The underloading group displayed prolonged involved limb T_2 relaxation times compared to the symmetric group in both the deep ($p = 0.096$) and superficial ($p = 0.032$) layers 24 months after ACLR (Figure 1). Larger between-limb asymmetries in T_2 relaxation times were also seen in the deep layer of the underloading group ($p = 0.039$) compared to symmetric group ($p = 0.255$, Figure 1). These data suggest that underloading of the patellofemoral compartment early after ACLR may be leading to early signs of OA development within patellar cartilage. Future work needs to examine a larger number of participants and include analysis of trochlear cartilage.

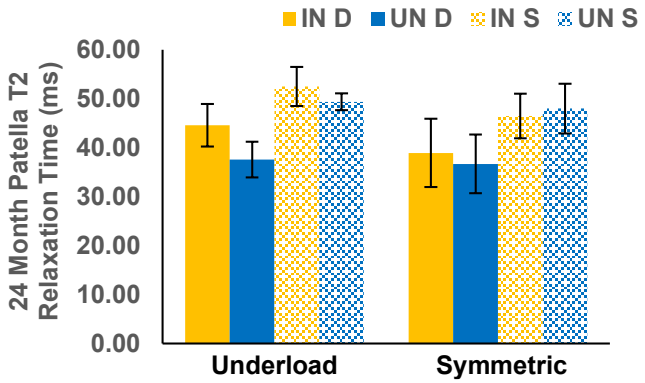

Figure 1: Deep (D, solid) and superficial (S, dashed) patella T_2 relaxation times 24 months after ACLR in those who underload their patellofemoral compartment (involved vs. uninvolved, IN vs. UN) and those who have symmetrical patellofemoral loading 6 months after ACLR. The involved limb (yellow) in the underloading group had prolonged relaxation times compared to the involved limb in the symmetric group Additionally, the underloading group had more asymmetrical relaxation times between limbs compared to the symmetric group.

Significance

Similar to the tibiofemoral compartment, underloading of the patellofemoral compartment 6 months after ACLR may leave individuals at risk for future patellofemoral OA development.

Acknowledgments

NIH R01-HD087459

References

[1] Wellsandt 2016, [2] Culvenor 2013 *AJSM*, [3] Buchanan 2004, [4] Yamaguchi 1989, [5] Gardinier 2013.

FEASIBILITY OF QUANTITATIVE SHOULDER ULTRASONOGRAPHY IN PEDIATRIC WHEELCHAIR USERS

Joshua M. Leonardis[1], Caleb M. A. Cordes[1], Alyssa J. Schnorenberg[1], Shubhra Mukherjee[2], Amee L. Seitz[3], and Brooke A. Slavens[1]
[1]University of Wisconsin-Milwaukee, Milwaukee, WI, USA
[2]Shriners Hospitals for Children, Chicago, IL, USA
[3]Northwestern University, Feinberg School of Medicine, Chicago, IL, USA
email: *leonarj@uwm.edu

Introduction

Children account for approximately 20% of all spinal cord injury (SCI) cases in the United States and most use manual wheelchairs for daily mobility [1]. Manual wheelchair propulsion is a physically demanding, repetitive task that is strongly associated with shoulder pain and pathology in adults [2]. However, limited knowledge exists regarding the relationship between shoulder pain and pathology in children with SCI [3]. Therefore, this study determined the feasibility of quantitative ultrasound assessment of the shoulder together with outcome measures in pediatric manual wheelchair users.

Methods

Two right-handed pediatric manual wheelchair users with SCI (1 male, age: 7.5 yrs, height: 1.10 m, weight: 23.1 kg, level of injury: T6, years since injury: 7.2 yrs; 1 female, age: 13.9 yrs, height: 1.35 m, weight: 50.2 kg, level of injury: T10, years since injury: 11.2 yrs) participated in a single experimental session. A GE LOGIQe ultrasound unit with a linear transducer set at 9 MHz captured B-mode images bilaterally to assess quantitative metrics including: acromiohumeral distance, supraspinatus and subscapularis tendon thicknesses measured from longitudinal images, supraspinatus muscle cross-sectional area, and occupation ratio (ratio of supraspinatus tendon thickness to acromiohumeral distance). Two images of each metric were obtained from each shoulder. Data were processed using standardized methods with previously established acceptable reliability for all the quantitative metrics [4]. Outcome measures included the Wheelchair User's Shoulder Pain Index (WUSPI), the Pediatric Spinal Cord Injury Activity Measures (PEDI SCI-AM), and the Pediatric Measure of Participation (PMoP).

Results and Discussion

All ultrasound imaging metrics could be obtained bilaterally from both participants (Table 1). The values obtained fit well with limited findings in the literature obtained from adults [5]. Generally, metrics were similar between shoulders within participant (mean difference across metrics (95% CI), male participant: 13.5% (6.5-20.5), female participant: 8.5% (2.7-14.2)). Between arm differences varied depending on the metric (acromiohumeral distance, male: 28.2%, female: 5.0%; subscapularis tendon thickness, male: 7.2%, female: 7.6%; supraspinatus tendon thickness, male: 2.5%, female: 17.3%; supraspinatus muscle area, male: 14.5%, female: 0.1%; occupation ratio, male: 16.4%, female: 12.3%).

Metrics were less similar between participants (mean difference across metrics (95% CI), dominant: 25.5% (12.1-39.0), non-dominant: 29.6% (10.3-48.9)). On the dominant and non-dominant shoulders, the metric with the greatest difference between subjects was supraspinatus muscle cross-sectional area (dominant: 41.4%, non-dominant: 49.8%). The metric with the smallest between-subject difference was subscapularis tendon thickness (dominant: 5.3%, non-dominant: 5.6%).

Outcomes measures were successfully obtained. WUSPI scores of 0 indicated both participants were pain free. Similar scores on the daily routines (male: 53.96, female: 61.62) and general mobility (male: 50.83 female: 58.75) domains of the PEDI SCI-AM indicated both were similarly mobile and capable of performing daily routines and self-care. The younger, male participant reported a 33% lower PEDI SCI-AM wheeled mobility score (male: 46.96, female: 65.46), indicating more difficulty performing wheelchair-related mobility tasks. Finally, both participants reported similar scores on the participation with friends domain (male: 53.72, female: 50.77) of the PMoP, whereas the younger, male participant reported a 51% lower score on the self-participation subsection (male: 42.32, female: 56.57), indicating a lower propensity to initialize participation.

Significance

Quantitative ultrasound imaging of the shoulder complex and outcome measures can be obtained from pediatric manual wheelchair users. The outcomes results provide valuable insight into the participants' free-living environment and indicate similar levels of independence and mobility. Work with a larger sample size is underway to develop methods for normalizing quantitative ultrasound metrics to participant size and investigate the prevalence of shoulder pathologies in pediatric wheelchair users.

Acknowledgments

This research was supported by the Eunice Kennedy Shriver National Institute of Child Health and Human Development (NICHD) of the NIH (1R01HD098698). Thank you to Tracy O'Brien at Shriners Hospitals for Children – Chicago and the Mobility Lab at the University of Wisconsin-Milwaukee.

References

1. American Spinal Injury Association, 2021.
2. Brose et al., Arch. of Phys. Med. & Rehab., 89, 2086-93, 2008.
3. Slavens et al., Front. Bioeng. Biotechnol., 3, 137, 2015.
4. Martinoli, Insights Into Imaging, 1(3), 99-141, 2010.
5. Belley et al., Arch. Phys. Med. & Rehab., 98(3), 517-24, 2017.

Table 1. Mean (SD) quantitative ultrasound imaging metrics.

		Acromiohumeral Distance (mm)	Supra. Tendon Thickness (mm)	Subsc. Tendon Thickness (mm)	Supra. Muscle Area (mm^2)	Occupation Ratio (%)
Female Participant	Dominant	13.3 (0.4)	4.2 (0.3)	4.4 (0.3)	78.4 (0.6)	34.1 (0.01)
	Non	13.6 (0.5)	3.5 (0.4)	4.7 (0.2)	78.2 (2.4)	34.3 (0.02)
Male Participant	Dominant	12.2 (0.8)	5.7 (0.3)	4.2 (0.2)	43.9 (2.5)	34.2 (0.01)
	Non	15.6 (0.1)	5.6 (0.2)	4.5 (0.03)	39.3 (1.8)	28.6 (0.01)

ARE SOLDIERS WHO START RUNNING UPON JOINING THE ARMY LESS SUSCEPTBLE TO INJURY?

A. Bloch*[1], M. Colpo[1], G. Freisinger[1], and R. Zifchock[1]
[1]United States Military Academy, Department of Civil & Mechanical Engineering, West Point, NY, USA
email: *audra.bloch@westpoint.edu

Introduction

Success in the Army is dependent upon Soldier physical fitness and readiness. Therefore, running is a key training technique as well as performance metric for members of the United States Army. Soldiers regularly complete a graded fitness test that includes a timed 2-mile run. Although running is a compulsory activity for all Soldiers, some start running from a young age before joining the Army, while others start because they are compelled to pass the fitness test. Susceptibility to running injuries, which can be particularly costly to both the individual soldiers and the greater Army, may be associated with running experience. Previous studies have examined the differences in kinetic and spatio-temporal parameters associated with running injuries, between experienced and novice runners [1, 2]. While there are mixed findings between studies, they focus upon years of running experience in a civilian population that chose to take up running, whereas the military represents a group of people who may be compelled to take up running. It is unclear whether there are differences in factors associated with injury susceptibility between those who chose to run for fitness before they joined the Army versus those who are compelled to run upon joining the Army. Thus, the purpose of this study was to determine the effect of running experience on factors that have previously been associated with injury susceptibility: peak vertical ground reaction force, ground contact time, and average loading rate.

Methods

A sample size of nine Soldiers were recruited to participate in this IRB-approved study. The sample consisted of four runners who had been running from a young age (Pre-Army, running start = 12.0 yrs, current age = 25 yrs, 1.79 m, 78 kg), and five who were compelled by the Army to run (Army, running start = 17.7 yrs, current age = 30 yrs, 1.74 m, 81 kg).

Participants wore their own sneakers and ran on an instrumented treadmill (Bertec FIT; Columbus, OH) at 75% of their typical 2-mile pace (pre-Army = 2.8 m/s, Army = 3.1 m/s). Subjects warmed up and then two running trials were recorded. Data were sampled at 1200 Hz (Vicon Nexus; Centennial, CO). Custom code written in MATLAB (Mathworks; Natick, MA) was used to analyze the ground reaction force data from six sequential foot strikes (including both left and right sides) to determine the ground contact time (GCT), average vertical loading rate (AVLR), and the peak vertical ground reaction force (pkVGRF). The variables of interest were calculated for all six foot strikes, and the data was averaged within a subject. Both AVLR and pkVGRF were normalized to body weight.

Two-tailed independent sample t-tests were conducted, and effect sizes were calculated to compare each variable of interest between groups (sig level, $p < 0.05$).

Results

No significant differences between Pre-Army and Army runners were found for any of the three variables of interest. However, there was a moderate-to-large effect size for GCT and AVLR. The data (Table 1) suggests that in our cohort, those who begin running when they join the Army tend to have lower AVLR and pkVGRF and longer GCT.

Table 1: Comparison between Army and Pre-Army runners

	pkVGRF, N/BW		GCT, s		AVLR, BW/s	
	Army	Pre-Army	Army	Pre-Army	Army	Pre-Army
Mean	2.32	2.39	0.30	0.27	55.47	72.86
SD	0.14	0.35	0.03	0.04	16.41	38.99
P-value	*0.69*		*0.26*		*0.39*	
Effect Size	*0.29*		*0.82*		*0.63*	

Discussion

The purpose of this study was to determine the effect of running experience on kinetic factors that have previously been associated with injury susceptibility. The data collected did not show any significant differences between Pre-Army and Army runners for the three variables of interest, but the effect size analysis suggests that there may be a tendency for runners who start running upon joining the Army to have a less risky movement patterns: lower AVLR and a longer GCT. The results of this study differ slightly from Quan et al [1], who suggested that novice runners may exhibit more risky movement patterns. One possible explanation for this is the formal running training that the new runners received upon entering the Army at West Point. This is a training program executed by professionals on proper running technique that new cadets receive.

A major limitation of this study was the small sample size. As suggested by the effect size, future analyses with a larger sample size might elucidate potential significant differences between groups. Additionally, utilizing a laboratory-based treadmill is effective for collecting data but can result in a different running pattern compared to running overground and in a more natural setting. Lastly, although subjects were allowed to run at a self-selected speed, future analyses might covary for speed to account for potential effects on the variables of interest.

Significance

Despite having less running experience, Soldiers who begin running upon joining the Army may exhibit less risky movement patterns. This may be the result of formal training programs that teach proper running form to new Soldiers, which may be more readily adopted by new runners as compared to those who have already established their running form. Further research with a larger sample size could support the expansion of this formal running technique training, and ultimately expand into other Army organizations.

References

[1] Quan, Applied Bionics and Biomechancs, 2021
[2] Agresta, Gait and Posture, 2018

INFLUENCE OF SLIP ONSET TIMING DURING STANCE ON FOOT YAW DURING TURNING SLIPS

Corbin M. Rasmussen[1] and Nathaniel H. Hunt[1]
[1]Department of Biomechanics, University of Nebraska at Omaha, Omaha, NE USA
email: cmrasmussen@unomaha.edu

Introduction

A number of slip recovery mechanisms have been elucidated, including trunk control, arm swing, and compensatory stepping (CS). Little research has considered foot yaw as a recovery mechanism, however, despite its stabilizing role in walking.[1] Utilizing foot yaw in recovery may provide more favorable center of pressure locations to counteract a slip, but it is unclear if foot yaw differs across different slip types. Previously, we have shown that slip onset timing during stance phase and the slipped foot relative to a turn strongly influence the perturbation that is experienced[2], providing a method of delivering a wide range of realistic slips. Therefore, here we examined how slip onset phase and the slipped foot influences slipping foot (SF) and CS yaw after a turning slip.

Methods

Eighteen young healthy adults performed 12 slip trials administered with WASP[3] as they walked over 180° curvilinear turns. Slips were delivered to both feet across early (0-33%, ES), middle (34-67%, MS) and late (68-100%, LS) stance phase. Kinematics were collected at 200 Hz via motion capture.

Kinematic data were used to determine slip onset timing, slip cessation, and gait events.[4] A line between the 2nd metatarsal head and calcaneus markers represented the foot segments. A SF yaw time series was calculated from slip onset to cessation, and the peak internal or external rotation from the foot's position at slip onset was extracted as the SF max yaw. To derive CS yaw change from unperturbed steps, the angle between the simplified CS foot segment and instantaneous heading direction at CS touchdown was compared to the average foot yaw during unperturbed steps under the same conditions.[5]

To investigate the influence of slip onset timing and slipped foot on SF and CS yaw, two linear mixed models were used. Onset timing and foot were treated as fixed effects and subject as a random effect. ES and outside foot slips were the baseline conditions to which others were compared in the models.

Results and Discussion

SF yaw was not impacted by the slipped foot ($t(140)=0.46$, $p=0.647$; Figure 1A). MS slips were significantly more externally rotated ($t(140)=3.05$, $p=0.003$; Figure 1A), but LS slips were not significantly different from those in ES ($t(140)=0.72$, $p=0.471$; Figure 1A). Notably, LS slips exhibited a large degree of variability in SF yaw. For CS yaw, the perturbed foot relative to the turn significantly influenced the direction of foot yaw ($t(133)=-9.57$, $p<0.001$; Figure 1B), with CS after outside and inside foot slips exhibiting increased external and internal rotation, respectively. Slip onset timing had no effect on CS yaw (MS: $t(133)=-0.89$, $p=0.378$; LS: $t(133)=-1.22$, $p=0.226$; Figure 1B).

Significance

The potential role of foot yaw in recovery from large balance disturbances has not been investigated in the literature. The dependence of SF yaw on MS onset timing and the large variability during LS provides further support for how diverse unconstrained slip perturbations can be.[2] SF yaw influences the initial conditions from which one must start to recover balance, and therefore may be an important factor to account for in slip-related fall prevention methods. The degree that SF yaw is actively controlled by the individual or the result of passive mechanics acting at the foot is still unclear. The lack of an effect of slip onset timing on CS yaw suggests that the increase in foot yaw compared to unperturbed steps is not specific to the direction of the perturbation[2] – that altering CS yaw is a "general" recovery strategy. Further research should relate center of pressure trajectories to SF and CS yaw to determine whether SF and/or CS foot yaw are truly mechanisms for balance recovery.

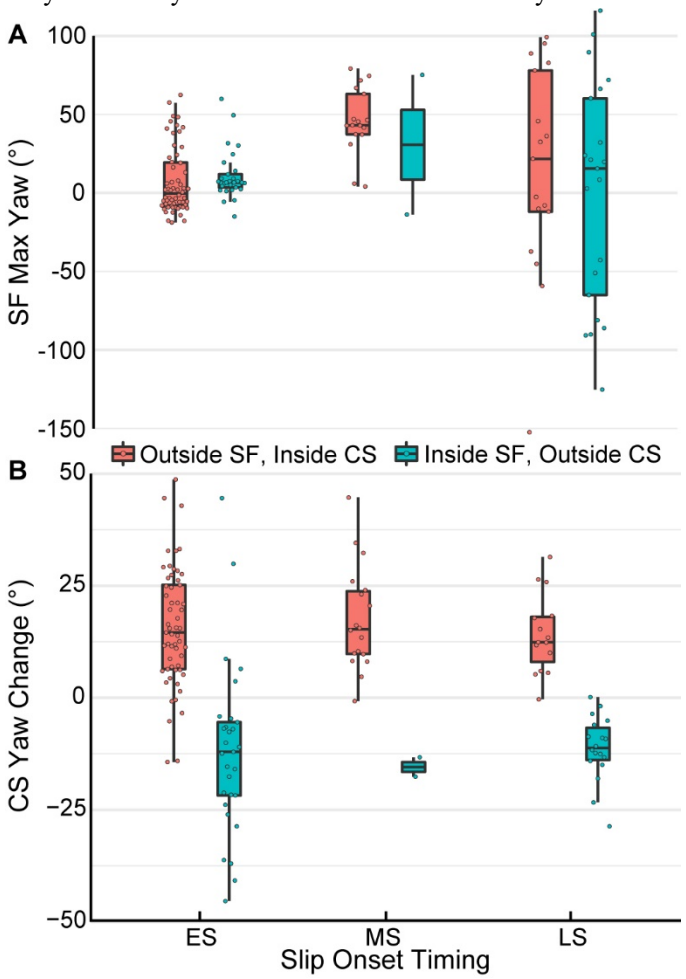

Figure 1: Boxplots depicting the influence of slip onset phase and perturbed foot on SF and CS yaw. Positive values represent external rotation, while negative values represent internal rotation.

Acknowledgments

Study funded by NIH grants R15AG063106 and P20GM109090.

References

1. Rebula JR et al. (2017). *J Biomech,* **53**: 1-8.
2. Rasmussen CM et al. (2019). *XXVII ISB/43rd ASB,* Calgary,CA
3. Rasmussen CM et al. (2019). *J Neuroeng Rehabil,* **16**: 118.
4. Zeni Jr. JA et al. (2008). *Gait Posture,* **27**: 710-4.
5. Courtine G et al. (2003). *Eur J Neurosci,* **18**: 177-90.

MEASURING PROSTHETIC FOOT USE BY CADENCE LEVEL WITH STEP ACTIVITY MONITORING

John M. Chomack[1], A. Sidiropoulos[1], M. Poppo[1], and J. Maikos[1]
[1]Veteran Affairs New York Harbor Healthcare System, New York, NY, USA
Email: john.chomack@va.gov

Introduction

As advanced prosthetic foot technology becomes more readily available, patients with lower limb amputation will have increased opportunities to access a range of energy storing, articulating, and powered devices. Therefore, it is critical to use objective measures for prosthetic prescription to meet the biomechanical and functional needs of each patient outside of the clinic. Capturing a patient's prosthetic performance while navigating his/her everyday environment is a key piece of information that has yet to be effectively utilized in the prescription process [1]. Activity monitoring devices, such as the Modus™, StepWatch 3™ (Modus Health LLC, Edmonds, WA) used in this study, offer the potential to capture this critical information due to their accuracy for those ambulating with a prosthesis [2]. This study sought to capture the community ambulation activity levels for individuals with transtibial amputation (TTA) while using 3 different types of prosthetic feet over 4 weeks. The purpose of the investigation was to determine if a specific foot type promoted higher activity levels as determined through cadence; and if the activity per level correlated with the outcome measures used in this study.

Methods

Fifty-eight individuals living with TTA (age 56.1±12.8 years, height 1.79±0.08 m, and weight 94.7±18.4 kg) with at least 1 year of prosthesis experience completed the protocol to-date. Participants were recruited from Veteran Affairs (VA) New York Harbor Healthcare System (NYHHS), James A. Haley VA Medical Center, VA Puget Sound Healthcare System, and Walter Reed National Military Medical Center. All procedures were approved by their respective Institutional Review Boards. Participants were randomized to wear 3 types of prosthetic feet: an energy storing and returning device (ESR), an ESR device with articulation (ART), and a powered articulating device (PWR). Each device was attached to a duplicated, well-fitting socket. Study participants wore each foot for a 1-week acclimation period and then separately completed a series of functional outcomes, questionnaires, and a biomechanical assessment for each device. After testing concluded for all devices, a Modus™, StepWatch 3™ step activity monitor (SAM) was affixed to each device and subjects were asked to use each prosthesis as desired for 4 weeks of home use. The SAMs were programmed to record the number of steps taken at each minute. Upon conclusion of the 4-week at-home portion, a close-out survey of the subject's device preference was conducted. Of the 58 participants, 45 used 2 or more feet during the at-home portion and were included in this analysis. Cadence was calculated at each minute, and then categorized into activity levels: low (1-15 steps/min), moderate (16-40 steps/min), and high (>40 steps/min). A one-way ANOVA and linear regression compared the effects of the percent of steps taken to each prosthetic type per activity level, and correlation to the FOs.

Results and Discussion

Figure 1 represents the frequency of the greatest percentage of steps taken at each activity level for each foot type as determined through cadence. Statistical analysis indicated there were no significant effects of prosthetic device type on percent steps taken at any activity levels ($p>0.05$). However, a trend towards significance occurred at the moderate activity level for ESR devices ($p=0.08$). While none of the 3 devices promoted greatest percent of steps at high activity, the trend of greatest percentage of steps taken at moderate activity by ESR devices may be

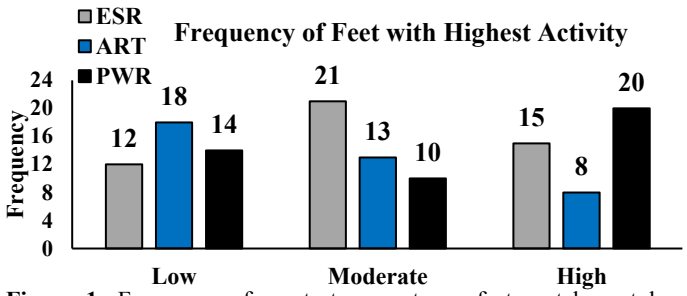

Figure 1: Frequency of greatest percentage of steps taken at low, moderate, and high activity levels by foot type.

partially explained by foot preference and self-selected walking speed. Based on data from the close-out survey regarding foot preferences, 47% of subjects who preferred the ESR device also performed their greatest percentage of steps at moderate activity with the ESR device. Because the majority of daily steps were taken at moderate activity levels, these findings suggests that participants may prefer to walk at this cadence and select/prefer the prosthetic device that matches the greatest percent of steps at moderate activity levels. Subjects had the most familiarity with the ESR device since they used their currently prescribed ESR device for this study. Lastly, the regression revealed that only the Time-Up & Go (TUG) was able to predict the percent steps at moderate activity ($p=0.03$) for the ESR device with moderate correlative strength ($R=0.60$).

This investigation sought to determine if a specific foot type promoted higher activity levels, and if those associated values correlated to objective metrics. While current results potentially indicate a correlation between moderate activity and use of the ESR device, factors such as the number of days of use or accounts of a device being used specifically for high level activities will need further investigation.

Significance

Step activity monitoring can be a valuable tool to use in the prosthetic prescription process since it can help evaluate community ambulation activities. Use of objective measures for prosthetic prescription can help meet the biomechanical and functional needs of each patient outside of the clinic.

Acknowledgments

Our work was supported by a DoD Orthotics and Prosthetics Outcomes Research Program Grant (W81XWH-17-2-0014). We acknowledge our co-investigators for their efforts.

References

[1] Halsne, E et al. *JRRD*, 30(4):515-530. (2013).
[2] Coleman, D et al. *JRRD*, 36(1):8-18. (1999).

UNILATERAL TRANSFEMORAL PROSTHESIS USERS RELY ON THEIR SOUND LIMB TO DRIVE CHANGES IN EXTERNAL BODY CENTER OF MASS WORK DURING WALKING

S. Pinhey[1], R. Amma[2,3], H. Murata[2,3], G. Hisano[3,4,5], D. Ichimura[4], H. Hobara[4], and M.J. Major[1,6]
[1]Northwestern University, Chicago, USA; [2]Tokyo University of Science, Japan; [3]National Institute of Advanced Industrial Science and Technology, Japan; [4]Tokyo Institute of Technology, Japan; [5]Research Fellow of Japan Society for the Promotion of Science, Japan; [6]Jesse Brown VA Medical Center, Chicago, USA
email: shaypinhey2021@u.northwestern.edu

Introduction

During human locomotion, each limb performs step-to-step work on the body center of mass (BCoM) to maintain forward walking (Donelan 2002). This efficient energy exchange involves alternating periods of negative and positive work that rely on physiological mechanisms to support limb collision following initial contact and push-off in late stance, respectively. Such mechanisms are altered or impaired in transfemoral prosthesis users (TFPUs) relative to able-bodied persons, which might explain their noted asymmetry and increased metabolic cost (Bonnet 2014). Modifications to step-to-step energy exchange displayed by TFPUs for achieving greater walking speeds may provide insight into their gait compensations and means for improving gait efficiency. This study characterized the effects of walking speed on BCoM work in unilateral TFPUs. It was hypothesized that collision work on both the sound and prosthetic limb would increase with walking speed and that participants would demonstrate reduced push-off work on their prosthetic limb as compared to their sound limb across all speeds.

Methods

Twenty-five unilateral TFPUs (19 M, 6 F, 31±10 yrs, 166±7 cm, 65.6±13.9 kg) wearing their customary prosthesis (n=15 mechanical, n=10 microprocessor knees, all dynamic response feet) walked on a split-belt instrumented treadmill (Tec Gihan Inc., Japan) that collected instantaneous ground reaction forces (GRFs) at 1000 Hz. Participants were first provided at least 7 minutes to accommodate to treadmill walking and then walked at 8 speeds (0.55-1.53 m/s with increments of 0.14 m/s) for 30 seconds each while GRF data were collected. Rest periods as requested were provided to minimize fatigue effects. All participants provided written informed consent prior to data collection. All GRF data were processed in MATLAB (Mathworks, USA) using the 'Individual Limbs Method' as outlined in Donelan (2002) to calculate work per step. Instantaneous power was calculated as the dot product of GRF and BCoM velocity (integration of BCoM acceleration with respect to time). Integration drift was removed using boundary conditions that assumed symmetry over a stride. Work (J/kg) for each limb was calculated by integrating power with respect to time over three phases of a step: collision (first double support phase), midstance (single support), and push-off (second double support). Two-way ANOVA were implemented in SPSS (v27, IBM, Armonk, USA) to assess the main and interaction effects of speed and limb side (sound, prosthetic) on work for each phase of walking (α=0.05), followed by simple main effect analysis if interactions were significant.

Results and Discussion

Figure 1 displays average collision, midstance, and push-off work for both limbs at each speed averaged across participants. Supporting our hypotheses, TFPUs displayed a significant ($p<0.001$) increase in collision work with walking speed on both limbs, and significantly ($p<0.001$) less push-off work generated by the prosthetic limb across all speeds. Midstance for the prosthetic limb remained nearly unchanged across speeds, but increased almost exponentially on the sound limb after 1.11 m/s. These results suggest that positive work is being maximized through mid and late stance on the sound limb to compensate for the greater negative sound limb collision work likely resulting from the absence of prosthetic limb push-off work (Figure 1b). While nearly equivalent across speeds, there was a significant ($p\leq0.033$) but small increase in prosthetic limb push-off work after 1.11 m/s that may suggest some element of prosthetic foot energy return at higher walking speeds.

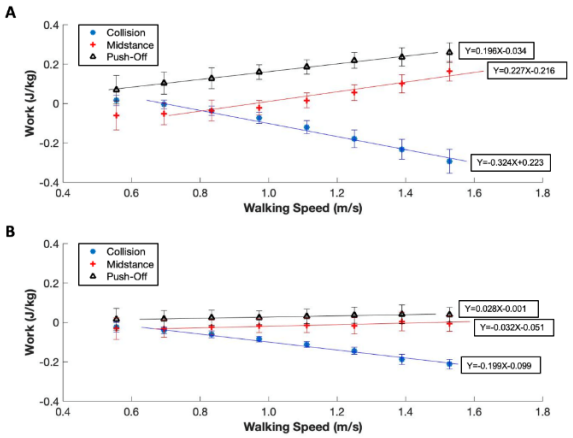

Figure 1: Average work at each speed for (A) sound and (B) prosthetic limbs. Error bars represent 95% confidence interval. Best fit linear models are included to visualize speed trends.

Significance

The results suggest that TFPUs gait inefficiency can be explained by the limited ability to generate prosthetic limb power during mid and terminal stance, relying more on the sound limb to drive energy changes during forward walking. The prosthetic limb served mainly to assume energy loss during collision and support the body as it transitions over that limb. This energy asymmetry emphasizes the need to assess the potential long term (overuse) effects of walking with a transfemoral prosthesis on sound limb musculoskeletal health. Interventions to address this asymmetry may include therapy to promote greater use of the prosthetic limb hip to generate work or prosthetic devices to aid late stance propulsion. A limit of our model is that it does not analyze joint or muscle level dynamics and future work should focus on these contributions to evaluate the physiological mechanisms used to compensate for minimal prosthetic limb power generation.

References

Bonnet X, J Eng Med 228(1), 60-66, 2014.
Donelan M, J Biomech 35(1), 117-124, 2002.

ALTERED JOINT POWERS DURING RUNNING AFTER TIBIAL BONE STRESS INJURY

Samuel M. Lyons[1], Jeffery J. Morgan[1], Salinda K. Chan[1], and Emily A. Kraus[1,2]
[1]Motion Analysis and Sports Performance Lab, Lucile Packard Children's Hospital, Stanford.
[2]Stanford University, School of Medicine, Department of Orthopaedic Surgery, Division of Paediatric Orthopaedics
email: SLyons@stanfordchildrens.org

Introduction

Walking and running mechanics are often used to investigate risk factors for overuse and acute injuries. Traditionally, kinetic measures are separated into the three cardinal planes. However, this can lead to misrepresentations when examining mechanical power[1]. A combined method has been used to examine limb power output during locomotion at varying speeds[2].

Farris and Sawicki found positive joint power contributions are proportional across speeds during running[2]. However, the presence of injury can affect running mechanics that may have the potential to alter a joint's power contribution.

Milner et al. found that runners with a history of tibial bone stress injury (BSI) have greater vertical loading rates compared to healthy controls[3]. Notably, the tibial BSI group ran with a more compliant ankle and stiffer knee joint than the healthy group[3]. This finding suggests that there may be a load shift between joints in runners who have experienced a BSI.

The purpose of this study was to examine the difference in total limb power and percent joint power contribution in healthy adolescent runners compared to their peers with a history of tibial BSI. It was hypothesized that runners with a history of BSI would have greater contribution of power production and absorption at the ankle and less at the hip and knee joints with no difference in total power compared to healthy controls.

Methods

Twenty-six runners were divided into groups: history of tibial BSI (n=14; male=10, female=4; age=16±2), and healthy controls (n=12; male=5, female=7; age=18±7). BSI's were diagnosed by one physician and were asymptomatic during testing. Subjects provided written/informed consent before being outfitted in a modified Plug-In Gait marker set and performing a five-minute warm-up. Participants then performed over ground jogging trials at a self-selected pace. Kinematic and kinetic data were collected using a Vicon camera system and embedded force plates.

Total limb power and percent joint contribution were calculated using a similar method to Farris and Sawicki[2]. Positive and negative joint work was summed from the integrations of the joint power-time curve in each plane. Joint work was divided by step time to obtain total joint power. Joint powers for the hip, knee, and ankle were summed to determine total limb power and percentage of limb power was calculated for each joint.

Variables were grouped by control limb (CON), uninvolved limb (UNI), and involved limb (BSI). The CON limb was a combination of left and right legs of the healthy group. A one-way ANOVA was used to compare the variables of limb and joint power, presented in Table 1. If significant main effects were determined, post-hoc testing was included to substantiate the difference within dependent variables.

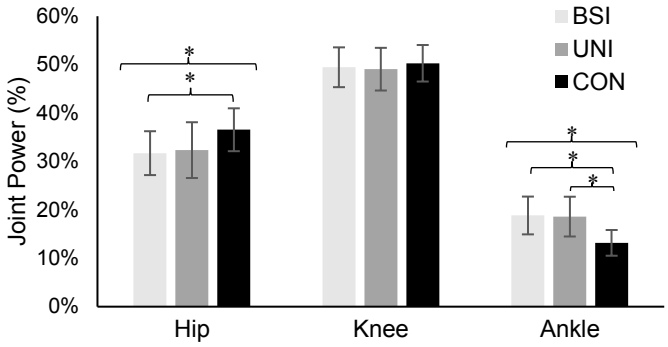

Figure 1: Negative power contribution during stance phase of running

Results and Discussion

The ANOVA revealed a significant main effect for group on Total Positive Power ($p=0.04$), Hip Negative Power ($p=0.04$), and Ankle Negative Power ($p<0.001$). There were no significant differences between groups for other variables. Post-hoc analysis revealed that the CON legs output greater Total Positive Power than the BSI legs ($p=0.03$) but was not significantly different than the UNI legs ($p>0.05$). Additionally, the CON legs had significantly greater Hip Negative Power than the BSI legs ($p=0.047$) but was not significantly different than the UNI legs ($p>0.05$). Lastly, the CON legs had significantly less Ankle Negative Power compared to both BSI ($p=0.001$) and UNI ($p=0.002$) legs. No significant differences were observed between the BSI and UNI legs for any variable measured.

The results support the hypothesis that adolescent runners with a history of BSI alter the power distributions between joints by increasing the involvement of the ankle and decreasing involvement of the hip. The knee joint appears less involved in a shift of power production or absorption after injury. Despite a significant difference in Total Power Production, alterations in positive joint power may be less sensitive than negative power.

Significance

This study is further evidence that history of tibial BSI can cause adaptations in running mechanics regardless of symptoms. Additionally, the changes that do occur are not limited to just the injured leg. Lastly, negative power appears to be more sensitive to change with the ankle joint increasing its contribution, comparatively. Clinicians and researchers should be aware of this adaptation after injury as it may influence treatment strategies.

References

1. Vigotsky, A.D., et al. J. Biomech, 93, 1-5. 2019.
2. Farris, D.J., et al. J. R. Soc. Interface 9(66), 110-118. 2012.
3. Milner, C.E., et al. Med. Sci. Sports Exerc, 38(2), 323. 2006.

Table 1. Mean±SD of power variables examined for each group. * Indicate significant main effects found.

	Positive Power				Negative Power			
Mean±SD	Total (W/kg)*	Hip (%)	Knee (%)	Ankle (%)	Total (W/kg)	Hip (%)*	Knee (%)	Ankle (%)*
CON	6.1 ± 1.3	46 ± 7	24 ± 6	30 ± 5	-5.4 ± 0.9	37 ± 4	50 ± 4	13 ± 3
BSI	5.1 ± 0.8	44 ± 6	21 ± 5	35 ± 5	-4.7 ± 0.7	32 ± 6	49 ± 4	19 ± 4
UNI	5.4 ± 0.7	43 ± 4	23 ± 4	34 ± 4	-4.9 ± 0.6	32 ± 5	49 ± 4	19 ± 4

AN EXAMINATION OF POWER IN THOSE WITH CHRONIC ANKLE INSTABILITY

Amanda N. Delaney[1], Bethany Wisthoff[1], Joseph J. Glutting[2], Kathy Liu[3], and Thomas W. Kaminski[1]
[1]Athletic Training Research Laboratory, University of Delaware, Newark, Delaware
[2]School of Education, University of Delaware, Newark, Delaware
[3]Department of Health Sciences, University of Colorado Colorado Springs, Colorado Springs, Colorado
email: adelaney@udel.edu

Introduction

Ankle injuries are very common in competitive sports and can over time lead to Chronic Ankle Instability (CAI) [1]. To help identify individuals with CAI, a score of less than or equal to 25 on the Cumberland Ankle Instability Tool (CAIT) can be used [2]. While research has sought to analyze the impact CAI has on ankle strength, not much has been done to examine its effects on ankle power. Time to peak torque (TTPT) is considered a measure of explosive power and may play a role in identifying the factors that contribute to CAI. Biomechanical analysis of acute ankle sprains suggest that peak inversion is reached between 0.09 and 0.17 seconds [3]. The purpose of this research was to determine if differences in TTPT occur in individuals with unilateral CAI. We hypothesized that the unstable ankle in our cohort of CAI subjects would take longer to reach peak torque, indicating a decrease in ankle power.

Methods

To assess the factors contributing to ankle sprains, a retrospective cohort design was used to measure ankle strength along with other variables. The study recruited a total of 712 Division 1 student-athletes (SA). During the protocol, every athlete was screened for CAI using the CAIT and 82 SAs [31 females (age: 18 ± 0.5 yrs, ht: 169.2 ± 8.9 cm, and mass: 65.3 ± 8.8 kg) and 51 males (age: 18.7 ± 0.93 yrs, ht: 182.8 ± 6.4 cm, and mass: 86.1 ± 15.7 kg)] were identified as having unilateral CAI. Ankle strength was measured using a KinCom 125 AP isokinetic dynamometer (Isokinetic International, Chattanooga, TN). Concentric (CON) and eccentric (ECC) strength was assessed in all four ankle motions [dorsiflexion (DF), plantar flexion (PF), inversion (INV), and eversion (EV)] at test velocities 30°/s and 120°/s. Testing procedures followed that of Morrison and Kaminski [4].

TTPT measures were compared using a within subjects design with the unstable ankle being compared against the stable ankle. Differences in TTPT values were analyzed using dependent samples T-test computed using SPSS (SPPS Version 26, IBM, Chicago, IL).

Results and Discussion

TTPT values are shown in Table 1. A significant difference in TTPT was determined comparing both ankles for ECC EV at 120°/s (t = 2.294, df[77], p < 0.024). The effect size was small (Cohen's, 1988, d = 0.26), however, the difference of 0.04 seconds is clinically meaningful especially given the time demonstrated for inversion ankle sprains to occur. Interestingly the ECC EV at 30°/s was trending towards significance.

Appropriate muscular power generated by the ankle evertors (peroneals) is important in opposing the violent inversion moments that occurs with a majority of acute ankle sprains. Our results suggest that although the differences in TTPT between stable and unstable ankles were small, it points to the importance of focusing rehabilitation efforts on power output in those with unilateral CAI.

Significance

Although biomechanists and clinicians generally argue for improving muscular strength post ankle sprain to prevent future episodes, this research study suggests that considerations for muscular power also be made. Suggestions for improving muscular power after an ankle sprain include activities that focus on the ballistic components of IN, EV, PF, and DF movements, as well as exercises that produce repetitive loading of these muscle groups. Additionally, interventions that involve speed training are recommended.

References

[1] Hertel J. et al., (2019), *J Athl Train*, **54**(6): 572–588.
[2] Wright C. et al., (2014). *Arch Phys Med Rehabil,* **95**(10): 1853-1859.
[3] Fong D. et al., (2012). *Am J Sports Med*, **40**(11), 2627-2632.
[4] Kaminski TW. et al., (2007). *J Athl Train,* **42**(1): 135-142.

Table 1: TTPT Means and Standard Deviations for all 4 Directions

	Plantar Flexion TTPT (s)				Dorsiflexion TTPT (s)			
	CON30	ECC30	CON120	ECC120	CON30	ECC30	CON120	ECC120
Unstable	0.38 ± 0.12	1.29 ± 0.22	0.14 ± 0.14	0.41 ± 0.30	0.55 ± 0.16	0.81 ± 0.23	0.15 ± 0.14	0.29 ± 0.24
Stable	0.39 ± 0.13	1.30 ± 0.18	0.15 ± 0.15	0.40 ± 0.28	0.56 ± 0.17	0.81 ± 0.21	0.13 ± 0.11	0.28 ± 0.22
	Inversion TTPT (s)				**Eversion TTPT (s)**			
	CON30	ECC30	CON120	ECC120	CON30	ECC30	CON120	ECC120*
Unstable	0.36 ± 0.13	1.17 ± 0.29	0.12 ± 0.13	0.37 ± 0.28	0.42 ± 0.16	1.09 ± 0.30	0.17 ± 0.22	0.31 ± 0.20
Stable	0.36 ± 0.14	1.20 ± 0.30	0.14 ± 0.19	0.36 ± 0.27	0.43 ± 0.15	1.17 ± 1.40	0.16 ± 0.16	0.35 ± 0.25

*Statistically significant difference between unstable and stable times

Age-related difference in corticospinal drive during split-belt walking is muscle-specific

Sumire Sato[1, 2, *], Julia T. Choi[1,2]
[1]Neuroscience and Behavior Program, University of Massachusetts Amherst, Amherst, MA
[2]Department of Applied Physiology and Kinesiology, University of Florida, Gainesville, FL
E-mail: *ssato@umass.edu

Introduction

Corticospinal drive quantified by coherence between two surface electromyography (EMG) signals in the beta-gamma band (15-45 Hz) is increased in the slow leg during early split-belt walking in healthy young adults and associated to temporal asymmetry.[1] With increased age, there are known age-related deterioration in corticospinal input,[2] which may influence locomotor adaptation. The objective of this study was to examine the age-related differences in (1) spatiotemporal kinematic adaptations and (2) corticospinal drive to the ankle dorsi- and plantar-flexors during split-belt treadmill walking. Based on previous studies[2,3] we hypothesized that (1) older adults will adapt kinematics slower and (2) demonstrate lower corticospinal drive compared to young adults.

Methods

Seven young (Age: 26.4 ± 4.6 years) and eight older healthy adults (Age: 72.4 ± 3.3 years) participated in this study. Participants walked on an instrumented treadmill for 5 conditions: 5 min at 0.5 m/s for familiarization, 5 min at 1.0 m/s for baseline pre-fast, 5 min at 0.5 m/s baseline pre-slow, 10 min split-belt adaptation with the slow leg at 0.5 m/s and the fast leg at 1.0 m/s, and 10 min post-adaptation at 0.5 m/s.

Kinematics were measured with reflective markers on the lower extremity, and step length (SL) and double support (DS) symmetry = [Fast leg – Slow leg] / [Fast leg + Slow leg] was quantified for each stride. For each symmetry measure, we examined the following time epochs during adaptation: (1) initial (first 5 strides), (2) early (stride # 6-30), (3) late (stride #31-100) and (4) plateau (last 30 strides).

EMG electrodes were placed on the proximal and distal ends of the tibialis anterior, the medial gastrocnemius and the soleus. EMG-EMG coherence between the two tibialis anterior electrodes and between the medial gastrocnemius and soleus electrodes was calculated for the dorsi-flexor during swing and plantar-flexor during stance, respectively, for each leg over 100 strides. For each condition, the natural logarithm of the cumulative sum of coherence for the beta-gamma (15-45 Hz) and was calculated to quantify corticospinal drive.

Results and Discussion

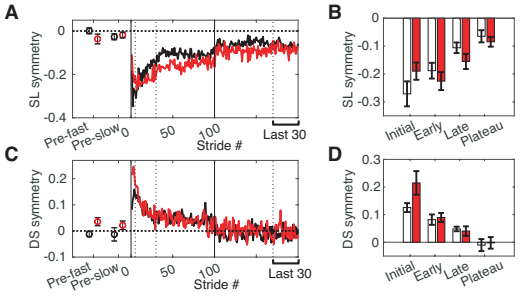

Figure 1: Step length (SL) symmetry (A-B) and double support (DS) symmetry (C-D) during adaptation. SL: All time epochs except for initial and early adaptation were significantly different from each other. DS: All time epochs were significantly different from each other. **Black** = young adults; **Red** = older adults.

Participants adapted SL symmetry and DS symmetry on the split-belt treadmill (Figure 1; SL: $F(3, 39)= 22.1$, $p < 0.001$; DS: $F(3,39) = 33.2$, $p < 0.001$). There was no evidence of a group effect (SL: $p = 0.847$; DS: $p = 0.321$), but time epoch × group interaction effect was significant for both symmetry measures (SL: $F(3,39) =3.8$, $p= 0.017$; DS: $F(3,39)= 2.9$, $p =0.049$).

There was a significant main effect of condition in tibialis anterior beta-gamma coherence in the slow leg, but not in the fast leg (Figure 2; Slow leg: $F(3,39) = 4.1$, $p = 0.013$; Fast leg: $p = 0.262$). Tibialis anterior coherence was lower in older adults compared to younger adults (Slow leg: $F(1,13) = 6.4$, $p = 0.025$; Fast leg: $F(1, 13) = 11.9$, $p = 0.004$), but there was no interaction effect (Slow leg: $p = 0.509$; Fast leg: $p = 0.841$) .

In contrast to the tibialis anterior, plantar-flexor beta-gamma coherence not different between conditions (Slow leg: $p = 0.036$, but post-hoc Bonferroni tests were all $p > 0.05$; Fast leg: $p = 0.525$). PF coherence was lower in older adults in the fast leg only (Slow leg: $p = 0.291$, Fast leg: $F(1,13) = 5.6$, $p = 0.035$), and there was no interaction effect (Fast leg: $p =0.092$, Slow leg: $p = 0.566$) .

Older adults may prioritize spatial symmetry at the beginning of split-belt adaptation. In line with previous studies[1] healthy adults increased corticospinal drive to the tibialis anterior during early adaptation in the slow leg. However, this was not observed in older adults. Age-related differences were greater in the tibialis anterior compared to the plantar-flexors, which may suggest an important role of the dorsi-flexors during split-belt adaptation.

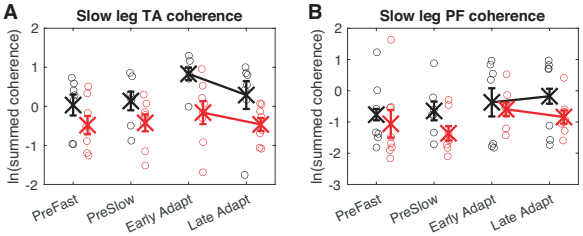

Figure 2: Tibialis anterior (A) and plantar-flexor (B) EMG-EMG coherence in the slow leg. Slow leg TA coherence was greater during early adaptation compared to pre-fast and pre-slow. **Black** = young adults; **Red** = older adults.

Significance

This study demonstrated age-related differences in corticospinal drive during split-belt locomotor adaptation. Further understanding of differences in neural mechanism with age may lead to gait interventions to reduce the fall risk in older adults.

Acknowledgments

We thank Chris Lamprecht and Joanne Lee for assistance with data processing, our participants, and support from American Society of Biomechanics Graduate Student Grant-In-Aid.

References

[1]Sato and Choi, 2019. J Neurophysiol 122, 1097-1109. [2] Spedden et al, 2019. Neurobiol Aging 78, 29-41. [3]Bruijn et al, 2012. J Neurophysiol 108, 1149-1157.

INFLUENCE OF UPPER LIMB MODEL PARAMETERS IN ISOMETRIC AND ISOKINETIC TASKS

Maximillian T. Diaz,[1] Joel B. Harley,[2] and Jennifer A. Nichols[1]
[1]J. Crayton Pruitt Family Department of Biomedical Engineering, University of Florida, Gainesville, FL, United States
[2]Department of Electrical & Computer Engineering, University of Florida, Gainesville, FL, United States
email: mdiaz40@ufl.edu

Introduction

Subject-specific models could assist physicians in diagnosing impairments and informing personalized care. Yet, most subject-specific models are hindered by a limited understanding of how model parameters influence predictions [1]. Although parameter sensitivity has been explored for gait [2], little is known about parameter sensitivity for upper limb tasks. Additionally, to what extent current upper limb models can accurately represent both healthy and pathologic populations is unknown. Thus, the objective of this study was to characterize how muscle and bone parameters influence predicted muscle activations during isometric versus isokinetic upper limb tasks. We specifically evaluated a broad range of bone densities (BD), optimal fiber lengths (OFL), physiological cross section areas (PCSA), and pennation angles (PA) due to their influence on muscle force production and recruitment [3-5].

Methods

A total of 401 parameter sets were defined to characterize healthy and pathologic BD, OFL, PCSA, and PA. First, a baseline parameter set was defined based on a validated upper limb model that represents an average adult male [6]. Then, the other 400 parameter sets were defined by varying each parameter from the baseline 100 times. Parameter values varied in equal steps across reported ranges of upper limb atrophy, hypertrophy, osteoporosis, and osteopetrosis [3-5].

To assess how parameters influenced predicted muscle activations, computed muscle control simulations were performed in OpenSim 4.1. For these simulations, each parameter set was applied to two models (a full arm model [6] and a thumb model [7]) and 3 tasks (1 isometric, 2 isokinetic) were simulated. The isometric task was a 40N lateral pinch task. The isokinetic tasks consisted of a distal task (wrist extension from 0º to 50º to 0º), and a proximal task (elbow flexion from 90º to 110º to 90º). To minimize simulation time, the full arm model was used for the isokinetic tasks, while the thumb model was used for the isometric task. Given 401 parameter sets and 3 tasks, a total of 1,203 simulations were performed.

We compute the Pearson correlation coefficient between each of our four parameters (BD, OFL, PCSA, and PA) and the area under the muscle activation curve (AUC) for the 14 muscles shared across both models. A high correlation indicates predicted muscle activations are sensitive to changes in the parameter, whereas low correlation indicates little to no effect on muscle activations. To identify differences between parameters and baseline, an ANOVA was performed followed by multiple comparisons with a Bonferroni correction.

Results and Discussion

During the isometric task, BD and PA did not influence muscle activation during lateral pinch. BD and PA exhibited no correlation with AUC (r=0) for most muscles (Fig. 1). Post hoc testing found no significant difference (p>0.99) from baseline. This suggests that for subject-specific lateral pinch models, it may be superfluous to incorporate subject-specific PA and BD.

In contrast, BD and PA were influential during isokinetic tasks. Despite little correlation between AUC and parameters during the distal isokinetic task, post hoc testing revealed AUC significantly ($p<0.01$) differed from baseline for all parameters. Further, during the proximal isokinetic task, BD was strongly correlated ($r>0.75$, $p<0.001$) for three muscles, suggesting isokinetic tasks informs identification of subject-specific BD.

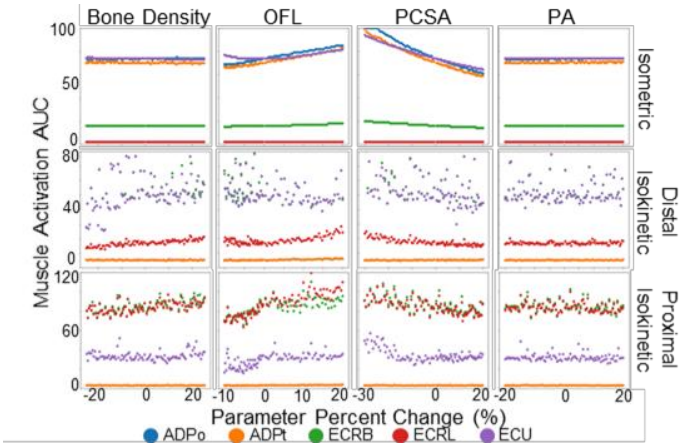

Figure 1: AUC of the muscle activation curve versus each parameter represented as percent change from baseline. Only five representative muscles are plotted due to space constraints. Correlations are indicated by non-horizontal lines. For example, OFL and PCSA have strong correlation ($|r|>0.8$, $p<0.01$) with AUC for most muscles during the isometric task. BD is correlated with AUC in the isokinetic tasks.

A difference between the isokinetic and isometric tasks is that muscle activations during isometric tasks were highly sequential, but isokinetic tasks resulted in increased variability (Fig. 1, higher spread in isokinetic tasks). It is believed the additional 41 muscles in the full arm model used for the isokinetic tasks provided compensatory solutions causing the variation. Due to strong correlations, it may be possible to create algorithms that identify subjects' PCSA and OFL from isometric tasks, and then use an isokinetic task to compute BD.

Significance

This work utilizes large datasets to capture the diversity of the human population and upper limb tasks to understand how subject-specific parameters influence hand model predictions.

Acknowledgments

Funding from NIH NIBIB Trailblazer Award (R21 EB030068).

References

[1] Valente et al. 2014. *PLoS One., 9*(11)
[2] Ackland et al. 2012. *J. Biomech*., 45(8):1463-1471
[3] Blake et al. 2005. *Osteoporos Int*., 16:2149–2156
[4] Erskine et al. 2014. *Eur J Appl Physiol*., 114(6):1239-49
[5] McPhee et al. 2018. *J Gerontol A Biol Sci Med Sci*, 73(10):1287-1294
[6] Saul et al. 2015. *Comp Methd Biomech Biomed Engin* 18(13):1445-58
[7] Nichols et al. 2017. *J. Biomech*., 58:97-104

INSTANTANEOUS CENTER OF ROTATION BEHAVIOR DURING LIGAMENT REMOVAL IN THORACIC SPINE

Michael Polanco[1], Stacie I. Ringleb[1], Michel Audette[1], Carl St. Remy[2], James Bennett[2], and Sebastian Bawab[1]
[1]Old Dominion University, Norfolk, VA, USA, [2]Children's Hospital of the King's Daughters, Norfolk, VA, USA
email: sbawab@odu.edu

Introduction

The Instantaneous Center of Rotation (ICR) is used to describe how a joint moves compared to Range of Motion which describes the quantity of joint motion and can assist in diagnosing spinal deformity and instability [1]. Finite element analysis can provide a clinician with a non-invasive approach in deciding how to best impose spinal flexibility pre-surgery, including ligament removal. Prior studies showed serial ligament removal in a lumbar functional unit of the spine affecting ICR location [2]. Limited investigations have taken place in the thoracic spine [3], which possesses different geometric and stiffness properties due to the costovertebral connections between the ribcage and thoracic columns. The purpose of the study is to assess the variance of the ICR of a thoracic functional unit during ligament removal in a finite element model. The hypothesis is the greatest shift in ICR will occur when the stiffest ligament, or flaval ligament, is removed.

Methods

A Finite Element model of an asymptomatic T7-T8 functional unit was utilized for this study (Figure 1). Ribcage, Vertebral, and Intervertebral Geometry for the model was acquired from CG Hero (CG Hero Ltd., Manchester, UK), and the finite element model created using Hypermesh (Altair Engineering, Troy, MI). Quasi-static analyses were run using LS-DYNA (Livermore Software Technology, Livermore, CA), where all intervertebral and costovertebral ligaments were characterized using tension-only elements [4-6], while vertebral and disc material properties were acquired from the literature [7]. A pure moment of ±9 N-m was applied over a rigid body element in flexion and extension encompassing the superior endplate and facet processes of T7 while the inferior endplate and facet processes of T8 were fully constrained. To reflect the steps taken for spinal flexibility gain in a posterior spinal fusion, the model was run with the interspinous and supraspinous ligaments removed, followed by facet joint removal, and finally ligamentum flavum removal. In each step, motion data was taken from a pair of nodes posteriorly and anteriorly along the superior endplate. From this, the ICR was assessed using the perpendicular bisector method [8] and its shift along the sagittal plane was analyzed.

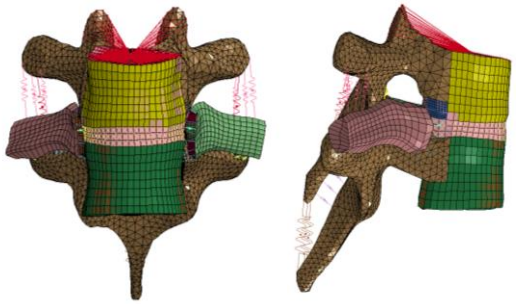

Figure 1. Finite Element Model of T7-T8 FSU

Results and Discussion

The greatest shift in the mean ICR occurred in flexion when the flaval ligament was removed, creating approximately a 30% shift from the mean position when the facet joint was removed, and 41% from the intact position. In extension, however, the only shift in mean ICR occurred when the facets were removed, having only shifted approximately 4% in the superior direction compared to intact, while no significant change is denoted in the posterior-anterior direction (Figure 2).

The results summarized here are sensible as a gradual removal of ligaments from posterior to anterior in flexion led to a shift in ICR in that direction, with the greatest shift happening with the flaval ligament removal because it was the stiffest ligament in the group. The ICR trends described here assume a given sequence of ligaments which are removed. ICR behavior could be altered directly with a procedure. Despite these differences, the shift in direction for flexion is in general agreement with similar assessments [2].

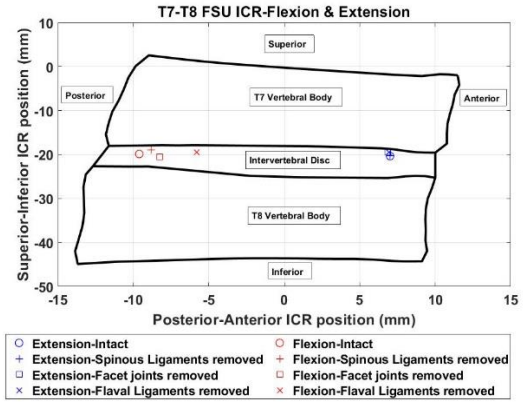

Figure 2. ICR calculations at different ligament removal stages

Significance

As little is known about ICR in the thoracic spine, results presented provide a first step by which its behavior can further be investigated when polysegmental models of the spine are incorporated with the ribcage. Kinematic comparisons can be compared between healthy spines and those with thoracic musculoskeletal disorders such as scoliosis. Ultimately, the ICR may lead to a guide for clinicians to find the optimum treatment for thoracic deformities and properly diagnose the level of spinal severity on patients based on symptomatic evaluation.

Acknowledgments

This work was funded by a SMART scholarship received by M. Polanco and the Children's Research Foundation.

References

[1] Lee, S.W. et al. *Spine* **22**(6), 641-7, 1997.
[2] Alapan, Y. et al. *Neurosurg Spine* **18**(6), 617-26, 2013.
[3] Panjabi, M.M. et al. *J Orthop Res* **1**(4), 387-94, 1984.
[4] Chazal, J. et al. *Biomechanics* **18**(3), 167-76, 1985.
[5] Pintar, F. *Dissertation*, 1986.
[6] Aira, J. et al. *Traffic Inj Prev* **20**(sup2), S1-S6, 2019.
[7] Naserkhaki, S. et al. Biomechanics 70, 33-42, 2018.
[8] Pearcy, M.J. and Bogduk, N. *Spine* **13**(9), 1033-41, 1988.

AN UNANTICIPATED SIDE-STEP CUT PRODUCES ALTERED KNEE MECHANICS

S. McCrory[1], N. Cortes[1], E. Nijmeijer[2], J. Bosma[2], J. Bombach[2], A. Benjaminse[2]
[1] George Mason University, Manassas, VA USA
[2] University of Groningen, The Netherlands
email: ncortes@gmu.edu

Introduction

Anterior cruciate ligaments (ACL) injuries are common in athletes and can have significant affects to quality of life in those affected. Jump landings and changes-of-direction movements are common mechanisms of injury for the ACL, which in turn, has helped in the development of tests that can be used to assess ACL injury risk. A common task used to assess ACL injury risk is the sidestep cut (SSC)[1]. Additionally, altered biomechanics are present during unanticipated variations of similar movements[2,3], suggesting that varying tasks produce distinct mechanics. While some variations have been explored, there are many others that have not been investigated to determine their effects on biomechanics. The present study introduces a novel version of unanticipated SSC task to determine potential biomechanical changes.

We hypothesized that athletes would have altered knee biomechanics when performing unanticipated (UNT) and anticipated (ANT) versions of the SSC.

Methods

19 recreationally active athletes (age = 22 ± 1.6 years, height = 186 ± 7 cm, mass = 80 ± 8.6 kg) completed both ANT and UNT versions of an SSC task. Subjects were outfitted with 21 retroreflective markers that were tracked using an 8-camera VICON system. The ANT SSC began with a 5m approach and a 5m follow-through after a 45-degree change-of-direction on a force plate. The change of direction was performed in the direction opposite of the subject's dominant leg and was performed by cutting with the dominant leg on a force plate. The UNT condition introduced 2 alternative tasks to each trial, with randomized light gates presenting the required version of the task to the subject directly after beginning the 5m approach. The UNT SSC task included the original task (change of direction toward non-dominant side), a change of direction to the dominant side (opposite direction of ANT), and a stopping task in which participants would stop and jump straight up once they reached the force plates. Only UNT trials that matched the ANT version of the task were recorded. Participants completed five valid trials of the task for ANT and UNT scenarios.

Analysis was completed using a custom pipeline in Visual 3D software to calculate knee flexion at initial contact (IC), knee flexion at midstance (MS), and knee flexion moment at MS. Descriptive statistics were computed. A one-way multivariate analysis of variance (MANOVA) was performed to determine differences between ANT and UNT conditions of the SSC task for all three variables.

Variable	ANT Mean ± SD	UNT Mean ± SD	p-value
Knee Flexion Angle (IC)	-23.7° ± 7.14°	-26.2° ± 6.06°	<0.05
Knee Flexion Angle (MS)	-43.4° ± 8.76°	-49.6° ± 7.89°	<0.001
Knee Flexion Moment (MS) (N*m/Kg)	-0.93 ± 0.36	-0.77 ± 0.29	<0.001
Total Knee Flexion (MS – IC)	19.7° ± 1.62°	23.4° ± 1.83°	

Table 1: Descriptive Statistics of SSC variables.

Results and Discussion

The results indicated a significant difference between ANT and UNT conditions for all three variables. Univariate analyses demonstrated that all variables were significantly different between the ANT and UNT conditions ($p<0.05$). This indicates that athletes will alter their knee biomechanics to complete tasks when having to make decisions quickly about the task, supporting our initial hypothesis.

These results suggest that unanticipated SSC tasks may replicate more realistic knee biomechanics, with regard to ACL injury risk, than the anticipated version of the same task. These findings differ from previous research that found decreased knee flexion during unanticipated cutting tasks.[4]

Significance

Due to the inherent uncertainty of the movement requirements of sports, understanding how the body moves differently may be beneficial in helping prevent ACL injuries. Introducing novel movement decision-making patterns into research may help in identifying types of movements that may cause athletes to be more at-risk for injury. These findings suggest that the introduction of increased cognitive strain (i.e., deciding what task to perform) may produce altered knee biomechanics in recreational athletes.

References

1. Jones et al. (2017) *Prof Strength Cond 47:37-42*
2. Zhang et al. (2019) *J Human Kinet, 67:25-35*
3. Norte et al. (2020) *J Athl Train, 55(8):834-842*
4. Meinerz et al. (2015) *J Athl Train, 50(9):905-913*

THE EFFECT OF COSTOVERTEBRAL JOINTS ON THE MOTION OF A THORACIC SPINE FUNCTIONAL UNIT

Michael Polanco[1], Stacie Ringleb[1], Michel Audette[1], Carl St. Remy[2], and James Bennett[2], Sebastian Bawab[1]
[1]Old Dominion University, Norfolk, VA, USA, [2]Children's Hospital of the King's Daughters, Norfolk, VA, USA
email: sbawab@odu.edu

Introduction

The costovertebral (CV) joint helps to reinforce the ribs to the vertebral column while providing stability to the thoracic spine [1]. Their proper representation, made of costocentral and costotransverse joints, in a finite element model can assist a clinician's understanding behind decisions made towards treatment options for musculoskeletal disorders [2]; however, in-vitro experimental data is needed for accurate development. Specimen preparation conditions vary for in-vitro experiments examining thoracic kinematics, including those who have left ribs and the CV joint intact [1]; or removed in their testing [3]. In addition, the ways that CV joints are represented in a finite element model is sometimes simplified to a spherical joint with rotational stiffnesses prescribed [4]. The purpose of the study is to examine the sensitivity of the CV joint on the motion of a thoracic functional unit.

Methods

A Finite Element Model of an asymptomatic T7-T8 (Figure 1) functional unit was utilized for this study. Model geometry for the ribs, vertebral body, and the intervertebral disc were obtained from CG Hero (CG Hero Ltd., Manchester, UK) and prepared using Hypermesh (Altair Engineering, Troy, MI). Quasi-static analyses were conducted using LS-DYNA (Livermore Software Technology, Livermore, CA). Vertebral and disc material properties were acquired from literature [5]. Intervertebral ligament [6,7] and CV joint ligament properties [8] were characterized as tension-only elements. Ribs in the model containing the CV joint were shortened to approximately 3 cm in length to maintain the ligamentous connections between ribs and the vertebral body. The facet, rib head, and rib to transverse process interfaces were represented using a surface penalty contact algorithm within LS-DYNA. A pure moment of ±7.5 N-m was applied over a rigid body element in flexion, extension, left/right lateral bending, and left/right axial rotation. Each case was first run with the CV joints present and repeated with the CV joints and ribs removed.

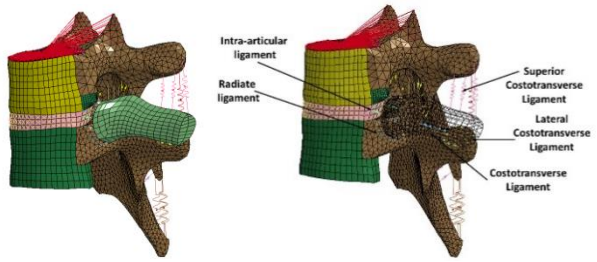

Figure 1: T7-T8 functional unit with CV joints

Results and Discussion

The smallest percent decrease in Range of Motion with the CV joints present occurred in both directions of axial rotation with less than 3%. The largest percent decrease in Range of Motion with the CV joints occurred in both directions of lateral bending, with approximately 8% and 14% for left and right lateral bending respectively. Finally, an approximate 5 and 7% reduction in Range of Motion occurred in flexion and extension respectively.

In comparison with similarly conducted experiments [9], the kinematics match well in axial rotation and flexion, but not in lateral bending and extension (Figure 2), which could be tied to facet behavior. Nonetheless, the findings are qualitatively in agreement with similarly conducted experiments [1]. While the differences are evident, further reduction in Range of Motion can be obtained when the ribcage is incorporated [1]. Future work will investigate stiffness differences with the entire ribcage connected to the spine. In addition, due to positional differences along the spinal column, the role of the CV joint in the motion of different intervertebral spinal units should be investigated.

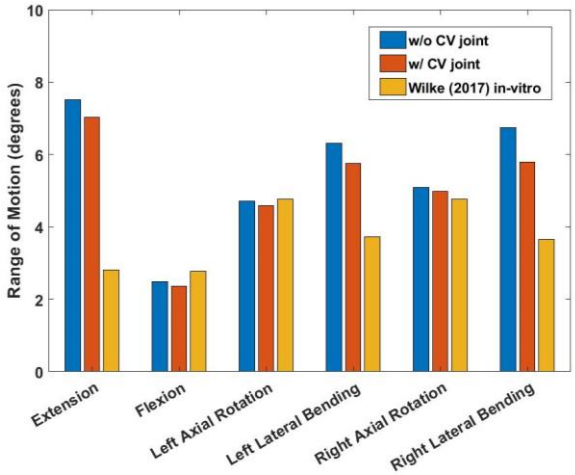

Figure *2:* Range of Motion comparison with and without CV joints

Significance

Biomechanical investigations of the thoracic spine for clinical applications presently remain limited. Accurate knowledge of thoracic spine anatomy and their testing conditions can enhance development of finite element models for surgical planning. This study confirms proper stiffening behavior by the CV joint which will aid in further model development and validation of the thoracic spine and could be utilized for clinical applications such as scoliosis treatment.

Acknowledgments

This work was funded by a SMART scholarship received by M. Polanco and the Children's Research Foundation.

References

[1] Oda, I. et al. *Spine* **21**(12), 1423-9, 1996.
[2] Schlager, B. et al. Comp Meth Biomech **21**(14), 2018.
[3] Wilke, H.J. et al. *Eur Spine J* **29**(1), 179-85, 2020.
[4] Kindig, M. et al. Comp Meth Biomech **18**(5), 2015.
[5] Naserkhaki, S. et al. Biomechanics 70, 33-42, 2018.
[6] Chazal, J. et al. *Biomechanics* **18**(3), 167-76, 1985.
[7] Pintar, F. *Dissertation*, 1986.
[8] Aira, J. et al. *Traffic Inj Prev* **20**(sup2), S1-S6, 2019.
[9] Wilke, H.J. et al. PloS One 12(5), e0177823, 2017.

DIFFERENCES IN MUSCLE DEMAND BETWEEN SKIPPING AND RUNNING

Sarah A. Roelker[1], John D. Willson, Paul DeVita, and Richard R. Neptune
[1]Department of Kinesiology, University of Massachusetts Amherst, Amherst, MA
email: sroelker@umass.edu

Introduction

Skipping has been proposed as a viable cross-training exercise to running due to its lower knee contact forces and higher metabolic cost.[1,2] However, it is not clear how individual muscle demand is differentially affected by the different gait modes. Thus, the purpose of this study was to identify differences in individual muscle force impulses and metabolic cost between skipping and running.

Methods

Five young adults (2 female; 22.4 ± 2.2 y; 1.70 ± 0.06 m; 74.5 ± 12.7 kg) provided written informed consent to participate in this study protocol approved by the East Carolina University IRB. Experimental 3D marker and ground reaction force data were collected during 10s running and skipping trials at 2.5 m/s on an instrumented dual-belt treadmill with right leg electromyography (EMG) data captured from 8 muscles. For each participant, the most representative running (Run) and skipping (Skip) cycles were identified.[3] The Skip cycle included the leading limb hop (Skip 1) and trailing limb step (Skip 2).[1,2] In OpenSim[4] 3.3 a full-body 12 segment model[5] was scaled to each participant's anthropometry. For each representative Run and Skip cycle, joint angles were determined using inverse kinematics.[6] A residual reduction algorithm fine-tuned the model mass properties and joint kinematics to make them dynamically consistant.[6] Muscle forces were estimated by computed muscle control[7] with constraints such that the muscle excitation timing and patterns were consistent with those of the measured EMG data.[8] Muscle force impulses were computed over each step (i.e., Run, Skip 1, and Skip 2) and then normalized to distance traveled to compare impulses between Run and Skip (Skip 1 + Skip 2) cycles (cumulative load per km). Muscle metabolic power was determined by the Umberger2010MuscleMetabolics probe[9] and integrated over each cycle to quantify metabolic cost. Muscle force impulses and metabolic cost were summed within functional groups (Fig. 1 caption). Repeated measures ANOVAs tested for between-step differences in muscle group impulses. Tukey's post-hoc tests identified pairwise differences. Paired t-tests assessed differences in muscle group impulses and metabolic cost between cycles. For all statistical tests $\alpha=0.05$.

Results and Discussion

All muscle groups had lower muscle force impulses in Skip 1 and/or Skip 2 than in the Run step (Fig. 1A). The trunk, gastrocnemii, and soleus impulses were also greater in the Run cycle than in the Skip cycle (Fig. 1B). Thus, per step and per cycle, skipping requires lower muscle forces than running. In contrast, skipping had a greater overall metabolic demand than running, with rectus femoris, vasti, gastrocnemii, and tibialis anterior all being significantly higher in skipping (Fig. 1C). Further analysis revealed that several muscles have greater active volume (greater fiber length and/or activation) during skipping. Also, shorter contact times during skipping[1] suggest higher rates of force development requiring greater muscle activations. Further, differences in the mechanics between running and skipping likely influence each muscle's force-length-velocity relationships, which alters the level of muscle force generation for a given activation level.

Significance

Consistent with previous studies, we found skipping has a higher metabolic demand relative to running at the muscle level, although the required muscles force impulses were lower. This further supports skipping as a viable alternative to running. Future work will investigate the influence of intrinsic muscle properties on these relationships as well as differences in joint loading at the hip, knee and ankle joints between the two gaits.

References

[1]McDonnell, *J Biomech*, 2017. [2]McDonnell, *Gait Posture*, 2019. [3]Sangeux, *Gait Posture,* 2015. [4]Delp, *IEEE Trans Biomed Eng*, 1990. [5]DeMers, *J Orthop Res,* 2014. [6]Delp, *IEEE Trans Biomed Eng,* 2007. [7]Thelen, *J Biomech*, 2003. [8]Roelker, *J Biomech*, 2019. [9]Umberger, *J R Soc Interface*, 2010.

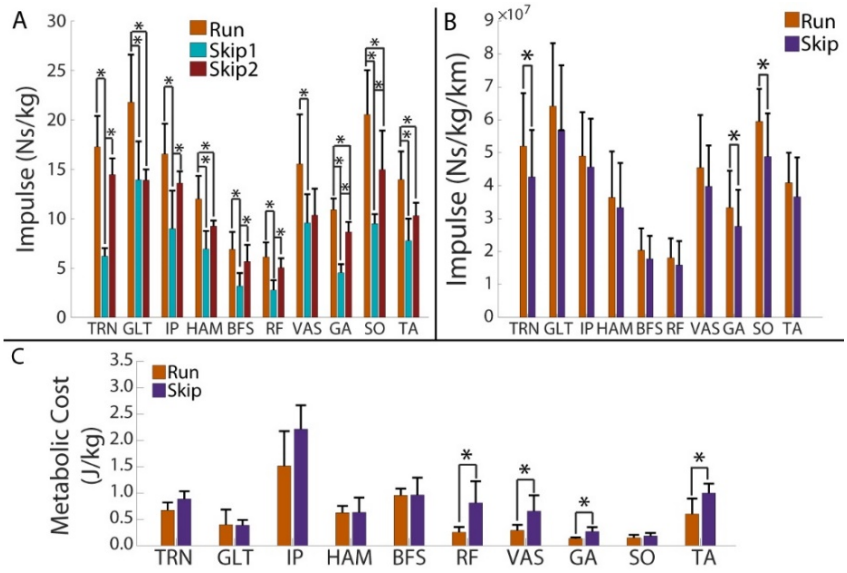

Figure 1: Muscle force impulses for running and skipping steps (A) and cycles (B) and muscle metabolic cost over Run and Skip cycles (C). Abbreviations: TRN: erector spinae, external obliques, internal obliques; GLT: gluteus maximus, gluteus medius, gluteus minimus; IP: iliacus, psoas; HAM: biceps femoris long head, semitendinosus, semimembranosus, gracilis; RF: rectus femoris; VAS: vastus medialis, vastus lateralis, vastus intermedius; BFS: biceps femoris short head; GA: medial and lateral gastrocnemius; SO: soleus, tibialis posterior, flexor digitorum, flexor hallucis, peroneus brevis, peroneus longus; TA: tibialis anterior, extensor digitorum, extensor hallucis, peroneus tertius. * $p < 0.0\,5$.

THE EFECT OF PROSTHETIC ANKLE STIFFNESS CHANGES ON GAIT AND STANDING IN PEOPLE WITH UNILATERAL TRANSTIBIAL AMPUTATIONS

M. Vaca, M.S.[1,2], R. Stine, M.S.[1,2] and S. Gard, Ph.D.[1,2]
[1] Department of Biomedical Engineering - Northwestern University, Evanston, IL
[2] Jesse Brown VA Medical Center, Chicago
email: miguelvm@u.northwestern.edu

Introduction

Modular prosthetic ankle components have been shown to improve walking in transtibial prosthesis users, but they may reduce stability during standing. Therefore, the stiffness of the prosthetic foot-ankle components may need to be appropriately tuned to provide optimal balance between mobility for walking and stability for standing. The present research investigates both concepts to improve our knowledge about how the prosthetic ankle stiffness influences standing and walking performance.

One method is to identify a mechanical property that directly influences the performance of the amputee (Major et al, 2012). Roll Over Shape (ROS) has been reported to accomplish it. (Gard et al, 2011; Hansen et al, 2010). Obtaining a prosthetic radius of ROS similar to the radii of able-bodied individuals may provide an overall improvement during gait.

Methods

This project was reviewed and approved by the Northwestern University IRB. All subjects provided informed consent before they were enrolled in the study.

Subjects: Eight individuals with unilateral transtibial amputation (3 males and 5 females; 48.1±13.9 years, 75.1±17.6 kg, 1.68±0.09m) participated.

Apparatus: Kinematic and kinetic data were collected at 120 Hz and 960 Hz, respectively, using a digital motion capture system (Motion Analysis Corp, CA) and force platforms (AMTI, MA).

Procedures: Three different levels of ankle stiffness (Firm, Medium and Soft) were tested using the College Park Venture foot (College Park, MI).

Data Analysis: The data were grouped and analysed using three separate procedures based upon data type: kinetic and kinematic calculations, ROS radii and sway area. Statistical analyses were performed using SPSS with repeated measures ANOVA for ROS radii data.

Results and Discussion

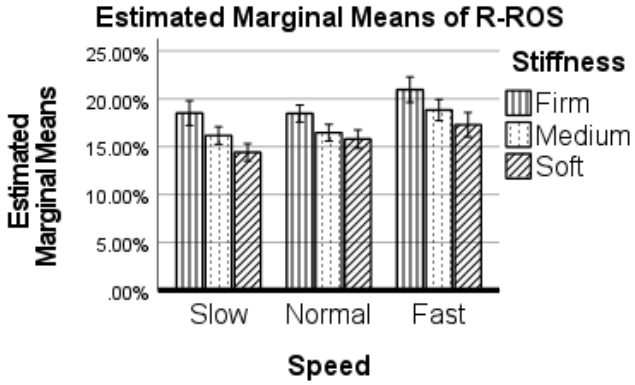

Figure 1: Radius of ROS (Normalized) at different stiffness conditions and self-selected walking speeds.

Radius of ROS was significantly different due to ankle stiffness ($p<0.001$) and walking speed ($p<0.001$). These results suggest that the Firm stiffness condition best replicated the ankle-foot ROS radius of able-bodied individuals (19%).

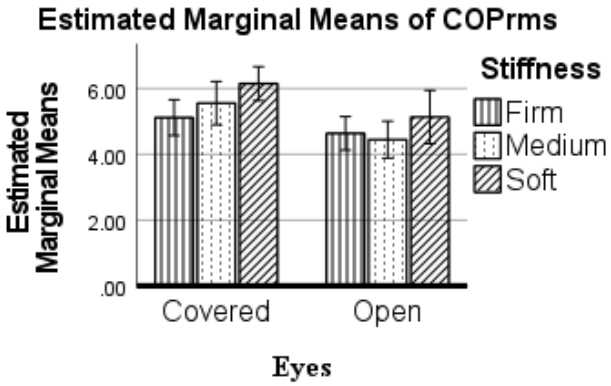

Figure 2: Root Means Square Distance of Center of Pressure during quiet standing at different stiffness conditions.

Sway movement of the COP at the Firm condition (5.18±1.74mm) was significantly smaller ($p<0.001$) compared to the Soft condition (6.28±1.64mm).

One of the key findings from the analyses was that walking speed had an influence on the ROS radius of a passive prosthetic foot-ankle mechanism. Contrary to what is observed on able-bodied ambulators, passive prosthetic components are not capable of maintaining a constant ROS geometry at different speeds, particularly when the forces applied are directly influenced by walking speed.

The ROS radius provided by the Firm condition was the closest approximation to able-bodied ROS radius (19%) and produced better performance compared to the other stiffness configurations. Additionally, the performance for standing balance favored the Firm stiffness condition. Taking into consideration the results from both sets of analyses, the Firm stiffness could be considered the most desirable for both walking and standing.

Significance

Improved understanding of how ankle stiffness influences walking and standing performance could help to establish guidelines for optimally fitting ankle units with prosthetic feet.

Acknowledgments

This study was supported by Veterans Health Administration Rehabilitation Research and Development Service
(grant no. RX002107).

References

Gard, S. JRRD 48(9), 1037, 2011.
Hansen, A. Disability and Rehabilitation 32(26), 2201, 2010.
Major, M. JRRD 49(6), 815, 2012

Put a Sock on It!: Investigation of Various Sock Types on Locomotive Patterns

Hannah Houde[1], Christopher M. Wilburn[1], John W. Fox[2], Adam E. Jagodinsky[3], Brandi E. Decoux[4] Elizabeth Hartfield[1], Sarah Carter[1], Ryan Bracher[1], and Wendi H. Weimar[1]

[1]Auburn University, Auburn, AL
[2] Methodist University, Fayetteville, NC
[3]Illinois State University, Normal, IL
[4]Bridgewater State University, Bridgewater, MA
Email: czw0043@auburn.edu

Introduction

Formerly perceived as an accessory in fashion, specialized socks and hosiery have a functional role in locomotive tasks. Clinically, modern textile advancements and composition of socks have provided kinetic attenuating benefits to individuals with diabetes, neuropathy, and rheumatoid arthritis [1-3]. Alterations in these compositional properties have also been implemented in commercially available socks and have been suggested to provide personalized podiatric comfort. These improvements have included but are not limited to graduated compression, enhanced moisture wicking, and minimized friction between the shoe-foot interface, in recreational and competitive activities [1,3]. However, further examination toward the influence of these socks on anatomical response and locomotive tasks within healthy populations remain limited. Thus, this study examined how socks of different compositional properties can effect locomotive outcomes and foot function.

Methods

Eighteen healthy participants (1.78 ± .07; mass: 84.4 ± 10.34) volunteered to walk at a self-selected paced across an instrumented walkway under three sock conditions: barefoot, traditional socks and athletic socks. The traditional socks were composed of 100% cotton while, the athletic sock had a reinforced arch band and was composed of 60% polyester, 25% polypropylene, 10% spandex, and 5% rubber.

Spatiotemporal parameters, such as walking velocity, normalized stride length, cadence, stance time, and stance percentage of cycle, were analyzed across each condition. Center of pressure deviations were used to examine the effect each sock condition had on foot function, as mentioned in previous literature [4-5]. Further, foot anthropometrics were taken to investigate the impact of sock conditions on specified foot architecture [6].

Results and Discussion

A series of mixed-factorial ANOVAS were employed to investigate spatiotemporal differences amongst the sock conditions, arch classifications, and determine any interactions. The results indicate significant differences in center of pressure deviations amongst sock conditions and arch classifications. Specifically, center of pressure path deviated from the center of the foot the least in the athletic sock condition, followed by the cotton sock and the condition that yielded the most deviation was barefoot (Figure 1). Additionally, lower arches displayed a greater deviated points when compared to neutral arches.

Overall, the findings in this study indicate that the use of various sock types decrease mediolateral center of pressure deviation, without altering spatiotemporal parameters, when compared to barefoot during walking gait. Despite the lack of significance between the athletic and cotton sock conditions and interaction amongst the sock conditions and arch classification, the athletic sock condition yielded smaller mediolateral center of pressure deviations. Thus, specialized sock use can provide some improvements to locomotive patterns.

	Barefoot	Athletic Sock	Cotton Socks		
	M (SD)	*M (SD)*	*M (SD)*	*F*	*p*
Walking Velocity (cm/s)	121.16 (15.02)	122.53 (13.13)	120.81 (15.80)	1.347	.516
Cadence (steps/min)	108.53 (5.98)	109.61 (3.96)	108.28 (4.81)	2.273	.119
Normalized Stride Length (% of body height)	74.62 (6.98)	75.11 (6.29)	74.15 (7.15)	1.007	.377
Stance Time (s)	.694 (.04)	.688 (.04)	.686 (.04)	2.375	.109
Stance % of Cycle (%)	62.77 (1.44)	62.77 (1.29)	63.03 (1.45)	1.885	.168
Center of Pressure Mediolateral Deviations	**104.28 (24.38)$^{*,+}$**	**91.73 (25.66)***	**93.49 (26.54)$^{+}$**	**9.930**	**< 0.001**
Center of Pressure Mediolateral Deviations (Neutral Arches)	**93.22 (27.99)$^{\#}$**	**79.16 (25.90)$^{\#}$**	**78.21 (28.88)$^{\#}$**	**5.027**	**.039**
Center of Pressure Mediolateral Deviations (Lower Arches)	**113.13 (17.84)**	**101.78 (22.57)**	**105.71 (17.55)**		

Figure 1. Results of Spatiotemporal Parameters Comparison Across Conditions and Arch Classifications

* indicates significance between barefoot and athletic sock condition; + indicates significance between barefoot and athletic sock condition; # indicates significance between low and neutral arches

Significance

While previous studies have demonstrated the influence cushioning properties of socks on force attenuation, this project suggests that various sock types can improve the function and stability of the foot during gait. Specifically, the knitting and structural components found in the athletic sock condition improve foot function regards of specific arch classifications. The use of athletic sock can serve as an inexpensive and accessible podiatric assistive device that promotes healthy foot mechanics during locomotion.

References

[1] Clinc. Biomech (2013) 28 (7): 825-830.
[2] Foot (1996) 6 (1): 5-9.
[3] Clinc. Biomech 2007; 21: 314-321.
[4] Gait Posture. 2008; 27 (4): 669-675.
[5] JAPMA. 1999; 89(6): 278-291.
[6] JAPMA. 2008. 98(2), 102-106.

Exploring the Functional Boundaries and Metabolism of Triceps Surae Force-Length Relations during Walking

Callum J. Funk[1], Rebecca L. Krupenevich[1], Gregory S. Sawicki[2], Jason R. Franz[1]
[1]Joint Department of Biomedical Engineering, UNC Chapel Hill and NC State University, Chapel Hill, NC
[2]George W. Woodruff School of Mechanical Engineering, Georgia Tech, Atlanta, GA, USA
email: jrfranz@email.unc.edu

Introduction

Older adults exhibit reduced ankle push-off intensity and higher metabolic energy costs during walking than younger adults [1]. During walking, triceps surae (TS) muscle fascicles in young adults operate near the peak of their force-length (F-L) relation, which acts to maximize force capacity (i.e., the maximum possible force at a fascicle length) and minimize the active muscle volume necessary to meet force demands [2]. However, older adults tend to operate at shorter lengths that are associated with higher metabolic costs in isolated contractions [3]. Theoretically, increasing or decreasing activation should be capable of steering muscle fascicles to shorter or longer lengths, respectively, with implications for force capacity, active muscle volume, and thus metabolic energy cost. However, the relations between muscle activation, muscle mechanics, and whole-body metabolic energy cost in walking have yet to be fully elucidated. There are two translational implications that motivate this work. First, energetics models informed by such relations may help guide the personalized prescription of assistive devices. Second, clarifying the local muscle neuromechanical determinants of walking metabolism in young adults might provide a mechanistic framework to elucidate those in older adults. Thus, the purpose of this study was to establish cause-and-affect relations between volitional changes in TS activation prescribed using biofeedback and walking metabolic cost, muscle mechanics, and force capacity. We hypothesized that (1) increased TS activation would increase metabolic cost via shorter muscle fascicle operating lengths and thus reduced force capacity and that (2) decreased TS activation would decrease metabolic cost via longer muscle fascicle operating lengths and thus increased force capacity.

Methods

26 young adults (23±4 yrs., 12F/14M) walked on an instrumented treadmill at 1.25 m/s using electromyographic (EMG) biofeedback to match targets corresponding to ±20 and ±40% TS (medial gastrocnemius [MG] and soleus) activation during push-off (late stance). B-mode ultrasound imaged subjects' MG. Subjects also performed maximal voluntary isometric plantar flexor contractions in a dynamometer at 5 joint angles to estimate individual F-L relations. We have thus far analyzed muscle data in n=9 participants using deep learning software [4]. We report net metabolic power, TA activation, MG force, force capacity, and MG fascicle lengths, averaged from the last two minutes of each walking trial, analyzed using repeated measures correlations [5].

Results and Discussion

In partial support of Hypothesis 1, subjects increased net metabolic power by up to 95% when targeting higher than normal TS activation ($p<0.01$; Fig. 1A). However, contrary to Hypothesis 2, they also increased net metabolic power by up to 23% when targeting lower than normal TS activation. At the instant of peak MG force (*i.e.*, t_{peak}), MG fascicle length was 6% shorter ($r=-0.60$, $p<0.001$) and MG force was 5% larger ($r=0.50$, $p=0.002$) on average when targeting +40% TS activation. Not surprisingly, net metabolic power positively correlated with peak MG force ($r=0.35$, $p=0.04$; Fig. 1B). However, as hypothesized, and consistent with the association between activation and operating length, net metabolic power most strongly correlated with shorter fascicle lengths at t_{peak} ($r=-0.55$, $p=0.001$; Fig.1C). Consistent with prior work in isolated contractions [3], those results suggest that shifts to shorter fascicle lengths may mediate activation-induced increases in metabolic cost. More surprisingly, these determinants (*i.e.*, MG force and fascicle length at t_{peak}) were not themselves well correlated ($p=0.17$; Fig. 1D). Finally, force capacity at t_{peak} and net metabolic power tended to positively correlate ($r=0.32$, $p=0.06$), alluding to higher metabolic cost of operating the MG at higher force capacity (Fig. 1E). This specific outcome is unlikely to apply to older adults who habitually operate further down the ascending limb.

Significance

We interpret our findings thus far to suggest that: (1) volitional changes in TS activation augment the metabolic cost of walking via relatively predictable alterations in muscle force and operating lengths but (2) activation-induced changes in muscle force and length, and their respective contributions to metabolic cost, may not be directly interdependent during complex, functional activities such as walking.

Acknowledgments

Supported by a grant from NIH (R01AG058615).

References

1. Franz JR. *Exerc. Sport Sci. Rev.* 44(4), 2016.
2. Rubenson J et al. *J. Exp. Biol.* 214, 2011.
3. Beck ON et al. *bioRxiv*, 2021.02.10.430661, 2021.
4. Cronin NJ et al. *arXiv*, 2009.04790, 2020.
5. Bakdash JZ & Maurisch LR. *Frontiers in Psych.* 8, 2017

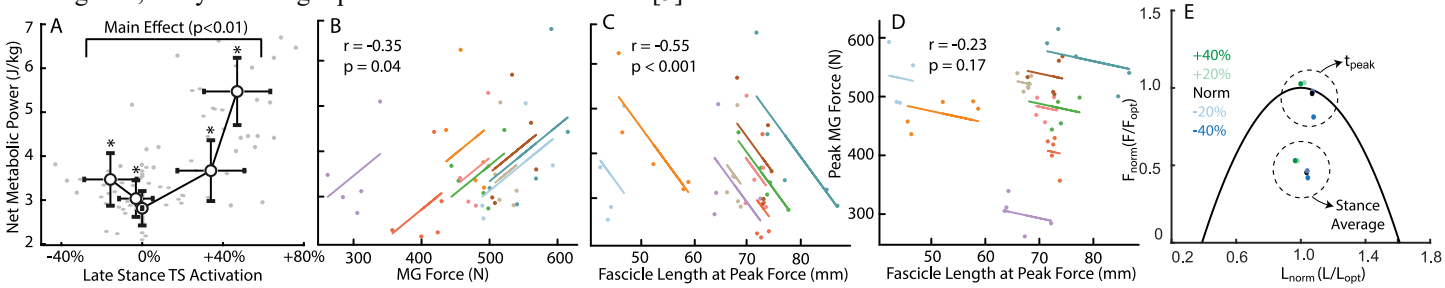

Figure 1: (A) Metabolic responses to altered triceps surae activation in walking (n=26). *significant pairwise difference compared to normal walking. (B-D) Repeated measures correlations between muscle dynamics and energetic outcomes, where each color represents an individual subject (n=9). (E) MVIC MG F-L relation compared to physiological loading during walking conditions, averaged across subjects (n=9).

HEALTHY HIP KINEMATICS DURING GAIT: SEX DIFFERENCES AND ASYMMETRY REVEALED THROUGH DYNAMIC BIPLANE RADIOGRAPHY

Camille Johnson, Ethan Ruh, Naomi Frankston, Shaquille Charles, Michael McClincy, William Anderst
Department of Orthopaedic Surgery, University of Pittsburgh, Pittsburgh, PA, USA
Email: ccj17@pitt.edu

Introduction

The contralateral hip is a common reference for clinical evaluation of hip pathologies and has implications for surgical planning and evaluation[1]. Symmetry in kinematics cannot be reliably identified using skin marker-based motion capture due to errors of up to 9.5° in rotation and 16.6 mm in translation when compared to underlying bone motion measured using biplane radiography[3,4]. Previous biplane radiography studies measured differences between operated and native hips or studied symptomatic cohorts[2], but there is a lack of data describing side-to-side differences (SSD) in healthy hip kinematics during gait.

The objectives of the study were 1) Determine the SSD in healthy hip kinematics during gait; 2) Determine kinematic differences between males and females. We hypothesized that SSD in kinematics would be smaller than previously reported in the knee and ankle and there would be no difference in kinematics waveforms between males and females during gait.

Methods

14 healthy young adults (6M, 8F; age: 21.6±2.2 years, BMI 22.0±1.9 kg*m^2/s) participated in this IRB-approved study. Synchronized biplane radiographs were collected at 50 images/sec for 1 second during treadmill walking (self-selected speed, 3 trials/hip). Femur and pelvis position were determined by matching subject-specific CT bone models to each frame of the radiographs using a validated volumetric model-based tracking technique (bias: 0.2˚, 0.2 mm; precision: 0.8˚, 0.3 mm)[5]. Anatomic coordinate systems were established in each femur and hemi-pelvis[6], mirrored to the contralateral side, and co-registered to produce identical coordinate systems for each hip. Six degree-of-freedom (DOF) rotations and translations were calculated[6], filtered, and normalized to standing posture. Translations were calculated as displacement of the femoral head center from the acetabulum center along the pelvis anatomical axis[6].

Symmetry was determined by calculating average absolute SSD in kinematic waveforms for each participant. Sex differences in kinematic curves were identified using statistical parametric mapping (SPM) unpaired Student's t-tests (α=0.05)[7].

Results and Discussion

Average treadmill walking speed was 1.01±0.16 m/s. Rotational SSD were 3.8±0.8°, 3.0±0.6°, and 4.5±0.5° for flexion-extension, abduction-adduction, and internal-external rotation, respectively. Translational SSD were 0.7±0.2mm, 0.4±0.1mm, and 0.4±0.1mm for anterior-posterior, superior-inferior, and medial-lateral translation, respectively. No significant sex differences in kinematics were identified (Figure 1).

This preliminary data illustrates that hip rotational SSD are comparable to those in the knee (3.8°) and ankle (4.1°), but translational SSD are smaller at the hip compared to the knee (1.3 mm) and ankle (1.5 mm) during walking[8,9]. These differences may be due to bony constraints (facilitating joint stability and weight bearing) and/or joint location in the kinetic chain. The lack of sex-based kinematic differences indicates that asymptomatic individuals may not exhibit different motion patterns at the hip during minimally demanding tasks such as level walking, despite known sex differences in pelvis anatomy.

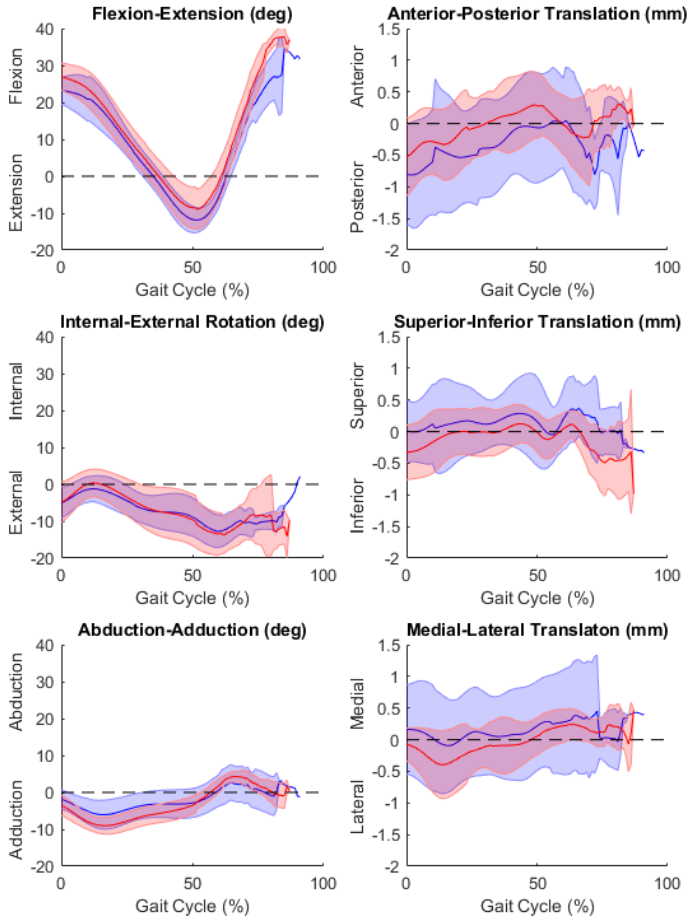

Figure 1: Average rotational (left) and translational (right) kinematics for males (blue) and females (red) during walking (shaded areas indicate standard deviation, horizontal dotted line indicates neutral standing position). 0% is foot strike, 100% is ipsilateral foot strike.

Significance

SSD in hip kinematics of up to 4.5° in rotation and 0.7 mm in translation are typical in healthy hips and may not be indicative of underlying pathology. Hip kinematics do not appear to be different between asymptomatic young adult males and females during gait.

References

1) Suh, *J Arthroplasty.* 2006. 2) Tsai, *JBiomech.* 2015. 3) Florentino, *G&P.* 2017. 4) Zugner, *J Orthop Res.* 2017. 5) Martin, *J Arthroplasty.* 2011. 6) Wu, *JBiomech.* 2002. 7) Pataky, *JBiomech.* 2014. 8) Gale, *JOR.* 2019. 9) Yang, *JBiomech.* 2020.

No Difference in Gait Symmetry Between Age Groups in Healthy Adults that Maintain Gait Speed

[1]Nicole E. Stark, [2]Daniel Schmitt, and [1]Robin M. Queen
[1]Department of Biomedical Engineering and Mechanics, Virginia Tech, Blacksburg, VA, USA
[2]Department of Anthropology, Duke University, Durham, NC, USA
Email : *nestark@vt.edu

Introduction

Historically bilateral symmetry in gait has been assumed and data was captured unilaterally [1]. However, Heydar et. al illustrated the importance of evaluating gait bilaterally, arguing that gait asymmetry is the norm because of limb dominance and independent limb coordination [1]. The normal amount of gait symmetry has since been evaluated, but results have been inconsistent due to differences in calculation methods, lack of specificity regarding the collection of symmetry measures during a trial, and the operational definition for healthy [2,3,4].

A normative baseline has not been established for gait symmetry and it is unknown how age affects symmetry making it hard to establish gait symmetry rehabilitation benchmarks for injured or diseased populations of varying ages. The purpose of this study was to determine the impact of age on gait symmetry, and we hypothesize that with age participants would be more symmetric. Symmetry in this study was defined as the difference in limb mechanics between the right and left limbs.

Methods

Eighty-two (24 males, 58 females) healthy adults between the ages of 18 and 85 (mean and standard deviation (SD) for Age= 45.46± 20.0 years, BMI=24.21± 3.81) signed institutional review board approved informed consent prior to study participation. Healthy was operationally defined as no history of serious lower extremity injury or surgery, no lower extremity injury in the past 12 months, and were able to walk unassisted from more than 10 minutes. Each participant completed between four and seven walking trials at a self-selected speed. Gait speed was measured using timing gates, motion capture data was collected using a modified Helen-Hayes marker set and a ten-camera system (Qualisys, Sweden; 120 Hz), and vertical ground reaction forces (GRF) were captured with four AMTI force plates (AMTI, Watertown, MA, 1200 Hz).

Gait symmetry was calculated using the Normalized Symmetry Index (NSI), in which 0% indicates full symmetry, over two consecutive steps for each trial [5]. NSI values were calculated for peak knee flexion, hip extension, ankle plantar flexion (A-PF), vertical GRF at weight acceptance (WA-GRF) and propulsive phase of gait (P-GRF) as well as knee and hip range of motion (ROM). Participants were split into 3 age groups 18-31 (22.07±1.6, N=29), 32-57 (48.6±7.6, N=27) and 58-85 (68.3±7.2, N=26) for analysis [6]. A three-way ANOVA was performed to compare each symmetry variable across age groups and post-hoc Games-Howell test was completed for all significant findings. All statistical test were done in SPSS V26 (IBM,Chicago, IL) with an α level of 0.05.

Table 1: Three Age Group ANOVA *p-value < 0.05

Age Group	18-32		33-57		58-85		p-
NSI (%)	Mean	SD	Mean	SD	Mean	SD	value
Knee Flex.	5.85	4.05	9.07	7.11	6.15	5.04	0.065
Hip Exten.	26.05	25.42	15.19	14.57	17.64	12.84	0.080
Ankle PF	23.19	19.81	12.66	10.37	17.45	16.18	0.049*
Knee ROM	5.39	4.25	5.94	4.58	6.25	4.88	0.777
Hip ROM	4.36	3.38	3.11	2.98	4.21	3.50	0.351
WA-GRF	2.76	2.20	3.02	1.88	3.28	2.51	0.690
P-GRF	2.46	1.72	1.37	1.13	2.56	1.77	0.011*

Results and Discussion

Gait speed was not different between age groups (18-31 1.28± 0.2 m/s; 32-57 1.32± 0.2 m/s; 32-57 1.37± 0.3 m/s; p=0.690), which is contrary to previous literature that indicates a decline of gait speed with age [7]. When comparing age groups, P-GRF and A-PF showed significant differences (p=0.011, p=0.049) (Table 1). The post-hoc analysis showed that a significant difference between the 18-32 and 33-57 groups for P-GRF and A-PF (p=0.018, p=0.041) and for P-GRF the 33-57 and 58-85 groups were also different from each other (p=0.016). Hip ROM, WA-GRF, and P-GRF all had mean symmetry values under 5%. Peak knee flexion and knee ROM were under 10% asymmetry. This data suggests that the commonly used value for healthy functional task asymmetry of under 10% [8,9] may be appropriate for many variables and across a wide age range of healthy vital adults. The older adults in this cohort maintained healthy gait speed comparable to the participants in the youngest age group, therefore, these findings may not apply to all older adults. In addition, our findings of large asymmetry for healthy peak hip extension and peak ankle PF indicate that an overall symmetry cutoff for every variable should not be used and that the cutoff should be variable specific [10].

This study was limited as it did not evaluate individuals as they age and instead used a cohort model in which individuals were grouped by age and compared. It is unclear if asymmetry present in the younger age group are indicative of healthy symmetry or disease/injuries that have yet to present themselves or have not completely healed. These findings indicate the need for a longitudinal study of gait symmetry during the aging processes as well as a detailed tracking of injury history to determining the impact of injury on gait symmetry. Future studies should assess symmetry in an older adult cohort that is not as fit and demonstrates the typical walking speed decline with age [7].

Significance

We hypothesized that with aging participants would become more symmetric, which was unsupported by study results. These findings show that evaluating gait kinetic and kinematic symmetry can be used as an evaluation tool for disability in reference to normative values like those presented here.

Acknowledgments

NIH grant AR074149 supported Nicole Stark on this project.

References

[1] Sadeghi et al. 2000 *Gait & Posture* [2] Gundersen et al. 1989 *Phys Ther* [3] Lathrop-Lambach et al.2014 *Gait and Posture* [4] Forczek et al. 2012 *J Hum Kinet* [5] Queen et al. 2020 *J Biomech* [6] Seung-uk et al. 2012 *J Arch Ger* [7] Buchner et al. 1996 *J Gerontol A Biol Sci Med Sci* [8] Schmitt et al. 2012 *JOSPT* [9] Kvist 2004 *Sports Med* [10] Herzog et al. 1989 *MSSE*

Optimized Unilateral Deep Brain Stimulation Improves Motor Capacity in Parkinson's Disease

Christopher P Hurt[1], D Kuhman[1], M Wade[1], and H Walker[1]
[1]University of Alabama at Birmingham
email: *cphurt@uab.edu

Introduction

For individuals with Parkinson's disease (PD), a progressive neurological disorder, pharmacologic interventions are initially effective at treating the symptomology of the disease. With disease progression, these interventions may lose their efficacy in optimally controlling motor symptoms. With waning effectiveness, the amount of time spent "on" when motor symptoms are controlled between self-administered doses, decreases. Deep brain stimulation (DBS) can be an effective adjunct therapy for treating symptoms of PD[1]. However, the evidence for long-term effective treatment of axial motor features such as gait and balance dysfunction with DBS is more equivocal[2]. Many investigations on the effectiveness of DBS are reported after the DBS device has been programmed and it is unclear the extent to which axial function is optimized as part of standard of care. It is possible that a lack of optimization in programming the DBS device drives the equivocal nature reported. Indeed, recently we showed that individuals with unilateral DBS demonstrated patient specific stimulation configurations resulting in clinically important improvements in gait speed[3]. Our purpose was to test the hypothesis that optimized performance of simple but quantitative measures of movement would result in better performance of unilateral DBS compared to standard pharmacologic interventions.

Methods

Twenty-two participants with PD (age 58.1±7.6 years, MDS-UPDRS 26.6±8.7 **)** were enrolled in the study. Participants visited the lab prior to implantation to undergo a screening visit in the practically defined off medication state (> 12 hours without PD medications). Data was collected both in the off medicine state, and then, approximately 1 hour after participants self-administered their PD medication, in the on state. Individuals were tested with the following tasks along with their constructs: 10m comfortable walking test (CWS)-gait function, Timed Up and Go (TUG)-mobility, 9-hole pegboard test (PEG)-upper extremity dexterity task, the, Lower limb target task-lower extremity dexterity task, and quiet stance task where we quantified sway area (Static Posture)-static balance. Participants visited the lab again, one month after unilateral DBS implantation in the subthalamic nucleus, in the off state, for device activation. Each DBS electrode was tested for clinical benefit with a standardized pulse width of 60 µs and a frequency of 130 Hz by a trained nurse practitioner. The novel DBS device used in this investigation contains six individual contacts and two virtual rings formed by 3 directional contacts each, and individual dorsal and ventral rings. Contacts were tested in random order to avoid an ordering effect while individual performed the aforementioned tasks for a total of 10 DBS settings (6 directional contacts, 2 virtual rings, 2 individual rings). The best performance was selected for each task. To determine if unilateral DBS was more effective than off or on medications, we performed a repeated measures ANOVA. Post hoc comparisons were made using a Bonferroni correction.

Results and Discussion

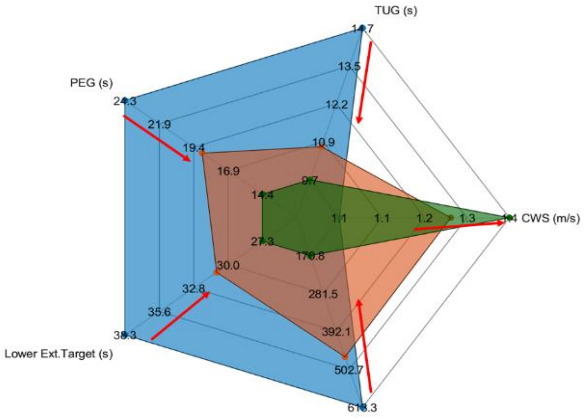

Figure 1. Spider plot of outcome measures under conditions of OFF meds (blue), ON meds (Red), and DBS (Green). The arrows represent the direction required to see improvement in the measure.

We observed improvements in performance measures with dopaminergic medicine as well as with DBS compared to off medicine and off DBS (Fig. 1). For some measures, unilateral DBS stimulation that was optimized for performance was superior to improvements with Dopaminergic medication. Participants' CWS was significantly faster with meds and with DBS. Post hoc analysis showed DBS was significantly faster than off and with meds (p=<0.001, p=0.032, respectively). The TUG also improved on meds and DBS (p<0,015 for both), although no difference was detected between meds and DBS (p=0.242). Both lower and upper extremity dexterity tasks were performed faster with DBS compared to off and on meds (p=0.003, p0.017, respectively). Finally, sway area was less with DBS than off or on medications (p=0.049, p=0.017). Despite the equivocal nature of previous research on the effect of DBS on axial movement function, we show that when DBS is optimized for performance, unilateral DBS results in clinically significant improvements in movement capacity compared to dopaminergic medications. Moreover, in contrast to clinical outcome measures, the use of continuous quantitative outcome measures may be more sensitive in detecting improvements in motor function.

Significance

The current investigation suggests that axial function can be significantly improved with unilateral DBS when movement function is optimized during DBS programming. Indeed the improvements we report are greater than established minimal clinical important differences.

Acknowledgments

Funding for this study is provided by the NIH (1UH3NS10053) to HW.

References

1. Walker H, Neurosurgery,2009. 2. Fasano A, Nat.Rev.Neurol. 2015. 3. Hurt C, Front Hum Neurosci, 2020.

CHARACTERIZATION OF GAIT DYNAMICS IN CHILDREN WITH HYPERMOBILE EHLERS-DANLOS SYNDROME

Anahita A. Qashqai[1], Joshua Leonardis[1], Michael Muriello[2], Donald Basel[2], and Brooke Slavens[1]
[1] University of Wisconsin-Milwaukee, Milwaukee, WI, USA
[2] Medical College of Wisconsin, Wauwatosa, WI, USA
Email: *Anahita@uwm.edu

Introduction

Hypermobile Ehlers-Danlos syndrome (hEDS) is a common heritable connective tissue disorder that affects an estimated 1 in every 5000 people worldwide [1]. hEDS is characterized by joint laxity, excessive joint ranges of motion (ROM), joint pain, fatigue, and joint instability during walking [1, 2]. Despite this clinical knowledge, there is limited biomechanical characterizations of gait in children with hEDS. Therefore, the purpose of this study was to quantify sagittal plane lower extremity joint kinematics, moments, and powers during overground walking in children with hEDS and compare them to typically developing children.

Methods

Eight children (4 males, 4 females, age: 14.5 ± 2.8 years) with hEDS participated. A 15-camera Vicon T-Series motion capture system, synchronized with four AMTI force plates, recorded marker trajectories and ground reaction forces while each subject completed 5 walking trials at a self-selected speed. The standard Vicon Plug-in Gait lower extremity inverse dynamics model was applied to compute joint dynamics [3]. An open-source dataset from 83 children (age: 10.5 ± 3.5 years) were used as a normative database of typically developing children [4]. Mann-Whitney U tests were applied to assess group differences in joint kinematics and moments in the sagittal plane, and joint powers ($p < 0.05$).

Results and Discussion

Spatio-temporal parameters were calculated (cadence: 56.3±2.2 strides/min, speed: 1.2±0.1 m/s, stride length: 1.3±0.1 m, single leg support 40.2±2.4%). Of the joint kinematics assessed, only peak hip extension significantly differed between the groups (hEDS: 10.3±5.2 deg vs. typically developing children (TD): 5.7±3.4 deg, p=0.04). We found significant differences in ankle plantarflexion moments and powers. Specifically, children with hEDS exhibited a significantly greater peak ankle plantarflexion moment (hEDS: 1.6±0.2 Nm/kg vs. TD: 1.1±0.1 N-m/kg) (p=0.02). Furthermore, children with hEDS exhibited significantly greater ankle power generation (hEDS: 30.1±15.4 J/kg vs. TD: 11.6±5.2 J/kg, p<0.01) and absorption (hEDS: 16.9±3.9 J/kg vs. TD: 4.7±0.2 J/kg, p<0.01), less knee power absorption (hEDS: 10.3±2.9 J/kg vs. TD: 19.5±3.2 J/kg, p<0.01), as well as less hip power generation (hEDS: 19.1±4.6 J/kg vs. TD: 11.4±2.1 J/kg) and more hip power absorption (hEDS: 7.9±3.4 J/kg vs. TD: 2.3±0.4 J/kg, both p<0.01 (Fig. 1).

Our results provide valuable insight into the characterization of gait in children with hEDS. While no significant differences occurred in peak ankle plantarflexion angle and peak knee flexion and extension, the hEDS group demonstrated altered moments and powers. This difference may be related to the fact that similar kinematic patterns can be produced by different underlying kinetics [5]. Moreover, our findings offer clinical significance. While we observed significantly greater ankle power generation in those with hEDS, less hip power generation and no significant difference in knee power generation were found. This may be the indication that the propulsion may be generated mainly by the ankle in this population.

Significance

This study aimed to fill a gap in knowledge by characterizing gait dynamics in children with hEDS. We identified differences in hip kinematics, ankle moments, and ankle powers compared to typically development children that may influence locomotion. Further research is underway with a larger population to determine a comprehensive biomechanical characterization of gait in children with hEDS.

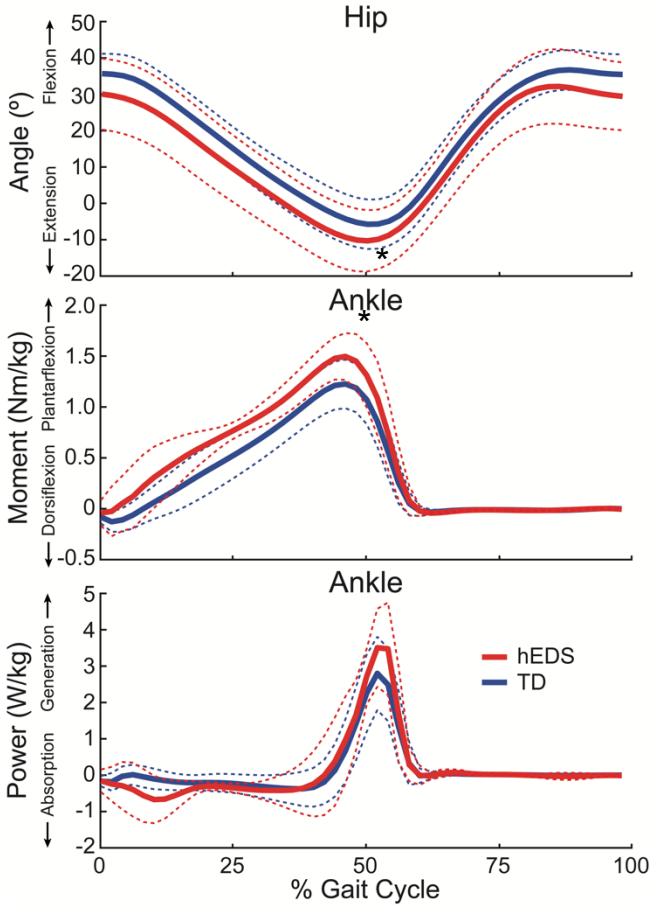

Figure 1. Hip flexion/extension angles, ankle plantarflexion/dorsiflexion moments, and ankle power generation/absorption during gait in children with hEDS and typically developing (TD) controls. Bold lines represent group means while dashed lines indicate one standard deviation.

References

1. Castori, M. (2010). Am J Hum Genet, A, 152(3).
2. Galli, M. (2011). Dev Disabil Res Rev, 32(5), 1663-1668.
3. Kadaba, M. (1990). J Orthop Res, 8(3), 383-392.
4. Schwartz, M. H. (2008). J Biomech., 41(8), 1639-16.
5. Sofuwa, O., (2005), *86*(5), 1007-1013.

EXOSKELETON TYPE AFFECTS WALKING IN INDIVIDUALS WITH SPINAL CORD INJURIES

Nicole E. Mattson[1], Leslie R. Morse[2], Nguyen Nguyen[2], Karen L. Troy[1]
[1]Department of Biomedical Engineering, Worcester Polytechnic Institute
[2]Department of Rehabilitation Medicine, University of Minnesota Medical School
email: nemattson@wpi.edu

Introduction

Individuals with spinal cord injuries (SCI) are at a high risk of fracture due to the bone loss that occurs as a result of their injuries [1-3]. Bone adapts to mechanical loads and in people with SCI, the lack of weight-bearing mobilization in the lower extremities contributes to bone loss [4]. Robotic exoskeletons provide mechanical assistance so that individuals with SCI can walk. Exoskeleton-assisted walking mechanically loads the skeleton, potentially contributing to bone health. Here, we used video gait analysis to quantify the kinematics and kinetics at the ankles and knees of individuals walking with assistance from an exoskeleton. The longer-term goal is to calculate a "bone loading dose" for each patient, which may modulate treatment effect.

Methods

Nine men with chronic spinal cord injury, drawn from a larger 12-month clinical trial, were video recorded at the end of their exoskeleton training (NCT02533713; age: 36.2 ± 8.3 years, height: 179.1 ± 6.1 cm, mass: 81.9 ± 14.9 kg.) Participants all wore pressure-sensing insoles (Orpyx LogR, Orpyx Medical Technologies, Calgary, Canada) to measure the total reaction force applied to the foot and the center of pressure location. All participants used either the Indego exoskeleton (Parker Hannifin, Cleveland, OH) or the EKSO (ekso Bionics, Richmond, CA).

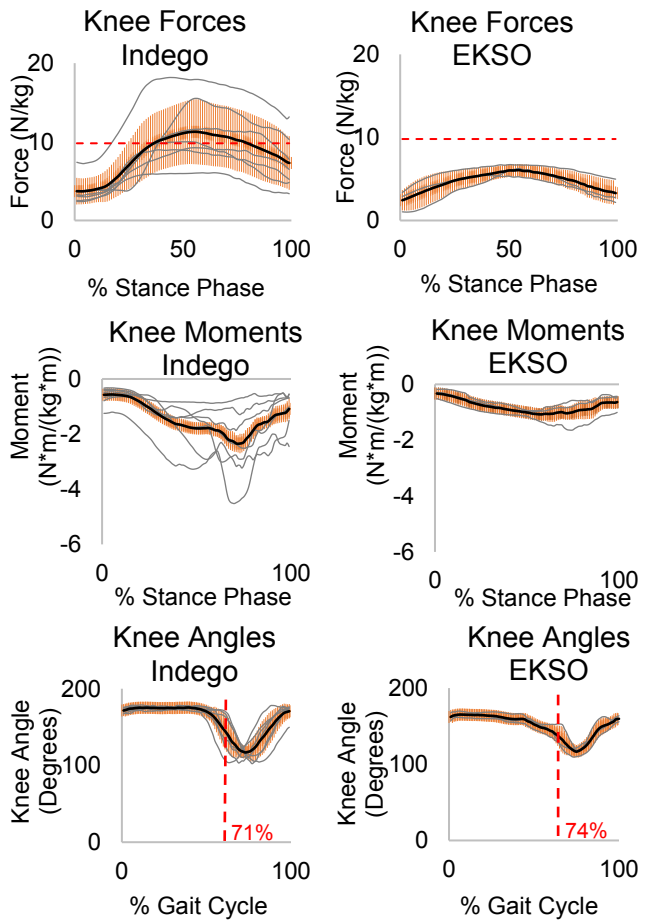

Figure 1: Kinematics, forces, and moments of the knee using the Indego and the EKSO for each patient (gray line), and the average (black line). Red dotted line represents one body weight and orange error bars represent standard deviation. Vertical red line on angle plots indicate where stance phase ends in the gait cycle.

Of the nine men, two were recorded using the EKSO, six using the Indego, and one using both. Sagittal plane knee and ankle kinematics were calculated from video based on the positions of fiducial markers during the gait cycle. Joint reaction forces and loading rates were calculated using SCI-specific anthropometric data [5], kinematics, and data from the insoles. We normalized the forces by dividing by body mass, and performed independent samples t-tests on each variable to compare the two exoskeletons.

Results and Discussion

Joint reaction forces depend on how much force is transmitted through the feet, as well as body position. These results suggest that walking in the EKSO may involve lower knee forces and moments, and less knee motion, compared to the Indego. The joint reaction forces and moments reported here reflect the total force that is transmitted through the user's skeleton, including inertial forces, but do not consider any muscle forces.

Variable	*Indego*	*EKSO*	p-value
Knee loading rate (N/kg/s)	25.06(11.06)	6.51(2.04)	0.022
Max. knee flexion angle (degrees)	177.29(1.73)	165.87(4.10)	0.000
Stride time (s)	2.38(0.287)	3.51(0.452)	0.001
Walking speed (m/s)	0.392(0.106)	0.259(0.073)	0.087

Table 1: Results of independent samples t-tests on variables comparing Indego and EKSO exoskeletons with corresponding p-values.

Significance

This research establishes a method to determine the forces applied to knee by different types of exoskeletons. Results can guide decisions regarding exoskeleton training to better facilitate mechanical re-loading of the skeleton for patients with SCI.

Acknowledgments

This work was funded by grant W81XWH-15-2-0078 (United States Department of Defense) to Leslie R. Morse.

References

[1] W. A. Bauman, et. Al. *Osteoporosis in Individuals with Spinal Cord Injury* 2015;7(2):188-201.
[2] A. Chantraine, et. Al. *Calcif Tissue Int*. 1986;38(6):323-327.
[3] S.D. Jiang, et Al. *Osteoporosis Int.* 2006; 17(2), 180–192.
[4] L. D. Carbone, et Al. *Osteoporosis Int.* 2013; 24(8), 2261–2267.
[5] Y. Fang et al. *J Biomechanics* 2017; 55(4), 11-17

COMPARISON OF WEARABLE DEVICES IN ASSESSING LEG STIFFNESS DURING TREADMILL RUNNING

Devin M. Green[1], Christopher J. Alfiero[1], Joshua P. Bailey[1]
[1]Department of Movement Sciences, University of Idaho, Moscow, ID
email: gree0130@vandals.uidaho.edu*

Introduction

Increased leg stiffness (K_{leg}) is suggested to be correlated with improved running performance [1], and reduced K_{leg} is thought to be closely related to fatigue in running [2]. Decreased leg stiffness during running may hinder performance and increase the risk of soft tissue injuries [2]. Therefore, assessing K_{leg} may be an important marker of fatigue and valuable in ascertaining injury risk. The gold standard for calculating K_{leg} is 3D motion analysis, but this technology is not capable of in-field assessments. Recently, a global positioning system (GPS) watch equipped with an accelerometer (Garmin™ HRM – Run: GR) has been validated as an in-field surrogate in calculating K_{leg} [3]. Other wearable devices have been validated in assessing temporospatial variables during running [4]; however, it remains speculative as to the agreement of K_{leg} estimations with validated technology. The purpose of this study was to assess the agreeability between two wearable devices GR and RunScribe™ (RS)) in calculating K_{leg} during running.

Methods

Seven endurance-trained male runners (28.5 ± 11.5 y; m 74.7 ± 7.1 kg; ht. 182.0 cm ± 6.4 cm; VO_{2max} 57.5 ± 5.7 ml/kg/min) were recruited. Participants performed a graded exercise test (GXT) on two separate occasions as part of a larger study. The first three stages of the GXT were used to assess K_{leg}, where participants ran at 3.13, 3.58, and 4.02 m/s and 1% incline. Data was sampled for 3 minutes during each stage via a Garmin Fenix 5 watch with a chest-mounted accelerometer, and RunScribe™ footpods and sacral pod mounted on top of each foot and on the waistband above the sacrum, respectively. RS pods were calibrated before each trial in accordance with the manufacturer's instructions. Cadence, contact, and flight time were extracted from the accelerometer-derived data from the GR-HRM-Run via GarminConnect™ platform. Extracted data was used, along with running speed, body mass & leg length, to calculate K_{leg} [5] for each of the first three GTX stages. K_{leg} was extracted from the RunScribe Dashboard™ and divided into the stages of the GXT. The agreeability of the wearables at each stage was assessed using intraclass correlation coefficients (ICC) and Bland-Altman analyses. One-sample t-tests and linear regressions were used to assess systematic and proportional biases at each stage with α=0.05.

Results and Discussion

Overall, there was no significant difference in K_{leg} between the two devices ($p = 0.969$). Bland-Altman plots indicated excellent agreement suggesting that when comparing the two devices, they are consistence in estimating K_{leg} during treadmill running. Bland-Altman plots indicated no significant systematic bias (Table 1). Additionally, there was no proportional bias detected ($\beta = -0.13$, $p = 0.46$), indicating that the mean differences remain constant with increases or decreases in K_{leg}. Mean K_{leg} and mean biases for each treadmill velocity are presented in Table 1.

Table 1
Agreement between wearables in K_{leg} estimation at varying treadmill velocities.

	K_{leg} (kN/m)			Limits of Agreement	
Velocity	Garmin	RunScribe	Mean Difference	Lower	Upper
3.13 (m/s)	11.4	11.2	0.18	-3.06	3.43
3.58 (m/s)	10.9	10.8	0.14	-3.74	4.02
4.02 (m/s)	10.3	10.6	-0.28	-4.40	3.85

K_{leg}, leg stiffness

Significance

As wearable devices continue to gain popularity among runners, there is an increasing need for validation in assessing in-field running metrics, such as K_{leg}. K_{leg} may be an important biomechanical parameter in assessing fatigability and risk of injury during running. The data from this study suggest that GR and RS reliably estimate K_{leg} during treadmill running. Considering GR has been validated as a surrogate for estimating K_{leg}, Given the lack of differences between the systems measure of K_{leg}, the determination of which system a researcher, athlete, or coach uses should depend upon what other metrics are important for their question. The main difference between these systems is the other run metrics they offer in addition to calculating K_{leg}.

Acknowledgments

We would like to thank the students and participants who helped make this project possible.

References

1. Dumke et al. (2010). *Int J Sp Phy Perf*, 5(2):249.
2. Butler et al. (2003). *Clin Biomech*, 18(6):511.
3. Polson et al. (2019). *J Orth Sp Phys*49(1).
4. Koldenhoven et al (2018). *Digit biomarkers*, 2(2):74.
5. Morin et al. (2005). *J Appl Biomech*, 21(2):167.

EFFECTS OF A POWERED ANKLE-FOOT PROSTHESIS ON INTACT KNEE ADDUCTION MOMENT

John M. Chomack[1], A. Sidiropoulos[1], M. Poppo[1], and J. Maikos[1]
[1]Veteran Affairs New York Harbor Healthcare System
Email: john.chomack@va.gov

Introduction

Individuals with a transtibial amputation (TTA) who use traditional energy storing and returning (ESR) devices often experience increased kinematic and kinetic asymmetries, particularly of their intact limb [1,2]. Experienced TTA prosthetic users have been shown to have increased intact 1st peak knee adduction moments (KAM) of 46% and 17% compared to the prosthetic side and normative data, respectively [3]. Research has correlated increased intact joint discomfort and knee osteoarthritis (OA) to abnormally high KAM of the intact limb [1,3]. Advanced prosthetic componentry, such as powered ankle foot devices that mimic that gastric-soleus complex, have the potential to reduce compensatory loading of the intact limb, which could reduce the risk of musculoskeletal injuries. The Empower foot (PWR) (Ottobock, Inc.) is the only commercially available prosthetic device able to provide the user with biomimetic power generation at push off. We hypothesized that use of a PWR device would significantly reduce the 1st peak of the intact KAM with respect to both ESR and articulating ESR (ART) devices and would be normalized to the control group.

Methods

Seventeen individuals living with TTA (age 52 ± 14.5 years, height 1.79 ± 0.1 m, and weight 85.9 ± 17.3 kg) with at least 1 year of prosthetic experience, as well as 6 control subjects were recruited from Veteran Affairs (VA) New York Harbor Healthcare System (NYHHS) and Walter Reed National Military Medical Center (WRNMMC). Study procedures were approved by each sites' respective Institutional Review Board. Participants were randomized to wear 3 types of prosthetic feet: ESR, ART, and PWR. Each device was randomly used for a 1-week acclimation period followed by biomechanical testing. Motion and force data were collected using an optical motion capture system (Qualisys, Goteborg, Sweden) and a force platform system (AMTI, Waterford, MA). Subjects were fit with 78 retroreflective markers and walked over level ground at 3 speeds: 1.0, 1.3, and 1.5 m/s. Data was analysed using Visual3D software (C-Motion Inc.) to derive kinetic results. A one-way, between subjects repeated measures ANOVA was used to determine if any significant differences ($p < 0.05$) were present for the 1st peak intact KAM values between each foot and the control data for all speeds.

Results and Discussion

Results show that the intact KAM for PWR device was 3.0%, 7.1%, and 0.1% lower compared to the ESR foot at 1.0, 1.3, and 1.5m/s, respectively, though results were not significant ($p = 0.135, 1.06, 0.76$). No other significant differences ($p < 0.05$) were found between the 1st peak of the ESR, ART, PWR devices, and the control at all speeds. Figure 1 shows KAM for all devices and control participants at 1.3 m/s. At 1.3 m/s, the percent difference of the 1st peak KAM between each device and the control were: ESR 2.2%, ART 8.8%, and PWR 9.2%, however the results were not significantly different ($p = 0.991$).

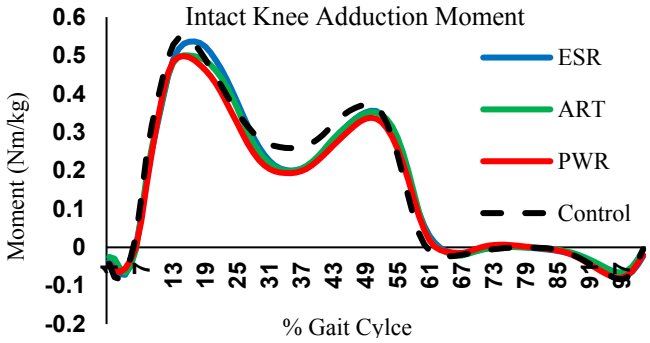

Figure 1: Average intact knee adduction moment at 1.3 m/s for ESR, ART, PWR, and control.

Previous research has shown that the 1st peak of the intact KAM for individuals with TTA who utilized a powered device was significantly reduced by 20.6% and 12.2% at walking speeds of 1.5 m/s and 1.75 m/s ($p = 0.03, 0.05$) compared to the ESR condition [1]. However, at slower walking speeds, comparable to the speeds used in this investigation, KAM was not significantly different between ESR and powered devices. These differences may be attributable to the net positive work performed at faster speeds by the powered prosthesis, whereas at slower speeds the net mechanical work is nearly zero across the entire stance phase [1]. Furthermore, while the powered device provided biomimetic push-off power, the uniaxial movement of the device cannot replicate the biarticular nature of the gastrocnemius, which may reduce the efficiency of the load transmission to the intact limb [2]. As such, the minimal reduction in intact KAM reported in this investigation could be the result of continued compensatory strategies of the intact limb and reduced stability in the knee frontal plane. Lastly, a longer acclimation period or the inclusion of a strength training/rehabilitation protocol could reduce some of the compensatory strategies. While the PWR device can produce biomimetic ankle power, device-specific training may need to be introduced to reduce joint loading on the intact side.

Significance

Biomimetic devices like the Empower have been shown to reduce some asymmetries during prosthetic gait, such as peak ankle power. However, this investigation did not indicate any significant reductions in peak KAM compared to ESR devices. Devices that could reduce peak KAM could potentially mitigate the risk of musculoskeletal injury, specifically knee OA of the unaffected leg.

Acknowledgments

This work was supported by a DoD Orthotics and Prosthetics Outcomes Research Program grant (W81XWH-17-2-0014). We also acknowledge our co-investigators at WRNMMC.

References

[1] Grabowski A. et al. J. NeuroEng & Rehab vol 10(49) (2013).
[2] Esposito E. et al. Pros & Orth Int vol 40(3) 311-19 (2016).
[3] Royer T. et al. Gait & Posture vol 23(3), 303-6 (2006).

Frontal-plane biomechanical model for predicting weight bearing during walking in older adults

Forouzan Foroughi[1], Mariah Smither[1], Erica A. Hedrick[2], Sheridan M. Parker[2], Brian A. Knarr[2], Hao-Yuan Hsiao [1]

[1]Department of Kinesiology and Health Education, University of Texas at Austin, Austin, TX, USA

[2]Department of Biomechanics, University of Nebraska at Omaha, Omaha, NE USA

Email: Frozen@utexas.edu

Introduction

Older adults commonly show decreased weight bearing during walking compared to younger adults. Deficits in weight bearing is associated with slower walking speed, lower-limb weaknesses, poor functional performance, and higher risk of falling that ultimately leads to reduced independence (1). Thus, identifying factors that contribute to weight bearing is an important goal.

Functional weight bearing requires sufficient vertical ground reaction force (VGRF) generated from the lower extremities. Factors that contribute to VGRF production have primarily been studied in the sagittal plane. In contrast, how frontal plane gait components affects VGRF production have received less attention. In a model-based simulation analysis, the hip abductor muscles in the frontal plane contributed significantly to the 1st peak of VGRF during early single-limb stance phase (2). In addition, frontal plane foot placement determines the orientation of the GRF vector and therefore affects the distribution of GRF in the mediolateral versus vertical directions (3). The primary purpose of this study is to develop and validate a biomechanical based model to predict the peak VGRF based on the hip abduction moment and lateral foot placement in older adults.

Methods

Twelve older adults (70 ± 5.87 years) walked on the split belt instrumented treadmill, at their preferred walking speed (1.01 ± 0.18 m/s). GRF data was acquired at 1200 Hz. Kinematic data was collected via a 10-camera motion analysis system. Hip abduction torque (τ_H) was calculated through inverse dynamics in Visual3D software. θ was determined as the angle between the horizontal and a vector joining the heel marker and the trunk center of mass (Figure 1). External moment arm (D) was measured as the medial-lateral distance between trunk center of mass and hip joint center. A quasi-static model including τ_H, (θ), and D was used to predict the 1st peak of VGRF during walking (Eq1&2).

$$\tau_H = F * D \quad \text{and} \quad \sin\theta = \frac{Fz}{F} \qquad \text{Eq1.}$$

$$\boldsymbol{Fz = \frac{\tau_h * \sin\theta}{D}} \qquad \text{Eq2.}$$

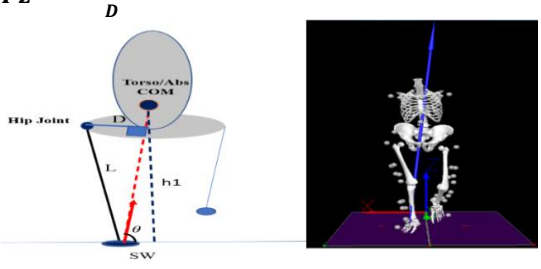

Figure 1: Diagram of VGRF model with associated frontal plane variables.

Data for each variable were averaged across gait cycles. Pearson's correlation coefficient and Root-mean-squared (RMS) errors were calculated for both legs to compare the model predicted VGRF versus the measured VGRF. All data was exported into MATLAB for further analysis.

Results and Discussion

The model explained over 75 % of the variances in measured VGRF for both limbs (r = 0.88 for the right and r = 0.94 for the left side). The RMS errors were 58.21 N (10 %) for the right and 42.79 N (10%) for the left side. The slopes of the regression line were close to 1 for both sides (Figure 2). These results demonstrated that hip abduction torque and lateral foot placement explained most of the variance in weight bearing during walking in older adults.

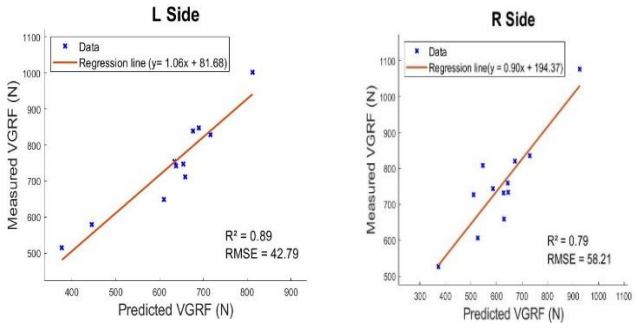

Figure 2: Predicted VGRF vs. Measured VGRF in older adults

Significance

To our knowledge, this is the first study that incorporates frontal plane hip torque and foot placement components to predict weight bearing. Our findings support previous studies by highlighting the importance of hip abduction torque and foot placement in producing VGRF. This model can be used to quantify the relative contribution of the hip abduction torque and lateral foot placement to changes in weight bearing during different walking conditions to reveal mechanisms underlying weight bearing deficits in older adults.

Acknowledgements

NIH R21-AG060034, P20-GM109090, R15-HD094194, and R01-NS114282

References

[1] Laroche D.P et al. (2011). Gait & Posture, 33(4), 668–672.
[2] Pandy, MG et al. (2003). Phil Trans R Soc Lond, 358: 1501 – 1509, 2003
[3] Brough, L et al. (2020). J of Biomechanics, 10.1016.

TOWARDS DETECTING THE INTENDED GAIT SPEED OF EXOSKELETON USERS

Roopak M. Karulkar[1] and Patrick M. Wensing[1]
[1]University of Notre Dame
email: rkarulka@nd.edu

Introduction

Robotic exoskeletons have been cleared by the FDA for gait rehabilitation due to their ability to accurately and repeatedly track joint trajectories necessary for gait rehabilitation. This dependence on the robot requires increased fluency in the Human Robot Interaction (HRI) for the user to convey their intent to the robot and accomplish desired goals. High fluency is indicated by the robot's ability to anticipate the user's actions [1] and provide timely assistance, and thus is only possible through accurate intent detection. Currently available exoskeletons rely on buttons and joysticks for the user to convey their intent. This project aims to create a framework that detects changes in desired gait speed more intuitively and without additional interfaces. Previously, Interacting Multi-Model Filtering was used to estimate the user's gait phase and velocity [2] by comparing exoskeleton sensor measurements to gaits generated by a Bipedal Spring-Loaded Pendulum model.

By contrast, the work herein hypothesizes that intent changes may be inferred primarily from footstep placement as the stability of gait is greatly influenced by ground contact. The work presents a Bayesian estimation framework that relies on measured changes in footstep placement to anticipate a user's intent to change speeds before it physically happens. This approach was evaluated on experimental data for walking trials of able-bodied (AB) and non-able-bodied (NAB) subjects in an Ekso GT exoskeleton.

Methods

This work considered estimating the desired velocity of the user v_x^d using state estimation strategies. State estimation was posed over an extended state vector $\boldsymbol{z} = [\boldsymbol{x}^T, v_x^d]^T$, where $\mathbf{x}$ is a vector containing the position and velocity of the exoskeleton's center of mass (CoM). This approach allows estimators to operate directly on the intent. The presented framework used a two-stage estimation approach to reinforce estimates by incorporating measurements at phase transitions.

It has been shown that velocity changes at midstance (MS) influence the foot placement at touchdown (TD) [3]. In the first stage, a simple data-driven model of step length was considered as a function of the velocity at the MS prior to TD v_x, desired velocity v_x^d, and leg length l_{leg}:

$$l_{step} = \left[v_x \left(v_x^d - v_x\right) l_{leg}\right]\boldsymbol{\kappa}, \qquad (1)$$

where $\boldsymbol{\kappa}$ is a vector of regression coefficients. A Bayesian update was applied to the CoM state at MS using the difference in the measured and estimated step lengths. The updated state was then passed to a Kalman filter to be updated at the next MS.

The estimation framework was evaluated using walking trials of highly proficient AB and NAB subjects in an Ekso GT exoskeleton [4]. Trial data was collected as part of a study approved by the IRB of the University of Notre Dame (Protocol 18-04-4650). The subjects walked at a self-selected speed using a walker before being issued a verbal speed-change command to speed up or slow down. Each subject underwent three speed-up (SU) and slow-down (SD) trials in a pseudo-random sequence.

The Ekso GT assists users by tracking a steady state trajectory and correcting deviations from it. Consequently, this assistance affected NAB users' step length, so the measured root mean square current of the hip motor during the swing phase, I_{RMS} was included as an additional measurement. It was modeled by:

$$I_{RMS} = \left[v_x \left(v_x^d - v_x\right)\right]\boldsymbol{\alpha}, \qquad (2)$$

where $\boldsymbol{\alpha}$ is a vector of regression coefficients.

Results and Discussion

Figure 1 shows the performance of the estimator for SU trials of AB and NAB users. The stem plot represents the user's intent at TD; positive/negative values indicate anticipated speed-up/slow-down. The vertical line represents the MS closest to the time the speed-change command was issued and a speed change is expected after this step. The estimator was able to anticipate the speed change before it manifested at MS for NAB and AB trials. For all trials, intent changes were generally detected within one step after the command was issued. Speed-up intent changes for NAB users were most difficult to estimate as these users may be at their physical limit [4]. Improving the measurement model may yield better metric precision in v_x^d estimates.

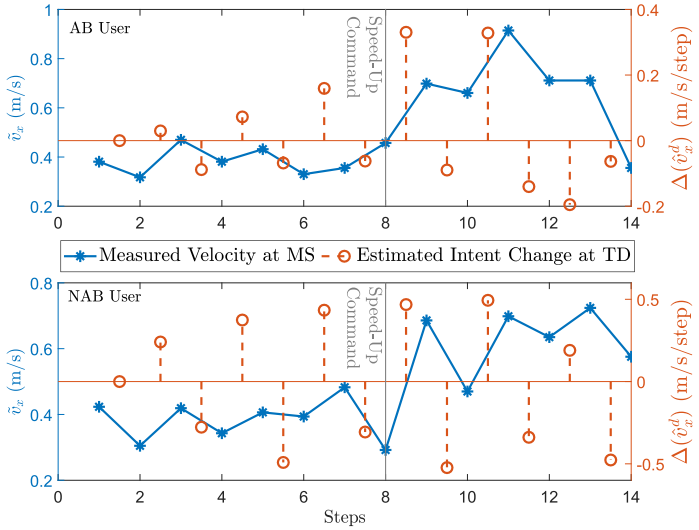

Figure 1: Estimator performance for Speed-Up trials for AB and NAB users.

Significance

The estimation framework presented in this work will enable exoskeleton users to make changes in their gait speed even when they may be physically unable to do so. This functionality presents an opportunity for exoskeleton users in late-stage rehabilitation to be more in control of their own rehab.

Acknowledgments

This work was supported by the National Science Foundation under Grant IIS-1734532

References

[1] Crandall et al., *IEEE Trans. On Systems, Man and Cybernetics-Part A*, **35**, 2005.
[2] Karulkar and Wensing, *IROS*, 2020.
[3] Wang and Srinivasan, *Biology letters*, **10**, 2014.
[4] Gambon et al., *IEEE Access*, **8**, 2020.

PRE AND POST-OP THORACOHUMERAL KINEMATICS OF SINGLE & MULTI-TENDON ROTATOR CUFF TEARS

Alyssa J. Schnorenberg[1,2], Dara Mickschl[3], Steven I. Grindel[3], and Brooke A. Slavens[1]
[1]Occupational Science and Technology, University of Wisconsin-Milwaukee, Milwaukee, WI, USA
[2]Biomedical Engineering, Marquette University, Milwaukee, WI, USA
[3]Orthopedic Surgery, Medical College of Wisconsin, Milwaukee, WI, USA
Email: *paulaj@uwm.edu *corresponding author

Introduction

Nearly 300,000 rotator cuff repair surgeries are performed each year in the U.S.A. [1]. Post-op rehabilitation must allow the repaired cuff to heal while restoring function and range of motion [2]. Normalization of the affected shoulder is defined as "changed kinematics toward symmetrical bilateral motion," as compared to the contralateral asymptomatic shoulder [3]. The potential for normalization of shoulder kinematics between 1 and 2 years after surgery has been demonstrated [3], but the process for how normalization occurs is unknown. This study evaluated the thoracohumeral joint motion of patients with single and multi-tendon rotator cuff tears to quantify the changes occurring within the first year of repair as compared to the non-injured arm.

Methods

Ten adults, five with a supraspinatus tear only (n=5; single) and five with tears in the supraspinatus and at least one other rotator cuff muscle (n=5; multi) participated in three test sessions: pre-op, and approximately three and six months after surgery. Average age was 63.2±7.9 years and 61.4±5.9 years, and average tear size was 1.2±0.2 cm and 3.0±1.4 cm for the single and multi tear groups, respectively. The American Shoulder and Elbow Surgeons Shoulder Score (ASES) was administered to assess self-perceived function and shoulder pain. A Vicon T-series system tracked reflective markers on the upper extremity while the participant performed five trials with each arm of maximal thoracohumeral (TH) external rotation from an adducted state, a challenging task with a rotator cuff tear. TH kinematics were calculated with our inverse kinematics model [4]. Group averages were computed for the peak TH external rotation angle for each arm and the shoulder pain and ASES score at each visit. Paired t-tests were used for within group comparisons between evaluations. Two sample t-tests were used for within evaluation comparisons between groups ($p<0.05$).

Table 1. Average (standard deviation) paing and ASES scores. *p<0.05

	Pain (0-10 scale)			ASES (0-100 scale)		
Group	Pre-Op	Post 1	Post 2*	Pre-Op	Post 1	Post 2
Single	4.4±1.5	2.4±2.5	0.2±0.4	60±8	67±19	93±4
Multi	5.4±2.5	4.2±1.8	2.0±1.8	48±14	51±18	82±15

Results and Discussion

Although on average the ASES score was 12.9 points higher for the single tear group, indicating better perceived function, there were no statistically significant differences between groups (Table 1). Shoulder pain was worse for the multi tear group than the single tear group across all visits (Table 1), but only significantly higher at six months post-op. Compared to the non-injured arm, both groups had significantly less TH external rotation of the injured arm at three months post-op, but only the single tear group had significantly less at six months post-op (Fig. 1). Results indicate the peak external rotation of the injured arm was significantly less than the non-injured arm for both groups at three months post-op, but only for the single tear group at six months post-op (Fig. 1). When comparing the average peak TH joint external rotation between groups at each visit, the multi tear group had significantly greater rotation of the injured arm than the single tear group at pre-op and six months post-op (Fig. 1).

Proper rehabilitation, particularly within three months post-op, is key to good functional outcomes [2]; however, the optimal rehabilitation protocol is still being deliberated [2,5]. Although most protocols aim to restore active range of motion by three to four months [5], this study showed this was not achieved by either group. Furthermore, only the multi tear group demonstrated normalization by six months post-op. While less external rotation was expected for the multi tear group as more muscles were torn, they had significantly greater motion at pre-op and six months post-op compared to the single tear group. This suggests that the pre-op range of motion may be indicative of the post-op rehab progress, regardless of the number of tendons involved.

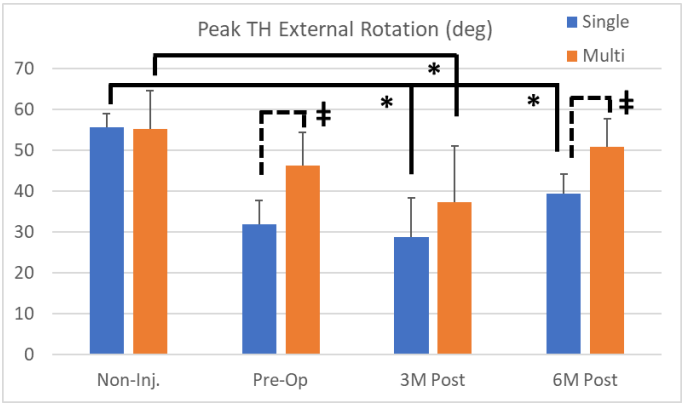

Figure 1: Group average (+1 standard deviation) peak external rotation for the single (blue), and multi (orange) tear groups at each session for both arms. * denotes significant within group differences; ± denotes significant between group differences ($p<0.05$).

Significance

Knowledge of pre-op shoulder complex motion alterations and post-op normalization is critical to understanding the rehabilitation process and recovery. This work helps identify the extent of recovery and potential timing for interventions. Further work is underway examining additional shoulder complex joints, tasks, and muscle activation.

Acknowledgments

This work was supported by a grant from the Medical College of Wisconsin, Department of Orthopedic Surgery.

References

[1] M. Crawford, AAOS Now, 34, 2014.
[2] H. Tonotsuka, et al., J Orthop Surgery, 25(3):1-8, 2017.
[3] A. Kolk, et al., J Shoulder Elbow Surg, 25:881-889, 2016.
[4] A. J. Schnorenberg, et al., J Biomech, 47:269-276, 2014.
[5] C. Jung, et al., Obere Extrem, 13:45-61, 2018.

ANATOMICAL CHARACTERISTICS CONTRIBUTING TO PATELLAR DISLOCATIONS FOLLOWING MPFL RECONSTRUCTION

John J. Elias[1], Jeffrey C. Watts[1], Lutul D. Farrow[2]
[1]Departments of Research and Orthopedic Surgery, Cleveland Clinic Akron General, Akron, OH,
[2]Department of Orthopaedic Surgery, Cleveland Clinic Foundation, Cleveland, OH
email: eliasj@ccf.org

Introduction

Medial patellofemoral ligament (MPFL) reconstruction is growing in popularity for surgical patellar stabilization following a lateral dislocation. Continued dislocations following MPFL reconstruction have been noted for approximately 5% of patients [1], and alternative procedures involving bone cuts are commonly considered for knees with high levels of anatomical pathology. The current study focuses on identifying anatomical characteristics that place the knee at risk of a patellar dislocation following MPFL reconstruction.

Methods

Knee function was simulated with thirteen multibody dynamic simulation models (RecurDyn) representing subjects being treated for recurrent patellar instability. The study was IRB approved. Ligaments, tendons, and retinacular structures were represented by tension-only springs, including assigned properties for stiffness, damping, and pre-strain at full extension (Fig. 1). Simplified Hertzian contact governed reaction forces at the patellofemoral and tibiofemoral joints. The models were individually validated for patellar tracking by comparisons to data measured from the subjects [2]. A pivot landing was simulated with each model. The quadriceps force increased from 180 N at 5° of flexion to 1000 N at 90°, with a 3200 N gravitational force applied at the hip, 40% of the quadriceps force applied through the hamstrings, and a 12 N-m external torque applied to the tibia. A gracilis tendon MPFL graft was represented by a rigid surface from the Schöttle point on the femur to a wrapping surface on the femur, with two springs extending to the medial edge of the patella.

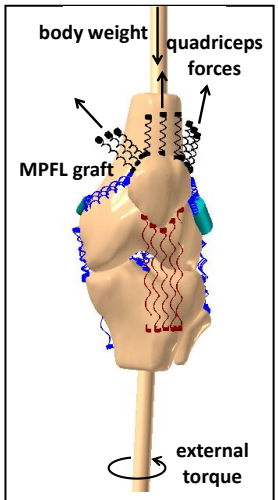

Figure 1: Model for dynamic simulation of knee function.

Multibody dynamic simulation output was post-processed with automated algorithms (Matlab) to characterize lateral patellar tracking in terms of bisect offset index (percentage of patellar width lateral to the deepest point of the trochlear groove) during knee flexion. Automated algorithms also quantified knee anatomy related to patellar height (Caton-Deschamps index), lateral position of the tibial tuberosity (tibial tuberosity to trochlear groove distance), and trochlear depth (lateral trochlear inclination angle). Linear regressions were used to relate patellar tracking to knee anatomy at both 5° and 45° of flexion. Tension within the graft was also quantified as the knee flexed.

Results and Discussion

The simulated pivoting maneuver produced a patellar dislocation for all thirteen models without an MPFL graft represented. Two of the models also experienced a dislocation with an MPFL graft represented, with dislocation occurring beyond 45° of flexion. The average (± standard deviation) tension within the graft peaked at 10° (52 ± 26 N) and varied dramatically among the knees at 45° (35 ± 63 N).

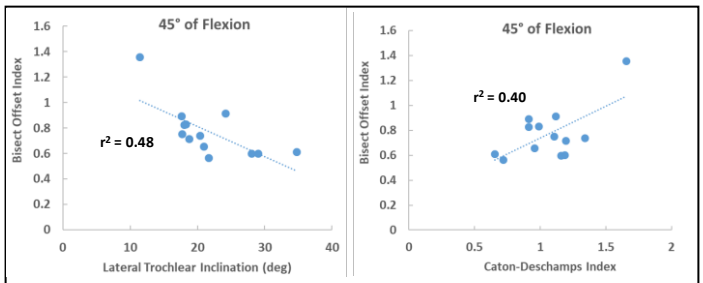

Figure 2: Correlations relating bisect offset index to lateral trochlear inclination and Caton-Deschamps index at 45° of flexion during simulated pivoting following MPFL reconstruction.

Patellar tracking was significantly correlated with anatomy at 45° of flexion, but not at 5°. At 45°, bisect offset index was significantly correlated with both Caton-Deschamps index (r^2 = 0.40, p = 0.02) and lateral trochlear inclination angle (r^2 = 0.48, p = 0.01), but not with tibial tuberosity to trochlear groove distance (p > 0.8). No significant correlations were identified between anatomy and patellar tracking at 5° (p > 0.1).

The analysis indicates that a high patella and a shallow trochlear groove are significantly correlated with lateral patellar maltracking at 45° of flexion for a pivot landing following MPFL reconstruction. At 45°, the patella should be captured by the trochlear groove, so lateral maltracking indicates a risk of post-operative patellar dislocations. Lack of significant correlations with the knee extended is likely related to relatively high and consistent graft tension.

Significance

The current study identifies two anatomical parameters associated with a high risk of a recurrent patellar dislocation following MPFL reconstruction. These are a high patella and shallow trochlear groove with the knee flexed. These parameters can help determine when alternative surgical procedures involving bone cuts are required to stabilize the patella.

Acknowledgments

Funding was provided by Department of Defense, Peer Reviewed Medical Research Program Discovery Award W81XWH2010040.

References

1. Schiphouwer et al. Knee Surg Sports Traumatol Arthrosc 2017; 25:245–250. 2. Tanaka et al. J Knee Surg doi: 10.1055/s-0040-1702185 [online ahead of print].

A PILOT STUDY ON THE RESPONSE OF UPPER LIMB PROSTHESIS USERS TO A SIMULATED TRIP

Clare Severe[1,2], Jenny A. Kent[1,2], Paul Hammond II[2], Noah Rosenblatt[3], and Matthew J. Major [1, 2]
[1]Northwestern University, Chicago IL; [2]Jesse Brown VA Medical Center, Chicago IL
[3]Rosalind Franklin University, North Chicago, IL
Email: claresevere2021@u.northwestern.edu

Introduction

Nearly half of persons with major upper limb loss (ULL) experience at least one fall per year [1] and almost a third will report an injury due to their most recent fall [1]. This evidence suggests that falls represent an important but often overlooked health hazard to this patient group. Importantly, while 25% of falls result from a trip, use of an upper limb prosthesis (ULP) increases likelihood of frequent falls (at least twice per year) by six times [1]. Additional biomechanical studies, which align with these findings on fall prevalence, suggest that persons with ULL experience impaired postural control and locomotor stability [2]. This pilot study aimed to characterize the locomotor response of persons with ULL to a simulated trip and assess effects of prosthesis use on that response.

Methods

After obtaining written informed consent, one male participant with unilateral transradial ULL (57 yrs, 178.0 cm, 95.8 kg, myoelectric prosthesis) completed two tasks while walking on a custom treadmill (Motek, Netherlands) and wearing a safety harness: 1) baseline walking at his self-selected speed and 1.0 m/s, and 2) 12 perturbation trials. Both tasks were completed under two conditions: with and without wearing his ULP. For each perturbation trial, the participant walked at 1.0 m/s and an unexpected treadmill belt disturbance was delivered during single limb support of either the sound or impaired limb side (6 on each side, random selection). Following a randomly selected step (between 21 and 40), the belt experienced an acceleration (up to 3.3 m/s over 400 ms) and deceleration back to 1.0 m/s. Perturbation trials ended after the participant regained steady walking and then completed 20 strides. Full-body kinematic data were collected with an optical motion capture system (Motion Analysis, CA) and custom marker set. A subject-customized biomechanical model in Visual 3D (C-Motion, MD) was used to estimate sagittal-plane whole-body angular momentum (*WAM*), trunk inclination (*TI*), and trunk inclination velocity (*TV*) *pre*- and *post*-perturbation.

Results and Discussion

The participant successfully recovered from all perturbations without a fall (i.e., full harness arrest). Example instantaneous. TI, TV and WAM (normalized by body mass, height and walking speed) for one perturbation trial are shown in Fig. 1.

Average max TI, max TV and WAM range across five trials (removing the first on both limb sides) are in Table 1. The perturbation induced a forward trunk lean, the magnitude of which was similar across all conditions. However, the trunk rotated forward faster and had a greater change from pre-perturbation behavior when perturbed during sound side single support. As intended, the perturbation generated a disturbance to WAM regulation (Fig. 1C) and while there was a greater post-perturbation WAM range when perturbed during sound side single support that aligned with trunk velocity changes, WAM range was considerably higher when the participant did not wear his prosthesis. Data collection is ongoing.

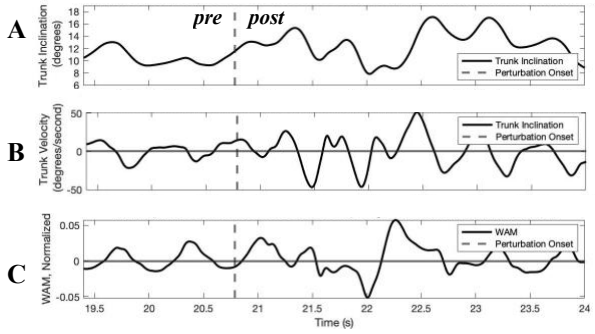

Figure 1: TI (A), TV (B) and WAM (C) for a perturbation trial (without ULP, impaired side leg); +=forward rotation.

Significance

Overall, findings suggest an asymmetric locomotor response following a trip disturbance that may share an interaction with ULP wear. These results could help us better understand the mechanisms underlying fall risk in this patient group. An enhanced understanding of locomotor stability and perturbation recovery can inform balance training that targets known deficits in postural control. Targeted training can help persons with ULL improve their postural control, thereby minimizing the risk of falls and fall-related injuries.

Acknowledgements

Work support by the US Dept. of VA (RX003290).

References

1. Major MJ. *Phys Ther* **4**, 377-387, 2019
2. Kent JA and Major MJ. *Clin Biomech* **76**, 105015, 2020

Table 1: Maximum TI, maximum TV and WAM range (mean±SD) separated by prosthesis condition and perturbation side.

		With Prosthesis		Without Prosthesis	
		Sound Side Perturbation	Impaired Side Perturbation	Sound Side Perturbation	Impaired Side Perturbation
TI (°)	*pre*	13.8±0.6	13.7±0.8	13.6±0.4	13.5±0.3
	post	17.7±1.3	17.3±0.7	17.0±1.6	15.7±1.2
TV (°/s)	*pre*	22.5±1.3	22.2±1.4	23.8±0.7	23.6±0.7
	post	40.0±6.6	31.3±3.3	41.8±10.1	35.0±11.0
WAM (norm.)	*pre*	0.045±0.001	0.036±0.021	0.047±0.001	0.045±0.001
	post	0.067±0.006	0.065±0.008	0.089±0.012	0.078±0.020

IMPACT OF ARCH HEIGHT ON ANKLE KINEMATICS DURING JUMPING TASK

Jerad J. Kosek[1], Christopher M. Wilburn[1], Imani N. Hill[1], Brandi E. Decoux[2], Portia T. Williams[3], Randy T. Fawcett[4], and Wendi H. Weimar[1]

[1]Auburn University, Auburn, AL
[2] Bridgewater State University, Bridgewater, MA
[3]North Carolina A&T State University, Greensboro, NC
[4]Virginia Tech University, Blacksburg, VA
Email: weimawh@auburn.edu

Introduction

Adequate foot mechanics are an essential tenet in the various phases of locomotive tasks. Acting the mediator, the medial longitudinal arch enables the foot alter closed-packed and loose-pack configurations that are beneficial toward conserving and directing energies [1-2]. The presence in medial longitudinal arch structural alterations have been demonstrated to provide kinematic disruptions that induce mechanical inefficiencies during the loading and propulsive phases, which ultimately predispose individuals to injuries [3-5]. While these findings have been thoroughly investigated in walking and running, such examination in other locomotive tasks, such as jumping and hopping remain limited. As jumping and hopping tasks are considered to act as an assessment in athletic performance outcomes and lower extremity function upon injury recovery, the additional influence specific arch classifications have on foot mechanics are often not considered. Thus, this project analyzed the effect arch height had on ankle kinematics during the loading and propulsive phases of various jumping and hopping tasks.

Methods

Twenty-two healthy, male collegiate Division I athletes volunteered to participate in this study. Each participant was instructed to perform a unilateral forward hop (FH), unilateral jump (LJ), and stationary hop (SH) on the dominant limb in a randomized order. During the SH task, the participants performed nine continuous hops. The FH task consisted of three trials of three consecutive forward hops. Within the LJ task, participants completed the following rhythmic sequence: jumping from the dominant leg to the non-dominant leg, to the dominant leg and back to the non-dominant leg.

Foot anthropometrics were taken using the Arch Height Measurement System device to classify the different arch types [6]. Bilateral retro-reflective markers were placed on the lower extremity to assess differences between sagittal and frontal ankle kinematics for each task. A force platform was also used kinetic patterns to specify loading and propulsive phase duration.

Results and Discussion

The results of a mixed-model ANOVA demonstrated no significant differences amongst in arch type amongst sagittal and frontal ankle kinematics during the tasks. Further detail associated with the statistical analysis can be found in Tables 1 and 2.

Skeletal alterations associated with the medial longitudinal arch are suggested to induce dysfunctional kinematic patterns during locomotive tasks [3-5] . However, the findings in this study suggest that different arch types produce similarities in locomotive mechanics. Specifically, low and neutral arches displayed comparable sagittal and frontal plane ankle kinematic patterns during loading and propulsive phases of jumping and hopping tasks. This outcome proposes the demand of additional research to investigate how and why these the kinematics differences have occurred.

	Normal Arch Height			Low Arch Height				
	Forward Hopping	Lateral Jumping	Stationary Hopping	Forward Hopping	Lateral Jumping	Stationary Hopping		
	M (SD)	*M (SD)*	*M (SD)*	*M (SD)*	*M (SD)*	*M (SD)*	*F*	*p*
Landing								
Plantarflexion (°)	60.41 (9.08)	55.41 (6.82)	55.70 (6.22)	65.65 (6.80)	61.31 (6.96)	57.83 (8.56)	0.470	0.628
Dorsiflexion (°)	93.12 (5.19)	89.60 (3.08)	94.02 (4.55)	96.68 (4.320)	91.42 (3.22)	97.34 (5.73)	0.451	0.640
Eversion (°)	-18.65 (14.07)	-33.08 (12.29)	-13.64 (11.28)	-9.91 (7.82)	-33.55 (7.13)	-8.33 (7.09)	0.470	0.628
Inversion (°)	-10.45 (6.82)	-20.54 (9.72)	-7.74 (5.22)	-4.45 (6.02)	-31.55 (6.22)	-7.04 (5.21)	3.272	0.078
Propulsion								
Plantarflexion (°)	40.48 (8.75)	41.39 (5.31)	43.73 (5.43)	47.75 (7.28)	46.28 (6.43)	48.22 (3.95)	0.504	0.608
Dorsiflexion (°)	93.77 (5.59)	88.85 (3.37)	94.21 (4.46)	98.37 (3.40)	90.44 (3.69)	97.10 (6.03)	1.063	0.355
Eversion (°)	-24.42 (11.33)	-34.52 (10.98)	-13.81 (6.40)	-12.86 (7.98)	-29.49 (20.59)	-8.16 (5.41)	0.735	0.451
Inversion (°)	-11.96 (5.33)	-24.638 (8.60)	-6.67 (4.60)	-9.17 (7.05)	-28.19 (6.50)	-5.44 (8.44)	2.136	0.131

Figure 1. Comparison of Peak Sagittal and Frontal Plane Ankle Kinematics Across Jumping and Hopping Tasks.

Significance

The notable differences observed within this study suggests that some of the kinematics patterns observed during walking and running tasks may be diminished in more ballistic locomotive tasks. Additionally, the use of a unique subject population may also suggest that higher competitive athletes develop locomotive mechanics that are different than non-athletic and less competitive populations. Further, the multiplanar demands associated with executing the jumping and hopping tasks could have reduced the impact loose and closed-packed joint positioning have on arch types completing the tasks. Thus, specific directional tasks and population may suggest the development of altered locomotive mechanics to execute task demands.

References

[1] Foot Ankle Int. 2005; 26 (12): 1081-1088.
[2] Curr. Orthop. 2002; 16 (3): 165-179
[3] Gait Posture. 2009; 30(3): 334–349.
[4] Gait Posture. 2008; 28(1): 29-37.
[5] Gait Posture. 2013; 38(3): 363-372
[6] J AM PODIAT MED ASSN. 2008. 98(2), 102-106.

THE INFLUENCE OF DISTAL THROWING ARM KINEMATICS ON MAXIMUM ELBOW VALGUS TORQUE IN YOUTH BASEBALL PITCHERS

Tessa C. Hulburt[1], Garrett S. Bullock[1], Arnel L. Aguinaldo[2], Kristen F. Nicholson[1]
1. Department of Orthopaedic Surgery, Wake Forest School of Medicine, Winston Salem, NC, USA
2. Department of Kinesiology, Point Loma Nazarene University, San Diego, CA, USA
Email: thulburt@wakehealth.edu

Introduction

Motion capture biomechanics has emerged as a vital tool to understand injury risk patterns and efficient mechanics in baseball pitching [1]. Biomechanics studies have investigated the lower extremity, trunk, and upper throwing arm, but little attention has been given to the distal throwing arm, particularly in youth pitchers [2]. The purpose of this study was to determine if distal throwing arm kinematics at maximum external rotation of the glenohumeral joint (MER) calculated from fastball (FB), breaking ball (BB) and off-speed (OS) pitches are related to maximum elbow valgus torque (EVT) in younger (13-15 years) and older youth athletes (16-18 years).

Methods

Motion capture analyses were conducted on 52 pitchers aged 13-15 years (age: 14.8 ± 0.65 years, height: 1.78 ± 0.07 m, weight: 71.5 ± 11.6 kg) and 52 pitchers aged 16-18 years (age: 16.7 ± 0.5 years, height: 1.85 ± 0.07 m, weight: 83.1 ± 11.5 kg). A 41 reflective markerset and twelve-camera motion analysis system (Qualisys AB, Göteborg, Sweden) were used to collect pitching mechanics data. Ball velocity (BV) was recorded with a Trackman device (Trackman, Scottsdale, Arizona). Distal throwing arm kinematics were calculated with Visual3D (C-Motion, Inc. Germantown, Maryland). Pitching models were created using the PitchTrak model [3], and segment coordinate systems were defined according to ISB recommendations [4]. EVT was normalized by body weight (N) and height (m). A generalized linear model with a lasso regularization was chosen due to dataset multicollinearity. The model calculated if kinematic predictor variables were associated with EVT response variable by weighting each variable coefficient. Larger coefficients indicated a stronger association with EVT. Predictor variable data were mean centered and scaled with standard deviation, so data were weighted by their relative influence.

Results and Discussion

Coefficients calculated using the generalized linear regression model with lasso regularization to determine distal throwing arm kinematics influence on EVT can be seen in Figure 1. The fastball model for the older youth players had a minimal explanation of variance with an (R^2 = 0.03) and showed minor influence of ulnar deviation angular velocity (UDV) at MER on EVT. The model of breaking ball pitches for older youth pitchers also had a minor explanation of variance (R^2 = 0.08) and showed that wrist flexion angle (WFA) at MER had the most influence on EVT compared to other kinematics. With an R^2 value of 0.41, a moderate explanation of variance, the model for off-speed pitches thrown by the younger youth group had the strongest relationship with EVT. All joint angles at MER had weaker associations with EVT compared to wrist flexion angular velocity (WFV) and UDV at MER, which had the strongest influences on EVT. The model for off-speed pitches in the older youth age group had a minimal explanation of variance (R^2 = 0.16) and showed that WFA, WFV and forearm pronation angular velocity (FPV) at MER had a relationship with EVT, with FPV having the strongest association comparatively.

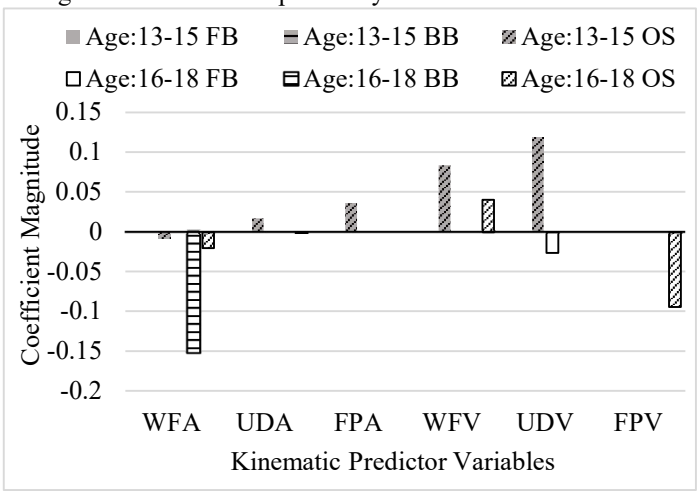

Figure 1. Kinematic coefficients associated with EVT for younger and older youth pitchers. Kinematic variables are wrist flexion angle (WFA), ulnar deviation angle (UDA), forearm pronation angle (FPA), wrist flexion angular velocity (WFV), ulnar deviation angular velocity (UDV), and forearm pronation angular velocity (FPV). All variables are at timepoint maximum external rotation of glenohumeral joint (MER).

The larger influence of WFV and UDV at MER on EVT in younger youth off-speed pitches compared to joint angles demonstrates that angular velocity is more important than distal arm position at MER. The weaker association of off-speed pitch distal arm kinematics with EVT in older youth pitchers could be due to lack of skill and coordination that exists in younger youth players during the average pubertal growth stage. Though a small age gap, skill and coordination obtained by age 16-18 compared to 13-15 years may result in reduced injurious distal arm kinematics in off-speed pitches.

Distal throwing arm kinematics had the most influence on EVT in younger youth off-speed pitches compared to other pitch types and older youth players. This work contributes knowledge of the influence of distal throwing arm mechanics on EVT, a metric of injury to the medial elbow.

Significance

Excessive EVT is related many common pitching elbow ailments such as elbow valgus overload syndrome, ulnar collateral ligament partial tear or rupture and avulsion injury at the UCL anterior bundle origin [5]. Results from this study call into question whether pitchers should wait until after the average pubertal growth stage to begin throwing off-speed pitches due to the higher potential for medial elbow injury.

References

[1] Davis JT et al. (2009). Am. J. Sports Med. 37: 1484-1491.
[2] Solomito MJ et al. (2004). Sport. Biomech. 13: 320-331.
[3] Aguinaldo AL et al. (2007). J. Appl Biomech. 23: 42-51.
[4] Wu G et al. (2005). J. Biomech. 38: 981-99
[5] Fleisig GS et al. (2012) Sports Health. 4: 419-424

DYNAMIC LIFTING TASKS YIELD LARGER THORACIC AND LUMBAR SPINAL LOADS COMPARED WITH QUASI-STATIC LIFTING

Katelyn A. Burkhart[1], M. Mehdi Alemi[1], Andrew C. Lynch[1], Brett T. Allaire[1], Mary L. Bouxsein[1], and Dennis E. Anderson*[1]
[1]Center for Advanced Orthopedic Studies, Beth Israel Deaconess Medical Center, Harvard Medical School, Boston MA
email: *danders7@bidmc.harvard.edu

Introduction

Inertial effects are a key component of dynamic motions, and prior studies in the lumbar spine have shown that spine loads can be underestimated if dynamic tasks are simplified to a quasi-static simulation (McGill and Norman 1985, Marras 1997). The differences will be amplified as velocity and/or mass lifted increases, as reported for lateral bending and lifting (Marras 1997, Bazrgari 2008). However, static analyses are increasingly applied in large datasets of subject-specific models based on medical imaging to study variations in spine loading or effects of loading activity in a population (Bruno and Mokhtarzadeh 2017). Thus, there is a need to understand the effect of dynamic vs. static simulations in these types of subject-specific models.

Therefore, the main objective of this study was to investigate thoracolumbar spine loads determined by subject-specific musculoskeletal models in static and dynamic simulations of the same lifting activity.

Methods

Six healthy participants aged 53-78 years (5F, 1M) underwent testing in our motion lab. Retroreflective markers were placed on anatomical regions, including clusters on T1, L1 and S2 spinous processes, a single marker on all other vertebrae from C7 to L5 spinous processes, pelvis, upper and lower limbs, and head. Subjects performed a sagittally symmetric 2-handed box lift with a mass equal to 10% of their body weight. We created subject-specific full-body musculoskeletal models with detailed thoracolumbar spines. Models were scaled from recorded neutral standing postures, distances between markers, and muscle and spine curvature were adjusted from CT-derived measurements.

Using the subject-specific models, we estimated vertebral compressive and anterior-posterior (AP) shear loading from T1 to L5 for the dynamic lifting task. During the lifting phase, we selected the single frame of inverse kinematics data that corresponded to maximum compressive spine load at T12 (Figure 1). This posture was extracted from the inverse kinematics and evaluated separately as a quasi-static lifting activity.

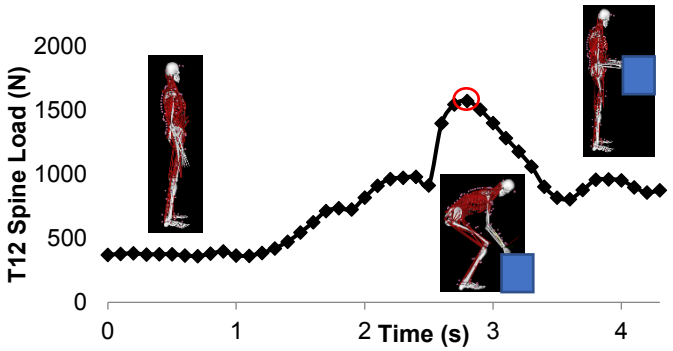

Figure 1: An example of a subject's compressive spine load at T12 during a dynamic lift. The red circle identifies the time point that was selected from the motion for a quasi-static comparison.

We compared spine loads between the dynamic and static simulations using paired Student's t-tests, with differences considered significant if $p < 0.05$.

Results and Discussion

In the frame identified as maximal compressive spine load during the lift, T1-L5 spine flexion angle, pelvis tilt, and hip flexion averaged 20.1±7.2º, 42.9±9.6º, and 69.1±13.0º respectively. Angular velocities varied greatly from subject-to-subject, with averages (range) of 7.4±8.3 (-4.9 to 16.5)º/s, 31.4±33.7 (-6.2 to 73.1)º/s, and 115.6±109.5 (-37 to 270)º/s respectively. Static simulations of the lifting activity consistently underestimated dynamic spine loads at every level of the spine from T1-L5 for compressive loading, and all levels except T12 and L2 in AP shear loading ($p<0.05$). In particular, dynamic compressive spine loads were an average of 21-36% larger across T1-L5 levels, with larger percent differences in the thoracic spine, but larger absolute differences in the lumbar spine (Figure 2). AP shear load (negative load indicates posterior direction) differences were minimal and relatively consistent throughout the spine, but notably larger at L5, likely due to higher shear loads at this level (Figure 2). Velocity of the lift was not controlled in this study, and likely contributes to some of the inter-subject variation between static and dynamic simulations that we observed.

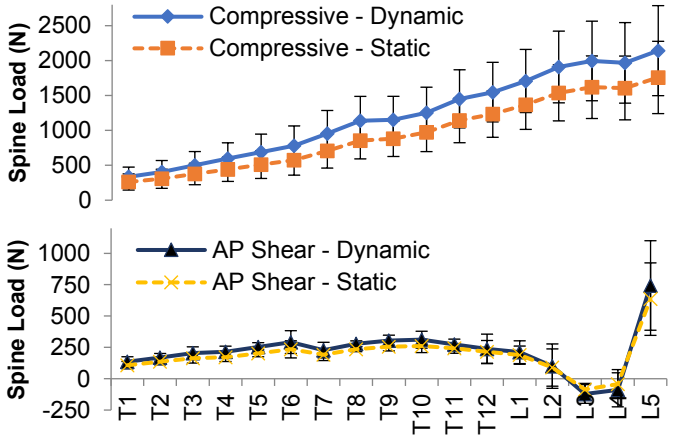

Figure 2: Mean dynamic and static spine loading in compression (top) and AP shear (bottom). Error bars indicate standard deviation.

Significance

The results demonstrate the substantial inertial effect that dynamic activities contribute to compressive and shear spine loading. This is significant for quasi-static modelling studies, as similar dynamic modelling could result in increased compressive spine loads across T1 to L5 spine levels. This difference in load could be meaningful for studies of injury risk or clinical biomechanics of the spine, and should be considered when quasi-static analysis are applied in large cohort studies.

Acknowledgments

This work supported by the National Institutes of Health (R01AR073019 and Harvard Catalyst - UL1TR001102).

References

McGill and Norman. 1985. Biomechanics 18. Marras et al. 1997. J. Biomech. 30, 697–703. Bazrgari, et al. 2008. J. Biomech. 41, 412–421. Bruno, A.G., 2017. J. Orthop. Res. 35, 2164–217

PERTURBATION DOSE-RESPONSE CURVES FOR STANDING BALANCE

Brandon J. Perry[1], D.M. Venema[2], J.B. Boron[3], J.M. Yentes[1]
[1]Department of Biomechanics, University of Nebraska at Omaha
email: brandonperry@unomaha.edu

Introduction

Prediction of falls in older adults remains a challenge for health care providers and researchers. Part of the difficulty is determining individual characteristics predictive of falling, and at what point the aging process becomes non-normative and increases fall risk for some individuals. Dose-response curves have been used extensively in pharmacological studies to determine drug effects. We propose that dose-response curves from varying magnitudes of perturbation may provide insight into the control of balance between middle (MA) and older-aged (OA) adults. Further, the dose-response methodology allows for stronger prediction models of fall-no fall.

Methods

Sixteen MA (male=3; 56.6yrs±7.5) and 12 OA (male=3; 71.5years±4.1) cohorts performed five, 60-sec standing trials on a moveable force platform (Neurocom Clinical Research System, Natus, Middleton, WI). All subjects were secured with a harness, wore noise blocking earphones, and foot placement was controlled between trials. The five trials involved surface perturbations while watching a static nature scene video at eye level. During the perturbation trials, the platform was displaced posteriorly at a velocity of 20cm/s by varying magnitudes of 2.54, 5.08, 7.62, 10.16, and 12.7cm. Time between perturbations were randomly varied between 16-27sec. Only one perturbation was given per trial and order of magnitudes were randomized. A five-min rest was given between each trial. Center of pressure data were collected, and response sway distance was calculated [1] over the entire trial. The first perturbation trial for each subject was discarded. Trials were considered a "fall" when subjects grabbed the harness, touched the wall or support columns, or stepped during the perturbation.

Response sway distance dose-response curves were generated for each subject and averages for each group was calculated. Changes in sway distances due to age and perturbation magnitudes were analyzed using 2x5 repeated ANOVA (significance: α=0.05). Survival analyses were used to compare the middle and older response sway distance data. Survival models are statistical models that use binary fail-no-fail data and continuous data such as insult, input, or response as inputs to create models capable of predicting the risk of failure. Inputs were binary fall-no fall response data and response sway distance.

Results and Discussion

The response sway distance of the dose-response curves did not differ between age groups (MA=0.59; OA=0.51; Figure 1). Sway distance differed by magnitude across both groups ($p<0.0001$). Although dose response curves were similar for both MA and OA, fallers in both age groups responded with a greater distance in sway at most perturbation magnitudes (Figure 1).

Survival models were fit to the MA and OA cohorts (Figure 2). The 50th percentile fall risk for the MA and OA cohorts was a 20.7mm and 15.5mm response sway distance, respectively, or a 34% decrease from the MA to OA cohorts. Although only ~5mm difference, at the 15.5mm response distance for the OA, the MA maintain a 75th percentile for not falling. Considered further, at the 20.7mm distance that places MA adults at the 50th percentile for not falling, the OA adult is at the 10th percentile for not falling.

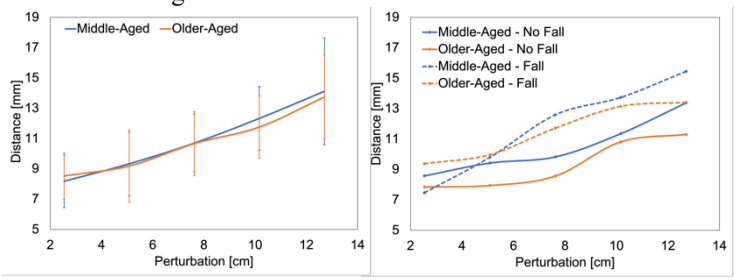

Figure 1 (left). Group average dose-response curves by age group. No difference in response distance was found between ages (p=0.54). All perturbation magnitudes were significantly different from each other (p's<0.05), except between 7.62 and 10.16 cm. **(right)**. Group average dose-response curves by age and faller group. A subject was marked as a faller if they fell during at least one of the trials. OA non-fallers also used less sway distance than did the MA non-fallers.

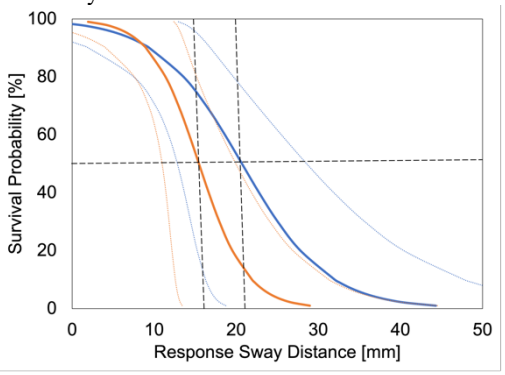

Figure 2. Survival analysis comparing the MA (blue) and OA (orange) cohorts. Thin lines represent 95th percentile confidence intervals. Black dashed lines demonstrate the 50th percentile fall risk for each group at 15.5mm and 20.7mm response sway distance.

Significance

While the dose-responses were similar between the two age cohorts at the given perturbations, the occurrence of requirement for additional stabilization or support from OA was higher. Further investigations should be given to dose-response curves divided by age and fall status. Data collections are ongoing. We anticipate that MA and OA cohorts' survival analyses will continue to diverge, with smaller confidence intervals. Dose-response designs may prove to be strong predictors of fall risk and in determining characteristics in midlife that may predict non-normative aging.

Acknowledgments

Funding provided by NIH (P20 GM109090), Dept of VA (I21RX003294), and UNO Science, Engineering, and Medicine grant. We would like to thank Judith Kim and Katie Chess for their help with data collections.

References

1. Prieto, et al. IEEE Trans Biomed Eng. 43(9):956-66, 1996.

Longitudinal Changes in Adjacent Segment Disc Deformation After Cervical Spine Fusion

Anna C. Martinez[1], Clarissa LeVasseur[2], Samuel Pitcairn[2], Jeremy Shaw[2], William Donaldson[2], Joon Lee[2], and William Anderst[2]
[1]Department of Bioengineering, University of Pittsburgh, Pittsburgh, PA
[2]Department of Orthopaedic Surgery, University of Pittsburgh, Pittsburgh, PA
Email: acm162@pitt.edu

Introduction

Approximately 150,000 cervical spinal fusion surgeries occur each year in the United States, with 25% of the patients requiring a second surgery within 10 years to address symptomatic adjacent segment disease (ASD)[1,2]. In vitro studies suggest that ASD may be due to excessive motion and disc loading post-surgery to compensate for the immobility in the fused vertebrae. However, it is unclear if adjacent segment disc deformation increases in vivo after fusion.

The aim of this study is to determine the change in adjacent segment disc deformation after cervical fusion. We hypothesized that compression, distraction, and shear deformation increase from before surgery to 3 years after surgery..

Methods

Thus far, 20 of the 80 anterior fusion patients who provided informed written consent to participate in this ongoing IRB-approved study have completed pre-surgical (PRE), 1-year post-surgical (1YR-POST) and 3-years post-surgical (3YR-POST) testing. On each test day, participants sat upright with their head in the neutral position for a single static image, then performed 3 trials of full range of motion (ROM) flexion/extension of their head followed by 3 trials of axial rotation while synchronized biplane radiographs of the cervical spine were collected at 30 images/s for 3 seconds for each trial. Three-dimensional vertebral motion was calculated using a previously validated model-based tracking technique that matched subject-specific bone models (obtained from CT) to the radiographs[3]. Adjacent segment disc deformation during the dynamic trials was calculated based upon vertebral body endplate motion and normalized to the static trial PRE with a validated precision of 0.4 ± 0.2 and 0.3 ± 0.2 mm above and below the fused segment, respectively.[3] The compressive/distraction strain was calculated for each instant during the vertebral movement using the equation: $\varepsilon_{cd} = \frac{l_{d(perp)} - l_{s(perp)}}{l_{s(perp)}}$, where $l_{d(perp)}$ and $l_{s(perp)}$ represent the dynamic and static length, respectively, of the disc perpendicular to the average plane of adjacent endplates. The shear deformation was calculated using the equation: $\varepsilon_{cd} = \frac{l_{d(par)} - l_{s(par)}}{l_{s(perp)}}$, where $l_{d(par)}$ and $l_{s(par)}$ represent the dynamic and static length, respectively, of the disc parallel to the average plane of adjacent endplates.[4] Five disc regions were identified based on endplate geometry (anterior, lateral, posterior-lateral, posterior, as well as the nucleus)[4]. The maximum intervertebral disc compression, distraction, and shear deformation of the superior adjacent segments were compared using a 2-way (test date by region) repeated-measures ANOVA with significance set at $p < 0.05$ with a post hoc tukey's multiple comparisons test.

Results and Discussion

During flexion/extension, the anterior region always underwent more compression and distraction than the lateral or nucleus regions, while the nucleus region underwent less compression than the posterior-lateral region (all $p < 0.03$, Figure 1A). Shear deformation was greater in the posterior, lateral and posterior lateral regions than in the nucleus and anterior regions (all $p < 0.027$). There were no differences in peak compression, distraction, or shear deformation across test days (all $p > 0.28$, Figure 1A), nor were there any interaction between region and test dates (all $p > 0.054$, Figure 1A).

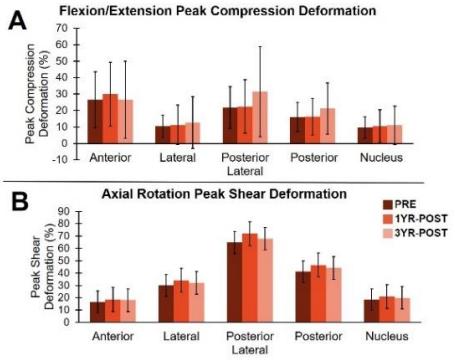

Figure 1: Peak disc compression experienced during flexion/extension (A) and peak shear deformation experienced during axial rotation (B) from each disc region. Each bar represents the test days: PRE (dark red), 1YR-POST (red), and 3YR-POST (light red). Error bars represent ±1 SD.

During axial rotation, there were no differences in compression or distraction deformation between regions or across test dates (all $p > 0.14$). Shear deformation was greater in the posterior lateral region that in the anterior and nucleus regions (all $p < 0.036$, Figure 1B) during axial rotation. This finding is indicative of a potential mechanical etiology for the common symptomatic pathology in the posterior-lateral region.

The main findings in this study include significantly larger disc deformations occurring in the posterior-lateral region, relative to the other disc regions, during flexion/extension and axial rotation head movements. There is no evidence to support the hypothesis that maximum disc compression, distraction, and shear deformation increase from PRE to 3YR-POST.

Significance

This study failed to support the hypothesis that adjacent segment disc deformation increases over the short-term after anterior cervical fusion. This is contrary to in vitro results.[6] Longer follow-up may be needed to observe the effects of excess load if it exists after fusion. Alternatively, factors other than excessive load may drive adjacent segment degeneration.

Acknowledgments

This work was supported by NIH Grant R01 AR069543.

References

(1) Olgesby et al., *Spine*, 2013. (2) Lawrence et al., *Spine*, 2012. (3) Anderst et al., *Spine*, 2011. (4) Anderst et al., *ABME*, 2015, 43. (5) Anderst et al., *JOR*, 2013. (6) Prasarn et al. *J. Neurosurg Spine.* 2012

THE INTERACTION OF SPEED, RESISTANCE, AND SPLIT-BELT WALKING TO INCREASE TRAILING LIMB ANGLE

Moll AN, Kuhman D, Baumann A, Jiang W, Marsh K, and Hurt CP[1]
[1]Department of Physical Therapy, University of Alabama at Birmingham, 1705 S. University Blvd, Birmingham, AL 35205
email: *amoll@uab.edu

Introduction

Trailing limb angle (TLA), the angle between the line joining the hip joint and ankle joint and the vertical axis normal to the treadmill surface, has been shown to relate to propulsive forces while walking[1]. Increasing walking speed and walking up a sloped surface have both been shown to increase TLA[2]. Split-belt treadmill walking whereby one belt moves at a faster speed than the other can also influence TLA[3-4]. For this study we systematically manipulated speed, slope, and split-belt treadmill walking to investigate which condition may be more favorable to increase TLA. We hypothesized that increasing the parallel forces that individuals experience would increase the TLA more than speed or split-belt walking alone.

Methods

Ten healthy, young adults (mean age: 25.3; mean height: 1.72 m; mean mass: 72.27 kg) participated in this study. Individuals were excluded if they had any lower extremity injury within 6 months prior to participation. Kinematics were collected simultaneously using an 8-camera motion capture system (Vicon) and a dual-belt, force instrumented treadmill (Motek). Data was processed in Visual 3D and TLA was analyzed with a custom script in Matlab. Participants performed 11 walking trials, with "wash out" trials included. Participants started at 0 degrees (°) incline with four belt speed configurations. Both belts tied at 0.5 m/s and at 1.0 m/s (Trials 1 and 2), belts split with the left belt at 1.0 m/s and the right belt at 0.5 m/s (Trial 3), and belts tied at 1.0 m/s to serve as a "wash out" trial (Trial 4). These trials were repeated for treadmill incline of 5° and 10°. For this abstract, all data except for the "wash out" trials for 0°, 5°, and 10° of incline are presented. A repeated measures ANOVA was used to assess the effect of slope, limb, and belt condition as well as any interaction that may occur on TLA (SPSS version 27). A Bonferoni post hoc analysis was performed to test difference between conditions.

Results and Discussion

For participants walking at 0° incline, TLA increased based on the belt condition: tied at 0.5 m/s, tied at 1m/s, and faster belt on the split condition (Figure 1: Left Panel). There was an interaction effect of belt condition and limb ($p = 0.001$), with participants having a stronger effect size from limb ($\eta^2 = 0.94$) than belt condition ($\eta^2 = 0.408$). TLA was significantly different based on the left or right limb ($p < 0.001$), with the biggest difference shown visually in Figure 1 on the split condition.

There were similar interactions observed for both studies of participants walking at a 5° and 10° incline on the treadmill. TLA increased most in the split belt condition (Figure 1: Middle and Right Panels). For participants walking at 5° incline, there was an interaction effect of belt condition and limb ($p < 0.01$), with participants having a stronger effect size on the TLA based on the belt condition ($\eta^2 = 0.350$) than limb ($\eta^2 = 0.004$). For participants walking at 10° incline, there was also an interaction effect of belt condition and limb ($p = 0.028$), with participants having a stronger effect size from belt condition ($\eta^2 = 0.397$). TLA was significantly different based on the belt condition (5°: $p = 0.04$; 10°: $p = 0.011$), with the biggest difference shown between the tied belt at 0.5 m/s and the split condition (5°: $p < 0.01$; 10°: $p < 0.001$ pairwise comparison).

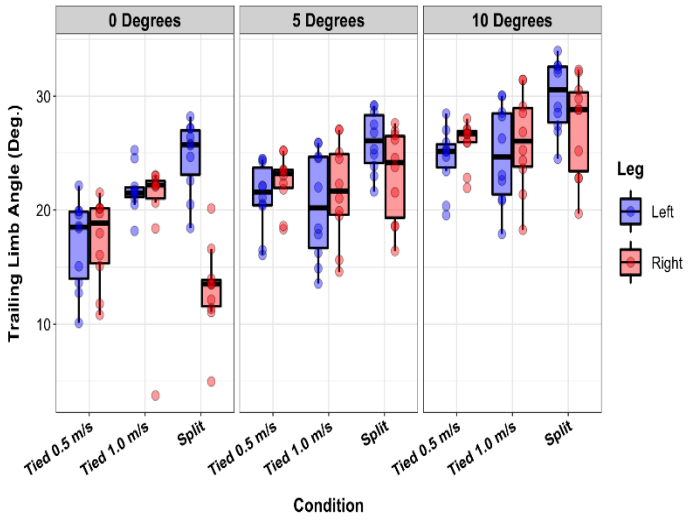

Figure 1. Trailing Limb Angle results of the tied and split belt incline conditions: 0° (Left Panel), 5° (Middle Panel), and 10° (Right Panel). For split condition in each incline position: left belt moved 1 m/s (fast belt) and right belt moved 0.5 m/s (slow belt). Results from the repeated measures ANOVA indicated significant differences in interaction between limbs and belt conditions for treadmill incline of 0°,5°, and 10°.

These results support our hypothesis that increasing resistive forces (i.e. increased parallel force) is more effective than speed for increasing TLA. The split belt condition has an increased positive affect on TLA for all conditions: 0°, 5°, and 10° incline. The combination of slope from treadmill belt incline and split belt conditions resulted in greatest change.

Significance

Split-belt treadmill walking with increased parallel forces can be used to create interventions to improve TLA. Previous investigations have shown that increasing TLA can increase propulsive forces. The overall results showed there was a bigger difference in TLA from changing the slope of the treadmill than walking at different speeds on a 0° incline. TLA did increase on the faster belt, which was the left foot in this study. That variable could be changed depending on the intervention required. This study adds increased knowledge required to implement a desired intervention in improving TLA.

References

1. Miyazaki T *et al.*, 2019, Biomed Res International
2. Hsiao H *et al.*, 2016, Journal of Biomechanics
3. Hsiao H et al., 2015, Human Movement Science
4. Sombric C et al., 2019, Frontiers in Physiology

HOW DOES THE MUSCLE FORCE-VELOCITY BEHAVIOR AFFECT MUSCLE STRAIN DISTRIBUTIONS?

Matthew D. DiSalvo[1], S.S. Blemker[1,2]
[1]Department of Biomedical Engineering, University of Virginia, Charlottesville, VA, USA
[2]Department of Mechanical Engineering, University of Virginia, Charlottesville, VA, USA
email: mdd5dn@virginia.edu

Introduction

The complexity and dynamics of muscle tissue has resulted in several variations of constitutive models for various applications[1]. Most muscle constitutive models incorporate the ability to represent quasi-static passive and active force-length behavior of muscle tissue, assuming a transversely isotropic material. These models have provided insights into the relationship between muscle morphology and strain distributions; however, it remains unclear if the force-velocity behavior influences the strain distributions. Therefore, the goals of this work are to (i) incorporate the force-velocity behavior into an already existing muscle constitutive law[2], and then (ii) examine the extent to which the force-velocity behavior influence strain distributions in a 3D muscle model.

Methods

A four-parameter, c1 continuous, force-velocity curve for normalized fiber lengths was chosen to model force-velocity behavior[3] for eccentric, isometric, and concentric conditions. This function was included as a new term in the calculation of fiber stress in an existing, commonly used uncoupled hyper-elastic transversely isotropic muscle material currently available as a material option in the finite element software FEBio[4].

Validation of the new muscle material as a FEBio capable material plugin was done with a model suite consisting of single hexahedral elements undergoing prescribed isovolumetric deformations representing eccentric, concentric, and isometric conditions. We verified that the stress and force predictions from the FE model were consistent with the theoretical force-velocity curve.

A simplified pennate muscle model was developed, consisting of a central muscle and two parallel tendon structures. The muscle portion consists of a composite of a Mooney-Rivlin material combined with our new material; the tendon regions use neo-Hookean parameters. One tendon underwent prescribed displacement to simulate eccentric velocity conditions. We performed simulations with the previous muscle model (which included no force-velocity effects) and the new muscle model (which included force-velocity effects). Two conditions were simulated with both models: a low lengthening velocity and a high lengthening velocity. In order to examine the strain distributions across the muscle, we determined the variation of along-fiber stretch as a function of the distance along the length of the muscle.

Results and Discussion

Validation of the FEBio implementation of the new material showed adherence theoretical force-velocity parameters in isometric conditions (RMSE = 0), and close adherence in the simulated concentric and eccentric behavior (RMSE = 0.12).

Strain distributions differed substantially when force-velocity effects were incorporated, as compared to when they are not incorporated. These differences are more pronounced at higher tendon displacement speeds (Fig. 1). Most notably, the peak along-fiber stretch was lower in the simulations that included force-velocity effects, and the range of along-fiber stretch was also lower in the force-velocity models.

Significance

While strains are not uniform through muscles, the force-velocity relationship attenuates the distribution by lowering both the peak and range of strains experienced. The new constitutive model developed in this project has many applications, and the code, once finalized, will be made available through FEBio.org.

Acknowledgments

U.S. DoD (DoD/USAMRAA W81XWH-16-R-BAA1)
NIH U01 1U01AR069393

References

[1] Dao, T.T. & M.-C.H.B. *App. Bionics and Biomechanics* (2018)
[2] Blemker, S.S. et al. *J Biomechanics* 38 (2005)
[3] Alcazar, J. et al. *Front. Physiol* (2019)
[4] Maas, S.A et al. *J Biomech Eng* 134 (2012)

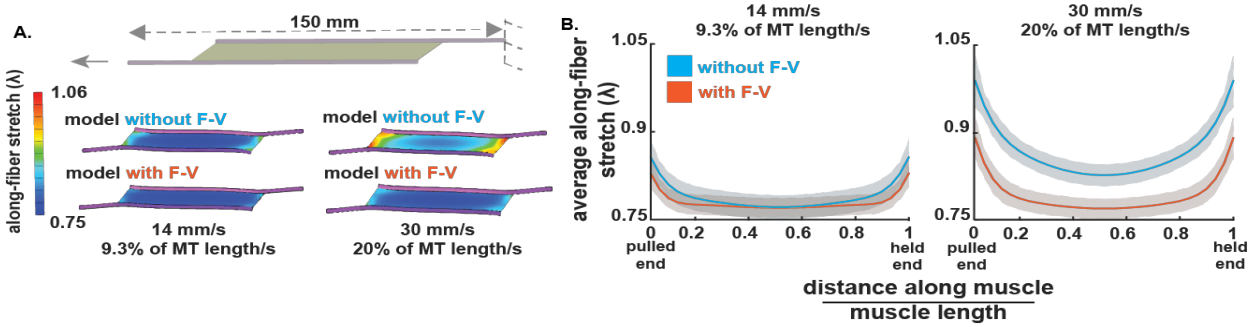

Figure 1: **A**. The pennate muscle model is a 150 mm long muscle-tendon unit with pennation angle of 45 degrees. A prescribed displacement is applied to left tendon after ramping up to maximum activation. The along-fiber stretch can be seen for two speeds, a "low" speed of 14 mm/s that produces comparatively smaller fiber stretch when compared to the "high" speed of 30 mm/s. The addition of the force-velocity behavior can be seen attenuating the magnitude and the distribution of the fiber stretch compared to the equivalent model lacking force-velocity behavior. **B**. The average along fiber-stretch is lower in the models with force-velocity behavior as compared to the models without force-velocity effects. The fiber strain distribution is noticeably less extreme towards either muscle ends in the force-velocity models, indicating a more uniform fiber strain distribution.

VIROTACTILE FEEDBACK FOR IMPROVED CONTROL OF MYOELECTRIC DEVICES

Sean P. Sanford [1'3], Brian D. Collins [2'3], Mingxiao Liu [1'3], and Raviraj Nataraj (PI) [1'3]
[1] Department of Biomedical Engineering, [2] Department of Computer Science, Stevens Institute of Technology, Hoboken, NJ 07030
[3] Movement Control Rehabilitation (MOCORE) Laboratory, Stevens Institute of Technology, email: ssanford@stevens.edu

Introduction

Sensory feedback in the form of visual, audio, or haptic cues can accelerate motor-learning and improve rehabilitation following neurotrauma [1]. Vibration, also known as vibrotactile feedback, applied directly to the muscle-tendon or muscle mid-belly is a unique form of haptic feedback that can be therapeutic in small doses [2]. Additionally, vibration can alter neurophysiological signals and the user's proprioception caused by muscle stretch reflexes, such as afferent signals and an increase in muscle spindle activation [3]. During isometric exercises, electromyographic (EMG) activity can be systematically altered based upon vibration location and magnitude [4]. Our objective was to optimize a machine-learning classifier used for controlling a virtual myoelectric prosthetic by modulating vibration in real-time to induce more distinct clusters of EMG activity. We hypothesized that vibration can be utilized to increase classification accuracy and improve myoelectric control.

Methods

In the preliminary study, three able-bodied participants donned a custom restrictive brace used to immobilize the upper-body for inducing isometric contractions (**Figure 1**). Participants applied orthogonal forces at two distinct force levels (30% and 50%) and four combinations of vibration (off/no vibration, upper-arm vibration only, torso vibration only, upper-arm and torso vibration). Small coin motors were used to vibrate both the agonist and antagonist muscles to maximize the vibration effect. For upper-arm vibration, the biceps and triceps brachii were palpated directly at the proximal and distal muscle-tendon junctions. The torso was vibrated on the muscle mid-belly of the pectoralis major and trapezius. Participants were positioned with their shoulder at approximately 45° abduction, elbow at 90°, and forearm directed forward with palm down. EMG activity was collected from fourteen upper-body muscles spanning from the forearm to the torso: upper trapezius, middle trapezius, lower trapezius, pectoralis major, anterior deltoid, posterior deltoid, serratus anterior, latissimus dorsi, biceps brachii, triceps brachii, brachioradialis, pronator teres, flexor digitorum, and extensor digitorum. For each combination of two force levels and four vibration modes, participants completed one trial of each orthogonal direction (up, down, left, right, back, forward), for a total of 48 trials. Each trial lasted 30-seconds and 10-seconds of 'on' EMG activity was collected for analysis. A break of 30-seconds separated each trial. An ANOVA test was used to determine significant changes in the magnitude of EMG activity of individual muscles across vibration modes at each force level. Principle component analysis was used to reduce dimensionality and K-means cluster analysis quantified the separability of EMG activity clusters. An optimal vibration pattern was chosen by the highest classification accuracy and muscle separability.

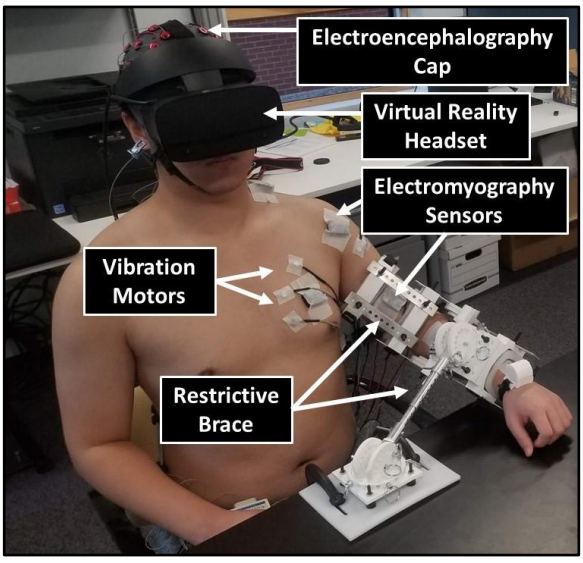

Figure 1. Demonstration of our experimental protocol utilizing a restrictive brace, vibration motors, and wearable sensors.

Results and Discussion

Significant differences were found between individual vibration groups and the no vibration condition at multiple muscle sites. Vibration significantly increased the magnitude of EMG activity at the biceps brachii, triceps brachii, and pectoralis major for multiple directions at each force level. This effect was most significant for the pectoralis major. Preliminary results suggest EMG activity can be systematically altered through vibration in real-time. Only the muscle sites palpated were influenced by vibration. No changes in EMG activity were found in the forearm muscles during any vibration mode. Major limitations include the lack of participant testing due to COVID protocols. Future studies include the implementation of a virtual reality environment for training greater independent function and improving control of myoelectric devices. Participants will be provided real-time visual feedback of virtual position and optimal vibration patterns to create a novel multi-sensory feedback rehabilitation paradigm. Additionally, electroencephalography data will be collected to evaluate cognitive factors including sense of agency and motivation.

Significance

Our objective was to utilize implicit vibration to increase the separability of EMG activity clusters and to create more distinct classes of inputs into a machine-learning algorithm with the intent to improve classification and subsequent myoelectric control. This work will advance the development of rehabilitation programs that leverage sensory feedback and the direct effects on neurophysiological signals for accelerating motor-learning. Following neurotrauma, clinical participants rehabilitating with our novel multi-sensory feedback approach will have (1) greater independent function of one's limbs during dynamic movements and (2) better control of remote or assistive myoelectric devices.

References

1. Sigrist R. *Psych. Bull. Rev.* 2013. 20(1). 21-53.
2. Alam M. M. *Work*. 2018. 59(4). 571-583.
3. Taylor M. W. *Multisensory Res.* 2017. 30(1). 25-63
4. Pujari A. N. *J. Rehab. Assist. Tech. Eng.*

THE EFFECT OF ADVANCED PREGNANCY ON GAIT ASYMMETRY: A CASE STUDY

Aude S. Lefranc[1], Glenn K. Klute[2,3], and Richard R. Neptune [1]
[1]Walker Department of Mechanical Engineering, The University of Texas at Austin, Austin, TX
[2]Center for Limb Loss and MoBility, VA Puget Sound, Seattle, WA
[3]Department of Mechanical Engineering, University of Washington, Seattle, WA
email: lefranc@utexas.edu

Introduction

During pregnancy, several biomechanical changes occur that alter the individual's gait pattern. As a result, females are at increased risk of falling during pregnancy, with 27% experiencing a fall at least once.[1] While most healthy individuals have some degree of gait asymmetry, severe asymmetry is a predictor of increased instability and fall risk. [2,3,4] However, it is unclear whether the biomechanical changes during pregnancy exacerbate pre-existing gait asymmetry, which may contribute to their increased risk of falling.

The purpose of this case study was to explore the effect of pregnancy on gait asymmetry, which was assessed by differences in step-length and ground reaction force (GRF) patterns between limbs. We anticipated that the participant would experience greater asymmetry during pregnancy compared to after pregnancy, and that the degree of asymmetry would increase as the pregnancy progressed.

Methods

Kinematic and kinetic data were collected from one healthy female (age: 25 years, height: 1.65 m, mass: 61.2 kg) during three stages of pregnancy (2nd trimester (2T), 3rd trimester (3T) and 6 months post-partum (PP)). The subject provided written informed consent to participate in this study protocol approved by the UT Austin IRB. Since data were not collected prior to pregnancy, the data at PP served as a baseline for the 2T and 3T data. A 10-camera motion capture system (VICON, USA) recorded full body kinematics during steady state treadmill walking. At each stage of pregnancy, the participant was asked to walk at her self-selected (SS) and a fixed (1m/s) speed. Motion data were processed in Visual3D (C-Motion, USA) and MATLAB (Mathworks, USA). Step length was defined as the distance between the heel contact point of one foot to that of the other foot while the GRF variables of interest were defined by the local and absolute extrema of each force (Table 1).[5]

$\mathbf{F_{max,1}}$	First local max of vertical and mediolateral (ML) GRFs
$\mathbf{F_{max,2}}$	Second local max of vertical and ML GRFs
$\mathbf{F_{max}}$	Absolute max of anterior-posterior (AP) GRFs
$\mathbf{F_{min}}$	Local min of vertical GRF, absolute min of ML and AP GRFs

Table 1: Definitions of GRF variables analyzed.

A symmetry index (SI) was used to quantify asymmetries between the step length and GRF variables (Eq. 1), where X_R is the variable for the right step and X_L is the variable for the subsequent left step. [6]

$$SI = \frac{X_R - X_L}{0.5 * (X_R + X_L)} * 100\% \quad (1)$$

A SI of 0% corresponds to perfect symmetry, while a positive/negative SI corresponds to right/left side dominance for a particular variable.

Results and Discussion

At baseline, the participant had a slightly longer left than right step length (Fig. 1). Her step length asymmetry increased at both

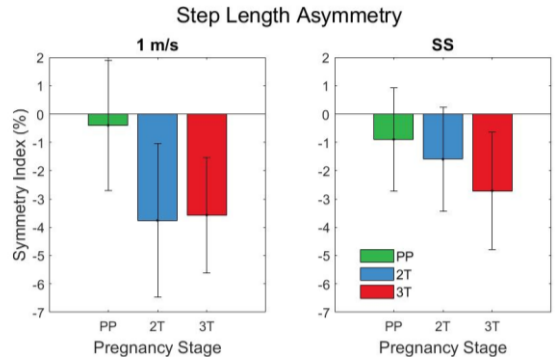

Figure 1: Mean step-length SI values (+/- one SD). Positive / negative SI corresponds to right/left side dominance. Her SS speed was 1.37, 1.30 and 1.26 m/s at PP, 2T and 3T, respectively.

2T and 3T at both walking speeds (SS and 1 m/s). The vertical GRF remained relatively symmetric throughout pregnancy. The most distinct increase in asymmetry occurred in the peak mediolateral GRF (Fig. 2; F_{min}, ML). At PP, there were additional asymmetries in the mediolateral ($F_{max,1}$, ML), peak braking (F_{min}, AP) and peak propulsive (F_{max}, AP) GRFs, which became more apparent during 2T and 3T for both speeds. However, there was minimal or no increase in asymmetry from 2T to 3T.

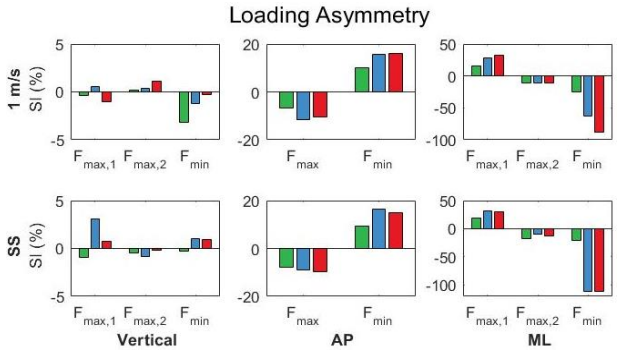

Figure 2: Mean asymmetry values for the Vertical, anteroposterior (AP) and mediolateral (ML) GRFs. Legend is the same as in Fig. 1.

Significance

This case study provides insight into the influence of pregnancy on gait asymmetry during walking, which showed for this individual that existing step-length and GRF asymmetries increased as their pregnancy progressed and may make her more susceptible to falling. Further study with more participants is needed to generalize these findings.

Acknowledgments

This research was supported in part by Dept. of Veterans Affairs, RR&D Service, award RX003138.

References

[1]Dunning K, et al. *Am J Ind Med.* 2003. [2]Yogev G, et al. *Exp Brain Res.* 2007. [3]Bautmans I, et al. *Gait Posture.* 2011. [4]Gillian S, et al. *Aging Clin Exp Res*. 2019. [5]Herzog W, et al. *Med Sci Sports Exerc.* 1989. [6]Robinson R O, et al. *J Manipulative Physiol Ther.* 1987.

STATISTICAL DYNAMIC FOOT SHAPE MODEL

Abhishektha Boppana[1], Allison P. Anderson[1]
[1]University of Colorado Boulder, Boulder, CO USA
email: *abhishektha@colorado.edu

Introduction

Finding a properly fit shoe can be difficult due to the wide distribution of foot shapes and sizes in the population, and limited footwear sizing options [1]. Foot shape also changes dynamically as the foot is loaded through stance phase [2]. Proper fit and comfort is important in reducing occupational footwear injuries [3] and improving performance in agility-based movements [4].

Capturing dynamic foot shape and identifying shape changes can help inform the design of better fitting footwear. This work presents a statistical shape model (SSM) to predict dynamic foot shape through stance phase while walking.

Methods

Thirty healthy subjects (15M/15F, ages 23.1 ± 3.7) were recruited using stratified sampling to maximize variance in foot length. Subjects' height, weight, foot length, foot width, and arch length were collected. Subjects walked on a treadmill at a speed of 1.4 m/s while six Intel RealSense D415 Depth Cameras to capture 3D foot shape point clouds at 90 frames-per-second with the DynaMo software package [5].

A single heel-strike to toe-off event was analysed for each subject. The foot was isolated from the point clouds, and then registered to a common static foot scan template. Kinematic variables, such as dorsi/plantarflexion, ankle inversion/eversion, ankle internal/external rotation, metatarsophalangeal (MTP) dorsi/plantarflexion, foot inversion/eversion, and foot internal/external rotation angles were calculated from foot features for every scan. The first eight principal components (PCs) were calculated for all registered foot scans, representing 95% of the total variance in the dataset. Elastic net regularization was used to build a linear regression model to predict PC scores from the anthropometric and kinematic predictors. PC scores were inversely transformed into predicted foot shapes. The model was validated through leave-one-out cross-validation.

Results and Discussion

The SSM consists of a linear regression model to predict PC scores that can be inversely transformed into a predicted foot shape. The model was able to predict foot shape across all collected scans with a root-mean-square error of 5.2 ± 2.0 mm. The model is available online to visualize predicted foot shape at: https://www.tinyfoot.cc/dynafootModel.

Each PC in the SSM is a shape mode representing an axis of variation. The first shape mode captures shape changes due to MTP and ankle dorsi/plantarflexion. The second and fourth shape modes capture shape changes from foot rotation in the frontal and transverse planes. Foot length variation is captured in the third shape mode. The fifth shape mode shows how the instep area decreases, and the heel area turns into a sharper shape as the MTP joint dorsiflexes through heel-off. Variation along the first and fifth shape mode is presented in Figure 1.

The presented SSM identifies dynamic foot shape changes during stance phase, and outputs predicted foot shapes during stance phase. These foot shape changes can be incorporated into footwear design to improve fit and comfort.

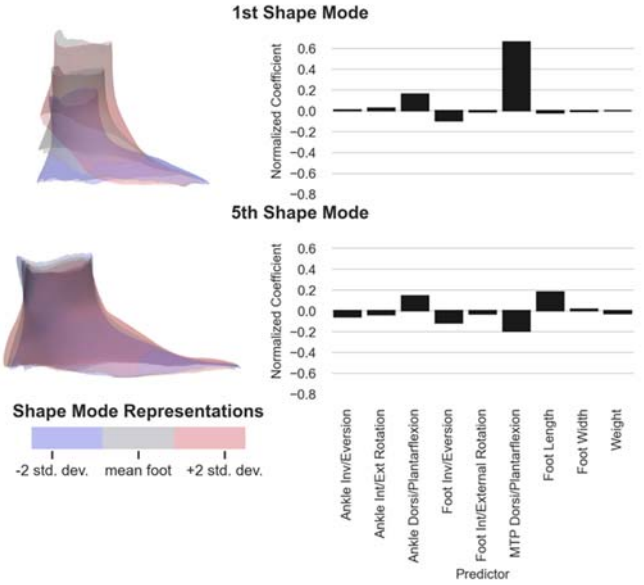

Figure 1: Left: Foot shape deformation at +2 and -2 standard deviations along the first and fifth shape mode. Right: Normalized coefficients from the model for each shape mode

Significance

Footwear can be designed to follow the shape changes identified in this model to ensure better capture of the foot, improving fit and comfort. Lacing over the instep area can be designed to provide additional tension during heel-off, accommodating the decrease in instep area and preventing the heel from lifting inside the shoe. While this study was limited to walking, future work can use these methods on motions such as running and agility movements for other footwear applications.

Acknowledgments

The authors would like to thank Dr. Matthew Reed and Dr. Daniel Park from the University of Michigan Transportation Research Institute for providing the template for foot shape registration and guidance on building the model's web tool.

References

[1] J. W. Wannop, et al, "Development of a Footwear Sizing System in the National Football League," *Sports Health*.
[2] B. Barisch-Fritz, et al, "The effects of gender, age, and body mass on dynamic foot shape and foot deformation in children and adolescents," *Footwear Sci.*
[3] J. A. Dobson, et al, "The three-dimensional shapes of underground coal miners' feet do not match the internal dimensions of their work boots," *Ergonomics*.
[4] M. K. Pryhoda *et al.*, "Alternative upper configurations during agility-based movements: part 1, biomechanical performance," *Footwear Sci.*
[5] A. Boppana and A. P. Anderson, "DynaMo: Dynamic Body Shape and Motion Capture with Intel RealSense Cameras," *J. Open Source Softw.*,

THE EFFECT OF PLANTAR FASCIA THICKNESS AT DIFFERENT FOOT POSITION IN A 3-D FINITE ELEMENT FOOT MODEL

Jinhyuk Kim, Sebastian Y. Bawab, Stacie I. Ringleb
Old Dominion University, Norfolk, VA, USA
email: sringleb@odu.edu

Introduction

The plantar fascia supports the arch and transfers loads during gait, exercise, or running. Therefore, it is subjected to varying stresses such as the repeated tension loading and shear stress. Pathologies and injuries, such as plantar fasciitis and diabetes change the properties of the plantar fascia [1]. The thickness of plantar fascia measured 2.0 ± 0.5mm for healthy people and 5.71 ± 1.3mm and 3.1 ± 1.0mm in patient with plantar fasciitis and diabetes, respectively [2, 3]. Furthermore, 15% - 100% higher plantar pressure in patient with diabetes were measured compared to healthy subjects [1]. Accordingly, the different material properties of the plantar fascia were also contributors to changes in deformation of foot. The purpose of this study was to examine the relationship between the deformation of foot with different plantar fascia thickness and three different foot positions in 3-D finite element foot model.

Methods

The 3D finite element (FE) models including soft tissue and plantar fascia were developed using Hypermesh (Altair, Troy, MI), and FEBio (FEBio, Salt Lake City, UT) segmented from CT images obtained from one cadaver (Figure 1). The FE models were created at three different foot positions (neutral position, 10° plantar flexion (PF), and 10° dorsiflexion (DF) with three different thickness of the plantar fascia (3mm, 4mm, and 5mm). The FE foot model was modeled with 4-node quadratic tetrahedral elements (TET4) and homogeneous isotropic elastic materials [4] and the second-order hyperelastic polynomial for the plantar soft-tissue [5]. A 700N axial load was applied to the top surface of tibia and fibula. The tied contact was applied between rigid plate and soft tissue and bones and cartilage.

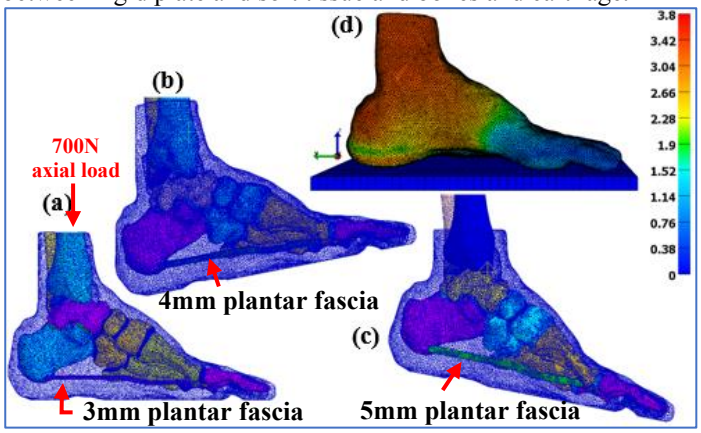

Figure 1: 3D FE Foot model with skin and three different thickness plantar fascia at three different foot positions. (a) The neutral position with 3mm thickness plantar fascia. (b) 10° DF foot position with 4mm thickness plantar fascia (c) 10° PF foot position with 5mm thickness plantar fascia. (d) The deformation of the foot with 3mm plantar fascia in the neutral position.

Results and Discussion

The deformation of the 3D FE models measured from 3.27mm to 3.59mm in neutral, from 3.35mm to 3.97mm in 10° DF, and from 3.03mm to 3.27mm in 10° PF under 700N axial load (Figure 2). In an *in vitro* experiment with same loading, the deformation using displacement transducer ranged from 4.71mm to 6.59mm (average 5.63mm) [6], however, the thickness of the plantar fascia was not reported. Depending on the thickness of the plantar fascia and the different foot position, the difference between the model and *in vitro* experiment varied by 15% - 50% in the same loading condition. The deformation in 10° PF decreased 11% compared to neutral foot positions. And, the deformation in 10° PF measured 6% higher deformation than neutral position FE model. (Figure 2). According to the simulation, the deformation was affected by the thickness of plantar fascia, but also affected by the position of foot. Further investigation in this model requires the analysis of the plantar pressure and stress on hindfoot. This model was also limited because the FE foot models were built based on the different cadaveric foot's CT images. More meaningful results can be obtained when the FE model is created based on a specific cadaveric foot's CT image. The plantar pressure must be compared to figure out the effect of thickness of plantar fascia or different foot position.

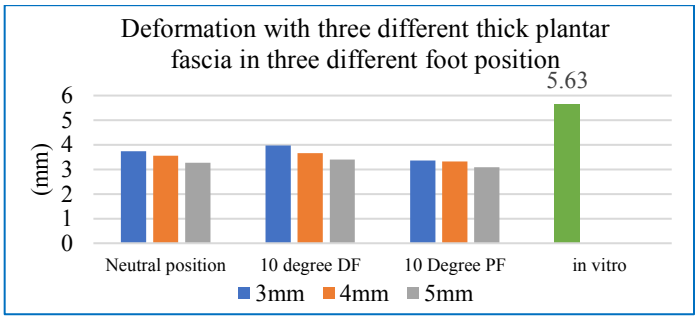

Figure 2: The deformation results based on three different thickness plantar fascia and three different foot positions compared with an *in vitro* experiment, with 700N axial load. The deformation in vitro measured from 4.71mm to 6.59mm.

Significance

3D finite element foot models with varying foot positions and plantar fascia thicknesses were created to examine changes that may occur in pathologies and injuries such as diabetes and plantar fasciitis. Because less flexible feet lead to higher plantar pressures the thicker plantar fascia that is measured in people with diabetes and plantar fasciitis, may contribute to foot ulceration, foot injury, or foot pain. In future iterations of the model, the plantar fascia will be conduced with non-linear material properties and the plantar pressure will be analyzed.

References

[1] A. Guiotto *et al.*, *J. Biomech,* 2014.
[2] S. Mahowald *et al.*, *J Am Podiatric Med Assoc*, 2011.
[3] E. D'Ambrogi *et al.*, *Diabetes Care,* 2003.
[4] H.-Y. K. Cheng *et al.*, *J. biomech. Eng*, 2008.
[5] W.-M. Chen *et al.*, *Med Eng Phys,* 2010.
[6] J. T.-M. Cheung *et al.*, *Clin Biomech,* 2006.

ADVANCING THE DEVELOPMENT OF SMART PROSTHETICS USING HUMAN REACH AND GRASP TOGETHER WITH STUDIES OF THE OCTOPUS

Garrett S. Weidig[1], Brittany Bush[1], Chris Sadler[1], Tyler VanBuren[1], Galit Pelled, PhD [1], Tamara Reid Bush, PhD[1]
[1]Michigan State University
email: weidigga@msu.edu, reditama@msu.edu

Introduction

Loss of limb is accompanied by loss of motor function: in order to restore function, robotic prosthetics being used by individuals [1-2]. However, complications such as misreading neurological signals into the prosthetic can arise in neuron-driven prosthetics. Since these rely on the body's ability to maintain an action potential, problems may arise in their reliability as well [3]. There is a need for prosthetics to work without input from the brain. Interestingly, one animal can move its limbs without direct brain input, the octopus.

The octopus is a muscular hydrostat whose arms have infinite degrees of freedom, but uses typical movements. The octopus also has an axial nerve in each arm that often reacts without the brain's input [4]. Investigating this 'disconnect' between the limbs and brain could be the key to the development of smarter prosthetics.

Therefore, the goals of this work were twofold 1) to determine the reach and grasp motions in human subjects and 2) to initiate a study of octopus reach and grasp movements for comparison to humans. Together, these unique studies have the potential to aid in the design of future smart prosthetics that parallel some natural components found in the octopus.

Methods

Human: Three male participants (average age 21.7 standard deviation 1.5) were tested using a motion capture system and reflective markers (10 individual and 5 marker pods). Participants completed different reaching and grasping motions using two different cylinders with radii of 76 and 152 mm. Participants grabbed in five orientations: in front, below, above, and two peripheral grabs (45° and 90°).

Motion data were analyzed to determine velocity and position profiles as well as eye gaze, determined by head orientation.

Figure 1: *Human (left):* Participant is reaching to grasp a bottle, bring it back to his chest, and put it back at a designated spot. Markers are worn on the upper extremities, torso, and head. *Octopus (right):* Four marker pods and one singular marker were placed on a cadaver octopus arm. Wave-like reaching motions were replicated above water.

Octopus: Preliminary work occurred with the octopus; species *Octopus bimaculoides.* The first step of this research was to evaluate the feasibility of obtaining movement of an octopus arm using motion capture. An amputated arm was manually moved to create typical reaching motions. Position and curvature profiles were obtained using the setup in Figure 1.

Results and Discussion

Initial data for eye positioning from human reaching is shown below for one of the participants. Figure 2 represents the distance between the plane of the eyes and the palm.

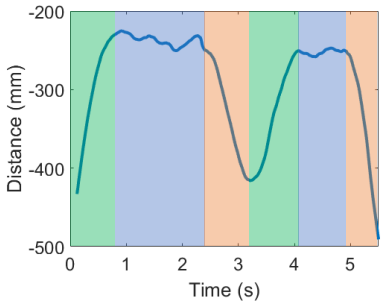

Figure 2: Distance between the eye plane and the palm during a reaching motion. Green represents reaching, blue represents grasping, and orange represents pulling.

Our data demonstrate the typical movements humans inherently perform when completing simple tasks. Here, those patterns are seen in the relative hand/head movements. Also, as these tasks become familiar, less visual attention needs to be paid to the hand and object.

Typical patterns are similarly relayed in an octopus' arm movements. Figure 3 shows that of an above water, amputated octopus arm. The manually simulated curvatures are similar to that of live octopus reaching motions.

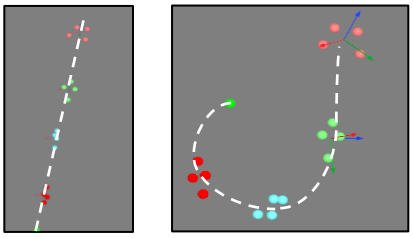

Figure 3: Motion capture visualization for a fully extended octopus arm (left) and an octopus arm during the whip-like motion (right). The white dotted line represents the position of the arm.

These above water tests allow for development of the analysis routines for position, velocity, curvature, and torsion data. Ongoing work is being conducted to gather the same data on living animals.

Significance

This work has the ability the fill the gap in functioning prosthetics by relating the octopus reach and grasp motions to processed use by humans. This work, combined with the neurological signal processing in both humans and octopus has the potential to produce higher functioning, predictive prosthetics.

References

[1] Bowrey, S et al., *Disability and Rehabilitation,* 26, 2009.
[2] Marks, L et al., *BMJ*, 323, 2001.
[3] Ngan, C et al. *Materials*, 12, 2019.
[4] Zullo, L et al. *Journal of Comparative Physiology*, 205, 2019

Muscle Activity in Postpartum Mothers Increases When Lifting Infant: Implications for Lumbopelvic Pain

Kathryn Havens, Ryan Zerega, Sonia Williams
Division of Biokinesiology and Physical Therapy at University of Southern California
email: khavens@usc.edu

Introduction

Lumbopelvic pain is common during pregnancy and does not dissipate following childbirth for many mothers.[1] Its source is not well understood but altered activation or coordination between lumbopelvic muscles may contribute.[2] The first step is to understand musculoskeletal demands during postpartum activities of daily living: lifting and caring for infants. Thus, we aimed to identify patterns of activation between pelvic floor, gluteal, and back muscles during infant lifting tasks in postpartum mothers. We hypothesized that lifting an infant in a car seat would be the most demanding task and elicit highest activation.[3,4]

Methods

6 healthy mothers (34.3 ± 2.6yr, 1.7 ± 0.1m, 62.5 ± 7.1kg) lifted their own infants (14.0 ± 2.4wks, 6.17 ± 0.8kg) in 3 ways: while in a car seat from the floor (10.3 ±1.1kg), from the floor, and from a changing-table height counter (**Figure 1**). Surface electromyography (EMG) was collected from the pelvic floor (Prometheus Pathway Vaginal EMG Sensor, Dover NH USA), bilateral gluteus maximus, and lumbar and thoracic erector spinae (ES) muscles (Noraxon Wireless EMG, Scottsdale AZ, 1500Hz). Equipment failure and cross talk reduced pelvic floor EMG data to 2 participants.

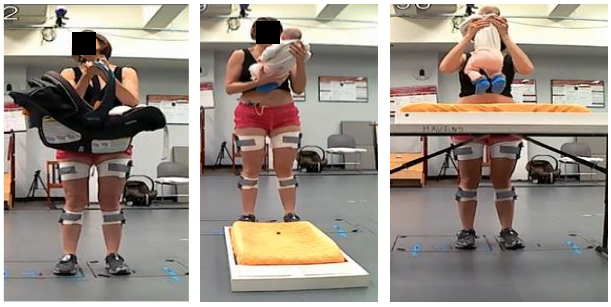

Figure 1: Lifting infant in car seat (left), from floor (middle), from changing table (right)

Raw EMG was band-pass filtered (4th order Butterworth, 10-500Hz), demeaned, and full wave rectified. One task repetition was defined from infant or car seat resting on the floor/surface to returning to surface, and the average of three repetitions were considered. Muscle activity amplitude was identified as mean processed EMG over each repetition, normalized to maximal voluntary contraction, and averaged bilaterally. Descriptive statistics were performed due to low sample size.

Results and Discussion

Compared to standing, muscle activity of pelvic floor, bilateral erector spinae and gluteus maximus was greater for all lifting tasks. Surprisingly, activation of pelvic floor was greatest during lifting from floor and reached 80% MVIC. It was also increased for lifting in car seat, while lifting off table was similar to standing. A similar pattern was identified in the erector spinae muscles. Gluteus maximus activity remained fairly low in all tasks, and greatest activity was found during lifting car seat (**Figure 2**).

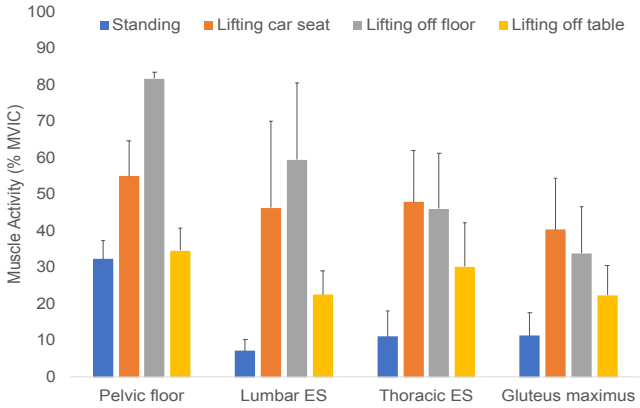

Figure 2: Mean (SD) muscle activity during infant lifting tasks

Because the car seat was heavier, we hypothesized mothers would exhibit the greatest activation during this task.[3,4] However, lifting their baby off the floor required mothers to squat low to the ground, and this also increased musculoskeletal demand. In both tasks, two bursts of activity were found in erector spinae activity, corresponding to the lifting and lowering phases of the task. Patterns of activation were more variable between participants for the pelvic floor and glutes. Lifting baby off of a changing table likely required more upper body strength, and mothers' muscle activity was low and more similar to standing. Upper body activity as well as timing and coordination of muscle activity during these common infant care tasks warrants further investigation.

Significance

Few studies have investigated postpartum mothers' biomechanics during infant care tasks. This pilot study suggests that mothers use strategies to lift infants that increase the demand of their lumbopelvic muscles. These data are exciting and encourage further exploration of application to medical and rehabilitative pain management, including postpartum lifting ergonomics, and strengthening and endurance protocols.

Acknowledgements

Thanks to the moms and babies who participated.

References

1. Wu *et al.*, *Obstet Gynecol*, 2014. 123: 1, 141–148. 2. Gutke et al., *J Rehabil Med,* 2008. 40: 4, 304–311. 3. Brown et al., *Physiotherapy*, 2004. 90: 4, 204–209. 4. Delitto & Rose, *Physical Therapy*, 1992. 72:6, 438-448.

WEARABLE SENSOR SUITE FOR LONG-TERM REAL-WORLD TRACKING

Yisen Wang[1], Lauro V. Ojeda[2], and Peter G. Adamczyk[1]
[1]University of Wisconsin-Madison, [2]Navigation Solutions, LLC
email: *peter.adamczyk@wisc.edu

Introduction

Biomechanics analysis may need abundant data from real world tracking, where more information can be extracted to enable scientific comparison of mobility interventions compared to pure lab testing. However, long-term tracking suffers from the trade-off of accuracy vs convenience as well as heading drift due to absence of GPS in indoor environments. As an attempt to resolve these problems, we are developing a sensor suite with a redundant high-accuracy IMU to mitigate long-term drift, three other low-cost IMUs and two Bluetooth devices for collecting motion and force data, as an extension to our previous method [1] with only a foot-mounted IMU. Here we describe the use of transfer alignment techniques to align and reconstruct knee and shank IMU motions which by themselves alone are impossible to build accurately.

Methods

Hardware: Our system incorporates 7 sensors with a total weight around 350 grams and similar diameter to the natural leg when attached on a prosthetic pylon. Various sources of data are collected to facilitate reliable reconstruction during long periods using sensor fusion techniques:

1) Five IMUs form the basis of sensor system. A low-cost cabled IMU is mounted on the instrumented foot and a Bluetooth Low Energy IMU on the other foot. The cabled IMU functions as the input of an Error State Kalman Filter for Pedestrian Dead Reckoning algorithm. Two more low-cost IMUs are attached to the shank and above the knee to reconstruct lower leg and upper leg motion. A high-accuracy low-drift IMU is installed together with the shank IMU, to maintain accurate heading during long-duration indoor motion.

2) Europa smart pyramid is an instrumented prosthetic pylon that monitors flexion and abduction bending moments and axial force via Bluetooth connection.

3) Environment sensors provide humidity, temperature and barometer data to distinguish indoor vs outdoor data and changes in height.

4) An RTK-GPS module provides centimeter-accuracy position measurements during outdoor movement to locate the system in the global frame.

Software: The sensor system runs on a Raspberry Pi Zero W and utilizes Robot Operating System to manage and monitor all sensors. A central node coordinates the data logging, error detection, timestamp synchronization and power management for sensor nodes.

Movement Reconstruction: The trajectory of each foot-mounted IMU is reconstructed using an Error State Kalman Filter [2], which leverages the Zero Velocity Update (ZUPT) [3] assumption at every foot fall to reduce error in absence of GPS data.

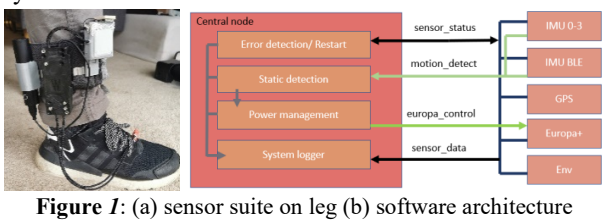

Figure *1*: (a) sensor suite on leg (b) software architecture

The more challenging part is the reconstruction for the shank and thigh IMUs, where the ZUPT is not valid, making it difficult to bound the velocity and heading error. However, we have the knowledge that these IMUs move with foot-mounted IMU, with error around 0.1m in horizontal plane due to leg motion. Thus, we use position results from the foot-mounted IMU as observations for the shank and thigh Kalman filters at every footfall to perform transfer alignment [4]. This process gradually aligns the shank and thigh IMUs with a global coordinate frame.

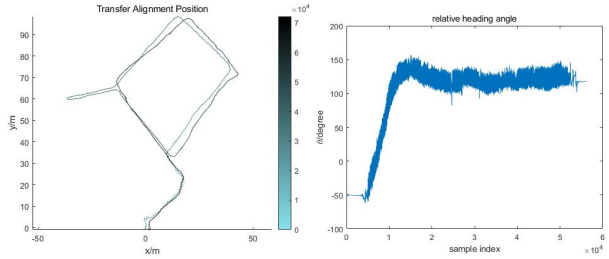

Figure *2*: (a) transfer alignment results (b) relative heading angle

Results and Discussion

Fig. 2 demonstrates convergence and bounded error of the shank's final heading with respect to foot-mounted IMU and position during testing on an intact subject. The wiggling part at the beginning is an effect of orientation error before the transfer alignment converges. Once the initialization stage finishes, the result is smooth and has bounded relative heading error.

It is worth mentioning that the sensor system housing is attached on pants, which is not as strong as attachment to a rigid object like a prosthesis or ankle-foot orthosis. At every footfall, the shank IMU endures significant shaking due to impact with the ground. However, even under this condition, the results still demonstrate a reliable reconstruction of heading and position.

In the special case of a prosthetic foot, there is a further rigid body relationship between the foot and shank IMUs during swing phase because the ankle joint angle is fixed. By applying orientation correction as an addition to position correction, the speed and accuracy of transfer alignment will be improved.

Reconstruction in indoor environments suffers most from heading error because of inevitable gyro drift. In both AFO and prosthesis cases, the previously aligned high-accuracy shank IMU can function as a low-drift reference during indoor periods to correct heading error in the foot-mounted IMU.

The preliminary results shown here demonstrate the effectiveness of transfer alignment in bringing multiple inertial sensors into long-term heading alignment for multi-body reconstruction. These techniques will be applied to compare different types of prosthetic feet and orthoses in a controlled test.

Acknowledgments

Funding provided by DOD W81XWH-19-2-0024

References

[1] Wang et al 2019 *Sensors*. [2] Solà 2017 *arXiv*.
[3] Ojeda et al 2007 *J Nav*. [4] Ojeda et al 2011 *Proc SPIE*

DO COGNITIVE DUAL-TASKS HAVE LIMB-DEPENDENT EFFECTS ON LANDING MECHANICS?

Jake J. Davis, Patrick D. Fischer, and Scott M. Monfort
Department of Mechanical and Industrial Engineering, Montana State University, Bozeman, MT, USA
Email: scott.monfort@montana.edu

Introduction

Landing mechanics during jump landing tasks have been used to gain insight into anterior cruciate ligament (ACL) injury mechanics [1, 2]. Performing a simultaneous secondary cognitive task (i.e. a dual-task) or reacting to a directional cue during these tasks can adversely affect lower extremity biomechanics [3,4]. However, the dependence of cognitive-motor effects to limb dominance is largely unknown, which limits the generalizability of this research and the ability to compare results between studies.

The purpose of this study was to determine the extent that cognitive tasks elicit different responses between dominant versus non-dominant limbs. We hypothesized that select landing mechanics variables would change similarly for dominant and non-dominant limbs when adding simultaneous cognitive tasks during the jump landing.

Methods

Female recreational soccer and basketball players (n = 40, 1.69 ± 0.07 m, 20.2 ± 2.57 yrs, 64.12 ± 8.29 kg) participated in the study. Participants jumped off a 30 cm high box onto two force plates and then jumped a second time in one of three directions (straight up, left, right), although, only the straight up direction is analyzed here [3]. These jump landings were performed under five randomly-ordered conditions: 1) **baseline (B)**: anticipated jump direction without any cognitive distraction; 2) **unanticipated (UA)**: participants were shown a direction for the second jump 250 ms before initial contact; 3) **anticipated recall (R)**: participants were told the direction of the second jump prior to the trial starting and, while standing on the box, were shown a circle of six letters for one second and after the trial they were asked to recall the position of one of the letters; 4) **anticipated identify/recall (IR)**: the same as R, but, instead of being asked for the position of a letter after the trial, one of the six letters appeared on a screen 250 ms before initial contact, then the participant was asked to recall the position of the presented letter after the trial; 5) **unanticipated IR (UIR)**: a combination of **IR** and **UA** where the same special memory task as **IR** is performed, but the jump direction is unknown and both the direction and letter are shown 250 ms before initial contact.

Motion capture data were collected, and an inverse kinematics model was used to calculate joint angles and moments. The outcome variables were peak external knee abduction moment (pKAbM), peak knee abduction angle (pKAbA), and peak knee flexion angle (pKFA). All were analyzed within the first 50 ms of initial contact [1,2].

Mixed effects models with 'Participant' as a random factor and 'Condition', 'Limb' and 'Condition*Limb' as fixed factors were used to test for an interaction between jump conditions and limb. A significance level of $\alpha = 0.05$ was chosen.

Results and Discussion

The Condition*Limb interaction term did not reach statistical significance for any of the dependent variables [pKAbM ($p = 0.673$), pKAbA ($p = 0.982$), or pKFA ($p = 0.426$)]. However, limb dominance had a significant effect on pKAbM ($p = 0.016$) and pKAbA ($p < 0.001$) but not on pKFA ($p = 0.957$), which partially corroborate previous findings on limb dominance [5]. That is, while participants showed significantly different pKAbM and pKAbA between dominant and non-dominant limbs, differences did not appreciably change across the dual-task conditions (**Figure 1**).

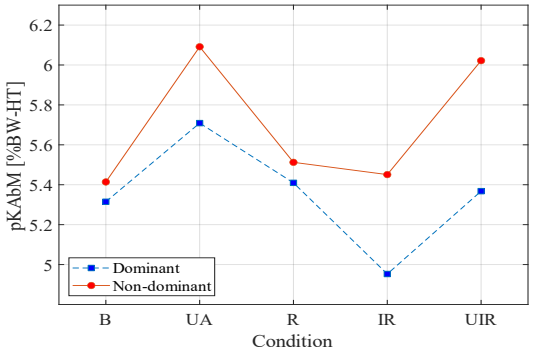

Figure 1: Interaction plot for mean pKAbM comparing the Condition*Limb interaction across the testing conditions.

These data support our hypothesis in that the effect of unanticipated, working memory, and visual constraint conditions during bilateral jump landings appeared to elicit similar responses in landing mechanics for both limbs. Thus, it appears that differences in how limb dominance is defined, or which limb is analysed, may not be a substantial confounding factor for these effects. Our study extends previous similar findings for an unanticipated single-limb landing [6]. Alternatively, our results also indicate that while there are differences in pKAbM and pKAbA between dominant and non-dominant limbs, these differences are not exacerbated by the addition of unanticipated, working memory, or visual constraint challenges.

Significance

The results of this study suggest that, while there is an appreciable difference in knee mechanics between dominant and non-dominant limbs when comparing raw values (e.g., pKAbM), dual-task effects may be more generalizable across limbs. Therefore, dual-task effects do not appear to be substantially confounded or sensitive to the choice of which limb is analysed during a bilateral jump-land-jump task within a population of healthy female athletes.

Acknowledgements

This material is based upon work supported by the NSF Graduate Research Fellowship under Grant No. W7834.

Reference

[1] Krosshaug *et al* (2007), *Am J Sports Med*. **35(3)** 359-67
[2] Koga H *et al* (2010), *Am J Sports Med.* **38(11)** 2218-25
[3] Herman DC *et al* (2016) *Am. J. Sports Med.* **44(9)** 2347-53
[4] Dai B *et al* (2018) *Sports Biomech.* **17(2)** 192-205
[5] Brophy R *et al* (2010) *Br. J. Sports Med.* **44(10)** 694-97
[6] Brown T *et al* (2009) *BJSM* **43**: 1049-10

EFFECTS OF PROPULSIVE FORCE BIOFEEDBACK ON OVERGROUND WALKING IN THOSE WITH PARKINSON'S DISEASE

Sidney T. Baudendistel[1], M. Pappas[1], A. Schmitt[2], J.R. Franz[3] and C. Hass[1]
[1]Department of Applied Physiology and Kinesiology, University of Florida, Gainesville, FL
[2] University of Arkansas, Fayetteville, AR
[3]Joint Dept. of Biomedical Engineering, UNC Chapel Hill and NC State University, Chapel Hill, NC
Email: sbaudendistel@ufl.edu

Introduction

Mobility impairments, such as slow gait speed and reduced stride length, are a top treatment priority for persons with Parkinson's disease (PD). The use of cueing to improve gait is widely used in clinical settings through focusing attention on spatial or temporal deficits associated with PD [1]. Treadmill use has also shown positive outcomes as the belts acts as an external pacemaker, regulating individuals' gait [2]. Unfortunately, positive results often fade after the provided feedback is removed.

While real-time visual biofeedback of propulsive force in walking (a determinant of speed and stride length) has been used to improve gait performance in other populations [3], it has not yet been applied to individuals with PD. Targeting force output allows individuals to focus on the underlying cause of movement deficits, insufficient force production, instead of kinematic outcomes such as step length or time. **The purpose of this study is to determine if overground walking speed and stride length improve following an acute bout of biofeedback training.**

Methods

Ambulatory individuals with PD participated in either: *Feedback* (n=5) [3] or *Control* (n=5). While walking at a preferred walking speed, baseline peak propulsive force was recorded during the last 30 seconds of 5 minutes of treadmill walking. A force target was displayed as a line (140% of baseline), used to encourage *Feedback* participants to increase their propulsive force. Intermittent feedback was given with each trial lasting 3 minutes, repeated 3 times, resulting in 9 minutes of targeting increased push-off force. *Control* participants walked on the treadmill for an equal amount of time without instruction or feedback. Following the protocols, both groups completed a minimum of five minutes of seated rest. All participants were then read the script already presented to the *Feedback* group, instructing individuals to increase push-off force with every step while walking on the treadmill for 2 minutes. No feedback was provided to either groups. No specific strategy was mentioned or declared during the entire study, referring participants to "interpret the instructions as best as possible" if asked specific questions. Treadmill speed was unchanged from baseline for the duration of the experiment. Both groups also participated in overground walking at their comfortable pace before and after completing all treadmill walking.

We analyzed the potential impact of propulsive force biofeedback on both instructed treadmill and habitual overground walking. Change scores for all measures were calculated so that positive values represent an increase compared to baseline. Mann-Whitney U tests compared change scores for treadmill walking (i.e., peak propulsive force, stride length, and stride time) and overground walking (i.e., speed, stride length, and stride time) between *Feedback* and *Control* groups ($p<.05$).

Results and Discussion

There were no significant differences between groups (*Feedback* vs *Control*; Mean±STD) for age (67±9 vs 65±6 years; p=.673) or disease duration (9±7 vs 11±4 years; p=.295). For treadmill walking, we found no differences in propulsive force, stride length, or stride time between groups when analyzing the change between baseline and instructed walking ($p \geq .465$). When combining groups, only propulsive force was different between time points (p=.007), showing both groups increased force production during instructed walking (17.2% vs 21.0%).

For overground walking, those who participated in the feedback protocol showed larger changes in speed (p=.047) and stride length (p=.047) compared to the control group (Fig 1). There were no between-group differences for change in stride time (p=.117).

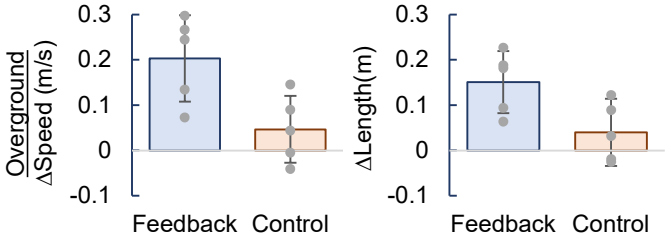

Figure 1: Overground walking speed and stride length before and after protocols, calculated as Post – Pre = Δ. Bar graphs represent group averages and standard deviation, while points represent individual data.

While both groups increased propulsive force with instruction (3% average), the protocol group appeared to better capitalize on those larger forces and exhibited larger increases in speed and stride length during "normal, comfortable" overground walking. Specifically, the feedback group increased speed 0.20m/s, which is above the moderate clinically meaningful difference [4], accompanied by longer stride lengths (0.15m). Changes in overground walking speed in the control group (0.05m/s) failed to exceed even the small clinically, meaningful level.

Significance

All participants were able to increase propulsive force using biofeedback and/or instruction. However, in this preliminary analysis, the biofeedback protocol resulted in consistently greater increases in overground speed and stride length across participants compared to the control group. Acute real-time visual biofeedback of propulsive force may be more efficacious for improving overground gait than treadmill walking alone.

Acknowledgments

This work was supported in part by: NIH T32-NS082128, Parkinson's Foundation (PF-VSA-SFW-1908), and the ASB Graduate Student Grant-in-Aid.

References

[1] Muthukrishnan et al., 2019. *Sensors*, 19(24), 5468.
[2] Mehrholz et al., 2015. *Cochrane Database Syst. Rev*, (8).
[3] Franz et al., 2014. *Clin Biomech.* 29(1), 68-74.
[4] Hass et al., 2014. *J Neurol Phys Ther.* 38(4), 233-238.

ENTRY ANGLE FOR JUMP-LAND-JUMP MOVEMENTS IMPACTS ACL INJURY RISK FACTORS

Shekoofe Saadat[1*], Mitchell L. Stephenson[2], Jason C, Gillette[1]
[1]Department of Kinesiology, Iowa State University
[b] Department of Health and Human Performance, University of Montana Western
Email: *shsaadat@iastate.edu

Introduction

Non-contact anterior cruciate ligament (ACL) injuries are common among young athletes. ACL injuries often happen during running and cutting movements that involve sudden change of direction and rapid deceleration when the knee is almost or fully extended and there is a dynamic valgus collapse [1,2]. Previous studies have concluded that during running and cutting movements, females showed smaller knee flexion angles [3] and greater knee external valgus moments when cutting to a sharper angle [3,4].

The purpose of the current study was to investigate the effects of jumping from different directions on landing mechanics and ACL injury risk factors in jump-land-jump movements. We hypothesized that as the angle of the jump was increased from the anterior, ACL injury risk factors would increase in the form of smaller knee flexion angles, larger knee valgus angles, larger lateral trunk lean, and larger peak external valgus moments.

Methods

Twenty-one uninjured, physically active females participated in this study. Facing anteriorly, participants jumped off a 28cm block, and the distance of this jump was 50% of their body height. Upon landing with each foot on a separate force platform, participants immediately performed a maximal vertical jump. The direction of the first jump was manipulated between seven different entry angles, from 90R (jump from 90° to the right) to 90L (jump from 90° to the left) in 30° increments. Participants performed 3 trials for each direction for a total of 21 jump-land-jump trials.

Reflective markers were placed on the participant to define the right foot, right calf, right thigh, and pelvis segments. Marker position data were recorded using 8 Vicon MX cameras at 160 Hz. In addition, ground reaction forces were recorded at 1600 Hz using two force platforms. All dependent variables were analyzed at the initial instant of landing from the first jump or during the first 100ms of landing [5].

Results and Discussion

When participants jumped from the 90R entry angle, they had significantly smaller initial knee flexion angles compared to the 90L entry angle. No significant differences were shown when comparing other entry angles. In addition, peak knee flexion angle was shown to be significantly smaller for right entry angles compared to 0 (forward) and left entry angles, with the 90R entry angle having the smallest peak knee flexion angle.

Initial knee valgus angles were significantly larger for right entry angles compared to forward and left entry angles, potentially putting the individual at higher risk for ACL injury (Figure 1) [1,2]. However, no significant differences in peak knee valgus angles were found as a function of entry angle.

Initial lateral trunk lean was significantly larger for the 90R entry angle as compared to other entry angles except the 0 and 90L entry angles (Figure 1). Peak lateral trunk lean from the 90R entry angle was significantly larger than all other entry

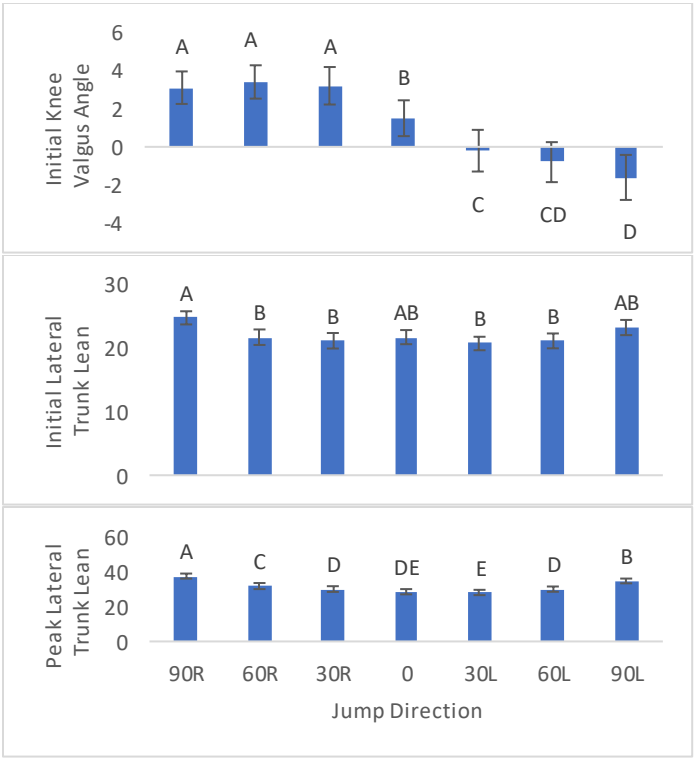

Figure 1: Initial knee valgus angle, initial lateral trunk lean, and peak lateral trunk lean (in degrees, mean ± standard error) as a function of entry angle. Significance ($p<0.05$) is shown as A>B>C>D>E.

angles. The 90L entry angle had significantly larger lateral trunk lean than all other entry angles except the 90R entry angle, indicating that jumping from a sharper angle results in greater peak trunk lateral lean. In addition, right entry angles resulted in significantly larger peak trunk lean compared to the equivalent left entry angle.

Peak external knee valgus moments were significantly larger for the right entry angles compared to the forward and left entry angles. Greater trunk lean and a resulting shift in the center of mass with right entry angles may be related to larger external knee valgus moments, potentially putting the ACL at higher injury risk [3,4].

Significance

Jumping from right entry angles may put the right knee at higher risk for ACL injury. We suggest athletes use caution when jumping lateral to a previously injured knee or jumps at sharp entry angles for individuals considered high risk for ACL injury.

References

[1] Hewett et al. (2006). *Am J Sports Med*, 34(2), 299-311.
[2] Hewett et al. (2009). *Br J Sports Med*, 43(6), 417-422.
[3] Schreurs et al. (2017). *J Biomech*, 63, 144-150.
[4] Sigward et al. (2015). *Clin J Sport Med*, 25(6), 529-534.
[5] Dai et al. (2015). *J Sport Health Sci*, 4(4), 333-340.

LESS LETHAL IMPACT MUNITIONS TO THE NASAL REGION – RISK OF INJURY ASSESSMENT USING THE FOCUS HEADFORM

Amanda Esquivel[1], Robert Macdonald[2], Don Sherman[2], and Cynthia Bir[2]
[1]University of Michigan – Dearborn, Dearborn MI
[2]Wayne State University, Detroit MI
email: aoe@umich.edu

Introduction

Serious injuries have been documented due to the use of less lethal impact munitions (LLIM). One recent study reported 45 injuries in two Minnesota health systems during a three-week period in 2020.[1] These included serious injuries to the head, neck, and face. The purpose of this study was to examine the risk of injury to the nasal from LLIM. Our hypothesis was that risk of injury to the nasal bone was high when these shots impacted this region.

Methods

Four different 37 mm bean bag rounds were fired 3-4 times from a launcher by a certified firearms instructor at a Facial and Ocular CountermeasUre for Safety Headform (FOCUS). (Table 1) This headform features eight discrete facial bones, two synthetic eye modules and 10 load cells. It has been previously validated using cadaveric specimens by examining force-deflection corridors for both the headform and specimens[2].

The headform was rigidly attached to a Hybrid III neck and secured to a linear trolley. Tri-axial nasal and uni-axial eye load cell data were collected at 20,000 Hz. The load cell data channels were filtered as recommended.[2] Risk of injury (ROI) was calculated based on previously developed injury risk curves, where F= maximum resultant force, λ = scale and γ = shape:

$$ROI = 1 - e^{-(\lambda * F)^{\gamma}} \qquad \text{Equation 1}$$

Table 1. Less lethal ammunition specifications

Round	Mass (g)	Velocity (fps)	Energy (J)
ALS 3702	100	216	218
ALS 3704	150	180	227
CTS 3580	60	300	251
DT 6225	75	220	169

Results and Discussion

The impact location of each shot is shown in Figure 1. Impacts were considered valid if they were confirmed to have impacted the nasal region via high speed camera and if the nasal load cell accounted for more than 60% of the impact load.

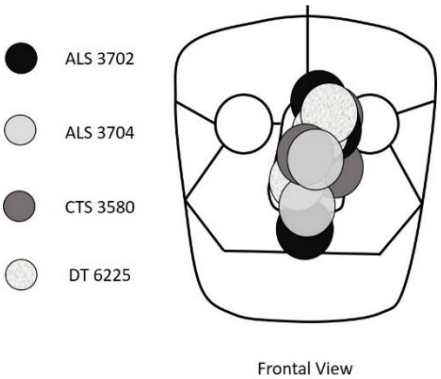

Figure 1. Impact locations of each trial

The resultant load to the nasal region ranged from 1335.2-4637.8 N. (Table 2) However, even loads to the nasal region in the 'lower' end of the spectrum resulted in a 92% risk of injury, specifically, nasal fracture. During validation of the FOCUS headform most nasal fractures due to impacts in the anterior/posterior direction were depressed and comminuted fractures.[2]

Even though the eye was not a region of interest for the current study, there was loading seen in the eye load cell for a number of cases. However, in the cases where any impact load occurred, the risk of injury to the eye, specifically, a globe rupture was 100%. This is consistent with a case series that examined eye injury due to less lethal projectiles and found that globe injury (closed and open) was the predominant eye injury seen.[3]

Table 2. Resultant force and risk of injury

Round	Velocity (fps)	Resultant Force Nasal (N)	Resultant Force Eye (N)	Risk of Injury (ROI) - Nasal	Risk of Injury (ROI) - Eye
ALS3702_01	192.7	2765.0	-	100.0%	-
ALS3702_02	196.2	3488.0	531.8	100.0%	100%
ALS3702_03	200.6	3151.9	756.9	100.0%	100%
ALS3702_04	206.5	1335.2	1125.0	91.7%	100%
ALS3704_01	145.4	3411.9	-	100.0%	-
ALS3704_02	168.4	2149.1	1273.8	99.6%	100%
ALS3704_03	150.9	4265.5	-	100.0%	-
CTS3580_01	326.9	3917.8	274.0	100.0%	100%
CTS3580_02	231.1	3009.2	362.4	100.0%	100%
CTS3580_03	223.9	2076.1	693.1	99.4%	100%
DT6225_01	199.0	2731.2	918.3	100.0%	100%
DT6225_02	201.3	4637.8	-	100.0%	-
DT6225_03	177.7	4057.3	-	100.0%	-

Significance

Less lethal weapons are not intended to be deployed to the facial region. However, numerous injuries due occur to the face and head. When a less lethal weapon impacts the nasal region, there is a very high chance this will result in a nasal fracture. If the impact is also near the eye region, this could result in a severe injury to the eye as well. This is supported clinically, in case series reports.

Acknowledgments

This material is based upon work supported by the National Science Foundation under grant no 1919416.

References

1. Kaske EA et al. Injuries from Less-Lethal Weapons during the George Floyd Protests in Minneapolis. N Engl J Med 2021
2. Weisenbach C et al. Summary of Available Craniomaxiollofacial Injury Criteria for Use with the FOCUS Headform. Army Technical Report 2020.
3. Rodriguez A et al. Ocular trauma by kinetic impact projectiles during civil unrest in Chile. Eye 2020.

REAL-TIME VISUAL BIOFEEDBACK TO INCREASE PROPULSIVE FORCE IN THOSE WITH PARKINSON'S DISEASE

Sidney T. Baudendistel[1], J.R. Franz[2] and C.J Hass[1]
[1]Department of Applied Physiology and Kinesiology, University of Florida, Gainesville, FL
[2]Joint Dept. of Biomedical Engineering, UNC Chapel Hill and NC State University, Chapel Hill, NC
Email: sbaudendistel@ufl.edu

Introduction

For the greater than 10 million people with Parkinson's disease (PD), declines in walking ability are a primary determinant of reduced quality of life. Slower gait velocity resulting from reduced propulsive force and shorter stride lengths is a cardinal feature of the disease. Currently, no pharmacological, surgical, or behavioural interventions restore gait performance to the levels of healthy peers. Strength training has received considerable attention as it increases strength but provides only limited improvements in habitual gait speed and length [1]; suggesting the inability to effectively utilize these gains to increase push-off force during walking.

While auditory cueing of stride frequency increases propulsive force in healthy older adults, real-time visual biofeedback of peak anterior-posterior ground reaction force (GRF) has been shown to encourage larger improvements in propulsive force than cueing alone [2]. Considering improvements in stride length with the use of visual and auditory cueing in individuals with PD [3], we hypothesized that real-time biofeedback that specifically targets propulsive force will effectively increase push-off force during walking with implications for improving our scientific understanding of mechanisms underlying gait impairment in those with PD. **The purpose of this study is to determine if individuals with PD can increase propulsive force using real-time biofeedback.**

Methods

Nine ambulatory individuals with PD (mean ± SD, age: 65±8 years, disease duration: 9±5 years) have thus far participated in a protocol based on Franz et al., 2014 [2]. First, participants selected a comfortable treadmill speed, at which they walked for all experimental trials. Five minutes of treadmill walking allowed for acclimatization and warm-up before explaining the biofeedback task. Baseline peak propulsive force was collected during the last 30 seconds of the 5-minute period via Matlab Plug-in for Qualisys. A propulsive force target was displayed as a bold line transecting the screen at 140% of each participant's individualized baseline with instantaneous force values averaged every two steps projected as a blue circle (Fig 1.). Participants were instructed to alter their propulsive force using a prewritten and standardized verbal script.

Fig 1: A bolded, red line transects the white plot at 40% above the baseline value achieved, allowing for a space of 20% between the top of the plot and the target line. The blue circle is the 2 step rolling average. The dashed line is not visible to participants but represents the individual's baseline value and is centered in the window.

Various target percentages were piloted to ensure 140% of baseline was feasible. Visual biofeedback was provided for 2 minutes and repeated 3 times, with breaks between as needed. Related-Samples Wilcoxon Rank Tests compared propulsive force (stride-averaged peak anterior GRF) and length of the last 20 strides of Baseline and the feedback trial which produced the largest average push-off force (significance defined as $p < 0.05$).

Results and Discussion

Participants successfully responded to real-time biofeedback and increased their propulsive force by an average of 4.8% body weight (BW) (Baseline: 16.3 %BW; Biofeedback: 21.1 %BW, $p = .011$; Fig. 1), representing 130 ± 28% of baseline values. Although not significantly different ($p>.515$), stride length tended to increase when participants walked with larger propulsive force using biofeedback (*i.e.*, 1.03m vs 1.07m).

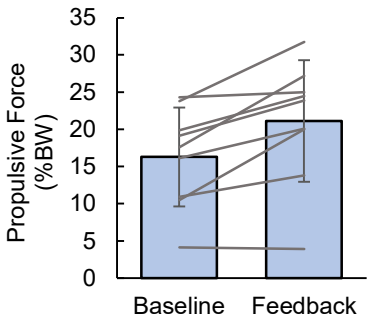

Fig 2: Peak Propulsive force averaged over the last 20 strides of each trial. Columns represent the average (SD) among the Baseline and the best biofeedback performance trial. Lines represent individual participant's average peak propulsive force.

In general, individuals with PD can use visual biofeedback to increase their propulsive force even when treadmill speed is unchanged. We interpret this finding to suggest that individuals with PD have an accessible propulsive force reserve. Interestingly, not all participants were able to increase propulsive force as effectively as others, evidenced by the variability between subjects in Figure 2. Investigating potential secondary determinants (e.g., balance, disease severity, strength, etc.) may explain the heterogeneity in our sample.

Significance

Further exploration into how to encourage individuals with PD to better use propulsive force may aid in future therapeutic interventions. Additionally, the use of real-time biofeedback as an experimental tool may help better understand underlying mechanisms related to gait dysfunction in those with PD.

Acknowledgments

This work was supported in part by: NIH T32-NS082128, Parkinson's Foundation (PF-VSA-SFW-1908) and the ASB Graduate Student Grant-in-Aid.

References

[1]Chung et al., 2016. *Clin Rehabil*, 30(1), 11-23.
[2] Franz et al., 2014. *Clin Biomech.* 29(1), 68-74.
[3] Muthukrishnan et al., 2019. *Sensors*, 19(24), 5468.

PREDICTIVE SIMULATION OF SIT-TO-STAND MOTION CONSIDERING THE EFFECT OF SPINE STIFFNESS

Ali A. MohammadiNasrabadi[1], J. McPhee[2]
[1]PhD candidate, Department of Systems Design Engineering, University of Waterloo, Ontario, Canada
[2]Professor, Department of Systems Design Engineering, University of Waterloo, Ontario, Canada
email: aliasgharmn@uwaterloo.ca

Introduction

Spine geometry, kinematics, and stiffness of the spinopelvic complex have significant effects on certain human movements [1]. For best results, these effects should be considered in planning surgeries such as total hip arthroplasty (THA). Experimental investigations have shown the importance of these parameters, especially in candidates for THA who have had previous spine fusion surgery [2], but the exact mechanism of how these parameters influence human movements is still unknown [3]. This research uses experiments, models, and predictive dynamic simulations of sit-to-stand movements to identify the effects of the spine on spinopelvic motion and lower-limb dynamics.

Methods

Different modelling approaches for the spine have been reviewed, and a gap between conceptual studies [2, 3] and modelling research [4, 5] is identified. To investigate the importance of including a spine model in predictive simulations of human movement, an experimental study has been carried out using a motion capture system. Reflective markers have been placed on the body segments of participants to extract joint angles. The results showed differences in spinopelvic motion resulting from different spinal stiffness and spinopelvic parameters. A multibody 6 degrees of freedom (DOF) sagittal human model has been developed that considers 4 DOF for the spine (S1-L5, L3-L2, L1-T12, T6-T5) and 2 DOF for the lower limbs (hip and knee joint angles). Dynamic optimization has been used to predict sit-to-stand motion using symbolic dynamic equations to compute gradients that speed up numerical convergence. For this purpose, trajectory optimization with 2 cost functions has been used. The first one uses joint torques and the second one is a modified version by adding joint jerks to smooth the trajectories.

$$J_1 = \sum_{i=1}^{n} \int_{t_0}^{t_f} u_i^2 , \qquad J_2 = \sum_{i=1}^{n} \int_{t_0}^{t_f} u_i^2 + \sum_{i=1}^{n} \int_{t_0}^{t_f} w_i \dddot{x}_i^2$$

where u_i are joint torques, $\dddot{x}$ are joint jerks, and w_i are weights.

The optimization results with both cost-functions were compared to the experiments and the one with lower error (J_2) has been used for further analysis in this research. To evaluate the effects of spine stiffness on the pelvic tilt, different stiffness factors are considered in the model with two scenarios: 1. Increasing the overall stiffness at L5 level of the spine 2. Fusion at L5 level with a restriction of the range of motion at this joint.

Results and Discussion

As shown in **Figure 1**, increasing the stiffness factor in the L5 joint causes an increase in the ROM of the hip joint with an approximately similar knee joint angle trajectory. Since the thigh has the same motion (same knee joint angle trajectory), the change in the hip joint ROM is because of a change in the pelvic tilt, which means that we have the same motion in the thigh with a more stationary pelvis. For the fusion scenario, the difference between the model with stiffer spine and the experimental results trajectory is about 15 degrees at the end point of motion. In the other scenario, there is a 30 degree reduction in the pelvic tilt at the final state. The stiffer spine not only caused a restriction to the pelvis tilt at the end of the motion (more stationary pelvis), but also caused more forward pelvic tilting in the middle of the motion. This increase in hip joint ROM will increase the risk of impingement or dislocation after THA surgery.

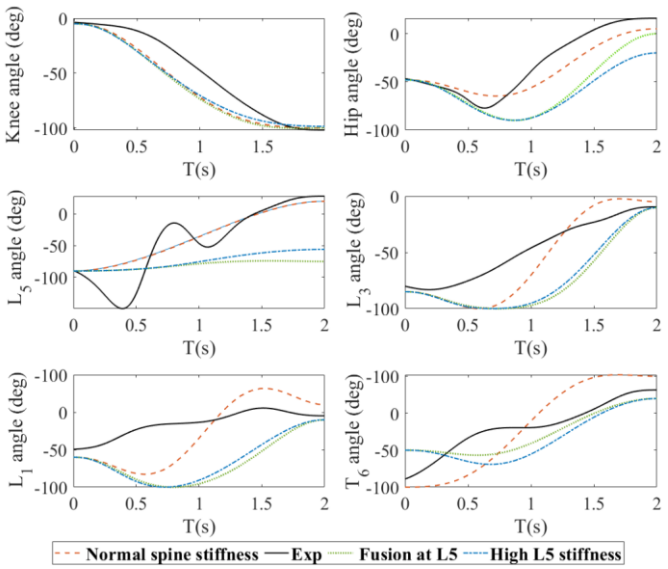

Figure 2: Comparison between optimization results of hip (top right), knee (top left), and spine joint angles with experimental results (black). The model is optimized for different spinal stiffnesses: normal (red), high stiffness at L5 (blue), and high stiffness with fusion at L5 (green).

Significance

In most dynamic models of human movements, the spine and pelvis are considered as one lumped link. Accordingly, the effects of the spine flexibility and pelvic tilt on lower limb dynamics are not implemented in such models. Different spine geometries and stiffnesses are factors that influence human movements. These effects are evaluated in this research and should be considered in future studies on dynamic analysis of human movements, e.g. surgery planning for THA to find the optimal position and orientation of the artificial cup and implant.

Acknowledgments

This research was funded by Intellijoint Surgical, the Natural Sciences and Engineering Research Council of Canada, and the Ontario Centres of Excellence.

References

[1] A.A. Sultan et al., The Journal of Arthroplasty, vol. 33, no. 5, pp. 1606-1616, 2018.
[2] A.L. Malkani et al., The Journal of Arthroplasty, vol. 33, no. 4, pp. 1189-1193, 2018.
[3] S.H. Lee, C.W. Lim, K.Y. Choi, Hip & pelvis, vol. 31, no. 1, pp. 4-10, 2019.
[4] A. Jalalian, I. Gibson, and E. H. Tay, Spine Deformity, vol. 1, no. 6, pp. 401-411, 2013.
[5] I. Shojaei, B. D. Hendershot, J. C. Acasio, C. L. Dearth, and M. Ballard, Clinical Biomechanics, vol. 63, pp. 95-103, 2019.

MODEL-BASED OPTIMIZATION OF ACETABULAR CUP ORIENTATION FOR TOTAL HIP REPLACEMENT

Behzad Danaei[1] and John McPhee [1]
[1]Systems Design Engineering, University of Waterloo, 200 University Ave. W, Waterloo, ON N2L 3G1
email: *bdanaei@uwaterloo.ca

Introduction

Total Hip Replacement (THR) is a surgical procedure in which the head and neck of a damaged hip joint are removed and replaced with artificial materials. Hip dislocation is the biggest problem that some patients experience after THR [1]. Two of the major causes of hip dislocation are (1) implant impingement where the edge of the femoral component collides with the edge of the cup or pelvis, and (2) edge loading when the hip joint contact force falls out of the cup surface. Proper acetabular cup orientation is reported as the most significant factor to reduce the risk of dislocation [1]. The objective of this research is to develop a model-based algorithm to determine the optimal orientation of the implant cup using motion capture data obtained from the patient while performing different daily activities.

Methods

Figure 1 depicts the main components of the method used in this research to determine the optimal cup orientation. By importing experimental motion capture data from different movements to the kinematic and dynamic model, the relative motion of the femur with respect to the pelvis along with the reaction force inside the hip joint are calculated. Then, by using the method of steepest descent optimization algorithm, the optimal orientation of the cup is obtained to maximize the minimum angular distance from impingement and edge loading for the combination of the provided motions.

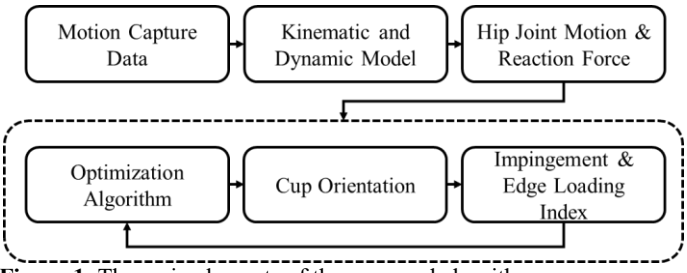

Figure 1: The main elements of the proposed algorithm.

Results and Discussion

Motion capture data for three different daily activities performed by a single subject are used in this study: (1) Running (2) Bending at hip from standing (3) Sit-to-Stand. The calculated optimal cup orientation for different combinations of the activities is shown in Table 1. As is evident, by combining more activities the optimal value of the orientation of the cup falls within the Lewinnek safe zone of anteversion of 40° ± 10° and 15° ± 10° [2] commonly used in THR surgeries. Other activities such as stepping up stairs and hip extension were also added, but the optimal orientation of the cup did not significantly change compared to the values obtained from using just the first three original activities. To investigate the impact of implant impingement and edge loading on the results, the optimal cup orientation was calculated for each individual criterion without the presence of the other one. The results are shown in Table 2. As can be observed, the optimal orientation of the cup for minimizing the risk of impingement could increase the risk of dislocation due to edge loading, and vice versa.

Table 2: The optimal orientation of the acetabular cup for different combinations of activities considering both impingement and edge loading criteria.

Movement	Optimal orientation of the cup	
	Anteversion	Inclination
Activity 1	18.8°	16°
Activity 1 & 2	21.7°	24.6°
Activity 1 & 2 & 3	16°	47.5°

Table 2: The optimal orientation of the acetabular cup using different criteria for the combination of all three activities.

Criterion	Optimal orientation of the cup		Minimum angular distance from the impingement	Minimum angular distance from edge loading
	Ant.	Inc.		
Impingement	27.5°	64.3°	23.3°	-19.8°
Edge loading	10.7°	8.7°	-29.1°	24.1°
Impingement & edge loading	16°	47.5°	15.7°	15.7°

Significance

The literature lacks effective mechanistic models to calculate the optimal acetabular cup orientation to minimize hip dislocation during dynamic movements of daily activities. In this research, a novel subject-specific model-based method was proposed for calculating the optimal orientation of the acetabular cup using motion capture data obtained from the patient. This method can be used in preoperative planning for THR surgery. The proposed method can improve current technologies and lead to new ones that can ultimately reduce the risk of dislocation following THR.

Acknowledgments

This research was funded by Intellijoint Surgical, the Natural Sciences and Engineering Research Council of Canada, and the Ontario Centres of Excellence.

References

[1] Biedermann, 2005. DOI: 10.1302/0301-620X.87B6.14745
[2] Lewinnek, 1978. PMID: 641088

EFFECT OF STRESS ON NECK MUSCLE ACTIVITY AND POSTURAL SWAY

Keaton Zimbelman[1], Anita N. Vasavada[1,2*]
[1]Department of Integrative Physiology and Neuroscience, and
[2]Voiland School of Chemical Engineering and Bioengineering, Washington State University, Pullman, WA, USA
email: *vasavada@wsu.edu

Introduction

Risk factors for neck pain include both biomechanical (*e.g.*, posture and muscle activity) and psychological factors (*e.g.*, depression and stress). Stress is associated with increases in trapezius muscle activity [1] and decrease in standing postural sway [2]. Characteristics of postural sway such as low amplitude and high frequency, may be related to increased joint stiffness and/or muscle activity [3]. This indicates that psychological factors can affect mechanical loads, and potentially musculoskeletal discomfort or pain, via changes in posture and/or muscle activity. This study examined how social-evaluative stress (SES) affects neck muscle activity and postural sway. We hypothesized that SES would cause (1) greater self-reported stress; (2) greater discomfort; (3) increase in neck muscle activation and (4) decrease in postural sway compared to a challenging cognitive task alone.

Methods

Ten young adults, five males, and five females (mean age 22±3.27 SD) with no history of severe neck pain or injury participated in this study. Subjects were unaware that the purpose of the study was to induce stress and were debriefed after the study. All subjects provided informed consent and the study was approved by the Washington State University IRB.

Two inertial measurement units (IMUs) were placed on the sternal notch and forehead, and 6 surface electrodes were placed bilaterally on the sternocleidomastoid, trapezius and semispinalis muscles (Trigno, Delsys, Natick, MA).

Social evaluative stress (SES) was imposed using the Montreal Imaging Stress Task (MIST) [4]. The MIST protocol consists of challenging mental arithmetic (MATH condition) and a condition of social evaluative stress (SES) added to the mental arithmetic. The SES condition involves time constraints and evaluative feedback to evoke a stress response in the participant. Performing this task has been found to increase participants' self-reported stress and cortisol levels [4].

Each participant first completed baseline measurements of postural sway and neck muscle activation with eyes closed for 15 seconds (REST). After a training session on the MIST task, the participant experienced either the control condition (MATH), or the experimental condition (SES), in a randomized order.

After each randomized condition, participants reported their levels of stress as well as discomfort in their neck, shoulders, arms, back, and legs using a Visual Analog Scale (VAS; 0 = no stress or discomfort and 10 = maximum stress or discomfort). Acceleromter data were high-pass filtered at 0.5 Hz and low-pass filtered at 60 Hz, and net acceleration magnitude and frequency were calculated. Root-mean-square (RMS) average muscle activity was calculated over a 50 ms moving window and normalized to maximum voluntary contraction. Stress and discomfort were compared after MATH and SES conditions with a significant p-value of 0.05. Muscle activity and postural sway were compared among REST, MATH and SES conditions with repeated-measures ANOVA and post-hoc t-tests using a Bonferroni correction (p- value of 0.05/3 = 0.0167).

Results and Discussion

Subjective stress and discomfort increased significantly between the MATH and SES conditions (p<0.05; Figure 1), confirming hypotheses 1 and 2.

Activity in the trapezius and semispinalis capitis muscles increased in both the MATH and SES conditions compared to REST, but there was no significant difference between MATH and SES conditions (Figure 1). The right trapezius muscle increased 63% from REST to MATH (p=0.04)and and 76% from REST to SES conditions (p=0.03), and the left semispinalis muscle increased 13% from REST to MATH (p=0.02) and 15 % from REST to SES (p=0.03). There was no significant change in the sternocleidomastoid. With the conservative Bonferroni criteria, the results did not support hypothesis 3.

Median head acceleration increased by 15% from REST to MATH and 30% from REST to SES (p=0.025). Head acceleration also increased by 14% in the SES condition compared to MATH (p=0.04). Median postural sway frequency was not different in MATH compared to SES (p>0.05). This result of greater head acceleration in SES vs. MATH is opposite to hypothesis 4. The differences between this and a previous study [2] may be due to seated vs. standing condition, and different methods of measuring postural sway (center of pressure measurements using sway referencing on a platform).

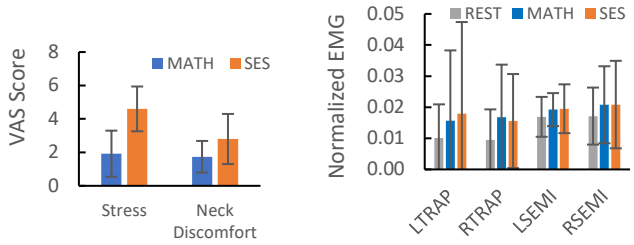

Figure 1: Left: Stress and neck discomfort after MATH and SES conditions. Right: Normalized muscle activity during REST, MATH and SES conditions.

Significance

We found that the MIST protocol induces stress and discomfort and that a challenging MATH task is an effective way to increase muscle activity and postural sway; however, added SES does not significantly change all of these biomechanical variables. MIST is a viable assay to evaluate the effects of cognitive demands and stress, as well as changes in response to interventions intended to improve workplace environment and responses to stress.

Acknowledgments

We thank Jordan Edwards for programming assistance.

References

[1] Shahidi *et al*., *J Electromyogr Kinesiol*, 2013. 23(5):1082-9.
[2] Doumas *et al*., *Exp Brain Res*, 2018. 236(1):305-314.
[3] Winter *et al., J Neurophysiol*, 1998. 80(3):1211-21.
[4] Dedovich *et al., J Psychiatry Neurosci*, 2005. 30(5):319-25.

Watch Your Step: Altered spatiotemporal strategies while negotiating unexpected obstacles under physical fatigue

Weise, M.A.[1], Cando, N.R.[1], Arzumanyan G.M.[1], Joo, J. [1], Stoehr, N.M.[1], Rogers, S.M.[1], Hinkel-Lipsker, J.W[1]
Move-Learn Lab, Department of Kinesiology[1], California State University, Northridge, CA USA
Email: michael.weise.60@my.csun.edu

Introduction

Slips, trips, and falls are all very common causes of non-fatal work-related injuries. For jobs that require large amounts of physical fatigue such as firefighting, it is crucial that they are able to react and respond to obstacles in unpredictable environments in order to avoid such injuries. Along with the unpredictability of the workplace environment in such professions, risk of slips, trips and falls can also be compounded by high levels of physical exertion leading to fatigue [1]. Such fatigue can alter both how a person perceives oncoming obstacles in their walking path, as well as their ability to mechanically negotiate an obstacle [1]. Moreover, it is unknown whether certain anthropometric and physiological factors influence one's ability to clear such obstacles [2]. For example, a person with a high level of physical fitness may be less affected by physical fatigue, and therefore not be at as great of a risk for slips, trips, and falls. Hence, this study sought to find the effects of physical fatigue on an individual's ability to quickly negotiate obstacles in unpredictable situations [3]. In addition, we investigated whether certain physiological and anthropometric variables would significantly predict spatiotemporal obstacle negotiation parameters. We hypothesized that individuals who are fatigued would exhibit more risky crossing behavior (e.g., lower foot clearance) compared to their rested state We also hypothesized that age, height, and estimated $VO2_{max}$ would significantly predict such parameters.

Methods

Twenty-one young (< 35 years old) participants with a moderate-to-high level of physical fitness were recruited for this study. Participants were instructed to walk through a darkened pathway over a randomly placed hurdle that upon approach (within 50 cm) would be illuminated by a motion-detecting light (Figure 1.), requiring a quick reaction to safely step over it. Following 5 such trials where the obstacle was moved to a new, unpredictable location, participants then engaged in a 32-minute fatiguing exercise protocol. They then completed 5 more obstacle negotiation trials. Three-dimensional marker coordinate data were collected at 60 Hz using an 8-camera motion capture system. These data were used to quantify multiple spatiotemporal obstacle negotiation parameters including leading and trailing heel and toe clearances, as well as horizontal foot placement on the step before the obstacle. A series of linear regression analyses were also performed to determine whether age, sex, height, and estimated $VO2_{max}$ could predict such parameters.

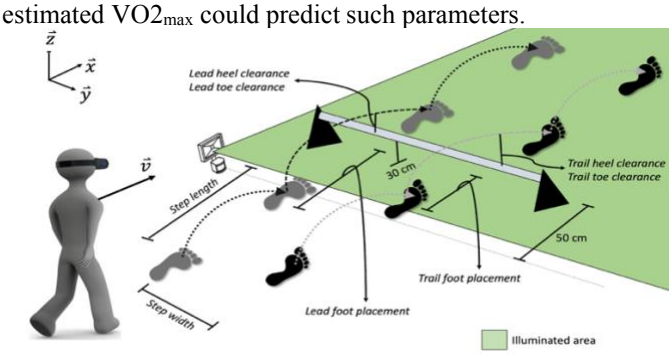

Figure 1. Representation of the obstacle and lab environment

Results and Discussion

Upon completion of fatigue-inducing exercise, participants exhibited a statistically significant decrease in trailing heel and leading toe clearance, along with a statistically-significant increase in leading heel clearance and gait velocity (Figure 2). This supports our hypothesis that participants would exhibit more risky obstacle negotiation behaviors when fatigued. Moreover, estimated $VO2_{max}$ was a significant predictor of leading and trailing horizontal foot placement, indicating that level of physical fitness has a direct relationship with certain obstacle negotiation parameters. In the context of physically-demanding occupations, these findings support the notion that physical fatigue plays a large role in one's ability to navigate difficult and changing terrain, and that ability may be less hampered if a person has a superior level of cardiovascular fitness.

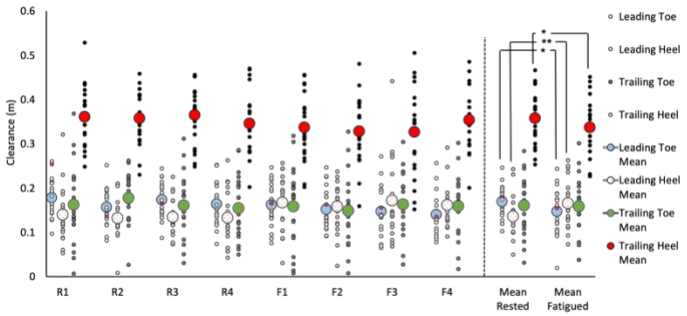

Figure 2. Statistical representation of leading and trailing foot values (heel and toe). * = $p < 0.05$, ** = $p < 0.001$

Significance

This study's results can provide a more comprehensive understanding of how physical fatigue can influence one's ability to negotiate obstacles in dynamic, unpredictable environments. Such understanding can guide future work geared towards the health and safety of workers in occupations involving high levels of physical exertion. In addition, these findings highlight the importance of maintaining workers' cardiovascular fitness as a means to reduce the risk for potential injuries from slips, trips, and falls in the workplace.

Acknowledgments

The authors gratefully acknowledge the Athletic Training department in assisting in the data collection process.

References

1. Park K, et al. (2011). Safety Sci, 49: 719-726.
2. Hancock, S, et al. (1986). Percept Mot Skills 39: 464-482.
3. Kesler, RM, et al. (2016). Appl Ergonomics: 52: 18-23.

PHYSICAL FATIGUE AFFECTS SPATIOTEMPORAL GAZE DYNAMICS DURING NEGOTIATION OF UNEXPECTED OBSTACLES

M. E. Ayala[1*], J. A. Vicente[1], M. Chavez[1], N. Vogt[1], P. L. Depur[1], N. M. Stoehr, M.S.[1], S. M. Rogers, D.A.T.[1], J. W. Hinkel-Lipsker, Ph.D.[1]

[1]Move-Learn Lab, Department of Kinesiology, California State University, Northridge, CA USA
Email: *Maria.ayala.324@my.csun.edu

Introduction

First responders are the community's primary relief from emergency situations (e.g., natural disasters, incidents of crime, accidents); navigating these unpredictably dynamic environments increases the incidence of mobility-related injury. A recent study found that firefighters have a 40% injury rate attributed to trips, slips, falls, and bodily obstacle collisions while on duty[1]. Previous work suggests the injury rate of firefighters may be attributed to the high physical exertion inherent in job-related tasks[1]. When negotiating obstacles during locomotion, people tend to direct their central gaze past the obstacle to plan future steps and use their peripheral vision to perceive the obstacle itself. However, this strategy changes when vision is compromised; those with peripheral vision impairments (e.g., retinitis pigmentosa) adopt a heavy reliance on central gaze to navigate obstacles[2,3], which does not allow them to focus their attention on other salient environmental cues. Healthy individuals may employ such a strategy in a fatigued state due to physiological changes, such as narrowing the peripheral visual field or impaired cognition. However, such an effect has yet to be studied. This study investigated how exercise-induced fatigue alters how one perceives their environment when confronted with an unexpected obstacle. We hypothesized that in a fatigued state, people would make greater use of central gaze to perceive obstacles and would have to cover a greater distance (i.e., greater gaze angular displacement) to do so. Further, we hypothesized that fatigued individuals would exhibit a delayed time to first fixation on the obstacle and a slower reaction time.

Methods

Twenty-one young, healthy subjects completed five obstacle negotiation trials in a rested state, followed by a fatiguing exercise protocol and immediate completion of five more obstacle negotiation trials in a fatigued state. For each obstacle negotiation trial, subjects walked through a darkened laboratory where they encountered a randomly placed obstacle that illuminated upon approach, requiring them to recognize it and negotiate it quickly. Wearable eye-tracking glasses were used to quantify pupillary movement during both rested and fatigued conditions at 100 Hz. In addition, these wearable glasses contained an embedded inertial measurement unit (IMU) that allowed for quantification of head rotation which, when combined with eye position, provided a combined head+eye gaze vector. This vector was used to identify angular gaze displacement, as well as onset of reaction to obstacle illumination. The obstacle itself was tagged as an area of interest (AOI) in post-processing, allowing us to determine if subjects directed their gaze towards the obstacle.

Results and Discussion

Results indicated a significant increase in the frequency of times when subjects used central gaze to perceive the obstacle while fatigued. Further, they had a greater angular gaze displacement, indicating they covered more area to use central gaze (i.e., it was not a more efficient strategy). There were no changes in reaction time or time to first fixation when fatigued.

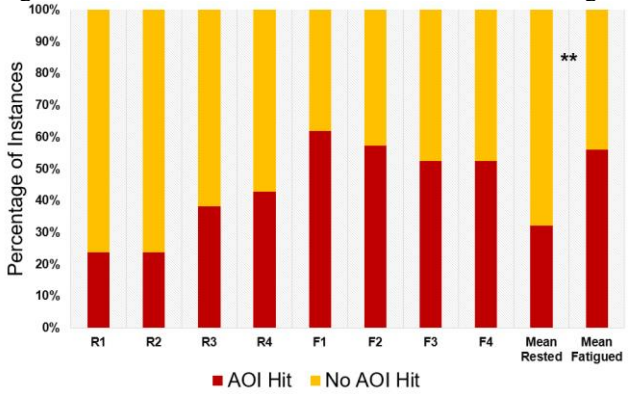

Figure 1. Frequency of use of central gaze to perceive obstacles across four rested (R1-R4) and four fatigued (F1-F4) trials ($p < 0.001$)

These findings reveal how fatigue reduces one's ability to use peripheral vision to perceive oncoming obstacles during locomotion. This could be due to physical exertion causing a narrowing of the peripheral visual field. While peripheral vision has lower acuity, it more rapidly detects the objects' location, leaving the central gaze to provide more detailed information about other salient environmental cues. Future work should investigate how the area of the visual field changes following fatiguing exercise.

Significance

Considering first responders encounter many high-stakes emergency situations, any inefficiency or deficit in the visual processes can be detrimental to their ability to ambulate safely. Understanding these inefficiencies may help develop alternative training strategies to adopt a more ergonomic gaze response for fatigued task performance (e.g., peripheral vision training). Advancement in these strategies may positively aid in the safety of physically demanding occupations. This study's results can further benefit the scientific community by providing insight into the role of vision during obstacle negotiation.

References

[1]Campbell, R. B. NFPA J, 2016.
[2]Timmis, M. A., et al. Invest Opthalmol Vis Sci 58, 2017.
[3]Turano, K. A., et al. Optom Vis Sci 78, 2001

IMPACT OF CALCANEAL PITCH ON MIDTARSAL JOINT KINEMATICS DURING GAIT

Paige F Paulus[1], Tom H Gale[1], Maria A Munsch[1], MaCalus V Hogan[1], and William J Anderst[1]
[1]University of Pittsburgh, Department of Orthopaedic Surgery
Email: pap82@pitt.edu

Introduction

Hindfoot kinematics during the stance phase of gait have been precisely measured using biplane radiography to provide novel insight into the dynamic kinematics of healthy and pathological feet [1, 2]. Less is known about midfoot kinematics during the gait cycle [3].

Calcaneal pitch is the angle between the inferior calcaneus and the horizontal plane (normal: 20-30°, pes planus: <18°). Diminished calcaneal pitch has been clinically associated with dysfunction such as plantar fasciitis and adult acquired flatfoot deformity [4].

The purpose of this pilot study was to explore the relationship between calcaneal pitch and talonavicular (TN) and calcaneocuboid (CC) kinematics during the stance phase of gait. We hypothesized that individuals with pes planus would have greater pronation (dorsiflexion (DF), eversion, and external rotation (ER)) and translation in CC and TN kinematics and this variation would be greater in the TN joint.

Methods

Five healthy volunteers (age: 26 to 41 years, weight: 103 to 181 lbs, and height 1.6 to 1.8 m) provided written informed consent prior to participating in this IRB-approved study. Subjects walked overground at a self-selected pace. Synchronized biplane radiographs of the foot and ankle were collected during static standing and during the full support phase of walking (heel strike (HS) to toe off (TO)) at 100 frames per second. Calcaneal pitch was measured in a static sagittal radiograph [4].

Computed Tomography scans were used to create subject-specific 3D models of the talus, calcaneus, cuboid, and navicular. A validated volumetric model-based tracking technique [5] was used to match these models to the biplane radiographic images with sub-millimeter accuracy. HS and TO were determined by a force plate under the foot.

Joint kinematics were filtered with a 4th order Butterworth filter with 10 Hz cut-off frequency and interpolated to percent stance phase. Dynamic kinematic data was normalized to the average static trial and participants grouped based on subject calcaneal pitch. Differences in kinematics between groups were evaluated using two sample t-test for static trials and statistical parametric mapping (SPM) [6] for dynamic trials with a significance set at $p < 0.05$ for all tests.

Results and Discussion

Based on calcaneal pitch assessment, two subjects were classified as normal calcaneal pitch (21.8° and 25.9°) and three were classified as pes planus (9.8° to 16.8°).

In the static standing position, the navicular was found to sit in greater dorsiflexion in relation to the talus (average difference = 24.5°, $p<0.001$) and more proximally in relation to the talus (average difference = 10.7 mm, $p<0.05$), and that the cuboid sits more medially in relation to the calcaneus (average difference = 8.4 mm, $p< 0.05$) in individuals with pes planus compared to those with normal calcaneal pitch.

The primary motion in the CC joint was dorsiflexion/plantarflexion rotation, while the primary motions in the TN joint were dorsiflexion/plantarflexion and inversion rotation (Table 1).

Table 1: Average Midtarsal Joint ROM over Stance Phase

	Talonavicular ± SD	Calcaneocuboid ± SD
Medial/Lateral Translation (mm)	4.4 ± 1.3	6.8 ± 2.4
Anterior/Posterior Translation (mm)	3.1 ± 1.1	2.3 ± 0.8
Proximal/Distal Translation (mm)	3.4 ± 0.9	7.7 ± 2.7
Dorsiflexion Rotation (°)	10.3 ± 3.8	10.0 ± 2.9
Inversion Rotation (°)	13.6 ± 3.2	7.8 ± 2.4
Internal Rotation (°)	9.6 ± 3.0	7.3 ± 3.7

During dynamic trials, the cuboid was found to move more laterally on the calcaneus ($p<0.001$) in individuals with pes planus during midstance and terminal stance (17-19% and 33-38% stance) (Figure 1).

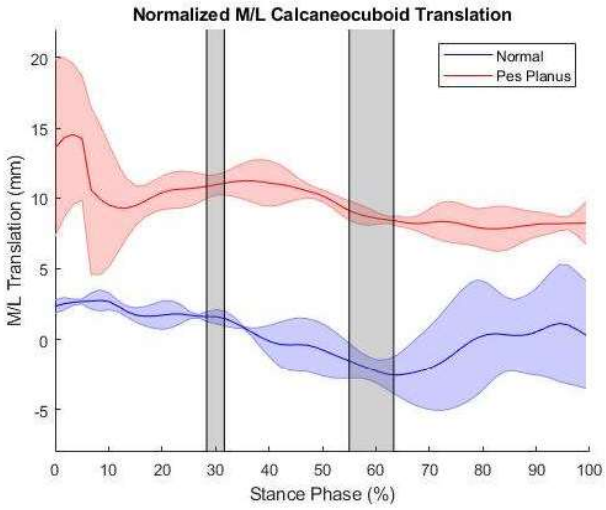

Figure 1: CC M/L translation (lateral (+), medial (-)) during dynamic trials. Gray shaded regions represent periods of significant differences ($p < 0.001$).

Significance

Results of this pilot study suggest calcaneal pitch can impact midtarsal motion during gait. This finding has implications for joint arthroplasty design and treatment of other foot pathologies. Further research on a larger cohort is justified to confirm these results.

Acknowledgments

This work was funded in part by NIH Grant R44HD066831.

References

[1] Lenz, et al, J of Biomech, 2021, [2] Yang, et al, J of Biomech, 2021 [3] Phan, et al, J. Biomech, 2019. [4] Flores, et al, RG, 2019. [5] Pitcairn et al, J. Biomech, 2020. [6] Friston, et al, Elsevier, 2007.

PRIOR EXPOSURE TO ENVIRONMENTAL UNCERTAINTY MAY LIMIT ADAPTATION OF PREDICTIVE CONTROL STRATEGIES DURING A GOAL-DIRECTED WALKING TASK

Aojun Jiang[1]*, Mary Bucklin[1], Jasjit Deol[2], Anna Shafer[2,3], and Keith E. Gordon[2,3]
[1]Northwestern University, Department of Biomedical Engineering, Evanston, IL, USA; [2]Northwestern University, Department of Physical Therapy and Human Movement Sciences, Chicago, IL, USA; [3]Edward Hines Jr. VA Hospital, Hines, IL, USA
*email: aojunjiang2021@u.northwestern.edu

Introduction

People form predictive internal models to control their center of mass (CoM) trajectory when walking in a novel and consistent environment[1]. Our purpose was to examine if exposure to external uncertainty (pseudorandom perturbations) impacts future formation of internal models used to control walking. During reaching exposure to pseudorandom perturbations can accelerate motor learning of a novel and consistent force field[2] by ensuring the limb remains close to its target trajectory via adaption of impedance control strategies that limit large kinematic errors. Alternatively, impedance control strategies could impair internal model formation by limiting kinematic errors known to drive some forms of motor learning. We hypothesize that prior exposure to pseudorandom perturbations will lead to the adaptation of control strategies that reduce initial kinematic errors when walking in a novel and consistent external force field. This reduction in kinematic errors will impede formation of a predictive internal model of CoM trajectory.

Methods

We evaluated locomotor adaptation to a novel and consistent force field as four healthy participants performed 70 repetitions of a discrete goal-directed forward-walking task, moving from a standing position to an end target located 1.5 meters (~2 steps) away. During the task, a cable-driven robot applied a laterally-directed force field to the CoM[3]. The applied forces were proportional in magnitude to forward walking velocity and directed towards the participant's right. Catch trials (no applied forces) interspersed with the consistent field trials were used to evaluate neural control strategies. Immediately prior to walking in the consistent field, participants performed 20 baseline trials (no applied forces), followed by 30 trials during which the robot applied pseudorandom perturbations of varying amplitude, duration, and direction. The current data were compared to a control group[1] consisting of thirteen healthy participants who adapted to an identical force field without prior exposure to pseudorandom perturbations. Participants were unaware of the external forces they would experience prior to starting each trial.

A motion capture system recorded 3D coordinates of markers on the pelvis and feet. We quantified signed area deviation of the CoM trajectory relative to a straight forward path originating from the lateral CoM position at first toe-off. Thus, the **CoM signed deviation** reflects directional biases in CoM trajectory by taking the difference between areas on either side of the straight path. We also quantified the CoM lateral offset during the anticipatory postural adjustment associated with gait initiation, as the difference in lateral COM position at start of trial and toe-off. The **CoM lateral offset** occurred prior to the initiation of forward movement and the application of external forces and thus reflects control strategies based purely on past experience.

Results and Discussion

All participants displayed large CoM signed deviations to their right (same direction as the force field) during early field trials (first 4 consistent field trials). Surprisingly, the pseudorandom perturbation group exhibited significantly larger CoM signed deviation errors than the control group (p=0.023) during the early field trials. By the late field trials (last 4 consistent field trials) the CoM signed deviation errors still tended to be larger in the pseudorandom perturbation group than the control group (p=0.068). In addition, unlike the control group, CoM signed deviation did not return to baseline levels by the late field trials for the pseudorandom perturbation group (p=0.004).

In addition, the control group CoM lateral offset became progressively more bias to the left from early to late field trials. In contrast, the pseudorandom perturbation group COM lateral offset did not change from early to late field trials. CoM lateral offset was significant larger in the control than the pseudorandom perturbation group (p=0.034) during late field trials. That by the late field trials the CoM signed deviation did not return to baseline, and CoM lateral offset did not increase in magnitude to offset the consistent force field for the pseudorandom perturbation group suggests that prior exposure to an unpredictable environment can limit future formation of a strong predictive internal model to control CoM walking trajectories.

However, when the force field was unexpectedly removed during catch trials all participants displayed large lateral COM signed deviations to their left suggesting that all participants had developed some predictive control strategies to offset the effects of the force field. The CoM signed deviation during catch trials were not different between the two groups (p=0.601).

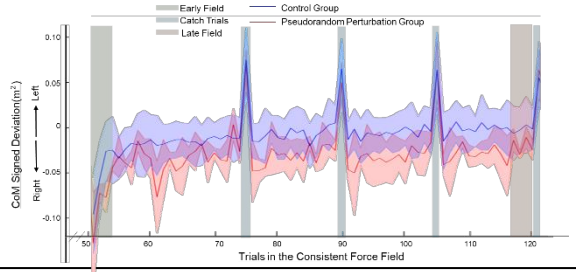

Figure 1: CoM Signed Deviation of the two groups during trials in the consistent force field. The pseudorandom perturbation group did not show a return of CoM Signed Deviation to baseline levels (0) by the late field trials.

Significance

Our preliminary research suggests that uncertainty may impede subsequent locomotor learning. Participants did not exhibit evidence of adapting an impedance control strategy in response to pseudorandom perturbations. To the contrary, larger COM signed deviation errors during the initial field trials suggest participants may have used an admittance control strategy. Our findings may provide a framework for structuring gait rehabilitation interventions, when the goal is to learn consistent aspects of gait (e.g. external environment or control of oneself) than additional external uncertainty should be minimized.

References

[1]Bucklin et al. 2019. Journal of Biomechanics, 2019. [2]Heald et al. 2018. Sci Rep. [3]Brown et al. 2017. *IEEE*.

EFFECTS OF CURVE RADII ON MAXIMUM CURVE SPRINTING VELOCITY IN ATHLETES WITH A LEG AMPUTATION

Gabriela B. Diaz[1], Ryan S. Alcantara[1], and Alena M. Grabowski[1]
[1]Applied Biomechanics Lab, University of Colorado Boulder, Boulder, CO USA
email: gabriela.diaz@colorado.edu

Introduction

People with and without transtibial amputation (TTA) run slower maximum velocities (v_{max}) on curves compared to straightaways, however the underlying biomechanical mechanisms that affect curve-running v_{max} are not completely understood [1]. Determinants of curve-running v_{max} are particularly relevant to athletic events such as the 200 m and 400 m sprint, where over half the race is along a curve. Faster curve-running v_{max} positively affects overall sprint performance. Greene (1985) developed a model that predicts curve compared to straightaway v_{max} based on a given curve radius [2]. However, the model has not been tested for conditions pertinent to competitive track and field events such as the 200 m and 400 m sprint and has not been validated on people with TTA.

Previous studies of non-amputee athletes propose that curve-running v_{max} is limited by the inside leg's ability to generate centripetal force [1]. Athletes with TTA use a running-specific prosthesis (RSP) to sprint, which results in lower stance average vertical ground reaction forces (GRFs) for the affected leg (AL) compared to the unaffected leg (UL) when running on a straightaway [3]. When athletes with TTA use an RSP to run on a flat regulation indoor track curve, their v_{max} is 3.9% slower when their AL is on the inside compared with outside of the curve [4], suggesting use of RSPs may also limit centripetal GRFs.

We hypothesized for athletes with TTA running on curve radii for Lane 1 of regulation 200 m (17.2 m) and 400 m (36.5 m) track curves: 1. v_{max} will slow according to Greene [2], resulting in an average 3% decrease in v_{max} on a 17.2 m compared to a 36.5 m radius curve, 2. running clockwise (CW) with the AL on the inside of the curve versus counter-clockwise (CCW) with the AL on the outside of the curve will decrease v_{max} by ~3.9% according to Taboga et. al. [4] regardless of curve radius, and 3. there will not be an interaction between curve radius and running direction on v_{max}.

Methods

8 competitive sprinters (7 M; 1 F) with a right TTA completed a randomized series of 40 m sprints on a flat indoor track and were provided with ≥8-min rest between trials. Athletes ran CCW and CW sprints along 40-m curves with radii of 17.2 m and 36.5 m. Athletes used spikes and ran across two mondo-covered adjacent force plates (AMTI; 1000 Hz) flush with the track surface. Lower body 3D kinematics were recorded using high-speed motion capture cameras (Vicon; 200 Hz). The force plates and capture volume (~2.5 x 5 m) were located halfway along the 40 m curve. Athletes adjusted their starting position to reach v_{max} within the capture volume. We instructed athletes to run as fast as possible for each trial. Trials were repeated until athletes successfully landed on the force plates at least once with the AL and with the UL. We calculated v_{max} as the average velocity of the pelvis markers within the capture volume. We constructed a linear mixed effects model to determine the effect of curve radius and running direction on v_{max}.

Results and Discussion

v_{max} decreased by 8.08% (0.57 ± 0.08 m/s) from the 36.5 m radius to the 17.2 m radius ($p < 0.001$). We also found that v_{max} decreased by 3.70% (0.27 ± 0.08 m/s) ($p < 0.001$) with the AL on the inside (CW direction) compared to the outside (CCW direction) of the curve. There was no significant interaction between curve radius and running direction, indicating the changes in v_{max} due to curve radii were similar across running directions ($p = 0.99$).

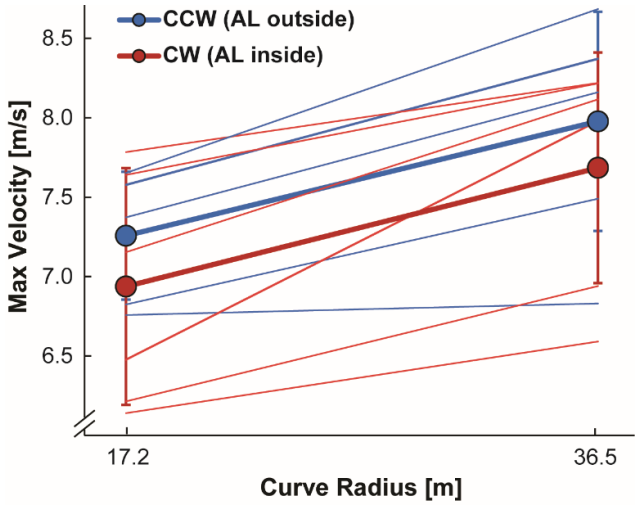

Figure 1. Maximum (Max) velocity across curve radii and running directions. Individual subject's values are displayed with thin lines. Counterclockwise (CCW) is blue and clockwise (CW) is red. Thicker lines show mean values for all subjects, with error bars as SD.

There was a greater reduction in v_{max} between curve radii than hypothesized. We found an 8% decrease in v_{max} when running on the 17.2 m curve compared to the 36.5 m curve, as opposed to the predicted 3% decrease. This suggests that athletes with TTA using an RSP slow more with smaller radius curves compared to non-amputees.

We found that athletes with TTA ran 3.7% slower on CCW versus CW curves, where their AL was on the outside compared to inside of the curve, respectively. Because all track and field competitions are run CCW and a previous study found that non-amputee sprinters ran 1.9% slower v_{max} on CW compared with CCW curves [4], the v_{max} differences for sprinters with right TTA may be attributed to training [4] in combination with the AL on the outside versus inside of the curve.

Significance

Our results show maximum velocity changes along typical regulation athletics curves for athletes with a transtibial amputation and can be used to inform future RSP designs used for sprinting along a curve. Additionally, our results show a greater reduction in v_{max} when the AL is on the inside compared to the outside of the curve, which can inform the International Paralympic Committee on fair competition between athletes with right versus left leg amputations.

References

[1] Y.-H. Chang and R. Kram, *J. Exp. Biol.*, Mar. 2007.
[2] P. R. Greene, *J. Biomech. Eng.,* May 1985
[3] A. M. Grabowski, *et al*, *Biol. Lett.,* Apr. 2010
[4] P. Taboga, R. Kram, & A. M. Grabowski, *J. Exp. Biol.*, 2016

Symmetry Differences in Stop Jump Landing Mechanics after Anterior Cruciate Ligament Reconstruction

[1]Michael A. Teater*, [2]Daniel O. Schmitt, [3]Douglas W. Powell, and [1]Robin M. Queen
[1]Department of Biomedical Engineering and Mechanics, Virginia Tech, Blacksburg, VA, USA
[2]Department of Anthropology, Duke University, Durham, NC, USA
[3]College of Health Sciences, University of Memphis, Memphis, TN, USA
Email: *michaelt20@vt.edu

Introduction

An estimated 350,000 anterior cruciate ligament reconstructions (ACLR) are performed annually in the USA (1). The risk of second ACL injury (tear of the graft or contralateral ACL) may be as high as 30% (2). Previous studies have reported increased asymmetry in the peak knee extension moment, vertical ground reaction force (vGRF), and deficits in postural stability in athletes who sustained a second ACL injury following return to activity (3,4). Limb stiffness and specifically limb stiffness symmetry during the landing phase of a stop jump (SJ) has not been considered as a potential risk factor for second ACL injuries. Given the importance of the vGRF in the determination of limb stiffness, joint work, and joint power, it is believed that examining limb stiffness could provide new insight on alterations to landing mechanics following ACLR that could be vital for identifying increased risk for second injuries. The purpose of the study was to compare SJ landing mechanics between ACLR patients and an asymptomatic control group to understand how limb stiffness, joint work, and joint power differ between groups. Limb symmetry was determined using the normalized symmetry index (NSI) (5). We hypothesized that the ACLR patients would be less symmetric (greater NSI values) when compared to the control participants.

Methods

40 ACLR (24 male and 16 female) and 60 control (30 male and 30 female) recreational athletes were recruited and signed institutional review board approved informed consent prior to testing. The ACLR patients were 5.9±1.4 months removed from primary, unilateral ACL reconstruction surgery and had an average age of 17.3±1.9 years, while the control group was 21.6±2.9 years old. Each participant completed between 7 and 10 SJ trials. Three-dimensional motion capture (240Hz) (Qualisys, Goteborg, Sweden) and force plate data (1920Hz) (AMTI, Watertown, MA, USA) were collected for each participant during each trial. A modified Helen-Hayes marker set was used for data collection (6). Participants were provided form fitting athletic clothing and neutral shoes (Air Pegasus; Nike Inc., Beaverton, Oregon) during testing. For the control group, limb dominance was defined as the foot used to kick a ball. Kinematic and kinetic parameters were analyzed during the first landing of the SJ. Limb stiffness, negative joint power, and negative joint work were calculated from initial contact to the lowest sacral position. The NSI was calculated for each outcome measure using previously reported methods (5). Independent samples t-tests ($p<0.05$) were completed in JMP Pro 15 (SAS Institute, Inc, Cary, NC, USA) to determine significant group differences in limb stiffness as well as hip/knee/ankle negative joint work and power.

Results and Discussion

Significant group differences existed for all outcome measures except for negative ankle work ($p=0.197$) (Table 1). ACLR patients have unique limb stiffness, joint power and joint work symmetry when compared to an uninjured control group. The decreased symmetry in ACLR patients demonstrates the need to develop intervention strategies focused on improving limb symmetry during landing to decrease second ACL injury risk. Future work will determine the joint mechanics that are driving these symmetry differences between groups with a focus on examining differences in limb loading, center of mass (COM) movement, joint coordination, individual joint stiffness, and kinematic asymmetry during a stop jump.

Significance

The asymmetry in limb stiffness, joint power, and joint work is greater in ACLR patients when compared to an uninjured control group during a stop jump. These findings indicate that ACLR patients land unevenly, which could alter dynamic stability and increase second ACL injury risk.

Acknowledgements

Supported by NIH grant AR069865

References

(1) Wojtys and Brower, J Athl Train, 2010 (2) Di Stasi et al., J Orthop Sports Phys Ther, 2013 (3) Lepley and Kuenze, J Athl Train, 2018 (4) Paterno et al., Am J Sports Med, 2016 (5) Queen et al., JOB, 2020 (6) Queen et al., FAI, 2012

	Surgical	Non-Surgical	ACLR NSI	Non-Dominant	Dominant	Control NSI	NSI P-value
Limb stiffness (N/m/kg)	9.12 ± 4.87	9.06 ± 5.03	14.0 ± 8.55	7.14 ± 4.23	7.05 ± 4.07	7.95 ± 6.84	<0.001*
Negative ankle work (Nm)	-0.53 ± 0.24	-0.55 ± 0.35	15.8 ± 10.3	-1.05 ± 0.70	-1.05 ± 0.69	18.8 ± 12.9	0.197
Negative knee work (Nm)	-1.36 ± 0.47	-1.38 ± 0.64	32.0 ± 18.8	-1.62 ± 0.43	-1.74 ± 0.57	15.7 ± 9.52	<0.001*
Negative hip work (Nm)	-0.44 ± 0.25	-0.43 ± 0.22	21.0 ± 13.2	-0.69 ± 0.32	-0.66 ± 0.32	13.8 ± 10.3	0.005*
Negative ankle power (J/s)	-4.82 ± 2.31	-5.09 ± 3.30	15.7 ± 11.8	-5.37 ± 3.69	-5.60 ± 3.62	11.1 ± 6.69	0.031*
Negative knee power (J/s)	-15.9 ± 6.00	-15.7 ± 7.09	32.8 ± 17.4	-9.91 ± 6.60	-9.70 ± 4.79	9.60 ± 5.85	<0.001*
Negative hip power (J/s)	-8.15 ± 3.63	-8.30 ± 3.93	17.1 ± 12.4	-10.9 ± 9.47	-9.24 ± 5.14	10.2 ± 6.54	0.002*

Table 1: NSI values (mean ± standard deviation) for ACLR and control group outcome measures. * indicates significant difference.

EFFECTS OF PHYSICAL THERAPY ON ANKLE-FOOT ROLLOVER SHAPE FOR A POWERED PROSTHESIS

Michael Poppo[1], A. Hansen[2,3], J. Chomack[1], and J. Maikos[1]
[1]Veterans Affairs New York Harbor Healthcare System, New York, NY
[2]Minneapolis Department of Veterans Affairs Health Care System, Minneapolis, MN
[3]Rehabilitation Medicine and Biomedical Engineering Departments, University of Minnesota, Minneapolis, MN
email: *michael.poppo@va.gov

Introduction

As prosthetic technology evolves, advanced devices for individuals with lower extremity amputation strive to offer more biomimetic features and benefits to users. The objective of this preliminary analysis was to determine the effects of an Empower (Ottobock, Germany) ankle-foot device (PWR), as well as a device-specific physical therapy (PT) intervention, on dynamic function (effective foot length ratio (EFLR), instantaneous radius of curvature (IROC), and radius of curvature (ROC)) for individuals with transfemoral amputation (TFA) compared to traditional energy storing and returning (ESR) prosthetic feet. We hypothesized that the PT group would generate improved roll-over shape characteristics at 4 and 8 weeks compared to the non-PT group.

Methods

Motion capture and kinetic data were captured for 5 people with unilateral TFA during overground walking at the Veterans Affairs New York Harbor Healthcare System (VA NYHHS). Participants were then randomized to two different groups during the initial 4 weeks of acclimation to the PWR foot. One group received the standard of care (non-PT group), which included training on the proper use and care of the foot by the study prosthetist and physical therapist (2 participants). The second group also received standard of care, but additionally underwent twice weekly, device-specific PT sessions with the study physical therapist (3 participants) (PT group). Neither group received PT between the 4-week and 8-week data collections. The PT program specifically targeted strengthening muscle groups to potentially improve the effectiveness of the PWR foot. Center of pressure (COP) data were transformed into the shank coordinate system during single limb stance. EFLR, a measure of the percentage of the foot that is effectively used during a step, was calculated as the distance from the prosthetic heel to the most anterior point of the COP progression divided by the overall length of the foot. Circular arcs of best fit were also applied to the COP data to determine roll-over shape characteristics, such as height-normalized ROC [1]. The IROC was calculated by evaluating the first derivative of COP forward travel with respect to shank angle. The peak IROC is representative of the fastest COP forward travel.

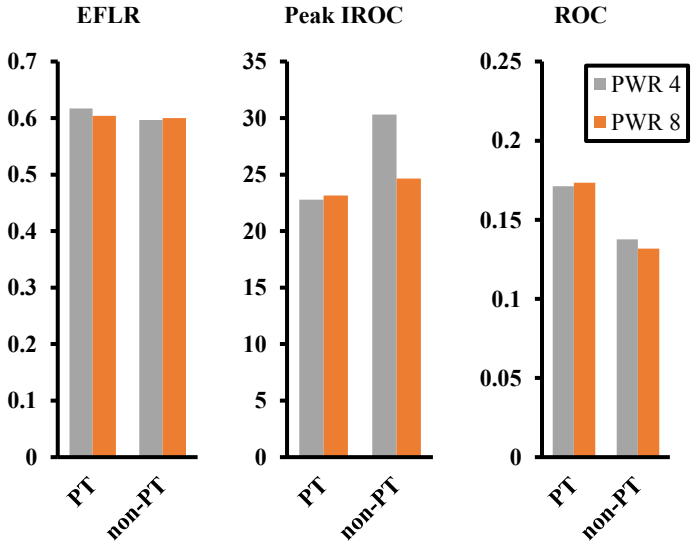

Figure 1: Comparison of PT and non-PT groups for average EFLR, Peak IROC (cm), and height-normalized ROC.

Results and Discussion

Although currently only a small sample size, PT intervention may slightly improve EFLR after the 4-week PT intervention (0.62) compared to the non-PT group (0.60). This may indicate that a device-specific PT intervention can improve anterior progression of the COP during single-leg stance, improving the walking efficiency of the PWR foot. However, the acute effects were not sustained beyond the PT intervention as shown by the lower EFLR (0.60) at 8-weeks in Figure 1. This suggests the need for a more-focused home exercise program to help sustain the long-term EFLR improvements. Figure 1 also shows that the non-PT group produced slightly higher peak IROC (PWR 4: 30.3 cm; PWR 8: 24.6 cm) compared to the PT group (PWR 4: 22.8 cm; PWR 8: 23.2 cm) which suggests improved stability in the non-PT group [2]. PT training focused on initiating pelvis movement may have promoted a smoother transition from heel to toe rocker. The non-PT group (PWR 4: 0.14; PWR 8: 0.13) showed reduced ROC compared to the PT group (PWR 4: 0.17; PWR 8: 0.17). This could suggest improved stability for the PT group during single leg stance because the foot is rotating about a larger rocker which may be resultant from focused muscle strengthening over the 4-week intensive PT program.

Significance

Although large changes in roll-over shape parameters have been shown to affect aspects of gait, it is unclear if the changes seen in this study are clinically relevant. The PT group is showing trends of improvement in some parameters and may generate benefits over the standard of care. These results can inform clinicians of the benefits of prescribing the PWR foot along with a device-specific treatment.

Acknowledgments

This work was supported by a DoD Orthotics and Prosthetics Outcomes Research Programs grant (W81XWH-17-1-0568). We would also like to acknowledge our collaborators at Walter Reed National Military Center.

References

[1] Hansen, A.. et al. *Clinical biomechanics (Bristol, Avon)*, *19*(4), 407–414, 2003.
[2] Curtze, C. Et al. *Journal of biomechanics*, *42*(11), 1746–1753, 2009.

LOCOMOTOR ADAPTATION IN HYPOGRAVITY RELIES ON A CENTRALIZED CONTROL ARCHITECTURE

Chase G. Rock[1], Kristy S. Yun[2], Angela Luo[1], Xiao Yang[1], and Young-Hui Chang[1,2]
[1]School of Biological Sciences, Georgia Institute of Technology, Atlanta, GA, USA
[2] BioEngineering Program, Georgia Institute of Technology, Atlanta, GA, USA
email: crock@gatech.edu

Introduction

Human motor control makes use of a gradient of centralized and decentralized mechanisms (*1*). Centralized mechanisms are generally responsible for coordinated, global behaviours while decentralized mechanisms govern relatively specific, localized movements (*2*). However, some motor tasks may be achieved by either mechanism, or a combination of both. If we knew which type of mechanism was governing a given task, we would gain valuable insight into how the motor system partitions its workload and could leverage this knowledge toward rehabilitation and robotics.

We previously validated the use of targeted, two-legged jumps to study locomotor adaptation to hypogravity (*3*). In the current study, we tested whether locomotor adaptation to hypogravity is due to a centralized or decentralized control mechanisms. After experiencing simulated hypogravity via one-legged jumping, the motor behaviour of both hypogravity-experienced (EXP) and hypogravity-naïve (NAÏ) legs was investigated for the existence of an adapted motor strategy. If centralized mechanisms were responsible for the adaptation, we would expect adaptation in both the experienced leg and the contralateral naïve leg. If decentralized mechanisms were responsible, we would not expect adaptation to be observed in the hypogravity-naïve leg.

Methods

Six right-leg dominant participants enrolled in this IRB-approved cross-over study. After being outfitted with EMG electrodes on muscles of both legs (vastus lateralis, lateral and medial gastrocnemius, and soleus muscles), participants performed 3 maximum effort, one-legged jumps on each leg. A virtual target was set at 75% of their max jump height, to which participants were given visual feedback on a monitor. They were instructed to jump to this virtual target for the remainder of the protocol.

Participants jumped to the target with their right leg 10 times at normal gravity (PRE). They were then placed in the hypogravity simulator (*3*), which attached to a harness and pulled vertically with a force equal to half of the participant's body weight. Participants performed 50 targeted one-legged jumps at 0.5g on their left leg. Immediately after the 50th jump, the hypogravity simulator was detached, and the participants again performed 10 jumps at 1g (POST) using their right leg (NAÏ). For comparison, the protocol was also completed with the right leg for all trials (EXP); PRE, simulated hypogravity, and POST.

After-effects in both EXP and NAÏ legs were investigated by comparing the muscle preactivation timing (i.e., time between muscle activation onset and ground contact; (*4*)) in the first POST trial with the average preactivation timing of the final 3 PRE trials. These results are presented in the context of our previous results on hypogravity adaptation in two-legged jumping (*3*).

Results and Discussion

Previously, our lab has shown a decrease in preactivation timing following two-legged adaptation to hypogravity (*3*). In the current study, preliminary results suggest a similar decrease for one-legged jumps in the gastrocnemii and soleus muscles (Fig. 1, EXP). Most importantly, locomotor adaptation is observed in the naïve leg without having motor experience in simulated hypogravity (Fig. 1, NAÏ).

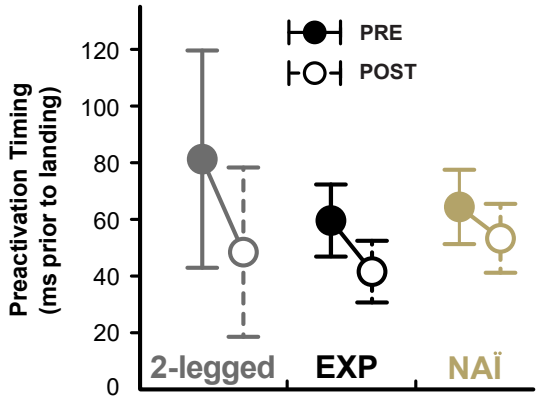

Figure 1: After hypogravity adaptation, aftereffects (n = 6) were observed in soleus preactivation timing (mean ± SD) on both the hypogravity-experienced leg (●) and on the hypogravity-naïve leg (●). These aftereffects reflect those observed in two-legged jumping (● ; n = 10).

Bilateral transfer of adaptation effects is known to occur in the upper limb (e.g., (*4*)), and evinces a centralized motor control strategy that is not end-effector specific. In the current study, it appears that the experience of using one leg for a locomotor task provides usable information for performing the same task with the naïve contralateral limb. A decentralized, limb-specific motor control strategy is unable to explain the observation of after-effects in the naïve leg. Instead, a centralized motor control strategy is likely responsible for the observed after-effects.

Adaptation to hypogravity relies on predictive, feedforward motor control. After-effects in the hypogravity-naïve leg contralateral to the leg that jumped in simulated hypogravity indicate a centralized locomotor control architecture.

Significance

Bilateral transfer of after-effects indicates a centralized control architecture for locomotor adaptation, which could be leveraged in rehabilitation interventions. Future work will investigate the extent to which centralized gravity adaptation of the lower body affects gravity-dependent motor behaviour throughout the body.

Acknowledgments

This material is based upon work supported by the NSF GRFP to CGR (DGE-1650044). Any opinions, findings, and conclusions or recommendations expressed in this material are those of the authors and do not necessarily reflect the views of the NSF.

References

1. K. Nishikawa *et al.*, *Integr. Comp. Biol.* **47**, (2007).
2. D. E. Koditschek *et al.*, *Arthropod Struct. Dev.* **33**, (2004).
3. C. G. Rock *et al., Virtual ASB*, (2020).
4. M. Santello, M. J. N. Mcdonagh, *Exp. Physiol.* **83**, (1998).

THE EFFECT OF SENSOR COMBINATIONS ON PREDICTING KNEE FLEXION ANGLE

David Hollinger[1*], Mark Schall[2], Howard Chen[1], Jordan Coker[1], and Michael Zabala[1]
[1]Department of Mechanical Engineering, Auburn University, Auburn, AL
[2]Department of Industrial & Systems Engineering, Auburn University, Auburn, AL
*Email: dzh0063@auburn.edu

Introduction

Recent trends in biomechanics research have focused on the intersection of wearable sensors and machine learning to optimize control of assistive devices. Wearable sensors (e.g. IMU, EMG) capturing subtle biomechanical signals are often used as feature labels for machine learning models to predict human motion [1]. Previous studies have explored how a combination of EMG and mechanical sensors can improve lower limb action classification [2-3]. However, previous analyses were optimized to predict cyclical movements (e.g. level walking, stair climbing, uphill walking) while numerous movements are non-cyclical (e.g. crouching, kneeling, stand-to-prone). Therefore, we examined sensor combinations that maximize joint angle prediction accuracy which can later be used for post hoc testing of non-cyclical movements patterns. We hypothesized that at least two EMG sensors are needed to reasonably predict knee flexion angle, but more than three sensors are redundant for this purpose.

Methods

Motion capture analysis was performed for 10 healthy volunteers during 15 walking trials at preferred walking speed. Six EMG sensors were placed on the left and right Rectus Femoris (RF), Vastus Lateralis (VL), Vastus Medialis (VM), Tensor Fasciae Latae (TF), Biceps Femoris (BF), and Semitendinosus (ST). An Artificial Neural Network (ANN) using Bayesian Regularization with EMG and flexion angle features was used to predict knee flexion angle at 50ms, 100ms, 150ms, and 200ms into the future. For each subject, data was split into 10 walking trials for training and 5 walking trials for testing. A time-series prediction for every permutation of six sensors was performed and compared to the actual knee flexion angle during walking. RMSE was calculated for the entire duration of each test trial to measure the knee flexion angle prediction accuracy. ANOVA ($p < 0.05$) was used to rank order the significance for the number of sensors and was repeated for each prediction time.

Results

Including additional EMG sensors did not significantly enhance prediction accuracy of knee flexion angle (Table 1). Adding a second EMG sensor reduced RMSE for predictions at 150ms and 200ms, however, a single EMG sensor was sufficient for 50ms predictions.

Discussion

To our surprise, multiple EMG sensors did not outperform a single EMG sensor for predicting knee flexion angle. Our results partially support our initial hypothesis that at least two EMG sensors provide considerable information for predicting joint angle, but more than three sensors do not significantly improve prediction accuracy. One sensor performed no worse than multiple sensors for predicting knee flexion angle.

Table I: Joint angle prediction comparison for a combination of EMG sensors based on amount and location

Knee Flexion Angle RMSE (deg.)						
Time (ms)	One Sensor	Two Sensors	Three Sensors	Four Sensors	Five Sensors	Six Sensors
50	0.50	0.51	0.50	0.51	0.51	0.59
100	4.74	4.69	4.54	4.81	4.68	5.21
150	15.69	13.78	14.70	15.42	15.86	17.02
200	27.49	24.42	25.35	24.27	25.46	25.95
Muscles Combination						
50	BF	BF, VM	BF, TFL, VL	BF, RF, ST, VM	RF, VM, VL, BF, ST	ALL
100	VM	BF, VL	RF, ST, VM	BF, TFL, VL, VM	RF, VM, VL, BF, ST	ALL
150	BF	BF, VM	BF,ST, VM	BF, RF, TFL, VM	BF, RF, ST, VL, VM	ALL
200	BF	RF, ST	VM, VL, ST	BF, RF, ST, VM	BF, ST, TFL, VL, VM	ALL

In the work by Young, et al., three EMG sensors were found to optimize classification for cyclical movements which indicates potential applications for combining action classifiers with joint angle predictions to identify movement transitions [2].

Although previous work has developed techniques to predict cyclical tasks with high accuracy, a general algorithm that detects non-cyclical tasks is needed. Future work will explore joint level prediction for two useful applications: (1) Predicting non-cyclical movement (e.g. stand-to-prone) (2) Identifying task transition (walk-to-run) by combining classifiers to detect task transition. The results of this study are useful for developing a generalized approach to predict movement that spans beyond cyclical movement patterns (e.g. walking). Researchers and practitioners can benefit from using a sensor reduction analysis to minimize cost of using redundant sensors and maximize prediction accuracy.

Significance

A sensor reduction analysis provides insight for optimal prediction accuracy for joint-level movement. In order to generalize an array of movements, an accurate joint-level classifier is useful to predict movement that an action level classifier may otherwise miss. Biomechanists incorporating machine learning models should consider the trade-off between prediction accuracy, feasibility, and the cost of the number and type of sensors to predict movement.

References

[1] Gurchiek et al.. *Sensors 2019,* 19(23), 5227
[2] AJ Young et al.. *Journal of neural engineering* 2014, 11 (5), 056021.
[3] Huang H et al. *IEEE Trans. Biomed. Eng*. 2011, 58 2867-75

WEARABLE TECH AND ELECTRONIC JOURNALS: ARE THEY CONSISTENT IN ADOLESCENT RUNNERS?

Micah C. Garcia[1*], David M. Bazett-Jones[1]
[1]University of Toledo, Toledo, OH, USA
email: * micah.garcia@rockets.utoledo.edu

Introduction

Running training plans are often developed based on external and internal loads. For external loads, runs may be prescribed according to distance or time, whereas internal loads may be prescribed according to running intensity (e.g., heart rate (HR) zones). Running journals are often used to manually recorded running sessions. However, wearable technology (e.g., GPS watches, HR monitors) has become popular among runners.[1] While external loads are measured similarly between running journals and GPS watches (i.e., same units), internal loads are captured differently. Running journals often use subject measures of intensity (e.g., session rating of perceived exertion [sRPE]) while GPS watches allow for the measurement of physiological measures (e.g., HR). Strong correlations have been found between sRPE and HR measures in soccer[2] and Australian football sessions,[3] but it is unknown if sRPE and HR are related in adolescent long-distance runners. Therefore, the purpose of our study was to compare the relationship of external and internal loads measured with running journals and GPS watches in adolescent runners. We hypothesized there would be stronger relationships between external loads than internal loads.

Methods

During the fall 2020, 23 high school cross-country runners (F=13, M=10, age=16.0±1.1 years) completed a prospective cohort study. Prior to the season, participants were issued a GPS watch (Garmin 45s) and were instructed to record all running sessions during the season with the GPS watch. After each running session, participants also self-reported distance, time, and sRPE (1=very easy, 10=maximal)[4] using an electronic running journal (Qualtrics). At the end of the season, GPS data (distance, time, average HR, and max HR) were extracted for each running session and matched with the running journal (distance, time, sRPE). We used Pearson's correlations to compare the relationships within external and internal loads between GPS watch and running journal data. HR and sRPE data were also grouped into five intensity zones (zone1: 50-60% HRmax, sRPE=1-2; zone2: 60-70% HRmax, sRPE=3-4; zone3: 70-80% HRmax, sRPE=5-6; zone4: 80-90% HRmax, sRPE=7-8; zone5: 90-100% HRmax, sRPE=9-10). Cohen's Kappa analysed the agreement between intensity zones for sRPE compared to intensity zones for average and max HR, respectively.

Results and Discussion

Strong positive relationships (Figure 1) were demonstrated between the GPS and running journal for distance (r=0.93) and time (r=0.88). However, poor relationships (Figure 1) were found between sRPE and average HR (r=0.11) and max HR (r=0.15). There was slight agreement between intensity zones for sRPE and average HR (κ=0.07) and max HR (κ=0.03).

As hypothesized, distance and time were strongly correlated between data from GPS watches and running journals. All runners had access to a GPS watch so they might have used the watch values when reporting in the running journal. However, there were poor and slight agreements between average or max HR from the GPS watch and sRPE from the running journal. These results were also expected as HR is a physiological measure while sRPE is a measure that may be influenced by person-level factors such as fatigue, stress, and nutrition.

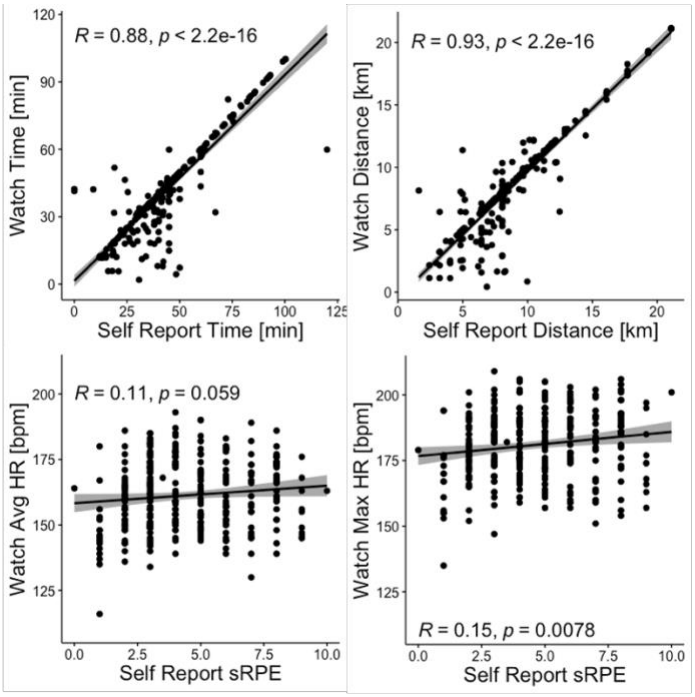

Figure 1: Correlations between GPS watch and running journal recorded external and internal loads.

The results should be considered in the context of their limitations. Previous studies that have compared HR to sRPE have used chest straps for recording HR.[3,4] GPS watches measure wrist-based HR, which may be less accurate at higher intensities. Further work is warranted to determine which method of quantifying internal loads is most important to runners.

Significance

External loads are captured similarly between GPS watches and running journals suggesting both methods measure the same construct in adolescent runners. However, internal load measures of intensity appear to be measured differently by GPS watch HR and running journal sRPE. This result indicates intensity measured by sPRE and intensity measured by HR provide different information. Prescribing runs according to HR intensity zones may not be an accurate representation of the perceived exertion of the adolescent runner.

References

1. Nielsen (2013) *J Strength Cond Res.*
2. Scott TR (2013) *J Strength Cond Res.*
3. Campos-Vazquez M (2014) *Int J Sports Physiol Perfom.*
4. Borg G (1998) *Borg's perceived exertion and pain scale.*

DEVELOPMENT OF A LOW COST MEASURE FOR LUMBAR-PELVIC COORDINATION

Derek H Nguyen[1,2] and Sara E Wilson[1,2]
[1]Bioengineering, University of Kansas
[2]Mechanical Engineering, University of Kansas
email: sewilson@ku.edu

Introduction

The coordination of the segments of the low back has been implicated in the etiology of low back pain (LBP). In repetitive lifting, experienced workers and weightlifters have been found to maintain a neutral coordination of the lumbar and pelvic segments relative to novice lifters who approach range of motion limits suggesting that such a neutral pattern may prevent injury[1-2]. In walking and running, subjects with a history of LBP have been found to have a decrease in lumbar and pelvic rotation[3-4].

Movement analysis research typically utilizes sophisticated 3-D motion capture systems. However, these cost of these systems and large size limits the research to a laboratory setting. In recent years, some have been utilizing inertial measurement units (IMUs) to conduct portable motion analysis for sports. This abstract describes the process of designing and developing an inexpensive technology for accurate measurement of lumbar-pelvic coordination patterns.

Methods

Each sensor in the designed system consists of an Arduino Nano, nRF24L0+ transmitter/receiver and the Adafruit BNO055 9-axis IMU. These have been incorporated into a printed circuit boards designed inhouse. The Adafruit BNO055 IMU sensor chip was chosen as it is a cheap inertial measurement sensor that provides absolute orientation. In addition to being inexpensive, the chip has an onboard sensor fusion algorithm that makes obtaining 3D space orientation easy. Adafruit also provides excellent documentation to use the chip with Arduino microcontrollers. The nRF2401+ chip was used to communicate between multiple Arduino devices to receive and transmit data.

To compare the accuracy of the device, validation testing was conducted against clinical-grade electromagnetic motion tracking system (Trakstar, Northern Digital, Waterloo, ON, Canada).

Results and Discussion

The overall dimensions of the device came out to be 3.5in by 2in. This current iteration may not be practical for some motion analysis application due to the current size and future iterations will look at reducing this size.

The system of IMU devices can communicate with each other to transmit orientation data in the form of quaternions to the host receiver. Communicating in quaternions allows for efficient transmission of sensor orientation (relative to rotation matrices) while avoid the issues of gimbal lock associated with Euler angles. Once transmitted to the Arduino Nano, data is converted to Euler angles and displayed using Python-based software. Our current device suffers from gimbal lock as pitch approaches 90 deg. Fortunately, the representation of orientation is easily convertible within the Python software depending on the application for the device.

The system sensors were assessed against the Trakstar electromagnetic sensor system in single plane rotations for yaw, pitch and roll. There was generally strong agreement between the measures except that yaw appeared to have an offset in angle (Figure 2). The source of this offset is unclear but may be due to sensor alignment. The next step will be to examine the use of this sensor system in assessing lumbar-pelvic coordination. In this the orientation of two sensors, one placed on the thoracic spine and another placed on the pelvis, will be used to assess coordination of these separate segments.

Significance

Differences in lumbar-pelvic coordination are thought to be associated with risk of LBP. The tool created here has been found to be accurate in detecting rotational motions. Future work will extend this towards creating a biofeedback platform for research into lumbar-pelvic coordination as well as rehabilitation and physical therapy.

Acknowledgments

This research was partially supported by the National Institutes of Health Postbaccalaureate Research Education Program (PREP) under award number R25GM078441.

References

1. Riley, A et al., J Biomech. 48(10):1693–1699, 2015.
2. Plamondon, A et al., Ergonomics, 53:1239-53, 2010.
3. Müller, R., et al., J. Biomech. 48:1009–1014, 2015.
4. Roncarati, A. Ergonomics. 11:158–164, 1988.

Figure 1: IMU device (Left) that transmits the orientation data back to the receiver/hub (right) for processing data in python.

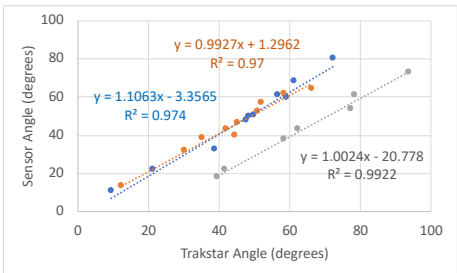

Figure 2: Pitch (blue), Roll (orange), and Yaw (grey) were found to have close agreement between the Trakstar system and the IMU sensors.

MECHANICAL PROPERTY CHANGES OF PEDIATRIC CORTICAL BONE DUE TO SALINE STORAGE TIME

Katarina Radmanovic[1], J. Fritz[1-3], C. Albert[1,3], J. Moore[4], T. Gilat Schmidt[1], S. Tarima[5], P. Smith[3], and G. Harris[1-4]
[1]Department of Biomedical Engineering, Marquette University/Medical College of Wisconsin, Milwaukee, WI, USA
[2]Department of Orthopaedic Surgery, Medical College of Wisconsin, Milwaukee, WI, USA
[3]Shriners Hospital for Children, Motion Analysis Center, Chicago, IL, USA
[4]Department of Mechanical Engineering, Marquette University, Milwaukee, WI, USA
[5]Division of Biostatistics, Medical College of Wisconsin, Milwaukee, WI, USA
email: katarina.radmanovic@marquette.edu

Introduction

In orthopedic research, bone specimens are often submerged in buffered saline solution while awaiting mechanical testing [1]. Zhang et al. observed changes in material properties of bovine cortical bone tissue collected after three-day saline preservation at room temperature [1]. The effects of saline storage time on the material properties of human healthy pediatric cortical diaphyseal bone have not been reported.

We hypothesized that macroscopic material properties of healthy pediatric cortical bone under refrigerated saline storage conditions remain constant for some time period before beginning to change.

Methods

One cortical bone specimen was collected from the femur of a deceased donor with no known musculoskeletal condition (10 year-old female). Twenty-four small beams (~5 mm x 1 mm x 0.65 mm) were machined with the long beam axis being parallel to the long diaphyseal axis [2]. Following machining, the beams were immediately submerged in buffered saline solution and stored in a refrigerator (4° C). A subset of three to four beams was loaded to failure in three-point bending daily for a duration of up to one week. Macroscopic material properties (including elastic modulus [E], yield strength [σ_y], yield strain [ε_y], and bending strength [σ_f]) were determined from the load-displacement data.

Multiple linear regression analyses were used to explore associations between each macroscopic property (dependent variable) and saline storage time (independent variable). These analyses assumed a slope of zero until an arbitrarily selected cut-off day (cut-offs at days 1 through 6 were assessed), after which a non-zero linear slope was fit to the data. This multiple linear regression model with a cut-off is the following:

$$Y_i = \beta_0 + \beta_1 * X_i + \varepsilon_i$$

where Y_i is a macroscopic metric; β_0 (intercept) and β_1 are the regression coefficients; X_i is time, which is zero prior to a selected cut-off value, or equal to the day number minus the cut-off day after that; and ε_i is zero mean Gaussian error.

The cut-off with the lowest corrected Akaike Information Criterion (AICc) was used in the regression model for each material property.

Results and Discussion

The best cut-off day for all material properties occurred at day 4. However, none of the models exceeded a decrease in the dependent variable (macroscopic property) beyond a mechanical testing variability of 12% until day 6 of saline storage (specifically, yield strength and bending strength each decreased by 13% on day 6). Therefore, testing of pediatric cortical bone beyond five days of storage in saline solution demonstrated a decline in strength. Bending strength versus saline storage time is presented in Fig. 1. The 12% mechanical testing variability was determined based on variability in elastic modulus with repeated testing of an acrylic beam, and accounts for user error in beam positioning and potential instrumentation error.

The current conclusions differ from those of Zhang et al. [1]. However, the current study differed from Zhang's in species (human) and storage temperature (refrigeration). Degradation of the macroscopic outcomes was within the testing variability through day 5 of refrigerated saline storage. Thus, mechanical testing of pediatric cortical bone should be performed within a five-day period following sample preparation to minimize material property degradation.

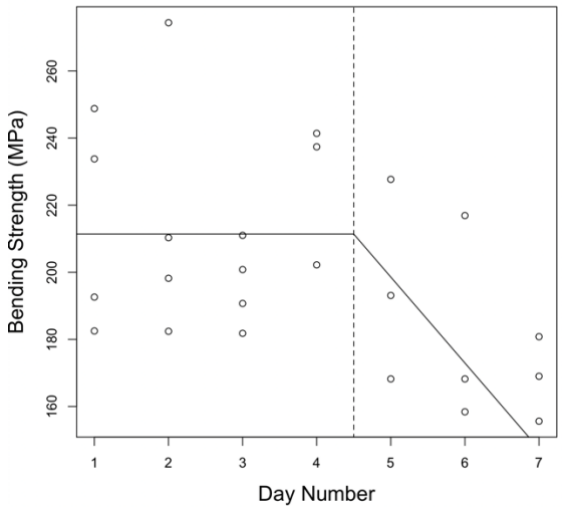

Figure 1: Bending strength (MPa) vs. saline storage time, for healthy pediatric cortical bone beams. The corresponding multiple linear regression model with a cut-off (dashed line) at Day 4 for the dataset is also shown (solid line). At Day 6, the model demonstrates a 13% decrease in bending strength from its initial intercept of 211 MPa.

Significance

The sample storage logistics surrounding material property characterization should be taken into consideration during experimental design of biomechanical testing. Saline storage time of pediatric cortical bone samples should be limited to no greater than five days prior to mechanical testing. If a five-day saline storage period is exceeded, cortical bone material properties may be altered.

Acknowledgments

OREC (MU, MCW) and US Dept. of Ed. P200A150271.

References

[1] Zhang et al (2018). *Clin Biomech*. **57**: 56-66.
[2] Albert et al (2013). *Proc Inst Mech Eng H*. **227**:105-13.

WEEKLY CHANGE IN RUNNING LOADS IN HIGH SCHOOL RUNNERS DURING A CROSS-COUNTRY SEASON

Micah C. Garcia[1*], Brett Pexa[2], Mitchell J. Rauh[3], Kevin R. Ford[2], David M. Bazett-Jones[1]
[1]University of Toledo, Toledo, OH, [2]High Point University, High Point, NC, [3]San Diego State University, San Diego, CA
email: * micah.garcia@rockets.utoledo.edu

Introduction

Running programs traditionally monitor external loads (e.g., time, distance) because they are simple to prescribe and measure. There has been a recent movement to encompass a more holistic approach to monitor running loads that considers internal loads (e.g., intensity measured by session rating of perceived exertion [sRPE])[1,2]. Workload incorporates both external and internal loads and accounts for the potential interaction between these types of loads. Running loads appear to be captured differently by external loads and workloads as weekly changes in running load were found to be different between types of loads in adult and high school runners[3,4]. However, the study which examined high school runners only investigated changes over a two-week period.[4] Therefore, the purpose of this study was to compare weekly change in running load among external loads and workloads during a full high school cross-country season. We hypothesized change in running load would be greater for workloads compared to external loads.

Methods

During the fall 2020, 13 high school cross-country runners (F=10, M=3, age=15.9±1.2 years) completed a prospective cohort study. Prior to the season, participants were issued a GPS watch (Garmin 45s) and were instructed to record all running sessions during the season. After each running session, participants self-reported distance, time, and sRPE (1=very easy, 10=maximal)[5] using an electronic running journal (Qualtrics). At the end of the season, external loads (time, distance, steps) were extracted from the GPS watch and matched with sRPE from the running journal. If the participant did not record their run with the GPS watch, distance and time were used from the running journal for that session, and steps were estimated from their average cadence.

Workload measures were calculated as the products of sRPE with time (timeRPE), distance (distanceRPE), and steps (stepsRPE), respectively. For each week in the season (n=8), external loads and workloads were summed, and the percentage change was calculated for each running load variable relative to the previous week.[3] This resulted in seven two-week cycles. For each runner, the average weekly percent change during the season was calculated among the seven cycles. Paired *t* tests compared average weekly percent change during the season between time-timeRPE, distance-distanceRPE, and steps-stepsRPE. Significance was set at $p<.05$.

Results and Discussion

During the season, the average weekly percent change for running load variables was time = 0.2±5.2%, distance = 0.5±5.5%, steps = 0.4±5.8%, timeRPE = 5.1±10.2%, distanceRPE = 5.8±10.6%, and stepsRPE = 5.5±11.4% (Figure 1). Paired *t* tests demonstrated significant differences between average weekly percent change in time-timeRPE, distance-distanceRPE, and steps-stepsRPE ($p\leq.02$) (Table 1).

To our knowledge, this is the first study to compare weekly change in external loads and workloads during a full cross-country season in male and female high school runners. Significant differences were found between the average weekly change in external loads and workloads during the season. Specifically, average weekly change in running load was significantly lower for external loads (time, distance, steps) compared to their respective workloads (timeRPE, distanceRPE, stepsRPE). These findings are in agreement with previous research in adult and male high school long-distance runners that also reported that percent change in running load was significantly lower when using external loads versus workloads.[3,4]

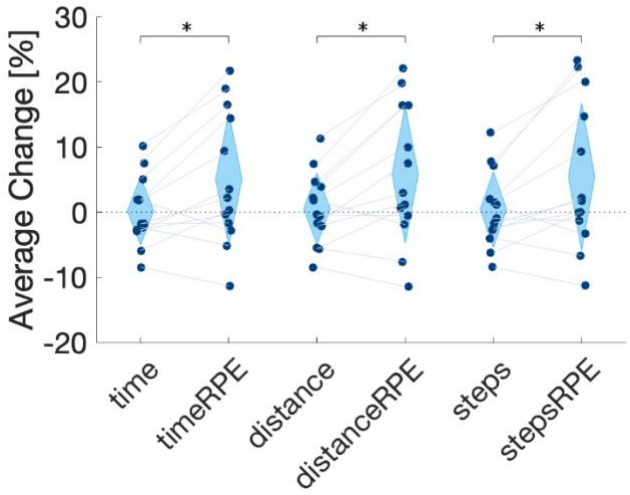

Figure 1: Average weekly percent change for running loads for each runner (dot) with mean±SD of all runners (blue diamond). *indicates significant difference.

Table 1. Paired *t* test mean difference [95% confidence interval].

Comparison	Mean Difference [95% CI]	*p*
time-timeRPE	-4.9% [-8.6%, -1.1%]	.01*
distance-distanceRPE	-5.3% [-9.0%, -1.6 %]	.01*
steps-stepsRPE	-5.0% [-9.1%, -1.0%]	.02*

Significance

Excessive progression in running load is believed to contribute to running-related injuries. Running programs are often designed to gradually increase running load to improve performance and reduce the risk of injury. However, these programs often only monitor external loads. Excluding the contribution of internal loads appear to underestimate the change in running load over a cross-country season. While prospective research is necessary to investigate if excessive progression in workload is a risk factor for sustaining a running-related injury, workload may better estimate running load than external loads alone.

References

1. Davis JJ (2019) *BMJ Open Sport Exerc Med.*
2. Paquette MR (2020) *JOSPT.*
3. Napier C (2019) *JAT.*
4. Ryan MR (2020) *Int J Sports Sci Coaching.*
5. Borg G (1998) *Borg's perceived exertion and pain scale.*

TRANSTIBIAL LIMB LOSS RETAINS A NORMAL METABOLIC COST IN 3-D SIMULATIONS OF WALKING

Ross H. Miller[1], Elizabeth Russell Esposito[2,3]
[1]Department of Kinesiology, University of Maryland, College Park, MD, USA
[2]DoD-VA Extremity Trauma & Amputation Center of Excellence, San Antonio, TX, USA
[3]Center for Limb Loss & Mobility, VA Puget Sound, Seattle, WA, USA
email: rosshm@umd.edu

Introduction

Below-knee limb loss and use of a prosthesis generally incurs a greater metabolic cost of walking than able-bodied individuals. However, high-functioning individuals with limb loss such as Service members do not experience this difference (Russell Esposito et al., 2014) and it is unclear how this is achieved.

We recently used optimal control simulations to show that walking with a transtibial prosthesis (i) does not increase metabolic cost when pre-limb loss levels of muscle strength are retained, particularly in the residual limb, and (ii) does not require large deviations from pre-limb loss gait mechanics (Russell Esposito & Miller, 2018). However, the musculoskeletal model was two-dimensional and many of the typical gait deviations of high-functioning individuals with transtibial limb loss occur outside of the sagittal plane (Rábago & Wilken, 2016).

Therefore, our purpose was to predictively simulate changes in metabolic cost of walking pre- vs. post-limb loss using a three-dimensional (3-D) musculoskeletal model. Based on previous human data (Russell Esposito et al., 2014), we expected that limb loss and transtibial prosthesis use would not increase the metabolic cost of walking above the pre-limb loss cost.

Methods

Optimal control simulations of walking were performed using a 3-D OpenSim model (Rajagopal et al., 2016). Muscle model parameter values were randomly assigned to define 36 "subjects" with different muscular strength and power capabilities. Optimizations were performed in Moco software using direct collocation to determine muscle excitations and associated model states that minimized a cost function (Dembia et al., 2020):

$$J = J_{track} + J_{effort}$$

where J_{track} was the mean squared deviation from average human kinetic and kinematic data from instrumented gait analysis (Miller et al., 2014). J_{effort} was the sum of squared muscle excitations, weighted by muscle mass.

In the pre-limb loss simulations, the models had two identical symmetric legs. In the post-limb loss simulations, the right ankle muscles were removed and the biological ankle/foot joints were replaced with linear spring-dampers representing a passive transtibial prosthesis (Russell Esposito & Miller, 2018). Metabolic costs pre- vs. post-limb loss were compared by two one-sided tests of equivalence, with a 2% change defined as the minimum effect of interest (Guidetti et al., 2018).

Results and Discussion

The change in metabolic cost pre- vs. post-limb loss (Fig. 1) was not significantly different from zero ($p = 0.38$) and fell within the equivalence bounds of ±2% ($p = 0.0001$). The simulated kinematics and ground reaction forces deviated from the able-bodied experimental means (Miller et al., 2014) by 0.51 standard deviations pre-limb loss and by 0.65 standard deviations post-limb loss. Differences in ground reaction forces pre- vs. post-limb loss (Fig. 2) were similar to those seen in individuals with and without transtibial limb loss (Sanderson & Martin, 1997).

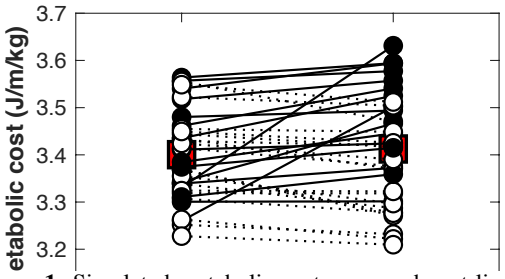

Figure 1: Simulated metabolic costs pre- and post-limb loss. Open circles/dashed lines had a decreased cost after limb loss and closed circles/solid lines an increased cost. Large squares are means.

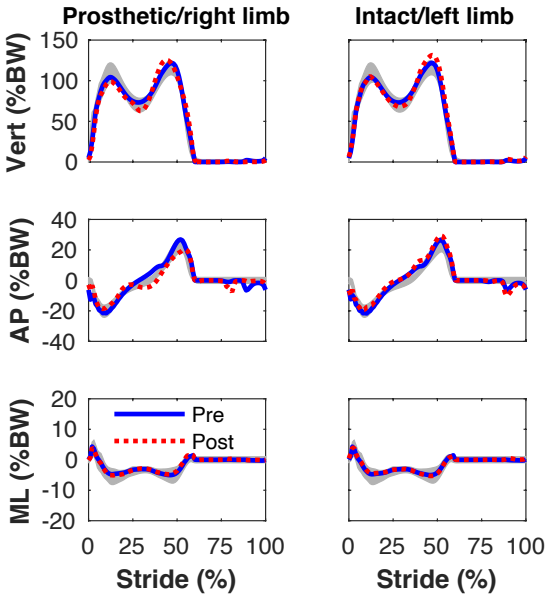

Figure 2: Ground reaction forces in % bodyweight (BW) pre- and post-limb loss. Shaded areas are mean±SD from Miller et al. (2014).

Significance

Transtibial limb loss *per se* may not directly increase the metabolic cost of walking.

References

Dembia et al. (2020): *PLoS Comp Biol* **16**, e1008493.
Guidetti et al. (2018): *PLoS One* **13**, e0209925.
Miller et al. (2014): *MSSE* **46**, 572-579.
Rábago & Wilken (2016): *Mil Med* **181**, 30-37.
Rajagopal et al. (2016): *IEEE TBME* **63**, 2068-2079.
Russell Esposito et al. (2014): *JRRD* **51**, 1287-1296.
Russell Esposito & Miller (2018): *PLoS One* **13**, e0191310.
Sanderson & Martin (1997): *Gait Posture* **6**, 126-136.

The views expressed herein are those of the authors and do not reflect the official policy or position of the US Army Medical Department, the US Army Office of the Surgeon General, Department of the Army, Department of Defense, Department of Veteran's Affairs or the US Government.

CERVICAL SPINE NEUROFORAMINAL CHANGES DURING A MULTI-AXIAL MOVEMENT: COMPARISON OF A COHORT WITH CHRONIC NECK PAIN AND HEALTHY CONTROLS

Craig C. Kage[1], Mathew R. MacEwen[1], Bryan Ladd[1], and Arin M. Ellingson[1]
[1]University of Minnesota, Minneapolis, USA
Email: ellin224@umn.edu

Introduction

Neck pain is a prevalent musculoskeletal condition with a myriad of potential contributing factors, one of which is neuroforaminal (NF) spacing [1]. Present evaluation of NF spacing is limited to static, planar, and/or superficial evaluation of the structures of the cervical spine. Biplane videoradiography is a method to capture *in vivo*, dynamic, 3D motion of the cervical spine [2]. Circumduction is a multi-axial task that investigates the unique coupling of the cervical spine, and mimics positions similar to Spurling's test during a dynamic physiologic loading motion [3]. The purposes of this study were to: 1) compare the NF height changes between those with chronic mechanical neck pain (MNP) and a healthy cohort (CTRL) and 2) to compare the *in vivo* kinematics during a multi-axial circumduction task.

Methods

After IRB approval and informed consent six participants were enrolled (recruitment and analysis ongoing) – three without neck pain (26.3±2.5 years, 1F, 2M) and three with a history of neck pain >12 weeks (32.7±7.8 years, 1F, 2M). CT's were acquired (0.2×0.2×0.6mm; 1.5mSv, Siemens Biograph), bone models of levels C5-C6 were segmented, and NF height landmarks were identified (MIMICS, Materialise) (C5: most superior point of the inferior pedicle, C6: most inferior point of the superior pedicle). Participants were trained in correct performance of a multi-axial left and right circumduction task (Fig 1) and completed three trials each during biplane videoradiography (160mA, 70-74kV, 3.5ms, 55° IBA, 174cm SID, 30Hz, 0.32mSv/trial to a metronome at 30 bpm. Calibration, undistortion, anatomic coordinate identification [4], and volumetric shape-matching were performed for levels C5-C6 for the final trial of right circumduction (DSX Suite, C-Motion Inc., USA). Data were filtered with a 4th order Butterworth filter (F_c = 3Hz) and relative kinematics and dynamic NF heights were extracted [5]. T-tests were performed in R/R Studio.

Results and Discussion

Kinematics were examined for C5 relative to C6 for each of the planar component motions (flexion/extension (FE), lateral bending (LB), axial rotation (AR)) of the circumduction task (Table 1). The MNP group demonstrated a significantly greater FE ROM ($p<0.001$) component of the circumduction task, but there were no significant differences in LB or AR motion components. The total time spent in extension (percentage of total motion) was not significantly different between groups (CTRL: 40.9±4.4%, MNP: 55.3±14.8%, p-value = 0.23).

Table 1: Total component ROM during R Circumduction

	FE C5/C6	LB C5/C6	AR C5/C6
CTRL	19.4±0.4	13.0±5.7	9.6±1.6
MNP	23.8±0.6	14.6±3.0	10.2±2.0
p-value	<0.001*	0.69	0.70

Percentage of NF height change from neutral are shown in Figure 1. Those with MNP demonstrated a trend towards greater time in diminished NF height (greater than -20% change from neutral) compared to controls (CTRL: 12.0±9.5%, MNP: 37.8%±14.5%, p-value = 0.06). This threshold was based on previous works showing a decrease of 20% NF area with physiological motion [6]. The timing of minimum NF height occurred between maximum right bending and extension. Although limited in scope and sample size, these results indicate that for the same multi-axial task – those with MNP tend to spend more time in a diminished NF position. This may be related to the significantly increased FE ROM observed at C5/C6 in those with MNP compare to the CTRL group; although time spent in extension was not significantly different between groups, those with MNP did trend towards more time in extension.

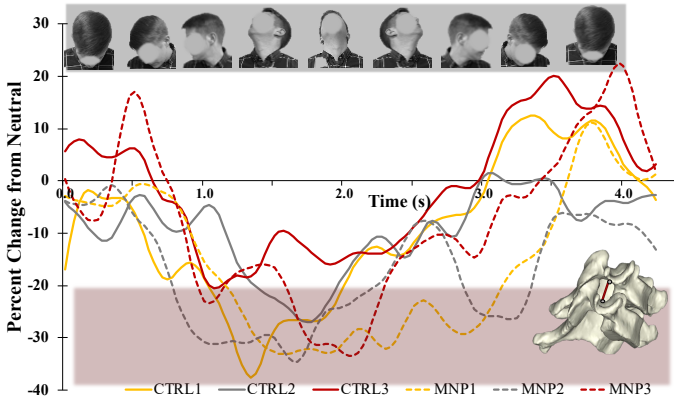

Figure 1: C5/C6 neuroforaminal height changes from neutral during a right circumduction task (top). Red shaded box highlights area with >20% closing of NF height from neutral.

Significance

Our preliminary results indicate that even with a limited sample size, differences were observed in a clinically relevant metric (NF height) between those with MNP and CTRL during a multi-axial, circumduction task. Further, this work demonstrates the feasibility of analyzing a complex, multi-axial task and extracting kinematic and dynamic NF data. Future research will expand to a broader population, additional levels of the cervical spine, and additional trials and repetitions.

Acknowledgments

Funding: NIH/NICHD R03 HD09771, NIH/NIAMS T32 AR050938 Musculoskeletal Training Grant, and Foundation for Physical Therapy Research (Promotion of Doctoral Studies II).

References

[1] Muhle, C., et al., Invest Radiol, 1998. [2] Kage, C.C., et al., PloS One, 2020. [3] Ellingson, A.M. et al., Clin Biomech, 2013. [4] Anderst, W.J., et al., Spine J, 2014. [5] Lawrence RL. MATLAB: Kinematics Toolbox. [6] Nuckley et al. Spine 2002.

MACHINE LEARNING PREDICTION OF PITCHING ARM STRESS

Kristen F. Nicholson[1], Gary S. Collins, Brian R. Waterman[1], and Garrett S. Bullock[1]
[1]Department of Orthopaedics, Wake Forest School of Medicine, Winston-Salem, USA
email: kfnichol@wakehealth.edu

Introduction

Musculoskeletal injuries in baseball players are a persistent and significant problem, with the greatest incidence attributed to the shoulder and elbow.[1] Pitching arm injuries are often contributed to excessive shoulder distraction force[5] and elbow valgus torque.[9] Over the past decade, research has attempted to elucidate the cause of these injuries. However, increasing velocity and performance is an equally important consideration. Theoretically, there are pitching mechanics that can optimize this balance of high pitch velocity and low joint stress. Optimal pitching mechanics, or pitching efficiency, is difficult to address due to the complex nature and large quantity of variables involved in the pitching motion.

Past research has examined how mechanics influence joint stress and pitching velocity, as well as how pitching velocity influences joint stress.[10] Much of the literature includes correlational studies with one or two variables. There is a lack of research investigating the relationship and influence of multiple variables on arm stress. Additionally, research suggests that a minimum of 40% of mechanical issues can be corrected once they are identified,[14] however there are no suggestions on which issues are the most important. The purpose of this study was to identify which variables have the most influence on elbow valgus torque and shoulder distraction force using a machine learning approach.

Methods

A retrospective review was performed on baseball pitchers who underwent biomechanical evaluation at the University biomechanics laboratory.

Regression models and four machine learning models were created for both elbow valgus torque and shoulder distraction force. All models utilized the same predictor variables, which included: pitch velocity and 17 pitching mechanics.

Results and Discussion

The analysis included a total of 168 pitchers with a mean age of 16.7 years (sd = 3.2). For both elbow valgus torque and shoulder distraction force, the gradient boosting machine models demonstrated the smallest RMSEs and the most precise calibrations compared to all other models (Table 1). The gradient boosting model for elbow valgus torque reported highest influence pitch velocity (relative influence: 28.4), maximum shoulder external rotation (9.23), lead leg maximum ground reaction force (6.6), shoulder abduction at foot strike (6.3), and maximum humeral rotation velocity (6.3). The gradient boosting model for shoulder distraction force reported highest influence for pitch velocity (20.4), maximum humeral rotation velocity (9.6), shoulder abduction at foot strike (6.5), maximum shoulder external rotation (6.5), shoulder abduction at release (5.7), difference of time to maximum trunk rotation velocity to pelvis rotation velocity (5.6), and trunk forward flexion at release (5.5).

While pitch velocity was the most influential variable, pitching mechanics revealed significant influence in both elbow and shoulder models. Pitchers and coaches should be aware that increases in velocity augment arm stress and should consider this in pitch counts at full intent. However, it is encouraging that there are modifiable mechanical factors that also influence arm stress. The elbow valgus torque model reported four variables in addition to pitch velocity with a relative influence greater than 5%. The shoulder distraction force model reported six biomechanical variables with relative influence over 5%. Maximum humeral rotation velocity, shoulder abduction at foot strike, and maximum shoulder external rotation were influential variables common to *both* elbow valgus torque and shoulder distraction force. Focusing on these three variables may be the best way to impact both elbow and shoulder stress.

Significance

The results of this study can be used to inform players, coaches, and clinicians on specific mechanical variables that may be optimized to mitigate elbow or shoulder stress that could lead to throwing related injury.

References

1. Agresta et al. *Orthop J Sport Med.* 2019
2. Bullock et al. *J Sci Med Sport.* 2020
3. Collins et al. *Eur J Cardio-toracic Surg.* 2013
4. Collins et al. *BMJ.* 2015
5. Fleisig et al. *Sport Biomech.* 2009

Table 1. Statistical and Machine Predictive Model Performance

Predictive Model	Root Mean Square Error		Calibration Slope	
	Elbow Valgus Torque	Shoulder Distraction Force	Elbow Valgus Torque	Shoulder Distraction Force
Generalized Regression	0.80	21	1.00 (95% CI: 0.86, 1.14)	1.00 (95% CI: 0.88, 1.12)
Random Forest	0.46	13	1.34 (95% CI: 1.26, 1.42)	1.25 (95% CI: 1.16, 1.34)
Gradient Boosting Machine	0.013	1.7	1.00 (95% CI: 0.999, 1.001)	1.00 (95% CI: 0.999, 1.001)
Support Vector Machine Regression	0.10	2.8	1.07 (95% CI: 1.06, 1.08)	1.08 (95% CI: 1.07, 1.09)
Artificial Neural Network	0.072	6.4	1.00 (95% CI: 0.92, 1.08)	1.00 (95% CI: 0.99, 1.01)

Elbow Valgus RMSE is reported as % body weight x height; Shoulder distraction RMSE is reported as % body weight

A COMPARISON OF THREE APPROACHES TO CALIBRATING INSTRUMENTED ORTHOPAEDIC DEVICES

Julia A. Henke[1], J. Kalshoven[1], J. J. Crisco[1]
[1]Brown University School of Engineering, Department of Orthopaedics, Warren Alpert Medical School, Brown University
email: julia_henke@brown.edu

Introduction

The joint between the trapezium and the first metacarpal, which gives the thumb much of its mobility, is the second most common site of osteoarthritis in American adults (Dahaghin et al., 2005). An instrumented trapezium, iTRAPZ, to measure *in vivo* loads on the joint using nine strain gages (three rosettes) is proposed to gain more insight into the joint and the loads it experiences regularly. Using strain gages requires transforming the strain gage voltage readings into relevant load data. There is no standardized way to do this, so we explored different supervised machine learning methods: a least squares approximation method, which is sometimes referred to as Bergmann's Matrix Method (Bergmann et al.,1988), a multiple linear regression (MLR) model, and a cascade-forward neural network method. The aim of this study was to evaluate and compare these potential load prediction methods.

Methods

The three methods, hereafter referred to as the BM (for Bergmann matrix), MLR, and NN methods, were all coded in MATLAB. Their load predictions were compared with the actual measured load using Bland-Altman analysis (Bland & Altman, 1986) and average relative error (Bergmann et al., 2008).

Bergmann Matrix Method

The matrix method uses least squares to solve for the calibration matrix. This was done using MATLAB® operator "/" (MATLAB, Mathworks, Natick MA, mrdivide/). An intercept (a row of ones) was added to the strain matrix before calibration to increase accuracy.

MLR Method

One regression was executed for each DOF component (Fx, Fy, Fz, Mx, My, Mz). The MATLAB® function "regress" was used (MATLAB, Mathworks, Natick MA, regress).

Supervised Neural Network Method

The supervised neural network method used two cascade-forward nets (MATLAB, Mathworks, Natick MA, cascadeforwardnet). The first network was trained with the Levenberg-Marquardt training function (trainlm) on all six components, and the first three rows of the resulting load matrix (Fx, Fy, Fz) were saved. The second network used the Bayesian Regularization training function (trainbr) for just the moment components. The two networks had a lower sum of average relative error than either alone.

Results and Discussion

All three methods were able to predict loads corresponding to strain values generated by analytical models of the iTRAPZ design with an average relative error (summed across all the load components) of 1.5%, and a limit of agreement range of about 1N for force components and 1Nm for moment components. The results of the three testing parameters showed a sharp decrease in error for the NN method after about 10,000 data points, while the other two methods remained stable. Most notably, the testing showed that good load predictions can still be made when removing some gages and not others. For example, if the 45° gages are removed from each rosette, the predictions are not adversely affected, but if two gages are removed from the same rosette and one of them is the 0° gage, error and limit of agreement range drastically increase (from 1N to around 30N) – for all methods except for the NN (Fig. 1).

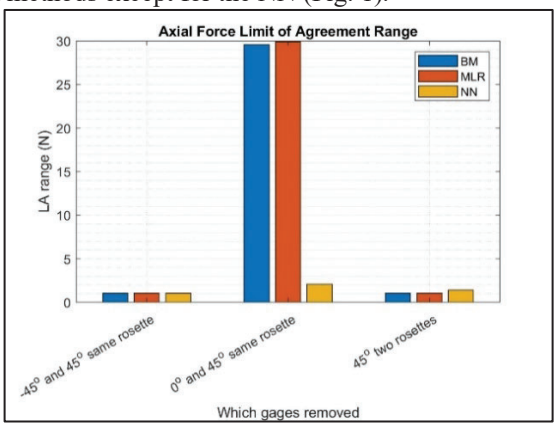

Figure 1: visualization of NN method robustness when removing certain strain gages

Although benchtop data collection and calibration are still ongoing, each method is able to predict applied loads and match the shape of the load application closely with a limit of agreement range that is smaller for moments and larger for force components, and also a larger bias than the tests done with generated data.

In summary, all methods yield good prediction results, but the NN method offers a new way to get accurate predictions given what would otherwise be considered incomplete data. The NN method, however, requires larger quantities of data and has a longer runtime.

Significance

This research presents novel means of calibrating instrumented orthopaedic implants, which could increase the robustness and ease of obtaining *in vivo* joint loading information.

Acknowledgments

This research was supported in part by funding from NIH R21 AR077201

References

Bergmann, G., et al. (2008). Design and calibration of load sensing orthopaedic implants. *Journal of Biomechanical Engineering*, *130*(2), 021009.

Bergmann, G., et al., (1988). Multichannel strain gauge telemetry for orthopaedic implants. *Journal of Biomechanics*, *21*(2), 169–176.

Bland, J. M., & Altman, D. G. (1986). Statistical methods for assessing agreement between two methods of clinical measurement. *Lancet (London, England)*, *1*(8476), 307–310.

Dahaghin, S., et al. (2005). Prevalence and pattern of radiographic hand osteoarthritis and association with pain and disability (the Rotterdam study). *Annals of the Rheumatic Diseases*, *64*(5), 682–687.

WEEK-TO-WEEK CHANGES IN RUNNING LOAD ARE DIFFERENT IN HIGH SCHOOL RUNNERS WHEN COMPUTED USING 1-, 2- AND 4-WEEK CYCLES

David M. Bazett-Jones,[1] Micah C. Garcia,[1] Max Paquette[2]
[1]University of Toledo, Toledo, OH, USA
[2]University of Memphis, Memphis, TN, USA
email: david.bazettjones@utoledo.edu

Introduction

Monitoring training stress in runners beyond weekly 'mileage' has become more and more popular with the improvement in wearable and other technologies. Long-distance runners and coaches traditionally only monitor external loads (e.g., distance, time) because they are simple to measure and prescribe. There has been an increased interest to monitor running loads that considers internal loads (e.g., physiological response to the external load).[1] Workload (i.e., measures of training stress) incorporates both external and internal loads and accounts for the potential interaction between these loads. Running workloads appear to yield different week-to-week changes depending on the external loads used in both adult and high school runners.[2,3] These studies used 1-week cycles to analyse week-to-week changes in running workload during a two-week cycle, but it is unknown if using longer monitoring cycles influences these results. Therefore, the purpose of this study was to compare 1-, 2- and 4-week cycles for computing weekly change in training stress among different external loads and workloads during a full high school cross-country season.

Methods

Eleven high school runners (F=9, M=2, age=16.0±1.3 years) recorded all running sessions with a GPS watch (Garmin 45s) during an entire cross-country season. After each running session, runners also self-reported distance, time, and rate of perceived effort (RPE) (1=very easy, 10=maximal)[4] using an electronic running log (Qualtrics). External loads (distance, time, steps) were extracted from GPS watch data. If the participant did not record their run with the GPS watch, distance and time were used from the running log for that session.

Workload measures were calculated as the products of RPE with distance (D-RPE), time (T-RPE) and steps (S-RPE), respectively. For each 1-, 2- or 4-week cycles in the season, external loads and workloads were summed, and the percentage change was calculated for each running load variable relative to the previous week.[2] ANOVAs were used to compare cycle lengths across all external load and workload variables. Sidak pairwise tests were used when significant main effects were identified ($p \leq .05$).

Results and Discussion

Significant main effects were found for all measures ($p<0.05$) except T-RPE ($p=0.08$). A significantly higher percent change was seen when using the 1-week compared to the 2-week cycle for distance ($p=0.005$), time ($p=0.001$), steps ($p=0.002$), D-RPE ($p=0.030$), and S-RPE ($p=0.046$; Figure 1). A significantly higher percent change was seen when using the 4-week compared to the 2-week cycle for distance ($p=0.009$), time ($p=0.003$), steps ($p=0.002$; Figure 1).

This is the first study to compare different methods of calculating weekly change in running loads. Previous studies have used 1-week cycles to measure percent change.[2,3] It is unknown what the most appropriate cycle length is for these analyses and which provides the most important information for running performance and/or injury risk detection. Although, it has been suggested that training load errors occur 3-4 weeks prior to the onset of a bone stress injury,[5] it is possible that currently used external and internal load variables are not sensitive enough to detect tissue damage using these monitoring approaches.

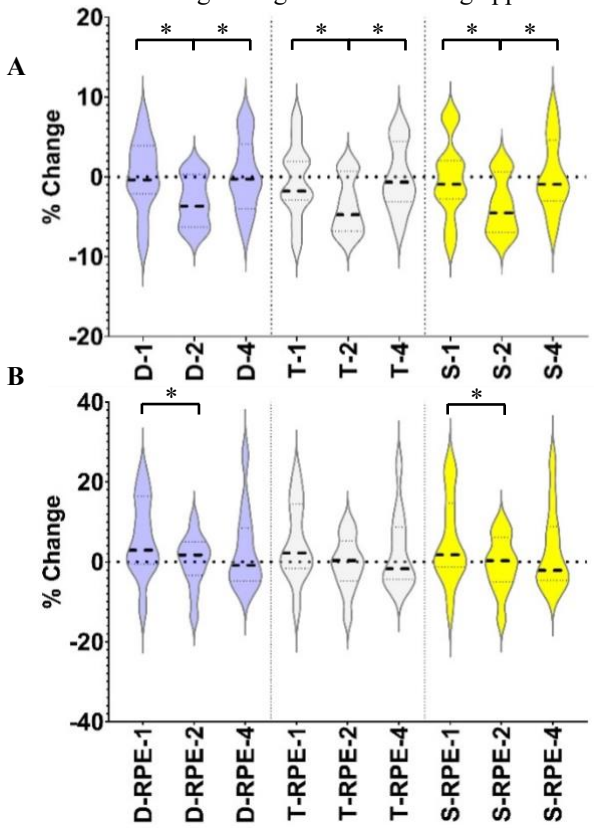

Figure 1: Average weekly percent change for running external loads (A; D=distance, T=time, S=steps) and workloads (B; D-RPE=distance•RPE, T-RPE=time•RPE, S-RPE=steps•RPE) compared across 1-, 2- and 4-week timeframes. *Significant difference.

Significance

Excessive progression in running load is believed to contribute to running-related injuries. Our findings indicate that the timeframe of calculating percent change results in different values. Understanding which timeframes are most relevant is required of future research.

References

1. Paquette MR (2020) *J Orthop Sports Phys Ther.*
2. Napier C (2019) *J Athl Train.*
3. Ryan MR (2020) *Int J Sports Sci Coaching.*
4. Borg G (1998) *Borg's perceived exertion and pain scale*
5. Warden S (2021) *Current Osteoporosis Reports*

PERFORMANCE EVALUATION OF K-MEANS AND HIERARCHICAL CLUSTERING ON LUMBAR KINEMATICS

Seth Higgins[1], Sandipan Dutta[1], Rumit Singh Kakar[1]
[1]Old Dominion University, Norfolk, Virginia USA
Email: shigg002@odu.edu

Introduction

As the amount of data in biomechanics and the interest in machine learning increases, we need to determine best practices to ensure accurate conclusions and reproducibility.[1] Biomechanics research tends to focus on analyzing movement patterns through discrete variables extracted from a time series because it is difficult to identify patterns in time-series movement data. Clustering algorithms provide a unique opportunity for biomechanists to analyze movement data from a time-series. Clustering algorithms can be used as a diagnostic tool by identifying non-pathological and pathological movement patterns. Clustering aims to take an unlabeled set of data and organize them into homogenous groups.[2]

There are many different clustering techniques to choose from, but k-means and hierarchical clustering analysis (HCA) are the most commonly used. k-means computes faster than HCA and can handle a large number of variables, but the number of clusters need to be specified beforehand and the results are dependent on the initial centroid definition.[3,4] HCA does not require any predefined number of clusters, but this method is more computationally expensive.[5] Agglomerative HCA merges similar time-series together forming a larger cluster.[5] This process continues until all time-series are arranged in similar groups clusters. In order to select the most appropriate algorithm, for biomechanical data set, different clustering approaches might need to be compared. Therefore, the purpose of this study was to compare clustering accuracy between k-means and HCA using lumbar segmental kinematics during lumbar flexion and extension motion.

Methods

87 healthy adults (Young (YA): n = 53; 26.4±6.6 yr; Middle-Age (MA): n = 34; 51.9±7.0 yr) performed maximal lumbar flexion and extension while 3D kinematics of the lumbar spine were calculated. Lumbar segmental kinematics were clustered using k-means and agglomerative HCA algorithms. Each algorithm was run using MATLAB's built-in function (k-means: *kmeans*; HCA with Ward linkage: *clusterdata*) Silhouette coefficients, using *evalcluster* function, were calculated to determine the appropriate number of clusters for each method and to determine which method provided the least error. Silhouette coefficients range from -1 to 1. Vectors with a coefficient value between 0 and 1 represent correct cluster match and vectors with value below zero are matched incorrectly. Silhouette coefficients were averaged across all clusters to produce an overall silhouette score. The greater overall silhouette score indicates a more accurate clustering result.

Results and Discussion

Each cluster in **figure 1** represents a group of subjects that moved their lumbar spine in similar manner. The difference between HCA 1-4 during flexion is the timing of maximum flexion and cluster 4 also had reduced lumbar flexion.

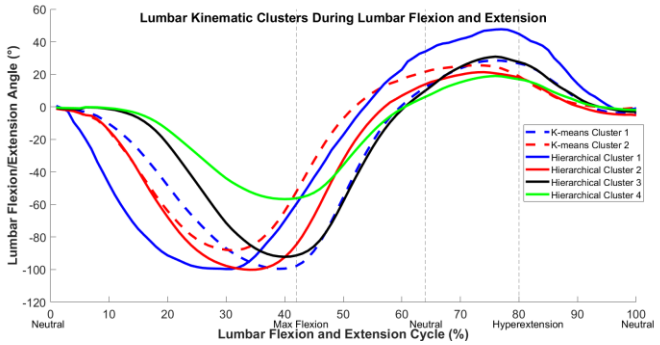

Figure 1: k-means and hierarchical clustering for lumbar kinematics.

During hyperextension, HCA 1 had greater lumbar hyperextension than clusters 2-4. For the k-means, cluster 1 had greater lumbar flexion, but no visual difference in hyperextension. The silhouette score determined that the appropriate number of clusters are 2 for k-means and 4 for HCA. For k-means, the number of participants in cluster 1 and 2 were 34 and 53, and for HCA 1, 2, 3 and 4 were 8, 37, 16 and 26, respectively. For both clustering methods, YA and MA adult participants were distrusted across all clusters. For k-means, cluster 1 had 21 YA and 13 MA adults and cluster 2 had 31 Y and 22 MA adults. For HCA, cluster 1 had 7 YA and 1 MA, cluster 2 had 21 YA and 16 MA, cluster 3 had 8 YA and 8 MA and cluster 4 had 16 YA and 10 MA. The silhouette score for k-means and HCA were 0.43 and 0.33, indicating that k-means with 2 clusters produced more accurate clusters.

Significance

k-means provided more accurate clusters than HCA. This shows that using k-means for this data set may be a better method when clustering lumbar kinematics than HCA. However, different situations may call for HCA, such as when the number of clusters are not known prior to analysis. HCA can be used to visualize the subclusters through a dendrogram to determine the appropriate number of clusters. HCA also does not depend on picking a random initial cluster, making this method more reproducible than k-means. Clustering can be used to determine patterns in biomechanical time series data such as running, throwing or jumping and is not limited to use with kinematic data. This study provides a basic framework for choosing clustering type.

References

1. Halilaj et al., 2018. *J. Biomech.* 81: 1-11.
2. Liao, 2005. *Pattern Recognit. Lett*. 38: 1857-74.
3. Dhanachandra et al., 2015. *Procedia Comput. Sci.*54: 764-771.
4. Aghabozorgi et al, 2015. *Inf. Syst. J.* 53: 16-38.
5. Bouguettaya et al., 2015. *Expert Syst Appl*. 45: 2785-2797

Implementation of Asymmetric Walking to Correct Between-Limb Gait Asymmetries in Post-ACLR Individuals

Yannis K. Halkiadakis*[,1], Helia Mahzoun Alzakerin[1], and Kristin D. Morgan[1]
[1]*Department of Biomedical Engineering, School of Engineering, University of Connecticut, Storrs, CT, USA*
Email: *yannis.halkiadakis@uconn.edu

Introduction

Anterior cruciate ligament (ACL) injuries are common, with over 250,000 tears occurring each year [1]. Despite ACL reconstruction (ACLR) and extensive rehabilitation, between-limb gait differences can persist in post-ACLR individuals. These gait differences lead to altered limb loading rate which contributes to detrimental knee loading and the initiation of post traumatic knee osteoarthritis [2]. Moreover, these changes likely reflect how post-ACLR individuals adopt compensatory strategies where they tend to either underload or overload their limb. Hence early rehabilitation efforts and return-to-sport criteria are often directed at restoring between-limb symmetry. While restoring between-limb symmetry is challenging, stroke research offers a promising approach that utilizes asymmetric walking [3]. Asymmetric walking occurs when an individual is made to intentionally walk with each limb moving at a different speed. This walking asymmetry functions to correct adverse between-limb gait differences. Since asymmetric walking has been little explored in post-ACLR, the objective of this study is to evaluate the effectiveness of the asymmetric walking in restoring between-limb loading rate symmetry. We hypothesized that the asymmetric walking would result in the adaptation of symmetric loading rate over time in the post-ACLR individuals.

Methods

Eight post-ACLR individuals (>1 year from return-to-sport clearance) with varying graft types (age 20.4 ± 0.9 yrs; height 1.76 ± 0.09 m; mass 73.0 ± 11.1 kg) participated in an asymmetric walking protocol. Participants walked on an instrumented split-belt treadmill (Bertec Corporation, Columbus, Ohio), with vertical ground reaction force (vGRF) data collected at 1200 Hz and low pass filtered at 35 Hz using a 4th order Butterworth filter. Participants performed a five-minute warm-up period at a self-selected walking speed to acclimate to the equipment. Participants then completed a ten-minute asymmetric walking trial, where one leg moved at 1.0 m/s and the other moved at 1.5 m/s and then the limb asymmetry protocol was reversed.

The loading rate was extracted from the vGRF using a custom MATLAB code (MATLAB R2019a, The MathWorks, Inc., Natick Massachusetts, USA). The loading rate data were divided into ten 1-minute segments and the mean loading rate was computed for each minute to assess the gait adaptation pattern over time (Table 1). The adaptive gait changes were assessed in the injured and non-injured limbs. A repeated measures ANOVA was performed to determine if the post-ACLR individuals adopted between-limb loading rate symmetry over time ($\alpha = 0.05$).

Results and Discussion

The results supported the hypothesis that post-ACLR individuals adopted symmetric between-limb loading rates in response to the asymmetric walking protocol over the ten-minute walking period (Fig. 1, Table 1). The repeated measures ANOVA (R^2= 0.97) rejected the null hypotheses that the loading rate did not change over time (p=0.003) and that there were no differences in the overall loading rate pattern over time for the two limbs (p=0.02). The repeated measures model predicted a higher average loading rate for the injured limb at minute 1. In addition, it predicted a decrease in the loading rate over time for the injured limb. As expected, there are significant differences between the participants.

The objective of this work is to demonstrate how the post-ACLR individuals adopted healthy, symmetric loading rate in response to the asymmetric walking protocol. Here, the asymmetric walking protocol was able to correct between-limb differences due to a 0.50 m/s gait perturbation. Moreover, this work revealed that the positive response to the asymmetric walking protocol was dependent on which limb is set at the faster speed. While this study was successful in identifying the adoption of healthy gait dynamics in post-ACLR individuals in response to an asymmetric walking protocol, future work will evaluate the long-term storage of the healthy gait dynamics once the asymmetric gait perturbation is removed.

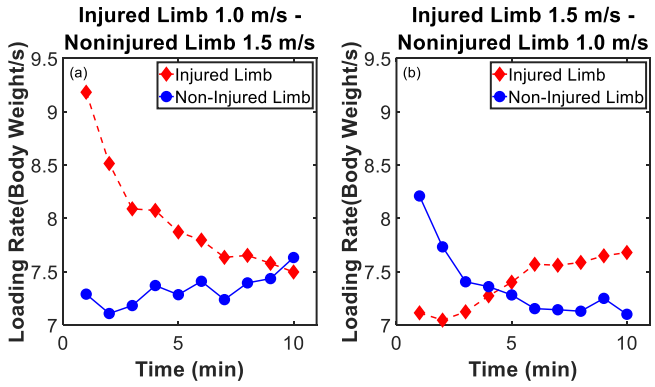

Figure 1. Comparison of the mean loading rate for each minute during the asymmetric walking trial when (a) the injured limb was set at the slower speed and (b) when the injured limb was set at the faster speed.

Significance

The overarching objective of this research is to develop a gait retraining protocol that can restore symmetric gait patterns in post-ACLR patients, in the hopes lowering risk of injury and risk of knee OA development.

References

[1] Noehren et al. (2013). *Med Sci Sports Exerc*, 45(7): 1340-1347.
[2] Hall et al. (2012). *Gait & Posture,* 36(1): 56-60
[3] Reisman et al. (2007). *Brain*, 130(7): 1861-1872.

Table 1. Average loading rate for injured and non-injured limbs during injured 1.0 m/s - non-injured 1.5 m/s trial (mean ± standard deviation

Limb	Minute 1	Minute 2	Minute 3	Minute 4	Minute 5	Minute 6	Minute 7	Minute 8	Minute 9	Minute 10
Injured Limb	9.2 ± 1.6	8.4 ± 1.6	8.1 ± 1.5	8.2 ± 1.8	8.0 ± 1.8	7.8 ± 1.8	7.8 ± 1.7	7.9 ± 1.7	7.7 ± 1.6	7.7 ± 1.5
Non-Injured Limb	7.3 ± 1.4	7.1 ± 1.5	7.2 ± 1.5	7.4 ± 1.4	7.3 ± 1.4	7.4 ± 1.5	7.2 ± 1.5	7.4 ± 1.5	7.4 ± 1.4	7.6 ± 1.5

COMPARISON OF FRONTAL PLANE ANGLES BETWEEN ADOLESCENT RUNNERS WHO RUN IN MOTION CONTROL AND NEUTRAL SHOES

Eryn L. Close[1*], Micah C. Garcia[1], and David M. Bazett-Jones[1]
[1] University of Toledo, Toledo, OH, USA
email: * eryn.close@rockets.utoledo.edu

Introduction

To accommodate consumer requests for comfort and ideas about injury prevention, running shoe manufacturers have developed many different models of running shoes, including motion control (MC) and neutral running shoes. MC shoes attempt to limit pronation through variations in medial and lateral sole support, while neutral shoes allow the foot to move freely[1,2]. Some studies reported that joint motion is reduced when running in MC shoes[2,3], while others have reported contradictory results[1]. Most footwear research has been collected on adult runners and results are generalized to adolescents. However, the potential confounding effects of growth and maturation may limit the application to younger runners. Therefore, the purpose of this study was to compare frontal plane running kinematics between adolescent runners who run in MC and neutral shoes. We hypothesized that adolescents who run in MC shoes would demonstrate smaller peak frontal plane angles than adolescents who run in neutral shoes.

Methods

59 uninjured adolescent long-distance runners (F=34, M=25; age=14.7±2.4 years) participated in this study. Participants were instrumented with reflective markers and ran over a 20-meter runway at a self-selected speed. Kinematic data were collected with a 12-camera system (Motion Analysis Corp) and exported to Visual3D (C-Motion, Inc.) for analysis. Right side stance phase data from a minimum of three trials were averaged for analysis. Dependent variables included peak hip adduction, knee abduction, and shoe eversion angles. ANCOVA tests using running speed as a covariate compared peak frontal plane joint angles between participants who ran in MC shoes (n=16) to participants who ran in neutral shoes (n=43). Running shoe type was determined according to manufacturer details that were retrieved online. Cohen's *d* effect sizes were also computed. Significance was set at $p<0.05$.

Results and Discussion

No significant differences were found in peak hip adduction (MC=13.9°±3.8°; neutral=13.6°±3.8°; p=.80, d=0.08), knee abduction (MC=-2.9°±2.7°; neutral=-2.8°±3.7°; p=.91, d=0.03), or shoe eversion angles (MC=6.7°±2.4°; neutral=7.9°±3.9°; p=.62, d=0.37) between shoe types (Figure 1). Our results indicate that peak frontal plane joint angles are not different between adolescent long-distance runners who run in MC and neutral shoes. MC shoes are designed to limit joint motion. However, the lack of significant difference between adolescents who ran in MC shoes compared to those who ran in neutral shoes questions if the shoe design actually limits motion. A previous study in adult runners also reported no significant difference between peak hip adduction, knee abduction, or shoe eversion between MC and neutral shoes[1]. Another study reported peak shoe eversion was significantly lower in MC shoes compared to neutral shoes[2]; however, the magnitude of the difference was only 0.9° between shoe types. While our study found peak shoe eversion that was 1.2° less for the MC shoe group, the large variability among runners and small sample size likely contributed to the non-significant difference compared to the neutral shoe group. The previous studies had their participants run in standard lab shoes[1-3] while our participants ran in their own preferred shoes, which increases the external validity of our findings because participants did not need to adapt to lab shoes.

Our results should be interpreted within the context of our limitations. First, markers were placed on the shoes rather than directly on the foot, similar to other studies[1]. While this acts as a surrogate measure of foot motion, we are unable to measure motion of the foot itself. Second, we did not record the age or distance run in the participants' shoes. Greater sole stiffness has been reported in running shoes that have been worn for greater running distances[4]. which may contribute to running kinematics.

Significance

To our knowledge, this was the first study to investigate running biomechanics between adolescent runners who ran in different types of shoes. It is reasonable to expect MC shoes would limit shoe eversion due to added support built into the shoe. However, we did not find significant differences in peak frontal plane angles at the hip, knee, or shoe between adolescent runners who ran in MC shoes compared to those who ran in neutral shoes. This suggests MC shoes may not actually control joint motion for adolescent runners.

References

1. Langley B (2019) *J of Applied Biomechanics*.
2. Lilley K (2013) *Gait & Posture*.
3. Rose A (2011) *Physiotherapy*.
4. Herbaut P (2017) *Gait & Posture.*

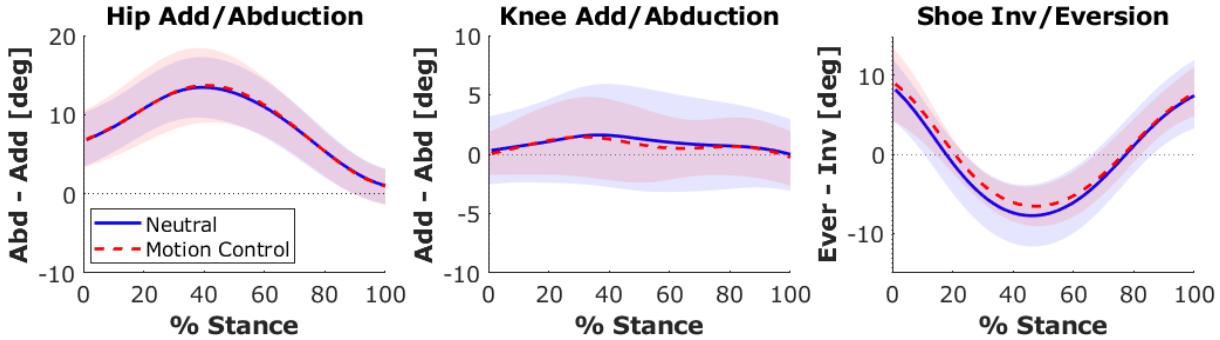

Figure 1. Ensemble average waveform (mean±SD) for frontal plane angles during stance phase between MC and neutral shoe groups.

FRONTAL-PLANE WHOLE-BODY ANGULAR MOMENTUM DURING PRE-PLANNED AND LATE-CUED TURNS

Mitchell Tillman and Antonia Zaferiou
Stevens Institute of Technology, Biomedical Engineering Dept., Hoboken, NJ USA
email: mtillman@stevens.edu

Introduction

Transitional maneuvers, like turning while walking, are performed daily and challenge balance. Turning requires the simultaneous maintenance of multiple contrasting mechanical objectives including translation, rotation, and balance. Often, an environmental cue to turn appears with less time for the motor system to pre-plan the turn. This is known as a late-cued turn.

Whole-body angular momentum (H) is a measure of balance control [1]. Excess angular momentum can lead to loss of balance and falls, especially in the frontal plane where balance cannot be easily recovered by stepping. The purpose of this study was to compare the effects of pre-planned and late-cued turns on frontal-plane balance control. We hypothesized that during late-cued turns, participants will use larger frontal-plane range of angular momentum than during pre-planned turns and straight-line gait.

Methods

Four healthy young adults participated in this study (2 female; age 27 ± 2 years; weight 68 ± 8 kg; height 1.75 ± 0.02 m) after providing informed consent in accordance with the IRB. A 14-segment whole-body kinematic model [2] was constructed using optical motion capture data (200 fps; Optitrack, USA). Participants were instructed to imagine that they were walking in a grocery store in three contexts. Tape on the floor marked walkways 0.915 m (36") wide (per ADA standards) in a "T", simulating a grocery store aisle intersection. First, participants walked straight for 10 m five times. Next, they performed a set of 10 pre-planned 90˚ turns to the left after walking 5 m. Finally, they performed 10 late-cued 90˚ turns to the left, randomly interspersed with 10 trials during which they did not turn. Upon reaching the intersection a visual late cue was provided on a 84" monitor at the end of the perpendicular aisle. Either the grocery item of interest (green broccoli) or a red "no" sign appeared, indicating whether to turn or continue straight, respectively.

3D angular momentum (H) about the body center of mass was expressed relative to a pelvis-fixed anterior axis to study frontal-plane H. Dividing H by the product of subject height (m), mass (kg), and $\sqrt{g * height}$ (m/s) normalized it to a dimensionless form [1]. Negative H indicated leftward rotation of the body above the center of mass, towards the inside of the turn (Fig. 1). The phase of interest in straight-line trials was during steady-state gait, between the third and third to last heel strike (approximately 5 strides). The phase of interest for pre-planned and late-cued trials was during the turn. Turns began at the heel strike prior to pelvis rotation about the vertical axis increasing three standard deviations above person-specific straight-line gait values. Turns ended at the first heel strike after pelvis rotation decreased below that same threshold, with respect to the new direction of travel. During these phases of interest, the median H was found within each footfall and the maximum magnitudes of the medians were used to calculate a range for each trial. Data were heteroscedastic, therefore the Kruskal-Wallis omnibus test compared the ranges within-subject across the three tasks (*Straight*, *Pre-Planned*, and *Late-Cued*) and post-hoc Mean Rank test pairwise multiple comparisons were performed.

Results and Discussion

Frontal-plane H fluctuated such that maxima occurred during double support after right foot heel strike, while the minima occurred during double support after left foot heel strike. Frontal-plane whole-body H magnitudes during straight-line gait were generally within 10% of the ranges reported by [3].

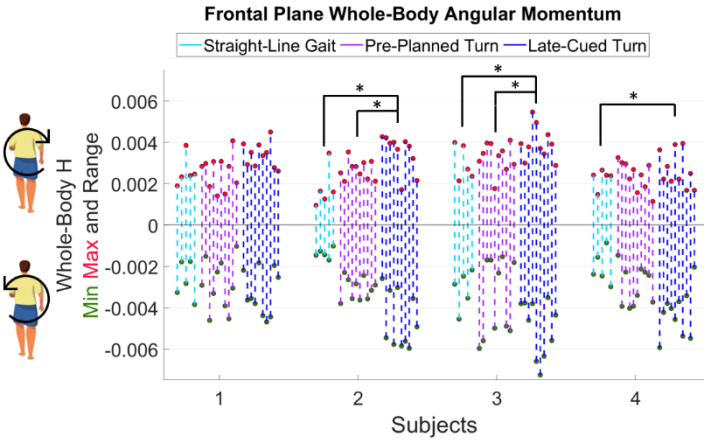

Figure 1: Whole-body frontal-plane H min (green), max (red), and range (dashed lines) for each trial for each participant during straight-line gait (cyan), pre-planned turns (purple), and late-cued turns (blue) tasks. Negative H indicates leftward rotation of the body above the center of mass, towards the inside of the turn.

Three of four participants significantly increased the range of frontal-plane H used during straight-line gait vs. late-cued turns ($p_{S2}<0.0001$, $p_{S3}=0.02$, $p_{S4}=0.03$), while two participants increased range during pre-planned vs. late-cued turns ($p_{S2}=0.01$, $p_{S3}=0.03$). No differences in range were observed between straight-line gait and pre-planned turns (min. $p\geq0.26$). Taken together, these preliminary results suggest that late-cued turns increase the range of frontal-plane H more than pre-planned turns. Though pre-planned turns have previously been found to alter mean frontal-plane H [4], we did not find this pattern in our small cohort. In the future, we will expand study enrollment and examine this phenomenon in older adults, who may respond differently due to age-related changes in balance control.

Significance

Control of angular momentum (H) is a proxy for balance control. Our novel finding that late-cued turns increased H in healthy young adults provides initial evidence that late-cued turns may challenge balance more than pre-planned turns. The current study suggests the need to consider late-cued transitional maneuvers as potential threats to balance during activities of daily living.

Acknowledgments

This research was supported by NSF (Award #1944207).

References

[1] Vistamehr et al. (2016). *Phys & Behav.* **3**: 396-400.
[2] de Leva (1996). *J of Biomech.* **9**: 1223-1230
[3] Herr, Popovic (2008). *J. of Exp. Biol.* **4**: 467-481
[4] Nolasco et al. (2019). *Gait and Posture*. **70**: 12-19.

RELIABILITY OF SMARTPHONE ACCELEROMETERS FOR MEASURING GAIT DURING DATA COLLECTION OVER ZOOM

Nancy Nguyen[1] and Jefferson W Streepey[1]
[1]Department of Kinesiology, School of Health and Rehabilitation Science, Indiana University Purdue University Indianapolis
Email : nanguy@iu.edu

Introduction

With the advancement of smartphone technology, the use of the smartphone's native accelerometers can be useful for clinicians and health care providers to track patient progress, especially when circumstances make it difficult for patients to travel for traditional assessment. Previous research has examined the use of accelerometers in a single type of smartphone in a tightly controlled laboratory setting and found the device acceptable as a stand-alone gait assessment tool [1-5]. It would be unlikely, however, that all patients would have exactly the same type of phone or access to a quiet laboratory setting. The purpose of this study is to examine whether smartphone technology can reliably capture characteristics of gait when the type of device is not controlled and done in the home under the direction of an online supervisor .

Methods

For this study, 30 healthy, young adults will meet with investigators through Zoom (Zoom Technologies, Inc, San Jose, CA). Subjects will be instructed to set up the experimental gait path that would allow them to walk forward, unobstructed, 8m turn 180 degrees and return to the starting position. Once the path is established, subjects will perform the gait task with half the subjects walking normally and the other half walking while also spelling words backwards. As the subjects complete the task, they will use their phones to record the accelerations which will be emailed to the investigators. A total of 8 trials will be done with 5 trials being recorded. Subjects will meet over Zoom with investigators again the following week to repeat the study.

The Vernier Graphical Analysis GW app (Vernier Software and Technology, Beaverton, OR) will be used to collect anterior-posterior (AP), medial-lateral (ML), and vertical accelerations collected at 50 Hz. A custon Matlab (Mathworks, Natick, MA) program will be used to lowpass filter the raw data at 12 Hz using a 4th order Butterworth filter. The program will then find the third step walking forward and the third step on the way back in each gait trial. Within these steps, the program will identify seven peak AP, ML, and vertical accelerations associated with events in the stance and swing phases of gait [2]. A 2x2 (direction x week) with repeated measures will be performed on the seven identfied peaks. ANOVA test will be run comparing the weeks and the steps chosen within a trial. A 7-item Cronbach's analysis will be used to determine the consistency of the gait assessments.

Results and Discussion

To date, nine subjects have completed two weeks of gait testing. These participants used an iPhone (Apple, Cupertino, CA) for their data collection. All nine completed the gait task while spelling backwards. The ANOVA revealed no differences between any of the dependent variables when testing the effect of walking direction (forward vs the walk back) or the week of data collection (Figure 1). The Cronbach alpha value for five of the seven metrics scored higher than 0.60, but with the alphas being 0.58 and 0.56 for the maximum and minimum AP peaks, respectively. These findings suggest that everyday smartphone technology may be able to reliably assess features of gait associated with medial lateral balance and vertical loading but might be more limited in its measurement of AP gait events.

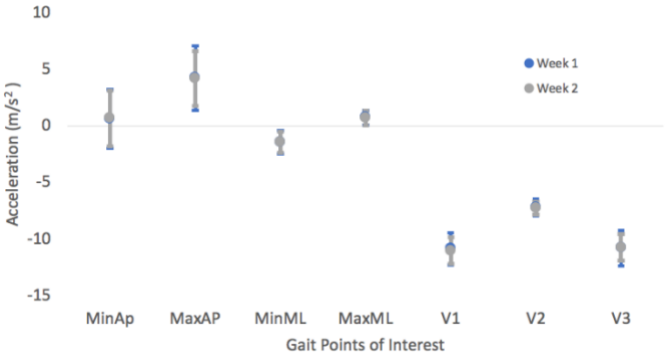

Figure 1: Average week one and week two minimum anterior-posterior (MinAP), maximum anterior-posterior peak (MaxAP), minimum medial-lateral peak (MinML), maximum medial-lateral peak (MaxML), and three peaks for the vertical acceleration data (V1, V2, and V3). There were no significant differences between the data collected on week one and week two.

Significance

The purpose of the study was to show that common smartphone technology can be reliably implemented in the home over Zoom to assess gait. The pandemic has changed the way medicine has worked and per the CDC, with an increase to the exposure of ill persons, healthcare systems must adapt to these changes using methods that do not rely on face-to-face interactions. With the smart-phone technology, clinicians may be able to collect accelerometer data with their patients virtually and better diagnose and treat their patients via long distance communication.

Acknowledgments

This research was supported by the Indiana University-Purdue University Post-Baccalaureate Research Education Program (IPREP), a NIH funded program intended to prepare recent college graduates, who are students from underrepresented minority or disadvantaged populations, for admission to graduate programs in the biomedical and behavioural sciences.

References

[1] Kim A. et al (2015). Gait Posture, 42:138-144
[2] Pitt W, Shou LS. (2019). GaitPosture71:279-283.
[3]Silsupadol P et al (2020) IEEE J Biomed HealthInform.24(4):1188-1195.
[4]Suffoletto B et al (2018) GaitPosture. 60:116-121.
[5]Sun B et al (2014) Sensors (Basel). 2014;14(9):17037-17054.

COMPARISON OF DYNAMIC LOW BACK STABILITY MODELS

Valerie R Jardon[1], Tong Chu[2], Sara E Wilson[1,2]
[1]Bioengineering, University of Kansas
[2]Mechanical Engineering, University of Kansas
email: sewilson@ku.edu

Introduction

Biomechanical trunk models are used to investigate the stability of the human trunk in order to understand the etiology of low back injuries. The methods used and the simplifications incorporated into the model may limit the ability of the model to predict the true dynamic behaviour of the trunk. In this work, the muscle models and stability methods are critically reviewed and compared for five published stability-based biomechanical trunk models.

Methods

Review of Literature: In order to determine the key papers that have been included in this work, a keyword search was completed in PubMed and Web of Science using the terms: "lumbar spine", "spine stability" and "muscle reflexes model". Additionally, literature-review software Research Rabbit was used to search citations. Five pivotal papers were selected for comparison (Table 1). To be included, the model must 1) be stability-based 2) model the lumbar spine/trunk 3) include muscles.

Model Analysis: For each of these papers, the muscle model and stability method used was compared to examine the impact of these modelling choices on the potential stability predictions that could be made.

Results and Discussion

Model Analysis: The stability models used in the five papers were either based on the second derivative of the potential energy calculated using the Hessian matrix or on the linearized state-space equation eigenvalues calculated from the Jacobian matrix (Table 1). These methods should give similar results for dynamic stability of the system.

However, the muscle models presented in the papers varied significantly. Three papers use some variant of Bergmark's model of short-range muscle stiffness[2-4]:

$$K = \frac{q}{lo}F \qquad \text{equation 1}$$

were lo is the neutral length of the muscle and F is the muscle force. The value selected for muscle stiffness coefficient (q) ranged from 5 to 40 in these papers. Crisco and Panjabi estimated q to range from 0.5 to 40[6]. Cholewicki's model used a crossbridge bond distributed model (DM) based on Huxley's 1957 model of crossbridge dynamics[1,7]. In terms of short-range stiffness, the model has a nonlinear stiffness as a function of force similar to that of Bergmark (Figure 1a). In the fifth paper by Wagner, muscle stiffness is that of a classic Hill-type model with a parallel elastic that doesn't appear to be a function of muscle force[5]. Examining the muscle models in a simple dynamic stability model, it can be seen that the muscle stiffness model used (here different values of q in the Bergmark model) can change the predicted stability (Figure 1b).

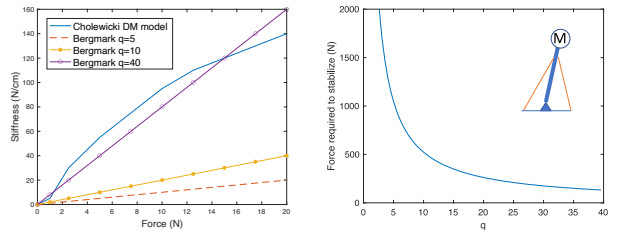

Figure 1: Comparison of the effects of the force-stiffness relationship in lumbar stability models. The first plot illustrates the force-stiffness relationships differences between the papers. The second plot shows how changing the value of q in the Bergmark muscle model can alter the force required to stabilize in a simple model.

Significance

Low back pain and injuries (LBP) are prevalent musculoskeletal conditions. It has been theorized that loss of dynamic stability of the spinal column contributes to such injuries. By reviewing and comparing five pivotal lumbar stability models, the limitations of the muscle models and the stability methods can be assessed to improve understanding of the general limitations of the models and direct future improvements in dynamic modelling of lumbar stability.

References

1. Cholewicki J, McGill SM. *Clin Biomech*. 1996;11(1):1-15.
2. Granata KP, Wilson SE. *Clin Biomech*. 2001;16(8):650-659.
3. Franklin TC, Granata KP. *J Biomech*. 2007;40(8):1762-1767.
4. Bergmark A. *Acta Orthop Scand Suppl*. 1989;230:1-54.
5. Wagner H, et al. *Pathophysiology*. 2005;12(4):257-265.
6. Crisco, JJ, Panjabi, MM. *Spine* 1991;16: 793–799.
7. Huxley, AF. *Prog Biophys Chem*. 1957;7:255-31

Table 1: Comparison of Models of Lumbar Stability

Reference Paper	Stability Method	Muscle Model
Cholewicki *et al.*[1]	Minimum Potential Energy Method*	Crossbridge bond distribution model (DM Model)°
Granata & Wilson[2]	Minimum Potential Energy Method*	Bergmark's stiffness (q=5)‡
Franklin & Granata[3]	Linear Stability Analysis†	Hill Model (CE+PE)§ + Bergmark's stiffness (q=10)‡
Bergmark[4]	Minimum Potential Energy Method*	Bergmark's stiffness (q=40)‡
Wagner *et al.*[5]	Linear Stability Analysis†	Hill's F-V Relation + PE

* A system is stable if the Hessian matrix, based on the second derivative of potential energy of the system, is positive definite[1].
† After linearizing a system about equilibrium, the eigenvalues of the Jacobian need to have negative real parts for the system to be stable[3,5].
°The crossbridge bond distribution model mathematically approximates Huxley's 2-state contraction dynamics[1].
‡ Active muscle stiffness estimated by Bergmark's $k=qF/L$ where F is muscle force, L is muscle length, and q is a dimensionless constant[2,4].
§ The Hill Model models muscle as a contractile element (CE) in parallel with a spring (PE), all in series with another spring (SE). The SE is not included in all works.

BIOMECHANICS OF ADOLESCENT RUNNERS WITH A HISTORY OF STRESS FRACTURE INJURY

Emily A. Jordan[1]*, Micah C. Garcia[1], David M. Bazett-Jones[1]
[1]University of Toledo, Toledo, OH, USA
email: * emily.jordan@rockets.utoledo.edu

Introduction

Long-distance running is popular among adolescents with approximately 12 million adolescents participating in running activities.[1] Running-related injuries (RRI) are common with up to 68% of adolescents reporting a prior RRI.[2] Adult long-distance runners who develop a stress fracture demonstrated differences in temporal-spatial parameters and ground reaction forces (GRFs) compared to uninjured runners.[3,4] Most RRI research has been conducted in adults and results are generalized to adolescents; however, growth and maturation are potential confounding factors. Therefore, the purpose of our study was to compare temporal-spatial parameters and GRFs between adolescent long-distance runners with a prior stress fracture and those with no history of RRI. We hypothesized runners with a history of injury would demonstrate lower cadence, longer step lengths, shorter stance duration, and larger GRFs than runners with no history of RRI.

Methods

48 adolescent long-distance runners (F = 27, M = 21, age = 14.5±2.4 years) participated. Participants were instrumented with reflective markers and ran over a 20-meter runway with floor embedded force plates (AMTI; Watertown, MA) at a comfortable, self-selected speed. Kinematic data were captured using a 12-camera motion capture system (Motion Analysis Corp.; Santa Rosa, CA) and exported to Visual3D (C-Motion, Inc; Germantown, MD) for analysis. Dependent variables included temporal-spatial parameters (cadence, step length, and stance duration) as well as peak braking GRF, vertical GRF, vertical impact peak GRF (VIP), vertical average loading rate (VALR), and vertical instantaneous loading rate (VILR).[5] Participants self-reported a prior stress fracture injury (Hx, n=10) or no history of RRI (No Hx, n=38). Differences between groups were assessed using ANCOVA models, with running speed as the covariate. Significance was set at $p<.05$. Cohen's *d* effect sizes between groups were also calculated.

Results and Discussion

Analyses indicated runners with no history of RRI demonstrated significantly greater VILR than runners with a history of stress fracture (Table 1). No significant differences were found for temporal-spatial parameters or the remaining GRFs.

Table 1: Temporal-spatial and GRF comparison between runners with a history of stress fracture (Hx) and no history of RRI (No Hx).

Variable	Hx	No Hx	p	*d*
Cadence [steps/min]	170 ± 13	169 ± 10	.65	0.09
Step Length [m]	1.28 ± 0.22	1.28 ± 0.21	.65	0.00
Stance Duration [s]	0.24 ± 0.04	0.23 ± 0.03	.14	0.28
Braking GRF [N/kg]	-0.39 ± 0.13	-0.40 ± 0.07	.63	0.10
Vertical GRF [N/kg]	2.44 ± 0.28	2.53 ± 0.23	.22	0.35
VIP [N/kg]	1.49 ± 0.40	1.67 ± 0.26	.07	0.53
VALR [N/kg/s]	0.11 ± 0.02	0.12 ± 0.01	.07	0.63
VILR [N/kg/s]	0.12 ± 0.02	0.14 ± 0.02	.01*	1.00

* indicates statistical significance ($p<.05$)

Previous studies in adults reported different temporal-spatial parameters and higher GRFs for runners who developed a stress fracture compared to uninjured runners.[3,4] We hypothesized that adolescent runners with a history of stress fractures would demonstrate larger GRFs than those with no history of RRI, however, we demonstrated that VILR was higher in those with no history of RRI. These findings are consistent with both VIP (d=0.53) and VALR (d=0.63) demonstrating moderate effect sizes for larger GRFs variables in those without a previous RRI. These results indicate that the biomechanical differences seen in adults with and without a history of stress fracture should not be generalized to adolescent runners.

Our results should be interpreted in the context of our limitations. First, we did not take into account the bone health of both injured and uninjured groups. Individuals with poor bone health are at higher risk of sustaining stress fracture injuries[6] but it is unknown if our groups had different bone health. There was also much variability in the time since stress fracture. The median time was 14 months (range = 4-30 months) and all runners were currently uninjured at the time of testing. It is possible the previously injured runners adapted their running mechanics since returning from the stress fracture to change how force is applied over their stride. We may also be underpowered due to our small sample size of runners with a history of stress fractures (n = 10). Prospective research is necessary to determine if adolescent runners who go on to sustain a stress fracture injury demonstrate different temporal-spatial parameters and GRFs than adolescent runners who remain injury-free.

Significance

To our knowledge, this is the first study to investigate running biomechanics in adolescent long-distance runners with a history of stress fractures. Results obtained from adult runners are often generalized to adolescent runners. However, differences in stress fracture healing time and recovery between adolescents and adults may limit the generalizability of adult research to adolescent runners.[7] Our results indicate adolescent long-distance runners with a history of stress fracture do not have different temporal-spatial parameters or larger GRFs than adolescent runners with no history of RRI. While stress fractures are multifactorial with non-biomechanical factors playing a role in injury. Prospective research that includes running mechanics, bone health, and training volume is necessary to improve understanding of stress fractures in adolescent long-distance runners.

References

1. Finley P (2017) *Sport J.*
2. Tenforde AS (2011) *PMR.*
3. Ceyssens L (2019) *Sports Med.*
4. Luedke LE (2016) *MSSE.*
5. Crowell HP (2011) *Clin Biomech.*
6. Krabak BJ (2020) *Br J Sports Med.*
7. Malone CA (2011) *J Forensic Sci.*

Analysis of EMG-EMG Connectivity in Muscular Activation of Lower Leg Muscles in Quiet Standing Positions

Gordon Alderink[1], Diana McCrumb[2], Yunju Lee[1,2], Samhita Rhodes[2],
[1]Department of Physical Therapy, Grand Valley State University, Grand Rapids, MI, USA
[2]School of Engineering, Grand Valley State University, Grand Rapids, MI, USA
Email: aldering@gvsu.edu

Introduction

To maintain control of balance, the center of mass (COM) must remain within its base of support (BOS) [1]. The CNS engages in multiple sensorimotor processes to control postural balance [2]. The single inverted pendulum model defines an ankle strategy, which the CNS uses to control postural stability. However, the exact nature of ankle muscle synergies related to the control of quiet standing is unknown. The signal that synchronously activitates these synergies is called a common neural drive [3]. EMG-EMG intermuscular coherence analyses have quantified postural control functional synergies for specific neural frequency bands [3]. Limited by linearity assumptions, magnitude squared coherence (MSC) analyses can be complemented by mutural information (MI), an information connectivity measure more suitable for the analysis of non-linear time series. The purpose of this study was to employ MSC and MI to examine the EMG-EMG connectivity of paired lower leg muscles during various quiet standing postures. We hypothesized that MSC and MI analyses would characterize the neural origin of a synchronized common neural drive.

Methods

Six healthy individuals (4 females; 24.8±3.3 yrs; 170.8±10.5 cm; 71.0±13.5 kg) participated. Approval was obtained from the Grand Valley State University Human Research Review Committee (#18-246-H). Surface EMG signals (Motion Lab Systems, Inc.), motion trajectories, and ground reaction forces (AMTI, Inc.) were synchronized using Vicon Nexus motion capture software v2.8 (Oxford Metrics, UK). Surface EMG was recorded (1200 Hz) for right and left tibialis anterior (TA), soleus (S), and medial gastrocnemius (MG). Raw data were processed using band-pass (10-500 Hz), and notch (60 Hz) filters. Data were collected for 30 seconds with participants standing on two force plates, under 6 conditions: 1) feet together eyes open (EO); 2) feet together eyes closed (EC); 3) dominant foot on rear plate EO; 4) dominant foot on rear plate EC; 5) dominant foot on fore plate EO; and 6) dominant foot on fore plate EC. MSC and MI were estimated from EMG-EMG for all muscle pairs in 6 neural frequency bands. For each individual, one-way ANOVAs were used to compare mean MSC and MI for each muscle pair in each frequency band, and all standing tasks. Dunnett's post-hoc, 2-sided t-test was used to examine connectivity value differences between the baseline condition and tandem positions.

Results and Discussion

Both MSC and MI demonstrated greatest connectivity in the delta band, followed by the theta band (Table). Previous work has shown that strong coherence in the delta band is indicative of postural control [4]. In general, connectivity did not appear to show clear patterns with regard to changed postural conditions. MI demonstrated significant connectivity in bilateral muscle pairs in the beta and gamma bands, which suggests organized neural drive [5]. Connectivity in the beta and lower gamma bands appears to be influenced by standing balance conditions, indicative of a neural drive originating from the motor cortex [6].

Changes in connectivity in the beta and gamma bands were found to be most significant in posterior muscle pairs of the rear leg in tandem, regardless of leg dominance. MI appears to be more sensitive to identifying connectivity between antagonistic pairs, e.g., TA:S, with greater connectivity in agonistic muscle pairs, e.g., MG:S, and all bilateral homologous muscle pairs, whereas MSC could only identify connectivity in agonist pairs. MSC connectivity for MG:S pairs may be influenced by cross-talk.

Table. Mean ± standard deviation for MSC and MI for all subjects/trials for eyes-closed tandem right foot on back force plate.

Frequency Band	MSC RTA:RMG	MSC RTA:RS	MSC RMG:LS
Delta (0 – 4 Hz)	0.19±.09	0.18±.03	0.17±.04
Theta (4 – 8 Hz)	0.07±.03	0.07±.01	0.06±.02
Alpha (8 – 13 Hz)	0.06±.01	0.07±.02	0.18±.21
Beta (13 – 30 Hz)	0.09±.02*	0.13±.08*	0.32±.22*
Lower Gamma (30 – 60 Hz)	0.09±.02*	0.13±.08*	0.27±.25*
Upper Gamma (60 – 100 Hz)	0.08±.02*	0.09±.03*	0.18±.19*
Frequency Band	**MI RTA:RMG**	**MI RTA:RS**	**MI RMG:RS**
Delta (0 – 4 Hz)	0.37±.02	0.37±.02	0.37±.02
Theta (4 – 8 Hz)	0.17±.01	0.17±.01	0.17±.01
Alpha (8 – 13 Hz)	0.10±.004	0.11±.004	0.15±.09
Beta (13 – 30 Hz)	0.07±.01*	0.17±.004*	0.13±.09*
Lower Gamma (30 – 60 Hz)	0.05±.01*	0.05±.01*	0.09±.07*
Upper Gamma (60 – 100 Hz)	0.04±.01*	0.04±.01*	0.07±.04*

MSC = Magnitude Squared Coherence; MI = Mutual Information; RTA = right tibialis anterior; RMG = right medial gastrocnemius; RS = right soleus. *p<0.05 vs. EO (feet together, eyes open).

Significance

Neural drives in the delta, beta and lower gamma bands appear to provide information about postural control. Both MSC and MI have demonstrated the ability to distinguish muscle connectivity in quiet standing postures in healthy participants. MI appears to be more sensitive to muscle synergies in antagonistic pairs and contralateral pairings. More research is needed using larger samples, and in measurement strategies for individuals with neuropathologies, e.g., post-concussion syndrome.

References

1. Winter, D. (1995). *Gait Posture*, 3, pp.193-214.
2. Ivanenko, Y. & Gurfinkel, V.S. (2018). *Front. Neurosci*.,12, pp. 1-9.
3. Boonstra, T.W. et al. (2008). *J. Neurophysiol*., 100, pp. 2158-2164.
4. Mochizuki, G. et al. (2006). *Exp. Brain Res*., 175, pp. 584-595
5. Danna-Dos-Santos et al. (2015). *Exp. Brain Res*., 233, pp. 657-669.
6. STEADI – Older Adult Prevention – CDC Injury Center, https://www.cdc.gov/steadi/materials.html.

EXPERIMENT DESIGN: EVALUATING KNEE MECHANISMS USING DEVICE MIGRATION AND INTERACTION FORCES

S. Patrick[1], N. Anil Kumar[1], and P. Hur[1,2]
[1]Texas A&M University, College Station, Texas, USA
[2]Gwangju Institute of Science and Technology, Gwangju, South Korea
*email: shawaneepatrick@tamu.edu

Introduction

The complex polycentricity of human joints, specifically the knee, has troubled exoskeleton and prosthetic designers for years. Some have designed polycentric knee mechanisms, but they mandate complex manufacturing and tedious fitment procedures during testing [1-3]. The latter is required because the centrode (i.e. the locus of the instantaneous center of rotation) is unique to the user [2]. Despite these attempts, the biomedical community still questions the need for polycentric knee joints citing that the centrode is merely 1-2cm. This study aims to conclusively answer this question through a case study of different knee mechanisms: (i) rigid single axis (*Rigid*), (ii) polycentric joint with meshed spur gears (*Geared*), and (iii) a novel polycentric mechanism that employs a single axis knee joint and compliance at the top and bottom cuffs (*Compliant*). The primary contribution of this study is the experiment protocol. Herein lies its details and some preliminary results.

Methods

Several steps were taken to limit the experiment's variables to only the mechanism designs listed above. Each knee mechanism was affixed within a compression knee brace. Doing so standardized the brace's material, weight, inherent compliance (or stretch), and brace-strap design across all three tests. During the first test, the brace was tightened to the user's comfort. The loads imposed by the brace's straps were measured using flexible force sensors (shown in Figure 1). These sensor readings were collected throughout the entire test using a wireless processing unit. In all tests that followed, the braces were fitted within ±1.0 N of the first test's readings.

After the brace was fitted, markers were placed on lower limb bony landmarks and the brace's hinge. Motion capture data (Vantage Vicon Cameras) was collected over a 15 minute walking trial at 2mph for each brace. Two metrics were used to compare the knee braces: (i) device migration – the difference in the distance between the brace marker and the shank marker at the beginning and end of the trial, (ii) range of interaction forces – the range of forces measured by the flexible force sensors across the walking trial. It is desired that the range of interaction forces be low. It is hypothesized that the two listed metrics are positively correlated. The experiment has been approved by the Institutional Review Board (IRB) at Texas A&M University. A pilot study was conducted with a young able-bodied subject (male, 1.70 m, 70 kg).

Results and Discussion

For the three knee braces (*Rigid, Geared, and Compliant*) the device migration was 1.25 mm, 1.00 mm and 0.59 mm respectively. At the top brace-strap, the range of interaction forces was lower with the *Compliant* than the *Rigid* and *Geared* brace. At the bottom brace-strap, the range of interaction forces measured with the *Compliant* brace was lower than the *Rigid* brace (Figure 1). The lower device migration along with the smaller range of interaction forces indicates that the *Compliant* brace has the potential to minimize interaction forces during the walking gait.

Despite the polycentric design, the *Geared* brace registered the highest interaction forces at the top brace-strap. This could likely be due to the uniqueness of the user's centrode and the mismatch between the mechanism's and the user's instantaneous center of rotation. If these preliminary results hold true, it would prove that there is no one-size-fits-all polycentric knee joint design and that incorporating compliant mechanisms is needed.

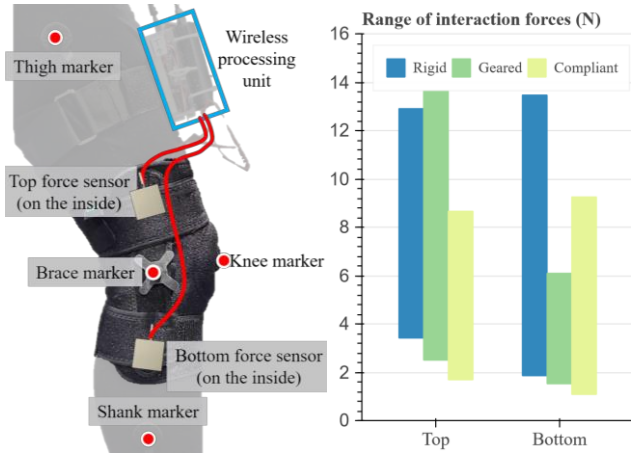

Figure 1: LEFT: Subject wearing the knee brace with mounted force sensors and a wireless processing unit. Figure also shows the marker placement. RIGHT: The range of interaction forces (N) at the top and bottom brace-straps for all three knee braces.

Significance

If successful, this study's results will quantify the effect of polycentric knee mechanisms vs. a single axis mechanism. The consequent inferences will help answer the long-standing question of whether the biomedical society will benefit from polycentric knee mechanisms. Additionally, while not discussed in this study, the *Compliant* knee mechanism is a novel design that is easier to manufacture and actuate (in motorized knee orthoses) than the state-of-the-art polycentric mechanisms. More importantly, the design's compliance would significantly reduce the amount of fitment time while minimizing potentially harmful interaction forces. This study will help validate the mechanism's design. Following which, it is hoped that said mechanism can be adopted in lower-limb exoskeletons.

References

[1] A. Stienen, et al., IEEE Transactions on Robotics, vol. 25, pp. 628–633, jun 2009.
[2] B. Celebi, et al., IEEE/RSJ International Conference on Intelligent Robots and Systems, pp. 996–1002, IEEE, nov 2013.
[3] V. A. D. Cai, et al., Meccanica, vol. 52, pp. 713–728, feb 2017.

Investigating the Windlass: Kinematic Coupling within the Foot

Lauren R. Williams[1], Kelsey Weaver[1], Kirk Bassett[1], Martha Gill[1], Dustin A. Bruening[1]
[1]Brigham Young University, Provo, UT, USA
Email: lauren.williams523@gmail.com

Introduction

Passively, metatarsophalangeal joint (MTP) extension exerts tension on the plantar fascia, pulling the midtarsal (MT) joint into plantarflexion and raising the arch. This coupling is known as the windlass mechanism.[1] However, it is unclear how much of this coupling contributes to midfoot motion during dynamic tasks. In this study we used a series of controlled tasks to investigate the extent of MTP and MT coupling. In addition, we included a range of arch stiffnesses to investigate the influence of foot structure on this coupling. We hypothesized that coupling would decrease as task complexity increased and that arch stiffness would be correlated with this coupling.

Methods

15 healthy subjects (age: 26±5.2 years, mass: 73.5±11.0 kg, height: 1.75±0.1 m) performed five tasks: (1) Seated Passive Extension, (2) Seated Active Extension, (3) Standing Passive Extension, (4) Standing Active Extension, and (5) Heel Raises. The participant's left lower limb was outfitted with a multi-segment foot marker set.[2] A motion analysis system (Qualisys) was used to collect kinematic data during all conditions. In the first four conditions, the participants' MTP joint was extended to the end range of motion both passively by an investigator and actively by the participant, with the participant either seated or standing. For the heel raises, participants performed bilateral heel raises instructed to achieve maximum height. All conditions were performed to a metronome of 40 bpm.

Participants' arch stiffness was measured using the arch-height-index measurement system and calculated as a function of the difference between arch height from sitting to standing.[3]

MTP and MT joint angles in the sagittal plane were calculated (Visual 3D software) for the upward phase of the heel raise (start to peak heel raise), and from neutral MTP joint position to peak MTP extension for all other conditions. From these angle curves, a distal foot coupling ratio was calculated as the slope of the line created by plotting the angle of these two joints against each other. This ratio (MT/MTP) can be used to describe the coupling motion at the MT and MTP joints, with a larger ratio indicating greater coupling.

A repeated measures ANOVA (α=0.05) with Bonferroni post-hoc tests was used to test the coupling ratio across the five different conditions. Bivariate correlations were used to assess the relationship between arch stiffness and coupling ratios.

Results and Discussion

Coupling generally decreased across the first four conditions, with statistical differences between seated conditions and Standing Active Extension. However, contrary to our hypothesis, the most complex task, Heel Raise, had the largest coupling ratio (0.80±0.16, Figure 1). But, in partial agreement with our hypothesis, Standing Active Extension (0.08±0.03) had a smaller coupling ratio than all other conditions ($p<0.01$), except for Standing Passive Extension (0.08±0.03). Additionally, Seated Passive Extension (0.12±0.03) had a larger coupling ratio than Standing Active Extension ($p<0.001$).

Arch stiffness (14.6±7.4 mm/kN) was moderately correlated with the coupling ratio during Heel Raises ($r=0.47$, Figure 2), nearing significance ($p=0.64$). This may indicate that flexible arches have greater coupling during dynamic and functional tasks, but more subjects are needed to confirm this. However, arch stiffness was only weakly correlated with all other conditions, suggesting that foot structure does not play as much of a role during less complex tasks.

Significance

The coupling ratio of the Seated Passive Extension was about 1/6 of that of the Heel Raises, suggesting that the windlass mechanism plays only a minor role in dynamic arch rise compared to active muscle contractions. However, the MTP and MT joints were tightly coupled during Heel Raises, showing the functional connection between them. Additional investigation into this coupling, including kinetics, is needed to fully understand the role of the distal foot and arch structure in dynamic motion.

Acknowledgments

This material is based upon work supported by the National Science Foundation Graduate Research Fellowship Program under Grant No. 1840996. Any findings and conclusions or recommendations expressed in this material are those of the author(s) and do not necessarily reflect the views of the National Science Foundation.

Figure 1. Distal foot coupling ratio (MT/MTP) across conditions

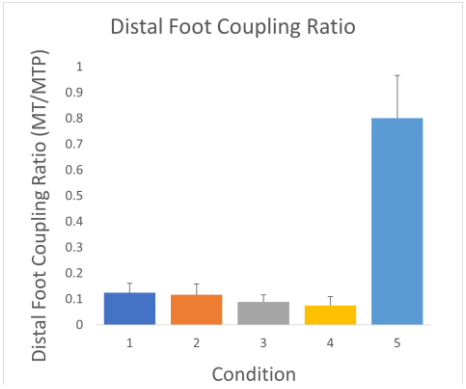

Figure 2. Arch stiffness versus Heel Raise coupling ratio (MT/MTP)

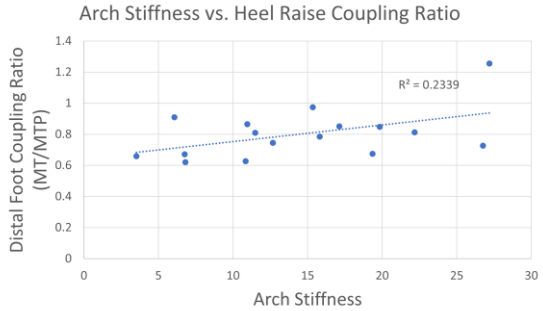

References

1. Hicks, *J. of Anatomy*. **88,** 25-30, 1954.
2. Bruening, et al. *Gait & Post*. **35**, 535-540, 2012.
3. Zifchock, et al. *J. Am Pod Med Ass.* **107,** 199-123, 2017.

RELIABILITY AND VALIDITY OF POSE ESTIMATION IN TWO-DIMENSIONAL KINEMATIC ANALYSIS

Lucas Haberkamp[1]*, Micah C. Garcia[1], David M. Bazett-Jones[1]
[1]University of Toledo, Toledo, OH, USA
email: lhaberk@rockets.utoledo.edu

Introduction

Three-dimensional (3D) motion capture is widely considered the gold standard of kinematic assessment as it provides the highest accuracy measurements. However, there are practical limitations to 3D motion capture, such as the costly equipment, need for operator proficiency, and the confinement to a laboratory setting. Due to these limitations, clinicians often rely on video-based two-dimensional (2D) motion capture, which has shown to be valid for evaluating movement patterns.[1] Free software (e.g., ImageJ) is available for users to manually process 2D video data; however, this can be time-consuming. There have been recent advancements using pose estimation models for 2D video motion capture purposes (e.g., OpenPose). OpenPose is a free and open source deep learning neural network that quickly identifies human body key points on a 2D video or image.[2-5] 2D pose estimation has been reported to be reliable and valid for determining sagittal plane kinematics during squatting and walking in adults.[6,7] It is unknown if the results are generalizable to adolescents or when analyzing frontal plane kinematics Therefore, the purpose of our study was to investigate the reliability and validity of using 2D pose estimation to calculate both sagittal and frontal plane measures during a single-leg squatting task in adolescents.

Methods

22 adolescents (F=14, M=8, age=16.5±1.2 years) participated in this study. During a single visit, participants were instrumented with reflective markers and completed a series of seven single-leg squats on their right leg. 3D kinematic data were recorded using a 12-camera system (Motion Analysis Corp, Santa Rosa, CA) and 2D sagittal and frontal plane videos were simultaneously recorded using an iPod Touch (Apple, Cupertino, CA) from each plane, respectively.

3D kinematic data were processed in Visual3D and exported to a custom MATLAB code. The 2D video data were processed with the OpenPose BODY_25 model and a custom Python code. For each squat repetition, peak sagittal (trunk forward lean, hip flexion, knee flexion, ankle dorsiflexion) and frontal plane angles (pelvic drop, hip adduction, knee abduction) were extracted at the instance of peak knee flexion. Joint angles were averaged across all squat repetitions for analysis. To assess reliability, 2D videos were re-processed with the 2D pose estimation model and Intraclass Correlation Coefficients (ICCs) were used to compare results to the initial measurements. For validity assessment, Pearson's correlation coefficients were used to compare the relationship between 3D and 2D measured joint angles.[8] Paired t-tests also compared joint angles between 3D and 2D measurements.

Results and Discussion

A key finding in this study was that the 2D pose estimation demonstrated excellent repeatability with an ICC of 1.0 for each kinematic variable. This indicates that 2D pose estimation consistently identified key points used to determine joint angles.

Moderate to strong positive relationships (r=.63-.95) were found for sagittal plane 3D and 2D joint angles (Table 1). However, poor relationships (r=-.51-.17) were found for frontal plane joint angles. These results are consistent with previous studies that reported strong correlations for sagittal plane angles, but poor correlations for frontal plane angles.[9] In the sagittal plane, the mean difference between methods was <5° for trunk forward lean, knee flexion, pelvic drop, and knee abduction, but >5° for hip flexion, ankle dorsiflexion, and hip adduction (Table 1). A possible explanation for these angle differences is different definitions of joint angle calculations between 3D and 2D measurements.

Significance

Using 2D pose estimation as a method to calculate kinematics offers unique benefits that could improve clinical use. The open-source code does not require coding knowledge. Processing of 2D video can require substantial manual processing for identifying landmarks; OpenPose removes the manual processing component. While OpenPose does not appear to correct the frontal plane limitations that are inherent with 2D motion analysis, it may be a more user and time-friendly option than some 2D analysis software.

References

1. Dingenen B (2018) *PT Sport.*
2. Cao Z (2021) *IEEE.*
3. Cao Z (2017) *CVPR.*
4. Wei S (2016) *CVPR.*
5. Simon T (2017) *CVPR.*
6. Ota M (2020) *Gait Posture.*
7. Stenum J (2020) *bioRxiv.*
8. Chan YH (20013) *Singap Med J.*
9. Simon M (2018) *Knee.*

Table 1. Reliability and validity of 2D sagittal plane joint angles at peak knee flexion measured with OpenPose. Reported as mean±SD.

Angle [°]	ICC	3D	2D	*r* (*p*)	Paired *t* test *p*-value
Trunk Forward Lean	1.0	34.6 ± 10.3	34.2 ± 10.5	.95 (<.001*)	.57
Pelvic Drop	1.0	4.7 ± 5.3	-0.1 ± 3.3	-.51 (.02*)	<.01*
Hip Flexion	1.0	76.3 ± 13.0	81.6 ± 15.4	.74 (<.001*)	.02*
Hip Adduction	1.0	19.5 ± 8.3	13.2 ± 9.9	.17 (.46)	.02*
Knee Flexion	1.0	80.4 ± 7.3	81.7 ± 6.9	.93 (<.001*)	.04*
Knee Abduction	1.0	9.0 ± 7.0	9.6 ± 13.5	.12 (.59)	.84
Ankle Dorsiflexion	1.0	36.1 ± 3.2	21.9 ± 3.3	.63 (.001*)	<.001*

* indicates statistical significance (p<.05), 2D=two-dimensional, 3D=three-dimensional, ICC=intraclass correlation coefficient

ESTIMATING TIBIAL BONE FORCE USING A WEARABLE IMU AND PRESSURE INSOLES SEGMENTED INTO REGIONS

Lauren M. Grohowski, Laura J. Elstub, Cameron A. Nurse, and Karl E. Zelik
Center for Rehabilitation Engineering and Assistive Technology, Vanderbilt University
email: lauren.m.grohowski@vanderbilt.edu

Introduction

The repetitive nature of running results in a high rate of lower limb injuries. Up to 30% of runners encounter overuse injuries such as stress fractures in the tibia [1], which result from an accumulation of microdamage due to repetitive bone forces. Ideally these bone forces could be monitored during running to better understand and manage injury risks. Matijevich et al. demonstrated that traditional ground reaction force metrics are often poor surrogate measures for the estimation of tibial bone force during running [2], highlighting the need for muscle force estimations alongside ground reaction forces.

We previously demonstrated the feasibility of combining wearable sensors (pressure-sensing insole and an inertial measurement unit (IMU) in each shoe) with musculoskeletal modelling and machine learning algorithms to accurately and noninvasively estimate tibial force [3]. Several important questions remain to facilitate development and translation into a wearable monitoring device for real-world use. One practical question is how does the accuracy of tibial force estimates change with a smaller number of pressure sensors, or segments, per insole? Research-grade pressure insoles often contain dozens of sensors per insole, whereas consumer pressure insoles may contain an order of magnitude less to meet user needs related to battery life, cost and complexity. Therefore, the aim of this research is to explore if insoles with fewer pressure sensors or segments have the potential to be used without compromising accuracy.

Methods

Three participants ran at varying slopes (0, +/-3, +/-6 degrees), speeds (2.7, 3, 3.3 m/s) and foot strike patterns (forefoot striking, rearfoot striking, regular gait). Data from 3D motion capture (Vicon) and a force-instrumented treadmill (Bertec) were combined to compute comparison standard *lab-based estimates* of tibial bone force. In addition, these signals were distilled to those we could expect to obtain from wearable sensors (e.g. insoles and IMU) to explore *simulated wearables*, and used to estimate tibial bone force [3]. The use of insoles affords the opportunity to partition forces under the feet into distinct segments of the foot, which cannot be achieved with force plates alone. Therefore, a *segmented wearables* condition was created using signals from pressure insoles (Novel) segmented into three distinct regions of the foot (heel, mid and fore) to estimate tibial force, using algorithms similar to [3].

For each region of the foot, peak force, impulse, and contact time were calculated. Mean absolute error (MAE) between tibial forces estimates from each wearable condition (simulated, and segmented) and the lab-based estimate of tibial force were computed and compared. In addition, a ranked list of input variables indicating their relative order of importance in estimating tibial bone force was used to gain insight on the inclusion of segmented forces in the estimation of tibial bone force during running.

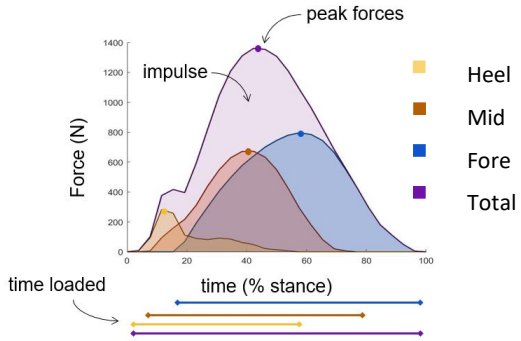

Figure 1: GRF profile (P02) representing segmented force features from each region of the foot for a single step.

Results and Discussion

The MAE for the simulated wearable feature set was 0.103 BW. This high level of accuracy was due to the signals being distilled from comparison standard lab-based signals, which are less noisy than typical wearable sensors. Interestingly, the segmented wearable feature set, using segmented data from the pressure insole, maintained this high accuracy (MAE = 0.102 BW). These preliminary findings suggest wearable sensors with relatively few pressure-sensing regions have the potential to maintain high accuracy in estimating tibial bone forces. In this ongoing study we will explore if these trends continue to hold for a larger sample.

In the segmented wearables analysis, peak forefoot force was ranked as the most important feature for estimating tibial force. Insole data may be influenced by foot strike patterns, running conditions, and foot shape. It is possible that peak forefoot force was the most important feature because all stance phases involve a push-off generating forefoot force, and thus this segmented region of the insole may provide a measurement commonality that can be exploited by algorithms to estimate tibial bone forces. This possibility warrants further investigation.

Significance

Preliminary evidence is promising that a fully wearable sensor system, with a relatively small number of pressure sensors or segments per insole, may provide accurate estimates of tibial bone force during running. Initial findings in this *N*=3 study suggest that forefoot pressure may be particularly important or useful in estimating tibial force across running conditions.

Acknowledgements

We are grateful for support from Vanderbilt Discovery Grant & Searle Systems Biology & Bioengineering Undergraduate Research Experience, & to Anna Wolfe & Emily Matijevich who assisted in the early stages of study development.

References

[1] Song and Koo. J. Korean Medical Sci. 2020.
[2] Matijevich et al. Plos One. 2019.
[3] Matijevich et al. Human Movement Sci. 2020.

INCREASING AGE ALTERS GAIT COMPENSATIONS FOLLOWING MENISCAL INJURY IN RATS

Kiara M. Chan[1], Taylor D. Yeater[1], and Kyle D. Allen[1,2]
[1]J. Crayton Pruitt Family Department of Biomedical Engineering, University of Florida, Gainesville, FL, USA
[2]Department of Orthopaedics and Sports Medicine, University of Florida, Gainesville, FL, USA
email: kiara.chan@ufl.edu

Introduction

Aging increases the susceptibility to osteoarthritis (OA)[1], and OA pain and joint dysfunction are often associated with motion. In clinical settings, distinct gait changes are observed in older adults with OA, yet not seen in younger OA-affected adults[2]. Like in OA patients, gait patterns shift in rodent models of OA to correct mechanical instabilities and protect the injured limb upon loading[3]. However, unlike in OA patients, it is unknown how age affects gait changes in rodent OA models. Previous work in preclinical OA models has only characterized changes in mechanical allodynia and mechanical hyperalgesia between young and old rodents[4,5]. In this work, gait compensations following meniscal injury in 3-, 6-, and 9-month old rats were evaluated to examine age-effects of OA-related joint dysfunction.

Methods

Male Lewis rats (N = 48) received either medial collateral ligament transection plus medial meniscus transection (MCLT+MMT) surgery or a skin-incision as a sham control. Surgeries were performed in 3-, 6-, and 9-month old rats (n = 8/age/surgery) and the right hind limb was operated in all animals. Using our lab's novel rodent gait system[6], rats underwent gait testing at 2, 4, 6, and 8 weeks after surgery. In total, 2646 gait trials were collected. After euthanasia, knees were processed to assess joint damage. Gait parameters were analysed using a linear mixed model allowing for fixed effects of velocity, surgery/limb, age, and timepoint and the random effects of animal. Linear mixed models were analysed with ANOVAs, and a Tukey's HSD post-hoc test was performed when indicated by the main effect or interaction ($p < 0.05$ considered significant).

Results and Discussion

For peak vertical force, the main effects of surgery/limb, age, and timepoint were significant. Overall, the MCLT+MMT right limb had significantly lower vertical loading compared to other limbs (Fig. 1A). The 6- and 9-month animals had significantly lower vertical loading, measured by % body weight, compared to the 3-month animals. Additionally, the age:surgery/limb and timepoint:age interactions were significant. The 6- and 9-month animals reduced loading in the MCLT+MMT right limbs, while the 3-month animals did not (Fig. 1B).

For stance time, the main effects of surgery/limb, age, and timepoint were significant. MCLT+MMT animals had longer stance times on both limbs, indicating a shuffle-step gait compensation. Stance time also generally increased with age. Additionally, the age:surgery/limb, timepoint:age, and timepoint:surgery/limb interactions were significant. The shuffle-step in MCLT+MMT animals was most apparent in the 6- and 9-month animals compared to the 3-month animals, and at the week 2 timepoint compared to all other timepoints.

Taken together, the results indicate the 6- and 9-month animals adopted different gait changes compared to the 3-month animals after meniscal injury. The older animals generally reduced the weight supported by the injured limb and increased the time spent on both limbs compared to the younger animals.

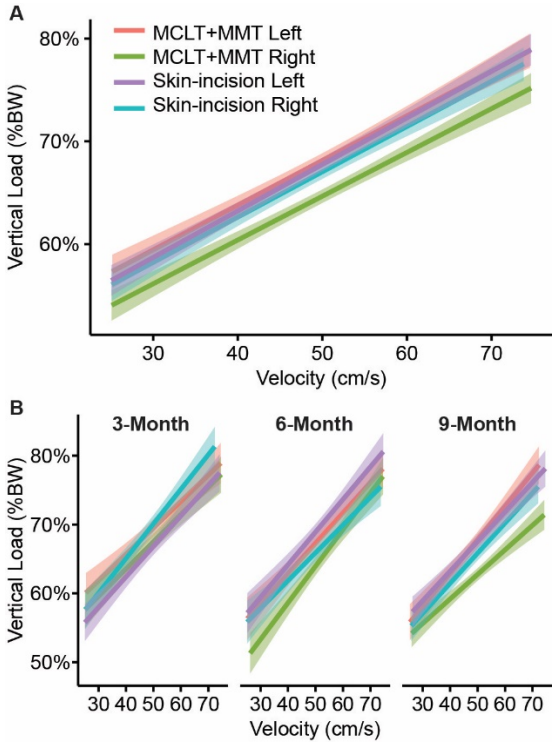

Figure 1: For vertical loading, the main effect of surgery/limb (A) and the interaction of age:surgery/limb (B) were significant. Vertical load measured as percent of animal body weight.

Significance

These data indicate animal age at the onset of injury affects gait changes in the OA-affected joint during walking. Our findings are consistent with clinical findings showing distinct gait changes only in older adults with OA. Interestingly, older animals had more severe cartilage damage compared to younger animals; however, it is unknown whether age-related gait changes are related to structural changes in the OA joint. Nevertheless, joint avoidance behaviours and joint dysfunction in a rodent OA model are affected by animal age.

Acknowledgments

This work was supported by the National Institutes of Health under grants R01AR071431 and R01AR068424 and by graduate student fellowships from the Herbert Wertheim College of Engineering and the J. Crayton Pruitt Family Department of Biomedical Engineering at the University of Florida.

References

[1]Loeser et al. *Nat Rev Rheumatol* (2016), [2]Duffell et al. *Gait Posture* (2017), [3]Kloefkorn et al. *Arthritis Res Ther* (2015), [4]Ogbonna et al. *Age* (2015), [5]Ro et al. *J Gerontol A Biol Sci Med Sci* (2020), [6]Jacobs et al. *Sci Rep* (2018)

HUMANS OPTIMALLY REGULATE MOMENTUM WHEN WALKING ON UNEVEN TERRAIN

Osman Darici[1], Arthur D. Kuo[1,2]
Faculty of Kinesiology[1], Biomedical Engineering Program[2], University of Calgary, Calgary, AB, Canada
Email: osman.darici1@ucalgary.ca

Introduction

Uneven terrain disrupts steady gait and requires compensatory control to maintain overall speed and momentum. It is unknown whether human compensations are dynamically composed for each step, or whether they are merely a matter of greater tonic effort. Dynamic adjustment could be advantageous for reducing energy expenditure or improving steadiness. However, it seems challenging for the human to survey upcoming terrain and dynamically compose the equivalent of an optimal control solution. But it is unclear whether such computation is indeed difficult. Perhaps human compensations for uneven terrain are optimal and dynamic, yet also straightforward to compose.

A simple dynamic walking model [1] suggests how control compensations could be simplified. The model requires push-off work to redirect the body center of mass (COM) between successive, pendulum-like stance phases. That work may be minimized to yield a push-off sequence that regulates momentum and maintains overall speed on uneven terrain. It predicts a sequence of speed fluctuations for a level walkway interrupted by single uneven upward step (*Up-step*) that agree well with human responses [1].

Further analysis of the model reveals dynamics that are approximately linear and superimposable. The compensation for a complex sequence of uneven steps could thus be composed quite easily, by superimposing a sequence of Up-step responses, each scaled for the height of one of the upcoming uneven steps. Conversely, the speed fluctuations for complex terrain could be deconstructed into a single Up-step disturbance waveform. Thus, the locally optimal control plan may be made global, and vice versa. We tested this by measuring speed fluctuations for humans walking over complex and simple terrains and comparing the speed responses with model prediction. We tested whether each terrain was predictive of human responses on the other and could be predicted by model.

Methods

We measured human (N = 11) speed fluctuations on two different terrains [1], and tested for linear superposition. Both terrains involved 15 meters flat ground before and after the uneven steps. The Up-step consisted of a single upward step (7.5 cm high) in the middle (Figure 1, top row left), whereas the Complex terrain had a pseudo-random pattern of 17 upward, downward, or level steps (Figure 1, top row right). We averaged each terrain's speed profiles across subjects (Figure 1, top row). We deconvolved the Complex waveform into a hypothetical Up-step kernel and tested whether that kernel could be superimposed to compose the Up-step and Complex responses (Figure 1, top row), and predict responses for a third, Independent terrain (Figure 1, bottom row right). We also used optimal control to predict speed profiles for the model [2]. for Up-step, Complex, and Independent terrain.

Results and Discussion

The Up-step speed fluctuation waveform was found to speed up over a few steps preceding the perturbation, lose speed atop it, and then to speed up again over a few subsequent steps (Fig. 1, top left). Decomposition of the Complex response yielded an Up-step kernel roughly similar to the empirical Up-step waveform (correlation coefficient R = 0.50, p = 1.4e-06 t-test N=11). That same kernel was also applied to the Complex terrain to re-compose the Complex speed waveform (R = 0.56, p = 2.2e-06). The same Up-step kernel was also able to predict the Independent terrain (R = 0.63, p = 4.7e-08). The model was also reasonably predictive of the Up-step (R = 0.45), and by superposition Complex (R = 0.27) and Independent (R = 0.57) terrains, all $p < 0.05$.

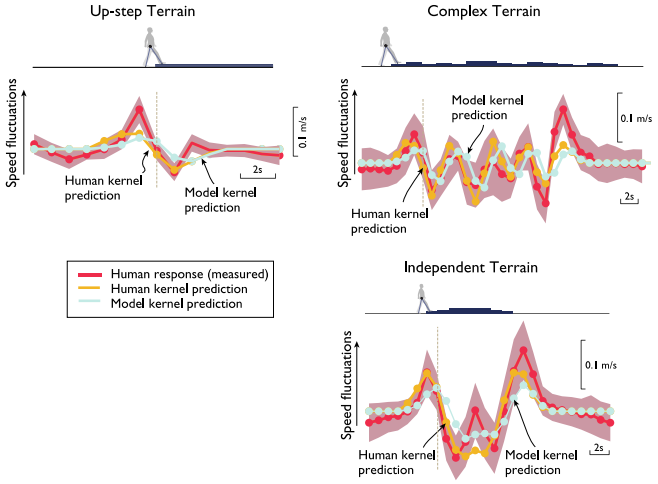

Figure 1: Top Row: Human speed fluctuations (mean N=11 subjects, shaded area ±1 std, vertical line denotes the first uneven step) on (left) Up-step and (right) Complex terrains, with predictions made from human Complex speed waveform, and by model. Bottom right: Measured and predicted speed (from human and model kernels) on an Independent terrain (mean ± s.d.).

Significance

Human speed adjustments on uneven terrain are not due to greater tonic effort, but are systematic and predictable. A single uneven step's response waveform may be composed into the response for many complex steps, and a complex waveform decomposed into a simpler one. The responses are also consistent with a model minimizing mechanical work. Humans can plan dynamic momentum control for complex terrain, perhaps to minimize work or energy expenditure, and the plan's composition could be as simple as linear superposition.

Acknowledgments

Supported by NSF DGE 0718128, ONR ETOWL program, NIH AG030815, the Dr. Benno Nigg Chair, NSERC (Discovery and CRC Tier I).

References

[1] Darici et al., 2017, *International Society of Biomechanics*.
[2] Darici et al., 2020, *Scientific Reports*, 10: 540

TOE JOINT EFFECT ON ANKLE KINEMATICS/KINETICS UNDER ACTIVE CONTROL

Woolim Hong[1], Namita Anil Kumar[1], and Pilwon Hur[1,2,*]
[1]Department of Mechanical Engineering, Texas A&M University, College Station, TX 77843, USA
[2]School of Mechanical Engineering, Gwangju Institute of Science and Technology, Gwangju 61005, South Korea
email: *pilwonhur@gist.ac.kr

Introduction

Toe joint is known as one of the important factors impacting the locomotor performance of humans [1], [2]. In [1], [2], researchers investigated the effect of toe joint on the ankle kinematics and kinetics by applying different stiffness conditions on the toe joint. According to their results, the rigid foot (i.e., without toe joint) showed more ankle push-off power compared to other toe stiffness conditions. To date, most studies of the toe joint effect have been done in the passive joint condition. Thus, in this study, the authors explore the toe joint effect on the ankle joint kinematics/kinetics under active control conditions using the fully actuated transfemoral prosthesis.

Methods

In this study, we used two different types of the prosthetic foot: without toe (WOT) and with toe (WT). The WOT foot is corresponding to the foot with the infinity stiffness in the toe joint, while the WT foot is corresponding to the foot with stiffness of 12 Nm/rad in the toe joint. The toe joint stiffness was given by putting four layers of flat-shaped spring steel [3].

For the prosthetic walking experiment, a custom-built fully actuated transfemoral prosthesis, AMPRO II [4], was used. To control the powered prosthesis, a hybrid control framework (i.e., impedance and tracking control) was utilized. In this study, we focus on ankle joint control because the ankle is more closely related to the toe joint compared to the knee [1]. Four equilibrium angles were set to the ankle for the impedance controller (see Table 1) [5]. Other impedance parameters (i.e., stiffness and damping) were controlled to be the same for both feet.

Table 1: Ankle equilibrium angles in four different walking phases. Heel-Strike (HS), Flat-Foot (FF), Heel-Off (HO), and Toe-Off (TO).

	Phase 1 (HS-FF)	Phase 2 (FF-HO)	Phase 3 (HO-TO)	Phase 4 (TO-HS)
WOT	0°	-2°	-10°	2°
WT	0°	-2°	-10°	2°

A healthy young subject (male, 170 cm, 70 kg) participated and was asked to walk on a treadmill using an L-shape simulator. The subject's safety was guaranteed by handrails on either side of the treadmill. The subject walked at 0.80 m/s for a minute and made over 30 consecutive steps during the experiment. All the joint kinematics data was recorded by two high-resolution optical encoders at each joint. This experimental protocol has been reviewed and approved by the Institutional Review Board (IRB) at Texas A&M University (IRB2015-0607F).

Results and Discussion

Figure 1 shows the ankle/knee joint angle and power results from the walking experiment. In Fig. 1A, the WOT shows earlier push-off than the WT foot. This can also be found in the ankle power curve in Fig. 1B. According to Table 2, when the toe joint is missing, the maximum ankle power is found 3.5% earlier than the WT foot ($p < 0.001$). Table 2 also shows that the maximum power of the WOT foot is 13.3% greater than that of the WT foot ($p > 0.05$), which is agreed with the previous studies [1], [2].

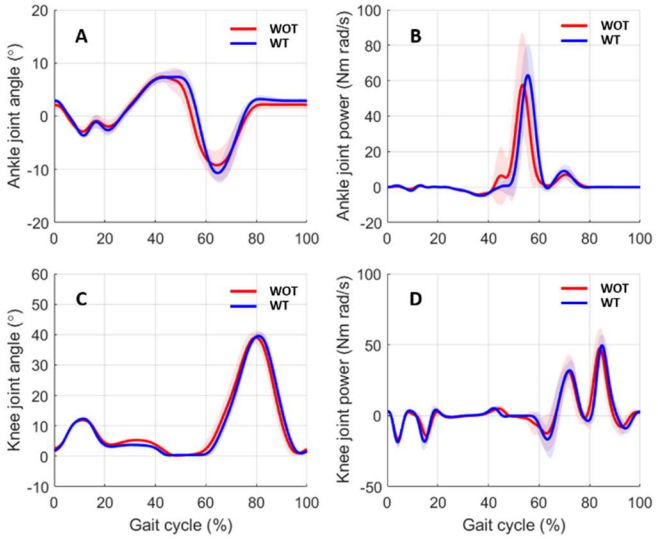

Figure 1: Ankle/knee joint angle and power profiles of two different types of the prosthetic foot (Red: WOT, Blue: WT). Solid lines and shaded regions indicate mean and ± 1 standard deviation of 30 consecutive steps, respectively.

Table 2: Maximum ankle power and the timing of the maximum ankle power for 30 consecutive steps.

	Maximum power (Nm*rad/s)	Maximum power timing (%)
WOT	80.21 ± 20.11	51.96 ± 3.43
WT	70.76 ± 16.55	55.48 ± 1.30

However, in Fig. 1B, the maximum value of the average power profile seems different from the result in Table 2. This is because the actual max ankle power (Table 2) didn't necessarily happen when the average profile was at its maximum (Fig. 1B). In the case of knee joint, there is no apparent difference between WOT foot and WT foot in general.

Since we have a limited number of subjects in this study, we plan to extend this study with a larger number of subjects (e.g., amputee subjects). Also, the authors believe the toe joint plays a more important role in faster walking, thus we plan to include different walking speed conditions when we conduct further experiment in the future.

Significance

By encompassing the idea of the passive toe joint and the active control at the ankle joint, the authors could achieve a better foot-rolling with a sufficient push-off time, resulting in a timely push-off with sufficient power to enhance the amputees' walking performance.

References

[1] E.C. Honert, et. al. (2018), *Bioinspiration & Biomimetics*, Vol. 13, No. 6
[2] K.A. McDonald, et. al. (2021), *Scientific Reports*, Vol. 11, No. 1
[3] W. Hong, et. al. (2018), *Americal Society of Biomechanics (ASB)*
[4] W. Hong, et. al. (2019), *IEEE ICRA*
[5] N. Anil Kumar, et. al. (2020), *IEEE ICRA*

INCREASES IN A RUNNER'S CUMULATIVE LOAD PRECEDE METATARSAL STRESS FRACTURE: A CASE STUDY

Ryan Alcantara[1] & Alena M. Grabowski[1]
[1]Applied Biomechanics Lab, University of Colorado Boulder, CO, USA
email: ryan.alcantara@colorado.edu

Introduction

Metatarsal stress fractures comprise 23% of stress fractures sustained by National Collegiate Athletic Association (NCAA) Cross Country runners [1]. Increases in a runner's workload (e.g., mileage and pace) affects cumulative bone loading and thus the risk of sustaining a stress fracture [2]. Cumulative bone loading is generally defined as the product of the magnitude of internal/external loads and the number of steps taken over a given duration of running [2]. The external cumulative bone loading can be estimated with wearable devices [3] and may be a viable measure of injury risk.

We sought to prospectively estimate external cumulative bone loading over the freshman year of an NCAA Cross Country runner who sustained a metatarsal stress fracture. Based on previous research that found military recruits sustained stress fractures ~1 month after undergoing a 2-month physical training program, we hypothesized that the runner would experience an increase in a surrogate of cumulative bone loading approximately 30-90 days prior to injury [4].

Methods

Data from a male NCAA Cross Country runner (18 yrs, 75 kg, 1.85 m) were analysed. The runner was diagnosed with a Grade 3 2nd metatarsal bone stress injury by a clinician. We analysed global positioning system (GPS) watch data collected at 3 Hz over 150 training runs during the 6 months prior to injury. The GPS watch measured running speed, cadence, and distance. We used these data to calculate the number of steps taken within 12 speed ranges (2-8 m/s in 0.5 m/s increments) for each run.

We conducted two data collections approximately 5 months and 1 month prior to injury. During these data collections, the runner ran on an instrumented treadmill (1000 Hz; Treadmetrix, Park City, UT) at 3.8, 4.1, and 5.4 m/s for 30 seconds each. We used a 30 N vertical ground reaction force (vGRF) threshold to identify stance phase and calculated peak vGRF for steps in the final 10 seconds of each trial. We used a linear mixed effects model to quantify the effect of running speed on peak vGRF. We then used the model to predict the peak vGRF for the speed ranges identified from the GPS watch data.

For each training run, we calculated cumulative load (CL) by multiplying the number of steps taken in each speed range by the corresponding predicted peak vGRF raised to the 4th power ($vGRF^4$) [5]. We used peak $vGRF^4$ to account for the relatively larger effect of load magnitude on bone fatigue life compared to the number of load cycles (steps) [2]. We used the predicted peak vGRF values based on the data collection closest to the date of a given training run. Thus, we incorporated longitudinal changes in the runner's vGRF production in our measures of CL.

Results and Discussion

In support of our hypothesis, the 7-day moving average CL increased 128% from approximately 90 to 60 days before injury and increased 161% from approximately 90 to 30 days before injury (Fig. 1). In contrast, the 7-day moving average running mileage increased 46% from approximately 90 to 60 days prior to injury and increased 87% from 90 to 30 days prior to injury. The weekly increase in the 7-day moving average running mileage was 0.2, 5.6, 45.2, and -4.8% from 3 to 2 months prior to injury but the weekly increase in the 7-day moving average CL was 14.2, 10.4, 41.3, and 41.5%. A 10% increase in weekly running mileage is traditionally used to define a safe increase in a runner's workload [2] but our findings illustrate how small changes in weekly mileage can result in large changes in CL. Relying on running mileage to determine injury risk does not account for disproportionate changes in bone loading due to running distance and speed [2] or how a runner's biomechanics may change over time.

NCAA Cross Country runners typically have three competitive seasons per year and can experience changes in workload when transitioning between seasons. Our findings indicate that a rapid increase in workload early in a competitive season may have contributed to the development of a stress fracture. Monitoring CL may help coaches quantify a runner's risk of stress fracture and inform changes in running mileage and pace. Moreover, an optimal workload depends on a runner's biomechanics, physiology, and musculoskeletal properties [2].

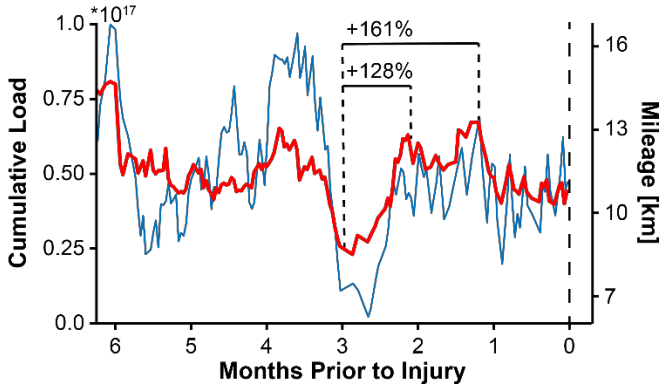

Figure 1. The 7-day moving average of a runner's cumulative load (CL; red line) and mileage (blue line) during the 6 months prior to developing a metatarsal stress fracture. From 3 to 2 months prior to injury, CL increased 128%. From 3 to 1 month prior to injury, CL increased 161%.

Significance

The number of steps taken and peak vGRF at a given speed may provide a viable surrogate for cumulative bone loading and could be used to inform a runner's risk of stress fracture injury. Longitudinally monitoring CL is feasible by leveraging data from a GPS watch and vGRF data collected in a laboratory.

Acknowledgments

Supported by the PAC12 Student-Athlete Health and Well-Being Grant Program (#3-03_PAC-12-Oregon-Hahn-17-02).

References

[1] Rizzone, K., et al. *J. Athl Training.* 2017; **52** (10), 966-75.
[2] Warden, S., et al. *Curr Osteoporos Rep.* 2021.
[3] Kiernan, D., et al. *J Biomech.*2018; **73** 201-9.
[4] Armstrong, DW., et al. *Bone*. 2004; **35**, 806-16.
[5] Ahola, R., et al. *J Biomech.* 2010; **43**, 1960-4.

AMONG GAIT QUALITY METRICS, GAIT DEVIATION INDEX BEST DISCRIMINATES CHANGES ASSOCIATED WITH TUNING OF A POWERED BELOW KNEE ROBOTIC PROSTHESIS

Kinsey Herrin*, Samuel T. Kwak, Chase G. Rock, Gautam Desai, Saranya Gourisetti, Isabella Turner, Margaret Berry, Young-Hui Chang
Georgia Institute of Technology
email: *kinsey.herrin@gatech.edu

Introduction

Powered robotic prostheses represent the latest advancement toward providing improved performance for individuals with amputation, and may improve metabolic cost, joint loading, and overall mobility[1], but the tuning process associated with a powered prosthesis for an individual user is problematic in that it is: 1. time consuming for busy clinicians and 2. currently completed in clinical settings based on subjective, observational metrics. To further complicate this process, there is an assumption that there is an ideal gait pattern for which clinicians should tune towards, but clinically based tuning often involves balancing patient comfort and capabilities as well as efforts to reduce habitual gait deviations. There are many ways to measure gait, making it challenging to determine a "gold standard" gait for a single individual. Studies have attempted to combine biomechanical measures (joint angles, kinetics, etc.) to create indices of gait quality, but it is unclear what measure is an optimal "gold standard" for which a robotic prosthesis should be tuned against. Therefore, in this study we investigate the ability of four common gait quality metrics to distinguish differences between a clinically prescribed, passive prosthesis and a tuned powered robotic prosthesis. Our hypothesis is twofold: 1) biomechanically based metrics will better distinguish gait differences than an observational metric between a passive foot and a powered foot and 2) a powered robotic prosthesis will improve gait quality according to the best metric as defined in hypothesis 1.

Fig 1. Powered prosthesis

Methods

Four subjects with below knee amputation provided informed consent according to the Georgia Institute of Technology IRB prior to study enrolment. Participants walked in their clinically prescribed, passive prosthesis over a split-belt treadmill (Bertec) at 1.0 m/s for three 15 second trials while full body biomechanics were collected. Then, a powered, tethered below knee prosthesis (Humotech PRO-001) was fit and aligned to each participant by a certified prosthetist (See Figure 1). The prosthesis was clinically tuned according to observational gait analysis and patient reported feedback. Full body biomechanics were recorded for 15 second trials following each tuning parameter change until the patient reported feeling comfortable and the gait was assessed to be visually appropriate at which point the final trial was collected. Gait quality was assessed post hoc using the Prosthetic Observational Gait Score (POGS)[2], the Gait Deviation Index (GDI[3]), trunk lateral sway[4], and impulse asymmetry[5]. Paired t-tests were used to compare differences between the passive and powered feet conditions with an alpha <0.05.

Results and Discussion

Of the four metrics analyzed, the GDI revealed significant differences between the passive foot and the powered foot for all subjects (see Table 1). Both impulse asymmetry and lateral sway were able to distinguish between the passive and powered feet in two subjects. Lateral sway improved in two subjects with use of the powered foot, but impulse asymmetry improved in one subject and worsened in another. Interestingly, as an observational clinical outcome, POGS could not distinguish between the passive and powered feet conditions.

GDI increased for three out of 4 subjects, which is a sign of improved gait quality. In one subject, GDI decreased from a normal gait pattern score (score ≥100) to a score of 98.3 which would also be considered a normal gait pattern. In this same subject, impulse asymmetry significantly decreased which would be indicative of improved symmetry during walking.

	GDI		Lateral Sway		Impulse Asymmetry		POGS	
Subject	*Passive*	*Powered*	*Passive*	*Powered*	*Passive*	*Powered*	*Passive*	*Powered*
BK01	87.2	98.2*	5.4	4.5*	42.6	23.7	5.0	5.0
BK02	86.0	90.7*	9.6	6.0*	25.8	36.6	3.0	3.0
BK04	96.6	104.0*	5.6	4.8	21.5*	62.6	3.0	0.0
BK06	106.7*	98.3	5.7	5.6	38.5	15.7*	0.0	0.0

Table 1. Results for GDI, Lateral Sway, Impulse Asymmetry and POGS in n=4 subjects with a below knee amputation. Significant improvements ($p<0.05$) are shaded in grey with an asterisk(*).

Our first hypothesis is accepted in that biomechanically based metrics were better at discriminating change in gait quality than an observational metric; however, we did see that GDI outperformed both impulse asymmetry and lateral sway indicating that there are varying levels of sensitivity among biomechanical metrics. For our second hypothesis, we saw improvements in the GDI of three subjects and a slight worsening of GDI in another subject. However, the decreased GDI did not indicate an abnormal gait. Moreover, we saw improvement in this subject's impulse asymmetry which would be indicative of a higher quality gait. Therefore, we accept our second hypothesis. It is worth mentioning that we saw a worsening of impulse asymmetry in another subject (BK04) with use of the powered foot; this underscores one of the biggest challenges in working with clinical populations- individuals may respond differently to varying technology and/or may require increased acclimation time to experience maximum benefit from a new device.

Significance

Given its sensitivity toward changes in gait, we believe GDI is an excellent metric for tuning robotic prostheses for 'optimal' gait. Interestingly, as a common, visually based clinical outcome measure, POGS still does not fully capture the nuances of standard clinical tuning for a powered prosthesis.

Acknowledgments

This work is supported through a grant from NSF NRI 1734416 and the authors gratefully acknowledge the GT PoWeR/EPIC labs for use of equipment.

References

1.Goldfarb, et al. (2013). *Sci. Trans. Med.*, **5**(210). 1-4.; 2. Hillman, et al. (2010). *Gait & Post.*, **32**(1), 39-45.; 3.Schwartz, et al. (2008) *Gait & Post.*, **28(**3), 351-357; 4. Lamoth, et al. (2010)Med Eng&Phys, (9):1009-14.; 5. Zmitrewicz, et al. (2006) Arch PM&R, 87(10), 1334-9.

QUANTIFYING PERIPHERAL NERVE INTERFACE AND RESIDUAL MUSCLE CONTROL DURING PHANTOM HAND MOVEMENT

Michael A. Gonzalez[1], A. Vaskov[1], P. Vu[1], C. Lee[1], C. Chestek[1], and D. Gates[1]
[1]University of Michigan, Ann Arbor, MI
email: magonzo@umich.edu

Introduction

Continuous control of advanced prosthetic hands is thought to require a well-defined model of the phantom hand and the ability to control it precisely. However, it is difficult to quantify an individual's level of phantom hand control. One approach to quantifying force and movement control is through Fitts' Law [1], a model of the relationship between task difficulty and task completion time. Faster and less variable performance results in a higher throughput, which represents more precise control. To better quantify and understand movement of the phantom, this approach can instead be applied to the electromyography (EMG) signals that would typically be present for that movement. For those muscles that no longer exist in individuals with amputation, it is possible to collect EMG from a biologic construct like a Regenerative Peripheral Nerve Interface (RPNI.). RPNIs are created by suturing a free muscle graft to a severed peripheral nerve. Following a period of revascularization and reinnervation, direct implantation of electrodes in RPNIs enables us to record amplified signals originating from the intrinsically innervating nerves [2].

However, the degree to which RPNI control may differ from that of residual muscles, or how these signals correspond to perceived phantom limb movement has yet to be studied. The purpose of this study was to quantify an individuals' ability to modulate RPNI and residual muscle signals during the perceived movement of their phantom limb.

Methods

One female with right transradial amputation participated. The participant underwent surgical intervention where RPNIs were created and 8 indwelling electrodes were implanted in these RPNIs and residual muscles. The participant was asked to flex her phantom thumb, with maximal effort, while viewing a visual display of the electroymography linear envelopes from her Flexor Pollicis Longus (FPL) and Median nerve RPNI. Muscle signals from indwelling electromyography (EMG) electrodes was collected at 1 kilosample/s. Envelopes were created by first bandpass filtering(100-500 Hz), rectifying, and smoothing signals with a 375ms moving average filter. The peak of the envelope during this trial was denoted maximum voluntary effort (MVC) and used for scaling signal targets.

The participant was presented with a random combination of target EMG amplitudes (25, 50% MVC) and widths (5, 10, 20, 40% MVC) (32 trials total) and asked to modulate her EMG amplitude so it fell within the target window as quickly as possible, within 4 seconds. She was provided continuous visual feedback of her EMG signals throughout the trial. The full protocol was completed twice, once with the residual muscle and once with the RPNI signal. For each trial, we measured peak EMG amplitude and time to peak amplitude. We then calculated the effective index of difficulty as:

$$ID_e = \log_2(A_e/W_e + 1)$$

where A_e is the mean peak amplitude across trials for a given target and W_e is calculated based on the variability of peak amplitudes for a given target. Throughput was then calculated using:

$$TP = \frac{1}{n}\sum\frac{ID_{e_i}}{Movement\ Time_i}\ ,where\ i\ the\ target\ MVC$$

We calculated the effect size for the differences between FPL and RPNI's peak amplitude and time to peak amplitude using Cohen's d.

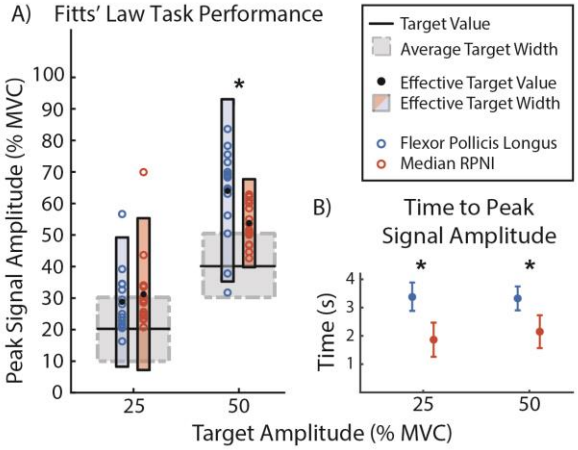

Figure 1: (A) Effective amplitude and width between channels. Grey boxes indicate target MVC and average target width. (B) Time to peak force between channels. * denotes a large effect size.

Results and Discussion

When matching her EMG to the targets, the participant was more accurate and less variable using her RPNI EMG than her residual muscle. This difference had a small effect for 25% targets (d = 0.36) and large effective for 50% targets (d = 1.13). The participant reached her peak amplitude faster with RPNI compared to with FPL for both targets (d_{25} = 1.82, d_{50} = 1.54).

The RPNI had a throughput that was nearly double that of the FPL (0.65 vs. 0.33 bits/s). Notably, the difference in throughput resulted from differences in time rather than differences in signal variability. This is relevant in the context of prosthetic control, as delays in control can disrupt the control loop [3]. Longer delays, or less predictable control, may necessitate more visual or sensory feedback to complete successful grasps.

Significance

This research provides the first direct comparison of control between RPNI and residual muscle signals in the context of a phantom limb movement. Our future work will focus on expanding this methodology to additional signals, as well as capturing surface EMG control. We hope this research will lead to a better understanding of how individuals with amputation control their phantom limb and if congruence between phantom and prosthetic hand position affects functional performance.

Acknowledgments

Thank you to Kelsey Ebbs. Our work is supported by NINDS grant R01NS105132

References

[1] Thumser et al. (2018). Front. Psych., 9:560
[2] Vu et al. (2020). Sci. Transl. Med. 12 :533560
[3] Saunders and Vijayakumar (2011). JNER, 8:60

RELATING FASCICLE DYNAMICS TO MUSCLE ACTIVITY AND MECHANICAL WORK DURING WALKING

Samuel T. Kwak[1]*, Young-Hui Chang[1]
[1]School of Biological Sciences, Georgia Institute of Technology, Atlanta, GA, USA
Email: *skwak@gatech.edu

Introduction

Controlling muscle fascicle dynamics during movement tasks is necessary for optimal performance and requires interaction between the muscle activation and the expected load (1,2). The correlation between fascicle timing and muscle activation has been observed in jumping (3), but it has not been addressed for muscles involved in absorbing negative work during the braking phase of walking in humans. Our goal was to understand how the timing and magnitude of activation of the tibialis anterior (TA) muscle relate to TA muscle fascicle dynamics during that task.

We predicted that during steady walking, peak TA muscle activity would correlate with TA muscle fascicle length change, peak fascicle velocity, and peak fascicle acceleration; and that negative work during heel strike would positively correlate with those three parameters. We also predicted that peak TA muscle activity would coincide with the time of peak fascicle velocity.

Methods

Eleven subjects (22.8 ± 3.6 years, 64.4 ± 9.7kg) gave written, informed consent prior to participating in our IRB approved protocol. Subjects walked at 1 m/s on an instrumented treadmill at 80% of their preferred step frequency. 3D joint kinematic (Vicon) and kinetic (AMTI) data were collected with ipsilateral TA ultrasound and EMG data (normalized to mean maximum EMG at 1.5 m/s). EMG data were collected from the contralateral leg on two subjects, where we assumed symmetry of mean TA EMG during steady-state walking. EMG data for two other subjects were corrupted and, therefore, not included in this study. TA muscle ultrasound images (60 Hz) were collected (Telemed) and manually digitized to obtain muscle fascicle lengths, velocities, and accelerations. We defined peak length change as the greatest amount of continuous fascicle lengthening from the initial heel contact until foot-flat gait events. Net length change, peak muscle activity, peak fascicle velocity, and peak fascicle acceleration were calculated in the same time window. We defined negative leg work as the negative mechanical work performed on the body center of mass by the lead leg from initial contact until COM power crossed zero. We used an ANOVA for linear regression correlations and a paired t-test for comparison of means to determine significance.

Results and Discussion

We accepted our hypotheses that peak TA muscle activity had a large effect on peak fascicle length change (f^2 = .78, p = .052) (Fig. 1B), peak velocity (f^2 = .76, p = .054), and peak acceleration (f^2 = .68, p = .039). In contrast, we rejected our hypotheses regarding correlations to lead limb negative work. Negative work did not correlate with peak fascicle length change (f^2 = .02, p = .690) (Fig. 1A), peak velocity (f^2 = .01, p = .757), or peak acceleration (f^2 = .05, p = .484). Negative work also did not correlate with peak muscle activity (f^2 = .06, p = .541). Although TA muscle lengthening during the stance phase of walking is related to its activation, the negative work experienced during weight acceptance does not appear to contribute to this relationship.

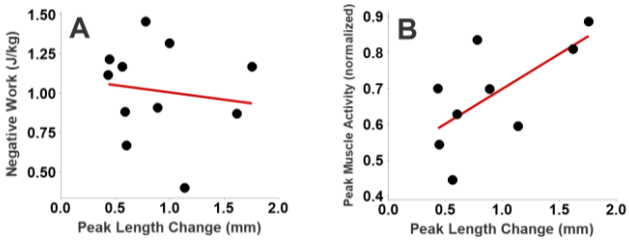

Figure 1: Lead limb negative work on COM (left) and peak TA muscle activity (right) with respect to TA muscle peak fascicle length change (linear fit, red line). Each dot represents the average of a single subject.

On average, peak TA muscle activity occurred 28 ms after initial heel contact (Fig. 2A), while mean peak fascicle velocity occurred 50 ms after heel contact (Fig. 2B). While the mean times of these events were different (d = 0.74, p < .001), the frequency of steps where peak EMG and fascicle velocity most often occurred overlapped in their timing (Fig 2). This timing (~40 ms) agrees with estimates of the short latency spinal reflex of the TA muscle (4). As net fascicle length change (0.24 ± 0.45 mm) was lower than peak length change (0.89 ± 0.45 mm, d = 1.19, p < .001), short-latency feedback from the TA muscle may be used as a protective mechanism to reduce overall fascicle stretching and avoid injurious strains.

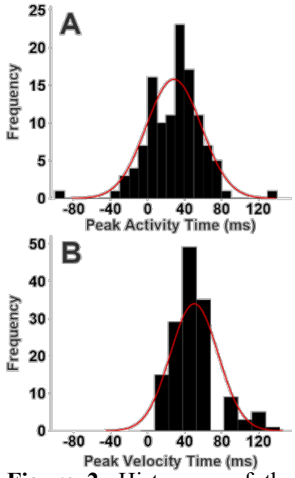

Figure 2: Histogram of the timing of peak TA activity (A) and peak fascicle lengthening velocity (B) across all steps with respect to initial contact at 0 ms, fitted with a normal distribution curve (red).

Significance

During normal human gait, many step-by-step adjustments are rapidly made to minimize energetic cost without the use of direct metabolic sensors (5). Proprioceptive feedback from leg muscles may play a major role in how these adjustments are made, particularly during the braking phase of walking when muscles are more likely to be eccentrically loaded. Elucidating the interaction between muscle activation and fascicle dynamics, and how it influences gait mechanics, will provide a more complete understanding of how locomotion is controlled, which could be leveraged toward improving rehabilitation techniques.

Acknowledgments

The authors thank Ashley Tran and Erika Sheng for assisting in data collections, and funding from NIH T32-HD055180.

References

1) Kawakami Y, et al. (2002). *J Physiol*, *540*(2), 635-646.
2) Lichtwark GA, et al. (2008). *J Theor Biol*, *252*(4), 662-673.
3) Wade L, et al. (2020). *J Appl Physiol*, *128*(3), 596-603.
4) Zuur AT, et al. (2009). *J Physiol*, *587*(8), 1669-1676.
5) Selinger JC, et al. (2015). *Curr. Biol. 25*(18), 2452-2456.

METHODS FOR ASSESSING SHOULDER DYNAMICS AND FUNCTION IN PEDIATRIC WHEELCHAIR ATHLETES

Matthew M. Hanks[1], Samantha R. Schwartz[1], Alyssa J. Schnorenberg[1], Kathryn A. Reiners[2], Shubhra Mukherjee[2], and Brooke A. Slavens[1]

[1]Department of Occupational Science & Technology, University of Wisconsin-Milwaukee, Milwaukee, WI, USA

[2]Shriners Hospitals for Children-Chicago, Chicago, IL, USA

email: *hanks@uwm.edu *corresponding author

Introduction

Approximately 20% of individuals living with spinal cord injuries (SCI) in the United States are children [1], and many use manual wheelchairs for mobility and physical activity. Exercise and physical activity are crucial to the long-term physical and mental health of pediatric manual wheelchair users [2]. However, limited knowledge exists regarding the relationship among physical activity, shoulder biomechanics, and function in children. This study examined the feasibility of characterizing clinically relevant shoulder biomechanics and function in pediatric wheelchair athletes and nonathletes.

Methods

Two pediatric manual wheelchair users with SCI (n = 1 male nonathlete, age: 7.5 years, height: 1.1 m, weight: 23 kg, level of injury: T6, time since injury: 7.2 years; n = 1 female athlete, age: 13.9 years, height: 1.35 m, weight: 50 kg, level of injury: T10, time since injury: 11.2 years) participated in a single experimental session approved by the institutional review board. Clinical examination consisting of active range of motion, isometric strength, and shoulder special tests was conducted. Participants propelled their personal wheelchair using a self-selected propulsion pattern and speed on tile floor. A Vicon motion capture system synchronized with Smartwheel instrumented wheelchair handrims were used to acquire three-dimensional (3-D) kinematics and kinetics. An established inverse dynamics model was applied to compute dominant limb 3-D glenohumeral joint dynamics during multiple propulsion cycles [3]. Function was measured using the validated Pediatric Spinal Cord Injury Activity Measure (PEDI SCI-AM).

Results and Discussion

Glenohumeral joint dynamics differed between the participants. On average, the wheelchair athlete exhibited less peak extension and internal rotation moment and greater flexion-extension range of motion than the nonathlete (Figure 1). Decreased shoulder range of motion is related to increased shoulder pain and decreased shoulder function in adult manual wheelchair users [4]. Similarly, high glenohumeral joint internal rotation moments are directly related to clinical shoulder pathology in adults [5]. Both of these trends occurred in the nonathlete relative to the athlete.

Previous research in adult manual wheelchair users suggests that physical activity is associated with increased strength and function [6]. We found that both participants had no pain or deficits in isometric strength and tested negative for supraspinatus and biceps weakness with the Empty Can and Speeds test, respectively. However, the wheelchair athlete scored higher on the PEDI SCI-AM compared to the nonathlete in the daily routines and self-care, wheeled mobility, and general mobility domains. These findings suggest that the pediatric wheelchair athlete is able to execute complex functions and perform everyday activities better than the nonathlete. Results from this experiment suggest that the proposed methods to assess glenohumeral joint dynamics and function can sensitively distinguish differences between pediatric wheelchair athletes and nonathletes and thus may help to evaluate function in a larger population of wheelchair users.

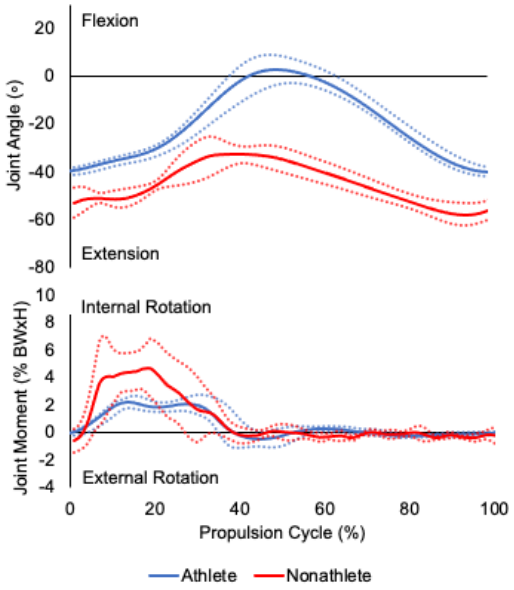

Figure 1: Mean ± 1 standard deviation glenohumeral joint flexion-extension angle (top) and normalized (body weight times height) internal-external rotation moment (bottom) during wheelchair propulsion in a pediatric wheelchair athlete (blue) and nonathlete (red).

Significance

These preliminary results serve as the basis to examine the relationship among physical activity, shoulder health, and mobility in pediatric manual wheelchair users. Shoulder pain and pathology become more concerning in manual wheelchair users with age and time since injury. Investigating the effects of physical activity on shoulder biomechanics and function in pediatric athletes may help identify strategies to enhance health and wellness across the lifespan. Research is underway with a larger sample size to better understand these relationships.

Acknowledgments

This research was supported by the Eunice Kennedy Shriver National Institute of Child Health and Human Development (NICHD) of the NIH (1R01HD098698). The authors would like to thank Dr. Kathy Zebracki at Shriners Hospitals for Children and the members of the UWM Mobility Laboratory.

References

[1] Facts on Pediatric Spinal Cord Injury. *ASIA*, 2021.
[2] Bloemen et al. *Dev Med Child Neurol*, 2015
[3] Schnorenberg et al. *J Biomech*, 2014.
[4] Ballinger et al. *Arch Phys Med Rehabil*, 2000.
[5] Mercer et al. *Clin Biomech*, 2006.
[6] Mulroy et al. *Phys Ther*, 2015.

Neuromuscular patterns change as a function of the temporal structure of metronomes during walking

João R. Vaz[1], Nelson Cortes[2], João S. Gomes[1], Pedro Pezarat-Correia[1], Nick Stergiou[3]
[1]Neuromuscular Research Lab, Faculty of Human Kinetics, University of Lisbon, Lisbon, Portugal
[3]George Mason University, Fairfax, VA USA
[3]Department of Biomechanics, University of Nebraska at Omaha, Omaha, NE USA
email: joaovaz@fmh.ulisboa.pt

Introduction

Variability is a fundamental feature of human movement. [1]. In particular, non-random fractal fluctuations during gait are present in a healthy gait. [1] Conversely, ageing alters these healthy fluctuations of human gait by turning them more random. [2] Gait rehab typically uses an isochronous stimulus that ignores the natural fluctuations of human gait. Several recent studies suggested that using a stimulus that embeds these natural fluctuations will improve this fundamental feature of human gait. [3-6] Despite the growing body of literature, the evidence of neuromuscular changes when walking to this stimulus is lacking. This is a fundamental next step to understand if and how this approach would lead to changes in the neuromuscular system. Therefore, this study aimed to investigate the effects of walking to different temporally structured metronomes on i) gait variability and ii) muscle activity variability. Additionally, it aimed to investigate if gait variability is associated with muscle activity variability.

Methods

Fourteen male participants (22.1±3.8yrs, 1.75±0.07m, 69.8±8.5kg) volunteered for this study. Participants walked four 10-minute trials on a treadmill. The first trial was an uncued trial at self-preferred speed; this was used for the calculation of preferred stride time (SPW). The stride time from this trial was then used to design individualized stimuli for 3 randomized cued trials: Isochronous (ISO), Fractal (FRC) and Random (RND). The stimulus was provided via a moving horizontal bar projected on a screen in front of the participant. Participants were instructed to synchronize their right heel strike to the top of the moving bar's path. [2,3] An accelerometer placed at the right foot's external malleoli was used to determine heel-strike events. Electromyography (EMG) was collected from the Gastrocnemius Medialis. Acceleration and EMG data were collected at 1kHz. We determined the inter-stride intervals (ISIs), defined as the time difference between two consecutive heel strikes. EMG signals were digitally filtered (10-500Hz), full-wave rectified, and low-pass filtered (12Hz, 4th Butterworth). Then, the peak of each gait cycle was detected to determine inter muscle peak intervals (IMPIs). Fractal scaling was calculated for each ISIs and IMPIs series and was used as a measure of the structure of variability. Detrended Fluctuation Analysis (DFA) was used to determine the fractal-scaling exponent (α) with window sizes of 16 to N/8. Repeated Measures ANOVA was used for both ISIs and IMPs. Pearson's Correlation Coefficient was used to test the association between ISIs and IMPIs.

Results and Discussion

In terms of α-ISIs, we have found a main effect for the condition (p<0.01). Pairwise comparisons revealed ISO and RND to be significantly lower than SPW (p<0.01) and FRC (p<0.01) – Table 1. Regarding α-IMPIs, we have also observed a main effect for condition (p<0.01). Pairwise comparisons showed ISO and RND to be lower than SPW (p<0.01) and FRC (p<0.01). α-ISIs and α-IMPIs were strongly correlated (R^2=0.83, p<0.001 – Fig. 1).

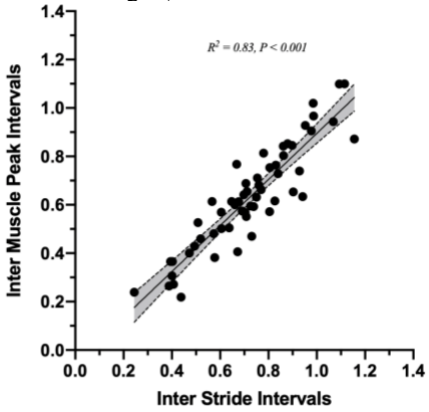

Fig. 1: Scatter plot *Inter Stride Intervals* vs. *Inter Muscle Peak Intervals*. Grey area represents confidence intervals.

Significance

The present study showed that a fractal metronome stimulated natural fluctuations during uncued, self-paced walking, while an isochronous and random metronome altered gait variability towards random fluctuations. Importantly, to the best of our knowledge, this is the first study to show this phenomenon occurring in the neuromuscular system (i.e., in muscle activity events). Furthermore, the relationship between gait and muscle activity variability suggests that when synchronizing to a metronome, the metronome's temporal structure also alters the neuromuscular patterns accordingly.

Acknowledgments

NS was supported by the NIH (P20GM109090 and R01NS114283)

References

1. Stergiou N, et al. *J Neurol Phys Ther* **30(3)**, 120-129, 2006
2. Vaz JR, et al. *Hum Mov Sci* **74**, 102677, 2020.
3. Vaz JR, et al. *Neurosci Let* **704**, 28-35, 2019.
4. Marmelat V, et al. *Plos One* **9**(3), e91949, 2014.
5. Hunt N, et al. *Sci Rep* **4**, 5879, 2014.
6. Vaz JR, et al. *Front Physiol* 11:67, 2020.

Table 1: Fractal-scaling (α) of Inter Stride Intervals and Inter Muscle Peak Intervals, per condition. Data are presented as M±SD.

	Self-Paced	Isochronous	Random	Fractal
Inter Stride Intervals **(ISIs)**	0.91 ± 0.16	0.52 ± 0.14	0.63 ± 0.12	0.83 ± 0.11
Inter Muscle Peak Intervals **(IMPIs)**	0.80 ± 0.19	0.41 ± 0.14	0.55 ± 0.12	0.76 ± 0.13

THE INFLUENCE OF HUNTINGTON'S DISEASE ON REACTIVE BALANCE MOVEMENT LATENCIES

J. Pitts[1], A. Gainer, C. Seidowski, C. Gwaltney, and C. A. Duncan[1]
[1]Department of Kinesiology and Integrative Physiology, Michigan Technological University
email: caduncan@mtu.edu

Introduction

Huntington's disease (HD) is a progressive, neurodegenerative disorder caused by a genetic defect that leads to atrophy in the caudate and putamen areas of the brain[1]. Physical symptoms of HD can challenge gait and balance[2], especially when coupled with cognitive impairments such as difficulties planning and coordinating movements[1]. Individuals with HD are more likely to experience fall injuries than healthy adults[3]. This is potentially due to decreased leg strength[4] and longer reaction times[5] that directly affect postural control. While reactive balance ability has been shown to decrease individuals with HD[6], the influence of HD on reactive stepping characteristics is unknown. The purpose of this research was to compare reactive balance in an individual with HD to a young adult free of conditions or injuries that would affect balance. We hypothesized that the individual with HD would show delayed responses and ability to recover from larger lean-and-release angles.

Methods

One female participant (67 y; 65 kg; 1.62 m) with a 12-year HD diagnosis (PwHD) was compared to one sex-matched healthy adult (20 y; 80.7 kg; 1.69 m) (HYA). Participants performed a series of lean-and-release balance recovery trials simulating a forward fall. Participants were horizontally tethered to the wall behind them while leaning forward in a plank-like position. The tether was released at a random time interval between 0-30 s, causing the individual to fall forward. For safety, participants wore a harness connected to an overhead gantry. Trials began at a 2° lean angle and increased by 2° each subsequent trial until the participant could not recover balance with only one step in three of five trials at that angle. Kinematic data were collected with an 11-camera optical motion capture system (Qualisys, Sweden). Surface electromyography (EMG) was collected bilaterally from the tibialis anterior (TA), rectus femoris (RF), and biceps femoris (BF) (Delsys Trigno, USA). Stepping and lower limb muscle onset latencies were calculated from kinematic and EMG data respectively. Stepping and muscle onset latencies of the PwHD lean angle (4°) where they began to take multiple steps were compared to equivalent angle of the HYA.

Results and Discussion

Our results indicate that the PwHD could only successfully recover from small release angle (2°) without taking the multiple steps, while implementing delayed recovery strategies. During the lean-and-release perturbations the PwHD could only reach a lean angle of 4°. This angle was far lower than the HYA (22°), and still lower than reported maximum lean angles for an older adult using similar lean-and-release protocols (13°)[7]. Muscle and stepping onset latencies were slower for the PwHD across all trials (Figure 1). Stepping onsets for the PwHD were 110-210msec slower than those of the HYA (Figure 1a). Corresponding muscle onset were approximately double those the healthy participant (Figure 1b).

These results support our hypotheses that the PwHD would show a delayed reactive response and resulting inability to recover from similar lean angles as healthy young and` older adults. These differences in response initiation may be related is potentially due to HD-related changes in sensorimotor integration ability.

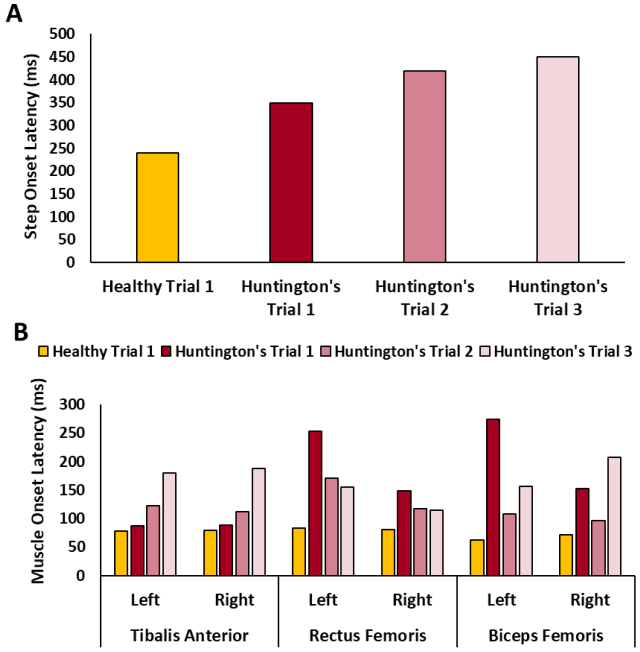

Figure 1: Stepping (A) and muscle (B) onset latencies for balance recovery trials at a 4° lean angle for a PwHD and HYA.

Significance

Ability to develop successful responses to regain balance are essential in preventing falls. To our knowledge, this is the first study to examine reactive stepping latencies of an individual with HD. Our results suggest that HD may affect the speed of reactive response initiation and ability to recovery balance during larger perturbations when compared to healthy older adults. These findings provide valuable insights to the nature of impaired reactive balance responses in individuals with HD that can help develop more focused interventions to improve balance control and prevent falls in individuals with HD.

References

1.Snowden JS (2017). Arch Clin Neuropsychol. 32(7):876-887.
2.Goodman & Fuller (2014). *Pathology: Implications for the Physical Therapist.* Elsevier Health Sciences; 2014.
3.Busse et. al. (2009). J. Neurol. Neurosurg. Psychiatry, 80(1):88-90.
4.Schell et al. (2019). NeuroRehabilitation.;44(1):85-93.
5.Goldberg et al. (2010) J. Neurol. Sci 298(1-2):91-95.
6. Tian et al. 1991*Acta Otolaryngol*. 1991;111(S481):333-336.
7.Carbonneau & Smeesters (2014). Gait & Posture. 39(1):365-371.

Biomechanical comparison of three implants used in the treatment of a fractured femur (31 A2.1) of an elderly patient

A..R. Vanegas[1], D.F. Villegas[2]
[1]Mechanical engineering student, Industrial University of Santander.
[2]P.H.D, Mechanical engineering professor, Industrial University of Santander.
email: adrianrangel20@gmail.com

Introduction

The election of the appropriate implant for the treatment of intertrochanteric fractures of the femur has been the subject of heated debate in the biomechanical field. And although some investigations have been carried and have determined the suitability of one or another method (namely, intramedullary or extramedullary osteosynthesis) in the treatment of fractures. The boundary conditions and the models used for said studies are part of a methodology that tends to idealize the true operating conditions of the implants, that is, the simplification of the models comes to consider healthy, long bones composed of a single material, which is not faithful to the biological reality described by the presence of cortical and trabecular tissue.

To avoid this limitation, our investigation performed a finite element analysis of the equivalent stresses (Von Mises) present in 3 common surgical arrangements in the treatment of a 31 A2.1 fracture (AO Classification) suffered by an elderly patient: PFNA nail, NAIL PFN and DHS plate. In this way we determine the implant that, in terms of reducing stress on the bone, provides better results for the patient.

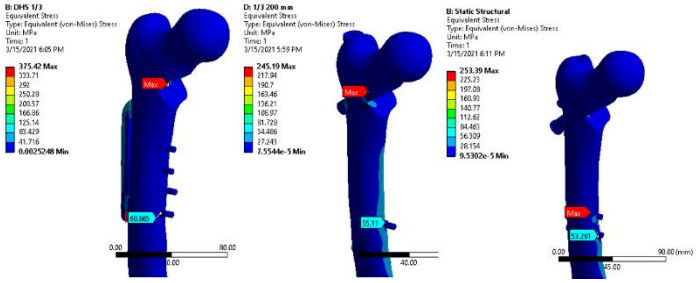

Figure 1: Equivalent stress distribution in the 3 assemblies a) DHS, the maximum effort in the bone was the highest of the 3, 68.665 Mpa b) PFNA, the maximum effort was 55.11 Mpa c) PFN, the maximum effort was 53,261.

Methods

The femur model was reconstructed using 3D Slicer and the tomographic images (TAC) of an elderly patient (female, 65 years old). The presence of cortical and trabecular tissue was considered. In this study, each of the materials was considered isotropic, elastic and linear. There were 3 materials considered: cortical bone, trabecular bone and stainless Steel for the implants. We construct a 31 A2.1 fracture in the femur model. In the Ansys Workbench suite, the bone and implant assemblies were performed for every case as well as the surgical procedure for each one of the implants. We take into account the surgical instructions consulted in the manufacturer's manuals and the recommendations of medical professionals. The distal end of the femur was fixed in all its degrees of freedom, the applied forces simulated the weight of a 65 kg woman in monopodal support. The contacts between the fractured fragments were frictional with a factor of 0.2. The remaining contacts were assumed to be bonded. A tetrahedral 10 node mesh was used in all three of the analysis, the results presented here converged after conducting a mesh convergence analysis.

Results and Discussion

The results of this research showed that the two implants that best reduced efforts were the intramedullary ones, the difference between the PFN (53,261 MPa) and PFNA (55,11 MPa), was only 1.8 MPa, while, on the other hand, the efforts in DHS-treated bone were 68.665 MPa. In all three cases, however, the stresses remained well below the ultimate assumed stress, 150 MPa. The appearance of maximum stress in all cases appear in the hole near the distal screws. Regarding the efforts experienced by the implants, the intramedullary nails delivered lower results (PFNA: 245.19 MPa and PFN: 253.39), while the effort in the DHS plate amounted to 375.42 MPa. Our study simulated the conditions in which a recently operated patient is found, that is, a patient who can barely practice monopodal support (without any type of gait) and whose fracture is not yet consolidated (hence the friction factor of 0.2) . Future work should consider another much higher force regime in which the bone-implant system is more demanding, although, of course, in this case, the degree of consolidation of the fracture should be taken into account, since only when the bone begins to heal can the patient undergo into harder gait conditions.

Significance

The importance of our work lies in the use of a reconstructed model based on one of the typical and most critical patients in the orthopedic world: an elderly woman. We used a method that considered the presence of two materials in the bone and the different surgical alternatives used by Colombian orthopedists in the treatment of this pathology. In this way, we propose a preoperative methodology that allows Colombian medical professionals to determine which implant is suitable for the treatment of fracture 31 A2.1

Acknowledgments

We thank Lineas Hospitalarias of Bucaramanga and CatMe S.A.S for allowing us access to implants and CT scans. Also, we appreciate the recommendations and support of Dr. Edna Buitrago.

References

Heller, M. O., Bergmann, G., Kassi, J. P., Claes, L., Haas, N. P., & Duda, G. N. (2005). Determination of muscle loading at the hip joint for use in pre-clinical testing. Journal of Biomechanics, 38(5), 1155–1163.

Henschel, J., Eberle, S., & Augat, P. (2016). Load distribution between cephalic screws in a dual lag screw trochanteric nail. Journal of Orthopaedic Surgery and Research, 11(1), 1–10.

Ardila, E., Guzmán, M., Cristancho, D. P., Méndez, L., Puig, Á., Medina, D. F., & Salazar, D. A. (2004). Características de las Fracturas de Cadera: A Propósito del Análisis de Historias Clínicas en Tres Hospitales Universitarios Colombianos Revista Metabolismo Óseo y Mineral, 2(2), 155–160.

Increased Abduction Range of Motion During Functional Activities is Associated with Improved Patient-Reported Outcomes After Reverse Shoulder Arthroplasty

Christopher J. Como[1], Brian Godshaw[2], Clarissa LeVasseur[2], Jonathan Hughes[2], William Anderst[2], Albert Lin[2]
1. University of Pittsburgh School of Medicine, Pittsburgh, PA, USA
2. Department of Orthopaedic Surgery, University of Pittsburgh, Pittsburgh, PA, USA
Email: cjc158@pitt.edu

Introduction

Reverse shoulder arthroplasty (RSA) is a common procedure used to restore function in patients with rotator cuff arthropathy.[1] Few studies have examined shoulder motion after RSA while performing functional activities, and most have not investigated associations between kinematics and patient-reported outcomes (PROs).[2-7] This study aimed to present a comprehensive description of functional motions in RSA patients, determine the repeatability of motion between and within subjects, and examine correlations between motion and PROs. It was hypothesized that increased range-of-motion would correlate with better patient-reported outcome scores.

Methods

Twenty-six patients received RSA (71.9 ± 7.2 yrs old; 2.4 ± 1.2 yrs post-op). Each subject completed 5 shoulder motions for at least 3 repetitions each: scapular plane abduction, hand-to-head, hand-to-back, internal/external rotation with the arm in 90° abduction, and circumduction. Reflective markers placed on the torso, shoulder and humerus were tracked using conventional motion capture (Vicon Vantage, 100 Hz) and used to calculate shoulder abduction, plane of elevation, and internal/external rotation for each motion. Total ROM and maximum/minimum ROM were calculated. Correlations between motion and implant characteristics of retroversion, tilt, eccentricity and lateralization, as well as PROs of ASES, Constant-Murley Score (CMS), VAS, and Brophy scores were determined.

Results

The largest rotation component during each motion was: 102.8 ± 24.9° of abduction during the abduction motion, 112.7 ± 62.4° of shoulder rotation during the hand-to-head motion, 73.2 ± 25.6° of internal/external shoulder rotation during the rotation motion, and 107.7 ± 29.2° in plane of elevation during the hand-to-back motion. During circumduction, the shoulder moved through 101.0 ± 13.6° of abduction, 101.5 ± 21.9° of plane of elevation, and 112.4 ± 17.0° of rotation (**Table 1**). Greater abduction was associated with improved CMS during abduction ($r = 0.467$, $p = 0.038$) and hand-to-back motions ($r = 0.456$, $p = 0.043$). Greater abduction during hand-to-back motion also correlated with better ASES scores ($r = 0.573$, $p = 0.008$). Increased humeral retroversion was associated with less abduction ($r = -0.470$, $p = 0.042$), lower plane of elevation ($r = -0.496$, $p = 0.031$), and less shoulder rotation ($r = -0.469$, $p = 0.043$) during circumduction. More humeral retroversion was also correlated with less abduction during hand-to-head motion ($r = -0.512$, $p = 0.025$). No correlations between ROM and tilt, lateralization, or eccentricity of the implant were found. Within subject variability in ROM was 10° or less all motions, indicating the movements were repeatable within subjects in spite of the large inter-subject variability.

Discussion

Few studies have investigated the association between kinematics and PROs after RSA. Increased abduction ROM during the tasks of abduction and hand-to-back motion was associated with better PROs, suggesting abduction during these movements is an important parameter in predicting outcomes post-operatively. The functional movements showed greater shoulder rotation ROM in the hand-to-head compared to hand-to-back motion, while the opposite trend was seen for plane of elevation indicating different strategies are used in these functional movements. Additionally, circumduction is a complex motion that has not previously been described and was shown to have a correlation with humeral retroversion for all measured rotations. The clinical implication of this finding is that humeral retroversion may be an important factor determining ROM for various movements.

Clinical Significance

Improving abduction ROM during functional tasks following RSA may be beneficial for optimizing outcomes. Humeral retroversion may be important for determining total ROM for complex functional motions.

References

(1) Churchill JL et al. *JBJS Rev.* 2016.
(2) Vidt ME et al. *J Biomech*. 2016.
(3) Jackson M et al. *J Biomech*. 2012.
(4) Mahfouz M et al. *JBJS*. 2005.
(5) Sheikhzadeh A et al. *JSES*. 2008.
(6) Kwon YW et al. *JSES*. 2012.
(7) Postacchini R et al. *J Biomech*. 2015

	Abduction	Hand-to-Head	Hand-to-Back	Int/Ext Rotation	Circumduction
Abduction	102.8 ± 24.9	97.1 ± 16.8	33.3 ± 10.0	10.6 ± 5.4	101.0 ± 13.6
Plane of Elevation	51.8 ± 23.8	45.4 ± 34.1	107.7 ± 29.2	14.3 ± 5.6	101.5 ± 21.9
Shoulder Rotation	77.2 ± 31.0	112.7 ± 62.4	55.4 ± 28.3	73.2 ± 25.6	112.4 ± 17.0

Table 1: Average total ROM (in degrees) for shoulder motions after reverse shoulder arthroplasty.

IDENTIFYING INITIAL CONTACT FOR TREADMILL RUNNING AT COMPETITIVE DISTANCE RUNNING SPEEDS

[1] Deborah L. King, [1]Meghan Beahan, [2]Neha Kapoor, [1]Elizabeth Steele, [1]Marley Baum, and [3]Rumit Singh Kakar
[1]Ithaca College, Ithaca, NY, USA; [2]Cornell University, Ithaca, NY, USA;
[3]Old Dominion University, Norfolk, VA, USA
Email: *dking@ithaca.edu

Introduction

Accurate determination of a runner's initial contact (IC) during the gait cycle is important for various biomechanical analyses including spatiotemporal characteristics and joint kinematics. Force plates or instrumented treadmills can reliably identify IC based on ground reaction forces while studies collecting data in the field or with a standard treadmill rely on kinematic data-based algorithms to determine IC.

Existing algorithms to identify IC from kinematic data are often limited to a specific foot strike pattern [1,4] or range of speeds [2,4,5,6]. An algorithm from Milner & Paquette, validated at 3.7 m/s for forefoot and rearfoot strikes, was found to be speed dependent [3,5]. A linear regression equation was proposed to adjust the algorithm based on running speed [3]. The adjusted algorithm has only been validated for speeds between 2.2 and 4.5 $m.s^{-1}$. While this may indicate reliability of the algorithm at recreational running speeds, competitive runners often train at faster speeds and validation of the algorithm at these speeds is essential. The purpose of this study was to validate the Milner & Paquette kinematic-based IC algorithm at speeds greater than 4.5 $m.s^{-1}$ and test the reproducibility of the adjusted algorithm at previously validated speeds.

Methods

Twenty-five healthy participants completed treadmill running at 7 speeds (3.58, 4.02, 4.47, 4.92, 5.36, 5.81, and 6.26 $m.s^{-1}$) for which complete sets of kinematic and force data were obtained. 3-D motion capture was performed using the Plug-in gait model (Vicon Nexus 2.9; 120 Hz). The rear feet of the treadmill were placed on two force platforms (AMTI 1080 Hz). Participants were asked to run 60 s at each speed and data was collected in the middle 45 s. Mean differences were determined between the speed-adjusted Milner and Paquette algorithms (IC_{calc_adj}) [3] and IC identified from force plates (IC_{FP}). Mean differences (95% CI) and percentage of ICs identified within 20 ms of IC_{FP} were calculated. Follow-up analysis fitting a polynomial equation to the mean differences of IC_{calc} and IC_{FP} were conducted to determine a valid algorithm for speeds 3.58-6.26 $m.s^{-1}$.

Results and Discussion

IC_{calc_adj} identified IC with an average error <0.000 s: ranging from 0.0007 [-0.023, 0.025] (3.58 $m.s^{-1}$) to 0.0003 [-.023, 0.023] (4.92 $m.s^{-1}$) for speeds up to 4.92 $m.s^{-1}$. At 5.26 $m.s^{-1}$ and above, mean errors increased linearly with a maximum mean difference of 0.0012 s [-.030, 0.052] at 6.26 $m.s^{-1}$ (Figure 1). Plotting IC_{calc_adj} mean differences revealed a non-linear relationship with speed (Figure 1). A 2nd order polynomial fit was applied to the IC_{calc_adj} data of 13 random runners: $y = 0.0034x^2 - 0.035x + 0.0957$ (R^2 = 0.968) to correct for running speed (IC_{calc_adj2}).

IC_{calc_adj2} was applied to the other 12 runners' data. Mean differences between IC_{calc_adj2} and IC_{FP} are reported in Table 1. Average error was 0.005 s. The percentage of ICs identified within 20 ms of IC_{FP} ranged from 72.6% (6.26 $m.s^{-1}$) to 94.9% (4.27 $m.s^{-1}$). Both 5.81 $m.s^{-1}$ and 6.26 $m.s^{-1}$ were below 82%.

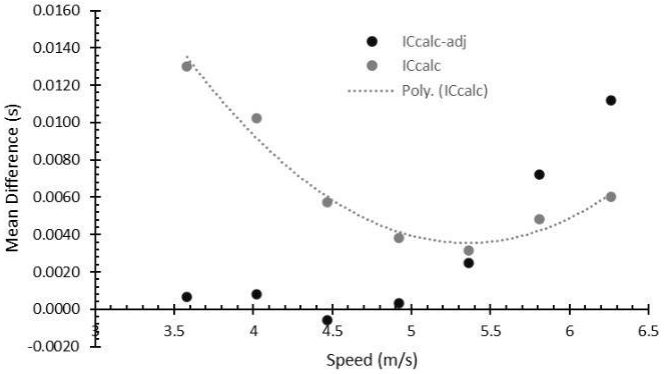

Figure 1. Mean difference between IC_{calc} and IC_{calc_adj} and IC_{FP} for 13 runners across 7 speeds with a 2nd order polynomial fit.

The Milner and Paquette algorithm [5] identifies IC at local minimums of the vertical velocity of the pelvis center of mass ($P\_CM_{vel\_v}$). Milner and Pacquette adjusted $P\_CM_{vel\_v}$ by 15 ms based on data collected at 3.7 $m.s^{-1}$ (IC_{calc}) [5]. From 2.68 to 4.47 $m.s^{-1}$, there is a linear relationship of $P\_CM_{vel\_v}$ to IC_{FP} with speed [3] with IC_{calc} occurring after IC by a greater magnitude at lower speeds. The current study found the linear relationship with speed extends to 5.36 $m.s^{-1}$. Above 5.36 $m.s^{-1}$, differences between IC_{calc} and IC_{FP} increase as does variability in IC_{calc}.

Significance

IC_{calc_adj} was found to be a valid method to identify IC for speeds up to 5.26 $m.s^{-1}$. This extends the range of speed for which IC can be adjusted using $P\_CM_{vel\_v}$ and IC_{calc_adj} to 5.36 $m.s^{-1}$ as compared to 4.47 m/s [3]. Despite a strong polynomial fit, IC_{calc_adj2} only corrects IC_{calc} up to 5.26 $m.s^{-1}$, providing little difference to IC_{calc_adj} at speeds under 5.26 $m.s^{-1}$. At speeds above 5.26 $m.s^{-1}$, a runner's biomechanics change and using IC_{calc_adj} or IC_{calc_adj2} is not a reliable method to identify IC.

References

1. Alvim et al. *J. Appl. Biomech*, **31**(5), 383–388, 2015.
2. Fellin et al. *J Sci Med Sport.,* **13**(6), 646–650, 2010.
3. King, McCartney, & Trihy. *J. Biomech.,* **90**, 119-122, 2019.
4. Leitch et al. *Gait and Posture*, **33**(1), 130–132, 2011.
5. Milner & Paquette. *J. Biomech.* **48**(12), 3502–3505, 2015.
6. Osis et al. *J. Biomech.,* **47**(11), 2786–2789, 2014

Speed ($m.s^{-1}$)	3.58	4.02	4.47	4.92	5.36	5.81	6.26
Mean Difference	0.015	0.012	0.008	0.007	0.007	0.009	0.008
[95% CI]	[-0.011, 0.041]	[-0.010, 0.035]	[-0.013, 0.029]	[-0.011, 0.025]	[-0.012, 0.026]	[-0.015, 0.032]	[-0.016, 0.032]

Table 1. Mean differences between IC_{calc_adj2} and IC_{FP}.

PROVIDING NEUROMUSCULAR TARGETS FOR RESHAPING DYNAMIC BALANCE OF LOCOMOTOR TRANSITIONS USING PREDICTIVE SIMULATIONS

Wentao Li[1] and Nicholas P. Fey[1]
[1]The University of Texas at Austin, Department of Mechanical Engineering
email: wentao.li@utexas.edu

Introduction

Anticipated and unanticipated changes of direction (i.e., maneuvers) are commonplace during our daily lives. The need for dynamic balance is amplified when the transition is performed with little to no prior knowledge of the future event [1]. Among different maneuvers, are crossover cuts which involve moving the trailing swing leg toward and in front of the leading stance leg. This style of transition increases the need for dynamic balance, relative to side-step cuts [1]. Individuals with mobility impairments or those that rely on the use of external assistive device such as lower-limb prostheses are especially challenged during these types of tasks. Improving how specific individuals can perform these potentially devastating tasks could lead to fewer falls/injuries, inspire greater confidence in the use of assistive devices for ambulation, and inform targeted rehabilitation protocols. One technique to help guide this process is musculoskeletal modeling and predictive simulation [2, 3]. In this study, we used predictive simulations and optimal control constructs to test a method for reshaping dynamic balance of unanticipated crossover cuts. We also compare how such improvements can be mediated at the musculotendon level.

Methods

Subject-specific as well as normative tracking data for this simulation approach was provided by a prior experiment [1] of five able-bodied subjects that performed unanticipated straight walking and 45° cutting tasks in response to random auditory cues. A musculoskeletal model (Fig. 1a) of each participant was created in OpenSim 4.0 by scaling the body segments in a generic model with 23 degrees of freedom and 92 Hill-type muscle-tendon actuators. Subtalar and metatarsophalangeal (MTP) joints were locked in each model. Foot-ground interaction was modeled as six Hunt-Crossley contact spheres under each foot. First, for each subject, an optimal tracking simulation was optimized according to the following objective function (1) and solved using direct collocation [4]:

$$J = w \int_0^{t_f} (w_1 \|a\|_2^2 + w_2 \|\Delta GRF\|_2^2 + w_3 \left\|\Delta q_{pelv}\right\|_2^2) dt \qquad (1)$$

where a is the muscle activation; ΔGRF is the tracking error of GRF; Δq_{pelv} is the tracking error of pelvic coordinates. Then, dynamic balance-reshaping simulations were performed for each subject, using the same initial conditions as the tracking simulation, and a new objective function (2):

$$J = w \int_0^{t_f} \begin{matrix} (w_1 \|a_i\|_2^2 + w_2 \|\Delta H\|_2^2 \\ + w_3 \left\|\Delta q_{pelv-xz}\right\|_2^2 + w_4 \left\|F_{penalty}\right\|_2^2) dt \end{matrix} \qquad (2)$$

where ΔH is the reshaping error of whole-body angular momentum relative a non-subject-specific normative profile (computed as the average of the remaining four subjects' experimental data in [1]); $\Delta q_{pelv-xz}$ is the tracking error of pelvic horizontal translations that is used to guide the turning direction; $F_{penalty}$ is the contact force between two feet that is penalized to avoid segment penetration during movements. The durations of all simulations were from toe-off of the trailing leg to the next heel strike of the leading leg, corresponding to roughly 1 stride that spanned each locomotor transition. For these ten simulations, average mechanical power of each muscle group was computed and then compared between tracking and reshaping simulations using one-tailed paired t-test (α=0.05).

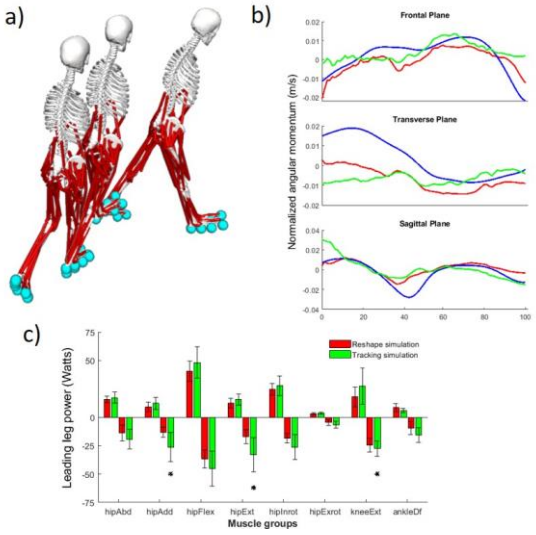

Figure 1: (a) A musculoskeletal model during an unanticipated crossover cut. (b) Average normalized H of the dynamic-balance reshape simulations (red), the data-tracking simulations (green), and the experiment anticipated crossover cut trials (blue). (c) Average positive and negative power of leading leg muscle group. "*" indicates significant changes between simulations. "Abd", "Add", "Flex", "Ext", "Introt", "Extrot", and "Df" refer to abduction, adduction, flexion, extension, interior rotation, exterior rotation, and dorsiflexion.

Results and Discussion

This study investigated whether individuals that perform unanticipated crossover cuts can reshape their dynamic balance while still completing these tasks, and a neuromuscular target for how do so. The reshaping simulations were able to reduce the need for dynamic balance (in the sense of H) of unanticipated crossover cuts (Fig. 1b), and did so (on average) by reducing the negative (i.e., eccentric) power of leading leg hip adductors, hip extensors and knee extensors (Fig. 1c), and without increasing the total average positive power across muscles.

Significance

This study shows that the performance of unanticipated crossover cuts can be optimized to improve dynamic balance, and highlight the potential for predictive simulations and optimal control to provide quantitative targets for reshaping dynamic balance in unanticipated crossover cuts—targets which are biologically-feasible. This approach could inform task-specific rehabilitation therapy by suggesting how to reshape an individual's dynamic balance and which joint-level kinematic adjustments and muscle groups would be optimal to engage in doing so.

References

[1]. Li, W., et al., (2020). *J. Neuroeng. Rehabil.*
[2]. Lin, Y. and Pandy, M., (2017). *J. Biomech.*
[3]. Nguyen, V., et al., (2019). *IEEE Int. Conf. Rehabil. Robot.*
[4]. Porsa, S., et al., (2016). *Ann. Biomed. Eng.*

ASSESSING BIOMECHANICS IN A CADAVERIC MODEL OF SCAPHOLUNATE INJURIES USING 4DCT

Taylor P. Trentadue[1,2,*], Cesar Lopez[1], Ryan E. Breighner[3], Mohsen Akbari-Shandiz[1], David Holmes III[4], Shuai Leng[5], Jay Smith[6], Andrew Thoreson[1], Kristin D. Zhao[1]

[1]Assistive and Restorative Technology Laboratory, Mayo Clinic, Rochester, MN; [2]Mayo Clinic Medical Scientist Training Program, Mayo Clinic, Rochester, MN; [3]Department of Radiology and Imaging, Hospital for Special Surgery, New York, NY; [4]Biomedical Imaging Resource, Mayo Clinic, Rochester, MN; [5]Computed Tomography Clinical Innovation Center, Mayo Clinic, Rochester, MN, [6]Department of Physical Medicine and Rehabilitation, Mayo Clinic, Rochester, MN — email: * trentadue.taylor@mayo.edu

Introduction

Scapholunate (SL) instability or dissociation is a prevalent cause of impaired wrist function. When untreated, it may progress to the SL advanced collapse pattern, a major contributor to radiocarpal osteoarthritis (OA).[1,2] Ligaments of the wrist are critical carpal stabilizers and motion constraints.[3] Primary stabilizers of the SL interval include intrinsic interosseous ligaments (SLIL).[4-6] Previous work has demonstrated that SLIL integrity contributes to normal SL motion.[4,6] Studies have reported that scaphoid and lunate contact areas change following SLIL injury,[4] with scaphoid pressure centroids translated dorsally and ulnarly and a decrease in scaphoid-to-lunate contact area ratio after injury.[7]

In predynamic or dynamic wrist instability,[1] diagnostic imaging modalities may not allow optimal SLIL injury diagnosis: traditional radiographs may not optimally capture diastasis, and MRI may lack sufficient sensitivity or specificity for detecting the ligament injury itself.[8] Four-dimensional (4D) CT, which involves 3D CT scanning over time, acquires CT volumes with high temporal resolution. Previous studies have used 4DCT to evaluate biomechanics at the SLIL.[9-12]

This study used 4DCT to assess changes in interosseous proximities in cadaveric specimens following sequential ligamentous compromise, simulating varying severities of ligament trauma. We hypothesize that median interosseous distances at the radioscaphoid, radiolunate, and scapholunate intervals will change with sequential ligament cuts at neutral as well as extrema of the motion cycle.

Methods

Data were collected from eight fresh-frozen cadaveric forearms procured through the institutional anatomic bequest program, excluding those with history of wrist pathology or evidence of bone trauma, fractures, or significant arthritis. The sample contained four males and four females (median [25th-75th percentile] age at time of death: 70.5 [66.3-74.8] years).

***Image acquisition*:** A second-generation dual-source CT scanner (SOMATOM Definition Flash, Siemens Healthcare, DE) was used to acquire neutral-static and dynamic CT scans of all specimens. Two independent but identical X-ray tubes were mounted on a rotating gantry at a 94-degree offset with opposing respective detector arrays. 4DCT imaging acquires high-temporal resolution (66 ms), continuous or intermittent images over the width of the detector arrays (57.6 mm) in the superior-inferior direction. Data were collected using dynamic, sequential, dual-source scanning mode, acquiring continuous imaging data of the moving wrist without table translation.

***Specimen preparation*:** Datasets were obtained with specimens intact and following five progressive ligamentous sectionings conducted under ultrasound guidance.[13] A custom motion simulator cyclically moved specimens between 45° flexion and 45° extension or 30° radial and 45° ulnar deviation at 0.5 Hz.

***Image processing*:** After image acquisition, static CT volumes were segmented to yield bone models for the radius, scaphoid, lunate, and capitate. For each movement in each condition, time series data for bone positions were found by registering static models to corresponding volumes at each time point of 4DCT acquisition. Proximity maps plotting magnitude of diastasis between vertices on bone surfaces were created for the radioscaphoid, radiolunate, and scapholunate intervals.

Results and Discussion

Proximity maps between bone pairs depict changes in diastasis and total contact area within or above given thresholds, allowing evaluation of changes in interosseous contact. For each ligament condition, interosseous distance patterns are altered compared to the intact state at motion extrema and as the wrist crosses through neutral (**Figure 1**). This study demonstrates that progressive ligament damage in cadaveric models, simulating various injuries, alter diastasis, which is detectable using 4DCT methods.

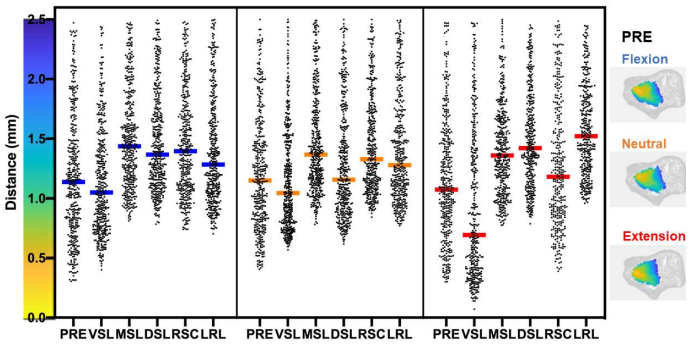

Figure 1: Violin plot representing distribution of interosseous distances between the radius and scaphoid (RS) during flexion-extension (FE) with sequential ligament sectionings in one cadaver. Horizontal lines in violin plots represent median RS distance in the given condition. Images represent scaphoid motion on the radius during FE of the intact wrist. Yellow represents minimum and blue maximum distance (2.5 mm).

Significance

SLIL injuries are a major contributor to wrist dysfunction. 4DCT-derived proximity maps quantify relationships between ligament injury severity and changes in diastasis in a cadaveric model. The distribution of interosseous distances at extrema of motion changes with ligament cuts. Patterns derived from these data may influence diagnosis of *in vivo* SL injury and surgical planning.

Acknowledgments

This work was supported by NIH R01 AR071338 (KDZ) and T32 GM065841 (Mayo Clinic Medical Scientist Training Program).

References

[1]Watson HK. *Hand Clin* (1997) [2]Watson HK. *J Hand Surg Am* (1984) [3]Berger RA. *Clin Orthop Relat Res* (2001) [4]Short WH. *J Hand Surg Am* (1995) [5]Short WH. *J Hand Surg Am* (2007) [6]Ruby LK. *J Hand Surg Am* (1987) [7]Viegas SF. *J Hand Surg Am* (1987) [8]Schmit M. *Radiology* (2005) [9] Kakar S. *J Wrist Surg* (2016) [10]Leng S. *Med Phys* (2011) [11] Brinkhorst M. *Skeletal Radiol* (2021) [12]de Roo MGA. *J Hand Surg Eur Vol* (2019) [13]Lee DJ. *Hand Clin* (2015).

THE EFFECTS OF MOBILITY-RELATED ANXIETY AND A COMMON DUAL TASK ON TURNING KINEMATICS: A VIRTUAL REALITY STUDY

Ashlee D. McBride[1], Caitlin R. Kane[1] , Peter C. Fino[1], A. Mark Williams[1], Keith R. Lohse[1] , Tiphanie E. Raffegeau[1]
[1] University of Utah Department of Health and Kinesiology
email: u1096151@utah.edu

Introduction

Walking while talking is a common every day dual-task (DT). However, mobility-related anxiety impairs cognitive-motor behaviors [1]. Healthy adults must flexibly trade-off cognitive and motor performance when speaking conversationally during complex walking tasks, and slow gait speed to continue speaking [2]. Therefore, performing a DT may be more challenging in anxiety-inducing settings, leading to impaired turning and speech performance. The purpose of this study was to investigate the effects of mobility-related anxiety on conversational speech performance when turning. We required healthy adults to perform a DT (walking and talking) at simulated low and high virtual heights using Virtual Reality (VR).We measured peak velocity and duration of turning, as well as silent pause number and duration during speech. We hypothesized that performing a DT while turning would lead to greater performance deficits at high compared to low height, reflected as slower and longer turns, and more frequent and longer silent pauses in speech.

Methods

Seven young adults with corrected to normal vision and hearing and no neurological diagnoses that affect gait participated (Age = 22.11 yrs, SD = 2.57 yrs). They wore a head-mounted VR system (HTC Vive v. 2.0) displaying a 0.4 x 5.2m virtual walkway matched to a physical walkway. Participants wore tri-axial inertial sensors (version 1.0, APDM Inc, Portland, OR, USA) on the sternum, lumbar, and both feet and wrists, to measure accelerations at 128 Hz, recording peak turn velocity and turn duration. Foot trackers (HTC Vive) worn around the ankle provided visual representations of their feet in VR. Participants performed six tasks with or without speech, where they walked back and forth on a walkway for one minute at a normal comfortable pace, beginning with a baseline walk (No VR). Participants were then randomly assigned to perform the VR or DT Block protocol. The DT Block began by choosing several topics (e.g., family, favorite sport) from a list of 21 provided. Participants performed a baseline speech task while seated (ST), before performing the gait and speech tasks (DT) in VR. Each task consisted of a different randomly assigned speech topic from their selections. Participants' responses were recorded using a wireless microphone (Movo, WMX-1). The recordings of the speech tasks were transcribed and the waveform and spectogram were analyzed in Praat (v 6.1.3) to identify pauses (>150ms) in speech. Each block of VR trials began at low height, before participants were transported to high height (15 m) while seated in a chair moving at 1 m/s. After each trial, they completed the Rating Scale of Mental Effort (RSME) [3], and the Mental Readiness Form (MRF) [4]. To better understand the interaction between mobility-related anxiety and DT on peak turning velocity, turn duration, and silent speech pause f and duration, we calculated Hedge's *g* to reveal effect sizes when comparing low walk to low DT walk, high walk to high DT walk, ST speech to DT low speech and ST speech to DT high speech.

Results and Discussion

The analysis revealed a medium to large effect of DT at low height on turning duration (Low = 2.24s, Low DT = 2.40s; g = -0.58), but not for peak turning velocity (Low = 157.91°/s, Low DT = 150.67°/s; g = 0.25). A medium effect of DT was detected on the duration of speech pauses (ST = 2.73s, Low DT = 2.39s; g = 0.44), but there was a minimal effect on number of speech pauses (ST = 17.6 , Low DT = 18.8; g = 0.24). The results suggest that the DT was challenging enough to increase the duration of turns and speech pauses, even at low height. At high height, there was no effect of mobility-related anxiety on turning duration (High = 2.61s, High DT = 2.63s; g = -0.04), but a medium to large effect was detected on peak turning velocity (High = 139.43°/s, High DT = 121.94°/s; g = 0.47). Mobility-related anxiety had a large effect on the duration of speech pauses (ST = 2.73s, High DT = 2.22s; g = 0.80), and a medium to large effect on the number of speech pauses (ST = 17.6, High DT = 20.0; g = 0.54). The results support that mobility-related anxiety influences DT performance so that participants adjust the motor task (slow peak turning velocity), and interrupt conversational speech (longer and more frequent pauses).

Our findings suggest that speaking conversationally in anxiety-inducing settings hindered turning and speech performance in healthy participants. In non-threatening settings (low height) the DT was challenging enough to slow turning duration and moderately degrade conversational speech performance. In the high height condition, participants were unable to achieve the same peak turning velocity as at low height. Although the motor and cognitive demands remained the same, motor kinematics changed and speech performance declined at high height, supporting the negative effect of mobility-related anxiety on cognitive-motor processes during turning [2]. Participants were not willing to increase the duration of their turns at high elevation during the DT, but they slowed their turn velocity and exhibited greater interference in speech performance than during the DT at low height. Due to our limited sample size, further investigation is needed to examine the interaction between mobility-related anxiety and DT, and how it effects turning and conversational speech performance. In the future, we will target older adults at fall-risk who struggle to walk and talk simultaneously [5]. We plan to explore the influence of mobility-related anxiety and conversational speech on older adult mobility, furthering our understanding of the effects of mobility-related anxiety on everyday DT in high-risk populations.

Aknowledgements

This project was supported by a Research Incentive Grant from the University of Utah Office of the Vice President for Research and the Undergraduate Research Opportunity Program.

References

1. Raffegeau, T. et al. (2018). Gait & Posture,64, 59-62.
2. Raffegeau T. et al. (2020). Gait & Posture, 238(11), 2653-2663.
3. Zijlstra, F., et al. (1985). [dissertation]. Maastricht University
4. Krane, V. (1994). Sport Psychologist, 8 (2) 189-189.
5. Montero-Odasso, M. et al., (2020). Falls Cogn. Older Pers. 3–20.

Do the Anterior Fascicles of the Soleus Influence Posterior Fascicle Behavior?

Katherine R. Knaus[1] and Silvia S. Blemker[1]
[1]Department of Biomedical Engineering, University of Virginia, Charlottesville, VA; Email: ker4e@virginia.edu

Introduction

The soleus muscle generates plantarflexion torque required for stability and locomotion. The soleus muscle has a complex 3D aponeurosis morphology[1], providing a framework for fascicles arranged in multiple compartments with different architecture and innervation[2]. The unipennate posterior compartment wraps around the deeper bipennate anterior compartment. Fascicles from both compartments originate on opposite sides of the broad anterior aponeurosis, separating them within the soleus volume.

Soleus muscle behavior is often measured *in vivo* using ultrasound and electromyography (EMG) to better understand its important function[3]. Ultrasound is used to track fascicles in a region of interest in the superficial portion of the muscle while EMG is used to estimate activation from measurements on the calf surface. While these measurements are insightful, they are unable to capture fascicle kinematics and activation of the deep anterior compartment or fully capture the posterior compartment.

These issues raise the question as to if contraction of the anterior compartment of the soleus influences behavior of fascicles in the posterior compartment. In order to answer this question, we used a finite element (FE) model of the soleus that represents its complex 3D structure to simulate varied activation in the anterior and posterior compartments during soleus muscle lengthening to explore how these portions of the muscle interact.

Methods

An image-based 3D finite element model (FEM) of the soleus muscle was previously constructed[4] with distinct structures for the anterior (AS) and posterior (PS) soleus muscle compartments and the anterior (AA) and posterior (PA) aponeuroses (Fig. 1A). The model was meshed as tetrahedral elements with fiber directions assigned to each element, using aponeuroses surfaces to define muscle fiber origins and insertions. Muscle and aponeuroses were transversely isotropic materials. Predicted architecture changes in simulations of passive lengthening were validated by creating fascicle tracts using streamlines (Fig. 1A) and comparing to soleus measurements made with diffusion tensor imaging (DTI)[2]. Tissue displacement in active lengthening was related to dynamic MRI[4].

The PS was either passive (α = 0%) or activated (α = 75%) while AS activation varied (α = 100%, 75%, 50%, 25%, 0%). Then soleus lengthening in ankle dorsiflexion was simulated by displacing the PA distal end by 20 mm, at the Achilles muscle-tendon junction (MTJ), while attachments of the AA to the tibia and fibula were fixed. Muscle force was measured at the MTJ.

Results and Discussion

PS fascicle strains determined during muscle lengthening (Fig. 1B) are similar with the PS passive (α = 0%) and active (α = 75%). With passive PS, varying AS activation changes PS fascicle lengths at the start of muscle lengthening, but has a lesser effect on PS fascicle length change. With active PS, varying AS activation has a low effect on starting PS fascicle lengths, but creates larger differences in PS fascicle length changes. There are greater differences in AS fascicle strains with varied AS activation. Differences in AS strains arise due to shorter fascicles lengths associated with activation prior to muscle stretch. With the PS active (α = 75%) there are greater differences between average strain in the PS and AS than when the PS is passive (α = 0%), regardless of the AS activation. Differences in activations also led to differences in muscle force during lengthening (Fig. 1C).

These results suggest activation of the anterior compartment does not influence the posterior compartment's fascicle behavior. However, only measuring the superficial soleus (i.e., with EMG and ultrasound) would not provide insight into the activation state or fascicle kinematics of the anterior compartment. Metrics of soleus mechanical behavior, i.e., muscle stiffness[3] calculated using force and posterior compartment fascicle length changes, during muscle lengthening are dependent on the activation state of the anterior compartment.

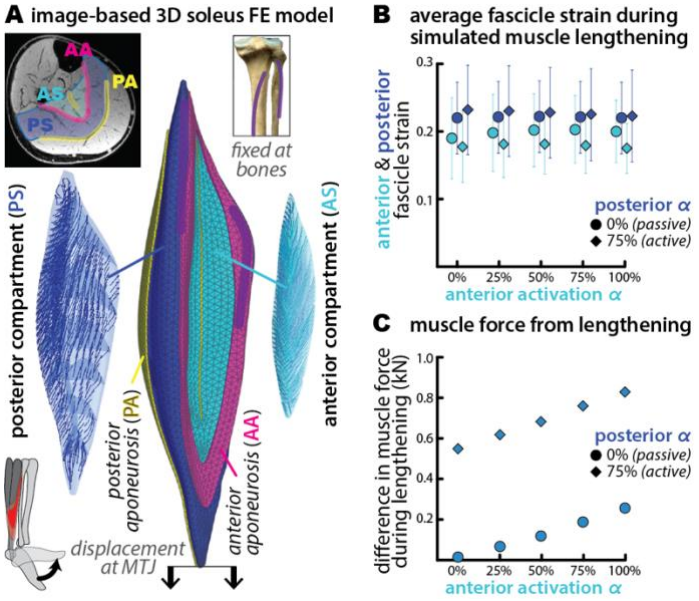

Figure 1: **A)** Image-based 3D soleus finite element (FE) model was used to simulate muscle lengthening after varied activation (α) in the anterior (AS) & posterior (PS) compartments. **B)** Average fascicle strains during lengthening were found & **C)** muscle force, normalized by passive force.

Significance

Model predictions help illuminate the relationship between the anterior and posterior compartments of the soleus which is currently unmeasurable. Model results can be used to better understand existing non-invasive measurements of human soleus function as there are no animals with equivalent soleus function or morphology that provides an alternative comparison. The model improves our ability to assess soleus changes in the context of ankle function which is critical for investigating gait alterations that result from aging or using wearable devices.

Acknowledgments

Thank you to Brian Jones, Darryl Thelen, Jason Franz, and other Tendonados and funding provided by grant #R01AG051748.

References

[1]Hodgson et al. (2006). *J Morphology* **267**:584-60 [2]Bolsterlee et al. (2018). *Peer J*, **6**:e4610; [3]Krupenevich et al. (2020). *J Biomech* **36(4)**:209-216; [4]Knaus et al. (in prep). *J Biomech*

Adaptive Control of Stride Length in Response to Perturbations While Walking in Older Women with Osteoarthritis

Yang Hu[1*], Rachneet Kaur[2], Alka Bishnoi[1], Richard Sowers[2], and Manuel E. Hernandez[1]
[1]Department of Kinesiology and Community Health, University of Illinois at Urbana-Champaign, IL
[2]Department of Industrial and Enterprise Systems Engineering, University of Illinois at Urbana-Champaign, IL
Email : *yangh3@illinois.edu

Introduction

Osteoarthritis (OA) is a musculoskeletal disease that affects balance control in older adults [1]. The ability to restore balance following sudden, unexpected perturbations is critical to avoid falls [1], particularly for persons with OA. To date, it is unclear how OA affects the ability to react and adapt to perturbations delivered while walking. Meanwhile, previous studies suggest that exposure to repeated perturbations can lead participants to better correct their loss of balance during the recovery phase (i.e., adaptation of the reactive strategy, assessed by differences in stride length) [2]. Thus, this study aims to investigate how OA affects the ability to respond to balance perturbations while walking and produce acute short-term effects to improve compensatory reactions in older women. We hypothesize that 1) older women with OA will be impacted more by anterior-posterior perturbations while walking as suggested by larger stride length errors compared to age-matched healthy controls (HOA); 2) OA group will demonstrate a slower adaptation rate compared to HOA, assessed by more perturbations needed to reach a constant stride length error and lower decay rate.

Methods

Nine older women with OA (OA, age: 67.9 ± 3.33 years) and eleven HOA (age: 69.33 ± 6.17 years) participated in this study. Participants were instructed to walk on an instrumented treadmill (C-Mill 3Q treadmill, Forcelink, Inc.) with a predefined comfortable walking speed. Participants first practiced walking on the treadmill and were then notified that they might experience slip perturbations in the experiment. Participants then went through two perturbation-walking (PW) trials. In each PW trial, custom belt speed profiles were used to simulate slips at pseudorandom intervals between 5 and 25 s, in which subjects were asked to recover from as best as possible. Customized Python scripts extracted stride length from the center of pressure data recorded by instrumented treadmill. Stride length error was calculated by stride length of five responsive strides after each perturbation subtracts the local baseline calculated before each perturbation. Stride length error was also standardized by the height and walking speed of each participant.

$$y = ae^{-bx} + c \quad (1)$$

A standard exponential model (eq. (1)) was applied to determine the constants of adaptation and decay. In equation (1), ***a*** denotes starting error. The constant ***-b*** denotes decay rate, while 1/b denotes the number of perturbations that an exponentially decaying quantity takes to decay by a factor of 1/e. The constant ***c*** denotes the end error converged to by the decay function.

Results and Discussion

Table 1 reported the model fitting parameters for each group in PW trials. The relevant error of the model constants suggested good fitting for starting error and end error, but not for decay rate. Consistent with the hypothesis, OA had a higher start error response to perturbation than HOA (Table 1). Higher start error suggests high risk of losing balance while encountering a novel balance perturbation, which confirmed the higher risk of falling associated with OA.[3]

Constants	Cohort	
	OA	HOA
a (error)	2.43 (0.68)	0.80(0.23)
b (error)	0.30(0.21)	0.28(0.25)
c (error)	1.98(0.38)	2.02(0.19)

Table 1: Exponential decay function fitting parameters for each group.

As expected, OA and HOA demonstrate different adaption patterns in response to perturbation. Both groups could improve recovery after the unexpected loss of balance as standard stride length error decreased along with perturbations and eventually converge to similar end errors (Figure 1). However, considering the higher start error in OA group, and similar decay rate between group, OA group might need more perturbation exposures to reach the similar performance as HOA.

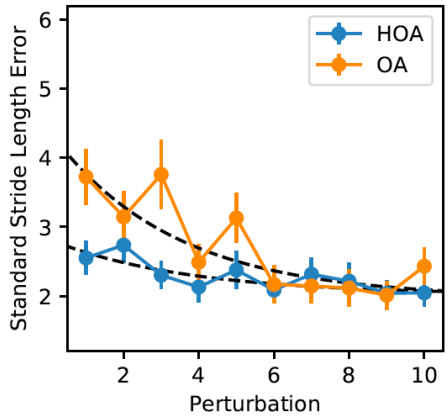

Figure 1: Adaptation curves for health older adult group (HOA) and osteoarthritis group (OA) in perturbation walking. Adaptation is shown by the progressive reduction in the standard stride length error across perturbations. Points, representing the group average with standard error for perturbation, are fitted by exponential function.

Our results suggest, while being cautious, unexpected slip perturbations during walking are still challenging for OA but not for HOA. As slip motion is a common experience in daily life, healthy older women have learned strategies to overcome slip motion, however, persons with OA may need additional training to acquire a similar ability.

Significance

This is the first study to examine the effect of osteoarthritis on adaptation to unexpected walking perturbations. This work suggests that OA impacts older women's ability to respond to perturbations while walking. While it is possible to improve compensatory reactions, OA patients may need more training blocks than age-matched controls. However, concerning the large relevant error in decay rate estimate, we will conduct additional analysis to address the OA's impact on adaptation rate.

Acknowledgments

We would like to thank all of the subjects and the MFPRL OA research team for their contributions to the study.

References

[1] Hinman et al. *Rheumatology*. 2002;41:1388–1394.
[2] Martelli et al. *Scientific Reports*. 2017; 7:17875.
[3] Doré et al. *Arthritis Care Res (Hoboken)*. 2-15; 67(5): 633–639.

UNDERLYING STRUCTURAL DIFFERENCES OF MULTIPLE HIP PATHOLOGIES RESULT IN ALTERED STRATEGIES FOR CONTROL OF BALANCE DURING SQUATS

Wentao Li[1], Ed Mulligan[2], Avneesh Chhabra[2], Joel E. Wells[2] and Nicholas P. Fey[1,2]
[1]The University of Texas at Austin, Dept. of Mechanical Engineering; [2]UT Southwestern Medical Center, Depts. of Orthopaedic Surgery, Radiology and School of Health Professions
email: wentao.li@utexas.edu

Introduction

There are multiple joint pathologies such as developmental dysplasia of the hip (DDH) and femoroacetabular impingement syndrome (FAI) that influence gait mechanics and overall quality of life [1, 2]. At the joint level, these pathologies are quite different. DDH is often congenital, associated with undercoverage of the femoral head relative by the acetabulum, and may result in structural injury and instability of the hip (i.e., an unconstrained joint). In contrast, FAI is typically-considered an abnormal morphological contact between the acetabulum and femoral head as a result of an overconstrained joint through either cam or pincer morphologies. Commonly, both DDH and FAI pathologies can lead to hip pain and long-term degradation of the hip including osteoarthritis and eventual total hip replacement [3]. The therapeutic and/or surgical treatment of these conditions differ. Thus, multiple studies attempt to highlight biomechanical differences that exist in these groups during ambulation and non-ambulatory tasks, such as single- and bilateral squats [1, 2].

Often the depth and style of squatting tasks are assessed in the clinic as additional metrics that are combined with medical imaging, physical examination and pain history to make accurate diagnoses and plans for treatment. Squats require a large range of motion of the hips [1]. Yet, they are also destabilizing tasks, which require control of balance. The mechanisms used by individuals with hip pathologies pertaining to balance are not well-understood. Therefore, this study investigated dynamic balance (computed as whole-body angular momentum, *H*) for individuals with DDH and FAI during bilateral and single-leg squats. Given the differing structure of the hip within these cohorts, we hypothesized that the dynamic balance would be less regulated (i.e. increased magnitude) for DDH, and more tightly-regulated (decreased) for FAI, relative to control subjects.

Methods

Nine control subjects and 30 (DDH=17; FAI=13, cam and pincer combined) patients performed three trials each of bilateral, left-leg, and right-leg squats on level platform, while kinematic data from 46 lower- and upper-body reflective markers were recorded at 120 Hz using a ten-camera Vicon motion capture system. All individuals within the patient cohorts were symptomatic, diagnosed and studied prior to undergoing hip preservation surgery at UT Southwestern. Age and gender within these cohorts were not controlled. Subjects were asked to perform a controlled squat as low as they could for all tasks and use their preferred style for single-leg squats, either with their swing leg forward or backward [4]. An eight-segment model was built in Visual3D and *H* was calculated using a common kinematic method [5], and normalized by body mass and height. Statistical parametric mapping (SPM) one-way ANOVA (α=0.05) was used to compare *H* of different groups in bilateral squats. SPM two-way ANOVA (α=0.05) with repeated measures of one factor was used to compare *H* in different groups and single-leg squat tasks (ipsilateral and contralateral). *Post-hoc* comparisons were performed using Bonferroni's correction.

Results and Discussion

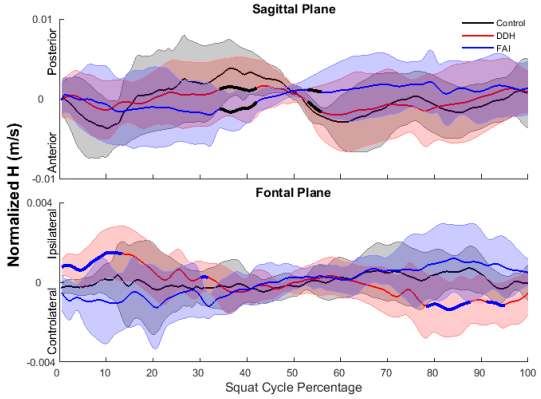

Figure 1: Group average (solid) and standard deviation (shaded) of *H* of DDH (red), FAI (blue) and control subjects (black) during bilateral squats. Data are time-normalized with standing positions representing 0% and 100% cycle, and 50% representing maximal squat depth. Black and blue "thick" line segments indicate significant differences relative to control and FAI groups during specific temporal regions.

Our hypotheses were partially supported. Individuals with DDH and FAI controlled their fore-aft (sagittal-plane) dynamic balance more tightly (i.e., decreased) than control subjects when they squatted bilaterally, near their maximal depth (Fig. 1), suggesting similar protective mechanisms may be used for fore-aft balance, despite large within-group variances. Previous investigations of FAI squats found reduced posterior pelvic tilt as they approached maximum depth [1], which may contribute to the increased anterior (i.e., reduced posterior) *H* of FAI group relative to control subjects before reaching maximum depth. Although prior studies observed few differences of frontal-plane hip biomechanics, our results suggest there are significant differences of frontal-plane *H* between DDH and FAI groups during the 1st half of bilateral squats, as the task was initiated (Fig. 1). Individuals with DDH had a tendency to allow their *H* to move toward their affected limb, while the FAI group's *H* tended to rotate away from their affect limb (Fig. 1).

Significance

This study is the first to show that individuals with DDH and FAI control sagittal-plane balance similarly but different from control subjects, and frontal-plane balance differently from each other during bilateral squats. These findings shed light on important biomechanical mechanisms used by these cohorts as well as the functional differences that arise from differing underlying hip morphologies. However, there was no difference between DDH, FAI, or control groups during different single-leg squat tasks, potentially due to the various single-squat styles each subject could employ [4].

References

[1]. Lamontagne, M., et al., (2009). *Clin. Orthop. Relat. Res.*
[2]. Chegini, S., et al., (2009). *J. Orthop. Res.*
[3]. Ganz, R., et al., (2003). *Clin. Orthop. Relat. Res.*
[4]. Khuu, A., et al., (2016). *Int J Sports Phys Ther*.
[5]. Li, W., et al., (2020). *J. Neuroeng. Rehabil*.

DeepLabCut Model Retraining Guidelines for Markerless Tracking in Bi-Planar X-Ray Videos

Nathan J. Kirkpatrick.[1], Robert J. Butera[1,2], and Young-Hui Chang[1,3]
[1]Coulter Department of Biomedical Engineering, Georgia Institute of Technology & Emory University, Atlanta, GA, USA
[2]School of Electrical and Computer Engineering, Georgia Institute of Technology, Atlanta, GA, USA
[3] School of Biological Sciences, Georgia Institute of Technology, Atlanta, GA, USA
Email: NK@gatech.edu

Introduction

Although researchers rely on the measurement of rat locomotion to better understand injury rehabilitation, diseases and more (1-3), existing workflows present a bottleneck that reduces study sample sizes, increases costs, and slows down the scientific process. Rodents present unique challenges with regards to kinematics measurements; their loose hindlimb skin makes optically tracking skin-mounted markers inaccurate (4), and their bones are too small to track surgically implanted markers via x-ray video (5). Traditionally, researchers interested in whole limb kinematics of rats have two options, both of which rely upon the collection of biplanar x-ray videos: manually track skeletal landmarks (4) or align μCT-derived 3D bone models for each bone of interest (rotoscoping, 6). Both of these options are tremendously time consuming and require sophisticated software and expertise to implement. Previously, we demonstrated how to increase the efficiency of rodent kinematic analysis by combining tools created for x-ray video analysis with DeepLabCut, a deep learning-based tool for markerless body part tracking designed for use with traditional optical video (7,8).

Here, we aim to determine how often, and under what conditions, brief retraining needs to be performed to maintain accuracy while minimizing the tedious and time-consuming processes of manually generating training data.

Methods

DeepLabCut was initially trained on 7 rat skeletal landmarks (Fig. 1B) from 724 pairs of frames of biplanar x-ray video (41-44kV, 80mA, 5ms, 100 fps) in Google Colab until performance plateaued (final test error 21 pixels).

After training, a new batch of x-ray videos from two Lewis rats across two recording sessions were analysed. The model was briefly retrained on 40 newly labelled frame pairs collected from only one of the animals during a single recording session. The performance of the model was assessed by analysing three different types of trial videos: videos containing these 40 labelled frames ("Partially Retrained", 228 total frames), novel videos of the same animal recorded during the same day as the "Partially Retrained" group that the model has never been trained on ("Novel Trial"), and novel videos of a different animal recorded during a different session as the "Partially Retrained" group ("Novel Animal"). A total of 692 frame pairs from 15 gait cycles were analysed by DeepLabCut in roughly 10 minutes. The percent of landmarks labelled correctly was determined by manual inspection. All animal work was performed in accordance with protocols approved by Georgia Institute of Technology's IACUC.

Results and Discussion

The model accurately labelled skeletal landmarks in "Partially Retrained" strides 97.3±2.2% of the time. The "Novel Trial" group reported an accuracy of 94.5±4.6%, and 72.5±8.1% of landmarks in the "Novel Animal" group were accurately labelled (Fig. 1C).

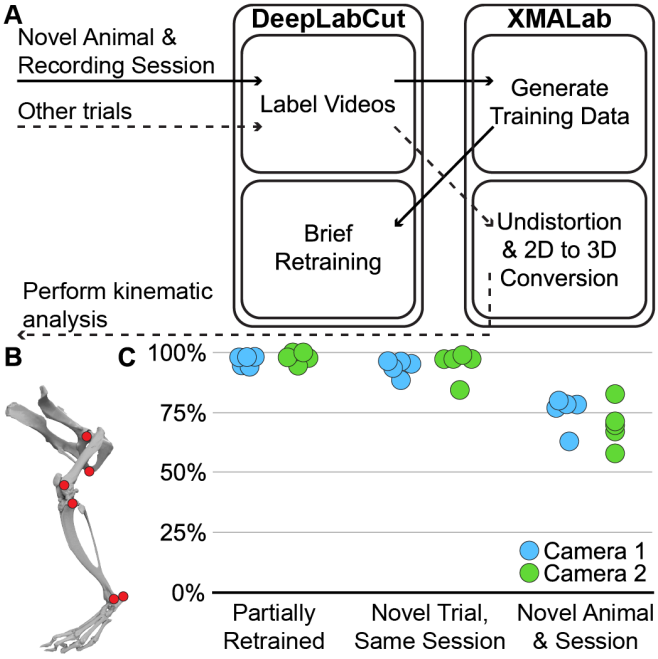

Figure 1: **A**, flowchart of pipeline for biplanar x-ray videos. Retraining is performed by following the black arrows. Trials from the same animal and recording session as the retraining data can be analyzed by following the dotted arrows. **B**, diagram of tracked skeletal landmarks **C**, Percent of landmarks identified correctly (N=15 gait cycles, 692 frame pairs) in trial videos that the model has varying levels of explicit familiarity with.

Based on these findings, we recommend that brief retraining be performed using a small subset of frames for each new animal and data collection session.

Significance

Reducing the analytical burden for rodent kinematic analysis can reduce costs, increase sample sizes and expand the possibility for new research collaborations to answer new questions related to movement analysis.

Acknowledgments

We would like to thank the members of the Comparative Neuromechanics Laboratory for their help and support.

References

1. J. M. Bauman, Y. H. Chang, *Biol Lett*. **9**, 1-5 (2013).
2. K. D. Allen, et al., *Arthritis Research & Therapy*. **14**, 1-14 (2012).
3. L. C. Tsai, et al., *Osteoarthritis & Cartilage.* **27**, 1851-1859 (2019).
4. J. M. Bauman, Y. H. Chang, *J Neurosci Methods.* **186(1),** 1-19 (2010).
5. B. J. Knörlein, et al., *J Exp Biol.* **219**, 3701-3711 (2016).
6. S. M. Gatesy, et al., *J Exp Zool.* **313**, 244-261 (2010).
7. A. Mathis, et al., *Nat Neuro*. **21**, 1281-1289 (2018).
8. N. Kirkpatrick, et al., American Society of Biomechanics (2020).

TIME TO CONTACT CAPTURES DECLINES IN POSTURAL CONTROL FOLLOWING FATIGUING ACTIVITY

Ross J. Brancati[1], Jane A. Kent[1], Katherine A. Boyer[1]
[1]Department of Kinesiology, University of Massachusetts Amherst, Amherst, MA
email: rbrancati@umass.edu

Introduction

Performance fatigability is a normalized metric of performance deterioration in response to a standardized activity.[1] Muscle fatigue, defined as an acute reduction in force and power output,[2] is a proposed contributor to greater fatigability.

The Advanced version of the Physical Performance Battery (SPPB-A) is a validated tool developed to evaluate mobility in older adults. It includes four 30-s balance tasks: side-by-side (SBS), semi-tandem (ST), full-tandem (FT), and single leg (SL).[3] The SPPB-A tests how long an individual can balance in a particular stance, but stance time alone may not be sensitive enough to detect changes in postural control. Moreover, activities of daily living often involve more challenging balance postures. Thus, it is of interest to quantify changes in postural control with muscle fatigue for all balance tasks of the SPPB-A.

Typical measures of postural control test either spatial or temporal aspects of balance.[4] Postural time-to-contact (TTC, s) is defined as the time it would take the center of pressure (COP), given its instantaneous trajectory, to contact a stability boundary and thus accounts for both spatial and temporal aspects of the COP.[5] TTC may provide greater sensitivity compared to traditional COP metrics and physiologically represents the time it would take to make corrective postural adjustments in response to, for example, a perturbation or potential fall.[4] The impact of balance task stance and muscle fatigue on TTC has not yet been quantified. Thus, the aim of this study was to quantify TTC in 4 balance task stances before and after a prolonged walk previously found to induce knee extensor muscle fatigue in younger and older adults[6,7] and changes in postural control in older adults.[7]

Methods

Three young healthy adults (age: 32.0±1.5 years, BMI: 21.9±5.2 kg m-2), sedentary participants were recruited for the study. Participants stood on a force plate (Advanced Medical Technology Inc., Watertown, MA, USA) in standardized lab footwear in 4 positions (SBS, ST, FT, and SL) for 30 s. A motion capture system (Qualysis, Gothenburg, Sweeden) collected marker data of both feet during each trial. Force data were sampled at 100 Hz and filtered with a second order low-pass Butterworth filter with a cut-off frequency of 10Hz. Participants then completed a 30-min treadmill walk[7] (30 MTW) at their preferred walking speed, determined by a 400m walk test. Following the 30MTW, the same four 30-s balance trials were repeated. Minimum and mean TTC were calculated for each stance using custom MATLAB code. TTC was calculated at each timepoint in each trial by solving for the time variable, τ, in the equation[5]: $P_i(\tau) = r(t_i) + P(t_i)\cdot\tau + a(t_i)\cdot\tau^2/2$. A one-way ANOVA was used to test for differences in baseline TTC for the 4 stances, with post-hoc tests as appropriate. Effect sizes for differences were calculated for each stance to assess the impact of the 30MTW.

Results and Discussion

Compared with the standard SBS stance, baseline mean and minimum (except ST) TTC were significantly lower in the 3 other stances (Figure 1). Mean TTC was also lower for FT compared to ST and minimum TTC was lower in FT and SL compared to ST. The decrease in TTC with increased stance difficulty suggests less postural stability. The effect sizes of mean TTC for differences pre to post 30MTW were nil for SBS (0.009), moderate for ST (0.788) and FT (-0.576), and small in SL (0.336) stance, suggesting that the 30MTW alters stability more in challenging dual stances.

Younger adults typically have a robust functional reserve and the change in muscle function with the 30MTW was likely not sufficient to require a large change in the postural control. In contrast, older adults have both a smaller functional reserve and may be more susceptible to muscle fatigue with a standardized exercise stimulus. Thus, TTC in the more challenging stances and following the 30MTW may yield greater insight as to the effects of fatigability in older adults.

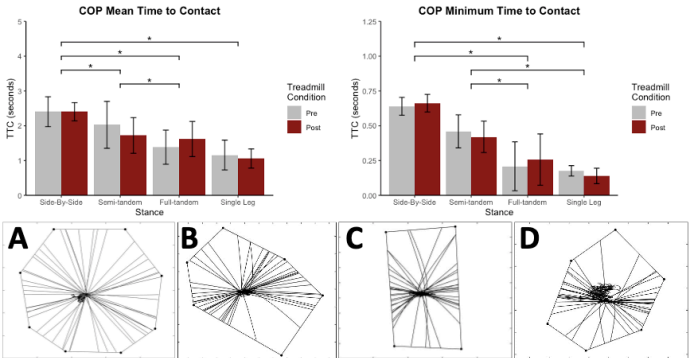

Figure 1: *Top:* Mean (left) and minimum (right) TTC for each stance. Mean and minimum (except for ST) TTC were different from TTC in the side-by-side stance (* p<.05). *Bottom:* plots of representative TTC trajectories for the 4 stances (A: SBS, B: ST, C: FT, and D: SL).

Significance

The mechanisms of performance fatigability have been suggested to involve neural and muscular processes[8]. These preliminary results suggest that difficult balance postures, along with advanced postural control measures such as TTC, may provide insight into the mechanisms of performance fatigability.

Acknowledgments

NIH R01AG058607. Recruitment: Charlie Gillon, data analysis: Aidan Gross.

References

1. Schrack, J. A. et al. J. Gerontol. A Biol. Sci. Med. Sci. 2020;75(9):e63-66.
2. Kent-Braun, J. A. et al. Compr. Physiol. 2012;2(2):997–1044
3. Simonsick, E. M. et al. J. Gerontol. A. Biol. Sci. Med. Sci. 2001;56A(1):M644-649
4. Richmond, S. B. et al. J. Sports Sci. 2020; 38(1):21–28
5. Slobounov, S. M. et al. J. Gerontol. A. Biol. Sci. Med. Sci. 1998;53A(1):B71–B80
6. Hafer, J. F. et al. Gait Posture. 2019;70:24-29
7. Foulis, S. A. et al. PLOS ONE. 2017;12(9): e0183483
8. Hunter, S. K. Cold Spring Harb. Perspect. Med. 2018;8:a029728

VALIDATION OF BODY-WORN INERTIAL MEASUREMENT UNITS FOR ASSESSING GAIT

Julie Rekant[1], Brandon Betts[2] and April Chambers[1,2]
1 Bioengineering, University of Pittsburgh, Pittsburgh, PA, USA
2 Health and Human Development, University of Pittsburgh, Pittsburgh, PA, USA
email: jur29@pitt.edu, web: https://www.engineering.pitt.edu/hmbl/

Introduction

Wearable sensors are a rapidly growing field for movement assessment however how they compare to the gold standard is not well described. Validation studies provide insight into how the information from wearable sensors can be interpreted in comparison to the gold standard and they inform future studies that rely on this wearable technology.

The Noraxon MyoMotion System (Noraxon USA Inc., Scottsdale, AZ) uses an array of inertial measurement units (IMUs) on rigid body segments to measure anatomical joint angles in natural and lab-based environments. How the portable Noraxon system performs compared to the gold standard motion capture system has not been extensively explored.

The goal of this study is to understand how kinematic outputs from the IMU-based system compare to existing gold-standard technology for assessing gait.

Methods

Ten healthy adults were included in this study with demographics (mean ± std dev): age 23 ± 2 years, height 167 ±11 cm, mass 66 ± 16 kg, and body mass index 23 ± 3 kg/m^2.

Participants performed a minimum of eight overground walking trials while equipped with both the Noraxon IMUs on the pelvis, thighs, shanks, and feet, and optokinetic markers on bony landmarks as has been described previously[1]. Participants walked at their comfortable gait speed across a tile floor while within the view of 14 Vicon motion capture cameras (Vicon Motion Systems Ltd., Centennial, CO).

Foot accelerometer data and heel marker positions were used to detect heel strikes and extract temporal features of gait. Kinematic outputs from the Noraxon MyoMotion System were automatically calculated with the company's proprietary software; this software calculates hip and ankle angles about the medial-lateral, anterior-posterior, and longitudinal axes, and sagittal plane knee angles. The International Society of Biomechanics (ISB) convension was used for calculating these joint angles from the motion capture data [2].

Results and Discussion

Kinematics as measured with the Noraxon MyoMotion System demonstrate a strong visual similarity to those measured with the gold standard Vicon motion capture (Figure 1). Sagittal plane kinematics were on average -5.3°, -10.6°, and 1.3° different at the hip, knee, and ankle, respectively for the Noraxon outputs when compared to Vicon kinematics. In the frontal plane, Noraxon outputs were an average of -1.1° and -2.1° different at the hip and ankle, respectively. Transverse plane kinematics were an average of -4.7° and -10.6° different at the hip and ankle, respectively, when compared to Vicon outputs.

The Noraxon MyoMotion System tended to underestimate lower-extremity joint angles when compared to the gold standard with the greatest disagreement seen for knee flexion and ankle external rotation. Visual inspection suggests differences in how the coordinate systems define kinematics in the anatomical position might be contributing to these differences. Differences in curve shapes might also be attributed to drift from the IMUs complicated by magnetic intefernece from data collection in a gait lab equipped a motion capture system.

Significance

IMU-based movement analysis shows promise for assessing lower extremity gait kinematics. Future work should explore best practices for aligning coordinate systems between analysis methods for improved comparison of results between data collection systems.

Acknowledgments

This work was supported by the University of Pittsburgh Human Movement and Balance Laboratory

References

1. Lerner ZF, et al. *Med Sci Sports Exerc.* 2014.
2. Wu G, et al. *J Biomech.* 2002.

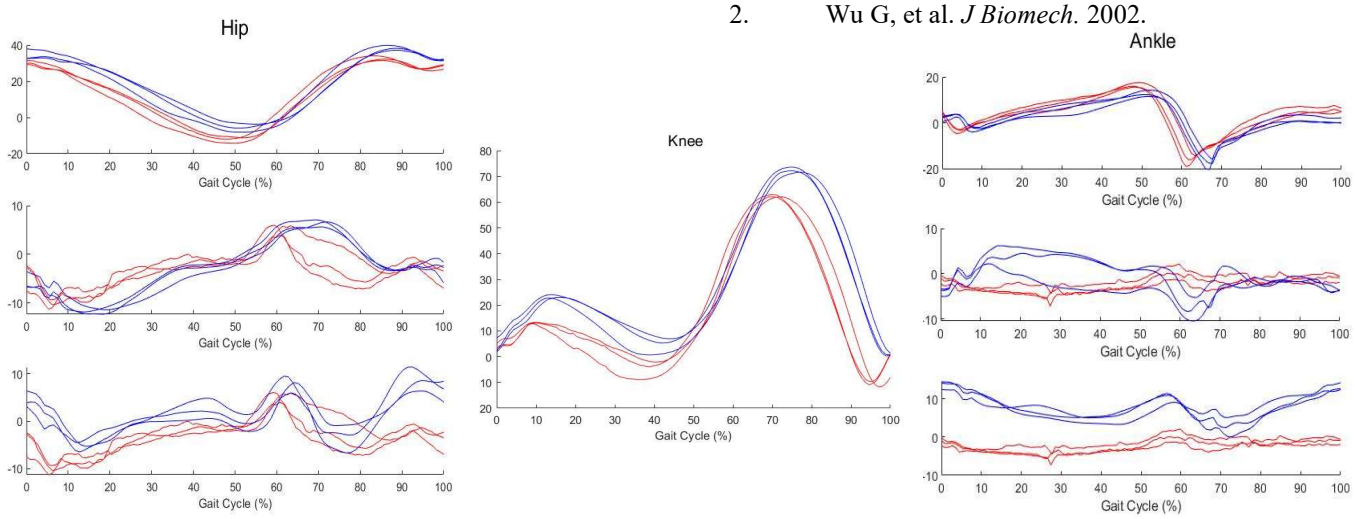

Figure 1. Noraxon (blue) and Vicon (red) kinematics in degrees vs percent of gait cycle for a sample participant. Left: Hip sagittal (top), frontal (middle), and transverse (bottom) plane kinematics. Middle: Knee sagittal plane kinematics. Right: Ankle sagittal (top), frontal (middle), and transverse (bottom) plane kinematics.

USE OF REAL-TIME VISUAL FEEDBACK OF PEAK PROPULSIVE FORCE IN PEOPLE WITH UNILATERAL TRANSTIBIAL AMPUTATION

Janet H. Zhang[1,*], Caelyn Hirschman[1], Alena M. Grabowski[1,2]
[1]University of Colorado Boulder, Boulder, CO, USA; [2]VA Eastern Colorado Healthcare System, Denver, CO, USA
email: *Hanwen.Zhang@colorado.edu

Introduction

During walking, people with transtibial amputation (TTA) using a passive-elastic prosthesis have more asymmetric peak vertical and horizontal ground reaction forces (GRFs) compared to non-amputees; specifically, they generate lower peak GRFs in their affected leg (AL) and higher peak GRFs in their unaffected leg (UL) [1]. Higher GRFs in the UL may lead to secondary disability such as osteoarthritis. To reduce asymmetry between legs, we provided real-time visual feedback of peak horizontal propulsive GRF (GRF_{prop}) of the AL to subjects with unilateral TTA using a passive-elastic prosthesis. We hypothesized that compared to no visual feedback (VF), participants would increase their peak GRF_{prop} and reduce asymmetry when provided with VF during walking. We further hypothesized that participants would retain the increased peak GRF_{prop} and reduced in asymmetry after the VF was removed.

Methods

Two subjects (S1, S2; 1M, 1F) with unilateral TTA walked on a dual-belt force-measuring treadmill (Bertec, Columbus, OH) at 1.25 m/s using their own passive-elastic prosthesis while we measured 3D GRFs (1000 Hz). We placed reflective markers bilaterally on the lower limbs and simultaneously recorded marker trajectories (Vicon, Centennial, CO; 100 Hz). Participants performed a 5-min baseline walking trial with no VF, and we calculated baseline peak GRF_{prop} from the AL as a reference training target. During VF trials, we placed a monitor at eye level ~1.5 m in front of each subject, and peak GRF_{prop} was displayed in real-time (Fig. 1). A red horizontal bar on the screen indicated the target AL peak GRF_{prop} (0%, +20% and +40% of baseline) [2]. We instructed subjects to modify their AL peak GRF_{prop} to meet the training target within 5%. Each VF trial lasted 5 min, followed by a 5-min rest, and then a 5-min retention trial with VF removed. We measured peak GRF_{prop} and calculated sagittal plane ankle power from both legs (Visual 3D, Germantown, MD). We also calculated inter-limb symmetry indices (SI) for these variables, where larger SI indicates greater asymmetry between the legs and 0% is perfect symmetry [3].

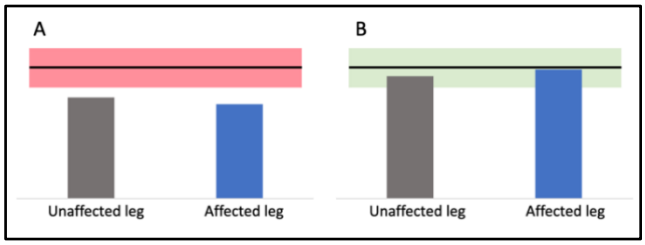

Figure 1: Example of VF. Grey and blue vertical bars represent peak GRF_{prop} measured in real-time during walking. Horizontal bar represents the training target. The color of the horizontal bar turns from red (A) to green (B) if the participant meets the training target within 5%.

Results and Discussion

S1 had higher AL peak GRF_{prop} than S2 during baseline walking (S1: 0.17 BW; S2: 0.11 BW). Compared to baseline walking, peak GRF_{prop} increased by up to 10.9% for S1 and by 12.4-58.2% for S2 in all VF walking trials (Fig. 2A). Neither subject retained this increase in peak GRF_{prop} in retention trials; peak GRF_{prop} increased by less than 4.2% for S1 and by 4.6-8.4% for S2 compared to baseline trials. S1 had a peak GRF_{prop} SI lower than 33.3% across all walking trials and S2 had more asymmetric peak GRF_{prop} during baseline walking (SI = 48.7%) and a less asymmetric peak GRF_{prop} when given real-time VF (SI = 5.9-30.6%). However, S2 walked with a more asymmetric peak GRF_{prop} during retention trials (Fig. 2B, SI = 40.6-44.7%) compared to baseline walking.

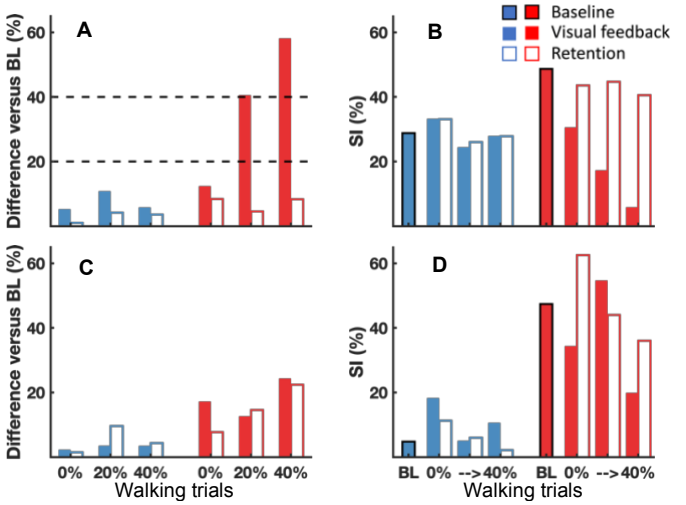

Figure 2. Subjects (S1 is blue, S2 is red) had increased AL peak GRF_{prop} (A) and decreased SI peak GRF_{prop} (B) during VF compared to baseline (BL) walking trials. Subjects had increased AL peak ankle power (C) and decreased SI peak ankle power (D) during VF compared to baseline (BL) walking trials. (A) 20% and 40% are indicated with dashed lines.

S1 had higher AL peak ankle power than S2 during baseline walking (S1: 3.46W/kg; S2: 1.72 W/kg). Compared to baseline trials, peak ankle power increased by 2.3-3.5% for S1 and by 12.7-24.4% for S2 during VF trials compared to baseline (Fig. 2C). S2 also maintained a 7.7-22.4% increase in peak ankle power during retention trials. Overall, S1 maintained peak ankle power SI across all walking trials (Fig. 2D, SI = 5.1-21.8%) and S2 reduced peak ankle power SI from 47.4% during baseline to 19.9% and 34.4% during 0%VF and 40%VF trials, respectively.

Significance

Our results suggest that when subjects with TTA using passive-elastic prostheses are given real-time VF of peak GRF_{prop}, they increase AL peak GRF_{prop} and walk with less inter-limb asymmetry. However, the effects of real-time VF may vary across individuals.

Acknowledgments

This study is funded by the Department of Veterans Affairs.

References

1. Grabowski & D'Andrea, *J NeuroEngin Rehab*, 2013
2. Franz et al., *Clinical Biomech*, 2014
3. Robinson & Nigg, *J Manipulative Physiol Ther*, 1987

STATIC OPTIMIZATION TO DETECT CHANGES IN MEDIAL KNEE CONTACT FORCE: A VALIDATION STUDY

Janelle M. Kaneda[1], Kirsten A. Seagers[1], Scott D. Uhlrich[1,2], Julie A. Kolesar[1,2], Kevin A. Thomas[1], and Scott L. Delp[1]
[1]Stanford University, Stanford, CA
[2]Department of Veterans Affairs Healthcare System, Palo Alto, CA
email: jkaneda@stanford.edu

Introduction

There are over 654 million individuals with knee osteoarthritis (KOA) worldwide.[1] KOA often occurs in the medial compartment. Increases in medial knee contact force (MCF) is thought to be associated with medial KOA progression;[2] however, most load-reducing gait modifications target a surrogate measure of MCF, the knee adduction moment (KAM), that does not fully capture medial compartment loading.[3] Gait modifications may be more effective if they target MCF instead of KAM. Thus, identifying if a gait modification increases or decreases MCF peaks can help evaluate their benefits for KOA treatment.[4] However, since MCF cannot be directly measured in a native osteoarthritic knee, musculoskeletal simulations are often used to estimate MCF. The ability of simulation techniques, like static optimization (SO), to predict changes in MCF needs to be validated against measurements from instrumented knee replacements (IKRs).[5] Previous work has shown that simulations can predict MCF changes for trunk sway gait,[6] but there is less work validating MCF changes across multiple gait modifications and multiple individuals. The purpose of this study is to evaluate whether SO can accurately estimate changes in MCF peaks induced by gait modifications.

Methods

We simulated MCF for two subjects with IKRs included in the 4th and 6th Knee Load Grand Challenge (GC).[7] Standing static calibration poses were used to scale a full-body musculoskeletal model[8] with a multi-compartment knee model.[9] Frontal-plane knee alignment was adjusted for the 6th GC subject, and knee contact points were adjusted for both subjects.[9,10]

We analysed baseline (natural) walking and five gait modifications (crouch, forefoot strike, bouncy, medial thrust, smooth) in total. We used a custom SO implementation using MATLAB and OpenSim 4.0[11] that includes passive muscle forces, estimates tendon compliance, and minimizes the sum of squared muscle activations. MCF from IKRs was calculated using regression equations.[12,13] The 1st and 2nd MCF peaks were defined as the maximum value in the first and last half of stance, respectively. Simulated and IKR MCFs were low-pass filtered at 15 Hz.

We evaluated how accurately SO could predict changes in MCF peaks above various simulated MCF thresholds. Changes in MCF peaks were computed by subtracting the average baseline MCF peak from the MCF peak of the gait modification for each of the simulated and IKR MCF values. This allowed us to evaluate whether clinically-meaningful changes in MCF could be correctly identified. We varied our threshold by 0.1 bodyweight (BW) increments of simulated MCF peak change and calculated accuracy for all changes beyond these thresholds. We computed accuracy for thresholds, above which, there were greater than three measurements. Mean absolute error (MAE) between simulated and IKR MCF peaks was also calculated.

Results and Discussion

MAE across all trials was 0.16 BW (10.9%) for the 1st peak of MCF, and 0.26 BW (20.8%) for the 2nd peak, which are within errors for simulation studies reported previously (0.2-0.3 BW).[6] The greater 2nd peak error may be due to the greater range of possible muscle coordination patterns in knee-crossing muscles during late stance.[14] SO predicted MCF changes with greater accuracy than chance for 0.25-0.5 BW 1st peak increases and for 0-0.4 BW 2nd peak reductions (Figure 1). These detectable changes are comparable to clinically-meaningful reductions in MCF induced by weight loss.[15] However, SO did not predict reductions in the 1st peak of MCF or increases in the 2nd peak of MCF with greater accuracy than chance.

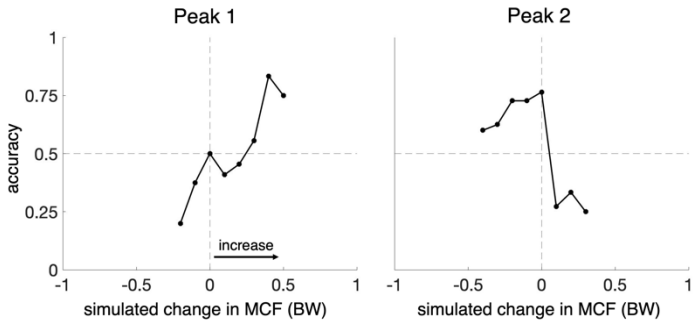

Figure 1: The accuracy of static optimization at predicting changes in peak medial knee contact force (MCF) for changes in MCF above varying thresholds. MCF changes are normalized by bodyweight (BW).

Significance

Accurately estimating the direction of changes in MCF peaks is important for evaluating gait modifications that aim to reduce knee loading. Here, we demonstrate that an SO algorithm can accurately detect some, but not all, changes in MCF peaks induced by gait modifications. A generic SO cost function may not accurately capture the coordination patterns adopted when subjects first learn a new gait pattern. Future work can evaluate whether different SO cost functions or the incorporation of electromyographic measurements can improve the ability of musculoskeletal simulations to estimate changes in MCF peaks.

Acknowledgments

This work was supported by NIH Grant P41EB027060.

References

[1] Cui et al., 2020. *EClinicalMedicine* **29.** [2] Andriacchi et al., 2004. *Ann Biomed Eng* **32.** [3] Walter et al., 2010. *J Orthop Res* **28.** [4] Kinney et al., 2013. *J Orthop Res* **31.** [5] Hicks et al., 2015. *J Biomech Eng* **137.** [6] Brandon et al., 2014. *J Biomech* **47.** [7] Fregly et al., 2012. *J Orthop Res* **30.** [8] Rajagopal et al., 2016. *IEEE Trans Biomed Eng* **63.** [9] Lerner et al., 2015. *J Biomech* **48.** [10] Winby et al., 2009. *J Biomech* **42.** [11] Seth et al., 2018. *PLoS Comput Biol* **14.** [12] Zhao et al., 2007. *J Orthop Res* **25.** [13] Meyer et al., 2011. ASME Summer BioE Conference. [14] DeMers et al., 2014. *J Orthop Res* **32.** [15] Aaboe et al., 2011. *Osteoarthr Cartil* **19.**

PATIENT-REPORTED KNEE PAIN IS ASSOCIATED WITH MEASURED QUADRICEPS TORQUE PRIOR TO TOTAL KNEE ARTHROPLASTY BUT NOT FOLLOWING SURGERY

Grant H. Berliner[1], Kenechukwu M. Okoye[1], Megan R. Hendricks[1], Gregory M. Freisinger[2], Jacqueline M. Lewis[1], Jeffrey F. Granger[1], Andrew H. Glassman[1], Matthew D. Beal[3], Laura C. Schmitt[1], Robert A. Siston[1], Ajit M.W. Chaudhari[1]
[1]The Ohio State University, Columbus, OH; [2] US Military Academy, West Point, NY; [3]Northwestern University, Evanston, IL
Email: berliner.26@buckeyemail.osu.edu

Introduction

Knee osteoarthritis (OA) is characterized by pain and loss of mobility of the knee that limits a patient's function. Previous studies have examined that a significant proportion of patients who elect a total knee arthroplasty (TKA) as the definitive treatment of their knee OA still report residual knee pain [1]. Researchers and clinicians have highlighted an individual's strength, specifically their lower limb strength, as important in determining an individual's knee function following TKA [2]. Other studies have examined specifically the cross-sectional area of the quadriceps muscles and its association with knee symptoms in individuals with knee OA [3]. During the course of rehabilitation, clinicians use measurements of individuals' quadriceps torque as an indicator of their strength and function. However, studies have already shown that failure of voluntary activation one month following TKA is a significant contributor to measured quadriceps "weakness", citing pain as one of the possible reasons for decreased activation [4].

However, less is known about how self-reported knee-related pain as captured by assessment tools like the Knee Osteoarthritis Outcome Score Pain (KOOS-Pain) subscale is associated with attenuated torque generation following TKA. The purpose of this study is to examine the association between an individual's knee-related pain and their torque-generating ability. We hypothesized that higher KOOS-Pain subscale (i.e. less pain) would positively correlate with quadriceps torque and greater improvement of KOOS Pain subscale would positively correlate with changes in quadriceps torque measurements at six months following TKA.

Methods

Twenty-seven individuals (18 female, age 63.0 ± 7.9 years) diagnosed with end stage OA were enrolled after giving informed consent per IRB guidelines as they awaited primary TKA. An isometric dynamometer (Biodex, Shirley, NY, USA) was used to evaluate the torque-generating capacity of the involved limb quadriceps within 30 days prior to their TKA (21.1 ± 24 days). The participants were seated with their knees flexed at 60 degrees and the participants' maximum voluntary isometric contraction normalized to body mass (qMVIC) were recorded with verbal encouragement throughout the task. The same knee extension evaluation was performed 6 months post-TKA.

Each participant also completed the KOOS Pain subscale to determine knee-related pain pre-operatively and 6 months post-operatively.

Pearson correlations (α = 0.05) assessed the correlation between the KOOS pain subscale and qMVIC at baseline and six-months post-TKA, as well as the absolute change between pre-TKA and six months post-TKA. We also examined the association between KOOS-pain at six months post-TKA and the change in qMVIC between pre-TKA and six months post-TKA.

Results and Discussion

Of the four analyses, we found a significant positive correlation between KOOS-Pain (less pain) at pre-TKA and qMVIC at pre-TKA (r = 0.548, r = 0.003). None of the other associations were significant.

Test	p-value	r
KOOS-Pain (@pre-op) vs Torque (@ pre-op)	0.003*	0.548
KOOS-Pain (@6 month change) vs Torque (6 month change)	0.484	0.138
KOOS-Pain (@ 6 months) vs Torque (6 months change)	0.058	-0.369
KOOS-Pain (@ 6 months) vs Torque (@ 6 months)	0.711	0.075

Table 1: Table of knee-related pain vs. torque correlations with corresponding correlation and p-values from Pearson Correlation statistical analysis.

These results suggest that in late-stage OA, prior to TKA, individuals' self-reported knee-related pain is associated with measured involved limb quadriceps torque. However, following TKA, that association does not persist. Similarly, changes with KOOS-pain are not associated with changes with qMVIC. Patient-reported knee-related pain appears to be more closely associated with measured quadriceps weakness in patients awaiting TKA than following TKA. Further study is required to better understand the factors that are more significantly related to measured knee extension torque in patients following TKA.

Significance

For patients post-TKA, patient-reported knee-related pain is less closely associated with measured quadriceps torque than pre-TKA. Residual knee pain may not be a significant contributor to observed quadriceps weakness post-TKA.

Acknowledgments

NIH NIAMS R01AR056700

References

1. Pagnano *Clin Orthop Rel Res* 1998
2. Petterson *Arthritis Care and Research* 2009
3. Ruhdorfer *Arthritis Care and Research* 2017
4. Mizner *Bone and Joint* 2005

FUNCTIONAL LEVEL IMPACTS THE USE OF ASSISTIVE DEVICES FOR INDIVIDUALS POST-STROKE

Erica A. Hedrick[1], Russell Buffum[1], Darcy S. Reisman[2], Samuel Bierner[3], and Brian A. Knarr[1]
[1]University of Nebraska at Omaha, Omaha, NE, USA,
[2] University of Delaware, Newark, DE, USA, [3]University of Nebraska Medical Center, Omaha, NE, USA
email: ehedrick@unomaha.edu

Introduction

Roughly 800,000 people experience a stroke every year in the United States, and about 30% of people require walking assistance (walker, cane, etc.) after a stroke [1]. While a cane can be used for body support overground, the criteria for optimal cane use in rehabilitation is not known. In addition, treadmill training is a common rehabilitation for individuals post-stroke. Handrails are typically used to assist with walking during this training, similar to a cane overground. While handrails are frequently used, subject interaction with these handrails are not usually considered and quantitatively reported. Individuals post-stroke frequently have a decreased propulsive force on their paretic side [2], which is correlated with a decreased walking speed [3].Therefore understanding the relationship between paretic propulsive force and anterior force on assistive devices is needed. The purpose of this study is to determine how the propulsive force generated through the paretic limb relates to the force generated on the assistive device. We hypothesize individuals with no experience with an assistive device will have a greater difference between propulsive limb force and assistive device force, compared to individuals that rely on using an assistive device.

Methods

Eight participants (3M, 5F; age 59.75.3±15.50 yrs.; 0.95±0.88 yrs. since stroke) from an ongoing study were included in this analysis: no history of assistive device use (N=2), past history of an assistive device use (N=2), and current dependence on an assistive device (N=4). Inclusion criteria included: age 19-80, single-chronic stroke, and ambulatory. Motion capture analysis using a full-body, 65-marker set was done both overground, using in-ground force plates and an instrumented cane, and with an instrumented treadmill and handrails. For the treadmill trials, subjects walked for two walking conditions (3 minutes each): light support handrail use (<5% BW) and self-selected handrail device use. The handrail on their nonparetic side was used. For the overground trials, subjects completed two conditions: walking with a cane using light pressure and walking with a cane comfortably. Real-time feedback of the cane and handrail forces were displayed for the light-support condition on a screen in front of the participant. Peak cane and handrail anterior forces and the difference between peak propulsive assistive device and paretic limb force were calculated for each group. Statistical analysis included a Wilcoxon signed rank test with a significance level of $\alpha \leq 0.05$.

Results and Discussion

The median peak propulsive (anterior) device force generated on the handrail (1.34% BW) was significantly more than on the cane (0.25% BW) ($p<0.001$). Canes are used primarily for body support [4], and handrails are fixed to the ground, which may be why individuals applied more propulsive force on the handrail compared to the cane. Individuals that had no history of assistive device use had the greatest difference between propulsive limb force and propulsive force applied to the assistive device (Figure 1). This suggests that these individuals are either able to generate more force with their limb than the other individuals, or they rely less on the assistive device. Previous assistive device users and current assistive device users had similar differences, although previous users had a slightly greater difference during overground walking. Previous and current assistive devices users may need the assistive device to supplement propulsive limb forces more than individuals that do not use an assistive device. Therefore, an individual's prior experience with assistive devices could change the relationship between propulsive force generated by the limb versus on the assistive device.

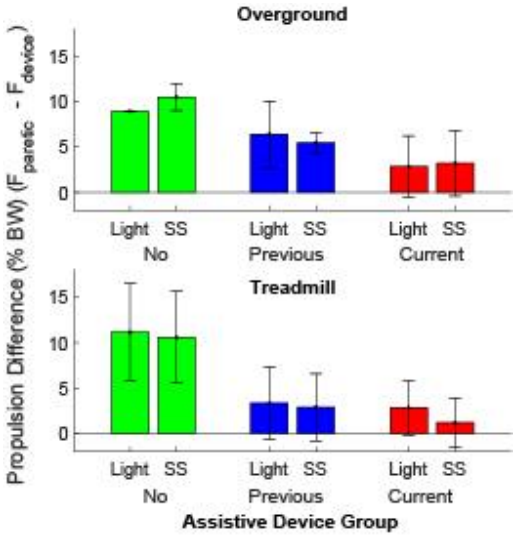

***Figure 1**. Differences between peak propulsive paretic limb force and propulsive device force for light and self-selected (SS) device use for each assistive device group: no history, previous history and current assistive device use during the overground conditions with the cane (top) and treadmill conditions with the handrail (bottom). Positive values indicate greater propulsive force generated by the paretic limb.*

Significance

These results suggest that assistive device use and prior experience with assistive devices can influence how these devices affect propulsive force generation in the paretic limb of individuals post-stroke. How this difference may change through the rehabilitation process may be a quantitative way to progress and guide clinical decision-making regarding transitions to independent walking.

Acknowledgments

This research was funded by the NIH (R15HD094194).

References

1. Go AS, et al., *Circulation*,**129**, 3, e28–e292, 2014 .
2. Lewek MD, et al., *Neurorehabil. Neural Repair*,**32**, 12, 1011–1019, 2018 .
3. Bowden MG, et al., *Stroke*,**37**, 872–876, 2006.
4. Chen G, et al., *Gait Posture*,**22**, 1, 57–62, 2005.

EARLY STRENGTH RECOVERY AFTER TKA PREDICTS STRENGTH RECOVERY AT TWO YEARS

Kenechukwu M. Okoye[1], Megan R. Hendricks[1], Grant H. Berliner[1],Gregory M. Freisinger[2], Jacqueline M. Lewis[1], Jeffrey F. Granger[1], Andrew H. Glassman[1], Matthew D. Beal[3], Laura C. Schmitt[1], Robert A. Siston[1], Ajit M.W. Chaudhari[1]
[1]The Ohio State University, Columbus, OH; [2]US Military Academy, West Point, NY; [3]Northwestern University, Evanston, IL;
Email: okoye.13@osu.edu

Introduction

Previous studies have shown that individuals with knee osteoarthritis who undergo total knee arthroplasty (TKA) exhibit initial involved limb quadriceps weakness after TKA, followed by increase in strength until six months [1]. At this six-month time point, patients often have not achieved significant gains in quadriceps strength over pre-TKA [1,2]. Perioperative quadriceps weakness is strongly associated with aberrant sagittal plane knee movement during high-demand tasks in this population [3], suggesting that strength improvement may be an important goal after TKA. However, no study has examined the relationship between early recovery of strength and long-term recovery of strength. Understanding this relationship could enable more personalized post-operative treatment recommendations for patients to improve long-term functional outcomes and patient satisfaction. The purpose of this study, therefore, was to examine whether initial quadriceps torque recovery in the first 6 months post-op predicted quadriceps torque recovery at 24 months post-TKA.

Methods

Twenty-seven individuals diagnosed with end stage OA were enrolled as they awaited primary TKA after providing IRB-approved informed consent. (18 female, age 63.0 ± 7.9 years) At 30 days pre-TKA, 6 months post-TKA, and 24 months post-TKA, the participants' involved limb quadriceps maximum voluntary isometric contraction (normalized to Nm/kg, qMVIC) was recorded using an electromechanical dynamometer (Biodex, Shirley, NY) with their knee flexed to 60 degrees.

Participants were stratified into three groups based on whether the difference in their qMVIC between pre-TKA and 6 months post-TKA exceeded the 95% confidence interval of the standard error of measurement (0.22 Nm/kg) [4]: Those whose qMVIC "Improved in 6mo" (n = 8), those whose qMVIC "Did not recover in 6mo" (n = 7), and those whose qMVIC "Recovered in 6mo" (n = 12). Individual regression analyses were conducted on each group to determine how strongly baseline qMVIC predicted qMVIC at 24 months. ANOVA was used to test for differences in baseline qMVIC between groups.

Results and Discussion

Baseline qMVIC predicted 24-month qMVIC in the "Recovered in 6mo" group (β_1 = .77 ± .25, R^2=.830, p < .001), with a relationship not significantly different from y=x across almost the entire range of observed baseline strength. In the "Improved in 6mo" group baseline qMVIC did not predict 24-month qMVIC (p = .357). Seven out of eight of these participants maintained an improved qMVIC at 24 months relative to baseline exceeding 0.22 Nm/kg.

Only one of the seven participants from the "Did not recover in 6mo" group showed a 24-month improvement of their qMVIC relative to baseline that exceeded 0.22 Nm/kg. This group also showed no significant relationship between baseline and 24-month qMVIC (p = .454). This group did have the highest average baseline qMVIC (p=.002), with all members being above the median for this cohort.

These results suggest that an incomplete six - month recovery of pre-TKA quadriceps strength is indicative of a slower or perhaps limited strength recovery remaining below baseline at 24 months. In contrast, early improvements in quadriceps strength were maintained by almost all participants at 24 months. While not investigated in this analysis, it is important to note that recovery from baseline may not be sufficient to achieve desired function, as all participants remained considerably below mean qMVIC of 2.1 Nm/kg for healthy adults of similar age [5].

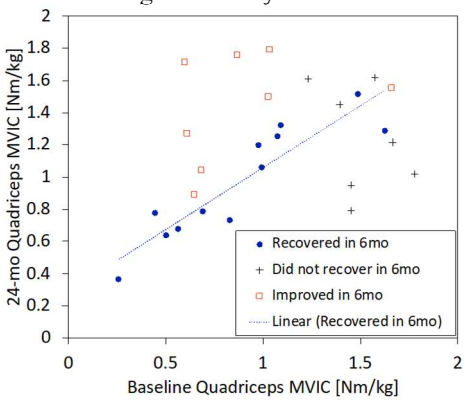

Figure 1: 24-month quadriceps MVIC (qMVIC, Nm/kg) vs. baseline qMVIC within groups based on 0-6 month change in qMVIC. Baseline qMVIC only predicted 24-mo qMVIC in the Recovered in 6mo group (blue line).

Significance

A patient's early recovery of quadriceps strength can give valuable insight into the course of long-term quadriceps recovery post-TKA. Considering patterns of strength recovery within this population based on quadriceps strength may prove useful to determine if and how to intervene to achieve better than baseline levels of quadriceps function. In general, patients who *only* recover to their baseline quadriceps strength at six months are likely to remain close to that level at 24 months. Those patients who have incomplete strength recovery relative to pre-TKA at 6 months are less likely to achieve baseline levels even at 24 months than those who arrive or exceed that benchmark by six months. Further study of the factors that lead to incomplete recovery and a lack of substantive gain in strength after this procedure as well as the implications of strength for daily function and quality of life are needed.

Acknowledgments

NIH NIAMS R01AR056700 | The Ohio State University MSTP

References

1. Mizner et al *J Orthop Sports Phys Ther* **35**(7), 2005
2. Cho *Knee Surg Sports Traumatol Arthrosc* **22,** 2014
3. Christensen et al *Knee* **26**(1), 2019
4. Kean et al *Arch Phys Med Rehabil* **91**(9), 2010
5. Bade et al. *J Orthop Sp Phys Ther* **40**(9), 2010

Training with Agency-Inspired Feedback from a Sensor Glove in Virtual Reality to Improve Grasp Performance

Mingxiao Liu[1,2], Sean P. Sanford[1,2], Samuel Wilder[1,2], and Raviraj Nataraj[1,2]
[1]Department of Biomedical Engineering, Stevens Institute of Technology, Hoboken, NJ, 07030
[2] Movement Control Rehabilitation (MOCORE) Laboratory, Stevens Institute of Technology, email: mliu26@stevens.edu

Introduction

Neuromuscular trauma including traumatic brain injury (TBI) and spinal cord injury (SCI) can significantly impair individuals' activities of daily living, especially hand movement [1]. As a traditional method, physical therapy (PT) often helped people to regain hand functions such as grasping. However, commitment to PT can be challenging, which involves repetitive and intensive movement training [2]. Also, traditional PT methods have yet to effectively leverage cognitive factors, whereas the emphasis is on the perception of self-control. *Sense of agency* or *agency* was studied previously to better motivate people to engage in movement training for rehabilitation [3]. Our preliminary study leveraged agency and presented a novel approach using a sensor glove to identify achievement of a "secure" grasp. Once identified, onboard training feedback would be provided to improve grasp performance [4]. In recent decades, virtual reality (VR) is involved in PT due to its advantage in customization, cost-effectiveness and ability to provide enhanced feedback [5]. In this study, we aim to integrate VR immersion with the sensor glove to further enhance the training effect and to effectively foster agency while accelerating motor gains during rehabilitation. We hypothesized that performance improvement will be more significant with VR immersion, compared to the preliminary results.

Methods

Ten participants performed a grasp-move-place task while receiving visual (color change) and audio (singular beep) feedback while immersed in a customized VR environment (*Unity, Unity Technologies*) during a training session (**Figure 1**). The task involved the participant grasping a small cubic object (both in VR and real-world) from the starting location and placing onto a designated target. A 2-layer feedforward neural network (NN) was used to assess the "secure" grasp from force and flex sensor signals based on offline training data. Once "secure" grasp was determined from the NN, feedback would be provided to the user during training across three distinct conditions: 1) 'Audio only' 2) 'Audio + Visual' 3) 'No Feedback'. In addition, to present as 'Decay' as the preliminary study, feedback was provided at progressively shorter time-intervals (from 1 to 0 s) after a "secure" grasp. The 'Decay' was intended to facilitate greater agency through intentional binding, whereby one builds a stronger perception to couple action ("secure" grasp) with a sensory consequence. The primary performance metrics were minimizing the completion time and pathlength in moving the object. Performance was assessed before and after training with the same task. A motion capture system (*LEAP, Ultraleap*) was used to track motion of the hand and the performance was assessed based on the position of the virtual object/hand. Lastly, electroencephalogram (*gUSBamp, g.tec*) and electromyography (*Delsys, Delsys Inc.*) were collected to examine the physiological changes with the training.

Results and Discussion

The preliminary study indicated significant ($p<0.05$) differences in completion time and pathlength before and after the training with 'No' feedback (where no feedback was provided during training) and 'Decay' feedback condition [4]. Current study is collecting additional subjects to increase sample size. A one-way repeated-measures ANOVA and Tukey post-hoc comparisons with Bonferroni correction will be performed for each performance metric across the training conditions and be compared with the preliminary results.

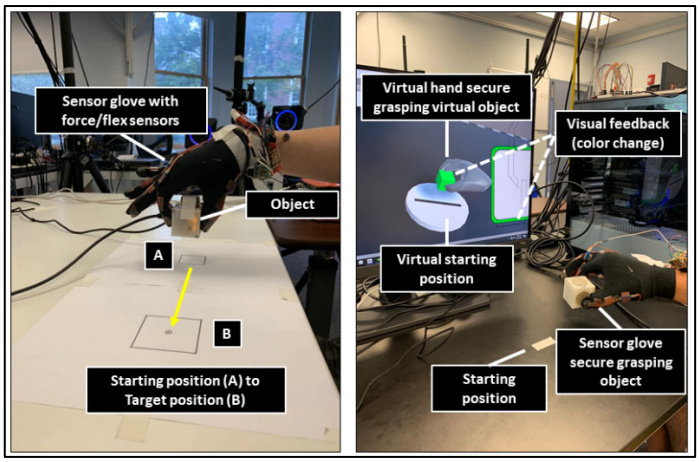

Figure 1: **Left)** Experimental procedure of the grasp-move-place task **Right)** VR and real-world setup of the task.

Significance

The preliminary study presented a novel method to predict and inform "secure" grasp from a sensor glove during a grasp-move-place task. Also, we demonstrated the effect of providing agency-inspired sensory feedback on grasp performance. In this study, we further examined the training effect and integrated the sensor glove with VR immersion. We hypothesized that the training effect would be greater with the VR immersion than our preliminary results. The next phase of the study is to test with clinical participants (TBI and incomplete SCI patients) to confirm the results of this study. Our objective is to develop a mixed-reality rehabilitative training paradigm that provide customizable and augmented feedback to improve grasp performance while leveraging agency for individuals following neurotrauma.

Acknowledgments

This research was funded by NEW JERSEY HEALTH FOUNDATION, grant number PC53-19. The authors would like to acknowledge the support from the Schaefer School of Engineering and Science, at the Stevens Institute of Technology.

References

1. Jia X. et al. J. Intensive Care Med. 2013;28(1):12-23.
2. Connell. L.A. et al. Phys. Ther. 2018;98(4):243-250.
3. Moore J.W. et al. Front. Psychol. 2016;7.
4. Liu M. et al. Sensors. 2021;21(4):1173.
5. Connelly L. et al. *IEEE Trans. Neural Syst. Rehabil. Eng.* 2010;18(5):551-559.

SIMULATING HIP STIFFNESS IN HEALTHY ADULTS DURING QUIET STANDING BY USE OF A HIP AND KNEE BRACE: PRELIMINARY RESULTS

Benjamin Hinkley, Aaron Tranquillo, Veronica Venezia, Niclas Sharp, Robert Creath*
Lewis Human Performance Lab, Department of Exercise Science, Lebanon Valley College, *creath@lvc.edu

Introduction

Human postural sway has been characterized as a two-segment inverted pendulum, where anteroposterior (A-P) sway occurs simultaneously around the ankles and hips. At higher body sway frequencies upper body (trunk) sway tends to be anti-phase (i.e., in opposition) to the lower body (legs) sway, while at lower frequencies trunk and legs sway tend to be synchronized (Creath et al. 2005, 2008). Older adults often exhibit reduced sway at the hip, suggesting a more rigid posture (Engelhart et al. 2016). Rigid posture may adversely affect balance control leading to falls, but little is known because within-subject postural rigidity is difficult to assess due to a lack of controlled experiments and differences in postural strategies observed within the population. The purpose of this experiment is to simulate hip stiffness in young healthy adults during quiet stationary stance using an adjustable, commonly available hip-knee orthotic brace (HKO) by comparing trunk and legs body sway for hip-restricted (HR), hip-unrestricted (UN), and without the HKO (NB) conditions.

Methods

* 18 healthy adults (7 m; 20.5±1.2 yrs.).
* A hip-knee orthotic brace (HKO) was used to immobilize hip and knee motion (Figure 1).
* 6, 130-second quiet-stance trials: 2-hip restricted (locked) (HR), 2-unrestricted (UN), and 2-without the brace (NB). The knee was always locked in position.
* Measures include 3D kinematics using 19 anatomical markers collected at 240Hz.
* Segment angles were determined using common trigonometric methods.
* Measures include power spectral density (PSD), coherence, and cophase (lead-lag between trunk and legs segments).
* T-tests at each frequency (α=0.05) with no multiplicity correction.

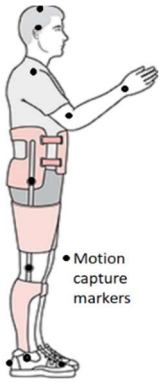

Figure 1: Subjects wore a hip and knee orthotic brace (HKO). Motion capture used 19 reflective body markers. Ankle motion was not restricted.

Results and Discussion

Persons experiencing minor physical impairments appear to perform normally because movement deficiencies are very small and easily compensated. Early data analyses included typical time-domain variables (e.g., mean, std dev.) which showed no differences. In the current analysis, spectral methods were used because they allow for frequency-by-frequency analysis.

Figures 2A&2B show the PSD estimates of trunk and legs sway angles relative to vertical. There were no significant statistical differences between conditions for either segment. Trunk spectral power at low frequencies was approximately 0.9 deg^2/Hz at 0.15 Hz, gradually decreasing to 10^{-5} deg^2/Hz at 5Hz. Legs spectral power at low frequencies was on the order of 10^{-4} deg^2/Hz at 0.15 Hz, gradually decreasing to physically insignificant levels at higher frequencies.

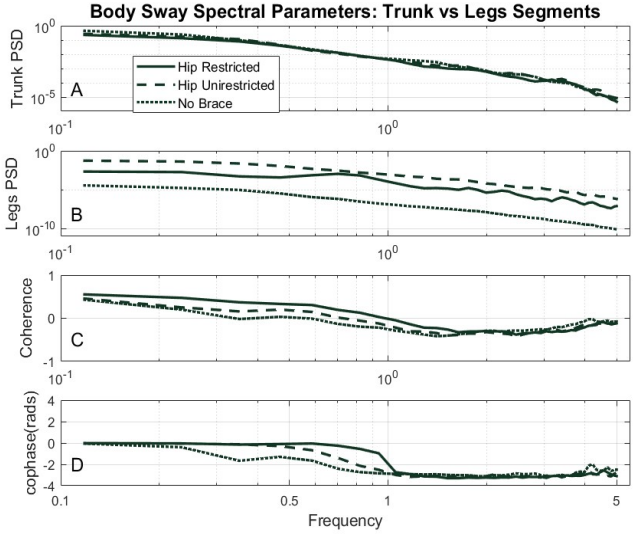

Figure 2: Body sway spectral parameters showing trunk and legs PSD (2A&2B), coherence (2C), and cophase (2D) for HR (solid lines), UN (dashed lines), and NB conditions (dotted lines).

Figure 2C shows the coherence between trunk and legs segments. There is a slight condition difference noted at lower frequencies between the HR and UN, and HR and NB conditions. Values below 0.33 are not significant.

Figure 2D shows the cophase between trunk and legs segments. At lower frequencies, the trunk and legs are in-phase while at higher frequencies the segments are antiphase to each other for all three conditions. Significant differences occur slightly below 1Hz between HR and NB suggesting that the trunk-legs phase relationship is altered at the transition between in-phase and antiphase due to restriction of hip motion.

Significant conditional differences indicate that simulated hip stiffness causes frequency-dependent changes in body sway.

Significance

Hip stiffness is common in older adults. This experiment demonstrates within-subject frequency-dependent differences occur between HR, UN and NB conditions. Based on these findings, future research can focus on specific body-sway frequencies to identify postural control deficiencies.

References

1. Engelhart D, Pasma JH, Scouten AC, Aarts RGKM, Meskers CGM, Maier AB, van der Kooij H. Adaptation of multijoint coordination during standing balance in healthy young and healthy old individuals. J Neurophysiol. 2016, Mar1: 115(3): 1422-1435.
2. Creath R, Kiemel T, Horak F, Peterka R, Jeka J. A unified view of quiet and perturbed stance: simultaneous co-existing excitable modes. *Neurosci Lett*. 2005; 377(2):75-80.
3. Creath R, Kiemel T, Horak F, Jeka JJ. The role of vestibular and somatosensory systems in intersegmental control of upright stance. *J Vestib Res*. 2008; 18(1):39-49.

EFFECT OF WEARING A BACKPACK ON SPEED AND KINEMATICS OF REACTIVE STEPPING

Jessica Pitts, D. Verbrigghe, C. Sisko, A. Smith, K. Elmblad, V. Komisar, M. A. Nussbaum, C. A. Duncan[1]
[1]Department of Kinesiology and Integrative Physiology, Michigan Technological University
email: caduncan@mtu.edu

Introduction

Backpacks are among the most common loads that people carry and typically place an additional load on the dorsum of the trunk[1]. Due to its position near or above the whole-body center of mass (COM), carrying this additional load may change postural control dynamics that can lead to instability and an increased risk of falls. During quiet standing, wearing a backpack increases COM movement[2], suggesting that unperturbed balance control is challenged. To our knowledge, however, it is unknown if wearing backpacks adversely affects postural control during instances of instability (e.g., a trip) during which people must regain their balance to avoid falling. In this study, we characterized how wearing a backpack affects reactive stepping following forward and backward lean-and-release perturbations. We hypothesized that changes to temporal-spatial characteristics of the reactive mechanism (e.g., step length, stepping onset) would be required to accommodate the increased load on the person. We also hypothesized that the maximum release angle that could be achieved without requiring multiple steps would decrease when wearing a backpack regardless of perturbation direction.

Methods

Twelve participants (6 men, 6 women; mean (SD) age: 24.3 (2.6) years; mass: 75.3 (13.5) kg; height: 170.3 (10.1) cm) performed a series of forward and backward lean-and-release balance recovery trials with and without wearing a backpack weighted with 15% of individual body weight. In each condition, participants started at release angles of 2º and 10º for backward and forward perturbations, respectively. The release angle was increased incrementally between trials by 2º until the participant could not recover their balance with only one step. During all trials, kinematics were recorded with an 11-camera optical motion capture system (Qualisys, Sweden).

COM kinematics (maximum velocity and acceleration), stepping temporal-spatial parameters (step length, and velocity), and stepping onset latency were obtained between loaded and unloaded conditions at the greatest lean angle. These measures were compared between conditions using paired *t* tests (significant effects identified when $p < 0.05$).

Results and Discussion

Maximum COM acceleration during the reactive response was significantly greater ($p = 0.008$) when wearing a backpack in both forward and backward perturbation trials (Figure 1a). This increase was accompanied by significant increases in step length and step height when wearing a backpack during both forward and backward perturbation (Figure 1b). No significant differences in maximum COM (0.93 (0.16) m/s) or stepping velocity (4.87 (0.69) m/s) or stepping height (0.27 (0.05) m) were found. However, there was a decrease in stepping onset latency of ~20 msec in the loaded vs. unloaded conditions for both perturbation directions that approached significance ($p = 0.093$). These kinematics changes while wearing a backpack did not result in decreases in the maximum lean angles from which participants could recover from either forward (22.9 (4.4)º) or backward (3.6 (3.0)º) perturbations.

These results suggest that reactive balance mechanisms must be modified to accommodate the greater COM acceleration to successfully regain balance. In the case of the current lean-and-release perturbations, modifications involved increasing the size of the base of support in the direction of COM movement by increasing step length.

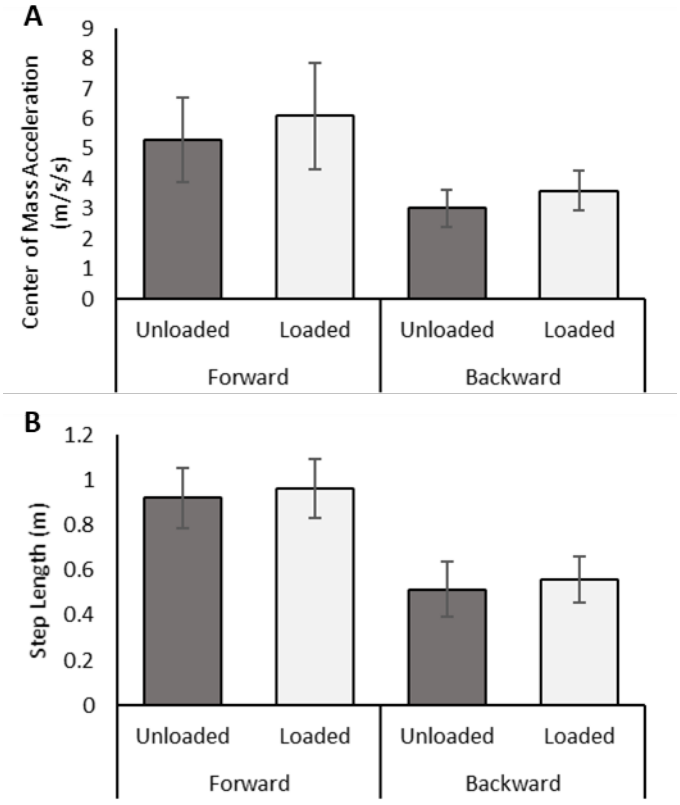

Figure 1: Maximum center of mass acceleration (A) and reactive stepping length (B) across loading conditions for forward and backward perturbation. Error bars represent SDs, and all paired differences between loading conditions were significant.

Significance

These findings provide evidence of the effect of wearing loads, like backpacks, on reactive balance control. Although the current young and healthy adults recovered balance equally as well while wearing a backpack, changes in response characteristics suggest that the additional load may be challenging for populations with musculoskeletal and neurological impairments, who may lack the strength or ability to quickly adapt a response to account for the additional load. This information can provide foundational insights to fuel future evidence-based practice related to carrying external loads, including clinical and ergonomic practice.

References

1. Qu, X. & Nussbaum, M.A. (2009). *Gait & Posture*, *29*(1), 23-30.
2. Chow et al. (2006). *Gait & Posture, 24*(2), 173-181.

MOVEMENT SMOOTHNESS WHEN WALKING, RUNNING, AND SKIPPING IN HEALTHY ADULTS AND INDIVIDUALS WITH MILD TRAUMATIC BRAIN INJURY

Selena Cho[1], Leland E. Dibble[1], Margaret W. Weightman[3], Lucy Parrington[2], Mark E. Lester[4], Carrie W. Hoppes[5], Laurie A. King[2], Peter C. Fino[1]
[1]University of Utah, Salt Lake City, UT
[2]Oregon Health & Science University, Portland OR
[3]Courage Kenny Research Center, Allina Health, Minneapolis MN
[4]Texas State University, Round Rock, TX
[5]Army-Baylor University Doctoral Program in Physical Therapy, For Sam Houston, TX
Email: u1365862@utah.edu

Introduction

Smooth movement is a characteristic feature of a healthy human motor control system. People with neurological diseases such as Parkinson's disease exhibit jerkier motions.[1] Smoothness is also an indicator of motor recovery in people following a neurological injury such as stroke.[2] Despite movement smoothness being a promising indicator of the integrity of the motor control system, it remains understudied in people with mild traumatic brain injury (mTBI), who also exhibit motor dysfunction following neurological injury.

Different locomotor tasks such as walking, running, and skipping should differ in kinematic smoothness because of unique swing phases, heel strikes, and kinetic impulses. But, clear evidence of this difference, or how it might change with neurological injury, is lacking. Inertial measurement units (IMUs) have been used to evaluate the quality of kinematics during a variety of locomotor tasks and infer the nature of motor control[3]. Therefore, we sought to quantify movement smoothness using IMUs during a variety of tasks that are clinically assessed in people with mTBI.

The purpose of this study was to (1) compare the utility of movement smoothness across fast walking, running, and skipping and (2) compare movement smoothness between healthy adults and those with persisting symptoms (>3 weeks) from mTBI. We expected the movements will be ranked from least to most smooth in the following order: skipping, walking, and running. Also, we hypothesized that the mTBI group would be less smooth than the control group across all tasks.

Methods

In this IRB approved study, 45 healthy adults [33F, mean (SD) age = 31.91 (9.84) years] and forty-one adults with mTBI [33F, mean (SD) age = 33.14 (9.52) years, time since injury = 341 (298) days] provided informed consent across two sites. Participants completed the revised High-Level Mobility Assessment Tool (HiMAT) during which they were instructed to walk, run, or skip as fast as possible for 20 m. IMUs (APDM Opals, Portland, OR) placed on the lumbar and forehead collected tri-axial angular velocity data at 128 Hz.

Trials were trimmed to discard stationary, non-movement related periods at the beginning and end of the trial recordings. Smoothness of angular motion was quantified using the spectral arc length (SPARC), which measures the arc length of the Fourier spectrum of movements to quantify smoothness[4]. The raw angular velocity from the gyroscope was input directly into SPARC. The SPARC Python modules were pulled into a customized MATLAB (R2020b) script for analysis.

Linear mixed-effects models were implemented with fixed effects for task, group, and their interactions with random effects for intercept and slope by task for each subject. Significance was set as $p<0.05$.

Results and Discussion

Main effects of task were observed in all models ($p < 0.001$). Angular motion of the lumbar and head was generally smoother during running than during walking or skipping (Fig 1). We suspect this difference is because the prolonged flight phase during running temporally separates braking and push-off impulses. Conversely, fast walking involves successive braking and push-off impulses during double support and skipping adds an additional ground contact phase of the swing limb.

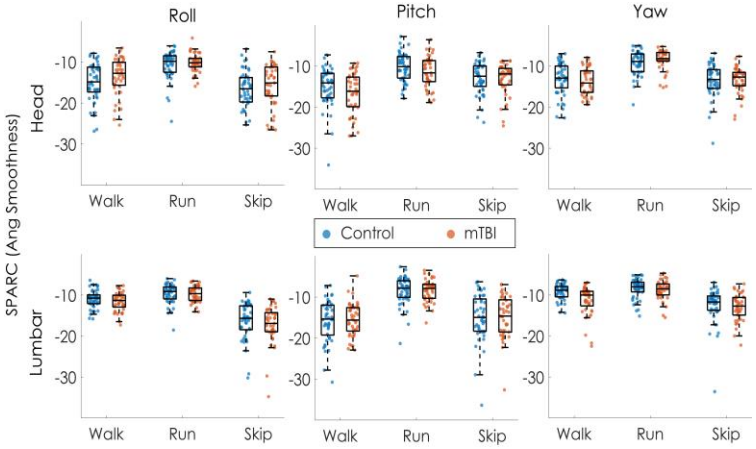

Figure 1: Distributions of SPARC for control (blue) and mTBI (orange) groups across each condition and body segment.

A group and group*task interaction were only observed in lumbar yaw; individuals with mTBI exhibited less smooth angular motion in lumbar yaw, but only while walking ($p < 0.001$). No other group differences were observed. The isolated difference in yaw may be caused by increased double support time or more variable step lengths in the mTBI group. Future work directly examining these spatiotemporal factors and examining linear motion using other measures such as log-dimensionless jerk is needed to confirm these interpretations.

Significance

While angular smoothness is sensitive to differences across fast locomotor tasks, people with persisting symptoms from mTBI are not less smooth than healthy control subjects.

Acknowledgments

This work was supported through the Congressionally Directed Medical Research Program (W81XWH1820049, PI: King).

References

1. Beck, Y. et al (2018). *J of Neuroeng Rehabil.* 15 (49).
2. Rohrer, B. et al (2002). *J of Neuroeng Rehabil.* 22 (18).
3. Fino, P. C. et al (2018). *Gait Posture*, 62, 157-166.
4. Balasubramanium, S. et al (2015). *J of Neuroeng Rehabil.* 12 (15).

Can Dynamic Plantar Pressure Parameters Characterize the Progression of Diabetes Mellitus?

Mathew Sunil Varre[1], Kenneth Izuora[2], Mohamed B. Trabia[3], Janet S. Dufek[1]
[1] Department of Kinesiology and Nutrition Sciences, University of Nevada – Las Vegas, NV, USA; [2] Department of Internal Medicine, University of Nevada – Las Vegas, NV, USA; [3] Department of Mechanical Engineering, University of Nevada – Las Vegas, NV, USA
Email: varre@unlv.nevada.edu

Introduction

Diabetic peripheral neuropathy (DN) is a common complication of type-2 diabetes mellitus (DM)[1]. Repetitive mechanical loading of the plantar surface combined with loss of sensation makes persons with DN prone to skin breakdown and foot ulcers (FU) [2]. Clinicians and researchers have used plantar pressure (PP) measurements such as peak plantar pressure (PPP), peak pressure gradient (PPG), and pressure time integral (PTI) to identify factors that may lead to skin breakdown and FUs[1-4]. Persons with DM have been found to have higher (PPP) compared to healthy people[2-4]. However, researchers have found that PPP alone may not be an adequate measure to predict the development of skin breakdown in individuals with DM[2]. PPG has been found to be a strong indicator of the onset of skin breakdown and FUs along with PPP in persons with DM[2]. Some studies have found higher PTI values in persons with DN compared with individuals with DM alone or healthy persons[4]. While past studies have made critical contribution in identifying differences between PP parameters, how PP parameters alter with the progression of DM is not well understood. It is vital to understand the changes in PP parameters in individuals with DM as the pathology advances from pre-diabetes (PD) to DM and development of DN thereafter. Therefore, we propose a quantitative approach that incorporates all three PP measures each of which would provide unique information that could be valuable in accurately characterizing the progression of DM and prevent foot related complications. The aim of this study was to investigate the differences in plantar pressure variables with the progression of diabetes mellitus. We hypothesized that there would be significant group differences in dynamic pressure parameters of three regions of the foot (rear, mid, and forefoot) during walking.

Methods

A convenience sample of fifty-seven individuals was used for the study representing three groups: PD [59.6 ± 11.4 Yrs, 93.7 ± 27.6 Kg, 1.68 ± 0.09 m, 9 male/10 female], Diabetic control (D) [61.0 ± 9.0 Yrs, 97.2 ± 23.7 Kg, 1.67 ± 0.07 m, 9 male/10 female], and DN [65.8 ± 7.4 Yrs, 99.1 ± 30.4 Kg, 1.68 ± 0.10 m, 11 male/8 female]. The subjects were briefed about the testing protocol and provided informed consent (IRB# 777036). The participants were fitted with thin socks and pressure measuring insoles (Medilogic, Schoenfeld, GE; 60 Hz). Pressure data were recorded for five trials as they walked at their preferred pace on a 6-10m walking path with a 4-m active test section.

Pressure data acquired were processed using Matlab v2019 b (MathWorks, MA, USA) by dividing the insole into 3 regions: rearfoot (RF), midfoot (MF), and forefoot (FF). Stance phase of the first three steps as the participant entered the 4-m test section were considered in the analysis. The value of peak pressure sensors in each region was recorded as PPP. PPG was calculated by computing the highest change in pressure at the peak pressure sensor and its neighboring 8 sensors[2]. PTI was calculated by summing the pressure at each time point for all sensors in each region. All PP parameters were normalized to body mass. Due to data non-normality, Kruskal-Wallis tests were performed to test differences of PP parameters at the three regions of the foot among the three groups (α =0.05).

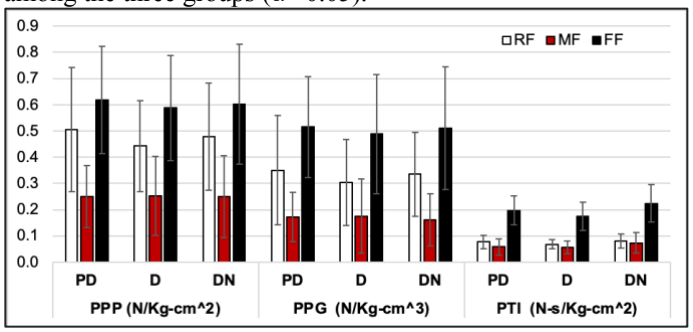

Figure 1: Average and standard deviation values of PP parameters for the three participant groups at three regions of the foot.

Results and Discussion

Statistical analysis did not show significant group differences for the demographics. Similarly, there were no statistically significant differences in the PP parameters. These non-significant findings for PPP, PPG, and PTI are similar to previously reported for D and DN groups[1,3,4]. However, comparisons of the PP parameters by region revealed significant differences for all PP parameters for the three groups (FF>RF>MF) (Fig 1). This was consistent with previous studies where they found PP parameters to be higher in FF region compared to other regions of the foot[1-4]. Also, visual check of the descriptives revealed large within-group variations in the PP parameters. Including a larger sample size in future analyses would perhaps reduce within-group differences. In conclusion, the preliminary results of this investigation show that plantar pressure parameters alone may not be able to characterize the progression of DM. A combination of PP parameters and subject-specific factors such as diagnosis duration, gait speed, and glycated hemoglobin may be able to distinguish the three groups and thereby disease progression in persons with DM.

Significance

Building on pilot findings, the potential application of this study to persons with DM is an approach to detect neuropathy at an early stage using dynamic plantar pressure. Subject specific parameters as predictors may be used and thereby prevent foot ulcers to provide additional insight. This may aid clinicians to provide better foot care management, treatment approaches, and footwear recommendations to individuals with DM to avoid foot related complications.

Acknowledgments

We would like to acknowledge funding support by National Institute of General Medical Sciences (GM 103440).

References

1. Gnanasundaram et al. *Foot & Ankle Surg.* **26**(2), 2020.
2. Mueller et al. *Physical Therapy,* **88**(11), 2008.
3. Fawzy et al, *Clin Med Insights: Endo & Diab*. **7**, 2014.
4. McPoil et al, *J Amer Pod Med Assn* **91**(6), 2001.

CONSIDERATION OF SUBTALAR JOINT AXIS LOCATION IN DYNAMIC MUSCULOSKELETAL MODEL

Julia M. Noginova, Hunter J. Bennett, Stacie I. Ringleb
Old Dominion University, Norfolk, VA
email: sringleb@odu.edu

Introduction

Frequently, the subtalar joint (STJ) is overlooked in biomechanical models by "locking" the joint out of the model during analysis or using a generic subtalar joint axis definition. Since the subtalar joint takes on much of the foot's load-acceptance, especially in dynamic tasks, involving a true STJ may be necessary to obtain accurate simulations. Furthermore, since the STJ is the beginning of the kinetic chain of the lower limb, the inclusion and accurate characterization of the STJ in models may improve understanding of the load-transmission through the ankle, knee, and hip.

The STJ significantly affected joint rotations at the knee and ankle as well as the predicted knee and ankle joint contact forces during running [1]. Additionally, the orientation of the STJ axis significantly affected ankle range of motion during walking and subtalar joint moments during walking and running [2]. In the OpenSim Lai model [3], the location of this 1DOF axis of rotation is based at the most distal part of the calcaneus. While there are no STJ specific standards, the ISB standards for ankle joint recommend that the calcaneus coordinate system origin should be coincident with that of the ankle, i.e. midway between the two malleoli of the talus [4]. Therefore, the purpose of this study was to determine how the subtalar joint axis location affects the kinetic chain from subtalar joint all the way to the knee during normal gait.

Methods

Overground walking was obtained from the 3rd, 4th, and 6th Grand Knee Challenge Competition [5]. The standard Lai model was scaled for each subject and adjusted to include the pelvis and lower instrumented limb. The STJ axis was modified by changing the location of the origin from the default location at the distal point of the calcaneus **(Heel)** to a new location at the talocrural axis **(Ankle).** The STJ axis orientation was set to match Inman's mean inclination/deviation angles in both conditions [6]. A two-tailed paired t-test was used to compare peak joint angles, moments, and loading forces that were computed for the lower kinetic chain using OpenSim's GUI toolbox. Significance was set at $p<0.05$. The *in vivo* knee load from the instrumented load cell (eTibia) was used to validate the models and compute RMS and Pearson's correlation (p^2) of the calculated knee joint reaction.

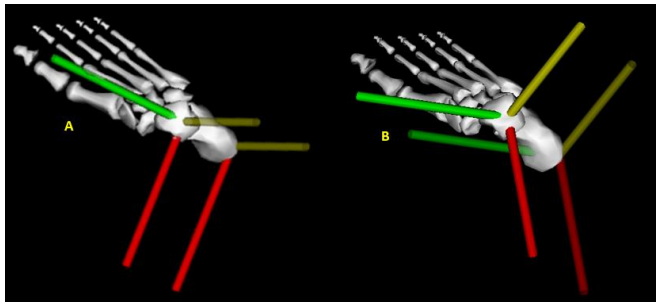

Figure 1: Distal calcaneus and talocrural joint origins with (A) default STJ orientation at both locations and (B) Max deviation angle defined by Inman at both locations. Green line is STJ's axis of rotation.

Results and Discussion

The default STJ oblique axis in the Lai model runs directly from the heel axis location through the ankle axis location. While this fits within Inman's description of where the axis extends through the talus to the heel, it does not match the reported STJ mean inclination and deviation angles. Changing the STJ origin location doesn't affect the axis of rotation (green) for the default orientation while changing the STJ origin for other orientations lead to differences in the axis of rotation and therefore of the joint calculations (Fig 1).

When utilizing Inman's mean orientation, there are significant differences between the Heel axis location and the Ankle location seen in the peak STJ moment ($p<0.02$), peak ankle contact force ($p<0.01$), as well as the 2nd peak of the knee contact force ($p<0.05$). When compared to the *in vivo* loading (eTibia), the Heel location gives an RMS of 314.21 N and p^2 of .72. By changing the axis location of the Inman orientation to match the suggestions by the ISB, the differences are minimized. The Ankle axis location gives an RMS of 276.32 N and p^2 correlation of .79.

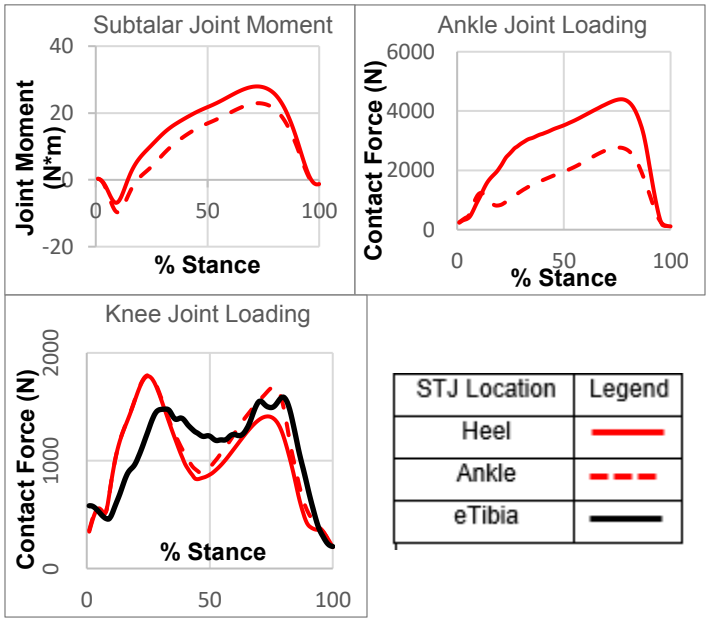

Significance

Subject-specificity is becoming increasingly more important in models, however unlike the attention that the knee and ankle receive, the subtalar joint is often under-appreciated. This work demonstrates that considerable attention needs to be placed on the location of the axes when using axes orientations that differ in inclination or deviation angles.

References

[1] Noginova, J. et al. ISB Conference. Calgary, AB, 2019.
[2] Noginova, J., et al. ASB Conference. Rochester, MN, 2018.
[3] Lai, A.K. et al. *Ann Biomed Eng*. 2017
[4] Wu et al. *J. Biomech.* 2002.
[5] Fregly et al. *J Orthop Res*. 2012
[6] Inman. The Joints of the Ankle. Williams & Wilkins, 1976.

Movement Variability during Dynamic Task in Individuals Suffering a Second ACL Injury

Jennifer Perry[1,2], Xenia Demenchuk[1], Mark Paterno[4], Robert Siston[1,2,3], and Laura Schmitt[2,3]
[1]Department of Mechanical and Aerospace Engineering, Ohio State University; [2]Sports Medicine Research Institute, Ohio State University; [3]School of Health and Rehabilitation Sciences, Ohio State University; [4]Division of Occupation Therapy and Physical Therapy, Cincinnati Children's Hospital
Email: perry.387@osu.edu

Introduction

Young, active individuals who undergo anterior cruciate ligament reconstruction (ACLR) after primary injury often experience suboptimal outcomes, including having a high risk of second ACL injury[1,2]. Atypical knee kinematics and kinetics observed in individuals after ACLR medical clearance to return to sport (RTS) have been related to suboptimal outcomes[2,3,4]. Since the lower extremity is a linked system, it may prove beneficial to look at the interactions between joints and their relative coordination in addition to single-joint biomechanics. Dynamic movement theory is one way to investigate the coordination between joints and proposes that there is a preferred range of coordination variability[4,5]. Abnormal coordination variability may be associated with suboptimal outcomes, but this is unknown. In young active individuals with ACLR, we hypothesized that 1) coordination variability at the time of RTS will be increased in those who subsequently sustained a second ACL injury compared to those without a second ACL injury and uninjured controls and 2) increased coordination variability will be associated with worse knee-related function at time of RTS.

Methods

A total of 116 young, active individuals cleared to RTS after ACLR were included as part of a secondary analysis of an on-going study, along with 55 healthy controls (Table 1). All participants, or parents/guardians, provided written informed consent. The ACLR group underwent data collection within 4 weeks of being medically cleared to RTS. The ACLR group was followed longitudinally in the study for at least 2 years after RTS. For this analysis, the ACLR group was subdivided based on occurrence of a second ACL injury (ipsilateral or contralateral) within 2 years of RTS. The ACLR group completed the International Knee Documentation Committee Subjective Knee Form (IKDC) to assess symptoms and function of the involved knee at RTS. Three-dimensional motion analysis was used to obtain lower extremity kinematics during a single leg landing task. Three trials were recorded for both limbs of each participant. The period from initial contact to lowest center of mass was examined. A vector coding technique was used to calculate coupling angles between two adjacent joints for each trial[4,5]. The overall root mean square of the resulting circular standard deviation between the three trials was computed to represent coordination variability in coupling angles during landing (Table 2). Kruskal-Wallis test was used to compare coordination variability and intra-participant limb difference of coordination variability between groups of healthy controls, ACLR with no second injury, and ACLR with second injury. Spearman's rho correlation coefficient was used to evaluate the association between IKDC scores and coordination variability at the time of RTS in the ACLR group.

	ACLR Without 2nd injury	ACLR with 2nd injury	Healthy Controls
Sex, M/F	34/55	5/22	15/40
Age, y	17.2±3.2	15.8±1.6	17.1±2.3
BMI	23.7±4.1	22.1±3.5	22.0±3.0
IKDC	87.8±11.4	90.9±7.3	-

Table 1: Group demographic data presented as mean ± STD.

Results and Discussion

In contrast to our hypothesis, we observed that those who had a second injury demonstrated lower variability of certain measures. There were no differences between groups in coordination variability on the involved limb. Those who sustained a second ACL injury demonstrated a significantly lower hip flexion-knee abduction (HF/KA) coordination variability on the uninvolved limb compared to both those without second injury and healthy controls (Table 2). HF/KA coordination variability can be interpreted as frontal plane knee control as the hip flexes during landing. Increased motion of the knee in the frontal plane has been shown to be a predictor of second ACL injuries[2]. ACLR participants without second injury showed a smaller difference in HF/KA coordination variability between limbs compared to both ACLR with second injury and healthy controls, with the uninvolved limb showing more variability than the involved limb. Since involved limb HF/KA coordination variability show no significant differences among the groups, the involved limb relative increase in variability compared to the uninvolved limb may be an important factor to look at when assessing risk of second ACL injury.

A lower score on the IKDC was correlated with higher involved limb HF/KA variability ($r = -0.23$, $p = 0.013$) in all ACLR participants at time of RTS. We previously reported that ACLR participants, regardless of second injury status, have higher HF/KA coordination variability on the involved limb, with both limbs showing greater variability that controls[5]. Increased variability of frontal plane knee coordination with hip flexion seen in ACLR participants may be contributing to self-reports of lower function and worse symptoms in the involved knee.

Coordination Variability	ACLR without 2nd injury	ACLR with 2nd injury	Healthy Controls	p-value
Uninvolved HF/KA	12.44 (17.2)	**7.44 (4.3)***	12.88 (11.6)	p = 0.001
Involved HF/KA	12.42 (15.0)	11.18 (11.4)	14.19 (22)	p = 0.053
ΔHF/KA	**-0.65 (16.6)***	4.15 (12.7)	3.29 (16.7)	p = 0.017

Table 2: Joint coordination variability results represented as median (IQR). P-value < 0.05* considered significant compared to other groups.

Significance

Of all the joint coupling angles we investigated, only HF/KA was associated with either second injury or knee-function. Clinicians should consider variability of dynamics task coordination during rehabilitation of young athletes after ACLR. Future work should consider how differences in coordination variability impact those who suffer an ipsilateral vs contralateral second injury.

Acknowledgments

This work was funded by the NIH grant F32-AR055844; the NFL Charities Medical Research Grants 2007, 2008, 2009, 2011.

References

1. Ardern et al. *BJSM*, 48(21), 1543–1552. **2.** Paterno et al. *AJSM*, 38(10) **3.** Schmitt et al. *MSSE.* 2015 Jul;47(7):1426-3 **4.** Davis et al. *Gait & Posture*, 67, 154–159, 2019. **5.** Demenchuk et al. *ASB*, 2020

THE RELATIONSHIP BETWEEN DYNAMIC POSTURAL INSTABILITY AND PHYSICAL ACTIVITY IN CHILDREN WITH CEREBRAL PALSY

Marley Castleberry[1], S. Wilhoite[1], K. Campbell[1], S. Thompson[1], T. Batson[1], L. Li[2], K. Newell[1], G. Colquitt[2], and C. Modlesky[1*]
[1]Department of Kinesiology, University of Georgia, Athens, GA
[2]Department of Kinesiology, Georgia Southern University, Statesboro, GA
Email: christopher.modlesky@uga.edu

Introduction

Cerebral palsy (CP) is a neurological condition caused by a brain lesion and is associated with musculoskeletal deficits. Postural instability is a typical impairment of children with CP and has negative implications on various functional movements.[1] Previous studies have suggested that static postural instability is negatively associated with functional activities that children perform during their daily routines. However, the relationship between dynamic postural control and physical activity (PA) has not yet been evaluated in children with CP[2]. Dynamic stability plays a vital role in maintaining balance during gait. However, it is unclear if instability within the gait cycle is linked to the low levels of PA in children with CP. Therefore, the purpose of this study was to assess dynamic instability between children with CP and typically developing children (TDC) and to determine if dynamic postural instability during gait is related to PA levels in children with CP. We hypothesized that children with CP have greater dynamic instability than TDC and that there is a negative relationship between the center of pressure (COP) variables (sway distance and velocity) and PA.

Methods

Eighteen ambulatory children with CP (8.8 ± 2.1 yrs, 130.3 ± 13.4 cm, 28.0 ± 6.0 kg), Gross Motor Function Classification Scale I – II, and 10 TDC (8.4 ± 2.0 yrs, 133.0 ± 12.8 cm, 31.7 ± 11.2 kg) were included in this study. Dynamic postural control was assessed using 4 force platforms (Bertec, 100 Hz; Columbus, OH) while participants completed 3 successful gait trials at a self-selected speed. A successful trial was considered when the foot landed completely on the surface of the force platform. Center of pressure measurements (sway velocity and distance) of each limb was calculated during the initial contact, midstance, and terminal stance phases of gait. Sway distance and velocity were calculated in the anterior-posterior (AP) and medial-lateral (ML) directions. Participants were instructed to wear two accelerometer-based PA monitors (Actigraph GT9X; Pensacola, FL) on the lateral aspect of the ankle on the more affected limb for children with CP and the non-dominant side for TDC. Monitors were worn for 3 weekdays and 1 weekend day, and total PA counts/day were averaged from the 2 monitors reported. Independent t-tests assessed group differences between PA counts and dynamic postural control measurements. Spearman rho correlations (r_s) assessed the relationship between postural control measurements and PA counts.

Results

Compared to TDC, children with CP had lower PA counts (p = 0.014). Additionally, children with CP exhibited greater sway distance in the ML direction during terminal stance (p = 0.031) and and a trend for greater sway distance during midstance (p = 0.057) than TDC. For children with CP, there was a negative correlation between PA counts and AP sway velocity on the more and less affected limbs during midstance (r_s = -0.53, p = 0.03; r_s = -0.59, p = 0.01; respectively) and on the less affected limb during terminal stance (r_s = -0.50, p = 0.04).

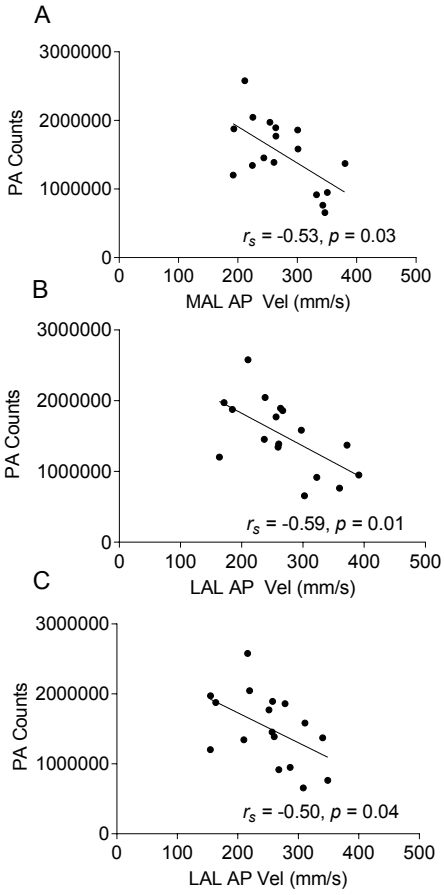

Figure 1. Significant relationships between PA and AP velocity (Vel) in the more (MAL) and less (LAL) affected limbs in children with CP. (A and B = midstance, C = terminal stance).

Significance

Children with CP are at a higher risk for falls. Dynamic instability presented during the midstance and terminal stance may increase this risk. Improvements in dynamic postural control may reduce this risk and improve overall levels of PA.

Acknowledgments

This research study was funded by the National Institutes of Health (HD090126).

References

1. Schless et al. (2019). *Gait & posture*, *68*, 531-537.
2. Pavão et al. (2014) *Braz J Phys Ther*, *18*(4), 300-307.

INDIVIDUALS WITH SYNDESMOTIC ANKLE SPRAINS MOVE DIFFERENTLY THAN MATCHED HEALTHY CONTROLS

Rachel L. Tatarski[1-2], L. Boucher[2], K. Evans[2], X. Pan[2], T. Miller[2], and S. Di Stasi[2]
[1]The University of Tennessee, Knoxville, [2]The Ohio State University
Email: rtatarsk@utk.edu

Introduction

In vivo biomechanics of the distal tibiofibular joint after a syndesmotic ankle sprain (SAS) are poorly understood but are critical to improving the recovery process and for making return-to-participation decisions. Even seemingly minor disruptions to the integrity of the joint may have substantial functional consequences. Given that the anterior tibiofibular ligament contributes the most to the stability of the distal tibiofibular joint,[1] its disruption during SAS may lead to mechanical instability of the joint and reduced function and quality of life. Thus, we hypothesized that participants with SAS would walk more slowly than the matched healthy control subjects, take shorter step lengths, and move with reduced ankle range of motion and reduced maximum external dorsiflexion moment during functional tasks.

Methods

14 patients with SAS (<1 year from injury) and 14 matched individuals without SAS (healthy control: HC), based on sex and activity level, aged 14-30 gave written informed consent and participated in this study (64% female).

Participants were outfitted with 87 retroreflective markers. Marker trajectories (240Hz) were measured with 12 motion analysis cameras and ground reaction forces were measured with 4 embedded force platforms (1200Hz). Participants performed three tasks during analysis: overground walking at a self-selected speed, single-leg anterior reach (SLAR) , and a double-leg deep squat (DLDS). Three successful trials of each task were collected. Primary variables of interest included sagittal plane ankle range of motion, the maximum external dorsiflexion moment, self-selected gait speed (gait), step length (gait), anterior reach distance (SLAR), and squat depth (DLDS).

Generalized estimating equations were used to test for group-by-limb interactions for each variable of interest for the three tasks ($\alpha = 0.05$). When group-by-limb interactions were significant, post-hoc paired and independent t-tests were used to evaluate limb and group differences. Main effects were used to evaluate limb or group differences.

Results and Discussion

Contrary to our hypothesis, there were no group differences in gait speed or step length. Even so, the participants with SAS walked with reduced ankle excursion (Fig. 1A) and reduced maximum external dorsiflexion moment (Fig. 1B) on the involved limb compared to the HC group. Importantly, participants with SAS demonstrated bilateral differences in ankle excursion. These differences may be compensatory mechanisms to increase stability of the ankle. This finding is similar to the way individuals with an acute lateral ankle sprain walk.[2]

During the SLAR, we found a group-by-limb interaction for ankle excursion (Fig. 1C), but no group or limb differences for maximum external dorsiflexion moment. The participants with SAS were likely hesitant to put the ankle into the extreme ranges of motion required for peak reaching performance. While there is a moderate correlation between ankle range of motion and reach performance, there is little consensus as to the discriminatory ability of the SLAR. As such, its clinical utility as a measure of functional performance in SAS is unknown.

For the DLDS, the SAS group squatted with less depth than the HC group and had reduced bilateral ankle excursion (Fig. 1D), even after accounting for squat depth. We suspected the SAS participants would offload the involved limb as is common in bilateral tasks like the DLDS, but there was not an effect of limb.

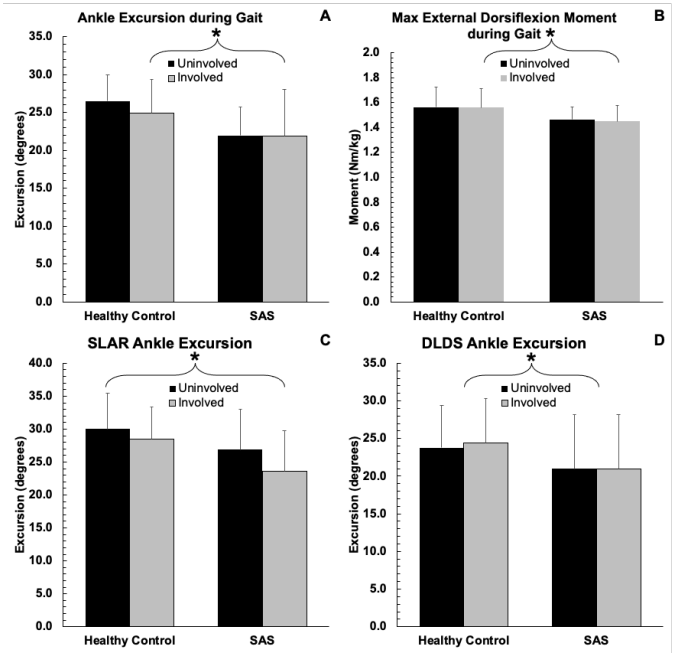

Figure 1: *An asterisk indicates a significant post-hoc test for limb or group.*

Significance

In summary, participants with SAS move differently than HC, even when they are relatively far along in the recovery process. Importantly, many of these differences persisted even when accounting for other factors like gait speed, reach distance, and squat depth. Biomechanical assessment of functional tasks should be considered when evaluating patient recovery and making return to participation decisions.

Acknowledgements

The authors would like to thank the American Society of Biomechanics for the Grant-in-Aid Award and the Alumni Grant for Graduate Research and Scholarship award from The Ohio State University.

References

1. Ogilvie-Harris D, et al. *Arthrosc J Arthoroscipic Relat Surg*. 1994;10(5):561-568.
2. Doherty C, et al. *J Electromyogr Kinesiol*. 2015;25(1):182-192.
3. Basnett CR, et al. *Int J Sports Phys Ther*. 2013;8(2):121-128.

FASTPITCH SOFTBALL BIOMECHANICS: STRIDE CHARACTERISTIC ALTERATIONS WHEN THROWING MOVEMENT PITCH TYPES

Jessica Gilliam[1] and Ajit Chaudhari[1]
[1]The Ohio State University
email: gilliam.159@osu.edu

Introduction

Softball pitching has several different pitch types including the fastball, rise, drop (DP), screw, and curve (CV) (Fig. 1). Like the fastball, the latter four pitches maintain the basic pitching blueprint with most of the bodily adjustments made at stride foot contact (SFC) and ball release (BR). The four movement pitch types are known conventionally to be more difficult to perform than the fastball [1]. Two of the most common movement pitch types thrown are the CV and DP. The CV is thrown by the pitcher's fingers snapping the ball at release, causing the ball to rotate in a corkscrew motion [1]. The pitching arm follows through across the body to the contralateral hip. The "Peel" drop is thrown by the hand and fingers pulling posteriorly and superiorly on the ball at the release point, creating a topspin motion on the ball[1]. Previous research has examined forces and torques on the throwing shoulder [2,3] as well as characteristics of the stride [3,4]. Due to the nature of the release, a conventional belief among coaches is that movement pitch types are associated with more stress on the throwing arm, but there is no scientific data to support that belief.

The purpose of this study was to identify if alterations to the pitching stride in the CV and DP pitches, relative to the fastball pitch, would be associated with greater forces and torques seen at the throwing shoulder.

Methods

Thirty-five female athletes (mean age, 14.7±1.6, mean height, 1.7±.07, mean mass, 67.8±14, dominant hand R/L, 30/5) participated after providing IRB-approved informed consent. Participants pitched while instrumented with reflective markers from a regulation softball pitching mound with embedded force plates (Fig. 1). Three-dimensional marker locations were recorded at 300 Hz and synchronized ground reaction forces collected at 1500 Hz (10 ViconMXF40 cameras, 4 Bertec4060 Force Plates). All analyses were conducted in Visual3D software.

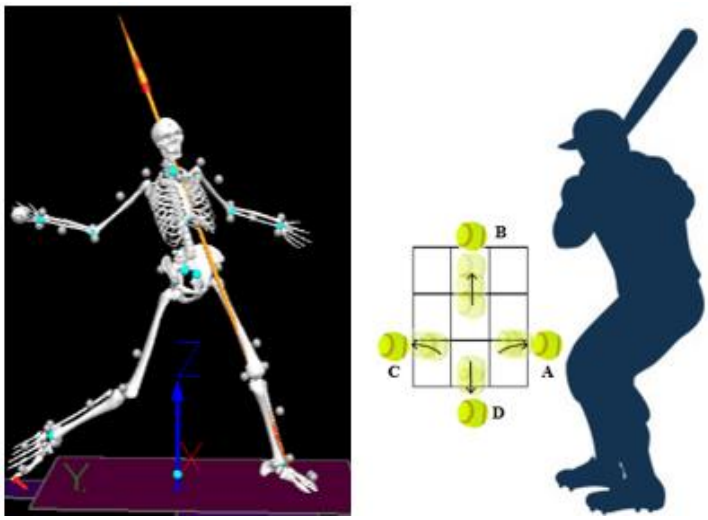

Figure 1: V3D model (left) and movement pitch types (right). The four main pitch types include Screw (A), Rise (B), Curve (C), and Drop (D). Displayed here as if pitching to a right-handed batter.

A Shapiro-Wilk normality test was conducted on each parameter of interest to determine data normality. Due to nonparametric data, Wilcoxon Rank Sums tests were conducted to compare parameters between pitch types. The significance level for all tests was set a priori ($\alpha<.05$). Due to the exploratory nature of this study, we did not apply any corrections for multiple comparisons.

Results and Discussion

At SFC, both superior ground reaction force (GRF) ($p=.007$) and stride foot angle ($p=.030$) differed between CV and fastball, but no other stride characteristics were different between CV vs fastball or DP vs fastball. The overall lack of differences between stride characteristics is consistent with the pitcher's goal of disguising alternating pitch types. This allows the pitcher to use deception as an added weapon during pitch delivery.

Changes to several shoulder joint reaction forces and moments occurred during ball release (BR) (all $p<.05$). As an example, Fig. 2 shows the medial shoulder joint reaction forces for fastball and CV ($p=.013$), and posterior shoulder joint reaction forces for fastball and DP ($p=.014$). In this population of youth softball pitchers, throwing the fastball led to higher shoulder forces and moments than either the CV or DP.

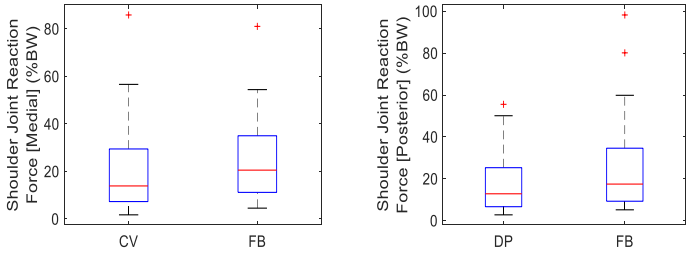

Figure 2: Medial shoulder joint reaction force [FB v. CV] (left) Posterior shoulder joint reaction force [FB v. DP] (right).

Significance

Across this group of female youth softball pitchers, there were no biomechanical reasons for concern of increased injury risk when throwing the CV or DP pitch types.

References

[1] Kingsbury, D. (2014) *Essential softball pitching grips [eBook].* 35pp.
[2] Barrentine, SW., et al. (1998) *J Orthop Sports Phys Ther* 28:405-414
[3] Werner, SL., et al. (2006) *Am J Sports Med* 34:597-603
[4] Oliver, GD., et al. (2011) *J Sports Sci* 29:1071-1077

DO THE EFFECTS OF COGNITIVE TASKS ON LANDING MECHANICS DEPEND ON JUMP DIRECTION?

Fatemeh Aflatounian, Patrick D. Fischer, and Scott M. Monfort*
Department of Mechanical and Industrial Engineering, Montana State University, Bozeman, Montana, USA
email: * scott.monfort@montana.edu

Introduction

Anterior cruciate ligament (ACL) injuries remain a major burden to athletes. Recent research supports the value of considering cognitive-motor function as a relevant factor for ACL injury risk, as athletes are often diverting attention and/or reacting to external information when ACL injuries occur [1]. Furthermore, cognitive function has been associated with ACL injury risk [2], and the additional of simultaneous cognitive tasks can influence knee mechanics associated with ACL injury risk [3,4]. While the relevance of cognitive-motor function for understanding ACL injury risk has been proposed, research linking simultaneous cognitive tasks to deleterious changes in knee mechanics have not determined whether jump-landing movement direction interacts with the effects of cognitive tasks. Therefore, the extent to which cognitive-motor function may differ across movement characteristics remains unknown. The purpose of this study was to determine how the effects of simultaneous cognitive challenges during a jump-land-jump movement differ based on the direction of a secondary jump. We hypothesized that knee mechanics during a jump-land-jump task would be similar regardless of the secondary jump direction.

Methods

Thirty-nine healthy, female, young adult, recreational athletes (20.2±2.6 years; 1.69±0.08 m; 64.6±7.9 kg; 9 basketball/30 soccer) participated in this study. All participants were right-limb dominant (preferred limb to kick ball farthest). Participants completed a jump-land-jump movement [4] that involved jumping off a 30-cm box over a distance of half the participants' height. Upon landing from the initial jump, participants immediately jumped as high as they could in one of three secondary jump directions: forward and to the left, forward and right, or straight up. This task was completed under five conditions. Baseline (**BL**) – anticipated secondary direction, no cognitive task. Working Memory (**WM**) – anticipated secondary direction, simultaneous working memory task. The working memory task involved remembering the locations of six letters arranged in a circular array (shown for 1 sec before jump started), with one random letter chosen to recall after completing the jump task was completed. Unanticipated (**UA**) – secondary jump direction was presented ~250 msec prior to initial contact using an arrow cue. Visually-constrained Working Memory (**VWM**) – same as **WM**, but the probe letter was presented ~250 msec prior to initial contact. Unanticipated Visually-constrained Working Memory (**UVWM**): - combination of **UA** and **VWM**.

Dependent variables were peak values of knee flexion angle (pKFA), knee abduction angle (pKAbA), and external knee abduction moment (pKAbM) for the dominant (right) limb from the first 50msec following initial contact from the initial jump due to ACL injuries commonly observed in this timeframe [1].

For each dependent variable, mixed effects models were used to test for an interaction between jump condition and secondary jump direction. Models included a random factor of 'Participant' and fixed effects of 'Condition', 'Direction', and 'Condition*Direction'.

Results and Discussion

The effect of cognitive load on landing mechanics interacted with secondary jump direction for pKFA ($p<0.001$), but not for pKAbA ($p=0.71$) or pKAbM ($p=0.25$). Post-hoc analysis identified that the unanticipated conditions had a greater impact on decreasing pKFA for the right jump direction (ipsilateral to dominant limb) compared to neutral or contralateral directions (**Figure 1**). Jump direction was a significant factor for all dependent variables (all $p < 0.001$). The Condition fixed factor was significant for pKFA ($p <0.001$), but not for pKAbA ($p=0.16$) or pKAbM ($p=0.36$).

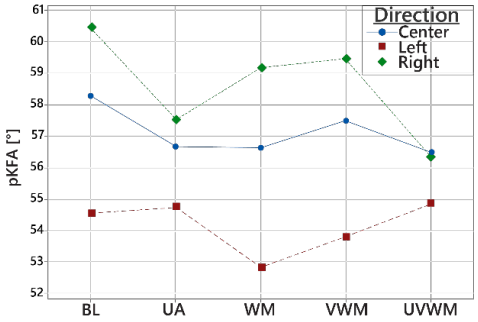

Figure 1: Condition*Direction interaction plot for pKFA.

The interaction between jump condition and secondary jump direction suggests that, while the anticipated conditions tended to be associated with greater knee flexion angle, larger decreases in knee flexion during unanticipated conditions were seen when jumping to the same side as the dominant limb. Therefore, secondary jump landing direction consideration is warranted when knee flexion angle is a variable of interest in cognitive-motor research.

Significance

Athletic performance often requires dynamic, multiplanar movements. Jump landings are used as a surrogate movement to gain insight into biomechanics used during these athletic tasks, but jump landing analyses are often restricted to jumping tasks that occur in the sagittal plane. The results of this study suggest analyses into cognitive-motor function during bilateral jump landings should keep in mind the potential interacting effects of secondary jump direction on sagittal plane kinematics.

Acknowledgments

This material is based upon work supported by the NSF Graduate Research Fellowship under Grant No. W7834.

References

[1] Krosshaug et. al. (2007) Am J Sports Med, 35(3):359-67
[2] Swanik et. al. (2018), Am J Sports Med, 35(6): 943-83
[3] Monfort et. al. (2019), Am J Sports Med, 47(6):1488–1495
[4] Herman DC et. al. (2016) Am J Sports Med, 44(9):2347-53

TRUNK CONTROL IN YOUNG HEALTHY ADULTS REQUIRES LARGE ADAPTATIONS DURING AND AFTER OBSTACLE AVOIDANCE WITH A COGNITIVE TASK

Masood Nevisipour[1], Thomas Sugar[1], Hyunglae Lee[2]
[1] The polytechnic school, Arizona State University, Mesa, AZ, USA
[2] School for Engineering of Matter, Transport, and Energy, Arizona State University, Tempe, AZ, USA
Email: mnevisip@asu.edu

Introduction

Older adults have shown diminished trunk control which is correlated to their high risk of falling [1]. When facing an obstacle, it is important to safely avoid the obstacle and not get tripped. While controlling trunk movements is critical for fall prevention [1], there is a lack of knowledge about trunk biomechanics during obstacle avoidance. Further, cognitive tasks have shown to negatively interfere with obstacle avoidance which increases risk of falling [2]. Our objective was to evaluate whole-body kinematics and kinetics during obstacle avoidance in the presence of a cognitive task to investigate how trunk control is affected compared to other joints. We studied young healthy adults to provide a baseline for future studies in older adults. We hypothesized that trunk would have the largest increase in peak flexion as well as peak extension torque during obstacle avoidance and a cognitive task would further increase those measures.

Methods

Ten young healthy adults walked for 2 mins at 1 m/s on a split-belt treadmill while fitted in a harness. A lightweight obstacle was released at the front of the treadmill at a random right heel strike moment 5 times during walking. The obstacle was wide and the subject was required to step over it with the lead leg – which was the right side for all the subjects – and then clear it with the trail leg (the left side). The same task was repeated while the subject was doing a cognitive task. Trunk, pelvis, hip, knee, and ankle angles and torques were calculated in the sagittal plane. A linear mixed effects model with the aforementioned variables as dependent variables and independent variable of condition was used. Conditions were: 1) walk (W), 2) walk with a cognitive task (WCT), 3) obstacle avoidance (OA), and 4) obstacle avoidance with a cognitive task (OACT). To evaluate the post-effects of obstacle avoidance, the absolute difference (GAP) between the start and end (0% vs. 100% of gait cycle) of each angle variable was calculated in the first gait cycle after completely passing the obstacle. This measure was normalized to the angular range of motion of the joint during walking.

Results and Discussion

During OA, trunk had the largest % increase (normalized to the variable range during walking) in peak flexion angle (163.0%) and peak extension torque (137.1%) compared to other joints adaptations (Table 1). These results show that during OA, trunk requires the largest adaptations in flexion as well as an additional large extension torque to retain its stability. These results raise concern for older adults who might have weakness and reduced control over trunk movements.

The cognitive task led to a larger increase in peak trunk flexion angle and extension torque. In OACT, peak trunk flexion angle was increased by 199.1%. Peak trunk extension torque was increased by 211.2% to compensate for this. Also, peak trunk flexion angle and extension torque were increased by 40.1% and 45.2% in WCT compared to W, respectively. These results suggest that trunk control is sensitive to and gets negatively impacted by a cognitive task. Subjects walk with a more flexed trunk doing the cognitive task which may put them at a higher risk of falling in case of obstacle contact. These results support our hypothesis and raise concern for older adults as their balance and walking have been shown to be more negatively impacted by a cognitive task [3].

Even after fully crossing the obstacle, the trunk was still adapting to return to its normal range of motion. The trunk flexion GAP in the first gait cycle after OA was 9.6% larger compared to W. While lead leg ankle had a 1.9% increase in GAP, hip and knee joints did not show any differences. Therefore, trunk and ankle appear to take longer returning to their normal range of motion. Older adults may need even more gait cycles to fully retain their normal trunk kinematics after obstacle avoidance.

In summary, during obstacle avoidance, trunk appears to require the largest adaptations which are associated with significantly larger extension torques. A cognitive task negatively affects trunk control. Lastly, trunk shows the largest post-effect adaptations that shows the trunk may need a longer time to stabilize after it is perturbed.

Significance

Our study provides a baseline for future studies in older adults and suggests that clinicians, researchers, and assistive device engineers should pay more attention to the trunk stabilization in challenging balance tasks. Further, it is very important to consider cognitive tasks when designing trunk training programs as well as wearable assistive devices as they might significantly affect the trunk control.

Acknowledgments

The authors gratefully acknowledge support of this work through a grant by "*The Global KAITEKI Center*" (TGKC) of the Global Futures Laboratory at Arizona State University.

References

[1] Grabiner, M. et al. *J of Electromyography and Kinesiology*; 18(2):197-204, 2008.
[2] Weerdesteyn, V. et al. *J of Motor Behavior*; 35(1):53-63, 2003.
[3] Beurskens, R. & Buck, O. Neural Plasticity; 131608, 2012.

Table 1. Whole-body kinematic and kinetic analysis during lead leg obstacle avoidance. (: p<0.05, ***: p<0.0001)*

Variables	W	WCT	OA	OACT	W-WCT	W-OA	OA-OACT	W-OACT
Peak R-Hip flexion (deg)	26.2 (1.3)	25.5 (1.3)	48.1 (1.7)	50.4 (1.6)	***	***		***
Peak R-Knee flexion(deg)	70.0 (1.7)	69.4 (1.7)	87.4 (2.0)	90.2 (2.0)	***	***		***
Peak R-Ankle dorsiflexion (deg)	-3.8 (0.4)	-3.7 (0.4)	-11.7 (0.9)	-12.5 (0.9)		***		***
Peak Trunk flexion (deg)	9.4 (1.0)	10.4 (1.0)	13.1 (1.1)	14.0 (1.1)	***	***	*	***
Peak Trunk extension torque (Nm/kg)	-0.16 (0.03)	-0.18 (0.03)	-0.24 (0.03)	-0.29 (0.04)	***	***	*	***

Design Optimization of a Shoulder-Assistive Device for Activities of Daily Living

Kaleb Burch[1], Jill Higginson[1]
[1]Department of Mechanical Engineering, University of Delaware, Newark, DE 19711
email: kburch@udel.edu

Introduction

Robotic exoskeletons are a proven rehabilitative tool that can improve upper extremity (UE) function in individuals who have had a stroke [1]. However, in order to assist activities of daily living (ADLs), an assistive device must be *wearable* and *portable*. Meeting wearability needs such as user comfort, low device mass, and low device profile is not a simple task, particularly when balanced with supplying sufficient moments about multiple degrees of freedom (DOF). Prior studies on UE assistive devices have sought to prevent singularities and misalignments, which improves comfort and range of motion [2]. Others have used musculoskeletal simulations to design passive devices to reduce muscle activations [3]. We propose a novel approach to design optimization for cable-driven assistive devices by representing wearability constraints in an inverse dynamics-based optimization.

Methods

In this study, we used the MATLAB *fmincon* function to optimize three-dimensional attachment locations at each end of a cable-driven actuator to minimize mean human-supplied biological joint moment ($\overrightarrow{M_{bio}}$) at the shoulder for abduction [4] and a forward reach motion [5]. First, the MoBL-Arms musculoskeletal model [5] in OpenSim [6] was used to compute shoulder joint moments ($\overrightarrow{M_{total}}$) via inverse dynamics. Then, the proximal attachment $\overrightarrow{r_p} = (x_p, y_p, z_p)$ fixed to the torso and distal attachment $\overrightarrow{r_d} = (x_d, y_d, z_d)$ fixed to the upper arm were generated (Fig. 1). Attachment locations were tracked using forward kinematics, cable moment arms ($\overrightarrow{r_c}$) were computed, and cable force ($\overrightarrow{F_c}$) was computed at each time point such that resultant biological moment, $\|\overrightarrow{M_{bio}}\| = \|\overrightarrow{M_{total}} - \overrightarrow{r_c} \times \overrightarrow{F_c}\|$, was minimized. Cable force was constrained to lie between 0 and 448 N (100lbs). Attachment locations were constrained to feasible and practical spaces around the body: $\overrightarrow{r_p}$ was confined to lie between spheres of radii 5 cm and 7 cm centred about the shoulder joint and $\overrightarrow{r_d}$ was confined to lie within cylinders that extended over the length of the humerus and had radii of 5 cm and 7 cm.

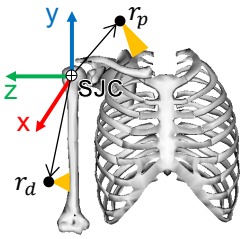

Figure 1. Direction conventions, neutral shoulder joint center (SJC) position, and attachment points.

Results and Discussion

Our optimization obtained reductions in mean biological joint moments of 69.8% for abduction and 31.1% for reaching; this is comparable to a prior UE assistive device simulation that obtained between 28% for abduction to 90˚ and 62% for an upward reach [3]. Maximum cable forces were 240.4 N during abduction and 349.6 N during reaching. For the abduction motion, attachment locations were identified at $\overrightarrow{r_p} = (0.96, 7.00, 3.46)$ and $\overrightarrow{r_d} = (0.86, -29.66, 4.64)$; units in centimeters. For the reaching motion, attachments were located at $\overrightarrow{r_p} = (7.00, 4.96, 2.74)$ and $\overrightarrow{r_d} = (5.78, -5.22, 0.34)$.

For both conditions, the optimal attachments tended to produce the largest moments about the shoulder elevation DOF, which had the largest mean moment (Fig. 2). Cable moments also offered some assistance about the elevation angle DOF in both motions. However, cable moments tended to increase the required biological moment about the shoulder rotation DOF.

This study showed that assistive devices can be designed to reduce joint moments during ADLs with a simple inverse dynamics-based optimization. Furthermore, moment reductions were accomplished while meeting wearability restrictions such as a low-profile design and low forces exerted on the user's body.

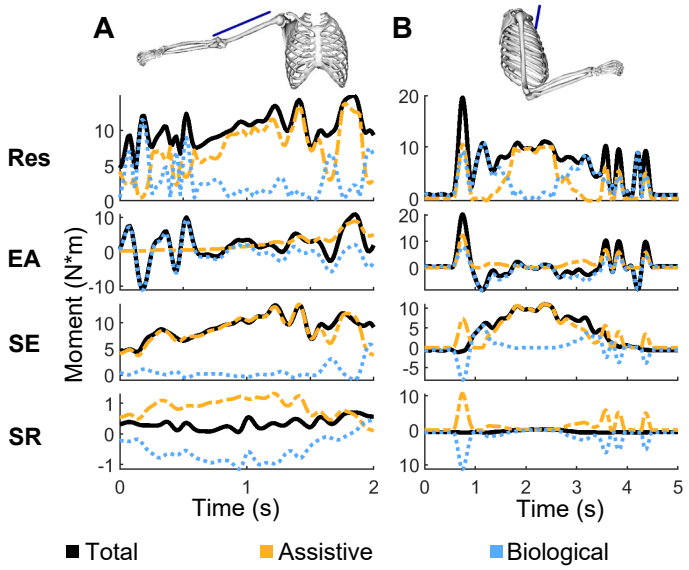

Figure 2. Total, biological, and assistive moments about each shoulder DOF and the resultant moment for (A) abduction up to 113º and (B) a forward reach. Elevation angle (EA), shoulder elevation (SE), shoulder rotation (SR), and resultant (Res) moments are shown.

Significance

This study demonstrated a simple approach for optimizing a shoulder-assistive device based on functional and practical criteria. Future work could be done to assess this approach for assisting specific impairments, to explore more design options, and to evaluate the effect of assistive moments on muscle function.

Acknowledgments

UNIDEL Foundation, Inc.

References

[1] Maciejasz et al. (2014) *J Neuroeng & Rehab,* **11**. [2] Schiele et al. (2006) *IEEE Trans on Neur Sys & Rehab Eng,* **14:** 456-469. [3] Nelson et al. (2020) *J Appl Biomech,* **36**: 59-67. [4] Richardson et al. (2017) *J Appl Biomech,* **33**: 469–473. [5] Saul et al. (2015) *Comp Methods in Biomech & Biomed Eng*, **18**: 1445-1458. [6] Delp et al. (2007) *IEEE Trans on Biomed Eng,* **54**: 1940-1950.

ARE LABORATORY-BASED OBSTACLE CROSSING MECHANICS APPLICABLE TO THE REAL WORLD?

Grace K. Kellaher[1], K. Balthaser[1], M. Jessell[1], F. Wade[1], A.C. Schmitt[2], and C.J. Hass[1]
[1]Department of Applied Physiology & Kinesiology, University of Florida, Gainesville, FL
[2]Department of Health, Human Performance, and Recreation, University of Arkansas, Fayetteville, AR
email: gkellaher@ufl.edu

Introduction

Successfully adapting walking to cross an obstacle is necessary to safely navigate everyday life (1-3). Typically, walking adaptability is studied in the controlled laboratory environment, and those findings are generalized to real-world mobility ability (4). Evaluations of obstacle crossing tasks conducted in laboratories are often used as a proxy to understand the walking characteristics that could lead to trips. However, it remains unknown whether laboratory-based mechanics of obstacle crossing mimic the mechanics of obstacle crossing in the natural environment. Thus, the purpose of this study was to compare gait parameters while crossing a variety obstacles outdoors to walking while crossing similar obstacles in a controlled laboratory environment.

Methods

Six healthy young adult women (22±2 yrs) provided informed written consent prior to participating. Participants performed four tasks: 1) unobstructed overground walking, 2) walking while crossing over a 10 cm dowel-rod obstacle, 3) walking while crossing over a 15 cm long x 31.5 cm wide x 10 cm tall foam block obstacle, and 4) walking and stepping up onto a standard height curb, in the laboratory and outdoors. Wireless sensors (APDM System) were placed on the top of each foot, and on the lower back over the lumbar spine to track motion. Spatiotemporal measures were calculated across the entire 6 m walking course. Planned comparison paired t-tests were run comparing mean gait speed, stride length variability (standard deviation) and single support variability. Comparisons included 1) indoor vs outdoor for each obstacle crossing task, 2) indoor and (3) outdoor overground walking vs each obstacle crossing task, and 4) indoor dowel obstacle crossing vs outdoor walking while stepping up onto a curb. Outcome measures reported were averaged across the entire walking trial for each task. After correcting for multiple comparisons significance was set at the level of $\alpha = .0167$.

Results and Discussion

When comparing indoor overground walking to each indoor obstacle crossing task, we found that variability of single support percent was significantly higher (all $p < .0167$) when obstacle crossing. When crossing obstacles outside, compared with outdoor unobstructed walking, single support variability was increased by up to 1.5% (all $p < 0.007$). Interestingly, when crossing manufactured obstacles outdoors (dowel and foam) gait speed was reduced by at least 0.12 m/s (all $p < 0.06$), but this was not the case when crossing a real-world obstacle (curb, $p > 0.0167$). Finally we found when crossing an outdoor curb, gait speed significantly increased by .17 m/s ($p = .004$) and single support percent variability significantly decreased by .72% ($p = .01$) when compared to the indoor dowel rod obstacle, often used to simulate the outdoor curb. Variability of stride length was not significantly different, regardless of the comparison being made ($p > .0167$). There were no significant differences in mean gait speed, variability of stride length, or variability of single support percent when comparing any indoor obstacle crossing task to its outdoor counterpart (all $p > .0167$).

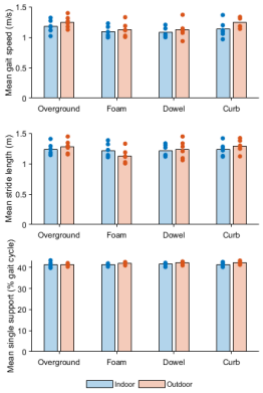

Figure 1. Mean gait speed, stride length, and single support % during each walking task. Individual mean values for gait speed, stride length, and single support %, are overlaid on their respective bar graphs.

When comparing task performance in an indoor setting versus an outdoor setting, spatiotemporal parameters did not differ (Figure 1). Despite our small sample size restricting our statistical power, we found that single support percent variability is affected by the presence of an obstacle, regardless of the environment the obstacle is encountered in. We also found mean gait speed is only impacted by manufactured obstacles (e.g. foam block, dowel rod) encountered in an outdoor environment, but not the real world (e.g. outdoor curb) obstacle, highlighted by comparing the indoor dowel obstacle and outdoor curb conditions, where both gait speed and single support variability were significantly different.. Our finding that gait speed does not change from overground walking to stepping onto a curb is different from a previous study, which has shown that when anticipating a raised surface, healthy young adults decrease both their speed and step length (1). We did not find any significant differences in stride length when comparing overground walking to any obstacle crossing task, regardless or environment, which is not consistent with previous obstacle crossing studies (2, 4) reporting gait speed decreases and step length increases during obstacle crossing compared to overground walking.

Significance

Overall, our results demonstrate that young adults adapted their mechanics for the type of obstacle and the environment the task is presented in. Further research in this area will allow us to understand the ecological validity of previous obstacle crossing research and improve our ability to identify behaviors that are at a greater risk for suffering a fall.

References

1. Laessoe et al. 2013. Aging Clin Exp Res. (25), 299–304.
2. Lowrey et al. 2007.Exp Brain Res. (182), 289–299.
3. Raffegeau et al. 2019 Exp Geron. (122), 60–66.
4. Galna et al. 2009. Gait & Posture. (30), 270–275.

LOWER BODY JOINT MOMENTS REDUCED WHILE WALKING WITH POSTERIOR WALKER

Evan A. Dooley[1] and Shawn D. Russell[1, 2]
[1]University of Virginia, Motion Analysis & Motor Performance Laboratory, Charlottesville, VA, USA
e-mail: dooley@virginia.edu

Introduction

Posterior walkers are prescribed to approximately 25% of children with cerebral palsy (CP), or 41,000 school-aged children in the United States (US CDC & NCES). Despite high usage, joint kinetics of patients using posterior walkers has not yet been investigated. This is challenging because we need to instrument the walker to collect the forces applied to the hands. Additionally, we need to create a model that allows these forces to be applied to the human. Understanding the reaction of the human to the device will allow devices to be designed that provide the best possible aid to the user. The aim of this work is to show the kinetic differences of the lower body between walking with and without a posterior walker.

Methods

A typical posterior walker (Nurmi Neo, Ottobock) was instrumented at both handles with a 6 DoF load cell (ATI) to capture the forces (1000 Hz) applied through the handles of the walker. 3 CP (14.7 ± 2.3 y.o.; 2F) and 3 typically developed (TD) (15.3 ± 7.2 y.o.; 1F) users walked with and without this instrumented walker, at their self-selected comfortable walking speed along a straight, level path. Walking kinematics were captured using a 12 camera motion capture system (Vicon) and ground reaction forces were captured by 5 in-ground force plates (Bertec). Joint kinetics were calculated in OpenSim using a subject-specific full-body model [2] with the addition of a novel posterior walker model to add forces at the hands (***Figure 1***). Joint kinetics were then normalized by body mass, filtered at 10 Hz, and splined to the gait cycle for comparison.

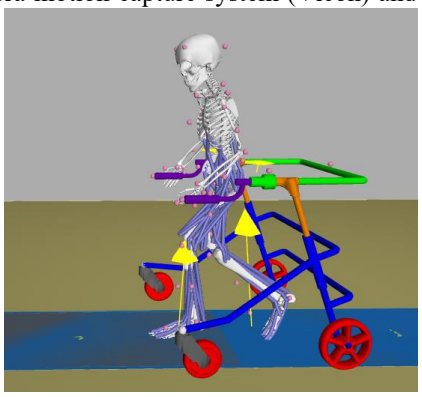

Figure 1. OpenSim model used in this study. Shown scaled to one CP subject. Ground and walker handle reaction forces shown in with yellow arrows.

Results and Discussion

For both the CP and TD users, walking with the posterior walker reduced the peak lower body sagittal joint moments of the user (***Table 1***). The largest reduction in the TD group was seen at peak in knee extension moment during early stance (50%), while the largest reduction in the CP group was seen at the peak knee extension moment during late stance (30%).

This joint moment reduction shows that walking with a posterior walker is not only useful for improving stability of the user but also for decreasing the loading of the lower body joints.

Future work is needed to investigate how much of this joint moment reduction is due to the user loading the walker to relieve weight from the lower body, and how much is due to the change in posture of the users while walking with and without the posterior walker. As the user loads the walker to relieve the lower body, the joint moments of the upper body increase. This increase in joint work, as well as the cost of pulling the walker along with the user will affect the efficiency of the human walking with the walker. These efficiency effects of walking with a walker is another direction for future work, as the CP population already has been shown to do 59% more work per unit mass on average than a TD group [3]. It is critical to account for the effort change, while providing stability to the user as we want to provide benefit, without increasing difficulty.

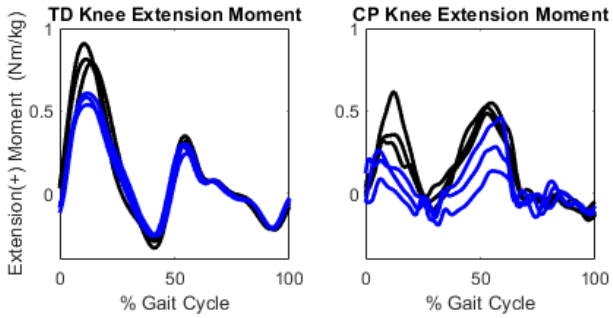

Figure 2. Representative knee moments from a TD (left) and CP subject (right). **Black** are without walker. **Blue** are trials using walker.

Significance

This work shows that walking with a posterior walker reduces the peak moments generated by the lower body during walking. This illuminates how using a posterior walker is not only beneficial for increasing the stability of the user, but also beneficial for any population with weakness in the lower body that may make unassisted walking more difficult (such as aging, CP, myelopathy). This suggests that posterior walkers could be useful to populations that may or may not have stability deficits to help them walk farther and longer.

Acknowledgments

This work was funded in part by a NIH Phase 1 SBIR.

References

[1] Park ES et al. (2001). *Yonsei Med. J.*, **42**: 180-184.
[2] Hamner SR et al. (2010). *J. Biomech*, **43**: 2709-2716.
[3] Russell SD et al. (2011). *J. Biomech*, **27**: 99-10

Table 1. Peak sagittal joint moments (Nm/kg) over the gait cycle for cerebral palsy (CP) and typically developed (TD) groups.

Peak Joint Moment Nm/kg (st.dev.)		**Hip Extension**	**Knee Extension Early Stance**	**Knee Extension Late Stance**	**Ankle Plantarflexion**
TD	Without	0.708 (0.039)	0.710 (0.080)	0.338 (0.108)	1.411 (0.150)
	With	0.579 (0.034)	0.352 (0.320)	0.248 (0.098)	1.289 (0.177)
CP	Without	0.490 (0.100)	0.444 (0.411)	0.716 (0.410)	1.241 (0.128)
	With	0.379 (0.096)	0.332 (0.288)	0.500 (0.366)	1.103 (0.105)

ANALYSIS OF NORMALIZATION TECHNIQUES: SURFACE ELECTROMYOGRAPHY SIGNALS FROM A CUTTING TASK OF A HAMSTRING STRENGTH TRAINING PROGRAM

Nathan Q. Holland[1], Z. Sievert[1], H. Bennett[1], and S. Ringleb[1]
[1]Old Dominion University, Norfolk, VA, USA
email: *nholland@odu.edu

Introduction

Hamstring muscle complex (HMC) injuries occur frequently in athletes who participate in professional and recreational sports like football and soccer [1]. For example, as of 2017, 12% of all injuries in British soccer were attributed to acute hamstring strains. For American National Football League sponsored training camps from 1998-2007, 2.2 hamstring injuries were sustained per 1000 athletes. Reinjury is just as elevated with a 1:3 occurrence [2]. Strength training programs help prevent injury of the hamstring through traditional exercises thought to increase strength and alter muscle architecture and stiffness [3]. Surface electromyography (EMG) is one method utilized to capture muscle excitations in these studies. EMG normalization is often incorporated to sustain repeatability and to establish a known scale to be shared and compared amongst other laboratories and researchers in the field [4]. EMG can be normalized using techniques such as maximum voluntary isometric contraction (MVIC), peak amplitude of the study for a given subject, etc., yet it is unclear which method might provide comparable results from a multi-week study. The purpose of this project was to investigate the application of normalization techniques on filtered EMG signal cutting tasks captured from a multi-week hamstring strength training program.

Methods

Five adults completed 6 weeks of a hamstring strength training program. The male subject's average age was 22.67±4.62, height: 1.87±0.01 m, and weight: 872.52±51.29 kg. The female's average age was 22.67±2.88, height: 1.66±0.08 m, and weight: 722.33±71.97 kg. Two days of resistance training and one day of plyometrics per week was required from study participants.

In the 1st and 6th weeks of the study, an anticipated cut (ac) task was staged leading up to a force plate and corresponding EMG signals collected using wireless surface electrodes (Trigno, Delsys Inc., Boston, MA) placed on the muscle belly of the lateral hamstring. MVICs were collected from a 10-second maximal isometric contraction each week.

MATLAB (MathWorks, Natick, MA) was used to filter and process the raw EMG signals of the subjects. The EMG signal during contact with the force plate was padded with zeros to account for the Butterworth filter's slow response to quick transitions, band-passed at 5-450 Hz, and then high-pass filtered at 20 Hz with a recursive 2nd order Butterworth filter. Full-wave rectification of the signal was applied, then a low-pass filter at 10 Hz using a recursive 2nd order Butterworth filter to create a linear envelope. 10 Hz cut-off was used to reduce damping for the onset of muscle signal excitation of the task. Trials according to each subject and week of the study were averaged to create a single linear envelope.

MVIC, max MVIC (mMVIC) across weeks for subject, mean MVIC (mnMVIC) (average of weeks) for subject, anticipated cut task for given subject and week (tsk), mean activation of the task (mTsk), max task across weeks for subject (mxTsk), and mean task (mnxTsk) for subject (average of weeks) were calculated in MATLAB and utilized to normalize each weekly ac task for each subject. Coefficient of variation (CV) was also calculated and compared to evaluate intra-individual variability of each normalization technique.

Results and Discussion

Subject	MVIC	mMVIC	mnMVIC	Tsk	mTsk	mxTsk	mnxTsk
S01							
Week 1	7	7	8	100	141	100	162
Week 6	7	5	6	100	126	66	107
S08							
Week 1	40	30	34	100	146	100	147
Week 6	27	27	31	100	135	91	133
S13							
Week 1	7	7	9	100	133	7	17
Week 6	187	94	125	100	126	100	235
S14							
Week 1	46	46	47	100	188	100	179
Week 6	43	41	42	100	152	89	159
S17							
Week 1	18	18	22	100	139	57	106
Week 6	52	31	39	100	149	100	185

Figure 1: Table featuring subject/week cut tasks, percentage of max effort for normalization type.

Subject	MVIC	mMVIC	mnMVIC	Tsk	mTsk	mxTsk	mnxTsk
S01	0.1008	0.2532	0.2532	0.1188	0.1013	0.2532	0.2532
S08	0.2398	0.0725	0.0725	0.0831	0.0691	0.0725	0.0725
S13	1.3518	1.2613	1.2613	0.1003	0.0945	1.2613	1.2613
S14	0.1755	0.1639	0.1639	0.1946	0.1760	0.1639	0.1639
S17	0.7327	0.3882	0.3882	0.0964	0.0910	0.3882	0.3882

Figure 2: Table featuring CV for each subject/ normalization type.

The results demonstrate that mTsk and mxTsk on average have less variation than the other methods. It could be a preferred method for normalizing for cutting tasks that involve the HMC. The data showed that by using mTsk for normalization, percentage of maximum effort may always be greater than 100%. Tsk normalization was always 100%, as the cutting task was normalized to its own peak. This may not be preferable for some researchers.

Significance

MVIC has been widely accepted and often assumed as the most appropriate method for normalization. Reproducibility and consistency are priority in EMG signal sharing. Emphasis toward other methods such as to the task itself may improve these desired outcomes. Exploration into other dynamic tasks should be considered for determining an appropriate normalization method seeing that MVIC was not proven the best regarding variation in this study.

Acknowledgments

The Neuromechanics Laboratory (ODU) provided raw EMG signals and insight toward the completion of this study.

References

[1] Made, A.D.V.D., et al. (2015) *Knee Surgery Sports Traumatology Arthroscopy* 23:p. 2115–2122.
[2] Chu, S., et.al. (2016), *Curr Sports Med Rep.*
[3] Delextrat, A., *Frontiers in Physiology* (2018) p.9.
[4] Halaki, M., *IntechOpen* (2012)

INFLUENCE OF OBJECT CHARACTERISTICS ON STABILITY DURING A PERTURBATION

Dorien Butter[1,2], Alexandra Ingram[1], Anna Florell[2], Bob Wong[3], Andrew Merryweather[1], and K. Bo Foreman[1,2]
[1]Mechanical Engineering Department, University of Utah, UT, USA
[2]Department of Physical Therapy, University of Utah, UT, USA
[3]College of Nursing, University of Utah, UT, USA
email: dorien.butter@utah.edu

Introduction

With over 700,000 patient falls occurring in US hospitals each year [1], understanding the cause is critical for fall prevention. The causes can be multi-faceted and are typically divided into intrinsic (age, sex, medication, etc.) and extrinsic (environment, training, education) risk factors [2]. To reduce falls, hospitals implement fall prevention strategies limiting exposure to extrinsic risk factors, identifying intrinsic fall risk factors, monitoring patients, and limiting unsupervised movement [3, 4] but fail to address extrinsic factors directly. Research on extrinsic fall risk factors focuses on flooring, lighting, and handrails [5, 6] and has influenced hospital room design. Additionally, a patient's location, task, and objects they interact with influence fall risk [7]. The interaction between the patient and the objects in the room is complex and not well understood.

To address the paucity of research in this area, we classified objects into defining characteristics to assess how they provide support during instability. This study aims to understand how the object characteristics of height, type of grasp, and resistance to movement provide stability to an individual during a moment of instability.

Methods

Healthy adults with no pre-existing conditions were recruited according to IRB 00099410. Participants were fitted with 69 retroreflective markers to track their full-body motion (15 segments) with motion capture (MoCap) (Vicon Nexus).

Participants were instructed to walk heel-toe along a 12ft line on the floor to create a narrow base of support for each trial while looking straight ahead. A 12ft long support structure was available to their left. It could be adjusted in height (30, 36, 42"), resistance to movement (locked or unlocked wheels), and type of grasp available (non-prehensile, parallel extension, medium wrap). Participants were instructed to hover or slide their hand over the support while walking. During each trial, participants experienced a lateral perturbation to the pelvis. The perturbation was created by dropping a 4.5kg weight vertically, which was connected by a rope to the participant. Participants also completed 6 perturbation trials with no support structure.

A total of 18 configurations of the support structure were tested three times each for 60 trials total. The order of the configurations was randomized for each participant. Data from each trial were collected with Vicon Nexus and post-processed in Visual3D, MATLAB, and RStudio. Data were normalized between the start of the perturbation and when participants regained stability. The outcome variable of interest was the minimum margin of stability (MoS) during the trial. One linear mixed-effects model (LME) was used to investigate the relationship between having a support object and having no support object. A second LME was used to investigate the types of support configurations. For both models, height, wheel status, and type of grasp were fixed effects; subjects were a random effect. Post-hoc pairwise comparisons were made with Tukey correction to investigate any significant effects.

Results and Discussion

Five participants are included in the analysis (4F, 1M, 26 ± 1.6yrs). The outcome metric, min MoS, was normally distributed. There was a significant difference between trials with support and trials with no support ($p = .014$), Table 1. The results suggest that having support reduces the level of instability.

Table 1. p values, and EMM comparing support and no support

Fixed Effect	p value	EMM (SE) [mm]
support	.014	-34.4 (1.90)
no support		-39.1 (2.57)

For the second LME investigating support characteristics, only the type of grasp was significant ($p < .001$). The estimated marginal mean (EMM) for min MoS, Table 2, suggests that participants became most unstable with the non-prehensile grasp (-37.8mm) and were the least unstable with medium wrap grasp (-30.6mm). Post-hoc test showed that all levels within type of grasp were approaching significance ($p = .06$).

Table 2. EMM (SE) for each level within type of grasp

Levels	EMM (SE) [mm]
non-prehensile	-37.8 (2.25)
parallel extension	-34.8 (2.25)
medium wrap	-30.6 (2.25)

Based on the results, the type of grasp available seems to be the driving factor influencing the quality of support an object can provide. The results suggest that a medium wrap helps minimize the instability during a perturbation. Data collection will continue for a total of 15 participants.

Significance

These results provide a more comprehensive understanding of how object characteristics influence quality of stability during a perturbation. Based on these results, and with further research, we can assign quality of support ratings to objects. Such ratings can then be implemented in fall risk models [8]. Understanding how objects provide support is the first step in integrating room design and layout into hospital fall prevention strategies.

Acknowledgments

This project was supported by the AHRQ (R18HS025606) and NIOSH (#2T42OH008141-13). The authors are solely responsible for this document's contents, findings, and conclusions, which do not necessarily represent the views of AHRQ or NIOSH.

References

1. Ganz, D., Agency for Healthcare Research and Quality, 2013.
2. Stevens, J.A., Journal of Safety Research, 2005. 36(4): p. 409-411.
3. Tideiksaar, R., Mt Sinai J Med, 1993. 60(6): p. 522-7.
4. Shorr, R.I., Annals of Internal Medicine, 2012. 157(10): p. 692-699.
5. Drahota, A.K., Age Ageing, 2013. 42(5): p. 633-40.
6. Komisar, V., Applied Ergonomics, 2019. 81: p. 102873.
7. Hitcho, E.B., J Gen Intern Med, 2004. 19(7): p. 732-9.
8. Chaeibakhsh, S., arXiv preprint arXiv:2101.03210, 2021

DYNAMIC BIPLANE RADIOGRAPHY AND MODEL-BASED TRACKING FOR EVALUATION OF THUMB KINEMATICS

Maria A. Munsch[1], Christopher J. Como[1], Tom H. Gale[1], John R. Fowler[1], and William J. Anderst[1]
[1]University of Pittsburgh Department of Orthopaedic Surgery
Email: munschma2@upmc.edu

Introduction

Dynamic biplane radiography (DBR) in conjunction with model-based tracking (MBT) has provided a suitable mechanism for biomechanical assessment of many joints but has not yet achieved widespread use at the thumb and wrist. While methods such as surface markers and implantation of metal beads have previously been utilized for kinematic analysis of many anatomic regions, these methods have many shortcomings[1,2]. Bead implantation requires invasive intervention, and surface markers are prone to soft tissue artifact. In addition, the small, overlapping carpal bones pose challenges to these traditional methods[3].

In order to verify that the challenges associated with the carpal bones will not preclude successful implementation of DBR with MBT, these strategies must be validated accordingly. The purpose of this work is to determine the accuracy of DBR with MBT for the evaluation of thumb and wrist joint kinematics.

Methods

Following institutional approval, three 0.6 mm stainless steel beads were implanted into the trapezium, scaphoid, first metacarpal, and radius of a cadaveric upper extremity from a 56-year-old female. The specimen was mounted in a PVC frame and then manipulated within the DBR system using fishing wire, which was tied to the specimen and pulled to move it in the desired manner (Figure 1.A). One static trial and three trials of thumb adduction-abduction were performed, with synchronized biplane radiographs collected at 100 Hz (Figure 1.B). Specimen-specific 3D bone models of the trapezium, scaphoid, first metacarpal, and radius were created from a CT scan (resolution 0.437 x 0.437 x 0.625 mm) (Figure 1.C). Anatomical landmarks were identified on the 3D bone models to establish an anatomic coordinate system (Figure 1.D). Bead-based tracking (BBT) and volumetric MBT were completed to track 3D bone motion (Figure 1.E). Joint kinematics were then calculated according to the anatomic coordinate systems and bone motion (Figure 1.F).

Precision of the BBT kinematic measurements was calculated with respect to the known distances between the implanted beads. Precision, bias, and root-mean-squared-error (RMSE) of the MBT kinematic measurements were calculated with respect to the BBT method. These values were computed for the static and dynamic trials for each of the four tracked bones and are reported in the bone anatomic coordinate systems.

Results and Discussion

Condition numbers for the bead distributions ranged from 21 to 82 indicating a good distribution of implanted beads to serve as a reference standard[4]. On average, the BBT system measured joint position for the static trials with precision of 0.037 mm and bias of 0.046 mm. For the dynamic trials, average BBT precision and bias were 0.068 mm and 0.10 mm, respectively.

On average, the MBT system measured joint position for the static trials with precision of 0.054 mm, bias of 0.48 mm, and RMSE of 0.48 mm. For the dynamic trials, average MBT precision, bias, and RMSE were 0.41 mm, 0.62 mm, and 0.77 mm, respectively. The precision of the MBT system was the worst for the trapezium, possibly due to the bone's arthritic nature in this particular cadaver specimen. Without the trapezium, the average precision and bias of the MBT system for the dynamic trials were 0.087 mm and 0.38 mm, respectively.

These measures of accuracy are comparable to those found with previous validation studies of the same MBT system for kinematic analysis of the ankle[5], knee[6], hip[7], lumbar spine[8], and cervical spine[9]. This study has demonstrated that DBR with MBT is a non-invasive and accurate method which can be utilized for kinematic analysis of the thumb and wrist. The results of this study are limited to one specific movement of the hand and wrist. Additional studies are needed to confirm these results are generalizable to other movements and to include cadaver specimens with varying levels of joint pathology.

Significance

Successful validation of DBR and MBT at the thumb and wrist will allow for its use in investigation of osteoarthritis (OA) and other upper extremity pathologies, injuries, and treatments.

References

1. Tashman, J BME 2003. 2. Selvik, Act Rad 1990. 3. Akhbari, J BME 2019. 4. Soderkvist, J BME 1993. 5. Pitcairn, J BME 2020. 6. Anderst, ME Phys 2009. 7. Martin, J Arth 2011. 8. Anderst, Spine 2008. 9. Anderst, Spine 2011.

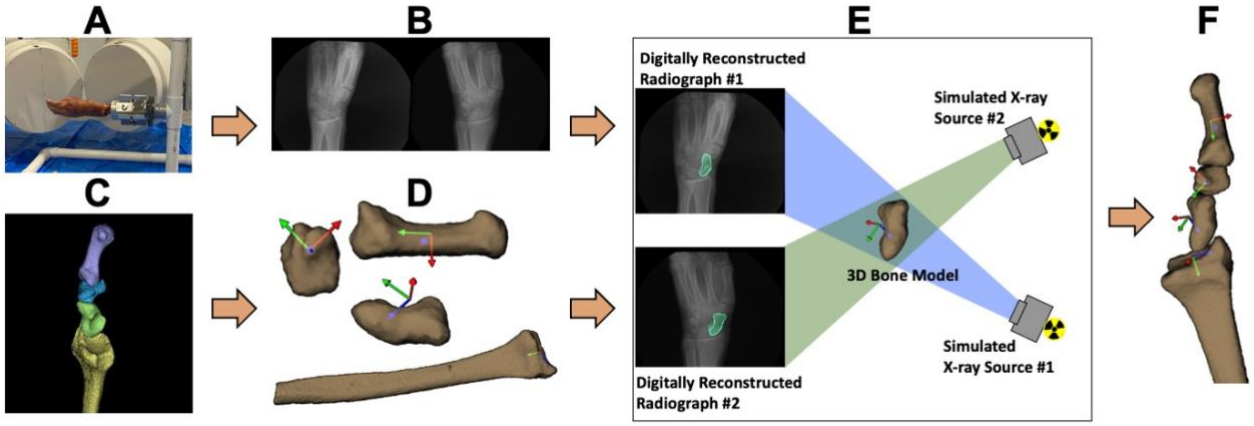

Figure 1. Data collection and model-based tracking workflow.

DRIVE LEG AND STRIDE LEG GROUND REACTION FORCES RELATIONSHIP TO MEDIAL ELBOW STRESS AND VELOCITY IN COLLEGIATE BASEBALL PITCHERS

Brett K. Smith, Hunter J. Bennett, Eva U. Maddox, Sebastian Y. Bawab, Stacie I. Ringleb
Old Dominion University
email : SRingleb@odu.edu

Introduction

Injuries to pitchers have become increasingly prevalent with 4.4 collegiate pitchers suffering an ulnar collateral ligament surgery per every 100 player-seasons in 2017[1]. Analyzing the biomechanics of pitching may help pitchers maximize velocity and reduce the kinetics in high injury risk regions. Ground reaction forces have been associated with pitch velocity[2,3]. Impulse of the drive leg in the anterior-posterior (AP) direction has been associated with increased pitch velocity and increased energy flow to the pelvis, trunk, and arm[3]. Peak ground reaction force of the stride leg in the AP direction has been associated with pitch velocity[2]. The following hypotheses were developed:
Hypothesis 1: There is a direct correlation between impulse of the drive leg in the AP direction and ball velocity.
Hypothesis 2: There is an inverse correlation between impulse of the drive leg in the AP direction and elbow varus torque.
Hypothesis 3: There is a direct correlation between stride leg peak ground reaction force in the AP direction and ball velocity.

Methods

12 collegiate baseball pitchers threw between 10 and 15 fastballs on an instrumented pitching mound (Fig 1). All available trials for each participant were used. Two force plates (2000Hz, Bertec FP-4060, Bertec Inc., OH, USA) were used to measure drive leg and stride leg ground reaction forces. A sleeve (motusBASEBALL Complete Package, Motus Global Inc., Massapequa, NY), containing an inertial measurement unit was used to calculate elbow torque. A radar unit (Rapsodo Pitching 2.0, Rapsodo Pte Ltd., Brentwood, MO) was used to measure pitch velocity. All ground reaction forces were normalized to body weight. Linear regressions were performed to analyze correlations between drive leg impulse in the AP direction with pitch velocity, drive leg impulse in the AP direction with elbow varus torque, and stride leg peak force in the AP direction with pitch velocity.

Figure 1: The instrumented pitching mound is shown with force plate 1 (FP1) under the drive leg and force plate 2 (FP2) under the stride leg.

Results and Discussion

This study found that impulse of the drive leg in the AP direction was significantly related to pitch velocity (p-value < 0.001, r = 0.366) (Fig 2(a)) and inversely related to elbow varus torque (p-value = 0.001, r = 0.299) (Fig 2(b)). The results show the importance of producing force over time (i.e., impulse) with the drive leg in the AP direction and not just a large peak force. Additionally, producing greater impulse may help maintain a stable drive leg, likely from a co-contracted back hip, and help generate more energy from the larger sections of the kinetic chain while reducing stress from the smaller segments of the chain such as the elbow. Stride leg peak force in the AP direction was significantly related to pitch velocity (p-value = 0.013, r = 0.222) shown in (Fig 2(c)). This result is in line with previous studies that found peak braking ground reaction force of the stride leg correlated with energy flow into the arm segment[3]. This finding suggests the importance of braking with the stride leg to transfer energy from lower extremity segments to upper extremity segments.

(a)

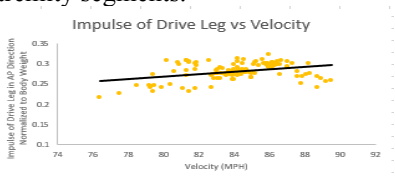

(b)

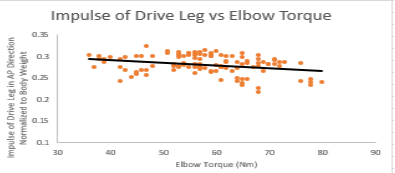

(c)

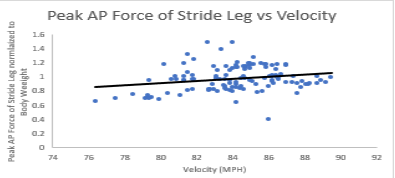

Figure *2:* Data from all participants and all available trials are shown.

Significance

The results of this study show how ground reaction forces relate to loads on the elbow and pitch velocity. Increasing the impulse on the drive leg may lead to greater pitch velocity and a decrease in elbow varus torque. Additionally, increasing stride leg peak ground reaction forces may lead to greater pitch velocity. Understanding these factors may help lead to increases in pitch velocity and decrease elbow varus torque.

This study focuses on how pitchers produce force leading up to ball release to maximize pitch velocity, however, a better understanding of forces after ball release may give more insight as to how these forces are optimally dissipated and how they are related to injury. These findings may also have an impact on other overhead throwing athletes such as football quarterbacks and javelin throwers. Future studies should be conducted to analyze the primary musculature that is activated to help produce these forces and could help impact strength training techniques.

References

1. Rothermich MA et al. (2018) JSM **6**: 4-9
2 McNally MP et al. (2015) JSCR **29**: 2708-2715
3 Howenstein J et al. (2020) JB **108**: 109909

SERIES-ELASTICITY DOES NOT ELIMINATE THE NEED FOR ACTIVE WORK IN RUNNING

Ryan T. Schroeder[1] and Arthur D. Kuo[1,2]
[1]Faculty of Kinesiology and, [2]Biomedical Engineering Program, University of Calgary
email: ryan.schroeder@ucalgary.ca

Introduction

Running costs considerable metabolic energy, despite savings from series elasticity. The savings come from tendons that passively store and return energy (e.g. 60% of shortening work in turkey lateral gastrocnemius[1]), such that muscle fascicles in series could largely operate isometrically. The classic spring-mass model[2] explains running based on elasticity alone, but fails to explain why fascicles actively perform any shortening work, or the metabolic cost of running on level ground or on slopes. We propose an extension of the spring-mass model to explain the energetic cost of running.

We extended the spring-mass model with passive dissipation and active actuation to restore losses. Energy cost was modelled proportional to work and a *force-rate* term for an empirically observed cost of rapid force production.[3] We aimed to identify features of optimal coordination between muscle and tendon, and thus help explain energetic cost despite elastic return.

Methods

We augmented the spring-mass model with active actuation to restore losses from passive dissipation (Fig. 1A). The actuator produced extension force and displacement in series with the spring. Its energy cost was proportional to work and a *force-rate* term for an empirically observed cost for rapid force production[3]. We used dynamic optimization to identify key features of coordination between muscle and tendon, and thus help explain energetic cost despite elastic return.

We modelled two types of passive dissipation (Fig. 1A). One was for foot-ground collision, modelled as a reduction of center of mass (CoM) momentum at contact. The second was tendon hysteresis, as a parallel, damping-like loss during loading of the spring. The actuator's force and displacement trajectories were optimized to minimize energy cost from active actuator work plus the force-rate cost (the time-derivative of force production).[4] We examined how active work must offset dissipation, and whether that work plus force-rate costs explain energy expenditure. The model was compared against human running features: CoM trajectory, leg power and energetic cost as a function of speed on flat ground.

Results and Discussion

We found that the model's passive energy dissipation must be restored with active actuator work. This is because periodic level gait requires zero net work over a stride. Relatively minor amounts of dissipation (3% collisional loss of momentum, 26% hysteresis loss) thus require compensatory active work, which is costly enough (assuming 25% work efficiency[6]) to substantially affect metabolic energy expenditure. With work as the only cost, the model avoids active negative work altogether, but an added force-rate cost makes it economical to actively perform negative and then positive power during stance (Fig. 1B) to reduce overall cost. With both work and force-rate costs, the model produces ground reaction forces and leg power similar to humans (Fig. 1B).

The model predicts similar energetic cost to humans, as a function of speed[5] (Fig. 1C). Cost is largely driven by active work for collision losses that increase with speed, and for hysteresis.

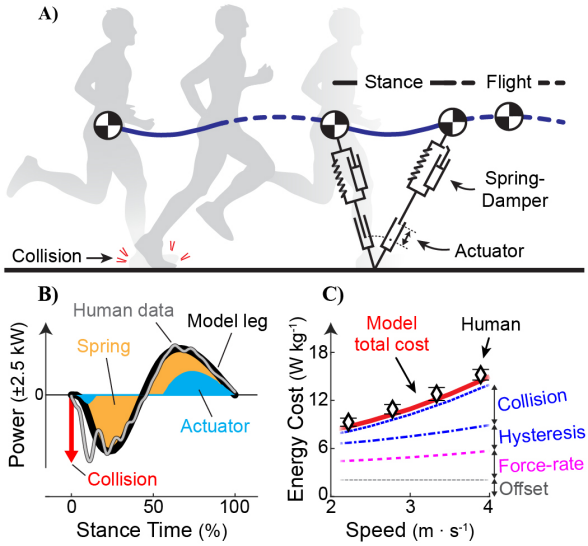

Figure 1: Spring-mass model of running extended to explain energetics. A) Active actuator in series with spring-damper and point-mass body, with collision loss at foot-ground contact. B) Net Leg power vs. time for Human (grey) and Model (black), with Actuator and Spring work (blue & orange shaded) and Collision loss (red arrow). C) Energy Cost vs. speed, including for work to restore Collision and Hysteresis, Force-rate cost and an Offset. Human data show mean ± 1 s.d.[5]

Actuator work makes up 70% of the model's net energetic cost, despite 53% elastic energy return, similar to humans.[6]

We found economy to depend on more than spring compliance. Minimizing work alone causes the optimal stiffness to increase with speed to reduce dissipation. But this is countered by the added force-rate cost, which penalizes short force bursts associated with stiffer springs. The force-rate cost has been characterized in other human movements,[3] but is not included in most running models. Our model suggests that without such a cost, running should benefit from a stiffer spring and more impulsive ground reaction forces at higher speeds.

Significance

A model with dissipation and active actuation identifies key features of running energetics. Even though economy is gained from spring-like elasticity, active work is still necessary to counter dissipative losses and avoid rapid force production. Active work appears critical for explaining running energetics.

Acknowledgments

Supported by Dr. Benno Nigg Research Chair, NSERC CRC (Tier 1), NSERC Discovery.

References

1. Roberts et al. (1997). *Science.* 275: 1113-1115
2. Blickhan (1989). *J. Exp. Biol.* 22: 1217-1227
3. Doke & Kuo (2007). *J. Exp. Biol.* 210: 2390-2398
4. Rebula & Kuo (2015). *PLoS ONE.* 10: e0117384
5. Kipp et al. (2018). *J. Exp. Biol.* 221: jeb184218
6. Riddick & Kuo (2020). *BioRxiv*
   doi: 10.1101/2020.09.22.309161

COMPARISON OF RESULTS FROM DIFFERENT FINITE ELEMENT SOFTWARE USED IN SPINE MODELLING

Isaac K. Kumi, Michael Polanco, Jinhyuk Kim, Sebastian Y. Bawab, Stacie I. Ringleb, Michel Audette
Old Dominion University, Norfolk, VA, USA

email: sringleb@odu.edu

Introduction

The Finite element (FE) method has allowed for the construction, simulation, and analysis of complex clinical conditions, avoiding the difficulties that have been associated with in-vitro experiments [1]. With the availability of several in-vitro experimental datasets, model validations have become easier to achieve, increasing the development and accessibility of published FE models. Because of this, different FE software has been introduced, providing a variety of options to run analyses for different applications. Although the software has allowed researchers to conduct several studies, it is important that the translation of results between software is consistent. The purpose of this study is to compare the kinematic results of two similar functional units using two different FE software.

Methods

Two L4-L5 3D FE functional unit models were obtained; one for analysis with FEBio [1] (FEBio, Salt Lake City, UT) (Fig 1a) and another for analysis with LS-DYNA [2] (Livermore Software Technology, Livermore, CA) (Fig 1b) for comparison. The vertebral body and material properties of both models were modeled similarly [2] except for the annulus fibrosus. While the model analyzed in LS-DYNA configured the matrix of the annulus using a Mooney Rivlin material [3] with the annulus fibres generated using a custom finite element code developed in MATLAB (The MathWorks Inc., Natick, MA)[4], the FEBio model characterised the matrix as a Holmes-Mow model with the exponential power law to describe the strain energy density of the fibres [5]. Ligaments for both models were represented as nonlinear tension-only springs and characterised with human ligament data from literature [6]. A torque of 7.5Nm was applied on the superior endplate of the L4 functional unit while all degrees of freedom on the inferior L5 endplate were constrained in both models. Quasi-static analyses were conducted, and range of motion (ROM) values were recorded for flexion, extension, right lateral bending and left axial rotation for both models.

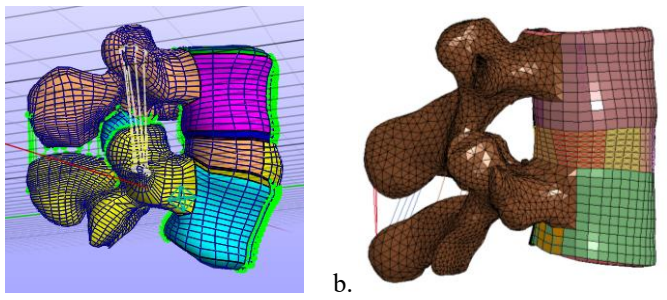

Figure 1: Sagittal view of the L4-L5 functional unit from both models (a) Open-source Functional unit model used for analysis in FEBio. (b) Functional unit model analyzed in LS-DYNA.

Results and Discussion

The ROM values obtained from both models were compared to results obtained from an in-vitro study [7] (Fig 2). The results showed the ROM values fell within the range of that presented by the study. The major difference between the two models were found with the right lateral bending and left axial rotation. The differences may be attributed to the different ways the annulus fibrosus was characterized between both models. The Holmes-Mow material in the FEBio model was modelled using the biphasic swelling theory [8] and describes the compressive nature of the annulus fibrosus needed for the model. The Mooney Rivlin material type in LS-DYNA is an incompressible uncoupled hyper-elastic material property, which alone is an incomplete representation of the annulus fibrosus. Nonetheless, the ROM values for both models fell within range provided by the in-vitro study. Future work could be done by looking at the lumbar spine while using different varying torques between both models.

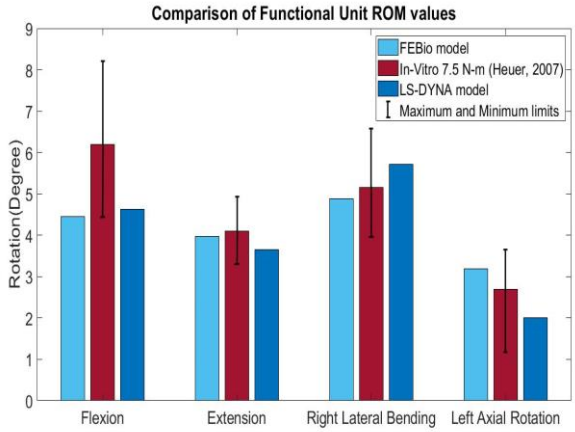

Figure 2: ROM for 7.5Nm torque for the L4-L5 functional units. The *in vitro* data reports the median value, where the error bars represent max and min values.

Significance

This comparison between FEBio and LS-DYNA has served as a validation of the models as their results are comparable and match that of the study reviewed [7]. FEBio was developed for biomechanical applications and is relatively new in development, so its comparison to established FE software is necessary to verify its use for specific applications. As the results obtained have been verified, either developed model could be used as a platform in future biomechanical studies.

References

[1] Finley, S. et al. *Comp. Method in Biom.* **21**(6), 444-52, 2018.
[2] Polanco, M. et al. ASB Conference, Atlanta, GA, 2020.
[3] Naserkhaki et al. *Biomechanics* **70**, 33-42, 2018.
[4] Shirazi-Adl, A. et al. *Spine* **9**,120-34, 1984.
[5] Jacobs, N.T. et al. *Biomechanics* **47**,2540-46,2014.
[6] Rohlmann, A. et al. *Biomechanics* **39**, 2484-90, 2016.
[7] Heuer, F et al. *Biomechanics* **40**, 271-80, 2007.
[8] Mow, V.C et al. *Biomechanical* **102**, 73-84, 1980.

THE EFFECT OF FOAM CHOICE ON QUIET-STANDING POSTUROGRAPHY

Kimberly E. Bigelow, A. Chaudhari[2], and D. Merfeld[2]
[1]University of Dayton, Dayton, OH, USA
[2]The Ohio State University, Columbus, OH, USA
email: kimberly.bigelow@udayton.edu

Introduction

In recent years, there has been an international push for increased standardization in the field of posturography, as there is concern that differing choices in testing protocols may lead to unequivocal findings [1]. Quiet-standing posturography protocols often incorporate the modified Clinical Test of Sensory Interaction on Balance (mCTSIB), with individuals standing quietly under both eyes open and eyes closed conditions and on both a flat surface and on a foam cushion. A large (N>5000) National Health and Nutrition Examination Survey (NHANES) found that individuals who failed to complete the eyes closed standing on foam ("vestibular") testing condition were 6.3 times more likely to report "difficulty with falling" (though posturography data was not collected in the NHANES study) [2]. Despite the seeming importance of this testing condition, the choice of foam pads used in posturography studies is not standardized, though the choice seems to influence results [3]. Our study sought to examine the effects of two foam surfaces commonly used in posturography testing: the memory foam-type compliant surface used in the NHANES study and a closed cell foam pad often used in physical therapy settings (brand: Airex).

Methods

Twenty healthy college-aged students participated in this study. The individuals tested included 8 men and 12 women, mean age: 20.3±1.3 (range: 18-22) years; mean height: 169.42±8.76 (range: 152.4-185.42) cm; and mean weight: 69.53±20.58kg (range: 44.48 to 132.68 kg). 70% of the study population was non-Hispanic, white; the remaining 30% of test participants came from other racial-ethnic groups.

Participants completed a sequence of 60 second trials while standing on a Bertec force-measuring platform. The tasks were: (1) Eyes Open, Comfortable Stance on the flat platform, (2) Eyes Closed, Comfortable Stance on the flat platform, (3) Eyes Open, Comfortable Stance on the Foam Pad, (4) Eyes Closed, Comfortable Stance on the Foam Pad, (5) Eyes Open, Narrow Stance (with heels and toes touching) on the Foam Pad, and (6) Eyes Closed, Narrow Stance on the Foam Pad. Participants completed this entire sequence for both foam pads, with allocation initially randomized and then counter-balanced. For all trials, study participants stood barefoot, with arms crossed across their chest, and looking straight ahead, trying not to talk or move for the trial duration. A two-minute break was given between the sets of six trials.

Anterior-posterior and medial-lateral center of pressure (COP) data were collected from the force plate at 1000 Hz. These data were filtered with a fourth-order low-pass Butterworth filter with 20 Hz. cutoff. A number of traditional postural sway measures were calculated; Root-mean square displacement (RMS) results are presented here.

Results and Discussion

Our results (Table 1) suggest that there are some statistically significant, albeit small, differences in sway results obtained depending on the foam used. The closed cell foam pad elicits smaller RMS COP displacements, which suggest that there is a higher likelihood of success of completing the more challenging trials. At the same time, the primary goal of providing the foam is to challenge balance by reducing the veracity of ankle proprioceptive cues. Reducing veracity of ankle proprioceptive cues would yield increased sway. Hence, both the increased RMS sway and increased standard deviations of sway metrics when standing on the memory foam would, on the surface, appear to be consistent with the memory foam reducing veracity of ankle proprioceptive cues. This could explain why the NHANES data set showed a strong correlation between "difficulty with falling" in the past year and failure to complete the "standing on memory foam with eyes closed" test condition [2].

Significance

Our findings suggest that the choice of foam used does matter and should therefore be reported in publications to allow for comparison across studies. Of the two foams we studied, we found that the memory foam does a better job of reducing veracity of ankle proprioceptive cues and may therefore be a better choice for quiet-standing posturography.

Acknowledgements

This study was funded by the Army Medical Research and Command, Congressionally Directed Medical Research Program (CDMRP), Award#W81XWH1920003.

References

1. Visser JE, et al. *Clin Neurophysiol*. **119**, 2424-2436, 2008.
2. Agrawal Y, et al. *Arch Intern Med*. **169,** 938-944, 2009.
3. Gosselin G, Fagan M. *Chiropract Man Ther*. **23,** 1-8, 2015.

Table 1: Mean ± Standard Deviation RMS (in mm) per trial, per foam condition

	Memory Foam (NHANES)	Closed Cell Foam (Airex)	Sig.
[Eyes Open, Comfortable Stance – No Foam]	*3.79 ± 1.1*	*4.37 ± 1.3*	*p=0.051]*
[Eyes Closed, Comfortable Stance – No Foam]	*5.99 ± 2.7*	*5.75 ± 2.1*	*p=0.735]*
Eyes Open, Comfortable Stance - Foam	10.41 ± 3.1	7.53 ± 2.2	**p=0.002***
Eyes Closed, Comfortable Stance – Foam	18.74 ± 7.5	11.80 ± 2.7	**p=0.001***
Eyes Open, Narrow Stance – Foam	10.23 ± 3.1	8.51 ± 1.6	**p=0.014***
Eyes Closed, Narrow Stance - Foam	19.37 ± 6.3	17.67 ± 3.7	p=0.267

QUANTIFYING RELATIONSHIPS BETWEEN LOWER-LIMB MUSCLE MORPHOLOGY AND GAIT KINEMATICS USING WEARABLE SENSORS

Akshay S. Chaudhari[1], Andrew Schmidt[1], Elka Rubin[1], Michael Ko[1], Lauren Watkins[1], Valentina Mazzoli[1]
1. Department of Radiology, Stanford University, Stanford, CA, United States
email: akshaysc@stanford.edu

Introduction

There is a large need to determine objective criteria for assessing rehabilitation efficacy following anterior cruciate ligament reconstruction (ACL-R) surgery[1]. While gauging lower-extremity gait asymmetry is one such method, most evaluations are qualitative and rely on visual assessments. Using gait labs to obtain quantitative measures is time-consuming and expensive. Furthermore, the impact between gait variations and rebalancing muscle mass in the injured and contralateral limbs is unknown. To address these challenges, here we describe a proof-of-concept **rapid** magnetic resonance imaging (MRI) protocol coupled with a **point-of-imaging** gait assessment using **wearable sensors**. We compare and describe sensitive metrics to **compare structural muscle morphology with functional gait asymmetries**.

Methods

Five healthy subjects (4 females) participated in this study (age: 26±2 years, BMI: 22±2). Each underwent a 5min upper thigh bilateral Dixon MRI scan on a 3T MRI scanner (SIGNA 750w Premier, GE Healthcare) to generate separate water and fat images[2]. Manual segmentations were performed for vastus medialis (VM) and vastus lateralis (VL) muscles in both limbs to compute the average cross-sectional area (CSA) and volume (Fig. 1). Muscle morphology asymmetries (MMA) were computed using volume and CSA ratios of the VM to the VL. Bilateral muscle asymmetries (B-MMA) were computed using the right MMA to left MMA ratios.

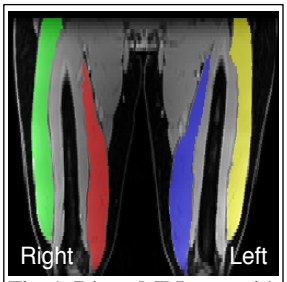

Fig. 1: Dixon MRI scan with vastus medialis (red, blue) and vastus lateralis (green, yellow) segmentations.

Immediately following the MRI scan, all subjects underwent a biomechanical assessment of gait kinematics using portable wearable sensors (Cionic, San Francisco, CA). A total of five inertial measurement units (IMUs) were attached to each shank and thigh, along with one IMU on the central pelvis via adjustable velcro straps (Fig. 2a). All subjects walked overground for approximately 30 seconds at a self-selected normal walking pace while wearing personal running shoes. The IMU data was used to calculate per-step kinematics of the knee and the hip (flexion/extension, abduction/adduction, and internal/external rotation) normalized by stride time[3]. Mean kinematics across all steps were computed as a percentage of the gait cycle.

Gait asymmetries for joint angles (normalized between -90° and 90°) between the right and leg legs for each of the six motions were computed using: (1) a symmetric Kullback–Leibler divergence (KLD) that quantifies the difference between two distributions, (2) a Wasserstein distance (WD) that describes the distributional energy required to transform one distribution to another, and 3) a Pearson correlation coefficient (R).

For our study outcome, we used Pearson's R to quantify the relationship between gait asymmetry and B-MMA inter-limb muscle morphology asymmetry. Mann-Whitney U-Tests were used for all statistical comparisons (significance level of α=0.05).

Results and Discussion

The VM was significantly smaller than the VL, with average MMA ratios of 0.77±0.12 and 0.78±0.09 for volume and CSA, respectively ($p<0.001$ for both). There were no significant inter-limb differences between MMA ratios for volume ($p=0.25$) or CSA ($p=0.60$). Comparatively, B-MMA asymmetry values were 0.90±0.06 for muscle volume and 0.98±0.13 for CSA. Gait asymmetries were smaller for hip kinematics compared to knee kinematics but did not exhibit statistical significance amongst the two for any of the three asymmetric metrics (lowest $p=0.14$ for KLD). Example knee kinematics for a subject with high inter-limb gait asymmetry (especially for abduction, R=0.20) and a high B-MMA of 0.78 is seen in Fig. 2b.

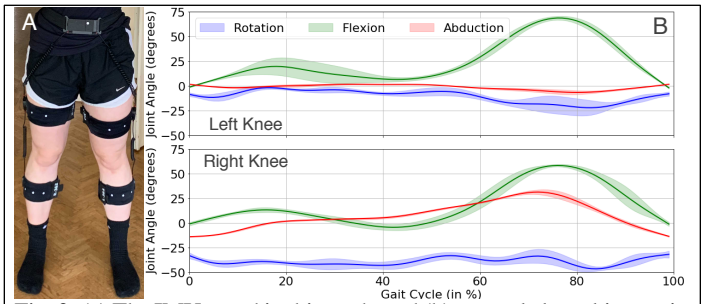

Fig. 2: (a) The IMUs used in this study and (b) example knee kinematics for a subject with high asymmetries, averaged over 27 gait cycles.

Correlations between B-MMA (for volume) and the three gait asymmetry metrics (Fig. 3) showed that decreased B-MMA (more right-left muscle asymmetry) was associated with increased gait asymmetry. Increased B-MMA resulted in higher positive KLD and WD correlations and negative R values. The KLD metric had the highest correlations, with all but knee flexion exhibiting statistical significance. Similar trends were seen for muscle CSA (not shown), but with reduced correlation strength.

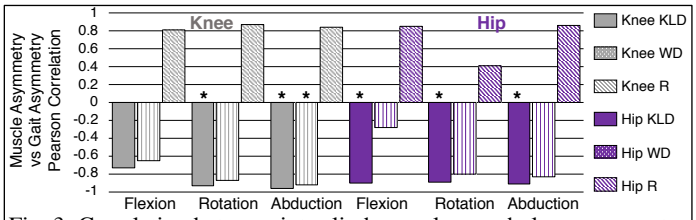

Fig. 3: Correlation between inter-limb muscle morphology asymmetry (B-MMA) and the three metrics of gait asymmetry. (*: $p<0.05$)

Significance

We showed the feasibility of assessing structural and functional lower-limb asymmetries at the point-of-imaging with wearable devices. Using KLD for gait asymmetry and VM/VL volume ratios was a sensitive metric to detect inter-limb structural-functional variations. This method that uses wearable devices and rapid MRI can be used for quantitative ACL-R assessment.

Acknowledgments

Research support: Philips, NWO. In-kind support: Cionic.

References

1:Myer JOSPT 2006 2:Reeder JMRI 2007 3:Winter Wiley 2009.

KINEMATIC MODEL FOR IDENTIFYING INITIAL CONTACT DURING TREADMILL RUNNING ACROSS COMPETITIVE RUNNING SPEEDS

[1] Deborah L. King, [1]Meghan Beahan, [2]Neha Kapoor, [1]Elizabeth Steele, [1]Marley Baum, and [3]Rumit Singh Kakar
[1]Ithaca College, Ithaca, NY, USA; [2]Cornell University, Ithaca, NY, USA; [3]Old Dominion University, Norfolk, VA, USA
email: dking@ithaca.edu

Introduction

Initial contact (IC) is a critical event commonly used to define a gait cycle in both walking and running. Joint kinematics associated with IC in running are used to identify foot contact angles and potential torques at the foot, which may be related to running economy and running-related injury [2,4]. While it is possible to identify IC using a force plate or instrumented treadmill, this instrumentation may not be available for testing overground running or running on a standard treadmill. In these cases, kinematic data must be used to estimate IC.

There are published kinematic models that estimate IC; however, many of these models are dependent on foot-strike angle [1,6] or are only valid at limited speeds [3,6,7,8]. The purpose of this study was to determine an algorithm to identify IC during treadmill running for different foot-strike angles across a range of competitive running speeds.

Methods

Twenty-five healthy recreational runners completed 7 treadmill trials at 7 different speeds (3.58, 4.02, 4.47, 4.92, 5.36, 5.81, and 6.26 ms^{-1}). Reflective markers were placed on the pelvis and lower extremities using the Plug-In Gait model (Vicon®:120 Hz). Each of the rear feet of the treadmill were placed directly over force plates (AMTI®:1080 Hz). Runners wore their own shoes, warmed up for as long as they needed, and were allowed rest between runs at different speeds. Runners ran at each speed in a self-selected order for 25-45 seconds and data was collected for the entire run after first 5 seconds.

Running kinematics were analyzed (Visual3D, C-motion) and IC for each gait cycle were predicted (IC_{pelv}) using raw pelvis center of mass (COM) displacement and measured simultaneously from the force curves (IC_{FP}). The mean difference was taken between IC_{pelv} and IC_{FP} for 13 random subjects and plotted for each speed. A curve was then fit to this data to adjust for speeds and compared to the mean differences (IC_{pelv}-IC_{FP}) for the remaining 12 runners for validation.

Results and Discussion

IC_{pelv} was predicted with a mean difference of 0.014 to 0.025 s (3-5 frames) as compared to IC_{FP} from 3.58 to 6.26 m/s (8-14 mph) speeds using the maximum downward velocity of the pelvis COM [7] (Figure 1). The mean difference decreased linearly with speed up to 5.36 m/s, which is consistent with the King et al [5] findings for 2.24 to 4.48 m/s. However, the linear pattern did not hold true at speeds above 5.36 m/s, so a polynomial fit was used to adjust for the entire range of speeds. This can be corrected with the quadratic

$$\boldsymbol{y = 0.003825x^2 - 0.0401x + 0.1203}$$

where, x is speed in m/s and y is mean difference (IC_{pelv}-IC_{FP}) in s. When compared to IC_{pelv} from the remaining 12 runners, the difference between IC_{pelv}-IC_{FP} and the best fit line ranged from 0.0002- 0.0013s (<0.16 frame at 120 Hz; Table 1).

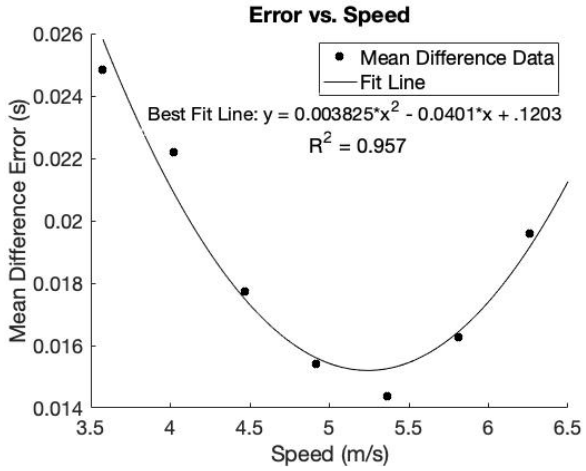

Figure 1: Mean difference between IC_{pelv} and IC_{FP} for 3.58-6.26 m/s (8-14mph) showing the quadratic fit to adjust for speed

Significance

It is recommended to use the maximum downward velocity of the pelvis COM with the quadratic fit $y = 0.003825x^2 - 0.0401x + 0.1203$ to predict the time of IC from 3.58 to 6.26 m/s in treadmill running when using kinematic data. Future research should validate this algorithm for overground running.

References

1. Alvim et al. *J Appl Biomech*, **31**(5), 383–8, 2015.
2. Bramah et al. *Am J Sport Med*, **46**(12), 3023-31, 2018.
3. Fellin et al. *J Sci Med Sport*, **13**(6), 646–50, 2010.
4. Hasegawa et al. *J Strength Cond Res*, **21**(3), 888-93, 2007.
5. King, McCartney, & Trihy. *J Biomech,* **90**, 119-22, 2019.
6. Leitch et al. *Gait Posture*, **33**(1), 130–2, 2011.
7. Milner & Paquette. *J Biomech*, **48**(12), 3502–5, 2015.
8. Osis et al. *J Biomech*, **47**(11), 2786–9, 2014.

Speed (m/s)	3.58	4.02	4.47	4.92	5.36	5.81	6.26
Mean Difference (10^{-3} s)	1.0	1.3	0.2	0.2	0.9	0.2	0.4
(95% CI) (10^{-3} s)	(-30.0, 32.0)	(-25.0, 27.0)	(-23.0, 23.0)	(-24.0, 25.0)	(-26.0, 28.0)	(-35.0, 35.0)	(-39.0, 40.0)

Table 1: Error (mean difference) between IC_{pelv}-IC_{FP} and the quadratic fit for 12 remaining runners at each speed.

INTERNAL FOOT MOTION OF TAA CANDIDATES OVER FOUR AMBULATORY EXERCISES

John Mead[1], Evan A. Dooley[2], Joseph S. Park M.D.[3], and Shawn Russell Ph.D.[1,2,3]
University of Virginia, Depts of [1]Biomedical Eng., [2]Mechanical Eng., and [3]Orthopaedic Surgery, Charlottesville, VA, USA
Email : dooley@virginia.edu

Introduction

Over the last two decades, total ankle arthroplasty (TAA), also known as replacement, has become the increasingly popular surgical treatment of end-stage ankle joint arthritis. Despite reports of TAA having improved patient outcomes [1, 2], little has been done to examine how TAA affects the motion of adjacent joints within the foot. Ankle replacements aim to return patients to full function, though we do not know how they change internal foot motion. The present study utilizes the validated four segment (tibia (TB), hindfoot (HF), forefoot (FF), hallux) Oxford foot model [3] to examine the differences in the foot kinematics in patients before TAA compared to a group of healthy ankles.

Methods

Motion capture data has been collected for 7 controls (5M, 2F: 30 ± 9.1 y.o.) and 5 TAA candidates (4M, 1F; 63 ± 4.7 y.o.). Subjects performed four activities: (A) Walking over level ground (15m); (B) Climbing 3 stairs; (C) Descending 3 stairs; and (D) Walking over a 15-degree laterally-inclined surface. Foot kinematics were determined by implementing the Oxford foot model to calculate the HF-TB, FF-HF, and FF-TB angles.

Results and Discussion

When walking over level ground (*Fig 1A*), TAA candidates have decreased range of motion (ROM) in their HF-TB joint while increased ROM FF-HF, which generated similar motion FF-TB between TAA and controls. This shows how TAA candidates compensate for lack of ROM at the ankle with the midfoot.

When climbing stairs (*Fig 1B*), decreased dorsiflexion is seen in the HF-TB joint as well as the FF-HF joint, compounding to have decreased dorsiflexion FF-TB. This is consistent with clinical reports that TAA candidates have difficulty clearing stairs while climbing them. Similarly, the TAA candidates show decreased dorsiflexion, and overall ROM, while descending stairs (*Fig 1C*). Dorsiflexion while descending is a means to decrease the speed at which the following stair is struck. This decrease in dorsiflexion presents an increased risk of falling.

Walking on the tilted surface shows increased inversion at push off, compared to controls (*Fig 1D*). Excessive motion at this point suggests that TAA candidates need improved stability in the frontal plane, as well as sagittal plane, and ankle replacement methods should improve both of these degrees of freedom.

Replacing the joint intends to return the ROM to the ankle joint. This is hypothesized to relieve the compensations in the adjacent foot joints and improve the stability of the patient. Further work is necessary to investigate how the ROM of the foot and ankle change after TAA. If TAA patients perform similarly to the control group across all activities, it can be concluded that TAA is a highly effective means for treating ankle joint arthritis.

Significance

Utilizing the Oxford foot model provides a view of how each segment functions in relation to one another as well as how the entire foot works during ambulatory exercises. More challenging tasks were included here to stress the ankle joint in multiple ways. This highlights the model's overall utility to aid in understanding internal foot motion. Further, using this multi-segment model will allow for increased understanding of how adjacent foot joints react to TAA. This will ultimately allow us to design better ankle replacement mechanisms targeting the specific ROM and degrees of freedom most useful to ambulation in a variety of settings.

Acknowledgments

UVA MAMP Lab and Integra Life Sciences

References

[1] Philippe (2008) F&A Int. [2] Norvell (2019) JB&JS.
[3] Carson (2001) J. Biomech.

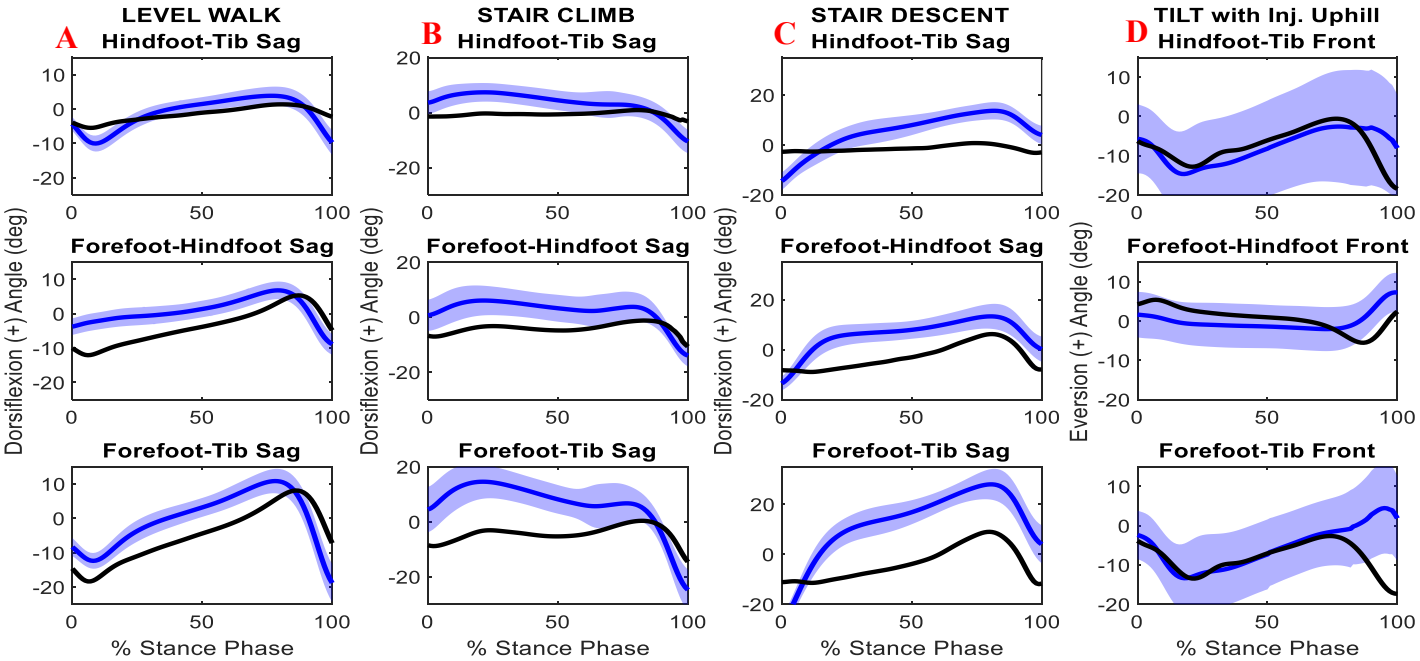

Figure 1. Kinematics of representative TAA patient (**black**) compared to the control database (**blue**) while performing four ambulatory activities.

GAIT SMOOTHNESS WHEN WALKING WITH AND WITHOUT VISION IN HEALTHY ADULTS AND INDIVIDUALS WITH MILD TRAUMATIC BRAIN INJURY

Nicholas Kreter[1], Selena Cho[1], Leland E. Dibble[1], Margaret W. Weightman[3], Lucy Parrington[2], Mark E. Lester[4], Carrie W. Hoppes[5], Laurie A. King[2], Peter C. Fino[1]
[1]University of Utah, Salt Lake City, UT
[2]Oregon Health & Science University, Portland OR
[3]Courage Kenny Research Center, Allina Health, Minneapolis MN
[4]Texas State University, Round Rock, TX
[5]Army-Baylor University Doctoral Program in Physical Therapy, For Sam Houston, TX
email: nick.kreter@utah.edu

Introduction

Sensorimotor impairments are common following mild traumatic brain injury (mTBI), and individuals may struggle with reweighting sensory information when one system is unavailable or unreliable.[1] For example, individuals with mTBI perform worse than healthy controls when sensory systems are challenged during static balance tasks.[2] How individuals with mTBI reweight sensory input during gait remains less clear.

During gait, humans rely heavily on vision to provide detailed information about features within the environment, the spatial orientation of the body, and the trajectory of movement.[3] Despite several investigation of the complex sensorimotor deficits during static balance following mTBI, the impact of mTBI on the use of visual information during gait remains unknown.

This study sought to compare gait smoothness and RMS acceleration, measures of movement control quality, in healthy adults and adults with persisting symptoms after mTBI when walking with and without vision. We hypothesized that the mTBI group would rely more on vision and exhibit a greater disruption to gait quality than the control group when walking with their eyes closed.

Methods

Forty-six healthy [33F, mean (SD) age = 31.91 (9.84) years] and forty-one concussed [33F, mean (SD) age = 33.14 (9.52) years, time since injury = 341 (298) days] adults across three different sites provided informed consent and participated in this IRB-approved study. As part of a larger study, participants completed an instrumented version of the Functional Gait Assessment (FGA). This abstract focuses on conditions one (gait on a level surface) and eight (gait with eyes closed) of the FGA.

Each participant was outfitted with inertial measurement units (IMUs) over the forehead, trunk, lumbar region, feet, and wrist to collect accelerations, angular velocities, and magnetic field potentials. Raw data were collected at a sampling frequency of 128 Hz. All data processing was done with custom MATLAB code (Matlab Inc., Natick Mass.). Data were aligned to the global frame and the start and end of movement were identified, and data during this time were isolated for analysis. The smoothness of angular velocity[4] and the root mean square (RMS) of linear acceleration were calculated for each axis of the head and lumbar sensors. Linear mixed-effects models were fit for each outcome with fixed effects for condition and group, their interaction, with random intercepts and slopes across condition by subject. A 0.05 significance level was used.

Results and Discussion

There were significant effects of condition on both smoothness and RMS. However, significant group effects were only present at the lumbar sensor. The mTBI group exhibited poorer smoothness about the pitch ($p<0.001$) and yaw ($p<0.001$) axes and smaller acceleration RMS values along ML ($p<0.001$) and vertical ($p<0.001$) axes. There were no significant interactions in any of the models tested.

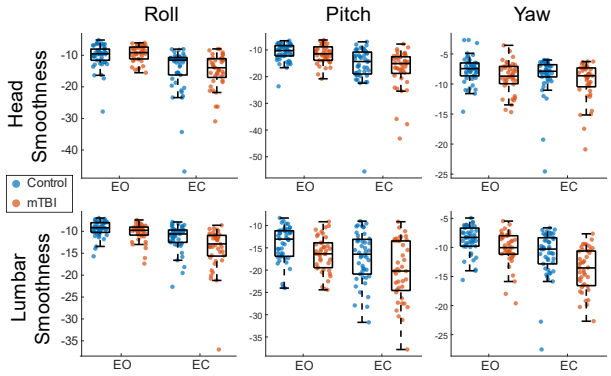

Figure 1: Comparison of healthy control (blue) and mTBI (orange) participant gait smoothness at head (top) and lumbar (bottom) sensors during eyes open (EO) and eyes closed (EC) walking tasks.

Both groups exhibited poorer smoothness and RMS of head and lumbar movement during the eyes closed walking task. The group differences we observed at the lumbar sensor are likely due to existing gait abnormalities in the mTBI group. But, the lack of any interaction effect does not support the idea that individuals with mTBI rely more on vision during gait. Given that concussed individuals sway more than healthy controls during static balance tasks without vision,[2] the lack of interaction between mTBI and condition in our study is surprising. However, vision plays a different role during gait than during static balance. While walking, vision is responsible for scanning the environment for upcoming obstacles and guiding foot placement when obstacles cannot be avoided. Participants were tested along a flat 6-meter-long walkway that may not have been challenging enough to force participants to rely on visual feedback. Future research may consider more complex environments.

Significance

Head and lumbar stability during gait is degraded by the absence of vison, however mTBI are not differntially affected.

Acknowledgments

This work was supported through the Congressionally Directed Medical Research Program (W81XWH1820049, PI: King).

References

1. Gera, G et al. *Mil. Med.* (2018) 183.sup_1:327-332.
2. Haran, FJ, et al. *J. Nneurotrauma* (2016) 33.7:705-711.
3. Patla, AE. *Gait Posture* (1997) 5.1:54-69.
4. Balasubramanian, S, et al. *JNER* (2015) 12.1:1-11.

REAL-TIME INTENT RECOGNITION ALGORITHM FOR ROBOTIC EXOSKELETONS VIA THE MAHALANOBIS DISTANCE

Taylor M. Gambon*, James P. Schmiedeler, and Patrick M. Wensing
All authors are from the University of Notre Dame
Corresponding author email: *tgambon@nd.edu

Introduction

Existing exoskeleton control strategies seek to identify the user's intended movements to better support that movement. While many rely on sensing the human directly through electrodes [1], recent work has shown that sensors already embedded in the exoskeleton are rich in intent-related information [2]. Taking the exoskeleton's motor encoder and commanded motor current signals as inputs, a new algorithm based on the Mahalanobis distance can indicate the user's desire to speed up or slow down [3]. While this algorithm has been tested with pre-recorded data from the EksoGT exoskeleton by Ekso Bionics, it has not yet been tested in real-time experiments. Pandemic constraints have driven real-time experiments to shift platforms to an XSens inertial motion capture suit that enables monitoring joint angles as subjects make speed changes while walking on a treadmill.

Figure 1: (Left) The EksoGT and its associated onboard signals. (Right) The XSens inertial motion capture suit and its associated signals.

Methods

In this pilot work, a single, healthy, male subject donned the XSens suit (Fig. 1) and first provided a five-minute training set of data by walking on a treadmill at a constant speed of 1.4 m/s. The XSens reports the left/right hip/knee angles in real time. A model of this subject's gait was formed by finding the mean and covariance matrices of these four signals for each time step of each gait phase. Next, the subject performed a series of intent changes by beginning to walk at 1.4 m/s for 15 s, increasing speed to 1.7 m/s for 15 s, and then returning to 1.4 m/s. This cycle was repeated three times. As the user made these speed changes, the intent recognition algorithm compared the incoming signals to the trained model by taking the squared Mahalanobis distance M between the model and the incoming datapoint,

$$M^2 = (\bar{x} - \bar{\mu})^T \Sigma^{-1} (\bar{x} - \bar{\mu})$$

where x is the new datapoint and the mean and covariance matrix of the model are μ and Σ, respectively. When M exceeded a pre-set threshold determined based on the average value of M from the training data set, the algorithm indicated a change in intent. Once indicated, the type of intent change (speed up/slow down) was determined based on timing discrepancies between the model and data. If more/less time was spent in a gait phase than expected from the model, a slow down/speed up was indicated.

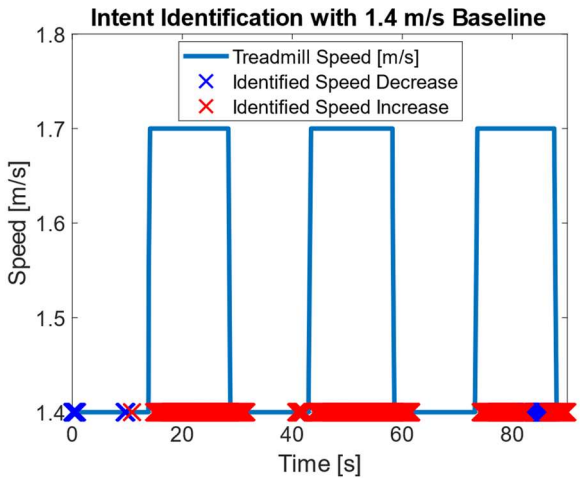

Figure 2: Representative output of the intent recognition algorithm.

Results and Discussion

The results illustrate that although the algorithm briefly mis-identified a slow-down intent change at several points during the trial (blue X's in Fig. 2), it was generally quite successful at indicating the user's desire to increase gait speed when the treadmill speed increased to 1.7 m/s (red X's inside the step increases in speed in Fig. 2). With 80% correct responses, the accuracy of the algorithm in recognizing intent change suggests that it may be successful at identifying speed changes less than the 0.3 m/s change shown here. The algorithm also correctly stops indicating an intent change when the user returns to walking at the same speed as in the training set (absence of X's in the gaps between step increases in speed in Fig. 2). Continued work includes the expansion to a larger number of human subjects and increasing to a total of 18 trials including three repetitions each of a small (0.1 m/s), medium (0.2 m/s), and large (0.3 m/s) increase/decrease in speed. The overall accuracy, time delay, and sensitivity of the algorithm will be assessed across subjects.

Significance

The ability to identify the user's intended gait speed will allow for a more user-friendly exoskeleton interface. Future control strategies will allow the user to fluidly and automatically change speeds to fit their desires, whether that is to get from point A to point B as quickly as possible or to match speeds with a companion. This would be especially empowering for individuals with a spinal cord injury since it could enable the device to sense the desire to change speed even when a user is unable to enact the speed change themselves.

Acknowledgments

This work is supported in part by the National Science Foundation under grant IIS-1734532.

References

[1] Tucker, et. al. *J Neuroeng Rehabil*, 12(1):1-30, 2015.
[2] Gambon, et. al. *IEEE Access*, 8:224071-224082, 2020.
[3] Gambon, et. al. *Proc. IEEE BioRob*, 1115-1121, 2020.

RELATIVELY SHORTER MUSCLE FASCICLES INCREASE THE METABOLIC COST OF CYCLIC FORCE PRODUCTION

Owen N. Beck[1*], Jordyn N. Schroeder[1], Lindsey H. Trejo[1], Jason R. Franz[2], & Gregory S. Sawicki[1]
[1]Schools of Mechanical Engineering & Biological Sciences, Georgia Institute of Technology, Atlanta, GA, USA
[2]Dept. Biomedical Engineering, University of North Carolina & North Carolina State University, Chapel Hill, NC, USA
Email: *obeck3@gatech.edu

Introduction

During locomotion, force-producing limb muscles are largely responsible for the whole-body's metabolic rate. One parameter that is not often considered to have a *measurable* effect on whole-body metabolism is relative muscle fascicle length. Perhaps, that is because muscle length is typically studied during steady isometric contractions [1], and it is difficult to isolate the metabolic effect of muscle length from other parameters during locomotor-like contractions (*e.g.,* mechanical work). To help link locomotion biomechanics to metabolic rate, our goal was to determine the metabolic influence of cyclically producing force at different muscle fascicle lengths (Fig. 1). We hypothesized that cyclically producing the same average force at relatively shorter fascicle lengths would increase metabolic rate.

Methods

Nine human participants cyclically produced ankle moments for five-minutes at two-distinct magnitudes and at three separate ankle angles (90°, 105°, 120°) on a fixed dynamometer using their soleus (Fig. 1). During these trials, we collected metabolic data, dynamometer torque data, motion capture data, soleus fascicle length and pennation angle via ultrasonography, and surface electromyography. We used linear mixed models and regressions to test the associations between independent and dependent variables (α=0.05).

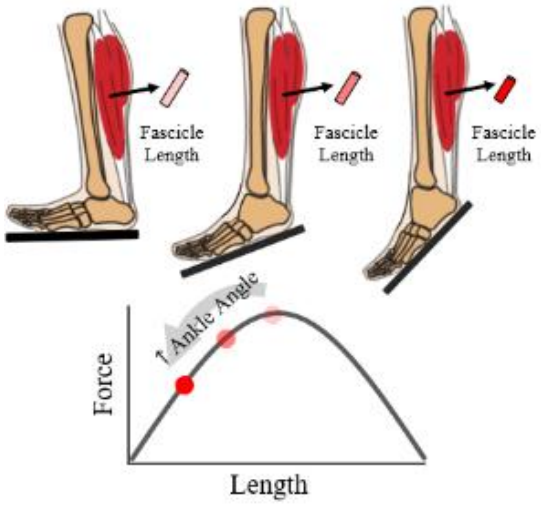

Figure 1. Three ankle angles (90°, 105°, and 120°) with the corresponding hypothetical soleus fascicle operating length and its region on a force-length curve.

Results & Discussion

Participants produced two distinct cycle average ± SD ankle moment magnitudes: 4.85 ± 0.72 Nm and 6.58 ± 0.94 Nm ($p<0.001$) (black & red symbols, respectively; Fig. 2). In each moment magnitude, the duration of active force production ($p\geq0.158$), force production cycle frequency ($p\geq0.375$), and cycle average ankle moment ($p\geq0.678$) were indistinguishable across ankle angles. Cycle average soleus fascicle force was unchanged within the lower ankle moment magnitude ($p=0.063$), but it increased with greater ankle angles within the higher ankle moment magnitude ($p=0.003$) due to systematic changes in Achilles tendon moment arm lengths [2]. Despite producing non-different and less cycle-average fascicle force within the lower and higher levels respectively, increasing participant ankle angle reduced average soleus fascicle length by 16% ($p<0.001$) and increased net metabolic power by 189% and 228%, respectively ($p<0.001$) (Fig. 2). Across moment magnitudes, metabolic power was not driven by fascicle mechanical work ($p=0.591$), fascicle force rate ($p\geq0.235$), or active muscle volume ($p\geq0.122$) [3]. Alternatively, supporting our hypothesis, net metabolic power was inversely related with participant average soleus fascicle operating length ($r=-0.72$ $p<0.001$).

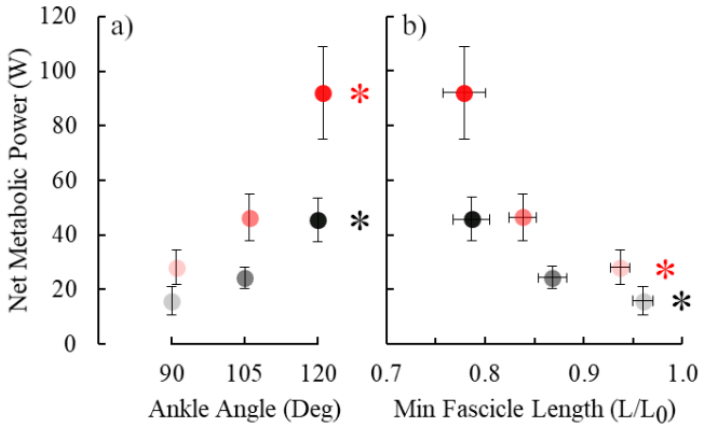

Figure 2: Average ± SE net metabolic power versus a) ankle angle & b) minimum soleus fascicle length. Black and red symbols indicate lower and higher ankle moment magnitude, respectively. Asterisks (*) indicate statistical significance ($p < 0.05$).

Significance

Enabling active muscle fascicles to operate at longer lengths may decrease metabolic rate during locomotion. These findings may help resolve why metabolic rate differs across and within animal species, in addition to informing biomechanical interventions that reduce user metabolic rate and consequently augment locomotor performance.

Acknowledgments

Supported by an NIH NIA fellowship (F32AG063460) to O.N.B. and an NIH NIA grant (R0106052017) to J.R.F. and G.S.S.

References

1. Hilber et al. (2001) *J Physiol* **531**: 771-80.
2. Bobbert et al. (1986) *J Biomech* **19**: 887-98.
3. Beck et al. (2019) *Exerc Sport Sci Rev* **47**: 237-45.

EMBODIED EFFECTS OF MUSIC ON POSTURAL CONTROL AMONG ADULTS WITH CONCUSSION

L. Worthen-Chaudhari[1], K. Quatman-Yates [2], E. Costa-Giomi[3], and W Mysiw[1]
[1]The Ohio State University Department of Physical Medicine & Rehabilitation
[2]The Ohio State University School of Health & Rehabilitation Sciences
[3]The Ohio State University Department of Music
email: *liseworthen@gmail.com

Introduction

Traumatic brain injury (TBI) can result in persistent deficits that impair functional skill and quality of life. The Lancet Neurology Commission reports that about half the world's population will sustain at least one TBI over their lifetime with consequences including loss of fundamental human functions such as movement, concentration, and emotional regulation [1]. Furthermore, the impact of neurotrauma extends to the social network of caregivers for TBI survivors (e.g., spouse, partner, family member), indicating an impact to society beyond loss of independence for the individual who is injured[1]. Alleviating chronic symptoms among persons with TBI is an important goal.

One potentially novel avenue through which we might be able to treat motor control deficits resulting from TBI involves active listening to rhythmic music. Current theories of music cognition predict that listening to music might improve both balance and pain for humans through mechanisms such as vestibular system [2–7], dopamine [8], and/or oxytocin [9] stimulation. Indeed, music that scored high in "groove", as measured by Janata's validated musical groove rating method, was found to regulate postural control responses in a healthy population[10]. However, no research to date has established the embodied effect of music on chronic motor deficits associated with TBI. Listening to music might prove to be a simple treatment for the persistent postural control deficits [11] experienced by persons with TBI[12].

The objective of this pilot project was to establish basic evidence regarding the impact of listening to music on postural control among adults with mild TBI (mTBI). We hypothesized that listening to music would modulate postural control while concussed individuals performed a task of quiet standing with eyes closed.

Methods

This research protocol was approved by The Ohio State University Institutional Review Board. Participants were recruited from The Ohio State University Physical Medicine and Rehabilitation Department outpatient concussion clinic. Eight adults (a) met criteria of 3-48 months post date of injury with persistent, chronic balance and pain symptoms (b) agreed to consent and (c) were able to perform the task of quiet standing with eyes closed for 30s. All participants (n=8) were unable to return to work following the concussion event. Postural control data was collected for 30s per condition, on 3 to 5 different days per participant (repeated measures) as described elsewhere [13].

We collected quiet standing with eyes closed (QEC) first and quiet standing with eyes closed and music playing (QEC_m) second in all cases. As described elsewhere[15], participants were instructed to close their eyes after the researcher counted down "3-2-1" for both conditions, For QEC_m conditions, we used Tango music. Per Ross et al. (2016), we instructed participants to listen to the beat of the music for approximately 15 seconds in order to acclimatize to the rhythm before commencing the countdown to close their eyes[10]. Per Will and Berg (2007) we used songs with a cadence of approximately 120 bpm, the periodic acoustic pace found to optimize central auditory-motor entrainment. Specifically, we played one of two songs for every data collection session: La Cumpartisa (118bpm) or La Maleva (125bpm).

Center of Pressure (COP) data were calculated as described elsewhere[13–15]. The following variables were calculated: COP area (COPa), COP mean velocity resultant (COPvelr), and COP variability resultant (COP_RMSr). Variables were analyzed across all data collection sessions using a paired t-test with Holms-Bonferroni post hoc correction (QEC v QEC_m).

Results and Discussion

Relative to performing QEC in silence, listening to Tango music while performing QEC was associated with reduced COP_RMSr ($p=0.001$), COP_velr ($p=0.002$), and COPa ($p=0.009$). Thus our hypothesis was found to be true within this cohort of n=8 adults with chronic concussion symptoms. We believe this to be the first evidence that music has the capacity to modulate postural control in the concussed human system.

Significance

The potential to modulate postural control simply by listening to music has exciting implications for treatment of motor control deficits among individuals with mTBI. More research is needed to explore the potential to induce positive train effects, simply through listening to music whether in a standing position, as in this research, or in a seated position. For chronic TBI neurorehabilitation, during which individuals may cycle between being immobilized and ambulatory, the ramifications of listening to music while seated as a treatment for postural control could be revolutionary.

Acknowledgments

This research was funded by a Pilot Grant from The Ohio State University Chronic Brain Injury (CBI) Discovery Theme Initiative as well as by The Ohio State University Department of Physical Medicine and Rehabilitation.

References

[1] Maas, et al., The Lancet Neurology (2017).
[2] Phillips-Silver & Trainor, Br & Cog 67 (2008) 94–102.
[3] Phillips-Silver & Trainor, Science 308 (2005) 1430.
[4] Todd & Cody, J Acoustic Soc Am 107 (2000) 496–500.
[5] Todd & Lee, Front Hum Neurosci 9 (2015) 444.
[6] Todd, et al., Hearing Research 309 (2014) 63–74.
[7] Todd, et al., Hearing Research 141 (2000) 180–188.
[8] Salimpoor, et al., Nature Neurosci. 14 (2011) 257.
[9] Grape, et al., Int Phys & Behav Sci. 38 (2002) 65–74.
[10] Ross, et al., J Exp Psy. 42 (2016) 308.
[11] Quatman-Yates, et al., Ped PhysTher 27 (2015) 316.
[12] Lahz & Bryant, APMR 77 (1996) 889–891.
[13] Worthen-Chaudhari, et al., G&P. 64 (2018) 141–146.
[14] Worthen-Chaudhari, et al. Clin Bio. 70 (2019) 257–264. https://doi.org/10.1016/j.clinbiomech.2019.08.010.
[15] Reed, et al., Plos One. 15 (2020) e0237246.
[16] Will & Berg, Neurosci Lett. 424 (2007) 55–60.

EFFECT OF PERTURBATION ON BRAIN ACTIVATION AND WALKING PERFORMANCE IN OLDER ADULTS WITH AND WITHOUT OSTEOARTHRITIS

Alka Bishnoi[1*], Yang Hu[1], and Manuel E. Hernandez[1]
[1]Department of Kinesiology and Community Health, University of Illinois at Urbana-Champaign, IL
Email : *abishn2@illinois.edu

Introduction

Falls and mobility impairment are the leading cause of injury among older adults and they are induced most frequently during walking [1]. Slipping and tripping during walking are most common causes of falls in older adults, representing failure to react to challenges in environment [2]. It can lead to more severe consequences in older adults with osteoarthritis (OA), who are already suffering from balance and gait impairment in daily life. However, it is still unknown if these perturbations have an effect on brain activation in older adults with and without OA.

This is the first study exploring the differences in brain activation during walking perturbations in adults with and without OA. We are also interested in seeing change in walking performance before and after perturbation. We hypothesize that 1) there will be increase in prefrontal cortical (PFC) activation during perturbation tasks relative to normal walking tasks; 2) there will be differences in prefrontal cortical activation among older adults with and without OA, particularly during perturbation tasks; 3) lastly, there will be changes in walking performance including stride time, stance time, stride length and stride width after perturbation tasks.

Methods

Nine older women with OA (OA group) and eleven older women without OA (HOA group) participated in this study. Participants walked on an instrumented treadmill (C-Mill 3Q treadmill, Forcelink, Inc.) with a predefined comfortable walking speed during normal walking trials (N1, N2) and two perturbation walking trials (P1, P2) while wearing functional near infrared spectroscopy (fNIRS) headband. PFC activation levels (oxygenated hemoglobin (HbO_2) and deoxygenated hemoglobin (Hb)) were recorded using fNIRS (fNIRS Imager 1200 system (fNIR) devices) during this order of trials: N1, P1, P2, N2. In each perturbation trial, custom belt speed profiles were used to simulate slips at pseudorandom intervals between 5 and 25 s, which subjects were asked to recover from as best as possible. Stride length, Stride time, Stride width, Stance time were extracted by customized Python scripts from center of pressure data recorded by the instrumented treadmill.

N=20	OA (N=9)	HOA (N=11)	P-value
Age (yrs)	67.9±3.33	69.33±6.17	>0.05
Gait speed (m/s)	1.23±0.32	1.41±0.31	<0.001
Womac pain score	3.74	0.35	<0.001
BMI	27.84	21.83	<0.001

Table 1 reported the descriptive characteristics of the participants

Results and Discussion

Consistent with hypothesis, linear mixed model analysis showed that PFC activation levels differed significantly during the perturbation tasks relative to normal walking tasks in both cohorts even after controlling for covariates (Gait speed, Womac score and BMI). Further, a significant interaction between cohort and task in P2 was found, as reported in Table 2.

Main Effects & Interaction (HbO_2)	β	SE	P-value
Task: P1	0.539	0.143	0.0001
Task: P2	1.424	0.138	<0.001
CohortOA : TaskP2	-0.500	0.238	0.036
Hb			
Task: P2	-0.359	0.136	0.001
CohortOA : TaskP2	-0.534	0.196	0.006

Table 2 reported the estimate (β) and standard error (SE) of PFC activation levels (HbO_2 & Hb) among both cohorts.

In addition to these increases in PFC activation in perturbation trials, we also found change in walking performance after perturbation. Post hoc analysis showed that there were PFC activation differences in between the tasks among both cohorts, but no overall changes between cohorts were found (Figure 1).

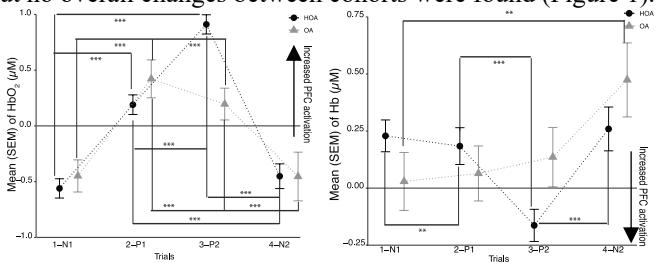

Stride time (β=0.025, SE=0.009, p=0.01), stance time (β=0.016, SE=0.006, p=0.01), and stride length (β=0.015, SE=0.007, p=0.04) changed significantly going from N1 to N2 trials for both cohorts, but no significant changes in stride width (β=0.004, SE=0.04, p=0.99) were found.

Significance

This is the first study examining the differences in PFC activation during normal walking and perturbation walking trials among older adults with and without osteoarthritis. The main outcome from this study was that we saw increases in PFC activation among both cohorts in perturbation tasks, and particularly by OA during the second perturbation trial, relative to normal walking trials. This is further explained by changes in their walking performance after perturbation as seen in stride time, stance time and stride length.

A short bout of perturbation trials led to increased brain activation and better walking performance in older adults. This research adds into the importance of using perturbation training in rehabilitation protocols in older adults. While we didn't see any overall differences in between cohorts, the increased brain activation observed in P2 by older women with OA merits further investigation.

Acknowledgments

We would like to thank all of the subjects and the MFPRL OA research team for their contributions to the study.

References

[1] Terroso et al. *Eur Rev Aging Phys Act*. 2014; 11(1):51-59
[2] Robinovitch et al. *Lancet*. 2013; 381(9860);47-54.

Cosimulation of the Extensor Hood with Finite Element and Musculoskeletal Models

*Christopher T. Jadelis[1], Derek Kamper[2], Katherine R. Saul[1]
[1]Department of Mechanical and Aerospace Engineering, North Carolina State University, Raleigh, NC, USA
[2]Joint Department of Biomedical Engineering, North Carolina State University and UNC-Chapel Hill, Raleigh, NC, USA
Email: *ctjadeli@ncsu.edu

Introduction

Evaluating manual dexterity and understanding the underlying mechanics responsible for hand function have long been foci of disability research [1]. Musculoskeletal modeling of the hand and fingers is one strategy that has been applied to explore hand dynamics and effects of injury or disease [2,3]. Anatomical factors such as small inertia, physiological pulleys, and viscoelastic damping from complex soft tissues, however, make traditional multibody dynamic approaches challenging [4]. The extensor mechanism of each finger is one such factor; it has multiple muscle insertions, varying stiffness, and ligamentous adhesions [5] which are not well captured by current models that typically assume a single tendinous insertion for a given muscle. To address this, our goal was to explore a cosimulation approach to integrate a rigid body dynamic model of the index finger with a finite element model of the extensor mechanism.

Methods

A previously developed rigid body musculoskeletal model of the hand, index finger, and thumb [2] implemented in OpenSim (v3.3) was adapted and integrated with an existing finite element (FE) model of the index finger extensor hood [6] implemented in FEBio. The FE model represents insertions for 4 muscles and includes the central slip (CS), terminal slip (TS), and adhesions, using material properties defined by [5]. Integration between the OpenSim and FEBio models was achieved using a custom MATLAB script. Simulations were designed to replicate a prior cadaveric experiment in which individual muscle tendons were loaded and the resulting fingertip forces recorded [7]. A forward dynamics simulation was initiated in the OpenSim model in which an excitation was applied to an individual muscle (extensor digitorum communis (EDC) or extensor indicus (EI)) so as to match the forces used in the cadaver study. The fingertip was fixed via a contact constraint (**Fig. 1**), and the predicted fingertip force was recorded as a baseline.

During cosimulation, the simulated muscle force from the rigid body simulation was applied as an initial condition on the corresponding muscle tendon in the FE model. Resulting reaction forces generated at the CS and TS attachments to the bones in the FE model were extracted. CS and TS forces were then applied to the OpenSim model as external forces in place of muscle actuators. The resulting fingertip forces were then compared to the simulation results from the rigid body dynamic model alone, as well as to the experimental forces to evaluate whether the cosimulation approach altered predicted fingertip forces.

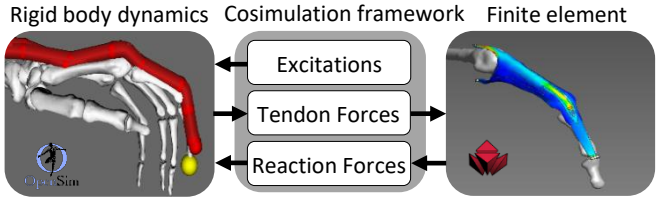

Figure 1. Flow of information used in the combined cosimulation model

Results and Discussion

Fingertip forces predicted with the cosimulation approach fell within 0.262N of the mean experimental values but tended to overpredict fingertip forces (cosimulation force greater than mean plus one standard deviation of experimental values, **Fig. 2)**. Cosimulation fingertip force vectors were oriented in the same direction as the rigid body simulation alone, which was within the experimental range for EDC but not EI. The forces generated by the FE model at TS and CS insertions had a force ratio (TS:CS) of 1.55, which was similar to the experimentally measured ratio of 1.7 [8].

This work provides a mechanism by which influence of complex soft tissue structures best evaluated in an FE framework can be incorporated into rigid body dynamic simulations better suited to exploring motor control. Limitations of the models include isotropic material assumptions. Simulations are sensitive to finger posture; small differences in equilibrium postures between FE and rigid body models may cause larger differences in predicted force. Current simulations examine a static task with a constrained fingertip; dynamic tasks, coordinated muscle activity, and finger motion will be explored in the future.

Significance

These models present a new method for simulating the complex extensor mechanism of the finger while integrated with rigid body dynamic modeling. This work can be applied to explore the effects of disease and injury states pertinent to the extensor mechanism on overall finger and hand function.

References

[1] M. T. Duruöz, *Hand Function*, 2014, pp. 41–51.
[2] A. J. Barry et al. *Biomech*. **77**, pp. 206–210, Aug. 2018.
[3] B. I. Binder-Markey et al. *J. Hand Surg*. **44**, Sep. 2019.
[4] B. I. Binder-Markey et al. *Biomech*., **61**, Aug. 2017.
[5] K. Qian et al. *Biomech*. **47**, Sep. 2014.
[6] B. Ellis et al. American Society of Biomechanics, 2011.
[7] D. Qiu. Illinois Institute of Technology, 2014.
[8] S. W. Lee, et al. *Biomech. Eng*. **130**, Oct. 2008.

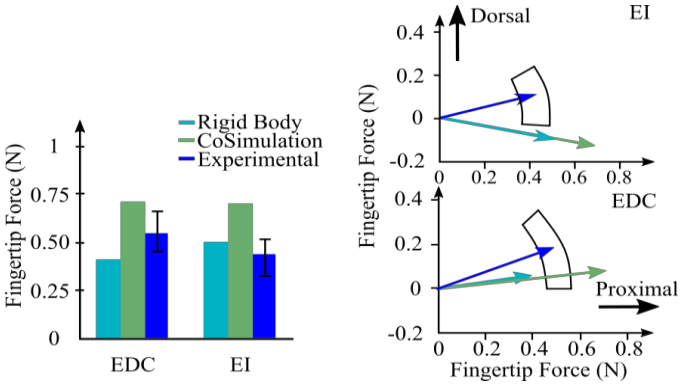

Figure 2. Fingertip forces for the rigid body dynamic musculoskeletal model and co-simulation model compared to experimental forces (Left: Magnitude. Right: force vectors in the sagittal plane ± 1 SD).

Influence of Fatigue on Postural Strategies to Gait Initiating Perturbations

D. Clark Dickin[1], Henry Wang[1], Matthew McClain[1]
[1]Biomechanics Laboratory, Ball State University, Muncie, Indiana USA
Email: dcdickin@bsu.edu

Introduction

Falls and fall-related injuries are a major concern for older adults and those with neuromuscular or musculoskeletal impairments[1]. Injuries resulting from a fall can include severe-fractures, internal injuries, and concussions. One way to assess postural stability is to perturb the support surface on which an individual stands[2]. During normal stance, an individual maintains their center of mass (COM) within their base-of-support (BOS). However, during a postural perturbation the COM is displaced and depending on the magnitude of the perturbation the response may necessitate a change in ones BOS. An individuals (in)stability is further exacerbated when experiencing muscular fatigue and can significantly alter postural control. Muscle fatigue can also influence gait mechanics and further increase the potential risk of falling. By understanding the internal and external factors contributing to postural control when challenged, clinicians can further improve the standard of care used to reduce overall fall risk.

Thus, the purpose of this study was to induce a postural perturbation during upright stance requiring an initiation of gait in rested and fatigued states. It was hypothesized that factors associated with gait stability and initiation would be impaired following muscle fatigue but would return towards baseline within 20 minutes of recovery. More specifically it was hypothesized that muscle fatigue would increase trunk lean, increase time to toe-off and initial foot-strike and increase loading rate of the first recovery step.

Methods

15 healthy young adults (7 female) participated in the study. Retroreflective markers were placed on body landmarks using a modified plug-in-gait with the addition of thigh, shank and pelvis clusters. To warm-up and familiarize with the treadmill participants walked for 5-minutes at 1.0 m/s (2.24 mph). Following the warm-up, 10 postural perturbation trials were performed on a force-instrumented treadmill that accelerated to 1.0 m/s in approximately 150 ms and continued for five seconds[3]. Immediately following the pre-fatigue perturbations, participants began the fatigue protocol consisting of a series of 3-minute bouts of the Queen's College Step Test and 1-minute bouts of bodyweight squats (both at 22 cycles per minute) until fatigued. Fatigue was determined participants failed to jump of at least 80% of maximum counter-movement vertical jump (MVJ) height. Post-fatigue testing consisted of 5-immediate post-fatigue perturbations, and five perturbations at 10- and 20-minute post fatigue. Data were analyzed using separate RM-ANOVA's for trunk lean at toe-off and foot-strike, time to toe off and foot-strike, and initial foot strike loading rate across the four times (PrePert, PostPert, 10Pert, 20Pert). Follow-up pairwise contrasts were performed where appropriate. Significance was set at $p \leq 0.05$ for all tests.

Results and Discussion

Significant differences were revealed for trunk angle at foot strike ($p=.05$) and the initial recovery step loading rate ($p=.001$). Follow-up contrasts revealed differences between PostPert and both 10Pert and 20Pert for trunk angle; and between PrePert and all Post perturbation conditions for loading rate. Trunk angle was more flexed immediately following fatigue but became more extended (upright) during the 10- & 20-minute recovery times. A more extended trunk position has been suggested to be a strategy used to assist in the control of whole-body angular motion (4) and may reflect a more restricted postural control strategy by limiting trunk motion during the initial recovery period. Reductions in loading rate across all post-fatigue trials suggest a more constrained initial step despite no significant differences in the timing of toe-off or foot-strike. Further analyses of joint kinetics and kinematics and muscle activation patterns may further delineate differences in gait initiation strategies adopted in response to muscular fatigue. Additional studies in older adult populations will further delineate differences in postural responses as a function of both age and fatigue.

Significance

Altered responses in trunk angle and loading rate following postural perturbation in a fatigued state provides preliminary insight into postural challenges necessitating a change in the base of support. Especially when overall strength is reduced (e.g., aging, musculoskeletal or neuromuscular disease, fatigue) understanding the differences in the mechanics of gait initiation may help to better design training interventions to help those at risk for falls.

References

1. Verma SK, et al., *PLoS One* 11(3): e0150939, 2016
2. Horak FB, et al. *Physical Therapy* **77**, 517-533, 1997.
3. Owings TM, et al. *Clinical Biomechanics,* **16**, 813-819, 2001.
4. Aminiaghdam et al., *PLoS One* 12(12); e0190135, 2017

Table 1: Summary data for postural perturbation responses following muscular fatigue

	Trunk Angle Toe-Off (deg)	Trunk Angle Heel-Strike (deg)	Time of Toe-Off (ms)	Time of Heel-Strike (ms)	Loading Rate (BW/s)
PrePert	7.85 (5.20)	13.77 (5.27)	0.24 (0.015)	0.43 (0.038)	33.76 (21.62)
PostPert	7.99 (4.57)	14.54 (4.89)	0.25 (0.029)	0.43 (0.043)	27.87 (16.62)
10Pert	7.68 (4.53)	13.15 (4.74)	.024 (0.016)	0.42 (0.034)	26.16 (19.12)
20Pert	7.47 (5.13)	12.49 (5.24)	0.25 (0.016)	0.42 (0.035)	24.35 (15.12)

ADIPOSE CHAMBER SIZE AND AUTOMATED FEATURE EXTRACTION IN DIABETIC PLANTAR SOFT TISSUE

Lynda Brady[1, 2], Yak-Nam Wang[1,5], Eric Rombokas[1,2,3], and William R. Ledoux[1,2,4]
[1]CLiMB, VA Puget Sound, Seattle, WA; Depts of [2]Mechanical Engineering, [3]Electrical Engineering, and [4]Orthopaedic Medicine,
[5]CIMU, Applied Physics Lab, University of Washington,Seattle, WA; University of Washington, Seattle, WA
email: lybrady@uw.edu

Introduction

Diabetes mellitus (DM) affects 9.4% of the U.S. population, and an additional 33.9% are pre-diabetic [1]. Lower extremity ulceration is a serious complication contributing to 108,000 amputations per year [1]. However, the mechanism of injury in ulceration is still unclear, making preventative treatment difficult. Within the plantar soft tissue, there is a superficial layer of adipose containing 'microchambers' of adipocytes, and a deep layer with 'macrochambers'. While these layers have been a benchmark for ultrasound mechanical studies [2], the chamber size has yet to be quantified. The purpose of this study was to measure these chambers and use an exploratory classification neural network to identify differences by disease state.

Methods

Plantar soft tissue specimens were obtained from 17 fresh cadaveric feet (6 DM, 11 non-DM, age 61-79 yr), sectioned, and prepared for histological analysis with Modified Hart's stain for elastin [2]. Digital whole-slide images (WSI) were obtained using a Nikon Eclipse i80 and a 12.6 megapixel digital camera.

WSI with significant plating artifacts were excluded from morphological analysis. If the muscle layer separating the superficial and deep adipose layers was present, superficial and deep adipose chambers were compared in addition to the disease state analysis. If the layer was absent, only the disease state analysis was performed. Full-size WSI were segmented by a modified U-Net [3] with a 50% tile overlap, and morphology characteristics area, perimeter, eccentricity, minimum and maximum diameter were calculated from segmented WSI using custom MATLAB code. Differences between groups were assessed with a 2-tailed Welch's t-test.

For classification, WSI were down sampled to 224x224 pixels using bicubic interpolation for input into the axial-deeplab network [4], which approximates a transformer by using row-wise and column-wise self-attention in sequential layers. The network attention was visualized using the Score-CAM method [5], and areas of attention were qualitatively assessed for patterns.

Results and Discussion

Adipose chambers were smaller on average in the superficial adipose layer compared to the deep layer for all size parameters ($p<0.01$ for all). This trend was consistent when data were split by disease state (Table 1). Adipose chambers in diabetic specimens were smaller on average than those in non-diabetic specimens ($p<0.01$). However, this phenomenon was stronger in the deep layer (Table1).

The network was able to achieve reasonable validation accuracy (84%, 18% above random) but did not provide consistent feature localization patterns. The areas of the image attended to by the network contained a variety of features from a variety of tissues within the image. Additionally, the network highlighted different areas on adjacent slices (Figure 1).

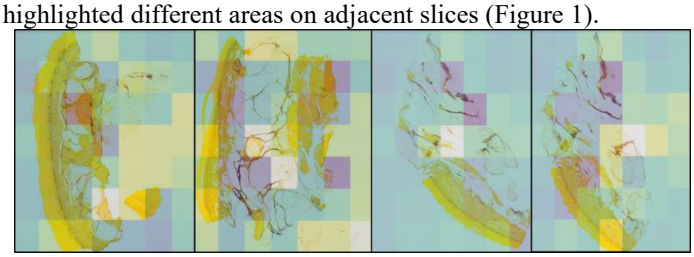

Figure 1. ScoreCAM of attention layer for example images. The network picks out different features on different images and on adjacent slices.

This transformer-style attention may be a poor architecture for identifying new features. A different attention classification network may provide more consistent human-interpretable features.

Significance

This quantitative work supports the common designation of smaller adipose chambers in the superficial adipose layer, and larger chambers in the deep layer of the plantar soft tissue. Additionally, this work demonstrates that these chambers are smaller in diabetic plantar soft tissue, particularly in the deep adipose layer. With the thicker, frayed elastic septae seen in diabetic samples [3], smaller adipose chambers may contribute to the increased modulus seen in diabetic adipose tissue in [6]. While the classification network with attention investigated did not yield novel features, such a technique could enable rapid discovery of clinically meaningful disease characteristics.

Acknowledgments

We would like to acknowledge Alyssa Ricketts and Christina Stender for help with image acquisition and exclusion analysis.

References

[1] CDCP. (2017) *National Diabetes Statistics Report*; US DHHS.
[2] Hsu, H. et al. (2007). J Appl Physiol. **102**(6):2227-31
[3] Wang, Y N et al. (2017). *Foot (Edinb),* **33**: 1-6
[4] Ronneberger, O et al. (2015). *Springer LNCS*, **9351**:234-241.
[5] Wang, H et al. (2020). *ECCV*.
[6] Pai, S and Ledoux, W. (2010). J Biomech. **43**(9): 1754-1760.

		Area (mm^2)	*Min Diameter (mm)*	*Max Diameter (mm)*	*Perimeter (mm)*	*Eccentricity*
Superficial	*Diabetic*	0.094	0.180	0.363	0.534	0.788
	Non-Diabetic (p)	0.108 (0.03)	0.184 (0.28)	0.376 (0.45)	0.540 (0.75)	0.797 (0.03)
Deep	*Diabetic*	0.211	0.247	0.498	0.753	0.790
	Non-Diabetic (p)	0.288 (<0.01)	0.276 (<0.01)	0.596(<0.01)	0.858(<0.01)	0.813(<0.01)
No Muscle	*Diabetic*	0.068	0.287	0.143	0.449	0.785
	Non-Diabetic (p)	0.151 (<0.01)	0.417 (<0.01)	0.206(<0.01)	0.617(<0.01)	0.796 (<0.01)

Table 1. Comparison of means for morphology parameters calculated.

Effects of forward forces at the center-of-mass on joint moments

Prokopios Antonellis*, Arash Mohammadzadeh Gonabadi, Kota Z. Takahashi, and Philippe Malcolm
Department of Biomechanics and Center for Research in Human Movement Variability
University of Nebraska at Omaha, Omaha, NE USA
email: *pantonellis@unomaha.edu, web: http://coe.unomaha.edu/brb

Introduction

Studies from Gottschall and Kram [1] and others [2,3] show that the metabolic cost of walking can be reduced using elastic tethers that provide constant forward forces at the waist. It was suggested that a future research direction could involve developing devices that allow assisting specifically during push-off. The present study investigated the joint moment mechanisms underlying the reduced metabolic rate of walking observed during non-constant, forward force profiles at the COM. We hypothesized that COM assistance during propulsion would result in higher reductions in positive ankle moment.

Methods

We developed a robotic waist tether that allows applying desired sinusoidal force profiles at the COM as a function of step time [4] (HuMoTech, Figure 1). Ten healthy participants walked on a treadmill at 1.25 $m \cdot s^{-1}$.

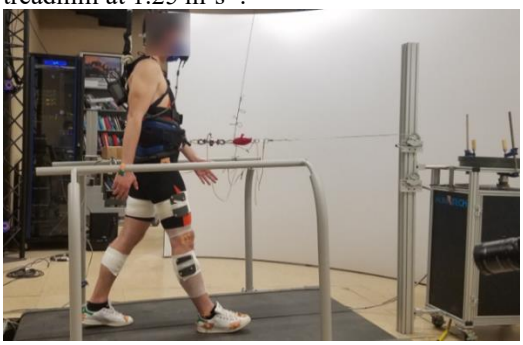

Figure 1: Experimental setup.

We tested 32 force profiles with different onset timings, durations, and peak force magnitudes. We measured joint kinetics (Vicon + Bertec) and metabolic rate (Cosmed).

Results and Discussion

The condition that minimized metabolic rate (48% reduction) had a peak force of 15% of body weight and a peak timing at 21% of the step (or at 11 and 61 % of the stride, i.e., during both double support phases). The metabolically optimal condition led to large decreases in peak plantarflexion moment and knee flexion moment that roughly coincided with the second actuation period during the second double stance. The metabolically optimal condition also reduced hip extension moment during the actuation period during the first double stance phase (differences between blue and black lines in Figure 2). Surprisingly, the condition that minimized metabolic rate led to increases in plantarflexion moment, knee extension moment, and hip flexion moment during the actuation period during the first half of stance. Thus, it appears that the combined effects of joint moment reductions at one portion of the gait cycle, with increases in joint moments at different portions of the gait cycle, can result in a net reduction in metabolic cost. Possibly this is because different muscles and movements have different metabolic costs; for example, the hip flexor moment - which was one of the increases - has been suggested to come mostly from tendon recoil and not cost any metabolic energy during normal walking [5,6].

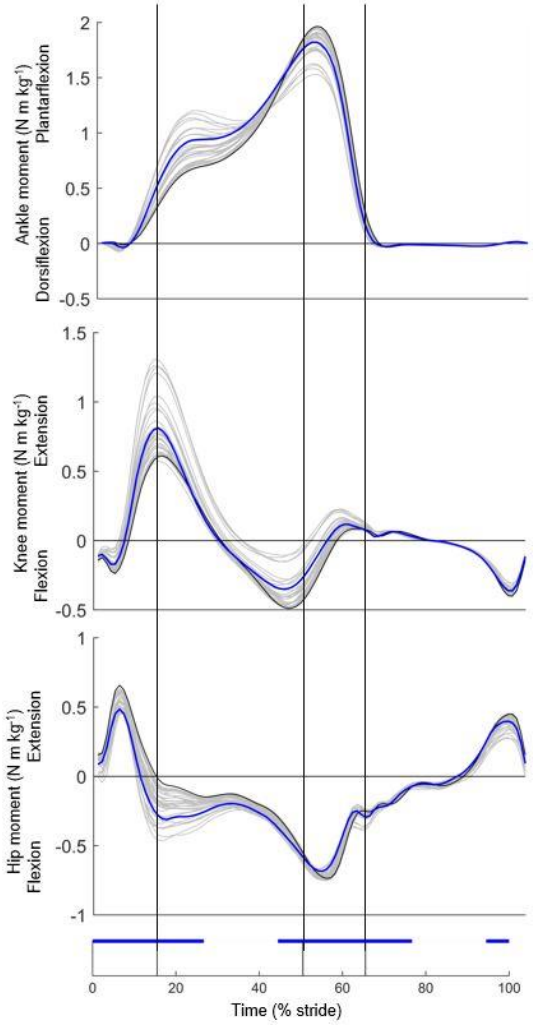

Figure 2: Joint moments. The thick gray line is the condition with zero aiding force. Blue line is the condition with the greatest reduction in metabolic cost. Gray lines represent all other conditions. Horizontal blue line shows the actuation periods of the condition with the greatest reduction in metabolic cost.

Significance

The finding that it is possible to reduce metabolic cost while increasing certain joint moments could be useful for exercise therapy in patients that require reducing metabolic cost while maintaining sufficient muscular effort.

Acknowledgments

EPSCoR OIA-1557417 and NIH P20GM109090. Graduate Research and Creative Activity and AMTI awards for PA.

References

1. Gottschall JS, Kram R. *J Appl Physiol*, **94**, 1766-1772, 2003.
2. Zirker CA, et al. *Appl Biomech*, **29**, 481-489, 2013.
3. Simha SN, et al. *IEEE TNSRE*, **27**, 1416-1425, 2019.
4. Gonabadi AM, Antonellis P, Malcolm P. *IEEE TNSRE*, **28**, 1353-1362, 2020.
5. Silder A, et al. *J. Biomech*, **40**, 2628-2635, 2007.
6. Gonabadi AM, Antonellis P, Malcolm P. *PLoS Comput Biol*, **16**, e1008280, 2020.

QUANTITATIVELY PRESCRIBED PASSIVE-DYNAMIC ANKLE-FOOT ORTHOSIS REDUCES TOTAL MECHANICAL COST-OF-TRANSPORT

Corey A. Koller[1,2], Darcy S. Reisman[1,3], and Elisa A. Arch[1,2]
[1]Biomechanics and Movement Science Interdisciplinary Program, University of Delaware, Newark, DE, USA
[2] Department of Kinesiology and Applied Physiology, University of Delaware, Newark, DE, USA
[3]Department of Physical Therapy, University of Delaware, Newark, DE, USA
email: ckoller@udel.edu

Introduction

Individuals post-stroke often have insufficient control of the shank's forward rotation during mid-to-late stance due to plantar flexor (PF) weakness [1]. Passive-dynamic ankle-foot orthoses (PD-AFOs) are commonly prescribed to these individuals post-stroke [2]. PD-AFO bending stiffness is a key orthotic characteristic that can assist the PFs [3] by providing the resistance needed to control the shank's forward rotation [2]. Controlling the shank's forward rotation allows mechanical energy to be stored that is returned during push-off to aid in forward progression [1]. Previous studies that have investigated AFO stiffness focused on standard-of-care AFOs (SOC-AFO) or AFOs with the same stiffness values for all participants [4,5]. We developed a prescription model that can quantitatively prescribe PD-AFO bending stiffness based on an individual's level of PF weakness [6]. We provided individuals quantitatively prescribed PD-AFOs to wear in the free-living environment for four-weeks. This study aimed to quantify and compare the gait strategies individuals post-stroke used to walk without their AFO, while wearing their SOC-AFO, and while wearing their quantitatively prescribed PD-AFO. We hypothesized that key joint-level biomechanical parameters (mean net peak paretic plantar flexion moment, mean paretic positive ankle joint work, mean paretic positive hip joint work) as well as global-level parameters (total mechanical cost-of-transport (COT), gait velocity) would improve (towards typical) while wearing the quantitatively prescribed PD-AFO compared to the other conditions.

Methods

Five individuals with chronic stroke (> six months post-stroke) underwent an instrumented gait analysis without wearing any AFO while walking at their self-selected walking velocity (No AFO velocity). From these baseline data, PD-AFO bending stiffness was prescribed based on each individual's level of PF weakness, and a PD-AFO with this stiffness was customized and manufactured for each participant [6]. Participants were given their PD-AFO to wear for four weeks after which time they returned to the lab to undergo another instrumented gait analysis while wearing their PD-AFO. Data were also collected as the participants walked with their SOC-AFO. While data were collected at the same velocity across conditions for each participant (No AFO velocity) to enable comparison of parameters across conditions, a 10-meter walk test was performed after each instrumented gait analysis to determine their self-selected gait velocity at each condition. This is the gait velocity parameter presented in the results. The joint-level biomechanical parameters and COT were calculated in Visual 3D software.

Results and Discussion

Five individuals post-stroke participated in the study (male: 2, age: 69.2 ± 4.8 yrs, mass: 82.3 ± 15.4 kg, height: 1.72 ± 0.1 m). The participants' average No AFO self-selected walking velocity was 0.55 ± 0.16.

All participants improved (decreased) their total mechanical COT and (increased) gait velocity while wearing the PD-AFO compared to wearing no AFO and their SOC-AFO (Table 1 – average results are presented in the table due to space limitations). However, only three out of five participants improved their net peak paretic plantar flexion moment and paretic positive hip work and none of the participants improved their paretic positive ankle work (Table 1).

Table 1: Participants' mean (± standard deviation) total mechanical COT, net peak PF moment, positive ankle joint work, positive hip joint work, and gait velocity across conditions.

Key Parameters:	No AFO	SOC-AFO	PD-AFO
Mechanical COT (J/kg/m)	2.400 ± 0.482	2.482 ± 0.639	2.217 ± 0.485
Net Peak PF Moment (Nm/kg)	-0.877 ± 0.250	-0.849 ± 0.248	-0.878 ± 0.241
Pos Ankle Joint Work (J/kg)	0.093 ± 0.015	0.068 ± 0.025	0.060 ± 0.028
Pos Hip Joint Work (J/kg)	0.103 ± 0.016	0.097 ± 0.030	0.087 ± 0.018
Gait Velocity (m/s)	0.55 ± 0.16	0.68 ± 0.28	0.77 ± 0.30

Significance

Even though the post-stroke population is heterogenous and there was variability in joint-level biomechanical parameters across participants, all five participants improved their global-level parameters with the PD-AFO. Further investigation is needed to understand the factors driving the improved global-level parameters, although it is likely that each individual (or groups of individuals) employs different biomechanical strategies. Still, given key goals of post-stroke gait rehab are to reduce the COT and improve gait velocity, this study's finding that the PD-AFO improved these critical parameters, at least for these five individuals, is exciting and supports the importance of properly prescribed PD-AFO bending stiffness.

Acknowledgments

UD Center for Composite Materials and Independence Prosthetic and Orthotics for helping manufacture and prepare the PD-AFOs.

References

[1] Perry J & Burnfield JM. (2010). *Gait Analysis: Normal & Pathological Function*; Slack Inc.
[2] Arch et al. (2015) *Ann Biomed Eng*, **43**: 442-450.
[3] Bregman DJJ et al. (2009). *Gait Posture*, **30**: 144-149.
[4] Bregmann DJJ et al. (2011). *Clin Biomech*, **26**: 955-961.
[5] Kerkum YL et al. (2016). *Gait Posture*, **46**: 104-111.
[6] Arch E & Reisman DS. (2016). *J Prosth Orthot*. **28**: 60-67.

Youth Walking Biomechanics: The Influence of Footwear on Kinetics and Kinematics.

Andrew G. Traut, MS, ATC[1,3], JJ Hannigan, PhD, ATC[2,3], Justin A. Ter Har, MS[1,3], Christine D. Pollard, PhD, PT[2,3]
[1]Program in Kinesiology, Oregon State University-Cascades, Bend, Oregon, USA.
[2]Program in Physical Therapy, Oregon State University-Cascades, Bend, Oregon, USA.
[3]School of Biological and Population Health Sciences, Oregon State University, Corvallis, Oregon, USA.
Email: trautan@oregonstate.edu

Introduction

The implementation of increased barefoot activity has been proposed as a strategy to improve health and physical performance [1]. Subsequently, "minimal" style shoes have been developed to approximate barefoot activity while providing the protection of a shoe [2]. This trend has carried over from adult to youth footwear. The biomechanical effects of different types of footwear has been extensively studied in adults but very little research has been conducted in youth. The purpose of this study was to compare walking biomechanics in male youth between 3 different footwear conditions The hypotheses of this study were that the walking biomechanics of youth would be significantly affected by changes in footwear, and that minimal shoe walking would demonstrate distinct similarities to being barefoot.

Methods

Eleven active male youth (8-12 years old) participants had walking biomechanics (ankle, knee, and hip kinematics and vertical ground reaction forces (vGRF)) analyzed using an 8-camera 3-D motion capture system (Vicon) and in-ground force plates (AMTI) in three footwear conditions (barefoot, traditional shoe: New Balance 880: drop: 13.3mm; heel height: 32.5mm; forefoot height: 19.2mm, and minimal shoe with no midsole cushioning: Xero Prio Youth: drop: 0mm; heel height: 11.0mm; forefoot height: 11.0mm). (Figure 1)

Figure 1: The two types of shoes used in this study. Left, minimal shoe (Xero Prio Youth). Right, traditional shoe (New Balance 880)

Variables of interest included the weight acceptance peak (initial peak) and propulsive peak (second peak) of the vGRF, and tri-planar hip, knee, and ankle kinematics (angle at initial contact, peak angle, excursion, angle at toe-off).

Results and Discussion

Sagittal plane knee and ankle, and frontal plane ankle kinematics were significantly different between footwear conditions. Youth displayed significantly ($p<0.001$) greater knee flexion at initial contact (KFIC) in the barefoot condition (6.18±3.44˚) as compared to the minimal (1.51±3.18˚) and traditional (1.13±3.08˚) shoe conditions (Figure 2A). Conversely, they displayed significantly ($p<0.001$) lower knee sagittal plane excursion (KSE) in the barefoot condition (24.87±4.69˚) compared to the minimal (37.29±4.61˚) and traditional (36.37±5.16˚) shoe conditions (Figure 2B). Similarly, youth exhibited significantly ($p<0.001$) less peak knee flexion in the barefoot (31.05±3.41˚) condition than in the traditional (37.51±3.72˚) and minimal (37.29±4.61˚) shoe.

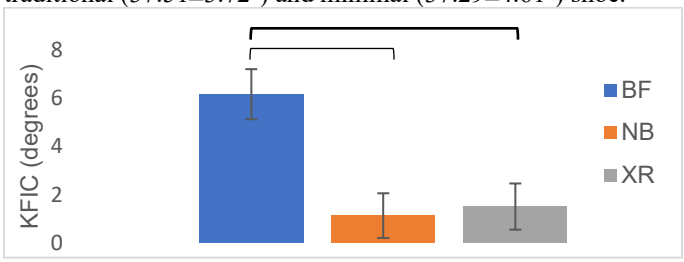

2A

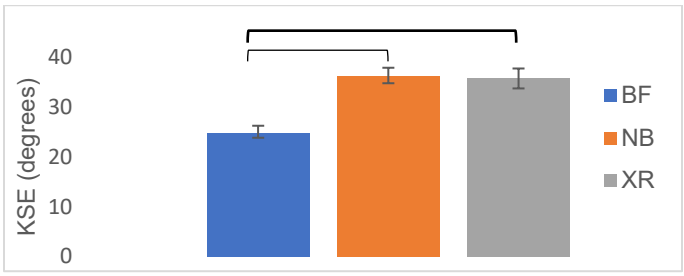

2B

Figure 2: Average Knee Flexion at Initial Contact Knee (2A) and Sagittal Plane Excursion (2B). Significant differences are bracketed.

The average propulsive peak of the vGRF was significantly ($p=0.024$) less when walking barefoot (1.12±0.07 bodyweights/second) compared to a traditional shoe (1.18±0.11 BW/s). There were no significant differences between the propulsive peak of the minimal shoe (1.14±0.10 BW/s) and the other footwear. These relationships indicate that minimal shoes cannot be expected to consistently replicate the biomechanics of barefoot walking in youth. In fact, youth exhibited walking biomechanics in the minimal shoe that were more similar to the traditional shoe, than barefoot. Also, shod walking is distinctly different from barefoot, which is in contrast to previous research that suggests that barefoot and shod walking biomechanics in youth can be assumed to be functionally identical [3].

Significance

Based on the results of this study, clinicians and others recommending footwear for youth, should not assume that minimal shoes will replicate the movement patterns of barefoot walking. Rather, lower extremity biomechanics are strikingly similar when youth walk in minimal shoes and traditional shoes, and substantially different when walking barefoot. This is a unique analysis of the effects of footwear on the walking biomechanics in youth, and the first study to specifically compare the effects of minimal and traditional shoes to barefoot walking in youth.

References

[1] Hollander et al. (2017). *Med Sci Sport Exer.* **49**:752-762
[2] Davis. (2014). *J Orthop Sports Phys Ther.* **44**: 775-784
[3] Oeffinger et al. (1999). *Gait & Posture.* **9**: 95-100

COMPARING THE VALIDITY OF A SOFT STRETCH SENSOR TO 3D MOTION CAPTURE FOR KNEE JOINT KINEMATICS

Alana J. Turner[1*], W. Carroll[2], L. Ramsey[1], S. Kodithuwakku Arachchige[1], H. Chander[1], A. Knight[1], & R. Burch[3]
[1]Mississippi State University, Department of Kinesiology
[2]Mississippi State University, Electrical Engineering
[3]Mississippi State University, Industrial Engineering & Athlete Engineering
email: *ajt188@msstate.edu

Introduction

3D-Motion Capture is considered the gold standard for analyzing joint angles. However, capturing joint angles by motion capture is limited to a laboratory setting and can be expensive to analyze. Therefore, a new type of technology, soft stretch sensors, have the capability to determine joint angles in real-life settings. This could be beneficial for injury prevention and identifying healthy joint movements during daily tasks. This new technology would benefit many populations, it needs to be validated for reliability of measurements. Moreover, the stretch sensor needs to be validated while performing simple movements like walking to test refresh rate and accuracy of joint angles. The purpose of this study is to compare soft stretch sensors to a 3D Motion Capture System measurement for real-time, gait measurements while collecting beneficial kinematics for general population.

Methods

Sixteen participants were marked with motion-capture sensors at the hip, knee, and ankle of both legs. Participants were then fitted with the knee brace on their right leg. One trial of three separate joint actions (knee flexion/extension) was performed along with one trial of three bodyweight squats. The 3D motion capture data was collected at 200 Hz and smoothed with a 30 Hz Butterworth filter. SRS data was initially sampled at 25 Hz, which was then up-sampled to 200 Hz to match the 3D motion capture data. Next, the two datasets were aligned overtime using cross-correlation.

Figure 1: Participant donning the knee brace.

Results and Discussion

Exercise	Mean R^2	Mean RMSE
Knee Flexion	0.799	5.470
Squat	0.957	8.127

Table 1: R-squared (R^2) values and root mean square error (RMSE) values for knee flexion and bodyweight squats.

From the data above results can be interpreted. The R^2 value for a bodyweight squat was higher when compared to just the knee joint flexion of 90º while participants were informed to perform a bodyweight squat at the parallel level. A greater R^2 value was reported because of the greater joint angle observed in this type of exercise. The soft stretch sensors may be accurate when the stretch from the movement is greater. Overall, this validation study was the first to be performed. A limitation we observed during data collection was the fit of the knee brace. In future studies, we intend to use a more structurally sound knee brace of multiple sizes for an improved fit for participants. We also intend to use the knee brace to look at clinical populations such as children with Autism Spectrum Disorder (ASD) to analyze abnormal gait movements possibly outside of a laboratory setting.

Figure 2: Example of data output during knee flexion for the soft stretch sensor and 3D-motion capture.

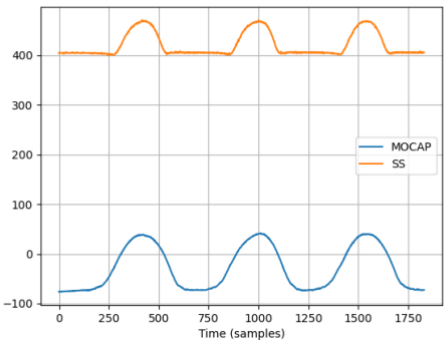

Significance

With this knee brace being one of the first of its kind using soft stretch sensors, more validation studies are needed for it to be considered a reliable data collection tool. However, a wearable such as an elastic knee brace could benefit several populations, from sport injury rehabilitation to gait rehabilitation for special population. The significance of wearable stretch sensors could change the process of data collection because of the ability to capture real-time movements outside of a laboratory setting.

Acknowledgments

We would like to acknowledge the hard work and commitment of students in the Neuromechanics Laboratory and the Electrical Engineering students that helped with this project.

References

1. Hopkins, J. Characterization of Multiple Movement Strategies in Participants with Chronic Ankle Instability. J. Athl. Train.
2. Kim, H. Altered movement biomechanics in chronic ankle instability, coper, and control groups: Energy absorption and distribution implications. J. Athl. Train.
3. Son, S. AlteredWalking Neuromechanics in Patients with Chronic Ankle Instability. J. Athl. Train.
4. Davarzani S. Closing the Wearable Gap—Part VI: Human Gait Recognition Using Deep Learning Methodologies. *Electronics*.
5. Talegaonkar, P. Closing the Wearable Gap-Part VII: A Retrospective of Stretch Sensor Tool Kit Development for Benchmark Testing. *Electronics*.

Optimal Design of a Parallel Rehabilitation Robot for the Lower-Limb based on Force-Space Matching

Alexander R. Dawson-Elli[1], and Peter G. Adamczyk[1]
[1]Department of Mechanical Engineering, University of Wisconsin-Madison
Email: dawsonelli@wisc.edu

Introduction

To date, serial robots like exoskeletons have been the dominant architecture in robotic rehabilitation of the lower-limb [1]. Serial robots offer the advantage of having large workspaces and congruent mechanics with the leg. By comparison, the application of parallel robots to lower-limb rehabilitation has been less explored. Parallel robots have many characteristics that make them desirable for rendering high-performance haptic environments, such as force fields and virtual channels. Due to their multiple connections to ground, they are stiff and may be actuated entirely using grounded motors (no motors on distal joints) and for this reason are also low inertia. The motivation for this simulation experiment is to design a parallel robot that has a high degree of force-space congruence with a human model, while retaining the desirable properties of a parallel robot.

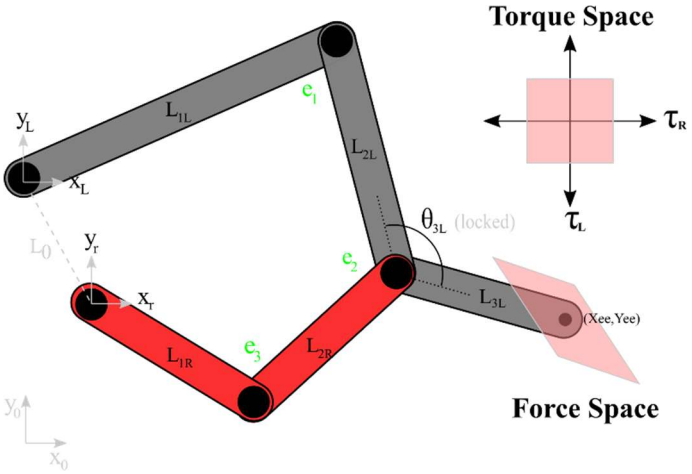

Figure 1: Parameters of the parallel robot model include the locations of the roots of the right and left robot segments, the link length parameters, the discrete states of the elbows. A polygon representing the torque space, or the set of all possible torques generated by robot motors, is mapped through the Jacobian into the end-effector force space.

Methods

We constructed a model of the forward, inverse, and instantaneous kinematics of a generalized 5-bar linkage (G5BL, Fig 1). We used the force Jacobian to map torques produced by the motors of the G5BL into cartesian force space at the end effector, where the G5BL interfaces with the human foot. We constructed a model of the human's force-production requirements in the sagittal plane by fitting an ellipse to force measurements from a prior experiment [3]. To assess the force-space compatibility of the G5BL to the human, we sampled the workspace of the human leg model on a cartesian grid. At each point on the grid, we rotated the leg's force ellipse to match the orientation of the endpoint relative to the hip, and calculated a congruence score as the fraction of area of the human force space that was covered by the robot's force space (Fig 2). When torque parameters were also allowed to vary within the simulation, the congruence score was normalized by the robot force space area.

Using the DIRECT (Divided Rectangles) optimization method [2], we calculated the robot design with maximal congruence summed over the sampling grid. Different parameterizations of the robotic model allow for constraining the solution space of robot. In Fig 2, the robot was limited to solutions with vertical root alignment ($x_r = x_l$), the minimum distance between the roots was set to 22cm, and θ_{3L} was set to π.

Results and Discussion

For this analysis, the mean congruence score across all points in the leg's workspace was 0.440, with a standard deviation of 0.042 using the area normalization criteria. The maximum torque of each motor was held at 100Nm. Congruence scores improved near the edge of the workspace, as the optimizer took advantage of the changing condition number of the robot Jacobian to better match the shape of the human force-space. The root of one branch of the parallel robot was placed near the hip, as was expected.

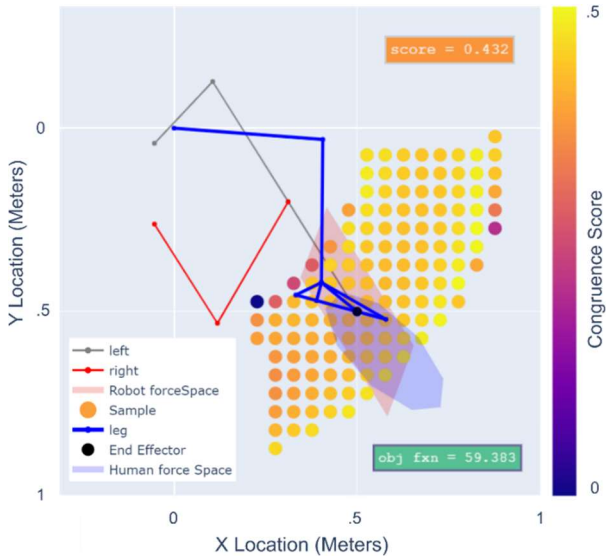

Figure 2: Results of an optimal force-space matching simulation. Constraints were placed on this simulation that the left and right robot roots are vertically oriented, and that the last L2l and L3l are parallel.

Significance

High congruence between the force-space requirements of the human and robot increase the inherent safety of human-robot interaction. The robot designed by our optimization routine allowed us to select a parallel robot which best matches the experimentally-determined force-space requirements of a human leg in the sagittal plane under realistic constraints on actuator placement, while retaining the advantages of a parallel robotic architecture. Our approach could be used in designing other parallel robots for human interaction, or more broadly in machine design where a parallel mechanism must achieve a force objective within a specified workspace.

Acknowledgments

We thank Patrick Dills, Michael Zinn, and Kreg Gruben for their input and advice, and funding from NSF CMMI-1830516.

References

[1] K.H. Low (2011) DSR2011.6026886
[2] Gablonski and Kelly (2001), J. Global Opt. **21**(1):27-37
[3] Gruben and Lopez-Ortiz (2003) Exp Brain Res, **148**:50–61

THREE-DIMENSIONAL COVERAGE MAPS IN THE ASSESSMENT OF CHOPART SUBLUXATION IN PROGRESSIVE COLLAPSING FOOT DEFORMITY

Andrew J. Behrens, Cesar de Cesar Netto, Kevin N. Dibbern
University of Iowa Orthopedic Functional Imaging Research Laboratory, Iowa City, IA
Email: andrew-behrens@uiowa.edu

Introduction

Progressive collapsing foot deformity (PCFD), formerly termed Adult-Acquired Flatfoot Deformity (AAFD), is a complex 3D deformity characterized by peritalar subluxation (PTS) of the hindfoot through the triple joint complex. In this context, adjacent structures may adopt different positions and boney relations can change, producing areas of increased contact or subluxation. The objective of this study was to develop 3D distance maps (DMs) and coverage maps (CMs) from weightbearing CT (WBCT)data to assess subluxation across the Chopart joint in PCFD patients. We hypothesized that CMs would show decreased coverage indicative of subluxation through certain regions of the Chopart joint in PCFD patients when compared to the controls.

Methods

In this IRB-approved, retrospective case-control study, we analyzed WBCT data of 18 consecutive patients with flexible PCFD and 10 controls. WBCT studies were performed with a cone-beam computed tomography (CT) scanner (PedCAT; Curvebeam). Participants were instructed to bear weight in a natural, upright standing position with the feet approximately at shoulder width and to distribute body weight evenly between the 2 lower limbs. WBCT technology allows a more accurate representation of loaded joints[1].

Using principal component axes, candidate coverage area was divided into nine regions on the talar head and 4 regions on the calcaneal-cuboid (CC) articular surface. This allowed precise quantification of percent coverage changes across the talar head and the CC articular surface. 3D distance mapping (DM) was used to objectively identify regions of joint coverage across the entire Chopart joint surface of the talus and calcaneus. Distance maps were computed as the perpendicular distance between surfaces in millimeters.

Areas with distances less than 4mm were defined to be covered, while areas without opposing surfaces or with distances greater than 4mm were considered to be uncovered. Joint coverage was defined as percentage of articular area with DMs lower than 4 mm. Coverage Maps (CM) were created to highlight areas of coverage (teal) versus non-coverage (pink). Comparisons were performed with independent t-tests, assuming unequal variances. P values <.05 were considered significant.

Results and Discussion

Changes in coverage percentages of PCFD cases relative to controls are indicated in figure 1. The middle lateral region of the talar head was found to have a 9% increase in coverage in PCFD cases relative to the controls (p = 0.011). The plantar region of the calcaneal-cuboid joint was found to have a 18% decrease in coverage compared to the controls. The medial side of the talar head generally saw decreases in coverage with the exception for the dorsal medial regions. However, these values were not statistically significant.

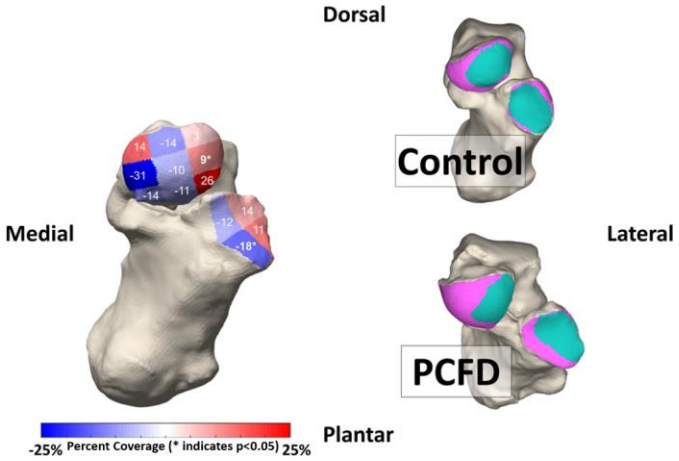

Figure 1: Summary of Percent Coverage changes and a sample Coverage Map. The red/blue scale indicates Percent Coverage changes.

On the calcaneus, the plantar region of the calcaneal-cuboid joint was found to have a significant coverage decrease of 18% relative to the controls (p = 0.017). There was also a decrease in coverage observed in the medial region of the calcaneal-cuboid joint and an increase in the dorsal and lateral areas.

Significance

Our results support the occurrence of significant Chopart joint changes in early flexible PCFD. Increased lateral and decreased medial/plantar talar head coverage point to internal rotation and plantarflexion of the talus. Associated dorsal migration of the cuboid where plantar and medial areas have decreased coverage indicate subluxation through the entirety of the Chopart joint. Novel usage of 3D distance maps to assess joint coverage enabled objective quantification of subluxation though the Chopart joint in early stage PCFD for the first time. These findings may assist clinical decision making regarding the restoration of normal joint alignment during PCFD corrections. Further studies are needed to establish thresholds of change associated with degeneration.

Acknowledgments

We thank the University of Iowa Department of Orthopedics and Rehabilitation for their continued support throughout this project.

References

1. Cody EA, Williamson ER, Burket JC, Deland JT, Ellis SJ. Correlation of talar anatomy and subtalar joint alignment on weightbearing computed tomography with radiographic flatfoot parameters. *Foot Ankle Int*. 2016;37(8):874-881.

UNCONSTRAINED DOUBLE-LIMB SLIP SEVERITY

Abderrahman Ouattas[1]*, Corbin M. Rasmussen[1] & Nathaniel Hunt[1]
[1]Department of Biomechanics, University of Nebraska at Omaha, Omaha, NE USA
Email: * aouattas@unomaha.edu , web: http://coe.unomaha.edu/brb

Introduction

More than 25% of older adults fall each year in the US [1]. Slips alone account for 25% of all falls [2]. Successful recovery depends on the severity of the slip and the individual's capacity to regain balance. When slips are unconstrained, the slipping feet travel in a variety of directions [3] which poses diverse challenges to supporting body weight and maintaining an upright trunk. However, previous research has focused on single limb slips at heel strike, and we lack the data to guide interventions on recovery from diverse double-limb slips. Preliminary data collected from a larger ongoing study [4] showed unconstrained and diverse feet velocities relative to the center of mass (CoM) during double-limb slips. We hypothesize that double-limb slip severity, characterized with the combination of velocities from both feet relative to CoM, will predict fall rates.

Methods

Six young adults (3M, 3F, 26.2 ± 2.8 years old, 1.71 ± 0.08 m, 80.94 ± 8.75 kg) participated in the study. Participants completed 3 sessions of 12 double limb slips each within one week (36 slips in total), that were triggered using a custom-built Wearable Apparatus for Slip Perturbations (WASP) [3-4]. The WASP induced slips to both limbs simultaneously while participants walked at a fixed gait speed of 1.3 ± 0.1 m/s on a 10 m walkway. Falls were identified if participants applied more than 30% of body weight to the harness, which was measured using a load cell [5]. Full body kinematics were recorded using an 18-camera motion capture system (Motion Analysis Corp., Santa Rosa, CA) and sampled at 100 Hz.

Data from the first three and last three slips were analyzed for each participant from slip onset until both feet reached a velocity of 0. Within this period of time, right and left feet velocities relative to the CoM were measured at the frame when each foot velocity was least similar to the CoM velocity. Such specific timepoint was chosen to quantify the maximum dissimilarity of the base of support relative to the CoM between falls and non-falls. To test our hypothesis, we used feet velocities in either the AP or ML direction relative to the CoM as inputs to a logistic regression classification model trained to discriminate trials in which the participant fell from non-falling trials. Custom Visual3D (C-Motion Inc., Germantown, MD, USA) pipelines were used for data analyses. Custom MATLAB codes (MathWorks, Natick, MA) were used for data visualization.

Results and Discussion

In the experimental data analyzed thus far, there have been 7 falls, and 27 recoveries. Load cell data did not record two slip trials from the total 36 trials. Using unconstrained slips to both feet simultaneously, slipping feet had substantial ML slipping speeds that ranged from 1% to 193% of the AP component. In the AP direction, feet showed diverse motions relative to one another (Figure 2), however, the COM always moved anteriorly during the slip faster than either foot (Figure 1). On the other hand, ML directions showed the slipping feet travelling in the same direction 73% of the time (Figure 2), and 88% of those times, both feet were moving opposite to the COM's direction (Figure 1).

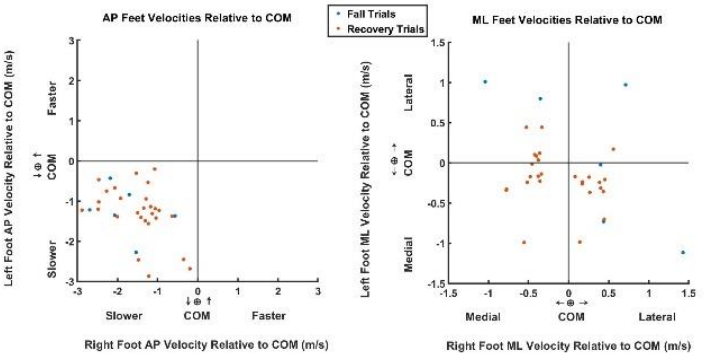

Figure 1: AP & ML Feet velocities relative to the CoM.

Overall, ML velocities of the slipping feet better predicted falls and recoveries compared to their AP velocities,. The logistic regression model based on ML slipping feet velocity (medial or lateral to the CoM), and positions relative to the CoM correctly predicted 4 of the 7 falls and all recovery trials with a deviance, a measure of the unexplained variance in the modeled data, of 17%. However, using only the AP feet velocity (model deviance 30.6%) and position (model deviance 25.7%) relative to the CoM poorly differentiated between fall and recovery trials and was only able to predict one fall trial.

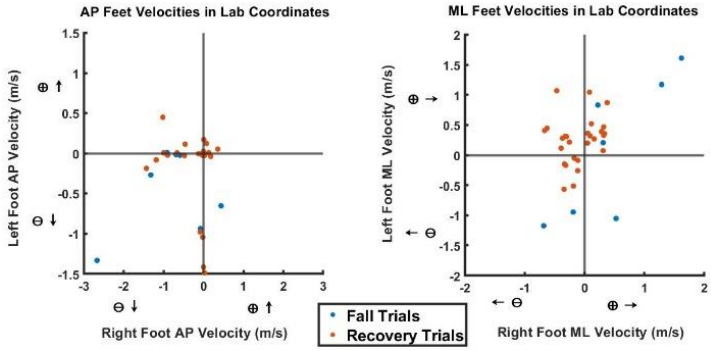

Figure 2: AP & ML Feet velocities in Lab Coordinates

Significance

The logistic regression model using ML feet velocities relative to the CoM, predicted four of the seven falls and all recoveries and outperformed the AP deviations, indicating ML movements during slipping may be more susceptible to deviations than AP movements within the recovery process of slip induced falls. If this hypothesis can be validated with adequate statistical power, then current methods to induce slips or slip like perturbation to assess balance or reduce falls must incorporate ML components, instead of only focusing on AP movements of the slipping feet.

Acknowledgments

NIH 2P20 GM109090-06; NIH R15AG063106-01

References

1. Bergen G, et al. *Morb. Mortal. Wkly. Rep*, 65, 993–998, 2016.
2. Berg WP, et al. *Age Ageing*, 26, 261-268, 1997.
3. Rasmussen CM, et al. *J. Neuroeng Rehab*, 16, 118, 2019.
4. Ouattas A, et al. *44th Virtual ASB*, 2020.
5. Yang F & Pai Y. *J. of Biomech*, 44, 2243–2249, 2011

The Effect of Electromyography Biofeedback Training on Scapular Stabilizer Muscles in Shoulder Impingement Patients

Eliot J. Mackay[1], N.J. Robey[1], D.N. Suprak[1], H.H. Buddhadev[1], and J.G. San Juan[1]
[1]Department of Health and Human Development, Western Washington University, Bellingham, WA, United States
Email: mackaye2@wwu.edu

Introduction

The shoulder is prone to injury in the general population and subacromial impingement syndrome (SAIS) is one of the highest diagnosed causes of impairment and pain in this region [1]. While SAIS is not entirely understood the pain from SAIS may be from the compression of soft tissue in the subacromial space [1]. Additionally, increased Upper Trapezius (UT), decreased Lower Trapezius (LT), and decreased Serratus Anterior (SA) activity may have a relationship with shoulder injury [2]. Management of SAIS may be treated through scapular focused exercise therapy to restore muscle performance and maintenance of optimal scapular positioning [3]. EMG biofeedback allows for visual feedback of muscle activity and has been an effective method in teaching various population groups about muscle activation [3]. It has also had kinematic effects when used in conjunction with exercise therapy [4].

The purpose of the study was to investigate how EMG biofeedback training with scapular rehabilitation exercises affected muscle activation of the injured shoulder and healthy shoulder of individuals. We hypothesized that after undergoing EMG biofeedback training, participants would experience a decrease in UT, an increase LT, and an increase in SA activation bilaterally.

Methods

A total of 10 participants (7 male and 3 female, 30.60 years ± 15.20 years, height 1.72 m ± 0.7 m, and mass of 75.65 kg ± 8.69 kg) were included in this study after passing two out of three clinical assessments (Hawkins-Kennedy, Neer, Empty Can) for SAIS. All 10 of the participants were right-hand dominant and 6 participants had right SAIS. Noraxon EMG (Scottdale, AZ, USA) electrodes were placed on the UT, LT, SA, and Lumbar Paraspinals (LP) to measure muscle activity sampled at 1500 Hz (Fig. 1). A maximal voluntary isometric contraction (MVIC) was conducted for each muscle group to normalize EMG data. Scapular kinematic testing was conducted for each participant that consisted of overhead humeral elevation at 35° in the scapular plane before and after biofeedback training [4]. Humeral elevation was measured with the Polhemus Liberty (Colchester, VT, USA) sampling at 240 Hz and EMG data was recorded at 30°, 60°, 90°, and 110° of elevation. The biofeedback training consisted of 10 repetitions of the I, W, T, and Y scapular rehabilitation exercises where participants were told to actively reduce UT muscle activation.

Figure 1. Experimental and participant set up.

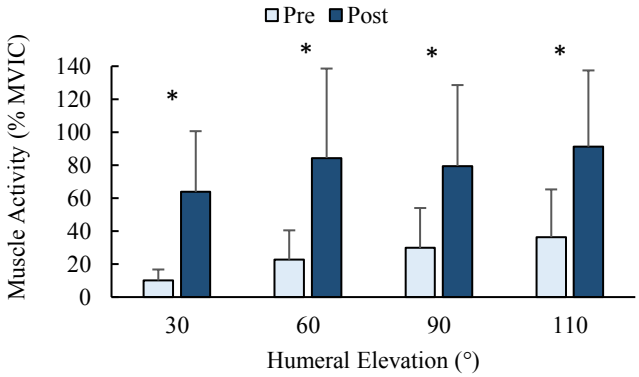

Figure 2. Mean Lower Trapezius muscle activation for healthy and impingement shoulder sides; * $p < 0.05$.

Results and Discussion

A repeated measures mixed ANOVA for each humeral angle and muscle showed no significant interaction between side and time. However, a main effect of time for each muscle group was found. UT activity was reduced at 60° and 90° ($p = 0.003$, and $p = 0.036$, respectively), LT activity (Fig. 2) was increased at all humeral angles ($p < 0.0005$), and SA muscle activity was increased at 110° ($p = 0.001$).

The findings of the present study support the hypothesis and are in accordance with previous research [3] which showed an increased ability to activate LT musculature and decreased UT activity level after biofeedback training. Increased activation of the primary upward rotators (LT and SA) may allow for decreased likelihood of impingement symptoms by maintaining optimal subacromial space during overhead activities [4]. Decreasing UT activity may reduce the degree of anterior tilting and resultant scapular impingement [4].

Healthy and SAIS shoulders included in the study were affected by EMG biofeedback training. Therefore, EMG biofeedback may be an effective tool to teach muscular control for scapular stabilization with overhead movement.

Significance

The results from this study provide a more thorough understanding of the effect a single session of EMG biofeedback has on muscular recruitment and control. It may now be possible to pursue further research to support this technology and implementation in a clinical setting.

Acknowledgments

We would like to thank Tyler Verrill, Nick Braman, and Audrey Goo for their involvement with this project.

References

[1] Michener et al. *Clin Biomech,* 18(5): 369-379, 2003.
[2] Chester et al. *BMC Musculoskelet Disord*, 11(1): 45, 2010.
[3] Wan-Yu et al. *J Athl Train, 55*(3): 265-273, 2020.
[4] San Juan et al. *J Biomech,* 49(9): 1881-1886, 2016

Multi-Segment Foot Joint Coordination Variability in Middle-Age Adults with Persistent Ankle Pain

Mohammed S. Alamri[1] and Stephen C. Cobb[1]
[1]Department of Kinesiology, University of Wisconsin-Milwaukee, Milwaukee, WI, USA
Email : msalamri@uwm.edu

Introduction

Persistent ankle pain is common following ankle sprain. The prevalence peaks in middle-aged adults, affecting an estimated 12.2% of adults 50-64 years old [1], and is associated with decreased health-related quality of life and mobility [2]. Joint coordination variability may be an important factor in persistent ankle pain in middle-aged adults, however, the majority of research has investigated chronic ankle instability (CAI) in young adults.

The previous studies have reported increased knee sagittal-ankle frontal plane [3] and shank transverse-ankle frontal plane [4] variability during mid and late stance in participants with CAI. The increased joint coordination variability has been theorized to be caused by CAI gait being less adaptable and more constrained due to weak musculature and/or the persistence of altered gait following an ankle sprain [5].

Although previous works have improved the understanding of the influence of persistent ankle symptoms on lower extremity-ankle coordination variability in young adults, none have investigated coordination variability within the foot of middle-aged adults. We hypothesized that middle-aged individuals with persistent ankle pain would show increased coordination variability during walking.

Methods

14 middle-aged adults (45 – 64 yo.) participated in the study (Table 1). Persistent ankle pain group participants (PAIN) had a history of at least one significant lateral ankle sprain, complained of at least moderately troublesome ankle pain on most days during the past month, and experienced pain for the previous three months [6]. Uninjured participants (CON) were sex and age matched with the PAIN group.

Following written informed consent, 35 markers (6.4 mm) were placed on each participant's foot and shank to define seven segments and six functional articulations (rearfoot, medial and lateral midfoot, medial and lateral forefoot, 1st metatarsophalangeal) [7]. Each participant then performed 5 barefoot overground walking trials at self-selected speeds along a 15 m walkway with 3 embedded force plates (1000 Hz), while marker position data were collected using a 14-camera motion analysis system (200 Hz). Joint coordination was calculated using the method proposed by Heiderscheit et al [8], and the variables calculated during weight acceptance, midstance, and push off are defined in Table 2. Multivariate Analysis of Variance (MANOVA) tests were performed to investigate group differences in the coordination variables ($\alpha = 0.05$).

Table 1. Study Participant Characteristics (Means ± SD).

Group	Sex (F/M)	Age (years)	Height (cm)	BMI (kg/m^2)
Control	7/1	53.3 ± 6.1	167.8 ± 6.4	24.9 ± 5.9
Pain	6/0	52.0 ± 5.0	169.7 ± 5.1	30.6 ± 7.5

Results and Discussion

The coordination variability for the two groups is presented in Table 2. We postulated that the persistent ankle pain group would show increased coordination variability within the foot segments during walking. Although the effect size of each ANOVA was moderate to large, none of the omnibus F-ratios were significant. This finding is contrary to studies in individuals with CAI [3-5]. The difference may be attributed to previous studies examining different joint coordination relationships, and/or the nature of persistent ankle pain versus CAI. Additionally, the small sample size may have limited the power of the current study.

Table 2. Joint Coordination Variability Mean (SD).

Coordination Variability	Group CON	Group PAIN
Rearfoot Frontal-Rearfoot Transverse-Plane		
-Weight Acceptance	8.34 (1.16)	7.98 (0.78)
-Midstance	7.89 (1.38)	7.35 (2.04)
-Push off	5.06 (1.61)	4.93 (0.83)
Medial Midfoot Frontal-Rearfoot Frontal-Plane		
-Weight Acceptance	7.26 (1.77)	8.22 (1.85)
-Midstance	6.77 (1.97)	6.34 (1.58)
-Push off	6.48 (0.93)	7.56 (1.14)
Lateral Midfoot Frontal-Rearfoot Frontal-Plane		
-Weight Acceptance	6.52 (0.59)	7.26 (1.42)
-Midstance	7.20 (1.91)	7.92 (1.50)
-Push off	6.99 (1.23)	7.11 (0.95)
Medial Forefoot Sagittal-Medial Midfoot Frontal-Plane		
-Weight Acceptance	5.64 (2.22)	7.38 (2.18)
-Midstance	5.25 (1.21)	4.46 (0.40)
-Push off	5.56 (2.41)	6.45 (1.47)
Lateral Forefoot Sagittal-Lateral Midfoot Frontal-Plane		
-Weight Acceptance	5.60 (1.43)	6.08 (1.39)
-Midstance	6.40 (1.66)	6.98 (1.57)
-Push off	6.32 (1.20)	6.18 (1.21)
Hallux Sagittal-Medial Midfoot Sagittal-Plane		
-Weight Acceptance	3.70 (2.43)	5.11 (2.89)
-Midstance	6.17 (1.42)	4.95 (1.35)
-Push off	5.33 (0.46)	5.04 (0.29)

Significance

Middle-aged adults with persistent ankle pain demonstrated no significant differences in coordination variability during walking gait. However, given the large effect size associated with the MANOVAs, further study is warranted to investigate lower extremity kinematic joint coordination variability in middle-aged adults with persistent ankle pain.

Acknowledgments

UW-Milwaukee CHS Student Research Grant Award.

References

[1] Murray C., et al. 2018. *PLoS One*, *13*(4): e0193662.
[2] Adamson J., et al. 2006. *Ann Rheum Dis, 65*(4):520–524.
[3] Lilley T., et al. 2018. *Sports Biomech, 17*(2), 261–272.
[4] Cornwall M., et al. 2019. *Gait & Posture, 70,* 130–135.
[5] Herb C., et al. 2014. *J Appl Biomech, 30*(3), 366–372.
[6] Parsons S., et al. 2006. *BMC Musculoskelet Disord, 7*:34.
[7] Cobb S., et al. 2016. *J Appl Biomech, 32* (6): 608–613.
[8] Heiderscheit C., et al. 2002. *J Appl Biomech, 18*, 110–12.

DEVELOPMENT OF A FULL-BODY MUSCULOSKELETAL MODEL INCORPORATING HEAD-MOUNTED DEVICE

Syed T. Mubarrat[1], Quinten Humphrey[2], Manoj Srinivasan[1], Thomas Chen[1], Kieran Binkley[1], and Suman K. Chowdhury[1]
[1]Industrial, Manufacturing, and Systems Engineering, Texas Tech University
[2]Mechanical Engineering, Texas Tech University
Email: suman.chowdhury@ttu.edu

Introduction

OpenSim, an open-source musculoskeletal modelling platform [1], has widely been used by the biomechanical researchers to create a broad range of *in-silico* models of the musculoskeletal system in order to estimate muscle and joint reaction forces. To date, however, there exists a limited number of full-body musculoskeletal models: full-lumbar spine model [2], Hammer's full body model [3], Christophy's lumbar spine model [4], Arnold's model [5] and Musculoskeletal Model for the Analysis of Spinal Injuries (MASI) [6]. Though these models are sufficient for analysing the lower body biomechanics, their simplified representations of the upper body—such as head, arms, trunk, and sometimes pelvis—are not sufficient to provide an accurate estimation of internal muscle and joint forces. Therefore, this study aimed to develop a full-body musculoskeletal model in OpenSim with multi-segmental muscle and joint representations of the upper body to investigate the effect of head-mounted virtual reality (VR) device on full-body gait biomechanics.

Methods

We developed a full-body musculoskeletal model in OpenSim v 4.1 based on the MASI model [6] by adding 32 muscles to the upper extremity representing the shoulder, elbow, and forearm, 43 muscles to the lower extremity containing the hip, knee, and ankle, and 20 hyoid muscles to the neck (Figure 1). The original MASI model had only 35 rigid anatomical segments, 78 upper and lower neck muscles, 34 joints, 30 kinematic constraints, and 43 degrees of freedom. Muscle parameters, i.e., optimal fiber length, peak force, tendon slack length, and pennation angle were taken from previous studies [7-9].

A total of 12 participants (weight: 174.41±5.00 lb, height: 72.96±6.90 in, age: 25.926±3.55 years) were recruited to perform multiple lifting tasks in virtual and real environments (virtual environment task (VET) and real environment task (RET)). A 10-camera motion capture system and two force plates were used to record participants' gait and ground reaction forces for the entire task duration, respectively. The gait and force data was then used to statically validate the model in the OpenSim modelling platform. We developed two different models for VET and RET, and scaled them according to the subjects' anthropomorphic data. The root mean squared (RMS) marker errors after the scaling process served as the static validation parameter. We also performed inverse dynamics simulation using our developed model and compared the moments around the shoulder, elbow, and knee joints between VET and RET. We are currently processing the dynamic validation of the model by comparing the results between inverse and forward dynamic simulations.

Results and Discussion

In this report, we present a novel full-body musculoskeletal model and statically validate it by scaling it for three male subjects. Averaged across all subjects, the scaling errors were found to be 3.17 ± 0.07 cm and 3.53 ± 0.52 cm for the models developed for RET and VET, respectively. Overall, the error was 3.35 ± 0.25 cm for both models, which is consistent with the findings of a previous study [10].

The inverse dynamics simulation exhibited RMS error of 2.91 ± 1.08 N-mm, 1.09 ± 0.31 N-mm, and 9.61 ± 1.31 N-mm between VET and RET for moments around shoulder, elbow, and knee joints, respectively. These results evinced the promise of the developed model in accurately simulating human motion biomechanics.

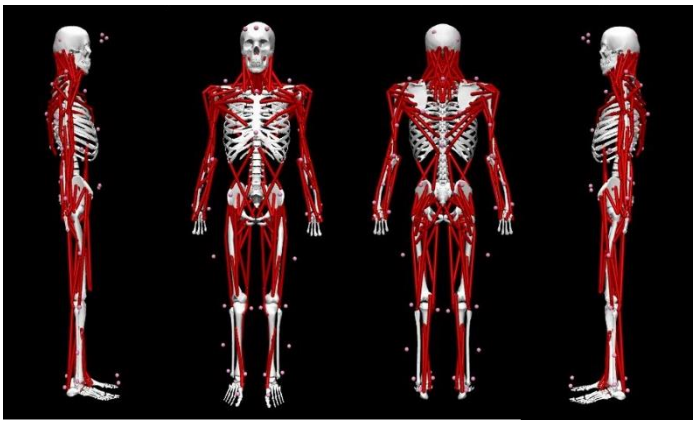

Figure 1: Right, front, back, and left view of the developed Opensim musculoskeletal model.

Significance

Our developed full-body OpenSim model can facilitate an accurate estimation of joint and muscle forces of both upper and lower bodies for various human-device (e.g., head-mounted VR device, exoskeleton, robotics, etc.) interactive gross-motor tasks and advance research in the areas of biomechanics, ergonomics, and rehabilitation science.

References

1. Delp, S.L., et al. IEEE transactions on biomedical engineering, 2007. **54**(11): p. 1940-1950.
2. Raabe, M.E. and A.M. Chaudhari. Journal of biomechanics, 2016. **49**(7): p. 1238-1243.
3. Hamner, S.R., A. Seth, and S.L. Delp. Journal of Biomechanics, 2010. **43**(14): p. 2709-2716.
4. Christophy, M., et al. Biomechanics and Modeling in Mechanobiology, 2012. **11**(1): p. 19-34.
5. Arnold, E.M., et al. Annals of Biomedical Engineering, 2010. **38**(2): p. 269-279.
6. Cazzola, D., et al. PLoS One, 2017. **12**(1): p. e0169329.
7. Delp, S.L., et al. IEEE Transactions on Biomedical engineering, 1990. **37**(8): p. 757-767.
8. Holzbaur, K.R., W.M. Murray, and S.L. Delp. Ann Biomed Eng, 2005. **33**(6): p. 829-40.
9. Mortensen, J.D., A.N. Vasavada, and A.S. Merryweather. PloS one, 2018. **13**(6): p. e0199912.
10. Kainz, H., et al. Journal of applied biomechanics, 2017. **33**(5): p. 354-360.

PREDICTION OF CHANGE OF DIRECTION GRF MEASURES USING EFFECTIVE FORCE MODELS

Nicholas M. Nelson[1], Bradley Davidson[1]
[1]University of Denver Human Dynamics Lab
Email: nick.nelson63@du.edu

Introduction

Evaluations of athletics or health based on joint kinetics are restricted to laboratory environments using camera-based motion capture and stationary force platforms. As a result, the true kinetics of *in situ* maneuvers ranging from basic sit-to-stand transitions to athletic changes of direction are generally unexplorable. Wearable motion capture might enable out-of-lab kinematic observation, but estimations of *in situ* joint kinetics are precluded without force platforms to characterize ground reaction forces (GRFs) as input to the inverse dynamics model.

The GRF—the net force on the body when no other external forces are present—can theoretically be replaced by the Effective Force of the link segment system where: $F_{GRF} = F_{Effective} = \sum_{i=1}^{n} m_i a_i$

Recent investigations have had some success in predicting vertical GRFs in walking with Effective Force Models (EFM) using a 13-segment optical motion capture (OMC) model [2] and a 17-segment inertial motion capture (IMC) model [3].

The objective of this investigation was to use EFM to predict GRF in an athletic change of direction movement and evaluate the effect of included segment kinematics in predicting two common biomechanical performance measures based on the GRF (Eccentric Rate of Force Development, Peak GRF).

Methods

Two participants, one male (age 24, mass 78.9 kg, height 182.9 cm) and one female (age 23, mass 55.5 kg, height 165.2) were instrumented with a collection of marker clusters placed on 13 body segments in The Motion Monitor (TMM) software. Each participant performed five repetitions of a lateral skater jump (LS) onto a force platform collecting GRF data at 1000 Hz. Three trials of the movement were collected for a total of 15 FP contacts per participant.

GRF and position data were filtered using a 4th order, lowpass zero phase lag Butterworth filter with cutoff frequencies of 30 Hz and 8 Hz, respectively. Center of mass accelerations were calculated using TMM software. Effective force models (EFMs) were created using 13 segments, 7 segments, and 1 segment with the HAT mass and total mass lumped into the pelvis for the 7-segment and 1-segment models, respectively. Agreement metrics from Bland-Altman (Biases and 95% Confidence Intervals) [3] were calculated using the differences between each EFM- and FP-derived measures of Peak ML force and ML rate of force development (RFD).

Results and Discussion

The ML GRFs predicted by each of the EFM models generally matched the shape of the ML FP data (Fig. 1). Biases (Fig 2.) are not consistent between subjects for either metric, indicating that more repetitions and subjects are likely needed.

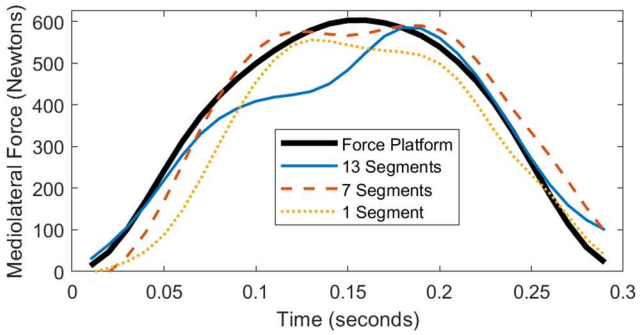

Figure 1. A typical effective force model prediction of mediolateral forces during a lateral skater jump

Limits of agreement (LoA) for RFD are large for all EFM configurations in each subject. The added step of differentiating force data with respect to time may have manifested additional error. Conversely, limits of agreement are much narrower for each prediction of peak vertical GRF. This is the point in agility movements where the high speed impact has slowed considerably, likely contributing to more accurate GRF predictions from kinematics.

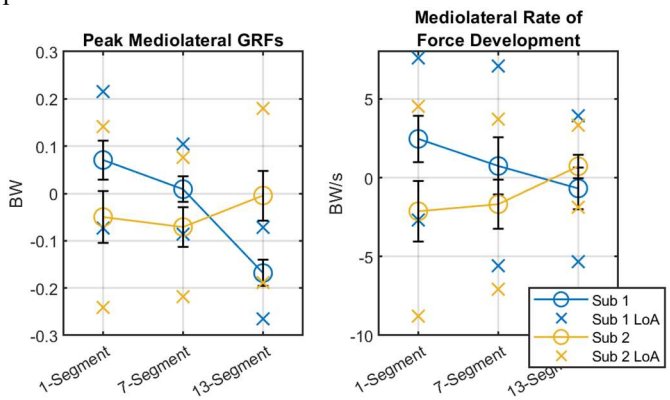

Figure 2. Metric biases with 95% confidence intervals

Significance

This investigation did not produce desirable agreements between FP and reduced segment EFM methods to validate EFMs as a replacement. Further investigation into the sensitivity of this method may yield an understanding of how to improve its predictions to provide GRF predictions for other complex movements.

References

[1] Mitiguy, P. *Advanced Dynamics & Motion Simulation.* 2019
[2] Ren, L. et al. *Whole body inverse dynamics over a complete gait cycle based only on measured kinematics.* 2008.
[3] Karatsidis, A. et al. *Estimation of Ground Reaction Forces and Moments During Gait Using Only Inertial Motion Capture.* 2016.
[4] Bland, J., Altman, D. *Statistical Methods for Assessing Agreement Between Two Methods of Clinical Measurement.* 1986.

HANDS-FREE INTERFACE FOR A SELF-BALANCING OMNIDIRECTIONAL RIDING BALLBOT

Seung Yun (Leo) Song, Chenzhang Xiao, Yu Chen, João Ramos, and Elizabeth T. Hsiao-Wecksler
Mechanical Science & Engineering, University of Illinois at Urbana-Champaign. email: ssong47@illinois.edu

Introduction

Our team is exploring a novel wheelchair based on a self-balancing, omnidirectional ball-based robot (ballbot) that uses upper body motions for hands-free lean-to-steer (LST) or lean-to-slide (LSL) driving control (Fig. 1) [1]. To enhance hands-free leaning control, the seat plate of the Force Sensing Seat (FSS) was instrumented with six load cells, i.e., making the FSS into a portable force plate. The FSS can estimate upper body motion (2D center of pressure (COP) and torso angle (θ)). Sagittal and frontal plane θ were derived from a statically-balanced point-mass model of the torso, FSS-derived resultant moments, and subject-specific anthropometric data (Fig. 2) [2]. COP and θ serve as reference signals to control the ballbot. Two studies have been piloted to improve/evaluate the accuracy of the FSS (validation study) and investigate the FSS feasibility for navigating a virtual human rider on a ballbot (simulation study).

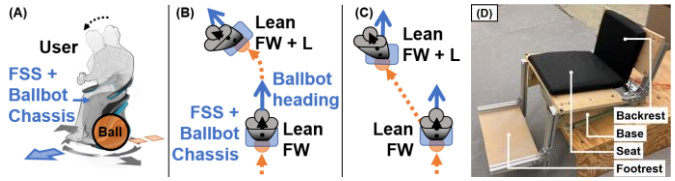

Figure 1: (A) Hands-free riding ballbot, (B) heading changes with lean-to-steer (LST), (C) lean-to-slide (LSL), (D) Force Sensing Seat (FSS).

Methods

In the validation study, currently three able-bodied males (26-28 yrs; 1.74 ± 0.04 m; 67.7 ± 7.1 kg) each performed four torso movements (forward/backward, left/right, diagonal left/neutral, diagonal right/neutral) of 10 cycles per motion and six repeated trials. FSS-derived values of COP and θ were compared to values derived from gold-standard equipment (Fig. 2). The FSS was mounted on a force plate (BP400600-1000-NC, AMTI). Markers were placed at four corners of the FSS seat and the subject's xyphoid, and captured with six cameras (Oqus 500+, Qualisys). Mocap-based torso angles θ^{MC} were derived from 2D projections of the vector **(H)** from the seat center to the xyphoid marker. To adjust FSS-derived values due to small off-axis coupling between load cells from assembly errors, resultant force, moment, and θ calculations from the FSS were linearly regressed to force plate and mocap data after pooling data across the first five trials of the 3 subjects. Trial 6 data for each subject were used to examine the accuracy of the regressed FSS estimations to gold standard data by computing error metrics: mean absolute error (MAE) and normalized MAE relative to max gold standard value (NMAE).

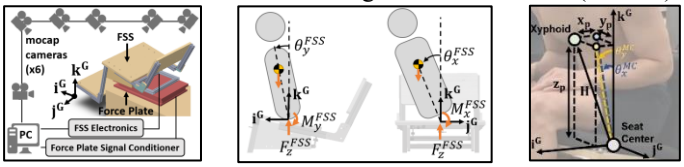

Figure 2: Test setup of validation study (left), computation of θ in x and y directions using FSS (middle) and motion capture system (right).

In the simulation study, we investigated the potential of using FSS-derived data to navigate a virtual human-ballbot system through obstacle courses using three control methods (two using FSS, one using a joystick) (Fig. 3). The two FSS methods (native (N) and enhanced (E)) used COP motion and resembled a Segway controller that tries to balance around a stationary equilibrium. An additional reference velocity signal proportional to the COP was added to E to encourage ballbot maneuverability and reduce rider effort. The joystick control method (J) served as a baseline. Switching between the LST and LSL drive modes was allowed for all control methods. Each of the 3 subjects navigated through training and testing courses, which consisted of different obstacles to realistically replicate an indoor environment (Fig. 3). Metrics (completion time (t_{cp}), mean of absolute resultant torso angles ($|\bar{\theta}_{xy}|$), percentage of sliding maneuvers ($SL\%$), and number of collisions (n_{col})) were computed for each method from the last of three trials in the testing course.

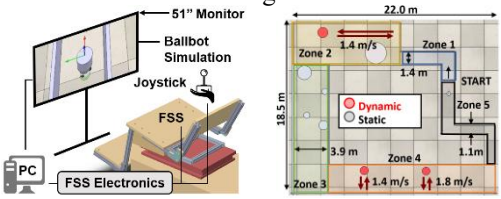

Figure 3: Test setup for simulation study (left), and virtual testing obstacle course divided into five zones (right)

Results and Discussion

Normalized mean absolute errors were below 10% (Table I). Largest errors were during rapid torso direction changes, which may not occur during usual operation of the ballbot. These results suggest that the FSS produced good estimates of torso movement.

Table I. MAE and (NMAE) of Force [N], Moment [Nm], COP [mm], and θ [°] for average of 3 subjects

F_x	F_y	F_z	M_x	M_y	COP_x	COP_y	θ_x	θ_y
1.74	1.02	2.07	1.68	0.93	1.69	2.55	1.21	1.98
(3.86)	(2.52)	(0.27)	(2.42)	(0.57)	(0.76)	(2.70)	(5.94)	(8.19)

Although the joystick controller J performed slightly better than the FSS controllers, the simulation study suggested that the FSS controllers are still viable and that the enhanced controller E was better than the traditional native controller N (Fig. 4). E displayed faster times, smaller lean angles, fewer collisions, and was ideal for quickly moving through obstacles or wide hallways than N. LSL was helpful to evade obstacles in front of the rider as it took less time to slide than to turn and then move.

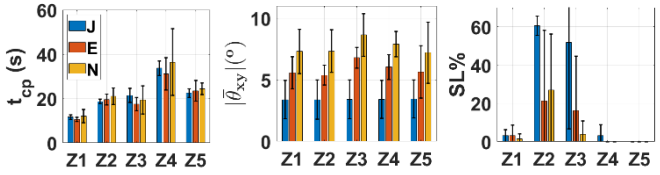

Figure 4: Average and SE bars of metrics for 3 subjects for each zone.

Significance

Preliminary results suggest the hands-free FSS interface could quantify torso motion and be used for navigating a riding ballbot.

Acknowledgments

NSF #2024905. Thanks to Adam Bleakney and Jeannette Elliot.

References

[1] Bleakney, AW, et al., U.S. Provisional Patent Application, 63/074,126.
[2] deLeva, P, J Biomech, 29(9):1223–1230, 1996.

SYSTEMATIC BIAS IN A PROBABILISTIC SPRING-MASS MODEL

John W. Fox[1], Adam E. Jagodinsky[2]
[1]Methodist University, Fayetteville, NC
[2]Illinois State University, Normal, IL
email: jfox@methodist.edu

Introduction

Human hopping is a bouncy form of locomotion in which kinematic and kinetic traces are homothetic to the spring-mass system.[1] Imperfections in the similarities have mostly been examined in running.[2,3] However, a recent review suggests that bipedal hopping may provide early detection of sensorimotor control loss in individuals with multiple sclerosis.[4] Such a proposition establishes a need to precisely describe a tolerable level of deviation from the spring-mass model in healthy subjects. Model bias may be estimated by evaluating paired differences in expectation and variance from a theoretical probability density function and empirical COM displacement. Therefore, the purpose of this study was to examine bias in a probabilistic spring-mass model. The null hypothesis was that there is no systematic bias in the theoretical spring-mass model when comparing the means and variances of COM displacement.

Methods

A total of 14 volunteers who signed the informed consent approved by the Methodist University IRB participated in the study. Participants (age = 18-40 yrs., mass = 77.87 ± 11.31 kg; height = 1.72 ± 0.07 m) performed six 20 second trials of bipedal hopping at preferred frequency. Ground reaction force (GRF) was measured via two Bertec force plates. Force signals from each force platform were summed and integrated twice to obtain COM displacement.[5] 2740 COM displacement traces during ground contact were trimmed for analysis.

Expectation and variance of COM displacement were computed from the empirical data and theoretical PDF given by:[6]

$$p(x) = \frac{2}{\pi\sqrt{A^2 - x^2}}$$

where p is density, A is amplitude, and x is displacement.

Limits of agreement (LoA) for the theoretical and empirical expectations and variances were estimated using a linear mixed effects model (lme4 1.1-26, R 4.0.4).[7] The total deviation index (TDI) provides a boundary in which paired differences are contained 95% of the time.[7] Confidences intervals around the mean bias and TDI from the linear mixed effects model were bootstrapped.[7]

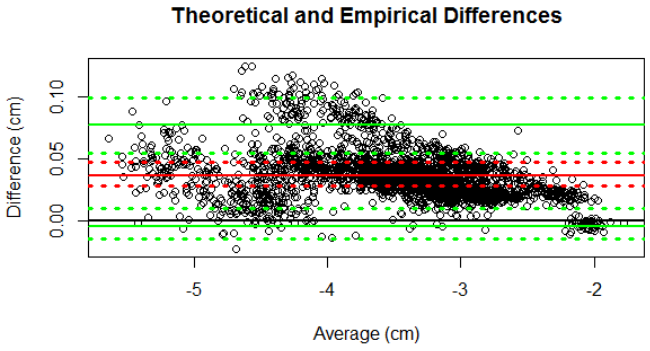

Figure 1: Bland-Altman plot showing paired differences between the theoretical and empirical expectation of COM displacement. Red solid line is the bias. Upper and lower limits of agreement are in green.

Results and Discussion

The mean bias in paired differences of COM displacement expectation was 0.036 cm (95% CI 0.028 to 0.047; 95% LoA -0.004 to 0.077 cm). The TDI was 0.539 cm (95% CI 0.478 to 0.591 cm). The mean bias in COM displacement variance was 0.066 cm^2 (95% CI 0.054 to 0.079 cm^2; 95% LoA 0.007 to 0.124 cm^2). The variance TDI was 0.955 cm^2 (95% CI 0.781 to 1.116 cm^2).

While the mean biases in paired differences for the expectation and the variance are small, zero is not contained in the confidence interval of either. Therefore, there is systematic bias in the spring-mass model as a predictor of COM displacement in bipedal hopping. In a spring-mass system the most probable displacement location is the amplitude.[6] The empirical data in this study suggests participants spend more time moving toward and away from the COM amplitude and less time at the amplitude compared to probabilistic spring-mass model predictions. However, the TDIs for the paired differences in expectation and variance was less than 1 cm and 1 cm^2. Therefore, 95% of the time paired differences in theoretical and empirical estimates of the distribution of COM displacement will be within ± 1 cm or ± 1 cm^2. Arguably the theoretical and empirical values are interchangeable.

Significance

Given that healthy participants coordinate COM displacement such that the distribution of displacements closely resembles the PDF of a spring-mass model, the spring mass model serves as a sound biomechanical model. Additionally, an empirical distribution of COM displacements that deviates too far from the spring mass model PDF may indicate a loss of motor control. This study is a step toward understanding the bias in the spring-mass model and how humans deviate from it to gain insight into loss of motor control.

Acknowledgments

Chelsie Miller, SPT, Sage Kim, SPT, and Kaitlyn Henley, SPT

References

1] Blickhan R. *J Biomech.* 1989; 22(11-12): 1217-1227. doi:10.1016/0021-9290(89)90224-8
2] Gill N, Preece SJ, Baker R. *Biomed Phys Eng Express* (2018); 4(5).
3] Bullimore SR, Burn JF. *J Theor Biol.* 2007; 248(4): 686-695. doi:10.1016/j.jtbi.2007.06.004.
4] Kirkland MC, Wadden KP, Ploughman M. *Disabil Rehabil.* 2020; 1-12. doi:10.1080/09638288.2020.1820585.
5] Cavagna GA. *J Appl Physiol.* 1975; 39(1): 174-179. doi:10.1152/jappl.1975.39.1.174.
6] Bao L, Redish EF. *Am J Phys.* 2002; 70(3): 210-217. doi:10.1119/1.1447541.
7] Parker RA, Scott C, Inácio V, Stevens NT. *BMC Med Res Methodol.* 2020; 20: 1-14. doi:10.1186/s12874-020-01022-x.

A COMPARISON OF KINEMATIC AND ANATOMICAL AXES OF THE FIRST METATARSOPHALANGEAL JOINT

Eric Thorhauer,[1,2] Mackenzie French,[1,4] Tadashi Kimura,[1,5] and William R. Ledoux[1,2,3]
[1]RR&D Center for Limb Loss and MoBility (CLiMB), VA Puget Sound, Seattle, WA; Departments of [2]Mechanical Engineering and [3]Orthopaedics & Sports Medicine, [4]School of Medicine, University of Washington, Seattle, WA; [5]Department of Orthopaedic Surgery, The Jikei University School of Medicine, Tokyo, Japan.
email: ericthor@uw.edu

Introduction

Consisting of the first metatarsal, the proximal phalanx, and two supporting sesamoids, the first metatarsophalangeal joint (MTPJ1) or great toe joint is essential to our mobility and kinetic interactions with the ground. Due to the limitations in motion capture, precise quantification of motion at this joint has been challenging. As technology and techniques, like biplane fluoroscopy, develop, the more precise descriptions of motion require coordinate frames embedded in the first metatarsal. Two common ways of deriving these coordinate systems are based on principal component analysis (PCA) of the bone and on fitting geometric primitives to bone subregions.

The aim of this study was to investigate spatial relationships between the kinematic (screw) and primary joint flexion axes defined using PCA and localized geometric fitting of cylinders.

Methods

Ten fresh frozen cadaveric foot and ankle specimens were biomechanically tested via a custom tendon-loading apparatus built around a weightbearing cone-beam CT scanner (LineUp, CurveBeam, USA). Appropriate tendon loads [1] were applied to induce motion simulating a toe flexion and a heel raise activity. Toe flexions were performed with an instrumented toeplate controlling dorsiflexion from neutral, in 10° increments, to the natural maximum (50° or 60°). Heel raises from neutral to maximum dorsiflexion, (5 intermediate poses) were performed with a CT scan acquired at each pose.

CT bone kinematics were determined via volumetric registration of specimen-specific templates [2]. Coordinate systems were embedded via the PCA method in the proximal phalanx, and the metatarsal, whose orientations were copied and placed at the center of mass for each sesamoid. Custom morphological-based metatarsal axes (CYL) were also separately defined by fitting cylinders to the articular surfaces of the metatarsal head.

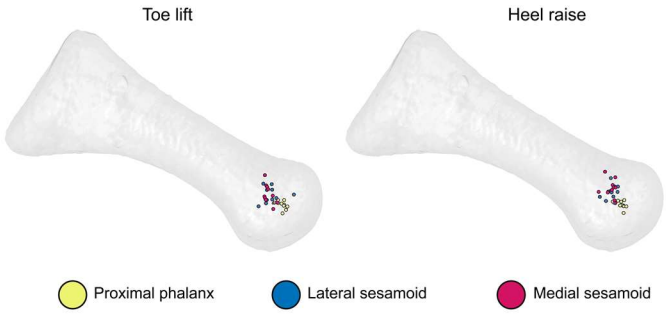

Figure 1: Each dot represents the median instantaneous center of rotation (ICR) for the proximal phalanx, and each sesamoid bone relative to the first metatarsal for a toe lift (dorsiflexion) and heel raise activity of a given foot.

The mean finite helical axes (mFHA) [3] and locations of the median instantaneous center of rotation (ICR) were determined for each of the three bones articulating with the metatarsal. All specimen data were spatially co-registered into a mean MTPJ1 representation. The orientations of the axes were compared in a spherical frame centered in the metatarsal head.

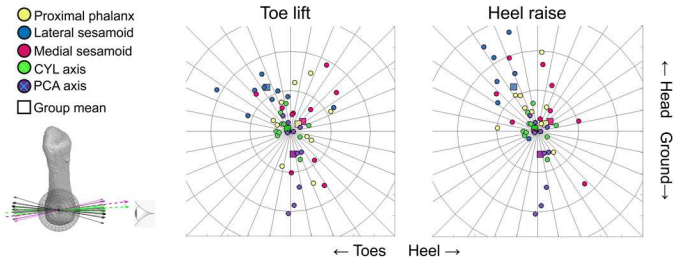

Figure 2: The intersection of the mean finite helical axes (mFHA) and flexion axes of the custom metatarsal anatomical coordinate systems based on two methods (PCA and CYL) with a unit sphere centered in the mean metatarsal model. Perspective from the medial side of a right metatarsal in a neutral foot position is shown.

Results and Discussion

All ICRs were clustered within the metatarsal head (Figure 1), like previously reported [4]. However, both sesamoid ICRs were distributed more proximally in the metatarsal body and with greater spread compared to the proximal phalanx. The distributions of the sesamoid ICRs were rotated between activities, while those of the proximal phalanx were largely unchanged.

The PCA-based flexion axes exhibited a more variable distribution than the CYL flexion axes, with some PCA axes tilted towards the ground. This is likely due to natural anatomical variation in metatarsal shape. The mFHA's of all bones were closer to the mean of the CYL flexion axes than PCA (Figure 2).

Flexion axes of a metatarsal anatomical coordinate system based on fitting cylinders to the distal articulations agree better with the orientations of the observed kinematic axes of the sesamoid bones and phalanx.

Significance

These data provide a basis of comparison for future in vivo studies of MTPJ1 motion. Joint coordinate systems for the first metatarsal bone may benefit from considering the geometric information of the articular surfaces.

Acknowledgments

Dept. of Veterans Affairs grant RX002357; University of Washington Medical School Scholarship of Discovery Program.

References

[1] Jackson LT, et al. J Biomech Eng. 2011 May;133(5):051005.
[2] Hu Y, et al. J Biomech Eng. 2011 Oct;133(10):101005.
[3] Ehrig RM, et al. J Biomech. 2019 Feb 14;84:4-10.
[4] Shereff MJ, et al. J Bone Joint Surg Am. 1986 Mar;68(3):392-8.

Human Gait and Motor Performance in a Physically Interactive Virtual Reality System

Syed T. Mubarrat[1], Manoj Srinivasan[1], Quinten Humphrey[2], Kieran Binkley[1], Thomas Chen[1], and Suman K. Chowdhury[1]
[1]Industrial, Manufacturing, and Systems Engineering, Texas Tech University
[2]Mechanical Engineering, Texas Tech University
Email: suman.chowdhury@ttu.edu

Introduction

Due to the recent advancement in the virtual reality (VR) technologies, some previous studies have focused on the utility of passive haptics—i.e., providing physical haptic interaction by mapping virtual objects to specific real objects—in the VR system. Though it was reported that the introduction of passive haptics enhanced both user experience and training effectiveness [1], a more comprehensive investigation of the technology in the context of motor output is warranted in order to explore how to maximize sensorimotor skill acquisition. Therefore, this study aimed to determine the impact of physically interactive VR usage on the sensory motor performance by comparing the movement kinematics and kinetics of the VR tasks with regard to same tasks performed in the real world. We hypothesize that the biomechanical parameters would exhibit no discrepancies between virtual and real environment tasks.

Methods

We designed a physically interactive VR system, in which the virtual environment (VE) was comprised of warehouse interiors, workers, forklifts, pallet racks, and four industrial collaborative robots (Cobots) and simulated a sequential time-and space-sharing human-robot collaborative pick-and-place task. Twelve healthy male participants (weight: 174.41 ± 5.00 lb, height: 72.96 ± 6.90 in, age: 25.926 ± 3.55 years) were recruited to perform three tasks while wearing a VR headset (VETs) and three tasks in the real environment (RETs). The task was to perform picking and placing of a box (weight: 20 lb; a total of 4 boxes; each placed at frontal and scapular planes of both left and right sides of the participants in the real world) within 8 seconds as soon as a Cobot deposited the box, each one at a time in a random order, either on the left-side or right-side pallet before the participant. A 10-camera motion capture system and two force plates were used to record participants' gait, ground reaction force, and centre of pressure. This gait data was then used to calculate the kinematics of the shoulder, elbow, and knee joints using the OpenSim modelling platform [2].

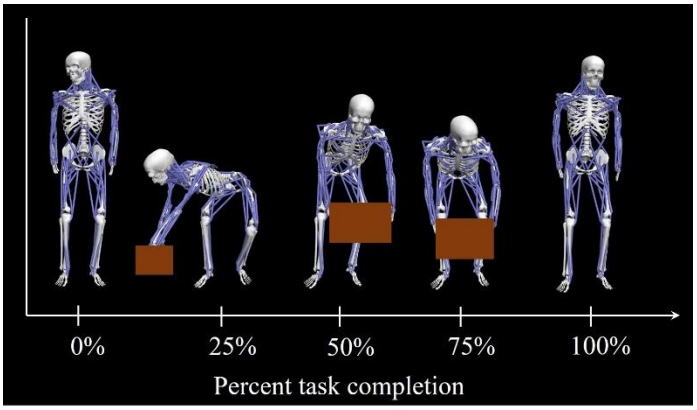

Figure 1: A visual demonstration of the simulated pick-and-place task in the Opensim modeling platform.

Results and Discussion

In this report, we present our conjecture of the differences between VET and RET based on the gait of three subjects. the RMSE of the COP of both feet between VET and RET were 33.42 ± 4.83 mm, 16.72 ± 1.66 mm, 44.98 ± 7.39 mm, and 20.30 ± 4.08 mm in the anterior-posterior (X) and medial-lateral (Y) direction for the right foot, and in the anterior-posterior (X) and medial-lateral (Y) direction for the left foot, respectively. For the complete task, the RMSE between VET and RET kinematics were 9.89 ± 0.71°, 10.69 ± 1.37°, and 8.77 ± 1.18° for shoulder, elbow, and knee joints, respectively. This discrepancies between VET and RET in terms of kinematics warrant a thorough analysis of perceptual-motor system to understand and improve the effectiveness of the VR skill acquisition.

Table 1: Comparison of biomechanical parameters between VET and RET for the box whose initial position was 30° right to mid-sagittal plane of the subjects.

		0%	25%	50%	75%	100%
R shoulder adduction (°)	RET	-20.14	-13.72	-10.69	-18.45	-18.58
	VET	-13.64	3.61	-7.30	-3.24	-15.80
L shoulder adduction (°)	RET	-21.39	-22.25	-14.04	-29.91	-17.16
	VET	-20.90	-45.15	-32.18	-27.17	-23.19
R elbow flexion (°)	RET	13.63	22.84	18.72	17.19	9.74
	VET	11.11	1.22	7.53	14.33	8.32
L elbow flexion (°)	RET	12.51	10.95	5.23	12.88	7.12
	VET	10.32	18.34	38.73	10.92	7.94
R knee bending (°)	RET	-7.28	-57.33	-28.31	-38.41	-6.06
	VET	-9.90	-52.69	-32.34	-28.81	-1.34
L knee bending (°)	RET	-8.31	-52.28	-20.32	-40.63	-6.37
	VET	-10.06	-55.09	-34.10	-40.40	-4.39
R COP X (mm)	RET	333.67	417.83	427.03	418.77	287.55
	VET	329.79	420.41	422.91	406.64	250.05
R COP Y (mm)	RET	-255.71	-204.55	-200.91	-208.51	-170.78
	VET	-244.23	-185.88	-204.36	-213.12	-187.04
L COP X (mm)	RET	338.68	409.06	417.53	438.76	295.16
	VET	326.65	422.89	409.71	428.39	247.76
L COP Y (mm)	RET	-600.89	-599.97	-617.22	-615.16	-498.37
	VET	-602.91	-617.72	-621.49	-650.72	-491.76

Significance

The study showed the promise of using physically interactive VR system that can provide operators with not only the first-hand experience of the real world task but also to retain relevant motor control, safety-awareness, and functional work capacity.

References

1. Cooper, N., et al. PloS one, 2018. **13**(2): p. e0191846.
2. Delp, S.L., et al. IEEE transactions on biomedical engineering, 2007. **54**(11): p. 1940-1950.

WHERE DOES STRETCH-SHORTENING CYCLE POTENTIATION OCCUR DURING A JUMP TEST PERFORMANCE?

Marzouq K. Almutairi[1,2], Mario Inácio[3], Gary Hunter[4], Harshvardhan Singh[1]
[1]University of Alabama at Birmingham, Department of Physical Therapy
[2]Qassim University, Department of Physical Therapy
[3]University Institute of Maia, Department of Physical Education and Sports Science
[4]University of Alabama at Birmingham, Department of Nutrition Science
email: marzouq@uab.edu

Introduction

Stretch shortening cycle potentiation (SSCP) is a basic muscle property positively related to the walking economy and increased physical activity. Typically, jump test performance (JTP) is used to assess SSCP[1]. JTP testing can involve three types of jump, countermovement jump (CMJ), static jump (SJ), and drop jump (DJ). Greater jump height achieved during DJ and CMJ compared to SJ is considered a surrogate marker of SSCP. While evidence indicates that the SSCP occurs early in the propulsion (i.e. concentric) phase during the jump, there is little information if SSCP is joint-specific[2]. Interestingly, nothing is known regarding joint-specific SSCP at the propulsion onset, which is defined as the first instant at which joint angular velocity becomes positive after the end of the eccentric phase. The identification of joint-specific SSCP would be highly relevant, as it could help understand joint-specific mechanics influencing JTP and could potentially help design joint-specific exercises to improve sports performance and physical activity. Thus, the purpose of this study was to assess joint-specific SSCP at the propulsion onset during JTP. We also sought to examine if the challenging nature of the jump task could affect joint-specific SSCP.

Methods

22 Healthy young adults (10 women, 12 men); age (years): 25.75±3.05; height (m): 1.71±.91; weight (kg): 71.90±16.34; performed the following jumps: maximal vertical jump from a standing position with a preliminary countermovement to their preferred depth (CMJ), maximal vertical jump after descending slowly from the standing position to the same depth achieved during CMJ and then remaining static for 2 seconds (SJ), and maximal vertical jump after dropping from a 15 cm high platform onto the force platforms (DJ). Hands were placed on the hips during all the jump trials. Full-body motion capture was used during all types of jumps. Joint kinetics and kinematics were calculated for the hip, knee, and ankle. Jump height (JH) was calculated from the greater trochanter data as its highest value achieved during the aerial phase minus standing upright height. The propulsion onset was defined as the first positive data point (after the end of the eccentric phase) of the joint angular velocity of the hip, knee, and ankle joints, respectively. Ratios of (i) jump height (JH) and (ii) respective joint-specific extension moments for different types of jump (CMJ/SJ; DJ/SJ; DJ/CMJ) were calculated as surrogate markers of SSCP.

One sample t-test was run to assess the presence of SSCP where a greater than 1 difference in a) JH ratio and b) respective ratios of joint moments (hip, knee, and ankle) at the propulsion onset between different types of jump (CMJ vs SJ; DJ vs SJ; CMJ vs DJ) indicated SSCP. Separate within-subjects repeated measures ANOVA were performed to compare joint-specific ratios of moments at the propulsion onset for a) CMJ/SJ, b) DJ/SJ, and c) DJ/CMJ.

Repeated measures for CMJ/SJ analysis were controlled for any difference in the knee angle between CMJ and SJ. For example, within-subjects repeated-measures ANOVA to compare joint-specific ratios of moments for CMJ/SJ were controlled for delta knee angle (CMJ-SJ).

Results and Discussion

Ratios of JH for CMJ/SJ, DJ/SJ, and DJ/CMJ were greater than 1 (all $P \leq 0.01$; **Figure 1**). Respective ratios of joint moments (hip, knee, and ankle) at the propulsion onset for CMJ/SJ and DJ/SJ were greater than 1 (all $P < 0.01$) while for DJ/CMJ, ratios of respective joint moments were greater than 1 for the ankle ($P = 0.028$) and hip ($P = 0.043$) but not for the knee ($P = 0.096$). We found the degree of SSCP was greatest at the ankle followed by the hip and knee for CMJ/SJ and DJ/SJ (all $P < 0.05$) (**Figure 2A and 2B**). No joint-specific differences in SSCP were noted for DJ/CMJ. To our knowledge, we are the first to report that SSCP is generated at the hip, knee, and ankle joints at the propulsion onset during JTP.

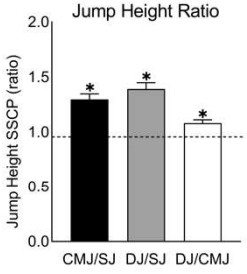

Figure1. *denotes significant difference from 1

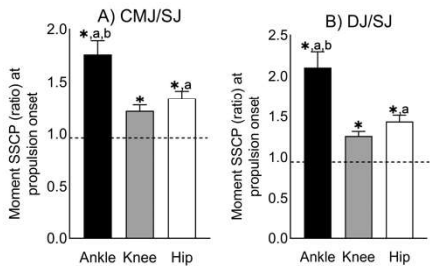

Figure2. *denotes significant difference from 1; [a]significantly different than the knee; [b]significantly different than the hip

Significance

Our findings show that at the propulsion onset during JTP, SSCP occurs at the hip, knee, and ankle, and is maximum at the ankle followed by hip and knee, in that order.

Acknowledgments

The authors wish to express gratitude to all the participants.

References

1. Bobbert MF, Gerritsen KG, Litjens MC, et al. Why is countermovement jump height greater than squat jump height? Med Sci Sports Exerc. 1996;28(11):1402-1412.
2. Kipp K, Krzyszkowski J, Heeneman J. Hip moment and knee power eccentric utilisation ratios determine lower-extremity stretch-shortening cycle performance. Sports Biomech. 2019:1-11.

SUBMAXIMAL SOLEUS FORCE LENGTH CHARACTERISTICS WITH AGING

Lindsey H. Trejo[1], Jordyn N. Schroeder[1], Owen N. Beck[1], and Gregory S. Sawicki[1]
[1]School of Mechanical Engineering and Biological Sciences, Georgia Institute of Technology, Atlanta, GA, USA
email: ltrejo@gatech.edu

Introduction

Older adults use more energy to walk than young adults. Reduced ankle push-off power leads to poor walking performance but the mechanism is unknown. Many age-related changes could cause reduced muscle power output such as loss of type 2 fiber percentage, loss of muscle mass, and increased connective tissue limiting gearing of the muscle. Instead, we believe reduced Achilles tendon stiffness in older adults is the structural bottleneck that disrupts muscle-tendon dynamics cascading into higher metabolic cost.

With reduced stiffness, tendon will have greater excursion and push muscles to shorter lengths.Shorter muscle lengths shift fascicles away from optimal lengths on the force-length (FL) curve. Then, to produce a given force at shorter lengths, required muscle activation is higher, which is more energetically costly.

It has been shown that at submaximal activations the optimal muscle length shifts to the right [1]. It is unclear whether this activation dependent, rightward shift in the FL curve is retained in aged muscle. We hypothesize that older adults would have less stiff tendons and optimal lengths shifted to the right at submaximal activations. The shape of the force length curve comes from the overlap of actin and myosin, changing the ability to form crossbridges. Assuming crossbridge formation is similar at matched relative actin-myosin overlaps across age, we expected no age-related differences in normalized force length curves.

Methods

One young (male, 30 years), and one older adult (female, 77 years) performed 2-3 plantarflexion (PF) contractions at 5 ankle joints (30°PF, 15°PF, 0°, 15° dorsiflextion (DF), maxDF) and 4 activations (0, 33, 66, 100% max voluntary contraction [MVC]). Force length curves were measured using a dynamometer. Muscle activity and muscle lengths of the soleus were measured using EMG and ultrasound, respectively. MVC were performed with visual torque feedback while 33% and 66% contractions were performed with EMG feedback. Two minutes of rest were taken between every contraction. For the passive curve, torque and length were measured at increments of 5° from 10°PF to maxDF after 45 seconds of resting in this position to mitigate history-dependent effects. Soleus active muscle force (F_{sol}^{act}) was calculated as follows.

$$F_{sol}^{act} = \frac{\tau_{total} - \tau_{pedal}}{r_{ank} \cdot \cos(\theta_{penn})} - F_{sol}^{pass}$$

τ_{total} is total torque, τ_{pedal} is pedal torque, r_{ank} is ankle moment arm, θ_{penn} is pennation angle, and F_{sol}^{pass} is passive force at the length during contraction. A 2nd or 3rd order polynomial was fit to the data for the active curves, and an exponential curve for the passive data [2]. For tendon stiffness, ultrasound was placed over the gastrocnemius - Achilles muscle tendon junction at 3 angles (0°, 15°, 30°) on the dynamometer and calculated as the slope of the force-displacement curve of the tendon. Submaximal FL curves were only obtained for the young adult.

Results and Discussion

As expected, the tendon stiffness was lower for the older adult (young: 156.2 kN/m, older: 115.9 kN/m) and the normalized max and passive force-length curves are similar between young and old. For the young adult at submaximal activations the optimal length shifted toward longer lengths (100%: 36.6 mm, 66%: 45.7 mm, 33%: 56.8 mm) in agreeance with our hypothesis. The absolute force-length curves for the older adult had lower maximum force (young: 6067.3 N, older: 2167.5 N), longer optimal length (young: 36.6, older: 44.5 mm), and a wider range (experimental range: young: 23.3 – 43.5, older: 26.4 – 53.8 mm; curve fit range: young: 21.9 – 51.4, older: 23.9 – 65.0 mm). Lower maximum force with aging has been reported previously. Since the normalized max curve was similar we would expect older adults submaximal curves to shift rightward proportionally.

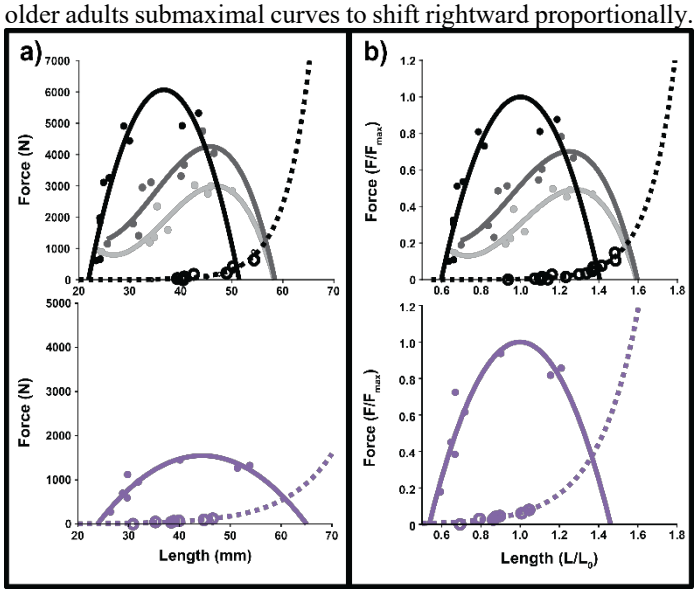

Figure 1: a) The force-length-activation curves of a young adult (top) and older adult (bottom) at 33%(grey), 66% (dark grey), and 100% (black/purple) activation and a passive curve (dotted). b) The normalized force-length-activation curves of a young adult (top) and older adult (bottom). Dots = experimental data.

Based on these preliminary data, we conclude older adults have less stiff tendons, have similar normalized force length curves at maximum capacity. Based on the similarity at maximum and the rightward shift in the young adult we would expect an activation dependent rightward shift in soleus optimal length in older adults.

Significance

Characterizing how muscle FL curves shift with aging is a critical aspect to understanding the mechanical and energetic implications of reduced tendon stiffness. Identification of such a shift can then inform training interventions and the design of assistive devices to address the mechanical and metabolic effects of aging.

Acknowledgments

NIH NIA Grant (R0106052017) and Alfred P. Sloan Foundation Graduate Scholarship

References

[1] N. C. Holt and E. Azizi, 2014, *Biol. Lett.*
[2] J. Rubenson et al., 2012 *J. Exp. Biol.*

WHICH JOINTS COMPENSATE FOR DESTABILIZING ENERGY DURING WALKING?

Pawel R. Golyski[1,2], Gregory S. Sawicki[1,2,3]
[1]Parker H. Petit Institute for Bioengineering and Biosciences, [2]The George W. Woodruff School of Mechanical Engineering
[3]School of Biological Sciences, Georgia Institute of Technology, Atlanta, GA, USA
email: *pgolyski3@gatech.edu

Introduction

Changing mechanical energy demand during walking is useful for investigating joint level contributions to whole-body mechanics. Because the net mechanical energy change of a person during a constant speed walking stride on level ground must be zero, the energy injected or extracted by a change in the net energy demand can be traced to each joint using mechanical energy accounting. A transient change in demand, such as falling in a hole [1], allows for exploring joint level contributions to stability where the objective is known (*e.g.* the dissipation of some known potential energy). A change in treadmill belt speed can also transiently inject or extract energy, depending on whether the treadmill velocity and anteroposterior GRF are in the same or opposite directions, respectively, at the time of the perturbation.

We evaluated which lower-limb joints compensate for the energy injected or extracted by a transient acceleration of a treadmill belt during walking. Based on previous research in humans and guinea fowl, we hypothesized changes in ankle work would compensate the most for changes in task demand. [1,2]

Methods

We had 1 subject (24 y/o, 89.3 kg, 1.05 m leg length) walk on a split-belt treadmill at 1.25 m/s while rapid (15 m/s^2, 0.2 sec duration) changes in belt speed to 2.5 m/s were applied to a single treadmill belt in a randomized order. While the participant walked, we transiently injected energy by delivering the perturbation at heel strike and extracted energy by delivering the perturbation at 20% of the gait cycle (2 legs x 10 trials per timing). Inverse dynamics were calculated in OpenSim. The stride preceding the perturbation (S -1), stride of the perturbation (S 0), and 3 strides following the perturbation (S +1-3) were analyzed. Sagittal plane joint powers from both limbs were integrated over each stride to calculate work of joints, and summed joint works were calculated as work of limbs. Treadmill work was calculated by integrating the product of both treadmill belt velocities and corresponding AP GRFs, with positive treadmill work being defined as energy flowing from the person to the treadmill.

Results and Discussion

Energy extraction and injection were both reflected in changes in whole limb and joint level work relative to the baseline (unperturbed) stride (Fig 1). The largest changes were observed on the stride of (S 0) and immediately following the perturbation (S +1). For both perturbations, pattern of generation and dissipation was similar across all joints on the perturbed stride (S 0). When dissipation was required (Fig 1A), it occurred primarily through net negative ankle work on the following stride (S +1). This distal joint dissipation supports our hypothesis and agrees with previous work. [1,2] When generation was required (Fig 1B), this primarily occurred at the hip joint on the stride following the perturbation (S +1). This was not consistent with our hypothesis and suggests proximal joints play an important role in stability during walking when energy must be produced (*e.g.* having to step out of a hole).

Significance

This work extends the paradigm of split-belt mechanical energetics for stability assessment. This approach is powerful because the stabilizing objective is known (*i.e.* return to steady-state levels of net mechanical energy = ~0). Further, the findings suggest the joint targets for wearable exoskeletons designed to improve stability may depend on whether energy is injected or extracted during the gait cycle and targeting a single joint may only allow for improvement of stability in certain cases.

Acknowledgments

PRG is supported by an NSF GRFP: DGE-165004.

References

[1] Dick et al. (2019) *J. R. Soc. Interface*
[2] Daley et al. (2007) *J. Exp. Biol*

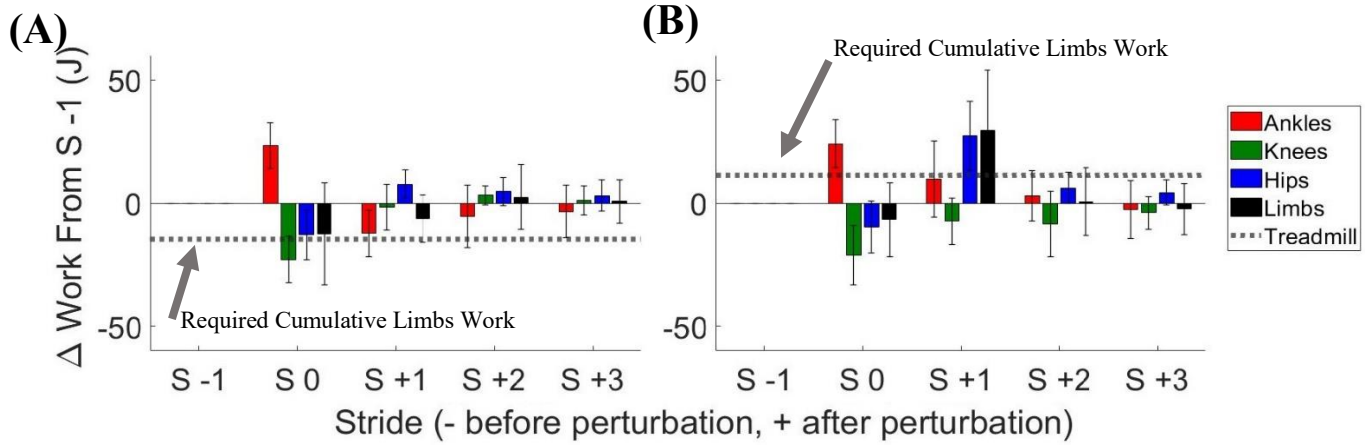

Figure 1: Work demand of the treadmill during the perturbed stride, as well as bilateral joint works and their sum ("Limbs"). **(A)** Perturbation onset at 0% of stride (energy injection by treadmill = person must dissipate energy) and **(B)** 20% of stride (energy extraction by treadmill = person must generate energy). Error bars represent ±1 standard deviation

THERE ARE UNIQUE JOINT KINEMATICS THAT EXIST DURING LOCOMOTOR TRANSITIONS FROM LEVEL WALKING TO STAIRS THAT ARE AFFECTED BY STAIR GRADE

Ross M. Neuman[1] and Nicholas P. Fey[1]
[1]The University of Texas at Austin, Department of Mechanical Engineering
email: ross.neuman@utexas.edu

Introduction

Human locomotion is typically characterized during isolated tasks (e.g., walking, running, stair ambulation). In these instances, repeated trials are often pooled to characterize the "steady-state" mechanics of given tasks. However, general human locomotion comprises continuous accommodation to new and varied terrains, as we complete our own activities of daily life. To fill an important gap in knowledge that may lead to improved therapeutic and device interventions for mobility-impaired individuals, identifying how the mechanics of individuals change as they transition between different locomotor tasks is vital. In this study, we characterize the transitions between level walking and stair ascent and descent, and their sensitivity to stair inclination angle. These transitions are a point of significant fall risk, particularly among the elderly [1], and are not well-handled by currently-available prosthetic and orthotic technologies [2]. We hypothesize that transition strides between level ground and stairs will possess joint kinematics that are unique from those in level and stair ambulation, and that these characteristics will be influenced by stair inclination angle.

Methods

Hip, knee and ankle angles were calculated from motion capture data (sampled at 120 Hz by a 10-camera Vicon system) of 10 able-bodied individuals (5 male, 5 female, 19-59 yrs., 53-87 kg). A Plug-In Gait lower-body markerset was used for these calculations, which were made using Vicon Nexus. These individuals completed 5 trials as they approached and ascended, then approached and descended a 4-step staircase at self-selected walking speeds. Trials were repeated at 20°, 25°, 30° and 35° stair inclination angles. Transition (TR) strides were defined as the first stride where terminal heel-strike occurred on the stairs following a toe-off on the level walking surface. To compare joint angles as function of the gait cycle, we used statistical parametric mapping (SPM) paired t-tests for each lower-limb joint, three times, to compare: TR strides and those of level walking (LW), TR and stair ascent (SA) strides, and TR and stair descent (SD) strides. Multiple non-transition stair strides that occurred on the staircase were pooled for these analyses, and a Bonferroni correction was used to adjust the significance level from α=0.05. Thus, *regions* of the gait cycle where statistically-significant differences occurred were identified, rather than choosing discrete data points [3]. TR strides were considered "unique" when significantly different from both TR and SA/SD strides.

Results and Discussion

Our hypotheses were supported. Unique TR joint kinematics were identified in at least one joint for each transition we compared, and usually in all three joints (e.g., Fig. 1). In general, TR strides tracked closely their preceding level walking task for much of stance, and tracked the following stair task during late swing. Uniqueness most often presented in late stance and early swing (Fig. 1), where rapid changes in mechanics are made. However, stair inclination was shown to influence both the timing and magnitude of these regions of significance.

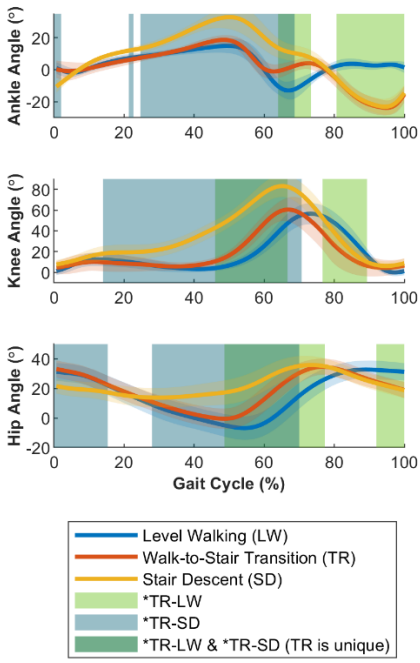

Figure 1: Comparison of kinematic trajectories for the transition from level walking to stair descent. Shaded regions represent significant difference between the TR stride and LW or SD. Overlapping regions represent kinematics unique to the TR stride. These data are shown for 35° stair inclination.

Our results appear to make intuitive sense—that transition strides are mostly a hybrid of their adjacent tasks—but importantly, they statistically quantify these relationships, as well as the additional, unique complexities that arise during these locomotor transitions. A salient example of these complexities can be seen in the ankle trajectories in Figure 1, from 60-80% of the gait cycle. Here, the TR stride shows the ankle depart from LW trajectory to hold a neutral position before plantarflexing prior to contact with the first descending step of the staircase. Such unique patterns may be vital to safely initiate stair descent from level walking.

Significance

This work is the first to statistically quantify uniqueness in lower-limb joint kinematics during locomotor transitions between level-ground walking and stairs, which contributes to our basic understanding of the biomechanics of human locomotion, and motivates future work to form a more complete picture of how humans negotiate variable terrains. These findings have potential implications in both clinical and technical fields, from informing fall-risk assessments and rehabilitative strategies, to highlighting vital transitory kinematics that designers of robotic prostheses and orthoses could incorporate into their devices.

References

[1] D. H. Blazewick, *et al.*, doi: 10.1016/j.ajem.2017.09.034.
[2] A. M. Simon *et al.*, doi: 10.1371/journal.pone.0099387.
[3] T. C. Pataky *et al.*, doi: 10.7717/peerj.2652.

MOTOR MODULE COMPARISON BETWEEN A COLLEGIATE & RECREATIONAL ATHLETE

Justin D. Lyon[1], J. Bailey.[2], Y. Chun[2], and C.P. McGowan[3]
[1]Department of Biological Sciences; [2]Department of Movement Sciences, University of Idaho, Moscow, ID
[3]Integrative Anatomical Sciences, University of Southern California
Email : lyon2142@vandals.uidaho.edu

Introduction

What inherent quality differentiates elite level college athletes from everyday active individuals? This study seeks to examine the neuromotor control patterns that underlie sprinting by college athletes. Muscle synergies have been defined as the physiological activation of a group of muscles that contribute to a particular movement, thus providing an insight into possible neuromotor control mechanisms used by the nervous system to simplify the coordination of movement tasks[1]. Elite level college athletes were used as the target population based on the belief that they have higher, more robust neuromuscular control patterns when compared to recreational athletes[2]. With the use of muscle synergy analysis, the purpose of this study is to be able to determine if there is a difference between the number of motor modules required to reconstruct the waveform of a given motor task between groups, or to what length the correlated values of the variance accounted for (VAF) group deviate from their calculated mean between groups. We hypothesize that because college athletes use highly repeatable muscle activation patterns to achieve consistent performance, then they will utilize a lower number of muscle synergies that account for a higher VAF over all strides compared to untrained individuals.

Methods

For this study, a recreational (athlete #1,167 cm, 57.65 kg, 21 years of age) and a collegiate level (athlete #1,180 cm, 80.65 kg,19 years of age) athlete were recruited from the University of Idaho student population. Wireless Delsys EMG surface electrodes (Avanti) were placed on each of the eight target muscles (TA, SOL, LG, VL, RF, ST, BF, and GM) on the right leg of each participant. Application and site preparation were in conjunction with Seniam guidance. Following the application of the EMG sensors, participants were provided a self-selected warm-up period of at least 5 minutes.

A standardized step-up/step-down task was used to normalize EMG signals across participants using a dynamic task. Participants ran a series of four 30-meter sprints on an outdoor track. Trials were recorded using Delsys EMG Works software, timing gates, and sagittal plane 2D video (GoPRo Hero 5). Tibial acceleration of the right leg was measured using the accelerometer channels of an Avanti sensor (Delsys) attached to the medial aspect of the right leg anterior tibial border. Using vertical accelerometer profiles, the location of 5 localized peaks were identified. One gait cycle was identified from one peak to the subsequent peak.

All EMG signals were then cycle divided into 4 cycles per trial. EMG signals were demeaned, full wave rectified, and then low pass filtered (6 Hz). EMG Data was then placed through a non-negative matrix factorization algorithm in order to determine the number of motor modules required to reconstruct the original EMG waveform. The number of motor modules used to reconstruct the sprinting wave form was determined based on a threshold VAF of >90% and whether adding a module led to a substantial change in the VAF.

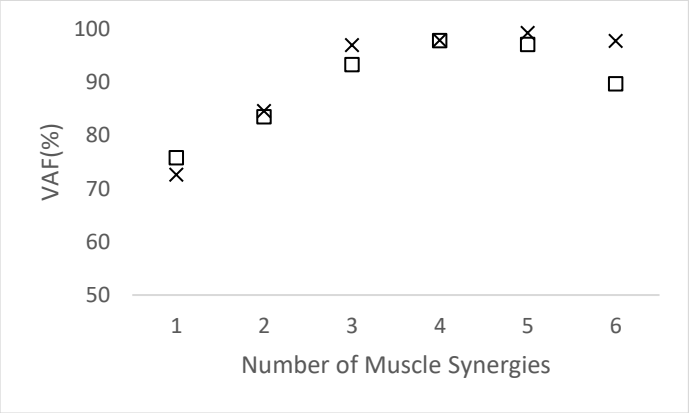

Figure 1: The number of muscle synergies selected accounted for > 90% of the overall variability accounted (VAF) as depicted by the plots from one recreational athlete (square) and one track athlete (X).

Results and Discussion

Applying six identified modules across one track athlete and one athlete represented that three modules were sufficient to recreate the muscle activation waveforms at a VAF > 90% with no substantial increase in VAF when adding another module. The exemplary recreational athlete achieved a VAF of 93% with three muscle synergies but experienced an increase of 4% when a fourth muscle synergy was added. When a fifth muscle synergy was applied to the recreational athlete there was not a substantial increase in VAF. Conversely, the track athlete achieved 97% VAF with three muscle synergies, and on substantial increase was observed with the addition of a fourth muscle synergy. For this reason, we concluded that in order to reconstruct the muscle activation waveform while sprinting, the track athlete was able to use three muscle synergies while the recreational athlete required four muscle synergies.

This exemplary analysis presents a possible insight into the more efficient motor control patterns of a trained, college sprinter when compared to a recreational athlete. The data presented is a pilot investigation of two individuals (one track and one recreational athlete) so the inclusion of further athletes may provide further evidence to support our findings.

Significance

These findings may support the theory that trained sprinters are more efficient in their movement patterns than non-trained sprinters.

Acknowledgments

Supported by the Arnold and Mabel Beckman Foundation through the Beckman Scholars Program

References

1.) Neptune et al. (2009). *ASME 2009 Summer Bioengineering Conference, Parts A and B*.
2.) Tillin, Neale A et al (2009). *Medicine & Science in Sports & Exercise*, Volume 42: Issue 4.

DETECTING SHIFTS IN MECHANICAL LOADING IN COLLEGIATE RUNNERS WITH AND WITHOUT IMPENDING LOWER EXTREMITY BONE STRESS RESPONSES

Harper E. Stewart[1], Kathryn A. Farina[3,4], Michael E. Hahn[3,4], and Jill McNitt-Gray[1,2]
[1]Department of Biomedical Engineering, [2]Department of Biological Sciences, University of Southern California, Los Angeles, CA,
[3]Bowerman Sports Science Clinic, [4]Department of Human Physiology, University of Oregon, Eugene, OR, USA
email: hestewar@usc.edu

Introduction

Running is the most popular form of physical activity in the USA and a primary reason people stop running is re-injury.[1] Stress-related fractures experienced by runners most commonly occur to the metatarsals or tibia, and in some cases the femur and pelvis.[2-4] Current approaches focus on group level analyses that relate loading rate with tibial acceleration by foot strike pattern or comparing tibial acceleration experienced by groups of individuals with a history of stress-related injury versus healthy controls.[5,6] An initial step in our exploratory, cross-institutional study focusing on NCAA DI runners, was to determine within-runner differences in variables used to characterize mechanical loading experienced by each leg over time. These within individual-differences in runners without a stress response can then be used to better understand observed differences in mechanical load experienced by individuals with a bone stress response.

Methods

12 NCAA DI mid- and long-distance runners from four different PAC 12 schools provided informed consent to participate in this cross-institutional study. Force data was collected using local instrumented outdoor track or treadmills (1000 Hz). Wearable inertial measurement units were used to measure accelerations at the sacrum and lateral shanks (iMeasureU, APDM, 500 Hz). Each runner participated in at least two collections separated by a minimum of 3 months. Nine or more steady-state contacts were collected per leg during each collection at different training paces. Mechanical loading was characterized by the average resultant GRF during contact (>30 N threshold) and the initial phase of contact (Fig 1).

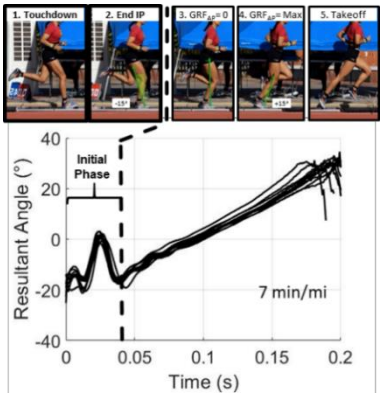

Figure 1: Initial phase defined from initial contact to largest posterior directed angle of the resultant GRF prior to propulsion.

Results and Discussion

Variables characterizing mechanical loading during foot contact of individuals without a bone stress response were found to be comparable over time within legs of runners (Fig 2), regardless of whether reaction forces were measured overground or using a treadmill. As this database of runners becomes more populated, insights regarding context for the observed differences in mechanical loading within individuals demonstrated by between variables, between legs, and between sessions can be elucidated as seen in Participants 1 and 12 (Fig 2).

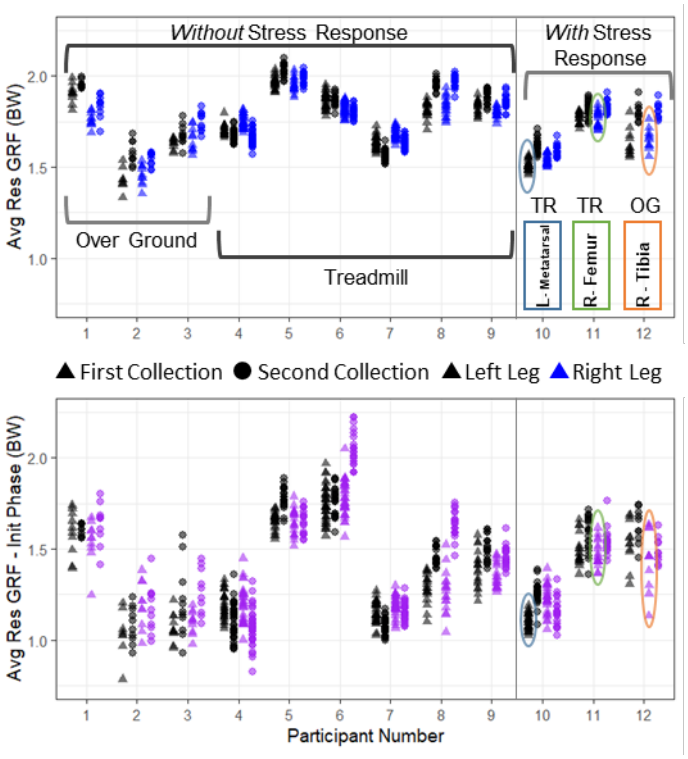

Figure 2: (*Top*) Average Resultant GRF during contact (*Bottom*) Average Resultant GRF during initial phase between collections, individuals, and legs at 7 min/mi pace (3.8 m/s). Collection prior to sustaining the stress response indicated by ovals.

Significance

This work in progress demonstrates the feasibility and utility of cross-institutional research that aims to prospectively determine injury risk by increasing sample size. By characterizing within runner-differences in mechanical loading experienced by individuals without a bone stress response, we have a foundation for detecting meaningful changes in mechanical loading characteristics in individuals with a bone stress response.

Acknowledgments

Supported by the PAC12 Student-Athlete Health & Well-Being Grant Program, Los Angeles Chapter of ARCS and USC WiSE. Thank you to our collaborators at the University of Colorado-Boulder.

References

[1] C. D. Johnson, et al. (2020) *Am. J. Sports Med.*
[2] T. Nusselt, et al. (2010) *Acta Orthop. Belg.*
[3] A. S. Tenforde *et al.*, (2018) *Med. Sci. Sports Exerc.*
[4] S. J. Koenig, et al. (2008) *Am. J. Orthop.*
[5] C. E. Milner, et al. (2006) *Med. Sci. Sports Exerc.*
[6] A. S. Tenforde et al. (2020) *PM R*

COORDINATION RIGIDITY IN GAIT, POSTURE, AND SPEECH IN PARKINSON'S DISEASE

Dobromir Dotov[1], V. Cochen de Cock[2], B. Bardy[3], and S. Dalla Bella[4]
[1]Psychology, Neuroscience and Behaviour, McMaster University, Hamilton, Canada
[2]Clinique Beau Soleil and CHU, Hôpital St Eloi, Montpellier, France
[3]EuroMov, Université de Montpellier, Montpellier, France
[4]International Laboratory for Brain, Music, and Sound Research, University of Montreal, Montreal, Canada
email: *dotovd@mcmaster.ca

Introduction

Parkinson's disease (PD) is associated with reduced coordination abilities. These can result either in random or rigid patterns of movement. The latter, described here as coordination rigidity (CR), have been studied less often. We investigated whether signatures of CR were present in walking, quiet stance, and speech—tasks involving coordination among multiple body parts. We used kinematic and voice recordings to compute theoretical variables from dynamic and complex systems. After clinical evaluation, moderate stage patients were compared against matched healthy participants.

Methods

The procedure involved clinical evaluation and a battery of walking, tapping and either postural or speech tests performed on a later day, see Figure 1. Participants (total N=78 across two studies) performed three-minute-long trials of over-ground walking in free condition or with rhythmic auditory cues. The postural task consisted of participants (N=38) maintaining standing posture for a minute in eyes-closed and eyes-open trials. Speech production (a subset of the participants, N=26) was recorded while reading a one-page article after one practice trial. All participants (N=78) performed a rhythmic tapping task with the instruction to keep a steady tempo without cueing.

We used the maximum Lyapunov exponent or log-divergence λ for a CR measure associated with instability in gait dynamics. For postural fluctuations, the choice of analysis method was similarly guided by theoretical and practical constraints. Sample entropy, the rate of generation of new information in a stochastic time-series, decreases when physiological control switches from complex to pathologically simple patterns. For speech, we captured the continuous variations in voice dynamics by analysing the smoothed amplitude envelope with recurrence quantification analysis. It detects recurrence points where the dynamic trajectory revisits locations in its embedded phase space. We used the predictability time measure (L_{AMP}).

Results and Discussion

PD was associated with decreased divergence in gait dynamics, reduced complexity of postural fluctuations, and increased predictability of voice dynamics, all consistent with CR, see Figure 1. The relevance of CR was confirmed by including features in automatic disease classification with supervised machine learning (81/81/86% accuracy/sensitivity/specificity).

Significance

We suggest the notion of CR, relevant for understanding the interplay between neural and biomechanical constraints on movement. Additionally, the present work makes a contribution with practical and clinical applications. We arrived at theoretically consistent results and satisfactory automatic classification by relying on affordable portable apparatus, a clinical setting, and tasks related to activities of daily living that in principle can be self-administered.

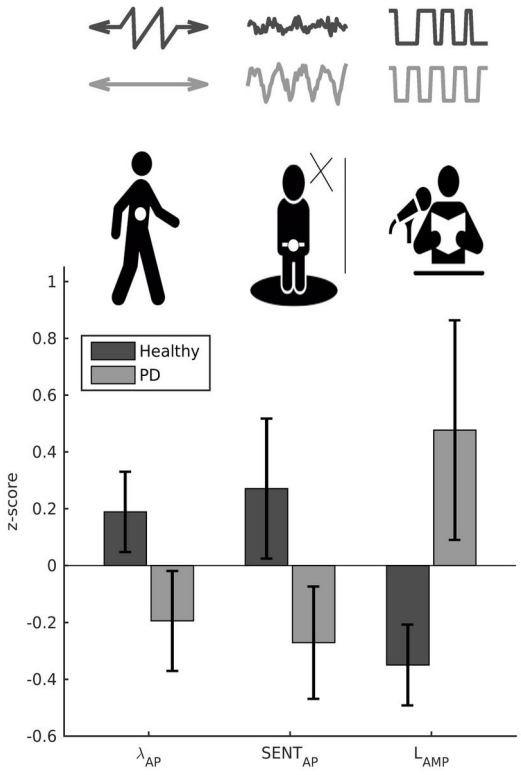

Figure *1*: Group means (SE) of measures sensitive to coordination rigidity in three activities of daily living: gait, postural control, and voice dynamics. Measures were normalized (z-score) for a common scale. The qualitative difference in movement is shown on top. Anterior-posterior (back and forth) upper body accelerations while walking become less dynamic (divergence rate λ). Anterior-posterior postural fluctuations while maintaining standing posture become more regular (SENT). The voice amplitude dynamics becomes more predictable (LAMP).

Acknowledgments

The authors were partly supported by grant FP7-ICT-2013-10 "Health and Wellness on the Beat" awarded to BB and SDB.

COMBINING AUDIOVISUAL AND SENSORIMOTOR BIOFEEDBACK IMPROVES PLANTARFLEXOR RECRUITMENT DURING WALKING IN CHILDREN WITH CEREBRAL PALSY

Alyssa M Spomer[1*], Benjamin C Conner[2], Michael H Schwartz[3], Zachry F Lerner[2-4], and Katherine M Steele[1]
[1]Department of Mechanical Engineering, University of Washington, Seattle, WA
[2]College of Medicine – Phoenix, University of Arizona, Phoenix, AZ
[3]Center for Gait & Motion Analysis, Gillette Children's Specialty Healthcare, St. Paul, MN
[4]Department of Mechanical Engineering, Northern Arizona University, Flagstaff, AZ
Email: *aspomer@uw.edu

Introduction

Cerebral palsy (CP) is a neuromuscular disorder that primarily impacts motor control, hindering independent gait. To improve mobility, children with CP often undergo surgical interventions; however, most interventions fail to improve function and impose large financial and emotional burdens on families [1]. As such, identifying alternative treatment options is critical to bolster clinical care for CP.

Biofeedback is a non-invasive alternative to traditional interventions. Commonly, biofeedback systems are designed to provide feedback on movement error via audio or visual cues; these systems have been used successfully to improve joint power [2], spatiotemporal parameters [3], and muscle activations [4]. However, developing strategies to provide sensorimotor (SM) feedback may be equally critical for facilitating user response and retention, particularly in CP where sensory processing is often impaired [5]. To this end, Conner et al recently demonstrated that an ankle exoskeleton that uses resistive torques to provide SM feedback during walking could elicit significant improvements in both muscle activity and motor control in CP [6]. While the success of each of these modalities highlights the promise of using biofeedback in CP, there is evidence to suggest that combining modalities may further amplify treatment effects [5].

The aim of this pilot study was to evaluate the effect of combined audiovisual (AV) and SM feedback (AV+SM) on muscle activity in individuals with CP. Secondarily, we evaluated whether changes in muscle activity corresponded to changes in motor control. We hypothesized that AV+SM feedback would have a larger effect than AV-only feedback.

Methods

Two subjects with diplegic CP (12,14 yrs; GMFCS II) walked at self-selected speed on a treadmill under two feedback conditions, performed in a non-randomized order: (1) AV and (2) AV+SM feedback. Participants performed one trial per condition which was separated into baseline (BASE; 2 min) and feedback (10 min) phases.

Both AV and SM feedback targeted soleus activity of the more affected limb, as the plantarflexors are critical for efficient propulsion but are often impaired in CP [7]. SM feedback was administered using an untethered ankle exoskeleton that has been previously validated in CP [8]. This device imparts a resistive dorsiflexion moment proportional to the user's estimated ankle moment during push-off to encourage plantarflexor activity. AV feedback provided real-time stance-phase activity from soleus electromyography (EMG) recordings. For each step, a tone played if soleus activity was 10% above BASE activity. During AV-only feedback, participants wore the exoskeleton in the zero-torque condition to reduce device-specific effects.

EMG data were collected bilaterally at 1000 Hz from the soleus, rectus femoris, semitendinosus, and tibialis anterior. Mean soleus activity was calculated from one-minute of data from the BASE and feedback trials. Muscle synergy analysis was performed to calculate the total variance accounted for by a one-synergy solution($tVAF_1$). The $tVAF_1$ captures motor control complexity; larger $tVAF_1$ values correspond to less complex motor control and have been shown to be associated with function and treatment outcomes in CP [9].

Results and Discussion

Participants increased soleus activity under both feedback conditions. However, AV+SM feedback resulted in a larger deviation in soleus activity from BASE (47.5%) than AV feedback alone (9.9%). In contrast, motor control complexity ($tVAF_1$) was minimally affected (deviation from BASE: +0.89% AV and +3.5% AV+SM).

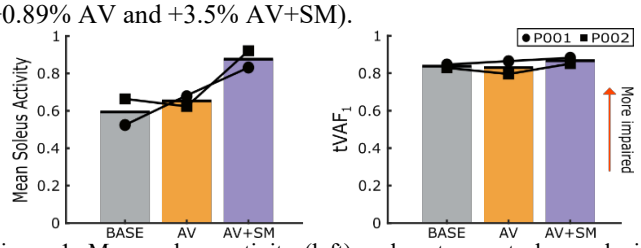

Figure 1: Mean soleus activity (left) and motor control complexity ($tVAF_1$; right) during BASE, AV, and AV + SM feedback conditions.

Integrating AV+SM feedback led to notable increases in soleus activity in a single session, suggesting that combining feedback modalities may be valuable for eliciting larger training responses than SM or AV feedback alone. There was minimal change in motor control, which aligns with our expectations that altering motor control requires longer duration training [6,10]. Future research will investigate whether the increased plantarflexor activity observed in AV+SM feedback is retained with additional training and amplifies improvements in motor control and function.

Significance:

This study demonstrates the potential for using exoskeleton resistance with AV feedback to improve plantarflexor recruitment during walking in CP. While further work with a larger cohort is needed, this is a promising early evaluation of a non-invasive treatment option to target muscle activity in CP.

Acknowledgments This work was funded under NIH Award 1R15HD099664, NIH NINDS Award R01NS091056, and NSF GRFP Award DGE-1762114.

References

[1] Schwartz MC, et al. Dev Med Child Neurol. **58**(11). 2016 [2] Booth ATC, et al. Gait Posture **52.** 2017. [3] Baram Y and Lenger R, Neuromodulation. **15.** 2012. [4] Dursun E, et al. Disabil Rehabil. **26**(2). 2004. [5] Shams L, Seitz AR. Trends Cogn. Sci. **12**(11). 2008. [6] Conner BC, et al. medRxiv 2020. [7] Brown JK, et al. Dev Med Child Neurol. **33**. 1991. [8] Conner BC, et al. Annals of Biomed Eng. **48.** 2020 [9] Steele KM, et al. Dev Med Child Neurol. **57**(12). 2015. [10] Rouston RL. Gait Posture. **38**(3). 2013.

PERTURBATION DIRECTION REVERSES THE EFFECT OF TIMING ON PEAK CENTER OF MASS SPEED

Jennifer K. Leestma[1,2], Gregory S. Sawicki[1,2,3], and Aaron J. Young[1,2]
[1]George W. Woodruff School of Mechanical Engineering, [2]Institute for Robotics and Intelligent Machines, and [3]School of Biological Sciences, Georgia Institute of Technology
email: *jleestma@gatech.edu

Introduction

Agile bipedal locomotion is crucial for humans to navigate the terrains and environments in daily life. However, we know relatively little about how individuals maintain balance in diverse environments, which would enable us to better treat populations with balance impairments and develop devices that augment balance. Previous work has employed perturbations to induce instability and study balance recovery [1]. However, no study has simultaneously evaluated the effects of perturbation *magnitude*, *direction*, and *timing* on balance, which would provide broad insight into the diversity of destabilizing scenarios that humans face during locomotion. Here, we investigate the combined effects of mediolateral (ML) perturbation direction and timing on balance, evaluated using peak ML center of mass (COM) speed. We hypothesize that perturbations beginning earlier in stance phase (*i.e.* longest time until next heel contact) will be followed by the largest peak ML COM speeds regardless of perturbation direction.

Methods

One healthy participant walked at 1.25 m/s on a treadmill mounted on a Stewart platform. We applied 96 translational perturbation conditions that varied in magnitude (5, 10, 15 cm), direction (mediolateral, anteroposterior, diagonals), and timing (50% double stance, 25, 50, 75% single stance, Fig. 1B). Gait events were calculated according to [2]. The participant walked in three consecutive sessions, with each session containing one perturbation per condition, for a total of 288 perturbations.

We determined ML COM velocity as the average of four pelvis markers. Peak ML COM speed was determined as the peak absolute velocity in all recorded steps after the initiation of the perturbation. Perturbations were binned into two categories; lateral perturbations resulted in COM movement to the medial side of the stance foot and widened step widths, while medial perturbations resulted in COM movement to the lateral side of the stance foot and narrowed step widths.

Results and Discussion

We evaluated linear relationships for both lateral and medial perturbations, including all perturbation magnitudes and all directions that had a mediolateral component (Fig. 1A). For lateral perturbations, we found a negative linear relationship between onset timing and peak ML COM speed ($p<0.001$). For medial perturbations, we found a positive linear relationship between onset timing and peak ML COM speed ($p<0.001$). The results indicate that timing has a significant effect on peak ML COM speed, but the effect is reversed by the perturbation direction (Fig. 1C). This indicates that double stance onset time is the most destabilizing for lateral perturbations, while late single stance onset time is the most destabilizing for medial perturbations.

Significance

These results begin to provide a more thorough understanding of how multiple variables interact to influence balance. The outcomes across *magnitude*, *direction*, and *timing* in healthy individuals will provide a reference to understand the limitations of those with balance impairments. Additionally, these data provide guidelines for the design of intelligent wearable robots that seek to augment human stability and reduce fall risk. Future work will extend this analysis to stability in *all* directions and use whole body angular momentum to more thoroughly quantify balance recovery.

Acknowledgments

The authors would like to acknowledge Pawel Golyski, Felicia Davenport, and the Human Balance Augmentation VIP team for their assistance in data collection. This work was funded by the NSF Research Traineeship: ARMS Award #1545287.

References

[1] S. M. Bruijn, et al., J R Soc Interface 10, (2013)
[2] J. A. Zeni, et al., Gait Posture 27, (2018)

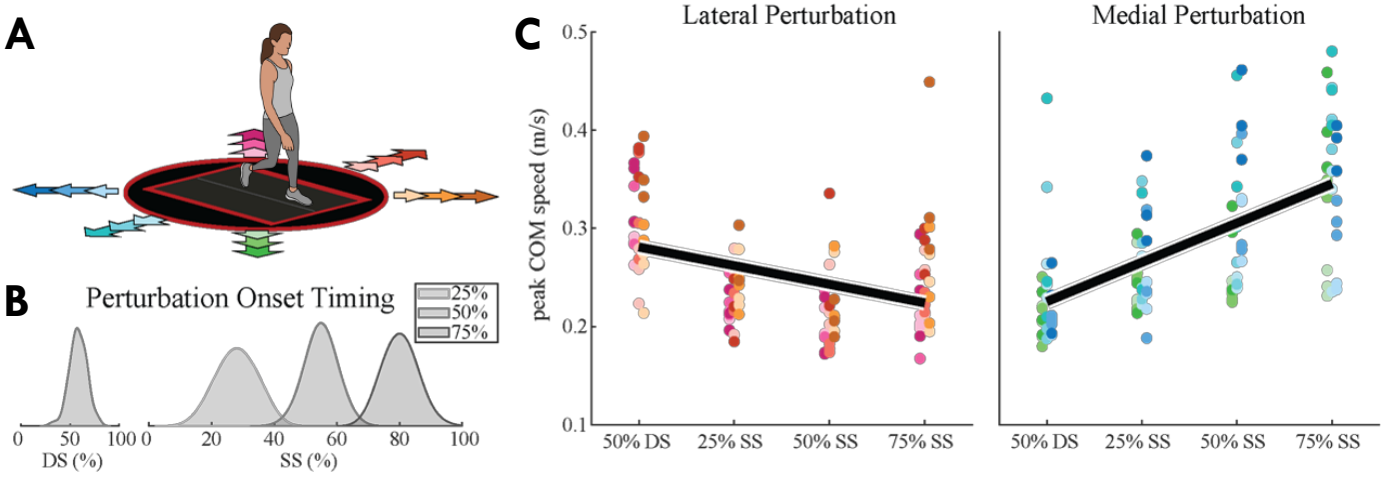

Figure 1: (A) Lateral (pink, red, orange) and medial (green, teal, blue) perturbations are shown. (B) The actual onset time distribution is plotted for each commanded onset time. (C) The effect of commanded onset time on peak ML COM speed is shown for lateral and medial perturbations.

MECHANICAL WORK AT THE KNEE JOINT FOR CASES WITH KNEE HEIGHT ASYMMETRY

Jacqueline C. Simon[1], Karen M. Kruger[1,2], Joseph J. Krzak[2,3], Ann Flanagan[2], Abdal Kawaiah[4], Robert Burnham Jr.[4], Susan Sienko[5], Cathleen Buckon[5], Jeremy Bauer[5], Gerald F. Harris[1,2]and Haluk Altiok[2]
[1]Marquette University
email: jacqueline.simon@marquette.edu

Introduction

Leg length discrepancy (LLD) affects a significant portion of the population [1-2]. It can be surgically corrected but often results in knee height asymmetry (KHA), knee joint misalignment in the coronal plane in the presence of equal limb lengths [3]. People with LLD develop compensation strategies during gait which tend to increase mechanical work in the sagittal plane [4-5]. Some have suggested that KHA less than four cm does not result in functional disability [6], but its biomechanical impact during common activities has not been extensively studied. The purpose of this study was to investigate the effect of KHA on gait biomechanics in children following limb equalizing surgery. The hypothesis is that degree of KHA can be used to predict mechanical work at the knee in the sagittal plane.

Methods

In an IRB approved study, gait data was collected for 10 patients with KHA following surgical correction of LLD (4M/6F, 17.4±2.0 yrs, BMI 26.7±6.8 kg/m^2) and 10 healthy control subjects (4M/6F, 16.4±1.8 yrs, BMI 22.4±2.7 kg/m^2). The Plug-in-Gait lower extremity model (Vicon Nexus) was used to calculate knee kinematics and kinetics. Standing lower extremity x-rays were measured to determine functional LLD. Scanograms were used to calculate the difference in tibia-to-femur (TF) ratio between the limbs (left-to-right).

Limb length measurement differences were compared with independent t-tests. Multiple linear regression was used to determine whether age, sex, BMI, functional LLD, TF ratio difference, and/or group (control vs. surgical) influenced work generated, work absorbed, and total work at the knee. Non-significant variables were removed from the final regression equations. Statistics were calculated in SPSS (version 26).

Results and Discussion

Subjects with KHA had a greater difference in standing limb length and TF ratio between the left and right sides than controls (Tbl. 1). There were no significant differences between groups

Table 1: Absolute value of between-limb difference.

	KHA Patients	Control Subjects	p-value
T/F ratio	0.039 ± 0.028	0.006 ± 0.007	0.002
Functional Limb Length (cm)	0.79 ± 0.40	0.32 ± 0.39	0.017

in between-limb difference in work generated, work absorbed, and total work (p≥0.300). Multiple regressions were run to predict difference in work generated, work absorbed, and total work at the knee from age, sex, BMI, functional LLD, TF ratio difference, and group (control vs. surgical). The independent variables could not significantly predict difference in work absorbed (p=0.475) or total work. However, for total work, the difference in TF ratio between limbs did show significant effect, so the regression analysis was repeated with this as the only independent variable. This time, difference in TF ratio did predict difference in total work at the knee with statistical significance (p=0.016) and with R^2_{adj}=0.241. Additionally, the regression analysis with all the independent variables was able to significantly predict difference in work generated at the knee (p=0.002) and with R^2_{adj}=0.597. The only independent variable of significance was the difference in TF ratio between limbs (p<0.001). Removing the nonsignificant variables, difference in TF ratio predicted difference in work generated at the knee (p<0.001) with R^2_{adj}=0.602 (Figure 1).

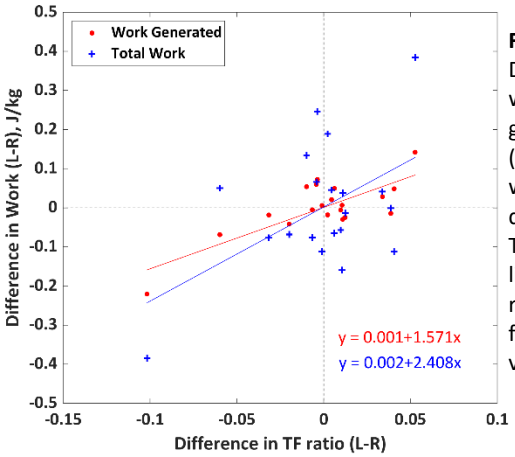

Figure 1: Difference in work generated (·) and total work (+) vs. difference in TF ratio. Left limb minus right limb for all values.

We expected to be able to predict mechanical work at the knee. While not the case for work absorbed, we found that the difference in TF ratio between limbs to explain 60.2% of the variability in the work generated at the knee and 24.1% of the variability in total work during stance.

Because the coefficients are positive, when the difference in TF ratio is negative (R>L), the difference in work generated is also negative (R>L) and vice versa, indicating that more work is generated in the limb with the more proximal knee than the limb with the more distal knee, thus increasing the total work in the proximal knee.

Weinberg and Liu [7] determined that TF ratios were significantly correlated with hip and knee arthritis. The difference in work generated and total work between proximal and distal knees in KHA might indicate an increased risk for arthritis in the proximal knee.

Significance

This research supports attention to knee height asymmetry following surgical correction of LLD.

Acknowledgments

Support for this study was provided by a startup grant from the Pediatric Orthopaedic Society of North America and by an ARRT Grant (#90AR5022-05-00).

References

[1] Subotnick.1981. *J. Orthop. Sports Phys. Ther.*, 3:1(11–16) [2] Woerman & Binder-Macleod, 1984 *J. Orthop. Sports Phys. Ther.*, 5:5(230–39) [3] Veilleux, et al. 2018. *Int. Orthop.*, 42:8(1979–85) [4] Song, et al. 1997. *J. Bone Joint Surg. Am.*, 79:11(1690–98) [5] Aiona, et al. 2015. *J. Pediatr. Orthop.*, 35:3(280–84) [6] Stanitski. 1999. *J. Am. Acad. Orthop. Surg.*, 7:3(143–53) [7] Weinberg & Liu. 2017 *J. Pediatr. Orthop.*, 37:5(317–22)

COORDINATION VARIABILITY IN PEOPLE WITH AND WITHOUT UNILATERAL TRANSTIBIAL AMPUTATION

Ryan D. Wedge[1*], A. Andrejchak[1], and S. Meardon[1]
[1]Department of Physical Therapy, East Carolina University (Greenville, NC)
email: *wedger19@ecu.edu

Introduction

People with a unilateral transtibial amputation have a structural asymmetry that contributes to walking asymmetries [1]. Current goals of rehabilitation are to minimize observable asymmetries to restore gait patterns similar to able-bodied individuals [2], but an asymmetric gait pattern may afford better function in those with unilateral transtibial amputation using a passive prosthesis[3].

Preferred walking limb coordination patterns vary across individuals, and the amount of coordination variability may represent motor system flexibility [4]. Extremes in the variation of stride-to-stride segment coordination may indicate poor control (e.g. high), or reduced degrees of freedom linked with injury (e.g. low) [4]. Reduced motor system flexibility for people with unilateral transtibial amputation may explain common secondary issues such as knee osteoarthritis [5].

The purpose of this study was to compare preferred stance time asymmetry and segmental coordination variability between people with and without unilateral transtibial amputation. We hypothesized that people with unilateral transtibial amputation would have greater stance time asymmetry and less coordination variability across thigh-shank couplings of the prosthetic limb compared to the intact limb and able-bodied limbs.

Methods

We collected walking data at preferred speed on a treadmill for three people with unilateral transtibial amputation (2 men, 1.79 ± 0.11 m, 68.3 ± 7.6 kg) and three people without amputation (3 men, 1.79 ± 0.04 m, 81.8 ± 3.2 kg). Amputations were due to non-vascular causes and all participants were able to walk community distances with variable cadences.

After 30 minutes of treadmill acclimatation, we collected full body kinematics with marker-based motion capture (240 Hz. Segment angles were calculated using Visual 3D. Thigh-shank segment coupling angle variability (CAV) was calculated from 15 consecutive strides for each limb and was evaluated during early (1-20% stride), mid (21-40%) and late stance (41-60%) and terminal swing (85-100%) [6]. Between limb CAV differences (prosthetic vs intact, prosthetic vs able-bodied and intact vs able bodied limbs) during each gait period were examined using t-tests ($\alpha = .05$) and effect sizes (d).

Results and Discussion

As expected, people with amputation (3.5 ± 0.5%) had greater stance asymmetry than able-bodied people (1.6 ± 0.2%) ($p = .003$, d = 5.3%) at preferred walking speed (1.00 ± 0.27 m/s & 1.48 ± 0.11 m/s). Our hypotheses for limb CAV differences during the gait cycle periods examined were partially supported (Figure 1). Thigh-shank CAV differences were observed at mid- and late-stance, when decreased push-off capability of a passive prosthesis affects gait. Lower CAV was observed (based on plots) in the prosthetic limbs when compared to the intact and able-bodied limbs for couples involving sagittal and transverse segment motions, potentially indicating less adaptability of the prosthetic limb in these planes. In addition to a larger sample size, future work should examine CAV across stride using curve analysis techniques such as statistical parametric mapping.

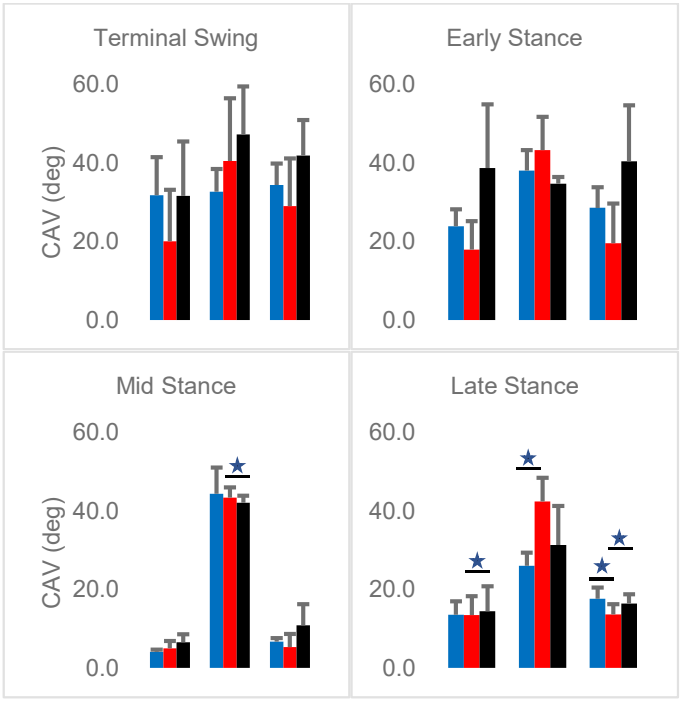

Figure 1: Mean +95% CI of CAV during four parts of the gait cycle for three thigh-shank segment couples (sag-sag (left columns), fr-fr (middle columns), and sag-trans (right columns)) across three limbs (able-bodied (blue), prosthetic (red), and intact (black)). During mid stance, fr-fr CAV was significantly more for the prosthetic limb than the intact limb ($p = .007$, $d = 2.29$). During late stance, sag-sag, fr-fr, and sag-trans CAV was significantly less for the prosthetic limb than the intact limb ($p = 0.03$, $d = 1.03$), the able-bodied limbs than the prosthetic limb ($p = .02$, $d = 3.28$), and the prosthetic limb relative to both the able-bodied ($p = .05$, $d = 2.19$) and intact ($p = .01$, $d = 2.38$) limbs, respectively.

Significance

Prosthetic use may contribute to decreased prosthetic limb motor system adaptability during late stance, potentially leading to asymmetric walking and load distribution. Future prostheses and rehabilitation paradigms should seek to optimize function and adaptability of the prosthetic limb.

Acknowledgments

The study was partially funded by a University of Massachusetts Amherst dissertation grant.

References

1. Sanderson & Martin 1997 G&P
2. Childers & Koger 2014 J Rehabil Res Dev
3. Winter & Sienko 1988 J Biomech
4. Heiderscheit et al., 2002 J Appl Biomech
5. Jakubowitz et al., 2019 PLoS One
6. Hafer et al., 2017 G&P

IMPACT OF REACH HEIGHT ON ESTIMATE SUPRASPINATUS RISK IN MANUAL WHEELCHAIR USERS

Kylee Schaffer[1], Stefan Madansingh, PhD, Emma Fortune, PhD, Melissa Morrow, PhD, Kristin Zhao, PhD, and Beth Cloud-Biebl, PT, DPT, PhD[1,2]
[1]Assistive and Restorative Technology Laboratory, Rehabilitation Medicine Research Center, Department of Physical Medicine and Rehabilitation; [2]Program in Physical Therapy, Mayo Clinic School of Health Sciences
email: Cloud.Beth@mayo.edu

Introduction

Manual wheelchair (MWC) users with spinal cord injury (SCI) commonly experience shoulder pain due, in part, to the frequent use of their upper extremities.[1] Shoulder pain may be caused by compression of rotator cuff tendons[2,3,4] between the proximal humerus and the structures of the coracoacromial (CA) arch (acromion, CA ligament, and coracoid). The thickness of the supraspinatus tendon is approximately 5 mm[5], so the tendon would likely be compressed when the distance between its insertion on the proximal humerus and CA arch is less than 5mm.

The amount of humeral elevation is considered a contributing factor in causing compression of rotator cuff tendons[2], but this effect of elevation may vary by type of task performed. The purpose of this study was to compare an estimate of rotator cuff compression risk and the humeral elevation at which it occurred between functional reaching tasks of different heights.

Methods

MWC users with SCI were recruited to participate in this IRB-approved study. Electromagnetic sensors (Liberty, Polhemus, Inc.) placed on the thorax, scapula, and humerus were used to collect shoulder kinematics at 120 Hz while subjects reached for a can on a high (54" from floor) and low (36" from floor) shelf. The reaching task was performed five times for each shelf height. Glenohumeral kinematics were used to animate CT-bone models of the humerus and scapula to determine the minimum distances between the supraspinatus tendon footprint and both the acromion and the CA ligament throughout the activity.

Data analysis focused on the first portion of the reaching task: from hand in lap to contacting the can. The outcome variables were the smallest minimum distance during this portion of the task for the supraspinatus relative to the acromion (Supra-Acr) and CA ligament (Supra-CAL) and the corresponding HT elevation angles. For each participant, the trial with the median Supra-Acr value and trial with the median Supra-CAL value were used for analysis. Outcome variables were compared between the high and low reaching conditions using a paired t-test ($\alpha = 0.05$).

Results and Discussion

Data from eight participants (7 male) were analyzed. Median age was 35.5 years (IQR = 25-38.5) and median years of MWC use was 9.3 years (IQR = 2.2-17.2). Level of SCI ranged from C5 to T6.

In high reaching, mean (SD) HT elevation at start was 23.4° (6.7) and at end was 115.5° (9.8). In low reaching, average HT elevation at start was 21.6° (6.4) and at end was 69.3° (7.8).

The average difference between high and low reaching conditions for smallest minimum distance of Supra-Acr was 0.12mm (95%CI: -0.58-0.82, p = 0.704, Fig. 1A). The HT elevation angle at which the smallest Supra-Acr minimum distance occurred was on average 12.7° (95%CI: 7.8-17.5, p = 0.000, Fig. 1B) less elevated in the low reach condition compared to the high reach condition.

The average difference between high and low reaching conditions for smallest minimum distance of Supra-CAL was -0.07mm (95%CI: -0.68-0.54, p = 0.790, Fig. 1A). The HT elevation angle at which the smallest Supra-CAL minimum distance occurred was 19.4° (95%CI: -8.9-47.8, p=0.150, Fig. 1B) less elevated in the low reach condition compared to the high reach condition. The lack of significance in this test despite the relatively large difference in elevation angles may be due to a high level of variability in the data due to the small sample size.

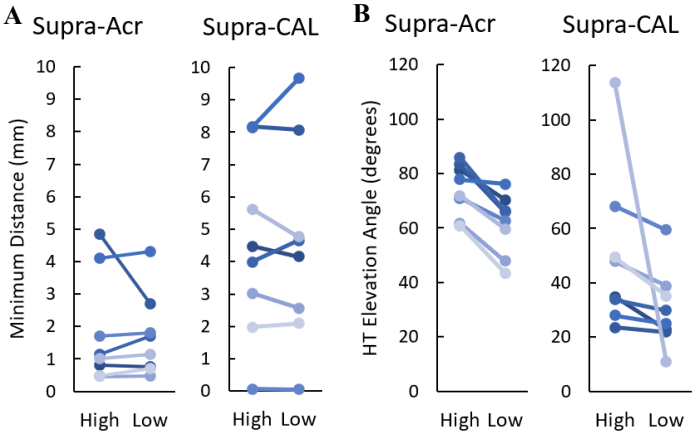

Figure 1: Comparison of high and low reaching conditions for smallest minimum distance (A) and for HT elevation angle at which the smallest minimum distance occurred (B) for both Supra-Acr and Supra-CAL. Individual participant data shown.

Significance

This study examines the differences between functional reaching tasks at two different heights. The results indicate that height of the reaching task may affect the HT elevation angle at which the supraspinatus most closely approximates the CA arch. It is possible that the difference in reach height influences more than amount of elevation needed to complete the task. This highlights the need to specifically evaluate functional tasks, as estimates of rotator cuff compression risk determined from planar motions (such as a flexion arm raise) may not apply.

Acknowledgments

Funded by the Mayo Clinic Rehabilitation Medicine Research Center, Craig H. Neilsen Fund for Spinal Cord Injury Care and Research Honoring Robert D. Brown Jr., M.D., CT bone model funded by NIH K01 HD042491 (P. Ludewig, University of Minnesota).

References

[1] T.A. Dyson-Hudson, S.C. Kirshblum. (2004) J Spinal Cord Med. 27(1): 4-17.
[2] R.L. Lawrence et al. (2017) J Orthop Res. 35(10): 2329-2337.
[3] F. Dal Maso et al. (2016) Man Ther. 25: 94-99.
[4] L.A. Michener et al. (2003) Clin Biomech. 18(5): 369-379.
[5] T. Matsuhashi et al. (2014) Clin Anat. 27(5): 702-706.

EFFECTS OF DUAL-TASKING ON FORCE PRODUCTION DURING FIVE-TIMES SIT-TO-STAND TASK IN HEALTHY YOUNG ADULTS

Srikant Vallabhajosula, Sarah Henderson, Brandi Wiltshire, Andrew Whyte, Susan Chinworth
Department of Physical Therapy Education, Elon University
email: svallabhajosula@elon.edu

Introduction

Sit-to-Stand (STS) task is an essential action of independent daily living that is also commonly transferred into the clinic to assess balance, power and muscle efficiency in the lower extremities of various populations using the five-times sit-to-stand (FTSTS) assessment.[1] Elements that comprise this action can assess fall risk, severity of disability, and/or shifts in posture that create compensations during physical activities in those with injury, physical or mental disability, and aging populations.[1,2] Previous research has focussed on examining discrete trials of sit-to-stand movement but not the FTSTS task as a whole.[3] To perform functional tasks like the STS, a certain level of attentional demand is required to perform the multiple components that are involved in completing a transitional movement. Adding a cognitive task could challenge the participant by redirecting attention away from the STS task. This is especially important for fall risk assessments because various populations within this cohort commonly present with cognitive/neurological impairments. While effects of dual-task on other functional tests like Timed Up and Go have been investigated, research is sparse on how dual-tasking affects FTSTS task which focusses more on lower extremity power production.[3] The purpose of our study was to examine the effects of a concurrent cognitive task on force production during FTSTS in healthy young adults. We hypothesized that when performing FTSTS under dual-task condition, participants will take longer time, produce lesser peak force, greater impulse, and lesser power during standing compared to performing FTSTS under single task condition. We also hypothesized the dual-task performance would show more variability than single-task performance.

Methods

10 healthy adults (mean age 24 (4.1) years) participated. Each participant stood up and sat down five times as fast as possible as part of FTSTS assessment. The participants were seated in a backless chair of standard height such that each foot was positioned on separate force plates. Ground reaction force data were collected at 960Hz. Three trials were completed without a cognitive task and then with a concurrent cognitive task of counting backwards by 3 starting from a random number. Time to complete FTSTS was measured using stopwatch. For each of the five times within the FTSTS task, peak force (N/BW), impulse (Ns/BW) and power (Nm/BW.s) variables were calculated using Visual3D script. An average and coefficient of variation of these five values were computed for each of the three trials. Coefficient of variation was defined as the % of SD over mean. One-tailed paired samples t-tests were conducted to compare single and dual-task performances.

Results and Discussion

Data are presented in Table 1. Participants took significantly longer time to complete FTSTS task while dual-tasking. Participants also produced significantly lesser power while dual-tasking. However, peak force and impulse were similar between both the conditions. None of the variability measures were significantly different between the two conditions.

In line with previous results on effects of dual-tasking on a functional task, results from the current study indicate that even healthy young adults take significantly longer time to complete the task when presented with a concurrent cognitive task. However, they do this without altering the peak force or impulse but rather lowering the rate at which this force is produced. Since FTSTS task is a functional task indicative of lower extremity power rather than lower extremity strength of an individual, adding a dual-task component could give additional insights into why this task is difficult for some individuals to perform. Further, our results also show that even though the rate of force production is altered between single- and dual-task conditions, the consistency with which force, impulse or power are produced is unaffected by the demands of an additional cognitive task.

In summary, healthy young adults took longer time with lesser power to complete FTSTS task while dual-tasking.

Table 1. Mean (SD) of Dependent Variables

	Single Task	Dual-Task	*P*
Time to complete FTSTS *	7.38 (1.08)	8.16 (1.77)	0.025
Peak force (N/BW)	1.35 (0.09)	1.37 (0.10)	0.053
CV of Peak force %	2.97 (1.15)	2.80 (0.98)	0.328
Impulse (Ns/BW)	0.57 (0.08)	0.58 (0.11)	0.139
CV of Impulse %	6.21 (1.68)	6.40 (3.07)	0.432
Power * (Nm/BW.s)	0.99 (0.14)	0.94 (0.15)	0.046
CV of Power %	8.32 (2.24)	8.60 (4.64)	0.431

* significance ($P < 0.05$); FTSTS – Five-times Sit-to-Stand; CV – Coefficient of variation

Significance

Results from the current study provide a baseline for future assessments of FTSTS while dual-tasking in several populations where FTSTS assessment is commonly used. Understanding the role of attention while performing an important clinical assessment like FTSTS could add additional insight into fall-risk associated with activities of daily living in several populations like older adults.

References

1. Whitney et al. *Phys. Ther.* 2005; 85 (10): 1034-1045
2. Chorin et al., *Aging Clin Exp Res*. 2016;28:871-879
3. Vander Linden et al., *Arch Phys Med Rehabil*. 1994;75(6):653-6

Impact Characteristics of Two Different American Football Helmet Types During Collisions

Brianna Roberts[3], Jenna Hawk[2], and Brian Wallace[1]
[1]Department of Kinesiology, University of Wisconsin Oshkosh, USA, [2]School of Physical Therapy and Athletic Training, Pacific University, USA, [3]Department of Kinesiology, Louisiana State University, USA
Email: wallaceb@uwosh.edu

Introduction

Since its inception, American football has been a high collision sport associated with head injuries, including concussions and more recently the identification of and link to Chronic Traumatic Encephalopathy (CTE). Many studies have attempted to determine the mechanisms behind head injuries, such as the angular and liner accelerations of the head or helmet during collisions. A 10g threshold has been identified as a commonly reported impact threshold for collisions (King et al. 2016). A modern helmet has been compared to a leather style helmet design, however, few studies have attempted to compare the collision characteristics of modern helmet types (Rowson et al. 2013). Therefore, the purpose of this study was to measure and compare the collision biomechanics of two commonly used modern helmet models (Vicis Zero1 and Riddell Speedflex). A secondary aim was to validate the Riddell InSite helmet monitoring system (version 2.0). We hypothesized that the Zero1 helmet would attenuate impact biomechanics better than the Speedflex helmet, and that the InSite system would validly quantify and categorize impacts.

Methods

We conducted linear drop tests of two helmet types at four heights (1.52m, 1.98m, 2.59m, & 3.05m). Three trials were conucted in random order at each height for each helmet model. A 5kg dummy headform was used to mimic head mass (Johnston et al. 2014). A custom apparatus was used to drop the helmets. The helmet was placed upside down and dropped in a manner that resulted in minimal pre-collision rotation of the helmet and a collision to the forehead region of the helmet. Helmets were weighed using a standard beam scale.

Kinetic data were recorded at 1800 Hz using a strain gauge force plate (model OR6-7-2000, AMTI Corporation) integrated into a standard motion capture system (Nexus v2.9, Vicon Corporation). During trials with the Speedflex helmet, the InSite system was active and recording the impacts.

Impulse, velocity, and acceleration (g) were calculated from vertical ground reaction forces in Excel (Microsoft Corporation). The InSite system measures g forces and categorizes them as "low" (15-28g), "medium" (29-62g) or "high" (≥63g). These categories were compared to actual g forces on a per-trial basis. Data were collapsed within helmet type. Independent t-tests were performed in Minitab (version 19) to compare between helmet types for each dependent variable. Alpha was set at $p \leq 0.05$.

Results and Discussion

Dependent variable data for both helmet models are presented in Table 1. Total impulse and peak velocity were significantly higher for the Zero1 helmet than the Speedflex helmet ($p=0.004$, 0.04). The Speedflex helmet resulted in higher peak accelerations ($p=0.000$), however, the Zero1 helmet resulted in higher mean accelerations ($p=0.05$). InSite registered 19 of the 24 impacts, reporting 12 as "high." All of the peak and six of the mean accelerations were above 63g. An in-helmet validation method may be more appropriate to account for the placement of the InSite sensors in the lining of the helmet.

The Zero1 helmet had a greater mass (2.27kg vs. 2.09kg), which may have influenced the total impulse values. The softer external structure of the Zero1 helmet enables it to preferentially absorb impacts as compared to more rigid helmet materials. The acceleration data indicate that the Zero1 sustains sub-maximal accelerations longer, while the Speedflex helmet absorbs impact energy more abruptly, resulting in higher peak accelerations .

Significance

The Zero1 helmet has reduced peak accelerations vs. the Speedflex helmet. This difference was independent of drop height. The Zero1 helmet may result in lower incidence of collision related head injury based on measured impact biomechanics.

Acknowledgments

We thank the UW Oshkosh football program for loaning the helmets used in this study. We also would like to thank Bryce Herlache for his assistance with data collection.

References

Johnston, J. M., et al. (2014). Simulation, fabrication and impact testing of novel football padding system that decreases rotational acceleration. *Sports Engineering, 18*, 11-20. doi: 10.1007/s12283-014-0160-4

King, D., et al. (2016). The influence of head impact threshold for reporting data in contact and collision sports: systematic review and original data analysis. *Sports Medicine, 46,* 151-169. doi: 10.1007/s40279-015-0423-7

Rowson, S., et al. (2013). Biomechanical performane of leather and modern football helmets. *J Neurosurg, 119,* 805-809. doi: 10.3171/2013.3.JNS121735

Table 1: Impulse, velocity, and acceleration data for Zero1 and Speedflex helmets. Mean±SD. *p≤0.05.

Model	Impulse (Ns)	Peak Velocity (m/s)	Mean Velocity (m/s)	Peak Acceleration (g)	Mean Acceleration (g)
Zero1	42.14±6.97*	18.56±3.07*	13.11±2.81	127.15±0.06*	57.60±17.10*
Speedflex	33.13±6.84	15.82±3.19	12.14±2.28	138..26±0.31	45.20±12.00

PROSTHETIC LEGS ARE SHORTER THAN BIOLOGICAL LEGS DURING RUNNING AND SPRINTING

Paolo Taboga[1*], Owen N. Beck, Janet H. Zhang, Joshua R. Tacca, & Alena M. Grabowski
[1]Dept. of Kinesiology, California State University, Sacramento, CA; Email: *paolo.taboga@csus.edu

Introduction

Recently, the governing body of Olympic track and field (World Athletics) banned an athlete with bilateral prosthetic legs from competing in sanctioned events because he was 'too tall'. Specifically, the respective athlete set their running-prostheses at heights that elicit an overall standing height taller than their MASH (maximum allowable standing height). MASH, a rule put forth by the International Paralympic Committee, estimates an athlete's stature based on 'proportional' body dimensions [1]. Hence, the maximum allowable prosthetic height (and leg length) that each athlete with bilateral leg amputations can use during sanctioned competition is presumably the value that elicits their MASH [1]. Aside from the difficulty of predicting an athlete's 'normally proportioned' leg lengths, we hypothesized that the MASH rule makes athletes with bilateral prosthetic legs *run* using shorter legs than non-amputees who have the same standing leg length (Fig. 1). This hypothesis is based on two factors. First, non-amputees can compete using shoes that have 2 or 2.5 cm thick soles depending on race distance, whereas the MASH for athletes with prosthetic legs uses *barefoot* stature [1]. Second, biological ankles can effectively lengthen the leg during running by actively plantar-flexing, whereas passive running-prostheses cannot actively lengthen. To test our hypothesis, we quantified the standing and running leg lengths of athletes with unilateral transtibial amputation and thus compare biological and prosthetic leg lengths within the same individual.

Methods

7 athletes with unilateral transtibial amputation using an 1E90 Sprinter running-prosthesis (Ottobock, Germany) participated. Each athlete performed a set of treadmill running trials that began at 3 m/s and increased 1 m/s until 9 m/s or maximum speed on a force measuring treadmill. Athletes performed running trials using recommended prosthetic length and ±2 cm. During each trial, we recorded biological and prosthetic leg length at touchdown, midstance, and take-off as the distance between the hip-joint center and the shoe or prosthesis marker that was closest to the ground, respectively (Fig. 1) during stance. We identified stance using a 50 N vertical ground reaction force threshold. We normalized running leg length to each participant's standing leg length (L_{ratio}=running leg length/standing leg length) to compare leg length changes during running relative to standing. Standing prosthetic leg length was measured in a loaded condition (~0.5 body weight applied to the prosthesis). We compared standing and running leg lengths, as well as L_{ratio} and differences across speeds using paired t-tests and linear mixed models (α=0.05).

Results and Discussion

Recommended standing prosthetic leg length was 3% longer than standing biological leg length ($p<0.001$).

Across all trials, biological leg length increased with faster running speeds at touchdown ($p<0.001$; Fig. 2). Alternatively, prosthetic leg length *decreased* with faster running speeds at touchdown ($p=0.030$) and midstance ($p<0.001$). From 3 to 7 m/s, biological L_{ratio} was 2-7% greater than prosthetic L_{ratio} throughout stance ($p\leq0.019$; Fig. 2). Also, at 8 and 9 m/s biological L_{ratio} was 4-7% greater than prosthetic L_{ratio} at touchdown and midstance ($p\leq0.0373$), but there was no difference at between L_{ratio} at take-off ($p\geq0.067$; Fig. 2). Moreover, for touchdown, midstance, and take-off, biological L_{ratio} was ~3.6-5.3% greater than prosthetic L_{ratio} (average biological L_{ratio} – average prosthetic L_{ratio} = 0.028+speed·0.0028; $p<0.001$; Fig. 2). Hence, if athletes with unilateral transtibial amputation match their standing leg lengths, their prosthetic leg length will be shorter than their biological leg during running.

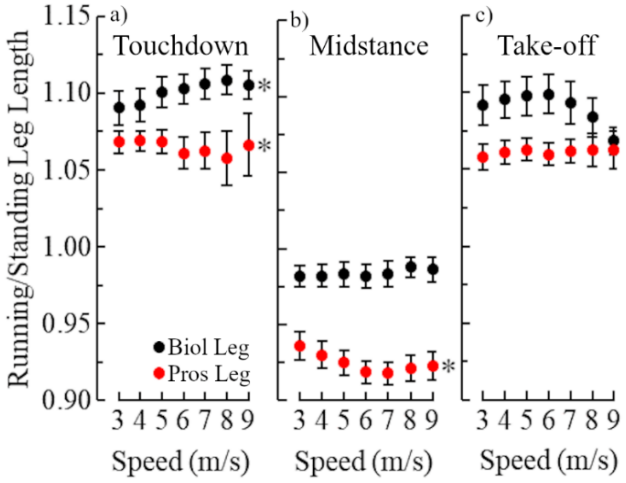

Figure 2. Ratio of running to standing leg length at touchdown, midstance, and take-off for biological (Biol) and prosthetic (Pros) legs across speed. Asterisk (*) indicates effect of speed on the respective leg length ratio.

Significance

These results suggest that biological legs are longer than prosthetic legs in athletes with unilateral transtibial amputation during running and the current MASH rule enforced by World Athletics likely requires athletes with bilateral prosthetic legs to run using shorter legs than non-amputees – especially at faster running speeds and when non-amputees use shoes.

References

1. Connick et al. (2015) *Scand J Med Sci Sports* **26**: 1353-59.

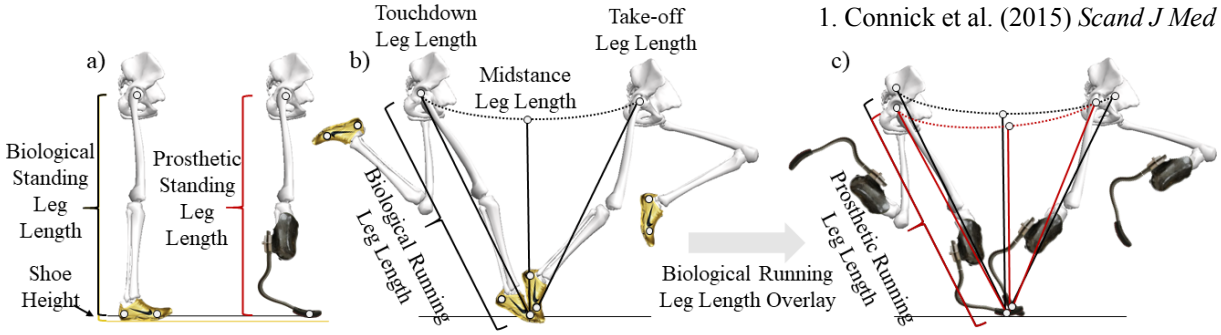

Figure 1. Illustration of biological and prosthetic leg length during a) standing and b) and c) running. In c) biological leg length (black) is superimposed to prosthetic leg length (red) for comparison.

DIFFERENCES IN TIBIAL ACCELERATIONS BETWEEN RUNNERS WITH AND WITHOUT A LOWER-LEG INJURY

Caleb D. Johnson, Irene S. Davis
Spaulding National Running Center, Harvard Medical School, Cambridge, MA 02138
email: cdjohnson@mgh.harvard.edu

Introduction

Peak tibial accelerations (TA) during running have gained recent interest in running biomechanics research. They have consistently shown strong correlations with vertical ground reaction force loading rates, which have been linked with running injuries.[1] As such, they may offer more a simple and portable measure of the loading to musculoskeletal tissues during running, and subsequently, risk for overuse injuries. However, very few studies have examined the direct association of TA with running injuries, and most have focused specifically on tibial stress fractures.[2,3] Therefore, our purpose was to examine differences in peak TA between runners with a lower-leg (knee and below) injury and healthy controls. We hypothesized that injured runners would show higher TA.

Methods

Participants included 30 injured runners (men/women= 16/14, age= 36±13yrs) and 28 healthy controls (men/women= 18/10, age= 33±10yrs). We included runners with injuries at the knee or below, as we felt that these injuries may be most affected by peak accelerations measured at the distal tibia. All participants were habitual rearfoot strikers and wore cushioned running footwear.

An inertial measurement unit containing a triaxial accelerometer (sampling rate= 1000Hz) was attached over each participant's distal medial tibia, just above the medial malleolus. Participants were given a 3-minute warm-up at a self-selected speed, followed by 16-seconds of data collection. Mean self-selected speeds were similar between groups: **injured**= 2.59m/s, **healthy**= 2.62 m/s.

Resultant TA were calculated as the root sum of squares of tri-axial accelerations. Peak vertical and resultant TA were extracted and averaged across all available strides (≈20 on average). Peaks that were ±2.5 median absolute deviations from the median were considered outliers and removed. Data from the injured leg was used for the injured group. A random leg was chosen for the healthy group, counterbalanced to match the number of right/left legs for the injured group.

Mann-Whitney U and Chi-Square tests were used to compare groups for potential confounders, including age, running speed, and sex. Mann-Whitney U tests were used to test for group differences in vertical and resultant TA.

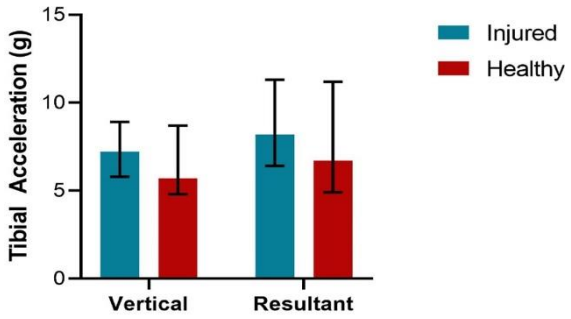

Figure 1. Median tibial accelerations (± IQR) by group

Results

The injured and healthy groups were comparable for mean age (p= 0.27) and running speeds (p=0.37), as well as proportions of men to women (p= 0.40). Median TA are depicted in Figure 1. Vertical (p= 0.06) and resultant (p= 0.25) TA were not found to be statistically different between groups. However, median vertical and resultant TA values were 26% and 22% higher, respectively, in the injured group.

Discussion

We did not find statistically different values for TA between injured and healthy runners, although median differences were in the hypothesized direction. These findings are in contrast to two previous studies, finding higher vertical TAs in runners with retrospective tibial stress fractures.[2,3] It should be noted that these studies were conducted with markedly smaller and lighter wired accelerometers that were tightly overwrapped to the tibia. The wearable sensors used in this study are larger and heavier, and thus potentially more prone to this artefact. Additionally, data for both groups were collected over a number of years and by different testers. Therefore, the fixation and location of sensor attachment to the lower leg may have varied across the data collection period. Efforts should be made in future studies to control for this.

Several studies have found higher vertical ground reaction force loading rates in injured runners.[4,5] Given the correlations between loading rates and TA, we expected that they would show similar differences. However, recent evidence has suggested that certain injuries may show stronger associations to loading rates. Therefore, another explanation for our findings is that TA are, similarly, more related to certain running injuries, compared to general injury. This should be studied further.

Significance

Our results add to the limited previous research establishing whether there is a direct association between peak TA and running-related injuries. While our results do not provide evidence that this is the case, there are a number of limitations that may have resulted in these findings. Along with the limited number of studies, future work is needed to establish the role of TA in running injuries.

References

[1] Sheerin, K. (2019). *Gait & Posture*, 67: 12-24
[2] Pohl, M. (2008). *J Biomech*, 41(6): 1160-1165
[3] Milner, C. (2006). *Med Sci Sports and Exerc*, 38(2):323-328
[4] Johnson, C. (2020). *Am J Sports Med*, 48(12): 3072-3080
[5] Futrell, E. (2018). *Med Sci Sports and Exerc*, 50(9): 1837-1841

A SYSTEMATIC STUDY OF REDUCED-ORDER PHYSIOLOGICAL BOUNCING MODELS WITH TRAJECTORY OPTIMIZATION

Zachary W. Mercer[1] and Christian M. Hubicki[1]
[1]Mechanical Engineering Department, FAMU-FSU College of Engineering, Florida State University
email: *hubicki@eng.famu.fsu.edu

Introduction

Robotic assistive devices hold enormous promise for augmenting and rehabilitating human locomotion (e.g. exoskeletons). Existing control techniques for lower-body exoskeletons, however, take significant time to design and tune because they are dependent on training with human subjects for hours or more [1]. To build a theoretical foundation for faster-tuned model-based exoskeleton control, this work explores simple and fast-to-compute math models for predicting how human behavior will adapt to forcing from external devices.

Specifically, we take a reduced-order modeling approach to find a generalizable model that is dependent on fewer subject-specific parameters. This work investigates the predicted behavior patterns of these models for a simple human locomotion task: bouncing up and down on two feet. We test a variety of minimalist math models and objective functions (used to model hypotheses about human control preferences) and assess the degree to which they explain observed human behaviors.

Using trajectory optimization, we systematically generate optimal bouncing strategies for each combination of math model and objective function at a variety of bounce frequencies. The work concludes by analyzing patterns in thousands of numerical optimizations of hypothetical bouncing tasks and compares their features to the experimental literature on human bouncing.

Methods

Our aim is to create a general physiological model that can be applied to a variety of specific tasks, constraints, and objectives while maintaining accuracy to the equivalent human motion. Our muscle model is structured as the plantar flexor performing a 2D bouncing task (Figure 1). We vary the bouncing frequency, MTU model, and objective function of the model to analyze trends in movement patterns generated by trajectory optimization. Each trajectory is defined by 151 node points and solved using IPOPT with user-supplied gradients.

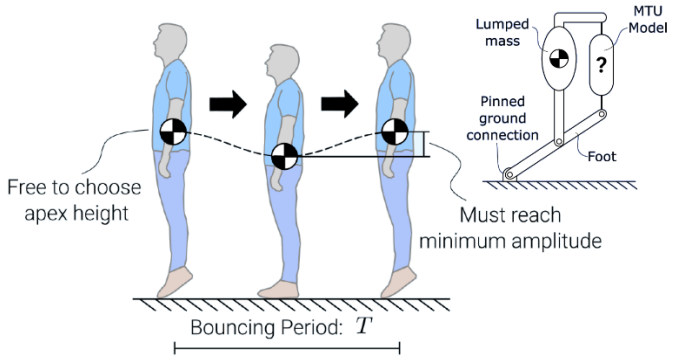

Figure 1: Model-based optimization of a periodic human bouncing task actuated by an MTU model. Formulated using direct collocation, the optimization chooses its starting mass height and velocity as well as defines the actuation patterns of the MTU.

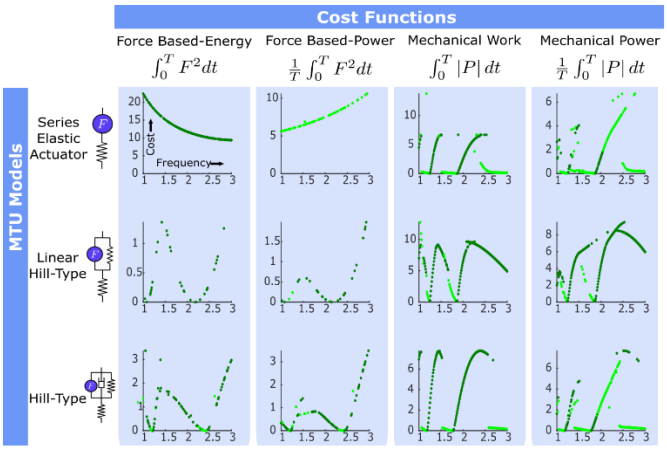

Figure 2: The results of 3,216 trajectory optimizations, showing the cost of bouncing over a range of prescribed frequencies when varying MTU models and cost functions.

Results and Discussion

Optimal movement strategies found with the minimal models were able to capture key trends that have been observed in real human bouncing as a function of frequency [2]. The Hill-Type model while optimizing for force-based objectives was able to find a preferred bouncing frequency closest to that observed in human studies. However, the most physiologically accurate behavior was shown when SEA, Linear Hill-type, and Hill-Type models solved for mechanical work and mechanical power objectives. Specifically, near the model's minimum-cost bouncing frequencies, the contractile element would be practically isometric. Moreover, the lengthening of the contractile element would remain in phase with the lengthening of the MTU overall while at the preferred frequency. Therefore, it is possible that a Hill-Type model optimizing for a combination of force-based and work-based objectives could provide an accurate analogue for human bouncing.

Significance

We are systematically exploring the limits of optimized simple models as parsimonious explanations of human movement patterns. This work also provides the first steps toward a robust and fast-solving algorithm able to predict how human movement strategies will adapt to forcing from external dynamics.

Acknowledgments

Supported by the FAMU-FSU Mechanical Engineering Department. Scientific assistance by Laksh Kumar.

References

[1] Zhang et al. “Human-in-the-loop optimization of exoskeleton assistance during walking”. Science (2017).
[2] Dean & Kuo. “Energetic costs of producing muscle work and force in a cyclical human bouncing task”. J. Appl. Physiol. (2011).

RECOVERY OF STABILITY AFTER TAKING A STEP IN CHILDREN WITH CEREBRAL PALSY

Katelyn S. Campbell[1], S. Wilhoite[1], S. Thompson[1], K. Newell[1], Li Li[2], G. Colquitt[2], and C. Modlesky[1]
[1]Department of Kinesiology, University of Georgia, Athens, GA
[2]Department of Health Sciences and Kinesiology, Georgia Southern University, Statesboro, GA
Email: christopher.modlesky@uga.edu

Introduction

Cerebral palsy (CP) is a neurological disorder affecting movement, posture, and muscle tone, often resulting in balance and coordination deficits.[1] Because postural control is an integral part of motor abilities,[2] improvements in posture could lead to improvements in function. Recovery from taking a step, one of the most common dynamic activities of daily living, may provide insight into the postural control and fall risk of children with CP. While studies have shown that other groups with postural deficits, such as aging adults, take longer to recover from taking step[3], no studies have examined step recovery in children with CP. The purpose of this study was to investigate recovery after taking a single step in children with hemiplegic CP. It was hypothesized that children with CP would take longer to recover from taking a step than typically developing children.

Methods

Nine ambulatory children (5-11 y; Gross Motor Function Classification System I-II) with spastic hemiplegic CP and 13 typically developing children (TDC) were studied. Two force platforms (Bertec, Columbus, OH; 100 Hz) were used to assess COP of the more affected (MAL) and less affected (LAL) limbs for CP and nondominant (ND) and dominant limbs (Dom) for TDC, during QS and step recovery (SR) tests.

Participants completed 3 trials of an eyes open QS test for 30 seconds, 3 trials of a SR test in which a step forward leading with the LAL/Dom was taken, and 3 trials of a SR test in which a step forward with the MAL/ND was taken. During the SR tests, participants were instructed to stand quietly after the step for 20 seconds. Data were filtered using a 5 *Hz* 4th order Butterworth lowpass filter. All data were processed using Matlab R2018b (Mathworks, Inc., Natick, MA). SR data was divided into an adjustment phase, which began when their foot contacted the platform and ended when the foot achieved weight stabilization, and a stabilization phase which began immediately after the adjustment phase. To reduce the potential influence of factors unrelated to balance, such as attention deficits, only the first 5 seconds of the stabilization phase were evaluated. The end of the adjustment phase and beginning of the stabilization phase were determined using this average peak to trough difference in ground reaction force (GRF) during quiet stance ± 2 SD of the range for each limb. The beginning of the stabilization phase was defined as the moment when the GRF peak-to-trough difference returned to the range determined for each participant in QS for at least 3 seconds; the beginning of the 3 seconds was then deemed the start of stabilization. Average GRF was calculated for MAL/ND and LAL/Dom during QS and the stabilization phase of SR. A review of the SR procedure is described in Figure 1.

Independent t-tests or Mann Whitney tests were used to assess between-group differences. Paired t-tests or Wilcoxon signed-rank tests were used to assess within-group differences in GRF between QS and the stabilization phase of SR.

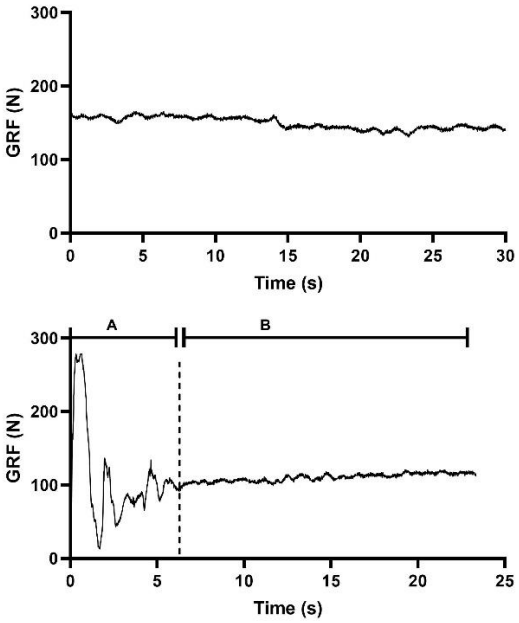

Figure 1: Procedure used to assess step recovery. (Top) Ground reaction force (GRF) was determined during 3 trials of quiet stance. (Bottom) The average GRF determined during quiet stance was used to determine the adjustment (A) and stabilization (B) phases of step recovery.

Results and Discussion

There were no differences between GRF during QS and GRF during the stabilization phase of SR, indicating that stabilization was reached during the SR test. When the MAL was stepping, the adjustment phase was longer for the MAL of children with CP than the ND of TDC (5.5 ± 1.6 vs 3.6 ± 1.7 s; $p = 0.019$) and longer for the LAL of children with CP than the ND of TDC (5.1 ± 1.9 vs 3.2 ± 1.6 s; $p = 0.022$). The finding suggests that compared to TDC, children with hemiplegic CP take longer to recover from taking a step.

Significance

Recovering balance after taking a step is necessary to maintain functional mobility. In the present study, it was demonstrated that, compared to typically developing children, children with hemiplegic CP take ~ 50 % longer to reach weight recovery from taking a step. Whether the longer step recovery period is related to the higher rate of falls in individuals with CP is unknown.

Acknowledgments

Funded by the National Institutes of Health (HD090126).

References

1. Rosenbaum et al. (2005). *Dev Med Child Neurol Suppl*, *109*, 8-14.
2. Ferdjallah et al. (2002). *Clin Biomech, 17*, 203-210.
3. Kilby et al. (2014). Gait Posture. *40*, 701-706.

RHYTHMIC AUDITORY STIMULATION IMPROVES COST OF TRANSPORT AND ASYMMETRY AFTER STROKE

Ashley N. Collimore[1+], Anna V. Roto[1+], Karen Hutchinson[1], Brian Harris[2], and Louis N. Awad[1*]
[1]College of Health and Rehabilitation Sciences, Boston University, Boston, Massachusetts, USA; [2]MedRhythms Inc.
+authors contributed equally to this work; email: *louawad@bu.edu

Introduction

There is a U-shaped relationship between walking cadence and the metabolic cost of transport (COT), such that walking at either a slower or faster cadence than optimal will increase metabolic cost (i.e., speed and mass-normalized energy consumption)[1]. While able-bodied individuals self-select an energetically-optimal walking cadence that approximates the resonant frequency of the leg, individuals post-stroke walk at slower cadences, leading to an increased COT. Additionally, spatiotemporal walking asymmetries characteristic of post-stroke walking may also contribute to a higher COT[3].

Rhythmic Auditory Stimulation (RAS) is an emerging gait therapy that has been shown to improve post-stroke walking[4]. Our group recently demonstrated that a music-based digital therapeutic could automate the delivery of a progressive and individualized RAS protocol. We found that a single 30-minute digital RAS session could meaningfully improve post-stroke walking speed by way of increasing cadence[5]. To expand upon this work, and drawing on the known relationship between walking cadence, spatiotemporal asymmetries, and the COT, the primary aims of this study were to evaluate if a single session of digital RAS locomotor training could improve the COT (ml O_2/kg/m) and spatiotemporal walking asymmetries after stroke. We hypothesized that there would be improvements in both COT and spatiotemporal asymmetries following digital RAS training. A second exploratory aim was to investigate if changes in each outcome (i.e., percent change in COT or spatiotemporal asymmetries) could be predicted by baseline measures (i.e., baseline speed and COT, or spatiotemporal parameters, respectively).

Methods

Participants completed one 30-minute digital RAS session. Indirect calorimetry (K5, Cosmed) and kinematic data (Qualisys) were collected concurrently during two, 3-minute speed-matched treadmill trials before and after training. Treadmill speed for both trials was set to each participant's comfortable walking speed measured prior to training, to isolate biomechanical and energetic changes from changes in speed. Indirect calorimetry data were converted into COT (ml O_2/kg/m) using standard methods[3]. Thirty seconds of steady state metabolic data (based on SD[6] and visual inspection) from the final 90 seconds of each walking bout were averaged to calculate pre-and post- COT. Step length, step time, stance time, and swing time were calculated using twenty steps time matched to the metabolic data. Asymmetry measures were calculated as the absolute difference in pre- to post-metrics divided by the sum.

Statistical analyses were calculated using RStudio Version 1.3.1056. To answer our primary aims, Wilcoxon Ranked Sum Tests were conducted between pre- and post-session measures of COT and spatiotemporal asymmetries. For exploratory analyses, we investigated Spearman's rank-order correlations between percent change in COT and baseline measures of speed and COT, and between percent change in spatiotemporal asymmetries and baseline spatiotemporal parameters for individual limbs. Alpha was set at 0.05.

Results and Discussion

Data were available from 10 individuals post-stroke (56.7±14 yrs. old, 8.9±5 yrs. post-stroke, 3 females, 6 right paretic). Training resulted in an average 9% reduction in the COT ($p = 0.027$) and ~20% reductions in step time, stance time, and swing time asymmetries (p's < 0.027) (Fig. 1). Changes in step length asymmetry were not observed ($p = 0.16$). Percent change in cost of transport was predicted by baseline COT ($\rho = -0.85$, $p = 0.004$), but not by baseline walking speed ($\rho = 0.43$, $p = 0.22$). More specifically, a higher COT prior to training was associated with a larger improvement after training. There were no baseline predictors of percent change in temporal asymmetries.

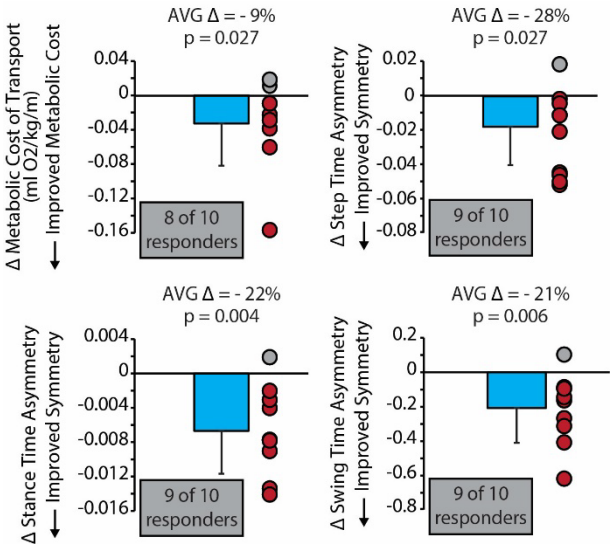

Figure 1: A majority of participants significantly improved metabolic cost of transport, step time asymmetry, stance time asymmetry, and swing time asymmetry after a single session.

Significance

A single session of digital RAS significantly reduced COT and concurrently improved post-stroke spatiotemporal asymmetries. Taken together with our previous finding of improvements in overground walking speed, the music-based digital therapeutic may be a useful paradigm for retraining gait patterns after stroke.

Acknowledgments

We thank our participants for their generous time.

References

1. Holt, K. G.,et al. 1995 *J. Mot. Behav.* DOI: 10.1080/00222895.1995.9941708
2. Franceschini, M. et al. 2013 *PLoS One* DOI:10.1371/journal.pone.0056669
3. Awad, L. N., et al. 2015 *NNR* DOI: 10.1177/1545968314552528
4. Magee W. L., et al. 2017 *CDSR* DOI:10.1002/14651858.CD006787.pub3
5. Hutchinson, K., et al. 2020 NNR *DOI: 10.1177/1545968320961114*
6. Taylor, H., et al. 1955 *J. Appl. Physiol.* DOI: 10.1152/jappl.1955.8.1.73

TOTAL ANKLE REPLACEMENT IN-VIVO KINEMATICS: A BIPLANE FLUOROSCOPY IMAGING STUDY

Amy L. Lenz, Rich J. Lisonbee, Andrew C. Peterson, Koren E. Roach, K. Bo Foreman, Alexej Barg, and Andrew E. Anderson
Department of Orthopaedics, University of Utah, Salt Lake City, UT, USA
email: amy.lenz@utah.edu

Introduction

Total ankle replacement (TAR) is one surgical option to treat ankle osteoarthritis. Unfortunately, TAR survival rates are lower than knee or hip arthroplasty (89% survival 10 years post-surgery, with an annual failure rate of 1.2% [1]). TAR failure may in part be caused by altered biomechanics. Motion capture studies using skin markers have demonstrated reduced range of motion in treated limbs [2]. However, this approach lacks the ability to independently differentiate tibiotalar and adjacent subtalar joint motion. In response, we developed techniques to measure in-vivo subtalar and tibiotalar motion of native joints [3] as well as TAR implants [4] using biplane fluoroscopy. The objective of this study was to evaluate the kinematics of the TAR prosthesis as well as ipsilateral subtalar joint in patients treated for ankle OA with unilateral TAR and compare these results to the contralateral untreated limb as well as to healthy controls.

Methods

Six asymptomatic participants with a unilateral Zimmer TAR (4 men; 68.2 ± 7.1 years; BMI 28.9 ± 6.7 kg/m^2; 5.4 ± 1.9 years post-op) and six control participants (3 male; 30.9 ± 7.2 years; BMI 23.5 ± 3.5 kg/m^2) provided informed consent to participate in this IRB-approved study. A validated high-speed biplane fluoroscopy system measured tibiotalar and subtalar kinematics [3] for one trial of overground walking at a self-selected speed and a double heel-rise activity. A computed tomography (CT) scan of each patient was acquired (Siemens Medical Solutions) from mid-tibia through metatarsals at a 0.6 mm slice thickness. For each participant, the tibia, talus, and calcaneus were segmented (Amira 6.0; Visage Imaging). Combined implant/bone models were developed for the TAR participants to perform model-based tracking [4]. Kinematics were normalized from heel-strike to toe off and reported as a percentage of normalized stance/activity. Confidence intervals (CIs) visualized group profiles and statistical parametric mapping (SPM) evaluated differences between groups ($p < 0.05$). Range of motion (ROM) was calculated between groups and statistically evaluated with a t-test ($p < 0.05$).

Results and Discussion

During walking, patients had symmetric motion for the tibiotalar and subtalar joints between the TAR and untreated limbs (Figure 1). When comparing the TAR side to healthy controls, the tibiotalar joint in patients with a TAR demonstrated reduced dorsiflexion, but only during 63.9 to 69.7% of stance (Figure 1); the subtalar joint had increased dorsiflexion and eversion, but only during 79.5 – 85.7% of stance. The tibiotalar ROM for dorsi-plantarflexion was lower for the TAR limb (10.3 ± 3.1°) compared to controls (17.8 ± 4.6°) ($p = 0.01$) (Table 1).

During the double heel-rise activity, patients had symmetric motion for the tibiotalar and subtalar joints between the TAR and untreated limbs. When comparing the TAR side to healthy controls, the tibiotalar joint in patients with a TAR demonstrated reduced dorsiflexion from 0 – 6.4 and 90.6 – 100%, reduced plantar flexion from 43.3 – 62.5%, and increased external rotation from 39.1 – 50.1% and 62.9 – 64.7% of the activity. The tibiotalar ROM for dorsi-plantarflexion was 14.8 ± 5.7° for the TAR limb, compared to 24.7 ± 6.3° for the untreated limb ($p = 0.04$), and 34.4 ± 9.5° for healthy controls ($p = 0.0001$). However, there were no significant differences in subtalar joint kinematics.

To our knowledge, this is the first study to investigate in-vivo tibiotalar and subtalar kinematics following TAR using biplane fluoroscopy. Minimally altered TAR kinematics still yielded a significant ROM reduction in the sagittal plane, which provides evidence that implant facilitated motion deviates slightly from healthy individuals. However, patients with a TAR had symmetric kinematics between treated and untreated limbs, which could be a clinically positive outcome of surgery. The bicondylar TAR design utilized herein is intended to mimic normative motion in the sagittal and transverse planes. Yet, participants did not utilize full sagittal plane motion, which may be related to implant design or secondary to habitual gait pattern tendencies persisting from pre-operative tibiotalar functional limitations.

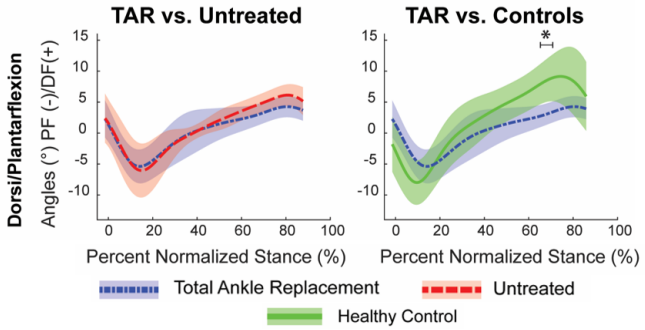

Figure 1: Mean (±95% confidence intervals) tibiotalar angles during overground walking (TAR limb = black line; controls = white line). Data are normalized to percent stance.

Significance

Altered TAR kinematics and compensatory subtalar motion may contribute to persisting postoperative pain, implant loosening, instability or secondary subtalar osteoarthritis.

Table 1. Range of motion for the tibiotalar and subtalar joints during walking and a double heel-rise activity.

Tibiotalar Range of Motion	Walking			Double Heel-rise		
	TAR	No TAR	Controls	TAR	No TAR	Controls
Dorsi/Plantarflexion	10.3 ± 3.1°	13.6 ± 4.5°	17.8 ± 4.6°	14.8 ± 5.7°	24.7 ± 6.3°	34.4 ± 9.5°
Ev/Inversion	2.5 ± 0.6°	2.9 ± 1.0°	3.8 ± 1.7°	2.3 ± 1.3°	3.0 ± 1.4°	6.6 ± 2.9°
Ext/Internal Rotation	4.8 ± 1.7°	8.9 ± 3.2°	5.3 ± 1.3°	5.6 ± 0.8°	6.7 ± 2.0°	10.9 ± 3.3°
Subtalar Range of Motion	Walking			Double Heel-rise		
	TAR	No TAR	Controls	TAR	No TAR	Controls
Dorsi/Plantarflexion	3.3 ± 1.6°	5.8 ± 2.0°	4.6 ± 1.5°	5.6 ± 2.2°	5.4 ± 2.1°	5.5 ± 3.1°
Ev/Inversion	4.1 ± 2.0°	8.5 ± 1.6°	7.6 ± 2.4°	4.2 ± 2.0°	5.1 ± 2.9°	6.7 ± 3.0°
Ext/Internal Rotation	4.7 ± 1.5°	5.9 ± 1.8°	6.5 ± 2.1°	6.7 ± 3.8°	6.2 ± 2.6°	7.4 ± 2.4°

Acknowledgments
Funding from Stryker/ORS Postdoctoral Fellowship and the National Institutes of Health (NIH R21 AR069773) is gratefully acknowledged.

References

[1] Zaidi et al. Bone Joint J 2013. [2] Brodsky et al. Foot & Ank Int. 2013. [3] Wang et al. Gait Post 2015. [4] Blair et al. Frontiers 2020.

Bi-linear Natural Ankle Quasi-Stiffness During Walking: Characterization & Implications for Orthosis Design

Luke Nigro[1], Elisa S. Arch, PhD[2]
[1]Dept. of Mechanical Engineering, University of Delaware, Newark, DE, USA
[2]Dept. of Kinesiology & Applied Physiology, University of Delaware, Newark, DE, USA
Email: lnigro@udel.edu

Summary

This research expands on an existing definition of natural ankle-quasi stiffness (NAS) as *bi-linear* – using two distinct portions of the loading phase of stance instead of one single region – to understand how ankle joint mechanics change during stance. A bi-linear ankle-foot orthosis (BL-AFO) prototype was constructed and tested as proof-of-concept for future AFO designs that can implement bi-linear stiffness.

Introduction

Natural ankle quasi-stiffness (NAS), defined as a linear regression of the sagittal ankle moment vs. ankle angle during the loading (second rocker) phase of stance, can be used as a design parameter to customize passive-dynamic AFO (PD-AFO) bending stiffness. This spring-like stiffness can substitute for lost plantar flexor (PF) function for individuals with PF weakness [1]. Historically, a single NAS value has been defined over the entire loading phase of stance [2]. NAS increases during the loading phase of stance in healthy gait [3] often with two regions of nearly linear stiffness – a lower stiffness early in loading and higher stiffness later in loading (Fig. 1). Tuning a single PD-AFO bending stiffness to the entire loading phase of stance may result in a device stiffness that is too stiff to initiate bending, or not stiff enough to provide appropriate support in late loading. This research focuses on characterizing *bi-linear* NAS – or dividing the loading phase into two distinct regions of stance, each with its own stiffness [4]. A PD-AFO prototype with bi-linear bending stiffness (BL-AFO) was then built as proof-of-concept that such a device could be designed around this concept of bi-linear NAS.

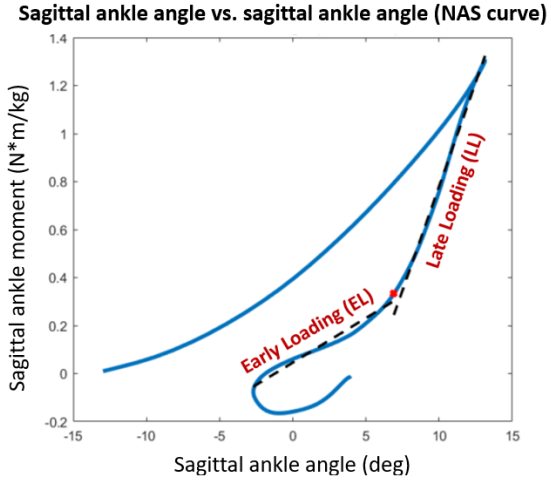

Figure 1: NAS curve of typical stance phase with the loading phase divided into EL and LL phases.

Methods

10 individuals walked at three speeds (0.6, 0.8, and 1.0 statures/s) over level ground. Sagittal ankle angles and moments were calculated from 3D kinematics and ground reaction forces (GRFs). Early loading (EL) and late loading (LL) phases were separated at the instant at which the vertical GRF reached a local minimum in the typical M-shaped profile at ~50% stance [4]. Ankle angles at the transition were calculated as the difference between the angle at that instant and the angle at which loading phase began. NAS was calculated for EL and LL regions separately for each trial and each speed. One-way ANOVA tests were used to determine significant differences in speed conditions. A BL-AFO was constructed from a single-stiffness PD-AFO with steel strips attached to a rear strut. As the BL-AFO flexes, only the rear strut bends initially. An adjustable grabber engages the steel strips once a certain angle is reached, thus adding their stiffness to the rear strut.

Results and Discussion

Average EL-NAS was 0.056 N*m/deg/kg and did not change significantly with walking speed. Average LL-NAS was 0.113, 0.162, and 0.210 N*m/deg/kg at 0.6, 0.8, and 1.0 statures/s, respectively, which is significantly greater than LL-NAS at every speed ($p<0.001$). The average transition angles for each speed were 8.7, 9.1, and 8.1 degrees for 0.6, 0.8, and 1.0 stat/s, respectively. Transition angles were significantly different from 0.8 to 1.0 stat/s only ($p<0.001$). The BL-AFO was able to achieve distinct bi-linear stiffness properties with an EL stiffness of 2.2 N*m/kg and LL stiffness of 4.2 N*m/kg and an adjustable transition angle (7-11 deg).

Conclusions

This research presents a thorough investigation of bi-linear NAS and its changes with walking speed. It also presents a BL-AFO prototype as a proof-of-concept that bi-linear stiffness can be used as design criteria for AFOs in the future.

Acknowledgments

Luke Nigro acknowledges the National Science Foundation's Graduate Research Fellowship no. 1940700 for funding, and Ralph Nigro, MS, for assistance with device construction. None of the authors have conflicts of interest to disclose.

References

[1] Arch & Reisman (2016), *J.Prosthet.Orthot.*, 28(2):60-67.
[2] Davis & DeLuca (1995), *Gait & Posture,* 4:224-231.
[3] Nigro et al. (2021), *Gait & Posture*, 84:58-65.
[4] Shamaei et al. (2013), *PLOS One,* 8(3).

The effects of joint quasi-stiffness on leg stiffness during sloped running

Caelyn Hirschman[1] & Alena M. Grabowski[1,2]
[1]Applied Biomechanics Lab, University of Colorado Boulder, CO USA; [2]VA Eastern Colorado Healthcare System, Denver, CO USA
email: Caelyn.Hirschman@colorado.edu

Introduction

Level-ground running has been well-described by a spring mass model, where body mass is a point mass, and the legs are massless linear springs [1]. Leg stiffness (k_{leg}) is the quotient of peak vertical force and leg displacement and adjusts to accommodate changes in uphill and downhill slope [2]. Further, the ankle and knee joints have been characterized as springs with angular stiffness [1]. During level running, joint stiffness (k_{joint}) is modified to increase speed and relates to k_{leg} [3]. k_{leg} and k_{joint} changes during running on slopes could provide information for biomimetic assistive device designs such as prostheses. However, the contribution of k_{joint} to k_{leg} is unknown for sloped running. We therefore determined k_{leg} and ankle (k_{ank}), knee (k_{knee}), and hip (k_{hip}) joint stiffness, and calculated theoretical leg stiffness (k_{legT}) using a novel equation [3] during running on slopes to provide insight and inform running prosthesis design. We hypothesized that when running uphill compared to level, k_{ank} and k_{hip} during the 2nd half of stance (final) will contribute more to overall k_{leg} and when running downhill compared to level, k_{knee} during the 1st half of stance (initial) will contribute more to overall k_{leg}.

Methods

20 runners (11M, 9F; mean ± SD: age 25±5 yrs; 68.5±8 kg; 175±8 cm) provided informed consent and ran on a force-treadmill (Treadmetrix, Park City, UT) at -6° and 0° at 3 m/s and +6° at 2 m/s. We measured 3D ground reaction forces (GRFs; 1000 Hz) and lower body motion (100 Hz; Vicon, Centennial, CO). We calculated joint angles (θ) and moments (M) during ground contact using Visual 3D (C-Motion, Germantown, MD). We calculated initial k_{joint} (k_{jointI}) from touch down to mid-stance and final k_{joint} (k_{jointF}) from mid-stance to toe off as $\Delta M/\Delta\theta$. To determine how k_{joint} affects k_{leg}, we used an equation derived by Moholkar (Eq. 1) to calculate initial and final k_{legT} [4]. The external moment arm of each joint (R) equals the average perpendicular distance from the GRF vector to the joint center of rotation.

$$k_{legT} = \left(\frac{R_{ank}^2}{k_{ank}} + \frac{R_{knee}^2}{k_{knee}} + \frac{R_{hip}^2}{k_{hip}}\right)^{-1} \qquad \text{Eq.1}$$

We used a one-way ANOVA and Bonferroni post hoc analyses to determine significant differences with $p<0.05$.

Results and Discussion

k_{ankleI} and k_{ankleF} did not change at +6° or -6° compared to 0° ($p>0.05$; Fig 1b & Table 1). k_{kneeI} increased at +6° ($P<0.01$) and k_{kneeF} increased at -6° ($p<0.01$) compared to 0° (Fig 1c & Table 1). k_{hipF} increased at +6° ($p<0.01$) compared to 0° (Fig 1d & Table 1). The contribution of k_{ankleI} and k_{ankleF} to k_{legT} did not change at +6° or -6° compared to 0° ($p>0.05$; Fig 2). k_{kneeF} contributed to k_{legT} 15% more at -6° compared to 0° (Fig 2) and k_{hipF} contributed to k_{legT} 15% more at +6° compared to 0° (Fig 2). In general, initial k_{legT} decreased at +6° ($p<0.05$) and final k_{legT} increased at -6° ($p<0.05$) compared to 0°.

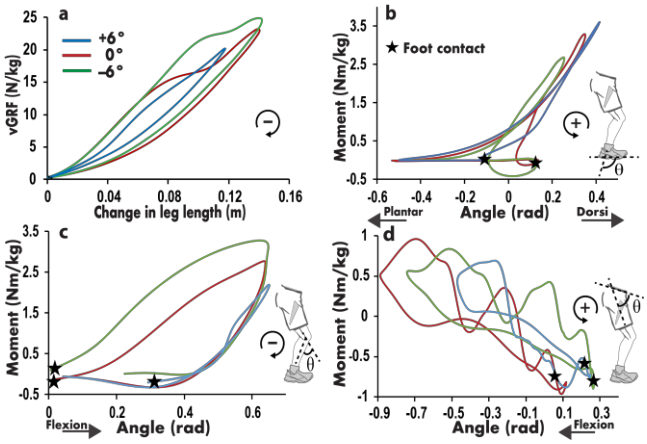

Fig 1. Representative lines indicate **a.** k_{leg} **b**. k_{ank} **c**. k_{knee}, and **d**. k_{hip} during running at 0° and ±6°. Area within each curve is net mechanical work. Static angles are 0 rad. Positive ankle, knee, and hip angle is dorsiflexion, flexion, and extension, respectively. * is foot contact and arrow is direction of net mechanical work.

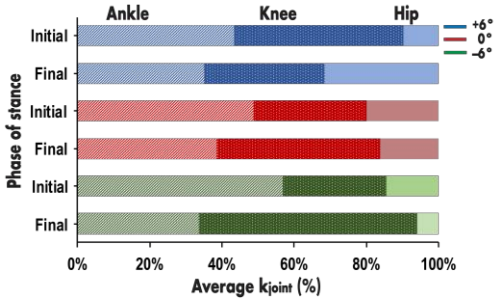

Fig 2. Average k_{joint} contributions during initial and final half of stance phase. 100% is the sum of average k_{ankle}, k_{knee} and k_{hip} used for Eq.1.

Table 1. k_{ank}, k_{knee}, and k_{hip} in N*m/kg/rad and k_{legT} in N/m/kg during running at 0° and ±6°. * indicates $p<0.05$ compared to 0°.

	-6°		0°		+6°	
	Initial	**Final**	**Initial**	**Final**	**Initial**	**Final**
k_{ank}	10.0 ± 4.5	7.3 ± 2.6	9.7 ± 3.1	6.1 ± 1.5	8.1 ± 2.4	5.2 ± 0.9
k_{knee}	5.0 ± 1.0	13.1 ± 4.7 *	6.2 ± 3.1	7.2 ± 1.1	8.8 ± 1.9 *	5.0 ± 1.9
k_{hip}	2.5 ± 2.6	1.3 ± 1.0	3.9 ± 7.4	2.6 ± 1.7	1.8 ± 1.7	4.7 ± 2.6*
k_{legT}	309.4 ± 130	476.2 ±241*	337.3 ± 153	337.9 ±78.2	217.0 ±112*	284.2 ± 111

Significance

Our results suggest that during uphill running, an assistive device should be less stiff initially then more stiff after mid-stance at the hip and during downhill running, an assistive device should be more stiff after mid-stance at the knee.

Acknowledgments

Work supported by a VA Career Development Award.

References

1 McMahon & Cheng. *J Biomech.* **23**, 65-78, 1990
2 Ferris et al. *Proc Biol Sci*. **265**, 989-994, 1997
3 Moholkar. PhD dissertation. *UC Berkeley*, 2004

The effects of real time visual feedback on metabolic cost during walking in people with transtibial amputation.

Caelyn Hirschman[1], Janet Zhang[1] & Alena M. Grabowski[1,2]
[1]Applied Biomechanics Lab, University of Colorado Boulder, CO USA
[2]Eastern Colorado Healthcare System, Department of Veterans Affairs, Denver, CO USA
email: Caelyn.Hirschman@colorado.edu

Introduction

People with unilateral transtibial amputation (TTA) using a passive-elastic prosthesis have a higher metabolic cost [1] and greater biomechanical asymmetry during walking than non-amputees [2]; peak horizontal and vertical ground reaction force (GRF) produced by the affected leg (AL) are lower compared to the unaffected leg (UL) [2]. We provided real time visual feedback (VF) of AL peak propulsive GRF during walking and hypothesized that 1. when using a passive elastic prosthesis, participants with TTA would increase average AL peak propulsive GRF to meet the training targets 20% and 40% higher, decrease asymmetry, and incur a greater metabolic cost than baseline trials; 2. participants with TTA would not retain increased AL peak propulsive force when VF was removed and thus asymmetry and net metabolic power would return to baseline.

Methods

Two subjects (S1, S2; 1M, 1F) with unilateral TTA provided informed consent and walked on a dual-belt force treadmill (Bertec, Columbus. OH) at 1.25 m/s using their own passive elastic prosthesis while we measured vertical and horizontal GRFs (1000 Hz) and normalized to body weight. We measured rates of oxygen consumption and carbon dioxide production via indirect calorimetry (ParvoMedics TrueOne2400, Sandy, UT) throughout each 5-min trial and averaged them during the last 2 min. We calculated net metabolic power (NMP) using a standard equation [Brockway 1987] and by subtracting metabolic power during standing.

During VF trials, we placed a monitor at eye level ~1.5 m in front of each subject and plotted real time peak propulsive GRF (Fig. 1). We asked subjects to match a target indicating 0%, +20% and +40% of their baseline AL peak propulsive force. Baseline (0%) AL peak propulsive GRF was measured during the first 5-min walking trial. Each VF trial was 5 min, followed by a 5-min rest and a 5-min retention trial where VF was removed. We calculated AL peak propulsive GRF, symmetry index (SI) of peak propulsive GRF between legs [3] and net metabolic power during each trial. SI is the percent difference between the UL and AL and 0% is perfect symmetry.

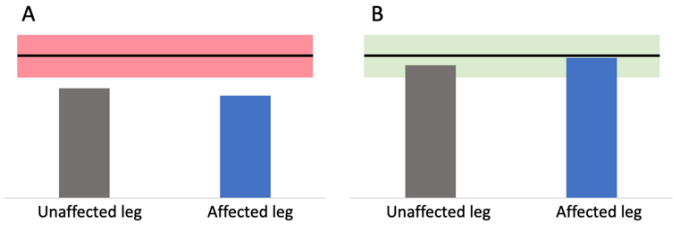

Figure 1: Example of VF provided. Gray and blue vertical bars represent each leg's peak propulsive GRF measured in real-time. Horizontal bar represents the training target and turns from red (A) to green (B) if the subject meets the target within 5%.

Results and Discussion

Compared to baseline walking, S1 increased AL peak propulsive GRF by up to 10.9% (Fig 2a) and had a lower SI in +20% (SI=24.5%) and +40% (SI = 28%) VF trials (Fig 2b). S2 increased AL peak propulsive GRF by 12.4-58.2% in all VF walking trials (Fig 2a) and had lower peak propulsive GRF SI (SI = 30.6-5.9%; Fig 2b). Both subjects exhibited greater net metabolic power (NMP) during the VF trials compared to baseline, where S1 had 5.5-6.9% and S2 had 8.2-12.9% greater NMP (Fig 2c). During retention trials neither subject retained AL peak propulsive GRF exhibited during VF trials, where S1 increased AL peak propulsive GRF by 0.9-4.2% (Fig 2a) and had an SI closer to baseline (SI = 27.8-33.1%; Fig 2b) and S2 increased AL peak propulsive GRF by 4.5-8.4% (Fig 2a) and had more asymmetric peak propulsive GRF (SI = 0.6-44.7%; Fig 2b) compared to retention trials. During retention trials, S1 increased NMP by 0.6-7.4% compared to baseline and subject 2 decreased NMP by 0.3-2.7% compared to baseline (Fig 2c).

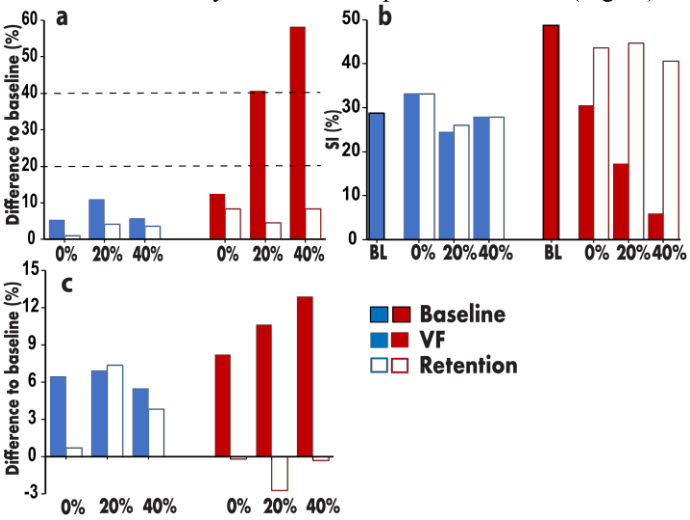

Figure 2. (**a**) AL peak propulsive GRF percent difference versus baseline and (**b**) SI of peak propulsive GRF, where lower SI is more symmetric and (**c**) NMP percent difference versus baseline from VF and retention trials for S1 (blue) and S2 (red). Horizontal dashed lines in (a) indicate +20 & +40% target for AL peak propulsive GRF.

Significance

Our results suggest that real time VF of AL peak propulsive GRF could increase AL peak propulsive force and reduce asymmetry for people with TTA. However, subjects increased net metabolic power during VF trials using a passive-elastic prosthesis. Thus, use of a stance-phase powered ankle prosthesis combined with VF may potentially improve symmetry and reduce metabolic power during walking.

Acknowledgments

Funding from the VA RR&D Service.

References

1. Huang et al., *Physical Medicine and Rehabilitation,* 1979
2. Grabowski & D'Andrea, *J NeuroEngineering Rehabil*, 2013
3. Robinson & Nigg, *J Manipulative Physiol Ther*, 1987

WHAT IS THE MOST EFFICIENT SEAT TUBE ANGLE FOR UPHILL SEATED CYCLING?

Ross D. Wilkinson[1], Todd Carver[2], and Rodger Kram[1]
[1]Locomotion Laboratory, University of Colorado, Boulder, CO, USA
[2]Specialized Bicycle Components Inc., Boulder, CO, USA
Email: ross.wilkinson@colorado.edu

Introduction

When riding uphill, many cyclists sit further forward on the saddle presumably because they experience an increased level of comfort, performance, and/or stability—but no empirical evidence exists. This forward shift of the hip joint center relative to the bottom bracket, in effect, steepens the seat tube angle (STA) of the bicycle frame (See Figure 1). Data on the effect of changing STA on the metabolic efficiency of level and uphill cycling are sparse and contradictory [1, 2, 3].

We investigated if the most efficient STA is specific to the incline of the terrain during level and uphill cycling on a stationary trainer and a treadmill.

Methods

Twenty-one healthy recreational cyclists volunteered (17M/4F, age= 33 ± 14 y, height= 1.77 ± 0.08 m, mass= 70 ± 9 kg, mean $\pm$ sd). Subjects rode an appropriately sized mountain bicycle (Chisel, Specialized Bicycle Components, Inc., Morgan Hill, CA, USA), fitted with a crank-based mechanical power meter (Quarq DZero, SRAM, Corp. Chicago, IL, USA). We set saddle height for each subject using a Retul Vantage fitting system and it remained constant for all conditions. Saddle tilt angle was -2° nose down relative to the riding surface for all conditions.

Testing comprised two sessions on separate days: one day riding on a trainer (KickR, Wahoo Fitness LLC, Atlanta, GA, USA) and a second day on a large, custom-built, motorized treadmill. Each day, subjects performed a total of six, 5-min bouts of seated cycling at ~ 3 W kg^{-1}, comprised of three bouts on a level surface and three on a 5° (8%) incline in three STA conditions: 74°, 79°, and 84°. The order of sessions and trials were randomized. Subjects used their freely chosen cadence.

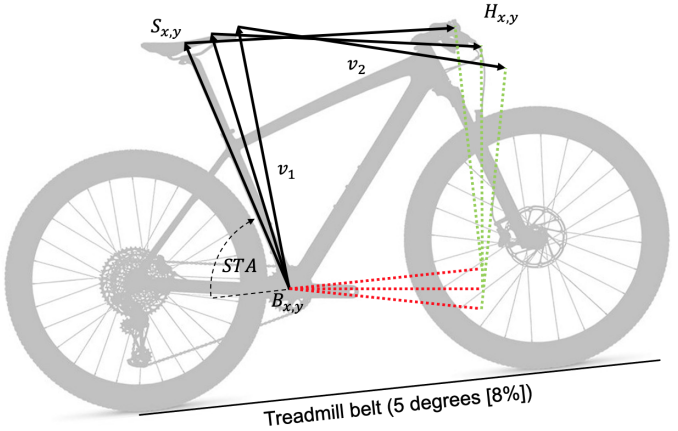

Figure 1: We altered the effective STA by rotating both v_1 and v_2. In this design, $\Delta S_{x,y} \neq \Delta H_{x,y}$ and $\Delta\theta \neq \Delta\angle BSH$ (*i.e.* the mean hip angle remains constant).

We calculated metabolic power[4] from the rates of oxygen consumption and carbon dioxide production during the last 2 min of each 5-min trial as measured by an open-circuit, expired gas analysis system (TrueOne 2400, ParvoMedics, Sandy, UT, USA).

Statistical analysis comprised a repeated-measures, three-way ANOVA ($apparatus \times incline \times STA$) with multiple comparisons (theory-wise Dunn-Sidak correction).

Results and Discussion

On the level trainer, the differences in gross efficiency between each STA were inconclusive. On a 5° inclined trainer, riders were 0.9% more efficient at 79° *vs.* 74° (t=2.0, p=.04, $CI_{95\%}[0.1,1.9]$). On the level treadmill, riders were 1.4% less efficient at 79° *vs.* 74° (t=2.5, p=.01, $CI_{95\%}[-0.3,-2.5]$). On a 5° inclined treadmill, the difference in gross efficiency between 79° and 74° was inconclusive. On both the level and inclined treadmill, riders were less efficient at 84° compared to 74° and 79°.

		STA		
		74°	79°	84°
Trainer	Level	21.7(0.2)	21.8(0.2)	21.5(0.3)
	Uphill	$21.5(0.2)^{b}$	$21.7(0.3)^{a}$	21.5(0.3)
Treadmill	Level	$21.6(0.2)^{b,c}$	$21.3(0.2)^{a,c}$	$20.9(0.3)^{a,b}$
	Uphill	$20.9(0.2)^{c}$	$21.1(0.3)^{c}$	$20.6(0.3)^{a,b}$

^{a,b,c}statistically different to 74°, 79°, and 84°, respectively (corrected p$<$ .05).

Table 1: Group mean results of gross efficiency in all conditions. Data are mean (standard error).

Significance

We find that riders improved their efficiency by using a 79° STA when cycling up a 5° incline. But, the most efficient STA varies with the incline of the terrain.

Acknowledgments

Supported by an unrestricted gift from Specialized Bicycle Components, Inc. TC is an employee of Specialized Bicycle Components, Inc.

References

[1] Heil et al. *Med Sci Sport Exer*, 27(5):730–735, 1995.
[2] Heil et al. *Eur J Appl Physiol O*, 75(2):160–165, 1997.
[3] Price and Donne. *J Sport Sci*, 15(4):395–402, 1997.
[4] Péronnet and Massicotte. *Can J Sport Sci*, 16:23–29, 1991.

NOSE-DOWN SADDLE TILT IMPROVES GROSS EFFICIENCY DURING SEATED UPHILL CYCLING

Ross D. Wilkinson and Rodger Kram
Locomotion Laboratory, University of Colorado, Boulder, CO, USA
Email: ross.wilkinson@colorado.edu

Introduction

The exciting penultimate stage of the 2020 Tour de France featured a time-trial with a steep 6 km uphill finish. Many racers switched to an uphill-specific bicycle before the final climb [1] to enhance their performance [2]. One aspect of bike setup that allegedly improves uphill cycling performance is nose-down saddle tilt. Some suggest that nose-down saddle tilt can reduce oxygen consumption and elbow flexor activity but supporting data are sparse [3]. Here, we tested the null hypothesis that there would be no effect of tilting the saddle 8° nose down on a cyclist's gross efficiency when cycling up an 8° incline.

Methods

Nineteen healthy recreational cyclists (18M/1F, age= 31 ± 9 y, height= 1.80 ± 0.06 m, mass= 74 ± 11 kg, mean $\pm$ sd) performed six, 5-min bouts of seated cycling at $\sim$ 3 W kg^{-1} on a large custom-built, motorized treadmill (length 3.2 m, width 0.9 m) inclined to 8°. The six trials consisted of three replicates of two saddle tilt angle conditions: parallel to the riding surface and 8° nose down. All subjects rode the same 56 cm road bicycle (Roubaix, Specialized Bicycle Components Inc., Morgan Hill, CA, USA), which was equipped with a crank-based mechanical power meter (Quarq DZero, SRAM, Corp. Chicago, IL, USA). We calculated metabolic power [4] from the rates of oxygen consumption and carbon dioxide production during the last 2 min of each 5-min trial as measured by an open-circuit, expired gas analysis system (TrueOne 2400, ParvoMedics, Sandy, UT, USA). Due to the steep incline, all subjects chose to ride in the "easiest" gear combination available (30x42).

We averaged the metabolic power values for the three replicates of the two conditions. A Jarque-Bera test with Monte Carlo simulation confirmed that the data matched a normal distribution (p= 0.879). Thus, a paired t-test was used to test the null hypothesis at the 5% significance level.

Results and Discussion

Our data provides statistically significant evidence that tilting the saddle nose down by 8° is associated with an improvement in gross efficiency when cycling up an 8° incline ($t = 5.9$, $p < 0.001$, $CI_{95\%}$ [0.2,0.4], ES = 1.3). Thus, we reject our null hypothesis. Gross efficiency improved for 16 out of 19 subjects in the nose-down condition compared to parallel with a mean relative improvement of $1.4 \pm 1.0\%$. Based on the probability distribution of our data, $\sim 91\%$ of cyclists are likely to improve their gross efficiency by tilting the saddle nose down by 8° when cycling up an 8° incline. Furthermore, $\sim 28\%$ of cyclists are likely to experience a $\geq 2\%$ improvement in gross efficiency. The mean mechanical power (Parallel= 2.87 ± 0.21, Nose down= 2.88 ± 0.22 W kg^{-1}), cadence (Parallel= 59 ± 4, Nose down= 59 ± 4 RPM), and RER (Paralllel= 0.90 ± 0.03, Nose down= 0.90 ± 0.03) were virtually identical between the two conditions.

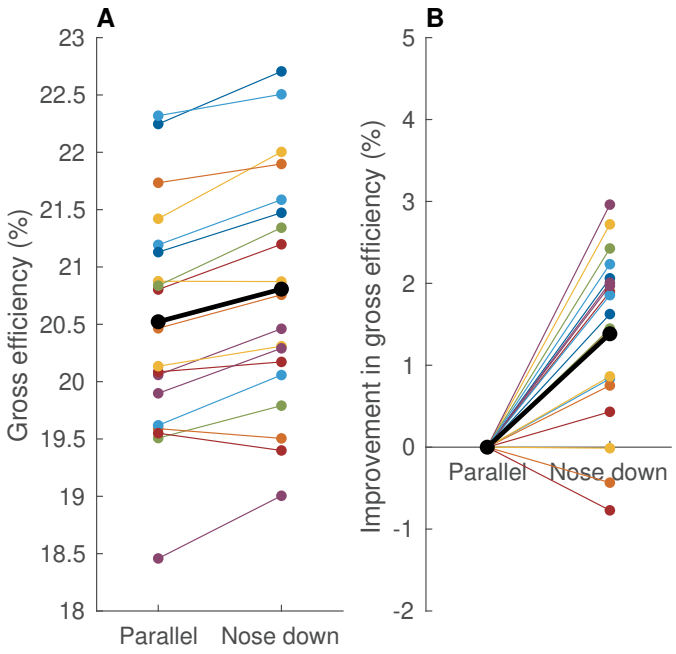

Figure 1: Individual (color) and group mean (black) gross efficiency (A) and percentage improvement in gross efficiency (B).

Significance

Current UCI (Union Cycliste Internationale) regulations allow a maximum saddle tilt angle of 9° in road cycling and there are no restrictions on mountain bikes. Our results suggest that riders could significantly improve their gross efficiency by tilting their saddle nose down by 8° on an 8° incline. We speculate that improvements in gross efficiency due to tilting the saddle nose down may be greater on steeper inclines. Further research is required to reveal the mechanism(s) responsible for the improvements in gross efficiency and to confirm that matching nose down tilt angle to surface incline maximizes gross efficiency.

Acknowledgments

Supported by an unrestricted gift from Koch Bein, LLC.

References

[1] Robinson. *WSJ*, https://tinyurl.com/2iqczo95, 2020.
[2] Roa and Muñoz. *Proc Inst Mech Eng*, 231(3):207–19, 2017.
[3] Fonda and Ŝarabon. *Kinesiology*, 44(1):5–17, 2012.
[4] Péronnet and Massicotte. *Can J Sport Sci*, 16:23–29, 1991.

RUNNING SHOES WITH A CARBON PLATE VS. TRADITIONAL CYCLING SHOES: EQUAL PERFORMANCE IN CYCLING SPRINTS?

Kyle Sterns[1], James W. Hurt III[2], Ross D. Wilkinson[1], and Rodger Kram[1]
[1]Locomotion Laboratory, University of Colorado, Boulder, CO, USA
[2]Hustle Bike Labs LLC, Crowley, TX, USA
Email: kyle.sterns@colorado.edu

Introduction

The sport of triathlon has historically catalyzed many new shoe designs because shoes need to maximize performance within each discipline but must also facilitate quick transitions. To maximize performance within the respective disciplines, professional triathletes typically use rigid-soled cycling-specific shoes with cleats that attach to the pedals and then transition to running-specific shoes for the running portion of the triathlon. Previous studies have demonstrated that, at sub-maximal efforts, shoe flexibility has no effect on cycling metabolic efficiency [1]. However, flexible shoes lacking a shoe-pedal attachment decrease maximal cycling power output by 26% [2]. Newly developed running shoes containing a stiff carbon fiber plate may present a new option especially for triathletes. Completing the cycling leg of a triathlon in running shoes would greatly reduce the bike-to-run transition time. We tested the null hypothesis that such running shoes and cycling shoes would have equal performance during cycling sprints.

Methods

Fourteen healthy cyclists (age $= 25 \pm 11$ y, height $= 1.80 \pm 0.06$ m, mass $= 69 \pm 7$ kg, mean $\pm$ sd) performed eight all-out cycling sprints, 50 m up a 4.9% incline, from a rolling start at 20 km hr^{-1}. Trials consisted of four sprints in each shoe condition. (traditional cycling shoes and hybrid running shoes). The traditional cycling shoes were Specialized S-Works 6 with carbon fiber soles and a standard Shimano SPD-SL cleat and pedal interface. The hybrid shoes were modified Nike 4% Vaporflys with a small steel plate attached to the carbon fiber plate that interfaced with prototype magnetic mountain bike pedals (Hustle Bike Labs LLC, Crowley, TX, USA). All subjects rode the same 56 cm road bicycle (Roubaix, Specialized Bicycle Components Inc., Morgan Hill, CA, USA), which was equipped with a crank-based mechanical power meter (Quarq DZero, SRAM, Corp. Chicago, IL, USA). We calculated peak 1-s and 50-m average crank power over the sprint interval. We averaged the peak 1-s and 50-m average power values for the replicates of the two conditions and used paired t-tests to evaluate the null hypothesis at the 5% significance level.

Results and Discussion

Peak 1-s crank power was lower for 12 of 14 subjects in the running shoes compared to the cycling shoes but was only $8.4 \pm 6.5\%$ less ($p < 0.001$). Similarly, 50-m average power decreased for 11 of 13 subjects but only by $6.9 \pm 5.9\%$ ($p = 0.002$). Sprinting is rare in triathlons, so even though some power would be lost during accelerations after turns, the bike-run transition time would be slashed. We believe that the lower power output with the hybrid shoe was due partly to rider skepticism about the magnetic pedals. The hybrid shoes closed the gap in power lost from 26% [1] to 8.4%, and with improved rider confidence and shoe design, there is potential to further close this gap.

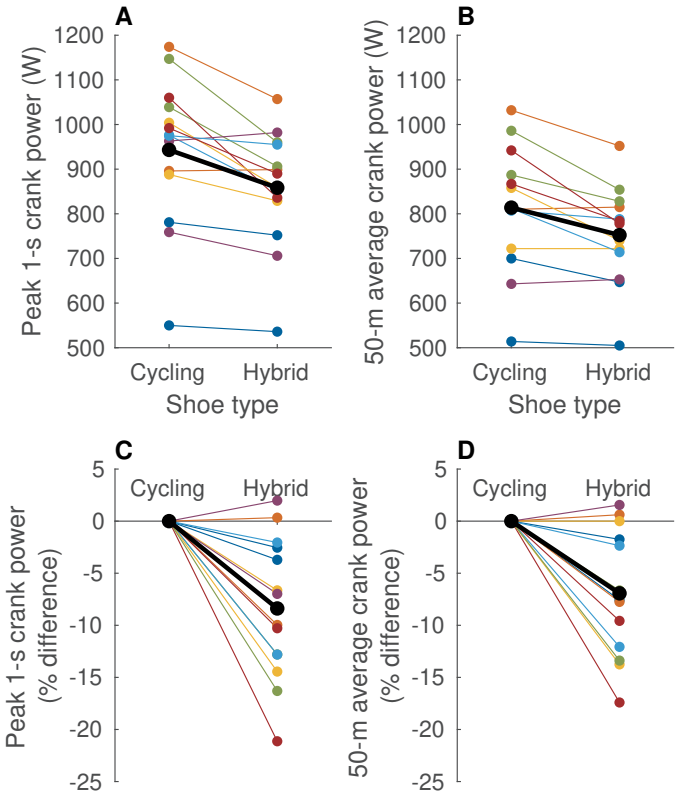

Figure 1: Individual (color) and group mean (black) peak 1-s crank power (A), 50-m average crank power (B), percentage change in peak 1-s crank power (C), and percentage change in 50-m average crank power (D).

Significance

We find that for producing maximal crank power, cycling shoes are superior. However, hybrid running shoes could clearly save time during the bike-run triathlon transition. Further research and development of hybrid run-cycling shoes are needed to fully explore their potential as a footwear replacement for triathlon.

Acknowledgments

Supported by the Undergraduate Research Opportunities Program (UROP) at the University of Colorado. RK is a paid consultant to Nike Inc. Specialized Bicycle Components Inc. supports the CU Locomotion Lab. JWH is employed by Hustle Bike Labs LLC.

References

[1] Straw and Kram. *Footwear Sci*, 8(1):19–22, 2016.
[2] Burns and Kram. *Footwear Sci*, 12(3):185–192, 2020.